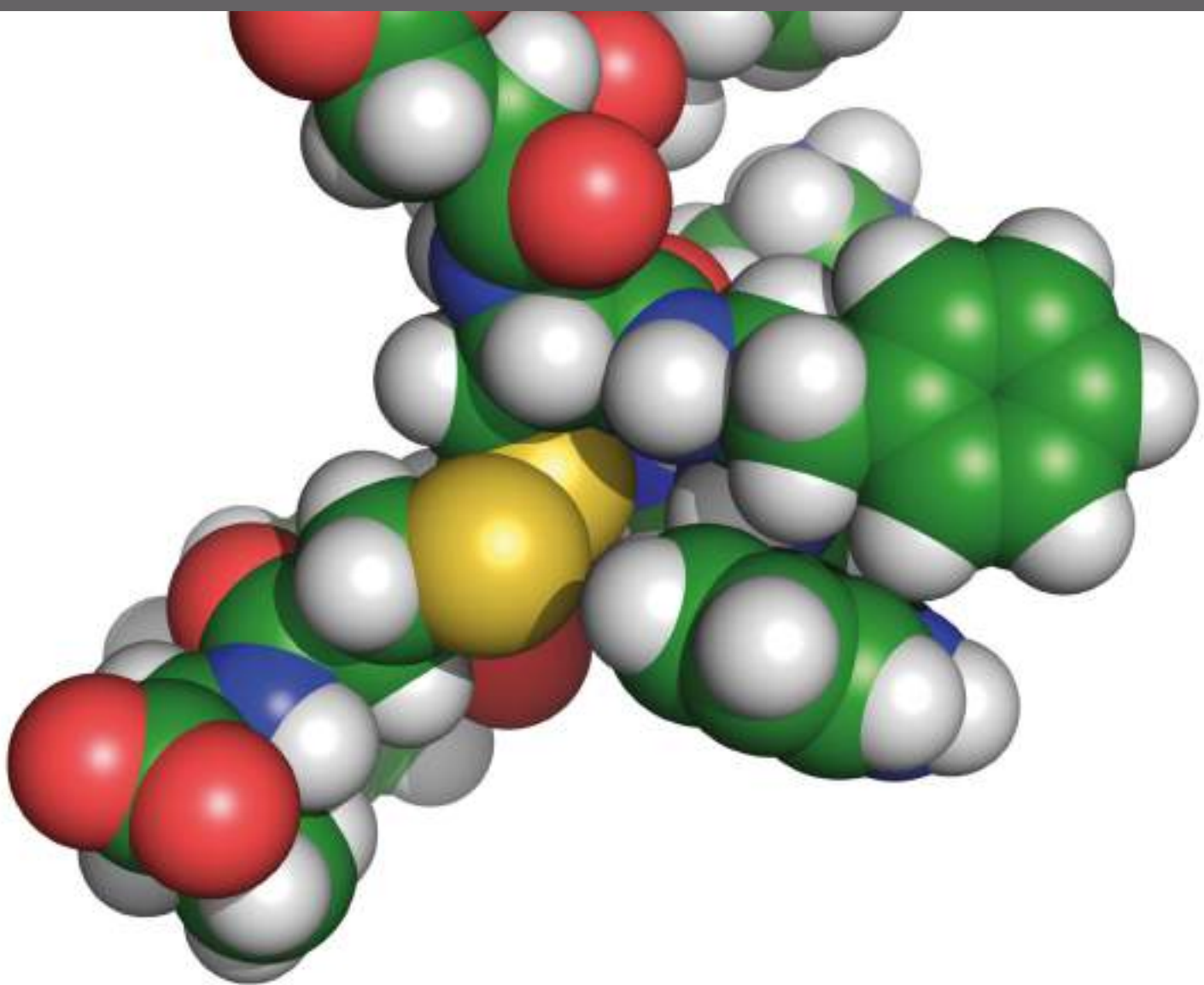
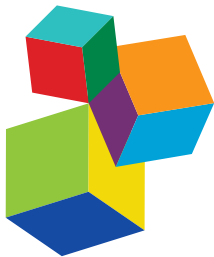


TRENDS IN REGULATORY PEPTIDES

EDITED BY: Hubert Vaudry, Marie-Christine Tonon and David Vaudry

PUBLISHED IN: Frontiers in Endocrinology and Frontiers in Neuroscience





Frontiers Copyright Statement

© Copyright 2007-2018 Frontiers Media SA. All rights reserved.

All content included on this site, such as text, graphics, logos, button icons, images, video/audio clips, downloads, data compilations and software, is the property of or is licensed to Frontiers Media SA ("Frontiers") or its licensees and/or subcontractors. The copyright in the text of individual articles is the property of their respective authors, subject to a license granted to Frontiers.

The compilation of articles constituting this e-book, wherever published, as well as the compilation of all other content on this site, is the exclusive property of Frontiers. For the conditions for downloading and copying of e-books from Frontiers' website, please see the Terms for Website Use. If purchasing Frontiers e-books from other websites or sources, the conditions of the website concerned apply.

Images and graphics not forming part of user-contributed materials may not be downloaded or copied without permission.

Individual articles may be downloaded and reproduced in accordance with the principles of the CC-BY licence subject to any copyright or other notices. They may not be re-sold as an e-book.

As author or other contributor you grant a CC-BY licence to others to reproduce your articles, including any graphics and third-party materials supplied by you, in accordance with the Conditions for Website Use and subject to any copyright notices which you include in connection with your articles and materials.

All copyright, and all rights therein, are protected by national and international copyright laws.

The above represents a summary only. For the full conditions see the Conditions for Authors and the Conditions for Website Use.

ISSN 1664-8714
ISBN 978-2-88945-537-9
DOI 10.3389/978-2-88945-537-9

About Frontiers

Frontiers is more than just an open-access publisher of scholarly articles: it is a pioneering approach to the world of academia, radically improving the way scholarly research is managed. The grand vision of Frontiers is a world where all people have an equal opportunity to seek, share and generate knowledge. Frontiers provides immediate and permanent online open access to all its publications, but this alone is not enough to realize our grand goals.

Frontiers Journal Series

The Frontiers Journal Series is a multi-tier and interdisciplinary set of open-access, online journals, promising a paradigm shift from the current review, selection and dissemination processes in academic publishing. All Frontiers journals are driven by researchers for researchers; therefore, they constitute a service to the scholarly community. At the same time, the Frontiers Journal Series operates on a revolutionary invention, the tiered publishing system, initially addressing specific communities of scholars, and gradually climbing up to broader public understanding, thus serving the interests of the lay society, too.

Dedication to quality

Each Frontiers article is a landmark of the highest quality, thanks to genuinely collaborative interactions between authors and review editors, who include some of the world's best academicians. Research must be certified by peers before entering a stream of knowledge that may eventually reach the public - and shape society; therefore, Frontiers only applies the most rigorous and unbiased reviews.

Frontiers revolutionizes research publishing by freely delivering the most outstanding research, evaluated with no bias from both the academic and social point of view. By applying the most advanced information technologies, Frontiers is catapulting scholarly publishing into a new generation.

What are Frontiers Research Topics?

Frontiers Research Topics are very popular trademarks of the Frontiers Journals Series: they are collections of at least ten articles, all centered on a particular subject. With their unique mix of varied contributions from Original Research to Review Articles, Frontiers Research Topics unify the most influential researchers, the latest key findings and historical advances in a hot research area! Find out more on how to host your own Frontiers Research Topic or contribute to one as an author by contacting the Frontiers Editorial Office: researchtopics@frontiersin.org

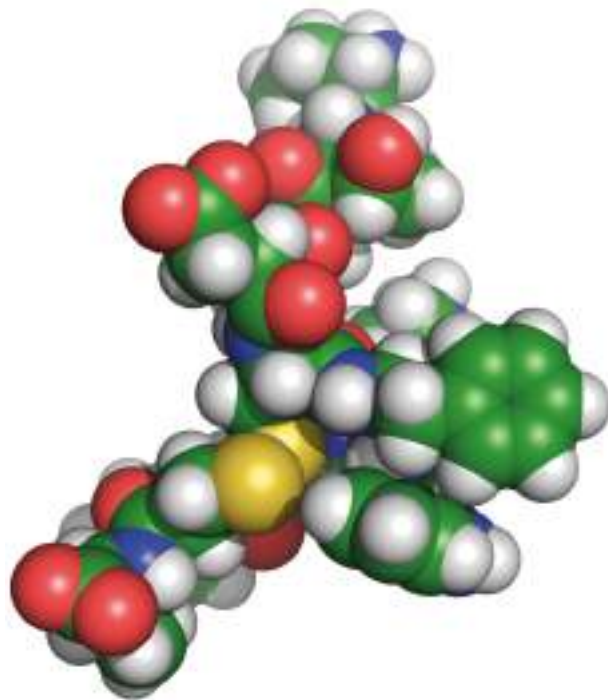
TRENDS IN REGULATORY PEPTIDES

Topic Editors:

Hubert Vaudry, University of Rouen, France

Marie-Christine Tonon, University of Rouen, France

David Vaudry, University of Rouen, INSERM U1239, France



Secondary structure of the regulatory peptide urotensin II. Three articles in this eBook are dedicated to the cardiovascular and chemotactic activities of urotensin II in fish and mammals.

Image: Nicolas Doucet, Jérôme Leprince, Chitra Narayanan, Jana Sopkova-de Oliveira Santos, and Marie-Christine Tonon.

Regulatory peptides represent the most diverse and versatile family of messenger molecules. They are produced by all living organisms from bacteria to mammals. They are involved in a wide variety of biological functions. Biologically active peptides and their receptors thus constitute an unlimited source of inspiration for the development of innovative drugs and cosmetics.

The present eBook is a unique collection of research articles and reviews that provide a representative exemplification of the latest progress in regulatory peptide research.

Citation: Vaudry, H., Tonon, M-C., Vaudry, D., eds. (2018). Trends in Regulatory Peptides. Lausanne: Frontiers Media. doi: 10.3389/978-2-88945-537-9

Table of Contents

06 Editorial: Trends in Regulatory Peptides

Hubert Vaudry, Marie-Christine Tonon and David Vaudry

G PROTEIN-COUPLED RECEPTORS

11 A Practical Guide to Approaching Biased Agonism at G Protein Coupled Receptors

Jaimee Gundry, Rachel Glenn, Priya Alagesan and Sudarshan Rajagopal

17 Distinct Conformational Dynamics of Three G Protein-Coupled Receptors Measured Using FlAsH-BRET Biosensors

Kyla Bourque, Darlaine Pétrin, Rory Sleno, Dominic Devost, Alice Zhang and Terence E. Hébert

NEUROPEPTIDES AND GLIOPEPTIDES

28 Activation of Brain Somatostatin Signaling Suppresses CRF Receptor-Mediated Stress Response

Andreas Stengel and Yvette F. Taché

38 Role of Transient Receptor Potential Ankyrin 1 Ion Channel and Somatostatin sst₄ Receptor in the Antinociceptive and Anti-inflammatory Effects of Sodium Polysulfide and Dimethyl Trisulfide

István Z. Bátkai, Ádám Horváth, Erika Pintér, Zsuzsanna Helyes and Gábor Pozsgai

50 NPY1 Receptor Agonist Modulates Development of Depressive-Like Behavior and Gene Expression in Hypothalamus in SPS Rodent PTSD Model

Lidia Serova, Hannah Mulhall and Esther Sabban

57 Involvement of the Bradykinin B₁ Receptor in Microglial Activation: In Vitro and In Vivo Studies

Keren Asraf, Nofar Torika, Abraham Danon and Sigal Fleisher-Berkovich

66 Hemoglobin-Improved Protection in Cultured Cerebral Cortical Astroglial Cells: Inhibition of Oxidative Stress and Caspase Activation

Fatma Amri, Ikram Ghouili, Marie-Christine Tonon, Mohamed Amri and Olfa Masmoudi-Kouki

76 The Eight and a Half Year Journey of Undiagnosed AD: Gene Sequencing and Funding of Advanced Genetic Testing Has Led to Hope and New Beginnings

Illana Gozes, Marc C. Patterson, Anke Van Dijck, R. Frank Kooy, Joseph N. Peeden, Jacob A. Eichenberger, Angela Zawacki-Downing and Sandra Bedrosian-Sermone

GASTROINTESTINAL PEPTIDES

90 Cholecystokinin—From Local Gut Hormone to Ubiquitous Messenger

Jens F. Rehfeld

98 Ghrelin Is a Regulator of Glucagon-Like Peptide 1 Secretion and Transcription in Mice

Andreas Lindqvist, Liliya Shcherbina, Ann-Helen Thorén Fischer and Nils Wierup

- 104 Protein Digestion-Derived Peptides and the Peripheral Regulation of Food Intake**
Juliette Caron, Dorothée Domenger, Pascal Dhulster, Rozenn Ravallec and Benoit Cudennec
- 115 Loss of Vagal Sensitivity to Cholecystokinin in Rats Born with Intrauterine Growth Retardation and Consequence on Food Intake**
Marième Ndjim, Camille Poinsignon, Patricia Parnet and Gwenola Le Dréan

PEPTIDES AND CANCER

- 126 Enhanced Mortality to Metastatic Bladder Cancer Cell Line MB49 in Vasoactive Intestinal Peptide Gene Knockout Mice**
Niely Mirsaidi, Matthew P. Burns, Steve A. McClain, Edward Forsyth, Jonathan Li, Brittany Dukes, David Lin, Roxanna Nahvi, Jheison Giraldo, Megan Patton, Ping Wang, Ke Lin, Edmund Miller, Timothy Ratliff, Sayyed Hamidi, Scott Crist, Ken-Ichi Takemaru and Anthony Szema
- 132 AM-37 and ST-36 Are Small Molecule Bombesin Receptor Antagonists**
Terry W. Moody, Nicole Tashakkori, Samuel A. Mantey, Paola Moreno, Irene Ramos-Alvarez, Marcello Leopoldo and Robert T. Jensen
- 140 Gastrin and Gastric Cancer**
Helge L. Waldum, Liv Sagatun and Patricia Mjønes
- 147 Receptor-Mediated Melanoma Targeting with Radiolabeled α-Melanocyte-Stimulating Hormone: Relevance of the Net Charge of the Ligand**
Jean-Philippe Bapst and Alex N. Eberle
- 158 Inhibition of Ectopic Arginine Vasopressin Production by Phenytoin in the Small Cell Lung Cancer Cell Line Lu-165**
Takahiro Ohta, Mitsuo Mita, Shigeru Hishinuma, Reiko Ishii-Nozawa, Kazuhisa Takahashi and Masaru Shoji
- 164 The Role of Endocrine G Protein-Coupled Receptors in Ovarian Cancer Progression**
Qingyu Zhang, Nadine Ellen Madden, Alice Sze Tsai Wong, Billy Kwok Chong Chow and Leo Tsz On Lee
- 173 The Autophagy Machinery: A New Player in Chemotactic Cell Migration**
Pierre-Michaël Coly, Pierrick Gandolfo, Hélène Castel and Fabrice Morin

CARDIOVASCULAR PEPTIDES

- 184 [Pyr¹]Apelin-13₍₁₋₁₂₎ Is a Biologically Active ACE2 Metabolite of the Endogenous Cardiovascular Peptide [Pyr¹]Apelin-13**
Peiran Yang, Rhoda E. Kuc, Aimée L. Brame, Alex Dyson, Mervyn Singer, Robert C. Glen, Joseph Cherian, Ian B. Wilkinson, Anthony P. Davenport and Janet J. Maguire
- 198 Role of the Vasopressin/Apelin Balance and Potential Use of Metabolically Stable Apelin Analogs in Water Metabolism Disorders**
Adrien Flahault, Pierre Couvineau, Rodrigo Alvear-Perez, Xavier Iturrioz and Catherine Llorens-Cortes
- 212 Central and Peripheral Effects of Urotensin II and Urotensin II-Related Peptides on Cardiac Baroreflex Sensitivity in Trout**
Frédéric Lancien, Gilmer Vanegas, Jérôme Leprince, Hubert Vaudry and Jean-Claude Le Mével

222 *The G Protein-Coupled Receptor UT of the Neuropeptide Urotensin II Displays Structural and Functional Chemokine Features*

Hélène Castel, Laurence Desrues, Jane-Eileen Joubert, Marie-Christine Tonon, Laurent Prézeau, Marie Chabbert, Fabrice Morin and Pierrick Gandolfo

MICROBIAL AND ANTIMICROBIAL PEPTIDES

238 *Membrane Active Antimicrobial Peptides: Translating Mechanistic Insights to Design*

Jianguo Li, Jun-Jie Koh, Shouping Liu, Rajamani Lakshminarayanan, Chandra S. Verma and Roger W. Beuerman

256 *Substance P and Calcitonin Gene-Related Peptide: Key Regulators of Cutaneous Microbiota Homeostasis*

Awa N'Diaye, Andrei Gannessen, Valérie Borrel, Olivier Maillot, Jeremy Enault, Pierre-Jean Racine, Vladimir Plakunov, Sylvie Chevalier, Olivier Lesouhaitier and Marc G. J. Feuilloley

263 *Peptides as Quorum Sensing Molecules: Measurement Techniques and Obtained Levels In vitro and In vivo*

Frederick Verbeke, Severine De Craemer, Nathan Debuinne, Yorick Janssens, Evelien Wynendaele, Christophe Van de Wiele and Bart De Spiegeleer



Editorial: Trends in Regulatory Peptides

Hubert Vaudry*, **Marie-Christine Tonon** and **David Vaudry**

University of Rouen, Mont-Saint-Aignan, France

Keywords: biologically active peptides, G protein-coupled receptors, neuropeptides, gliopeptides, gastrointestinal peptides, peptides and cancer, cardiovascular peptides, antimicrobial peptides

Editorial on the Research Topic

Trends in Regulatory Peptides

Regulatory peptides play crucial roles in the transfer of information within cells and tissues, between tissues and organs in the body, or between different organisms. They are produced by all species belonging to the different phylums, from bacteria to mammals. They display, by far, the most diverse structures of all signaling molecules. Regulatory peptides exert a broad spectrum of biological effects, acting notably as neurotransmitters, neuromodulators, hormones, pheromones, growth factors, cytokines, toxins, antibiotics, etc. In the animal kingdom, they control all physiological activities including neurophysiological, cardiovascular, gastrointestinal, renal, urogenital, respiratory, and immune functions. Not surprisingly, they are implicated in a number of physiopathological conditions such as pain transmission, Alzheimer's disease, autism, stroke, tumorigenesis, infertility, diabetes, metabolic disorders, and cardiovascular and gastrointestinal diseases. Thus, a large proportion of drugs target peptide receptors including opiate, vasopressin, oxytocin, somatostatin, gonadotropin-releasing hormone (GnRH), melanocortin, growth hormone, insulin, glucagon, parathyroid hormone, and calcitonin receptors. In addition, a number of pharmacological compounds regulate the production or breakdown of regulatory peptides, e.g., angiotensin-converting enzyme (ACE) inhibitors, dipeptidyl peptidase IV (DPP-IV) inhibitors, and enkephalinase inhibitors. Various peptides are also currently used as vaccines, antibiotics, sweeteners, cosmetic ingredients, and food additives. As a result, biologically active peptides represent a fascinating multidisciplinary research field for chemists, biochemists, physiologists, and pharmacologists with strong potential for novel therapeutic approaches and drug development.

This Research Topic is a compilation of contributions from the Regulatory Peptide meeting (RegPep2016) held in Rouen, Normandy, France that illustrates the diversity of the investigations currently conducted across the world on biologically active peptides.

Many regulatory peptides exert their biological effects through G protein-coupled receptors (GPCRs) which, not surprisingly, are targeted by a large proportion of the drugs currently on the market. Pharmaceutical compounds acting through a given GPCR can differentially activate its downstream signaling pathways (1). This functional selectivity of GPCR agonists is called biased signaling. Gundry et al. described two examples of drug-biased ligands, i.e., dopamine D2 receptor agonists and μ-opioid receptor agonists, which could have practical implications for the treatment of psychiatric disorders and pain. They highlighted the potential limitations in the characterization of biased agonists and provided a general approach to assessing biased agonists that should help the development of this promising new class of drugs.

Fluorescence resonance energy transfer (FRET) and bioluminescence resonance energy transfer (BRET) technologies are widely applied to study GPCR activation and dimerization (2). Using fluorescent biarsenical hairpin binders as acceptors for BRET-based biosensors, Bourque et al. have compared the responses of type 1 angiotensin receptor, prostaglandin F_{2α} receptor, and β₂-adrenergic receptor to their respective ligands. Their data revealed marked differences in the magnitude and

OPEN ACCESS

Edited and Reviewed by:

Liliane Schoofs,
KU Leuven, Belgium

*Correspondence:

Hubert Vaudry
hubert.vaudry@univ-rouen.fr

Specialty section:

This article was submitted to
Neuroendocrine Science,
a section of the journal
Frontiers in Endocrinology

Received: 26 February 2018

Accepted: 12 March 2018

Published: 26 March 2018

Citation:

Vaudry H, Tonon M-C and Vaudry D (2018) Editorial: Trends in Regulatory Peptides. *Front. Endocrinol.* 9:125.
doi: 10.3389/fendo.2018.00125

kinetics of the receptor responses to ligand stimulation. This study demonstrates conformational heterogeneity of three GPCRs that belong to the same receptor family, i.e., class A GPCRs.

Neuropeptides represent one of the largest families of regulatory peptides and regulate many physiological functions in the central nervous system (CNS) and in peripheral organs. For instance, corticotropin-releasing factor (CRF) initiates the hormonal response to stress by stimulating the pituitary adrenocortical axis and the sympathetic system. CRF also acts as a neuromodulator within the brain to elicit stress-related behaviors (3). Stengel and Taché reviewed the different mechanisms through which somatostatin signaling suppresses CRF receptor-mediated stress response. Somatostatin acts at the pituitary level to inhibit CRF-induced corticotropin secretion. Concurrently, somatostatin acts centrally to suppress stress-induced activation of the sympathetic system. Somatostatin attenuates the stress response caused by food restriction. Finally, somatostatin agonists counteract the inhibitory effect of CRF on gastrointestinal motor functions. Specific somatostatin receptor agonists can thus be used in preclinical studies to selectively modulate the different components of stress responses.

Somatostatin-producing sensory neurons express the non-selective cation channel TRPA1, a member of the transient receptor potential ankyrin channel family. The activity of TRPA1 can be modulated by inorganic sodium polysulfide (POLY) and dimethyl trisulfide (DMTS), an organic compound naturally occurring in garlic (4). Bátai et al. have compared the effects of POLY and DMTS on sensory neurons in carrageenan-evoked hind paw inflammation. Using genetically modified mice lacking either TRPA1 or the sst₄ somatostatin receptor, they show that somatostatin, acting through sst₄, is an important mediator of the antihyperalgesic effect of POLY and DMTS.

There is strong evidence that neuropeptide Y (NPY) also attenuates stress responses, anxiety, fear, and autonomic regulations (5). Serova et al. showed that intranasal administration of the Y1R-preferring NPY receptor agonist [Leu³¹Pro³⁴]NPY prevents stress-induced depressive-like behavior. Both NPY and [Leu³¹Pro³⁴]NPY inhibit the effect of a single prolonged stress on CRF mRNA expression. In contrast, [Leu³¹Pro³⁴]NPY enhances, while NPY attenuates, stress-induced glucocorticoid receptor (GR) mRNA expression. The significance of the differential effects of NPY and its Y1R-preferring agonist on CRF and GR expression is discussed.

A number of neuropeptides play key roles in the regulation of glial cell function. Microglial cells, which are responsible for immune surveillance within CNS, express the two types of bradykinin receptors, B₁R and B₂R (6). Asraf et al. have examined the role of these receptors in microglial activation. *In vitro*, the B₁R antagonist R-175, but not the B₂R antagonist HOE 140, enhances the production of NO and the release of the pro-inflammatory cytokine TNF- α in lipopolysaccharide-stimulated BV2 microglial cells. In transgenic Alzheimer's disease mice, intranasal administration of R-175, but not HOE 140, augments amyloid burden and causes microglia accumulation in the cortex. These observations support the view that B₁R modulation may be considered as a potential therapeutic strategy for Alzheimer's disease.

Both neurons and astroglial cells express hemoglobin (Hb) (7), and the transcription of the Hb gene is enhanced during

the preconditioning phase of ischemia (8). Amri et al. showed that Hb exerts a protective effect on hydrogen peroxide-induced oxidative stress and apoptosis in cultured rat astrocytes. The glioprotective activity of Hb is mediated through the PKA, PKC, and MAK signaling pathways. These data suggest that Hb may confer neuroprotection in neurodegenerative diseases.

Activity-dependent neuroprotective protein (ADNP) is a glioprotein which mediates the neuroprotective action of vasoactive intestinal polypeptide (VIP). Mutations of the ADNP gene have been reported in autistic patients (9). In their case report article, Gozes et al. described the clinical phenotype of an 11-year-old girl carrying an ADNP p.Tyr719* mutation, also known as the Helsmoortel–Van der Aa syndrome. The patient exhibits craniofacial asymmetry, autistic stereotypes, global developmental delay, motor skill deficit, and inability to talk. A short bioactive peptide fragment of ADNP, called NAP, represents a possible therapeutic option for patients with the Helsmoortel–Van der Aa syndrome.

Rehfeld has been involved for four decades in the study of the gastrointestinal regulatory peptide cholecystokinin (CCK) (10). In a comprehensive review, Rehfeld summarized the current knowledge regarding CCK and its receptors. CCK is expressed not only in intestinal endocrine I cells but also in brain neurons, peripheral nerves, endocrine cells, cardiocytes, kidney cells, and male germ cells, as well as in the immune system. Consistent with the widespread distribution of CCK and the CCK1 and CCK2 receptors, CCK and related peptides exert a large array of biological effects. Expression of CCK in various types of tumors suggests that CCK could serve as a tumor marker.

Various peptide hormones from the gastrointestinal tract are involved in the control of appetite and energy homeostasis (11), but little is known regarding the possible interplay between these different hormones. Lindqvist et al. have investigated the effect of ghrelin on glucagon-like peptide 1 (GLP-1), glucose-dependent insulinotropic peptide (GIP), and insulin secretion in mice. They show that intravenous injection of ghrelin induces a significant increase in plasma GLP-1 during a glucose tolerance test, but does not affect circulating levels of GIP, insulin, and glucose. *In vitro*, ghrelin inhibits proglucagon mRNA expression in the GLUTag cell line derived from a glucagon-producing enteroendocrine tumor. These data suggest that ghrelin exerts opposite effects on GLP-1 gene transcription and GLP-1 secretion.

Besides their role as nutrients, food-derived peptides can exert multiple regulatory actions. In particular, protein digestion-derived peptides may control appetite through modulation of gut hormone secretion (12). Caron et al. summarized the literature concerning the action of bioactive peptides originating from dietary proteins on the biosynthesis and release of the gastrointestinal hormones CCK and GLP-1. Alimentary peptides can also regulate the activity of the ubiquitous enzyme DPP-IV, which inactivates GLP-1 and GIP by cleaving off their N-terminal residues. Finally, peptides from food proteins can act as agonists of peripheral opioid receptors, whose activation inhibits gastric emptying and causes food intake-induced satiety. Food protein fragments thus represent a cornucopia of regulatory peptides for the control of food intake and glucose homeostasis.

The satiety effect of CCK is mediated by the vagal nerve that conveys the anorexic signal from the gut to the hindbrain (13).

Ndjim et al. hypothesized that vagal sensitivity to CCK could be impaired in rats suffering from perinatal malnutrition. They showed that low-protein diet increases food intake after a fasting period, enhances the postprandial plasma CCK level, attenuates the sensitivity to CCK, and reduces the CCK1 receptor level in nodose ganglia. These data support the notion that reduced vagal sensitivity to CCK contributes to food intake disorders in undernourished rats.

Several peptides participate in the regulation of tumor cell proliferation and migration. In particular, VIP inhibits proliferation of small-cell lung carcinoma (SCLC) (14). Since VIP receptors are expressed in bladder carcinoma, Mirsaidi et al. have studied the effect of VIP on bladder cancer cell proliferation *in vivo* and *in vitro*. Intramuscular injection of MB49 bladder cancer cells causes increased mortality in VIP-KO mice as compared to wild-type animals. *In vitro*, VIP reduces the growth of cultured MB49 cells. These data suggest that VIP could be of therapeutic value for the treatment of bladder carcinoma.

Gastrin-releasing peptide (GRP) and neuromedin B are two mammalian counterparts of the frog skin peptide bombesin. All three peptides act through three types of GPCRs designated BB₁R, BB₂R, and BRS-3. Numerous cancer cells, including SCLC, express GRP, neuromedin B, and/or their receptor(s), and the peptides act as autocrine factors stimulating tumor growth (15). Moody et al. have synthesized small-molecule bombesin receptor antagonists and tested their ability to antagonize BB₁R, BB₂R, and BRS-3 in various cancer cell lines. Two compounds, AM-37 and ST-36, inhibit bombesin agonist (BA)1 binding and (BA)1-induced cancer cell proliferation *in vitro*. These compounds may thus be useful agents for the treatment of BB₁R-, BB₂R-, and/or BBS-3-expressing tumor cells.

Gastrin is a peptide hormone produced by the stomach that stimulates gastric acid secretion. Gastrin is also produced by a number of malignant carcinomas called gastrinomas (16). Waldum et al. reviewed the literature on the role of gastrin in the etiology of gastric cancer. Their report points out the predominant role of gastrin in gastric carcinogenesis. It thus appears that gastrin antagonists may prove useful for the prophylaxis of gastric cancer.

Melanoma cells overexpress the melanocortin type 1 receptor (MC1R). Since α -melanocyte-stimulating hormone (α -MSH) is the natural ligand of MC1R, several radiolabeled α -MSH analogs have been proposed for the diagnosis and/or radiopharmaceutical treatment of melanoma. However, high uptake of the labeled peptides in the kidney hampers their clinical applications (17). Bapst and Eberle have designed a new radiolabeled MC1R ligand, [¹¹¹In]-DOTA-Phospho-MSH2-9, with an overall net charge of -1, which exhibits lower kidney uptake and retention. This compound is an attractive novel lead MC1R ligand for the development of clinically relevant melanoma targeting radiopeptides.

The SCLC cell line LU-165 expresses the antidiuretic peptide arginine-vasopressin (AVP) gene. Phenytoin, a voltage-gated sodium (Na_v) channel antagonist, inhibits AVP release from the isolated rat neurohypophysis and is effective in the treatment of syndrome of inappropriate AVP secretion (18). Ohta et al. showed that phenytoin inhibits AVP mRNA expression in LU-165 cells and suppresses secretion of the C-terminal fragment of pro-AVP

from these cells. This study suggests that Na_v channels play a key role in AVP expression and secretion in neuroendocrine tumors.

There is clear evidence that GPCRs are implicated in various aspects of tumorigenesis including proliferation, survival, and migration of cancer cells, as well as promotion of angiogenesis (19). Various hormones, acting through GPCRs, play a critical role in progression and metastasis of ovarian cancers. Zhang et al. summarized the literature pertaining to the role of estrogens, GnRH, follicle-stimulating hormone, luteinizing hormone, thyroid-stimulating hormone, and kisspeptin GPCRs in ovarian tumorigenesis, as well as angiotensin II and endothelin GPCRs in neovascularization of ovarian tumors. The diversity of GPCRs regulating growth and metastasis of ovarian tumor cells allows the development of novel chemotherapeutic agents for the benefit of patients with ovarian neoplasms.

Autophagy is a catabolic lysosomal process through which cell compartments are degraded and recycled to maintain energy homeostasis (20). Autophagy plays a key role in cell expansion, chemotactic migration, and invasion (21). Coly et al. summarized the organization and molecular dynamics of the autophagy machinery and elaborated on the implication of chemokine and neuropeptide GPCRs (e.g., CXCR4 and UT, respectively) in the control of autophagosome biogenesis and cancer cell metabolism.

Regulatory peptides exert multiple functions in the cardiovascular system (22). In particular, the vasoactive peptide apelin enhances cardiac contractility and induces the release of vasodilators. The major molecular form of apelin circulating in the plasma is pyroglutamyl apelin 13 ([Pyr¹]apelin-13). Yang et al. reported that incubation of [Pyr¹]apelin-13 with recombinant human ACE2 generates the [Pyr¹]apelin-13₍₁₋₁₂₎ peptide *in vitro* and that endogenous [Pyr¹]apelin-13₍₁₋₁₂₎ is present in the human cardiovascular endothelium. [Pyr¹]apelin and [Pyr¹]apelin-13₍₁₋₁₂₎ bind to human heart with similar affinity, and both peptides induce contraction of the saphenous vein with similar potency. In human volunteers, [Pyr¹]apelin and [Pyr¹]apelin-13₍₁₋₁₂₎ provoke similar dose-dependent increases in forearm blood flow. This study indicates that deletion of the C-terminal phenylalanine residue of [Pyr¹]apelin-13 by ACE2 does not affect the cardiovascular activity of the peptide.

In plasma, apelin peptides have a short half-life of about 5 min (23). Flahault et al. described the development of metabolically stable and potent apelin analogs that can be used to investigate the cardiovascular and diuretic activities of the native peptide. They provided an extensive and critical look at the physiological effects of apelin on the hydromineral balance and focused on the central and peripheral actions of apelin agonists on cardiorenal functions.

In teleost fish, receptors for the vasoactive neuropeptide urotensin II (UII) are expressed in the brainstem, in the spinal cord, and in the cardiovascular system, suggesting that UII may act both centrally and peripherally to control cardiovascular activity. Consistent with this hypothesis, intracerebroventricular (ICV) or intra-arterial (IA) injection of UII in trout increases blood pressure (BP) (Vanegas et al.). Lancien et al. have studied the effect of UII on the cardiac baroreflex sensitivity (BRS) in unanesthetized trout. They showed that ICV administration of low picomolar doses of UII not only increases BP and heart rate

but also reduces BRS, whereas IA administration of UII elevates BP and decreases heart rate without affecting BRS. It thus appears that only the central urotensinergic system is implicated in regulation of BRS.

In addition to its well established vasoactive properties, UII may exert various other biological effects (24). In particular, the genes encoding UII and its receptor UT are expressed in several tumoral cell lines, and UII triggers cancer cell motility. Based on these observations, Castel et al. hypothesized that the UII/UT system could exert chemotactic activities. In support of this hypothesis, they point out the existence of a common proline residue in transmembrane domain 2 (P2.58) shared by UT and chemokine receptors. They also discuss recent studies suggesting that UII may exert pro-inflammatory and pro-migratory effects on tumor cells.

The antimicrobial peptide database (<http://aps.unmc.edu/AP>) contains currently over 2,850 antimicrobial peptides (AMPs) that generate hope for the treatment of bacterial resistant infections. However, to date, no AMP has led to the development of pharmaceutically useful compounds. Li et al. highlighted the importance of understanding the mechanisms of action of AMPs on the bacterial membrane at the atomic level for the rational design of AMP-derived antibiotics.

The skin, which produces a number of biologically active peptides and expresses their cognate receptors, can be regarded as an authentic neuroimmunoendocrine organ (25, 26). For instance, in the human skin, sensory afferent C-fibers contain the neuropeptides substance P (SP) and calcitonin gene-related peptide (CGRP). N'Diaye et al. described the regulatory actions that SP and CGRP exert on the cutaneous bacterial microflora. This report provides evidence for immunomodulatory functions of SP and CGRP in the maintenance of skin microbiota homeostasis.

Quorum sensing is a chemical communication process by which bacteria regulate gene expression in response to fluctuations

in cell population density. Quorum sensing bacteria synthesize different types of auto-inducers: Gram-negative bacteria mainly produce homoserine lactone molecules while Gram-positive bacteria use modified oligopeptides (27). Verbeke et al. described various methods currently available for the identification and measurement of quorum sensing molecules with special emphasis on autoinducer peptides.

The review articles and original research papers gathered in the present e-book illustrate the importance of regulatory peptides in basic research and their huge potential for drug development. We hope that this Research Topic will become a major set of references for all scientists involved in this rapidly expanding field.

AUTHOR CONTRIBUTIONS

All the authors have made a substantial, direct, and intellectual contribution to the work and approved it for publication.

ACKNOWLEDGMENTS

We want to thank all the authors of this Research Topic for their excellent contributions, and the dedicated reviewers for their insightful comments that helped maintain the articles at the highest standards. We also gratefully acknowledge the excellent secretarial assistance of Mrs. Catherine Beau and the continuous support of the Frontiers staff. RegPep2016 was organized under the aegis of the International Regulatory Peptide Society, the International Neuropeptide Society/Society for Biologically Active Peptides, the Summer Neuropeptide Conferences, the European Neuropeptide Club, the Groupe Français des Peptides et des Protéines, and the Société Française des Peptides Antimicrobiens. RegPep2016 was generously supported by the Conseil Régional de Normandie, the Métropole Rouen Normandie, and the GEFLUC Rouen-Normandie.

REFERENCES

- Kenakin T, Christopoulos A. Signalling bias in new drug discovery: detection, quantification and therapeutic impact. *Nat Rev Drug Discov* (2013) 12:205–16. doi:10.1038/nrd3954
- Lohse MJ, Nuber S, Hoffmann C. Fluorescence/bioluminescence resonance energy transfer techniques to study G-protein-coupled receptor activation and signaling. *Pharmacol Rev* (2012) 64:299–336. doi:10.1124/pr.110.004309
- Chrousos GP, Zoumakis E. Milestones in CRH research. *Curr Mol Pharmacol* (2017) 10:259–63. doi:10.2174/1874467210666170109165219
- Hatakeyama Y, Takahashi K, Tominaga M, Kimura H, Ohta T. Polysulfide evokes acute pain through the activation of nociceptive TRPA1 in mouse sensory neurons. *Mol Pain* (2015) 11:24. doi:10.1186/s12990-015-0023-4
- Wu G, Feder A, Wegener G, Bailey C, Saxena S, Charney D, et al. Central functions of neuropeptide Y in mood and anxiety disorders. *Expert Opin Ther Targets* (2011) 15:1317–31. doi:10.1517/14728222.2011.628314
- Fleisher-Berkovich S, Filipovich-Rimon T, Ben-Shmuel S, Hülsmann C, Kummer MP, Heneka MT. Distinct modulation of microglial amyloid β phagocytosis and migration by neuropeptides (i). *J Neuroinflammation* (2010) 7:61. doi:10.1186/1742-2094-7-61
- Biagioli M, Pinto M, Cesselli D, Zaninello M, Lazarevic D, Roncaglia P, et al. Unexpected expression of alpha- and beta-globin in mesencephalic dopaminergic neurons and glial cells. *Proc Natl Acad Sci U S A* (2009) 106:15454–9. doi:10.1073/pnas.0813216106
- He Y, Hua Y, Liu W, Hu H, Keep RF, Xi G. Effects of cerebral ischemia on neuronal hemoglobin. *J Cereb Blood Flow Metab* (2009) 29:596–605. doi:10.1038/jcbfm.2008.145
- Larsen E, Menashe I, Ziats MN, Pereanu W, Packer A, Banerjee-Basu S. A systematic variant annotation approach for ranking genes associated with autism spectrum disorders. *Mol Autism* (2016) 7:44. doi:10.1186/s13229-016-0103-y
- Rehfeld JF, Larsson LI, Goltermann NR, Schwartz TW, Holst JJ, Jensen SL, et al. Neural regulation of pancreatic hormone secretion by the C-terminal tetrapeptide of CCK. *Nature* (1980) 284:33–8. doi:10.1038/284033a0
- Tan T, Bloom S. Gut hormones as therapeutic agents in treatment of diabetes and obesity. *Curr Opin Pharmacol* (2013) 13:996–1001. doi:10.1016/j.coph.2013.09.005
- Horner K, Drummond E, Brennan L. Bioavailability of milk protein-derived bioactive peptides: a glycaemic management perspective. *Nutr Res Rev* (2016) 29:91–101. doi:10.1017/S0954422416000032
- Dockray GJ. Gastrointestinal hormones and the dialogue between gut and brain. *J Physiol* (2014) 592:2927–41. doi:10.1113/jphysiol.2014.270850
- Vacas E, Muñoz-Moreno L, Fernández-Martínez AB, Bajo AM, Sánchez-Chapado M, Prieto JC, et al. Signalling pathways involved in antitumoral effects of VIP in human renal cell carcinoma A498 cells: VIP induction of p53 expression. *Int J Biochem Cell Biol* (2014) 53:295–301. doi:10.1016/j.biocel.2014.05.036
- Cuttitta F, Carney DN, Mulshine J, Moody TW, Fedorko J, Fischler A, et al. Bombesin-like peptides can function as autocrine growth factors in human small-cell lung cancer. *Nature* (1985) 316:823–6. doi:10.1038/316823a0

16. Epelboym I, Mazeh H. Zollinger-Ellison syndrome: classical considerations and current controversies. *Oncologist* (2014) 19:44–50. doi:10.1634/theoncologist.2013-0369
17. de Visser M, Verwijnen SM, de Jong M. Update: improvement strategies for peptide receptor scintigraphy and radionuclide therapy. *Cancer Biother Radiopharm* (2008) 23:137–57. doi:10.1089/cbr.2007.0435
18. Miyagawa CI. The pharmacologic management of the syndrome of inappropriate secretion of antidiuretic hormone. *Drug Intell Clin Pharm* (1986) 20:527–31. doi:10.1177/106002808602000701
19. Dorsam RT, Gutkind JS. G-protein-coupled receptors and cancer. *Nat Rev Cancer* (2007) 7:79–94. doi:10.1038/nrc2069
20. Hale AN, Ledbetter DJ, Gawriluk TR, Rucker EB III. Autophagy: regulation and role in development. *Autophagy* (2013) 9:951–72. doi:10.4161/auto.24273
21. Veale KJ, Offenhäuser C, Whittaker SP, Estrella RP, Murray RZ. Recycling endosome membrane incorporation into the leading edge regulates lamellipodia formation and macrophage migration. *Traffic* (2010) 11:1370–9. doi:10.1111/j.1600-0854.2010.01094.x
22. Yang P, Maguire JJ, Davenport AP. Apelin, Elabala/Toddler, and biased agonists as novel therapeutic agents in the cardiovascular system. *Trends Pharmacol Sci* (2015) 36:560–7. doi:10.1016/j.tips.2015.06.002
23. Gerbier R, Alvear-Perez R, Margathe JF, Flahault A, Couvineau P, Gao J, et al. Development of original metabolically stable apelin-17 analogs with diuretic and cardiovascular effects. *FASEB J* (2017) 31:687–700. doi:10.1096/fj.201600784R
24. Vaudry H, Leprince J, Chatenet D, Fournier A, Lambert DG, Le Mével JC, et al. International union of basic and clinical pharmacology. XCII. Urotensin II, urotensin II-related peptide, and their receptor: from structure to function. *Pharmacol Rev* (2015) 67:214–58. doi:10.1124/pr.114.009480
25. Roosterman D, Goerge T, Schneider SW, Bunnett NW, Steinhoff M. Neuronal control of skin function: the skin as a neuroimmunoendocrine organ. *Physiol Rev* (2006) 86:1309–79. doi:10.1152/physrev.00026.2005
26. Haslam IS, Roubos EW, Mangoni ML, Yoshizato K, Vaudry H, Kloepfer JE. From frog integument to human skin: dermatological perspectives from frog skin biology. *Biol Rev Camb Philos Soc* (2014) 89:618–55. doi:10.1111/brv.12072
27. Whiteley M, Diggle SP, Greenberg EP. Progress in and promise of bacterial quorum sensing research. *Nature* (2017) 551:313–20. doi:10.1038/nature24624

Conflict of Interest Statement: The authors declare that the research was conducted in the absence of any commercial or financial relationship that could be construed as a potential conflict of interest.

Copyright © 2018 Vaudry, Tonon and Vaudry. This is an open-access article distributed under the terms of the Creative Commons Attribution License (CC BY). The use, distribution or reproduction in other forums is permitted, provided the original author(s) and the copyright owner are credited and that the original publication in this journal is cited, in accordance with accepted academic practice. No use, distribution or reproduction is permitted which does not comply with these terms.



A Practical Guide to Approaching Biased Agonism at G Protein Coupled Receptors

Jaimee Gundry¹, Rachel Glenn¹, Priya Alagesan¹ and Sudarshan Rajagopal^{2*}

¹ Trinity College of Arts and Sciences, Duke University, Durham, NC, USA, ² Department of Medicine and Biochemistry, Duke University Medical Center, Durham, NC, USA

OPEN ACCESS

Edited by:

Hubert Vaudry,
University of Rouen, France

Reviewed by:

Lan Ma,
Fudan University, China
Helene Castel,
University of Rouen, France
Bernard Mouillac,
Institut National de la Santé et de la
Recherche Médicale (INSERM),
France

*Correspondence:

Sudarshan Rajagopal
sudarshan.rajagopal@dm.duke.edu

Specialty section:

This article was submitted to
Neuroendocrine Science,
a section of the journal
Frontiers in Neuroscience

Received: 27 November 2016

Accepted: 09 January 2017

Published: 24 January 2017

Citation:

Gundry J, Glenn R, Alagesan P and
Rajagopal S (2017) A Practical Guide
to Approaching Biased Agonism at G
Protein Coupled Receptors.
Front. Neurosci. 11:17.
doi: 10.3389/fnins.2017.00017

Biased agonism, the ability of a receptor to differentially activate downstream signaling pathways depending on binding of a “biased” agonist compared to a “balanced” agonist, is a well-established paradigm for G protein-coupled receptor (GPCR) signaling. Biased agonists have the promise to act as smarter drugs by specifically targeting pathogenic or therapeutic signaling pathways while avoiding others that could lead to side effects. A number of biased agonists targeting a wide array of GPCRs have been described, primarily based on their signaling in pharmacological assays. However, with the promise of biased agonists as novel therapeutics, comes the peril of not fully characterizing and understanding the activities of these compounds. Indeed, it is likely that some of the compounds that have been described as biased, may not be if quantitative approaches for bias assessment are used. Moreover, cell specific effects can result in “system bias” that cannot be accounted by current approaches for quantifying ligand bias. Other confounding includes kinetic effects which can alter apparent bias and differential propagation of biological signal that results in different levels of amplification of reporters downstream of the same effector. Moreover, the effects of biased agonists frequently cannot be predicted from their pharmacological profiles, and must be tested in the *vivo* physiological context. Thus, the development of biased agonists as drugs requires a detailed pharmacological characterization, involving both qualitative and quantitative approaches, and a detailed physiological characterization. With this understanding, we stand on the edge of a new era of smarter drugs that target GPCRs.

Keywords: G protein coupled receptor, biased agonism, arrestins, G proteins, GRKs

INTRODUCTION

G protein-coupled receptors (GPCRs) are the most common receptors in the genome and one of the largest drug targets for neuroendocrine disease (Overington et al., 2006). Classically, drugs targeting these receptors have been considered along the spectrum from antagonists to partial agonists to full agonists, which block, partially activate or fully activate, respectively, all of the signaling pathways downstream of a receptor. Over the past two decades, we have now appreciated a different phenomenon, biased agonism (in contrast to “balanced agonism”), the ability of some ligands to selectively activate some signaling pathways while blocking others (Rajagopal et al., 2010). Biased agonism was first noted as a reversal of the order of potencies for different ligands between alternative G protein signaling pathways (Kenakin, 1995). While the study of biased

agonism has largely focused on GPCRs, it is likely to occur in other receptor types as well (Zheng et al., 2012). A biased response is due to a combination of two distinct phenomena, ligand bias and system bias (Kenakin and Christopoulos, 2013b). Ligand bias, or “true” biased agonism, refers to differences in signaling due to the molecular variation that governs the interaction between the ligand and the transduction proteins at the receptor. Ligand bias is thought to be due to the stabilization of distinct receptor conformational states that differentially activate these alternative signaling pathways (Kahsai et al., 2011; Liu et al., 2012; Wacker et al., 2013). For GPCRs, the easiest bias to observe is that between selective activation of heterotrimeric G proteins (G protein-bias) and β -arrestin (β -arrestin-bias) adapter proteins (Wei et al., 2003). This is because G proteins and β -arrestins typically activate distinct signaling pathways, with G proteins typically activating second messengers and β -arrestins regulating receptor desensitization, internalization and activation of MAP kinases (DeWire et al., 2007). In contrast, system bias, or “apparent” biased agonism, is a reflection of the differences in measurements of biochemical amplification at the tissue, cellular, or *in vitro* level between the assays that are being used (Onaran and Costa, 2012). Thus, system bias has contributions from true differential amplification of signaling pathways (amplification bias) and the assays used to assess these signaling pathways (observation bias). In the development of biased agonists, it is critical to apply approaches that can separate ligand bias, which should be present across different assays, from system bias.

Biased agonists are expected to have different functional and physiological consequences from conventional balanced agonists, given that they activate only a select portion of a receptor’s signaling cascade while inhibiting others (Whalen et al., 2011). Because so many drugs target GPCRs, biased agonism holds the promise of developing a whole new class of “smarter” drugs that selectively target therapeutically relevant signaling pathway with fewer side effects from non-selective activation or blockade of other signaling pathways. A few therapeutics in the clinic have since been shown to act as biased agonists, which may explain why some drugs have greater efficacy than others within the same class (Kim et al., 2008). Conversely, failure to account for the potential of biased agonism may lead to the development of pharmaceuticals that may target the relevant signaling pathway while, at the same time, activating pathways leading to intolerable side effects. The goal of this perspective is to highlight examples of drug development of biased agonists, current limitations in their characterization and a general approach to characterizing the pharmacology of this promising new class of drugs.

THE PROMISE OF BIASED AGONISM

For biased agonists to be developed as drugs, a clear understanding of their physiological effects must be determined. Biased agonists targeting a number of disease states have been and are currently being developed (reviewed in Whalen et al., 2011; Kenakin and Christopoulos, 2013b), and a review of all of those studies is beyond the scope of this perspective. Rather, we will focus on biased drug development at two receptors

that are important in the nervous system: The dopamine D₂ receptor and the μ -opioid receptor (μ OR). Dopamine D₂ receptors were originally thought to affect schizophrenia through $G\alpha_i/G\alpha_0$ -mediated inhibition of adenylyl cyclase (Girault and Greengard, 2004). Based on that understanding, one would expect that blockade of G protein-mediated D₂ signaling would be sufficient to treat schizophrenia. However, behavioral and biochemical evidence has since shown a central role of β -arrestin 2 in signal transduction by D₂ dopamine receptors through the regulation of the AKT-GSK3 pathway (Beaulieu et al., 2007), through the formation of a protein complex composed of β -arrestin 2, AKT, and PP2A that promotes the dephosphorylation of AKT in response to dopamine. Lithium, a common drug used to treat bipolar disorder and other psychiatric illnesses, targets this protein complex, as do a wide array of antipsychotic medications (Masri et al., 2008). In β -arrestin 2 knockout mice, the behavioral effects of lithium treatment are lost, and the mice display defects in behaviors known to be regulated by dopamine (Beaulieu et al., 2008). More recently, a β -arrestin-biased D₂ receptor agonist has been developed (Allen et al., 2011) that has distinct effects from balanced agonists in a mouse model of schizophrenia (Park et al., 2016).

The μ OR is the target for endogenous enkephalin peptides and exogenous opioid analgesics including morphine, which act as agonists. Enkephalins are balanced agonists for G protein- and β -arrestin-mediated pathways, whereas morphine is biased toward G protein-mediated signaling, with a considerable reduction of receptor phosphorylation and internalization (Bohn et al., 2004). However, β -arrestin 2 knockout mice have demonstrated amplified and prolonged morphine-induced analgesia compared to wild type mice, consistent with the presence of morphine-induced β -arrestin-mediated desensitization (Bohn et al., 1999). Furthermore, β -arrestin 2 knockout mice are protected from the side effects of morphine such as respiratory depression and constipation, which suggests that β -arrestin-mediated pathways control these peripheral side effects (Bohn et al., 2000). Recently, G protein-biased μ OR agonists have been developed using different strategies (DeWire et al., 2013; Manglik et al., 2016). These drugs provide analgesia in animal models without the side effects of respiratory depression and tolerance (DeWire et al., 2013; Manglik et al., 2016), and one of these compounds has already shown promise in early phase clinical trials in humans (Soergel et al., 2014).

LIMITATIONS TO IDENTIFYING BIASED AGONISTS

While there is considerable promise in the development of biased agonists as therapeutics, there are a number of considerations that must be addressed when characterizing a biased agonist, from the pharmacological to the physiological levels (Table 1).

Make Sure Your Ligand is Actually Biased

Many older studies assumed that a ligand was biased compared to a balanced agonist if there was a significant difference in efficacies or potencies through different signaling pathways.

TABLE 1 | Limitations to the assessment of biased agonism and approaches to minimize them.

Problem	Solution
Ensure that the ligand is biased	<ul style="list-style-type: none"> Choose assays to minimize difference in amplification Use qualitative and quantitative approaches for assessing ligand bias and removing effects of system bias
Confounding by cell-specific effects	<ul style="list-style-type: none"> Use cells that are as close to physiological as possible Validate findings from heterologous system in more physiologically relevant cell type
Unexpected propagation of bias	<ul style="list-style-type: none"> Obtain data from multiple time points to ensure that bias persists over biologically relevant time scale Assess different reporters downstream of the same effector to ensure similar degrees of bias
Complex/Unexpected physiology	<ul style="list-style-type: none"> Test effects of biased agonists in physiologically relevant cell types and animal models of disease

However, large differences in potency and efficacy can be due to system bias and not ligand bias (Onaran and Costa, 2012). One of the first methods for properly identifying biased ligands was by identifying a change in the rank order of potency of ligands (Kenakin, 1995). Over the past few years, a number of approaches have been developed to identify and quantify ligand bias through the calculation of “bias factors” (reviewed in Kenakin and Christopoulos, 2013a). While a full discussion of the details of these different approaches is beyond the scope of this perspective, we discuss some of their advantages and disadvantages below (see *General Approach*).

Avoid Confounding by Cell-Specific Effects

Even with our current approaches for assessing bias, it is still possible that the effects of system bias cannot be fully accounted for. For example, the bias factor approaches based on the operational model are best suited for cases in which the major difference is a change in receptor number or immediate downstream amplification, as the τ factor (an estimate of efficacy) is equal to receptor concentration divided by a constant for system amplification (Black and Leff, 1983). The operational model cannot correct for examples in which other cofactors that affect signaling, such as GRKs, are differentially expressed. For example, GRK2 overexpression is known to phosphorylate the μ OR and increase β -arrestin recruitment to the receptor in response to morphine (Zhang et al., 1998). However, a recent study has shown that GRK2 activity at the μ OR generates a unique conformation of the receptor that is associated with differential activity (Nickolls et al., 2013). This type of behavior cannot be accounted for using pharmacological methods for quantifying bias.

Watch for Unexpected Propagation of Bias

A recent study by Klein Herenbrink et al. (2016) highlighted that apparent bias may change depending on the time and pathway assessed. At the D2 dopamine receptor, they found that there was a significant effect of ligand-binding kinetics and the

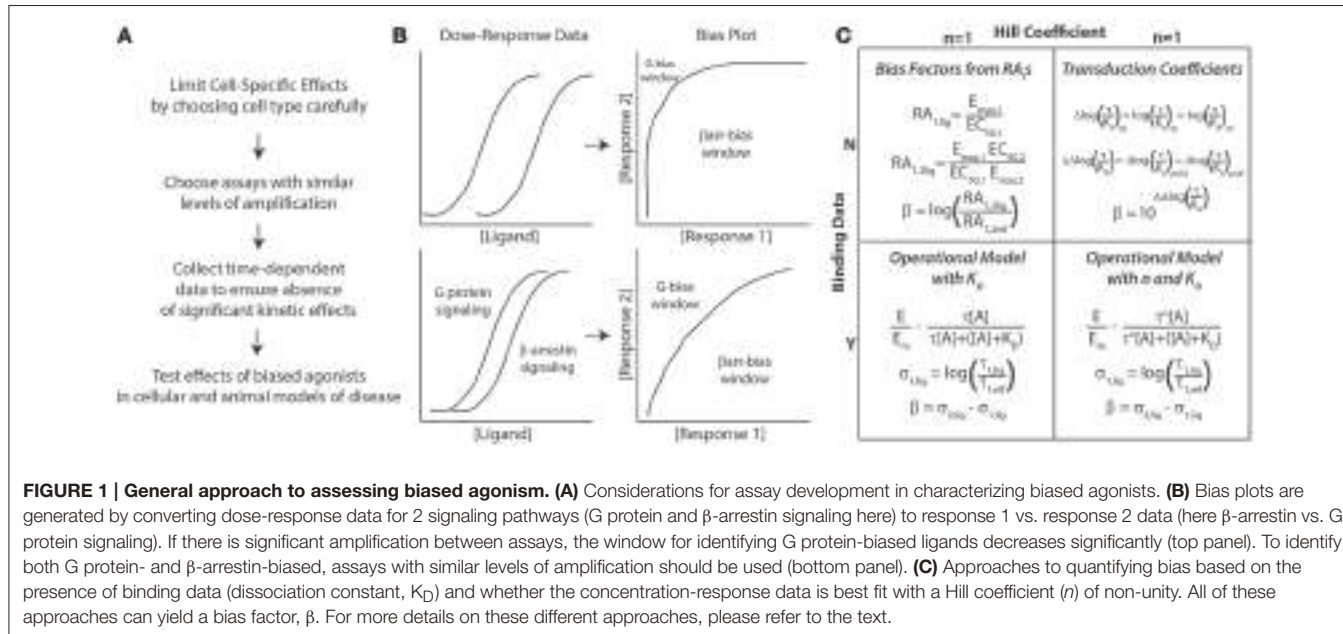
temporal pattern of receptor-signaling processes on the observed bias of different ligands. These differences even led to some examples of reversals in the direction of bias. Most methods for determining bias factors assume equilibrium conditions, a situation which is clearly absent when there is a significant kinetic effect. Also, the authors found that different reporters of the same pathway could have different degrees of amplification and estimated bias. At the μ OR, a robust correlation was found between off-rate kinetics for ligands and slower receptor dephosphorylation and β -arrestin dissociation (Sianati, 2014), suggesting similar behaviors at other GPCRs. These kinetic effects must be considered in the assessment of bias.

Characterize the Physiological Effects of the Biased Agonist

It is common for the pharmacological effects of a drug to not correspond with its *in vivo* activity, due to off-target effects or unexpected biology. This is especially true for biased agonists, which have more complex effects than simple agonists or antagonists. For example, SII angiotensin is a synthetically modified form of angiotensin II that binds the angiotensin type 1A receptor (AT₁AR) (Holloway et al., 2002). SII is unable to activate G α_q signaling but retains the ability to recruit β -arrestin 2, which would be expected to result in a loss of calcium signaling with increased desensitization (Wei et al., 2004). However, SII was found to act as a calcium sensitizer in cardiomyocytes (Rajagopal et al., 2006; Monasky et al., 2013) through a novel β -arrestin regulatory mechanism. Subsequent work, however, has shown that the signaling pattern induced by SII is much more complex, and involves activation of other G protein-dependent effects, suggesting that the relationship between observed bias and physiological effects is more complex (Sauliere et al., 2012). Thus, sometimes it can be difficult to establish a clear connectivity between biased coupling and cellular behavior. For example, at the urotensin receptor, ligands which differentially activated G α_q , G α_{13} , G α_i , and β -arrestin, do not display clear patterns for their effects on cell death, migration and adhesion (Brule et al., 2014). It is critical to characterize signaling pathways activated by biased agonists in physiologically relevant tissues, as these can be very different from heterologously expressed cells.

A GENERAL APPROACH TO IDENTIFYING AND CHARACTERIZING BIASED AGONISTS

Based on these considerations, we recommend the following approach to identify biased agonists (**Figure 1A**). First, to limit possible cell-specific effects, cells that are as close to physiologically relevant as possible should be used for the assays used to test bias. This can be difficult, however, as most physiologically relevant cell lines are difficult to transfect and not suited to most pharmacological assays. Therefore, it is important to confirm, after a potential biased agonist has been identified, that its biochemical effects are observed in a physiological relevant cell type. Second, in choosing



the assays for different signaling pathways, they should have similar levels of amplification, i.e., these assays should generate similar signals for the same concentration of ligand (Rajagopal et al., 2010). This provides a larger window for identifying biased agonists (Figure 1B). For example, assays that measure second messengers downstream of G proteins, such as cyclic AMP (cAMP) or calcium, have significant amplification. This is in contrast to recruitment assays of G proteins or β-arrestins to the receptor using bioluminescence resonance energy transfer (BRET), in which the spatial proximity of a luciferase (RLuc)-tagged receptor to a yellow fluorescent protein (YFP)-tagged effector results in energy transfer. In a BRET assay, the YFP:RLuc ratio indicates the degree of recruitment, with virtually no amplification. Assays that report on receptor internalization can be useful in determining receptor distribution in response to ligand stimulation, as shortly after β-arrestin recruitment, receptors undergo endocytosis and rapid or slow recycling. Using reporters that are significantly distal to the receptor runs the risk that they may report on other effectors, e.g., MAP kinase activation is regulated both by G proteins and β-arrestins. Third, to avoid confounding from potential kinetic effects, it is important to collect time-dependent data to ensure that any bias persists across a valid biological time scale. Lastly, the effects of biased agonists should be tested in cellular and animal models, as little may be known about the physiological effects of a biased agonist.

With respect to the specific methods used to quantify ligand bias, both qualitative and quantitative methods should be used to identify potentially biased ligands (Rajagopal et al., 2011). Most quantitative approaches for bias result in the calculation of a “bias factor” that quantifies the degree of ligand bias numerically. The details of bias factor calculations are beyond the scope of this perspective, and the interested reader should refer to the specific citations below. First, use “bias plots” to qualitatively

identify potentially biased ligands (Figure 1B) (Gregory et al., 2010). If a ligand does not demonstrate bias on the bias plot (has a similar response-response curve on the bias plot to the balanced agonist) but does have a significant bias factor, it is likely that the bias factor calculation is in error. This is because errors in a bias factor can be introduced at multiple stages in the fitting of concentration-response data depending on the technique used. If the data is fit well with a simple dose-response equation with a Hill coefficient of 1, the most straightforward approach to calculate a bias factor is by the logarithm of ratios of relative intrinsic activities (Griffin et al., 2007; Rajagopal et al., 2011) (Figure 1C). This calculation does not require additional information on ligand binding nor a complex fitting routine (it just requires E_{max} s and EC_{50} s for the different assays) that could introduce errors into the bias factor. An alternative approach is to calculate transduction coefficients (Kenakin et al., 2012), although that should be mathematically identical with bias factors obtained from intrinsic relative activities when the Hill coefficient is 1 (Griffin et al., 2007).

If binding data for ligands and a reference agonist are available, fitting to an operational model (Black and Leff, 1983) can yield both bias factors and estimates of efficacy. This estimate of efficacy (the effective signaling, σ) (Rajagopal et al., 2011), is closely related to intrinsic efficacy, ϵ , from classic pharmacological theory (Onaran et al., 2014). The advantage of this estimate of efficacy is that it provides information to the degree of agonism of the ligand tested, e.g., whether the ligand is a weak partial agonist or a full agonist. This data is not provided by a bias factor, which only gives an estimate of the relative efficacies of two signaling pathways compared to one another for a single ligand. As an example, a bias factor cannot differentiate between a weak partial agonist that is biased and a similarly biased full agonist; comparing their effective signaling can differentiate between such drugs. This approach

should provide efficacy estimates even if the Hill coefficient is not unity.

If binding data is not unavailable and the Hill coefficient is not one, then the best approach to use is the calculation of transduction coefficients (Kenakin et al., 2012). In this approach, transduction coefficients [$\log(\tau/K_A)$] are fit to the data along with an “apparent” dissociation constant; bias factors can be calculated from these transduction coefficients. For a partial agonist, in which the E_{max} for the ligand does not approach the maximal effect of the system, the EC_{50} approaches the dissociation constant for the ligand, K_D . In that situation, the data will be well fit with the transduction coefficient equation. However, for full agonists, where E_{max} approaches the maximal effect of the system, there may not be a clear relationship between EC_{50} and K_D . This can result in an ambiguous fit associated with relatively larger errors for estimates in transduction coefficients and bias factors.

CONCLUSIONS

Drug discovery of biased agonists is an active area of research which has exploded over the past 5 years. In the development

of biased agonists, it is critical that potential limitations in their characterization should be minimized. This means that we must confirm that the ligand is actually biased using qualitative and quantitative approaches, that there is no significant confounding from cell-specific effects, that there is not unexpected propagation or kinetic effects in signaling and that we understand the physiological effects of the biased agonists in cellular and animal models of disease. Using this general approach, a broad understanding of signaling by biased agonists from the pharmacological to the physiological level can be obtained and we can move forward in the development of these promising agents as novel therapeutics.

AUTHOR CONTRIBUTIONS

All authors listed, have made substantial, direct and intellectual contribution to the work, and approved it for publication.

FUNDING

SR is funded by NIH HL114643 and a Burroughs Welcome Career Award for Medical Scientists.

REFERENCES

- Allen, J. A., Yost, J. M., Setola, V., Chen, X., Sassano, M. F., Chen, M., et al. (2011). Discovery of beta-arrestin-biased dopamine D2 ligands for probing signal transduction pathways essential for antipsychotic efficacy. *Proc. Natl. Acad. Sci. U.S.A.* 108, 18488–18493. doi: 10.1073/pnas.1104807108
- Beaulieu, J. M., Gainetdinov, R. R., and Caron, M. G. (2007). The Akt-GSK-3 signaling cascade in the actions of dopamine. *Trends Pharmacol. Sci.* 28, 166–172. doi: 10.1016/j.tips.2007.02.006
- Beaulieu, J. M., Marion, S., Rodriguez, R. M., Medvedev, I. O., Sotnikova, T. D., Ghisi, V., et al. (2008). A beta-arrestin 2 signaling complex mediates lithium action on behavior. *Cell* 132, 125–136. doi: 10.1016/j.cell.2007.11.041
- Black, J. W., and Leff, P. (1983). Operational models of pharmacological agonism. *Proc. R. Soc. Lond. B. Biol. Sci.* 220 141–162. doi: 10.1098/rspb.1983.0093
- Bohn, L. M., Dykstra, L. A., Lefkowitz, R. J., Caron, M. G., and Barak, L. S. (2004). Relative opioid efficacy is determined by the complements of the G protein-coupled receptor desensitization machinery. *Mol. Pharmacol.* 66, 106–112. doi: 10.1124/mol.66.1.106
- Bohn, L. M., Gainetdinov, R. R., Lin, F. T., Lefkowitz, R. J., and Caron, M. G. (2000). Mu-opioid receptor desensitization by beta-arrestin-2 determines morphine tolerance but not dependence. *Nature* 408, 720–723. doi: 10.1038/35047086
- Bohn, L. M., Lefkowitz, R. J., Gainetdinov, R. R., Peppel, K., Caron, M. G., and Lin, F. T. (1999). Enhanced morphine analgesia in mice lacking beta-arrestin 2. *Science* 286, 2495–2498. doi: 10.1126/science.286.5449.2495
- Brule, C., Perzo, N., Joubert, J. E., Sainsily, X., Leduc, R., Castel, H., et al. (2014). Biased signaling regulates the pleiotropic effects of the urotensin II receptor to modulate its cellular behaviors. *FASEB J.* 28, 5148–5162. doi: 10.1096/fj.14-249771
- DeWire, S. M., Ahn, S., Lefkowitz, R. J., and Shenoy, S. K. (2007). Beta-arrestins and cell signaling. *Annu. Rev. Physiol.* 69, 483–510. doi: 10.1146/annurev.physiol.69.022405.154749
- DeWire, S. M., Yamashita, D. S., Rominger, D. H., Liu, G., Cowan, C. L., Graczyk, T. M., et al. (2013). A G protein-biased ligand at the mu-opioid receptor is potently analgesic with reduced gastrointestinal and respiratory dysfunction compared with morphine. *J. Pharmacol. Exp. Ther.* 344, 708–717. doi: 10.1124/jpet.112.201616
- Girault, J. A., and Greengard, P. (2004). The neurobiology of dopamine signaling. *Arch. Neurosci.* 61 641–644. doi: 10.1001/archneur.61.5.641
- Gregory, K. J., Hall, N. E., Tobin, A. B., Sexton, P. M., and Christopoulos, A. (2010). Identification of orthosteric and allosteric site mutations in M2 muscarinic acetylcholine receptors that contribute to ligand-selective signaling bias. *J. Biol. Chem.* 285, 7459–7474. doi: 10.1074/jbc.M109.094011
- Griffin, M. T., Figueroa, K. W., Liller, S., and Ehlert, F. J. (2007). Estimation of agonist activity at G protein-coupled receptors: analysis of M2 muscarinic receptor signaling through Gi/o/Gs, and G15. *J. Pharmacol. Exp. Ther.* 321, 1193–1207. doi: 10.1124/jpet.107.120857
- Holloway, A. C., Qian, H., Pipolo, L., Ziogas, J., Miura, S., Karnik, S., et al. (2002). Side-chain substitutions within angiotensin II reveal different requirements for signaling, internalization, and phosphorylation of type 1A angiotensin receptors. *Mol. Pharmacol.* 61, 768–777. doi: 10.1124/mol.61.4.768
- Kahsai, A. W., Xiao, K., Rajagopal, S., Ahn, S., Shukla, A. K., Sun, J., et al. (2011). Multiple ligand-specific conformations of the beta(2)-adrenergic receptor. *Nat. Chem. Biol.* 7, 692–700. doi: 10.1038/nchembio.634
- Kenakin, T. (1995). Agonist-receptor efficacy. II. Agonist trafficking of receptor signals. *Trends Pharmacol. Sci.* 16, 232–238. doi: 10.1016/S0165-6147(00)89032-X
- Kenakin, T., and Christopoulos, A. (2013a). Measurements of ligand bias and functional affinity. *Nat. Rev. Drug Discov.* 12:483. doi: 10.1038/nrd3954-c2
- Kenakin, T., and Christopoulos, A. (2013b). Signalling bias in new drug discovery: detection, quantification and therapeutic impact. *Nat. Rev. Drug Discov.* 12, 205–216. doi: 10.1038/nrd3954
- Kenakin, T., Watson, C., Muniz-Medina, V., Christopoulos, A., and Novick, S. (2012). A simple method for quantifying functional selectivity and agonist bias. *ACS Chem. Neurosci.* 3, 193–203. doi: 10.1021/cn200111m
- Kim, I. M., Tilley, D. G., Chen, J., Salazar, N. C., Whalen, E. J., Violin, J. D., et al. (2008). Beta-blockers alprenolol and carvedilol stimulate beta-arrestin-mediated EGFR transactivation. *Proc. Natl. Acad. Sci. U.S.A.* 105, 14555–14560. doi: 10.1073/pnas.0804745105
- Klein Herenbrink, C., Sykes, D. A., Donthamsetti, P., Canals, M., Coudrat, T., Shonberg, J., et al. (2016). The role of kinetic context in apparent biased agonism at GPCRs. *Nat. Commun.* 7:10842. doi: 10.1038/ncomms10842
- Liu, J. J., Horst, R., Katritch, V., Stevens, R. C., and Wuthrich, K. (2012). Biased signaling pathways in beta2-adrenergic receptor characterized by 19F-NMR. *Science* 335, 1106–1110. doi: 10.1126/science.1215802
- Manglik, A., Lin, H., Aryal, D. K., McCory, J. D., Dengler, D., Corder, G., et al. (2016). Structure-based discovery of opioid analgesics

- with reduced side effects. *Nature* 537, 185–190. doi: 10.1038/nature19112
- Masri, B., Salahpour, A., Didriksen, M., Ghisi, V., Beaulieu, J. M., Gainetdinov, R. R., et al. (2008). Antagonism of dopamine D2 receptor/beta-arrestin 2 interaction is a common property of clinically effective antipsychotics. *Proc. Natl. Acad. Sci. U.S.A.* 105, 13656–13661. doi: 10.1073/pnas.0803522105
- Monasky, M. M., Taglieri, D. M., Henze, M., Warren, C. M., Utter, M. S., Soergel, D. G., et al. (2013). The beta-arrestin-biased ligand TRV120023 inhibits angiotensin II-induced cardiac hypertrophy while preserving enhanced myofilament response to calcium. *Am. J. Physiol. Heart Circ. Physiol.* 305, H856–H866. doi: 10.1152/ajpheart.00327.2013
- Nickolls, S. A., Humphreys, S., Clark, M., and McMurray, G. (2013). Co-expression of GRK2 reveals a novel conformational state of the micro-opioid receptor. *PLoS ONE* 8:e83691. doi: 10.1371/journal.pone.0083691
- Onaran, H. O., and Costa, T. (2012). Where have all the active receptor states gone? *Nat. Chem. Biol.* 8, 674–677. doi: 10.1038/nchembio.1024
- Onaran, H. O., Rajagopal, S., and Costa, T. (2014). What is biased efficacy? Defining the relationship between intrinsic efficacy and free energy coupling. *Trends Pharmacol. Sci.* 35, 639–647. doi: 10.1016/j.tips.2014.09.010
- Overington, J. P., Al-Lazikani, B., and Hopkins, A. L. (2006). How many drug targets are there? *Nat. Rev. Drug Discov.* 5, 993–996. doi: 10.1038/nrd2199
- Park, S. M., Chen, M., Schmerberg, C. M., Dulman, R. S., Rodriguez, R. M., Caron, M. G., et al. (2016). Effects of beta-arrestin-biased dopamine D2 receptor ligands on schizophrenia-like behavior in hypoglutamatergic mice. *Neuropsychopharmacology* 41, 704–715. doi: 10.1038/npp.2015.196
- Rajagopal, K., Whalen, E. J., Violin, J. D., Stiber, J. A., Rosenberg, P. B., Premont, R. T., et al. (2006). Beta-arrestin2-mediated inotropic effects of the angiotensin II type 1A receptor in isolated cardiac myocytes. *Proc. Natl. Acad. Sci. U.S.A.* 103, 16284–16289. doi: 10.1073/pnas.0607583103
- Rajagopal, S., Ahn, S., Rominger, D. H., W., Gowen-McDonald, Lam, C. M., Dewire, S. M., et al. (2011). Quantifying ligand bias at seven-transmembrane receptors. *Mol. Pharmacol.* 80, 367–377. doi: 10.1124/mol.111.072801
- Rajagopal, S., Rajagopal, K., and Lefkowitz, R. J. (2010). Teaching old receptors new tricks: biasing seven-transmembrane receptors. *Nat. Rev. Drug Discov.* 9, 373–386. doi: 10.1038/nrd3024
- Sauliere, A., Bellot, M., Paris, H., Denis, C., Finana, F., Hansen, J. T., et al. (2012). Deciphering biased-agonism complexity reveals a new active AT1 receptor entity. *Nat. Chem. Biol.* 8, 622–630. doi: 10.1038/nchembio.961
- Sianati, S. (2014). *Mu-opioid Receptor Signalling Mechanisms: Quantifying Bias and Kinetics*. University of Sydney, Faculty of Medicine, Pharmacology.
- Soergel, D. G., Subach, R. A., Burnham, N., Lark, M. W., James, I. E., Sadler, B. M., et al. (2014). Biased agonism of the mu-opioid receptor by TRV130 increases analgesia and reduces on-target adverse effects versus morphine: a randomized, double-blind, placebo-controlled, crossover study in healthy volunteers. *Pain* 155, 1829–1835. doi: 10.1016/j.pain.2014.06.011
- Wacker, D., Wang, C., Katritch, V., Han, G. W., Huang, X. P., Vardy, E., et al. (2013). Structural features for functional selectivity at serotonin receptors. *Science* 340, 615–619. doi: 10.1126/science.1232808
- Wei, H., Ahn, S., Barnes, W. G., and Lefkowitz, R. J. (2004). Stable interaction between beta-arrestin 2 and angiotensin type 1A receptor is required for beta-arrestin 2-mediated activation of extracellular signal-regulated kinases 1 and 2. *J. Biol. Chem.* 279, 48255–48261. doi: 10.1074/jbc.M406205200
- Wei, H., Ahn, S., Shenoy, S. K., Karnik, S. S., Hunyady, L., Luttrell, L. M., et al. (2003). Independent beta-arrestin 2 and G protein-mediated pathways for angiotensin II activation of extracellular signal-regulated kinases 1 and 2. *Proc. Natl. Acad. Sci. U.S.A.* 100, 10782–10787. doi: 10.1073/pnas.1834556100
- Whalen, E. J., Rajagopal, S., and Lefkowitz, R. J. (2011). Therapeutic potential of beta-arrestin- and G protein-biased agonists. *Trends Mol. Med.* 17, 126–139. doi: 10.1016/j.molmed.2010.11.004
- Zhang, J., Ferguson, S. S., Barak, L. S., Bodduluri, S. R., Laporte, S. A., Law, P. Y., et al. (1998). Role for G protein-coupled receptor kinase in agonist-specific regulation of mu-opioid receptor responsiveness. *Proc. Natl. Acad. Sci. U.S.A.* 95, 7157–7162. doi: 10.1073/pnas.95.12.7157
- Zheng, H., Shen, H., Oprea, I., Worrall, C., Stefanescu, R., Girnita, A., et al. (2012). Beta-Arrestin-biased agonism as the central mechanism of action for insulin-like growth factor 1 receptor-targeting antibodies in Ewing's sarcoma. *Proc. Natl. Acad. Sci. U.S.A.* 109, 20620–20625. doi: 10.1073/pnas.1216348110

Conflict of Interest Statement: The authors declare that the research was conducted in the absence of any commercial or financial relationships that could be construed as a potential conflict of interest.

The reviewer HC and handling Editor declared their shared affiliation, and the handling Editor states that the process nevertheless met the standards of a fair and objective review.

Copyright © 2017 Gundry, Glenn, Alagesan and Rajagopal. This is an open-access article distributed under the terms of the Creative Commons Attribution License (CC BY). The use, distribution or reproduction in other forums is permitted, provided the original author(s) or licensor are credited and that the original publication in this journal is cited, in accordance with accepted academic practice. No use, distribution or reproduction is permitted which does not comply with these terms.



Distinct Conformational Dynamics of Three G Protein-Coupled Receptors Measured Using FlAsH-BRET Biosensors

Kyla Bourque, Darlaine Pétrin, Rory Sleno, Dominic Devost, Alice Zhang and Terence E. Hébert*

Department of Pharmacology and Therapeutics, McGill University, Montreal, QC, Canada

OPEN ACCESS

Edited by:

Hubert Vaudry,
University of Rouen, France

Reviewed by:

Xavier Iturrioz,
Institut National de la Santé et de la Recherche Médicale (INSERM), France
Kazuhiro Takahashi,
Tohoku University, Japan
David Chatenet,
Institut National de la Recherche Scientifique, Canada

*Correspondence:

Terence E. Hébert
terence.hebert@mcgill.ca

Specialty section:

This article was submitted to
Neuroendocrine Science,
a section of the journal
Frontiers in Endocrinology

Received: 20 January 2017

Accepted: 21 March 2017

Published: 07 April 2017

Citation:

Bourque K, Pétrin D, Sleno R, Devost D, Zhang A and Hébert TE (2017) Distinct Conformational Dynamics of Three G Protein-Coupled Receptors Measured Using FlAsH-BRET Biosensors. *Front. Endocrinol.* 8:61.
doi: 10.3389/fendo.2017.00061

A number of studies have profiled G protein-coupled receptor (GPCR) conformation using fluorescent biarsenical hairpin binders (FlAsH) as acceptors for BRET or FRET. These conformation-sensitive biosensors allow reporting of movements occurring on the intracellular surface of a receptor to investigate mechanisms of receptor activation and function. Here, we generated eight FlAsH-BRET-based biosensors within the sequence of the β_2 -adrenergic receptor (β_2 AR) and compared agonist-induced responses to the angiotensin II receptor type I (AT1R) and the prostaglandin F2 α receptor (FP). Although all three receptors had FlAsH-binding sequences engineered into the third intracellular loops and carboxyl-terminal domain, both the magnitude and kinetics of the BRET responses to ligand were receptor-specific. Biosensors in ICL3 of both the AT1R and FP responded robustly when stimulated with their respective full agonists as opposed to the β_2 AR where responses in the third intracellular loop were weak and transient when engaged by isoproterenol. C-tail sensors responses were more robust in the β_2 AR and AT1R but not in FP. Even though GPCRs share the heptahelical topology and are expressed in the same cellular background, different receptors have unique conformational fingerprints.

Keywords: G protein-coupled receptors, G proteins, conformational profiling, biosensors, signaling

INTRODUCTION

Understanding the dynamic nature of G protein-coupled receptors (GPCRs) is critical given their capacity to modulate numerous biological responses in health and disease. Largely localized to the plasma membrane, GPCRs respond to an array of extracellular stimuli including photons, odors, hormones, peptides, lipids, and sugars (1). With over 800 genes expressed in the human genome, they are found in nearly every organ of the body (2, 3). The β_2 -adrenergic receptor (β_2 AR) is one of the most studied GPCRs and is tightly regulated as part of elaborate multicomponent signaling networks. Upon ligand binding, the receptor undergoes a conformational change that stimulates the exchange of guanine diphosphate for guanine triphosphate in the G α s subunit leading to the functional dissociation of the G $\beta\gamma$ dimer from G α (1). These G proteins then independently act on downstream effector molecules in a number of signaling cascades. This simplified notion of receptor activation provides only a glimpse into the complex processes of signal transduction, of which we have much to learn.

Understanding GPCR function involves determining how agonist binding translates into receptor activation. The traditional view of receptor activation has evolved from where it was initially

thought of as a switch from a single inactive state to a single active state. Now it is widely accepted that the receptor pool in any given cell can occupy a number of different inactive and active conformations (4–6). At equilibrium, there are numerous conformations within the receptor population and different orthosteric and allosteric ligands can stabilize diverse receptor states. The fundamental mechanisms of GPCR activation have been investigated by several groups using diverse techniques, including but not limited to nuclear magnetic resonance, double electron-electron resonance, and fluorescence spectroscopy (4, 7–9). Both fluorescence and bioluminescence resonance energy transfer (FRET and BRET) approaches have also been used to explore the conformational dynamics of GPCRs (9–14). The site specific introduction of the short tetracysteine motif CCPGCC within the coding frame of a receptor when labeled with a fluorescein derivative can be used in resonance energy transfer (RET) applications to report on conformations adopted by the receptor upon ligand binding in living cells (15, 16).

We have explored the use of FlAsH BRET in the conformational profiling of the prostaglandin F₂α receptor [FP; (11)], and the angiotensin II type I receptor [AT1R; (17)]. Here, we introduced this tetracysteine tag at various locations within the coding sequence of the β₂AR in order to report on conformational changes upon agonist stimulation. Eight such biosensors were constructed; two within the second intracellular loop, three in the third intracellular loop, and three in the carboxyl terminus of the receptor. In a previous study, the β₂AR was tagged using FlAsH FRET (18). In that work, the third intracellular loop was tagged with the FlAsH motif and the carboxyl terminus with CFP after having truncated the C-tail at amino acid 343 (18). Upon agonist stimulation, an increase in the FRET ratio was observed suggesting that the third intracellular loop approaches the C-terminus (18). Other groups have also attempted to understand the conformational dynamics of the β₂AR while using fluorescence-based probes as indicators of conformational changes occurring in real-time. Lohse and colleagues have generated FRET-based biosensors incorporating YFP in the third loop and CFP in the C-terminus of the β₂AR (19). Again, the receptor was truncated at amino acid 369. To our knowledge, our study is the first report of using the full-length β₂AR tagged with reporter proteins to monitor conformations adopted by the receptor upon agonist stimulation. Further, we compare and contrast three distinct GPCRs and show that even though they share a similar seven transmembrane architecture, they behave very differently in regards to the magnitude and kinetics of their BRET responses.

MATERIALS AND METHODS

Materials

Primers

All primers were synthesized and purchased by Integrated DNA Technologies (Coralville, IA, USA, see **Table 1**).

Constructs

The recombinant receptors used in this paper are as follows: SP-FLAG-hAT1R-CCPGCC-ICL3-p3-RlucII or SP-FLAG-hAT1R-CCPGCC-C-tail-p1-RlucII in a pIRESH plasmid backbone

TABLE 1 | List of primers used for the generation of the β₂-adrenergic receptor (β₂AR) FlAsH-BRET-based recombinant biosensors.

Position	Sequence (5' → 3')
ICL2 p1	F: TGCTGCCCCGGCTGCTGCAGCCTGCTGA R: GCAGCAGCGGGGGCAGCACTGGTACTTG
ICL2 p2	F: TGCTGCCCCGGCTGCTGCCCTTCAGTAATGGCAAAGTAGC R: GCAGCAGCGGGGGCAGCATGAAGTAATGGCAAAGTAGC
ICL3 p1	F: TGCTGCCCCGGCTGCTGCATGTCCAGA R: GCAGCAGCGGGGGCAGCAGAAGCAGGCC
ICL3 p2	F: TGCTGCCCCGGCTGCTGCCAGCAGGATG R: GCAGCAGCGGGGGCAGCACACCTGGCT
ICL3 p3	F: TGCTGCCCCGGCTGCTGCCAGCAATGCCCGT R: GCAGCAGCGGGGGCAGCAATGCCCGT
C-tail p1	F: TGCTGCCCCGGCTGCTGCCCTATGGGA R: GCAGCAGCGGGGGCAGCACTCAAAGA
C-tail p2	F: TGCTGCCCCGGCTGCTGCAATAACTGCG R: GCAGCAGCGGGGGCAGCATTCTTCTCC
C-tail p3	F: TGCTGCCCCGGCTGCTGCCATCAAGGTA R: GCAGCAGCGGGGGCAGCAGCCCACAAA
Name	Sequence (5' → 3')
BamHI β ₂ AR	F: CAGTGGATCCATGGGGCAACCCGGGAAC
β ₂ AR EcoRI	R: CTCCGGATCCGAATTCCAGCAGTGAGTC
BamHI	
NheI Xhol Kozak	F: CCTAGCTAGCTCGAGGCCACCATGAA
SP	

(17) along with SP-HA-hFP-CCPGCC-ICL3-p4-RlucII in a pcDNA3.1(−) backbone (11), in addition to the panel of eight β₂AR biosensors expressed in a pIRESpuro3 plasmid backbone.

Generation of FlAsH-BRET-Based Biosensors

The intramolecular biosensors were designed to harbor the tetracysteine tag positioned at various locations within the intracellular surface of the receptor in addition to a C-terminally fused *Renilla* luciferase. More precisely, the CCPGCC tag was inserted in two positions within the second intracellular loop, three within the third, and three within the carboxyl terminus domain of the receptor. For ease of cloning, compatible restriction sites were introduced by polymerase chain reaction (PCR) at the 5' and 3' ends of the receptor to facilitate its insertion into its corresponding mammalian expression vector. Briefly, HA-tagged hβ₂AR (20) in a pcDNA3.1(−) backbone vector was used as a template and amplified by PCR using the BamHI-β₂AR forward and the β₂AR-EcoRI-BamHI reverse primers. The resulting PCR product was cloned into an accepting vector; pIRESpuro3-signal peptide-HA-RlucII using BamHI. We screened for correct orientation using PstI. The introduction of the CCPGCC motif was accomplished by overlapping PCR where the wild-type receptor was flanked by the appropriate primers (**Table 1**) in order to introduce the desired TC tag within the coding sequence (11). In the first round, fragment one was generated using NheI-XhoI-forward primer and the appropriate FlAsH internal reverse primer. Fragment 2 was generated using the appropriate FlAsH internal forward primer and β₂AR-EcoRI-BamHI reverse primer. Both fragments were then combined in equal portions and used as templates for the second round of PCR using NheI-XhoI-Kozak-β₂AR forward and β₂AR-EcoRI-BamHI reverse primer. This product was cloned

into pIRESpuro3-SP-HA-RlucII backbone using *NheI* and *EcoRI*. All constructs were confirmed by bidirectional sequencing (Génome Québec).

Cell Culture

HEK 293 SL cells were cultured in Dulbecco's Modified Eagle's medium (DMEM) supplemented with 5% vol/vol fetal bovine serum and 1% w/v penicillin-streptomycin from Wisent. The cells were maintained in a controlled environment, 37°C in a humidified atmosphere at 95% air and 5% CO₂.

Transient Transfection

HEK 293 SL cells were plated at a density of 2.0×10^5 cells per well in clear 6-well plates (Thermo Scientific, 140675) prior to transfection. On the following day, cells were transfected with 1 µg of each of the eight β₂AR FlAsH biosensors along with pcDNA3.1(–) for a total of 1.5 µg per well using Lipofectamine 2000 (Invitrogen) following the manufacturer's instructions. Alternatively, 1 µg of AT1R-ICL3-p3-RlucII or AT1R-C-tail-p1-RlucII and 500 ng of the FP-ICL3-p4-RlucII biosensor was also used.

Immunofluorescence

The day following transfection, cells were detached with 0.25% Trypsin-EDTA (Wisent) and 2.0×10^4 cells were re-plated onto a poly-L-ornithine (Sigma-Aldrich) treated clear bottom black 96-well plate (Thermo Scientific, 165305). The next day, the cells were washed once with phosphate-buffered saline (PBS) and fixed with 2% paraformaldehyde (Sigma-Aldrich) for 10 min at room temperature. Successively, the cells were blocked with a 1% bovine serum albumin (Fisher Scientific) PBS solution for 1 h at room temperature to prevent non-specific interactions of the antibodies. Cells were then incubated with a monoclonal mouse anti-HA primary antibody for 1 h (BioLegend, 1:200, previously Covance). Afterward, the cells were washed three times with PBS and an Alexa fluor-488 goat anti-mouse IgG secondary antibody (Life Technologies, 1:1,000) was used to label cells. To confirm the ability of recombinant receptors to localize to the cell surface, the Operetta High Content Imaging system (Perkin Elmer) with a 20× WD objective was used. The excitation filter was set at 475/15 nm and its corresponding emission filter at 525/25 which permitted to capture the signal produced by Alexa fluor-488.

Gαs Coupling and Downstream cAMP Production

HEK 293 SL cells were transfected with 1 µg of each of the eight β₂AR FlAsH biosensors and the β₂AR-WT-RlucII construct supplemented with 0.5 µg of the previously described H188 EPAC FRET sensor (21) using Lipofectamine 2000 (Invitrogen) following the manufacturer's instructions. The day following transfection, cells were detached with 0.25% Trypsin-EDTA (Wisent) and 4.0×10^4 cells were re-plated onto a poly-L-ornithine (Sigma-Aldrich) treated black flat bottom 96-well plate (Costar, 3916). The day of the experiment, cells were washed once in 150 µL of Krebs buffer and the cells then sat in 90 µL of Krebs at 37°C prior to the start of the assay. A Synergy 2 plate reader (Biotek) was used to assay coupling of the β₂AR FlAsH biosensors to

Gαs by investigating accumulation of cAMP. The temperature of the instrument was set at 37°C and kinetic measurements were taken. The 420/50 excitation filter was used to excite the donor molecule, mTurquoise2, and light was captured by the emission filters 485/20 (mTurquoise2) and 528/20 (Venus). Basal FRET was measured continuously every 5 s for a total of 20 s. Cells were then treated with either the vehicle (ascorbic acid) or the full agonist, 10 µM isoproterenol (in ascorbic acid) using the injector module. Stimulated FRET readings were then captured every 5 s for a total time of 2 min. FRET ratios were computed by dividing the Venus emission channel by the mTurquoise2 emission channel. ΔFRET ratios were calculated by subtracting the averaged isoproterenol stimulated FRET ratio by the averaged basal FRET ratio, as shown; ΔFRET = (avgFRET_{stimulated} – avgFRET_{basal}).

ERK1/2 MAP Kinase Activation

Twenty-four hours post-transfection, cells were detached with 0.25% Trypsin-EDTA (Wisent) and 400 µL of cell suspension was re-plated onto a clear 12-well plate (Costar, 3513). On the day of the experiment, the cells were starved in DMEM without serum supplementation for 5 h. Afterward, cells were stimulated with either vehicle or 10 µM isoproterenol for 5 min at 37°C. The plate was then placed on ice, where the cells were washed once with an ice-cold PBS solution. The cells were lysed in 200 µL of 4× Laemmli buffer (2% SDS, 10% glycerol, 60 mM Tris pH 6.8, 0.02% bromophenol blue, 5% β-mercaptoethanol). In order to shear the genomic DNA, lysates were sonicated three times, each repetition for 5 s at 3 W using a Sonication 3000 (Misonix). Lysates were then heated at 65°C for 15 min.

MAP kinase activation was measured by western blot. Correspondingly, 30 µL of cell lysate was loaded and proteins were, respectively, separated by SDS-PAGE and then transferred onto a PVDF membrane via a wet transfer technique. To prevent non-specific binding of the primary antibody, the membrane was blocked in a 5% non-fat milk solution in Tris-buffered saline and 0.0005% Tween20 solution. An anti-phospho-ERK1/2 rabbit primary antibody was used (Cell Signalling Technologies, 1:1,000) followed by an anti-rabbit polyclonal IgG peroxidase secondary antibody (Santa Cruz Biotechnology, 1:20,000). Immuno-detection was accomplished via chemiluminescence using Western Lightning plus-ECL (Perkin Elmer) or ECL-Select western blotting detection reagent (GE Healthcare) given that the secondary antibody was conjugated to the horseradish peroxidase enzyme.

FlAsH Labeling

Twenty-four hours post-transfection, cells were detached with 0.25% Trypsin-EDTA (Wisent) and 4.0×10^4 cells were re-plated onto a poly-L-ornithine (Sigma-Aldrich) treated white 96-well plate (Thermo Scientific, 236105). The next morning, a 25 mM solution of 1,2-ethanedithiol (EDT) was prepared by diluting it in dimethyl sulfoxide. Then, one volume of FlAsH reagent (2 mM) was added to two volumes of EDT to make a 667 µM FlAsH (Invitrogen) solution, which was incubated for 10 min at room temperature. Following the incubation, 100 µL of Hank's balanced salt solution (HBSS) without phenyl red, with sodium bicarbonate, calcium, and magnesium was added to the 667 µM FlAsH

solution and further incubated for 5 min at room temperature (Wisent). Then, HBSS was added to make a solution with final concentration of 750 nM FlAsH-EDT₂. In parallel, cells were washed in 150 µL of HBSS prior to the FlAsH labeling. Subsequently, 60 µL of the 750 nM FlAsH-EDT₂ solution was added to the cells and incubated for 1 h at 37°C, protected from any source of direct light. Following the incubation, cells were washed once with 100 µL of 1 M 2,3-dimercapto-1-propanol (BAL, Invitrogen) diluted in HBSS buffer and then incubated for 10 min at 37°C. The cells were washed once again with BAL without incubation. Afterward, cells were washed once with 150 µL of the assay buffer: Krebs (146 mM NaCl, 4.2 mM KCl, 0.5 mM MgCl₂, 1 mM CaCl₂, 10 mM HEPES pH 7.4, 0.1% glucose). The cells then sat in 80 µL of Krebs for 2 h at room temperature, in an environment protected from light, prior to the BRET assay. The FlAsH labeling procedure has been previously described elsewhere (11).

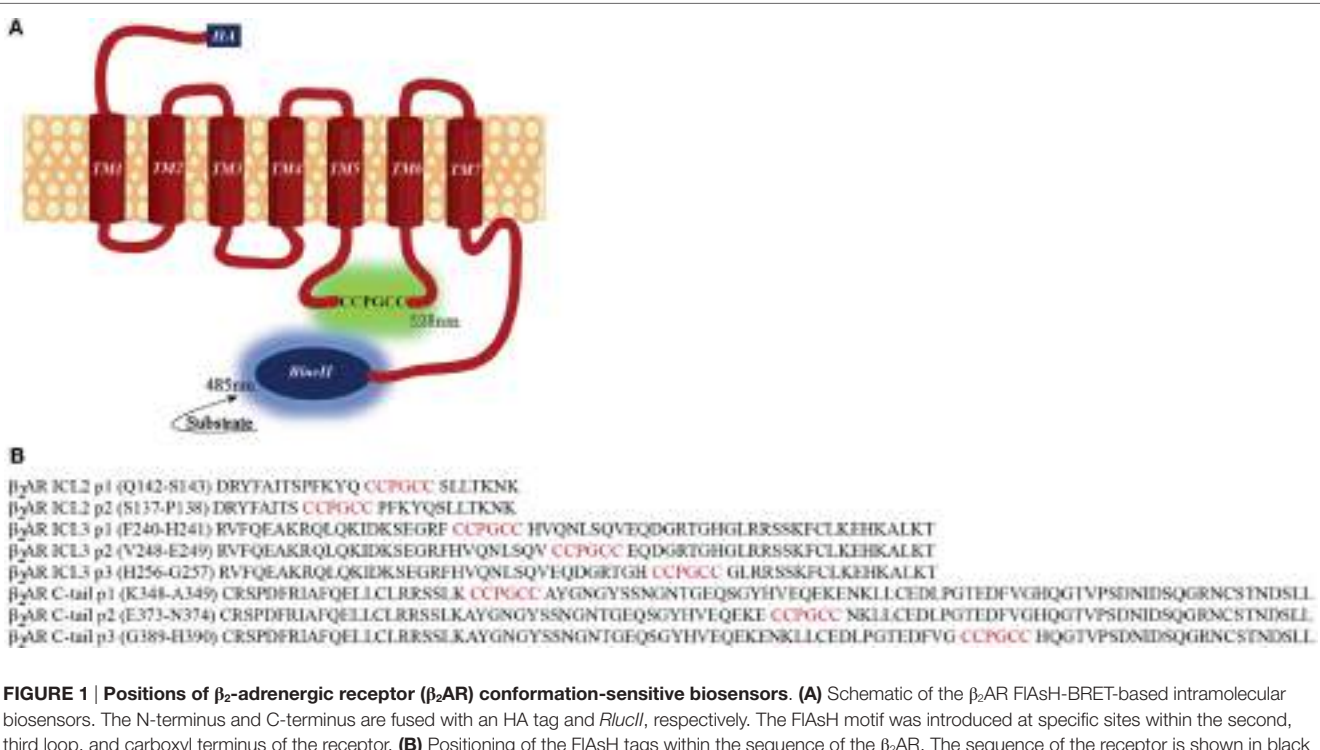
BRET Measurements

A TriStar² LB 942 multimode plate reader from Berthold Technologies was used to measure BRET using the pre-determined BRET¹ filter pair F485 and F530. Light was produced *via* enzymatic catalysis of the luciferase substrate coelenterazine h by the donor RlucII. Accordingly, 10 µL of a 2 µM coelenterazine h solution (NanoLight Technologies) was added to the cells and incubated for 5 min whereafter the luminescence was measured. Basal BRET corrected from spectral overlap of the donor and acceptor channels were calculated by subtracting the BRET value obtained from unlabeled cells expressing solely the donor from the corresponding BRET value obtained from the labeled FlAsH recombinant receptors. Additionally, ligand-induced changes were investigated

and kinetic readings were reported. Correspondingly, the counting time of the two filters was analyzed continuously every 0.2 s for a total of 50 repeats. Subsequently, either vehicle or a saturating concentration of the agonist, 10 µM isoproterenol, was injected using the injector module. For the AT1R, 1 µM angiotensin II was used and 1 µM PGF2α for FP. Thereafter, the luminescence was again captured every 0.2 s and a total of 100 repeats. The change in BRET, as a response to the addition of agonist or the ΔBRET, as referred to in this paper, was computed by subtracting the average BRET across all reads pre-injection from the average BRET across all reads post-injection: $\Delta\text{BRET} = (\text{avgBRET}_{\text{post-injection}}) - (\text{avgBRET}_{\text{pre-injection}})$.

Statistical Analysis

All statistical analysis was performed using GraphPad Prism 7.0 software. Data are reported as mean ± SE. The Prism software performed a Brown–Forsythe test to determine if parametric or non-parametric statistics should be performed. The degree of Gαs coupling was evaluated using a one-way analysis of variance (ANOVA) followed by Dunnett's multiple comparisons test comparing the various FlAsH positions to the wild type (Figures 3A,B). When determining the basal BRET exhibited by each of the recombinant β₂AR biosensors, a one-way ANOVA was performed. A Dunnett's *post hoc* test was successively completed with the purpose of comparing the basal BRET of the eight recombinant constructs to the wild-type receptor (Figure 4A). When evaluating the agonist-induced BRET response, a two-way ANOVA was carried out followed by a Bonferroni corrected Student's *t*-test aimed at comparing the response of the vehicle to the response of the agonist for each individual sensor position (Figure 4B).



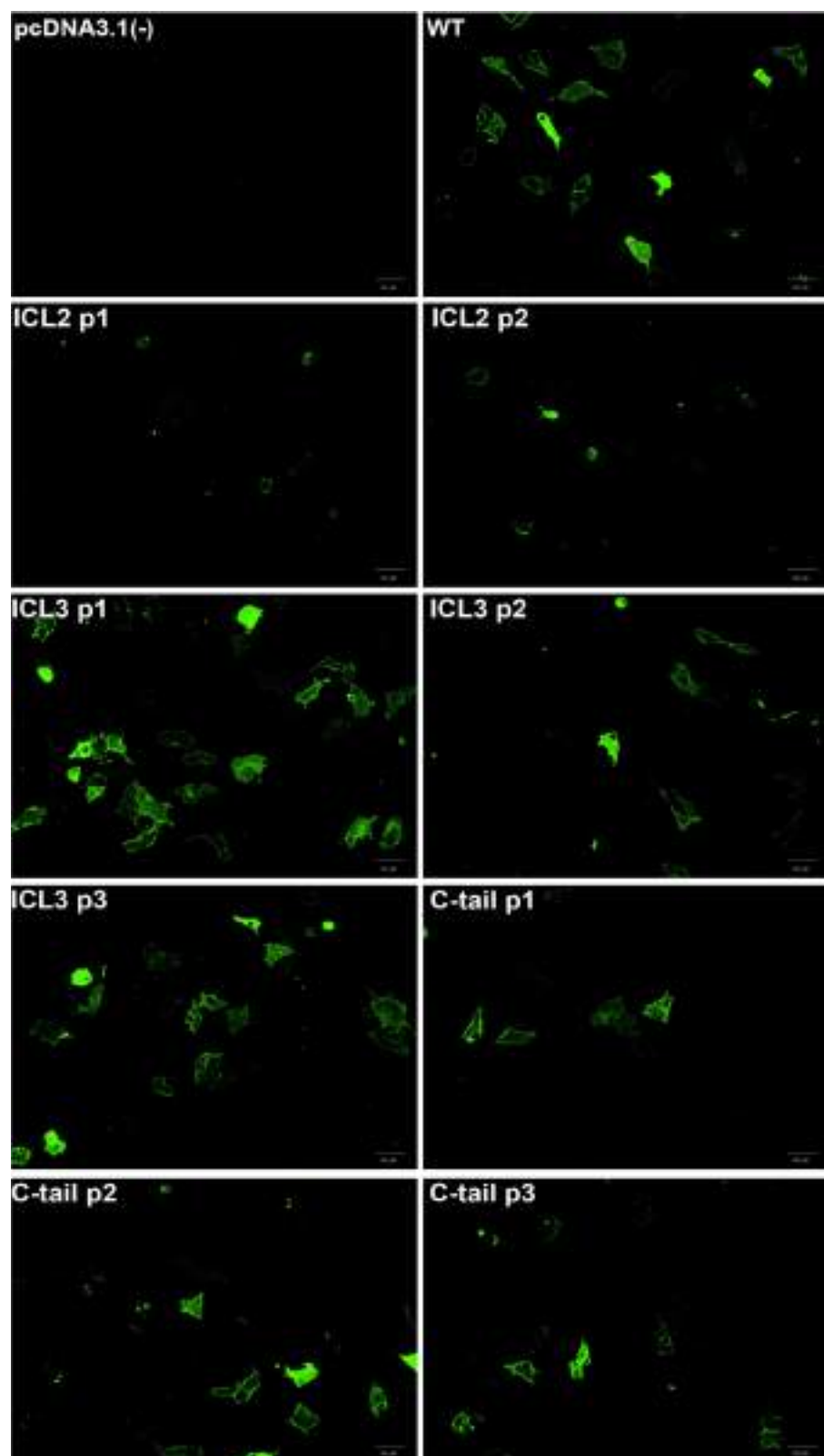
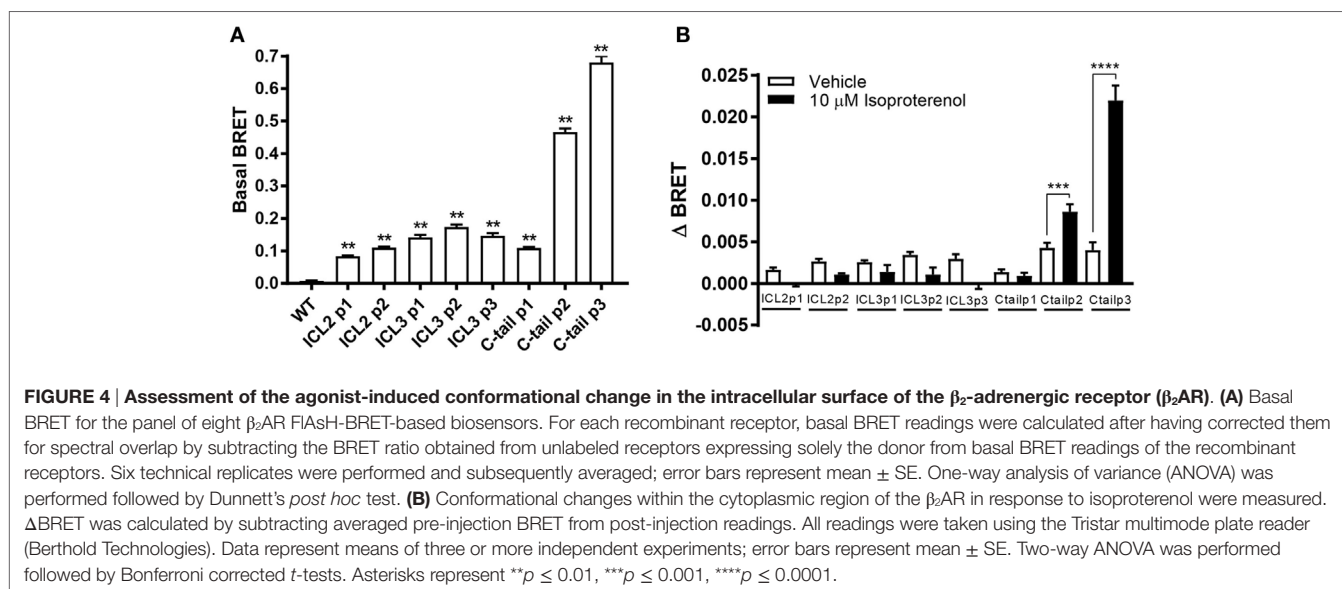
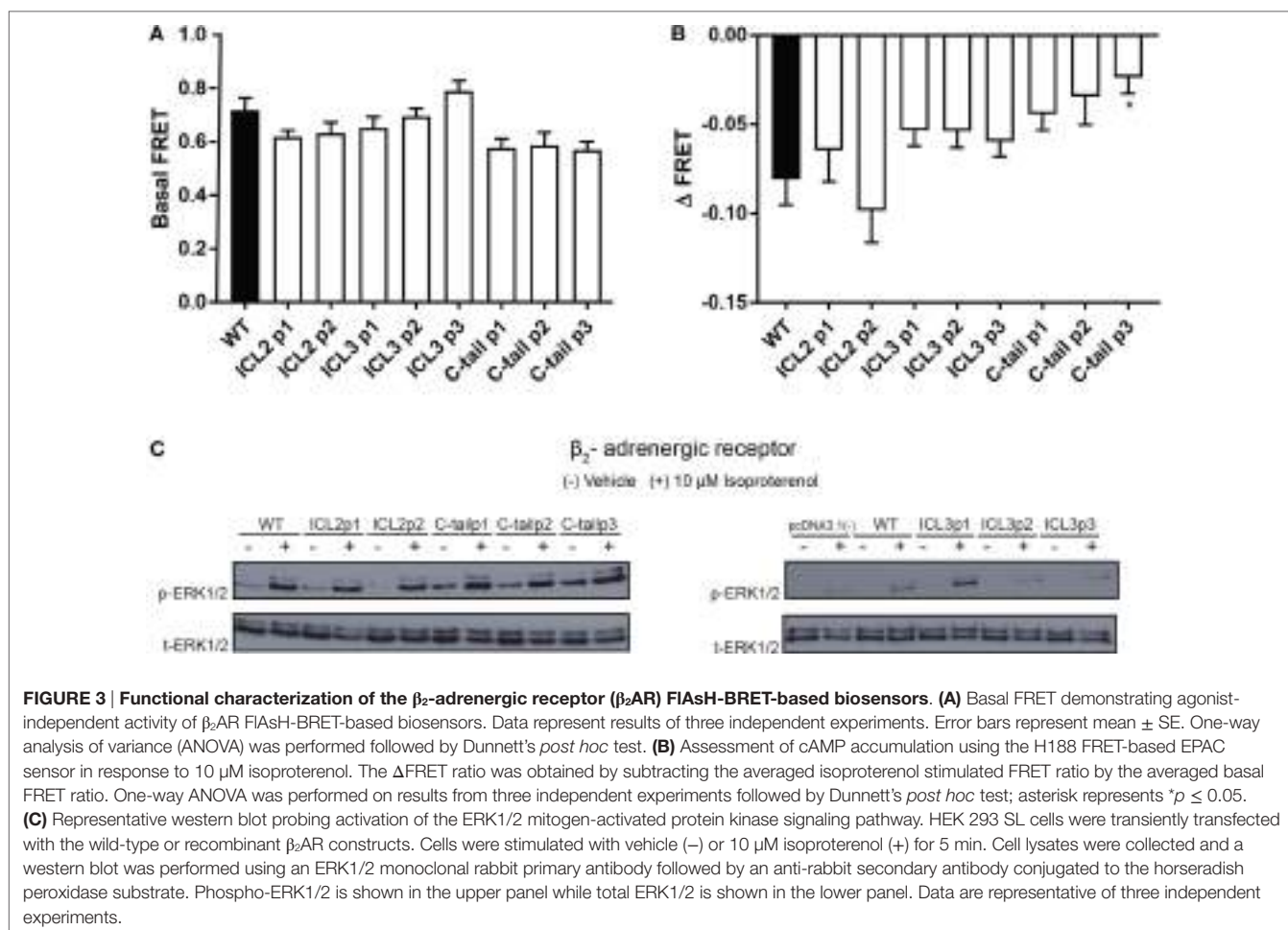


FIGURE 2 | Cell surface localization of the β_2 -adrenergic receptor (β_2 AR) FlAsH-BRET-based biosensors. Fluorescence microscopy validating cell surface localization of the FlAsH-tagged intramolecular β_2 AR biosensors. Immunofluorescence images of non-permeabilized HEK 293 SL cells transiently transfected with the recombinant β_2 AR constructs demonstrating their membrane localization. The cells were incubated with an anti-HA primary antibody and then stained with an Alexa fluor-488 conjugated secondary antibody. Images were taken using the Operetta high content microscope (Perkin Elmer).



RESULTS

Biosensor Validation

We constructed a number of FlAsH-BRET biosensors in the β_2 AR with a FlAsH-binding site engineered into various intra-

cellular sites and *Renilla* luciferase placed on the carboxy terminus (Figure 1). If the biosensor components are positioned at appropriate sites within the receptor then this would allow profiling of conformational changes in the receptor upon ligand stimulation. In order for our intramolecular BRET constructs

to be meaningful tools for the study of receptor conformational dynamics, recombinant receptors must maintain their native function. If they do not function in a manner similar to the wildtype receptor, then conformational analysis will be meaningless. Immunofluorescence was first used to verify the surface localization of the recombinant receptors generated. An anti-HA antibody was used to label the recombinant receptors, followed by an Alexa fluor-488 conjugated secondary antibody. As illustrated in **Figure 2**, almost all the FlAsH-tagged β_2 AR constructs trafficked to the cell surface. Receptors tagged within the second intracellular loop were less robustly expressed compared to the wild type. However, the fluorescence intensity for all other positions was similar to the wild type providing us with at least six positions to carry forward.

Next, to further validate the functionality of each construct, we measured isoproterenol-mediated cAMP accumulation as well as ERK1/2 MAPK activation. We studied the relative accumulation of cAMP as an indication of G α s activation using the H188 FRET-based EPAC sensor. FRET was used as BRET-based EPAC biosensors could not be used with the BRET-based conformational biosensors (as both would be activated). As shown in **Figures 3A,B**, the majority of constructs displayed similar levels of cAMP accumulation (measured as a decrease in FRET) as compared to the untagged wild-type receptor. As the β_2 AR shows agonist-independent basal activity, we examined both basal (**Figure 3A**) and agonist-stimulated FRET (**Figure 3B**). We observed that certain sensor positions exhibited high basal

activity as shown as the reduced FRET ratio at baseline. This may have been as a result of higher expression levels of these biosensors. For example, the C-tail P3 position may seem as though there is less cAMP production than the wild type in response to agonist; however, the lack of a robust decrease in FRET as a response to agonist is probably due to having attained the threshold of detection at basal levels.

We then examined a more distal readout of receptor functionality; the β_2 AR-mediated MAPK (Raf/Ras/MEK/ERK) signaling pathway that has been previously characterized by various groups (22, 23). As demonstrated by **Figure 3C**, all the recombinant β_2 AR constructs exhibited MAPK activation at similar intensities as the wild-type receptor. As a result, the third intracellular loop sensors as well as the C-tail sensors passed the validation stage although some caution again must be taken when interpreting results using the sensors engineered into the second intracellular loop. It must be noted here that all our transfections were transient and no attempt was made to normalize levels of expression *per se*.

BRET Measurements

Next, we measured basal BRET between the FlAsH-labeled receptors and the C-tail luciferase. Basal BRET or the BRET ratio after it has been corrected for spectral overlap of the donor and acceptor channels was determined by subtracting BRET where cells were not labeled with FlAsH. All receptor biosensors showed basal BRET to varying degrees (**Figure 4A**). The

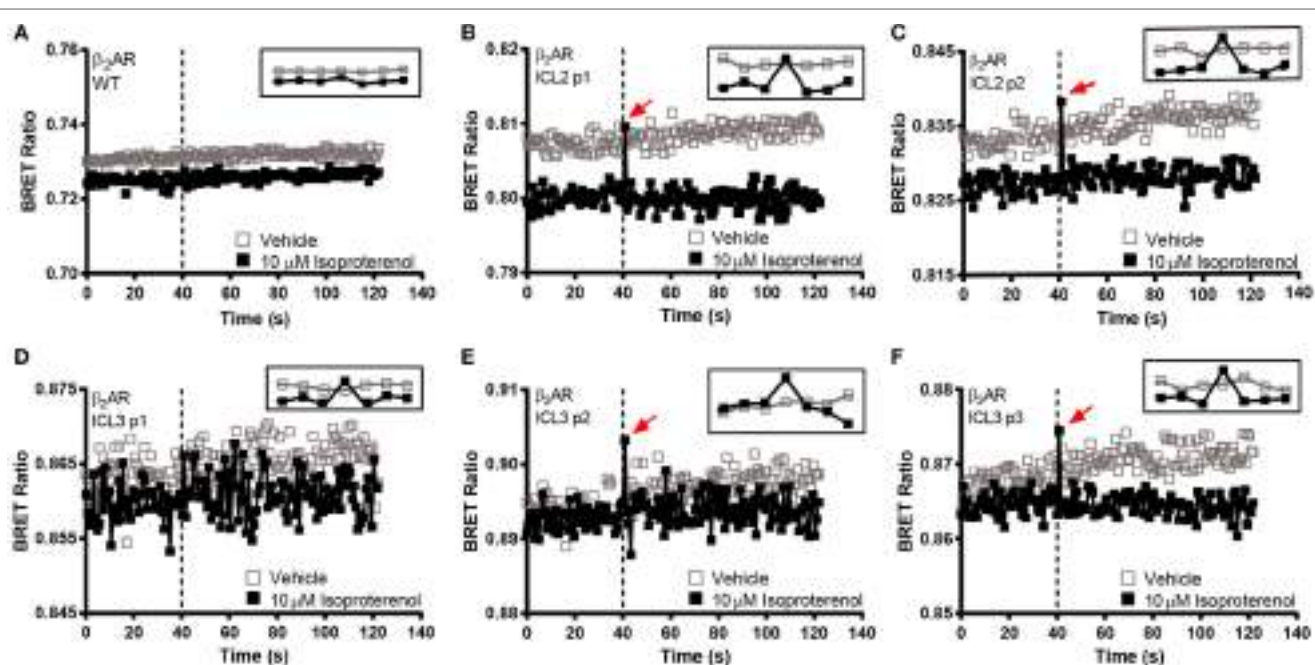


FIGURE 5 | BRET kinetics in the second and third intracellular loops of the β_2 -adrenergic receptor (β_2 AR). HEK 293 SL cells transiently expressing the ICL2 and ICL3 β_2 AR biosensors were labeled with the FlAsH reagent. **(A)** WT untagged receptor, **(B)** ICL2 p1, **(C)** ICL2 p2, **(D)** ICL3 p1, **(E)** ICL3 p2, and **(F)** ICL3 p3. Open boxes refer to vehicle and solid boxes refer to isoproterenol treatment. Basal BRET was captured prior to the injection of the full agonist, 10 μ M isoproterenol. After ligand stimulation, data were continuously captured to observe the corresponding change in the BRET signal. The BRET ratio was calculated by dividing the fluorescence by the luminescence and plotted as a function of time. The dotted line represents the time at which the injection took place. The inset at the top right corner of each graph zooms in at the time points close to the injection. The data are representative of three or more independent experiments.

larger the basal BRET, the closer the donor–acceptor pair was at the outset. As a result, there is a greater dynamic range to capture relative changes in receptor conformation. The β_2 AR biosensor with the greatest basal BRET was the third position within the C-tail. There was a position-dependent increase in the basal BRET, as one moves farther down the tail of the receptor, as acceptor and donor moieties get closer together. As for the third loop, the second position showed the largest basal BRET which is in accordance to its position in the middle of the loop (**Figure 4A**).

Δ BRET in response to ligand was measured by subtracting the averaged post-injection BRET from the averaged pre-injection BRET readings. BRET ratios could potentially increase or decrease depending on the ligand used and the subsequent conformation adopted by the receptor. It was hoped that our biosensors would differentially respond to ligands and provide a conformational fingerprint to better understand the dynamic nature of the receptor which could be exploited for validating new drugs in early phases of development. Of all the biosensors tested, only the C-tail positions P2 and P3 showed a robust conformational change upon isoproterenol stimulation (**Figure 4B**). The lack of response in ICL3 was somewhat of a surprise but the functional

data (**Figures 2 and 3**) suggested that ICL2 sensors may not be correctly folded.

In order to make a comprehensive assessment of the isoproterenol induced responses of the β_2 AR biosensors, we also examined the underlying kinetics. As mentioned, neither the second or third loop positions captured a sustained conformational change in response to isoproterenol (**Figures 4B** and 5). Oddly, a small spike was a consistent feature of the ligand-induced response in these sensors with the exception of ICL3 P1 (**Figures 5D–F**). The presence of this spike was not an artifact originating from the sampling instrument as no such spikes were seen when vehicle was similarly injected and it was also absent from kinetic traces of the wild-type receptor expressing RlucII with no FIAsH-binding sequences (**Figure 5A**). The C-tail P1 sensor displayed similar features as the second and third loop positions (**Figures 5 and 6A**). However, the responses in the other C-tail sensors were much more robust and sustained (**Figures 6B,C**). We have previously analyzed responses to ligand in both FP (11) and in the AT1R (17). Responses in ICL3 in AT1R and FP were both robust and sustained (**Figures 6D,E**) compared to the β_2 AR. Further, robust sustained responses have also been detected in both ICL2 and the C-terminus of AT1R

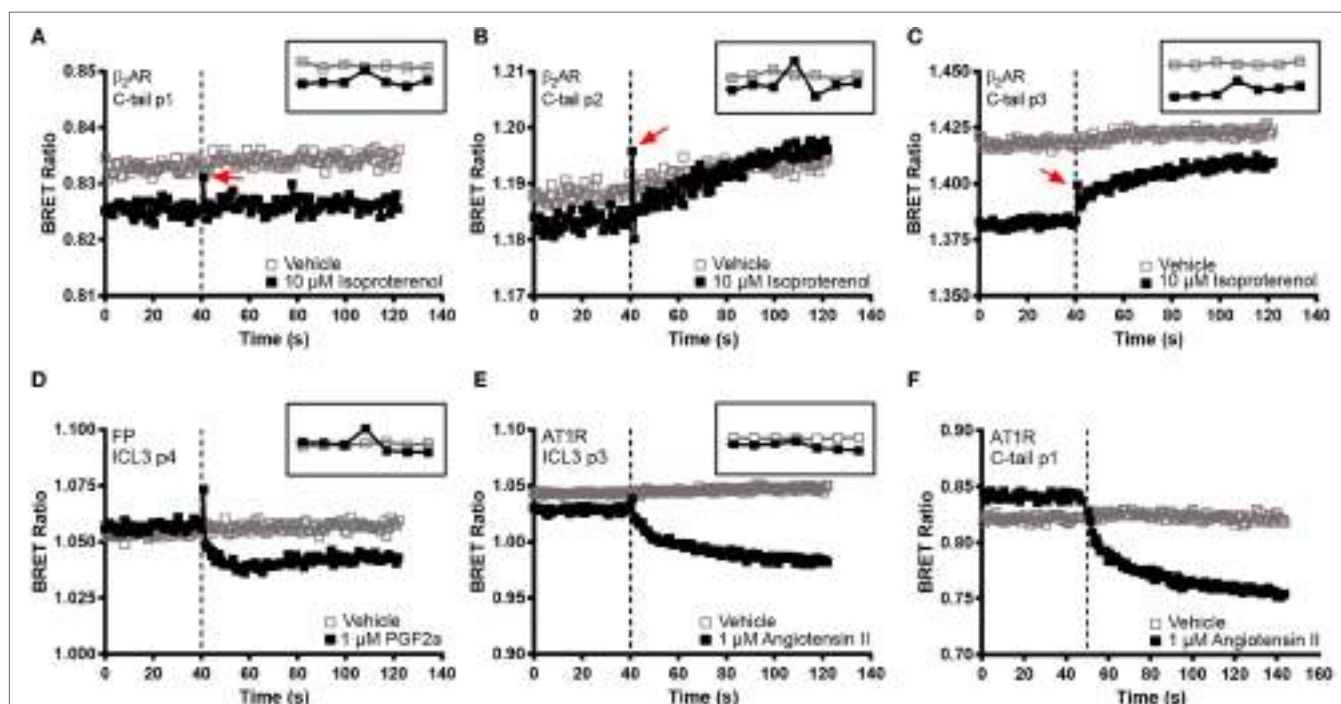


FIGURE 6 | BRET kinetics in the C-terminal β_2 -adrenergic receptor (β_2 AR) FIAsH constructs as well as in AT1R and FP biosensors. HEK 293 SL cells transiently transfected with the three C-tail β_2 AR recombinant biosensors or with FP ICL3 p4 or AT1R ICL3 p3 and C-tail p1 and then labeled with the FIAsH reagent. **(A)** C-tail p1, **(B)** C-tail p2, **(C)** C-tail p3, **(D)** FP ICL3 p4, **(E)** AT1R ICL3 p3, and **(F)** AT1R C-tail p1. Open boxes refer to vehicle and solid boxes refer to agonist treatment. Basal BRET was captured prior to the injection of each receptor's respective full agonist, 10 μ M isoproterenol, 1 μ M PGF2 α , or 1 μ M angiotensin II. After ligand stimulation, data were continuously captured to observe the corresponding change in the BRET signal. The BRET ratio was calculated by dividing the fluorescence by the luminescence and plotted as a function of time. The dotted line represents the time at which the injection took place. The inset at the top right corner of each graph zooms in at the time points close to the injection. Measurements were recorded on 40,000 cells except for the AT1R C-tail p1 where 30,000 cells were used. All readings were taken using the Tristar multimode plate reader (Berthold Technologies) except the AT1R C-tail p1 which was assayed on the Victor X Light (Perkin Elmer). The data are representative of three or more independent experiments.

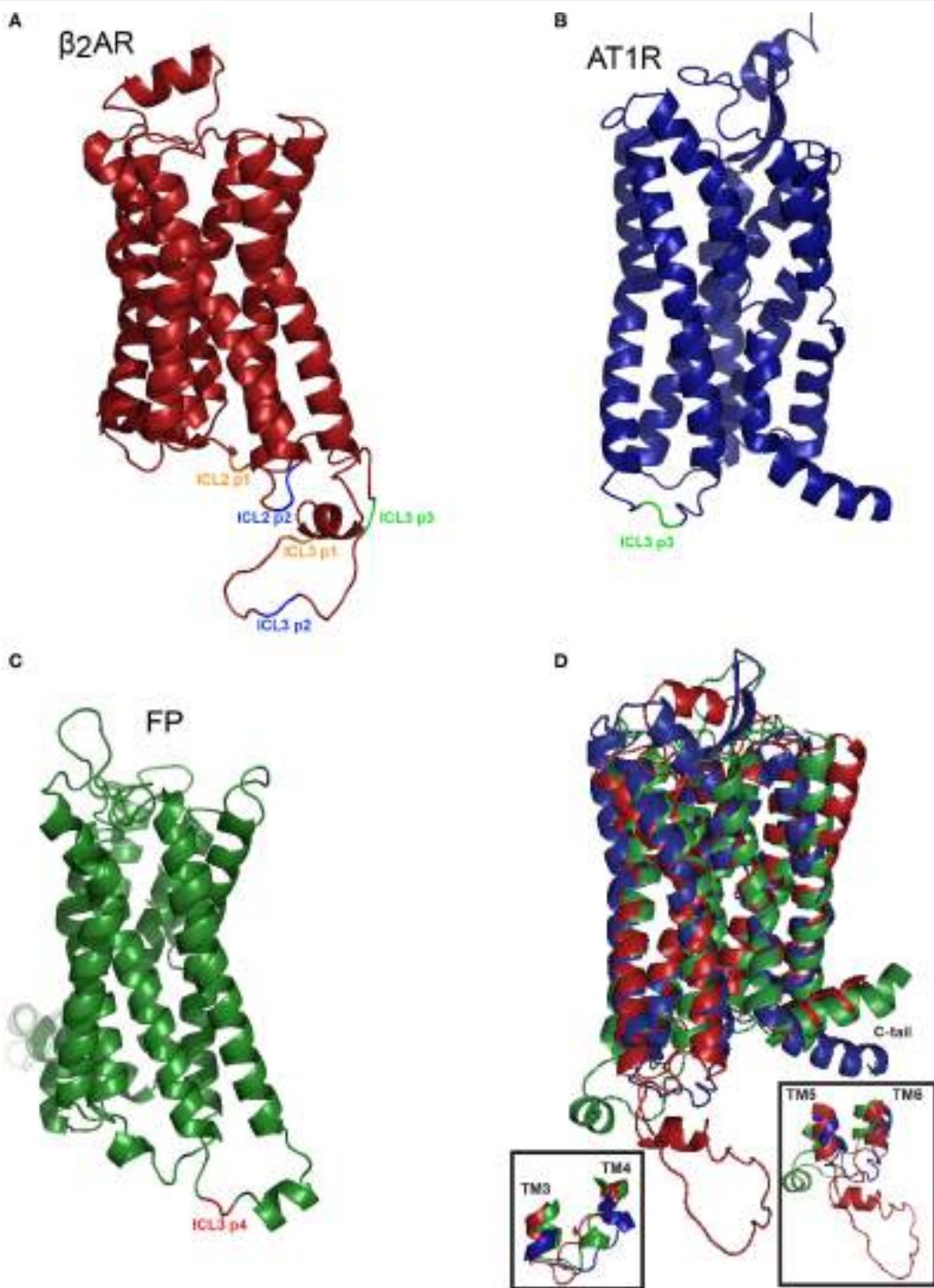


FIGURE 7 | Homology-based representation of the positioning of the FlAsH tag in three class A G protein-coupled receptors. (A) Homology model of the h β 2AR (P07550-1) based on PDB identifier: 2rh1A with truncated C-tail. Positions highlighted in orange correspond to the first position, in blue the second position, and in green the third position within each respective loop structure. **(B)** Homology model of the human angiotensin II type 1 receptor (P30556-1) modeled upon the existing crystal structure with PBD accession 4yayA, the C-tail was then truncated (25). The ICL3 p3 biosensor is shown in green. **(C)** Homology model of the human FP (P43088-1) based on the PBD ID: 3emlA. Insertion of the TC tag in ICL3 position 4 is shown in red. **(D)** Superimposing the models of the h β 2AR, AT1R, and FP. Overlay of three receptors reveals the relative similarities in the transmembrane domains and differences in the cytoplasmic regions. Approximately 20 residues were removed from the N-terminus and the C-terminus was truncated to facilitate the visualization of the overall structure. Inset shows expanded versions of ICL2 (left) or ICL3 (right). The I-TASSER models (26, 27) were exported into PyMOL where the CCPGCC motifs were inserted at their respective positions and color coded to facilitate the visualization of the FlAsH tags.

[(17); **Figure 6F**]. Interestingly, no responses were detected in similar constructs built into either ICL2 or the C-tail of FP (data not shown). Taken together, our data paint a picture which highlights the conformational heterogeneity of different GPCRs in response to ligand stimulation.

DISCUSSION

Crystal structures offer snapshot images of receptor structure that can be complemented using more dynamic measures such as RET approaches. Kobilka and coworkers reported that transmembrane domain VI experiences a 14 Å outward movement when comparing the inactive carazolol bound β_2 AR versus the active-G α s bound crystal structure (24). We show here that three different GPCRs show distinct patterns of BRET in response to ligand even when biosensors are placed in similar positions (**Figure 7**).

For the β_2 AR, our data showed that ICL2 and ICL3 did not respond to the full agonist isoproterenol, whereas two of our C-tail biosensors exhibited sustained BRET responses. As the acceptor was progressively walked down the C-terminus, resonance energy was more efficiently transferred from donor to acceptor under basal conditions and this may explain why BRET was not detected in biosensors with acceptor and donor farther apart. This pattern was distinct in the AT1R and in FP receptor. The AT1R exhibits the most conformational heterogeneity in that sensors engineered into ICL2, ICL3, or the C-tail all reported robustly on conformational changes in response to either canonical (Ang II or Ang III) or biased (SI) ligands (17). Further, only ICL3 biosensors reported responses upon stimulation with PGF2 α in FP (11, data not shown for ICL2 or the C-tail). This may suggest that the movement of the intracellular loops in the β_2 AR or FP is constrained by a protein within the vicinity of the fifth, sixth or seventh transmembrane domain. Even if this constrained conformation does not allow us to use these biosensors in this cellular background, it does highlight the advantage of using a six amino acid tag since this reduced size allows us to probe receptor conformation. For instance, if GFP or one of its variants were used instead of the FlAsH tag, perhaps the 238 amino acid (27 kDa) insertion would have significantly distorted receptor structure.

G protein-coupled receptors have many associated interacting partners that may pose conformational constraints on the receptor which translates into distinct conformational profiles. One of the major differences between the three receptors is that both the AT1R and FP couple to G α q whereas the β_2 AR couples to G α s. The β_2 AR has also been reported to differentially couple to G α i (28–30). It may be interesting to explore the propensity of the receptor to couple to different G proteins in a particular biological context. Such differential coupling may lead to distinct conformations adopted by the receptor. Alternatively, it is well known that all three GPCRs form oligomers (31–35). Homo- and heterodimers or larger oligomers are not fully characterized and their physiological roles are not fully understood. Perhaps the formation of such larger arrays imposes additional conformational

constraints on the receptor. These effects must be considered as early as events occurring in receptor biosynthesis (36, 37). Further exploring the lifecycle of a receptor is merited since oligomerization can alter several aspects of receptor function (37). Likewise, the β_2 AR experiences a high level of basal activity which some believe is due to the higher availability of G proteins and other effectors; proteins that might restrict receptor movement (38).

The length of intracellular loops in each receptor may also be related to measured conformational flexibility. The β_2 AR has a much longer third loop than the other two receptors. Taking this into account, we could imagine that the β_2 AR might be more free to adopt a larger range of conformations compared to the AT1R and FP (**Figure 7**). This may be a contributing factor explaining the different conformational patterns exhibited by all three receptors. These receptors are all classed into the same family of class A GPCRs, yet, they show different conformational behaviors. It must also be noted that this method is limited by the orientation of the reporter proteins. If the receptor folds in such a way where the enzymatic pocket of RlucII orients itself facing away from the FlAsH tag, the transfer of resonance energy will be less efficient with respect to RET.

In conclusion, we have demonstrated that the β_2 AR, AT1R, and FP display distinct conformational signatures when assayed in HEK 293 cells. Certainly cell context will matter in such experiments. The introduction of these BRET-based biosensors into diverse cell types may result in the detection of multiple different conformations adopted by the receptor depending on the cellular and subcellular contexts. Such receptor-based biosensors will be portable in this regard. Combined with genome editing approaches, these sensors are simple tools that could be used to uncover the complex mechanisms of GPCR activation and function.

AUTHOR CONTRIBUTIONS

KB, DD, RS, and TH designed the study, and wrote and edited the paper. KB, DD, RS, DP, and AZ performed experiments. KB, DD, and RS analyzed the data. KB, DD, RS, and DP generated figures.

ACKNOWLEDGMENTS

This work was supported by a grant from the Consortium Québécois sur la Découverte du Médicament and a grant from the Canadian Institutes of Health Research (CIHR, MOP-130309, TEH). RS was supported by a scholarship from the McGill-CIHR Drug Development Training Program. The authors thank Dr. Kees Jalink at the Netherlands Cancer Institute for the generous gift of the H188 EPAC FRET sensor and Mr. Jace Jones-Tabah for assistance in interpreting the data from these experiments. The authors thank Dr. Wolfgang Reitsch for assistance with high content microscopy. The authors thank Phan Trieu for technical and logistical assistance. The authors thank Dr. Jean-François Trempe and Mr. Andrew Bayne for assistance with PyMOL software.

REFERENCES

- Marinissen MJ, Gutkind JS. G-protein-coupled receptors and signaling networks: emerging paradigms. *Trends Pharmacol Sci* (2001) 22:368–76. doi:10.1016/S0165-6147(00)01678-3
- Fredriksson R, Lagerstrom MC, Lundin LG, Schioth HB. The G-protein-coupled receptors in the human genome form five main families. Phylogenetic analysis, paralogon groups, and fingerprints. *Mol Pharmacol* (2003) 63: 1256–72. doi:10.1124/mol.63.6.1256
- Salon JA, Lodowski DT, Palczewski K. The significance of G protein-coupled receptor crystallography for drug discovery. *Pharmacol Rev* (2011) 63:901–37. doi:10.1124/pr.110.003350
- Manglik A, Kim TH, Masureel M, Altenbach C, Yang Z, Hilger D, et al. Structural insights into the dynamic process of β_2 -adrenergic receptor signaling. *Cell* (2015) 161:1101–11. doi:10.1016/j.cell.2015.04.043
- Ye L, Van Eps N, Zimmer M, Ernst OP, Prosser RS. Activation of the A2A adenosine G-protein-coupled receptor by conformational selection. *Nature* (2016) 533:265–8. doi:10.1038/nature17668
- Staus DP, Strachan RT, Manglik A, Pani B, Kahsai AW, Kim TH, et al. Allosteric nanobodies reveal the dynamic range and diverse mechanisms of G-protein-coupled receptor activation. *Nature* (2016) 535:448–52. doi:10.1038/nature18636
- Nygaard R, Zou Y, Dror RO, Mildorf TJ, Arlow DH, Manglik A, et al. The dynamic process of β_2 -adrenergic receptor activation. *Cell* (2013) 152:532–42. doi:10.1016/j.cell.2013.01.008
- Ambrosio M, Zurn A, Lohse MJ. Sensing G protein-coupled receptor activation. *Neuropharmacology* (2011) 60:45–51. doi:10.1016/j.neuropharm.2010.08.006
- Lohse MJ, Nuber S, Hoffmann C. Fluorescence/bioluminescence resonance energy transfer techniques to study G-protein-coupled receptor activation and signaling. *Pharmacol Rev* (2012) 64:299–336. doi:10.1124/pr.110.004309
- Borroto-Escuela DO, Flajolet M, Agnati LF, Greengard P, Fuxe K. Bioluminescence resonance energy transfer methods to study G protein-coupled receptor-receptor tyrosine kinase heteroreceptor complexes. *Methods Cell Biol* (2013) 117:141–64. doi:10.1016/B978-0-12-408143-7.00008-6
- Sleno R, Pétrin D, Devost D, Goupil E, Zhang A, Hébert TE. Designing BRET-based conformational biosensors for G protein-coupled receptors. *Methods* (2016) 92:11–8. doi:10.1016/j.jmeth.2015.05.003
- Rebois RV, Maki K, Meeks JA, Fishman PH, Hébert TE, Northup JK. D2-like dopamine and β -adrenergic receptors form a signaling complex that integrates Gs- and Gi-mediated regulation of adenylyl cyclase. *Cell Signal* (2012) 24:2051–60. doi:10.1016/j.cellsig.2012.06.011
- Maier-Peusel M, Frolich N, Dees C, Hommers LG, Hoffmann C, Nikolaev VO, et al. A fluorescence resonance energy transfer-based M2 muscarinic receptor sensor reveals rapid kinetics of allosteric modulation. *J Biol Chem* (2010) 285:8793–800. doi:10.1074/jbc.M109.098517
- Ziegler N, Batz J, Zabel U, Lohse MJ, Hoffmann C. FRET-based sensors for the human M1-, M3-, and M5-acetylcholine receptors. *Bioorg Med Chem* (2011) 19:1048–54. doi:10.1016/j.bmc.2010.07.060
- Griffin BA, Adams SR, Tsien RY. Specific covalent labeling of recombinant protein molecules inside live cells. *Science* (1998) 281:269–72. doi:10.1126/science.281.5374.269
- Adams SR, Campbell RE, Gross LA, Martin BR, Walkup GK, Yao Y, et al. New biarsenical ligands and tetracycysteine motifs for protein labeling *in vitro* and *in vivo*: synthesis and biological applications. *J Am Chem Soc* (2002) 124:6063–76. doi:10.1021/ja017687n
- Devost D, Sleno R, Pétrin D, Zhang A, Shinjo Y, Okde R, et al. Conformational profiling of the AT1 angiotensin II receptor reflects biased agonism, G protein coupling and cellular context. *J Biol Chem* (2017). doi:10.1074/jbc.M116.763854
- Nakanishi J, Takarada T, Yunoki S, Kikuchi Y, Maeda M. FRET-based monitoring of conformational change of the β_2 -adrenergic receptor in living cells. *Biochem Biophys Res Commun* (2006) 343:1191–6. doi:10.1016/j.bbrc.2006.03.064
- Reiner S, Ambrosio M, Hoffmann C, Lohse MJ. Differential signaling of the endogenous agonists at the β_2 -adrenergic receptor. *J Biol Chem* (2010) 285: 36188–98. doi:10.1074/jbc.M110.175604
- Lavoie C, Mercier JF, Salahpour A, Umapathy D, Breit A, Villeneuve LR, et al. β_1/β_2 -adrenergic receptor heterodimerization regulates β_2 -adrenergic receptor internalization and ERK signaling efficacy. *J Biol Chem* (2002) 277: 35402–10. doi:10.1074/jbc.M204163200
- Klarenbeek J, Goedhart J, van Batenburg A, Groenewald D, Jalink K. Fourth-generation epac-based FRET sensors for cAMP feature exceptional brightness, photostability and dynamic range: characterization of dedicated sensors for FLIM, for ratiometry and with high affinity. *PLoS One* (2015) 10:e0122513. doi:10.1371/journal.pone.0122513
- Galandrin S, Bouvier M. Distinct signaling profiles of β_1 - and β_2 -adrenergic receptor ligands toward adenylyl cyclase and mitogen-activated protein kinase reveals the pluridimensionality of efficacy. *Mol Pharmacol* (2006) 70:1575–84. doi:10.1124/mol.106.026716
- Shenoy SK, Drake MT, Nelson CD, Houtz DA, Xiao K, Madabushi S, et al. β -arrestin-dependent, G protein-independent ERK1/2 activation by the β_2 adrenergic receptor. *J Biol Chem* (2006) 281:1261–73. doi:10.1074/jbc.M506576200
- Rasmussen SG, DeVree BT, Zou Y, Kruse AC, Chung KY, Kobilka TS, et al. Crystal structure of the β_2 adrenergic receptor-Gs protein complex. *Nature* (2011) 477:549–55. doi:10.1038/nature10361
- Zhang H, Unal H, Gati C, Han GW, Liu W, Zatsepina NA, et al. Structure of the angiotensin receptor revealed by serial femtosecond crystallography. *Cell* (2015) 161:833–44. doi:10.1016/j.cell.2015.04.011
- Yang J, Yan R, Roy A, Xu D, Poisson J, Zhang Y. The I-TASSER Suite: protein structure and function prediction. *Nat Methods* (2015) 12:7–8. doi:10.1038/nmeth.3213
- UniProt Consortium. UniProt: a hub for protein information. *Nucleic Acids Res* (2015) 43:D204–12. doi:10.1093/nar/gku989
- Kilts JD, Gerhardt MA, Richardson MD, Sriram G, Mackensen GB, Grocott HP, et al. β_2 -adrenergic and several other G protein-coupled receptors in human atrial membranes activate both G(s) and G(i). *Circ Res* (2000) 87:705–9. doi:10.1161/01.RES.87.8.705
- Daaka Y, Luttrell LM, Lefkowitz RJ. Switching of the coupling of the β_2 -adrenergic receptor to different G proteins by protein kinase A. *Nature* (1997) 390:88–91. doi:10.1038/36362
- Xiao RP. β -adrenergic signaling in the heart: dual coupling of the β_2 -adrenergic receptor to G(s) and G(i) proteins. *Sci STKE* (2001) 2001:re15. doi:10.1126/stke.2001.104.re15
- Hébert TE, Moffett S, Morello JP, Loisel TP, Bichet DG, Barret C, et al. A peptide derived from a β_2 -adrenergic receptor transmembrane domain inhibits both receptor dimerization and activation. *J Biol Chem* (1996) 271:16384–92. doi:10.1074/jbc.271.27.16384
- Salahpour A, Bonin H, Bhalla S, Petaja-Repo U, Bouvier M. Biochemical characterization of β_2 -adrenergic receptor dimers and oligomers. *Biol Chem* (2003) 384:117–23. doi:10.1515/BC.2003.012
- Goupil E, Fillion D, Clément S, Luo X, Devost D, Sleno R, et al. Angiotensin II type I and prostaglandin F2 α receptors cooperatively modulate signaling in vascular smooth muscle cells. *J Biol Chem* (2015) 290:3137–48. doi:10.1074/jbc.M114.631119
- AbdAlla S, Lother H, Quitterer U. AT1-receptor heterodimers show enhanced G-protein activation and altered receptor sequestration. *Nature* (2000) 407:94–8. doi:10.1038/35024095
- AbdAlla S, Lother H, Abdel-tawab AM, Quitterer U. The angiotensin II AT2 receptor is an AT1 receptor antagonist. *J Biol Chem* (2001) 276:39721–6. doi:10.1074/jbc.M105253200
- Salahpour A, Angers S, Mercier JF, Lagace M, Marullo S, Bouvier M. Homodimerization of the β_2 -adrenergic receptor as a prerequisite for cell surface targeting. *J Biol Chem* (2004) 279:33390–7. doi:10.1074/jbc.M403363200
- Terrillon S, Bouvier M. Roles of G-protein-coupled receptor dimerization. *EMBO Rep* (2004) 5:30–4. doi:10.1038/sj.emboj.7400052
- Milligan G. Constitutive activity and inverse agonists of G protein-coupled receptors: a current perspective. *Mol Pharmacol* (2003) 64:1271–6. doi:10.1124/mol.64.6.1271

Conflict of Interest Statement: The authors declare that the research was conducted in the absence of any commercial or financial relationships that could be construed as a potential conflict of interest.

Copyright © 2017 Bourque, Pétrin, Sleno, Devost, Zhang and Hébert. This is an open-access article distributed under the terms of the Creative Commons Attribution License (CC BY). The use, distribution or reproduction in other forums is permitted, provided the original author(s) or licensor are credited and that the original publication in this journal is cited, in accordance with accepted academic practice. No use, distribution or reproduction is permitted which does not comply with these terms.



Activation of Brain Somatostatin Signaling Suppresses CRF Receptor-Mediated Stress Response

Andreas Stengel^{1*} and Yvette F. Taché^{2,3}

¹ Division of Psychosomatic Medicine, Charité Center for Internal Medicine and Dermatology, Charité-Universitätsmedizin Berlin, Berlin, Germany, ² Vatche and Tamar Manoukian Digestive Diseases Division, CURE Digestive Diseases Research Center, G Oppenheimer Center for Neurobiology of Stress and Resilience, Department of Medicine, University of California, Los Angeles, Los Angeles, CA, USA, ³ VA Greater Los Angeles Health Care System, Los Angeles, CA, USA

OPEN ACCESS

Edited by:

Jacques Epelbaum,
Institut National de la Santé et de la
Recherche Médicale, France

Reviewed by:

James A. Carr,
Texas Tech University, USA
Jean-Louis Guillou,
University of Bordeaux 1, France

*Correspondence:

Andreas Stengel
andreas.stengel@charite.de

Specialty section:

This article was submitted to
Neuroendocrine Science,
a section of the journal
Frontiers in Neuroscience

Received: 01 February 2017

Accepted: 06 April 2017

Published: 25 April 2017

Citation:

Stengel A and Taché YF (2017)
Activation of Brain Somatostatin
Signaling Suppresses CRF
Receptor-Mediated Stress Response.
Front. Neurosci. 11:231.
doi: 10.3389/fnins.2017.00231

Corticotropin-releasing factor (CRF) is the hallmark brain peptide triggering the response to stress and mediates—in addition to the stimulation of the hypothalamus-pituitary-adrenal (HPA) axis—other hormonal, behavioral, autonomic and visceral components. Earlier reports indicate that somatostatin-28 injected intracerebroventricularly counteracts the acute stress-induced ACTH and catecholamine release. Mounting evidence now supports that activation of brain somatostatin signaling exerts a broader anti-stress effect by blunting the endocrine, autonomic, behavioral (with a focus on food intake) and visceral gastrointestinal motor responses through the involvement of distinct somatostatin receptor subtypes.

Keywords: brain-gut axis, food intake, gastrointestinal functions, HPA, hypothalamus, stress

INTRODUCTION

The past years have witnessed major advances in our understanding of the underlying mechanisms involved in the bodily response to stress (Chrousos and Zoumaki, 2017). Namely, the corticotropin-releasing factor (CRF) systems in the brain play a major role in coordinating an array of stress-related behavioral, endocrine, autonomic and visceral changes as well as the stress recovery through activation of distinct CRF receptor subtypes (Bale and Vale, 2004; Taché and Million, 2015; Henckens et al., 2016). This was established by monitoring alterations of CRF systems occurring during stress exposure in specific brain nuclei and the impact of pharmacological or targeted genetic manipulations of CRF ligands and/or receptors on the stress response (Suda et al., 2004; Chen et al., 2014; Rivier and Rivier, 2014; Taché and Million, 2015; Henckens et al., 2016). Simultaneously, other brain pathways are recruited by stress that exert stress-relieving effects (Bali et al., 2014). Among them, the activation of brain neuropeptide Y₁ and oxytocin receptors have been implicated in stress adaptation processes as recently reviewed (Zheng et al., 2010; Reichmann and Holzer, 2016). Earlier reports by Brown et al. showed that the injection of somatostatin-28 into the lateral brain ventricle blocked acute stressors-induced rise of ACTH and epinephrine plasma levels in rats (Brown et al., 1984). The present review will summarize mounting evidence indicating that activation of brain somatostatin signaling at different brain sites exerts an anti-stress action that extends to several components of the stress response through distinct somatostatin receptor subtypes.

Brain Corticotropin Releasing Factor Signaling

In 1950, Harris and colleagues reported that different stressors stimulate the release of adrenocorticotrophic hormone (ACTH) *via* a yet unknown hypothalamic factor (de Groot and Harris, 1950; Harris, 1950). Five years later, Guillemin and coworkers purified a factor able to stimulate pituitary ACTH secretion using a large sample of bovine hypothalamus (Guillemin and Rosenberg, 1955; Saffran et al., 1955). This factor was named CRF (Guillemin and Rosenberg, 1955; Saffran et al., 1955). However, it took another 26 years to identify and sequence the 41-amino acid peptide that plays a pivotal role in the stress-related pituitary release of ACTH and β -endorphin (Vale et al., 1981; Bale and Chen, 2012). Besides acting as a secretagogue of the hypothalamus-pituitary-adrenal (HPA) axis, CRF was subsequently implicated in stress-related alterations of autonomic (Yang et al., 2010; Bardgett et al., 2014), visceral (Taché and Million, 2015), behavioral (Bale and Vale, 2004), and also immune (Gravanis and Margioris, 2005) responses.

Following the characterization of CRF, additional structurally related members of the CRF peptide family were identified, namely urocortin 1 (Ucn 1, 40 amino acids, 45% sequence homology with rat/human CRF) (Vaughan et al., 1995), Ucn 2 (39 amino acids, 34% sequence homology with rat/human CRF) (Reyes et al., 2001) and Ucn 3 (38 amino acids, 26% sequence homology with rat/human CRF) (Lewis et al., 2001). These peptides are encoded by distinct genes highly conserved across mammalian and non-mammalian species (Lovejoy and de Lannoy, 2013).

Mapping studies identified prominent CRF expression in the cerebral cortex, amygdala, hippocampus and the Barrington's nucleus in rodents (Wang et al., 2011). Likewise, urocortins display broad distribution although there is little overlap with that of CRF. Ucn 1 immunoreactivity is mainly expressed in the Edinger-Westphal nucleus (Bittencourt et al., 1999), while Ucn 2 mRNA (due to the lack of a specific antibody) has been detected in the supraoptic nucleus, the paraventricular and arcuate nucleus of the hypothalamus, the locus coeruleus, several cranial nerve motor nuclei and the ventral horn of the spinal cord (Reyes et al., 2001; Mano-Otagiri and Shibasaki, 2004). Lastly, Ucn 3 mRNA and peptide expression have been identified in the amygdala, lateral septum, ventromedial hypothalamus and paraventricular nucleus of the hypothalamus, basomedial nucleus of the stria terminalis, dorsal raphe nucleus and the area postrema (Lewis et al., 2001; Li et al., 2002; Mano-Otagiri and Shibasaki, 2004; Venihaki et al., 2004).

The various biological effects of CRF and Ucns are mediated by binding to and activating two distinct seven-transmembrane domain (TMD) G-protein-coupled receptor subtypes, CRF₁ and/or CRF₂ that belong to the B1 subfamily (Perrin and Vale, 1999). CRF ligands display distinct affinity to CRF receptors with CRF binding preferentially to CRF₁ and with lesser affinity to CRF₂ (Hillhouse and Grammatopoulos, 2006), while Ucn 1 displays equal high affinity to both CRF₁ and CRF₂ and Ucn 2 and 3 are selective CRF₂ agonists (Grace et al., 2007). Both CRF receptors are encoded by distinct genes which exhibit diverse alternative pre-mRNA splicing patterns resulting in

multiple variants derived from partial or total exon deletions or insertions (Grammatopoulos et al., 1999; Pisarchik and Slominski, 2001; Wu et al., 2007, 2011; Zmijewski and Slominski, 2010; Grammatopoulos, 2012; Yuan et al., 2012, 2016). With regard to the nine human CRF₁ variants, CRF_{1a-i}, described, CRF_{1a} being the main wild type functional receptor while the other isoforms may modulate CRF signaling (Zmijewski and Slominski, 2010; Wu et al., 2011). For the CRF₂, three functionally active splice variants, CRF_{2a-c}, have been described in humans (Hillhouse and Grammatopoulos, 2006).

In line with the widespread expression of CRF ligands, CRF₁ and CRF₂ are also widely distributed in the rodent brain (Van Pett et al., 2000; Justice et al., 2008). CRF₁ is prominently expressed in the forebrain including the isocortex throughout cortical layers II-VI, hippocampal formation at the CA1 level, basal ganglia within the globus pallidus and striatum, sensory systems and the amygdala (Justice et al., 2008; Kuhne et al., 2012), while basal levels are low in the hypothalamus (Bonaz and Rivest, 1998) and spinal cord (Kuhne et al., 2012). Moreover, CRF₁ was also detected in all segments of the mouse spinal cord throughout laminae II-V (Korosi et al., 2007). The CRF₂ shows a wide distribution in the brain, most notably in the amygdala, lateral septum, supraoptic nucleus, ventromedial hypothalamus, dorsal raphe nuclei, area postrema, the nucleus of the solitary tract and the spinal cord (Bittencourt and Sawchenko, 2000; Korosi et al., 2007; Lukkes et al., 2011).

Brain Somatostatin Signaling

Somatostatin-14 was isolated in 1973 from ovine hypothalamus and shown to inhibit growth hormone secretion *in vitro* (Brazeau et al., 1973). Seven years later, the N-terminally extended form, somatostatin-28, generated by differential posttranslational processing from a common precursor molecule, was identified (Pradayrol et al., 1980). The somatostatinergic system also encompasses cortistatin, an evolutionary-related peptide that shares high structural and functional similarity to somatostatin although derived from a distinct gene (de Lecea et al., 1996; Gahete et al., 2008). In the rat brain, the pre-pro-hormone gives rise to cortistatin-14 and -29, while in humans, it leads to a 17-amino acid peptide (Hannon et al., 2002a).

Besides the initially described expression site in the hypothalamus, somatostatin is widely distributed in the rodent brain with dense expression in the cortex, amygdala, limbic and sensory system, periaqueductal central gray and paraventricular, ventromedial and arcuate hypothalamic nuclei (Finley et al., 1981; Johansson et al., 1984; Moga and Gray, 1985; Viollet et al., 2008).

Somatostatin-14 and somatostatin-28 bind to five receptor subtypes (sst_{1-5}), all belonging to G-protein-coupled TMD receptors encoded by different non-allelic and intronless genes (Theodoropoulou and Stalla, 2013). Different functionally active isoforms have been described for the sst_2 and sst_5 . The full length sst_{2a} and the truncated sst_{2b} differ only in the length and composition of their C-terminal domains (Cole and Schindler, 2000). The truncated sst_5 variants differ by their shorter C-terminal tails and display less than seven TMD which vary between species and have been named

accordingly (rat sst₅TMD1; mouse sst₅TMD1, sst₅TMD2 and sst₅TMD4; pig sst₅TMD3 and sst₅TMD6; human sst₅TMD4 and sst₅TMD5) (Duran-Prado et al., 2009, 2012; Cordoba-Chacon et al., 2010).

In line with the mapping of the ligand, the sst receptors are widely expressed in the rodent brain with the following regional pattern: all layers of the cerebral cortex (sst₁, sst_{2a/b}, sst₃, sst₄), bed nucleus of the stria terminalis (sst₁, sst_{2a/b}, sst₄), hippocampus (sst₁, sst_{2a/b}, sst₃, sst₄), basolateral amygdaloid nucleus (sst₁, sst_{2a/b}, sst₃, sst₄), medial amygdaloid nucleus (sst₁, sst₂, sst₃), ventromedial hypothalamic nucleus (sst₁, sst₂, sst₃), dorsomedial hypothalamic nucleus (sst₁, sst₃), paraventricular nucleus (sst_{2a}, sst₃) and arcuate nucleus of the hypothalamus (sst₁, sst_{2a}, sst₃, sst₄), substantia nigra (sst₁, sst_{2a/b}, sst₃), dorsal raphe nucleus (sst₁, sst₂, sst₃), locus coeruleus (sst₂, sst₃), granular layer of the cerebellum (sst₁, sst_{2b}, sst₃, sst₄, sst₅), dorsal motor nucleus of the vagus nerve (sst_{2a/b}, sst₄, sst₅) and nucleus of the solitary tract (sst₁, sst₂, sst₃) (Schindler and Humphrey, 1999; Fehlmann et al., 2000; Schulz et al., 2000; Hannon et al., 2002b; Videau et al., 2003; Spary et al., 2008; Kumar, 2012). With regards to the truncated sst₅ variants, they show a distinct distribution with a high abundance of full length sst₅ in mouse hypothalamus and cerebellum followed by sst₅TMD2 and sst₅TMD1, whereas sst₅TMD4 is not detectable (Hannon et al., 2002b; Cordoba-Chacon et al., 2010). By contrast, in the mouse cortex full length sst₅ is absent, while all truncated variants are expressed (sst₅TMD2, sst₅TMD4, sst₅TMD1) (Cordoba-Chacon et al., 2010) indicative of a prominent role of truncated sst₅ variants in this brain area. The distinct expression pattern is important in the context of pharmacological characteristics of truncated variants. Indeed, *in vitro* studies showed that cells expressing the sst₅TMD2 mainly respond to cortistatin, whereas those expressing sst₅TMD4 were exclusively activated by somatostatin and those bearing the sst₅TMD1 responded to both ligands (Cordoba-Chacon et al., 2010, 2011). It is to note that species differences exist since in humans, cortistatin activates sst₅TMD4, while somatostatin activates the sst₅TMD5 (Duran-Prado et al., 2009; Cordoba-Chacon et al., 2011).

Somatostatin in the brain exerts a wide variety of physiological functions besides the initially described inhibitory effect on growth hormone release. Its actions include increased locomotor activity (Viollet et al., 2008), memory and learning (Vecsei and Widerlov, 1988; Gastambide et al., 2009), and sleep (Steiger, 2007; Xu et al., 2015), as well as changes in autonomic cardiovascular and gastric functions (e.g., sympatho-inhibitory effect with lowering of heart rate and blood pressure, stimulation of gastric secretion and transit) (Brown and Taché, 1981; Martinez et al., 2000; Bou Farah et al., 2016), immune functions (Gonzalez-Rey et al., 2015) and ingestive behaviors (e.g., increased feeding and drinking; Stengel et al., 2015). Of importance in relation with stress, injection of somatostatin into the brain influences emotional processes exerting anxiolytic and anti-depressant effects (Engin and Treit, 2009; Scheich et al., 2016). However, in contrast to other anxiolytics such as benzodiazepines, somatostatin exerts pro-cognitive effects under healthy (Liguz-Lecznar et al., 2016) and Alzheimer's disease conditions (Epelbaum et al., 2009).

RESPONSE TO STRESS

Activation of CRF Signaling

CRF expression is upregulated in the hypothalamus and the peptide released into the median eminence under conditions of stress leading to pituitary ACTH and subsequently adrenal glucocorticoid hormone release (cortisol in humans and corticosterone in rodents) (Turnbull and Rivier, 1997; Smith and Vale, 2006; Kageyama and Suda, 2009). Moreover, hypothalamic CRF₁ receptors are also upregulated in rodents exposed to acute or chronic stress by a CRF feed-forward mechanism (Bonaz and Rivest, 1998; Imaki et al., 2001; Konishi et al., 2003; Wan et al., 2014; Eraslan et al., 2015). The use of selective CRF receptor subtype agonists and antagonists as well as transgenic animal models established the primary role of CRF₁ receptor in driving the stress-related HPA, behavioral, autonomic and visceral responses (Turnbull and Rivier, 1997; Luckey et al., 2003b; Farrokhi et al., 2007; Kehne and Cain, 2010; Taché, 2015).

Activation of Somatostatin Signaling

Somatostatin signaling is also activated by different stressors. In particular, immobilization (Negro-Vilar and Saavedra, 1980; Arancibia et al., 2000), handling (Arancibia et al., 1984), maternal separation (Polkowska and Wankowska, 2010), hypoxia (Chen and Du, 2002), pain (Arancibia et al., 1984), and injection of endotoxin (Priego et al., 2005) increase hypothalamic somatostatin mRNA levels and peptide release. Somatostatin release also occurred in the dorsal dentate gyrus in rats subjected to immobilization (Arancibia et al., 2001). Moreover, rats exposed to an elevated plus maze displayed an activation of somatostatin positive neurons in the basolateral amygdala (Butler et al., 2012). The activation of somatostatin signaling under conditions of stress is not restricted to the ligand but also occurred at the receptor level. In the amygdala and anterior cingulate cortex, sst₂ mRNA was upregulated following acute exposure of rats to a potential predator (Nanda et al., 2008), a finding recently also observed in the medial habenula following chronic mild stress (Faron-Gorecka et al., 2016).

SUPPRESSION OF THE CRF-MEDIATED STRESS RESPONSE BY ACTIVATION OF SOMATOSTATIN SIGNALING

Endocrine Response

Initial reports by Brown et al. showed that intracerebroventricular (icv) injection of the pan-sst agonist, somatostatin-28 or the oligo-somatostatin agonist, des-AA_{1,2,4,5,12,13}-[D-Trp₈]somatostatin (ODT8-SST) (Erchegyi et al., 2008) prevented the increase of ACTH plasma levels induced by tail suspension or exposure to ether in rats (Brown et al., 1984). By contrast, the intravenous (iv) injection of ODT8-SST had no effect indicating a centrally-mediated inhibitory action of somatostatin-28 (Brown et al., 1984). The somatostatin action may involve a component upstream of CRF signaling. This is most likely due to the inhibition of hypothalamic release of CRF induced by tail suspension (Brown et al., 1984). This is also supported by *in vitro* studies showing that octreotide

($sst_5 = sst_2 > sst_3$ agonist) (Grace et al., 2008) and the pan-sst agonists, somatostatin-14 and cortistatin ($sst_2 = sst_3 = sst_4 = sst_5 > sst_1$) (Fukusumi et al., 1997) blunt basal and KCl-induced CRF release from hypothalamic and hippocampal explants (Tizabi and Calogero, 1992; Tringali et al., 2012).

With regards to the receptor subtype(s) involved, in addition to the $sst_5 = sst_2 > sst_3$ agonist, octreotide (Tringali et al., 2012), recent studies indicate that intra-hippocampal infusion of the sst_2 agonist, L-054,264, and sst_4 agonist, L-803,087 lowered the elevated corticosterone levels in the plasma and hippocampal dialysate induced by acute foot shock in mice (Prévôt et al., 2017). By contrast, under the same conditions, the sst_1 agonist L-797,591 and sst_3 agonist, L-796,77 had no effect (Prévôt et al., 2017). The activation of these somatostatin- sst_2 and - sst_4 signaling pathways was shown to have physiological relevance in dampening the hippocampal corticosterone elevation induced by acute foot shock. In sst_2 knockout mice, the rise in hippocampal corticosterone after an acute foot shock had a shorter onset, higher maximum and delayed recovery compared to wild type mice (Prévôt et al., 2017). Moreover, the sst_4 agonist microinjected into the hippocampus in sst_2 knockout mice exposed to foot shock shortened the return to basal corticosterone levels, while not influencing the elevation to the peak rise (Prévôt et al., 2017). These data point toward distinct inhibitory actions of sst subtypes with sst_2 dampening the initial stress-corticosterone response, while sst_4 activation accelerates the recovery.

It is likely that somatostatin may have an additional sst_2 -mediated inhibitory action at the pituitary level where ACTH-secreting cells express the sst_2 (Day et al., 1995; Mezey et al., 1998). *In vitro* studies showed that somatostatin-14 (Heisler et al., 1982; Richardson, 1983) and somatostatin-28 (Strowski et al., 2002) as well as selective sst_2 and sst_5 agonists, unlike sst_1 , sst_3 , or sst_4 (Strowski et al., 2002) block the CRF-stimulated ACTH release from pituitary AtT-20 cells. Moreover, the pituitaries of sst_2 knockout mice display a higher ACTH release *in vitro* compared to that of wild type littermates (Viollet et al., 2000) and *in vivo*, sst_2 knockout mice have elevated basal levels of plasma corticosterone, while those of sst_4 knockout mice were unchanged (Prévôt et al., 2017). Taken together, the somatostatin receptors-induced reduction of HPA activation and elevation of hippocampal corticosterone in response to stress may be primarily mediated by brain sst_2 and sst_4 and pituitary sst_2 (Figure 1).

Autonomic Response

Convergent reports in rats indicate that the activation of brain somatostatin signaling blocked the stress-related sympathetic activation. Brown et al. initially showed that icv injection of somatostatin-28 or ODT8-SST abolished the plasma epinephrine elevation elicited by a variety of stressors including acute exposure to tail suspension, intermittent loud noise, ether stress, or metabolic hypoglycemic stress induced by the injection of 2-deoxyglucose or insulin in rats (Fisher and Brown, 1980; Brown et al., 1982, 1984; Gotoh et al., 2001).

The centrally mediated action of the SST-agonists was demonstrated by the lack of effect when ODT8-SST was

administered peripherally at a dose 100-times higher than icv (Fisher and Brown, 1980; Gotoh et al., 2001). Microinjection of ODT8-SST into specific brain nuclei further established that the dorsal hypothalamic area is a brain site responsive to suppress elevated epinephrine secretion in dogs (Brown, 1983). In addition, the direct electrophysiological recording in the adrenal branch of the splanchnic nerve corroborated that icv injection of somatostatin suppresses adrenal sympathetic efferent activity in rats (Somiya and Tonoue, 1984).

With regards to the somatostatin receptor subtype(s) involved, icv injection of octreotide ($sst_5 = sst_2 > sst_3$) prevented the rise in serum catecholamines induced by 2-deoxyglucose and short exposure to cold swim stress (Gotoh et al., 2001). Recent neuroanatomical and electrophysiological findings support a role of the sst_2 to induce sympathoinhibitory actions in presympathetic neurons located in the rostroventrolateral medulla (RVLM). The sst_{2a} is the receptor most abundantly expressed at this site compared to other subtypes and microinjection of somatostatin into the RVLM induces a sympatho-inhibitory response mimicked by the sst_2 agonist, lanreotide and prevented by an sst_2 antagonist, BIM-23627 in rats (Burke et al., 2008).

Behavioral Response—Focus on Food Intake

Brain CRF receptors are involved in the stress-related reduction of food intake in rodents (Krahn et al., 1986; Shibasaki et al., 1988b) through the activation of both CRF₁ and CRF₂ (Hotta et al., 1999; Sekino et al., 2004; Stengel and Taché, 2014b). This inhibitory effect is counteracted by brain somatostatin as the pan-sst agonists, somatostatin-14 and somatostatin-28 or the oligo-somatostatin agonist, octreotide injected icv blunted the icv CRF-induced reduction of refeeding after a fast in rats (Shibasaki et al., 1988a). Moreover, somatostatin-14 and octreotide also blocked the robust anorexigenic response to restraint stress (Shibasaki et al., 1988b). Likewise, we reported that the intracisternal (ic) injection of ODT8-SST prevented the inhibition of food intake induced after abdominal surgery in fasted rats (Stengel et al., 2011b). This effect is recapitulated by the selective peptide sst_2 agonist, S-346-011 (Stengel et al., 2011b; Figure 1). We also found that ic ODT8-SST or an sst_2 agonist, unlike selective sst_1 or sst_4 agonists, restored plasma levels of the orexigenic hormone, acyl ghrelin (Hosoda et al., 2002) that were inhibited by abdominal surgery (Stengel et al., 2011b). However, the restoration of food intake after surgery by ic ODT8-SST is not secondary to the normalization of circulating acyl ghrelin as the ghrelin receptor antagonist, [D-Lys³]-GHRP-6 injected intraperitoneally (ip) did not alter ic ODT8-SST's action (Stengel et al., 2011b).

We previously established that abdominal surgery activates hypothalamic CRF neurons (Bonaz and Taché, 1997; Wang et al., 2011). Therefore, it may be speculated that the activation of brain sst_2 by ic ODT8-SST suppresses brain CRF release and the related inhibition of food intake (Stengel and Taché, 2014b). Whether the recently established robust dipsogenic response to brain sst_2 activation (Karasawa et al., 2014) also contributes to the increased

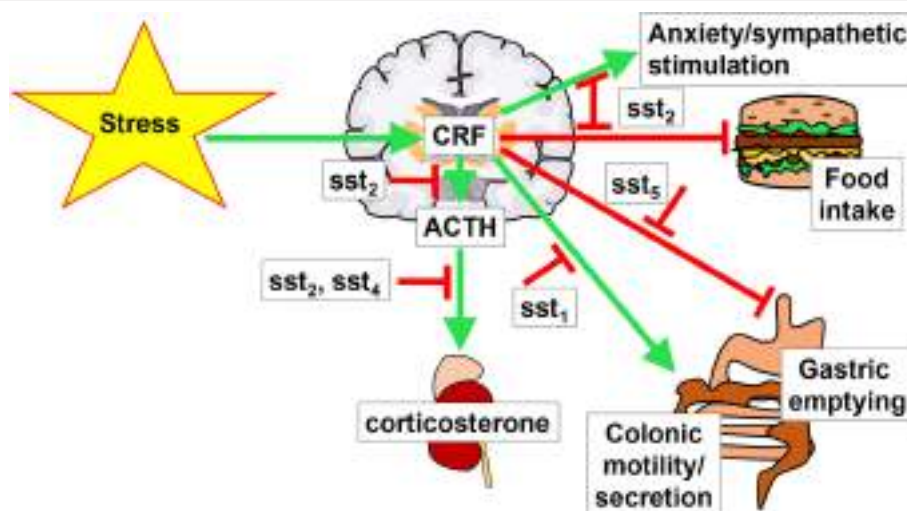


FIGURE 1 | Brain interaction of CRF and somatostatin signaling. Stress activates the hypothalamus-pituitary-adrenal gland axis by stimulating the hormones corticotropin-releasing factor (CRF), adrenocorticotrophic hormone (ACTH) and corticosterone. This stimulation is modulated by somatostatin signaling via different somatostatin receptors (sst). Green arrows indicate a stimulatory effect, red arrows depict an inhibition.

feeding behavior (Kissileff, 1969) inhibited by stress will have to be further investigated.

Visceral Response—Focus on Gastrointestinal Motor Functions

A multitude of stressors (physical, psychological, and immunological) alter gastrointestinal transit resulting in an inhibitory effect in the upper gastrointestinal tract, while stimulating colonic propulsive motor function (Stengel and Taché, 2009). These effects involve the activation of brain CRF receptors (Taché and Bonaz, 2007). Likewise, CRF and urocortin 1 injected into the brain ventricle or paraventricular nucleus of the hypothalamus suppress gastric emptying (Taché et al., 1987; Mönnikes et al., 1992; Coskun et al., 1997; Lee and Sarna, 1997) and shorten colonic transit time (Mönnikes et al., 1993; Martinez and Taché, 2001). Conversely, the blockade of CRF receptor signaling, namely CRF₂ and/or CRF₁ in the upper and CRF₁ in the lower gastrointestinal tract, prevented the delayed gastric emptying and the stimulation of colonic motility and defecation induced by various stressors in rodents (Taché and Bonaz, 2007).

By contrast to the ic injection of CRF, that of the pan-sst agonist, ODT8-SST accelerates gastric emptying in rats, an effect recapitulated by the preferential sst₅ agonist, BIM-23052 injected ic and blocked by subdiaphragmatic vagotomy or atropine (Martinez et al., 2000). The sst₅ is likely the main receptor mediating this action as ic injection of the selective sst₁, sst₂, sst₃ or sst₄ agonists CH-275, DC-32-87, BIM-23056 and L-803,087, respectively did not modify gastric emptying (Martinez et al., 2000). Lastly, intravenous (iv) injection of the predominant sst₅ agonist, BIM-23052 had no effect (Martinez et al., 2000). The prominent expression of the sst₅ in the dorsal motor nucleus of the vagus nerve (Thoss et al., 1995) along with

functional data are consistent with the activation of the sst₅ in the hindbrain inducing a vagal cholinergic-dependent stimulation of gastric propulsive motor function (Martinez et al., 2000). The sst₅ has been shown to form heterodimers with sst₁ or sst₂ that potentiates signaling efficiency (Rocheville et al., 2000). Whether ODT8-SST acts through these heterodimers cannot be ruled out. In addition, as the μ opioid receptor antagonist, naloxone was shown to block the ODT8-SST-induced acceleration of gastric emptying in rats (Stengel et al., 2010), it will be important to investigate whether heterodimers of the sst₅ with the μ opioid receptor also expressed in the dorsal motor nucleus (Mansour et al., 1995) occur as shown before with the sst_{2a} (Pfeiffer et al., 2002).

Under stress conditions, the activation of somatostatin receptors restores the inhibited gastric emptying. Abdominal surgery is a well-established physical stressor suppressing the initial neurogenic phase of postoperative gastric ileus through activation of brain CRF signaling (Luckey et al., 2003a; Stengel and Taché, 2014a). We showed that injection of somatostatin-28 icv and ODT8-SST icv or ic prevented the abdominal surgery-induced delayed gastric emptying (Stengel et al., 2011b). This effect is mimicked by ic injection of the selective sst₅ agonist, BIM-23052, while under the same conditions, ic injection of sst₁ (S-406-062), sst₂ (S-346-011), or sst₄ (S315-297) peptide agonists had no effect (Stengel et al., 2011b). It is important to note that the prevention of surgery-induced inhibition of the prokinetic hormone acyl ghrelin (De Smet et al., 2009) by ic ODT8-SST primarily involves the sst₂ (Stengel et al., 2011b). Additionally, we demonstrated that blockade of ghrelin signaling using the ghrelin receptor antagonist, [D-Lys³]-GHRP-6 did not modify the ODT8-SST-induced prevention of postoperative gastric ileus (Stengel et al., 2011b). Taken together these data argue against the preventive action of ic ODT8-SST against postoperative gastric ileus being secondary to the normalization of circulating

prokinetic hormone acyl ghrelin. The mechanisms may involve stimulation of vagal efferent activity and/or an interaction with other transmitters such as opioids that will have to be further established.

Several stressors exert a brain CRF₁-mediated stimulatory action on colonic motor functions in rodents (Taché and Million, 2015). The activation of brain somatostatin signaling inhibits the colonic response to exogenously administered CRF or CRF endogenously released by stress (Stengel et al., 2011a). We reported that icv injection of ODT8-SST inhibits the icv CRF- and water avoidance stress-induced increased fecal pellet output and colonic contractions evoked by semi-restraint in mice (Stengel et al., 2011a). Pharmacological characterization of receptor supports a primary involvement of the sst₁. Acute anesthesia stress in mice, that led to a pronounced increase of fecal pellet output, is inhibited by icv injection of somatostatin-28 and ODT8-SST or the selective peptide sst₁ agonist, S-406-062 (Stengel et al., 2011a). In contrast, the oligo-sst agonist, octreotide (sst₅ = sst₂ > sst₃) or selective peptide sst₂ or sst₄ agonists, S-346-011 and S-315-297, respectively did not modify the acute stress-induced stimulation of fecal pellet output (Stengel et al., 2011a). This assumption is further corroborated by the expression of this receptor (among other receptors) in the hypothalamus and the brainstem (Fehlmann et al., 2000) in nuclei modulating colonic motility.

SUMMARY

Mounting evidence supports that the activation of brain sst alleviates many components of the stress response involving brain CRF signaling. The receptor subtype(s) have been characterized by the use of selective peptide agonists and antagonists or genetic manipulations in rodents. The sst₂ subtype is primarily involved in preventing the acute stress-induced

endocrine (rise of ACTH and corticosterone), autonomic (sympatho-inhibition) and behavioral (suppression of food intake and anxiety) responses. With regards to the brain-gut axis, the hindbrain sst₅ plays a key role in counteracting the stress-induced suppression of gastric emptying, whereas forebrain sst₁ reduces the stress-related stimulation of propulsive colonic motor function (Figure 1). These data provide clear evidence that exogenous activation of brain sst receptors by pharmacological administration of somatostatin and selective agonists have anti-stress properties; however, the role of endogenous brain somatostatin released by stress (Arancibia et al., 1984, 2000) or exogenous CRF (Mitsugi et al., 1990) in attenuating or terminating the stress response has still been little investigated (Prévôt et al., 2017). Likewise, our knowledge of specific brain sites through which selective activation of somatostatin receptors alleviates the stress response is still limited to sst₂ signaling in the hippocampus to suppress the rise in plasma corticosterone and to induce anxiolytic behavior (Prévôt et al., 2017) and in the RVLM to elicit sympatho-inhibition (Pilowsky et al., 2008; Prévôt et al., 2017).

AUTHOR CONTRIBUTIONS

All authors listed, have made substantial, direct and intellectual contribution to the work, and approved it for publication.

ACKNOWLEDGMENTS

This work was supported by funding of the German Research Foundation STE 1765/3-2, Charité University Funding UFF 89/441-176 (AS) and National Institute of Health grants (R01 DK -57238), P30 Center grant DK-41301 (Animal Model Core) and VA Senior Career Scientist Award (YT).

REFERENCES

- Arancibia, S., Epelbaum, J., Boyer, R., and Assenmacher, I. (1984). *In vivo* release of somatostatin from rat median eminence after local K⁺ infusion or delivery of nociceptive stress. *Neurosci. Lett.* 50, 97–102. doi: 10.1016/0304-3940(84)90469-5
- Arancibia, S., Payet, O., Givalois, L., and Tapia-Arancibia, L. (2001). Acute stress and dexamethasone rapidly increase hippocampal somatostatin synthesis and release from the dentate gyrus hilus. *Hippocampus* 11, 469–477. doi: 10.1002/hipo.1061
- Arancibia, S., Rage, F., Grauges, P., Gomez, F., Tapia-Arancibia, L., and Armario, A. (2000). Rapid modifications of somatostatin neuron activity in the periventricular nucleus after acute stress. *Exp. Brain Res.* 134, 261–267. doi: 10.1007/s002210000462
- Bale, T. L., and Chen, A. (2012). Minireview: CRF and Wylie Vale: a story of 41 amino acids and a Texan with grit. *Endocrinology* 153, 2556–2561. doi: 10.1210/en.2012-1273
- Bale, T. L., and Vale, W. W. (2004). CRF and CRF receptors: role in stress responsivity and other behaviors. *Annu. Rev. Pharmacol. Toxicol.* 44, 525–557. doi: 10.1146/annurev.pharmtox.44.101802.121410
- Bali, A., Singh, N., and Jaggi, A. S. (2014). Neuropeptides as therapeutic targets to combat stress-associated behavioral and neuroendocrinological effects. *CNS Neurol. Disord. Drug Targets* 13, 347–368. doi: 10.2174/1871527313666140314163920
- Bardgett, M. E., Sharpe, A. L., and Toney, G. M. (2014). Activation of corticotropin-releasing factor receptors in the rostral ventrolateral medulla is required for glucose-induced sympathoexcitation. *Am. J. Physiol. Endocrinol. Metab.* 307, E944–E953. doi: 10.1152/ajpendo.00291.2014
- Bittencourt, J. C., and Sawchenko, P. E. (2000). Do centrally administered neuropeptides access cognate receptors? An analysis in the central corticotropin-releasing factor system. *J. Neurosci.* 20, 1142–1156.
- Bittencourt, J. C., Vaughan, J., Arias, C., Rissman, R. A., Vale, W. W., and Sawchenko, P. E. (1999). Urocortin expression in rat brain: evidence against a pervasive relationship of urocortin-containing projections with targets bearing type 2 CRF receptors. *J. Comp. Neurol.* 415, 285–312.
- Bonaz, B., and Rivest, S. (1998). Effect of a chronic stress on CRF neuronal activity and expression of its type 1 receptor in the rat brain. *Am. J. Physiol.* 275, R1438–R1449.
- Bonaz, B., and Taché, Y. (1997). Corticotropin-releasing factor and systemic capsaicin-sensitive afferents are involved in abdominal surgery-induced Fos expression in the paraventricular nucleus of the hypothalamus. *Brain Res.* 748, 12–20. doi: 10.1016/S0006-8993(96)01281-4
- Bou Farah, L., Bowman, B. R., Bokiniec, P., Karim, S., Le, S., Goodchild, A. K., et al. (2016). Somatostatin in the rat rostral ventrolateral medulla: origins and mechanism of action. *J. Comp. Neurol.* 524, 323–342. doi: 10.1002/cne.23846
- Brazeau, P., Vale, W., Burgus, R., Ling, N., Butcher, M., Rivier, J., et al. (1973). Hypothalamic polypeptide that inhibits the secretion of immunoreactive pituitary growth hormone. *Science* 179, 77–79. doi: 10.1126/science.179.4068.77

- Brown, M. R. (1983). Central nervous system sites of action of bombesin and somatostatin to influence plasma epinephrine levels. *Brain Res.* 276, 253–257. doi: 10.1016/0006-8993(83)90732-1
- Brown, M. R., Fisher, L. A., Spiess, J., Rivier, C., Rivier, J., and Vale, W. (1982). Corticotropin-releasing factor: actions on the sympathetic nervous system and metabolism. *Endocrinology* 111, 928–931. doi: 10.1210/endo-111-3-928
- Brown, M. R., Rivier, C., and Vale, W. (1984). Central nervous system regulation of adrenocorticotropin secretion: role of somatostatins. *Endocrinology* 114, 1546–1549. doi: 10.1210/endo-114-5-1546
- Brown, M., and Taché, Y. (1981). Hypothalamic peptides: central nervous system control of visceral functions. *Fed. Proc.* 40, 2565–2569.
- Burke, P. G., Li, Q., Costin, M. L., McMullan, S., Pilowsky, P. M., and Goodchild, A. K. (2008). Somatostatin 2A receptor-expressing presynaptic neurons in the rostral ventrolateral medulla maintain blood pressure. *Hypertension* 52, 1127–1133. doi: 10.1161/HYPERTENSIONAHA.108.118224
- Butler, R. K., White, L. C., Frederick-Duus, D., Kaigler, K. F., Fadel, J. R., and Wilson, M. A. (2012). Comparison of the activation of somatostatin- and neuropeptide Y-containing neuronal populations of the rat amygdala following two different anxiogenic stressors. *Exp. Neurol.* 238, 52–63. doi: 10.1016/j.expneurol.2012.08.002
- Chen, N. A., Jupp, B., Sztainberg, Y., Lebow, M., Brown, R. M., Kim, J. H., et al. (2014). Knockdown of CRF1 receptors in the ventral tegmental area attenuates cue- and acute food deprivation stress-induced cocaine seeking in mice. *J. Neurosci.* 34, 11560–11570. doi: 10.1523/JNEUROSCI.4763-12.2014
- Chen, X. Q., and Du, J. Z. (2002). Increased somatostatin mRNA expression in periventricular nucleus of rat hypothalamus during hypoxia. *Regul. Pept.* 105, 197–201. doi: 10.1016/S0167-0115(02)00022-8
- Chrousos, G. P., and Zoumakis, E. (2017). Milestones in CRH research. *Curr. Mol. Pharmacol.* [Epub ahead of print].
- Cole, S. L., and Schindler, M. (2000). Characterisation of somatostatin sst₂ receptor splice variants. *J. Physiol. Paris.* 94, 217–237. doi: 10.1016/S0928-4257(00)00207-2
- Cordoba-Chacon, J., Gahete, M. D., Duran-Prado, M., Luque, R. M., and Castano, J. P. (2011). Truncated somatostatin receptors as new players in somatostatin-cortistatin pathophysiology. *Ann. N.Y. Acad. Sci.* 1220, 6–15. doi: 10.1111/j.1749-6632.2011.05985.x
- Cordoba-Chacon, J., Gahete, M. D., Duran-Prado, M., Pozo-Salas, A. I., Malagon, M. M., Gracia-Navarro, F., et al. (2010). Identification and characterization of new functional truncated variants of somatostatin receptor subtype 5 in rodents. *Cell Mol. Life Sci.* 67, 1147–1163. doi: 10.1007/s00018-009-0240-y
- Coskun, T., Bozkurt, A., Alican, I., Ozkutlu, U., Kurtel, H., and Yegen, B. C. (1997). Pathways mediating CRF-induced inhibition of gastric emptying in rats. *Regul. Pept.* 69, 113–120. doi: 10.1016/S0167-0115(96)02066-6
- Day, R., Dong, W., Panetta, R., Kraicer, J., Greenwood, M. T., and Patel, Y. C. (1995). Expression of mRNA for somatostatin receptor (sstr) types 2 and 5 in individual rat pituitary cells. A double labeling *in situ* hybridization analysis. *Endocrinology* 136, 5232–5235.
- de Groot, J., and Harris, G. W. (1950). Hypothalamic control of the anterior pituitary gland and blood lymphocytes. *J. Physiol.* 111, 335–346. doi: 10.1113/jphysiol.1950.sp004483
- de Lecea, L., Criado, J. R., Prospero-Garcia, O., Gautvik, K. M., Schweitzer, P., Danielson, P. E., et al. (1996). A cortical neuropeptide with neuronal depressant and sleep-modulating properties. *Nature* 381, 242–245. doi: 10.1038/381242a0
- De Smet, B., Mitselos, A., and Depoortere, I. (2009). Motilin and ghrelin as prokinetic drug targets. *Pharmacol. Ther.* 123, 207–223. doi: 10.1016/j.pharmthera.2009.04.004
- Duran-Prado, M., Gahete, M. D., Delgado-Niebla, E., Martinez-Fuentes, A. J., Vazquez-Martinez, R., Garcia-Navarro, S., et al. (2012). Truncated variants of pig somatostatin receptor subtype 5 (sst5) act as dominant-negative modulators for sst2-mediated signaling. *Am. J. Physiol. Endocrinol. Metab.* 303, E1325–E1334. doi: 10.1152/ajpendo.00445.2012
- Duran-Prado, M., Gahete, M. D., Martinez-Fuentes, A. J., Luque, R. M., Quintero, A., Webb, S. M., et al. (2009). Identification and characterization of two novel truncated but functional isoforms of the somatostatin receptor subtype 5 differentially present in pituitary tumors. *J. Clin. Endocrinol. Metab.* 94, 2634–2643. doi: 10.1210/jc.2008-2564
- Engin, E., and Treit, D. (2009). Anxiolytic and antidepressant actions of somatostatin: the role of sst₂ and sst₃ receptors. *Psychopharmacology (Berl)* 206, 281–289. doi: 10.1007/s00213-009-1605-5
- Epelbaum, J., Guillou, J. L., Gastambide, F., Hoyer, D., Duron, E., and Viollet, C. (2009). Somatostatin, Alzheimer's disease and cognition: an old story coming of age? *Prog. Neurobiol.* 89, 153–161. doi: 10.1016/j.pneurobio.2009.07.002
- Eraslan, E., Akyazi, I., Ergul-Ekiz, E., and Matur, E. (2015). Noise stress-induced changes in mRNA levels of corticotropin-releasing hormone family molecules and glucocorticoid receptors in the rat brain. *Folia Biol. (Praha)* 61, 66–73.
- Erchegyi, J., Grace, C. R., Samant, M., Cescato, R., Piccand, V., Riek, R., et al. (2008). Ring size of somatostatin analogues (ODT-8) modulates receptor selectivity and binding affinity. *J. Med. Chem.* 51, 2668–2675. doi: 10.1021/jm701444y
- Faron-Gorecka, A., Kusmider, M., Kolasa, M., Zurawek, D., Szafran-Pilch, K., Gruba, P., et al. (2016). Chronic mild stress alters the somatostatin receptors in the rat brain. *Psychopharmacology (Berl)* 233, 255–266. doi: 10.1007/s00213-015-4103-y
- Farrokhi, C. B., Toyote, P., Blanchard, R. J., Blanchard, D. C., Litvin, Y., and Spiess, J. (2007). Cortagine: behavioral and autonomic function of the selective CRF receptor subtype 1 agonist. *CNS Drug Rev.* 13, 423–443. doi: 10.1111/j.1527-3458.2007.00027.x
- Fehlmann, D., Langenegger, D., Schuepbach, E., Siehler, S., Feuerbach, D., and Hoyer, D. (2000). Distribution and characterisation of somatostatin receptor mRNA and binding sites in the brain and periphery. *J. Physiol. Paris* 94, 265–281. doi: 10.1016/S0928-4257(00)00208-4
- Finley, J. C., Maderdrut, J. L., Roger, L. J., and Petrusz, P. (1981). The immunocytochemical localization of somatostatin-containing neurons in the rat central nervous system. *Neuroscience* 6, 2173–2192. doi: 10.1016/0306-4522(81)90006-3
- Fisher, D. A., and Brown, M. R. (1980). Somatostatin analog: plasma catecholamine suppression mediated by the central nervous system. *Endocrinology* 107, 714–718. doi: 10.1210/endo-107-3-714
- Fukusumi, S., Kitada, C., Takekawa, S., Kizawa, H., Sakamoto, J., Miyamoto, M., et al. (1997). Identification and characterization of a novel human cortistatin-like peptide. *Biochem. Biophys. Res. Commun.* 232, 157–163. doi: 10.1006/bbrc.1997.6252
- Gahete, M. D., Duran-Prado, M., Luque, R. M., Martinez-Fuentes, A. J., Vazquez-Martinez, R., Malagon, M. M., et al. (2008). Are somatostatin and cortistatin two siblings in regulating endocrine secretions? *In vitro* work ahead. *Mol. Cell. Endocrinol.* 286, 128–134. doi: 10.1016/j.mce.2007.11.013
- Gastambide, F., Viollet, C., Lepousez, G., Epelbaum, J., and Guillou, J. L. (2009). Hippocampal SSTR4 somatostatin receptors control the selection of memory strategies. *Psychopharmacology (Berl)* 202, 153–163. doi: 10.1007/s00213-008-1204-x
- Gonzalez-Rey, E., Pedreno, M., Delgado-Maroto, V., Souza-Moreira, L., and Delgado, M. (2015). Lulling immunity, pain, and stress to sleep with cortistatin. *Ann. N.Y. Acad. Sci.* 1351, 89–98. doi: 10.1111/nyas.12789
- Gotoh, M., Takagi, J., Mori, S., Yatoh, M., Hirooka, Y., Yamanouchi, K., et al. (2001). Octreotide-induced suppression of the hyperglycemic response to neostigmine or bombesin: relationship to hypothalamic noradrenergic drive. *Brain Res.* 919, 155–159. doi: 10.1016/S0006-8993(01)03018-9
- Grace, C. R., Erchegyi, J., Samant, M., Cescato, R., Piccand, V., Riek, R., et al. (2008). Ring size in octreotide amide modulates differently agonist versus antagonist binding affinity and selectivity. *J. Med. Chem.* 51, 2676–2681. doi: 10.1021/jm701445q
- Grace, C. R., Perrin, M. H., Cantle, J. P., Vale, W. W., Rivier, J. E., and Riek, R. (2007). Common and divergent structural features of a series of corticotropin releasing factor-related peptides. *J. Am. Chem. Soc.* 129, 16102–16114. doi: 10.1021/ja0760933
- Grammatopoulos, D. K. (2012). Insights into mechanisms of corticotropin-releasing hormone receptor signal transduction. *Br. J. Pharmacol.* 166, 85–97. doi: 10.1111/j.1476-5381.2011.01631.x
- Grammatopoulos, D. K., Dai, Y., Randeva, H. S., Levine, M. A., Karteris, E., Easton, A. J., et al. (1999). A novel spliced variant of the type 1 corticotropin-releasing hormone receptor with a deletion in the seventh transmembrane domain present in the human pregnant term myometrium and fetal membranes. *Mol. Endocrinol.* 13, 2189–2202. doi: 10.1210/mend.13.12.0391

- Gravanis, A., and Margioris, A. N. (2005). The corticotropin-releasing factor (CRF) family of neuropeptides in inflammation: potential therapeutic applications. *Curr. Med. Chem.* 12, 1503–1512. doi: 10.2174/0929867054039008
- Guillemain, R., and Rosenberg, B. (1955). Humoral hypothalamic control of anterior pituitary: a study with combined tissue cultures. *Endocrinology* 57, 599–607. doi: 10.1210/endo-57-5-599
- Hannon, J. P., Nunn, C., Stoltz, B., Bruns, C., Weckbecker, G., Lewis, I., et al. (2002a). Drug design at peptide receptors: somatostatin receptor ligands. *J. Mol. Neurosci.* 18, 15–27. doi: 10.1385/JMN:18:1-2:15
- Hannon, J. P., Petrucci, C., Fehlmann, D., Viollet, C., Epelbaum, J., and Hoyer, D. (2002b). Somatostatin sst2 receptor knock-out mice: localisation of sst1-5 receptor mRNA and binding in mouse brain by semi-quantitative RT-PCR, *in situ* hybridisation histochemistry and receptor autoradiography. *Neuropharmacology* 42, 396–413. doi: 10.1016/S0028-3908(01)00186-1
- Harris, G. W. (1950). The hypothalamus and endocrine glands. *Br. Med. Bull.* 6, 345–350. doi: 10.1093/oxfordjournals.bmb.a073628
- Heisler, S., Reisine, T. D., Hook, V. Y., and Axelrod, J. (1982). Somatostatin inhibits multireceptor stimulation of cyclic AMP formation and corticotropin secretion in mouse pituitary tumor cells. *Proc. Natl. Acad. Sci. U.S.A.* 79, 6502–6506. doi: 10.1073/pnas.79.21.6502
- Henckens, M. J., Printz, Y., Shamgar, U., Dine, J., Lebow, M., Drori, Y., et al. (2016). CRF receptor type 2 neurons in the posterior bed nucleus of the stria terminalis critically contribute to stress recovery. *Mol. Psychiatry*. doi: 10.1038/mp.2016.133. [Epub ahead of print].
- Hillhouse, E. W., and Grammatopoulos, D. K. (2006). The molecular mechanisms underlying the regulation of the biological activity of corticotropin-releasing hormone receptors: implications for physiology and pathophysiology. *Endocr. Rev.* 27, 260–286. doi: 10.1210/er.2005-0034
- Hosoda, H., Kojima, M., and Kangawa, K. (2002). Ghrelin and the regulation of food intake and energy balance. *Mol. Interv.* 2, 494–503. doi: 10.1124/mi.2.8.494
- Hotta, M., Shibasaki, T., Arai, K., and Demura, H. (1999). Corticotropin-releasing factor receptor type 1 mediates emotional stress-induced inhibition of food intake and behavioral changes in rats. *Brain Res.* 823, 221–225. doi: 10.1016/S0006-8993(99)01177-4
- Imaki, T., Katsumata, H., Miyata, M., Naruse, M., Imaki, J., and Minami, S. (2001). Expression of corticotropin-releasing hormone type 1 receptor in paraventricular nucleus after acute stress. *Neuroendocrinology* 73, 293–301. doi: 10.1159/000054646
- Johansson, O., Hokfelt, T., and Elde, R. P. (1984). Immunohistochemical distribution of somatostatin-like immunoreactivity in the central nervous system of the adult rat. *Neuroscience* 13, 265–339. doi: 10.1016/0306-4522(84)90233-1
- Justice, N. J., Yuan, Z. F., Sawchenko, P. E., and Vale, W. (2008). Type 1 corticotropin-releasing factor receptor expression reported in BAC transgenic mice: implications for reconciling ligand-receptor mismatch in the central corticotropin-releasing factor system. *J. Comp. Neurol.* 511, 479–496. doi: 10.1002/cne.21848
- Kageyama, K., and Suda, T. (2009). Role and action in the pituitary corticotroph of corticotropin-releasing factor (CRF) in the hypothalamus. *Peptides* 30, 810–816. doi: 10.1016/j.peptides.2008.12.007
- Karasawa, H., Yakabi, S., Wang, L., Stengel, A., Rivier, J., and Taché, Y. (2014). Brain somatostatin receptor 2 mediates the dipsogenic effect of central somatostatin and cortistatin in rats: role in drinking behavior. *Am. J. Physiol. Regul. Integr. Comp. Physiol.* 307, R793–R801. doi: 10.1152/ajpregu.00248.2014
- Kehne, J. H., and Cain, C. K. (2010). Therapeutic utility of non-peptidic CRF1 receptor antagonists in anxiety, depression, and stress-related disorders: evidence from animal models. *Pharmacol. Ther.* 128, 460–487. doi: 10.1016/j.pharmthera.2010.08.011
- Kissileff, H. R. (1969). Food-associated drinking in the rat. *J. Comp. Physiol. Psychol.* 67, 284–300. doi: 10.1037/h0026773
- Konishi, S., Kasagi, Y., Katsumata, H., Minami, S., and Imaki, T. (2003). Regulation of corticotropin-releasing factor (CRF) type-1 receptor gene expression by CRF in the hypothalamus. *Endocr. J.* 50, 21–36. doi: 10.1507/endocrj.50.21
- Korosi, A., Kozicz, T., Richter, J., Veening, J. G., Olivier, B., and Roubos, E. W. (2007). Corticotropin-releasing factor, urocortin 1, and their receptors in the mouse spinal cord. *J. Comp. Neurol.* 502, 973–989. doi: 10.1002/cne.21347
- Krahn, D. D., Gosnell, B. A., Grace, M., and Levine, A. S. (1986). CRF antagonist partially reverses CRF- and stress-induced effects on feeding. *Brain Res. Bull.* 17, 285–289. doi: 10.1016/0361-9230(86)90233-9
- Kuhne, C., Puk, O., Graw, J., Hrabe De Angelis, M., Schutz, G., Wurst, W., et al. (2012). Visualizing corticotropin-releasing hormone receptor type 1 expression and neuronal connectivities in the mouse using a novel multifunctional allele. *J. Comp. Neurol.* 520, 3150–3180. doi: 10.1002/cne.23082
- Kumar, U. (2012). Immunohistochemical distribution of somatostatin and somatostatin receptor subtypes (SSTR1-5) in hypothalamus of ApoD knockout mice brain. *J. Mol. Neurosci.* 48, 684–695. doi: 10.1007/s12031-012-9792-7
- Lee, C., and Sarna, S. K. (1997). Central regulation of gastric emptying of solid nutrient meals by corticotropin releasing factor. *Neurogastroenterol. Motil.* 9, 221–229. doi: 10.1046/j.1365-2982.1997.d01-58.x
- Lewis, K., Li, C., Perrin, M. H., Blount, A., Kunitake, K., Donaldson, C., et al. (2001). Identification of urocortin III, an additional member of the corticotropin-releasing factor (CRF) family with high affinity for the CRF2 receptor. *Proc. Natl. Acad. Sci. U.S.A.* 98, 7570–7575. doi: 10.1073/pnas.121165198
- Li, C., Vaughan, J., Sawchenko, P. E., and Vale, W. W. (2002). Urocortin III-immunoreactive projections in rat brain: partial overlap with sites of type 2 corticotrophin-releasing factor receptor expression. *J. Neurosci.* 22, 991–1001.
- Liguz-Lecznar, M., Urban-Ciecko, J., and Kossut, M. (2016). Somatostatin and somatostatin-containing neurons in shaping neuronal activity and plasticity. *Front. Neural. Circuits* 10:48. doi: 10.3389/fncir.2016.00048
- Lovejoy, D. A., and de Lannoy, L. (2013). Evolution and phylogeny of the corticotropin-releasing factor (CRF) family of peptides: expansion and specialization in the vertebrates. *J. Chem. Neuroanat.* 54, 50–56. doi: 10.1016/j.jchemneu.2013.09.006
- Luckey, A., Livingston, E., and Taché, Y. (2003a). Mechanisms and treatment of postoperative ileus. *Arch. Surg.* 138, 206–214. doi: 10.1001/archsurg.138.2.206
- Luckey, A., Wang, L., Jamieson, P. M., Basa, N. R., Million, M., Czimber, J., et al. (2003b). Corticotropin-releasing factor receptor 1-deficient mice do not develop postoperative gastric ileus. *Gastroenterology* 125, 654–659. doi: 10.1016/S0016-5085(03)01069-2
- Lukkes, J. L., Staub, D. R., Dietrich, A., Truitt, W., Neufeld-Cohen, A., Chen, A., et al. (2011). Topographical distribution of corticotropin-releasing factor type 2 receptor-like immunoreactivity in the rat dorsal raphe nucleus: co-localization with tryptophan hydroxylase. *Neuroscience* 183, 47–63. doi: 10.1016/j.neuroscience.2011.03.047
- Mano-Otagiri, A., and Shibasaki, T. (2004). Distribution of urocortin 2 and urocortin 3 in rat brain. *J. Nippon Med. Sch.* 71, 358–359. doi: 10.1272/jnms.71.358
- Mansour, A., Fox, C. A., Burke, S., Akil, H., and Watson, S. J. (1995). Immunohistochemical localization of the cloned mu opioid receptor in the rat CNS. *J. Chem. Neuroanat.* 8, 283–305. doi: 10.1016/0891-0618(95)00055-C
- Martinez, V., Rivier, J., Coy, D., and Taché, Y. (2000). Intracisternal injection of somatostatin receptor 5-preferring agonists induces a vagal cholinergic stimulation of gastric emptying in rats. *J. Pharmacol. Exp. Ther.* 293, 1099–1105.
- Martinez, V., and Taché, Y. (2001). Role of CRF receptor 1 in central CRF-induced stimulation of colonic propulsion in rats. *Brain Res.* 893, 29–35. doi: 10.1016/S0006-8993(00)03277-7
- Mezey, E., Hunyady, B., Mitra, S., Hayes, E., Liu, Q., Schaeffer, J., et al. (1998). Cell specific expression of the sst2A and sst5 somatostatin receptors in the rat anterior pituitary. *Endocrinology* 139, 414–419. doi: 10.1210/endo.139.1.5807
- Mitsugi, N., Arita, J., and Kimura, F. (1990). Effects of intracerebroventricular administration of growth hormone-releasing factor and corticotropin-releasing factor on somatostatin secretion into rat hypophysial portal blood. *Neuroendocrinology* 51, 93–96. doi: 10.1159/000125322
- Moga, M. M., and Gray, T. S. (1985). Evidence for corticotropin-releasing factor, neurotensin, and somatostatin in the neural pathway from the central nucleus of the amygdala to the parabrachial nucleus. *J. Comp. Neurol.* 241, 275–284. doi: 10.1002/cne.902410304
- Mönnikes, H., Raybould, H. E., Schmidt, B., and Taché, Y. (1993). CRF in the paraventricular nucleus of the hypothalamus stimulates colonic motor activity in fasted rats. *Peptides* 14, 743–747. doi: 10.1016/0196-9781(93)90107-R

- Mönnikes, H., Schmidt, B. G., Raybould, H. E., and Taché, Y. (1992). CRF in the paraventricular nucleus mediates gastric and colonic motor response to restraint stress. *Am. J. Physiol.* 262, G137–G143.
- Nanda, S. A., Qi, C., Roseboom, P. H., and Kalin, N. H. (2008). Predator stress induces behavioral inhibition and amygdala somatostatin receptor 2 gene expression. *Genes Brain Behav.* 7, 639–648. doi: 10.1111/j.1601-183X.2008.00401.x
- Negro-Vilar, A., and Saavedra, J. M. (1980). Changes in brain somatostatin and vasopressin levels after stress in spontaneously hypertensive and Wistar-Kyoto rats. *Brain Res. Bull.* 5, 353–358. doi: 10.1016/S0361-9230(80)80004-9
- Perrin, M. H., and Vale, W. W. (1999). Corticotropin releasing factor receptors and their ligand family. *Ann. N.Y. Acad. Sci.* 885, 312–328. doi: 10.1111/j.1749-6632.1999.tb08687.x
- Pfeiffer, M., Koch, T., Schroder, H., Laugsch, M., Hollt, V., and Schulz, S. (2002). Heterodimerization of somatostatin and opioid receptors cross-modulates phosphorylation, internalization, and desensitization. *J. Biol. Chem.* 277, 19762–19772. doi: 10.1074/jbc.M110373200
- Pilowsky, P. M., Abbott, S. B., Burke, P. G., Farnham, M. M., Hildreth, C. M., Kumar, N. N., et al. (2008). Metabotropic neurotransmission and integration of sympathetic nerve activity by the rostral ventrolateral medulla in the rat. *Clin. Exp. Pharmacol. Physiol.* 35, 508–511. doi: 10.1111/j.1440-1681.2008.04906.x
- Pisarchik, A., and Slominski, A. T. (2001). Alternative splicing of CRH-R1 receptors in human and mouse skin: identification of new variants and their differential expression. *Faseb J.* 15, 2754–2756. doi: 10.1096/fj.01-0487fje
- Polkowska, J., and Wankowska, M. (2010). Effects of maternal deprivation on the somatotrophic axis and neuropeptide Y in the hypothalamus and pituitary in female lambs. The histomorphometric study. *Folia Histochem. Cytophiol.* 48, 299–305. doi: 10.2478/v10042-010-0024-0
- Pradayrol, L., Jornvall, H., Mutt, V., and Ribet, A. (1980). N-terminally extended somatostatin: the primary structure of somatostatin-28. *FEBS Lett.* 109, 55–58. doi: 10.1016/0014-5793(80)81310-X
- Prévôt, T. D., Gastambide, F., Viollet, C., Henkous, N., Martel, G., Epelbaum, J., et al. (2017). Roles of hippocampal somatostatin receptor subtypes in stress response and emotionality. *Neuropsychopharmacology*. doi: 10.1038/npp.2016.281. [Epub ahead of print].
- Priego, T., Ibanez De Caceres, I., Martin, A. I., Villanua, M. A., and Lopez-Calderon, A. (2005). Endotoxin administration increases hypothalamic somatostatin mRNA through nitric oxide release. *Regul. Pept.* 124, 113–118. doi: 10.1016/j.regpep.2004.07.001
- Reichmann, F., and Holzer, P. (2016). Neuropeptide Y: a stressful review. *Neuropeptides* 55, 99–109. doi: 10.1016/j.nep.2015.09.008
- Reyes, T. M., Lewis, K., Perrin, M. H., Kunitake, K. S., Vaughan, J., Arias, C. A., et al. (2001). Urocortin II: a member of the corticotropin-releasing factor (CRF) neuropeptide family that is selectively bound by type 2 CRF receptors. *Proc. Natl. Acad. Sci. U.S.A.* 98, 2843–2848. doi: 10.1073/pnas.051626398
- Richardson, U. I. (1983). ACTH secretion in mouse pituitary tumor cells in culture: inhibition of CRF-stimulated hormone release by somatostatin. *Life Sci.* 33, 1981–1988. doi: 10.1016/0024-3205(83)90736-1
- Rivier, J. E., and Rivier, C. L. (2014). Corticotropin-releasing factor peptide antagonists: design, characterization and potential clinical relevance. *Front. Neuroendocrinol.* 35, 161–170. doi: 10.1016/j.yfrne.2013.10.006
- Rocheville, M., Lange, D. C., Kumar, U., Sasi, R., Patel, R. C., and Patel, Y. C. (2000). Subtypes of the somatostatin receptor assemble as functional homo- and heterodimers. *J. Biol. Chem.* 275, 7862–7869. doi: 10.1074/jbc.275.11.7862
- Saffran, M., Schally, A. V., and Benfey, B. G. (1955). Stimulation of the release of corticotropin from the adenohypophysis by a neurohypophysial factor. *Endocrinology* 57, 439–444. doi: 10.1210/endo-57-4-439
- Scheich, B., Gaszner, B., Kormos, V., Laszlo, K., Adori, C., Borbely, E., et al. (2016). Somatostatin receptor subtype 4 activation is involved in anxiety and depression-like behavior in mouse models. *Neuropharmacology* 101, 204–215. doi: 10.1016/j.neuropharm.2015.09.021
- Schindler, M., and Humphrey, P. P. (1999). Differential distribution of somatostatin sst2 receptor splice variants in rat gastric mucosa. *Cell Tissue Res.* 297, 163–168. doi: 10.1007/s00410051344
- Schulz, S., Handel, M., Schreff, M., Schmidt, H., and Hollt, V. (2000). Localization of five somatostatin receptors in the rat central nervous system using subtype-specific antibodies. *J. Physiol. Paris* 94, 259–264. doi: 10.1016/S0928-4257(00)00212-6
- Sekino, A., Ohata, H., Mano-Otagiri, A., Arai, K., and Shibasaki, T. (2004). Both corticotropin-releasing factor receptor type 1 and type 2 are involved in stress-induced inhibition of food intake in rats. *Psychopharmacology (Berl)* 176, 30–38. doi: 10.1007/s00213-004-1863-1
- Shibasaki, T., Kim, Y. S., Yamauchi, N., Masuda, A., Imaki, T., Hotta, M., et al. (1988a). Antagonistic effect of somatostatin on corticotropin-releasing factor-induced anorexia in the rat. *Life Sci.* 42, 329–334. doi: 10.1016/0024-3205(88)90642-X
- Shibasaki, T., Yamauchi, N., Kato, Y., Masuda, A., Imaki, T., Hotta, M., et al. (1988b). Involvement of corticotropin-releasing factor in restraint stress-induced anorexia and reversion of the anorexia by somatostatin in the rat. *Life Sci.* 43, 1103–1110. doi: 10.1016/0024-3205(88)90468-7
- Smith, S. M., and Vale, W. W. (2006). The role of the hypothalamic-pituitary-adrenal axis in neuroendocrine responses to stress. *Dialogues Clin. Neurosci.* 8, 383–395.
- Somiya, H., and Tonoue, T. (1984). Neuropeptides as central integrators of autonomic nerve activity: effects of TRH, SRIF, VIP and bombesin on gastric and adrenal nerves. *Regul. Pept.* 9, 47–52. doi: 10.1016/0167-0115(84)90006-5
- Spary, E. J., Maqbool, A., and Batten, T. F. (2008). Expression and localisation of somatostatin receptor subtypes sst1-sst5 in areas of the rat medulla oblongata involved in autonomic regulation. *J. Chem. Neuroanat.* 35, 49–66. doi: 10.1016/j.jchemneu.2007.06.002
- Steiger, A. (2007). Neurochemical regulation of sleep. *J. Psychiatr. Res.* 41, 537–552. doi: 10.1016/j.jpsychires.2006.04.007
- Stengel, A., Coskun, T., Goebel, M., Wang, L., Craft, L., Alsina-Fernandez, J., et al. (2010). Central injection of the stable somatostatin analog ODT8-SST induces a somatostatin2 receptor-mediated orexigenic effect: role of neuropeptide Y and opioid signaling pathways in rats. *Endocrinology* 151, 4224–4235. doi: 10.1210/en.2010-0195
- Stengel, A., Goebel-Stengel, M., Wang, L., Larauche, M., Rivier, J., and Taché, Y. (2011a). Central somatostatin receptor 1 activation reverses acute stress-related alterations of gastric and colonic motor function in mice. *Neurogastroenterol. Motil.* 23, e223–e236. doi: 10.1111/j.1365-2982.2011.01706.x
- Stengel, A., Goebel-Stengel, M., Wang, L., Luckey, A., Hu, E., Rivier, J., et al. (2011b). Central administration of pan-somatostatin agonist ODT8-SST prevents abdominal surgery-induced inhibition of circulating ghrelin, food intake and gastric emptying in rats. *Neurogastroenterol. Motil.* 23, e294–e308. doi: 10.1111/j.1365-2982.2011.01721.x
- Stengel, A., Karasawa, H., and Taché, Y. (2015). The role of brain somatostatin receptor 2 in the regulation of feeding and drinking behavior. *Horm. Behav.* 73, 15–22. doi: 10.1016/j.yhbeh.2015.05.009
- Stengel, A., and Taché, Y. (2009). Neuroendocrine control of the gut during stress: corticotropin-releasing factor signaling pathways in the spotlight. *Annu. Rev. Physiol.* 71, 219–239. doi: 10.1146/annurev.physiol.010908.163221
- Stengel, A., and Taché, Y. (2014a). Brain peptides and the modulation of postoperative gastric ileus. *Curr. Opin. Pharmacol.* 19, 31–37. doi: 10.1016/j.coph.2014.06.006
- Stengel, A., and Taché, Y. (2014b). CRF and urocortin peptides as modulators of energy balance and feeding behavior during stress. *Front. Neurosci.* 8:52. doi: 10.3389/fnins.2014.00052
- Strowski, M. Z., Dashkevitz, M. P., Parmar, R. M., Wilkinson, H., Kohler, M., Schaeffer, J. M., et al. (2002). Somatostatin receptor subtypes 2 and 5 inhibit corticotropin-releasing hormone-stimulated adrenocorticotropin secretion from AtT-20 cells. *Neuroendocrinology* 75, 339–346. doi: 10.1159/000059430
- Suda, T., Kageyama, K., Sakihara, S., and Nigawara, T. (2004). Physiological roles of urocortins, human homologues of fish urotensin I, and their receptors. *Peptides* 25, 1689–1701. doi: 10.1016/j.peptides.2004.03.027
- Taché, Y. (2015). Corticotrophin-releasing factor 1 activation in the central amygdala and visceral hyperalgesia. *Neurogastroenterol. Motil.* 27, 1–6. doi: 10.1111/nmo.12495
- Taché, Y., and Bonaz, B. (2007). Corticotropin-releasing factor receptors and stress-related alterations of gut motor function. *J. Clin. Invest.* 117, 33–40. doi: 10.1172/JCI30085
- Taché, Y., Maeda-Hagiwara, M., and Turkelson, C. M. (1987). Central nervous system action of corticotropin-releasing factor to inhibit gastric emptying in rats. *Am. J. Physiol.* 253, G241–G245.

- Taché, Y., and Million, M. (2015). Role of corticotropin-releasing factor signaling in stress-related alterations of colonic motility and hyperalgesia. *J. Neurogastroenterol. Motil.* 21, 8–24. doi: 10.5056/jnm14162
- Theodoropoulou, M., and Stalla, G. K. (2013). Somatostatin receptors: from signaling to clinical practice. *Front. Neuroendocrinol.* 34, 228–252. doi: 10.1016/j.yfrne.2013.07.005
- Thoss, V. S., Perez, J., Duc, D., and Hoyer, D. (1995). Embryonic and postnatal mRNA distribution of five somatostatin receptor subtypes in the rat brain. *Neuropharmacology* 34, 1673–1688. doi: 10.1016/0028-3908(95)00135-2
- Tizabi, Y., and Calogero, A. E. (1992). Effect of various neurotransmitters and neuropeptides on the release of corticotropin-releasing hormone from the rat cortex *in vitro*. *Synapse* 10, 341–348. doi: 10.1002/syn.890100409
- Tringali, G., Greco, M. C., Lisi, L., Pozzoli, G., and Navarra, P. (2012). Cortistatin modulates the expression and release of corticotrophin releasing hormone in rat brain. Comparison with somatostatin and octreotide. *Peptides* 34, 353–359. doi: 10.1016/j.peptides.2012.02.004
- Turnbull, A. V., and Rivier, C. (1997). Corticotropin-releasing factor (CRF) and endocrine responses to stress: CRF receptors, binding protein, and related peptides. *Proc. Soc. Exp. Biol. Med.* 215, 1–10. doi: 10.3181/00379727-215-44108
- Vale, W., Spiess, J., Rivier, C., and Rivier, J. (1981). Characterization of a 41-residue ovine hypothalamic peptide that stimulates secretion of corticotropin and beta-endorphin. *Science* 213, 1394–1397. doi: 10.1126/science.6267699
- Van Pett, K., Viau, V., Bittencourt, J. C., Chan, R. K., Li, H. Y., Arias, C., et al. (2000). Distribution of mRNAs encoding CRF receptors in brain and pituitary of rat and mouse. *J. Comp. Neurol.* 428, 191–212.
- Vaughan, J., Donaldson, C., Bittencourt, J., Perrin, M. H., Lewis, K., Sutton, S., et al. (1995). Urocortin, a mammalian neuropeptide related to fish urotensin I and to corticotropin-releasing factor. *Nature* 378, 287–292. doi: 10.1038/378287a0
- Vecsei, L., and Widerlov, E. (1988). Effects of intracerebroventricularly administered somatostatin on passive avoidance, shuttle-box behaviour and open-field activity in rats. *Neuropeptides* 12, 237–242. doi: 10.1016/0143-4179(88)90061-3
- Venihaki, M., Sakihara, S., Subramanian, S., Dikkes, P., Weninger, S. C., Liapakis, G., et al. (2004). Urocortin III, a brain neuropeptide of the corticotropin-releasing hormone family: modulation by stress and attenuation of some anxiety-like behaviours. *J. Neuroendocrinol.* 16, 411–422. doi: 10.1111/j.1365-2826.2004.01170.x
- Videau, C., Hochgeschwender, U., Kreienkamp, H. J., Brennan, M. B., Viollet, C., Richter, D., et al. (2003). Characterisation of [125I]-Tyr0DTrp8-somatostatin binding in sst1- to sst4- and SRIF-gene invalidated mouse brain. *Naunyn Schmiedebergs Arch. Pharmacol.* 367, 562–571. doi: 10.1007/s00210-003-0758-8
- Viollet, C., Lepousez, G., Loudes, C., Videau, C., Bluet-Pajot, M. T., Ungerer, A., L'heritier, A., et al. (2000). Involvement of sst2 somatostatin receptor in locomotor, exploratory activity and emotional reactivity in mice. *Eur. J. Neurosci.* 12, 3761–3770. doi: 10.1046/j.1460-9568.2000.00249.x
- Wan, Q., Gao, K., Rong, H., Wu, M., Wang, H., Wang, X., et al. (2014). Histone modifications of the Crhr1 gene in a rat model of depression following chronic stress. *Behav. Brain Res.* 271, 1–6. doi: 10.1016/j.bbr.2014.05.031
- Wang, L., Goebel-Stengel, M., Stengel, A., Wu, S. V., Ohning, G., and Taché, Y. (2011). Comparison of CRF-immunoreactive neurons distribution in mouse and rat brains and selective induction of Fos in rat hypothalamic CRF neurons by abdominal surgery. *Brain Res.* 1415, 34–46. doi: 10.1016/j.brainres.2011.07.024
- Wu, S. V., Yuan, P. Q., Lai, J., Wong, K., Chen, M. C., Ohning, G. V., et al. (2011). Activation of Type 1 CRH receptor isoforms induces serotonin release from human carcinoid BON-1N cells: an enterochromaffin cell model. *Endocrinology* 152, 126–137. doi: 10.1210/en.2010-0997
- Wu, S. V., Yuan, P. Q., Wang, L., Peng, Y. L., Chen, C. Y., and Taché, Y. (2007). Identification and characterization of multiple corticotropin-releasing factor type 2 receptor isoforms in the rat esophagus. *Endocrinology* 148, 1675–1687. doi: 10.1210/en.2006-0565
- Xu, M., Chung, S., Zhang, S., Zhong, P., Ma, C., Chang, W. C., et al. (2015). Basal forebrain circuit for sleep-wake control. *Nat. Neurosci.* 18, 1641–1647. doi: 10.1038/nn.4143
- Yang, L. Z., Tovote, P., Rayner, M., Kockskamper, J., Pieske, B., and Spiess, J. (2010). Corticotropin-releasing factor receptors and urocortins, links between the brain and the heart. *Eur. J. Pharmacol.* 632, 1–6. doi: 10.1016/j.ejphar.2010.01.027
- Yuan, P. Q., Wu, S. V., Pothoulakis, C., and Taché, Y. (2016). Urocortins and CRF receptor type 2 variants in the male rat colon: gene expression and regulation by endotoxin and anti-inflammatory effect. *Am. J. Physiol. Gastrointest. Liver Physiol.* 310, G387–G398. doi: 10.1152/ajpgi.00337.2015
- Yuan, P. Q., Wu, S. V., and Taché, Y. (2012). Urocortins and CRF type 2 receptor isoforms expression in the rat stomach are regulated by endotoxin: role in the modulation of delayed gastric emptying. *Am. J. Physiol. Gastrointest. Liver Physiol.* 303, G20–G31. doi: 10.1152/ajpgi.00547.2011
- Zheng, J., Babygirija, R., Bulbul, M., Cerjak, D., Ludwig, K., and Takahashi, T. (2010). Hypothalamic oxytocin mediates adaptation mechanism against chronic stress in rats. *Am. J. Physiol. Gastrointest. Liver Physiol.* 299, G946–G953. doi: 10.1152/ajpgi.00483.2009
- Zmijewski, M. A., and Slominski, A. T. (2010). Emerging role of alternative splicing of CRF1 receptor in CRF signaling. *Acta Biochim. Pol.* 57, 1–13.

Conflict of Interest Statement: The authors declare that the research was conducted in the absence of any commercial or financial relationships that could be construed as a potential conflict of interest.

Copyright © 2017 Stengel and Taché. This is an open-access article distributed under the terms of the Creative Commons Attribution License (CC BY). The use, distribution or reproduction in other forums is permitted, provided the original author(s) or licensor are credited and that the original publication in this journal is cited, in accordance with accepted academic practice. No use, distribution or reproduction is permitted which does not comply with these terms.



Role of Transient Receptor Potential Ankyrin 1 Ion Channel and Somatostatin sst4 Receptor in the Antinociceptive and Anti-inflammatory Effects of Sodium Polysulfide and Dimethyl Trisulfide

István Z. Báta¹, Ádám Horváth², Erika Pintér², Zsuzsanna Helyes² and Gábor Pozsgai^{1*}

Department of Pharmacology and Pharmacotherapy, Medical School, University of Pécs, Pécs, Hungary

OPEN ACCESS

Edited by:

Hubert Vaudry,
Université de Rouen, France

Reviewed by:

Nils Lambrecht,
University of California, Irvine,
United States

Gábor B. Makara,
Hungarian Academy of Sciences
(MTA), Hungary

*Correspondence:

Gábor Pozsgai
gabor.pozsgai@aok.pte.hu

Specialty section:

This article was submitted to
Neuroendocrine Science,
a section of the journal
Frontiers in Endocrinology

Received: 31 October 2017

Accepted: 06 February 2018

Published: 27 February 2018

Citation:

Báta IZ, Horváth Á, Pintér E,
Helyes Z and Pozsgai G (2018)

Role of Transient Receptor
Potential Ankyrin 1 Ion Channel
and Somatostatin sst4 Receptor
in the Antinociceptive and
Anti-inflammatory Effects of Sodium
Polysulfide and Dimethyl Trisulfide.

Front. Endocrinol. 9:55.
doi: 10.3389/fendo.2018.00055

Transient receptor potential ankyrin 1 (TRPA1) non-selective ligand-gated cation channels are mostly expressed in primary sensory neurons. Polysulfides (POLYs) are Janus-faced substances interacting with numerous target proteins and associated with both protective and detrimental processes. Activation of TRPA1 in sensory neurons, consequent somatostatin (SOM) liberation and action on sst4 receptors have recently emerged as mediators of the antinociceptive effect of organic trisulfide dimethyl trisulfide (DMTS). In the frame of the present study, we set out to compare the participation of this mechanism in antinociceptive and anti-inflammatory effects of inorganic sodium POLY and DMTS in carrageenan-evoked hind-paw inflammation. Inflammation of murine hind paws was induced by intraplantar injection of carrageenan (3% in 30 µL saline). Animals were treated intraperitoneally with POLY (17 µmol/kg) or DMTS (250 µmol/kg) or their respective vehicles 30 min prior paw challenge and six times afterward every 60 min. Mechanical pain threshold and swelling of the paws were measured by dynamic plantar aesthesiometry and plethysmometry at 2, 4, and 6 h after initiation of inflammation. Myeloperoxidase (MPO) activity in the hind paws were detected 6 h after challenge by luminescent imaging. Mice genetically lacking TRPA1 ion channels, sst4 receptors and their wild-type counterparts were used to examine the participation of these proteins in POLY and DMTS effects. POLY counteracted carrageenan-evoked mechanical hyperalgesia in a TRPA1 and sst4 receptor-dependent manner. POLY did not influence paw swelling and MPO activity. DMTS ameliorated all examined inflammatory parameters. Mitigation of mechanical hyperalgesia and paw swelling by DMTS were mediated through sst4 receptors. These effects were present in TRPA1 knockout animals, too. DMTS inhibited MPO activity with no participation of the sensory neuron–SOM axis. While antinociceptive effects of POLY are transmitted by activation of peptidergic nerves via TRPA1, release of SOM and its effect on sst4 receptors, those of DMTS partially rely on SOM release triggered by other routes. SOM is responsible for the inhibition of paw swelling by DMTS, but TRPA1 does not contribute to its release. Modulation of MPO activity by DMTS is independent of TRPA1 and sst4.

Keywords: transient receptor potential ankyrin 1, sst4, somatostatin, dimethyl trisulfide, polysulfide, carrageenan, luminol, IR-676

INTRODUCTION

Inorganic polysulfides (POLYs; hydrogen polysulfide) have been demonstrated to be synthesized in the human body (1). These species possess antioxidant and radical scavenging properties. Beside *in vitro* systems, these findings were confirmed in lung tissue from patients suffering from chronic obstructive pulmonary disease too (2–5). According to some opinions inorganic POLYs might mediate persulfidation of cysteine residues of proteins, a process traditionally attributed to hydrogen sulfide (H_2S) (6). Dimethyl trisulfide (DMTS) is an organic trisulfide compound naturally occurring in garlic. It is used widely as a food additive (7). Recently, DMTS has been patented in the US as a parenteral antidote of cyanide poisoning (8). This adds vastly to the translation potential of the drug. We have reported lately antinociceptive properties of DMTS against mechanical hyperalgesia evoked by heat injury in mice. Transient receptor potential ankyrin 1 (TRPA1) ion channels and somatostatin (SOM) sst₄ receptors contribute pivotally to these effects (9). Chemically, alkyl trisulfides (such as DMTS) produce tri/disulfide metabolites with the thiol groups of cysteine amino acids (unlike inorganic POLYs leading to protein persulfidation). Others propose organic trisulfides to be sources of hydrogen sulfide (H_2S) (10). Based on the latest findings, H_2S in concert with nitric oxide reacts with thiol residues of proteins (11, 12). H_2S released from organic trisulfides might influence protein-associated metal atoms too (13). Organic trisulfides were reported to exert antioxidant and anti-inflammatory effects mostly studied in animal models of inflammatory bowel disease (14–16). Inorganic POLYs are known to interact with functional cysteines of the TRPA1 ion channel (17). As mentioned above our previous work suggests that one of the targets of DMTS is the ion channel TRPA1 as well (9).

Transient receptor potential ankyrin 1 is a non-selective cation channel permeable to Ca^{2+} and Na^+ . TRPA1 is a member of transient receptor potential ankyrin subfamily of ion channels, itself being a subdivision of the transient receptor potential family. TRPA1 is the only ankyrin-type TRP channel to be found in mammals. Polymodal TRPA1 channels might be opened by chemical substances, temperature, mechanical stimuli, potential difference, or changes of pH. Electrophilic agents—most probably including organic trisulfide compounds—excite TRPA1 by forming covalent bonds with cysteine residues (18). TRPA1 is mostly expressed in primary nociceptor neurons, but it was evinced in the cornea, skin, pancreas, spleen, lung, kidney, testis, and the human endometrium (19). Expression of TRPA1 channels in polymorphonuclear granulocytes of patients suffering from chronic inflammatory disease was shown to correlate with nociception (20). The role of TRPA1 is known in complete Freund's adjuvant-induced inflammation. However, no involvement was detected in carrageenan-evoked paw inflammation (21, 22). TRPA1 channels are typically expressed by sensory neurons containing neuropeptides (e.g., SOM). Activation of the channel leads to Ca^{2+} influx into the nerve endings and release of peptides. Earlier we found SOM liberation from murine sensory neurons upon stimulation with DMTS (9).

Somatostatin is a cyclic peptide with important endocrine function besides its presence in the sensory nervous system

(23). SOM is expressed in 17.8% of human dorsal root ganglion neurons. The peptide might be liberated by TRPA1 agonists (24). Unlike most neuropeptides, SOM is distributed by the bloodstream and exerts antinociceptive and anti-inflammatory effects distant from the release site in numerous animal models of inflammatory disease (25). These could be ameliorated by depletion of peptides from sensory nerves, administration of anti-SOM antibody or SOM receptor antagonist (24). According to previous data, these effects are mediated by one of five SOM receptors: sst₄ (9, 26–29). Antinociceptive and anti-inflammatory effects could be mimicked by two different agonists (TT-232, J-2156) of sst₄ receptors. The agonists were ineffective in animals lacking the corresponding functional receptor (24, 30). Sst₄ is present in sensory neurons, lymphocytes, and vascular endothelial cells enabling the transmission of the aforementioned beneficial effects of SOM (25).

In the present study, we set out to investigate the effect of inorganic sodium POLY and DMTS on the sensory-SOM-sst₄ system in carrageenan-induced hind paw inflammation in genetically engineered mice lacking either functional TRPA1 or sst₄. Both mechanical nociception and inflammatory parameters, such as paw swelling and myeloperoxidase (MPO) activity of accumulated neutrophil granulocytes, were assessed.

MATERIALS AND METHODS

Animals

Experiments were conducted on genetically modified male mice lacking functional TRPA1 or sst₄ receptors (KO) and their wild-type counterparts (WT; 2–4 months, 20–25 g) (27, 31). Age-matched animals were used in the study. The original heterozygous TRPA1 breeding pair was a generous gift from Pierangelo Geppetti (University of Florence, Italy). These mice were originally generated and characterized by Bautista and colleagues (31). Neither the strain with genetic modification of TRPA1 nor that with modified sst₄ gene is available commercially. TRPA1 and sst₄ WT and KO breeding lines were produced by crossing respective heterozygote animals. WT and KO animals were chosen from the resulting litter and used for further breeding (i.e., WT mice were mated with WT ones and KO mice with KO ones). For the fifth-generation clean WT and KO breeding lines were established and maintained by inbreeding. All animals were genotyped until generation 5 and random sentinel litters of the WT and KO lines afterward. Due to poor breeding performance of the sst₄ colony, heterozygotes were used in the breeding even after the fifth generation and all offspring were genotyped for an extended period of time. Animals were bred and kept in the Laboratory Animal Centre of University of Pécs under standard pathogen free conditions at 24–25°C, 12 h light/dark cycles. Mice were housed in groups of 5–10 in polycarbonate cages (330 cm² floor space, 12 cm height) on wood shavings bedding. Animals were provided standard diet and water *ad libitum*. All experimental procedures were carried out according to the European Communities Council Directive of 2010/63/EU. The studies were approved by the Ethics Committee on Animal Research, University of Pécs (license number: BA02/2000-47/2017).

Carrageenan-Induced Hind Paw Inflammation

Inflammation of one hind paw was triggered by intraplantar injection of carrageenan ($20 \mu\text{L}$, 3% in saline). The contralateral paw received saline. The side of carrageenan injection was randomized. Animals were treated with either POLY ($17 \mu\text{mol/kg}$, i.p.) or DMTS ($250 \mu\text{mol/kg}$, i.p.) or the respective vehicle 30 min before challenge of the paws and every 60 min afterward (seven times altogether). POLY was prepared freshly before each application. DMTS was prepared daily.

Preparation of POLY and DMTS Solutions

Polysulfide was prepared as described earlier (32). Stock solutions of hypochlorous acid and sodium sulfide nonahydrate were prepared in distilled water using polypropylene tubes blown with nitrogen gas beforehand. All later dilutions and reactions were performed in similar tubes. Reagents were kept on ice. Concentration of hypochlorous acid was calculated from the light extinction of the solution at 292 nm wavelength ($E_{292} = 350 \text{ M}^{-1}\text{cm}^{-1}$). Concentration of sulfide was derived from the extinction at 230 nm ($E_{230} = 7700 \text{ M}^{-1}\text{cm}^{-1}$) and the reaction with 5,5'-dithiobis(2-nitrobenzoic acid) (DTNB). Extinction of the reaction product of sulfide and DTNB was measured at 412 nm ($E_{412} = 28,200 \text{ M}^{-1}\text{cm}^{-1}$). Sulfide concentration was calculated as the mean of the two values yielded by direct spectrophotometry and reaction with DTNB. Stock solutions of hypochlorous acid and sulfide were prepared daily. Sulfide stock solution was diluted further in distilled water to 60 mM . Hypochlorous acid solution was added slowly under stirring to produce 20 mM in the final volume. The reaction of sulfide and hypochlorous acid produces POLY. This POLY solution was diluted to twofold in distilled water containing 4.17% v/v $10\times$ concentrated phosphate-buffered saline (PBS, pH 7.4). This amount of PBS renders the POLY solution isosmotic. Concentrated hydrochloric acid was then added by $5 \mu\text{L}$ under stirring to set the pH to 7.4 (app. $25\text{--}30 \mu\text{L}$, as required). Concentration of the resulting POLY solution was measured by cold cyanolysis, as described earlier (33). Shortly, the isosmotic and isohydric POLY solution was alkalinized by the addition of NH_4OH and reacted with KCN. After 25 min incubation at room temperature formaldehyde and Goldstein reagent (FeCl_3 dissolved in 18.38% HNO_3) were added. Absorbance of the formed orange product was detected after 15 min reaction time at room temperature at 460 nm . POLY concentration was calculated using a standard curve constructed with KSCN. The buffered solution was found to contain 3.3 mM POLY, yielding a dose of $17 \mu\text{mol/kg}$ at 5 mL/kg . Isosmotic and isohydric POLY solution was injected into the mice immediately after production. PBS was used as vehicle control.

A DMTS solution of 1 M was prepared in dimethyl sulfoxide (DMSO). This solution was diluted to 100 mM in saline containing 2% v/v polysorbate 80. After slow dissolution, a further dilution commenced in saline to 25 mM . The 25 mM solution was injected at 10 mL/kg i.p. resulting in a dose of $250 \mu\text{mol/kg}$. In vehicle, DMSO was applied instead of 1 M DMTS solution. Final DMTS solutions contained 2.24% v/v DMSO and 0.45% v/v polysorbate 80. Vehicle had 2.5% v/v DMSO.

Measurement of Mechanical Pain Threshold of the Hind Paws

Mechanical hyperalgesia evoked by carrageenan was assessed by dynamic plantar aesthesiometry (DPA, Hugo Basile, Italy) 2, 4, and 6 h after the initiation of inflammation. Baseline values were taken on three separate days before paw challenge. Stimulator of the instrument reached 10 g "force" in 4 s.

Detection of Paw Swelling by Plethysmometry

Swelling of inflamed and control hind paws was measured by plethysmometry (Hugo Basile, Italy). These measurements were performed following DPA experiments to prevent stressing the animals before aesthesiometry. Control measurements were conducted right after control DPA experiments on three separate days preceding paw challenge. Paw volumes were measured in cm^3 .

Detection of MPO Activity in the Hind Paws by Luminescent Imaging

Animals were anesthetized with ketamine and xylazine (120 and 12 mg/kg) 6 h after hind paw challenge. Mice were injected i.p. with sodium luminol (5-amino-2,3-dihydro-1,4-phthalazine-dione; 150 mg/kg) dissolved in sterile PBS. Luminol signals reactive oxygen species correlated with MPO activity of neutrophil granulocytes via luminescence (34). Bioluminescence of luminol was captured 10 min after administration. Measurements were conducted in an IVIS Lumina II (PerkinElmer, Waltham, USA; 120 s acquisition, F/stop = 1, Binning = 8) instrument and Living Image® software (Perkin-Elmer, Waltham, USA). Identical regions of interest (ROIs) were applied to both hind paws and calibrated units of luminescence (total radiance = total photon flux/s) originating from the ROIs were detected (35).

Chemicals

All chemicals were purchased from Sigma Aldrich, Hungary unless otherwise stated. DMSO was from Reanal, Hungary. Ketamine was from Richter Gedeon, Hungary. Xylazine was from Eurovet Animal Health BV, Netherlands.

Statistics

Data are presented as mean \pm SEM. Two-way repeated-measure ANOVA followed by Bonferroni's test was used for mechanonociceptive threshold and paw volume data. Some data on mechanonociceptive threshold were analyzed by plain one-way ANOVA followed by Tukey's test. Results on MPO activity were analyzed by plain one-way ANOVA and Bonferroni's test. Statistical analysis was performed by GraphPad Prism 5 software.

RESULTS

Inhibition of Carrageenan-Evoked Mechanical Pain by POLY Is TRPA1 and *sst₄* Receptor-Dependent

Carrageenan-injected paws of TRPA1 WT and KO mice undergoing vehicle administration developed significantly lowered mechanical pain threshold compared to saline-treated ones

($n = 6-7$; **Figures 1A,B**). POLY significantly reduced mechanical hyperalgesia in carrageenan-injected feet of TRPA1 WT animals in comparison with those of vehicle-treated ones (4.89 ± 0.36 vs. 6.22 ± 0.81 g at 4 h after challenge; $n = 6-7$; **Figure 1A**). Inhibitory effect of POLY on mechanical nociception in carrageenan-treated hind paws was lacking in TRPA1 KO animals compared to WT ones (7.12 ± 0.6 vs. 5.16 ± 0.44 g, 6.22 ± 0.81 vs. 4.64 ± 0.4 g, 5.97 ± 0.37 vs. 4.46 vs. 0.26 g at 2, 4 and 6 h after challenge; $n = 6-7$; **Figure 1B**). POLY had no effect on the mechanical pain thresholds of saline-injected feet of TRPA1 WT and KO animals (**Figures 1A,B**).

Similar to the above, both sst4 receptor WT and KO animals treated with the vehicle of POLY responded with reduced mechanical pain threshold to carrageenan administration ($n = 6-8$; **Figures 1C,D**). POLY significantly relieved mechanical nociception 6 h after challenge in carrageenan-injected feet of sst4 WT animals compared to those of vehicle-treated ones (3.85 ± 0.27 vs. 5.35 ± 0.45 g at 6 h after challenge; $n = 7-8$; **Figure 1C**). No effect of POLY was observed in sst4 KO mice. POLY did not affect mechanical pain thresholds of saline-treated paws of sst4 receptor WT and KO animals (**Figures 1C,D**).

No Exclusive Role of TRPA1 Ion Channel in the Protective Effect of DMTS in Carrageenan-Induced Mechanical Hyperalgesia

Carrageenan-injected hind paws of TRPA1 WT and KO animals treated with vehicle of DMTS developed mechanical

hyperalgesia compared to saline-injected contralateral paws ($n = 6-7$; **Figures 2A,B**). Carrageenan-treated hind paws of TRPA1 WT mice undergoing DMTS administration showed significantly less hyperalgesia than those administered vehicle ($n = 6-7$; **Figure 2A**). Protective effect of DMTS was reduced in carrageenan-injected feet of TRPA1 KO animals compared to those of TRPA1 WT ones ($n = 6-7$; **Figure 2B**). However, DMTS still alleviated mechanical hyperalgesia in carrageenan-treated feet of TRPA1 KO mice at 2 and 4 h after challenge in comparison with vehicle-treated animals ($n = 7$; **Figure 2B**). Saline-injected paws of DMTS and vehicle-treated TRPA1 WT and KO animals did not differ from one another (**Figures 2A,B**).

Carrageenan-injected hind paws of sst4 receptor WT and KO animals being administered vehicle of DMTS exhibited mechanical hyperalgesia compared to saline-injected control feet ($n = 7-8$; **Figures 2C,D**). Carrageenan-treated hind paws of sst4 receptor WT mice injected with DMTS developed significantly smaller hyperalgesia than those of vehicle-treated control animals ($n = 7$; **Figure 2C**). Mechanical pain threshold of saline-treated paws of DMTS and vehicle-injected sst4 receptor WT animals did not differ statistically (**Figure 1C**). DMTS did not inhibit nociception in carrageenan-treated feet of sst4 receptor KO animals compared to those of their WT counterparts (**Figure 2D**). Saline-treated feet of vehicle-injected sst4 receptor KO animals developed significantly larger mechanical pain threshold at 6 h than those of DMTS-treated ones ($n = 7-8$; **Figure 1D**).

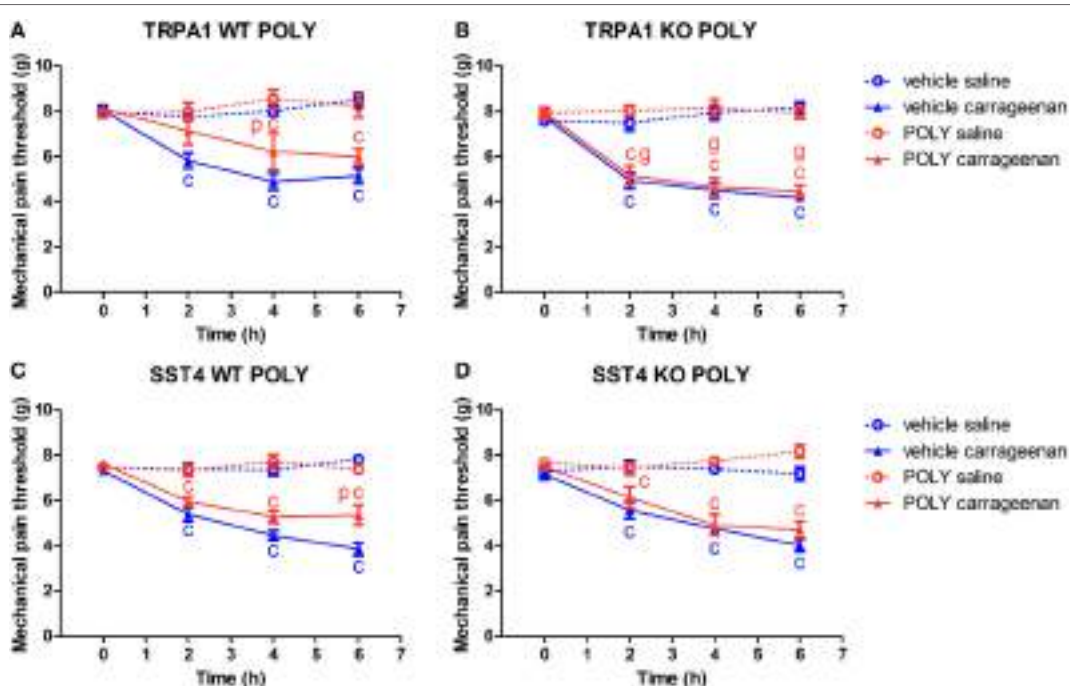


FIGURE 1 | Antinociceptive effect of sodium polysulfide (POLY, 17 $\mu\text{mol/kg}$) in carrageenan-induced paw inflammation is mediated by transient receptor potential ankyrin 1 (TRPA1) and sst4 receptors. Mechanical pain threshold of saline or carrageenan-injected (3% in 20 μL saline) hind paws of **(A)** TRPA1 WT, **(B)** TRPA1 KO, **(C)** sst4 receptor WT, and **(D)** sst4 receptor KO animals in response to POLY or vehicle treatment. Data are shown as mean \pm SEM. $n = 6-8$. $^{\circ}p < 0.05$ vs. saline-injected paws. $^{\circ}p < 0.05$ vs. vehicle of POLY. $^{\circ}p < 0.05$ vs. TRPA1 WT animals. Two-way repeated-measure ANOVA followed by Bonferroni's multiple comparison test.

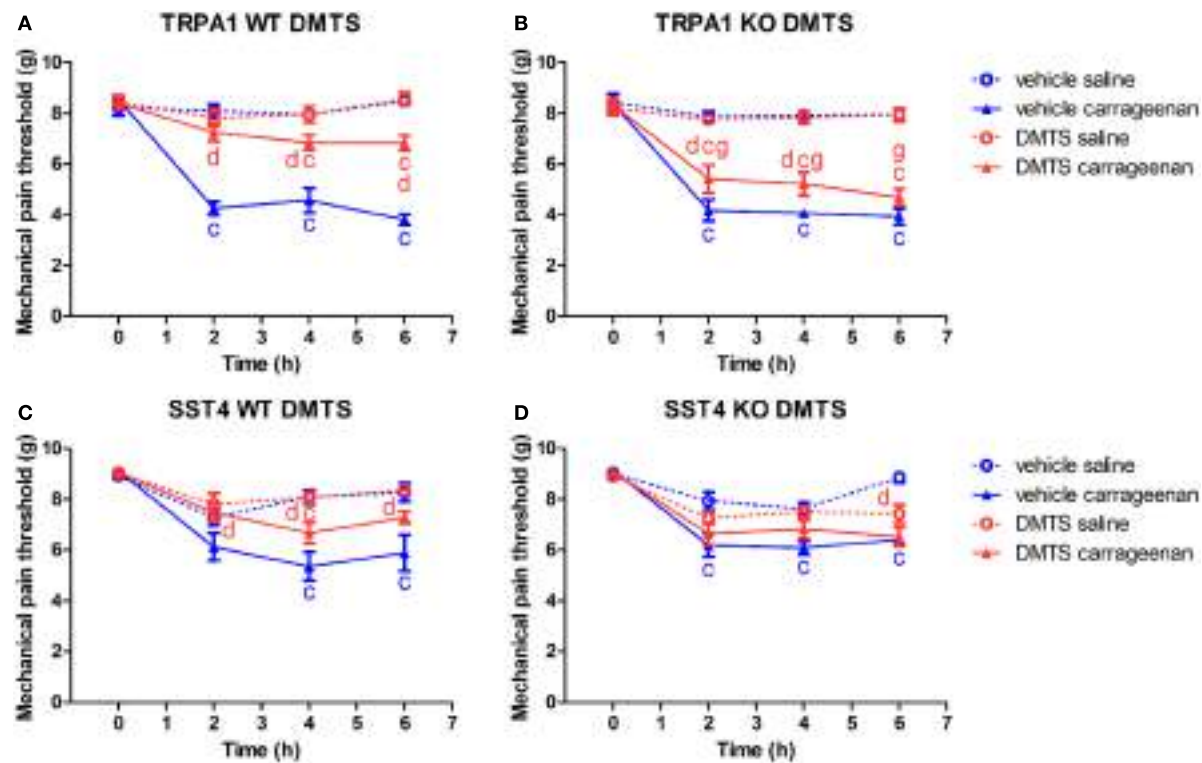


FIGURE 2 | Antinociceptive effect of dimethyl trisulfide (DMTS, 250 μ mol/kg) in carrageenan-evoked paw inflammation is independent of the transient receptor potential ankyrin 1 (TRPA1) ion channel, but is mediated by somatostatin (SOM) sst₄ receptors. Effect of DMTS or vehicle treatment on mechanical pain threshold of either saline or carrageenan-treated (3% in 20 μ L saline) hind paws of (A) TRPA1 WT, (B) TRPA1 KO, (C) sst₄ receptor WT, and (D) sst₄ receptor KO mice. Data are shown as mean \pm SEM. $n = 6\text{--}8$. $^{\circ}p < 0.05$ vs. saline-injected paws. $^{\circ}p < 0.05$ vs. vehicle of DMTS. $^{\circ}p < 0.05$ vs. TRPA1 WT animals. Two-way repeated-measure ANOVA followed by Bonferroni's multiple comparison test.

POLY Does Not Affect Paw Swelling Evoked by Carrageenan

Both vehicle and POLY-treated TRPA1 WT and KO mice exhibited significant paw swelling upon carrageenan stimulation of the hind paws. POLY had no statistically significant inhibitory effect on the swelling of the feet in TRPA1 WT or KO animals. T-values of two-way ANOVA followed by Bonferroni's test for the comparison of POLY- and vehicle-treated carrageenan-injected paws of TRPA1 KO animals are the following: 0 h, 0.04846; 2 h, 0.8061; 4 h, 1.573; and 6 h, 1.018. A trend for inhibition by POLY can be seen in carrageenan-injected feet of TRPA1 KO mice in comparison to those of vehicle-treated ones that does not reach the level of statistical significance ($n = 6\text{--}7$; Figures 3A,B). POLY or vehicle treatment did not change paw volumes of saline-injected control paws. Similar results were obtained in sst₄ receptor WT and KO mice regarding lack of statistically significant effect of POLY in either saline or carrageenan-injected paws compared to vehicle ($n = 6\text{--}8$). Volume of carrageenan-injected hind feet of sst₄ KO mice was significantly smaller at 4 and 6 h post challenge than those of WT ones ($n = 8$; Figures 3C,D).

Protective Effect of DMTS in Carrageenan-Evoked Paw Swelling Is Independent of TRPA1, but Is Mediated Through sst₄ Receptors

Transient receptor potential ankyrin 1 WT and KO mice developed significant swelling of the hind feet irrespectively of DMTS or vehicle treatment ($n = 6\text{--}7$). DMTS ameliorated swelling at 6 h in carrageenan-injected feet of TRPA1 WT mice compared to those of vehicle-treated ones ($n = 6\text{--}7$; Figure 4A). DMTS significantly relieved swelling in carrageenan-treated paws of TRPA1 KO mice at 4 and 6 h after challenge in comparison with those of vehicle-treated ones ($n = 7$; Figure 4B). DMTS produced a stronger inhibition of swelling in the carrageenan-injected feet of TRPA1 KO animals at 4 h than in those of TRPA1 WT mice ($n = 7$; Figure 4B). Edema formation in saline-injected feet of TRPA1 WT and KO mice was not affected by DMTS or vehicle treatment.

Carrageenan challenge lead to significant paw swelling in sst₄ receptor WT and KO mice irrespectively of vehicle or DMTS treatment ($n = 7\text{--}8$). DMTS relieved edema formation in carrageenan-treated paws of sst₄ WT animals at 6 h in comparison with those of vehicle-treated ones ($n = 7$; Figure 4C). DMTS did not show any protective effect in sst₄ receptor KO mice (Figure 4D).

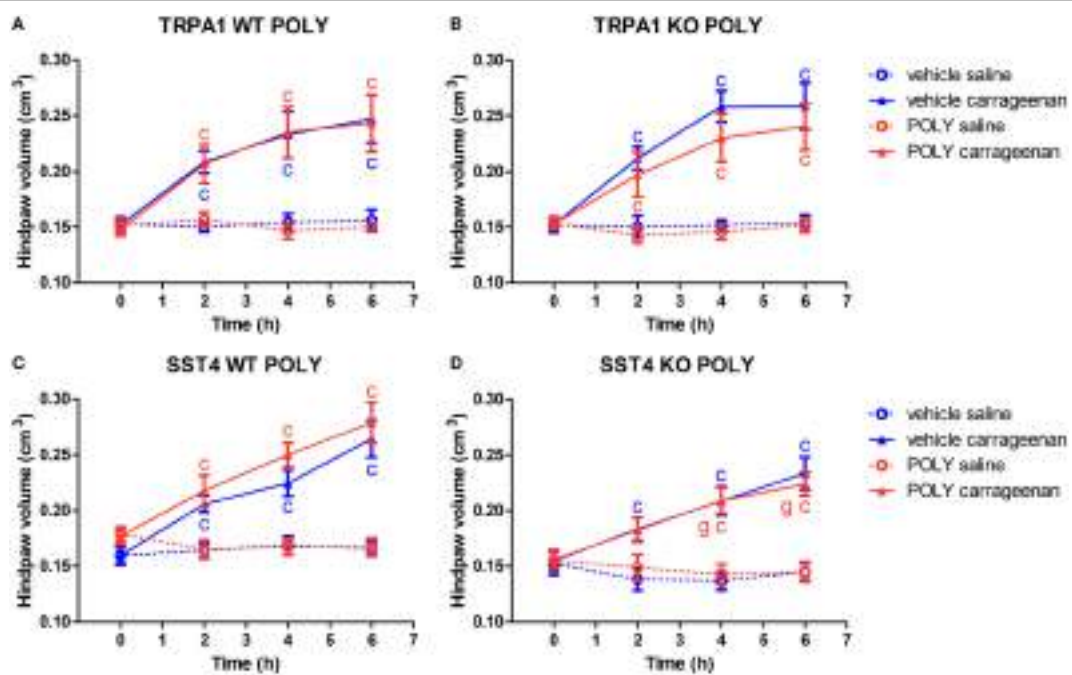


FIGURE 3 | Sodium polysulfide (POLY; 17 $\mu\text{mol/kg}$, i.p.) does not affect paw swelling detected by plethysmometry in carrageenan-induced hind paw inflammation. Effect of POLY or vehicle treatment on paw swelling of either saline or carrageenan-treated (3% in 20 μL saline) hind paws of **(A)** transient receptor potential ankyrin 1 (TRPA1) WT, **(B)** TRPA1 KO, **(C)** sst4 receptor WT, and **(D)** sst4 receptor KO mice. Data are shown as mean \pm SEM. $n = 6\text{--}8$. $^{\circ}\text{p} < 0.05$ vs. saline-injected paws. Two-way repeated-measure ANOVA followed by Bonferroni's multiple comparison test.

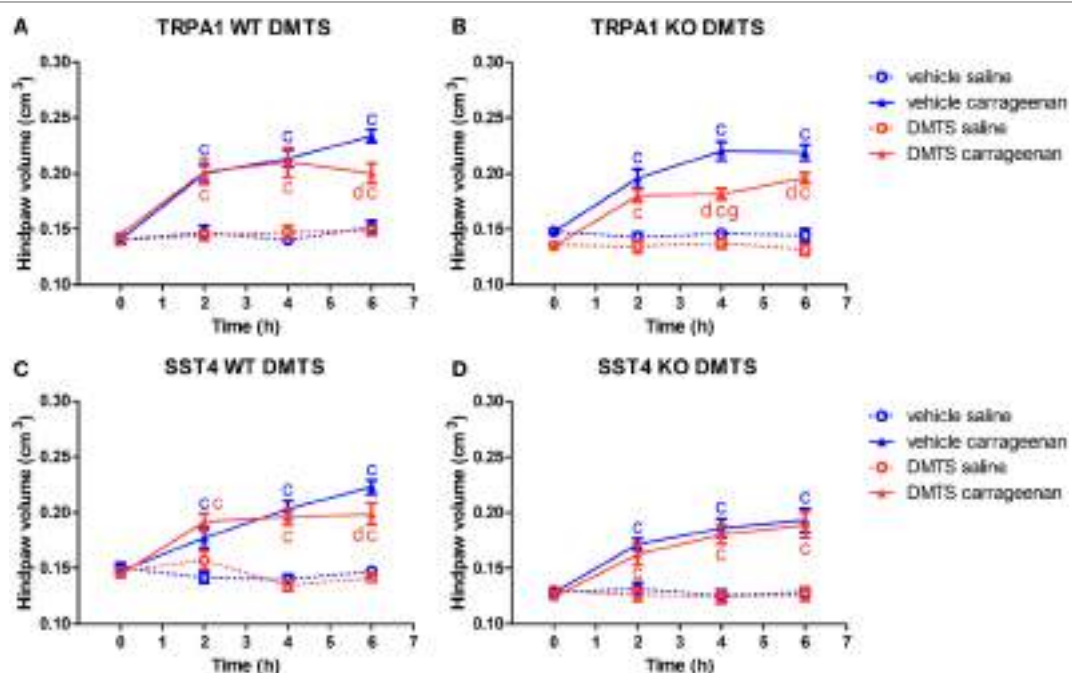


FIGURE 4 | Alleviating effect of dimethyl trisulfide (DMTS, 250 $\mu\text{mol/kg}$, i.p.) on edema formation in carrageenan-induced hind paw inflammation is independent of the transient receptor potential ankyrin 1 (TRPA1) ion channel, but is mediated by somatostatin (SOM) sst4 receptors. Effect of DMTS or vehicle treatment on hind paw edema detected by plethysmometry in saline or carrageenan-treated (3% in 20 μL saline) feet of **(A)** TRPA1 WT, **(B)** TRPA1 KO, **(C)** sst4 receptor WT, and **(D)** sst4 receptor KO mice. Data are shown as mean \pm SEM. $n = 6\text{--}8$. $^{\circ}\text{p} < 0.05$ vs. saline-injected paws. $^{\circ}\text{p} < 0.05$ vs. vehicle of DMTS. $^{\circ}\text{p} < 0.05$ vs. TRPA1 WT animals. Two-way repeated-measure ANOVA followed by Bonferroni's multiple comparison test.

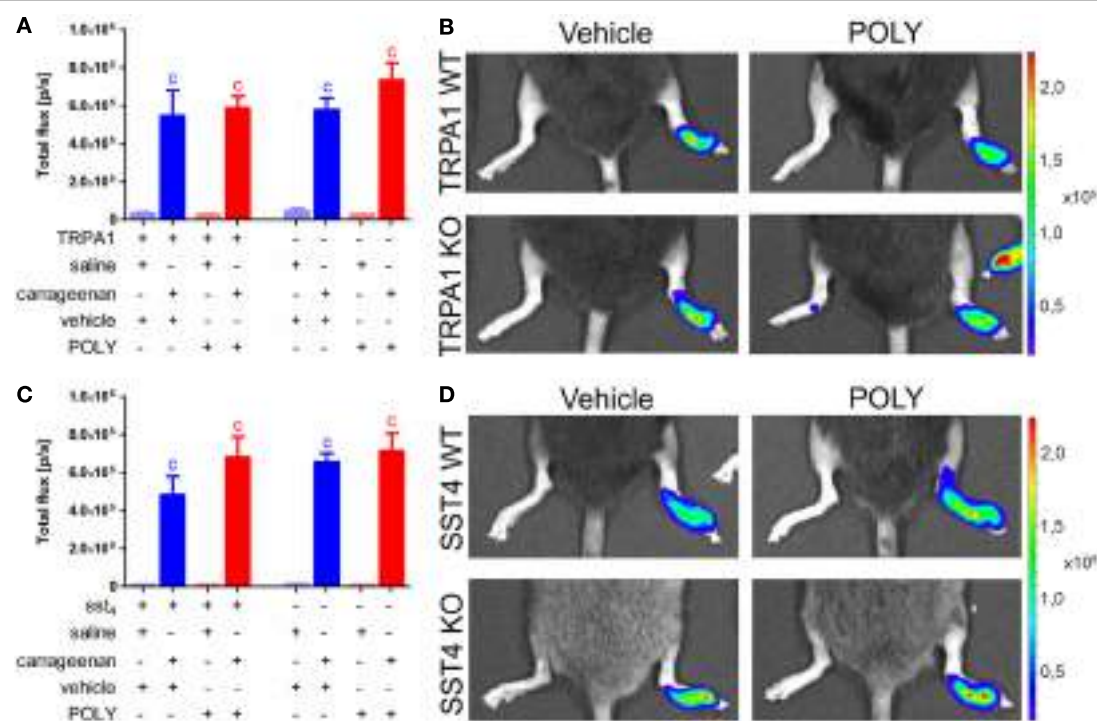


FIGURE 5 | Polysulfide (POLY) treatment (17 $\mu\text{mol/kg}$, i.p.) does not alter myeloperoxidase (MPO) activity shown by luminal bioluminescence in murine hind paws with carrageenan-induced inflammation. **(A)** Bioluminescence in saline and carrageenan-injected (3% in 20 μL saline) hind feet of transient receptor potential ankyrin 1 (TRPA1) WT and KO animals. **(B)** Representative bioluminescent images of saline and carrageenan-treated (3% in 20 μL saline) hind paws of TRPA1 WT and KO mice illustrating MPO activity. **(C)** Luminal bioluminescence in saline and carrageenan-treated (3% in 20 μL saline) hind feet of sst4 receptor WT and KO mice. **(D)** Representative bioluminescent images of saline and carrageenan-treated (3% in 20 μL saline) hind paws of sst4 WT and KO animals. Data are shown as mean \pm SEM. $n = 7-8$. $^{\circ}p < 0.05$ vs. saline-injected paws. One-way ANOVA followed by Bonferroni's multiple comparison test.

Carrageenan-Evoked MPO Activity of Accumulated Neutrophil Cells Is Unaffected by Administration of POLY

Both TRPA1 WT and KO animals developed significantly elevated MPO activity in carrageenan-injected hind paws independently from vehicle or POLY administration ($n = 7$). POLY did not ameliorate MPO activity in any animal groups nor did it affect the values of saline-injected control paws (Figures 5A,B). Similar data were produced in sst4 receptor WT and KO mice ($n = 7-8$; Figures 5C,D). Fluorescent determination of plasma extravasation following measurement of MPO activity produced no significant difference in either POLY or DMTS treated groups of any genetic background. (Datasheet 1 in Supplementary Material).

DMTS Inhibits MPO Activity of Accumulated Neutrophil Granulocytes Independently of sst4 Receptors

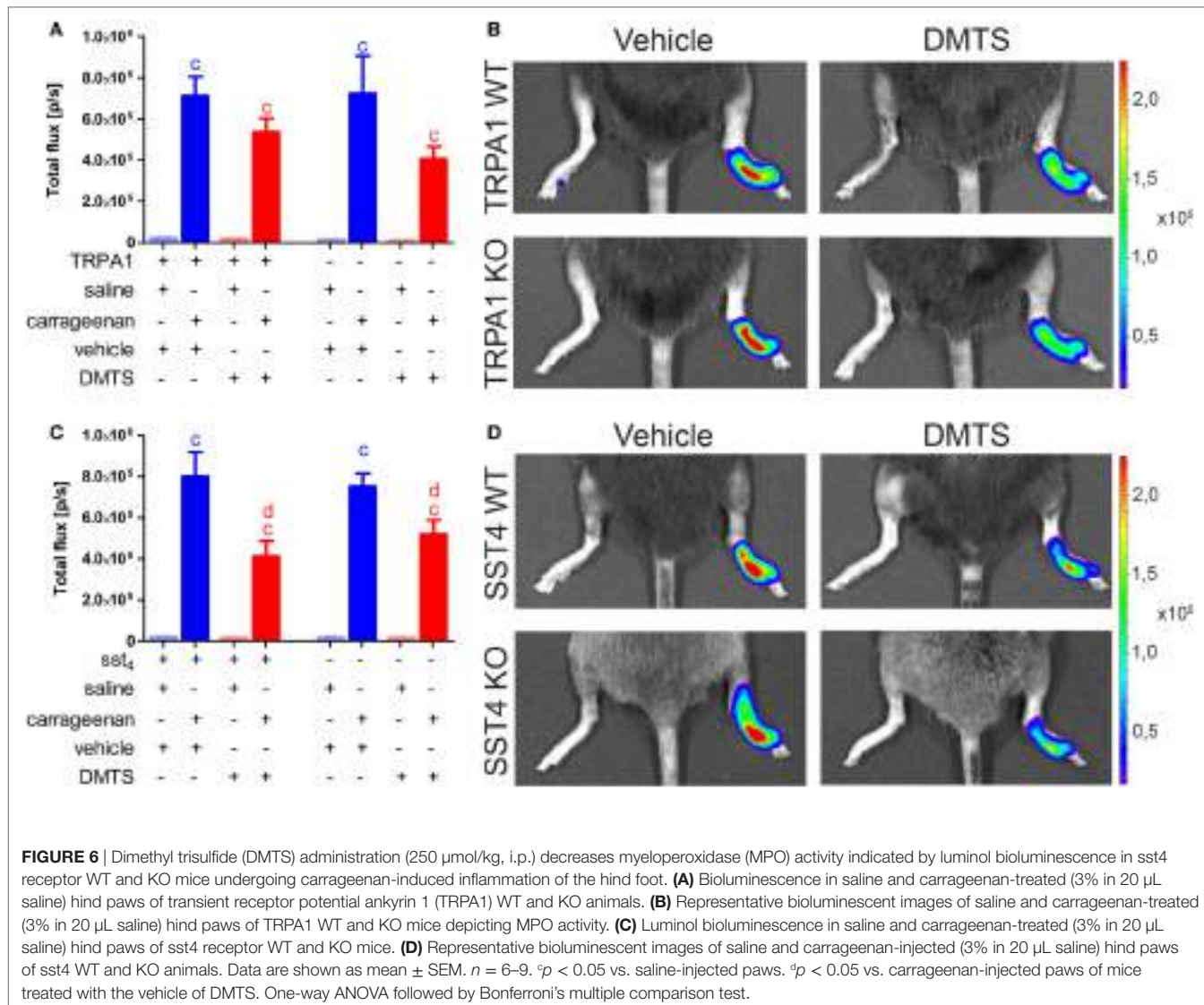
Carrageenan-injected feet of TRPA1 WT and KO animals developed significantly increased MPO activity irrespectively of vehicle or DMTS administration ($n = 6-7$). MPO activity in carrageenan-injected hind paws of DMTS-treated TRPA1 WT and KO mice tends to be smaller than in those of vehicle-treated

ones (Figures 6A,B). Sst4 WT and KO mice showed significantly elevated MPO activity upon carrageenan injection independently of vehicle or DMTS treatment ($n = 7-9$). DMTS did not alter MPO activity of saline-injected control paws. DMTS ameliorated MPO activity in carrageenan-treated feet of both sst4 WT and KO mice compared to those of vehicle-treated ones ($n = 7-9$; Figures 6C,D).

DISCUSSION

The main novel findings of the current study are the following:

- Antinociceptive effect of POLY in carrageenan-evoked paw inflammation depends on TRPA1 ion channel opening by the drug, release of SOM from the activated peptidergic sensory nerve fibers and subsequent activation of sst4 receptors, as the antihyperalgesic effect of POLY was absent in TRPA1 and sst4 KO mice.
- Organic trisulfide DMTS possessed an antinociceptive effect not only in TRPA1 and sst4 receptor WT animals, but also in TRPA1 KO ones. Protective activity was significantly weaker in TRPA1 KO mice than in WT ones. These findings imply target molecules of DMTS on sensory nerve endings other than TRPA1 leading to activation of the fibers and SOM release.



- iii. Polysulfide administration exhibited no statistically significant effect on carrageenan-induced paw edema, unlike DMTS that ameliorated swelling in TRPA1 WT, KO, and *sst4* receptor WT mice. These data point toward other mediators of DMTS effect than TRPA1 on peptidergic nociceptors.
- iv. Polysulfide had no effect on MPO activity of the inflamed hind paws. Interestingly, DMTS significantly lowered MPO activity characterizing neutrophil accumulation in *sst4* receptor WT and KO animals. A similar trend emerged in TRPA1 WT and KO animals not breaching the limit of statistical significance. Our results indicate a mechanism of action of DMTS regarding MPO activity differing completely from the one suggested by data on mechanical nociception and paw swelling. Activation of TRPA1, release of SOM and its effect on *sst4* receptors do not contribute to the inhibition of MPO activity by DMTS.

Most authors familiar with the area agree that activation of TRPA1 ion channels on nociceptor sensory nerve endings by H_2S , POLYs, or other agonists is painful due to activation of the ascending pain pathway (17, 36, 37). We do not debate that TRPA1 receptor activation is acutely painful. Intraperitoneal administration of POLY and DMTS surely evoked abdominal discomfort in our experimental animals. However, it is not only well documented scientifically, but exploited clinically that activation of peptidergic primary sensory neurons mediates a later onset antinociceptive effect (we refer to the dermal patch Qutenza® with high capsaicin content used in the therapy of neuropathic pain and relying on a different mechanism of action than that suggested for POLY and DMTS by the present work).

It was reported earlier that peptidergic sensory nerve endings release neuropeptides upon activation, among them SOM. Beside a population of nociceptors SOM is expressed in the central nervous system and peripheral tissues, too (23, 38). Treatment

with TRPA1 receptor agonists or nociceptor activation by other means leads to SOM release from primary sensory neurons and the peptide reaches significant concentration in the bloodstream (9, 39–42). SOM exerts antinociceptive and anti-inflammatory effects at parts of the body distant from the site of release. These effects were shown to be mediated by somatostatin sst₄ receptors (9, 25, 28, 40). Antinociceptive and anti-inflammatory SOM effects are obviated by somatostatin receptor antagonist, depletion of SOM from sensory nerves, an antibody catching the peptide and genetic lack of the sst₄ receptor. On the other hand, sst₄ receptor agonists induce similar beneficial effects to those of SOM (24, 30). Sst₄ receptors expressed in sensory neurons, lymphocytes, and vascular endothelial cells might contribute to the protective effect (25). Non-neuronal sources of TRPA1 activation-induced surge of SOM in the circulation shall not be taken into account, hence denervation or defunctionalization of the area exposed to TRPA1 agonist prevented such effects (39, 43).

Somatostatin is a prerequisite of antihyperalgesic and anti-inflammatory effects mediated by peptidergic nerve endings. It is known that other mediators contribute too. The sensory neuron-dependent antinociceptive effect was abolished by antagonism of opioid receptors. Opioid peptides might be released from sensory neurons and leukocytes (39).

According to our data activation routes of the sensory neuron-somatostatin axis other than TRPA1 ion channels are in play in case of DMTS, as the organic trisulfide elicited antinociceptive effect and inhibited paw swelling independently of TRPA1, but still *via* sst₄ receptors. Similar mechanisms might have been in play leading to the trend of inhibition of hind paw edema detected by plethysmometry in TRPA1 KO mice treated with POLY (**Figure 3B**). Several such mechanisms were suggested for H₂S. TRPV1 channels co-expressed with TRPA1 can be ruled out because DMTS failed to produce Ca²⁺ signals in CHO cells expressing the channel (9). Taken into account that organic trisulfides are donors of H₂S, these mechanisms might be valid for DMTS as well (10). Conversion of inorganic POLY into sulfide in living cells is an active field of research and remains to be elucidated. H₂S was reported to activate T-type CaV 3.2 channels of sensory neurons (36). These ion channels modulate pain sensation by regulating the activity of sensory neurons (44). It has to be noted that inhibition of CaV 3.2 channels by H₂S was detected, too. Supraphysiological concentration of H₂S behaves rather as an activator, while normal concentration leads to inhibition of T-type Ca²⁺ channels (45). Voltage-gated K⁺ channels are potential mediators of the effects of DMTS too. KV 4.3 voltage-gated K⁺ channels are expressed in DRG neurons (46). H₂S was reported to contract murine gastric smooth muscle by persulfidation of KV 4.3 channels. Inhibition of KV 4.3 channels was reproducible in H293 cells and could be diminished by a reducing agent and a blocker of free thiol groups that prevent protein persulfidation (47). Ability of the organic trisulfide DMTS to inhibit voltage-gated K⁺ channels could contribute to depolarization of peptidergic sensory neurons and SOM release from these cells.

Sodium POLY is an anionic compound, thus it most probably cannot penetrate into the central nervous system. It reacts readily with cysteine amino acids of proteins and loses its negative charge. However, proteins are excluded from the brain and cannot

transport POLY there. This way the effects of POLY described in the present study might rely on a peripheral mechanism (even SOM released from the sensory nerves is excluded from the central nervous system). Potassium POLY was found to enter intact HEK293T cells and produce protein persulfidation (6). Organic trisulfides such as DMTS are highly lipophilic and penetrate the blood-brain barrier freely. An uptake *via* facilitated diffusion or active transport has been proposed in case of DMTS too (48). Target proteins in the spinal cord and brain available for DMTS might contribute to its differing effect on nociception from that of POLY.

Mechanical pain threshold data of carrageenan-injected feet of TRPA1 and sst₄ WT and KO animals treated with vehicle of POLY or DMTS were analyzed by one-way ANOVA followed by Tukey's test. Statistically significant difference was found between POLY- and DMTS-treated TRPA1 WT mice at 2 h ($p < 0.05$), POLY- and DMTS-treated sst₄ WT animals at 0 ($p < 0.05$) and 6 h ($p < 0.01$), POLY- and DMTS-treated sst₄ KO mice at 0 ($p < 0.05$) and 6 h ($p < 0.01$). It is needless to state that it makes no sense to compare TRPA1 and sst₄ strains. The above differences do not influence the power of conclusions on the mechanism of either DMTS or POLY action because conclusions were drawn from within either POLY- or DMTS-treated groups, where influencing factors were homogeneous.

Interestingly, a smaller paw volume was detected at 4 and 6 h in the carrageenan-injected hind paws of POLY-treated sst₄ KO mice compared to the WT ones. This might conflict with protective nature of SOM discussed above. Compensatory changes in the expression of inflammatory genes in knockout animals might be responsible. Unfortunately, the sst₄ receptor gene-modified mouse strain utilized in the present study has not been characterized yet in that regard. However, similar results were published on another protective neuropeptide and its receptor: pituitary adenylate cyclase-activating polypeptide (PACAP) and VPAC1 receptor. PACAP is usually known as a protective peptide. Experimental autoimmune encephalomyelitis (EAE) was found to be more severe in PACAP peptide knockout mice (49). Mirroring our findings on sst₄ SOM receptors, animals genetically lacking VPAC1 PACAP receptors exhibited ameliorated responses in the same EAE model and in dextran sulfate-evoked colonic inflammation too (50, 51). VPAC1 KO mice had decreased mRNA levels of T_h2 cytokines and chemokines (50). A similar compensatory mechanism in sst₄ KO animals might influence the activation of neutrophils and macrophages—the dominant cells involved in carrageenan-induced paw edema inflammation—and decrease edema formation (52).

An inhibitory effect of DMTS on MPO activity was found that is mediated by neither TRPA1 nor SOM. Sulfide potentially being released from DMTS directly inhibits MPO activity of neutrophil granulocytes offering a straightforward mechanism (10, 53). Sulfide was documented to inhibit neutrophil cell accumulation and formation of reactive oxygen species in murine ventilator-induced lung injury, as well as to interfere with Ca²⁺-dependent cytoskeletal activities (chemotaxis and release of azurophilic granules) of human neutrophils (54, 55). H₂S suppressed adherence of rat neutrophil granulocytes in the mesenteric blood vessels detected by intravital microscopy. The effect was found

to be mediated by the inhibition of K_{ATP} ion channels (56, 57). Similarly, recruitment of human neutrophil cells was reduced by sulfide by the stimulation of L-selectin shedding. L-selectin is necessary for the adhesion of the inflammatory cells to endothelium. Activation of TNF- α -converting enzyme (ADAM-17) is supposed to be responsible (58).

We conclude that activation of peptidergic sensory neurons, release of SOM and subsequent activation of sst4 receptors are important mediators of antihyperalgesic effect of both POLY and DMTS. Unlike POLY, DMTS possesses anti-inflammatory activity too. The aforementioned mechanism contributes to the amelioration of edema formation by DMTS complemented by other means of peptidergic-nerve activation as the effect depends on the presence of functional sst4 receptors. DMTS is able to suppress MPO activity of neutrophil granulocytes at the site of inflammation without the involvement of the sensory neuron-SOM axis. Superior chemical stability, favorable pharmacokinetic properties, and significant translational potential—due to being a recognized food additive and having been patented as cyanide antidote—set DMTS in front of sodium POLY as a candidate of drug development which is only set back by the characteristic odor of the substance.

ETHICS STATEMENT

All experimental procedures were carried out according to the European Communities Council Directive of 2010/63/EU. The studies were approved by the Ethics Committee on Animal Research, University of Pécs (license number: BA02/2000-47/2017).

AUTHOR CONTRIBUTIONS

IB designed and performed *in vivo* experiments, as well as fluorescent and luminescent imaging. He was involved in sodium

REFERENCES

1. Kimura H. Hydrogen sulfide and polysulfide signaling. *Antioxid Redox Signal* (2017) 27(10):619–21. doi:10.1089/ars.2017.7076
2. Abiko Y, Shinkai Y, Unoki T, Hirose R, Uehara T, Kumagai Y. Polysulfide Na2S4 regulates the activation of PTEN/Akt/CREB signaling and cytotoxicity mediated by 1,4-naphthoquinone through formation of sulfur adducts. *Sci Rep* (2017) 7(1):4814. doi:10.1038/s41598-017-04590-z
3. Numakura T, Sugiura H, Akaike T, Ida T, Fujii S, Koarai A, et al. Production of reactive persulfide species in chronic obstructive pulmonary disease. *Thorax* (2017) 72(12):1074–83. doi:10.1136/thoraxjnl-2016-209359
4. Misak A, Grman M, Bacova Z, Rezuchova I, Hudecova S, Ondriasova E, et al. Polysulfides and products of H2S/S-nitrosoglutathione in comparison to H2S, glutathione and antioxidant Trolox are potent scavengers of superoxide anion radical and produce hydroxyl radical by decomposition of H2O2. *Nitric Oxide* (2017). doi:10.1016/j.niox.2017.09.006
5. Ikeda M, Ishima Y, Kinoshita R, Chuang VTG, Tasaka N, Matsuo N, et al. A novel S-sulfhydrated human serum albumin preparation suppresses melanin synthesis. *Redox Biol* (2018) 14:354–60. doi:10.1016/j.redox.2017.10.007
6. Greiner R, Pálinkás Z, Bäsell K, Becher D, Antelmann H, Nagy P, et al. Polysulfides link H2S to protein thiol oxidation. *Antioxid Redox Signal* (2013) 19(15):1749–65. doi:10.1089/ars.2012.5041
7. Roth M, Meiringer M, Kollmannsberger H, Zarnkow M, Jekle M, Becker T. Characterization of key aroma compounds in Distiller's grains from wheat as a basis for utilization in the food industry. *J Agric Food Chem* (2014) 62(45):10873–80. doi:10.1021/jf503281x
8. Bartling CM, Andre JC, Howland CA, Hester ME, Cafmeyer JT, Kerr A, et al. Stability characterization of a polysorbate 80-dimethyl trisulfide formulation, a cyanide antidote candidate. *Drugs R D* (2016) 16(1):109–27. doi:10.1007/s40268-016-0122-3
9. Pozsgai G, Payrits M, Sághy É, Sebestyén-Bátai R, Steen E, Szőke É, et al. Analgesic effect of dimethyl trisulfide in mice is mediated by TRPA1 and sst4 receptors. *Nitric Oxide* (2017) 65:10–21. doi:10.1016/j.niox.2017.01.012
10. Benavides GA, Squadrato GL, Mills RW, Patel HD, Isbell TS, Patel RP, et al. Hydrogen sulfide mediates the vasoactivity of garlic. *Proc Natl Acad Sci U S A* (2007) 104(46):17977–82. doi:10.1073/pnas.0705710104
11. Cortese-Krott MM, Pullmann D, Feelisch M. Nitrosopersulfide (SSNO-) targets the Keap-1/Nrf2 redox system. *Pharmacol Res* (2016) 113:490–9. doi:10.1016/j.phrs.2016.09.022
12. Cortese-Krott MM, Kuhnle GGC, Dyson A, Fernandez BO, Grman M, DuMond JF, et al. Key bioactive reaction products of the NO/H2S interaction are S/N-hybrid species, polysulfides, and nitroxyl. *Proc Natl Acad Sci U S A* (2015) 112(34):E4651–60. doi:10.1073/pnas.1509277112
13. Kolluru GK, Shen X, Yuan S, Kevin CG. Gasotransmitter heterocellular signaling. *Antioxid Redox Signal* (2017) 26(16):936–60. doi:10.1089/ars.2016.6909

polysulfide synthesis and cold cyanolysis and evaluation of data. HÁ performed fluorescent and luminescent imaging. HZ and PE contributed to the conception and design of the study and provided financial background. PG designed the study, performed *in vivo* experiments, contributed to sodium polysulfide synthesis, and drafted the manuscript. He provided funding too.

ACKNOWLEDGMENTS

We wish to thank Prof. Péter Nagy, Virág Bogdáni, and Zoltán Pálinkás from the Department of Molecular Immunology and Toxicology, National Institute of Oncology, Budapest, Hungary for introducing us to polysulfide chemistry and detection. We would like to thank Mr. Alexander Bragvin Aaleskjaer from the Medical School, University of Pécs, Pécs, Hungary for his practical help.

FUNDING

This study was funded by the following grants of the National Research, Development and Innovation Office—NKFIH, Hungary: OTKA PD 112171, OTKA NN 114458. This work was funded by the grants GINOP-2.3.2-15-2016-00048 STAY ALIVE and EFOP-3.6.2-16-2017-00006 LIVE LONGER from the European Regional Development Fund. This project was supported by the János Bolyai Research Scholarship of the Hungarian Academy of Sciences (GP).

SUPPLEMENTARY MATERIAL

The Supplementary Material for this article can be found online at <http://www.frontiersin.org/articles/10.3389/fendo.2018.00055/full#supplementary-material>.

14. Bai A-P, Ouyang Q, Hu R-W. Diallyl trisulfide inhibits tumor necrosis factor-alpha expression in inflamed mucosa of ulcerative colitis. *Dig Dis Sci* (2005) 50(8):1426–31. doi:10.1007/s10620-005-2857-5
15. Lee HGH-J, Lee HGH-J, Choi K-S, Surh Y-J, Na H-K. Diallyl trisulfide suppresses dextran sodium sulfate-induced mouse colitis: NF-κB and STAT3 as potential targets. *Biochem Biophys Res Commun* (2013) 437(2):267–73. doi:10.1016/j.bbrc.2013.06.064
16. Miltonprabu S, Sumedha NC, Senthilraja P. Diallyl trisulfide, a garlic polysulfide protects against as-induced renal oxidative nephrotoxicity, apoptosis and inflammation in rats by activating the Nrf2/ARE signaling pathway. *Int Immunopharmacol* (2017) 50:107–20. doi:10.1016/j.intimp.2017.06.011
17. Hatakeyama Y, Takahashi K, Tominaga M, Kimura H, Ohta T. Polysulfide evokes acute pain through the activation of nociceptive TRPA1 in mouse sensory neurons. *Mol Pain* (2015) 11:24. doi:10.1186/s12990-015-0023-4
18. Zygmunt PM, Högestätt ED. TRPA1. In: *Handbook of Experimental Pharmacology*. Berlin, Heidelberg: Springer (2014). p. 583–630.
19. Fernandes ES, Fernandes MA, Keeble JE. The functions of TRPA1 and TRPV1: moving away from sensory nerves. *Br J Pharmacol* (2012) 166(2):510–21. doi:10.1111/j.1476-5381.2012.01851.x
20. Pereira I, Mendes SJF, Pereira DMS, Muniz TF, Colares VLP, Monteiro CRA, et al. Transient receptor potential ankyrin 1 channel expression on peripheral blood leukocytes from rheumatoid arthritic patients and correlation with pain and disability. *Front Pharmacol* (2017) 8:53. doi:10.3389/fphar.2017.00053
21. Horváth Á, Tékus V, Boros M, Pozsgai G, Botz B, Borbely É, et al. Transient receptor potential ankyrin 1 (TRPA1) receptor is involved in chronic arthritis: in vivo study using TRPA1-deficient mice. *Arthritis Res Ther* (2016) 18(1):6. doi:10.1186/s13075-015-0904-y
22. Fernandes ES, Russell FA, Alawi KM, Sand C, Liang L, Salamon R, et al. Environmental cold exposure increases blood flow and affects pain sensitivity in the knee joints of CFA-induced arthritic mice in a TRPA1-dependent manner. *Arthritis Res Ther* (2016) 18(1):7. doi:10.1186/s13075-015-0905-x
23. ten Bokum AM, Hofland LJ, van Hagen PM. *European Cytokine Network*. (Vol. 11). Montrouge, France: John Libbey Eurotext Ltd (2000). p. 161–76.
24. Szolcsányi J, Pintér E, Helyes Z, Pethő G. Inhibition of the function of TRPV1-expressing nociceptive sensory neurons by somatostatin 4 receptor agonism: mechanism and therapeutic implications. *Curr Top Med Chem* (2011) 11(17):2253–63. doi:10.2174/156802611796904852
25. Pintér E, Helyes Z, Szolcsányi J. Inhibitory effect of somatostatin on inflammation and nociception. *Pharmacol Ther* (2006) 112(2):440–56. doi:10.1016/j.pharmthera.2006.04.010
26. Helyes Z, Pintér E, Németh J, Sándor K, Elekes K, Szabó A, et al. Effects of the somatostatin receptor subtype 4 selective agonist J-2156 on sensory neuropeptide release and inflammatory reactions in rodents. *Br J Pharmacol* (2006) 149(4):405–15. doi:10.1038/sj.bjp.0706876
27. Helyes Z, Pintér E, Sándor K, Elekes K, Bánvölgyi A, Keszthelyi D, et al. Impaired defense mechanism against inflammation, hyperalgesia, and airway hyperreactivity in somatostatin 4 receptor gene-deleted mice. *Proc Natl Acad Sci U S A* (2009) 106(31):13088–93. doi:10.1073/pnas.0900681106
28. Markovics A, Szöke É, Sándor K, Börzsei R, Bagoly T, Kemény Á, et al. Comparison of the anti-inflammatory and anti-nociceptive effects of cortistatin-14 and somatostatin-14 in distinct in vitro and in vivo model systems. *J Mol Neurosci* (2012) 46(1):40–50. doi:10.1007/s12031-011-9577-4
29. Sándor K, Elekes K, Szabó Á, Pintér E, Engström M, Wurster S, et al. Analgesic effects of the somatostatin sst4 receptor selective agonist J-2156 in acute and chronic pain models. *Eur J Pharmacol* (2006) 539(1–2):71–5. doi:10.1016/j.ejphar.2006.03.082
30. Schuelert N, Just S, Kuelzer R, Corradini L, Gorham LCJ, Doods H. The somatostatin receptor 4 agonist J-2156 reduces mechanosensitivity of peripheral nerve afferents and spinal neurons in an inflammatory pain model. *Eur J Pharmacol* (2015) 746:274–81. doi:10.1016/j.ejphar.2014.11.003
31. Bautista DM, Jordt S-E, Nikai T, Tsuruda PR, Read AJ, Poblete J, et al. TRPA1 mediates the inflammatory actions of environmental irritants and proalgesic agents. *Cell* (2006) 124(6):1269–82. doi:10.1016/j.cell.2006.02.023
32. Nagy P, Winterbourne CC. Rapid reaction of hydrogen sulfide with the neutrophil oxidant hypochlorous acid to generate polysulfides. *Chem Res Toxicol* (2010) 23(10):1541–3. doi:10.1021/tx100266a
33. Wood JL. Sulfane sulfur. *Methods Enzymol* (1987) 143:25–9. doi:10.1016/0076-6879(87)43009-7
34. Botz B, Bölcseki K, Kereskai L, Kovács M, Németh T, Szigeti K, et al. Differential regulatory role of pituitary adenylate cyclase-activating polypeptide in the serum-transfer arthritis model. *Arthritis Rheumatol* (2014) 66(10):2739–50. doi:10.1002/art.38772
35. Borbely É, Botz B, Bölcseki K, Kenyér T, Kereskai L, Kiss T, et al. Capsaicin-sensitive sensory nerves exert complex regulatory functions in the serum-transfer mouse model of autoimmune arthritis. *Brain Behav Immun* (2015) 45:50–9. doi:10.1016/j.bbi.2014.12.012
36. Fukami K, Fukami K, Sekiguchi F, Sekiguchi F, Kawabata A, Kawabata A. Hydrogen sulfide and T-type Ca²⁺ channels in pain processing, neuronal differentiation and neuroendocrine secretion. *Pharmacology* (2017) 99(3–4):196–203. doi:10.1159/000444944
37. Andersen HH, Lo Vecchio S, Gazerani P, Arendt-Nielsen L. Dose-response study of topical allyl isothiocyanate (mustard oil) as a human surrogate model of pain, hyperalgesia, and neurogenic inflammation. *Pain* (2017) 158(9):1723–32. doi:10.1097/j.pain.0000000000000979
38. Gamse R, Leeman SE, Holzer P, Lembeck F. Differential effects of capsaicin on the content of somatostatin, substance P, and neurotensin in the nervous system of the rat. *Naunyn Schmiedebergs Arch Pharmacol* (1981) 317(2):140–8. doi:10.1007/BF00500070
39. Pethő G, Bölcseki K, Füredi R, Botz B, Bagoly T, Pintér E, et al. Evidence for a novel, neurohumoral antinociceptive mechanism mediated by peripheral capsaicin-sensitive nociceptors in conscious rats. *Neuropeptides* (2017) 62:1–10. doi:10.1016/j.npep.2017.02.079
40. Helyes Z, Szabó Á, Németh J, Jakab B, Pintér E, Bánvölgyi Á, et al. Antiinflammatory and analgesic effects of somatostatin released from capsaicin-sensitive sensory nerve terminals in a Freund's adjuvant-induced chronic arthritis model in the rat. *Arthritis Rheum* (2004) 50(5):1677–85. doi:10.1002/art.20184
41. Antal A, Nemeth J, Szolcsányi J, Pozsgai G, Pinter E. Abdominal surgery performed under general anesthesia increases somatostatin-like immunoreactivity in human serum. *Neuroimmunomodulation* (2008) 15(3):153–6. doi:10.1159/000151528
42. Suto B, Bagoly T, Börzsei R, Lengl O, Szolcsányi J, Nemeth T, et al. Surgery and sepsis increase somatostatin-like immunoreactivity in the human plasma. *Peptides* (2010) 31(6):1208–12. doi:10.1016/j.peptides.2010.03.018
43. Bölcseki K, Tékus V, Dézsi L, Szolcsányi J, Pethő G. Antinociceptive desensitizing actions of TRPV1 receptor agonists capsaicin, resiniferatoxin and N-oleoyldopamine as measured by determination of the noxious heat and cold thresholds in the rat. *Eur J Pain* (2010) 14(5):480–6. doi:10.1016/j.ejpain.2009.08.005
44. Todorovic SM, Jevtovic-Todorovic V. T-type voltage-gated calcium channels as targets for the development of novel pain therapies. *Br J Pharmacol* (2011) 163(3):484–95. doi:10.1111/j.1476-5381.2011.01256.x
45. Elies J, Scragg JL, Boyle JP, Gamper N, Peers C. Regulation of the T-type Ca²⁺ channel Cav3.2 by hydrogen sulfide: emerging controversies concerning the role of H₂S in nociception. *J Physiol* (2016) 594(15):4119–29. doi:10.1113/jphysiol.2016.20963
46. Yunoki T, Takimoto K, Kita K, Funahashi Y, Takahashi R, Matsuyoshi H, et al. Differential contribution of Kv4-containing channels to A-type, voltage-gated potassium currents in somatic and visceral dorsal root ganglion neurons. *J Neurophysiol* (2014) 112(10):2492–504. doi:10.1152/jn.00054.2014
47. Liu D-H, Huang X, Meng X-M, Zhang C-M, Lu H-L, Kim Y-C, et al. Exogenous H₂S enhances mice gastric smooth muscle tension through S-sulphydrylation of Kv43, mediating the inhibition of the voltage-dependent potassium current. *Neurogastroenterol Motil* (2014) 26(12):1705–16. doi:10.1111/nmo.12451
48. Kiss L, Bocsik A, Walter FR, Ross J, Brown D, Mendenhall BA, et al. In vitro and in vivo blood-brain barrier penetration studies with the novel cyanide antidote candidate dimethyl trisulfide in mice. *Toxicol Sci* (2017) 160(2):398–407. doi:10.1093/toxsci/kfx190
49. Tan Y-V, Abad C, Lopez R, Dong H, Liu S, Lee A, et al. Pituitary adenylate cyclase-activating polypeptide is an intrinsic regulator of Treg abundance and protects against experimental autoimmune encephalomyelitis. *Proc Natl Acad Sci U S A* (2009) 106(6):2012–7. doi:10.1073/pnas.0812257106

50. Abad C, Jayaram B, Becquet L, Wang Y, O'Dorisio MS, Waschek JA, et al. VPAC1 receptor (Vipr1)-deficient mice exhibit ameliorated experimental autoimmune encephalomyelitis, with specific deficits in the effector stage. *J Neuroinflammation* (2016) 13(1):169. doi:10.1186/s12974-016-0626-3
51. Yadav M, Huang M-C, Goetzel EJ. VPAC1 (vasoactive intestinal peptide (VIP) receptor type 1) G protein-coupled receptor mediation of VIP enhancement of murine experimental colitis. *Cell Immunol* (2011) 267(2):124–32. doi:10.1016/j.cellimm.2011.01.001
52. Tejada MA, Montilla-García A, Cronin SJ, Cikes D, Sánchez-Fernández C, González-Cano R, et al. Sigma-1 receptors control immune-driven peripheral opioid analgesia during inflammation in mice. *Proc Natl Acad Sci USA* (2017) 114(31):8396–401. doi:10.1073/pnas.1620068114
53. Pálinkás Z, Furtmüller PG, Nagy A, Jakopitsch C, Pirker KF, Magierowski M, et al. Interactions of hydrogen sulfide with myeloperoxidase. *Br J Pharmacol* (2015) 172(6):1516–32. doi:10.1111/bph.12769
54. Mariggò MA, Pettini F, Fumarulo R. Sulfide influence on polymorphonuclear functions: a possible role for CA²⁺ involvement. *Immunopharmacol Immunotoxicol* (1997) 19(3):393–404. doi:10.3109/08923979709046984
55. Spassov SG, Donus R, Ihle PM, Engelstaedter H, Hoetzel A, Faller S. Hydrogen sulfide prevents formation of reactive oxygen species through PI3K/Akt signaling and limits ventilator-induced lung injury. *Oxid Med Cell Longev* (2017) 2017:3715037. doi:10.1155/2017/3715037
56. Fiorucci S, Antonelli E, Distrutti E, Rizzo G, Mencarelli A, Orlandi S, et al. Inhibition of hydrogen sulfide generation contributes to gastric injury caused by anti-inflammatory nonsteroidal drugs. *Gastroenterology* (2005) 129(4):1210–24. doi:10.1053/j.gastro.2005.07.060
57. Zanardo RCO, Brancaleone V, Distrutti E, Fiorucci S, Cirino G, Wallace JL. Hydrogen sulfide is an endogenous modulator of leukocyte-mediated inflammation. *FASEB J* (2006) 20(12):2118–20. doi:10.1096/fj.06-6270fje
58. Ball CJ, Reiffel AJ, Chintalapani S, Kim M, Spector JA, King MR. Hydrogen sulfide reduces neutrophil recruitment in hind-limb ischemia-reperfusion injury in an L-selectin and ADAM-17-dependent manner. *Plast Reconstr Surg* (2013) 131(3):487–97. doi:10.1097/PRS.0b013e31827c6e9c

Conflict of Interest Statement: The authors declare that the research was conducted in the absence of any commercial or financial relationships that could be construed as a potential conflict of interest.

Copyright © 2018 Bátai, Horváth, Pintér, Helyes and Pozsgai. This is an open-access article distributed under the terms of the Creative Commons Attribution License (CC BY). The use, distribution or reproduction in other forums is permitted, provided the original author(s) and the copyright owner are credited and that the original publication in this journal is cited, in accordance with accepted academic practice. No use, distribution or reproduction is permitted which does not comply with these terms.



NPY1 Receptor Agonist Modulates Development of Depressive-Like Behavior and Gene Expression in Hypothalamus in SPS Rodent PTSD Model

Lidia Serova, Hannah Mulhall and Esther Sabban *

Department of Biochemistry and Molecular Biology, New York Medical College, Valhalla, NY, USA

OPEN ACCESS

Edited by:

Hubert Vaudry,
University of Rouen, France

Reviewed by:

James A. Carr,
Texas Tech University, USA
Tamas Kozicz,
Radboud University Nijmegen,
Netherlands

*Correspondence:

Esther Sabban
sabban@nymc.edu

Specialty section:

This article was submitted to
Neuroendocrine Science,
a section of the journal
Frontiers in Neuroscience

Received: 06 December 2016

Accepted: 24 March 2017

Published: 19 April 2017

Citation:

Serova L, Mulhall H and Sabban E

(2017) NPY1 Receptor Agonist

Modulates Development of
Depressive-Like Behavior and Gene
Expression in Hypothalamus in SPS
Rodent PTSD Model.

Front. Neurosci. 11:203.

doi: 10.3389/fnins.2017.00203

Delivery of neuropeptide Y (NPY) to the brain by intranasal infusion soon after traumatic stress has shown therapeutic potential, and prevented development of many behavioral and neuroendocrine impairments in the single prolonged stress (SPS) animal model of PTSD. Therefore, we examined whether the Y1R preferring agonist [$\text{Leu}^{31}\text{Pro}^{34}$]NPY is sufficient to prevent development of SPS induced depressive-like behavioral changes, and hypothalamic gene expression as obtained with intranasal NPY intervention. Male Sprague-Dawley rats were given intranasal infusion of either NPY (150 $\mu\text{g}/\text{rat}$), a low (68 $\mu\text{g}/\text{rat}$), or high (132 $\mu\text{g}/\text{rat}$) dose of [$\text{Leu}^{31}\text{Pro}^{34}$]NPY or vehicle immediately following the last SPS stressor, left undisturbed for 1 week and then tested for depressive-like behavior together with naïve unstressed controls. Vehicle treated animals had elevated immobility forced swim test (FST) and reduced sucrose preference, which were not observed in animals given NPY or the higher dose of [$\text{Leu}^{31}\text{Pro}^{34}$]NPY. This dose of [$\text{Leu}^{31}\text{Pro}^{34}$]NPY, like NPY, also prevented the SPS-elicited induction of CRF mRNA in the mediobasal hypothalamus. However, [$\text{Leu}^{31}\text{Pro}^{34}$]NPY did not prevent, but rather enhanced, the SPS-triggered induction of GR and FKBP5 mRNA levels in the mediobasal hypothalamus. Thus, [$\text{Leu}^{31}\text{Pro}^{34}$]NPY may be as effective as NPY and displays therapeutic potential for preventing development of depressive-like behaviors and dysregulation of the CRF/HPA system in PTSD. However, due to its different effects compared to NPY on GR and FKBP5 a broader agonist, such as NPY, may be more desirable.

Keywords: stress, neuropeptide Y, corticotropin releasing factor, glucocorticoid receptor, FKBP5, depression, PTSD

INTRODUCTION

Considerable evidence indicates that in the CNS neuropeptide Y (NPY) can attenuate the response to stress, and has therapeutic potential for PTSD as well as for depression (reviewed in Heilig, 2004; Morales-Medina et al., 2010; Wu et al., 2011; Sah and Geraciotti, 2013; Enman et al., 2015; Reichmann and Holzer, 2016; Sabban et al., 2016; Schmeltzer et al., 2016). Our recent studies revealed proof of concept that delivery of NPY to the brain shortly before or immediately after

exposure to traumatic stress can prevent the development of many PTSD associated behavioral and neuroendocrine impairments. Intranasal infusion of NPY after exposure to traumatic stress in the single prolonged stress (SPS) protocol, rodent model of PTSD, averted the elevation of anxiety, depressive-like behavior and hyperarousal observed in vehicle treated animals a week or more afterwards. Intervention with intranasal NPY also provided resistance against prolonged activation of the hypothalamic pituitary adrenal (HPA) axis, and molecular changes in multiple brain regions, including the mediobasal hypothalamus (Serova et al., 2013; Laukova et al., 2014; Sabban et al., 2015a, 2016).

At least four NPY receptors, Y1R, Y2R, Y4R, and Y5R, mediate the biological effects of NPY (Michel et al., 1998; Hirsch and Zukowska, 2012). The Y6 subtype is truncated, non-functional in humans and absent in the rat. The NPY receptors associate with Gi/Go and regulate several signaling cascades leading to hyperpolarization by inhibiting calcium channels and activation of GIRK or I_H channels, inactivation of adenylyl cyclase and thus cAMP dependent pathways and mobilization of intracellular calcium by phospholipase C and phosphatidyl inositol kinase. NPY can lead to changes ERK or CREB signaling resulting in alterations in gene expression (reviewed in Brothers and Wahlestedt, 2010; Sah and Geraciotti, 2013).

Y1R, Y2R, and Y5R are abundantly expressed in brain areas implicated in anxiety and depression (reviewed in Kask et al., 2002; Heilig, 2004; Eva et al., 2006). The importance of Y1 transmission in depressive disorders was emphasized in the Flinders Sensitive Line, a genetic model of depression. In these animals, hippocampal and hypothalamic Y1 receptor mRNA levels were lower and Y1 receptor binding higher than in the control Flinders Resistant Line (Jiménez-Vasquez et al., 2007). The beneficial effect of NPY was also observed in the acute model of depression, likely mediated by the Y1 receptors (Redrobe et al., 2002; Goyal et al., 2009). Moreover, antidepressant like effects of agmatine occur via the NPYergic system and probably by stimulation of the Y1 receptor subtype (Kotagale et al., 2013). Immunohistochemistry showed that neuroendocrine CRF neurons in the PVN coexpress Y1R. Direct infusion of the Y1 preferring agonist [Leu³¹Pro³⁴]NPY into the PVN increased c-Fos and phosphorylated CREB expression in populations of CRF/Y1r-ir cells and elevated plasma corticosterone levels (Dimitrov et al., 2007). This suggests that NPY afferents and subsequent activation of NPY Y1 receptors play an important role in the regulation of the HPA.

Due to the widespread distribution of NPY into the brain following intranasal infusion (Sabban et al., 2016), it remains to be determined the activation of what receptor subtypes are sufficient for NPY's stress-reductive and therapeutic effects. In addition, a more selective agonist than NPY may able to be effective at low dose, and provide less opportunity for potential side effects.

In this study we examined whether the Y1 receptor preferring agonist [Leu³¹Pro³⁴]NPY is able to provide selective protective effects on traumatic stress triggered depressive-like behaviors and changes in hypothalamic gene expression.

MATERIALS AND METHODS

Materials

[Leu³¹Pro³⁴]-Neuropeptide Y (human, rat) was purchased from Tocris. NPY was synthesized by NeoScientific (Cambridge, MA). They were stored lyophilized at -80°C and dissolved in distilled water immediately before infusion.

Animals

All experiments were performed in accordance with the National Institute of Health Guide for the Care and Use of Laboratory Animals and approved by Institutional Animal Care and Use Committee at NYMC and the USAMRMC Animal Care and Use Review Office. Male Sprague-Dawley rats (150–160 g) were purchased from Charles River (Wilmington, MA) and housed (4 per cage) in a barrier area on 12 h light/dark cycle at $23 \pm 2^{\circ}\text{C}$ with *ad libitum* access to food and water.

Experimental Design

The experimental design is shown in **Figure 1**. After 2 week acclimation period, the rats were randomly assigned to the experimental or control groups (10 rats per group). SPS was performed between 9 a.m. and 2 p.m. as previously described (Serova et al., 2013). First, rats were subjected to a 2 h immobilization on metal board by taping the limbs with a surgical tape and restricting the motion of the head. Immediately afterwards, they were subjected to a 20 min forced swim in a plexiglass cylinder (50 cm height, 24 cm diameter, Stoelting, Wood Dale, IL) filled to two-thirds with 24°C fresh water. The animals were dried and allowed to recuperate for 15 min and then exposed to ether vapor until loss of consciousness.

While still under the influence of ether from the last SPS stressor, each rat received intranasal infusion of either: (1) 150 μg NPY; (2) 68 μg [Leu³¹Pro³⁴]NPY; (3) 132 μg [Leu³¹Pro³⁴]NPY, or (4) vehicle (distilled water). The infusion was administered, 10 μl into each nare, with pipetteman and disposable plastic tip. Extreme care was taken to avoid contact with the intranasal mucosa. Following administration, the head of the animal was held in a tilted back position for approximately 15 s.

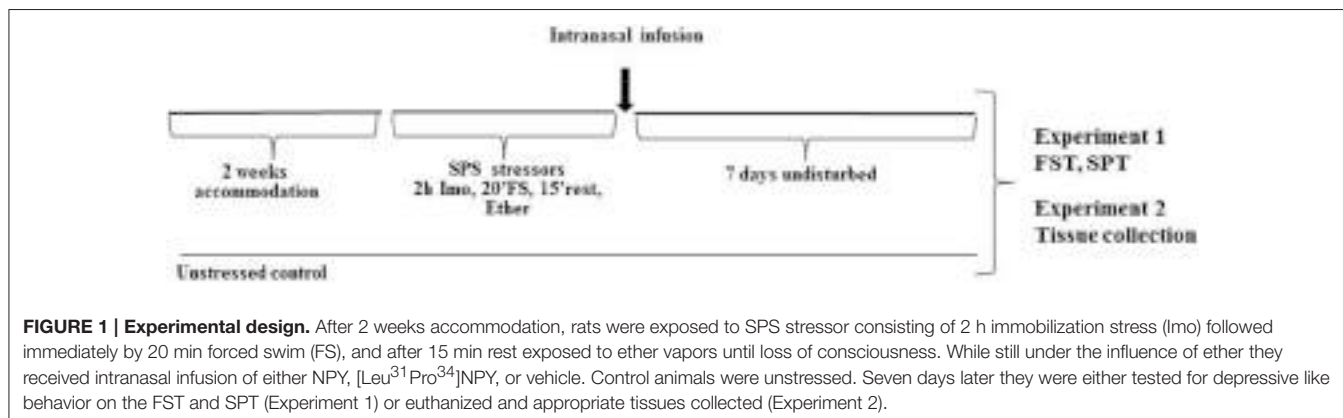
Following the SPS procedure, animals left undisturbed (2 per cage) for 7 d and were then tested on the forced swim test and sucrose preference test (Experiment 1) or euthanized to determine changes in gene expression in the mediobasal hypothalamus (Experiment 2).

Forced Swim Test (FST)

Rats were examined in a modified version of the Porsolt swim test (Cryan et al., 2002) as previously described (Serova et al., 2013). They were put into the same plexiglass cylinders filled to two-thirds with 24°C fresh water for 5 min and their behavior was recorded. A trained individual blinded to the experimental group scored the time spent swimming, defined as movement of the forelimbs and hind limbs and the time spent immobile when the animal showed no movement, or only movements needed to keep its head above the water.

Sucrose Preference Test (SPT)

For the sucrose preference test (Briones and Woods, 2013), rats were trained to a two-bottle choice of drinking water and 1%



sucrose solution for 2 days followed by 2 days of testing. On the day of testing, two pre-weighted bottles of 5% sucrose solution and tap water were presented. To prevent possible effects of side preference in drinking behavior, the position of the bottles was switched after 24 h of training or testing. No food or water deprivation was applied before or during the test. Liquid consumption from each bottle corrected by body weight was used to calculate sucrose solution intake, water intake and total consumption by the end of the 48-h period. Sucrose preference was calculated using the following equation: sucrose preference (%) = sucrose intake/(sucrose intake + water intake) × 100.

Gene Expression in Mediobasal Hypothalamus

A week after the SPS stressors, the rats were sacrificed and the mediobasal hypothalamus containing paraventricular nucleus (PVN) without the arcuate nucleus was isolated and immediately frozen in liquid nitrogen at kept at -80°C. Total RNA was isolated with RNeasy Plus Mini Kit (Qiagen, Valencia, CA). This kit has been designed to isolate total RNA from animal tissues and obtain optimal RNA yield and purity. It also allows eliminating contamination by genomic DNA using gDNA eliminator columns. Briefly, the frozen samples were homogenized in lysate buffer containing β-mercaptoethanol with Polytron PT 1200E (Kinematica AG, Switzerland). After centrifugation the supernatant was transferred and centrifuged through gDNA eliminator spin columns. After addition of 70% ethanol, RNA was precipitated on the RNeasy spin columns, washed and eluted with RNase-free water. RNA concentration was evaluated by spectrophotometry (NanoDrop 2000, Thermo Fisher Scientific, Pittsburgh, PA). The ratio of absorbance at 260 to 280 nm was about 2.0. Overall average yield of isolated total RNA was 5–8 μg per 10 mg of brain tissue which is within in the best range provided by Qiagen's protocol.

The relative levels of CRF, GR, and FKBP5 mRNAs were determined by RT-qPCR. Reverse transcription of 1,000 ng of RNA was performed with the RevertAid First Strand cDNA Synthesis kit (Thermo Fisher Scientific, Hanover Park, IL) using an oligo dT primer at 42°C for 60 min in MyCycler (BioRad, Hercules, CA). For qPCR, the cDNA (33.2 ng in 2 μl) was mixed with 12.5 μl of FastStart Universal SYBR Green Master Rox (Roche Diagnostics, Indianapolis, IN) and

1 μl of the following primer sets: CRF (Crh, NM_031019.1, cat. no. PPR44803B, Qiagen); glucocorticoid receptor (GR) (Nr3c1, NM_012576.2, cat no. PRR52805B, Qiagen); FKBP5 (Fkbp5, NM_001012174.1, cat. no. PPR51629B, Qiagen) and glyceraldehyde-3-phosphate dehydrogenase (GAPDH; Gapdh, NM_017008.4, forward 5'-TGGACCACCCAGCCCAGCAAG-3', reverse 5'-GGCCCCTCCTGTTATGGGGT-3'), to a final volume 25 μl in PCR-96-Microplate (Axygen Scientific, Union City, CA). The primers for CRF, GR and FKBP5 were validated experimentally by Qiagen to amplify a single amplicon (125, 81, 96 bp respectively) with uniform PCR efficiency. The amplicon for GAPDH (140 bp) was shown to be proportional to RNA input. PCR was performed on ABI7900HT Real-Time PCR instrument (Applied Biosystems, Carlsbad, CA). The data were analyzed with SDS Software 2.4 (Applied Biosystems). The melting curves were examined to verify a single amplicon at the expected melting temperature. Ct values were in the range of 27–29 for CRF, 25–28 for GR and FKBP5, and 16–17 for GAPDH. Data were normalized to GAPDH mRNA (not altered by experimental conditions) and expressed as the relative fold changes calculated using the ΔΔCt method (Livak and Schmittgen, 2001).

Statistical Analysis

Data were analyzed using Prism 4 (GraphPad) software. Following confirming normality with D'agostino and Pearson Omnibus Normality Test, and data were analyzed by one way ANOVA followed by Tukey's Multiple Comparison Test for differences among the groups. Values of $p \leq 0.05$ were considered significant.

RESULTS

Intranasal Administration of [Leu³¹Pro³⁴]NPY Prevented the SPS Elicited Depressive-Like Behavior

Initially, we examined the ability of two doses of the Y1R preferring agonist [Leu³¹Pro³⁴]NPY to change despair or depressive-like behavior in forced swim test (FST) of rats subjected to SPS stressors (Figure 2). Animals were given intranasal infusion of either: NPY (150 μg/rat), low (68 μg/rat)

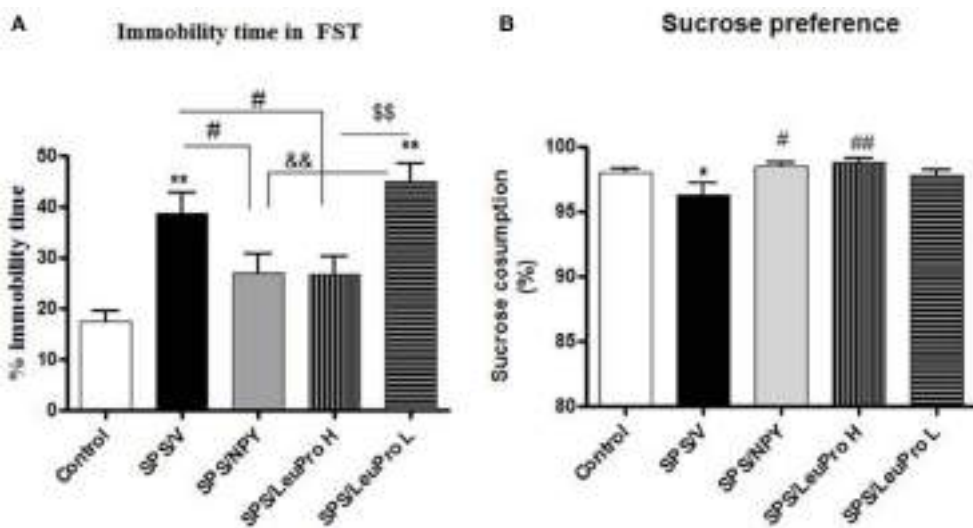


FIGURE 2 | Depressive-like behavior. Immediately after the last SPS stressor rats were infused with vehicle (SPS/V), 150 µg NPY (SPS/NPY), 132 µg [Leu³¹Pro³⁴]NPY (SPS/LeuPro H), or 64 µg [Leu³¹Pro³⁴]NPY (SPS/LeuPro L) or unstressed (Controls). Testing for depressive-like behavior began 7 days later. **(A)** Immobility time on FST. **(B)** Sucrose preference. Data are presented as mean ± SEM. $n = 8$ –10 per group. * $p < 0.05$, ** $p < 0.01$ compared to Controls; # $p < 0.05$, ## $p < 0.01$ compared to SPS/V; && $p < 0.01$ compared to SPS/NPY; §§ $p < 0.01$ compared to SPS/LeuPro H.

or high (132 µg/rat) dose of [Leu³¹Pro³⁴]NPY, or vehicle immediately following the last stressor (ether) of the SPS protocol. They were left undisturbed for 1 week and then tested on the FST (Figure 2A) together with naïve unstressed controls. One way ANOVA showed a significant impact of treatment on time immobile ($F = 9.5$, $p < 0.0001$). Rats that received vehicle (SPS/V) spent longer time immobile compared to the unstressed controls ($p < 0.01$). Administration of NPY, as previously observed (Serova et al., 2013), prevented development of this despair behavior. Despite similar body weight in all the SPS treated groups, the SPS/NPY group of rats spent less time immobile compared to the SPS/V group ($p < 0.05$) and did not differ from the unstressed controls. The results with [Leu³¹Pro³⁴]NPY depended on the dose used. The low dose was not effective to change SPS-induced immobility time in FST ($p > 0.05$, SPS/LeuPro L vs. SPS/V). However, the immobility time with the higher dose was different than with the low dose ($p < 0.01$) and significantly reduced compared to the vehicle treated group ($p < 0.05$, SPS/LeuPro H vs. SPS/V). Similarly, treatment with NPY as well as the higher, but not the lower, dose of [Leu³¹Pro³⁴]NPY prevented the reduction in sucrose reference observed in the vehicle treated group (Figure 2B). Therefore, only the higher dose was used in the further experiments.

Effects of NPY and [Leu³¹Pro³⁴]NPY on Single Prolonged Stress (SPS) Elicited Molecular Changes in the Mediobasal Hypothalamus

In the next experiment, we examined the effect of early intervention with intranasal NPY, or [Leu³¹Pro³⁴]NPY on SPS-elicited changes in expression of several genes in the mediobasal hypothalamus, an integrative center in the regulation of HPA axis

(Figure 3). One way ANOVA revealed significant differences in CRF mRNA levels among animals with different treatments ($F = 10.0$, $p < 0.0001$, Figure 3A). Tukey's multiple comparison test showed that [Leu³¹Pro³⁴]NPY was similar to NPY in preventing the elevation of CRF mRNA. An induction of CRF mRNA was observed only in the vehicle treated group ($p < 0.01$ compared to controls, SPS/NPY or SPS/LeuPro).

Since the GR plays a crucial role in the negative feedback regulation of HPA axis we examined GR mRNA levels. ANOVA showed significant impact of treatment ($F = 15.0$, $p < 0.0001$, Figure 3B). While, significantly increased by SPS in vehicle infused animals compared to controls ($p < 0.01$) this did not occur in rats given NPY infusion. They had GR mRNA levels similar to the controls and decreased compared to the SPS/V group ($p < 0.01$). Surprisingly, in animals with [Leu³¹Pro³⁴]NPY infusion, GR mRNA levels were significantly higher than in controls, SPS/V or SPS/NPY groups ($p < 0.001$).

The levels of FKBP5 mRNA were also affected by treatment ($F = 10.0$, $p < 0.0001$, Figure 3C). In agreement with our previous published results (Laukova et al., 2014), similar to CRF and GR, mRNA levels of FKBP5 are also elevated by SPS in the mediobasal hypothalamus. The pattern of changes in FKBP5 gene expression was analogous to those of GR mRNA levels. There was elevation of gene expression of FKBP5 by SPS as shown in vehicle treated group but not in animals given NPY ($p > 0.01$ vs. controls or SPS/NPY). However, rats administered [Leu³¹Pro³⁴]NPY had a greater induction of FKBP5 mRNA levels, which was higher than in any of the other groups.

DISCUSSION

The results of this study suggest an important role for the Y1R in protection from development of the depression-like

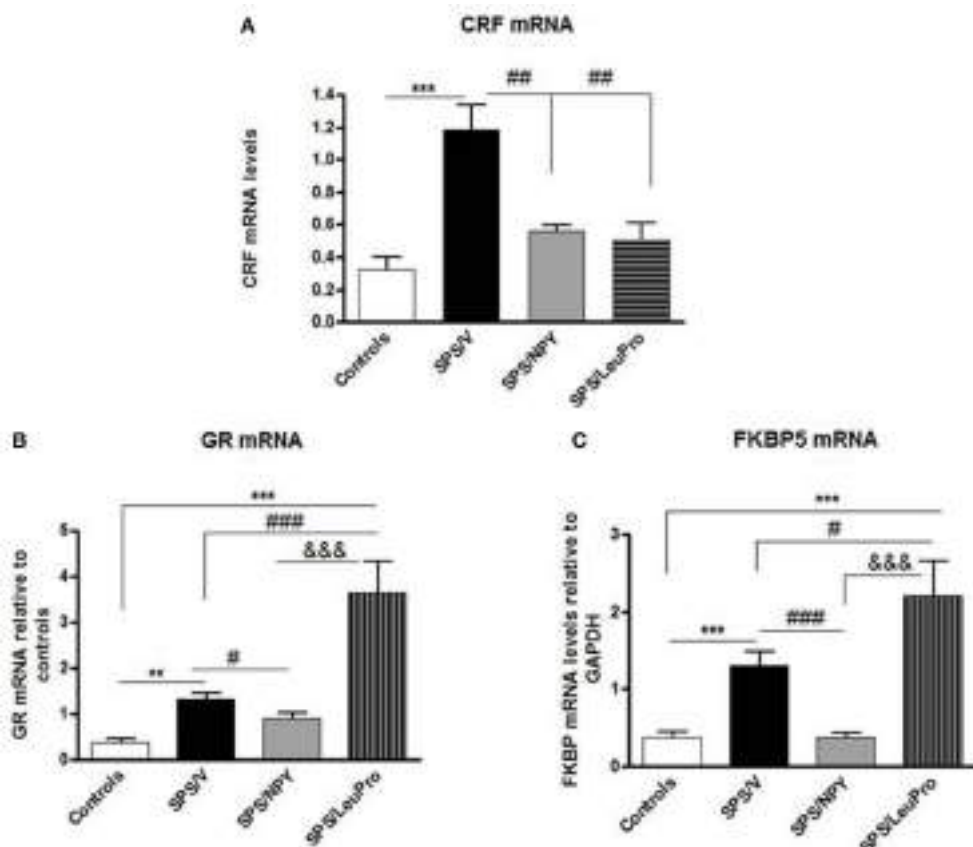


FIGURE 3 | Changes in mRNA levels for several genes in the mediobasal hypothalamus. Data are presented as mean \pm SEM. $n = 8\text{--}10$ per group. **(A)** CRF mRNA levels. *** $p < 0.001$ compared to controls; ## $p < 0.01$ compared to SPS/V. **(B)** GR mRNA levels. ** $p < 0.01$, *** $p < 0.001$ compared to controls; # $p < 0.05$, ## $p < 0.001$ compared to SPS/V; &&& $p < 0.001$ compared to SPS/LeuPro. **(C)** FKBP5 mRNA levels. *** $p < 0.001$ compared to Controls; # $p < 0.05$, ## $p < 0.001$ compared to SPS/V; &&& $p < 0.001$ compared to SPS/LeuPro.

symptoms following the exposure to severe stress. Infused immediately after the application of SPS stressors, the higher dose of [Leu³¹Pro³⁴]NPY was able to prevent development of SPS-induced increase in immobility time in FST. This dose was also protective against long lasting elevation of CRF mRNA levels in the mediobasal hypothalamus. However, the Y1R preferring agonist did not prevent the SPS elicited effects on gene expression of GR and FKBP5 in this brain region, which were even higher than in SPS group treated with vehicle.

The findings demonstrated that [Leu³¹Pro³⁴]NPY, when given at a similar dose as NPY, is equally effective to ameliorate the development of SPS-elicited depressive-like behavior as shown by both the FST and sucrose preference test. The importance of the Y1R on basal activity on FST has previously been observed. Intracerebral infusion of the Y1R agonist [Leu³¹Pro³⁴]PYY, or NPY, 30 min before the test significantly increased time mice spent swimming compared to controls (Redrobe et al., 2002). Administration of [Leu³¹Pro³⁴]NPY in olfactory bulbectomized rat model of depression reduced depressive related features in open field test (Goyal et al., 2009). Moreover, Y1R deficient mice ($-/-$) displayed greater immobility time in FST than the

+/+ wild type controls (Karlsson et al., 2008) confirming the importance of the Y1R. Our data revealed for the first time that stimulation of Y1R immediately after exposure rats to SPS stressors provides a long-lasting anti-depressive-like effect. It remains to be determined whether Y1R agonists are sufficient to also produce the reduction in SPS triggered symptoms of anxiety obtained with intranasal NPY.

The results also suggest that beneficial effects of intranasally infused NPY in SPS-induced despair or depressive-like behavior is mediated by its activation of Y1 receptors. Although [Leu³¹Pro³⁴]NPY is assumed to be specific for the Y1 receptor we cannot rule out a contribution of the Y5 receptor subtype. It has been shown that [Leu³¹Pro³⁴]NPY also has efficacy at the Y5R (Gerald et al., 1996). The rat hypothalamus also expresses Y5R to some extent. In rat hypothalamic homogenates approximately 20% of specific binding fit the pharmacological profile of Y5 receptors (Widdowson et al., 1997). It is also have been found that endogenous NPY acts via PVN Y1 and Y5 receptors to change sympathetic nerve activation and heart rate (Cassaglia et al., 2014). Thus the Y1R preferring agonist, [Leu³¹Pro³⁴]NPY given in relatively high dose could also interact

with Y5 receptors. Therefore, our data with [Leu³¹Pro³⁴]NPY may represent additive activation of both receptors. Further studies with more doses of [Leu³¹Pro³⁴]NPY and different agonists will help determine the lowest effective dose and distinguish their selective roles.

[Leu³¹Pro³⁴]NPY was sufficient to prevent the SPS elicited rise of CRF gene expression. CRF plays a key role in integrating neural, endocrine, and behavioral responses to stressful stimuli. During stress, CRF initiates the activation of the HPA axis. Released from the hypothalamus, CRF stimulates ACTH synthesis and release from the anterior pituitary. This evokes glucocorticoid secretion from the adrenal cortex into circulation. Glucocorticoids, via GR, mediate many of their physiological responses to stress. Within the hypothalamus, GR plays a crucial role in direct glucocorticoid feedback by repressing CRF biosynthesis and release and thus enabling appropriate termination of the stress response.

Elevated expression of CRF in the mediobasal hypothalamus has been linked to a depressive-like state. Many antidepressant drugs have delayed onset of clinical efficacy and in rats, long-term administration of clinically effective antidepressant drugs resulted in reduction in CRF mRNA expression levels in the hypothalamic PVN (Brady et al., 1991). The over-expression of CRF in the PVN appears to be a common neuroendocrine abnormality for depressive states in animals (Mironova et al., 2013). Depression and PTSD are frequently co-morbid. Patients with PTSD and animal models of PTSD display dysregulations of the HPA axis on several levels, such as blood glucocorticoid and ACTH concentration, expression of GR receptors in many brain regions as well as GR receptor modulator glucocorticoid sensitive co-chaperone FK506-binding protein 5 (FKBP5) (Yehuda, 2009; Mehta et al., 2011; Knox et al., 2012; Laukova et al., 2014). We previously observed that SPS has a long lasting effect on activation of the HPA axis. A week after exposure to SPS stressors, corticosterone and ACTH in plasma and CRF, GR, and FKBP5 mRNAs in the mediobasal hypothalamus were still significantly above levels in unstressed animals (Laukova et al., 2014; Sabban et al., 2015b).

The results of experiments presented here revealed than activation of Y1 receptors with [Leu³¹Pro³⁴]NPY immediately after exposure to SPS stressors can prevent development of abnormal expression of CRF in the PVN which might also related to physiologically normal immobility time in the FST in these rats. In contrast to rats treated with NPY, rats infused with [Leu³¹Pro³⁴]NPY still had robustly elevated mRNA levels for GR and FKBP5. Moreover the levels of these two mRNAs were even

higher than in the rats administered with vehicle. A dissociation of the effects on CRF gene expression from those on GR and FKBP5 in the mediobasal hypothalamus was also observed with the melanocortin 4 receptor antagonist, HS014 (Serova et al., 2014).

Although hypothalamic GR plays a major role in glucocorticoid-dependent feedback mechanism regulating CRF gene expression, our results suggest that normalization of CRF gene expression with [Leu³¹Pro³⁴]NPY may be mediated by other pathways. The PVN receives inputs from the medial amygdala indirectly via the bed nucleus of the stria terminalis and from the ventral hippocampus via interneurons (López et al., 1999; Ulrich-Lai and Herman, 2009) which indirectly control CRF expression. In this regard, disruption of GR in the PVN led to HPA hyperactivity but did not affect anxiety and despair-like behavior (Laryea et al., 2013). In contrast to CRF, GR synthesis in the mediobasal hypothalamus is not restricted to the PVN (Aronsson et al., 1988). Thus, our findings with GR may reflect stimulation of Y1 receptors on different mediobasal hypothalamic cell types other than the PVN.

Overall the results indicate that while [Leu³¹Pro³⁴]NPY can be similarly effective as NPY with therapeutic potential in PTSD for preventing development of depressive-like behaviors and dysregulation of CRF/HPA system at the level of the PVN. However, issues relating to its effect on GR and FKBP5 gene expression indicate that it might not be as useful therapeutically as NPY.

AUTHOR CONTRIBUTIONS

Each of the authors made a significant contribution to the manuscript. ES and LS, design, analysis, interpretation of the data and writing the manuscript. HM, performance of experiment on gene expression, participation in interpretation of data, and in review of manuscript.

ACKNOWLEDGMENTS

We thank Matt Forman for assistance with the behavioral tests. This work was supported by the funds from the NYMC/Touro Bridge Funding Program and by Office of the Assistant Secretary of Defense for Health Affairs through the DOD Department of Defense Broad Agency Announcement for Extramural Medical Research under Award No W81XWH-16-1-0016. Opinions, interpretations, conclusions and recommendations are those of the authors and not necessarily endorsed by the Department of Defense or the US Army.

REFERENCES

- Aronsson, M., Fuxé, K., Dong, Y., Agnati, L. F., Okret, S., and Gustafsson, J. A. (1988). Localization of glucocorticoid receptor mRNA in the male rat brain by *in situ* hybridization. *Proc. Natl. Acad. Sci. U.S.A.* 85, 9331–9335. doi: 10.1073/pnas.85.23.9331
- Brady, L. S., Whitfield, H. J., Fox, R. J., Gold, P. W., and Herkenham, M. (1991). Long-term antidepressant administration alters corticotropin-releasing hormone, tyrosine hydroxylase, and mineralocorticoid receptor gene expression in rat brain. Therapeutic implications. *J. Clin. Invest.* 87, 831–837. doi: 10.1172/jci115086
- Briones, T. L., and Woods, J. (2013). Chronic binge-like alcohol consumption in adolescence causes depression-like symptoms possibly mediated by the effects of BDNF on neurogenesis. *Neuroscience* 254, 324–334. doi: 10.1016/j.neuroscience.2013.09.031
- Brothers, S. P., and Wahlestedt, C. (2010). Therapeutic potential of neuropeptide Y (NPY) receptor ligands. *EMBO Mol. Med.* 2, 429–439. doi: 10.1002/emmm.201000100

- Cassaglia, P. A., Shi, Z., Li, B., Reis, W. L., Clute-Reinig, N. M., Stern, J. E., et al. (2014). Neuropeptide Y acts in the paraventricular nucleus to suppress sympathetic nerve activity and its baroreflex regulation. *J. Physiol.* 592, 1655–1675. doi: 10.1113/jphysiol.2013.268763
- Cryan, J. F., Markou, A., and Lucki, I. (2002). Assessing antidepressant activity in rodents: recent developments and future needs. *Trends Pharmacol. Sci.* 23, 238–245. doi: 10.1016/S0165-6147(02)02017-5
- Dimitrov, E. L., DeJoseph, M. R., Brownfield, M. S., and Urban, J. H. (2007). Involvement of neuropeptide Y Y1 receptors in the regulation of neuroendocrine corticotropin-releasing hormone neuronal activity. *Endocrinology* 148, 3666–3673. doi: 10.1210/en.2006-1730
- Enman, N. M., Sabban, E. L., McGonigle, P., and Van Bockstaele, E. J. (2015). Targeting the neuropeptide Y system in stress-related psychiatric disorders. *Neurobiol. Stress* 1, 33–43. doi: 10.1016/j.ynstr.2014.09.007
- Eva, C., Serra, M., Mele, P., Panzica, G., and Oberto, A. (2006). Physiology and gene regulation of the brain NPY Y1 receptor. *Front. Neuroendocrinol.* 27, 308–339. doi: 10.1016/j.yfrne.2006.07.002
- Gerald, C., Walker, M. W., Criscione, L., Gustafson, E. L., Batzl-Hartmann, C., Smith, K. E., et al. (1996). A receptor subtype involved in neuropeptide-Y-induced food intake. *Nature* 382, 168–171. doi: 10.1038/382168a0
- Goyal, S. N., Upadhyay, M. A., Kokare, D. M., Bhisikar, S. M., and Subhedar, N. K. (2009). Neuropeptide Y modulates the antidepressant activity of imipramine in olfactory bulbectomized rats: involvement of NPY Y1 receptors. *Brain Res.* 1266, 45–53. doi: 10.1016/j.brainres.2009.02.033
- Heilig, M. (2004). The NPY system in stress, anxiety and depression. *Neuropeptides* 38, 213–224. doi: 10.1016/j.npep.2004.05.002
- Hirsch, D., and Zukowska, Z. (2012). NPY and stress 30 years later: the peripheral view. *Cell. Mol. Neurobiol.* 32, 645–659. doi: 10.1007/s10571-011-9793-z
- Jiménez-Vasquez, P. A., Diaz-Cabiale, Z., Caberlotto, L., Bellido, I., Overstreet, D., Fuxe, K., et al. (2007). Electroconvulsive stimuli selectively affect behavior and neuropeptide Y (NPY) and NPY Y(1) receptor gene expressions in hippocampus and hypothalamus of flinders sensitive line rat model of depression. *Eur. Neuropsychopharmacol.* 17, 298–308. doi: 10.1016/j.euroneuro.2006.06.011
- Karlsson, R. M., Choe, J. S., Cameron, H. A., Thorsell, A., Crawley, J. N., Holmes, A., et al. (2008). The neuropeptide Y Y1 receptor subtype is necessary for the anxiolytic-like effects of neuropeptide Y, but not the antidepressant-like effects of fluoxetine, in mice. *Psychopharmacology (Berl.)* 195, 547–557. doi: 10.1007/s00213-007-0945-2
- Kask, A., Harro, J., von Hörsten, S., Redrobe, J. P., Dumont, Y., and Quirion, R. (2002). The neurocircuitry and receptor subtypes mediating anxiolytic-like effects of neuropeptide Y. *Neurosci. Biobehav. Rev.* 26, 259–283. doi: 10.1016/S0149-7634(01)00066-5
- Knox, D., Nault, T., Henderson, C., and Liberzon, I. (2012). Glucocorticoid receptors and extinction retention deficits in the single prolonged stress model. *Neuroscience* 223, 163–173. doi: 10.1016/j.neuroscience.2012.07.047
- Kotagale, N. R., Paliwal, N. P., Aglawe, M. M., Umekar, M. J., and Taksande, B. G. (2013). Possible involvement of neuropeptide Y Y1 receptors in antidepressant like effect of agmatine in rats. *Peptides* 47, 7–11. doi: 10.1016/j.peptides.2013.04.018
- Laryea, G., Schütz, G., and Muglia, L. J. (2013). Disrupting hypothalamic glucocorticoid receptors causes HPA axis hyperactivity and excess adiposity. *Mol. Endocrinol.* 27, 1655–1665. doi: 10.1210/me.2013-1187
- Laukova, M., Alaluf, L. G., Serova, L. I., Arango, V., and Sabban, E. L. (2014). Early intervention with intranasal NPY prevents single prolonged stress-triggered impairments in hypothalamus and ventral hippocampus in male rats. *Endocrinology* 155, 3920–3933. doi: 10.1210/en.2014-1192
- Livak, K. J., and Schmittgen, T. D. (2001). Analysis of relative gene expression data using real-time quantitative PCR and the $2^{-\Delta\Delta C_T}$. *Methods* 25, 402–408. doi: 10.1006/meth.2001.1262
- López, J. F., Akil, H., and Watson, S. J. (1999). Neural circuits mediating stress. *Biol. Psychiatry* 46, 1461–1471. doi: 10.1016/S0006-3223(99)00266-8
- Mehta, D., Gonik, M., Klengel, T., Rex-Haffner, M., Menke, A., Rubel, J., et al. (2011). Using polymorphisms in FKBP5 to define biologically distinct subtypes of posttraumatic stress disorder: evidence from endocrine and gene expression studies. *Arch. Gen. Psychiatry* 68, 901–910. doi: 10.1001/archgenpsychiatry.2011.50
- Michel, M. C., Beck-Sickinger, A., Cox, H., Doods, H. N., Herzog, H., Larhammar, D., et al. (1998). XVI. International Union of Pharmacology recommendations for the nomenclature of neuropeptide Y, peptide YY, and pancreatic polypeptide receptors. *Pharmacol. Rev.* 50, 143–150.
- Mironova, V., Rybnikova, E., and Pivina, S. (2013). Effect of inescapable stress in rodent models of depression and posttraumatic stress disorder on CRH and vasopressin immunoreactivity in the hypothalamic paraventricular nucleus. *Acta Physiol. Hung.* 100, 395–410. doi: 10.1556/APhysiol.100.2013.4.4
- Morales-Medina, J. C., Dumont, Y., and Quirion, R. (2010). A possible role of neuropeptide Y in depression and stress. *Brain Res.* 1314, 194–205. doi: 10.1016/j.brainres.2009.09.077
- Redrobe, J. P., Dumont, Y., Fournier, A., and Quirion, R. (2002). The neuropeptide Y (NPY) Y1 receptor subtype mediates NPY-induced antidepressant-like activity in the mouse forced swimming test. *Neuropsychopharmacology* 26, 615–624. doi: 10.1016/S0893-133X(01)00403-1
- Reichmann, F., and Holzer, P. (2016). Neuropeptide Y: a stressful review. *Neuropeptides* 55, 99–109. doi: 10.1016/j.nep.2015.09.008
- Sabban, E. L., Alaluf, L. G., and Serova, L. I. (2016). Potential of neuropeptide Y for preventing or treating post-traumatic stress disorder. *Neuropeptides* 56, 19–24. doi: 10.1016/j.npep.2015.11.004
- Sabban, E. L., Laukova, M., Alaluf, L. G., Olsson, E., and Serova, L. I. (2015a). Locus coeruleus response to single-prolonged stress and early intervention with intranasal neuropeptide Y. *J. Neurochem.* 135, 975–986. doi: 10.1111/jnc.13347
- Sabban, E. L., Serova, L. I., Alaluf, L. G., Laukova, M., and Peddu, C. (2015b). Comparative effects of intranasal neuropeptide Y and HS014 in preventing anxiety and depressive-like behavior elicited by single prolonged stress. *Behav. Brain Res.* 295, 9–16. doi: 10.1016/j.bbr.2014.12.038
- Sah, R., and Geraciotti, T. D. (2013). Neuropeptide Y and posttraumatic stress disorder. *Mol. Psychiatry* 18, 646–655. doi: 10.1038/mp.2012.101
- Schmeltzer, S. N., Herman, J. P., and Sah, R. (2016). Neuropeptide Y (NPY) and posttraumatic stress disorder (PTSD): a translational update. *Exp. Neurol.* 284, 196–210. doi: 10.1016/j.expneurol.2016.06.020
- Serova, L. I., Tillinger, A., Alaluf, L. G., Laukova, M., Keegan, K., and Sabban, E. L. (2013). Single intranasal neuropeptide Y infusion attenuates development of PTSD-like symptoms to traumatic stress in rats. *Neuroscience* 236, 298–312. doi: 10.1016/j.neuroscience.2013.01.040
- Serova, L. I., Laukova, M., Alaluf, L. G., and Sabban, E. L. (2014). Blockage of menanocortin-4 receptors by intranasal HS014 attenuates single prolonged stress-triggered changes in several brain regions. *J. Neurochem.* 131, 825–835. doi: 10.1111/jnc.12847
- Ulrich-Lai, Y. M., and Herman, J. P. (2009). Neural regulation of endocrine and autonomic stress responses. *Nat. Rev. Neurosci.* 10, 397–409. doi: 10.1038/nrn2647
- Widdowson, P. S., Buckingham, R., and Williams, G. (1997). Distribution of [Leu31,Pro34]NPY-sensitive, BIBP3226-insensitive [¹²⁵I]PYY(3-6) binding sites in rat brain: possible relationship to Y5 NPY receptors. *Brain Res.* 778, 242–250.
- Wu, G., Feder, A., Wegener, G., Bailey, C., Saxena, S., Charney, D., et al. (2011). Central functions of neuropeptide Y in mood and anxiety disorders. *Expert Opin. Ther. Targets* 15, 1317–1331. doi: 10.1517/14728222.2011.628314
- Yehuda, R. (2009). Status of glucocorticoid alterations in post-traumatic stress disorder. *Ann. N.Y. Acad. Sci.* 1179, 56–69. doi: 10.1111/j.1749-6632.2009.04979.x
- Conflict of Interest Statement:** The authors declare that the research was conducted in the absence of any commercial or financial relationships that could be construed as a potential conflict of interest.
- Copyright © 2017 Serova, Mulhall and Sabban. This is an open-access article distributed under the terms of the Creative Commons Attribution License (CC BY). The use, distribution or reproduction in other forums is permitted, provided the original author(s) or licensor are credited and that the original publication in this journal is cited, in accordance with accepted academic practice. No use, distribution or reproduction is permitted which does not comply with these terms.



Involvement of the Bradykinin B₁ Receptor in Microglial Activation: *In Vitro* and *In Vivo* Studies

Keren Asraf, Nofar Torika, Abraham Danon and Sigal Fleisher-Berkovich*

Department of Clinical Biochemistry and Pharmacology, Ben-Gurion University of the Negev, Beer-Sheva, Israel

OPEN ACCESS

Edited by:

Hubert Vaudry,
University of Rouen, France

Reviewed by:

Mami Noda,
Kyushu University, Japan
Laurent Gautron,
University of Texas Southwestern
Medical Center, USA
Marie-Christine Tonon,
University of Rouen, France

*Correspondence:

Sigal Fleisher-Berkovich
fleisher@bgu.ac.il

Specialty section:

This article was submitted to
Neuroendocrine Science,
a section of the journal
Frontiers in Endocrinology

Received: 14 November 2016

Accepted: 30 March 2017

Published: 19 April 2017

Citation:

Asraf K, Torika N, Danon A and
Fleisher-Berkovich S (2017)
Involvement of the Bradykinin B₁
Receptor in Microglial Activation:
In Vitro and *In Vivo* Studies.
Front. Endocrinol. 8:82.
doi: 10.3389/fendo.2017.00082

The importance of brain inflammation to Alzheimer's disease (AD) pathogenesis has been accepted of late, with it currently being held that brain inflammation aggravates AD pathology. One important aspect of brain inflammation is the recruitment and activation of microglia, a process termed microgliosis. Kinins and bradykinin (BK), in particular, are major pro-inflammatory mediators in the periphery, although all of the factors comprising the kinin system have also been described in the brain. Moreover, it was shown that the amyloid β (A β) peptide (a component of AD plaques) enhances kinin secretion and activates BK receptors that can, in turn, stimulate A β production. Still, the role of bradykinin in modulating brain inflammation and AD is not completely understood. In this study, we aimed to investigate the roles of the bradykinin B₁ receptor (B₁R) and bradykinin B₂ receptor (B₂R) in regulating microglial secretion of pro-inflammatory factors *in vitro*. Furthermore, the effects of intranasal administration of specific B₁R and B₂R antagonists on A β burden and microglial accumulation in the brains of transgenic AD mice were studied. The data obtained show that neither R-715 (a B₁R antagonist) nor HOE 140 (a B₂R antagonist) altered microglial cell viability. However, R-715, but not HOE 140, markedly increased lipopolysaccharide-induced nitric oxide (NO) and tumor necrosis factor-alpha (TNF- α) release, as well as inducible nitric oxide synthase expression in BV2 microglial cells. Neither antagonist altered NO nor TNF- α production in non-stimulated cells. We also showed that intranasal administration of R-715 but not HOE 140 to 8-week-old 5X familial AD mice enhanced amyloid burden and microglia/macrophage accumulation in the cortex. To conclude, we provide evidence supporting a role of B₁R in brain inflammation and in the regulation of amyloid deposition in AD mice, possibly with microglial/macrophage involvement. Further studies are required to test whether modulation of this receptor can serve as a novel therapeutic strategy for AD.

Keywords: bradykinin, brain inflammation, HOE 140, microglia, R-715

INTRODUCTION

Alzheimer's disease (AD) is a prevalent neurodegenerative disease (1) that is characterized by two neuropathological hallmarks, namely the deposition of amyloid β plaques and the accumulation of neurofibrillary tangles (2, 3). The role that brain inflammation plays in AD pathogenesis has only recently been appreciated. Currently, brain inflammation is thought to contribute to and to exacerbate AD pathology (4, 5). One important aspect of the central immune response to brain inflammation is microglial activation.

Microglia are the resident phagocytes of the brain. These cells use their processes to scan the brain for pathogens and debris (6). Microglia also maintain brain plasticity and remodel synapses (7, 8). In AD, microglia bind soluble amyloid β (A β) oligomers and fibrils and become activated. The activated microglia then start to engulf A β fibrils by phagocytosis. Inefficient phagocytosis of A β has been identified as a major pathogenic pathway (5). Microglia are likely to exist in a range of phenotypic states during chronic inflammation in AD. Upon binding to A β , microglia release pro-inflammatory molecules, such as interleukin-1 β (IL-1 β), tumor necrosis factor-alpha (TNF- α), and IL-12, as well as reactive oxygen species, like nitric oxide (NO) (9–11). In turn, pro-inflammatory conditions promote neuronal damage mediated by A β and decrease the phagocytosis of these oligomers and their degradation by microglia (12, 13).

Although much is known of the molecular basis of initiating signals and pro-inflammatory chemical mediators in brain inflammation, it has only recently become apparent that endogenous stop signals are critical players at early checkpoints during the various stages of brain inflammation. Some neuropeptides that are produced during the ongoing inflammatory response have emerged as endogenous anti-inflammatory agents that participate in the regulation of processes that ensure self-tolerance and/or inflammation resolution. Neuropeptides, such as kinins, can regulate brain inflammation and affect microglial functions both *in vitro* and *in vivo* (14, 15). Thus, the release of these factors can determine whether microglia assume a neuroprotective phenotype.

Kinins, in particular bradykinin (BK), are pro-inflammatory mediators in the periphery. At peripheral sites, BK can elicit all of the major signs of inflammation, namely pain, hyper-perfusion, and increased vascular permeability (16–19). All kinin system components have also been described in the central nervous system (20). Indeed, high BK levels are found after brain trauma and ischemia (21). Furthermore, it was shown that A β upregulates BK receptors and kinin release, followed by BK-induced A β synthesis (22). Still, the role that bradykinin plays in AD modulation is not completely understood. BK activates two types of receptors, namely, the B₁ receptor [bradykinin B₁ receptor (B₁R)] and the B₂ receptor [bradykinin B₂ receptor (B₂R)] (23, 24). B₂R is a constitutive receptor and has high affinity for BK, while B₁R is generally upregulated following tissue injury and binds with high affinity to des-Arg⁹-BK, a kinin metabolite (24). In the brain, microglial cells express both receptors (14, 25).

In the present study, our intent was to investigate the contributions of B₁R and B₂R in mediating microglial inflammation *in vitro*. Moreover, the *in vivo* influence of intranasal administration of specific B₁R and B₂R antagonists on A β burden and microglial accumulation in brains of transgenic AD mice was considered.

MATERIALS AND METHODS

Cell Cultures

The BV2 microglial cell line (provided by Prof. Rosario Donato, Department of Experimental Medicine and Biochemical Sciences, University of Perugia) was seeded in 6-well, 24-well, or 96-well

plates at densities of 1×10^6 , 3×10^5 , and 2×10^4 cells per well, respectively. Cells were maintained in RPMI-1640 supplemented with 10% fetal calf serum and 0.4 mM L-glutamine. To create a sterile environment, 100 U/ml of penicillin and 100 μ g/ml of streptomycin were added. Cells were grown in humidified atmosphere of 5% CO₂ at 37°C. At the beginning of each experiment, the cells were incubated with serum-free medium (SFM) for 4 h, followed by a 22-h incubation with the indicated test agents in SFM supplemented with 0.1% bovine serum albumin (BSA) and 10 mM HEPES (pH 7.4). BV2 cells were treated with R-715, a B₁R selective antagonist, and HOE 140, a B₂R selective antagonist, both purchased from GL Biochem (Shanghai, China), lipopolysaccharide (LPS) from *Escherichia coli* serotype 055:B5 was purchased from Sigma Aldrich (St. Louis, MO, USA).

Cell Count

At the end of each experiment, cells were harvested after incubation with 1 ml SFM for 1 h at 4°C and counted using a Z1 Coulter counter (Coulter Electronics, Miami, FL, USA).

Cell Viability

Cell viability was determined by a Cell Proliferation Kit (XTT) (Biological Industries, Kibbutz Beit-Haemek, Israel) according to the manufacturer's instructions. The assay was performed using a microplate reader (Bio-Rad model 680).

Determination of NO Levels

(Griess Reaction)

Nitrite levels were determined in the culture supernatants using the Griess reaction. Nitrite standard curve samples or supernatants (100 μ l each) were mixed with 100 μ l Griess reagent (Sigma-Aldrich) in 96-well plates. Thereafter, the plates were incubated for 15 min in the dark at room temperature. Nitrite levels were measured with a microplate reader at 540 nm.

Determination of TNF- α Levels (ELISA)

Tumornecrosisfactor- α levels were measured using an enzyme-linked immunosorbent assay (ELISA) kit (BD Biosciences, San Diego, CA, USA) according to the manufacturer's instructions.

SDS Polyacrylamide Gel Electrophoresis and Western Blot Analysis

The expression levels of inducible nitric oxide synthase (iNOS) protein in BV2 microglial cells were analyzed by Western blot (26). Briefly, cells were harvested using lysis buffer (20 mM HEPES pH 7.4, 150 mM NaCl, 1 mM EDTA, 1 mM EGTA, 10% glycerol, 1 mM MgCl₂, 1% Triton X-100, and 1% deoxycholic acid) containing a protease inhibitor cocktail. Cells lysates were incubated at 4°C for 30 min, followed by a 15 min centrifugation (12,000 g) at 4°C. Thereafter, protein levels were determined by Bradford assay (Bio-Rad). Aliquots of whole cell lysates containing 40 μ g protein were denatured and separated on 7.5% polyacrylamide-SDS gels and transferred to nitrocellulose membranes. Non-specific sites were blocked by 4% BSA (90 min incubation at room temperature). This was followed by overnight incubation at 4°C with rabbit anti-iNOS antibodies (1:500;

Cayman Chemicals, Ann Arbor, MI, USA). After washing, the membranes were incubated with IgG-horseradish peroxidase (HRP)-conjugated donkey anti-rabbit antibodies (1:5,000; GE Healthcare, Buckinghamshire, UK) for 90 min at room temperature. Finally, enhanced chemiluminescence solution was added, and the membranes were exposed to X-ray film (Fuji medical X-ray film, FujiFilm). Protein levels were normalized to β -actin levels using mouse monoclonal anti- β -actin antibodies (1:25,000; MP Biological, Santa Ana, CA, USA) and HRP-conjugated goat anti-mouse antibodies (1:20,000; Jackson ImmunoResearch Laboratories, West Grove, PA, USA). A computerized image analysis system (EZ Quant-Gel 2.2, EZQuant Biology Software Solutions, Israel) was used for semi-quantitative analysis.

Mice

Wild-type (WT) C57BL/6 mice were purchased from Harlan Israel (Jerusalem, Israel). Transgenic 5X familial AD (5XFAD) mice were provided by Prof. Robert Vassar (Department of Cell and Molecular Biology, Northwestern University). 5XFAD mice include five mutations under the transcriptional control of the neuron-specific mouse Thy-1 promoter, with three mutations in the human APP695 gene (Swedish K670N, M671L, Florida I716V and London V717I) and two mutations in the human presenilin-1 gene (M146L, L286V). At the age of 2 months, 5XFAD mice evolve A β accumulation and gliosis (27). The human APP gene was detected by PCR analysis of mice tail tissue DNA. Mice were placed in cages at temperatures of $22 \pm 2^\circ\text{C}$ and 65% humidity. Food and water supply was made available, and a 12 h light/dark cycle was maintained. All animal studies were performed according to the recommendations of Institutional Animal Care and Use Committee of Ben-Gurion University of the Negev. The protocol employed was approved by this committee (approval number IL-30-08-2011).

In the first experiment, 8-week-old mice were divided into three groups, namely WT mice treated with R-715, 5XFAD mice treated with saline, and 5XFAD mice treated with R-715. In the second experiment, mice were again divided into three groups, namely WT mice treated with HOE 140, 5XFAD mice treated with saline, and 5XFAD mice treated with HOE 140. The mice received daily intranasal treatment of 1 mg/kg per day for 18 days (5 days/week).

Immunohistochemistry

Mice were anesthetized upon intra-peritoneal injection of 0.2 ml ketamine–xylazine mixer (1:1). Brains were removed following cold PBS cardiac perfusion and were divided into two hemispheres. One hemisphere from each mouse brain was incubated overnight in 4% paraformaldehyde solution at 4°C , followed by incubation in 30% sucrose solution at 4°C for 2 days. The hemispheres were then frozen in molds containing tissue adhesive (O.C.T. compound, Tissue-Tek, Torrance, CA, USA) at -80°C . All hemispheres were cut into sagittal sections (40 μm) using a cryostat and maintained at -20°C in PBS:ethyleneglycol:glycerol (2:1:1) non-freezing solution. Free-floating sections were washed using 0.05% PBS/Tween 20 and permeabilized using 0.5% PBS/Triton X-100. After blocking non-specific binding using antibody diluent solution (GBI Labs, Mukilteo, WA, USA), sections were

incubated for 2 h at room temperature with rabbit anti-human A β (1:250; a gift from Prof. Alon Monsonego, The Shraga Segal Department of Microbiology and Immunology, Faculty of Health Sciences and the National Institute of Biotechnology in the Negev, Ben-Gurion University of the Negev) and rat anti-mouse/human CD11b antibodies (1:25, Biolegend). Primary antibodies were diluted in antibody diluent solution. Thereafter, the sections were rinsed and incubated for 1 h at room temperature with the appropriate secondary antibody, i.e., Cy³-conjugated donkey anti-rabbit IgG (1:1,000) or Alexa fluor 488-conjugated goat anti-rat IgG (1:250), both from Jackson ImmunoResearch Laboratories. Secondary antibodies were diluted in 0.05% PBS/Tween 20. After washes, the sections were mounted with mounting medium containing DAPI (Vector labs) on charged slides and stored at 4°C . An Olympus Fluoview FV1000 confocal microscope (Olympus, Hamburg, Germany) at $1,024 \times 1,024$ pixel resolution with a $\times 10$ objective was used for imaging. In each experiment, five sections from the cortex of each animal were analyzed. A β and CD11b staining was quantified using the ImageJ software version 1.40C (NIH). Average fluorescent A β - and CD11b-containing areas were calculated for each treated group.

Statistical Analysis

For each experiment, results are presented as the mean \pm SEM. To assess the statistical significance of differences between treatment groups, one-way analysis of variance was performed, followed by a *post hoc* multiple comparison test (Tukey–Kramer Multiple Comparison Test). $P < 0.05$ was considered statistically significant.

RESULTS

Serving as a positive control, actinomycin D, significantly reduced BV2 microglial cell viability (Figure 1). By contrast, neither the B₁R antagonist R-715 at concentrations of 10^{-7} and 10^{-6} M (Figure 1A) nor the B₂R antagonist HOE 140 at a concentration of 10^{-6} M (Figure 1B) altered microglial cell viability, as measured with XTT assay.

The production of NO (Figure 2A) and TNF- α (Figure 2B) in non-stimulated BV2 cells or in BV2 cells induced by LPS (7 ng/ml) and treated with R-715 (10^{-7} and 10^{-6} M) was next considered. LPS markedly enhanced NO and TNF- α production, as compared with controls. R-715 at concentrations of 10^{-7} and 10^{-6} M significantly increased LPS-induced NO secretion (Figure 2A). R-715, at concentrations of 10^{-7} and 10^{-6} M, also increased LPS-induced TNF- α secretion (Figure 2B). By contrast, R-715 did not alter NO (Figure 2A) or TNF- α (Figure 2B) production in non-stimulated cells. However, the selective B₂R antagonist HOE 140 failed to alter NO (Figure 3A) or TNF- α (Figure 3B) release from either non-stimulated or LPS-stimulated cells.

As shown in Figure 4, a 24-h treatment of BV2 cells with LPS (7 ng/ml) significantly increased iNOS expression levels. 10^{-6} M of R-715 increased the LPS-induced iNOS expression by up to 102%.

As anticipated, the cortex of WT mice intranasally administered with R-715 did not show any A β plaques (Figure 5A). Levels of both A β and CD11b (marker for microglial accumulation)

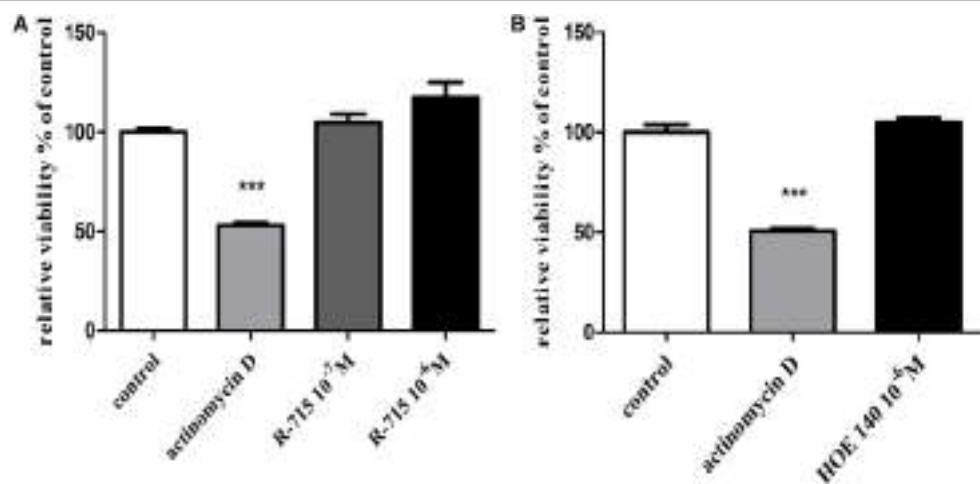


FIGURE 1 | Effects of bradykinin B₁ receptor (B₁R) and bradykinin B₂ receptor (B₂R) antagonists on the viability of BV2 cells. Cells were incubated with (A) the B₁R antagonist R-715 (10^{-7} and 10^{-6} M) or (B) the B₂R antagonist HOE 140 (10^{-6} M) for 24 h. At the end of the experiment, viability was assessed by the XTT assay. Results are given as mean \pm SEM, $n = 4$; a one-way analysis of variance and Tukey–Kramer Multiple Comparison Test were performed to determine statistical significance; *** $P < 0.001$ versus the control.

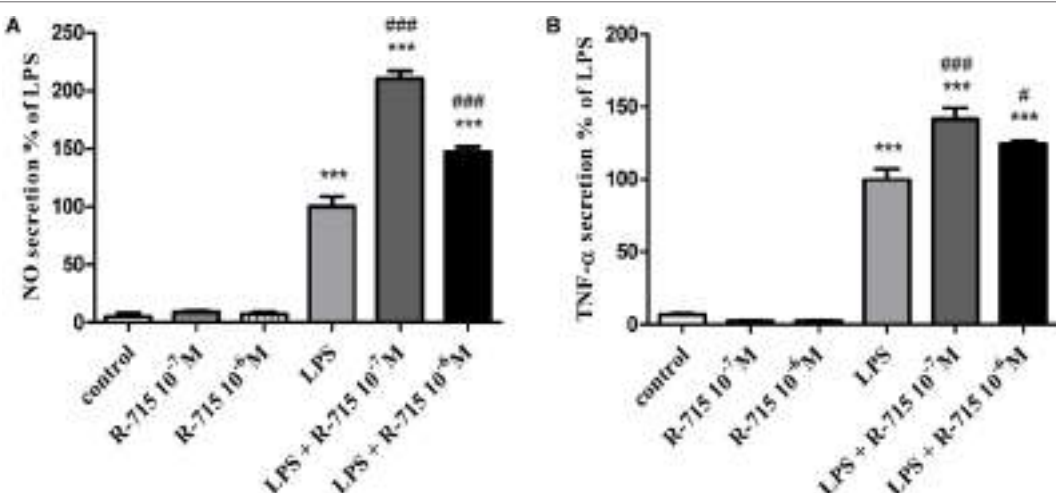


FIGURE 2 | Effects of the bradykinin B₁ receptor (B₁R) antagonist on basal and lipopolysaccharide (LPS)-induced NO and tumor necrosis factor-alpha (TNF- α) release from BV2 cells. Cells were incubated with the B₁R antagonist R-715 (10^{-7} and 10^{-6} M) in the presence or absence of LPS (7 ng/ml) for 24 h. NO (A) and TNF- α (B) levels were measured in the media, and the cells were counted. Results are representatives of three independent experiments and are presented as mean \pm SEM, $n = 3$ –6; statistical significance was assessed by one-way analysis of variance followed by a Tukey–Kramer Multiple Comparison Test; *** $P < 0.001$ versus the control, ## $P < 0.001$ versus LPS, and # $P < 0.05$ versus LPS.

were significantly enhanced in age-matched 5XFAD mice treated intranasally with the vehicle (Figure 5). However, as compared to 5XFAD mice treated with the vehicle, age-matched 5XFAD mice treated intranasally with R-715 (1 mg/kg/day) showed close to 100 and 50% increases in A β burden (Figures 5A,D) and CD11b staining (Figures 5B,D), respectively. 5XFAD mice intranasally treated with HOE 140 did not display any differences in plaque burden (Figures 6A,D) or CD11b staining (Figures 6B,D) in the cortex, as compared to vehicle-treated mice. Modified Figures 5 and 6 are adapted with permission from Asraf et al. (28).

DISCUSSION

Although BK is generally viewed as a central pro-inflammatory mediator (25, 29, 30), a possible protective role for BK in the brain has been proposed. Recently, we showed a dual effect of kinins on the production of prostaglandin (PG), a pro-inflammatory mediator, in cultured glial cells (i.e., microglia and astrocytes) (31). Specifically, the activation of B₂ receptors increased PG synthesis, whereas B₁R agonists inhibited synthesis of these pro-inflammatory mediators. We have, therefore, suggested that a regulatory loop exists in which B₂ receptors mediate enhanced-glial inflammation.

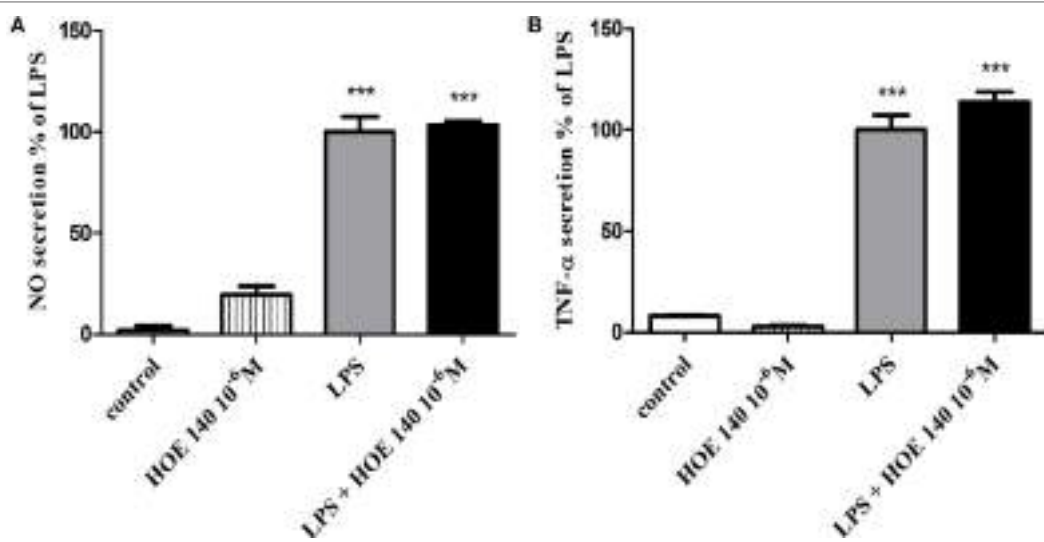


FIGURE 3 | Effect of the bradykinin B₂ receptor (B₂R) antagonist on basal and lipopolysaccharide (LPS)-induced NO and tumor necrosis factor-alpha (TNF- α) release from BV2 cells. Cells were incubated with the B₂R antagonist HOE 140 (10^{-6} M) in the presence or absence of LPS (7 ng/ml) for 24 h. NO (A) and TNF- α (B) levels were measured in the media, and the cells were counted. Results are representatives of three independent experiments and are presented as mean \pm SEM, $n = 3–6$; statistical significance was assessed by one-way analysis of variance followed by a Tukey-Kramer Multiple Comparison Test; *** $P < 0.001$ versus control.

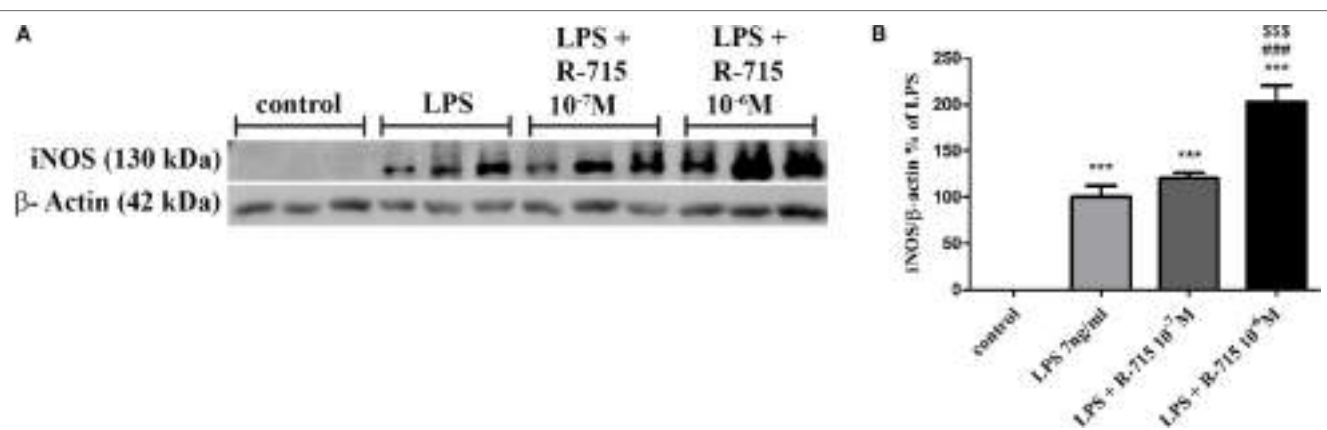


FIGURE 4 | Effect of the bradykinin B₁ receptor (B₁R) antagonist on iNOS expression in lipopolysaccharide (LPS)-stimulated BV2 cells. Cells were incubated with the B₁R antagonist R-715 (10^{-7} and 10^{-6} M) and LPS (7 ng/ml) for 24 h. Whole cell lysates (40 μ g) were examined by Western blot analysis using anti-iNOS or β -actin antibodies. The results shown here represent three independent experiments (A). The graph represents the mean \pm SEM of three experiments (B), $n = 3$. One-way analysis of variance and a Tukey-Kramer Test were used to determine statistical significance: *** $P < 0.001$ versus the control, *** $P < 0.001$ versus LPS, and **** $P < 0.001$ versus LPS + R-715 (10^{-7} M).

B₁ receptors are subsequently upregulated and are involved in the attenuation of glial inflammation (31). These findings were confirmed in part by Noda et al., who documented reduced microglial inflammation upon BK treatment of LPS-induced cells (32, 33). More recently, we also showed that a B₁ receptor agonist abrogated NO and TNF- α production in LPS-treated BV2 microglial cells (26).

In the present study, R-715 significantly enhanced iNOS expression and release of TNF- α and NO from BV2 microglia. Using immunocytochemistry, we previously demonstrated the expression of both B₁ and B₂ receptor sub-types in BV2 microglia (34). In the present study, B₁Rs are blocked by R-715, and no regulatory

feedback inhibition exists through B₁ receptors. This suggests that endogenous BK, possibly released from BV2 cells, activates B₂ receptors and contributes to the amplification of inflammation (TNF- α and NO synthesis) induced by LPS. Interestingly, BK and LPS were shown to induce B₂R expression and synergistically enhance nitrosative stress and inflammation in epithelial cells (35). Induction of activated microglial TNF- α and NO release is of particular relevance, as these pro-inflammatory cytokines are both associated with neuronal loss. iNOS expression and NO generation have been described in several brain pathologies, including AD (36). Microglial iNOS is induced by A β both *in vitro* and *in vivo* and activated iNOS-expressing microglia were found

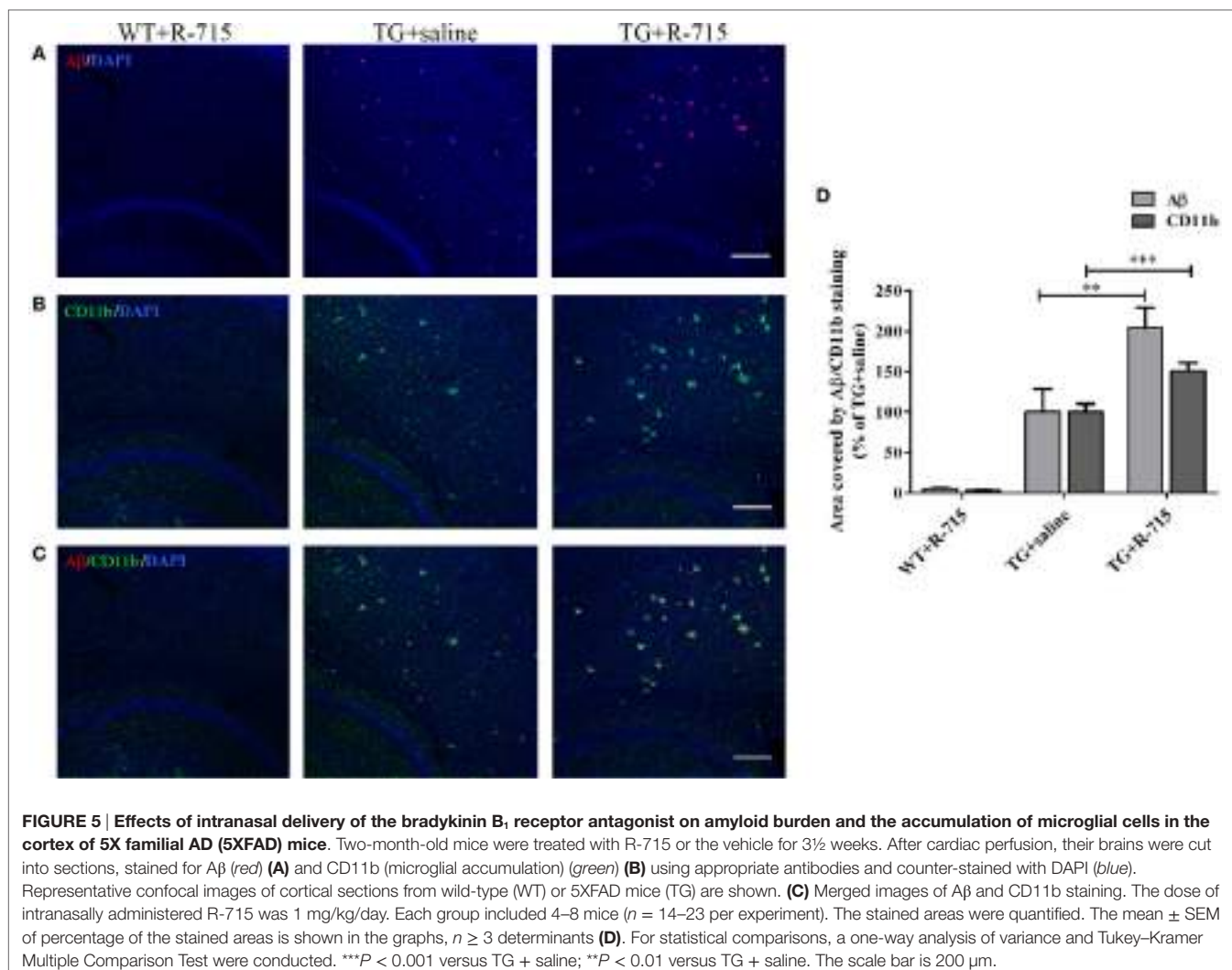


FIGURE 5 | Effects of intranasal delivery of the bradykinin B₁ receptor antagonist on amyloid burden and the accumulation of microglial cells in the cortex of 5X familial AD (5XFAD) mice. Two-month-old mice were treated with R-715 or the vehicle for 3½ weeks. After cardiac perfusion, their brains were cut into sections, stained for A β (red) (**A**) and CD11b (microglial accumulation) (green) (**B**) using appropriate antibodies and counter-stained with DAPI (blue). Representative confocal images of cortical sections from wild-type (WT) or 5XFAD mice (TG) are shown. (**C**) Merged images of A β and CD11b staining. The dose of intranasally administered R-715 was 1 mg/kg/day. Each group included 4–8 mice ($n = 14$ –23 per experiment). The stained areas were quantified. The mean \pm SEM of percentage of the stained areas is shown in the graphs, $n \geq 3$ determinants (**D**). For statistical comparisons, a one-way analysis of variance and Tukey–Kramer Multiple Comparison Test were conducted. *** P < 0.001 versus TG + saline; ** P < 0.01 versus TG + saline. The scale bar is 200 μ m.

in amyloid plaques surrounded by dead and dystrophic neurons. Various modes and mechanisms by which NO can lead to neuronal death have been described (37, 38). TNF- α is also associated with neurodegeneration and furthermore induces the expression of amyloid precursor protein and promotes its cleavage by stimulating secretase activity to release A β . Reciprocally, A β induces TNF- α synthesis in neurons and glial cells. In addition, A β has been shown to physically bind TNFR-1, thereby inducing neuronal death (39).

For *in vivo* studies, the five familial Alzheimer's disease (5XFAD) mouse model was employed. These mice develop rapid A β deposits alongside microglial accumulation beginning at 2 months of age, with plaques initially accumulate in the cortex. As shown in Figure 5, intranasal treatment of these mice with R-715 for 3.5 weeks significantly enhanced amyloid burden and CD11b expression in the cortex. Intranasal application of this B₁R antagonist was chosen since this mode of delivery likely increases the direct action of the compound by bypassing the blood–brain barrier. Moreover, clinical studies involving nasal application of other compounds, such as insulin, to AD patients showed improvement in memory skills (40). However, peripheral effects of the antagonist cannot be ruled out. Furthermore, the effectiveness of the passage of peptides from

nose to brain is controversial (41). Intranasal delivery of B₁R or B₂R antagonists has been tried here, for the first time. Similar results as those reported here were, nonetheless, reported by Passos et al., who showed that an 8 month-long treatment of triple mutant APP (Tg-SwDI) mice with R-715 resulted in enhanced amyloid burden (42). Antagonism of B₁R using R-715 also resulted in significantly greater severity of multiple sclerosis in a mouse model of the disease (43). On the other hand, there is evidence suggesting a role for B₂Rs in regulating brain inflammation and AD. Upregulation of B₁ and B₂ receptors in A β -infused rats was observed, mainly in brain regions such as the hippocampus and cortex, suggesting the possible involvement of kinins in AD (44). In a mouse model of AD, Prediger et al. showed improvement of cognitive deficits by genetic deletion or pharmacological antagonism of B₁ or B₂ receptors (45). Blockage of B₂ receptor, as shown by Bicca et al., prevented A β -induced cognitive impairment by inhibiting brain inflammation (46). Moreover, differential roles of B₁ and B₂ receptors in memory consolidation were observed during aging in mice.

B₁ and B₂ receptors transduce their signals through similar cellular pathways. They both are generally described as signaling through G α q and G α i. However, B₂ receptors also interact with

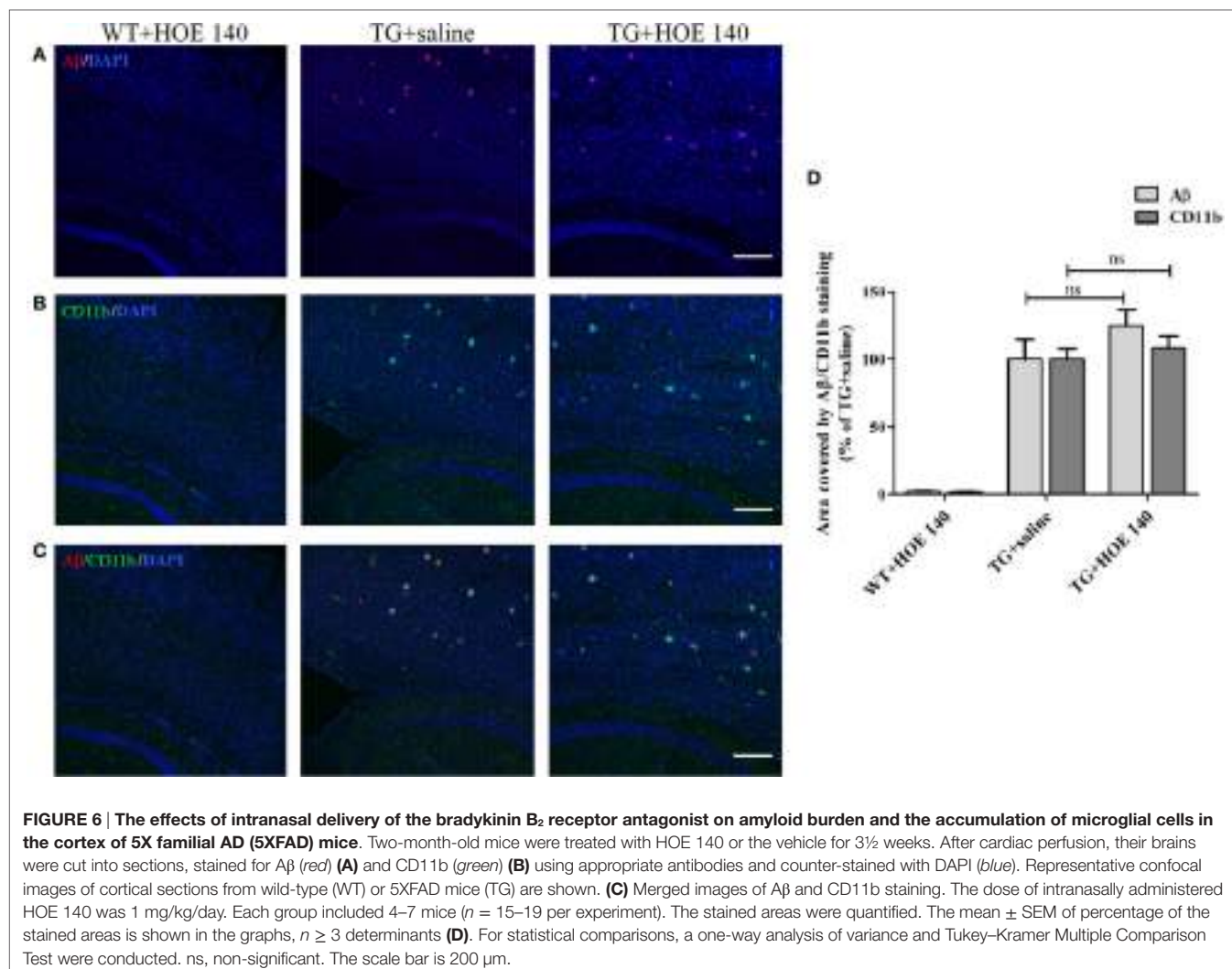


FIGURE 6 | The effects of intranasal delivery of the bradykinin B₂ receptor antagonist on amyloid burden and the accumulation of microglial cells in the cortex of 5X familial AD (5XFAD) mice. Two-month-old mice were treated with HOE 140 or the vehicle for 3½ weeks. After cardiac perfusion, their brains were cut into sections, stained for A_β (red) (**A**) and CD11b (green) (**B**) using appropriate antibodies and counter-stained with DAPI (blue). Representative confocal images of cortical sections from wild-type (WT) or 5XFAD mice (TG) are shown. (**C**) Merged images of A_β and CD11b staining. The dose of intranasally administered HOE 140 was 1 mg/kg/day. Each group included 4–7 mice ($n = 15$ –19 per experiment). The stained areas were quantified. The mean \pm SEM of percentage of the stained areas is shown in the graphs, $n \geq 3$ determinants (**D**). For statistical comparisons, a one-way analysis of variance and Tukey–Kramer Multiple Comparison Test were conducted. ns, non-significant. The scale bar is 200 μ m.

other G proteins as well, including G α s and G α 12/13. The signaling patterns are also different for both receptors. For example, in vascular smooth muscle cells, activating B₂R induced transient increase in intracellular Ca²⁺ signaling, whereas B₁ receptor stimulation was sustained (47). The specific way of signaling is possibly the result of different extent of regulation that these receptors are dependent on. Further studies are required to find out whether any of these differences explains differential involvement of BK receptors in modulation of amyloid burden and glial accumulation *in vitro* and *in vivo*.

To achieve better insight into mechanisms by which amyloid deposition is modulated by B₁R, the effect of B₁R antagonism on microglial/macrophage accumulation was investigated. R-715 distinctly augmented microglial/macrophage accumulation in the cortex of 5XFAD mice. Lee et al., similar to us, showed that reduced microglial activation was associated with less amyloid accumulation (48). Specific characterization of the microglia/macrophage phenotype(s) was not done here, although one can envision that a more complete analysis of microglial markers might point to a given functional or activation state that is more favorable for reducing amyloid accumulation.

To conclude, we have presented evidence supporting a role for B₁R in brain inflammation and in the regulation of amyloid deposition in AD mice, possibly with microglial/macrophage involvement. Further studies are required to test whether modulation of this receptor can serve as a novel therapeutic strategy for AD.

ETHICS STATEMENT

This study was carried out in accordance with the recommendations of the Institutional Animal Care and Use Committee of Ben-Gurion University of the Negev, Beer-Sheva, Israel. The protocol was approved by this committee: approval number IL-30-08-2011.

AUTHOR CONTRIBUTIONS

SF-B and KA designed the experiments. KA performed the experiments. KA and NT analyzed data and prepared figures. SF-B and KA wrote the manuscript.

ACKNOWLEDGMENTS

The authors would like to thank Prof. Abraham Danon for his useful advice.

REFERENCES

- Hebert LE, Weuve J, Scherr PA, Evans DA. Alzheimer disease in the United States (2010–2050) estimated using the 2010 census. *Neurology* (2013) 80(19):1778–83. doi:10.1212/WNL.0b013e31828726f5
- Hardy J, Selkoe DJ. The amyloid hypothesis of Alzheimer's disease: progress and problems on the road to therapeutics. *Science* (2002) 297(5580):353–6. doi:10.1126/science.1072994
- Holtzman DM, Morris JC, Goate AM. Alzheimer's disease: the challenge of the second century. *Sci Transl Med* (2011) 3(77):77sr1. doi:10.1126/scitranslmed.3002369
- Akiyama H, Barger S, Barnum S, Bradt B, Bauer J, Cole GM, et al. Inflammation and Alzheimer's disease. *Neurobiol Aging* (2000) 21(3):383–421. doi:10.1016/S0197-4580(00)00124-X
- Heneka MT, Carson MJ, El Khoury J, Landreth GE, Brosseron F, Feinstein DL, et al. Neuroinflammation in Alzheimer's disease. *Lancet Neurol* (2015) 14(4):388–405. doi:10.1016/S1474-4422(15)70016-5
- Kettenmann H, Hanisch UK, Noda M, Verkhratsky A. Physiology of microglia. *Physiol Rev* (2011) 91(2):461–553. doi:10.1152/physrev.00011.2010
- Ji K, Akgul G, Wollmuth LP, Tsirka SE. Microglia actively regulate the number of functional synapses. *PLoS One* (2013) 8(2):e56293. doi:10.1371/journal.pone.0056293
- Parkhurst CN, Yang G, Ninan I, Savas JN, Yates JR III, Lafaille JJ, et al. Microglia promote learning-dependent synapse formation through brain-derived neurotrophic factor. *Cell* (2013) 155(7):1596–609. doi:10.1016/j.cell.2013.11.030
- Bamberger ME, Harris ME, McDonald DR, Husemann J, Landreth GE. A cell surface receptor complex for fibrillar beta-amyloid mediates microglial activation. *J Neurosci* (2003) 23(7):2665–74.
- Paresce DM, Ghosh RN, Maxfield FR. Microglial cells internalize aggregates of the Alzheimer's disease amyloid beta-protein via a scavenger receptor. *Neuron* (1996) 17(3):553–65. doi:10.1016/S0896-6273(00)80187-7
- Stewart CR, Stuart LM, Wilkinson K, van Gils JM, Deng J, Halle A, et al. CD36 ligands promote sterile inflammation through assembly of a toll-like receptor 4 and 6 heterodimer. *Nat Immunol* (2010) 11(2):155–61. doi:10.1038/ni.1836
- Liu Y, Walter S, Stagi M, Cherny D, Letiembre M, Schulz-Schaeffer W, et al. LPS receptor (CD14): a receptor for phagocytosis of Alzheimer's amyloid peptide. *Brain* (2005) 128(Pt 8):1778–89. doi:10.1093/brain/awh531
- von Bernhardi R, Ramirez G, Toro R, Eugenin J. Pro-inflammatory conditions promote neuronal damage mediated by amyloid precursor protein and decrease its phagocytosis and degradation by microglial cells in culture. *Neurobiol Dis* (2007) 26(1):153–64. doi:10.1016/j.nbd.2006.12.006
- Noda M, Kariura Y, Amano T, Manago Y, Nishikawa K, Aoki S, et al. Expression and function of bradykinin receptors in microglia. *Life Sci* (2003) 72(14):1573–81. doi:10.1016/S0024-3205(02)02449-9
- Ifuku M, Farber K, Okuno Y, Yamakawa Y, Miyamoto T, Nolte C, et al. Bradykinin-induced microglial migration mediated by B1-bradykinin receptors depends on Ca²⁺ influx via reverse-mode activity of the Na⁺/Ca²⁺ exchanger. *J Neurosci* (2007) 27(48):13065–73. doi:10.1523/JNEUROSCI.3467-07.2007
- Bhoola KD, Figueiroa CD, Worthy K. Bioregulation of kinins: kallikreins, kininogens, and kininases. *Pharmacol Rev* (1992) 44(1):1–80.
- Lai J, Luo MC, Chen Q, Porreca F. Pronociceptive actions of dynorphin via bradykinin receptors. *Neurosci Lett* (2008) 437(3):175–9. doi:10.1016/j.neulet.2008.03.088
- Cruden NL, Newby DE. Therapeutic potential of icatibant (HOE-140, JE-049). *Expert Opin Pharmacother* (2008) 9(13):2383–90. doi:10.1517/14656566.9.13.2383
- Abraham WM, Scuri M, Farmer SG. Peptide and non-peptide bradykinin receptor antagonists: role in allergic airway disease. *Eur J Pharmacol* (2006) 533(1–3):215–21. doi:10.1016/j.ejphar.2005.12.071
- Walker K, Perkins M, Dray A. Kinins and kinin receptors in the nervous system. *Neurochem Int* (1995) 26(1):1–16. doi:10.1016/0197-0186(94)00114-A
- Kamiya T, Katayama Y, Kashiwagi F, Terashi A. The role of bradykinin in mediating ischemic brain edema in rats. *Stroke* (1993) 24(4):571–5. doi:10.1161/01.STR.24.4.571
- Iores-Marcal LM, Viel TA, Buck HS, Nunes VA, Gozzo AJ, Cruz-Silva I, et al. Bradykinin release and inactivation in brain of rats submitted to an experimental model of Alzheimer's disease. *Peptides* (2006) 27(12):3363–9. doi:10.1016/j.peptides.2006.08.012
- Regoli D, Barabe J. Pharmacology of bradykinin and related kinins. *Pharmacol Rev* (1980) 32(1):1–46.
- Calixto JB, Cabrini DA, Ferreira J, Campos MM. Kinins in pain and inflammation. *Pain* (2000) 87(1):1–5. doi:10.1016/S0304-3959(00)00335-3
- Gimpl G, Walz W, Ohlemeyer C, Kettenmann H. Bradykinin receptors in cultured astrocytes from neonatal rat brain are linked to physiological responses. *Neurosci Lett* (1992) 144(1–2):139–42. doi:10.1016/0304-3940(92)90735-P
- Sarit BS, Lajos G, Abraham D, Ron A, Sigal FB. Inhibitory role of kinins on microglial nitric oxide and tumor necrosis factor-alpha production. *Peptides* (2012) 35(2):172–81. doi:10.1016/j.peptides.2012.03.026
- Oakley H, Cole SL, Logan S, Maus E, Shao P, Craft J, et al. Intraneuronal beta-amyloid aggregates, neurodegeneration, and neuron loss in transgenic mice with five familial Alzheimer's disease mutations: potential factors in amyloid plaque formation. *J Neurosci* (2006) 26(40):10129–40. doi:10.1523/JNEUROSCI.1202-06.2006
- Asraf K, Torika N, Roasso E, Fleisher-Berkovich S. Differential effect of intranasally administrated kinin B1 and B2 receptor antagonists in Alzheimer's disease mice. *Biol Chem* (2016) 397(4):345–51. doi:10.1515/hsz-2015-0219
- Austinat M, Braeuninger S, Pesquero JB, Brede M, Bader M, Stoll G, et al. Blockade of bradykinin receptor B1 but not bradykinin receptor B2 provides protection from cerebral infarction and brain edema. *Stroke* (2009) 40(1):285–93. doi:10.1161/STROKEAHA.108.526673
- Couture R, Harrisson M, Vianna RM, Cloutier F. Kinin receptors in pain and inflammation. *Eur J Pharmacol* (2001) 429(1–3):161–76. doi:10.1016/S0014-2999(01)01318-8
- Levant A, Levy E, Argaman M, Fleisher-Berkovich S. Kinins and neuroinflammation: dual effect on prostaglandin synthesis. *Eur J Pharmacol* (2006) 546(1–3):197–200. doi:10.1016/j.ejphar.2006.06.074
- Noda M, Kariura Y, Pannasch U, Nishikawa K, Wang L, Seike T, et al. Neuroprotective role of bradykinin because of the attenuation of pro-inflammatory cytokine release from activated microglia. *J Neurochem* (2007) 101(2):397–410. doi:10.1111/j.1471-4159.2006.04339.x
- Noda M, Sasaki K, Ifuku M, Wada K. Multifunctional effects of bradykinin on glial cells in relation to potential anti-inflammatory effects. *Neurochem Int* (2007) 51(2–4):185–91. doi:10.1016/j.neuint.2007.06.017
- Fleisher-Berkovich S, Filipovich-Rimon T, Ben-Shmuel S, Hulsmann C, Kummer MP, Heneka MT. Distinct modulation of microglial amyloid beta phagocytosis and migration by neuropeptides (i). *J Neuroinflammation* (2010) 7:61. doi:10.1186/1742-2094-7-61
- Ricciardolo FL, Sorbello V, Benedetto S, Defilippi I, Sabatini F, Robotti A, et al. Bradykinin- and lipopolysaccharide-induced bradykinin B2 receptor expression, interleukin 8 release and “nitrosative stress” in bronchial epithelial cells BEAS-2B: role for neutrophils. *Eur J Pharmacol* (2012) 694(1–3):30–8. doi:10.1016/j.ejphar.2012.07.051
- Brown GC. Mechanisms of inflammatory neurodegeneration: iNOS and NADPH oxidase. *Biochem Soc Trans* (2007) 35(Pt 5):1119–21. doi:10.1042/BST0351119
- Gibbons HM, Dragunow M. Microglia induce neural cell death via a proximity-dependent mechanism involving nitric oxide. *Brain Res* (2006) 21(1):1–15. doi:10.1016/j.brainres.2006.02.032
- Diaz A, Mendieta L, Zenteno E, Guevara J, Limon ID. The role of NOS in the impairment of spatial memory and damaged neurons in rats injected with amyloid beta 25–35 into the temporal cortex. *Pharmacol Biochem Behav* (2011) 98(1):67–75. doi:10.1016/j.pbb.2010.12.005

FUNDING

This study was supported by the Israel Science Foundation (grant no. 101/11-16).

39. Wang WY, Tan MS, Yu JT, Tan L. Role of pro-inflammatory cytokines released from microglia in Alzheimer's disease. *Ann Transl Med* (2015) 3(10):136. doi:10.3978/j.issn.2305-5839.2015.03.49
40. Freiherr J, Hallschmid M, Frey WH II, Brunner YF, Chapman CD, Holscher C, et al. Intranasal insulin as a treatment for Alzheimer's disease: a review of basic research and clinical evidence. *CNS Drugs* (2013) 27(7):505–14. doi:10.1007/s40263-013-0076-8
41. Leng G, Ludwig M. Intranasal oxytocin: myths and delusions. *Biol Psychiatry* (2016) 79(3):243–50. doi:10.1016/j.biopsych.2015.05.003
42. Passos GF, Medeiros R, Cheng D, Vasilevko V, Laferla FM, Cribbs DH. The bradykinin B1 receptor regulates Abeta deposition and neuroinflammation in Tg-SwDI mice. *Am J Pathol* (2013) 182(5):1740–9. doi:10.1016/j.ajpath.2013.01.021
43. Schulze-Töpphoff U, Prat A, Prozorovski T, Siffrin V, Paterka M, Herz J, et al. Activation of kinin receptor B1 limits encephalitogenic T lymphocyte recruitment to the central nervous system. *Nat Med* (2009) 15(7):788–93. doi:10.1038/nm.1980
44. Viel TA, Lima Caetano A, Nasello AG, Lancelotti CL, Nunes VA, Araujo MS, et al. Increases of kinin B1 and B2 receptors binding sites after brain infusion of amyloid-beta 1–40 peptide in rats. *Neurobiol Aging* (2008) 29(12):1805–14. doi:10.1016/j.neurobiolaging.2007.04.019
45. Prediger RD, Medeiros R, Pandolfo P, Duarte FS, Passos GF, Pesquero JB, et al. Genetic deletion or antagonism of kinin B(1) and B(2) receptors improves cognitive deficits in a mouse model of Alzheimer's disease. *Neuroscience* (2008) 151(3):631–43. doi:10.1016/j.neuroscience.2007.11.009
46. Bicca MA, Costa R, Loch-Neckel G, Figueiredo CP, Medeiros R, Calixto JB. B(2) receptor blockage prevents Abeta-induced cognitive impairment by neuroinflammation inhibition. *Behav Brain Res* (2015) 278: 482–91. doi:10.1016/j.bbr.2014.10.040
47. Mathis SA, Criscimagna NL, Leeb-Lundberg LM. B1 and B2 kinin receptors mediate distinct patterns of intracellular Ca²⁺ signaling in single cultured vascular smooth muscle cells. *Mol Pharmacol* (1996) 50(1): 128–39.
48. Lee DC, Rizer J, Hunt JB, Selenica ML, Gordon MN, Morgan D. Review: experimental manipulations of microglia in mouse models of Alzheimer's pathology: activation reduces amyloid but hastens tau pathology. *Neuropathol Appl Neurobiol* (2013) 39(1):69–85. doi:10.1111/nan.12002

Conflict of Interest Statement: The authors state that the study was conducted without any commercial or financial relationships that could be construed as a potential conflict of interest.

The reviewer, M-CT, and handling editor declared their shared affiliation, and the handling editor states that the process nevertheless met the standards of a fair and objective review.

Copyright © 2017 Asraf, Torika, Danon and Fleisher-Berkovich. This is an open-access article distributed under the terms of the Creative Commons Attribution License (CC BY). The use, distribution or reproduction in other forums is permitted, provided the original author(s) or licensor are credited and that the original publication in this journal is cited, in accordance with accepted academic practice. No use, distribution or reproduction is permitted which does not comply with these terms.



Hemoglobin-Improved Protection in Cultured Cerebral Cortical Astroglial Cells: Inhibition of Oxidative Stress and Caspase Activation

Fatma Amri¹, Ikram Ghouili¹, Marie-Christine Tonon², Mohamed Amri¹ and Olfa Masmoudi-Kouki^{1*}

¹University of Tunis El Manar, Faculty of Sciences of Tunis, UR/11ES09 Laboratory of Functional Neurophysiology and Pathology, Tunis, Tunisia, ²INSERM U1239, Laboratory of Neuronal and Neuroendocrine Communication and Differentiation, Institute for Research and Innovation in Biomedicine (IRIB), University of Rouen Normandie, Mont-Saint-Aignan, France

OPEN ACCESS

Edited by:

Maria M. Malagón,
Instituto Maimónides de
Investigación Biomédica
de Córdoba, Spain

Reviewed by:

Luis Miguel García-Segura,
Consejo Superior de Investigaciones
Científicas (CSIC), Spain
Julie A. Chowen,
Hospital Infantil Universitario Niño
Jesús, Spain

*Correspondence:

Olfa Masmoudi-Kouki
olfa.masmoudi@fst.utm.tn

Specialty section:

This article was submitted to
Neuroendocrine Science,
a section of the journal
Frontiers in Endocrinology

Received: 19 January 2017

Accepted: 23 March 2017

Published: 10 April 2017

Citation:

Amri F, Ghouili I, Tonon M-C, Amri M and Masmoudi-Kouki O (2017) Hemoglobin-Improved Protection in Cultured Cerebral Cortical Astroglial Cells: Inhibition of Oxidative Stress and Caspase Activation. *Front. Endocrinol.* 8:67. doi: 10.3389/fendo.2017.00067

Oxidative stress plays a major role in triggering astroglial cell death in diverse neuro-pathological conditions such as ischemia and neurodegenerative diseases. Numerous studies indicate that hemoglobin (Hb) is expressed in both resting and reactive glia cells, but nothing is known regarding a possible role of Hb on astroglial cell survival. Thus, the purpose of the present study was to investigate the potential glioprotective effect of Hb on hydrogen peroxide (H_2O_2)-induced oxidative stress and apoptosis in cultured rat astrocytes. Our study demonstrates that administration of graded concentrations of Hb (10^{-12} to 10^{-6} M) to H_2O_2 -treated astrocytes reduces cell death in a concentration-dependent manner. H_2O_2 treatment induces the accumulation of reactive oxygen species (ROS) and nitric oxide (NO), a drop of the mitochondrial membrane potential, and a stimulation of caspase-3/7 activity. Exposure of H_2O_2 -treated cells to Hb was accompanied by marked attenuations of ROS and NO surproductions, mitochondrial membrane potential reduction, and caspase-3/7 activity increase. The protective action of Hb was blocked by the protein kinase A (PKA) inhibitor H89, the protein kinase C (PKC) inhibitor chelerythrine, and the mitogen-activated protein (MAP)-kinase kinase (MEK) inhibitor U0126. Taken together, these data demonstrate for the first time that Hb is a glioprotective factor that protects astrocytes from apoptosis induced by oxidative stress and suggest that Hb may confer neuroprotection in neurodegenerative diseases. The anti-apoptotic activity of Hb on astrocytes is mediated through the PKA, PKC, and MAPK transduction pathways and can be accounted for by inhibition of oxidative stress-induced mitochondrial dysfunctions and caspase activation.

Keywords: hemoglobin, oxidative stress, astrocytes, apoptosis, cell protection

INTRODUCTION

Hemoglobin (Hb) is a heme protein mainly present in erythrocytes of vertebrates (1, 2). Hb is known to function as a carrier protein of oxygen (O_2) and carbon monoxide (CO), and thus ensures transport of O_2 to the tissues, cell oxygen-consuming, and catalysis of redox reactions (3–6).

Abbreviations: Hb, hemoglobin; H_2O_2 , hydrogen peroxide; MAPK, mitogen-activated protein kinase; NO, nitric oxide; PKA, protein kinase A; PKC, protein kinase C; ROS, reactive oxygen species.

It was traditionally thought that release of Hb from erythrocytes was deleterious for the brain during intracerebral hemorrhage and trauma (2, 7, 8) and that free Hb induced a strong oxidative stress and inflammation, which were responsible for neuronal apoptosis (9–12). However, increasing evidences suggest that neurotoxicity associated to Hb derives from erythrocyte breakdown and may be accounted for iron accumulation in tissue neighboring hematomas (9, 13), rather than an accumulation of Hb molecule by itself (8, 14). In fact, iron chelators provide neuroprotection in intracerebral hemorrhage (15, 16), or in cultured astrocytes or neurons incubated with higher doses of Hb (9, 17, 18). Moreover, it has been reported that low doses of Hb maintain nitric oxide (NO) homeostasis and act as scavenger of reactive oxygen species (ROS) such as hydrogen peroxide (H_2O_2) (19–22) to protect cells from oxidative damages. Indeed, it has been reported that Hb prevents death of presenilin-1-deficient neurons induced by oxidative stress (23). In addition, overexpression of Hb has been found to be protective in rat models of ischemia and thereby increases neuron survival in hypoxic conditions (24). Altogether, these observations suggest that endogenous Hb could exert a strong protective effect and attenuate cellular ROS accumulation.

There is now clear evidence that Hb is expressed not only in erythroid cells but also in other cell types including neurons and glia cells (6, 25, 26). The occurrence of Hb-like immunoreactivity and Hb mRNA has been visualized in different regions of the brain, notably in the cortex, hippocampus, and cerebellum (13, 25–27). In particular, it has been shown that Hb transcript and protein levels are increased in cortical neurons and astroglial cells during the preconditioning phase of ischemia both *in vivo* and *in vitro* (28, 29). On the other hand, high concentrations of Hb mRNA and protein are found in human gliomas (30), indicating that over expression of Hb may have a role in promoting cell proliferation. An age-related decline in Hb expression in astrocytes has been found, suggesting that loss of this protein may increase susceptibility to age-related neurological disorders (31). Moreover, it has been indicated that induction of glia Hb expression contributes to reduce neuronal cell death under hypoxia conditions (24). Altogether, these results suggest that upregulation of astrocytic Hb may play a critical role in the pathogenesis of brain disorders; however, the function of endogenous astroglial Hb, which is present in much lower concentrations than found in blood, in astrocyte proliferation and/or survival is still not clear.

Since astrocytes play prominent role in the protection of neurons against oxidative injury, loss of astroglial cells may critically impair neuronal survival (32, 33). Thus, protection of astrocytes from oxidative insult appears essential to maintain brain function. Although there is clear evidence that Hb expression is upregulated in astroglial cells after traumatic brain injury and stroke (24, 29) and could exert neuroprotective activity (23, 30), a possible effect of Hb on astrocyte survival has never been investigated.

The purpose of the present study was thus to examine the potential protective action of Hb against H_2O_2 -induced astroglial cell death and to investigate some of the mechanisms involved in this effect.

ANIMALS AND METHODS

Animals

Wistar rats (Pasteur Institute, Tunis) were kept in a temperature-controlled room ($21 \pm 1^\circ\text{C}$), under an established photoperiod (lights on 0700–1900 hours) and with free access to food and water.

Reagents

Dulbecco's modified Eagle's medium (DMEM), Ham F12 culture medium, D(+)-glucose, L-glutamine, N-2-hydroxyethylpiperazine-N-2-ethane sulfonic acid (HEPES), fetal bovine serum (FBS), and the antibiotic-antimycotic solution, were obtained from Life Technologies (Grand Island, NY, USA). H89, chelerythrine, fluorescein diacetate-acetoxymethyl (FDA-AM), dimethyl sulfoxide (DMSO), insulin, Triton X-100, and bovine Hb were purchased from Sigma-Aldrich (St. Louis, MO, USA). The lactate dehydrogenase (LDH; EC 1.1.1.27) assay kit was obtained from Bio-Maghreb (Tunis, Tunisia). 5-6-chloromethyl 2'-7'dichlorodihydrofluorescein diacetate (CM-H₂DCFDA), JC-10, and 4,5-diamino fluorescein diacetate (DAF-FM) were from Molecular Probes (Eugene, OR, USA). U0126 and Apo-ONE Homogeneous Caspase-3/7 assay kit were supplied by Promega (Charbonnières, France).

Cell Culture

Secondary cultures of rat cortical astrocytes were prepared from 1- or 2-day-old Wistar rats of both sexes as previously described (34). Briefly, cerebral hemispheres were dissected, meninges removed, and tissues collected in DMEM/Ham F12 (2:1; v/v) culture medium supplemented with 2 mM glutamine, 1% insulin, 5 mM HEPES, 0.4% glucose (final concentration of glucose in culture media is 4.5 g/L), and 1% of the antibiotic-antimycotic solution. The tissues were dissociated mechanically with a syringe equipped with a 25 G gage needle, and filtered through a 100-μm sieve (Falcon, Franklin Lakes, NJ, USA). Dissociated cells were resuspended in culture medium supplemented with 10% FBS, plated in 75-cm² flasks (Greiner Bio-one GmbH, Frickenhausen, Germany) at the density of 17×10^6 cells/mL and incubated at 37°C in 5% CO₂/95% air. After 7–8 days, the cultures became confluent and loosely attached microglia cells and oligodendrocytes were removed by shaking the flasks on an orbital agitator (250 rpm, 18 h). Adhesive cells (mostly astrocytes) were detached by trypsinization, harvested and plated on 24- or 96-well plates at a density of 8×10^4 cells/mL. All experiments were performed on 5- to 7-day-old secondary cultures and more than 98% of the cells were labeled with antibodies against glial fibrillary acidic protein (35).

Experimental Design

All experiments were performed on DIV 5–7 astroglial cells grown up in culture medium containing 10% of FBS. After removal of medium, cells were incubated at 37°C with fresh serum-free culture medium in the absence or presence of the test substances for 24 h. Previous data indicated that incubation of astrocytes during 24 h with 50 μM H₂O₂ induces about 40% of cell death (36). Thus, a dose of 50 μM H₂O₂ was used in the present study to evaluate the effect of Hb on astrocyte survival. On the basis of the

results shown in **Figures 1, 2 and 3A**, a concentration of 10^{-9} M Hb, which prevents the deleterious effects of H_2O_2 , was used in all subsequent experiments. It has been previously demonstrated that 2×10^{-5} M H89, 10^{-6} M chelerythrine, and 10^{-6} M U0126 blocked the protective effects of some neuropeptides on cultured astrocytes (35, 37). Thus these concentrations were also used in the present study.

Measurement of Cell Survival

At the end of the treatment period, cells were washed twice with phosphate-buffered saline (PBS, 0.1 M, pH 7.4) and incubated for 8 min with 15 $\mu\text{g}/\text{mL}$ FDA-AM in the dark, rinsed twice with PBS, and lysed with a Tris/HCl solution containing 1% sodium dodecyl sulfate. Fluorescence was measured with excitation at 485 nm and emission at 538 nm using a fluorescence microplate reader FL800TBI (Bio-Tek Instruments, Winooski, VT, USA). Experiments were carried out on 16 different wells from four independent experiments.

Measurement of Intracellular ROS Formation

ROS were detected by measuring the fluorescence of 2',7'-dichlorofluorescein (DCF), which is derived from the deacetylation and oxidation of the non-fluorescent compound DCFH₂-DA. At the end of the treatment period, cells were washed twice with PBS, and then incubated with 10 μM DCFH₂-DA for 30 min at 37°C in the dark. Fluorescence was measured with excitation at 485 nm and emission at 538 nm using a fluorescence microplate reader. Experiments were carried on 18 different wells from three independent experiments.

Measurement of NO Accumulation

Relative changes in cytosolic NO concentration in astrocytes were monitored using the fluorescent probe 4,5-diamino fluorescein diacetate (DAF). At the end of the treatment period, cells were washed twice with PBS and then incubated with 10 μM DAF-FM diacetate for 30 min. Fluorescence was measured with excitation at 485 nm and emission at 538 nm using a fluorescence microplate reader. Experiments were carried out on 18 different wells from three independent experiments.

Measurement of Mitochondrial Activity

Mitochondrial membrane potential was quantified using the JC-10 probe. Cells seeded into 96-well plates were incubated in the absence or presence of H_2O_2 with or without Hb. At the end of the treatment, astrocytes were incubated in the presence of the JC-10 probe (10 $\mu\text{g}/\text{mL}$) at 37°C for 1 h, and then washed twice with PBS. In healthy astrocytes, the intact membrane potential allows the lipophilic dye JC-10 to enter into the mitochondria where it aggregates and produces an intense orange signal. In dead cells, mitochondrial membrane potential collapses so that the monomeric JC-10 probe remains cytosolic and emits a green signal. Fluorescence intensity was measured with fluorescence microplate reader and expressed as a ratio of the emission at 610 nm (orange) over 530 nm (green) to evaluate mitochondrial

integrity (38). Experiments were carried out on 12 different wells from three independent experiments.

Measurement of Caspase 3 Activity

The effect of Hb on H_2O_2 -induced increase of caspase 3 activity was measured by using Apo-ONE Homogeneous Caspase-3/7 kit (Promega). At the end of the incubation, 100 μL of the cell suspension was incubated with 100 μL of kit buffer and caspase substrat. Caspase-3 activity was calculated from the slope of the fluorescence measured every 15 min for 3 h with excitation at 485 nm and emission at 530 nm. Experiments were carried out on 12 different wells from three independent experiments.

Cell Cytotoxicity Measurement

The cytotoxicity of H_2O_2 on astrocytes was determined by measuring the activity of LDH released into the culture medium, using a LDH assay kit (Bio-Maghreb, Tunis, Tunisia) according to the manufacturer's instructions. LDH activity was measured at 340 nm with a spectrophotometric microplate reader. The results were expressed as a percentage of total LDH release after cell lysis with 1% Triton X-100 in PBS. Experiments were carried out on 16 different wells from four independent experiments.

Statistical Analysis

The data were presented as mean \pm SEM of at least three independent experiments ($n \geq 3$). The statistical analysis of the data was performed using Student's *t*-test for single comparisons and by ANOVA followed by Bonferroni's test, and two-way ANOVA test for multiple comparisons with the GraphPad software (La Jolla, CA, USA). In all cases a *p*-value of 0.05 or less was considered as statistically significant.

RESULTS

Protective Effect of Hb against H_2O_2 -Induced Astroglial Cell Death

Incubation of cultured astrocytes with 50 μM H_2O_2 for 24 h induced a decrease ($-37.2 \pm 1.9\%$; $p < 0.001$) of the proportion of surviving cells. Administration of graded concentrations of Hb (10^{-12} to 10^{-6} M), which did not affect cell viability by themselves, dose-dependently prevented cell death induced by 50 μM H_2O_2 (**Figure 1A**). Examination of cultures by phase-contrast microscopy revealed that H_2O_2 induced cell shrinkage and disturbance of the astrocyte network with appearance of retracted processes (**Figure 1B, b**). The effect of H_2O_2 on morphological alterations was slightly attenuated with low concentration (10^{-12} M) of Hb (**Figure 1B, c**) and totally prevented with higher concentrations of Hb, condition in which cells exhibited a flat polygonal morphology similar to that of untreated-astrocytes (**Figure 1B, a,d**).

Effect of Hb on H_2O_2 -Induced Intracellular ROS and NO Accumulation in Cultured Astrocytes

To examine whether Hb could block H_2O_2 -induced intracellular ROS accumulation, astrocytes were labeled with CMH₂DCFDA,

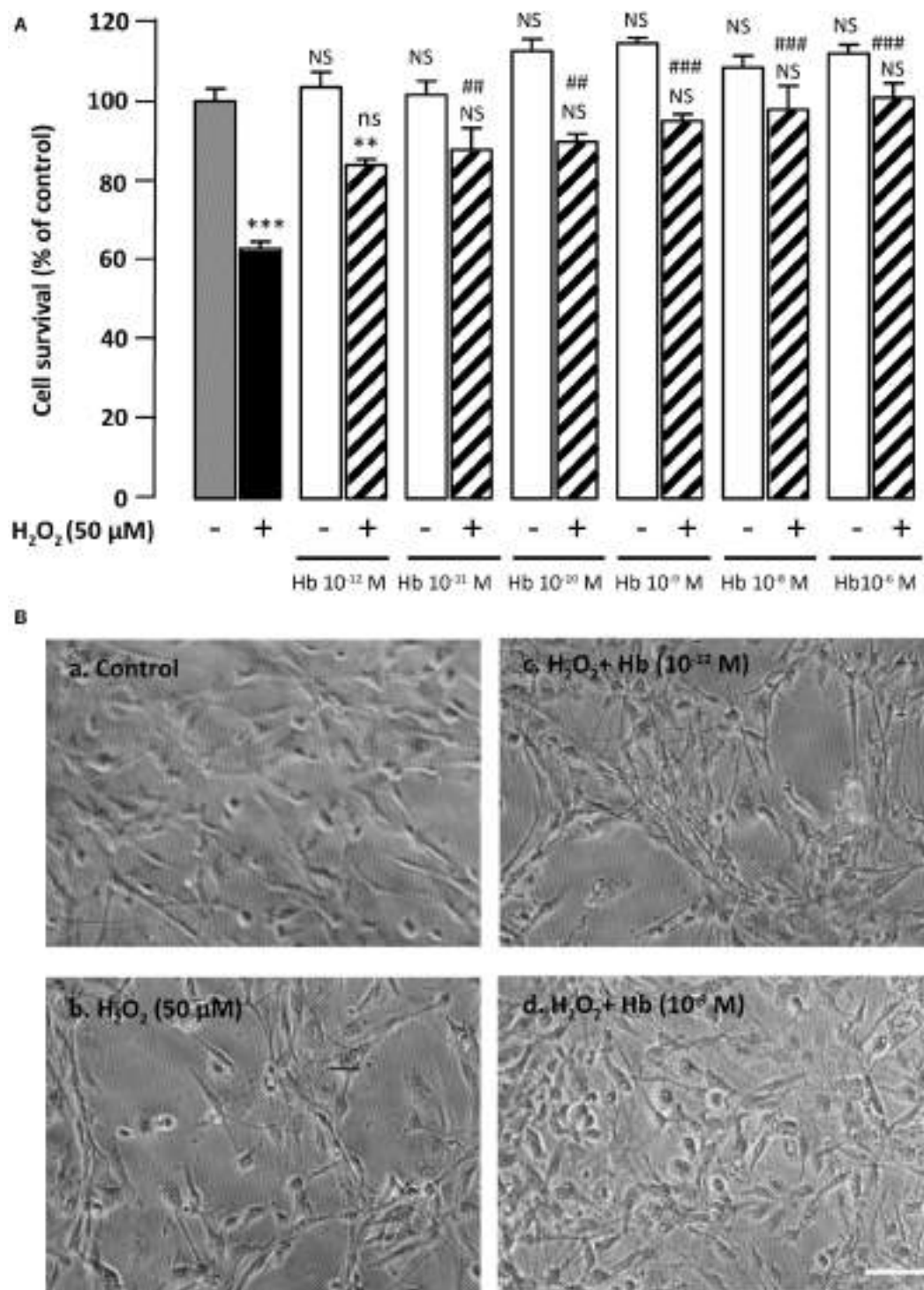


FIGURE 1 | Glioprotective effect of Hb on H_2O_2 -induced cell death. (A) Cells were co-incubated for 24 h with medium alone (white bar) or with H_2O_2 ($50 \mu\text{M}$) in the absence (black bar) or presence of graded concentration of Hb (10^{-12} to 10^{-6} M , hatched bars). Cell survival was quantified by measuring FDA fluorescence intensity, and the results are expressed as percentages of the control. Data are means \pm SEM of four independent experiments. ANOVA followed by Bonferroni's test *** $p < 0.001$; NS, not statistically different from control cells (absence of H_2O_2 and absence of Hb). # $p < 0.01$; ### $p < 0.001$; ns, not statistically different vs. H_2O_2 -treated cells. **(B)** Typical phase-contrast images illustrating the effect of Hb on H_2O_2 -induced morphological changes in cultured rat astrocytes. Cells were incubated for 24 h with medium alone (a), or $50 \mu\text{M}$ H_2O_2 in the absence (b), or presence of 10^{-12} M Hb (c), or 10^{-9} M Hb (d). Scale bar 100 μm .

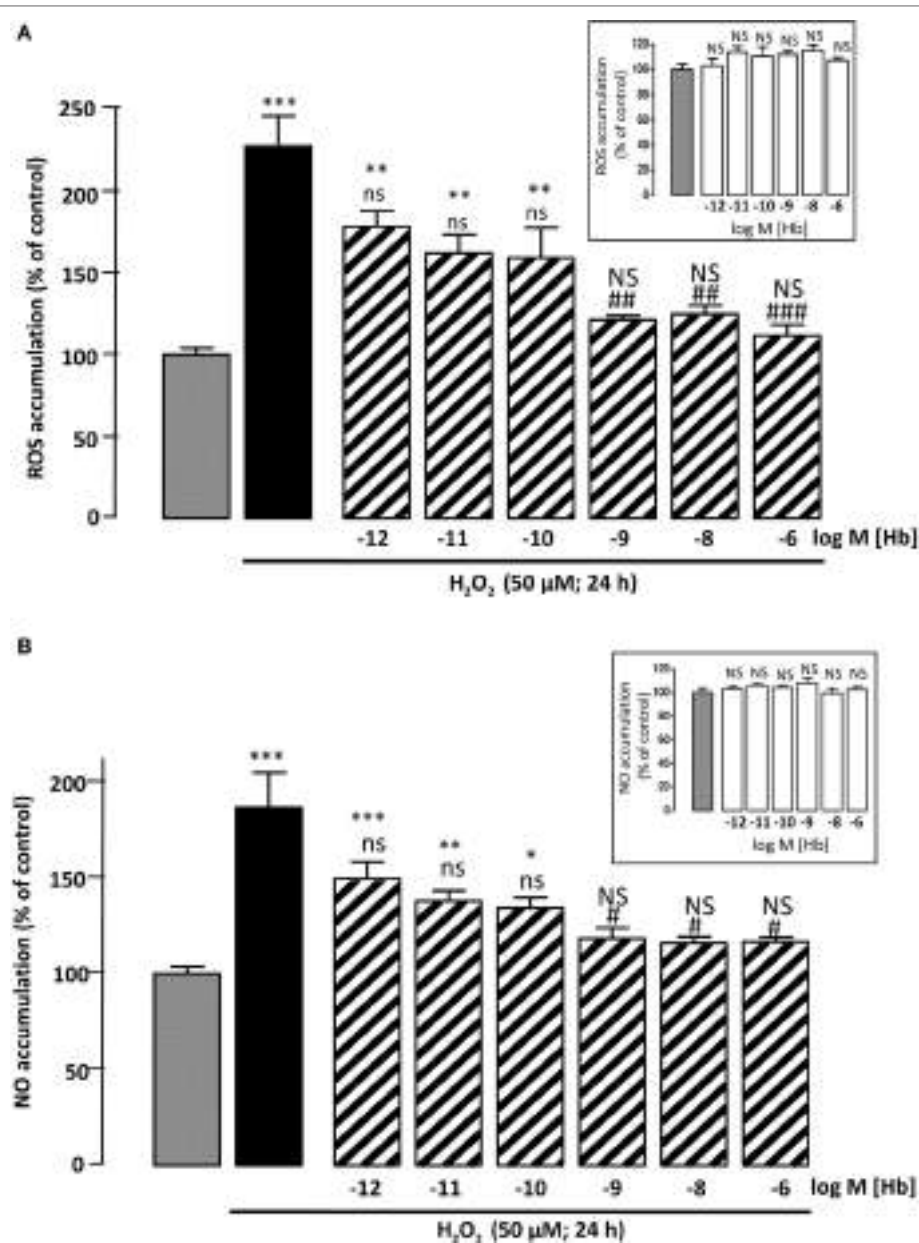
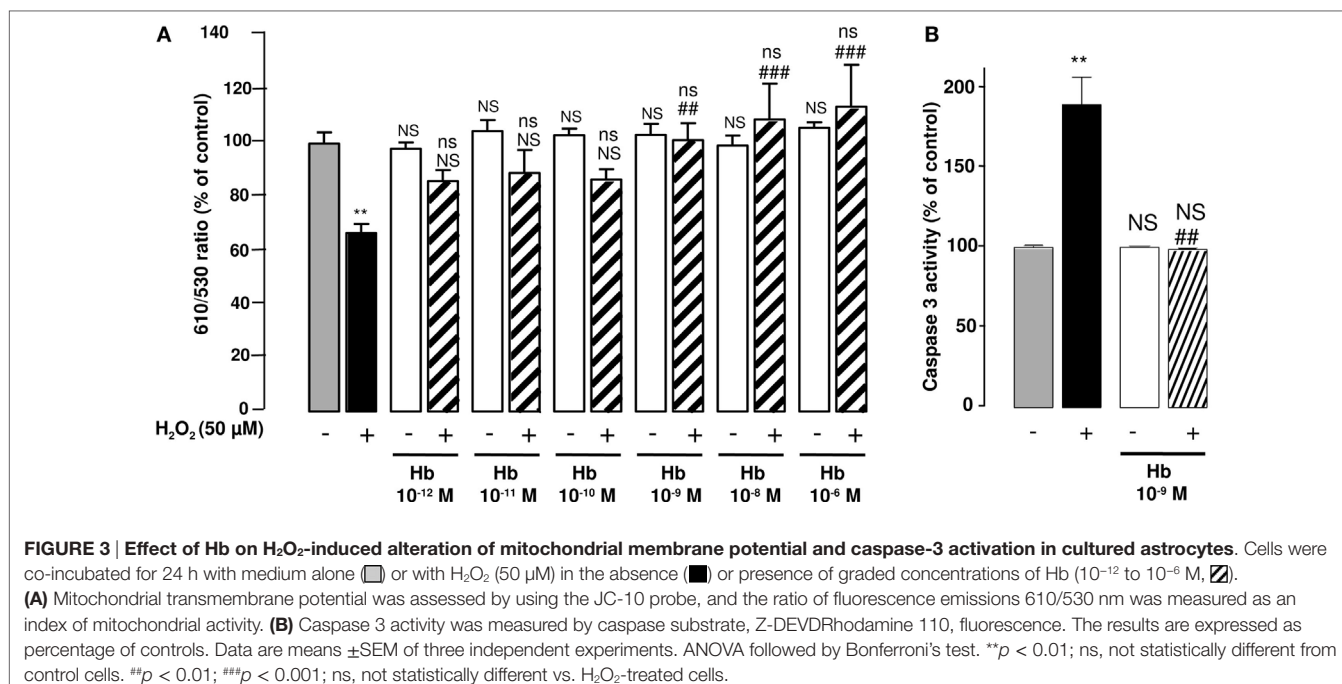


FIGURE 2 | Effect of Hb on H₂O₂-induced ROS and NO intracellular accumulations. Cells were co-incubated for 24 h with medium alone (■) or with H₂O₂ (50 μM) in the absence (■) or presence of graded concentration of Hb (10⁻¹² to 10⁻⁶ M, ▨). **(A)** Cellular ROS level was quantified by measurement of DCF fluorescence intensity. **(B)** Cellular NO level was quantified by measurement of DAF fluorescence intensity. Inset, effect of graded concentration of Hb (10⁻¹² to 10⁻⁶ M; ▨) on intracellular ROS accumulation (**A**) and NO formation (**B**). The results are expressed as percentages of the controls. Data are means ± SEM of three independent experiments. ANOVA followed by Bonferroni's test **p* < 0.05; ***p* < 0.01; ****p* < 0.001; NS, not statistically different from control cells. #*p* < 0.05; ##*p* < 0.01; ###*p* < 0.001; ns, not statistically different vs. H₂O₂-treated cells.

which forms the fluorescent DCF compound by oxidation with ROS. Incubation of cultured astrocytes with 50 μM H₂O₂ alone for 24 h, induced an increase in DCF fluorescence intensity (+127 ± 18%; *p* < 0.001). Incubation of cells with graded concentrations of Hb (10⁻¹² to 10⁻⁶ M) had no effect on DCF fluorescence intensity (Inset), but reduced in a dose-dependent manner, the effect of H₂O₂ on DCF formation (Figure 2A). Since large amounts of NO are produced by cells under oxidative stress status (39), we

have investigated the effect of Hb on H₂O₂-induced NO formation in astroglial cells. By using the DAF-FM probe, which forms the fluorescent DAF compound upon oxidation by NO, we found that H₂O₂ induced a significant increase (+86.6 ± 18.23%; *p* < 0.001) of NO production and, in the same range of concentrations, Hb was also able to reduce in a dose-dependent manner the effect of 50 μM H₂O₂ on DAF formation (Figure 2B). In contrast, all concentrations of Hb tested did not affect, by themselves, NO production (inset).



Effect of Hb on H₂O₂-Induced Mitochondrial Potential Alteration and Caspase-3 Activation

Considering the major action of oxidative stress in the alteration of mitochondria functions, we have examined the effect of Hb on the integrity of mitochondria by using the fluorescent ratio-metric probe JC-10. Treatment of astrocytes with 50 μM H₂O₂ alone induced a significant reduction ($-32.6 \pm 3.4\%$; $p < 0.01$) of the 610/530 nm ratio, indicating that the mitochondrial integrity was impaired by oxidative stress. Incubation of cells with graded concentrations of Hb (10⁻¹² to 10⁻⁶ M) did not affect 610/530 nm fluorescence ratio, but dose-dependently reduced the deleterious effect of H₂O₂ on the mitochondrial membrane potential, and the 610/530 nm ratio was restored to control values for concentrations greater than 10⁻⁹ M (Figure 3A). H₂O₂-induced reduction of membrane potential was associated with an increase of caspase 3 activity ($+89.3 \pm 17.19\%$; $p < 0.05$). Addition of Hb (10⁻⁹ M) in the incubation medium totally suppressed the stimulatory effect of H₂O₂ on caspase 3 activation (Figure 3B).

Identification of the Signal Transduction Pathways Involved in the Glioprotective Effect of Hb on H₂O₂-Induced Astroglial Death

Incubation of astrocytes with 50 μM H₂O₂ for 24 h induced an increase of LDH levels in the culture medium ($+82.6 \pm 7.55\%$; $p < 0.01$) (Figure 4A). Addition of Hb at the dose of 10⁻⁹ M to the culture medium abolished the effect of H₂O₂ on LDH leakage ($100.2 \pm 0.9\%$) (Figure 4A). To investigate the signaling cascade involved in the protective action of Hb, we have used

pharmacological inhibitors of adenylyl cyclase (AC)/protein kinase A (PKA), phospholipase C (PLC)/protein kinase C (PKC), or mitogen-activated protein kinase (MAPK) transduction pathways. Incubation of astrocytes with the PKA inhibitor H89 (2×10^{-5} M), the PKC inhibitor chelerythrine (10^{-6} M) or the mitogen-activated protein kinase kinase (MEK) inhibitor U0126 (10^{-6} M), which had no effect by themselves on cell damage and cell death induced by H₂O₂, abrogated the protective action of Hb (10⁻⁹ M) on H₂O₂-provoked toxicity and cell death (Figures 4A,B).

DISCUSSION

The main finding of the present study is to demonstrate for the first time that Hb protects astroglial cells against oxidative stress and death induced by H₂O₂ exposure. It has been found that Hb is effective at very low concentrations and exerts its glioprotective effect through inhibition of ROS and NO generation, mitochondrial dysfunctions, and caspase-3 activation.

In agreement with previous reports (35, 40, 41), we observed that H₂O₂-treated astrocytes exhibited modifications of cell morphology such as cell shrinkage and appearance of thin processes. In parallel, H₂O₂ induced an increase of LDH in the medium and a decrease of cell survival. Here, we showed that Hb dose-dependently prevented H₂O₂-induced cell death and abolished H₂O₂-evoked morphological changes. These data could be seemed in contradiction with previous studies indicating that Hb released from red blood cells in intracerebral hemorrhage is neurotoxic (9, 30, 42–44). Nevertheless, it can be noted that the concentration of Hb detected in this pathology is 10,000 times higher than that used in the present study. In addition, the concentration of Hb needed to prevent

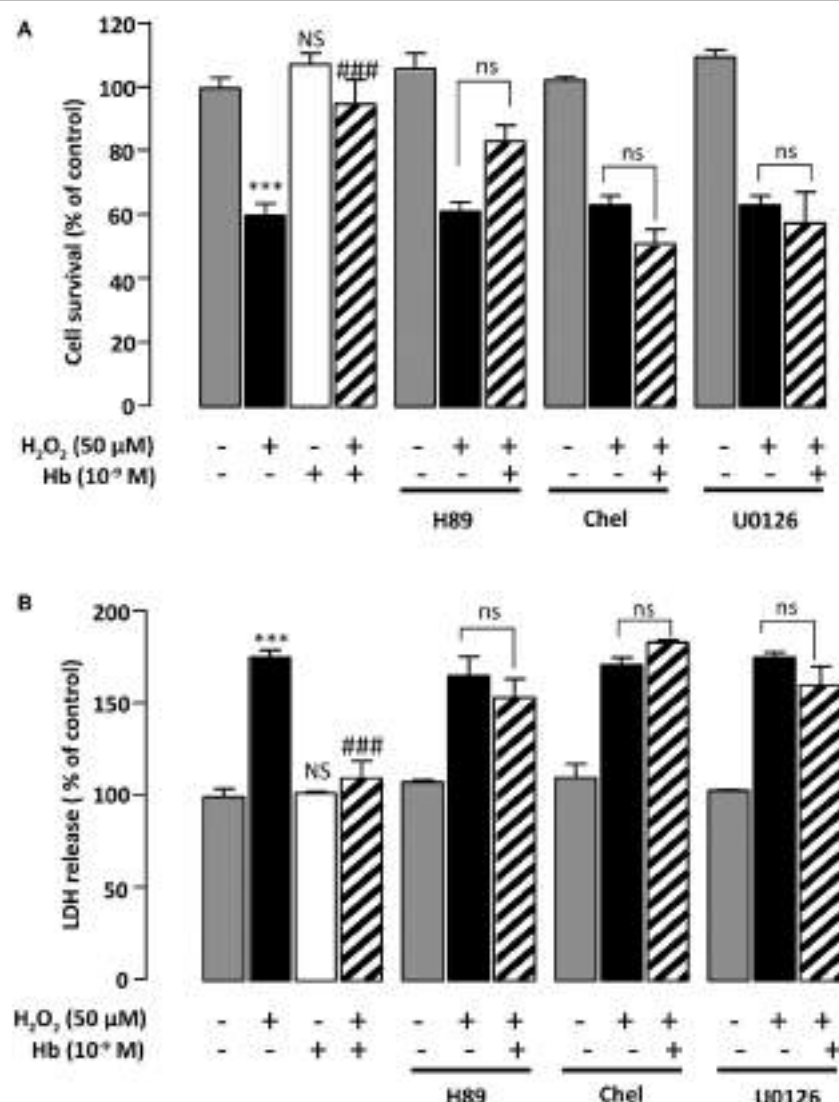


FIGURE 4 | Characterization of intracellular pathways involved in the protective effect of Hb on astroglial cells. Cells were pre-incubated for 30 min in the absence or presence of H89 (2×10^{-5} M), chelerythrine (10^{-6} M; Chel), or U0126 (10^{-6} M) and then incubated for 24 h with medium alone (□) Hb (10^{-9} M) alone or with H_2O_2 (50 μM) in the absence (■) or presence of Hb (▨). **(A)** Cell death was determined by measuring LDH activity in culture media, and the results are expressed as percentage of LDH released in Triton-lysed cells. **(B)** Cell survival was quantified by measuring FDA fluorescence intensity, and the results are expressed as percentages of control. Data are means \pm SEM of four independent experiments. ANOVA followed by Bonferroni's test *** $p < 0.001$; NS, not statistically different from control cells. #** $p < 0.001$; ns, not statistically different vs. H_2O_2 -treated cells.

the deleterious effects of H_2O_2 on astroglial cells (the present data) was in the same range as that produced by neuronal cells brain, i.e., cortical and hippocampal neurons and astrocytes (25, 45, 46). Furthermore, there is now mounting evidence indicating that endogenous neuronal Hb is not detrimental in brain diseases (30) and even may exert beneficial effects on neuronal cells in *in vivo* and *in vitro* models of ischemia (24, 45). While, the precise roles of Hb in brain physiology and in neurodegenerative diseases are not well understood. Since, astrocytes produce neuroprotective compounds, that Hb protects glial cells against moderate injuries could be benefit for brain neuronal populations. As in the case of Hb, the potency and efficacy of others oxygen-binding globins, neuroglobin,

and myoglobin, in preventing neuronal cell death have been proven against various neurotoxins, including H_2O_2 , and brain injuries induced by hypoxia, ischemia, or stroke (30, 47–51). It is noteworthy that subnanomolar concentrations of Hb were still effective to protect astrocytes from the cytotoxic effect of H_2O_2 after 24 h of treatment, indicating that this globin exhibits a strong cytoprotective activity.

It is well documented in numerous cell types including astrocytes that H_2O_2 exerts its cytotoxic effect *via* the production of highly reactive species inside the cell (34, 51–53). The present study reveals that treatment of astrocytes with Hb reduced, in a concentration-dependent manner, intracellular ROS and NO levels, phenonenum, which is likely responsible for a reduction

of cell death induced by H₂O₂. In agreement with the fact that Hb may protect astrocytes from oxidative stress, it has been demonstrated that (i) Hb strongly scavenges ROS and NO (6), (ii) Hb overexpression prevents H₂O₂-induced ROS surproduction and cell death in primary rat mesangial cells (54), and (iii) increasing expression of neuronal Hb prior to hypoxia insult enhances neuronal cell viability by decreasing oxidative stress process (45, 55). It cannot be excluded that peroxidase activity of Hb (56, 57) could be in part responsive for its protective effect against H₂O₂.

It is widely accepted that ROS can induce cell death by multiple intracellular mechanisms including mitochondrial dysfunction leading to the formation of mitochondrial permeability transition pores and thus activation of caspases, the effectors of apoptotic cell death (37, 58, 59). In agreement with this notion, measurement of mitochondria activity, with the membrane potential-sensitive probe JC-10, revealed that treatment of astrocytes with H₂O₂ resulted in a decrease of the proportion of active mitochondria, and that co-administration of nanomolar concentration of Hb prevented the deleterious effect of H₂O₂ on mitochondria. Concurrently, Hb suppressed stimulation of caspase-3/7 activity induced by H₂O₂. That Hb exerts its glioprotective effect through the intrinsic mitochondrial pathway is supported by a study showing that Hb blocks the effects of NO on (i) the decrease of procaspase-2 protein levels, an inactive form of caspase-2, (ii) the stimulation of caspase-3 activity, (iii) the cleavage of poly (ADP-ribose) polymerase (PARP) and the DNA fragmentation, and (iv) the apoptotic cell death in human neuroblastoma SH-SY5Y cells (60, 61). In addition, Hb reverses heme oxygenase-1/CO-provoked neuronal cell death through inhibition of caspase-3-dependent apoptotic pathway (62). Thus, collectively, these data strongly suggest that Hb rescues astrocytes from oxidative stress by preventing ROS accumulation, which in turn preserves mitochondrial activity and prevents caspase-3 activation. In support of this hypothesis, it has been shown that the globin neuroglobin, the neuropeptides octadecaneuropeptide, and pituitary adenylate cyclase-activating polypeptide, which can rescue astrocytes from oxidative damages, inhibit the effects of H₂O₂ on alteration of mitochondrial integrity and stimulation of caspase3/7 activity (35, 37, 51, 63).

That Hb, by itself, might peroxidate H₂O₂ in culture media, and that this effect might be responsible for the protective effect of Hb, cannot be totally excluded. Nevertheless, in the present study, the protective effect of Hb was shown at very low doses (10⁻¹¹ to 10⁻⁶ M) and peroxidation of H₂O₂ by Hb has been found at doses 1,000- to 10,000 times higher than that used in the present study (56, 57). In addition, the peroxidase activity of Hb is optimal at pH 5.5, and dramatically falls down at physiological pH (57).

Although our understanding of the precise signaling pathways that trigger apoptosis of neuronal cells is still fragmentary, it has been demonstrated that activation of the AC/PKA and the PLC/PKC transduction pathways contributes to reduce intracellular ROS levels and to protect cells against oxidative stress-induced apoptosis in cultured neurons and astrocytes (34, 64, 65). Here, we show that treatment of astrocytes with

the PKA inhibitor H89 or the PKC inhibitor chelerythrine abrogated the effects of Hb on H₂O₂-evoked caspase-3/7 activation and cell death apoptosis. We have previously demonstrated that the MAPK signaling cascade is involved in apoptotic death of astrocytes (37, 51), and it has been shown that survival of astrocytes requires phosphorylation of extracellular signal-regulated kinase (43). Consistently, we show that the protective action of Hb on astrocytes against H₂O₂ was abolished by the MEK inhibitor U0126. Collectively, these data suggest that the glioprotective activity of Hb can be accounted for by activation of the PKA, PKC, and MAPK transduction pathways. The receptor through which Hb might modulate intracellular pathways in astrocytes and exert its glioprotective effect is currently unknown. Alternatively, it can be proposed that Hb, in the same way as neuroglobin, could directly interact with G proteins and thus modulates transduction pathways (66–68). However, such hypothesis raises the question how Hb crosses the membrane. The delivery of Hb inside astrocytes might result to its interaction with the scavenger receptor CD163, which acts as a Hb transporter in macrophages (69). That CD163, or other receptor or mechanism, might be involved in the uptake of Hb by astrocytes merits further investigations.

The protective effect of low doses of Hb on astroglial cells might have a physiopathological significance in neurological disorders including neurodegenerative diseases, like ischemia and stroke. Clinical studies have shown that the neuronal Hb expression is reduced in brain of patient with Alzheimer disease, Parkinson disease, or dementia with Lewy Bodies (27). Along these lines, it has been reported that treatment of rat with rotenone, neurotoxin used to reproduce features of Parkinson's disease (70), induces downregulation of Hb expression in selected neuronal populations, i.e., nigral, cortical, and striatal neurons, associated with an elevation of oxidative stress damages and mitochondria dysfunction (55, 71). In contrast, upregulation of neuronal expression of Hb is accompanied by enhanced resistance to oxidative stress under hypoxic conditions (45). Despite their high antioxidative activities, astroglial cells cannot survive and protect neurons under insurmountable oxidative stress (32). Thus, upregulation of Hb expression in astrocytes might increase protection of cells from oxidative insults and might delay neuronal damages in various cerebral injuries involving oxidative neurodegeneration.

In conclusion, the present study demonstrates that Hb at low concentrations acts as endogenous protective agent against oxidative and nitrosative stress inducing apoptosis of cultured astrocytes. The antiapoptotic effect of this globin is attributable, at least in part, to the reduction of ROS formation, which preserves mitochondrial functions and prevents caspase 3 activation.

ETHICS STATEMENT

Approval for these experiments was obtained from the Medical Ethical Committee for the Care and Use of Laboratory Animals of Pasteur Institute of Tunis (approval number: FST/LNFP/Pro152-012).

AUTHOR CONTRIBUTIONS

FA, MA, and OM-K conceived and designed the experiments. FA, IG, and OM-K performed the experiments. FA, M-CT, MA, and OM-K analyzed the data. FA, IG, M-CT, MA, and OM-K contributed to reagents/materials/analysis tools. FA, M-CT, and OM-K wrote the paper.

ACKNOWLEDGMENTS

FA and IG were recipients of fellowships from the University of Tunis El Manar, a France-Tunisia exchange program and France-Tunisia exchange programs PHC-Utique.

REFERENCES

- Edsall JT. Understanding blood and hemoglobin: an example of international relations in science. *Perspect Biol Med* (1986) 29:S107–23. doi:10.1353/pbm.1986.0052
- Zhou Y, Wang Y, Wang J, Anne Stetler R, Yang QW. Inflammation in intracerebral hemorrhage: from mechanisms to clinical translation. *Prog Neurobiol* (2014) 115:25–44. doi:10.1016/j.pneurobio.2013.11.003
- Rahaman MM, Straub AC. The emerging roles of somatic globins in cardiovascular redox biology and beyond. *Redox Biol* (2013) 1:405–10. doi:10.1016/j.redox.2013.08.001
- Burmester T. Evolution of respiratory proteins across the pancrustacea. *Integr Comp Biol* (2015) 55:792–801. doi:10.1093/icb/icv079
- Cook SA, Hill EA, Borovik AS. Lessons from nature: a bio-inspired approach to molecular design. *Biochemistry* (2015) 54:4167–80. doi:10.1021/acs.biochem.5b00249
- Quaye IK. Extracellular hemoglobin: the case of a friend turned foe. *Front Physiol* (2015) 6:96. doi:10.3389/fphys.2015.00096
- Laird MD, Wakade C, Alleyne CH Jr, Dhandapani KM. Hemin-induced necroptosis involves glutathione depletion in mouse astrocytes. *Free Radic Biol Med* (2008) 45:1103–14. doi:10.1016/j.freeradbiomed.2008.07.003
- Jaremk KM, Chen-Roetling J, Chen L, Regan RF. Accelerated hemolysis and neurotoxicity in neuron-glia-blood clot co-cultures. *J Neurochem* (2010) 114:1063–73. doi:10.1111/j.1471-4159.2010.06826.x
- Vanderveldt GM, Regan RF. The neurotoxic effect of sickle cell hemoglobin. *Free Radic Res* (2004) 38:431–7. doi:10.1080/10715760310001638010
- Lara FA, Kahn SA, da Fonseca AC, Bahia CP, Pinho JP, Graca-Souza AV, et al. On the fate of extracellular hemoglobin and heme in brain. *J Cereb Blood Flow Metab* (2009) 29:1109–20. doi:10.1038/jcbfm.2009.34
- Sukumari-Ramesh S, Laird MD, Singh N, Vender JR, Alleyne CH Jr, Dhandapani KM. Astrocyte-derived glutathione attenuates hemin-induced apoptosis in cerebral microvascular cells. *Glia* (2010) 58:1858–70. doi:10.1002/glia.21055
- Wang YC, Zhou Y, Fang H, Lin S, Wang PF, Xiong RP, et al. Toll-like receptor 2/4 heterodimer mediates inflammatory injury in intracerebral hemorrhage. *Ann Neurol* (2014) 75:876–89. doi:10.1002/ana.24159
- Bishop GM, Robinson SR. Quantitative analysis of cell death and ferritin expression in response to cortical iron: implications for hypoxia-ischemia and stroke. *Brain Res* (2001) 907:175–87. doi:10.1016/S0006-8993(01)02303-4
- Bamm VV, Lanther DK, Stephenson EL, Smith GS, Harauz G. In vitro study of the direct effect of extracellular hemoglobin on myelin components. *Biochim Biophys Acta* (2015) 1852:92–103. doi:10.1016/j.bbadi.2014.10.009
- Huang FP, Xi G, Keep RF, Hua Y, Nemoianu A, Hoff JT. Brain edema after experimental intracerebral hemorrhage: role of hemoglobin degradation products. *J Neurosurg* (2002) 96:287–93. doi:10.3171/jns.2002.96.2.0287
- RighyC, BozzaMT, OliveiraMF, BozzaFA. Molecular, cellular and clinical aspects of intracerebral hemorrhage: are the enemies within? *Curr Neuropharmacol* (2016) 14:392–402. doi:10.2174/1570159X14666151230110058
- Regan RF, Rogers B. Delayed treatment of hemoglobin neurotoxicity. *J Neurotrauma* (2003) 20:111–20. doi:10.1089/08977150360517236
- Owen JE, Bishop GM, Robinson SR. Phenanthrolines protect astrocytes from hemin without chelating iron. *Neurochem Res* (2014) 39:693–9. doi:10.1007/s11064-014-1256-8
- Masuoka N, Kodama H, Abe T, Wang DH, Nakano T. Characterization of hydrogen peroxide removal reaction by hemoglobin in the presence of reduced pyridine nucleotides. *Biochim Biophys Acta* (2003) 1637:46–54. doi:10.1016/S0925-4439(02)00213-2
- Goldstein S, Samuni A. Intra- and intermolecular oxidation of oxymyoglobin and oxyhemoglobin induced by hydroxyl and carbonate radicals. *Free Radic Biol Med* (2005) 39:511–9. doi:10.1016/j.freeradbiomed.2005.04.003
- Chen K, Piknova B, Pittman RN, Schechter AN, Popel AS. Nitric oxide from nitrite reduction by hemoglobin in the plasma and erythrocytes. *Nitric Oxide* (2008) 18:47–60. doi:10.1016/j.niox.2007.09.088
- Schechter AN. Hemoglobin research and the origins of molecular medicine. *Blood* (2008) 112:3927–38. doi:10.1182/blood-2008-04-078188
- Nakajima M, Shirasawa T. Presenilin-1-deficient neurons are nitric oxide-dependently killed by hydrogen peroxide in vitro. *Neuroscience* (2004) 125:563–8. doi:10.1016/j.neuroscience.2004.01.016
- Tezel G, Yang X, Luo C, Cai J, Kain AD, Powell DW, et al. Hemoglobin expression and regulation in glaucoma: insights into retinal ganglion cell oxygenation. *Invest Ophthalmol Vis Sci* (2010) 51:907–19. doi:10.1167/iovs.09-4014
- Biagioli M, Pinto M, Cesselli D, Zaninello M, Lazarevic D, Roncaglia P, et al. Unexpected expression of alpha- and beta-globin in mesencephalic dopaminergic neurons and glial cells. *Proc Natl Acad Sci U S A* (2009) 106:15454–9. doi:10.1073/pnas.0813216106
- Chuang JY, Lee CW, Shih YH, Yang T, Yu L, Kuo YM. Interactions between amyloid-beta and hemoglobin: implications for amyloid plaque formation in Alzheimer's disease. *PLoS One* (2012) 7:e33120. doi:10.1371/journal.pone.0033120
- Ferrer I, Gomez A, Carmona M, Huesa G, Porta S, Riera-Codina M, et al. Neuronal hemoglobin is reduced in Alzheimer's disease, argyrophilic grain disease, Parkinson's disease, and dementia with Lewy bodies. *J Alzheimers Dis* (2011) 23:537–50. doi:10.3233/JAD-2010-101485
- He Y, Hua Y, Liu W, Hu H, Keep RF, Xi G. Effects of cerebral ischemia on neuronal hemoglobin. *J Cereb Blood Flow Metab* (2009) 29:596–605. doi:10.1038/jcbfm.2008.145
- He Y, Hua Y, Keep RF, Liu W, Wang MM, Xi G. Hemoglobin expression in neurons and glia after intracerebral hemorrhage. *Acta Neurochir Suppl* (2011) 111:133–7. doi:10.1007/978-3-7091-0693-8_22
- Xie LK, Yang SH. Brain globins in physiology and pathology. *Med Gas Res* (2016) 6:154–63. doi:10.4103/2045-9912.191361
- Orre M, Kamphuis W, Osborn LM, Melief J, Kooijman L, Huitinga I, et al. Acute isolation and transcriptome characterization of cortical astrocytes and microglia from young and aged mice. *Neurobiol Aging* (2014) 35:1–14. doi:10.1016/j.neurobiolaging.2013.07.008
- Belanger M, Magistretti PJ. The role of astroglia in neuroprotection. *Dialogues Clin Neurosci* (2009) 11:281–95.
- L'Episcopo F, Tirolo C, Testa N, Caniglia S, Morale MC, Marchetti B. Glia as a turning point in the therapeutic strategy of Parkinson's disease. *CNS Neurol Disord Drug Targets* (2010) 9:349–72. doi:10.2174/187152710791292639
- Masmoudi-Kouki O, Douiri S, Hamdi Y, Kaddour H, Bahdoudi S, Vaudry D, et al. Pituitary adenylate cyclase-activating polypeptide protects astroglial cells against oxidative stress-induced apoptosis. *J Neurochem* (2011) 117:403–11. doi:10.1111/j.1471-4159.2011.07185.x

FUNDING

This study was supported by the Laboratory of Functional Neurophysiology and Pathology (UR/11ES09) and alternance scholarship of Tunisian Higher Education Ministry, a France-Tunisia exchange program CMCU-Campus France PHC Utique grant number 16G0820/34940PK (to OM-K and David Vaudry), France-Tunisia exchange program CMCU-Utique (grant number 13G0815), a France-Tunisia exchange program No. SSHN2016, and the Institute for Medical Research and Innovation (IRIB). The funders had no role in study design, data collection and analysis, decision to publish, or preparation of the manuscript.

35. Douiri S, Bahdoudi S, Hamdi Y, Cubi R, Basille M, Fournier A, et al. Involvement of endogenous antioxidant systems in the protective activity of pituitary adenylate cyclase-activating polypeptide against hydrogen peroxide-induced oxidative damages in cultured rat astrocytes. *J Neurochem* (2016) 137:913–30. doi:10.1111/jnc.13614
36. Moriyama M, Jayakumar AR, Tong XY, Norenberg MD. Role of mitogen-activated protein kinases in the mechanism of oxidant-induced cell swelling in cultured astrocytes. *J Neurosci Res* (2010) 88:2450–8. doi:10.1002/jnr.22400
37. Hamdi Y, Kaddour H, Vaudry D, Bahdoudi S, Douiri S, Leprince J, et al. The octadecapeptide ODN protects astrocytes against hydrogen peroxide-induced apoptosis via a PKA/MAPK-dependent mechanism. *PLoS One* (2012) 7:e42498. doi:10.1371/journal.pone.0042498
38. Liu YY, Sparatore A, Del Soldato P, Bian JS. H2S releasing aspirin protects amyloid beta induced cell toxicity in BV-2 microglial cells. *Neuroscience* (2011) 193: 80–8. doi:10.1016/j.neuroscience.2011.07.023
39. Quincozes-Santos A, Bobermin LD, Latini A, Wajner M, Souza DO, Goncalves CA, et al. Resveratrol protects C6 astrocyte cell line against hydrogen peroxide-induced oxidative stress through heme oxygenase 1. *PLoS One* (2013) 8:e64372. doi:10.1371/journal.pone.0064372
40. Ferrero-Gutierrez A, Perez-Gomez A, Novelli A, Fernandez-Sanchez MT. Inhibition of protein phosphatases impairs the ability of astrocytes to detoxify hydrogen peroxide. *Free Radic Biol Med* (2008) 44:1806–16. doi:10.1016/j.freeradbiomed.2008.01.029
41. Hamdi Y, Masmoudi-Kouki O, Kaddour H, Belhadj F, Gandolfo P, Vaudry D, et al. Protective effect of the octadecapeptide on hydrogen peroxide-induced oxidative stress and cell death in cultured rat astrocytes. *J Neurochem* (2011) 118:416–28. doi:10.1111/j.1471-4159.2011.07315.x
42. Regan RF, Guo Y, Kumar N. Heme oxygenase-1 induction protects murine cortical astrocytes from hemoglobin toxicity. *Neurosci Lett* (2000) 282:1–4. doi:10.1016/S0304-3940(00)00817-X
43. Rollins S, Perkins E, Mandybur G, Zhang JH. Oxyhemoglobin produces necrosis, not apoptosis, in astrocytes. *Brain Res* (2002) 945:41–9. doi:10.1016/S0006-8993(02)02562-3
44. Tejima E, Zhao BQ, Tsuji K, Rosell A, van Leyen K, Gonzalez RG, et al. Astrocytic induction of matrix metalloproteinase-9 and edema in brain hemorrhage. *J Cereb Blood Flow Metab* (2007) 27:460–8. doi:10.1038/sj.jcbfm.9600354
45. Schelhorn DW, Schneider A, Kuschinsky W, Weber D, Kruger C, Dittgen T, et al. Expression of hemoglobin in rodent neurons. *J Cereb Blood Flow Metab* (2009) 29:585–95. doi:10.1038/jcbfm.2008.152
46. Russo R, Zucchielli S, Codrich M, Marcuzzi F, Verde C, Gustincich S. Hemoglobin is present as a canonical $\alpha_2\beta_2$ tetramer in dopaminergic neurons. *Biochim Biophys Acta* (2013) 1834:1939–43. doi:10.1016/j.bbapap.2013.05.005
47. Li RC, Morris MW, Lee SK, Pouranfar F, Wang Y, Gozal D. Neuroglobin protects PC12 cells against oxidative stress. *Brain Res* (2008) 1190:159–66. doi:10.1016/j.brainres.2007.11.022
48. Li RC, Guo SZ, Lee SK, Gozal D. Neuroglobin protects neurons against oxidative stress in global ischemia. *J Cereb Blood Flow Metab* (2010) 30:1874–82. doi:10.1038/jcbfm.2010.90
49. Watanabe S, Takahashi N, Uchida H, Wakasugi K. Human neuroglobin functions as an oxidative stress-responsive sensor for neuroprotection. *J Biol Chem* (2012) 287:30128–38. doi:10.1074/jbc.M112.373381
50. Qiu XY, Chen XQ. Neuroglobin – recent developments. *Biomol Concepts* (2014) 5:195–208. doi:10.1515/bmc-2014-0011
51. Amri F, Ghoulili I, Amri M, Carrier A, Masmoudi-Kouki O. Neuroglobin protects astroglial cells from hydrogen peroxide-induced oxidative stress and apoptotic cell death. *J Neurochem* (2017) 140:151–69. doi:10.1111/jnc.13876
52. Le HT, Sin WC, Lozinsky S, Bechberger J, Vega JL, Guo XQ, et al. Gap junction intercellular communication mediated by connexin43 in astrocytes is essential for their resistance to oxidative stress. *J Biol Chem* (2014) 289:1345–54. doi:10.1074/jbc.M113.508390
53. Ramalingam M, Kim SJ. Insulin on hydrogen peroxide-induced oxidative stress involves ROS/Ca²⁺ and Akt/Bcl-2 signaling pathways. *Free Radic Res* (2014) 48:347–56. doi:10.3109/10715762.2013.869588
54. Nishi H, Inagi R, Kato H, Tanemoto M, Kojima I, Son D, et al. Hemoglobin is expressed by mesangial cells and reduces oxidant stress. *J Am Soc Nephrol* (2008) 19:1500–8. doi:10.1681/ASN.2007101085
55. Saha D, Patgaonkar M, Shroff A, Ayyar K, Bashir T, Reddy KV. Hemoglobin expression in nonerythroid non-erythroid cells: novel or ubiquitous? *Int J Inflamm* (2014) 2014:803237. doi:10.1155/2014/803237
56. Kapralov A, Vlasova II, Feng W, Maeda A, Walson K, Tyurin VA, et al. Peroxidase activity of hemoglobin-haptoglobin complexes: covalent aggregation and oxidative stress in plasma and macrophages. *J Biol Chem* (2009) 284:30395–407. doi:10.1074/jbc.M109.045567
57. Grigorjeva DV, Gorudko IV, Sokolov AV, Kosmachevskaya OV, Topunov AF, Buko IV, et al. Measurement of plasma hemoglobin peroxidase activity. *Bull Exp Biol Med* (2013) 155:118–21. doi:10.1007/s10517-013-2094-4
58. Wang JY, Shum AY, Ho YJ, Wang JY. Oxidative neurotoxicity in rat cerebral cortex neurons: synergistic effects of H₂O₂ and NO on apoptosis involving activation of p38 mitogen-activated protein kinase and caspase-3. *J Neurosci Res* (2003) 72:508–19. doi:10.1002/jnr.10597
59. Sastre J, Serviddio G, Pereda J, Minana JB, Arduini A, Vendemiale G, et al. Mitochondrial function in liver disease. *Front Biosci* (2007) 12:1200–9. doi:10.2741/2138
60. Uehara T, Nomura Y. [Possible involvement of caspase activation in nitric oxide-induced neuronal apoptosis in SH-SY5Y cells]. *Nihon Yakurigaku Zasshi* (1998) 112(Suppl 1):118–22. doi:10.1254/fpj.112.supplement_118
61. Uehara T, Kikuchi Y, Nomura Y. Caspase activation accompanying cytochrome c release from mitochondria is possibly involved in nitric oxide-induced neuronal apoptosis in SH-SY5Y cells. *J Neurochem* (1999) 72:196–205. doi:10.1046/j.1471-4159.1999.0720196.x
62. Yang CM, Hsieh HL, Lin CC, Shih RH, Chi PL, Cheng SE, et al. Multiple factors from bradykinin-challenged astrocytes contribute to the neuronal apoptosis: involvement of astroglial ROS, MMP-9, and HO-1/CO system. *Mol Neurobiol* (2013) 47:1020–33. doi:10.1007/s12035-013-8402-1
63. Hamdi Y, Kaddour H, Vaudry D, Douiri S, Bahdoudi S, Leprince J, et al. The stimulatory effect of the octadecapeptide ODN on astroglial antioxidant enzyme systems is mediated through a GPCR. *Front Endocrinol* (2012) 3:138. doi:10.3389/fendo.2012.00138
64. Seaborn T, Masmoudi-Kouki O, Fournier A, Vaudry H, Vaudry D. Protective effects of pituitary adenylate cyclase-activating polypeptide (PACAP) against apoptosis. *Curr Pharm Des* (2011) 17:204–14. doi:10.2174/138161211795049679
65. Kaddour H, Hamdi Y, Vaudry D, Basille M, Desrues L, Leprince J, et al. The octadecapeptide ODN prevents 6-hydroxydopamine-induced apoptosis of cerebellar granule neurons through a PKC-MAPK-dependent pathway. *J Neurochem* (2013) 125:620–33. doi:10.1111/jnc.12140
66. Takahashi N, Watanabe S, Wakasugi K. Crucial roles of Glu60 in human neuroglobin as a guanine nucleotide dissociation inhibitor and neuroprotective agent. *PLoS One* (2013) 8:e83698. doi:10.1371/journal.pone.0083698
67. Guidolin D, Agnati LF, Tortorella C, Marcoli M, Maura G, Albertini G, et al. Neuroglobin as a regulator of mitochondrial-dependent apoptosis: a bioinformatics analysis. *Int J Mol Med* (2014) 33:111–6. doi:10.3892/ijmm.2013.1564
68. Takahashi N, Wakasugi K. Identification of residues crucial for the interaction between human neuroglobin and the alpha-subunit of heterotrimeric Gi protein. *Sci Rep* (2016) 6:24948. doi:10.1038/srep24948
69. Schaer CA, Schoedon G, Imhof A, Kurrek MO, Schaer DJ. Constitutive endocytosis of CD163 mediates hemoglobin-heme uptake and determines the noninflammatory and protective transcriptional response of macrophages to hemoglobin. *Circ Res* (2006) 99: 943–50. doi:10.1161/01.RES.0000247067.34173.1b
70. Sherer TB, Betbaro R, Testa CM, Seo BB, Richardson JR, Kim JH, et al. Mechanism of toxicity in rotenone models of Parkinson's disease. *J Neurosci* (2003) 23:10756–64.
71. Richter F, Meurers BH, Zhu C, Medvedeva VP, Chesselet MF. Neurons express hemoglobin alpha- and beta-chains in rat and human brains. *J Comp Neurol* (2009) 515:538–47. doi:10.1002/cne.22062

Conflict of Interest Statement: The authors declare that the research was conducted in the absence of any commercial or financial relationships that could be construed as a potential conflict of interest.

Copyright © 2017 Amri, Ghoulili, Tonon, Amri and Masmoudi-Kouki. This is an open-access article distributed under the terms of the Creative Commons Attribution License (CC BY). The use, distribution or reproduction in other forums is permitted, provided the original author(s) or licensor are credited and that the original publication in this journal is cited, in accordance with accepted academic practice. No use, distribution or reproduction is permitted which does not comply with these terms.



The Eight and a Half Year Journey of Undiagnosed AD: Gene Sequencing and Funding of Advanced Genetic Testing Has Led to Hope and New Beginnings

Illana Gozes^{1*}, Marc C. Patterson², Anke Van Dijck³, R. Frank Kooy³, Joseph N. Peeden⁴, Jacob A. Eichenberger⁵, Angela Zawacki-Downing⁶ and Sandra Bedrosian-Sermone⁶

¹The Lily and Avraham Gildor Chair for the Investigation of Growth Factors, Elton Laboratory for Neuroendocrinology, Department of Human Molecular Genetics and Biochemistry, Sackler Faculty of Medicine, Adams Super Center for Brain Studies and Sagol School for Neuroscience, Tel Aviv University, Tel Aviv, Israel, ²Division of Child and Adolescent Neurology, Pediatrics and Medical Genetics, Mayo Clinic Children's Center Rochester, Rochester, MN, USA, ³Cognitive Genetics Group, Department of Medical Genetics, University of Antwerp, Antwerp, Belgium, ⁴Diagnostic Clinic, East Tennessee Children's Hospital and Clinical Assistant Professor of Medicine at the University of Tennessee, Knoxville, TN, USA, ⁵Physician Informaticist, Children's Hospital of Georgia at Augusta University, Augusta, GA, USA, ⁶ADNP Kids Research Foundation, Brush Prairie, WA, USA

OPEN ACCESS

Edited by:

Hubert Vaudry,
University of Rouen, France

Reviewed by:

Lidia V. Gabis,
Sheba at Tel Hashomer, Israel
Nils Lambrecht,
University of California at Irvine,
United States

*Correspondence:

Ilana Gozes
igozes@post.tau.ac.il

Specialty section:

This article was submitted to
Neuroendocrine Science,
a section of the journal
Frontiers in Endocrinology

Received: 15 September 2016

Accepted: 02 May 2017

Published: 19 May 2017

Citation:

Gozes I, Patterson MC, Van Dijck A, Kooy RF, Peeden JN, Eichenberger JA, Zawacki-Downing A and Bedrosian-Sermone S (2017) The Eight and a Half Year Journey of Undiagnosed AD: Gene Sequencing and Funding of Advanced Genetic Testing Has Led to Hope and New Beginnings. *Front. Endocrinol.* 8:107. doi: 10.3389/fendo.2017.00107

Background: Activity-dependent neuroprotective protein (ADNP) is one of the most prevalent *de novo* mutated genes in syndromic autism spectrum disorders, driving a general interest in the gene and the syndrome.

Aim: The aim of this study was to provide a detailed developmental case study of ADNP p.Tyr719* mutation toward improvements in (1) diagnostic procedures, (2) phenotypic scope, and (3) interventions.

Methods: Longitudinal clinical and parental reports.

Results: AD (currently 11-year-old) had several rare congenital anomalies including imperforate anus that was surgically repaired at 2 days of age. Her findings were craniofacial asymmetries, global developmental delay, autistic behaviors (loss of smile and inability to make eye contact at the age of 15 months), and slow thriving as she gradually matures. Comprehensive diagnostic procedures at 3 years resulted in no definitive diagnosis. With parental persistence, AD began walking at 3.5 years (skipping crawling). At the age of 8.5 years, AD was subjected to whole exome sequencing, compared to the parents and diagnosed as carrying an ADNP p.Tyr719* mutation, a causal recurring mutation in ADNP (currently ~17/80 worldwide). Brain magnetic resonance imaging demonstrated mild generalized cerebral volume loss with reduced posterior white matter. AD is non-verbal, communicating with signs and word approximations. She continues to make slow but forward developmental progress, and her case teaches newly diagnosed children within the ADNP Kids Research Foundation.

Conclusion: This case study emphasizes the importance of diagnosis and describes, for the first time, early motor intervention therapies. Detailed developmental profile of selected cases leads to better treatments.

Keywords: activity-dependent neuroprotective protein, case study, mutation, nonsense, motor delays, autism spectrum disorder

INTRODUCTION

Looking at neuroglial interactions, we (Gozes group) discovered activity-dependent neuroprotective protein (ADNP), as a protein secreted from glial cells in the presence of vasoactive intestinal peptide (VIP), which mediates VIP's neuroprotective activity (1). Further cloning (2) revealed high conservation and specificity to vertebrates (3). The large human ADNP (hADNP) gene structure (~40 kb) includes five exons and four introns with alternative splicing of an untranslated second exon (chromosome 20q12-13.2, a region associated with aggressive tumor growth). As we described (2, 3), hADNP is also mutated in cancer.

Knocking out ADNP in mice resulted in embryonic death at the time of neural tube closure, revealing that ADNP is crucial for brain formation (4). ADNP haploinsufficient mice survive but show learning and memory deficits (5), in a sex-dependent manner (6). At the protein level, we have shown multiple crucial interactions for ADNP including direct binding to the chromatin remodeling complex SWI/SNF and interaction with heterochromatin protein 1 alpha (7, 8). This study was extended to show that ADNP interacts with all HP1 proteins toward histone posttranslational modification (9). At the transcriptional level, ADNP binds to the locus control region of the beta globin gene to regulate globin transcription (10) as well as the promoter regions of apolipoprotein E, cathepsin C, cathepsin Z, metallothionein 1, neurogenin 1, and myosin regulatory light chain 2 (8). At the RNA splicing level (11), ADNP interacts with Brahma, a component of the SWI/SNF complex regulating alternative splicing that shows a similar developmental expression pattern to ADNP. Immunoprecipitations further suggested binding between ADNP and polypyrimidine tract-binding protein-associated splicing factor (PSF), with PSF being a direct regulator of the microtubule-associated tau transcript splicing. Further interaction with the protein translation machinery was shown with the eukaryotic translation initiation factor 4E (eIF4E) (6) through direct binding as well as sex and age-dependent regulation. Notably, eIF4E is linked to autism (12). In the neuronal cell cytoplasm, ADNP is critical for neurite outgrowth and maintenance (13) through direct interaction by its SIP motif with microtubule end binding proteins (14, 15). The microtubule system is tightly associated with the autophagy system (16), and ADNP binds the microtubule-associated protein 1 light chain 3B (17). With these key regulatory functions ADNP controls the expression of >400 genes during embryonic development (8) and of thousands of hippocampal genes postnatally, impacting pathways associated with ion channels-synaptic transmission in a sex- and age-dependent manner (18).

From a clinical point of view, an ADNP gene deletion was first implicated in delayed cognitive development in a case study in 2007 (19). Further findings included the first *de novo*

p.Lys408Valfs*31 mutation in the ADNP gene in a large cohort of autistic patients (20). Large-scale sequencing study (21), analyzing 2,446 probands, identified an additional p.Tyr719* *de novo* ADNP mutation and this is the subject of our current publication. Helsmoortel et al. (22) grouped 10 patients with mutations in ADNP. As all patients suffered from autism with intellectual deficiencies and shared characteristic facial features, it was concluded that mutations in ADNP cause a syndromic form of autism. Two additional patients were further described, sharing the reported characteristics (23, 24). Interestingly, Pescosolido et al. described another case of p.Tyr719* *de novo* ADNP mutation, suggesting that this is a recurrent mutation. Coe et al. (25) also reported five patients with a truncating ADNP mutation in a screening of 4,716 patients with autism/ID. De Rubeis et al. (26) identified three more patients of a total of 3,871 screened and the DDD project reported four novel cases out of 1,133 screened (27). We have summarized the above in an introductory remark to the story of Tony Sermone, presenting an additional ADNP mutation L349Rfs*49 (28). A short synopsis of the clinical phenotype was recently published (29), additional mutations are discovered and information extended (27, 30–33) and an extensive description is in preparation (Van Dijck et al., in preparation). Interestingly, a recent publication suggested that ADNP is one of three major genes associated with autism spectrum disorder (ASD) (34), complementing the original estimation of the ADNP-related syndrome constituting 0.17% of ASD cases (22). These findings mark ADNP as one of the most frequent ASD-associated genes known to date. Therefore, further understanding of the ADNP-related syndrome is of general interest both from a case study point of view as well as from a population perspective. Here, we chose to present one case study and concentrate, for the first time, on delays in motor development.

METHODS

Longitudinal clinical and parental reports were collected focusing on diagnosis, phenotypic scope, and interventions. Time points of emphasis: birth, 1–3.5 years and 8.5 to date. All materials were given with parental informed consent.

RESULTS

Initial Clinical Data

Father's and mother's age at birth was 32 and 31, respectively. No consanguinity. No affected siblings—parents were carriers of CF. AD was born at 37–38 weeks vaginally (October 1, 2005). She was 50 cm in length and weighed 3.475 kg. Her head circumference was 34 cm. She had Apgar scores of 7 and 8 at 1 and 5 min of life. She was noticed to have low anal atresia and had surgery to repair

TABLE 1 | Parental/caregiver observations/clinician observations.

A: Gross physical anomalies											
Age (years)	0	1	2	3	4	5	6	7	8–10		
	Imperforate anus (surgery at 2 days, 12-day stay)—5 months anal dilation										
Legs	Extreme small feet and toes. At 9 years and 8 months: trunk and upper extremities appear larger than lower extremities. Left leg is 2 cm shorter than the right leg and 9 cm less in width at the midthigh. Her left foot is smaller than her right. She has fifth finger clinodactyly. She has proximal implantation of the thumbs										
Hair	White/blonde (silver) forelock of hair (remaining hair is brown), hair growth pattern discrepancy (left side). Low hairline. She has a posterior parietal hair whorl. She has an irregular hair part to the left										
Face	Facial asymmetry, flat face and a slant mouth (left side), small low-set ears posteriorly rotated, facial palsy (age 15 months–8.5 years of age)										
Head and face	Flat back/head side (plagiocephaly). Treated with helmet cranial technologies. Frequent otitis as an infant/young child	Stopped smiling, had trouble with eye contact (~15 months)			Stopped head helmet treatment, suggested microcephaly				Eye defects: she has intermittent left esotropia (a right gaze preference). Prominent upper buccal frenulum. Widely spaced and asymmetric size of teeth. Mandibular dimple upon her chin that is to the left of the midline		
Stature	60th percentile (%)							10%	"Short" stature	0% short stature	
Weight					48–50%						
B: Motor disabilities and sleep disturbances											
Age (years)	0	1	2	3	4	5	6	7	8	9	10
Legs	Leg length discrepancy (left leg), extreme small feet and toes, low tone, hypotonic throughout the body Left side weakness "abnormal gait" favoring right side										
Muscles	Legs showing signs of atrophy—not growing until 2.5 years Extreme muscle tightness (warm baths, stretching, braces, treadmill, and orthopedic shoes, >300 treatments)										
Mobility	Sitting up at 9 months and severe delays starting at 11 months. Minimal progress	Most severe motor delay minimal progress—bearing weight to stand was severely delayed until 3 years of age									
Walking		Therapy began at 15 months		Begin independent walking (3.5)						Running!	
Fine muscle tone	Made improvements, still struggling										
Sleep disturbance	Until 3 years of age, terrible spells (stopped breathing) required ambulatory care/inpatient hospital visits. Apnea tests revealed nothing. Nightly awakening 1–4 a.m., muscle cramps and dystonia, until the age of 5 years of age						Improved after 5		Normal sleep	Hypotonia	
C: Clinical tests											
Karyotype (skin biopsy):						(46,XX)—no chromosome abnormality was apparent.					
Array Comparative Genomic Hybridization						arr cgh 1-22(39,986 oligos)x2,X(2,745 oligos)x2,Y(367 oligos)x0. The result is normal. No abnormality was detected by array CGH analysis					
Prader-Willi–Angelman analysis						MLPA demonstrated a normal methylation pattern. No deletions or duplications were detected. This indicates that both the maternally and paternally derived copies of the PWAS critical region are present					

(Continued)

TABLE 1 | Continued

Fragile X analysis	CGG repeat: 23 and 29; methylation status: normal; final result: normal
CFTR gene, full gene analysis	A mutation was NOT detected. Intron 8 poly T alleles are: 7T/7T
Endocrine studies (for growth deceleration) (2 years, 5 months): the sedimentation rate was normal. Calcium was normal at 9.7, and the phosphorus was normal as well at 4.7 mg/dL Reference range for the calcium is 9.6–10.6, and the reference range for the phosphorus is 4.3–5.4. Normal thyroid function: TSH was 2.7 with a reference range of 0.3 to 5, and the free T4 was 1.3 with a reference range of 0.8–1.8	Growth factors were also in the normal range. Specifically, the IGF-1 was 54 ng/mL The reference range is 51–303. The IGFBP-3 is at 3.7 mcg/mL with a normal range being 0.8–3.9. The skeletal survey showed bone age at 2.5 years using the RUS method; there was no evidence of skeletal dysplasia
Echocardiogram (2 years, 5 months)	Normal
Upper GI endoscopy and flexible sigmoidoscopy (2 years, 5 months)	The upper endoscopy was completely normal on both visualization and histology. During the flexible sigmoidoscopy, the presence of a significant amount of stool was noted, and AD was disimpacted
Retroperitoneal ultrasound (2 years, 5 months): additional evaluation at 9 years, 8 months: delayed bladder training	Both kidneys are in normal position and have normal appearance. No hydronephrosis or parenchymal loss. The right kidney measures 6.8 cm; left, 6.9 cm. These are normal measurements for a patient of this age. Ureters are not seen. Incidentally noted is an enlarged spleen with several calcified granulomas within it. The spleen measures 9.6 cm

D: Psychology performed at 3 years, 2 months

Bayley Scales of Infant Development, Third Edition: AD was able to attend to a picture, squeeze object to make a sound, retrieve an object of interest, stack two blocks, scribble on paper with crayon, make forward progress by crawling, and make coordinated, alternating step movements (language assessment was performed separately by Speech Pathology)

Autism Diagnostic Observation Schedule: AD had limited language, including three signs (more, all-done, and bubbles) and a few verbalizations (babbling, whining, groan, and words "go," "da-da," and "ma-ma"). She did not have a distal point. She had poor eye contact; rarely or never directed facial expressions at others; and did not coordinate eye contact, verbalizations, and gestures to communicate social intent. She occasionally moved closer to person as a request for more or would moan indirectly when frustrated. She did not respond to name, except when her father implied he was going to tickle her. She signed "more" for bubbles and snacks. She was generally aloof and passive and did not exhibit giving, showing, or initiate joint attention. She responded to joint attention when toy was activated but not in response to gaze or pointing by examiner. She played with cause and effect toys and tended to perseverate on musical phone toy. She exhibited many self-stimulatory, repetitive behaviors including: (a) holding her hands out in front of her and waving her hand while staring and smiling at it, (b) slapping her belly hard then holding her hand up in the air and shaking and staring at it while laughing, and (c) putting her head back, shaking her hair, and staring at the lights. She also peered at objects out of the corner of her eyes, banged her head on floor, and exhibited rigid body and flapping hands when excited about bubbles

Clinical report at 9 years and 8 months

Has several autistic behaviors: swishing of her head and hair back and forth. Head banging. She looks at objects out of the corner of her eyes in a stereotypical fashion. She has inconsistent response to her name (despite normal hearing). Her play behavior is largely perseverative play with basic toys. She enjoys music. She does not have pretend play. She will clap her feet together and stomp when excited. She clinches her hands together with excitement. She can be friendly and loving; however, she may also have aggressive periods

E: Evaluation by Speech Pathology at 3 years, 2 months

The Verbal Language Development Scale was administered: this is a developmental scale that is completed via observation of the child as well as through parent report. AD exhibited a language age equivalent of 12 months on this instrument. Those items which she exhibited that would be expected by the first year of age include laughing, smiling, producing consonant sounds reflexively, understanding the word "bye-bye", and following simple directions. She was inconsistently responding to her name. She did not yet imitate sounds or imitate words. Those items that she exhibited that would be expected between the first and second year of age include an expressive vocabulary of two words and recognizing the name of familiar objects; marking with a pencil or crayon was emerging. Items that would be expected by the second year of age that she did not yet exhibit included an expressive vocabulary of at least 25 words, using the names of familiar objects, identifying common pictures when they are named, talking in short sentences, and naming common pictures

Expressive language: a spontaneous language sample was taken throughout this session. Much of this was done while AD was playing with toys or interacting with her parents or interacting with her sister. A number of instances of non-verbal communication including nodding yes to a question and using a sign to indicate that her parents were being bad were observed. A number of isolated syllables using the neutral schwa vowel and /m/ and /n/ were heard. As well as one instance of "da". She also used the vowel /i/ in isolation in a non-meaningful way. By parent report, she also produced a repetitive "dib, dib, dib." Therefore, her phonetic inventory is constrained to /n/, /m/, /d/, /b/, and /p/. Vowels were constrained to primarily the schwa, /i/, and an isolated /i/. Mr. and Mrs. parents report they have not heard additional vowels at home. Syllable shapes noted included consonant-vowel and reduplicated syllables

(Continued)

TABLE 1 | Continued

Oral structural functional exam: physical examination of the oral mechanism was done via observing AD during vocal play. She had facial symmetry at rest. Range of motion of the lips is full bilaterally for retraction and for lip rounding. Tongue movement was not observed. Given her good production of "da," she shows good strength of lingual movement for the plosive sound. She also is reported to produce /b/ and /p/ showing good labial strength. There did not appear to be any reduction in range of motion. The presence of oral non-verbal apraxia could not be ascertained as she was not yet able to follow verbal directions or imitate blowing, clicking her tongue, puckering lips on command, etc. (This was diagnosed later at ~10 years of age)

Speech production: spontaneous speech is characterized by adequate respiratory support and a mildly hoarse phonatory quality (+1). Resonance is normal. There was no evidence for dysarthria

Behavioral and communication observations: AD showed fleeting eye contact. She played appropriately with a number of toys. She showed good attention to her sister's face as her sister engaged her in attempts at imitation of sounds. She sought attention both from her parents and from the clinician. A couple of spontaneous signs were noticed. She did babble sounds as noted above but less frequently than would be expected even for a child 9–12 months of age. There were some moments of joint attention but this was inconsistent. Her parents reported frequent head banging; however, this was not observed during the clinical session

F: Behavior dysfunctions											
Age (years)	0	1	2	3	4	5	6	7	8	9	10
Autistic-like		15 months (lack of smile)	Non-verbal, began head banging (self-injury)	3.5 began walking, smile develops	Much injurious behavior disappeared (reduced) as she started walking, communication cards and voice technologies	Some injurious behavior			Non-verbal, being trained and can sign and use voice technology, increased vocalization and independency. Receptive language grew with aggressive repetition. Her participation increased with adaption of her needs. Anxiety is subsiding		
Treatment benefits			Greatly benefited from developmental playgroups prior to age 3.		Parental observation: AD is known to smile and any display positive body language toward normally developing peers (she smiles and even waves hi and tries to approximate goodbye "beh" to other children and now as she ages she no longer needs prompting for the social interactions). Multiple therapies are the best treatment. She benefited and grew in independence both in mobility and functionality with the public school system						
Sensory		Dysfunction disorder diagnosed prior to the age of 2. Difficulties with maintaining temperature, keeping on gloves, hats, shoes, etc.									

(A) Gross physical anomalies and sleep disturbances. (B) Motor disabilities (including pictures at toddler age with walker and running at the age of 10). Findings are arranged by age (years) 1–10. (C)–(E) Clinical observation: AD was seen in multidisciplinary consultation at Mayo Clinic in 2008, at 3 years of age. The multidisciplinary team at that time included Pediatric Neurology, Pediatric Endocrinology, Physical Medicine and Rehabilitation, Medical Genetics, Social Work, Pediatric Allergy, Pediatric Cardiology, Pediatric Gastroenterology, Pediatric Otorhinolaryngology, Pediatric Dermatology, Orthopedics, Developmental and Behavioral Pediatrics, and Neuropsychology. (C) Clinical tests. (D) Psychology performed at 3 years, 2 months. (E) Evaluation by speech pathology at 3 years, 2 months. (F) Behavioral dysfunctions (findings are arranged by age in years: 1–10).

this at 2 days of age [Table 1 (A), physical anomalies]. She had significant GERD as an infant and young child. At 2 years of age, AD was diagnosed with autism.

Developmental Delay: Focus on Motor Function

AD started sitting at 7–9 months. While her younger brother walked at 1 year of age, she continued to lag severely behind, she could not crawl, walk, or even bare weight to stand on her legs. It seemed that at about 2 years of age, AD's legs began to show some signs of atrophy,

not increasing in shoe size (unlike her siblings), until she began to walk. Currently, at the age of 11, one can still see the disproportion of AD's small tapered legs from the knees to the feet, compared to the rest of her body. This finding attests to the importance of ADNP in muscle and bone development and to the regulation of key gene/proteins beyond embryonic development (8, 18).

AD started walking with a walker at 2.5 years of age, skipping crawling [Table 1 (B); Figure 1A]. Walking short distances resulted in skin redness and muscle pain. She began walking independently at the age of 3.5 years. The following year presented daily challenges in her “functional” walking. She often could not

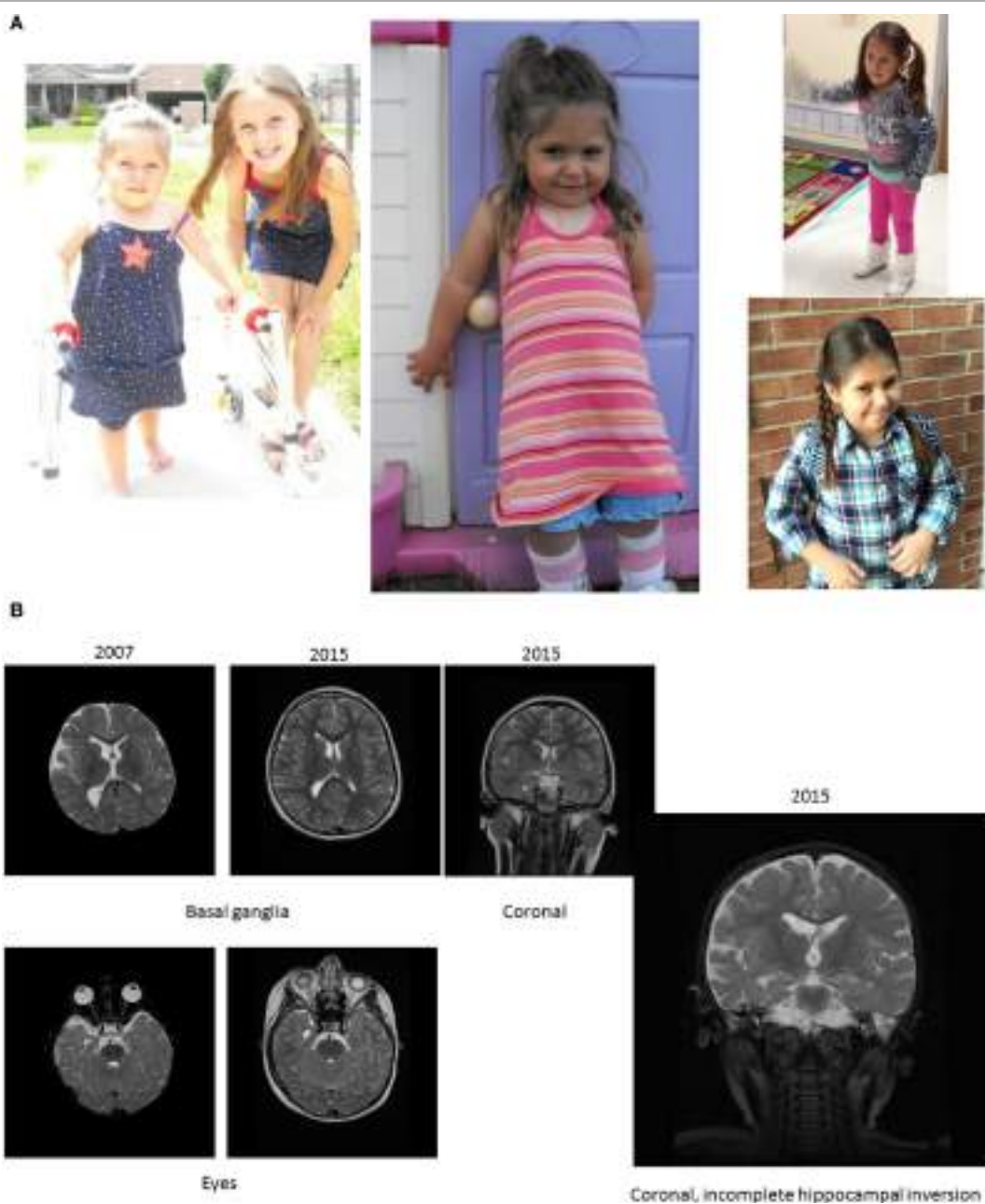


FIGURE 1 | Continued



FIGURE 1 | Pictures depicting AD's development, brain development, and comparison to other children with the same mutation. (A) AD's development in pictures: starting top left: young AD with her sister's "push" to walk. AD is barefoot and her legs turned red from a very short walk. Her muscles in her ankles got tight and she exhibited low muscle tone and needed to be stretched several times a day, or she would suffer excruciating pain at night. The painful day walk and nights were full of crying periods. At the same time, a picture was taken, when she finally could lean against things with her leg braces and at a similar time point. Third picture on the top, AD at her first beauty pageant, after months of her sister and mother teaching her how to spin and dance with a baton ribbon. Fourth picture on the bottom, AD at her eighth birthday, just before her diagnosis and submission to brain scans. AD is successful at attending regular primary schools. Her smile keeps the family and caregivers going. (B) Magnetic resonance imaging results (volumetric T2 performed at 2007 and 2015). (C) Pictures of additional children with ADNP p.Tyr719* mutation (featured also in Table 2 (E), all materials given with parental informed consent).

stand for more than a few seconds. Climbing stairs was a third milestone, using the strong leg and pushing the weaker leg after. Until about the age of 5, AD had severe muscle tightness that mimicked symptoms of a neuromuscular disorder. The muscle tightness was associated with severe sleep disturbances [Table 1 (B), last raw]. At 9 years and 3 months, the parents noticed that she had more of a delay with gross motor skills than with fine (albeit both delayed). She walked independently, but with a broad based and antalgic gait [Table 1 (B); Figure 1A]. At 10.5 years of age, she was ambulatory and quite flexible with increased range of motion noted particularly in the small joints. Physically, hands were broad, with short and broad fingers and fifth finger clinodactyly. Distal phalanges appeared short and fingernails were spatulate. Feet showed short fourth and fifth toes and deep setting. Toe tip and fingertip pads were prominent [see also Table 1 (A)]. Through parental persistence and AD's willpower (see treatments below), now at age 11, she is running and riding a bicycle. She still struggles with reciprocating down stairs and is mostly non-verbal (see below).

Clinical Test Results and Growth Curve

Age of 3 Years and 2 Months: (Mayo Clinic)

1. Static encephalopathy of presumed antenatal onset and genetic etiology
2. Severe global developmental delay (the diagnosis of intellectual disability is typically not made at this age)

3. ASD
4. Multiple congenital anomalies (imperforate anus, dental anomalies, facial asymmetry, and poliosis)
5. Microcephaly [head circumference, 45.5 cm (<2%)]
6. Generalized hypotonia, axial greater than appendicular
7. Normal stature and mass [weight 14.7 kg (61%); length, 90 cm (10%)]
8. Hyperopic astigmatism

Extensive investigations showed normal or negative results [Table 1 (C)], those also included tests for Rett syndrome and a skeletal survey (bone, age 2.5 years). Psychological and speech evaluations were also included showing global delays as indicated below.

At 9 Years and 3 Months

AD's weight was 27.1 kg. Her height 114.7 cm, occipitofrontal circumference 50 cm. She has continued problems with constipation/obstipation.

At 10.5 Years of Age

She was short statured (height 128 cm)¹ with normal weight and head circumference (34.5 kg and 52 cm, respectively). She was still mostly non-verbal. She communicated with her family

¹<https://www.cdc.gov/growthcharts/data/set1clinical/cj41c022.pdf>.

TABLE 2 | Activity-dependent neuroprotective protein (ADNP) phenotype data questionnaire (Facebook™, A–D); (E) selected children with ADNP p.Tyr719* mutation (featured also in Figure 1C); Facebook data.

A	
cDNA/nucleotide	c.2157C>G
Protein—pchange	p.Y719
Zygosity	Heterozygous
Inherited/de novo	<i>De novo</i>
Location	USA
Sex	Female
Birthday	01/10/2005
Pregnancy or birth complications?	Meconium stained from AD imperforate anus
Birth weight	7.8 lbs
Developmental	
Gross motor delay	Yes
Intellectual disability	Originally diagnosed as severe—at the age of 10 diagnosed as moderate
Speech delay (has under 25 understandable words)	Apraxia/speech delay
Have you done prompt, rest, or other “oral motor planning” types of therapy or “general speech therapy”	Yes
Can your child write?	Age 10: now writes her name with hand over hand assistance and used handwriting with no tears program. Primarily a “motor planning issue” needs repetition and tracing. She is also able at age 10 to recognize certain site words on Flashcards especially written in red which helps her cortical vision impairment (CVI)
Can your child feed him/herself with utensils?	Yes, with spoon
Neurological/brain	
Has your child had a magnetic resonance imaging (MRI) brain scan?	At 2 years (no findings) and at 9 years (Figure 1A)
Does your child have a brain abnormality?	Slight diminishing of white matter in the cerebellum (9 years of age)
Regression of skill?	Slight when not working consistently
Facial palsy/bells palsy?	Left side facial palsy
B	
Behavior	
Autism spectrum disorder (ASD) diagnosis?	At 2 years of age
Did you have a hard time getting an ASD diagnosis?	No—however, socializes with adults important: at 3.5 years of age when she achieved stages of independent and functional walking and attained mobility, she started opening up and was able to access her environment and peers. She grows and flourishes (and still does at age 10) having “inclusion” and access to her normally developing peers. AD “wants” to play but her lack of speech makes connecting difficult on many levels.

(Continued)

TABLE 2 | Continued

Rocks back and forth or shakes head when excited	No (claps her hands and makes noise or word approximation)
Like to rub or twirl fingers and hands, sometimes close to face for stimulation?	Yes
Does/did your child love to be around most adults, not just family (loving, eye contact, happy with adults, especially as an infant/young toddler)?	Yes
Does your child interact or directly socialize with other children?	No (starting to develop as she attained mobility)
Does your child like “indirect” interaction with children? (prefers to play alone by other children, but not with them)	Yes
Does/did your child have an extremely loving, friendly, affectionate/cuddles demeanor as a baby/young toddler?	Yes
Does your child line up or stack items compulsively?	No
Does your child have an extreme love for music?	Yes!!
Does your child have an extreme love for water (in water or splashing/playing with water)?	Yes
Sensory processing disorder?	Yes
Enjoys/loves “swinging” = vestibular stimulation	Yes
ADHD diagnosis?	No
OCD diagnosis?	No
Anxiety disorder?	No
BAD Behavior, does/did your child have increased BB in early childhood?	Yes
What age did “bad” behaviors begin (symptoms)	2 (head banging, hair pulling, copying with waiting, violent behavior—improvements as she matures)
C	
Vision	
Vision impairment	Yes
CVI	Yes
Farsightedness	Yes (farsighted for many years—however, with further maturation, this is diminished and now she is tending toward near sightedness)
Near sightedness	Developed to some degree with further maturation (age 10)
Astigmatism	Yes
Glasses?	Transient
Will your child wear the glasses?	No
Light-gazer (stared/stares at lights)	Yes
Strabismus (occasional eye crossing)	Yes
Ptosis (drooping or falling eyelid)	No

(Continued)

TABLE 2 | Continued

Hearing	
Developmental hearing impairment. Update October 2016: she has healed and passed the functional hearing tests for the first time in 5 years. She will not need a third set of permanent tubes	Started failing traditional tests at age 5 even after tubes—auditory brainstem response (ABR) performed—normal. Asymmetric, better on the right ear ABR performed with MRI at age 9 and it was normal. 2016 her final (second set) ear tubes were removed and will follow-up this to see how she does without them. Repeat ABR is necessary each year.
Sleeping	
Did or does your child have any "prolonged sleeping problems?"	Yes (severe ages birth to age 5 waking at 1–4 a.m.). Sleeping issues decreased after the age of 5, the parents refused medication
Gastrointestinal and feeding	
Childhood feeding problems?	Could not latch, bottle was ok, breast milk ok reflux and still regurgitates food back up in mouth and obstipation
Feeding tube	No
GERD or reflux	Yes
Oral movement difficulties	Yes
Oral drinking liquid problems (thicken liquids)	Yes
Does not seem to "getfull"	Yes
Aspiration difficulties	Yes
Is your child overweight?	Yes
Constipation problems	Yes
D	
Body and skeletal	
Teeth: did teeth come in-early? (baby teeth, including molars approximately at age 1)	NO
Feet: shape or abnormality—describe all	Short little toes, chubby/puffy, flat
Feet: (circulation) cold (abnormally cold)	Yes
Feet: size	Very small
Hand: shape or abnormality, describe all	Fifth finger clinodactyly tested by X-ray and confirmed by Mayo ClinicGenetics
Hands: puffy/pudgy	Small and toddler like
Hands: fifth finger clinodactyly? (pinky finger bends inward at the last joint)	Yes
Ankles: pronate inward/bow inward	
Heart: congenital heart defect?	At/after birth it took longer for a valve to close. Murmur now not heard at age 9. Checked out ok for cardiology with recent ADNP diagnosis and ultrasound 2015
Endocrinology and growth	
Growth delays/"short stature" (below 25% percentile)	YES (diagnosed at the age of 3)
Growth Hormone - LOW?	Growth hormone was low around age 7

(Continued)

TABLE 2 | Continued

Others			
Has your child had "breath holding" episodes?	Started at 4 weeks old, stopped around 3 years old (ambulatory care needed and coded at hospital)		
Autoimmune: did/does your child get sick often?	At young ages, high fever, RSV, kidney infection, UTI		
Insensitivity to pain/high pain threshold	Yes		
Temperature regulation issues	Yes		
Circulation: does your child get cold hands and feet?	Yes		
Toilet trained? Daytime?	In the process—76% trained		
Toilet trained? Night time?	No		
Hyperphagia? Excessive appetite—obsessed with eating even if not hungry...	Yes		
Abnormal obsession or desires of drinking water	Yes		
E. Selected p.Tyr719* ADNP-mutated children			
ID	8	10	13
cDNA/nucleotide	c.2157 C>A	c.2157 C>A	c.2157 C>G
Protein—pchange	p.Tyr719*	p.Tyr719*	p.Tyr719*
Sex	Male	Female	Male
Birth Year	2012	2014	2008
Gross motor delay	Yes	Yes	Yes
Fine motor delay	Yes	Yes	Yes
Intellectual disability	Yes	Unknown—too young	Yes
Speech delay	Yes	YES	Yes
ASD diagnosis	Yes	unknown—too young	No
Brain abnormality on MRI	No	YES	Yes
Type of brain abnormality	n/a	Widening of ventricles, cerebral atrophy (volume loss), thinning of the corpus callosum	Frontal atrophy and some volume loss all over. Wide frontal and temporal horns. Small/ fine corpus callosum

with signs and word approximations. She demonstrated autistic stereotypies as well as sensory-seeking behaviors including head banging and skin picking.

Currently, AD continues to make slow but forward developmental progress, demonstrating the importance of early and extensive therapies (see below).

Psychological Test Results (3 Years and 2 Months, Mayo Clinic)

Bayley Scales of Infant Development, Third Edition: (SS = 55, first percentile) 11-month-old level [Table 1 (D)]. Motor skills

(SS = 49, <0.1st percentile) 15-month-old level for fine motor skills to 9-month-old level for gross motor skills.

Child Development Inventory (MCDI): general development 16-month-old level, social maturity, 23-month-old level; self-help skills, 15-month-old level; fine motor and language skills, 16-month-old level; and gross motor skills 11–12 months.

Behavior Assessment System for Children, Second Edition–Parent and Teacher Rating Scales: “at risk” for attention problems and sad/irritable mood.

Connors Teachers Rating Scale, Revised: limited adaptive skills, including socialization and functional communication.

School Situation Questionnaire: AD’s behavior was not reported to be problematic in most school situations.

Autism Diagnostic Observation Schedule: communication (RS = 4, cutoffs = 2/4), reciprocal social interaction (RS = 14, cutoffs = 4/7), combined algorithm (RS = 18, cutoffs = 7/12); limited play skills (RS = 4) and stereotyped behavior and restricted interests (RS = 5). Consistent with ASD [Table 1 (D)].

Evaluation by Speech Pathology (3 Years and 2 Months)

The Verbal Language Development Scale: age equivalent of 12 months.

Expressive language: a number of instances of non-verbal communication observed and a number of isolated syllables; no recognizable words.

Oral structural functional exam: facial symmetry at rest; range of motion of the lips was full bilaterally for retraction and for lip rounding; reported adequate tongue movement and labial strength. No reduction in range of motion.

Speech production: adequate respiratory support and a mildly hoarse phonatory quality (+1). Resonance is normal. No evidence for dysarthria.

Behavioral and communication observations: fleeting eye contact; played appropriately with a number of toys; good attention to her sister; sought attention both from her parents and from examiner. Babbled sounds less frequently than would be expected even for a child of 9–12 months. Inconsistent joint attention. At ~10 years of age, verbal apraxia was diagnosed [Table 1 (E)].

Brain Magnetic Resonance Imaging (MRI) Results: Mild Generalized Cerebral Volume Loss with Reduced Posterior White Matter at 15.5 Months and at 9 Years

Scans demonstrated mild generalized cerebral volume loss with reduced posterior white matter. The 2007 study showed periatrivial signal hyperintensity that had resolved by 2015. The corpus callosum appeared relatively proportional to the overall volume loss but slightly foreshortened, consistent with brachycephaly. The right lateral ventricle was more asymmetric than normal and much of that can be attributed to the incompletely inverted hippocampus on that side with a low-lying fornix. The frontal and temporal extra-axial spaces were enlarged in 2007, but had resolved by 2015. Craniofacial dysmorphism (prominent forehead, broad nose, and thin upper lip) was apparent on the 2015 scan [Table 1 (A); Figure 1B]. Similarly, at 10.5 years clinical

observations, craniofacies showed tall forehead with high anterior hairline, heavy brows giving eyes a deep-set appearance, right exotropia, and long eyelashes. Philtrum was short and deep, and the upper lip was thin. There were creases on the earlobes.

Molecular Test Results: Part of a Growing Syndrome

Primary diagnosis (Dr. Peeden) was obtained at 8.5 years showing ADNP *de novo* gene mutation: g.49509094G>C; cDNA: c.2157C>G; protein: p.Tyr719*. Diagnosis was obtained by whole exome sequencing compared to the parents. With the ADNP kids belonging to a family of affected children suffering many similar abnormalities, further solutions are on the horizon. To provide information, advocacy and emotional support to families worldwide [e.g., Ref. (28)], an ADNP Syndrome Parents Group was established on the social networking site Facebook™. This is facing the time, like other support groups, for versatile diseases (35). Currently ~80 families are assembled, connected through the original set up of ADNP ASD mutations². The parents formed a table of traits³, which are shown for AD [Table 2 (A–D)]. Several other ADNP-associated traits are visible when looking at Table 2 including auditory impediments, suggesting an involvement of ADNP in the development of all senses. AD was spared heart abnormalities and seizures; however, as these affect other ADNP children, she is closely observed (28).

AD shares the same mutation with several other children [e.g., Ref. (24)]. A parent questionnaire of 17 individuals with ADNP p.Tyr719* or a close mutation indicated cognitive (including speech) and motor delays, as well as autistic features and >50% brain abnormalities, which are further investigated. Figure 1C shows representative pictures of three additional ADNP p.Tyr719* children exhibiting potential facial similarities and using standing and walking devices [Table 2 (E)]. The ADNP p.Tyr719* is an integral part of the ADNP-related syndrome encompassing other ADNP mutations (Van Dijck et al., in preparation).

Treatment Modalities and Future Perspectives

In general, a helmet treatment was implemented for cranial asymmetry [Table 1 (A)].

Treatments for Motor Disabilities

Proved to be successful and should be implemented in future cases. In this respect, all children with ADNP mutations show motor delays (see text footnote 3).

The painful doubt whether AD would be wheelchair bound drove the parents to seek help. Physical therapy began at the age of 15 months. She had multitude therapies at home, collaborative clinic, early intervention, developmental playgroups, and private clinic/water therapy. For example, she had physical and occupational therapy, hippotherapy (involving an occupational therapist, a physiotherapist, or a speech and language therapist working with AD and a horse to present challenges and to

²<http://www.omim.org/entry/611386>.

³<http://www.adnlpkids.com/>.

promote different postural responses) and aquatic therapy. At one point, she was given up to 10 therapies a week. At the age of 2.5, her therapist and the orthotics⁴ tailor made shoes with an inside lift to accommodate her left leg shortness. She then began to wear ankle foot orthosis brace to her knee, covering her entire foot. The physical therapist devised fabric braces with Velcro with metal bars that did not allow her to bend her knee, forcing her to bare weight. Her father has further built a “standing device” made of wood and PVC pipes to aid in her “timed” standing to ensure that she would not incur atrophy in her lower limbs/legs. Following this, parents were advised of gait trainers and other newly engineered products that help children like AD. AD further used a surfboard therapy machine that helped her core balance and many mirrors and began making a connection. Basic standing on her own was her first milestone, followed by the use of a pediatric walker [Table 1 (B), picture].

Walking short distances resulted in skin redness and muscle pain, which were relieved with warm baths and pool therapy. The parents further used a treadmill program (e.g., <http://www.taap-project.com/>) in physical therapy to strengthen AD and built new pathways and signals to help her motor planning and focus on the repetition of steps. Metronome was a program⁵ that they have also used that proved to be successful. Notably, the physical therapist persisted, despite AD’s severe unknown motor movement disorder and continued to increase the “frequency” of land and water therapies toward success.

She was treated with over 300 h combined physical and aquatic therapies between the ages of 1–5 years. Without a medical billing code for doctors to use, the term “global delay” did not guarantee insurance coverage nor did it describe the medical complexity of AD. This resulted in expenses of over \$2,000 per summer during the walk therapies. Currently, AD gets biweekly physical therapies to maintain and further improve her mobility and has begun growth hormone therapy (age 10), aiming to bring her back to the growth chart.

Treatment of Speech Disabilities

AD was recently diagnosed with apraxia of speech [Table 1 (E)] and traditional speech therapy may not benefit her as much as focus on oral motor “planning.” She is now receiving this specialized therapy as her evaluation showed she desires to speak, tries and makes approximations, but similar to walking cannot put it together.

The Z-VIBES⁶ oral motor tool has been most successful for the children with ADNP mutation who speak (closed ADNP Syndrome PARENTS GROUP, Facebook). AD has used it as a small child, with no obvious results, but now it seems to be having a significant effect.

Additionally, the Kaufmann kit,⁷ which uses cards to teach children to combine consonants and vowels to form words while controlling for oral-motor difficulty, is also helping AD. As a

small child she was not able to understand, but now these cards are used in combination with PROMPT therapy (Prompts for Restructuring Oral Muscular Phonetic Targets⁸). With physical cueing and repetition of the cards, AD now has some approximations for sounds such as “meh,” “na,” and “beh,” for “me,” “no,” and “bye,” respectively.

Over the years, AD’s educational team has indicated that the autism symptoms have become less prevalent. With access to a speaking device (a card system) and multimodal communication system, AD is now flourishing. Her improved communication shows an amazing personality, which is humorous and lively.

Face to the Future: Treatment Using Novel Biologically Active ADNP Peptides

From a scientific point of view, we strive to have tailored drugs to treat the ADNP children, early enough to avoid confounding developmental delays. In this respect, we (Gozes) have been developing NAP (NAPVSIPQ) the shortest active snippet of ADNP (1). NAP increases ADNP’s activity at the cellular level in terms of cellular protection (14) as well as synaptic plasticity (14). On the whole animal level, it provides cognitive protection in mice with ADNP deficiencies (5). NAP has also shown protective activity in over 20 cell culture systems and in over 25 animal models. Notable examples include schizophrenia (36–38), Alzheimer’s disease (39–41), frontotemporal dementia (42, 43), amyotrophic lateral sclerosis (44), and most importantly cognitive deficiencies associated with ASD (5) as well as developmental delays linked to prenatal and postnatal toxicities (45–47). NAP, also called davunetide, has shown activity in clinical trials. It increased cognitive scores in a Phase IIa clinical trial in patients suffering from amnestic mild cognitive impairment (48, 49) and protected functional daily activities (50) as well as brain cellular activity (measured by MRI) (51), in schizophrenia patients. NAP (davunetide) is safe and bioavailable (52, 53). Clinical studies in the ADNP-related syndrome are currently planned with NAP—now called CP201 (Coronis Neurosciences⁹).

CONCLUSION

The described complex syndrome of motor dysfunction, autism, speech delay, and facial dysmorphism should trigger gene sequencing and early diagnosis of children with the ADNP syndrome (also known as the Helsmoortel–Van der Aa syndrome¹⁰).

The case of AD highlights global developmental delays, with emphasis on motor functions, which was not described before. While AD had not always been referred to the appropriate specialized therapies, her family persistence and ultimate success in motor development should help guide newly diagnosed children. This report teaches modes of interventions and paves the path to basic discoveries on ADNP’s involvement in muscle development.

AD’s major impediment nowadays is her inability to talk, a trait that has been lagging behind. In this respect, better understanding

⁴<https://en.wikipedia.org/wiki/Orthotics>

⁵<https://www.youtube.com/watch?v=WR1lC6UYh9I>

⁶<http://www.arktherapeutic.com/z-vibes-all/>.

⁷<http://www.northernspeech.com/early-intervention-language-and-speech/kaufman-k-slp-treatment-kit-1-ndash-basic-level/>.

⁸<http://www.promptinstitute.com/?page=FamiliesWIP>.

⁹<http://www.coronisns.com/>.

¹⁰<https://rarediseases.info.nih.gov/diseases/12931/adnp-syndrome>.

of ADNP's association with muscle development may shed light on speech development as well.

The more we understand about the ADNP protein and gene, the better we can help the families and patients with syndromic developmental dysfunctions gain enhanced functionality and integration into a healthy society coupled with ADNP replacement/enhancement therapies, such as CP201 (Coronis Neurosciences; see text footnote 9).

ETHICS STATEMENT

This study was supported by Tel Aviv University, the study is descriptive the parent is an author. Informed consents were given for all data by the respective parents.

AUTHOR NOTES

Recently (at about age 11) AD was diagnosed with a suspected form of dysarthria—<https://www.ncbi.nlm.nih.gov/pubmed-health/PMHT0027115/>. The number of ADNP syndrome children has now increased to 107 within the ADNP network (<http://www.adnfpfoundation.org/>), including 23 children sharing a similar mutation with AD (**Table 2**).

AUTHOR CONTRIBUTIONS

IG compiled the data and wrote/edited the paper; MP provided the in-depth clinical analysis at 3 years of age and the

longitudinal MRI data; AVD and FK read the manuscript and provided clinical input; JP provided the diagnosis and longitudinal clinical data, JE provided critical editorial inputs; AZ-D initiated the study and provided the most extensive parental story, and SB-S compiled the data in **Table 2**, read, and commented on the paper.

ACKNOWLEDGMENTS

We thank Dr. Sara S. Cathey, Clinical Geneticist, Greenwood Genetic Center, Charleston Office, North Charleston, SC, USA, AD's current geneticist. We also thank for his input Dr. Gonzalez-Lamuño Leguina, Domingo, Hospital U. "Marqués de Valdecilla," Santander, Spain. We further thank Gal Hacohen Kleiman and Shlomo Sragovich for critical reading of the manuscript. This study was supported by ERA-NET Neuron, Grant acronym AUTISYN, AMN Foundation and the Spanish, French (Drs. Ronith and Armand Stemmer) and Canadian Friends of Tel Aviv University Additional support was obtained from the ADNP Kids Research Foundation <http://www.adnfpfoundation.org/>. CP201 is planned for clinical trials (Coronis Neuroscience, Coronis Neurosciences, <http://www.coronisns.com/>, IG, Chief Scientific Officer). From the family point of view, AD's story is told expressively and with great sensitivity on the parent WEB page—<http://www.adnfpkids.com/>. We thank the reviewers of this paper for excellent input. A comprehensive description of the ADNP-related syndrome is currently in preparation (Van Dijck et al., 2017).

REFERENCES

- Bassan M, Zamostiano R, Davidson A, Pinhasov A, Giladi E, Perl O, et al. Complete sequence of a novel protein containing a femtomolar-activity-dependent neuroprotective peptide. *J Neurochem* (1999) 72:1283–93. doi:10.1046/j.1471-4159.1999.0721283.x
- Zamostiano R, Pinhasov A, Gelber E, Steingart RA, Seroussi E, Giladi E, et al. Cloning and characterization of the human activity-dependent neuroprotective protein. *J Biol Chem* (2001) 276:708–14. doi:10.1074/jbc.M007416200
- Gozes I, Yeheskel A, Pasmanik-Chor M. Activity-dependent neuroprotective protein (ADNP): a case study for highly conserved chordata-specific genes shaping the brain and mutated in cancer. *J Alzheimers Dis* (2015) 45:57–73. doi:10.3233/JAD-142490
- Pinhasov A, Mandel S, Torchinsky A, Giladi E, Pittel Z, Goldswieig AM, et al. Activity-dependent neuroprotective protein: a novel gene essential for brain formation. *Brain Res Dev Brain Res* (2003) 144:83–90. doi:10.1016/S0165-3806(03)00162-7
- Vulih-Shultzman I, Pinhasov A, Mandel S, Grigoriadis N, Touloumi O, Pittel Z, et al. Activity-dependent neuroprotective protein snippet NAP reduces tau hyperphosphorylation and enhances learning in a novel transgenic mouse model. *J Pharmacol Exp Ther* (2007) 323:438–49. doi:10.1124/jpet.107.129551
- Malishkevich A, Amram N, Hacohen-Kleiman G, Magen I, Giladi E, Gozes I. Activity-dependent neuroprotective protein (ADNP) exhibits striking sexual dichotomy impacting on autistic and Alzheimer's pathologies. *Transl Psychiatry* (2015) 5:e501. doi:10.1038/tp.2014.138
- Mandel S, Gozes I. Activity-dependent neuroprotective protein constitutes a novel element in the SWI/SNF chromatin remodeling complex. *J Biol Chem* (2007) 282:34448–56. doi:10.1074/jbc.M704756200
- Mandel S, Rechavi G, Gozes I. Activity-dependent neuroprotective protein (ADNP) differentially interacts with chromatin to regulate genes essential for embryogenesis. *Dev Biol* (2007) 303:814–24. doi:10.1016/j.ydbio.2006.11.039
- Mosch K, Franz H, Soeroes S, Singh PB, Fischle W. HP1 recruits activity-dependent neuroprotective protein to H3K9me3 marked pericentromeric heterochromatin for silencing of major satellite repeats. *PLoS One* (2011) 6:e15894. doi:10.1371/journal.pone.0015894
- Dresner E, Malishkevich A, Arivit C, Leibman Barak S, Alon S, Ofir R, et al. Novel evolutionary-conserved role for the activity-dependent neuroprotective protein (ADNP) family that is important for erythropoiesis. *J Biol Chem* (2012) 287:40173–85. doi:10.1074/jbc.M112.387027
- Schirer Y, Malishkevich A, Ophir Y, Lewis J, Giladi E, Gozes I. Novel marker for the onset of frontotemporal dementia: early increase in activity-dependent neuroprotective protein (ADNP) in the face of Tau mutation. *PLoS One* (2014) 9:e87383. doi:10.1371/journal.pone.0087383
- Gkogkas CG, Khoutorsky A, Ran I, Rampakakis E, Nevarko T, Weatherill DB, et al. Autism-related deficits via dysregulated eIF4E-dependent translational control. *Nature* (2013) 493:371–7. doi:10.1038/nature11628
- Mandel S, Spivak-Pohin I, Gozes I. ADNP differential nucleus/cytoplasm localization in neurons suggests multiple roles in neuronal differentiation and maintenance. *J Mol Neurosci* (2008) 35:127–41. doi:10.1007/s12031-007-9013-y
- Oz S, Kapitansky O, Ivashco-Pachima Y, Malishkevich A, Giladi E, Skalka N, et al. The NAP motif of activity-dependent neuroprotective protein (ADNP) regulates dendritic spines through microtubule end binding proteins. *Mol Psychiatry* (2014) 19:1115–24. doi:10.1038/mp.2014.97
- Gozes I, Sragovich S, Schirer Y, Idan-Feldman A. D-SAL and NAP: two peptides sharing a SIP domain. *J Mol Neurosci* (2016) 59(2):220–31. doi:10.1007/s12031-015-0701-8
- Esteves AR, Gozes I, Cardoso SM. The rescue of microtubule-dependent traffic recovers mitochondrial function in Parkinson's disease. *Biochim Biophys Acta* (2014) 1842:7–21. doi:10.1016/j.bbadic.2013.10.003

17. Merenlender-Wagner A, Malishkevich A, Shemer Z, Udwawa M, Gibbons A, Scarr E, et al. Autophagy has a key role in the pathophysiology of schizophrenia. *Mol Psychiatry* (2015) 20:126–32. doi:10.1038/mp.2013.174
18. Ponting CP, Goodstadt L. Separating derived from ancestral features of mouse and human genomes. *Biochem Soc Trans* (2009) 37:734–9. doi:10.1042/BST0370734
19. Borodzin W, Graham JM Jr, Böhm D, Bamshad MJ, Spranger S, Burke L, et al. Multigene deletions on chromosome 20q13.13-q13.2 including SALL4 result in an expanded phenotype of Okihiro syndrome plus developmental delay. *Hum Mutat* (2007) 28:830. doi:10.1002/humu.9502
20. O'Roak BJ, Vives L, Girirajan S, Karakoc E, Krumm N, Coe BP, et al. Sporadic autism exomes reveal a highly interconnected protein network of de novo mutations. *Nature* (2012) 485:246–50. doi:10.1038/nature10989
21. O'Roak BJ, Vives L, Fu W, Egertson JD, Stanaway IB, Phelps IG, et al. Multiplex targeted sequencing identifies recurrently mutated genes in autism spectrum disorders. *Science* (2012) 338:1619–22. doi:10.1126/science.1227764
22. Helsmoortel C, Vulsto-van Silfhout AT, Coe BP, Vandeweyer G, Rooms L, van den Ende J, et al. A SWI/SNF-related autism syndrome caused by de novo mutations in ADNP. *Nat Genet* (2014) 46:380–4. doi:10.1038/ng.2899
23. Vandeweyer G, Helsmoortel C, Van Dijck A, Vulsto-van Silfhout AT, Coe BP, Bernier R, et al. The transcriptional regulator ADNP links the BAF (SWI/SNF) complexes with autism. *Am J Med Genet C Semin Med Genet* (2014) 166C:315–26. doi:10.1002/ajmgc.31413
24. Pescosolido MF, Schwede M, Johnson Harrison A, Schmidt M, Gamsiz ED, Chen WS, et al. Expansion of the clinical phenotype associated with mutations in activity-dependent neuroprotective protein. *J Med Genet* (2014) 51:587–9. doi:10.1136/jmedgenet-2014-102444
25. Coe BP, Witherspoon K, Rosenfeld JA, van Bon BW, Vulsto-van Silfhout AT, Bosco P, et al. Refining analyses of copy number variation identifies specific genes associated with developmental delay. *Nat Genet* (2014) 46:1063–71. doi:10.1038/ng.3092
26. De Rubeis S, He X, Goldberg AP, Poultney CS, Samocha K, Cicek AE, et al. Synaptic, transcriptional and chromatin genes disrupted in autism. *Nature* (2014) 515:209–15. doi:10.1038/nature13772
27. Deciphering Developmental Disorders Study. Large-scale discovery of novel genetic causes of developmental disorders. *Nature* (2015) 519:223–8. doi:10.1038/nature14135
28. Gozes I, Helsmoortel C, Vandeweyer G, Van der Aa N, Kooy F, Sermone SB. The compassionate side of neuroscience: Tony Sermone's undiagnosed genetic journey-ADNP mutation. *J Mol Neurosci* (2015) 56:751–7. doi:10.1007/s12031-015-0586-6
29. Van Dijck A, Helsmoortel C, Vandeweyer G, Kooy F. ADNP-Related Intellectual Disability and Autism Spectrum Disorder. In: Pagon RA, Adam MP, Ardinger HH, Wallace SE, Amemiya A, Bean LJH, et al., editors. *GeneReviews® [Internet]*. Seattle, WA: University of Washington (2016).
30. Krajewska-Walasek M, Jurkiewicz D, Pieikutowska-Abramczuk D, Kucharczyk M, Chrzanowska KH, Jezela-Stanek A, et al. Additional data on the clinical phenotype of Helsmoortel-Van der Aa syndrome associated with a novel truncating mutation in ADNP gene. *Am J Med Genet A* (2016) 170:1647–50. doi:10.1002/ajmg.a.37641
31. Alvarez-Mora MI, Calvo Escalona R, Puig Navarro O, Madrigal I, Quintela I, Amigo J, et al. Comprehensive molecular testing in patients with high functioning autism spectrum disorder. *Mutat Res* (2016) 78(4–785):46–52. doi:10.1016/j.mrfmmm.2015.12.006
32. D'Gama AM, Pochareddy S, Li M, Jamuar SS, Reiff RE, Lam AT, et al. Targeted DNA sequencing from autism spectrum disorder brains implicates multiple genetic mechanisms. *Neuron* (2015) 88:910–7. doi:10.1016/j.neuron.2015.11.009
33. Iossifov I, Levy D, Allen J, Ye K, Ronemus M, Lee YH, et al. Low load for disruptive mutations in autism genes and their biased transmission. *Proc Natl Acad Sci U S A* (2015) 112:E5600–7. doi:10.1073/pnas.1516376112
34. Larsen E, Menashe I, Ziats MN, Pereanu W, Packer A, Banerjee-Basu S. A systematic variant annotation approach for ranking genes associated with autism spectrum disorders. *Mol Autism* (2016) 7:44. doi:10.1186/s13229-016-0103-y
35. Craig D, Strivens E. Facing the times: a young onset dementia support group: facebook style. *Australas J Ageing* (2016) 35:48–53. doi:10.1111/ajag.12264
36. Merenlender-Wagner A, Pikman R, Giladi E, Andrieux A, Gozes I. NAP (davunetide) enhances cognitive behavior in the STOP heterozygous mouse – a microtubule-deficient model of schizophrenia. *Peptides* (2010) 31:1368–73. doi:10.1016/j.peptides.2010.04.011
37. Vaisburd S, Shemer Z, Yeheskel A, Giladi E, Gozes I. Risperidone and NAP protect cognition and normalize gene expression in a schizophrenia mouse model. *Sci Rep* (2015) 5:16300. doi:10.1038/srep16300
38. Merenlender-Wagner A, Shemer Z, Touloumi O, Lagoudaki R, Giladi E, Andrieux A, et al. New horizons in schizophrenia treatment: autophagy protection is coupled with behavioral improvements in a mouse model of schizophrenia. *Autophagy* (2014) 10:2324–32. doi:10.4161/15548627.2014.984274
39. Matsuoka Y, Gray AJ, Hirata-Fukae C, Minami SS, Waterhouse EG, Mattson MP, et al. Intranasal NAP administration reduces accumulation of amyloid peptide and tau hyperphosphorylation in a transgenic mouse model of Alzheimer's disease at early pathological stage. *J Mol Neurosci* (2007) 31:165–70.
40. Matsuoka Y, Jouroukhin Y, Gray AJ, Ma L, Hirata-Fukae C, Li HF, et al. A neuronal microtubule-interacting agent, NAPVSIPQ, reduces tau pathology and enhances cognitive function in a mouse model of Alzheimer's disease. *J Pharmacol Exp Ther* (2008) 325:146–53. doi:10.1124/jpet.107.130526
41. Gozes I, Giladi E, Pinhasov A, Bardea A, Brenneman DE. Activity-dependent neurotrophic factor: intranasal administration of femtomolar-acting peptides improve performance in a water maze. *J Pharmacol Exp Ther* (2000) 293:1091–8.
42. Shiryaev N, Jouroukhin Y, Giladi E, Polyzoidou E, Grigoriadis NC, Rosenmann H, et al. NAP protects memory, increases soluble tau and reduces tau hyperphosphorylation in a tauopathy model. *Neurobiol Dis* (2009) 34:381–8. doi:10.1016/j.nbd.2009.02.011
43. Quraishi S, Cowan CM, Mudher A. NAP (davunetide) rescues neuronal dysfunction in a *Drosophila* model of tauopathy. *Mol Psychiatry* (2013) 18:834–42. doi:10.1038/mp.2013.32
44. Jouroukhin Y, Ostritsky R, Assaf Y, Pelleg G, Giladi E, Gozes I. NAP (davunetide) modifies disease progression in a mouse model of severe neurodegeneration: protection against impairments in axonal transport. *Neurobiol Dis* (2013) 56:79–94. doi:10.1016/j.nbd.2013.04.012
45. Sokolowska P, Passemard S, Mok A, Schwendimann L, Gozes I, Gressens P. Neuroprotective effects of NAP against excitotoxic brain damage in the newborn mice: implications for cerebral palsy. *Neuroscience* (2011) 173:156–68. doi:10.1016/j.neuroscience.2010.10.074
46. Rotstein M, Bassan H, Kariv N, Speiser Z, Harel S, Gozes I. NAP enhances neurodevelopment of newborn apolipoprotein E-deficient mice subjected to hypoxia. *J Pharmacol Exp Ther* (2006) 319:332–9. doi:10.1124/jpet.106.106898
47. Spong CY, Abebe DT, Gozes I, Brenneman DE, Hill JM. Prevention of fetal demise and growth restriction in a mouse model of fetal alcohol syndrome. *J Pharmacol Exp Ther* (2001) 297:774–9.
48. Gozes I, Stewart A, Morimoto B, Fox A, Sutherland K, Schmechel D. Addressing Alzheimer's disease tangles: from NAP to AL-108. *Curr Alzheimer Res* (2009) 6:455–60. doi:10.2174/156720509789207895
49. Morimoto BH, Schmechel D, Hirman J, Blackwell A, Keith J, Gold M, et al. A double-blind, placebo-controlled, ascending-dose, randomized study to evaluate the safety, tolerability and effects on cognition of AL-108 after 12 weeks of intranasal administration in subjects with mild cognitive impairment. *Dement Geriatr Cogn Disord* (2013) 35:325–36. doi:10.1159/000348347
50. Javitt DC, Buchanan RW, Keefe RS, Kern R, McMahon RP, Green MF, et al. Effect of the neuroprotective peptide davunetide (AL-108) on cognition and functional capacity in schizophrenia. *Schizophr Res* (2012) 136:25–31. doi:10.1016/j.schres.2011.11.001
51. Jarskog LF, Dong Z, Kangarlu A, Colibazzi T, Girgis RR, Kegeles LS, et al. Effects of davunetide on N-acetylaspartate and choline in dorsolateral prefrontal cortex in patients with schizophrenia. *Neuropsychopharmacology* (2013) 38:1245–52. doi:10.1038/npp.2013.23
52. Gozes I, Morimoto BH, Tiong J, Fox A, Sutherland K, Dangoor D, et al. NAP: research and development of a peptide derived from activity-dependent neuroprotective protein (ADNP). *CNS Drug Rev* (2005) 11:353–68. doi:10.1111/j.1527-3458.2005.tb00053.x

53. Morimoto BH, Fox AW, Stewart AJ, Gold M. Davunetide: a review of safety and efficacy data with a focus on neurodegenerative diseases. *Expert Rev Clin Pharmacol* (2013) 6:483–502. doi:10.1586/17512433.2013.827403

Conflict of Interest Statement: Coronis Neurosciences is developing NAP (davunetide, CP201) for autism. Professor Gozes is the Chief Scientific Officer (Consultant).

Copyright © 2017 Gozes, Patterson, Van Dijck, Kooy, Peeden, Eichenberger, Zawacki-Downing and Bedrosian-Sermone. This is an open-access article distributed under the terms of the Creative Commons Attribution License (CC BY). The use, distribution or reproduction in other forums is permitted, provided the original author(s) or licensor are credited and that the original publication in this journal is cited, in accordance with accepted academic practice. No use, distribution or reproduction is permitted which does not comply with these terms.



Cholecystokinin—From Local Gut Hormone to Ubiquitous Messenger

Jens F. Rehfeld*

Department of Clinical Biochemistry, Rigshospitalet, University of Copenhagen, Copenhagen, Denmark

Cholecystokinin (CCK) was discovered in 1928 in jejunal extracts as a gallbladder contraction factor. It was later shown to be member of a peptide family, which are all ligands for the CCK₁ and CCK₂ receptors. CCK peptides are known to be synthesized in small intestinal endocrine I-cells and cerebral neurons. But in addition, CCK is expressed in several endocrine glands (pituitary cells, thyroid C-cells, pancreatic islets, the adrenals, and the testes); in peripheral nerves; in cortical and medullary kidney cells; in cardiac myocytes; and in cells of the immune system. CCK peptides stimulate pancreatic enzyme secretion and growth, gallbladder contraction, and gut motility, satiety and inhibit acid secretion from the stomach. Moreover, they are major neurotransmitters in the brain and the periphery. CCK peptides also stimulate calcitonin, insulin, and glucagon secretion, and they may act as natriuretic peptides in the kidneys. CCK peptides are derived from proCCK with a C-terminal bioactive YMGWMDFamide sequence, in which the Y-residue is partly O-sulfated. The plasma forms are CCK-58, -33, -22, and -8, whereas the small CCK-8 and -5 are potent neurotransmitters. Over the last decades, CCK expression has also been encountered in tumors (neuroendocrine tumors, cerebral astrocytomas, gliomas, acoustic neuromas, and specific pediatric tumors). Recently, a metastatic islet cell tumor was found to cause a specific CCKoma syndrome, suggesting that circulating CCK may be a useful tumor marker.

OPEN ACCESS

Edited by:

Hubert Vaudry,
University of Rouen, France

Reviewed by:

Pascal Favrel,
University of Caen Normandy, France
Daniel Fourmy,
University of Toulouse, France

***Correspondence:**

Jens F. Rehfeld
jens.f.rehfeld@regionh.dk

Specialty section:

This article was submitted to
Neuroendocrine Science,
a section of the journal
Frontiers in Endocrinology

Received: 08 December 2016

Accepted: 24 February 2017

Published: 13 April 2017

Citation:

Rehfeld JF (2017) Cholecystokinin—
From Local Gut Hormone to
Ubiquitous Messenger.
Front. Endocrinol. 8:47.
doi: 10.3389/fendo.2017.00047

INTRODUCTION

Cholecystokinin (CCK) is member of a family of regulatory peptides with a remarkably well preserved C-terminal sequence (1–3). The family also includes frog skin peptides (caerulein and phyllocaerulein) and the protochordate neuropeptide cionin, but in mammals, CCK and gastrin are the only family members (**Figure 1**).

After the discovery in 1928 (6), CCK became part of the classical troika of gut hormones together with secretin and gastrin. The last decades, however, have shown that CCK, in addition to its local acute functions in digestion (gallbladder emptying and pancreatic enzyme secretion), is also a growth factor, a neurotransmitter in the brain and peripheral neurons [for reviews, see Ref. (7–9)], and besides, it may be a spermatozoan fertility factor, a natriuretic kidney peptide, an anti-inflammatory cytokine in the immune system, and a cardiac marker of heart failure. The long history has made the CCK literature comprehensive and at some points also confusing because impure CCK preparations with little attention paid to species differences and to physiological levels were used initially. In addition, most assays for measurement of CCK in plasma and elsewhere lacked specificity and sensitivity (10–12).

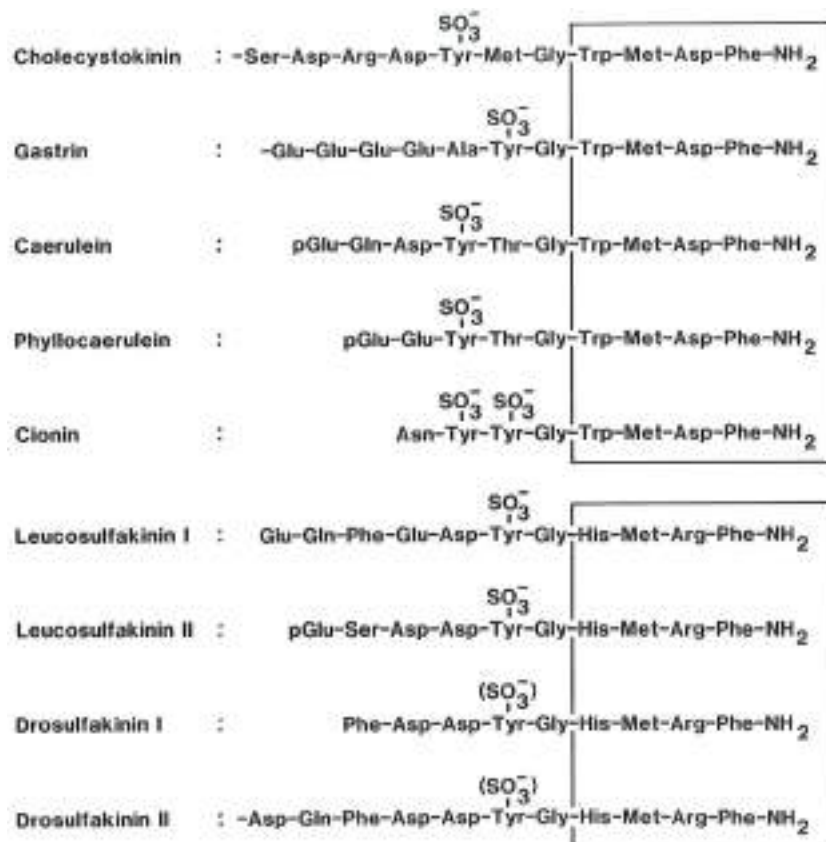


FIGURE 1 | The homologous bioactive sequences of peptide systems belonging to the cholecystokinin (CCK) family (upper panel). CCK and the antral hormone, gastrin, are the only mammalian members of the family. Caerulein and phyllocaerulein are identified from frogskin extracts. Clonin is a neuropeptide isolated from the central ganglion of the protochord, *ciona intestinalis*. Note the unique disulfated sequence, which might suggest that clonin may resemble a common ancestor of CCK and gastrin. The core of the bioactive sequences, the common C-terminal tetrapeptide amide, is boxed. The lower panel shows the bioactive sequences of the insect peptides, the sulfakinins, which display some homology with vertebrate and protochordian members of the CCK family (4, 5). Also their C-terminal tetrapeptide amide sequence is boxed.

The biochemical concept of CCK as a single hormonal peptide from the small intestine has also changed considerably. Now CCK is known to be synthesized and released in multiple molecular forms. And the CCK gene is expressed at peptide level in a cell-specific manner in neurons, endocrine cells, and epithelial cells outside the gastrointestinal tract (Table 1). All known biological effects of CCK peptides reside in the conserved C-terminal heptapeptide sequence (Figure 1). Modification of this sequence grossly reduces or abolishes receptor binding and biological effects (13–15). The N-terminal extensions of the common C-terminus increase the biological potency and the specificity for receptor binding. Of particular importance is the tyrosyl residue in position seven [as counted from the C-terminus (Figure 1)]. The tyrosyl residue is rarely completely sulfated (16–20). The CCK₂ receptor binds sulfated and unsulfated ligands equally well, whereas the CCK₁ receptor is exclusive and requires Y-sulfation of the ligand.

The following is a short review about the biology of CCK with emphasis on the recently recognized widespread expression (Table 1) and besides an update on the classic gastrointestinal effects of CCK peptides.

BIOGENESIS

As described earlier (9), “the exonal unit of the CCK gene is seven kilobases interrupted by two introns (23). The first of the three exons is small and non-coding. Several conserved regulatory elements have been identified in first 100 bp of the promoter, including an E-box element, a combined cAMP response element (CRE)/12-O-tetradecanoylphorbol-13-acetate response element (TRE), and a GC-rich region (24, 25). Whereas the function of the E-box and the GC-rich region is not fully clarified (26, 27), the combined CRE/TRE sequence plays an important role in the regulation of CCK transcription. The CRE/TRE binds the transcription factor CREB, which is activated by phosphorylation by several signaling pathways, including cAMP, fibroblast growth factor, pituitary adenylate cyclase-activating polypeptide, calcium, hydrolyzates, and peptones to ultimately induce CCK transcription (28–32). Only one CCK mRNA molecule has been found, and the CCK peptides are thus fragments of the same proCCK protein. The mRNA has 750 bases, of which 345 are protein coding (33, 34). The concentrations of CCK mRNA in cerebrocortical tissue are similar to that of the duodenal

TABLE 1 | The widespread expression of cholecystokinin (CCK) peptides in normal adult mammalian tissue.

Tissue	Tissue content ^a (pmol/g)	Precursor percentage ^c
Intestinal tract		
Duodenal mucosa	200	5
Jejunal mucosa	150	20
Ileal mucosa	20	50
Colonic mucosa	5	50
Central nervous system		
Cerebral cortex	400	2
Hippocampus	350	2
Hypothalamus	200	2
Cerebellum	2	90
Spinal cord	40	10
Peripheral nervous system		
Vagal nerve	25	5
Sciatic nerve	15	5
Nerveplexes in colonic wall	5	20
Extraintestinal endocrine glands		
Adenohypophysis	25	100
Neurohypophysis	20	10
Thyroid gland	2	20
Adrenal medulla	1	50
Urogenital tract		
Renal cortex ^b	+++	–
Renal medulla ^b	+++	–
Testicles	5	80
Spermatozoa	1	50
Cardiovascular system:		
Atrial myocytes	10	95
Ventricular myocytes	2	95
Mononuclear immune cells^b		
	++	–

^aOrders of magnitude based on measurement of tissue extracts from different mammalian species.

^bExpression determined only by immunocytochemistry.

^cThe precursor percentage was estimated by subtraction of the sum of bioactive, α -amidated CCK peptides (11, 12) from the total procholecystokinin product using the principle of processing-independent analysis (21, 22).

mucosa (34), and in the brain, there is a rapid synthesis of CCK peptides (35).

The primary translational product, preproCCK, has 115 amino acid residues. The first part is the signal peptide. The second part with considerable species variation is a spacer peptide. The bioactive CCK peptides are derived from the subsequent 58 amino acid residues (16, 18, 36–38), and the species variation is small in this sequence. The processing of proCCK is cell-specific: endocrine cells contain a mixture of the medium-sized CCK-58, -33, -22, and -8, whereas neurons mainly release CCK-8 and to some extent CCK-5 (16, 39). The endoproteolysis of proCCK occurs mainly at monobasic sites. Y-77 is mostly O-sulfated (16–20, 40), which is decisive for CCK₁ receptor binding.

In the small intestine, CCK peptides are synthesized in endocrine I-cells (41), whose apical membrane is in contact with the intestinal lumen and whose basal region contains secretory granules with CCK peptides. CCK is also synthesized in pituitary corticotrophs and melanotrophs, in thyroid C-cells (17), and in adrenal medullary cells (42, 43). In the pituitary cells, CCK constitutes a small fraction of the hormones. Tumors originating from pituitary corticotrophs, however, produce larger amounts of CCK (44)."

It is the brain that expresses most CCK (16, 39, 42). Moreover, cerebral CCK neurons are more abundant than neurons of other neuropeptides (42, 45, 46). While most peptidergic neurons occur in subcortical regions, CCK is expressed in the highest concentrations in neocortical neurons (39, 42, 47). The perikarya of the cortical CCK nerves are distributed in layers II–VI, with the highest frequency in layers II and III (42, 48). CCK in mesencephalic dopamine neurons projecting to the limbic area of the forebrain (45) has aroused clinical interest because these neurons are supposed to be involved in schizophrenia.

Outside the brain, the colon contains numerous CCK neurons, whereas jejunum and ileum are less innervated (42). Colonic CCK fibers occur in the circular muscle layer, which they penetrate to form a plexus in the submucosa (42). In accordance with these locations, CCK peptides excite colonic smooth muscles and release acetylcholine from neurons in both plexus myentericus and submucosa (49). Ganglionic cell somas in pancreatic islets are also surrounded by CCK nerves (50). Moreover, CCK nerve terminals also surround pancreatic islets (51). Finally, afferent vagal nerve fibers also contain CCK (52, 53).

ENDOCRINE AND NEURONAL RELEASE

Also mentioned before (9), "CCK in circulation originates mainly from intestinal endocrine cells. The release to blood was not possible to examine until specific assays were developed (10–12, 54). The assays have confirmed that protein- and fat-rich food is the most important stimulus (11, 54). Of the constituents, protein and L-amino acids as well as digested fat cause significant CCK release (54, 55). Carbohydrates only release small amounts of CCK (54), but hydrochloric acid also stimulates release (55).

The release from neurons has been examined directly in brain slices and synaptosomes (56, 57). Potassium-induced depolarization caused a calcium-dependent release of CCK-8. Similarly, depolarization releases CCK peptides from the hypothalamic dopamine neurons that innervate the intermediate lobe of the pituitary (58). By analogy with other neuropeptides, it is possible that overflow from peripheral CCK neurons may contribute slightly to CCK in plasma.

By comparison with identified CCK peptides, it has been possible to deduce the molecular pattern of CCK in plasma. The picture has varied (12) due to species differences and because the molecular pattern along the gut varies (59, 60). Furthermore, the distribution may vary during stimulation. In man, CCK-33 predominates in plasma, but CCK-58, -22, and -8 are also present (11, 61).

In the basal state, the concentration of CCK in plasma is around 1 pmol/l, but often less. The concentration increases within 20 min to 3–5 pmol/l during meal stimulation, and then declines gradually only to reach a second peak after 1.5–2 hours. In comparison with most other pancreatic and gastrointestinal hormones (62), the concentrations of CCK in plasma are low. When food-induced CCK in plasma is mimicked by infusion of exogenous CCK, the same degree of gallbladder contraction and release of enzymes as seen during meals occurs (54, 62–64). Therefore, the low circulating concentrations of CCK are sufficient to account for the gallbladder contraction and pancreatic enzyme secretion during meals.

Because the cholecystokinetic and pancreozymic potency of CCK-33 and CCK-8 on a molar base are identical (65), it may seem less important what I-cells release during digestion.” On the other hand, CCK-58, -33, and -22 are cleared from blood at a significantly slower rate than CCK-8.

RECEPTORS

The cellular effects of CCK peptides are mediated via two receptors (66, 67). The “alimentary” CCK-A or CCK₁ receptor (66) mediates gallbladder contraction, relaxation of the sphincter of Oddi, pancreatic growth and enzyme secretion, delay of gastric emptying, and inhibition of gastric acid secretion via fundic somatostatin (68). CCK₁ receptors have been found also in the anterior pituitary, the myenteric plexus, and areas of the mid-brain (69, 70). The CCK₁ receptor binds with high affinity CCK peptides that are amidated and sulfated, whereas the affinity for non-sulfated CCK peptides and gastrins is negligible.

The CCK-B or CCK₂ receptor (the “brain” receptor) is the predominant CCK receptor in the brain (67, 71). It is less specific than the CCK₁ receptor and binds also non-sulfated CCK, gastrins, and C-terminal fragments such as CCK-5. It has been shown that the gastrin receptor cloned from the stomach (67) and CCK₂ receptors are identical (71, 72). The gastrin/CCK₂ receptor is expressed also in substantial amounts in pancreatic islet cells in man (73).

GASTROINTESTINAL EFFECTS

The defining functions of CCKs in digestion have been detailed regularly [for instance, see Ref. (6, 7)].

Gallbladder and Pancreas

“CCK peptides stimulate hepatic secretion mainly as bicarbonate from hepatic ductular cells (74) and act on gallbladder muscles with a potency correlated to the low plasma concentrations of sulfated CCK. From the liver and gallbladder, bile is released into the duodenum via CCK-mediated rhythmic contraction and relaxation of muscles in the common bile duct and the sphincter of Oddi. CCK regulates the secretion of pancreatic enzymes so potently that it seems sufficient to account for all enzyme secretion (63–65). CCK is also capable of releasing several small intestinal enzymes such as alkaline phosphatase (75), disaccharidase (76), and enterokinase (77). In addition, CCK stimulates the biosynthesis of pancreatic amylase, chymotrypsinogen, and trypsinogen (78–80).

While the interest in the effect of CCK on the exocrine pancreas was for many years restricted to enzyme secretion, it is now well established that CCK also stimulates fluid and bicarbonate secretion. The effect on bicarbonate secretion is in itself weak, but because CCK potentiates the secretin-induced bicarbonate secretion in the same way as secretin potentiates the CCK-induced enzyme release (81), the effect of CCK peptides on bicarbonate and fluid secretion is potent. There are species differences, so it is now assumed that CCK in man stimulates pancreatic enzyme secretion through a cholinergic pathway that is less significant in rodents (82–84).

There are also species differences regarding the endocrine pancreas. CCK peptides release insulin and glucagon more potently in man and pig than in dog and rat (51, 85–87). The difference is partly due to neurons in pancreatic islets that release CCK-8 and CCK-5 in man and pig (51), whereas rat and dog islets have no such innervation (50, 51). Moreover, islet cells in man and pig also express the CCK₂ receptor abundantly (73), whereas rat islet cells express mainly the CCK₁ receptor (88).

Already in 1967, Rothman and Wells (80) noted that CCK increased pancreatic weight and enzyme synthesis. Also the output of bicarbonate and protein from the hypertrophic pancreas was increased (89). Although secretin in itself is without trophic effects, the combination of secretin and CCK showed trophic effect on ductular cells with increased secretin-induced bicarbonate output (89)."

Gut Motility

Cholecystokinin contributes to control intestinal motility. The distal part of the gut is as mentioned abundantly innervated with CCK neurons (42, 90). It is therefore likely that an increase of intestinal motor activity by exogenous CCK (91) reflects neuronal control of intestinal muscles by CCK peptide transmission. Neuronal CCK acts both indirectly via acetylcholine release from postganglionic parasympathetic nerves and directly on muscle cells (49). The observation that CCK peptides stimulate intestinal blood flow is in harmony with the occurrence of CCK nerve terminals around blood vessels in the basal lamina propria and the submucosa (42).

Satiety

“In 1973, Gibbs et al. discovered that exogenous CCK inhibits food intake (92). The effect mimicked the satiety induced by food and was not seen with other gut peptides known then. The effect could be demonstrated in several mammals. Vagotomy studies indicate that peripheral CCK induces satiety via CCK₁ receptors relaying the effect into afferent vagal fibers (93). The satiety signal then reaches the hypothalamus from the vagus via the nucleus tractus solitarius and area postrema.

Gastric Acid Secretion

The effect of CCK on gastric acid secretion has been uncertain. On one hand, it has been suggested that intestinal CCK was an acid inhibitor (an enterogastrone). On the other hand, the results of CCK infusions have been inconsistent. The gastrin/CCK double “knock-out” mice have now shed further light on the problem showing that circulating CCK stimulates somatostatin release from fundic D-cells via CCK₁ receptors, which then inhibits acid secretion from parietal cells (68)."

NOVEL SITES OF EXPRESSION

The major sites of CCK expression are as mentioned endocrine cells in the gut, the brain, and in peripheral nerves. But the last decades have uncovered additional sites and cell types that also express the CCK gene at peptide level (Table 1). In some of these sites, proCCK is not processed to the known α -amidated

peptides. Their functions are therefore still unknown. But since CCK receptors also have such widespread expression (66, 67, 70–73, 94, 95), there is both room and need for delineation of the roles of CCK released from the “new” sites.

Extraintestinal Endocrine Cells

Pituitary corticotrophs and melanotrophs express significant amounts of proCCK fragments, but the posttranslational processing results in only trace amounts of conventional α -amidated CCK peptides (43, 96). Also, thyroid C-cells produce CCK, but mainly as non-sulfated but amidated CCK-8 (17). Since C-cells are well equipped with CCK₂ receptors (97), thyroid CCK-8 is probably an autocrine stimulator of growth of normal and not least malignant C-cells. Adrenal medullary cells produce small amounts of CCK, although amidated and with a low degree of sulfation (98). The significance of adrenal CCK is unknown.

Male Germ Cells

Spermatogenic cells express transiently the CCK gene in most mammals (99, 100). Less than 25% of the amidated CCK is sulfated. Interestingly, the CCK peptides in mature spermatozoa are concentrated in the acrosomal granule, which opens the possibility that CCK may play a role in fertilization due to the acrosomal reaction (100). The acrosomal expression is species-specific, as human spermatozoa in addition to CCK also express its homolog, gastrin (101).

Kidney Cells

In rodent kidneys (rat, mice, and guinea pigs), CCK has recently been shown by immunohistochemistry to be expressed both in the renal cortex and in the medulla. The cortical expression occurs in distal tubular cells and glomeruli, and the medullar CCK expression is confined to collecting ducts (102, 103). The discovery of renal CCK expression may have been stimulated by earlier findings of significant CCK₁ and CCK₂ receptor expression also in human kidney tissue (104, 105). It has led to suggestions of local regulatory functions of natriuresis and inflammation in the kidneys. Remarkably, the expression in diabetic mice and rat kidneys is grossly increased. This increase has been suggested to protect the diabetic kidneys somewhat against inflammatory actions of macrophages (103).

Immune Cells

Cholecystokinin immunoreactivity has consistently been found to be expressed in human and rat mononuclear cells in blood (106, 107). Moreover, CCK-8 (sulfated as well as non-sulfated) has been reported to exert a wide specter of stimulation and inhibition on lymphocytes, macrophages, and cytokine release, with ensuing anti-inflammatory effects (108–111). The field is complex due to the many players; but the clinical impact of CCK in inflammatory diseases and endotoxin shock may be significant.

Cardiac Myocytes

Fetal mice express high levels of CCK mRNA in cardiac myocytes (112). Accordingly, adult cardiomyocytes in mice, rats, and

pigs contain substantial amounts of proCCK protein (113). The processing, however, of cardiac proCCK is unique, as the result is a long triple-sulfated and N-terminally truncated fragment 25–94 with only trace amounts of the conventionally amidated and sulfated CCK peptides (113). The tissue concentration of the long proCCK fragment is higher in atrial than ventricular myocytes. The long proCCK fragment is released to plasma and may find use as a marker of the risk of mortality in heart failure patients (113).

Tumor Expression

Cholecystokinin is expressed at highly variable amounts in different neuroendocrine tumors, especially corticotrophic pituitary tumors (44), medullary thyroid carcinomas (17), phaeochromocytomas (98), and pancreatic islet cell tumors of which some may cause a specific CCKoma syndrome (114–117). CCK is also expressed in Ewing's Sarcomas, where proCCK measurements may be used to monitor the treatment (118). Cerebral gliomas, astrocytomas, and acoustic neuromas also express CCK (119–121). The present knowledge about tumor expression of CCK was recently summarized in a review that also discussed measurements of CCK and proCCK in plasma as tumor markers (122).

CONCLUSION

Since the identification of CCK half a century ago as a single peptide with a sequence of 33 amino acid residues (CCK-33), the CCK story has been loaded with major revelations: first, it was shown that the C-terminus of CCK was similar to that of gastrin, and that CCK and gastrin peptides share the same receptor, the CCK₂ receptor. Then, it was demonstrated that bioactive CCK occurs in multiple molecular forms—from CCK-58 to CCK-5 with and without tyrosyl O-sulfations. At variable intervals, it has since been shown that CCK peptides are expressed all over the body: in central and peripheral neurons, in intestinal and extraintestinal endocrine cells, in germ cells, kidney epithelial cells, cardiac myocytes, and immune cells. Moreover, the proCCK maturation appears to be cell specific, and tumors expressing CCK release correspondingly varying multifaceted patterns of CCK peptides. Thus, today CCK should be seen as an almost ubiquitous system of intercellular messenger peptides. The complex biology is probably characteristic for many regulatory peptides, for which the CCK system may serve as a source of inspiration for further research.

AUTHOR CONTRIBUTIONS

The author confirms being the sole contributor of this work and approved it for publication.

ACKNOWLEDGMENTS

The skillful and patient secretarial assistance of Connie Bundgaard (cand.phil.) is gratefully acknowledged.

REFERENCES

- Larsson LI, Rehfeld JF. Evidence for a common evolutionary origin of gastrin and cholecystokinin. *Nature* (1977) 269:335–8. doi:10.1038/269335a0
- Johnsen AH. Phylogeny of the cholecystokinin/gastrin family. *Front Neuroendocrinol* (1998) 19:73–99. doi:10.1006/frne.1997.0163
- Johnsen AH, Rehfeld JF. Cionin: a disulfotyrosyl hybrid of cholecystokinin and gastrin from the neural ganglion of the protostome ciona intestinalis. *J Biol Chem* (1990) 265:3054–8.
- Nachman RJ, Holman GM, Haddon WF, Ling N. Leucosulfakinin, a sulfated insect neuropeptide with homology to gastrin and cholecystokinin. *Science* (1986) 234:71–3. doi:10.1126/science.3749893
- Nichols R, Schneuwly SA, Dixon JE. Identification and characterization of a *Drosophila* homologue to the vertebrate neuropeptide cholecystokinin. *J Biol Chem* (1988) 263:12167–70.
- Ivy AC, Oldberg E. A hormone mechanism for gallbladder contraction and evacuation. *Am J Physiol* (1928) 86:559–613.
- Jorpes JE, Mutt V. Secretin, cholecystokinin and pancreozymin. In: Jorpes JE, Mutt V, editors. *Handbook of Experimental Pharmacology*. (Vol. 34), New York: Springer Verlag (1973). p. 1–179.
- Rehfeld JF. Cholecystokinin. *Best Pract Res Clin Endocrinol Metab* (2004) 18:569–86. doi:10.1016/j.beem.2004.07.002
- Rehfeld JF, Friis-Hansen L, Goetze JP, Hansen TV. The biology of cholecystokinin and gastrin peptides. *Curr Top Med Chem* (2007) 7:1154–65. doi:10.2174/156802607780960483
- Rehfeld JF. How to measure cholecystokinin in plasma? *Gastroenterology* (1984) 87:434–8.
- Rehfeld JF. Accurate measurement of cholecystokinin in plasma. *Clin Chem* (1998) 44:991–1001.
- Rehfeld JF. How to measure cholecystokinin in tissue, plasma and cerebrospinal fluid. *Regul Pept* (1998) 78:31–9. doi:10.1016/S0167-0115(98)00133-5
- Mutt V, Jorpes JE. Structure of porcine cholecystokinin-pancreozymin. 1. Cleavage with thrombin and with trypsin. *Eur J Biochem* (1968) 6:156–62. doi:10.1111/j.1432-1033.1968.tb00433.x
- Mutt V, Jorpes JE. Hormonal polypeptides of the upper intestine. *Biochem J* (1971) 125:57–8. doi:10.1042/bj1250057P
- Morley JS, Tracy HJ, Gregory RA. Structure-function relationships in the active C-terminal tetrapeptide sequence of gastrin. *Nature* (1965) 207:1356–9. doi:10.1038/2071356a0
- Rehfeld JF, Hansen HF. Characterization of preprocholecystokinin products in the porcine cerebral cortex. Evidence of different processing pathways. *J Biol Chem* (1986) 261:5832–40.
- Rehfeld JF, Johnsen AH, Ødum L, Bardram L, Schifter S, Scopsi L. Non-sulphated cholecystokinin in human medullary thyroid carcinomas. *J Endocrinol* (1990) 124:501–6. doi:10.1677/joe.0.1240501
- Bonetto V, Jörnwall H, Andersson M, Renlund S, Mutt V, Sillard R. Isolation and characterization of sulfated and nonsulfated forms of cholecystokinin-58 and their action on gallbladder contraction. *Eur J Biochem* (1999) 264:336–40. doi:10.1046/j.1432-1327.1999.00599.x
- Reeve JR Jr, Liddle RA, McVey DC, Vigna SR, Solomon TE, Keire DA. Identification of nonsulfated cholecystokinin-58 in canine intestinal extracts and its biological properties. *Am J Physiol Gastrointest Liver Physiol* (2004) 287:G326–33. doi:10.1152/ajpgi.00520.2003
- Agersnap M, Rehfeld JF. Nonsulfated cholecystokinins in the small intestine of pigs and rats. *Peptides* (2015) 71:121–7. doi:10.1016/j.peptides.2015.07.010
- Bardram L, Rehfeld JF. Processing-independent radioimmunoanalysis: a general analytical principle applied to progastrin and its products. *Anal Biochem* (1988) 175:537–43. doi:10.1016/0003-2697(88)90580-5
- Paloheimo LI, Rehfeld JF. A processing-independent assay for human procholecystokinin and its products. *Clin Chim Acta* (1994) 229:49–65. doi:10.1016/0009-8981(94)90228-3
- Deschenes RJ, Haun RS, Funckes CL, Dixon JE. A gene encoding rat cholecystokinin. Isolation, nucleotide sequence, and promoter activity. *J Biol Chem* (1985) 260:1280–6.
- Nielsen FC, Pedersen K, Hansen TV, Rourke IJ, Rehfeld JF. Transcriptional regulation of the human cholecystokinin gene: composite action of upstream stimulatory factor, Sp1, and members of the CREB/ATF-AP-1 family of transcription factors. *DNA Cell Biol* (1996) 15:53–63. doi:10.1089/dna.1996.15.53
- Hansen TV. Cholecystokinin gene transcription: promoter elements, transcription factors and signaling pathways. *Peptides* (2001) 22:1201–11. doi:10.1016/S0196-9781(01)00443-0
- Rourke IJ, Hansen TV, Nerlov C, Rehfeld JF, Nielsen FC. Negative cooperativity between juxtaposed E-box and cAMP/TPA responsive elements in the cholecystokinin gene promoter. *FEBS Lett* (1999) 448:15–8. doi:10.1016/S0014-5793(99)00320-8
- Hansen TV, Rehfeld JF, Nielsen FC. Function of the C-36 to T polymorphism in the human cholecystokinin gene promoter. *Mol Psychiatry* (2000) 5:443–7. doi:10.1038/sj.mp.4000705
- Hansen TV, Rehfeld JF, Nielsen FC. Mitogen-activated protein kinase and protein kinase A signaling pathways stimulate cholecystokinin transcription via activation of cyclic adenosine 3', 5'-monophosphate response element-binding protein. *Mol Endocrinol* (1999) 13:466–75. doi:10.1210/mend.13.3.0257
- Deavall DG, Raychowdhury R, Dockray GJ, Dimaline R. Control of CCK gene transcription by PACAP in STC-1 cells. *Am J Physiol Gastrointest Liver Physiol* (2000) 279:G605–12.
- Bernard C, Sutter A, Vinson C, Ratineau C, Chayvialle J, Cordier-Bussat M. Peptides stimulate intestinal cholecystokinin gene transcription via cyclic adenosine monophosphate response element-binding factors. *Endocrinology* (2001) 142:721–9. doi:10.1210/endo.142.2.7924
- Gevrey JC, Cordier-Bussat M, Nemoz-Gaillard E, Chayvialle JA, Abello J. Co-requirement of cyclic AMP- and calcium-dependent protein kinases for transcriptional activation of cholecystokinin gene by protein hydrolysates. *J Biol Chem* (2002) 277:22407–13. doi:10.1074/jbc.M201624200
- Hansen TV, Rehfeld JF, Nielsen FC. KCl and forskolin synergistically up-regulate cholecystokinin gene expression via coordinate activation of CREB and the co-activator CBP. *J Neurochem* (2004) 89:15–23. doi:10.1046/j.1471-4159.2003.02252.x
- Deschenes RJ, Lorenz L, Haun RS, Roos BR, Collier KJ, Dixon JE. Cloning and sequence analysis of cDNA encoding rat preprocholecystokinin. *Proc Natl Acad Sci U S A* (1984) 81:726–30. doi:10.1073/pnas.81.3.726
- Gubler U, Chua AO, Hoffman BJ, Collier KJ, Eng J. Cloned cDNA to cholecystokinin mRNA predicts an identical preprocholecystokinin in pig brain and gut. *Proc Natl Acad Sci U S A* (1984) 81:4307–10. doi:10.1073/pnas.81.14.4307
- Goltermann N, Rehfeld JF, Roigaard-Petersen H. In vivo biosynthesis of cholecystokinin in rat cerebral cortex. *J Biol Chem* (1980) 255:6181–5.
- Jorpes JE, Mutt V. Cholecystokinin and pancreozymin, one single hormone? *Acta Physiol Scand* (1966) 66:196–202. doi:10.1111/j.1748-1716.1966.tb03185.x
- Dockray GJ, Gregory RA, Hutchinson JB, Harris JL, Runswick MJ. Isolation, structure and biological activity of two cholecystokinin octapeptides from sheep brain. *Nature* (1978) 274:711–3. doi:10.1038/274711a0
- Reeve JR Jr, Eysselein V, Walsh JH, Ben-Avram CM, Shively JE. New molecular forms of cholecystokinin. Microsequence analysis of forms previously characterized by chromatographic methods. *J Biol Chem* (1986) 261:16392–7.
- Rehfeld JF. Immunochemical studies on cholecystokinin. II. Distribution and molecular heterogeneity in the central nervous system and small intestine of man and hog. *J Biol Chem* (1978) 253:4022–30.
- Agersnap M, Zhang MD, Harkany T, Hökfelt T, Rehfeld JF. Nonsulfated cholecystokinins in cerebral neurons. *Neuropeptides* (2016) 60:37–44. doi:10.1016/j.npep.2016.08.003
- Buffa R, Solcia E, Go VL. Immunohistochemical identification of the cholecystokinin cell in the intestinal mucosa. *Gastroenterology* (1976) 70:528–30.
- Larsson LI, Rehfeld JF. Localization and molecular heterogeneity of cholecystokinin in the central and peripheral nervous system. *Brain Res* (1979) 165:201–18. doi:10.1016/0006-8993(79)90554-7
- Rehfeld JF. Procholecystokinin processing in the normal human anterior pituitary. *Proc Natl Acad Sci U S A* (1987) 84:3019–23. doi:10.1073/pnas.84.9.3019
- Rehfeld JF, Lindholm J, Andersen BN, Bardram L, Cantor P, Fenger M, et al. Pituitary tumors containing cholecystokinin. *N Engl J Med* (1987) 316:1244–7. doi:10.1056/NEJM198705143162004
- Hökfelt T, Rehfeld JF, Skirboll L, Ivemark B, Goldstein M, Markey K. Evidence for co-existence of dopamine and CCK in meso-limbic neurons. *Nature* (1980) 285:476–8. doi:10.1038/285476a0

46. Crawley JN. Comparative distribution of cholecystokinin and other neuropeptides. Why is this peptide different from all other peptides? *Ann N Y Acad Sci* (1985) 448:1–8. doi:10.1111/j.1749-6632.1985.tb29900.x
47. Fallon JH, Seroogy KB. The distribution and some connections of cholecystokinin neurons in the rat brain. *Ann N Y Acad Sci* (1985) 448:121–32. doi:10.1111/j.1749-6632.1985.tb29912.x
48. Hendry SH, Jones EG, Beinfeld MC. Cholecystokinin-immunoreactive neurons in rat and monkey cerebral cortex make symmetric synapses and have intimate associations with blood vessels. *Proc Natl Acad Sci USA* (1983) 80:2400–4. doi:10.1073/pnas.80.8.2400
49. Vizi SE, Bertaccini G, Impicciatore M, Knoll J. Evidence that acetylcholine released by gastrin and related peptides contributes to their effect on gastrointestinal motility. *Gastroenterology* (1973) 64:268–77.
50. Larsson LI, Rehfeld JF. Peptidergic and adrenergic innervation of pancreatic ganglia. *Scand J Gastroenterol* (1979) 14:433–7.
51. Rehfeld JF, Larsson LI, Goltermann N, Schwartz TW, Holst JJ, Jensen SL, et al. Neural regulation of pancreatic hormone secretion by the C-terminal tetrapeptide of CCK. *Nature* (1980) 284:33–8. doi:10.1038/284033a0
52. Dockray GJ, Gregory RA, Tracy HJ, Zhou WY. Transport of cholecystokinin-octapeptide-like immunoreactivity towards the gut in afferent vagal fibres in cat and dog. *J Physiol* (1981) 314:501–11. doi:10.1113/jphysiol.1981.sp013721
53. Rehfeld JF, Lundberg J. Cholecystokinin in feline vagal and sciatic nerves: concentration, molecular forms and transport velocity. *Brain Res* (1983) 275:341–7. doi:10.1016/0006-8993(83)90995-2
54. Liddle RA, Goldfine ID, Rosen MS, Taplitz RA, Williams JA. Cholecystokinin bioactivity in human plasma. Molecular forms, responses to feeding, and relationship to gallbladder contraction. *J Clin Invest* (1985) 75:1144–52. doi:10.1172/JCI111809
55. Himeno S, Tarui S, Kanayama S, Kuroshima T, Shinomura Y, Hayashi C, et al. Plasma cholecystokinin responses after ingestion of liquid meal and intraduodenal infusion of fat, amino acids, or hydrochloric acid in man: analysis with region specific radioimmunoassays. *Am J Gastroenterol* (1983) 78:703–7.
56. Dodd PR, Edwardson JA, Dockray GJ. The depolarisation-induced release of cholecystokinin octapeptide from rat synaptosomes and brain slices. *Regul Pept* (1980) 1:17–29. doi:10.1016/0167-0115(80)90003-8
57. Emson PC, Lee CM, Rehfeld JF. Cholecystokinin octapeptide: vesicular localization and calcium dependent release from rat brain in vitro. *Life Sci* (1980) 26:2157–63. doi:10.1016/0024-3205(80)90603-7
58. Rehfeld JF, Hansen HF, Larsson LI, Stengaard-Pedersen K, Thorn NA. Gastrin and cholecystokinin in pituitary neurons. *Proc Natl Acad Sci U S A* (1984) 81:1902–5. doi:10.1073/pnas.81.6.1902
59. Maton PN, Selden AC, Chadwick VS. Differential distribution of molecular forms of cholecystokinin in human and porcine small intestinal mucosa. *Regul Pept* (1984) 8:9–19. doi:10.1016/0167-0115(84)90024-7
60. Rehfeld JF, Holst JJ, Jensen SL. The molecular nature of vascularly released cholecystokinin from the isolated perfused porcine duodenum. *Regul Pept* (1982) 3:15–28. doi:10.1016/0167-0115(82)90003-9
61. Rehfeld JF, Sun G, Christensen T, Hillingsø JG. The predominant cholecystokinin in human plasma and intestine is cholecystokinin-33. *J Clin Endocrinol Metab* (2001) 86:251–8. doi:10.1210/jcem.86.1.7148
62. Hornnes PJ, Kühl C, Holst JJ, Lauritzen KB, Rehfeld JF, Schwartz TW. Simultaneous recording of the gastro-entero-pancreatic hormonal peptide response to food in man. *Metabolism* (1980) 29:777–9. doi:10.1016/0026-0495(80)90203-6
63. Anagnosides AA, Chadwick VS, Selden AC, Barr J, Maton PN. Human pancreatic and biliary responses to physiological concentrations of cholecystokinin octapeptide. *Clin Sci (Lond)* (1985) 69:259–63. doi:10.1042/cs0690259
64. Kerstens PJ, Lamers CB, Jansen JB, de Jong AJ, Hessels M, Hafkenscheid JC. Physiological plasma concentrations of cholecystokinin stimulate pancreatic enzyme secretion and gallbladder contraction in man. *Life Sci* (1985) 36:565–9. doi:10.1016/0024-3205(85)90638-1
65. Solomon TE, Yamada T, Elashoff J, Wood J, Beglinger C. Bioactivity of cholecystokinin analogues: CCK-8 is not more potent than CCK-33. *Am J Physiol* (1984) 247:G105–11.
66. Wank SA, Harkins R, Jensen RT, Shapira H, de Weerth A, Slattery T. Purification, molecular cloning, and functional expression of the cholecystokinin receptor from rat pancreas. *Proc Natl Acad Sci U S A* (1992) 89:3125–9. doi:10.1073/pnas.89.7.3125
67. Kopin AS, Lee YM, McBride EW, Miller LJ, Lu M, Lin HY, et al. Expression cloning and characterization of the canine parietal cell gastrin receptor. *Proc Natl Acad Sci U S A* (1992) 89:3605–9. doi:10.1073/pnas.89.8.3605
68. Chen D, Zhao CM, Häkanson R, Samuelson LC, Rehfeld JF, Friis-Hansen L. Altered control of gastric acid secretion in gastrin-cholecystokinin double mutant mice. *Gastroenterology* (2004) 126:476–87. doi:10.1053/j.gastro.2003.11.012
69. You ZB, Herrera-Marschitz M, Pettersson E, Nylander I, Goiny M, Shou HZ, et al. Modulation of neurotransmitter release by cholecystokinin in the neostriatum and substantia nigra of the rat: regional and receptor specificity. *Neuroscience* (1996) 74:793–804. doi:10.1016/0306-4522(96)00149-2
70. Honda T, Wada E, Battey JF, Wank SA. Differential gene expression of CCK(A) and CCK(B) receptors in the rat brain. *Mol Cell Neurosci* (1993) 4:143–54. doi:10.1006/mcne.1993.1018
71. Pisegna JR, de Weerth A, Huppi K, Wank SA. Molecular cloning of the human brain and gastric cholecystokinin receptor: structure, functional expression and chromosomal localization. *Biochem Biophys Res Commun* (1992) 189:296–303. doi:10.1016/0006-291X(92)91557-7
72. Lee YM, Beinborn M, McBride EW, Lu M, Kolakowski LF Jr, Kopin AS. The human brain cholecystokinin-B/gastrin receptor. Cloning and characterization. *J Biol Chem* (1993) 268:8164–9.
73. Saillan-Barreau C, Dufresne M, Clerc P, Sanchez D, Corominola H, Moriscot C, et al. Evidence for a functional role of the cholecystokinin-B/gastrin receptor in human fetal and adult pancreas. *Diabetes* (1999) 48:2015–21. doi:10.2337/diabetes.48.10.2015
74. Shaw RA, Jones RS. The choleretic action of cholecystokinin and cholecystokinin octapeptide in dogs. *Surgery* (1978) 84:622–5.
75. Dyck WP, Martin GA, Ratliff CR. Influence of secretin and cholecystokinin on intestinal alkaline phosphatase secretion. *Gastroenterology* (1973) 64:599–602.
76. Dyck WP, Bonnet D, Lasater J, Stinson C, Hall FF. Hormonal stimulation of intestinal disaccharidase release in the dog. *Gastroenterology* (1974) 66:533–8.
77. Götz H, Götz J, Adelson JW. Studies on intestinal enzyme secretion; the action of cholecystokinin-pancreozymin, pentagastrin and bile. *Res Exp Med (Berl)* (1978) 173:17–25. doi:10.1007/BF01851370
78. Bragado MJ, Tashiro M, Williams JA. Regulation of the initiation of pancreatic digestive enzyme protein synthesis by cholecystokinin in rat pancreas *in vivo*. *Gastroenterology* (2000) 119:1731–9. doi:10.1053/gast.2000.20242
79. Williams JA. Intracellular signaling mechanisms activated by cholecystokinin-regulating synthesis and secretion of digestive enzymes in pancreatic acinar cells. *Annu Rev Physiol* (2001) 63:77–97. doi:10.1146/annurev.physiol.63.1.77
80. Rothman SS, Wells H. Enhancement of pancreatic enzyme synthesis by pancreozymin. *Am J Physiol* (1967) 213:215–8.
81. Debas HT, Grossman MI. Pure cholecystokinin: pancreatic protein and bicarbonate response. *Digestion* (1973) 9:469–81. doi:10.1159/000197476
82. Soudah HC, Lu Y, Hasler WL, Owyang C. Cholecystokinin at physiological levels evokes pancreatic enzyme secretion via a cholinergic pathway. *Am J Physiol* (1992) 263:G102–7.
83. Ji B, Bi Y, Simeone D, Mortensen RM, Logsdon CD. Human pancreatic acinar cells lack functional responses to cholecystokinin and gastrin. *Gastroenterology* (2001) 121:1380–90. doi:10.1053/gast.2001.29557
84. Owyang C, Logsdon CD. New insights into neurohormonal regulation of pancreatic secretion. *Gastroenterology* (2004) 127:957–69. doi:10.1053/j.gastro.2004.05.002
85. Jensen SL, Rehfeld JF, Holst JJ, Nielsen OV, Fahrenkrug J, Schaffalitzky de Muckadell OB. Secretory effects of cholecystokinins on the isolated perfused porcine pancreas. *Acta Physiol Scand* (1981) 111:225–31. doi:10.1111/j.1748-1716.1981.tb06730.x
86. Hermansen K. Effects of cholecystokinin (CCK)-4, nonsulfated CCK-8 and sulfated CCK-8 on pancreatic somatostatin, insulin, and glucagon secretion in the dog: studies *in vitro*. *Endocrinology* (1984) 114:1770–5. doi:10.1210/endo-114-5-1770
87. Otsuki M, Sakamoto C, Yuu H, Maeda M, Morita S, Ohki A, et al. Discrepancies between the doses of cholecystokinin or caerulein-stimulating exocrine and endocrine responses in perfused isolated rat pancreas. *J Clin Invest* (1979) 63:478–84. doi:10.1172/JCI109325

88. Monstein HJ, Nylander AG, Salehi A, Chen D, Lundquist I, Häkanson R. Cholecystokinin-A and cholecystokinin-B/gastrin receptor mRNA expression in the gastrointestinal tract and pancreas of the rat and man. A polymerase chain reaction study. *Scand J Gastroenterol* (1996) 31:383–90. doi:10.3109/00365529609006415
89. Petersen H, Solomon T, Grossman MI. Effect of chronic pentagastrin, cholecystokinin, and secretin on pancreas of rats. *Am J Physiol* (1978) 234:E286–93.
90. Schultzberg M, Hökfelt T, Nilsson G, Terenius L, Rehfeld JF, Brown M, et al. Distribution of peptide- and catecholamine-containing neurons in the gastro-intestinal tract of rat and guinea-pig: immunohistochemical studies with antisera to substance P, vasoactive intestinal polypeptide, enkephalins, somatostatin, gastrin/cholecystokinin, neuropeptides and dopamine beta-hydroxylase. *Neuroscience* (1980) 5:689–744.
91. Gutiérrez JG, Chey WY, Dinoso VP. Actions of cholecystokinin and secretin on the motor activity of the small intestine in man. *Gastroenterology* (1974) 67:35–41.
92. Gibbs J, Young RC, Smith GP. Cholecystokinin elicits satiety in rats with open gastric fistulas. *Nature* (1973) 245:323–5. doi:10.1038/245323a0
93. Smith GP, Jerome C, Cushin BJ, Eterno R, Simansky KJ. Abdominal vagotomy blocks the satiety effect of cholecystokinin in the rat. *Science* (1981) 213:1036–7. doi:10.1126/science.7268408
94. Reubi JC, Waser B, Gugger M, Friess H, Kleeff J, Kayed H, et al. Distribution of CCK1 and CCK2 receptors in normal and diseased human pancreatic tissue. *Gastroenterology* (2003) 125:98–106. doi:10.1016/S0016-5085(03)00697-8
95. Dufresne M, Seva C, Fourmy D. Cholecystokinin and gastrin receptors. *Physiol Rev* (2006) 86:805–47. doi:10.1152/physrev.00014.2005
96. Rehfeld JF. Accumulation of nonamidated preprogastrin and preprocholecystokinin products in porcine pituitary corticotrophs. Evidence of post-translational control of cell differentiation. *J Biol Chem* (1986) 261:5841–7.
97. Reubi JC, Waser B. Unexpected high incidence of cholecystokinin-B/gastrin receptors in human medullary thyroid carcinomas. *Int J Cancer* (1996) 67:644–7. doi:10.1002/(SICI)1097-0215(19960904)67:5<644::AID-IJC9>3.0.CO;2-U
98. Bardram L, Hilsted L, Rehfeld JF. Cholecystokinin, gastrin and their precursors in pheochromocytomas. *Acta Endocrinol* (1989) 120:479–84.
99. Persson H, Ericsson A, Schalling M, Rehfeld JF, Hökfelt T. Detection of cholecystokinin in spermatogenic cells. *Acta Physiol Scand* (1988) 134:565–6. doi:10.1111/j.1748-1716.1998.tb08534.x
100. Persson H, Rehfeld JF, Ericsson A, Schalling M, Pelto-Huikko M, Hökfelt T. Transient expression of the cholecystokinin gene in male germ cells and accumulation of the peptide in the acrosomal granule: possible role of cholecystokinin in fertilization. *Proc Natl Acad Sci U S A* (1989) 86:6166–70. doi:10.1073/pnas.86.16.6166
101. Schalling M, Persson H, Pelto-Huikko M, Odum L, Ekman P, Gottlieb C, et al. Expression and localization of gastrin messenger RNA and peptide in spermatogenic cells. *J Clin Invest* (1990) 86:660–9. doi:10.1172/JCI114758
102. Aunapuu M, Roosaar P, Järveots T, Kurrikoff K, Köks S, Vasar E, et al. Altered renal morphology in transgenic mice with cholecystokinin overexpression. *Transgenic Res* (2008) 17:1079–89. doi:10.1007/s11248-008-9204-5
103. Miyamoto S, Shikata K, Miyasaka K, Okada S, Sasaki M, Koderer R, et al. Cholecystokinin plays a novel protective role in diabetic kidney through anti-inflammatory actions on macrophage: anti-inflammatory effect of cholecystokinin. *Diabetes* (2012) 61:897–907. doi:10.2337/db11-0402
104. de Weert A, Jonas L, Schade R, Schöneberg T, Wolf G, Pace A, et al. Gastrin/cholecystokinin type B receptors in the kidney: molecular, pharmacological, functional characterization, and localization. *Eur J Clin Invest* (1998) 28:592–601. doi:10.1046/j.1365-2362.1998.00310.x
105. von Schrenck T, de Weert A, Bechtel S, Eschenhagen T, Weil J, Wolf G, et al. Evidence for CCK(B) receptors in the guinea-pig kidney: localization and characterization by ¹²⁵I-gastrin binding studies and by RT-PCR. *Naunyn Schmiedebergs Arch Pharmacol* (1998) 358:287–92. doi:10.1007/PL00005255
106. Okahata H, Nishi Y, Muraki K, Sumii K, Miyachi Y, Usui T. Gastrin/cholecystokinin-like immunoreactivity in human blood cells. *Life Sci* (1985) 36:369–73. doi:10.1016/0024-3205(85)90123-7
107. Sacerdote P, Breda M, Barcellini W, Meroni PL, Panerai AE. Age-related changes of beta-endorphin and cholecystokinin in human and rat mononuclear cells. *Peptides* (1991) 12:1353–6. doi:10.1016/0196-9781(91)90219-F
108. De la Fuente M, Carrasco M, Del Rio M, Hernanz A. Modulation of murine lymphocyte functions by sulfated cholecystokinin octapeptide. *Neuropeptides* (1998) 32:225–33. doi:10.1016/S0143-4179(98)90041-5
109. Carrasco M, Del Rio M, Hernanz A, De la Fuente M. Inhibition of human neutrophil functions by sulfated and nonsulfated cholecystokinin octapeptides. *Peptides* (1997) 18:415–22. doi:10.1016/S0196-9781(96)00338-5
110. Meng AH, Ling YL, Zhang XP, Zhang JL. Anti-inflammatory effect of cholecystokinin and its signal transduction mechanism in endotoxic shock rat. *World J Gastroenterol* (2002) 8:712–7. doi:10.3748/wjg.v8.i4.712
111. Li S, Ni Z, Cong B, Gao W, Xu S, Wang C, et al. CCK-8 inhibits LPS-induced IL-1 β ta production in pulmonary interstitial macrophages by modulating PKA, p38, and NF- κ B pathway. *Shock* (2007) 27:678–86. doi:10.1097/shk.0b013e3180ze26dd
112. Lay JM, Gillespie PJ, Samuelson LC. Murine prenatal expression of cholecystokinin in neural crest, enteric neurons, and enteroendocrine cells. *Dev Dyn* (1999) 216:190–200. doi:10.1002/(SICI)1097-0177(199910)216:2<190::AID-DVDY9>3.0.CO;2-K
113. Goetze JP, Johnsen AH, Kistorp C, Gustafsson F, Johnbeck CB, Rehfeld JF. Cardiomyocyte expression and cell-specific processing of procholecystokinin. *J Biol Chem* (2015) 290:6837–43. doi:10.1074/jbc.M114.622670
114. Madsen OD, Larsson LI, Rehfeld JF, Schwartz TW, Lernmark A, Labrecque AD, et al. Cloned cell lines from a transplantable islet cell tumor are heterogeneous and express cholecystokinin in addition to islet hormones. *J Cell Biol* (1986) 103:2025–34. doi:10.1083/jcb.103.5.2025
115. Madsen OD, Karlsson C, Nielsen E, Lund K, Kofod H, Welinder B, et al. The dissociation of tumor-induced weight loss from hypoglycemia in a transplantable pluripotent rat islet tumor results in the segregation of stable alpha- and beta-cell tumor phenotypes. *Endocrinology* (1993) 133:2022–30. doi:10.1210/endo.133.5.8404649
116. Rehfeld JF, Federspiel B, Bardram L. A neuroendocrine tumor syndrome from cholecystokinin secretion. *N Engl J Med* (2013) 368:1165–6. doi:10.1056/NEJMMc1215137
117. Rehfeld JF, Federspiel B, Agersnap M, Knigge U, Bardram L. The uncovering and characterization of a CCKoma syndrome in enteropancreatic neuroendocrine tumor patients. *Scand J Gastroenterol* (2016) 51:1172–8. doi:10.1080/00365521.2016.1183706
118. Reubi JC, Koefoed P, Hansen TV, Stauffer E, Rauch D, Nielsen FC, et al. Procholecystokinin as marker of human Ewing sarcomas. *Clin Cancer Res* (2004) 10:5523–30. doi:10.1158/1078-0432.CCR-1015-03
119. Oikonomou E, Buchfelder M, Adams EF. Cholecystokinin (CCK) and CCK receptor expression by human gliomas: evidence for an autocrine/paracrine stimulatory loop. *Neuropeptides* (2008) 42:255–65. doi:10.1016/j.npep.2008.02.005
120. Camby I, Salmon I, Danguy A, Pasteels JL, Brotchi J, Martinez J, et al. Influence of gastrin on human astrocytic tumor cell proliferation. *J Natl Cancer Inst* (1996) 88:594–600. doi:10.1093/jnci/88.9.594
121. Rehfeld JF, van Solinge WW, Tos M, Thomsen J. Gastrin, cholecystokinin and their precursors in acoustic neuromas. *Brain Res* (1990) 530:235–8. doi:10.1016/0006-8993(90)91288-R
122. Rehfeld JF. Cholecystokinin expression in tumors: biogenetic and diagnostic implications. *Future Oncol* (2016) 12:2135–47. doi:10.2217/fon-2015-0053

Conflict of Interest Statement: The author declares that the research was conducted in the absence of any commercial or financial relationships that could be construed as a potential conflict of interest.

Copyright © 2017 Rehfeld. This is an open-access article distributed under the terms of the Creative Commons Attribution License (CC BY). The use, distribution or reproduction in other forums is permitted, provided the original author(s) or licensor are credited and that the original publication in this journal is cited, in accordance with accepted academic practice. No use, distribution or reproduction is permitted which does not comply with these terms.



Ghrelin Is a Regulator of Glucagon-Like Peptide 1 Secretion and Transcription in Mice

Andreas Lindqvist, Liliya Shcherbina, Ann-Helen Thorén Fischer and Nils Wierup*

Department of Clinical Sciences, Lund University Diabetes Centre, Malmö, Sweden

The gut hormones ghrelin, glucagon-like peptide 1 (GLP-1), and glucose-dependent insulinotropic peptide (GIP) have been intensively studied for their role in metabolism. It is, however, not well known whether the hormones interplay and regulate the secretion of each other. In this study, we studied the effect of ghrelin on GLP-1, GIP, and insulin secretion during an oral glucose tolerance test (OGTT) in mice. Intravenous administration of ghrelin caused increased GLP-1 secretion during the OGTT. On the other hand, ghrelin had no effect on circulating levels of glucose, insulin, and GIP. Furthermore, ghrelin treatment reduced proglucagon mRNA expression in GLUTag cells. The effect of ghrelin on GLP-1 secretion and proglucagon transcription was reinforced by the presence of GHS-R1a in human and mouse ileal L-cells, as well as in GLUTag cells. In summary, ghrelin is a regulator of GLP-1 secretion and transcription, and interfering with GHS-R1a signaling may be a way forward to enhance endogenous GLP-1 secretion in subjects with type 2 diabetes.

OPEN ACCESS

Edited by:

Hubert Vaudry,
University of Rouen, France

Reviewed by:

Odile Viltart,
Lille University of Science and
Technology, France

Laurent Gautron,
University of Texas Southwestern
Medical Center, United States
Masayasu Kojima,
Kurume University, Japan

*Correspondence:

Nils Wierup
nils.wierup@med.lu.se

Specialty section:

This article was submitted to
Neuroendocrine Science,
a section of the journal
Frontiers in Endocrinology

Received: 20 January 2017

Accepted: 01 June 2017

Published: 19 June 2017

Citation:

Lindqvist A, Shcherbina L, Fischer A-HT and Wierup N (2017)
Ghrelin Is a Regulator of Glucagon-Like Peptide 1 Secretion and Transcription in Mice.
Front. Endocrinol. 8:135.
doi: 10.3389/fendo.2017.00135

INTRODUCTION

The gastrointestinal tract harbors an array of hormones and regulatory peptides, involved in control of processes ranging from food intake to glucose homeostasis (1). Although the biological significance of the major gut hormones is well established, the interplay between different gut hormones is not well known and needs further investigation. Glucagon-like peptide 1 (GLP-1) is a product of the proglucagon gene produced by L-cells in the distal intestine, mainly in the ileum and colon. GLP-1 is known to increase insulin secretion (2) and beta cell proliferation (3) and to inhibit intestinal motility (4), gastric emptying (5), and food intake (6). GLP-1 chemistry is an area targeted for the treatment of type 2 diabetes (T2D) and GLP-1 analogs and inhibitors of the GLP-1-degrading enzyme DPP-IV are successfully used in clinical practice (7). Glucose-dependent insulinotropic peptide (GIP) is, on the other hand, produced in K-cells mainly located to the proximal parts of the small intestine. GIP has many effects that are similar to those of GLP-1 including stimulating insulin secretion (8, 9) and promoting beta cell proliferation (10, 11). Increased understanding of the mechanisms regulating incretin secretion is important to understand normal physiology and may pave the way for new targets for the treatment of T2D. Ghrelin is a 28-amino acid peptide hormone produced by P/D1 cells in the oxyntic mucosa of the stomach (12), in the upper small intestine (13), and in a distinct cell type in the pancreatic islets (14). Normoglycemic lean humans have elevated ghrelin levels in response to fasting and the levels decrease upon meal ingestion (15). Central and peripheral administration of ghrelin in rodents and humans has been shown to increase food intake (16–18) and to inhibit insulin secretion (19). Furthermore, ghrelin has been shown to inhibit insulin secretion in isolated mouse islets (20, 21) and in clonal beta cells (22, 23). Obese individuals have lower fasting levels of ghrelin (24) and deranged suppression of ghrelin levels upon meal ingestion (25). Furthermore, lean T2D

patients have higher levels of fasting ghrelin, whereas obese T2D subjects have lower levels of fasting ghrelin, than do normoglycemic lean control subjects (26). The GLP-1 analog, exendin-4 reduces ghrelin levels in fasting rats (27) and GLP-2, another product of the proglucagon gene, suppresses ghrelin secretion in humans (28). Furthermore, ghrelin was reported to attenuate the effects of GLP-1 on food intake (29). Two studies have shown that ghrelin regulates GLP-1 secretion and production, but the available data are somewhat contradictory (30, 31). Here, we aimed to assess the effect of intravenously administered ghrelin on GLP-1 and GIP secretion in response to an oral glucose tolerance test (OGTT). Our results suggest that intravenous administration of ghrelin increases GLP-1 secretion during an OGTT and that ghrelin affects proglucagon transcription *in vitro* in GLUTag cells.

MATERIALS AND METHODS

Mice

Female C57BL/6NTac mice (approximately 25 g; 4–5 weeks of age) were housed in climate-controlled rooms ($23 \pm 1^\circ\text{C}$) with a 12:12 h light–dark cycle. Food and water were provided *ad libitum* unless otherwise stated. All the experiments in this study were approved by and performed in accordance with the Animal Ethics Committee, Lund and Malmö, Sweden (Ethical permit number M458-12).

Oral Glucose Tolerance Test

The mice were fasted for 4 h before the oral glucose tolerance test (OGTT). OGTTs were performed at 1300. The mice were anesthetized using an intraperitoneal injection of Hypnorm/Dormicum (10 µl/g BW; fentanyl 0.315 mg/ml, fluanisone 10 mg/ml, and midazolam 5 mg/ml). Basal blood samples (40 µl) were collected through retro-orbital puncture and ghrelin [50 nmol/kg (21); Phoenix Pharmaceuticals, Burlingame, CA, USA] or saline was injected intravenously in a tail vein 5 min prior to glucose administration (32, 33) ($n = 18$ and $n = 15$, respectively). At time 0, glucose [3 mg/g body weight (32, 33)] was given orally through gavage. Blood samples (40 µl/time point) were collected at 10, 20, 30, 60, and 90 min through retro-orbital puncture. After glucose tolerance tests, the mice were kept overnight under a heating lamp for recovery.

Blood Collection

Blood was collected in chilled tubes supplemented with 500 KIU/ml Aprotinin (Trasylol®; Leverkusen, Germany) and 100 µmol/ml of the DPP-IV inhibitor Diprotin A (Sigma Aldrich, St. Louis, MO, USA). Plasma ($1,500 \times g$, 3 min, 4°C) was stored at -80°C until analysis.

Hormone Analyses

Active GLP-1, total GIP, and total ghrelin were analyzed using ELISAs from Millipore (Darmstadt, Germany). Insulin was analyzed using an ELISA from Mercodia (Uppsala, Sweden), and glucose was analyzed using a commercially available kit (Infinity Glucose Oxidase) from Thermo Fisher Scientific (Lexington, MA, USA). Assays were performed according to the instructions provided by the manufacturers.

Cell Culture

The GLUTag cell line (provided by Dr. Daniel J. Drucker, Mount Sinai Hospital, Toronto, ON, Canada) was originally isolated from a glucagon-producing enteroendocrine tumor in mice. GLUTag cells were routinely cultured in Dulbecco's modified Eagle's medium, 1 g/l glucose, supplemented with 10% FBS, and 2 mM glutamine. For ghrelin treatment, cells were seeded in 24-well plates at a density of 250,000 cells/well and cultured for 24 h. Thereafter, medium was replaced by new medium with or without ghrelin at concentrations of 10 nM, 100 nM, and 1 µM and cells were incubated for 24 h.

Quantitative Real-time PCR

RNA was extracted from GLUTag cells using a commercially available kit (Nucleo Spin RNA II, Macherey Nagel, Bethlehem, PA, USA). cDNA was generated using a RevertAid First Strand cDNA Synthesis kit (Thermo Fisher Scientific, Waltham, MA, USA). Real-time PCR was run using TaqMan® assays [GLP-1, Mm1269055_m1; peptidylpropyl isomerase A (PPIA) Mm02342429_g1]. 25 ng of cDNA was run under the following conditions: 1 cycle of 50°C for 2 min and 95°C for 10 min followed by 40 cycles of 95°C for 15 s and 60°C for 1 min. The mRNA expression was calculated using the $2^{-\Delta\Delta(\text{CT})}$ formula and expressed as arbitrary units in relation to PPIA expression that was used as reference gene.

Tissue Collection

Mouse ileum was collected from female C57BL/6NTac mice (approximately 25 g body weight), and specimens from human terminal ileum were taken during colonoscopy as previously detailed (13). The studies were approved by the Human Ethics Committee in Lund.

Immunohistochemistry

Specimens of human and mouse ileum were fixed in 4% paraformaldehyde and embedded in paraffin. Sections (6 µm) were cut on a microtome, and slides were incubated with previously characterized primary antibodies for ghrelin receptor (GHS-R1a) (rabbit antibody; code: H-001-62, dilution: 1:400, Phoenix Pharmaceuticals, Burlingame, CA, USA), proglucagon (guinea pig antibody; code: M7807, dilution: 1:5,000, EuroDiagnostika, Malmö, Sweden), and GIP (goat antibody; code: sc-23554; dilution 1:500, Santa Cruz Biotechnology, Houston, TX, USA) overnight at 4°C. Thereafter, slides were incubated with secondary antibodies [donkey anti-rabbit Cy2 (1:400) for GHS-R1a, donkey anti-guinea pig Texas Red (1:400) for GLP-1, and donkey anti-goat Texas Red (1:400) for GIP] for 1 h at room temperature. GLUTag cells were cultured on cover slips and incubated with GHS-R1a antibody (code: 00020; dilution: 1:400) overnight at 4°C. Secondary antibody (donkey anti-rabbit Cy2; 1:400) was applied and incubated for 1 h at room temperature. Nuclei was stained with 1 µM DAPI (Thermo Fisher Scientific, Waltham, MA, USA).

Statistics

Data are presented as mean \pm SEM. Statistical significance was calculated using one-way or two-way ANOVA where appropriate using the software GraphPad Prism 6 (GraphPad Software Inc.,

La Jolla, CA, USA). Differences were considered significant if $p < 0.05$.

RESULTS

Effect of Intravenous Ghrelin on GLP-1, GIP, and Insulin Release during an OGTT

Ghrelin had no effect on basal GLP-1 levels, but glucose-stimulated GLP-1 secretion was found to be transiently increased in mice that had received intravenous administration of ghrelin (**Figure 1A**). Thus, AUC for GLP-1 was increased approximately 1.5-fold ($p < 0.05$; **Figure 1B**). On the other hand, basal and

glucose-stimulated plasma levels of insulin, GIP and glucose (**Figures 1C–E**) were unaffected by ghrelin administration. Elevated circulating ghrelin levels in ghrelin-treated mice were confirmed (**Figure 1F**).

Effects of Ghrelin on Proglucagon mRNA in GLUTag Cells

Having established that ghrelin affects GLP-1 plasma levels, we next assessed whether ghrelin impacts on proglucagon transcription. To this end, GLP-1-expressing GLUTag cells were used as a model. Ghrelin was added to the media at different concentrations (10^{-6} , 10^{-7} , and 10^{-8} M) and cells were cultured for 24 h.

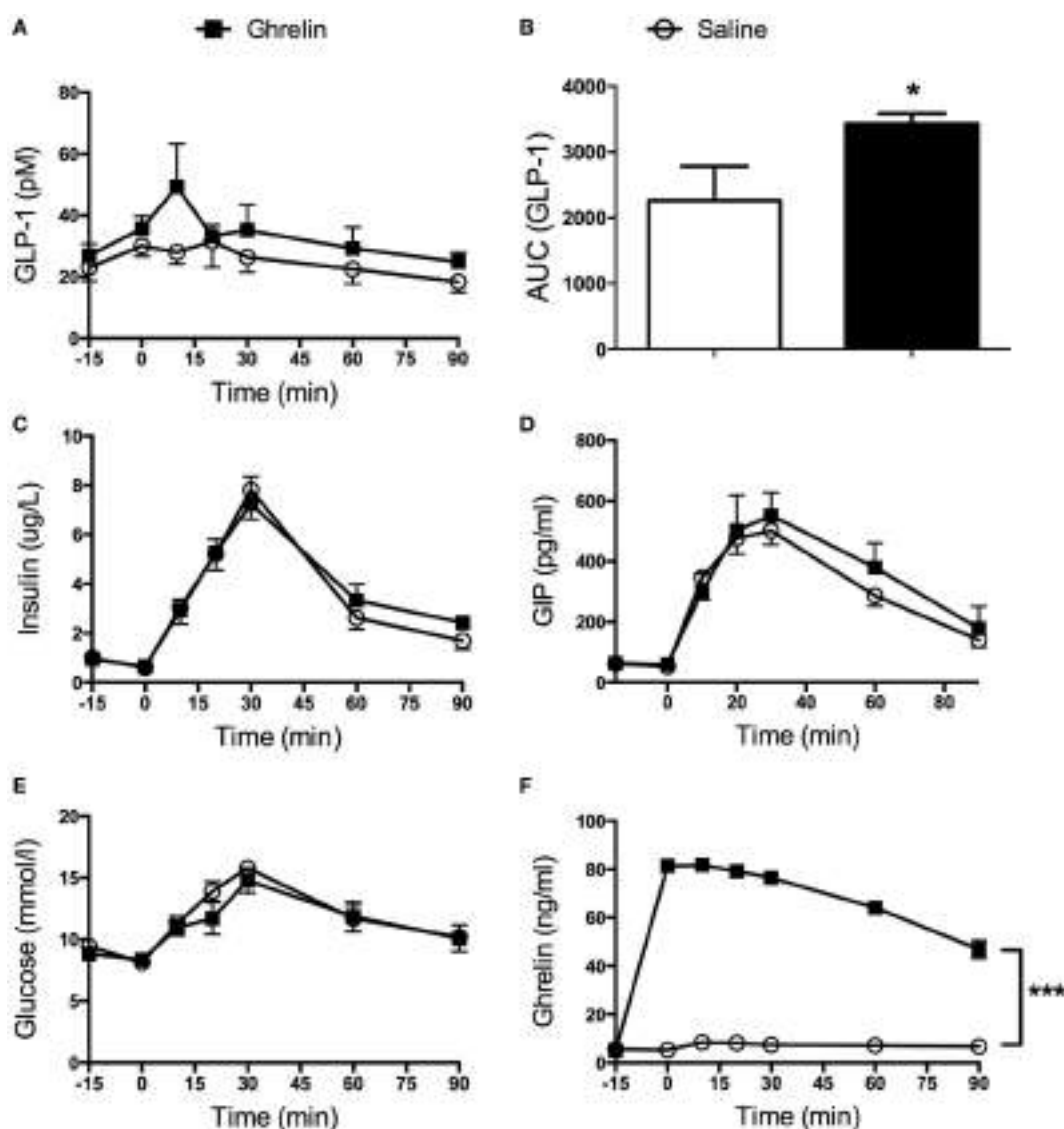


FIGURE 1 | Glucagon-like peptide 1 (GLP-1) secretion was increased in mice receiving ghrelin intravenously (50 nmol/kg) **(A)**. AUC calculations revealed a statistically significant increase in GLP-1 after ghrelin injection **(B)**. Insulin **(C)**, glucose-dependent insulinotropic peptide (GIP) **(D)**, and glucose **(E)** were unaffected by ghrelin treatment. Hyperghrelinemia in the mice was confirmed by significantly elevated levels of circulating ghrelin in the group of mice having received intravenous administration of ghrelin **(F)**. * $p < 0.05$; *** $p < 0.001$. All statistical analyses were performed using two-way ANOVA except for **(B)** where Student's *t*-test was applied.

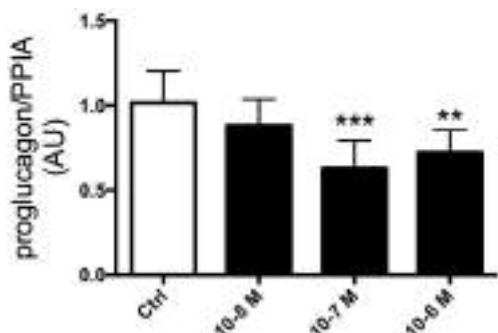


FIGURE 2 | GLUTag cells were incubated with 10⁻⁶, 10⁻⁷, or 10⁻⁸ M ghrelin for 24 h. Cells treated with 10⁻⁶ and 10⁻⁷ M ghrelin displayed reduced proglucagon mRNA expression compared to control cells. *** $p < 0.01$; ** $p < 0.001$. Statistical analysis was performed using one-way ANOVA. Experiments were repeated in eight passages of cells ($n = 8$).

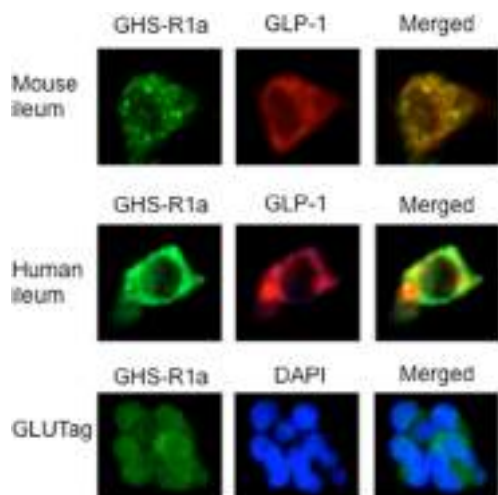


FIGURE 3 | The presence of the ghrelin receptor, GHS-R1a, was confirmed in mouse and human ileum using immunohistochemistry. Double staining with glucagon-like peptide 1 (GLP-1) revealed that GHS-R1a is colocalized with GLP-1 in mouse and human ileum (upper panel). GHS-R1a immunoreactivity was also evident in GLUTag cells (lower panel).

This revealed that addition of ghrelin (10⁻⁶ or 10⁻⁷ M) resulted in reduced proglucagon mRNA expression compared with vehicle-treated control cells ($p < 0.01$ and $p < 0.005$, respectively; Figure 2).

GHS-R1a Expression in Mouse and Human Ileum

Our data on the effect of ghrelin on GLP-1 secretion imply that L-cells express ghrelin receptors (GHS-R1a). To test this, we double stained mouse and human ileal sections for GHS-R1a and proglucagon. This revealed that GLP-1-producing L-cells harbored GHS-R1a expression in both species (Figure 3). On the other hand, GIP-producing K-cells were devoid of

GHS-R1a (data not shown). Furthermore, stainings for GHS-R1a confirmed GHS-R1a expression also in GLUTag cells (Figure 3).

DISCUSSION

The gut hormones ghrelin and GLP-1 have been extensively studied the last decade. However, it is still not fully understood how they interplay. Here, we show that intravenously administered ghrelin stimulates secretion of GLP-1 *in vivo* in mice, as well as that ghrelin affects GLP-1 transcription in an *in vitro* model of L-cells. On the other hand, ghrelin had no effect on plasma levels of GIP, insulin, or glucose.

Our data on the stimulatory effect of ghrelin on GLP-1 gain support from a recent study by Gagnon et al. who reported stimulatory effects of ghrelin on GLP-1 secretion *in vivo* in mice and *in vitro* in GLUTag and NCI-H716 cell lines via MAPK-dependent pathways (30). Furthermore, the authors demonstrated a role for endogenous ghrelin as a regulator of GLP-1 since treatment with a ghrelin receptor antagonist reduced circulating GLP-1 levels. In contrast to our present data, Gagnon et al. found ghrelin administration to reduce glucose levels paralleled by a minute increase in insulin secretion. Interestingly, these effects were absent in mice lacking the GLP-1 receptor and in wild-type mice cotreated with a GLP-1 receptor antagonist (30). The divergent data with respect to insulin and glucose levels may be related to differences in study design between the study by Gagnon et al. and the present study. First, different doses of ghrelin were used; Gagnon et al. used a fourfold higher dose of ghrelin (200 vs 50 nmol/kg). Second, the timing of ghrelin injection differed. Gagnon et al. injected ghrelin at -15 min, whereas in the present study, ghrelin was injected at -5 min. Third, the administration route differed. Whereas ghrelin was administered intravenously in the present study, Gagnon et al. administered ghrelin intraperitoneally. Also, in the present study, active GLP-1 was measured, while Gagnon et al. measured total GLP-1. Although it is difficult to compare the effect of acute administration of ghrelin with that of life long absence of the ghrelin receptor, our data and the data by Gagnon et al. are not in accordance with the data, presented by Xu et al., on increased circulating levels of GLP-1 in GHS-R1A null mice. However, it needs to be mentioned that Xu et al. only reported basal levels of GLP-1 and did not assess GLP-1 levels during a glucose tolerance test (31).

The two previous reports also assessed GLP-1 secretion from cell lines, but there is no consensus on the direction of the effect. Thus, Xu et al. (31) showed that ghrelin suppresses active GLP-1 secretion in STC-1 cells, whereas Gagnon et al. found ghrelin to increase GLP-1 secretion in GLUTag cells and NCI-H716 cells (30).

Our present *in vivo* data are in agreement with a study in humans by Tong et al. (34) who elegantly showed that during a meal tolerance test, infusion of a high dose of ghrelin increased the postprandial response of GLP-1, without affecting GIP, peptide YY, or glucagon. On the other hand, ghrelin had no effect on GLP-1 levels during an intravenous glucose tolerance test (IvGTT) (34). Furthermore, insulin secretion rate adjusted for glucose was reduced by ghrelin infusion.

In this study, ghrelin administration had no effect on insulin and glucose levels during the OGTT. This is in contrast to previous reports showing that ghrelin inhibits insulin secretion in different models and settings, including IvGTT in mice (21), *in vitro* studies in isolated islets and clonal cells (21–23, 35), as well as *in vivo* in humans (34, 36). To the best of our knowledge, the effect of intravenously administered ghrelin on insulin secretion during an OGTT in mice has not been reported previously. Fusco et al. administered ghrelin intravenously to obese patients with or without polycystic ovary syndrome and found ghrelin to suppress insulin secretion during an OGTT (37). However, incretin levels were not measured (37). We suggest that a possible explanation for the lack of effect of ghrelin on insulin in this study may be a result of the stimulatory actions of GLP-1 masking the inhibitory effect of ghrelin on the beta cell.

Furthermore, intravenous ghrelin administration had no effect on circulating levels of GIP during the OGTT. This is in line with the data presented by Tong et al. in healthy human subjects (34). As the half-life of ghrelin is approximately 85 min (38), it seems unlikely that this would contribute to the observations presented here.

We also showed that ghrelin reduced proglucagon mRNA expression in GLUTag cells, an *in vitro* model of L-cells. This observation was unexpected in light of the stimulatory effects of ghrelin on GLP-1 secretion *in vivo*. There is no ready explanation for the divergent data, and it is not known whether ghrelin has the same effect in L-cells *in vivo*. However, our present data gain support from similar observations in STC-1 cells (31). It should be mentioned that the effect on circulating levels of GLP-1 *in vivo* was evident within minutes, whereas the effect of ghrelin on proglucagon mRNA in GLUTag cells was seen after 24 h of culture. Furthermore, the effect of ghrelin on proglucagon mRNA integrity is not known. Further studies are needed to understand the impact of ghrelin on GLP-1 transcription and production.

Nevertheless, our functional data gain support from our confirmatory finding of GHS-R1a expression in L-cells in human

and murine ileum, as well as in GLUTag cells. Thus, providing anatomical prerequisites for a direct effect of ghrelin on L-cells. Gagnon et al. demonstrated GHS-R1a mRNA expression in GLUTag and NCI-H716 cells (30). In this study, we confirm the previous findings of Xu et al. who demonstrated the presence of GHS-R1a in L-cells in murine ileum (31). The lack of effect of ghrelin on GIP secretion shown here and reported by Tong et al. (34) is most likely explained by our present finding of lack of GHS-R1a in K-cells.

In summary, during an oral glucose challenge, intravenously administered ghrelin stimulates circulating levels of GLP-1, without affecting levels of GIP, insulin, or glucose. Furthermore, ghrelin affects GLP-1 transcription and we confirm previous observations that murine L-cells express GHS-R1a and also show that human ileal L-cells express GHS-R1a.

ETHICS STATEMENT

The experiments were approved by the Animal Ethics Committee, Lund and Malmö, Sweden.

AUTHOR CONTRIBUTIONS

AL performed analyses and co-wrote the manuscript. LS performed analyses. A-HF performed surgeries. NW conceptualized the study and wrote the manuscript.

FUNDING

This work was supported by grants from the Swedish Research Council (Dnr. 2008-4216 and 521-2012-2119). This project is financially supported by the Swedish Foundation for Strategic Research. In addition, the project was also funded by the Albert Pahlsson Foundation, the Swedish Diabetes Foundation, ALF, the Novo Nordisk Foundation, the Royal Physiographical Society in Lund, and the Medical Faculty at Lund University.

REFERENCES

- Tan T, Bloom S. Gut hormones as therapeutic agents in treatment of diabetes and obesity. *Curr Opin Pharmacol* (2013) 13:996–1001. doi:10.1016/j.coph.2013.09.005
- Kjems LL, Holst JJ, Volund A, Madsbad S. The influence of GLP-1 on glucose-stimulated insulin secretion: effects on beta-cell sensitivity in type 2 and nondiabetic subjects. *Diabetes* (2003) 52:380–6. doi:10.2337/diabetes.52.2.380
- Xu G, Stoffers DA, Habener JF, Bonner-Weir S. Exendin-4 stimulates both beta-cell replication and neogenesis, resulting in increased beta-cell mass and improved glucose tolerance in diabetic rats. *Diabetes* (1999) 48:2270–6. doi:10.2337/diabetes.48.12.2270
- Hellstrom PM, Naslund E, Edholm T, Schmidt PT, Kristensen J, Theodorsson E, et al. GLP-1 suppresses gastrointestinal motility and inhibits the migrating motor complex in healthy subjects and patients with irritable bowel syndrome. *Neurogastroenterol Motil* (2008) 20:649–59. doi:10.1111/j.1365-2982.2007.01079.x
- Wettergren A, Schjoldager B, Mortensen PE, Myhre J, Christiansen J, Holst JJ. Truncated GLP-1 (proglucagon 78–107-amide) inhibits gastric and pancreatic functions in man. *Dig Dis Sci* (1993) 38:665–73. doi:10.1007/BF01316798
- Gutzwiller JP, Goke B, Drewe J, Hildebrand P, Ketterer S, Handschin D, et al. Glucagon-like peptide-1: a potent regulator of food intake in humans. *Gut* (1999) 44:81–6. doi:10.1136/gut.44.1.81
- Holst JJ. The physiology of glucagon-like peptide 1. *Physiol Rev* (2007) 87:1409–39. doi:10.1152/physrev.00034.2006
- Lu M, Wheeler MB, Leng XH, Boyd AE III. The role of the free cytosolic calcium level in beta-cell signal transduction by gastric inhibitory polypeptide and glucagon-like peptide I(7–37). *Endocrinology* (1993) 132:94–100. doi:10.1210/endo.132.1.8380389
- Siegel EG, Creutzfeldt W. Stimulation of insulin release in isolated rat islets by GIP in physiological concentrations and its relation to islet cyclic AMP content. *Diabetologia* (1985) 28:857–61. doi:10.1007/BF00291078
- Bocker D, Verspohl EJ. Role of protein kinase C, PI3-kinase and tyrosine kinase in activation of MAP kinase by glucose and agonists of G-protein coupled receptors in INS-1 cells. *Int J Exp Diabetes Res* (2001) 2:233–44. doi:10.1155/EDR.2001.233
- Trumper A, Trumper K, Trusheim H, Arnold R, Goke B, Horsch D. Glucose-dependent insulinotropic polypeptide is a growth factor for beta (INS-1) cells by pleiotropic signaling. *Mol Endocrinol* (2001) 15:1559–70. doi:10.1210/me.15.9.1559

12. Kojima M, Hosoda H, Date Y, Nakazato M, Matsuo H, Kangawa K. Ghrelin is a growth-hormone-releasing acylated peptide from stomach. *Nature* (1999) 402:656–60. doi:10.1038/45230
13. Wierup N, Bjorkqvist M, Westrom B, Pierzynowski S, Sundler F, Sjolund K. Ghrelin and motilin are cosecreted from a prominent endocrine cell population in the small intestine. *J Clin Endocrinol Metab* (2007) 92:3573–81. doi:10.1210/jc.2006-2756
14. Wierup N, Svensson H, Mulder H, Sundler F. The ghrelin cell: a novel developmentally regulated islet cell in the human pancreas. *Regul Pept* (2002) 107:63–9. doi:10.1016/S0167-0115(02)00067-8
15. Ariyasu H, Takaya K, Tagami T, Ogawa Y, Hosoda K, Akamizu T, et al. Stomach is a major source of circulating ghrelin, and feeding state determines plasma ghrelin-like immunoreactivity levels in humans. *J Clin Endocrinol Metab* (2001) 86:4753–8. doi:10.1210/jcem.86.10.7885
16. Tschoop M, Smiley DL, Heiman ML. Ghrelin induces adiposity in rodents. *Nature* (2000) 407:908–13. doi:10.1038/35038090
17. Wren AM, Seal LJ, Cohen MA, Brynes AE, Frost GS, Murphy KG, et al. Ghrelin enhances appetite and increases food intake in humans. *J Clin Endocrinol Metab* (2001) 86:5992. doi:10.1210/jcem.86.12.8111
18. Wren AM, Small CJ, Abbott CR, Dhillo WS, Seal LJ, Cohen MA, et al. Ghrelin causes hyperphagia and obesity in rats. *Diabetes* (2001) 50:2540–7. doi:10.2337/diabetes.50.11.2540
19. Tong J, Prigeon RL, Davis HW, Bidlingmaier M, Kahn SE, Cummings DE, et al. Ghrelin suppresses glucose-stimulated insulin secretion and deteriorates glucose tolerance in healthy humans. *Diabetes* (2010) 59:2145–51. doi:10.2337/db10-0504
20. Kurashina T, Dezaki K, Yoshida M, Sukma Rita R, Ito K, Taguchi M, et al. The beta-cell GHSR and downstream cAMP/TRPM2 signaling account for insulinostatic and glycemic effects of ghrelin. *Sci Rep* (2015) 5:14041. doi:10.1038/srep14041
21. Reimer MK, Pacini G, Ahren B. Dose-dependent inhibition by ghrelin of insulin secretion in the mouse. *Endocrinology* (2003) 144:916–21. doi:10.1210/en.2002-220819
22. Colombo M, Gregersen S, Xiao J, Hermansen K. Effects of ghrelin and other neuropeptides (CART, MCH, orexin A and B, and GLP-1) on the release of insulin from isolated rat islets. *Pancreas* (2003) 27:161–6. doi:10.1097/00006676-200308000-00009
23. Wierup N, Yang S, McEvilly RJ, Mulder H, Sundler F. Ghrelin is expressed in a novel endocrine cell type in developing rat islets and inhibits insulin secretion from INS-1 (832/13) cells. *J Histochem Cytochem* (2004) 52:301–10. doi:10.1177/002215540405200301
24. Tschoop M, Weyer C, Tataranni PA, Devanarayana V, Ravussin E, Heiman ML. Circulating ghrelin levels are decreased in human obesity. *Diabetes* (2001) 50:707–9. doi:10.2337/diabetes.50.4.707
25. le Roux CW, Patterson M, Vincent RP, Hunt C, Ghatei MA, Bloom SR. Postprandial plasma ghrelin is suppressed proportional to meal calorie content in normal-weight but not obese subjects. *J Clin Endocrinol Metab* (2005) 90:1068–71. doi:10.1210/jc.2004-1216
26. Shiota T, Nakazato M, Mizuta M, Date Y, Mondal MS, Tanaka M, et al. Plasma ghrelin levels in lean and obese humans and the effect of glucose on ghrelin secretion. *J Clin Endocrinol Metab* (2002) 87:240–4. doi:10.1210/jcem.87.1.8129
27. Perez-Tilve D, Gonzalez-Matias L, Alvarez-Crespo M, Leiras R, Tovar S, Dieguez C, et al. Exendin-4 potently decreases ghrelin levels in fasting rats. *Diabetes* (2007) 56:143–51. doi:10.2337/db05-0996
28. Banasch M, Bulut K, Hagemann D, Schrader H, Holst JJ, Schmidt WE, et al. Glucagon-like peptide 2 inhibits ghrelin secretion in humans. *Regul Pept* (2006) 137:173–8. doi:10.1016/j.regpep.2006.07.009
29. Chelikani PK, Haver AC, Reidelberger RD. Ghrelin attenuates the inhibitory effects of glucagon-like peptide-1 and peptide YY(3-36) on food intake and gastric emptying in rats. *Diabetes* (2006) 55:3038–46. doi:10.2337/db06-0730
30. Gagnon J, Baggio LL, Drucker DJ, Brubaker PL. Ghrelin is a novel regulator of glucagon-like peptide-1 secretion. *Diabetes* (2015) 64:1513–21. doi:10.2337/db14-1176
31. Xu G, Hong X, Tang H, Jiang S, Liu F, Shen Z, et al. Ghrelin regulates GLP-1 production through mTOR signaling in L cells. *Mol Cell Endocrinol* (2015) 416:9–18. doi:10.1016/j.mce.2015.08.016
32. Andersson U, Rosen L, Ostman E, Strom K, Wierup N, Bjorck I, et al. Metabolic effects of whole grain wheat and whole grain rye in the C57BL/6J mouse. *Nutrition* (2010) 26:230–9. doi:10.1016/j.nut.2009.06.007
33. Andersson U, Rosen L, Wierup N, Ostman E, Bjorck I, Holm C. A low glycaemic diet improves oral glucose tolerance but has no effect on beta-cell function in C57BL/6J mice. *Diabetes Obes Metab* (2010) 12:976–82. doi:10.1111/j.1463-1326.2010.01288.x
34. Tong J, Davis HW, Gastaldelli A, D'Alessio D. Ghrelin impairs prandial glucose tolerance and insulin secretion in healthy humans despite increasing GLP-1. *J Clin Endocrinol Metab* (2016) 101:2405–14. doi:10.1210/jc.2015-4154
35. Egido EM, Rodriguez-Gallardo J, Silvestre RA, Marco J. Inhibitory effect of ghrelin on insulin and pancreatic somatostatin secretion. *Eur J Endocrinol* (2002) 146:241–4. doi:10.1530/eje.0.1460241
36. Broglia F, Arvat E, Benso A, Gottero C, Muccioli G, Papotti M, et al. Ghrelin, a natural GH secretagogue produced by the stomach, induces hyperglycemia and reduces insulin secretion in humans. *J Clin Endocrinol Metab* (2001) 86:5083–6. doi:10.1210/jcem.86.10.8098
37. Fusco A, Bianchi A, Mancini A, Milardi D, Giampietro A, Cimino V, et al. Effects of ghrelin administration on endocrine and metabolic parameters in obese women with polycystic ovary syndrome. *J Endocrinol Invest* (2007) 30:948–56. doi:10.1007/BF03349243
38. Dornonville de la Cour C, Lindqvist A, Egecioglu E, Tung YC, Surve V, Ohlsson C, et al. Ghrelin treatment reverses the reduction in weight gain and body fat in gastrectomised mice. *Gut* (2005) 54:907–13. doi:10.1136/gut.2004.058578

Conflict of Interest Statement: The authors declare that the research was conducted in the absence of any commercial or financial relationships that could be construed as a potential conflict of interest.

Copyright © 2017 Lindqvist, Shcherbina, Fischer and Wierup. This is an open-access article distributed under the terms of the Creative Commons Attribution License (CC BY). The use, distribution or reproduction in other forums is permitted, provided the original author(s) or licensor are credited and that the original publication in this journal is cited, in accordance with accepted academic practice. No use, distribution or reproduction is permitted which does not comply with these terms.



Protein Digestion-Derived Peptides and the Peripheral Regulation of Food Intake

Juliette Caron[†], Dorothée Domenger[†], Pascal Dhulster, Rozenn Ravallec and Benoit Cudennec*

Université Lille, INRA, Université Artois, Université Littoral Côte d'Opale, EA 7394 – ICV – Institut Charles Viallette, Lille, France

The gut plays a central role in energy homeostasis. Food intake regulation strongly relies on the gut–brain axis, and numerous studies have pointed out the significant role played by gut hormones released from enteroendocrine cells. It is well known that digestive products of dietary protein possess a high satiating effect compared to carbohydrates and fat. Nevertheless, the processes occurring in the gut during protein digestion involved in the short-term regulation of food intake are still not totally unraveled. This review provides a concise overview of the current data concerning the implication of food-derived peptides in the peripheral regulation of food intake with a focus on the gut hormones cholecystokinin and glucagon-like peptide 1 regulation and the relationship with some aspects of glucose homeostasis.

Keywords: protein digestion, bioactive peptides, food intake regulation, gut hormones, dipeptidyl peptidase IV, enteroendocrine cells

OPEN ACCESS

Edited by:

Hubert Vaudry,
University of Rouen, France

Reviewed by:

Hiroshi Hara,
Hokkaido University, Japan
Leo T. O. Lee,
University of Macau, China

*Correspondence:

Benoit Cudennec
benoit.cudennec@univ-lille1.fr

[†]These authors have contributed equally to this work.

Specialty section:

This article was submitted to
Neuroendocrine Science,
a section of the journal
Frontiers in Endocrinology

Received: 25 January 2017

Accepted: 03 April 2017

Published: 24 April 2017

Citation:

Caron J, Domenger D, Dhulster P, Ravallec R and Cudennec B (2017) Protein Digestion-Derived Peptides and the Peripheral Regulation of Food Intake. *Front. Endocrinol.* 8:85.
doi: 10.3389/fendo.2017.00085

INTRODUCTION

Food intake regulation strongly relies on the gut–brain axis, and numerous studies have pointed out the significant role played by gut hormones in response to food digestion (1, 2). These hormones are involved in appetite regulation as short-term peripheral satiety signals. They promote satiety, i.e., diminish appetite and reduce food intake by endocrine and nervous paths activating different signaling pathways (3–5).

The increasing expansion of obesity-related diseases has led the scientific community to explore new therapeutic approaches. They need to promote long-term body weight decrease and stabilization, especially fat loss, as well as satiety while reducing caloric intake (6). Dietary proteins have a greater satiety effect than carbohydrates and fat when equally consumed (7). However, this effect may rely on the protein source (8). Satiating properties of dietary proteins come from various physiological effects such as gut hormone secretion stimulation, energy expenditure and amino acid circulating level increase, and gluconeogenesis stimulation (9). Nevertheless, the mechanisms occurring in the gut and leading to the release of peripheral signals (e.g., gut hormones) implicated in the short-term regulation of food intake are still unclear. In the context of obesity and type 2 diabetes mellitus (T2DM) management, protein intake has revealed interesting positive effects on glycemia decrease, insulin secretion, and body fat loss (10). So far, the beneficial effects of protein intake on energy homeostasis remain partially elucidated but have been mainly attributed to amino acid composition (6). Bioactive peptides have emerged as potential molecules accounting for the positive effects of protein intake on weight loss and glycemia management. The process of gastrointestinal (GI) digestion is able to release bioactive peptides at circulating levels that might exert significant physiological

effects on energy homeostasis. Unfortunately, their quantification *in vivo* still remains challenging. Some food protein-derived peptides, especially from dairy proteins, have demonstrated several biological activities, and these have been well characterized in relation to glycemia management (11). Nevertheless, the many bioactivities of food-derived peptides described so far still need to be better defined and integrated in a context of physiological function. Here, we review the involvement of protein-derived bioactive peptides in the short-term regulation of food intake and the mechanisms of protein-induced satiety, with a special focus on the gut hormones, cholecystokinin (CCK), and glucagon-like peptide 1 (GLP-1) on the one hand, and some aspects of glucose homeostasis on the other hand.

CCK SECRETION AND BIOACTIVE PEPTIDES

Cholecystokinin, mainly secreted by enteroendocrine I cells located in the upper intestinal tract, acts at different levels on food intake regulation. It retards gastric emptying, stimulates pancreatic secretion and decreases food intake. Several studies in rats or humans have proved that protein or protein hydrolyzate intake could stimulate CCK secretion correlated with a gastric emptying decrease (12, 13), inhibit intraluminal protease activity (14) or decrease food intake (15). The GI digestion process appears as a key step which emphasizes the satiating properties of dietary proteins. Several *in vivo* and *in vitro* studies with intact proteins, their hydrolyzates or corresponding amino acid mixtures illustrate this phenomenon. Indeed, peptides are sequentially released throughout GI digestion and are, with fatty acids, the main stimuli of CCK release. Sharara et al. have shown that a protein intake stimulated postprandial secretion of CCK in rats, though indirectly, whereas free amino acid intake had no effect (16). Soy protein or casein intake in rats caused a delay in food intake decrease compared to the one induced by the respective protein hydrolyzates. This might be due to a slower release of peptides occurring during intact protein GI digestion (17). *In vitro*, the STC-1 murine enteroendocrine cell (EEC) line is widely used for intestinal hormones synthesis and secretion studies. Using this model, the greater CCK stimulating potential of various peptones or protein hydrolyzates than the equivalent mixtures of free amino acids has been shown and further investigated. Amino acid mixtures representing the composition of various protein hydrolyzates such as soy protein (18), blue whiting or shrimp (19, 20) or various animal peptones (21) displayed lower CCK enhancing effects than their associated hydrolyzates. A beneficial effect of a longer pepsin hydrolysis time has been observed on the CCK enhancing potential of a soy protein hydrolyzate (18). The peptide structure thus seems a key determinant in the stimulation of CCK secretion, although this is still questionable (22). This brings light to the central role played by the GI digestion process in generating bioactive peptides from ingested dietary proteins. Proteins preloads studies have proved to decrease food intake during meals and to faster induce satiety. Interestingly, a preload of whey proteins administrated to healthy subjects significantly decreased food intake and stimulated satiety compared to a

preload of caseins, and this has been partially linked to a higher plasmatic CCK level (8). Thus, the type of protein source seems to influence the CCK enhancing potential, but this still needs to be clearly demonstrated.

Once released into the lumen, peptides come in contact with the brush border barrier where they can stimulate gut hormone secretion. All the known different pathways have been summarized in **Figure 1**.

Nishi et al. have isolated a peptide fragment of soy β -conglycinin (β 51–63) able to induce food intake decrease in rats correlated to enhanced CCK levels. This fragment showed *in vivo* to have the strongest ligand affinity for a rat intestinal membrane (estimated by surface plasmon resonance) compared to other β -conglycinin fragments whose CCK enhancing potentials were lower (23). The high occurrence of arginine residues in this particular bioactive fragment could partially account for the CCK enhancing effects (13). Concomitantly, a pork hydrolyzate showed a very high ligand affinity with rat brush border membrane correlated to a dose-dependent CCK enhancing effect on the murine STC-1 cell line. Moreover, an orogastric preload of this pork hydrolyzate significantly reduced food intake in rats (24). Dietary peptides could directly stimulate CCK secretion in I cells, or indirectly in the mucosa involving intermediate factors such as luminal CCK-releasing factor (LCRF) (25). Originally purified as a 70–75 amino-acid residue peptide from rat jejunum secretion (26), LCRF was found at the highest levels in the small intestine but is present in different parts throughout the GI tract (27). LCRF was identified after several studies showing that CCK release and pancreatic secretions were inhibited by trypsin, chymotrypsin, and elastases implying an intraluminal factor, sensitive to proteases, that elicits CCK secretion (28). Early studies tested the bioactivity of different LCRF fragments and highlighted the activity of fragment 11–25 but not 1–6 for instance, in accordance with the susceptibility of LCRF bioactivity to intestinal and pancreatic enzymes degradation (29). Further, it has been shown that LCRF acts directly on CCK-secreting cells also *via* an increase in intracellular calcium at least involving the L-type calcium channel (25). The intestinal mucosa possesses a wide variety of cells in addition to the EECs, which might be stimulated by peptides and be involved in CCK secretion. Receptors and signaling pathways involved have only been partially characterized so far. Intracellular calcium mobilization has been first pointed out using *in vitro* cell lines. Némoz-Gaillard et al. have demonstrated that egg white albumin peptones stimulated CCK secretion *via* a toxin pertussis sensitive G protein inducing a Ca^{2+} cytosolic input through voltage-dependent Ca^{2+} channels in STC-1 cells (30). Activation of Ca^{2+} channels can be the first step of the signaling pathway leading to CCK secretion: L-type channels are activated by diazepam-binding inhibitor (DBI), which has been isolated from rat intestinal mucosa, inducing CCK secretion (31). GPR93, also known as GPR92, is part of the G protein-coupled receptors (GPCR) investigated for their possible link between nutrient sensing and the transduction to GI cell functions. It is highly expressed in the intestine and has been found to respond to a protein hydrolyzate in rat enterocytes and non-tumorigenous rat enterocytes cell line (hBRIE380) (32). GPR93 is also endogenously expressed by STC-1 cells where its overexpression and

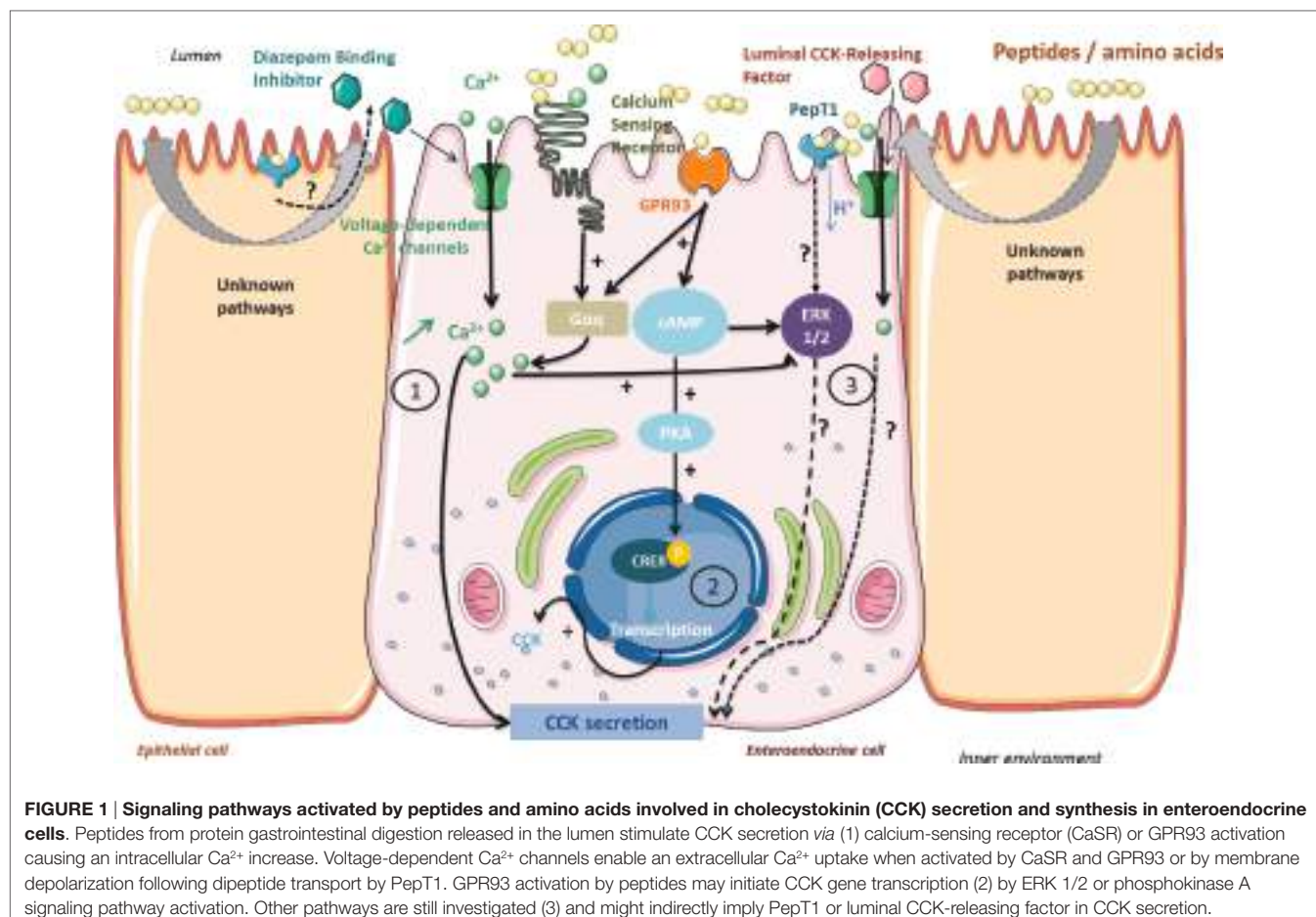


FIGURE 1 | Signaling pathways activated by peptides and amino acids involved in cholecystokinin (CCK) secretion and synthesis in enteroendocrine cells. Peptides from protein gastrointestinal digestion released in the lumen stimulate CCK secretion via (1) calcium-sensing receptor (CaSR) or GPR93 activation causing an intracellular Ca^{2+} increase. Voltage-dependent Ca^{2+} channels enable an extracellular Ca^{2+} uptake when activated by CaSR and GPR93 or by membrane depolarization following dipeptide transport by PepT1. GPR93 activation by peptides may initiate CCK gene transcription (2) by ERK 1/2 or phosphokinase A signaling pathway activation. Other pathways are still investigated (3) and might indirectly imply PepT1 or luminal CCK-releasing factor in CCK secretion.

activation by peptones lead to increases in CCK transcription and release (33). Further investigation of the transduction pathway revealed the involvement of G_α proteins, a dose-dependent intracellular Ca^{2+} increase and the ERK 1/2. The calcium-sensing receptor (CaSR) is the other receptor involved in luminal peptide detection linked to CCK secretion stimulation. Part of the C family of GPCR, CaSR possesses an N-terminal Venus fly trap (VFT) domain located in the extracellular side rich in cysteine residues (34). CaSR is activated by various metabolites, extracellular Ca^{2+} , and basic L-amino acids for which the VFT domain is required. CaSR is expressed in numerous tissues including the GI tract and is involved in calcium metabolism (35). CaSR is implicated in the stimulation of CCK secretion in the presence of L-phenylalanine, a well-known CCK secretion stimulator, in STC-1 cells (36). CaSR phenylalanine activation induces an intracellular Ca^{2+} increase ending up with CCK secretion (37). Peptide β 51–63 from β -conglycinin, a CCK-enhancing stimulator in STC-1 cells, provokes an intracellular Ca^{2+} increase mediated by CaSR (38). The authors later demonstrated that CaSR was also involved in protein hydrolyzate detection and CCK secretion stimulation. Treating cells with a specific CaSR antagonist significantly affected the CCK response in the presence of protein hydrolyzates (39). Even though protein hydrolyzates contain a significant part of free amino acids, low molecular weight peptides (>1,000 Da)

have been suggested to be the best stimuli of CCK secretion via CaSR activation. However, to the best of our knowledge, no peptide sequence has been characterized as CaSR specific.

Dietary peptides influence CCK secretion stimulation at different levels, but they also turn out to be influencing CCK gene transcription. Thus, Cordier-Bussat et al. showed that meat and egg albumin peptones had a dose-dependent effect on CCK secretion stimulation in STC-1 cells but also on the mRNA levels of the CCK gene (21). The authors later proved that peptones were able to stimulate cAMP release and to promote phosphokinase A (PKA) activation that induces CREB transcription factor phosphorylation, activating the CCK gene promoter in STC-1 cells (40). Choi et al. also noticed in STC-1 cells that GPR93 activation by peptones, or a specific agonist, led to an increase in CCK mRNA levels. Peptones were able to activate the PKA pathway that promoted the activation of the CCK gene promoter, and this has not been stated with the specific agonist. GPR93 activation by oligopeptides activates several signaling pathways that might influence both CCK synthesis and secretion (33). Indeed, Choi et al. studies in the STC-1 model implicated the ERK1/2 (MEK), PKA, and calcium/calmodulin-dependent protein kinase (CaMK) pathways in the mediation of CCK upregulation. Furthermore, Gevrey et al. work, also in STC-1 cells, had already shown peptone-induced involvement of the cAMP, PKA, and

CREB as the primary pathway, together with a Ca^{2+} dependent ERK1/2 (MEK) pathway and a minor involvement of CaMK on CCK gene promoter activity. They demonstrated a total inhibition of this promoter activity when all pathways were blocked, suggesting crosstalk between them. Previous evidence of possible interactions between the cAMP and ERK pathways in different cell types also exists (41–43).

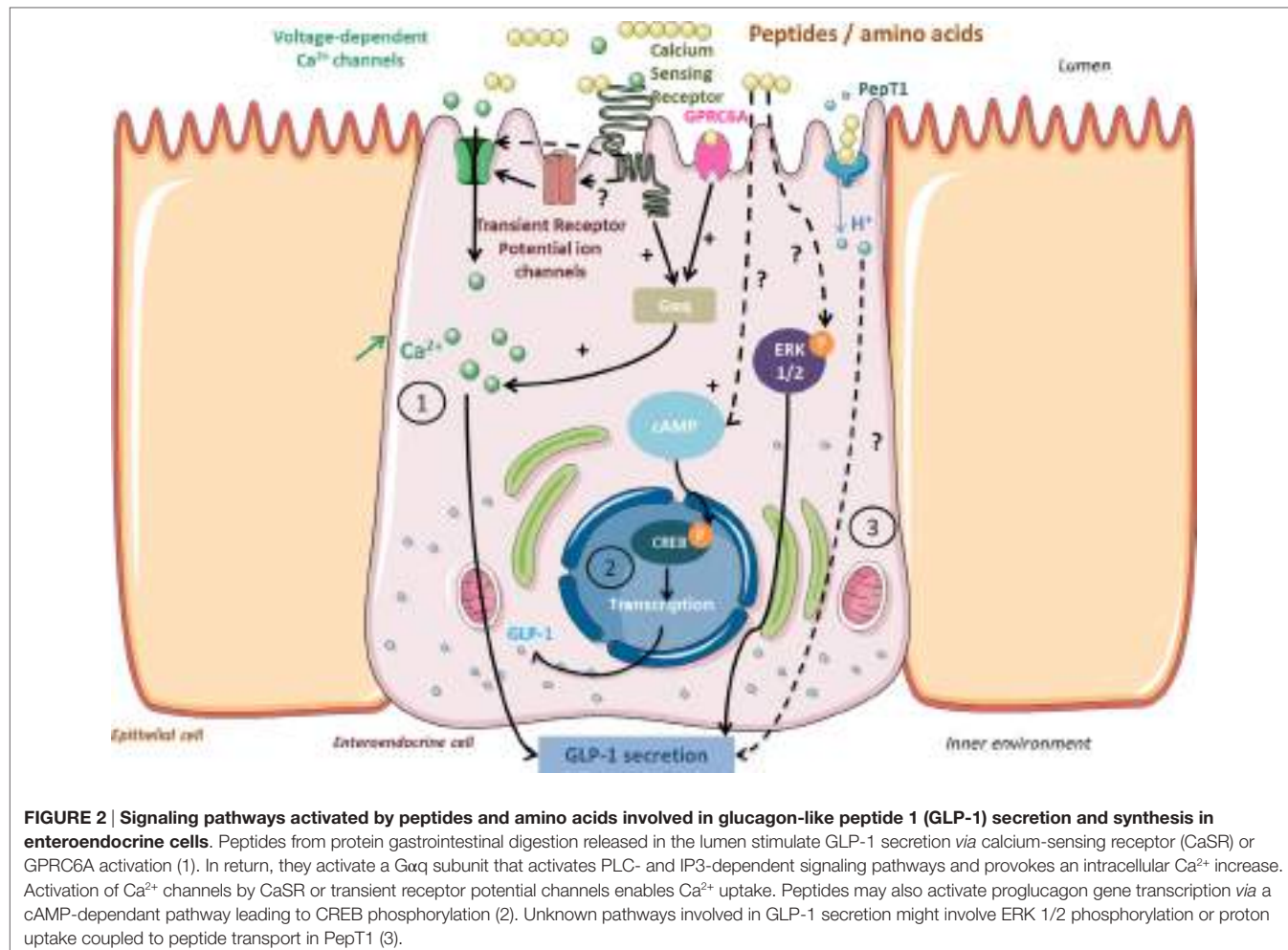
Anorexigenic effects of dietary peptides are also mediated by peripheral CCK-1R (13, 17, 44). Raybould et al. have proved that luminal nutrients stimulated CCK secretion that activates vagal afferents and inhibits gastric emptying (45). Later, Darcel et al. have pointed out that the di/tripeptides transporter PepT1 was also implied in the CCK secretion signaling pathway. The authors demonstrated that a duodenal infusion of meat peptones led to a vagal afferent discharge inhibited by a PepT1 inhibitor infused in the duodenal mucosa (46). The indirect role of PepT1 in CCK secretion induced by protein hydrolyzates was clearly pointed out in STC-1 cells as well as in native human intestinal I cells. Indeed, these cells were activated by PepT1 agonists, but this effect was not associated with CCK secretion alteration and was not affected by PepT1 antagonist treatment (47). These authors thus excluded a direct role of PepT1 in mediating the effect of peptone on CCK secretion. To account for an indirect role of PepT1, it was suggested that this transporter on enterocytes could promote a signaling factor release like the DBI that would trigger CCK release by I-cells. Moreover, although these authors found PepT1 transcripts in these cells, STC-1 expression of PepT1 could not be confirmed by another group (48). Remarkably, dietary peptides can also behave as CCK-1R agonists: soy or potato protein hydrolyzates known as CCK secretion stimuli in STC-1 cells, additionally act as partial agonists of CCK-1R in CCK-1R-overexpressing CHO cells. In the case of soy protein hydrolyzate, Staljanssens et al. demonstrated that the β -conglycinin hydrolyzates generated by GI digestion partially activate CCK-1R in CHO-CCK-1R cells but also probably other receptors involving an intracellular calcium response. Indeed, elevation of intracellular calcium was also noted in the native CHO cells, and more puzzling, this effect was decreased in the presence of a CCK-1R antagonist in both cell types (49). As the intestinal mucosa is densely innervated, vagal afferents expressing CCK-1R could be accessible to luminal content and be directly activated by dietary peptides (50). Lately, a study in vagotomized pigs has questioned the predominant role of the vagus nerve. CCK-1R blockade in abdominal vagal afferents did not abolish plasmatic CCK level increase and satiety after a liquid meal (51). This highlights that other peripheral CCK-1R could be involved and might have a greater role than the ones located in vagal afferent neurons.

To summarize, dietary peptides activate distinct signaling pathways involved in CCK secretion that promotes satiety and decrease food intake. They act in EECs by activating specific receptors (GPR93, CaSR) that, in response, induce CCK secretion stimulation *via* intracellular calcium mobilization. Peptides may indirectly act on the intestinal mucosa and stimulate the secretion of intermediate factors (LCRF) inducing CCK secretion in EECs. Another pathway stimulated by dietary peptides might involve PepT1 but has not been fully characterized yet. Peptides may also interact with CCK-1R either as partial agonist

in vagal afferents located in the intestinal mucosa or indirectly by activating a PepT1 involving signaling pathway. Finally, peptides regulate CCK synthesis at the CCK gene transcription level, but the pathways involved have to be further elucidated.

GLP-1 SECRETION AND BIOACTIVE PEPTIDES

Glucagon-like peptide 1 plays a significant role in energy homeostasis: it regulates blood glucose *via* its incretin action and promotes satiety and food intake decrease *via* its anorexigenic properties. That is why GLP-1 has recently emerged as an interesting therapeutic target in T2DM and obesity treatment approaches. Positive results from bariatric surgery on T2DM and obese subjects (sustainable weight loss, blood glucose regulation improvement) were partially attributed to elevated plasmatic GLP-1 levels, but these still remain partially unresolved (52). Dietary protein intake is one of the stimuli of GLP-1 secretion in EECs of the L-type, more abundant in the distal intestine, and activates several signaling pathways (Figure 2). GLP-1 effects were described after dietary protein intake from either animal sources, especially milk-derived proteins (53) or plant sources (54). A whey protein load before a meal led to a faster food intake decrease and satiety stimulation correlated to higher circulating GLP-1 levels in healthy subjects (55). A high-protein diet significantly increased postprandial GLP-1 levels compared to a conventional protein diet in healthy subjects, and extended satiety was partially attributed to these elevated GLP-1 levels (56). A preload of blue whiting administered to rats induced a short-term food intake decrease correlated to a plasmatic CCK and GLP-1 level increase (20). Beyond their satiating properties, dietary proteins can also improve blood glucose *via* GLP-1 secretion stimulation and plasmatic dipeptidyl peptidase IV (DPP-IV) activity inhibition (57–60). Whey proteins are a well-known source of bioactive peptides stimulating GLP-1 secretion, inhibiting plasma DPP-IV activity, and stimulating insulin secretion in pancreatic cells (61). However, the GLP-1-enhancing potential of proteins was found weaker than other macronutrients since lipid- or carbohydrate-based meals led to higher GLP-1 levels than after a high-protein diet (62). Moreover, an increase of the plasma GLP-1 level is not always associated with satiating effects (63). The reproducibility of GLP-1 satiating effects seems to strongly rely on several parameters such as the physiological state of the patient or experimental conditions of the study like the presence of other macronutrients, the protein source, and the delay duration after preload administration. This tends to make the comparison between different studies delicate (64). Regarding the secretion trigger mechanisms of GLP-1, two ways have been uncovered that explain the biphasic secretion of GLP-1. First, the activation of vagal afferents located in the duodenum, which indirectly stimulates GLP-1 secretion in distal EECs, then a direct contact with the EECs located in the ileum (65, 66). *In vitro* cell models have been widely developed to better understand the mechanisms of nutrient chemosensing. Animal (meat, egg white albumin) or plant protein (zein, rice) hydrolyzates have demonstrated GLP-1 enhancing properties in murine EEC lines such as STC-1 (67) and GLUTag (60, 66) or



human cell lines such as NCI-H716 (68). Free amino acids also have GLP-1 enhancing properties, but the resulting effect appears lower than for peptides (20, 67). Mechanisms of GLP-1 secretion triggered by free amino acids have been deeper investigated. L-Glutamine induces membrane depolarization and activation of a metabolic pathway involving intracellular calcium mobilization in GLUTag cells (69). This pathway has later been confirmed in primary intestinal cells where L-glutamine-induced membrane depolarization was associated to cAMP and intracellular calcium increases, probably mediated by a GPCR (70). However, in both healthy and T2DM patients, encapsulated L-glutamine ingestion did not influence GLP-1 levels to significantly induce beneficial metabolic effects. Surprisingly, L-glutamine intake was even followed by food intake increase and suggested that L-glutamine might interact with orexigenic pathways (71). CaSR, preferentially activated by aromatic amino acids and expressed in EECs, is one of the receptors involved in the GLP-1 secretion pathway. Indeed, amino acids such as phenylalanine, tryptophan, glutamine, or asparagine have shown a GLP-1 enhancing effect in isolated rat intestines, and this was strongly altered by a specific CaSR antagonist (72). Another GPCR, of the class C, named GPRC6A has been characterized as an amino acid chemodetector

more sensitive to basic amino acids exhibiting hydroxyl or sulfonyl groups. Extracellular binding of L-ornithine with GPRC6A triggered GLP-1 exocytosis by activating the intracellular calcium and inositol triphosphate related pathway in GLUTag cells (73).

Activation pathways triggered by peptides are under investigation but display certain similarities with those activated by amino acids such as intracellular calcium increase. One tetrapeptide of glycine residues stimulates GLP-1 secretion in NCI-H716 cells associated to intracellular calcium increase (74). Two distinct peptide sensing pathways have been highlighted in native L cells, one involving CaSR activation and intracellular calcium variation and the other peptide transport by PepT1 associated with membrane depolarization (75). Other transporters are involved in calcium regulation, such as voltage-dependent Q type channels or transient receptor potential channels and might be activated by protein hydrolyzates. Thus, they might participate in the GLP-1 secretion as suggested in a study realized in murine native EECs (76). Another intracellular signaling pathway has been characterized in NCI-H716 cells and involves MAP kinase metabolites: ERK1/2 phosphorylation activated by meat peptones triggers GLP-1 secretion (77). Finally, dietary peptides in the form of protein hydrolyzates are also able to positively influence proglucagon

gene transcription in both STC-1 and GLUTag cells (67, 78) by cAMP increase and CREB transcription factor phosphorylation (79). To the best of our knowledge, the tetra-glycine peptide was the only peptide sequence known for its GLP-1 enhancing properties until recently; our group identified three peptides, obtained from the GI digestion of bovine hemoglobin, able to highly stimulate GLP-1 secretion in STC-1 cells: ANVST, TKAVEH, and KAAVT (80).

BIOACTIVE PEPTIDES AND DPP-IV ACTIVITY: GLP-1 ACTIVITY REGULATION AND INDIRECT EFFECT ON GLUCOSE HOMEOSTASIS

Dipeptidyl peptidase IV is a serine exopeptidase that removes dipeptides from the N-terminal side of substrates, including GLP-1 and GIP, by cleaving post-proline or -alanine residues (81). It cleaves and *de facto* quickly inactivates GLP-1 following its secretion and therefore appears as a strong inhibitor of its activities (82). DPP-IV exists in transmembrane and soluble active forms and is expressed in various tissues and fluids. It has also been implicated in many other regulatory processes by its interaction with neuropeptides or chemokines (83). Today, DPP-IV inhibitors are thus considered an advanced class of agents for T2DM management due to their effects on the GLP-1 availability and recovery of the incretin effect. In this way, the oral administration of DPP-IV inhibitors (gliptins) is the most recent alternative treatment of T2DM (84). However, numerous works have pointed out the advantage to identify “natural” as in food-derived peptide inhibitors of DPP-IV activity as an alternative for synthetic inhibitors to reinstate the incretin effect in T2DM. GI dietary protein digestion is a natural enzymatic hydrolysis release of bioactive peptides that could exhibit DPP-IV inhibitory potentials close to those of peptides released under controlled enzymatic hydrolysis. IC₅₀ values of various digests generally range from 1 to 5 mg·mL⁻¹ like numerous protein hydrolyzates. As an example, several milk protein digests, generated under *in vitro* conditions, reached similar IC₅₀ values compared to protein hydrolyzates obtained with microbial enzymes such as Alcalase® or Flavourzyme® (85). Gruyere GI digestion has shown to be an interesting source of Ile-Pro-Ala, and Val-Ala-Pro-Phe-Pro-Glu-Val, two DPP-IV inhibitory peptides (86). Alaska pollock (*Theragra chalcogramma*) skin collagen, digested under *in vitro* GI conditions, has IC₅₀ values ranging from 1 to 2 mg·mL⁻¹ (87), and similar values have been measured with salmon collagen hydrolyzates obtained with a controlled enzymatic hydrolysis (88). A tetrapeptide Val-Ala-Ala-Ala has been recently isolated from an *in vitro* GI digest of bovine hemoglobin with an IC₅₀ of 0.141 ± 0.014 mM (80). A similar trend has been observed with plant protein GI digests. Amaranth (*Amaranthus hypochondriacus*) seed digests obtained by GI digestion have IC₅₀ values close to 1 mg·mL⁻¹ (89). Cowpea bean GI digestion (*Vigna unguiculata*), germinated or non-germinated, has produced digests with DPP-IV inhibitory properties at 0.58 mg·mL⁻¹ soluble protein. Two peptides Thr-Thr-Ala-Gly-Leu-Leu-Gln and Lys-Val-Ser-Val-Val-Ala-Leu, characterized by LC-MS-MS in

these isolated digests, could have interesting DPP-IV inhibitory properties. A docking study has revealed that these two peptides could strongly interact with the catalytic site of the DPP-IV (90). The process of GI digestion could be able to naturally generate bioactive peptides from dietary proteins with DPP-IV inhibitory properties. The inhibitory potential seems to increase along the progress of digestion: most of the intestinal digests of *in vitro* GI hemoglobin digestion exhibited lower IC₅₀ values than those of gastric digests (78). However, most of the studies focus on investigating DPP-IV inhibitory properties of protein hydrolyzates during their GI digestion. When digested, protein hydrolyzates often exhibit better DPP-IV inhibitory potentials than those of native proteins. This has been noticed with cuttlefish (91, 92), rice, pea, soy, hemp protein (92), or whey protein hydrolyzates (93). A similar observation has been made when comparing the DPP-IV inhibitory potential of cow’s milk yogurt from microbial fermentation and its respective GI-derived digests. The DPP-IV inhibitory potential of this yogurt GI digests was significantly better than the yogurt one and was constantly progressing over digestion time (94). GI digestion extends protein degradation and, as a consequence, promotes the release of new potential bioactive peptides. In that sense, most of the studies first focus on optimizing hydrolysis conditions to generate bioactive peptides and then investigate peptide or hydrolyzate stability and their associated bioactivities in simulated GI conditions. Bioactive peptides may be released exogenously (enzymatic hydrolysis and fermentation) or endogenously (GI digestion of dietary or endogenous proteins), but they need to survive GI conditions and to be absorbed, implying crossing the intestinal barrier, to exert their inhibitory potentials on circulating DPP-IV that would impact the most GLP-1 activity. Indeed, GI conditions may compromise their bioavailability and bioactivity. Thus, simulating *in vitro* GI digestion is a crucial preliminary step to predict the *in vivo* stability of peptides or protein hydrolyzates in proteolytic conditions. Three peptides were isolated from macroalga hydrolyzates (*Palmaria palmata*) Ile-leu-Ala-Pro, Leu-Leu-Ala-pro, and Met-Ala-Gly-Val-Asp-His-Ile and proved to keep their DPP-IV inhibitory properties after simulating gastric and intestinal digestion conditions (95). One fraction isolated from an α-lactalbumin hydrolyzate was not affected in terms of DPP-IV inhibitory properties after simulating GI digestion (1.20 ± 0.12 mg·mL⁻¹). Nevertheless, characterizing peptide sequences from various bioactive fractions (digested or not) by LC-MS-MS led to the conclusion that the DPP-IV inhibitory effect observed did not necessarily involve the same sequences before and after simulating GI digestion of the fractions (96). The action of GI enzymes can generate new sequences that might also reveal greater DPP-IV inhibitory properties than the native peptide. This was noticed for three peptides released from a cooked tuna juice hydrolyzate (*Thunnus tonggol*) obtained by enzymatic hydrolysis. Their DPP-IV inhibitory properties were enhanced after simulating GI digestion (97). Recently, a couple of studies have been investigating the potential bioactivity of endogenous peptides. Endogenous proteins represent a noticeable protein intake, and they are also degraded by GI digestion. Like dietary proteins, they can be regarded as a potential source of bioactive peptides. A human serum albumin hydrolyzate has exhibited

DPP-IV inhibitory effects that remained in enriched fractions and lysozyme GI digest of the same hydrolyzate (98). Two inhibitory peptides from endogenous proteins, predicted by *in silico* digestion, have confirmed *in vitro* their potentials: Met–Ile–Met from human serum albumin ($IC_{50} = 800.51 \pm 4.90 \mu\text{M}$) and Arg–Pro–Cys–Phe from endoribonuclease ($IC_{50} = 1,056.78 \pm 61.11 \mu\text{M}$). Although their IC_{50} values do not indicate a strong inhibitory potential compared to Ile–Pro–Ile, endogenous proteins are a complementary source of bioactive peptides (99).

Thus, dietary protein, protein hydrolyzate, or dietary peptide intake could be part of T2DM therapeutic approaches by specifically targeting DPP-IV activity. To date, few *in vivo* studies have confirmed DPP-IV inhibitory potentials measured *in vitro*. Studies in streptozotocin-induced obese, Zucker diabetic fatty rat, or lean rats have pointed out that protein hydrolyzate or peptide intake could improve blood glucose, circulating GLP-1 and insulin levels and also decrease plasma DPP-IV activity. This has been described with various hydrolyzates from zein (58), pork gelatin skin (100), salmon gelatin (59), and tilapia gelatin (101). The peptide Leu–Pro–Gln–Asp–Ile–Pro–Pro–Leu, a β -casein fragment isolated from Gouda cheese, exhibited a high DPP-IV inhibitory potential *in vitro* ($IC_{50} = 46 \mu\text{M}$) and significantly improved blood glucose in diabetic rats after an oral glucose tolerance test. However, the authors did not specify whether this effect was related to DPP-IV activity inhibition (102). Indeed, protein and protein hydrolyzate intake may also improve blood glucose in diabetic rats without reducing plasma DPP-IV activity. In diabetic rats, plasma DPP-IV activity remained higher than in control rats after a protein rich 6-week diet made of either casein or white egg hydrolyzate, although fasting blood glucose and circulating insulin levels were significantly improved (103).

BIOACTIVE PEPTIDES AND OPIOID RECEPTORS: INTESTINAL GLUCONEOGENESIS (IGN) AND PROTEIN-INDUCED SATIETY

Besides their interaction with gut hormones synthesis and secretion, food-derived peptides could interact with the peripheral opioid receptors and indirectly induce gluconeogenesis that participates in the maintenance of satiety and reduction of food intake. Peripheral opioid receptors are involved in gastric emptying inhibition and food intake-induced satiety by the release of endogenous opioid peptides that act in the CNS (104). Exogenous opioid peptides produced by the GI digestion of alimentary proteins could interact with these receptors and thus intervene in food intake regulation. Casein and soy protein ingestion induces food intake decrease mediated by two distinct signaling pathways, one involving CCK-1R receptors and the other, peripheral μ -opioid receptors (MOR). GI digestion seems to be the source of the release of peptides like β -casomorphin, derived from caseins and known for its opioid activities (17, 105). The name “nutropioids” has been coined for these opioid oligopeptides originating from the diet. Besides, it is known that products of alimentary protein digestion can act as antagonists of MOR present on afferent nerve endings in the intestinal mucosa

and portal vein. Detection of these oligopeptides is transmitted to the CNS and induces a decrease in food intake. This regulatory loop comes in complement to the action of the endogenous peptides released following food intake, like endorphins, and demonstrates the plurality of pathways engaged at the peripheral and central levels to promote satiety (106, 107). Mithieux et al. described a regulatory loop of food intake implicating portal vein MOR and IGN activated by alimentary protein GI digestion. This theory rests on the anorexigenic properties of glucose: the antagonistic action of oligopeptides in the portal vein MOR activates IGN *via* a gut–brain axis increasing glycemia that in turn activates hypothalamic regions involved in food intake regulation (108–113). However, only selected dipeptides have been tested so far in these studies to validate the portal vein MOR implication and no food-derived peptide motif has to date, been identified for its anorexigenic properties through this regulatory loop. In contrast, it is noteworthy that the vast majority of proteins investigated as a source of bioactive peptides, of very different animal and plant origins, have been found to produce opioid sequences when hydrolyzed/digested. These food-derived opioid peptides have not been systematically tested for their effect on opioid receptors, but agonistic activity seems to be preponderant, with only few and exclusively from milk products, opioid peptides with antagonist activity. However, it is striking again that all these food-derived opioid peptides have been shown to have a preference for MOR (114). Albeit controversial (115), particularly regarding the importance and relevance of the IGN (high-protein diet context) in comparison to hepatic gluconeogenesis production (116) and species discrepancies (117), this model of protein-induced satiety based on the portal vein MOR and IGN elegantly brings together two critical actors in the regulation of food intake, the opioid system, and glucose homeostasis. It reinforces the central role of the gut–brain axis in energy homeostasis and especially in food intake regulation and highlights the role of the process of digestion in producing food protein-derived bioactive peptides.

CONCLUSION

For decades, the process of GI digestion has been studied merely for its capacity to transform food into nutriments, the source of energy for our body. It is only recently that the GI tract has been considered a dynamic interface between the luminal environment and the internal environment. Interaction between nutriments and the intestinal barrier elicit the activation of multiple signaling pathways, including some involved in energy homeostasis regulation. With the exponential increase of people affected by diseases linked to the metabolic syndrome, alimentary proteins become the subject of increasing interest since they reduce food intake, induce satiety and increase energy expenditure. Yet, the underlying mechanisms are still not completely elucidated. The *in vitro* study of some mechanisms, notably the production and secretion of the GI hormones, highlighted the primary role of bioactive peptides originating from protein GI digestion. Regarding the existing links between these peptides and the regulation of intestinal hormones, some signaling pathways have been unveiled implicating a role for the GPCR family of receptors.

Thus, the presence of these receptors on the apical side of the EECs constitutes the first level of integration of the information on the luminal content. These receptors act as chemodetectors and initiate the translation of the detected information into a hormonal response. Hence, GPCRs attract particular attention as novel targets for obesity and type 2 diabetes treatments. With regards to the peptides, very few structural criteria are known to date to favor these receptors activation.

It is nowadays admitted that the GI tract has the capacity to release bioactive peptides that participate in the regulation of energy homeostasis, from ingested alimentary proteins. While the effects of these peptides confirming a decrease in food intake and an increase in satiety have been demonstrated *in vivo*, the correlation with an increase in intestinal hormone release or DPP-IV inhibition has not often been established. The presence of the peptides in the intestinal lumen and their potential crossing of the intestinal barrier could be the trigger of other food intake decreasing signaling pathways activation, like the indirect activation of IGN by the portal vein MOR antagonism, or the stimulation of not yet studied intestinal hormones release. Finally, *in vivo*

identification of the peptides produced during GI digestion and responsible for the described effects is still difficult to realize. Therefore, analytical strategies have been implemented *in vitro* in order to follow the release of peptides during GI digestion and meanwhile to reveal their bioactive potential.

AUTHOR CONTRIBUTIONS

JC and DD participated in all steps of preparation of this manuscript and contributed equally to this work. RR and PD participated in the editing of the manuscript and revised it critically. BC was awarded the funding and participated in the conception and in the editing of the manuscript and revised it critically.

FUNDING

This work was supported by the CPER “Albiotech” funding and a grant of the Nord Pas de Calais Region: “2nd appel à projet, Programme projets émergents.”

REFERENCES

- Cummings DE, Overduin J. Gastrointestinal regulation of food intake. *J Clin Invest* (2007) 117(1):13–23. doi:10.1172/JCI30227
- Sternini C, Anselmi L, Rozengurt E. Enteroendocrine cells: a site of ‘taste’ in gastrointestinal chemosensing. *Curr Opin Endocrinol Diabetes Obes* (2008) 15(1):73–8. doi:10.1097/MED.0b013e3282f43a73
- Morton GJ, Cummings DE, Baskin DG, Barsh GS, Schwartz MW. Central nervous system control of food intake and body weight. *Nature* (2006) 443(7109):289–95. doi:10.1038/nature05026
- Wren AM, Bloom SR. Gut hormones and appetite control. *Gastroenterology* (2007) 132(6):2116–30. doi:10.1053/j.gastro.2007.03.048
- Moran TH, Dailey MJ. Gut peptides: targets for antiobesity drug development? *Endocrinology* (2009) 150(6):2526–30. doi:10.1210/en.2009-0003
- Westerterp-Plantenga MS, Lemmens SG, Westerterp KR. Dietary protein – its role in satiety, energetics, weight loss and health. *Br J Nutr* (2012) 108(S2): S105–12. doi:10.1017/S0007114512002589
- Bensaid A, Tome D, Gietzen D, Even P, Morens C, Gausseres N, et al. Protein is more potent than carbohydrate for reducing appetite in rats. *Physiol Behav* (2002) 75(4):577–82. doi:10.1016/S0031-9384(02)00646-7
- Hall WL, Millward DJ, Long SJ, Morgan LM. Casein and whey exert different effects on plasma amino acid profiles, gastrointestinal hormone secretion and appetite. *Br J Nutr* (2003) 89(2):239–48. doi:10.1079/BJN2002760
- Westerterp-Plantenga MS. Protein intake and energy balance. *Regul Pept* (2008) 149(1–3):67–9. doi:10.1016/j.regpep.2007.08.026
- Layman DK, Boileau RA, Erickson DJ, Painter JE, Shiue H, Sather C, et al. A reduced ratio of dietary carbohydrate to protein improves body composition and blood lipid profiles during weight loss in adult women. *J Nutr* (2003) 133(2):411–7.
- Horner K, Drummond E, Brennan L. Bioavailability of milk protein-derived bioactive peptides: a glycaemic management perspective. *Nutr Res Rev* (2016) 29(1):91–101. doi:10.1017/S0954422416000032
- Shi G, Leray V, Scarpignato C, Bentoumiou N, Varannes S, Cherbut C, et al. Specific adaptation of gastric emptying to diets with differing protein content in the rat: is endogenous cholecystokinin implicated? *Gut* (1997) 41(5):612–8. doi:10.1136/gut.41.5.612
- Nishi T, Hara H, Tomita F. Soybean β -conglycinin peptone suppresses food intake and gastric emptying by increasing plasma cholecystokinin levels in rats. *J Nutr* (2003) 133(2):352–7.
- Liddle RA, Green GM, Conrad CK, Williams JA. Proteins but not amino acids, carbohydrates, or fats stimulate cholecystokinin secretion in the rat. *Am J Physiol* (1986) 251(2 Pt 1):G243–8.
- Brennan IM, Luscombe-Marsh ND, Seimon RV, Otto B, Horowitz M, Wishart JM, et al. Effects of fat, protein, and carbohydrate and protein load on appetite, plasma cholecystokinin, peptide YY, and ghrelin, and energy intake in lean and obese men. *Am J Physiol Gastrointest Liver Physiol* (2012) 303(1):G129–40. doi:10.1152/ajpgi.00478.2011
- Sharara A, Bouras EP, Misukonis M, Liddle RA. Evidence for indirect dietary regulation of cholecystokinin release in rats. *Am J Physiol* (1993) 265(1):G107–12.
- Pupovac J, Anderson GH. Dietary peptides induce satiety via cholecystokinin-A and peripheral opioid receptors in rats. *J Nutr* (2002) 132(9):2775–80.
- Nishi T, Hara H, Hira T, Tomita F. Dietary protein peptic hydrolysates stimulate cholecystokinin release via direct sensing by rat intestinal mucosal cells. *Exp Biol Med* (2001) 226(11):1031–6. doi:10.1177/153537020122601110
- Cudennec B, Ravallec-Plé R, Courois E, Foucheau-Peron M. Peptides from fish and crustacean by-products hydrolysates stimulate cholecystokinin release in STC-1 cells. *Food Chem* (2008) 111(4):970–5. doi:10.1016/j.foodchem.2008.05.016
- Cudennec B, Foucheau-Peron M, Ferry F, Duclos E, Ravallec R. In vitro and *in vivo* evidence for a satiating effect of fish protein hydrolysate obtained from blue whiting (*Micromesistius poutassou*) muscle. *J Funct Foods* (2012) 4(1):271–7. doi:10.1016/j.jff.2011.12.003
- Cordier-Bussat M, Bernard C, Haouche S, Roche C, Abello J, Chayvialle JA, et al. Peptones stimulate cholecystokinin secretion and gene transcription in the intestinal cell line STC-1. *Endocrinology* (1997) 138(3):1137–44. doi:10.1210/endo.138.3.5023
- Geraedts MC, Troost FJ, Fischer MA, Edens L, Saris WH. Direct induction of CCK and GLP-1 release from murine endocrine cells by intact dietary proteins. *Mol Nutr Food Res* (2011) 55(3):476–84. doi:10.1002/mnfr.201000142
- Nishi T, Hara H, Asano K, Tomita F. The soybean β -conglycinin β 51–63 fragment suppresses appetite by stimulating cholecystokinin release in rats. *J Nutr* (2003) 133(8):2537–42.
- Sufian MK, Hira T, Miyashita K, Nishi T, Asano K, Hara H. Pork peptone stimulates cholecystokinin secretion from enteroendocrine cells and suppresses appetite in rats. *Biosci Biotechnol Biochem* (2006) 70(8):1869–74. doi:10.1271/bbb.60046
- Wang Y, Prpic V, Green GM, Reeve JR Jr, Liddle RA. Luminal CCK-releasing factor stimulates CCK release from human intestinal endocrine and STC-1 cells. *Am J Physiol Gastrointest Liver Physiol* (2002) 282(1):G16–22.
- Spannagel AW, Green GM, Guan D, Liddle RA, Faull K, Reeve JR. Purification and characterization of a luminal cholecystokinin-releasing factor from rat intestinal secretion. *Proc Natl Acad Sci U S A* (1996) 93(9):4415–20. doi:10.1073/pnas.93.9.4415

27. Tarasova N, Spannagel AW, Green GM, Gomez G, Reed JT, Thompson JC, et al. Distribution and localization of a novel cholecystokinin-releasing factor in the rat gastrointestinal tract 1. *Endocrinology* (1997) 138(12):5550–4. doi:10.1210/endo.138.12.5554
28. Miyasaka K, Guan D, Liddle RA, Green GM. Feedback regulation by trypsin: evidence for intraluminal CCK-releasing peptide. *Am J Physiol* (1989) 257(2):G175–81.
29. Spannagel AW, Reeve JR Jr, Greeley GH Jr, Yanaihara N, Liddle RA, Green GM. Bioactivity of intraduodenally and intravenously infused fragments of luminal cholecystokinin releasing factor (LCRF). *Regul Pept* (1998) 73(3):161–4. doi:10.1016/S0167-0115(97)01074-4
30. Némoz-Gaillard E, Bernard C, Abello J, Cordier-Bussat M, Chayvialle JA, Cuber JC. Regulation of cholecystokinin secretion by peptones and peptidomimetic antibiotics in STC-1 cells. *Endocrinology* (1998) 139(3):932–8. doi:10.1210/en.139.3.932
31. Yoshida H, Tsunoda Y, Owyang C. Diazepam-binding inhibitor 33-50 elicits Ca²⁺ oscillation and CCK secretion in STC-1 cells via L-type Ca²⁺ channels. *Am J Physiol Gastrointest Liver Physiol* (1999) 276(3):G694–702.
32. Choi S, Lee M, Shiu AL, Yo SJ, Aponte GW. Identification of a protein hydrolysate responsive G protein-coupled receptor in enterocytes. *Am J Physiol Gastrointest Liver Physiol* (2007) 292(1):G98–112. doi:10.1152/ajpgi.00295.2006
33. Choi S, Lee M, Shiu AL, Yo SJ, Hallden G, Aponte GW. GPR93 activation by protein hydrolysate induces CCK transcription and secretion in STC-1 cells. *Am J Physiol Gastrointest Liver Physiol* (2007) 292(5):G1366–75. doi:10.1152/ajpgi.00516.2006
34. Conigrave AD, Hampson DR. Broad-spectrum amino acid-sensing class C G-protein coupled receptors: molecular mechanisms, physiological significance and options for drug development. *Pharmacol Ther* (2010) 127(3):252–60. doi:10.1016/j.pharmthera.2010.04.007
35. Conigrave A, Mun H-C, Brennan SC. Physiological significance of L-amino acid sensing by extracellular Ca²⁺-sensing receptors. *Biochem Soc Trans* (2007) 35(5):1195–8. doi:10.1042/BST0351195
36. Mangel AW, Prpic V, Wong H, Basavappa S, Hurst LJ, Scott L, et al. Phenylalanine-stimulated secretion of cholecystokinin is calcium dependent. *Am J Physiol* (1995) 268(1 Pt 1):G90–4.
37. Hira T, Nakajima S, Eto Y, Hara H. Calcium-sensing receptor mediates phenylalanine-induced cholecystokinin secretion in enteroendocrine STC-1 cells. *FEBS J* (2008) 275(18):4620–6. doi:10.1111/j.1742-4658.2008.06604.x
38. Nakajima S, Hira T, Eto Y, Asano K, Hara H. Soybean β51–63 peptide stimulates cholecystokinin secretion via a calcium-sensing receptor in enteroendocrine STC-1 cells. *Regul Pept* (2010) 159(1–3):148–55. doi:10.1016/j.regpep.2009.11.007
39. Nakajima S, Hira T, Hara H. Calcium-sensing receptor mediates dietary peptide-induced CCK secretion in enteroendocrine STC-1 cells. *Mol Nutr Food Res* (2012) 56(5):753–60. doi:10.1002/mnfr.201100666
40. Gevrey JC, Cordier-Bussat M, Némoz-Gaillard E, Chayvialle JA, Abello J. Co-requirement of cyclic AMP- and calcium-dependent protein kinases for transcriptional activation of cholecystokinin gene by protein hydrolysates. *J Biol Chem* (2002) 277(25):22407–13. doi:10.1074/jbc.M201624200
41. Saxena M, Williams S, Taskén K, Mustelin T. Crosstalk between cAMP-dependent kinase and MAP kinase through a protein tyrosine phosphatase. *Nat Cell Biol* (1999) 1(5):305–10. doi:10.1038/13024
42. Zanassi P, Paolillo M, Feliciello A, Avvedimento EV, Gallo V, Schinelli S. cAMP-dependent protein kinase induces cAMP-response element-binding protein phosphorylation via an intracellular calcium release/ERK-dependent pathway in striatal neurons. *J Biol Chem* (2001) 276(15):11487–95. doi:10.1074/jbc.M007631200
43. Alleaume C, Eychène A, Caigneaux E, Muller J-M, Philippe M. Vasoactive intestinal peptide stimulates proliferation in HT29 human colonic adenocarcinoma cells: concomitant activation of Ras/Rap1–B-Raf–ERK signalling pathway. *Neuropeptides* (2003) 37(2):98–104. doi:10.1016/S0143-4179(03)00020-9
44. Reidelberger RD, Heimann D, Kelsey L, Hulce M. Effects of peripheral CCK receptor blockade on feeding responses to duodenal nutrient infusions in rats. *Am J Physiol Regul Integr Comp Physiol* (2003) 284(2):R389–98. doi:10.1152/ajpregu.00529.2002
45. Raybould HE, Zittel TT, Holzer HH, Lloyd KK, Meyer JH. Gastroduodenal sensory mechanisms and CCK in inhibition of gastric emptying in response to a meal. *Dig Dis Sci* (1994) 39(12):41S–3S. doi:10.1007/BF02300368
46. Darcel NP, Liou AP, Tome D, Raybould HE. Activation of vagal afferents in the rat duodenum by protein digests requires PepT1. *J Nutr* (2005) 135(6):1491–5.
47. Liou AP, Chavez DI, Espero E, Hao S, Wank SA, Raybould HE. Protein hydrolysate-induced cholecystokinin secretion from enteroendocrine cells is indirectly mediated by the intestinal oligopeptide transporter PepT1. *Am J Physiol Gastrointest Liver Physiol* (2011) 300(5):G895–902. doi:10.1152/ajpgi.00521.2010
48. Matsumura K, Miki T, Jhomori T, Gonoi T, Seino S. Possible role of PEPT1 in gastrointestinal hormone secretion. *Biochem Biophys Res Commun* (2005) 336(4):1028–32. doi:10.1016/j.bbrc.2005.08.259
49. Staljanssens D, Van Camp J, Billiet A, De Meyer T, Al Shukor N, De Vos WH, et al. Screening of soy and milk protein hydrolysates for their ability to activate the CCK1 receptor. *Peptides* (2012) 34(1):226–31. doi:10.1016/j.peptides.2011.11.019
50. Foltz M, Ansems P, Schwarz J, Tasker MC, Lourbakos A, Gerhardt CC. Protein hydrolysates induce CCK release from enteroendocrine cells and act as partial agonists of the CCK1 receptor. *J Agric Food Chem* (2008) 56(3):837–43. doi:10.1021/jf072611h
51. Ripken D, Van der Wielen N, Van der Meulen J, Schuurman T, Witkamp R, Hendriks H, et al. Cholecystokinin regulates satiation independently of the abdominal vagal nerve in a pig model of total subdiaphragmatic vagotomy. *Physiol Behav* (2015) 139:167–76. doi:10.1016/j.physbeh.2014.11.031
52. Meek CL, Lewis HB, Reimann F, Gribble FM, Park AJ. The effect of bariatric surgery on gastrointestinal and pancreatic peptide hormones. *Peptides* (2016) 77:28–37. doi:10.1016/j.peptides.2015.08.013
53. Hutchison AT, Feinle-Bisset C, Fitzgerald PC, Standfield S, Horowitz M, Clifton PM, et al. Comparative effects of intraduodenal whey protein hydrolysate on antropyloroduodenal motility, gut hormones, glycemia, appetite, and energy intake in lean and obese men. *Am J Clin Nutr* (2015) 102(6):1323–31. doi:10.3945/ajcn.115.114538
54. Stringer DM, Taylor CG, Appah P, Blewett H, Zahradka P. Consumption of buckwheat modulates the post-prandial response of selected gastrointestinal satiety hormones in individuals with type 2 diabetes mellitus. *Metabolism* (2013) 62(7):1021–31. doi:10.1016/j.metabol.2013.01.021
55. Ma J, Stevens JE, Cukier K, Maddox AF, Wishart JM, Jones KL, et al. Effects of a protein preload on gastric emptying, glycemia, and gut hormones after a carbohydrate meal in diet-controlled type 2 diabetes. *Diabetes Care* (2009) 32(9):1600–2. doi:10.2337/dc09-0723
56. Lejeune MP, Westerterp KR, Adam TC, Luscombe-Marsh ND, Westerterp-Plantenga MS. Ghrelin and glucagon-like peptide 1 concentrations, 24-h satiety, and energy and substrate metabolism during a high-protein diet and measured in a respiration chamber. *Am J Clin Nutr* (2006) 83(1):89–94.
57. Diepvens K, Häberer D, Westerterp-Plantenga M. Different proteins and biopeptides differently affect satiety and anorexigenic/orexigenic hormones in healthy humans. *Int J Obes* (2008) 32(3):510–8. doi:10.1038/sj.ijo.0803758
58. Mochida T, Hira T, Hara H. The corn protein, zein hydrolysate, administered into the ileum attenuates hyperglycemia via its dual action on glucagon-like peptide-1 secretion and dipeptidyl peptidase-IV activity in rats. *Endocrinology* (2010) 151(7):3095–104. doi:10.1210/en.2009-1510
59. Hsieh C-H, Wang T-Y, Hung C-C, Chen M, Hsu K. Improvement of glycemic control in streptozotocin-induced diabetic rats by Atlantic salmon skin gelatin hydrolysate as the dipeptidyl-peptidase IV inhibitor. *Food Funct* (2015) 6(6):1887–92. doi:10.1039/c5fo00124b
60. Ishikawa Y, Hira T, Inoue D, Harada Y, Hashimoto H, Fujii M, et al. Rice protein hydrolysates stimulate GLP-1 secretion, reduce GLP-1 degradation, and lower the glycemic response in rats. *Food Funct* (2015) 6(8):2525–34. doi:10.1039/c4fo01054j
61. Power-Grant O, Bruen C, Brennan L, Giblin L, Jakeman P, Fitzgerald R. In vitro bioactive properties of intact and enzymatically hydrolysed whey protein: targeting the enteroinsular axis. *Food Funct* (2015) 6(3):972–80. doi:10.1039/c4fo00983e
62. Elliott RM, Morgan LM, Tredger JA, Deacon S, Wright J, Marks V. Glucagon-like peptide-1(7–36)amide and glucose-dependent insulinotropic polypeptide secretion in response to nutrient ingestion in man: acute post-prandial and 24-h secretion patterns. *J Endocrinol* (1993) 138(1):159–66. doi:10.1677/joe.0.1380159
63. Klaauw AA, Keogh JM, Henning E, Trowse VM, Dhillo WS, Ghatei MA, et al. High protein intake stimulates postprandial GLP1 and PYY release. *Obesity* (2013) 21(8):1602–7. doi:10.1002/oby.20154

64. Dougkas A, Östman E. Protein-enriched liquid preloads varying in macronutrient content modulate appetite and appetite-regulating hormones in healthy adults. *J Nutr* (2016) 146(3):637–45. doi:10.3945/jn.115.217224
65. Herrmann C, Göke R, Richter G, Fehmann H-C, Arnold R, Göke B. Glucagon-like peptide-1 and glucose-dependent insulin-releasing polypeptide plasma levels in response to nutrients. *Digestion* (1995) 56(2):117–26. doi:10.1159/000201231
66. Hira T, Mochida T, Miyashita K, Hara H. GLP-1 secretion is enhanced directly in the ileum but indirectly in the duodenum by a newly identified potent stimulator, zein hydrolysate, in rats. *Am J Physiol Gastrointest Liver Physiol* (2009) 297(4):G663–71. doi:10.1152/ajpgi.90635.2008
67. Cordier-Bussat M, Bernard C, Levenez F, Klages N, Laser-Ritz B, Philippe J, et al. Peptones stimulate both the secretion of the incretin hormone glucagon-like peptide 1 and the transcription of the proglucagon gene. *Diabetes* (1998) 47(7):1038–45. doi:10.2337/diabetes.47.7.1038
68. Reimer RA, Darimont C, Gremlich S, Nicolas-Metral V, Ruegg UT, Mace K. A human cellular model for studying the regulation of glucagon-like peptide-1 secretion. *Endocrinology* (2001) 142(10):4522–8. doi:10.1210/endo.142.10.8415
69. Reimann F, Williams L, da Silva Xavier G, Rutter G, Gribble F. Glutamine potently stimulates glucagon-like peptide-1 secretion from GLUTag cells. *Diabetologia* (2004) 47(9):1592–601. doi:10.1007/s00125-004-1498-0
70. Tolhurst G, Zheng Y, Parker HE, Habib AM, Reimann F, Gribble FM. Glutamine triggers and potentiates glucagon-like peptide-1 secretion by raising cytosolic Ca²⁺ and cAMP. *Endocrinology* (2011) 152(2):405–13. doi:10.1210/en.2010-0956
71. Meek CL, Lewis HB, Vergese B, Park A, Reimann F, Gribble F. The effect of encapsulated glutamine on gut peptide secretion in human volunteers. *Peptides* (2016) 77:38–46. doi:10.1016/j.peptides.2015.10.008
72. Mace OJ, Schindler M, Patel S. The regulation of K- and L-cell activity by GLUT2 and the calcium-sensing receptor CasR in rat small intestine. *J Physiol* (2012) 590(12):2917–36. doi:10.1113/jphysiol.2011.223800
73. Oya M, Kitaguchi T, Pais R, Reimann F, Gribble F, Tsuboi T. The G protein-coupled receptor family C group 6 subtype A (GPRC6A) receptor is involved in amino acid-induced glucagon-like peptide-1 secretion from GLUTag cells. *J Biol Chem* (2013) 288(7):4513–21. doi:10.1074/jbc.M112.402677
74. Le Nevé B, Daniel H. Selected tetrapeptides lead to a GLP-1 release from the human enteroendocrine cell line NCI-H716. *Regul Pept* (2011) 167(1):14–20. doi:10.1016/j.regpep.2010.10.010
75. Diakogiannaki E, Pais R, Tolhurst G, Parker HE, Horscroft J, Rauscher B, et al. Oligopeptides stimulate glucagon-like peptide-1 secretion in mice through proton-coupled uptake and the calcium-sensing receptor. *Diabetologia* (2013) 56(12):2688–96. doi:10.1007/s00125-013-3037-3
76. Pais R, Gribble FM, Reimann F. Signalling pathways involved in the detection of peptones by murine small intestinal enteroendocrine L-cells. *Peptides* (2016) 77:9–15. doi:10.1016/j.peptides.2015.07.019
77. Reimer RA. Meat hydrolysate and essential amino acid-induced glucagon-like peptide-1 secretion, in the human NCI-H716 enteroendocrine cell line, is regulated by extracellular signal-regulated kinase1/2 and p38 mitogen-activated protein kinases. *J Endocrinol* (2006) 191(1):159–70. doi:10.1677/joe.1.06557
78. Caron J, Domenger D, Belguesmia Y, Kouach M, Lesage J, Goossens J-F, et al. Protein digestion and energy homeostasis: how generated peptides may impact intestinal hormones? *Food Res Intern* (2016) 88(Pt B):310–8. doi:10.1016/j.foodres.2015.12.018
79. Gevrey JC, Malapel M, Philippe J, Mithieux G, Chayvialle JA, Abello J, et al. Protein hydrolysates stimulate proglucagon gene transcription in intestinal endocrine cells via two elements related to cyclic AMP response element. *Diabetologia* (2004) 47(5):926–36. doi:10.1007/s00125-004-1380-0
80. Caron J, Cudennec B, Domenger D, Belguesmia Y, Flahaut C, Kouach M, et al. Simulated GI digestion of dietary protein: release of new bioactive peptides involved in gut hormone secretion. *Food Res Intern* (2016) 89:382–90. doi:10.1016/j.foodres.2016.08.033
81. Jao C-L, Hung C-C, Tung Y-S, Lin P-Y, Chen M-C, Hsu K-C. The development of bioactive peptides from dietary proteins as a dipeptidyl peptidase IV inhibitor for the management of type 2 diabetes. *Biomedicine* (2015) 5(3):1–7. doi:10.7603/s40681-015-0014-9
82. Drucker DJ, Nauck MA. The incretin system: glucagon-like peptide-1 receptor agonists and dipeptidyl peptidase-4 inhibitors in type 2 diabetes. *Lancet* (2006) 368(9548):1696–705. doi:10.1016/S0140-6736(06)69705-5
83. Mulvihill EE, Drucker DJ. Pharmacology, physiology, and mechanisms of action of dipeptidyl peptidase-4 inhibitors. *Endocr Rev* (2014) 35(6):992–1019. doi:10.1210/er.2014-1035
84. Godinho R, Mega C, Teixeira-de-Lemos E, Carvalho E, Teixeira F, Fernandes R, et al. The place of dipeptidyl peptidase-4 inhibitors in type 2 diabetes therapeutics: a “me too” or “the special one” Antidiabetic class? *J Diabetes Res* (2015) 2015:28. doi:10.1155/2015/806979
85. Lacroix IME, Li-Chan ECY. Dipeptidyl peptidase-IV inhibitory activity of dairy protein hydrolysates. *Int Dairy J* (2012) 25(2):97–102. doi:10.1016/j.idairyj.2012.01.003
86. Kopf-Bolanz KA, Schwander F, Gijs M, Vergères G, Portmann R, Egger L. Impact of milk processing on the generation of peptides during digestion. *Int Dairy J* (2014) 35(2):130–8. doi:10.1016/j.idairyj.2013.10.012
87. Guo L, Harnedy PA, Zhang L, Li B, Zhang Z, Hou H, et al. In vitro assessment of the multifunctional bioactive potential of Alaska pollock skin collagen following simulated gastrointestinal digestion. *J Sci Food Agric* (2015) 95(7):1514–20. doi:10.1002/jsfa.6854
88. Li-Chan EC, Hunag S-L, Jao C-L, Ho K-P, Hsu K-C. Peptides derived from Atlantic salmon skin gelatin as dipeptidyl-peptidase IV inhibitors. *J Agric Food Chem* (2012) 60(4):973–8. doi:10.1021/jf204720q
89. Velarde-Salcedo AJ, Barrera-Pacheco A, Lara-Gonzalez S, Montero-Morán GM, Díaz-Gois A, de Mejia EG, et al. In vitro inhibition of dipeptidyl peptidase IV by peptides derived from the hydrolysis of amaranth (*Amaranthus hypochondriacus* L.) proteins. *Food Chem* (2013) 136(2):758–64. doi:10.1016/j.foodchem.2012.08.032
90. De Souza Rocha T, Hernandez LMR, Chang YK, de Mejia EG. Impact of germination and enzymatic hydrolysis of cowpea bean (*Vigna unguiculata*) on the generation of peptides capable of inhibiting dipeptidyl peptidase IV. *Food Res Intern* (2014) 64:799–809. doi:10.1016/j.foodres.2014.08.016
91. Cudennec B, Balti R, Ravallec R, Caron J, Bougatef A, Dhuister P, et al. In vitro evidence for gut hormone stimulation release and dipeptidyl-peptidase IV inhibitory activity of protein hydrolysate obtained from cuttlefish (*Sepia officinalis*) viscera. *Food Res Intern* (2015) 78:238–45. doi:10.1016/j.foodres.2015.10.003
92. Nonogierma A, FitzGerald R. Investigation of the potential of hemp, pea, rice and soy protein hydrolysates as a source of dipeptidyl peptidase IV (DPP-IV) inhibitory peptides. *Food Dig Res Curr Opin* (2015) 6:19–29. doi:10.1007/s13228-015-0039-2
93. Nonogierma AB, FitzGerald RJ. Dipeptidyl peptidase IV inhibitory properties of a whey protein hydrolysate: influence of fractionation, stability to simulated gastrointestinal digestion and food-drug interaction. *Int Dairy J* (2013) 32(1):33–9. doi:10.1016/j.idairyj.2013.03.005
94. Jin Y, Yu Y, Qi Y, Wang F, Yan J, Zou H. Peptide profiling and the bioactivity character of yogurt in the simulated gastrointestinal digestion. *J Proteomics* (2016) 141:24–46. doi:10.1016/j.jprot.2016.04.010
95. Harnedy PA, O'Keefe MB, FitzGerald RJ. Purification and identification of dipeptidyl peptidase (DPP) IV inhibitory peptides from the macroalga *Palmaria palmata*. *Food Chem* (2015) 172(0):400–6. doi:10.1016/j.foodchem.2014.09.083
96. Nonogierma AB, FitzGerald RJ. Prospects for the management of type 2 diabetes using food protein-derived peptides with dipeptidyl peptidase IV (DPP-IV) inhibitory activity. *Curr Opin Food Sci* (2016) 8:19–24. doi:10.1016/j.cofs.2016.01.007
97. Huang S-L, Jao C-L, Ho K-P, Hsu K-C. Dipeptidyl-peptidase IV inhibitory activity of peptides derived from tuna cooking juice hydrolysates. *Peptides* (2012) 35(1):114–21. doi:10.1016/j.peptides.2012.03.006
98. Dave LA, Hayes M, Mora L, Montoya CA, Moughan PJ, Rutherford SM. Gastrointestinal endogenous protein-derived bioactive peptides: an in vitro study of their gut modulatory potential. *Int J Mol Sci* (2016) 17(4):482. doi:10.3390/ijms17040482
99. Dave LA, Hayes M, Moughan PJ, Rutherford SM. Novel dipeptidyl peptidase IV inhibitory and antioxidant peptides derived from human gastrointestinal endogenous proteins. *Int J Pept Res Ther* (2016) 22(3):355–69. doi:10.1007/s10989-016-9515-y
100. Huang S-L, Hung C-C, Jao C-L, Tung Y-S, Hsu K-C. Porcine skin gelatin hydrolysate as a dipeptidyl peptidase IV inhibitor improves glycemic control in streptozotocin-induced diabetic rats. *J Funct Foods* (2014) 11(0):235–42. doi:10.1016/j.jff.2014.09.010

101. Wang Y, Landheer S, van Gilst WH, van Amerongen A, Hammes H-P, Henning RH, et al. Attenuation of renovascular damage in Zucker diabetic fatty rat by NWT-03, an egg protein hydrolysate with ACE-and DPP4-inhibitory Activity. *PLoS One* (2012) 7(10):e46781. doi:10.1371/journal.pone.0046781
102. Uenishi H, Kabuki T, Seto Y, Serizawa A, Nakajima H. Isolation and identification of casein-derived dipeptidyl-peptidase 4 (DPP-4)-inhibitory peptide LPQNIPPL from gouda-type cheese and its effect on plasma glucose in rats. *Int Dairy J* (2012) 22(1):24–30. doi:10.1016/j.idairyj.2011.08.002
103. Ochiai M, Kuroda T, Matsuo T. Increased muscular triglyceride content and hyperglycemia in Goto-Kakizaki rat are decreased by egg white hydrolysate. *Int J Food Sci Nutr* (2014) 65(4):495–501. doi:10.3109/09637486.2013.879288
104. Janssen P, Pottel H, Vos R, Tack J. Endogenously released opioids mediate meal-induced gastric relaxation via peripheral mu-opioid receptors. *Aliment Pharmacol Ther* (2011) 33(5):607–14. doi:10.1111/j.1365-2036.2010.04557.x
105. Froetschel M, Azain M, Edwards G, Barb C, Amos H. Opioid and cholecystokinin antagonists alleviate gastric inhibition of food intake by premeal loads of casein in meal-fed rats. *J Nutr* (2001) 131(12):3270–6.
106. Duraffourd C, De Vadder F, Goncalves D, Delaere F, Penhoat A, Brusset B, et al. Mu-opioid receptors and dietary protein stimulate a gut-brain neural circuitry limiting food intake. *Cell* (2012) 150(2):377–88. doi:10.1016/j.cell.2012.05.039
107. Pfleiderer PT, Schriever SC, Tschöp MH. Nutropioids, hedonism in the gut? *Cell Metab* (2012) 16(2):137–9. doi:10.1016/j.cmet.2012.07.011
108. Mithieux G, Misery P, Magnan C, Pillot B, Gautier-Stein A, Bernard C, et al. Portal sensing of intestinal gluconeogenesis is a mechanistic link in the diminution of food intake induced by diet protein. *Cell Metab* (2005) 2(5):321–9. doi:10.1016/j.cmet.2005.09.010
109. De Vadder F, Gautier-Stein A, Mithieux G. [Opioid receptors associated with portal vein regulate a gut-brain neural circuitry limiting food intake]. *Med Sci (Paris)* (2013) 29(1):31–3. doi:10.1051/medsci/2013291010
110. De Vadder F, Gautier-Stein A, Mithieux G. Satiety and the role of μ-opioid receptors in the portal vein. *Curr Opin Pharmacol* (2013) 13(6):959–63. doi:10.1016/j.coph.2013.09.003
111. Mithieux G. Crosstalk between gastrointestinal neurons and the brain in the control of food intake. *Best Pract Res Clin Endocrinol Metab* (2014) 28(5):739–44. doi:10.1016/j.beem.2014.03.004
112. Mithieux G. Nutropioids regulate gut-brain circuitry controlling food intake. In: Delhanty PJD, van der Lely AJ, editors. *How Gut and Brain Control Metabolism*. Karger Publishers (2014). p. 155–62.
113. Mithieux G. Metabolic effects of portal vein sensing. *Diabetes Obes Metab* (2014) 16(S1):56–60. doi:10.1111/dom.12338
114. Teschemacher H. Opioid receptor ligands derived from food proteins. *Curr Pharm Des* (2003) 9(16):1331–44. doi:10.2174/1381612033454856
115. Westerterp-Plantenga M, Luscombe-Marsh N, Lejeune M, Diepvens K, Nieuwenhuizen A, Engelen M, et al. Dietary protein, metabolism, and body-weight regulation: dose-response effects. *Int J Obes* (2006) 30:S16–23. doi:10.1038/sj.ijo.0803487
116. Watford M. Is the small intestine a gluconeogenic organ? *Nutr Rev* (2005) 63(10):356–60. doi:10.1111/j.1753-4887.2005.tb00114.x
117. L'Heureux-Bouron D, Tomé D, Rampil O, Even PC, Larue-Achagiotis C, Fromentin G. Total subdiaphragmatic vagotomy does not suppress high protein diet-induced food intake depression in rats. *J Nutr* (2003) 133(8):2639–42.

Conflict of Interest Statement: The authors declare that the research was conducted in the absence of any commercial or financial relationships that could be construed as a potential conflict of interest.

Copyright © 2017 Caron, Domenger, Dhulster, Ravallec and Cudennec. This is an open-access article distributed under the terms of the Creative Commons Attribution License (CC BY). The use, distribution or reproduction in other forums is permitted, provided the original author(s) or licensor are credited and that the original publication in this journal is cited, in accordance with accepted academic practice. No use, distribution or reproduction is permitted which does not comply with these terms.



Loss of Vagal Sensitivity to Cholecystokinin in Rats Born with Intrauterine Growth Retardation and Consequence on Food Intake

Marième Ndjim, Camille Poinsignon, Patricia Parnet and Gwenola Le Dréan*

UMR 1280 PHAN, INRA, Université de Nantes, Institut des Maladies de l'Appareil Digestif (IMAD), Centre de Recherche en Nutrition Humaine Ouest (CRNH Ouest), Nantes, France

Perinatal malnutrition is associated with low birth weight and an increased risk of developing metabolic syndrome in adulthood. Modification of food intake (FI) regulation was observed in adult rats born with intrauterine growth retardation induced by maternal dietary protein restriction during gestation and maintained restricted until weaning. Gastrointestinal peptides and particularly cholecystokinin (CCK) play a major role in short-term regulation of FI by relaying digestive signals to the hindbrain via the vagal afferent nerve (VAN). We hypothesized that vagal sensitivity to CCK could be affected in rats suffering from undernutrition [low protein (LP)] during fetal and postnatal life, leading to an altered gut-brain communication and impacting satiation. Our aim was to study short-term FI along with signals of appetite and satiation in adult LP rats compared to control rats. The dose-response to CCK injection was investigated on FI as well as the associated signaling pathways activated in nodose ganglia. We showed that LP rats have a reduced first-meal satiety ratio after a fasting period associated to a higher postprandial plasmatic CCK release, a reduced sensitivity to CCK when injected at low concentration and a reduced presence of CCK-1 receptor in nodose ganglia. Accordingly, the lower basal and CCK-induced phosphorylation of calcium/calmodulin-dependent protein kinase in nodose ganglia of LP rats could reflect an under-expressed vanilloid family of transient receptor potential cation channels on VAN. Altogether, the present data demonstrated a reduced vagal sensitivity to CCK in LP rats at adulthood, which could contribute to deregulation of FI reported in this model.

OPEN ACCESS

Edited by:

Hubert Vaudry,
University of Rouen, France

Reviewed by:

Miriam Goebel-Stengel,
HELIOS Klinikum Zerbst, Germany
Qingchun Tong,
University of Texas Health Science Center at Houston, USA

*Correspondence:

Gwenola Le Dréan
gwenola.ledrean@univ-nantes.fr

Specialty section:

This article was submitted
to Neuroendocrine Science,
a section of the journal
Frontiers in Endocrinology

Received: 10 January 2017

Accepted: 23 March 2017

Published: 10 April 2017

Citation:

Ndjim M, Poinsignon C, Parnet P and Le Dréan G (2017) Loss of Vagal Sensitivity to Cholecystokinin in Rats Born with Intrauterine Growth Retardation and Consequence on Food Intake. *Front. Endocrinol.* 8:65.
doi: 10.3389/fendo.2017.00065

INTRODUCTION

Metabolic pathologies such as obesity and type 2 diabetes are a worldwide public health problem especially in Western countries. Although life style, decreased physical activity and nutritional transition are the main causes of predisposition to obesity, a large body of epidemiological studies linked a low birth weight, consequence of intrauterine growth retardation (IUGR), to a higher

Abbreviations: BW, bodyweight; CART, cocaine amphetamine-regulated peptide; CaMKII, calcium/calmodulin-dependent protein kinase; CCK, cholecystokinin; CCK-1R, CCK-1 receptor; ERK, extracellular signal-regulated kinase; FI, food intake; GIP, glucose-dependent insulinotropic peptide; I.P., intraperitoneal; IUGR, intrauterine growth retardation; LP, low protein; MCH, melanin-concentrating hormone; NPY, neuropeptide Y; NTS, nucleus of the solitary tract; PYY, peptide YY; TRPV, vanilloid family of transient receptor potential; VAN, vagal afferent nerve; Y2-R, Y2 receptor.

risk of metabolic pathologies at adulthood. It is indeed well documented that low birth-weight babies present a higher susceptibility to develop obesity, insulin resistance, cardiovascular diseases, and type 2 diabetes later in life (1–3). More generally the metabolic programming concept proposes that a deleterious nutritional environment inflicted during fetal and early postnatal life could impact long-term health (4).

Animal studies have demonstrated that perinatal undernutrition may lead to a programmed hyperphagia that in the long term led to adult obesity (5). Previous studies in our laboratory demonstrated that low-protein (LP) rats eat more of a regular chow diet from weaning to 2-month old (6, 7). At adulthood despite a higher speed of ingestion (6, 8), a delay in appearance of satiety (satiation) is still observed with more food consumed during the first meal (7). LP rats have also a greater appetite for high-energy diet at adulthood (8) and a preference for high-fat food in the offspring of undernourished dams has also been reported (9), which could contribute to an increase of the body weight during adulthood and later on to obesity.

Food intake (FI) is a highly integrated behavior that relies on complex interactions between neuronal populations located in hypothalamic nuclei, brainstem, and cerebral nuclei implicated in hedonism, motivation, and activation of the peripheral autonomous system. In the central nervous system, the arcuate nucleus contains two well-characterized neuronal populations that act with opposite effects on feeding. Anorexigenic proopiomelanocortin neurons synthesize α -melanocyte-stimulating hormone and cocaine and amphetamine-regulated peptide (CART) whereas orexigenic neurons express neuropeptide Y (NPY) and agouti-related protein (10).

Animal studies have shown that altered maternal nutrition disturbs this hypothalamic system in offspring in favor of orexigenic activity predisposing to hyperphagia (6, 11). Long-term mechanisms of FI regulation by peripheral signaling (leptin, insulin) that monitor energy stores and availability to maintain homeostasis are particularly sensitive to perinatal nutrition. In LP rats, impaired leptin and insulin signaling in arcuate nucleus has been demonstrated to contribute to hyperphagia (12). By contrast, the short-term mechanisms of FI, which regulate on one hand anticipated appetite through ghrelin action and on the other hand meal size and the inter-meal time through peptides from the digestive tract have been poorly studied in maternal food-deprived offspring.

Short-term regulation of FI is controlled by the integration of digestive signals by the vagus nerve into the nucleus of the solitary tract (NTS) in the hindbrain that initiates satiation by a vago-vagal reflex (13). Among these signals, gastrointestinal peptides and mainly cholecystokinin (CCK) are key regulator of short-term FI (14). Vagal afferent nerves (VANs) are primary target of CCK and it is now well demonstrated that they represent a major site for integration of peripheral signals controlling FI (15). Indeed, CCK-1 receptors (CCK-1R) are expressed in nodose ganglia and CCK release after a meal stimulates expression of Y2 receptor (Y2-R), which responds to the anorexigenic gut peptide YY (PYY) and the release of CART in VAN while expression of the orexigenic peptide melanin-concentrating hormone (MCH) is suppressed. By contrast, during fasting, when plasma CCK concentration is low, MCH receptor expression increases while Y2-R and CART expression is reduced (16). As a gatekeeper, CCK

operates this vagal neurochemical phenotype switch according to the energy state (14). Interestingly, this normal switching between feeding and fasting states is blunted in diet-induced obesity rats as demonstrated by a loss of vagal sensitivity to leptin (17), which is known to act synergistically with CCK on VAN to potentiate the satiety effect of CCK (18).

Cholecystokinin suppression of FI involves numerous signaling pathways. In NTS neurons, CCK activity involves extracellular signal-regulated kinase (ERK) signaling cascade (19–21). In nodose neurons, CCK induces an increase in intracellular calcium mediated by members of the vanilloid family of transient receptor potential (TRPV)2–5 cation channels (22). Transient calcium signal is converted by calcium/calmodulin-dependent protein kinase (CaMKII), which autophosphorylates and functions as an intracellular signaling element. Prolonged phosphorylation of CaMKII reflects cellular activation (23).

We hypothesized that in LP rats, alteration of short-term FI and particularly satiation could be due to a loss of vagal sensitivity to CCK and/or an alteration of the vagal phenotype leading to a compromised integration of short-term satiety signals. Therefore, the aim of the present study was to investigate the reactivity to CCK in the adult offspring of dams fed a control or a LP diet during lactation and gestation. First-meal pattern following fasting was studied in physiological cages and plasma concentrations of various gastrointestinal peptides were measured in pre- and postprandial period. A dose-response to intraperitoneal (i.p.) CCK agonist (CCK-8S) injection was performed to quantify CCK sensitivity by measuring FI. Neurochemical vagal phenotype was determined in fasting/feeding states and vagal activation following CCK injection was analyzed by measuring phosphorylation of CaMKII and ERK in nodose ganglia.

ANIMALS AND METHODS

Animals

Pregnant females (gestation day 1) were obtained from Janvier (Le Genest Saint Isle, France), housed individually under standard laboratory conditions with free access to either a control (20% w/w protein, $n = 8$) or an isocaloric LP diet (8% protein, $n = 8$) through gestation and lactation. Both diets were purchased from AB diets (Woerden, The Netherlands) and composition is provided in Table S1 in Supplementary Material. At delivery, litter size was adjusted to eight male pups per dam. Pups were pooled and randomly attributed to foster mothers to create two experimental groups. Pups born from control dams were adopted by foster control ones (control, $n = 24$) and pups born from LP dams were attributed to foster LP dams (LP, $n = 24$). Control and LP offspring were weaned at 21 days of age and received a standard laboratory chow (A04, Safe, Augy, France) until adulthood. As previously described in this model (6, 24), birth weight of LP rats was 7–9% lower than control birth weight and this difference persisted until adulthood (130–160 days).

First-Meal Pattern Analysis

At 160 days of age, rats (8–12 animals/group) were individually housed ($22 \pm 2^\circ\text{C}$, 12:12-h light/dark cycle, lights on at 7:30)

for 3 days in plexiglas Phecomb cages (Bioseb, Vitrol, France) equipped to monitor meal pattern by continuous and automatic weighing of food. Phecomb system weights the food tray for each second. It allows precisely quantifying the food consumption and identifying feeding events. Artifacts as large vibrations when the rat enters in contact with the tray but without eating are taken into account by filters on the hardware and the software (Phecomb system monitoring software Compulse). A percentage of reliability of the quality signal was calculated by the software and only experiments with a percentage >80% have been used. A meal was defined with a minimal size of 0.5 g and a minimum inter-meal interval of 20 min. A meal is composed of several bouts. Meal parameters extracted from Compulse software included latency to eat, meal size, duration of the meal, inter-meal interval, and satiety ratio. After 48 h of fasting and 24 h of acclimatization to the cage, data were recorded from the beginning of the second day (8:00 a.m.) each 5 s over a 24-h period. This prolonged caloric restriction of 48 h was chosen on the basis of previous reports showing that 24–48 h duration of fasting triggers VAN to switch from anorectic to orexigenic phenotype (16, 25, 26). Other previous studies used this duration of fasting to promote feeding in adult rats weighting more than 500 g (6, 7).

Fasting-Feeding Experiment

Control ($n = 16$) and LP rats ($n = 16$) were fasted for 48 h (water *ad libitum*) and then divided into two subgroups: one group not refed and the second group refed during 2 h. Rats were killed by CO₂ inhalation and cervical dislocation. Stomach, duodenum, ileum, and nodose ganglia were rapidly dissected and collected for further analysis. Portal blood sample was collected in EDTA-containing tubes (Coveto, Montaigu, France). To preserve active form of gastrointestinal peptides, portal blood (200 µL) was collected in less than 30 s and directly flushed within EDTA tubes containing a mix of protease inhibitors including dipeptidyl peptidase IV inhibitor (diprotin A 100 µM, Sigma, Saint Louis, MO, USA), serine protease inhibitors (aprotinin, approx. 400 TIU/L, Sigma), and protease cocktail inhibitors (diluted 1/100, Sigma). After centrifugation, plasma (50 µL) was then aliquoted in microtube containing the same mix of protease inhibitors and immediately frozen at -80°C.

Plasma Gastrointestinal Peptides

Plasma concentration of rat non-sulfated CCK-8 (CCK-8NS) and desacylated ghrelin was analyzed by ELISA (EIA kit, Phoenix France, Strasbourg and SpiBio, Montigny le Bretonneux, France, respectively). Plasma total glucose-dependent insulinotropic peptide (GIP) and total PYY were assayed by Milliplex mag (Rat metabolic magnetic bead panel kit, Millipore, MA, USA).

Kinetics of CCK Release

Rats ($n = 9$ –12 animals/group) were fasted for 15 h and refed (chow) at the beginning of the dark phase. This duration of fasting was chosen to induce hunger in adult rats while limiting leptin deficiency that attenuated response to meal-related satiety signals (27). Their FI was measured by food tray weighing at 60, 90, and 150 min post-refeeding. Concomitantly, blood was collected from

the tail vein in EDTA-containing tubes (Microvette CB300 EDTA 3K, Sarstedt, Marnay, France) at 0 (15 min before refeeding), 15, 30, 60, 90, and 150 min after the beginning of the meal.

Sensitivity to CCK

Rats were deprived of food during 15 h and were intraperitoneally injected with either sterile NaCl 0.9% (saline) or CCK octapeptide, sulfated (CCK-8S, Bachem, Germany) just before light off and refeeding. FI and spillage were weighed every 30 min during 90 min. The satiating effect of CCK-8S was tested on distinct animals, for three doses [0.25, 2.5, and 7.5 nmol/kg of bodyweight (BW)] vs vehicle (saline) on consecutive days. It means that each rat received one of the treatment on a given test day followed by a period of 3–5 days of wash out and resting between each injection. Therefore, the whole experiment extended over 3 weeks. Doses of CCK were chosen on the basis of previous published data. The low dose (0.25 nmol/kg BW) reduces 1-h FI by 25% in standard fed rats (28). The 10-fold higher dose (2.5 nmol/kg BW) is necessary to induce FI reduction in diet-induced obesity rats (29) and the higher dose (7.5 nmol/kg BW) is used to induce anorectic effect in MC4R^{-/-} obese rats (30).

CCK-Vagal Activation

Rats were fasted for 15 h and then received an intraperitoneal (i.p.) injection with either CCK-8S (0.25 nmol/kg BW) or saline 5 min before refeeding and light off. Twenty minutes after injections, rats were killed by CO₂ inhalation followed by cervical dislocation and nodose ganglia were rapidly collected for Western blot analysis.

Western Blot Analysis

Nodose ganglia were homogenized at 4°C in RIPA lysis and extraction buffer as previously described (31). Protein concentration was determined using the Bio-Rad protein assay (Bio-Rad, Marnes la Coquette, France). Fifteen micrograms of protein was solubilized in electrophoresis sample buffer, loaded in ready-to-use (4–15%) polyacrylamide gels (Mini-protean TGX, Bio-Rad) and transferred onto Trans-Blot Turbo membrane (Bio-Rad). Protein was probed with anti-pCaMKII mouse polyclonal antibody (diluted 1/2,000, pT286, Thermo Scientific) and anti-CaMKII rabbit monoclonal antibody (diluted 1/1,000, Abcam, France). Following de-hybridization, membrane was probed with rabbit polyclonal anti-pERK and total ERK antibodies (diluted 1/1,000, Abcam). Immunoreactive bands were visualized with DyLight™680- and 800-conjugated antibodies, respectively (KPL, Eurobio, France). Band intensities were quantified by infrared scanning densitometry (Odyssey Imaging Systems, LI-COR, Germany). Data are expressed as the ratio of phosphorylated protein relative to total protein. Protein load was controlled with anti-actin mouse monoclonal antibody (diluted 1/2,000, Sigma).

Immunohistochemistry

Cryostat sections (7 µm) of fixed nodose ganglia in 4% paraformaldehyde were mounted on SuperFrost Plus Gold slides (Thermo Scientific; Braunschweig, Germany). Sections were stained with a rabbit polyclonal antibody raised against CCK-1R diluted at 1/200 (Santa Cruz Biotechnology, CA, USA). The secondary antibody

used at appropriate dilution (1/1,000) was a goat biotinylated anti-rabbit polyclonal antibody (Vector Laboratories, Clinisciences, Nanterre, France) followed by Alexa Fluor® 488-conjugated streptavidin antibody (Molecular Probes, Life Technologies). Nuclei were counterstained with DAPI. Tissues sections were mounted in Prolong Gold antifading medium (Molecular Probes, Thermo Scientific, Courtaboeuf, France). Three to five sections of nodose ganglia per rat were analyzed by fluorescence microscopy (Zeiss Axiovert 200M, Carl Zeiss, France). Fluorescence was quantified on image mosaic representing the total surface of each longitudinal nodose ganglia section using Volocity software (Volocity 6.2.1, Perkin Elmer, France).

Real-time Quantitative Polymerase Chain Reaction (RT-qPCR)

Total RNA was isolated with TRIzol reagent (Invitrogen, Life Technologies) and treated for 45 min at 37°C with RQ1 DNase (Promega, Charbonnières-Les-Bains, France). One microgram RNA was reverse-transcribed using Superscript III Reverse Transcriptase (Invitrogen). Five microliters of a 1/20 (nodose ganglia) or 1/40 (intestinal tissue) dilution of cDNA solution were subjected to RT-qPCR in a Bio-Rad iCycler iQ system using the qPCR SYBR Green MasterMix (Fermentas, Courtaboeuf, France). Quantitative PCR consisted of 45 cycles, 30 s at 95°C and 30 s at 60°C each. Primers sequences are figured in Table S2 in Supplementary Material.

Statistical Analysis

All statistical analyses were carried out using GraphPad Prism 6 (GraphPad Software, Inc., San Diego, CA, USA) software. Comparisons between control and LP groups were performed with an unpaired, two-tailed, Mann–Whitney test. When measures were repeated (dose-response), Friedman test was applied following Wilcoxon signed rank test. A *P* value ≤ 0.05 was considered statistically significant.

RESULTS

First-Meal Pattern and Plasma Gastrointestinal Peptides

Following 48-h fasting, first-meal size (grams per kilogram BW) was significantly higher in LP rats and the inter-meal interval

preceding the second meal tended to be reduced, leading to a significant 30%-lower satiety ratio in LP rats as compared to the control group (**Figure 1**). Since these short-term parameters of FI are primarily regulated by gastrointestinal peptides, gene expression (Figure S1 in Supplementary Material) and plasma concentration of ghrelin (stomach), CCK, GIP (duodenum), and PYY (ileum) were performed in fasted and 2 h-refed control and LP rats (**Figure 2**). As expected, plasma desacylghrelin was significantly decreased 2 h post-feeding but there were no differences between control and LP rats. Basal plasma concentration of CCK-8NS was similar in the both groups suggesting no IUGR effect on CCK production by I-cells. By contrast, postprandial CCK in LP rats was significantly higher than basal concentration 2 h post-feeding whereas in control rats CCK concentration reached back the initial basal level. This result supports the hypothesis of an alteration in the postprandial feedback regulation of CCK secretion and could be related to failure in short-term mechanisms of FI observed in LP rats (enhanced meal size and reduced satiety ratio). Plasma concentration of GIP and PYY (secreted further distally in the gastrointestinal tract than CCK and GIP) were significantly higher 2 h post-feeding as compared to fasting but with no difference between control and LP groups. Neither basal nor postprandial gene expression of these gastrointestinal peptides was affected by perinatal LP diet (Figure S1 in Supplementary Material).

Since plasma CCK concentration remained higher than basal concentration 2 h post-feeding in LP rats, we sought for an alteration in the kinetic of production of CCK over the feeding period. Plasma concentration of CCK was measured from 15 min before and until 150 min after feeding. As shown in **Figure 3A**, CCK release in response to feeding was similar in both groups but from 1 h to 2 h 30 min after FI plasma concentration of CCK was significantly higher in LP rats as compared to control rats. While in control group CCK concentration reached basal value as soon as 60 min post-feeding, values in LP rats were still higher than basal concentration at 150 min post-feeding. The total release of plasma CCK evaluated by the area under curve over the completed period (0–150 min) was significantly higher in LP rats as compared to control rats (**Figure 3A**). These results clearly showed an alteration in the regulation of postprandial CCK release in LP rats.

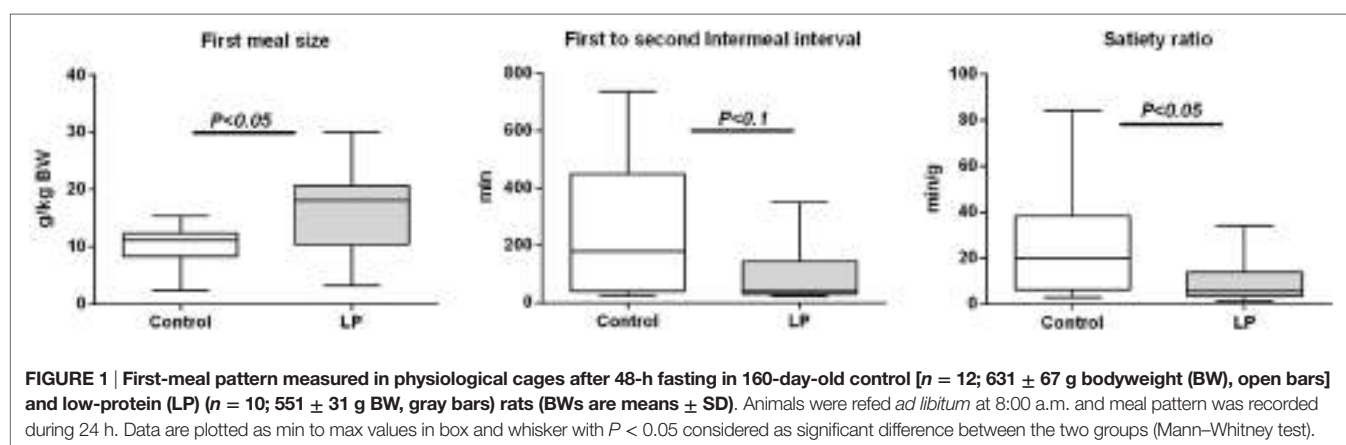


FIGURE 1 | First-meal pattern measured in physiological cages after 48-h fasting in 160-day-old control [$n = 12$; 631 ± 67 g bodyweight (BW), open bars] and low-protein (LP) ($n = 10$; 551 ± 31 g BW, gray bars) rats (BWs are means \pm SD). Animals were refed *ad libitum* at 8:00 a.m. and meal pattern was recorded during 24 h. Data are plotted as min to max values in box and whisker with $P < 0.05$ considered as significant difference between the two groups (Mann–Whitney test).

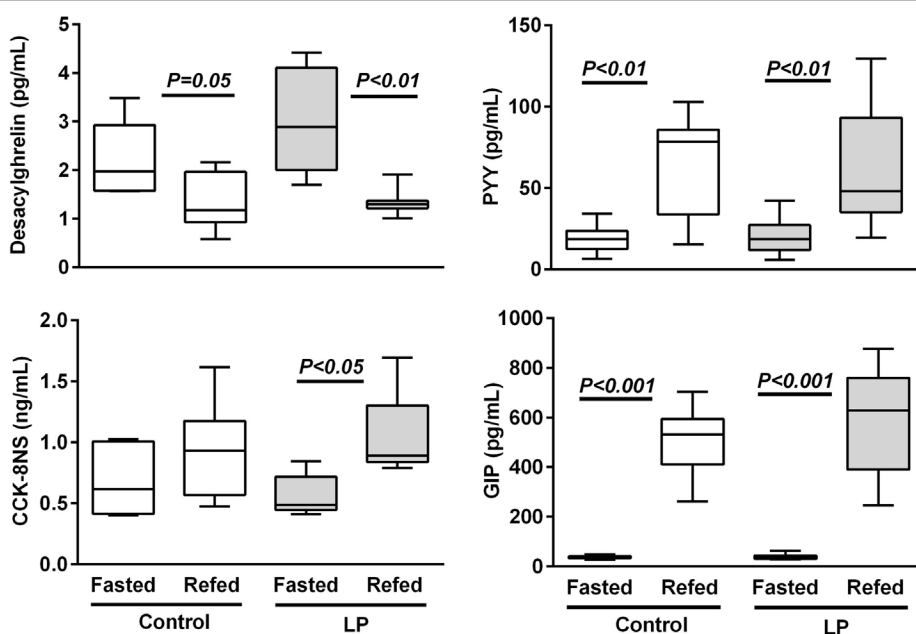


FIGURE 2 | Plasma gastrointestinal peptides in 48 h-fasted and 2 h-refed 160-day-old control and low-protein (LP) rats ($n = 8$ in each subgroup). Data are plotted as min to max values in box and whisker with $P < 0.05$ considered as significant difference between the fasted and refed subgroups (Mann–Whitney test).

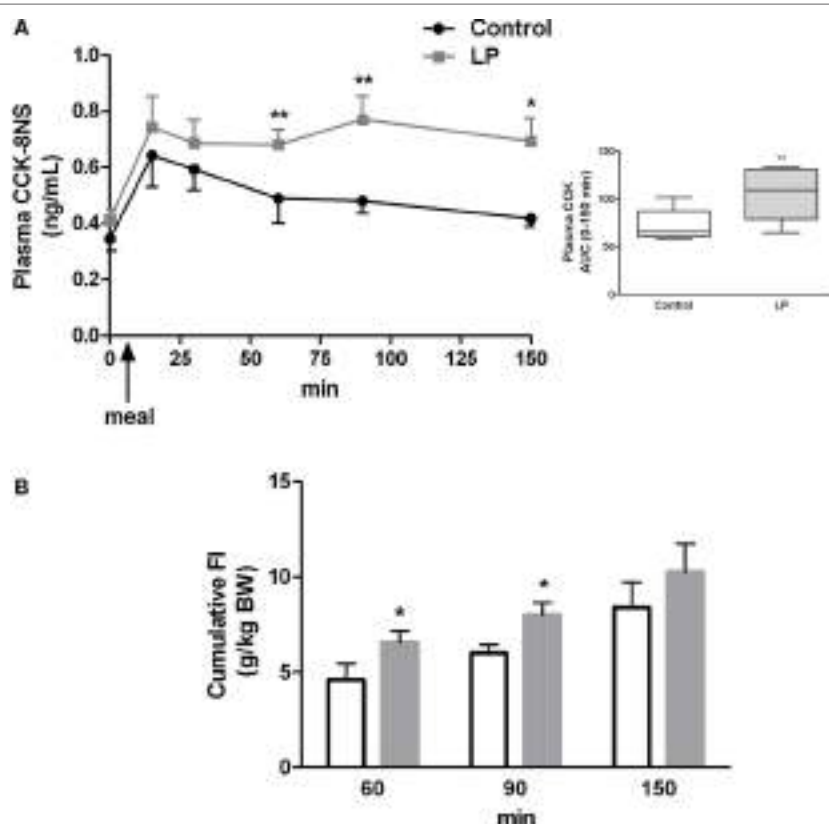


FIGURE 3 | (A) Basal and postprandial cholecystokinin (CCK) secretion measured in plasma at different times before and after refeeding by ELISA in control ($n = 9$) and low-protein (LP) rats ($n = 9$). In the box are represented the area under curve (AUC) calculated over the 0- to 150-min period. Rats were fasted 15 h before refeeding at light off indicated by an arrow. **(B)** Cumulative food intake [g/kg bodyweight (BW)] measured by food weighing in the same groups of rats. BWs (mean \pm SD) were 658 ± 57 and 621 ± 90 g in control and LP groups, respectively. Values are means \pm SEM. Significant differences between control and LP groups at $*P < 0.05$ and $**P < 0.01$, respectively (Mann–Whitney test).

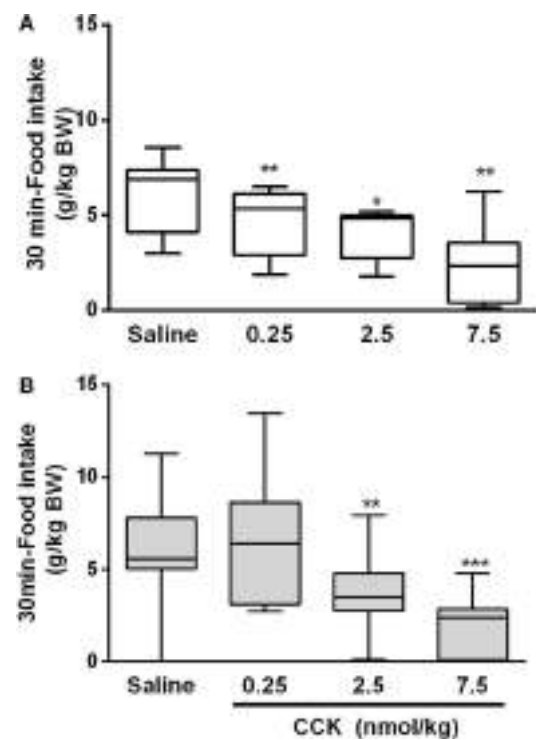


FIGURE 4 | Food intake during the first 30 min following i.p. injection of CCK and refeeding in control (A) and low-protein (LP) (B) groups. Bodyweights (mean \pm SD) were 655 ± 58 and 590 ± 81 g in control and LP groups, respectively. Each rat received all treatments at different days (repeated measures) with a minimum of 3-day wash out (recovery) between two treatments. * $P < 0.05$, ** $P < 0.01$ indicated significant differences vs saline group (Friedman and Wilcoxon signed rank tests).

Concomitant to higher CCK concentration at 60 and 90 min post-feeding in the LP group, cumulative FI measured for the same period was significantly higher in LP rats than control rats (**Figure 3B**). This result demonstrated that higher amount of plasma CCK was inefficient to reduce FI in LP rats.

Sensitivity to CCK-Induced Satiety

Since CCK is a major intestinal peptide of satiation, we examined its satietogenic effect by measuring FI after an i.p. administration of CCK-8S. As expected, in the control group, CCK induced a dose-dependent decrease of food ingestion in accordance with the normal sensitivity to satietogenic effect of CCK (**Figure 4A**). The minimal dose of CCK [0.25 nmol/kg; (28)] induced a 25% FI reduction ($P < 0.01$) on the first 30 min as compared to saline in the control group. In LP rats, this minimal dose had no effect on FI. A 10-fold higher dose (2.5 nmol/kg) was necessary to induce a significant reduction of FI in LP rats ($P < 0.01$). This suggested a resistance to the satiety effect of CCK (**Figure 4B**). At 60 and 90 min post-CCK injection and refeeding, FI was no more significantly different from saline in the both group except for the higher dose of CCK at 60 min ($P < 0.05$) (data not shown).

Vagal Neurochemical Phenotype and CCK-1R Signaling

Since short-term regulation of FI by CCK acts primarily *via* vagal nerve, the expression of CCK-1R was measured in nodose ganglia. The basal expression of vagal CCK-1R measured by immunofluorescence ($P < 0.01$) was lower in LP rats as compared to control rats and could contribute to the loss of sensitivity to CCK-induced satiety in LP rats (**Figures 5A,B**). No effect of

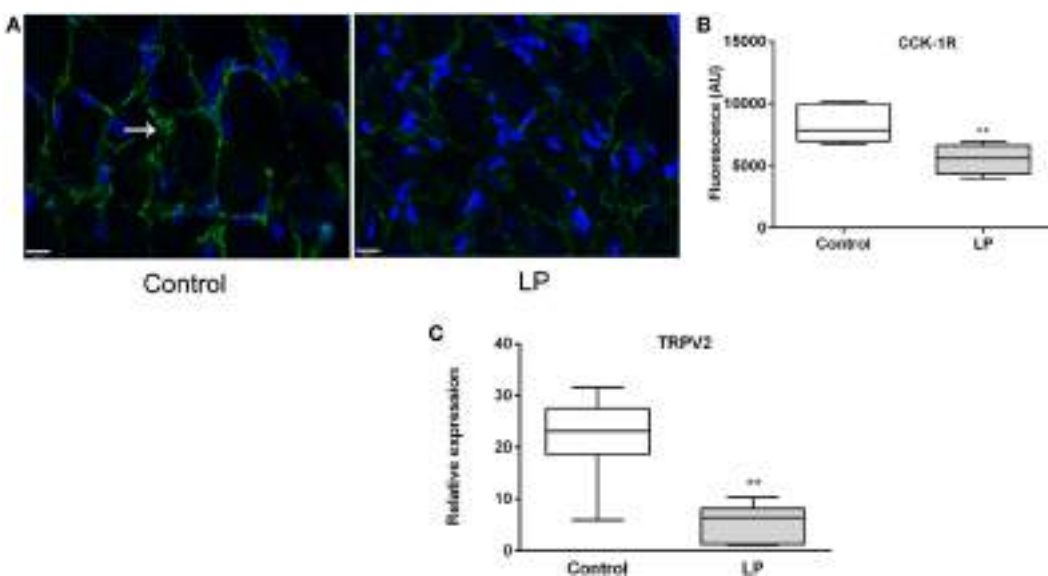


FIGURE 5 | (A) Immunofluorescence ($\times 63$) of CCK-1R (green) in nodose ganglia of control (left) and low-protein (LP) (right) rats at basal state (fasting). Nuclei are stained in blue with Dapi. **(B)** Corresponding histogram of quantification of fluorescence ($n = 3\text{--}4$). **(C)** Relative expression of TRPV2 expression at basal state. Values are means \pm SEM. * $P < 0.05$, ** $P < 0.01$ vs control (Mann–Whitney test).

refeeding on vagal CCK-1R expression was observed (data not shown) in the present experiment as previously reported (32). The neurochemical switch operated by CCK on VAN determines an anorexigenic vs orexigenic phenotype that mediates an appropriate response at the brain stem and hypothalamic levels to regulate FI (14, 15). Anorexigenic peptides (CART) and receptors (Y2-R) as well as orexigenic NPY were analyzed in nodose ganglia in response to refeeding in both groups. Unexpectedly, no significant difference was observed in expression of these genes between fasting and refed states, either in control or LP rats (Figure S2 in Supplementary Material).

Since CCK effects on VAN are mediated by TRPV2–5 cation channels (22), we determined gene expression of TRPV2 and found it significantly under expressed in LP nodose ganglia as compared to control (Figure 5C). Detection of phosphorylated CaMKII has been previously used as a marker of cellular activation in the nodose ganglia (23). Under basal conditions, the ratio pCaMKII/CaMKII was significantly lower in LP nodose ganglia as compared to control (0.4038 ± 0.06 vs 2.888 ± 0.47 , respectively, means \pm SEM, $P < 0.05$, Mann–Whitney test). Unexpectedly CCK-dependent pCaMKII/CaMKII ratio was reduced 20 min after injection in control rats, with no effect in LP rats (Figure 6).

Cholecystokinin activity on CREB phosphorylation in VAN (26) and phosphorylation of ERK in NTS is linked to the satiation effect of the peptide (21, 33). However, 20 min after exogenous administration of CCK, no activation of the ERK pathway was detected in nodose ganglia of control or LP rats (Figure 7).

DISCUSSION

Although some experimental studies testify alteration of FI and meal pattern in LP rats at adulthood, to the best of our knowledge the present data provide the first evidence that the sensitivity to CCK-induced satiation is impaired by perinatal undernutrition. The resistance to the satiation effect of CCK could be related to a lower expression of CCK-1R and TRPV2 in nodose ganglia in LP rats accredited by a lower basal and phosphorylated level of CaMKII as compared to control rats. The higher postprandial CCK release that we observed in LP rats possibly represents an adaptive mechanism that is partially inefficient at reducing the first meal after a fasting period.

Short-term FI and Postprandial CCK Are Altered in LP Rats

Alteration of short-term FI has been previously reported in perinatally malnourished rats. Protein restricted diet provided to dams during gestation and/or lactation modify the early appetite of their pups. They demonstrate a hyperphagic phase especially after weaning (7, 34) and during their catch-up growth (6, 7). At adulthood, FI seems grossly normal but a delay in satiation (7) and an increase of the first-meal size following 48-h fasting are still observed suggesting a persistent alteration of short-term regulation of FI. Such an alteration could predispose to obesity particularly when the animals are challenged with a high-calories diet (8). Interestingly, a very recent study showed that LP rats are hyperphagic at older age

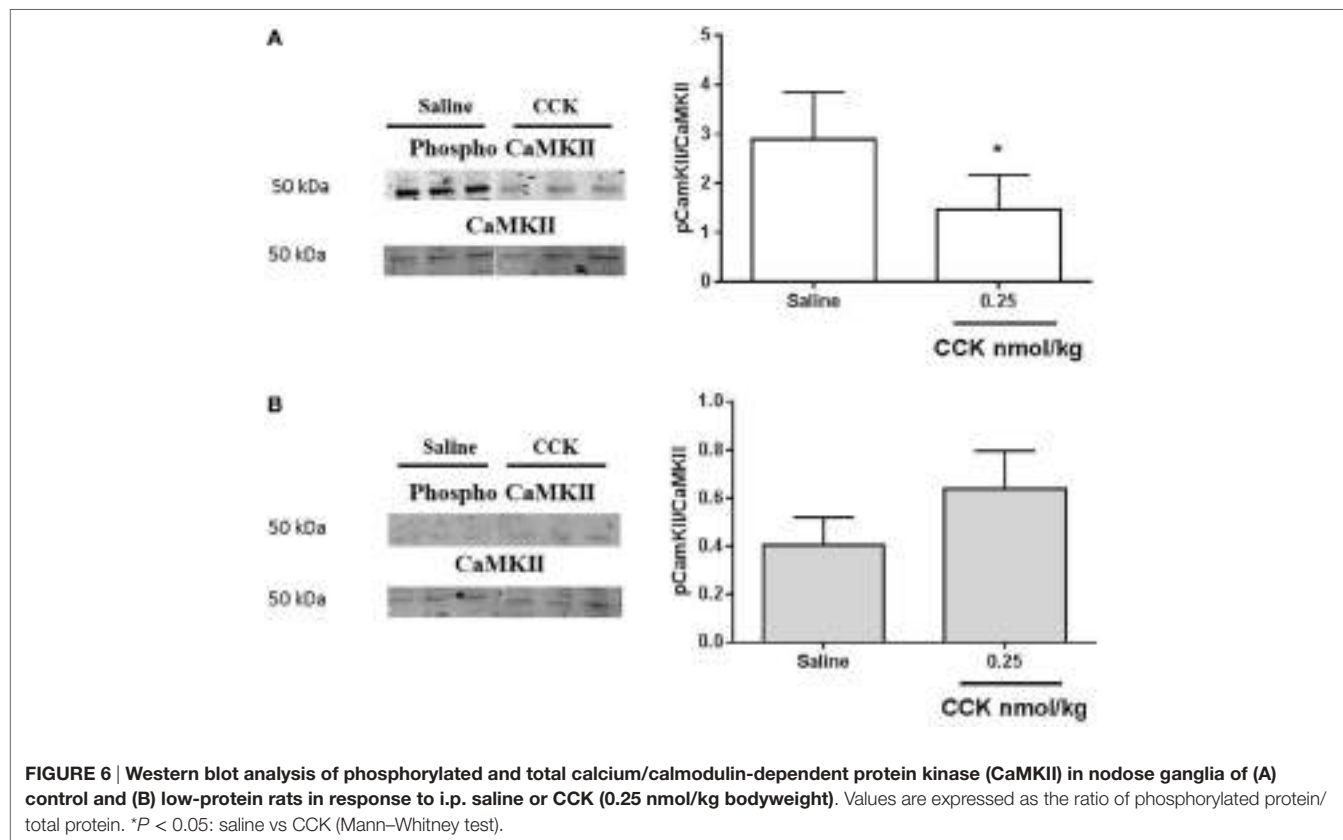


FIGURE 6 | Western blot analysis of phosphorylated and total calcium/calmodulin-dependent protein kinase (CaMKII) in nodose ganglia of (A) control and (B) low-protein rats in response to i.p. saline or CCK (0.25 nmol/kg bodyweight). Values are expressed as the ratio of phosphorylated protein/total protein. * $P < 0.05$: saline vs CCK (Mann–Whitney test).

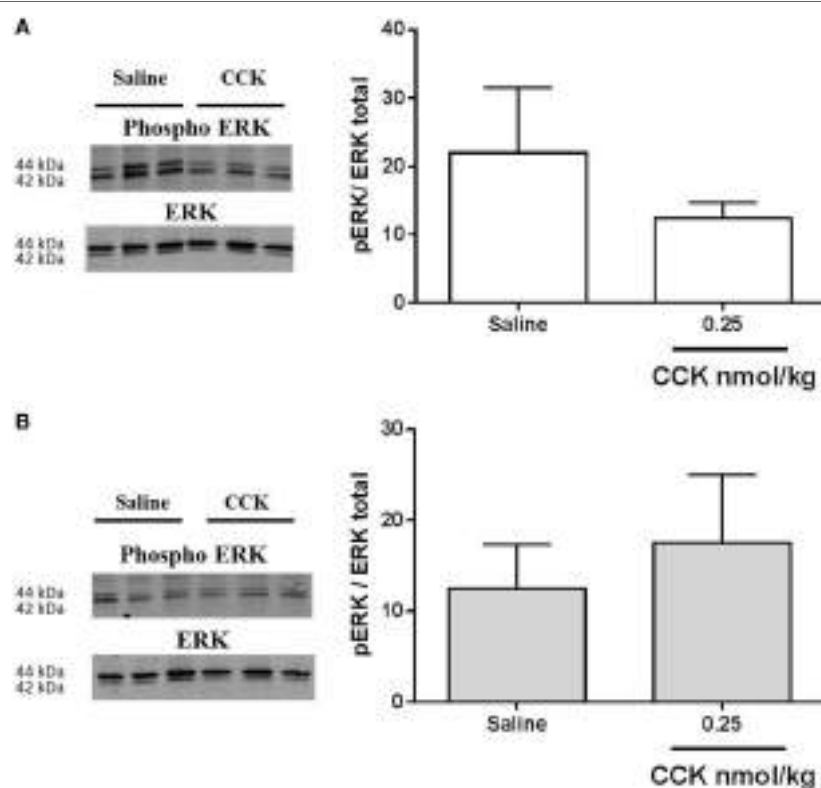


FIGURE 7 | Western blot analysis of phosphorylated and total ERK1/2 in nodose ganglia of (A) control and (B) low-protein rats ($n = 4\text{--}5$) in response to i.p. saline or CCK (0.25 nmol/kg bodyweight). Values are expressed as the ratio of phosphorylated protein/total protein. * $P < 0.05$: saline vs CCK (Mann-Whitney test).

(1-year old) than younger adult ages usually studied, reinforcing the importance of long lasting impact of programming hyperphagia by perinatal nutrition (35). In the present study using physiological cages that give precise information of meal pattern, we confirmed that adult (160-day old) LP rats present an altered regulation of the first-meal pattern after a long period of fast.

Short-term FI is regulated by a vago-vagal reflex initiated by arrival of food in the stomach and the upper intestine that are sensitive to both distension and nutrients. It ensues digestive secretion and release of appetite-regulating gut peptides (CCK, serotonin, GIP, PYY, glucagon like peptide-1, etc.), all known, at the exception of ghrelin, to reduce meal and delay the next meal (36). We first hypothesized that gene expression as well as the basal and postprandial release of those peptides may be altered in LP rats. A previous study reported elevated plasma ghrelin and reduced CCK and PYY in adult IUGR rats obtained by a 50%-caloric restriction of their dams diet during gestation and maintained restricted during lactation (37). These changes were paralleled to mRNA levels in gastric and intestinal tissues. In this drastic model, as previously shown by others (38), rats are hyperphagic during the whole period of the experiment (from weaning to 7- to 9-month olds). However, only fasting GI peptides concentrations were reported in that study. Therefore, no conclusions on their

dynamic change in relation to FI can be drawn. In the present work, offspring obtained by protein restriction of theirs dams during gestation and lactation showed no modification in gene expression of GI peptides, nor at basal or postprandial states. We then measured their plasma concentrations and found that only postprandial CCK was significantly higher than basal in 2-h-refed LP animals. This result seems in contrast with the increased first-meal size and the reduced satiety ratio we measured in LP rats but can be interpreted as if a higher CCK release was inefficient to correctly regulate FI. The kinetic of plasma CCK release post-refeeding was similar in both groups suggesting no delay in CCK secretion by I-cells. By contrast, the feedback regulation seen by the reduced FI 1 h post-refeeding in control rats seemed ineffective in LP rats. As previously mentioned, short-term regulation of FI is initiated by proximal gut mechano- and chemoreceptors, in association with GI peptides release. These initials signals are integrated by VAN to the hindbrain, which triggers a vago-vagal reflex to decrease FI by inhibiting gastric emptying, stimulating digestive secretion, etc. The release of GI peptides is supposed to be regulated by a classic downregulation of theirs receptors once stimuli (nutrients) have moved to distal parts of gut. Thus, the higher postprandial plasma CCK found in LP rats led us to propose the existence of a state of resistance to the satietogenic effect of CCK in these rats.

LP Rats Are Resistant to CCK-Induced Satiation

Exogenous administration of CCK-8S in LP rats at a dose previously shown to induce satiety in refed rats (28) was not efficient to reduce FI in contrast to control group where the consumption of food was 25% reduced. Since the satietogenic effect of CCK is mediated by CCK-1R on VAN, we hypothesized that perinatal malnutrition could affect CCK signaling *via* its receptor on the vagus nerve. We effectively found that CCK-1R immunoreactivity was significantly lower in nodose ganglia of LP rats compared to control rats probably contributing to the resistance to CCK. A reduced sensitivity to a satietogenic dose of CCK, leading to hyperphagia, has already been shown in obesity-prone rats receiving standard chow (39) as well as in high-fat diet fed rats (40). In diet-induced obese rats, neurochemical analysis of VAN supports a vagal resistance to CCK and leptin in this model in which hyperphagia occurred concomitantly with this resistance (29). In DIO mice, spontaneous activity of VAN innervating the jejunum is weaker as compared to control and the number of afferent neurons that respond to CCK is reduced (41). The impact of perinatal malnutrition on the activity/neurochemical phenotype of the vagus nerve is poorly documented. One study reported a reduced vagal firing rate in adult rats reared by mothers fed a LP diet leading to an impaired efferent vagal activity (42). Electrophysiological studies of nodose neurons of LP rats are in progress in our lab to better characterize the effect of perinatal malnutrition on the activity of the vagus nerve.

Dockray and collaborators have considered CCK as a gate-keeper of the vagal phenotype, switching from an orexigenic phenotype during fasting at low CCK concentration to an anorexigenic one when CCK is released at refeeding (16, 25, 43). Here, we did not observe any modifications of the vagal phenotype between fasting and refed states neither in control nor in LP rats. This discrepancy could be related to different duration of fasting between experiments, even if our conditions (48-h fasting) were close to that of the earlier studies (24–48 h). A very recent study in mice also failed to reproduce this metabolic switch of VAN from an anorectic to orexigenic phenotype (44). Using confocal microscopy to visualize all afferent visceral C-fibers of the vagus nerve, these authors showed that the neuropeptide CART was not regulated by metabolic challenge (fasting or high-fat diet). They also failed to detect any production of MCH, an orexigenic neuropeptide previously shown to be produced by CART neurons in fed state in response to fasting. In our study, we did not detect MCH (mRNA or protein) in nodose ganglia of control and LP rats, whatever they were in their fed or fasted state (data not shown). Thus, our data could not support the hypothesis of an alteration of the vagal phenotype switch by CCK in LP rats but led us to consider CCK signaling in nodose ganglia.

Following its receptor activation, in synergic interaction with leptin receptors, CCK induces a cascade of signal transduction pathways leading to neuronal firing (45). Among them, p-ERK1/2 in terminal endings of VAN in NTS is central to CCK-induced inhibition of FI (19, 21). In the present study, we did not measure any activation of ERK following CCK injection in nodose ganglia. Previous data showing CCK-induced phosphorylation of ERK in

NTS reported that the effect occurred very quickly, as soon as 6 min following injection (21). Here, we measured CCK signaling 20 min after stimulation, this may have contributed, in combination with the low dose used, to the absence of phosphorylation signal in nodose ganglia. An analysis on a shorter time needs to be further performed and CCK signaling measured at the afferent endings in the NTS may provide a better comprehension of the underlying mechanism. Concerning calcium signaling, we showed that LP lowered TRPV2 expression in nodose ganglia. This observation could be put in relation with the attenuated level of CaMKII and pCaMKII measured in this model as compared to normal birth-weight rats. Such a reduced expression of CaMKII has been previously reported in the frontal cortex in young adult LP rats (46). Similarly, in LP fetal brain, number of CaMKII immunopositive cells was decreased as compared to control (47). The major role of CaMKII in mediating glutamate signaling has been extensively studied in postsynaptic events implied in memorization and cognition, which are altered in IUGR infants and animal models (48). As proposed by Flores et al., underexpression of CaMKII in frontal cortex of LP rats could be related to altered synaptic plasticity and decreased learning performances in this model. In our study, the reduced expression of CaMKII in nodose ganglia may contribute, together with the reduced CCK-1R expression, to the hyposensitivity of afferent neurons to CCK. Actually, factors leading to this decreased basal expression related to perinatal LP environment are unknown. Epigenetic mechanism is now widely accepted as a memory of antenatal undernutrition exposure throughout life. Research of epigenetic marks on the promoter of the CaMKII gene would be of great interest to link early LP environment and CaMKII expression. More unexpectedly, exogenous CCK induced a decrease in phosphorylation of CaMKII in nodose ganglia of the control group of rats. It has been previously demonstrated in cultured nodose neurons that the CCK-induced increase in cytosolic calcium concentrations is dependent on extracellular calcium influx rather than mobilization on intracellular stores (49). In neurons of the dorsal root ganglia, such a decrease in CaMKII autophosphorylation has been reported *in vitro* by depleting extracellular calcium (50). The significance of this observation in the present study needs further investigation.

In conclusion, we showed for the first time in the present study that adult perinatally undernourished rats have a reduced first-meal satiety ratio associated to a higher postprandial plasmatic CCK release, a reduced sensitivity to CCK when injected at low concentration and a reduced presence of CCK-1R and TRPV2 in nodose ganglia. Altogether, the present data demonstrated a reduced vagal sensitivity to CCK in LP rats at adulthood, which could contribute to deregulation of FI reported in this model.

ETHICS STATEMENT

All experiments were conducted in accordance with the European Union regulations for the care and use of animals for experimental procedures (2010/63/EU). Protocols were approved by the local Committee on the Ethics in Animal Experiments of Pays de la Loire (France) and the French Ministry of Research (Projects

2011.4 and 0271.01). Animal facility is registered by the French Veterinary Department as A44276.

AUTHOR CONTRIBUTIONS

GLD designed the study, GLD and CP wrote the protocol, and MN wrote the first draft of the manuscript. MN and CP managed the literature searches and performed animal experiments and analyses. MN performed the statistical analyses. PP contributed for interpretation of data and revised the manuscript. All authors contributed to and have approved the final manuscript.

ACKNOWLEDGMENTS

Guillaume Poupeau and Blandine Castellano are greatly acknowledged for their contribution at managing animal experiment; Thomas Moyon for help in statistical analyses;

REFERENCES

- Barker DJ, Winter PD, Osmond C, Margetts B, Simmonds SJ. Weight in infancy and death from ischaemic heart disease. *Lancet* (1989) 2:577–80. doi:10.1016/S0140-6736(89)90710-1
- Ravelli G-P, Stein ZA, Susser MW. Obesity in young men after famine exposure in utero and early infancy. *N Engl J Med* (1976) 295:349–53. doi:10.1056/NEJM197608122950701
- Syddall HE, Sayer AA, Simmonds SJ, Osmond C, Cox V, Dennison EM, et al. Birth weight, infant weight gain, and cause-specific mortality: the Hertfordshire Cohort Study. *Am J Epidemiol* (2005) 161:1074–80. doi:10.1093/aje/kwi137
- Waterland RA, Garza C. Potential mechanisms of metabolic imprinting that lead to chronic disease. *Am J Clin Nutr* (1999) 69:179–97.
- Desai M, Li T, Han G, Ross MG. Programmed hyperphagia secondary to increased hypothalamic SIRT1. *Brain Res* (2014) 1589:26–36. doi:10.1016/j.brainres.2014.09.031
- Coupe B, Grit I, Darmaun D, Parnet P. The timing of “catch-up growth” affects metabolism and appetite regulation in male rats born with intrauterine growth restriction. *Am J Physiol Regul Integr Comp Physiol* (2009) 297:R813–24. doi:10.1152/ajpregu.00201.2009
- Orozco-Solis R, de Souza S, Barbosa Matos RJ, Grit I, Le Bloch J, Nguyen P, et al. Perinatal undernutrition-induced obesity is independent of the developmental programming of feeding. *Physiol Behav* (2009) 96:481–92. doi:10.1016/j.physbeh.2008.11.016
- Martin Agnoux A, Alexandre-Gouabau MC, Le Drean G, Antignac JP, Parnet P. Relative contribution of foetal and post-natal nutritional periods on feeding regulation in adult rats. *Acta Physiol (Oxf)* (2014) 210:188–201. doi:10.1111/apha.12163
- Dalle Molle R, Laureano DP, Alves MB, Reis TM, Desai M, Ross MG, et al. Intrauterine growth restriction increases the preference for palatable foods and affects sensitivity to food rewards in male and female adult rats. *Brain Res* (2015) 1618:41–9. doi:10.1016/j.brainres.2015.05.019
- Wynne K, Stanley S, McGowan B, Bloom S. Appetite control. *J Endocrinol* (2005) 184:291–318. doi:10.1677/joe.1.05866
- Ross MG, Desai M. Developmental programming of appetite/satiety. *Ann Nutr Metab* (2014) 64(Suppl 1):36–44. doi:10.1159/000360508
- Coupe B, Grit I, Hulin P, Randuineau G, Parnet P. Postnatal growth after intrauterine growth restriction alters central leptin signal and energy homeostasis. *PLoS One* (2012) 7:e30616. doi:10.1371/journal.pone.0030616
- Schwartz MW. Central nervous system regulation of food intake. *Obesity (Silver Spring)* (2006) 14(Suppl 1):1s–8s. doi:10.1038/oby.2006.275
- Dockray GJ. Gastrointestinal hormones and the dialogue between gut and brain. *J Physiol* (2014) 592:2927–41. doi:10.1113/jphysiol.2014.270850
- Dockray GJ. The versatility of the vagus. *Physiol Behav* (2009) 97:531–6. doi:10.1016/j.physbeh.2009.01.009
- Burdya G, de Lartigue G, Raybould HE, Morris R, Dimaline R, Varro A, et al. Cholecystokinin regulates expression of Y2 receptors in vagal afferent neurons serving the stomach. *J Neurosci* (2008) 28:11583–92. doi:10.1523/JNEUROSCI.2493-08.2008
- de Lartigue G, Barbier de la Serre C, Espero E, Lee J, Raybould HE. Diet-induced obesity leads to the development of leptin resistance in vagal afferent neurons. *Am J Physiol Endocrinol Metab* (2011) 301:E187–95. doi:10.1152/ajpendo.00056.2011
- Peters JH, Ritter RC, Simasko SM. Leptin and CCK modulate complementary background conductances to depolarize cultured nodose neurons. *Am J Physiol Cell Physiol* (2006) 290:C427–32. doi:10.1152/ajpcell.00439.2005
- Babic T, Townsend RL, Patterson LM, Sutton GM, Zheng H, Berthoud HR. Phenotype of neurons in the nucleus of the solitary tract that express CCK-induced activation of the ERK signaling pathway. *Am J Physiol Regul Integr Comp Physiol* (2009) 296:R845–54. doi:10.1152/ajpregu.90531.2008
- Campos CA, Wright JS, Czaja K, Ritter RC. CCK-induced reduction of food intake and hindbrain MAPK signaling are mediated by NMDA receptor activation. *Endocrinology* (2012) 153:2633–46. doi:10.1210/en.2012-1025
- Sutton GM, Patterson LM, Berthoud HR. Extracellular signal-regulated kinase 1/2 signaling pathway in solitary nucleus mediates cholecystokinin-induced suppression of food intake in rats. *J Neurosci* (2004) 24:10240–7. doi:10.1523/JNEUROSCI.2764-04.2004
- Zhao H, Simasko SM. Role of transient receptor potential channels in cholecystokinin-induced activation of cultured vagal afferent neurons. *Endocrinology* (2010) 151:5237–46. doi:10.1210/en.2010-0504
- Vincent KM, Sharp JW, Raybould HE. Intestinal glucose-induced calcium-calmodulin kinase signaling in the gut-brain axis in awake rats. *Neurogastroenterol Motil* (2011) 23:e282–93. doi:10.1111/j.1365-2982.2011.01673.x
- Fanca-Berthon P, Michel C, Pagniez A, Rival M, Van Seuningen I, Darmaun D, et al. Intrauterine growth restriction alters postnatal colonic barrier maturation in rats. *Pediatr Res* (2009) 66:47–52. doi:10.1203/PDR.0b013e3181a2047e
- Burdya G, Varro A, Dimaline R, Thompson DG, Dockray GJ. Feeding-dependent depression of melanin-concentrating hormone and melanin-concentrating hormone receptor-1 expression in vagal afferent neurons. *Neuroscience* (2006) 137:1405–15. doi:10.1016/j.neuroscience.2005.10.057
- de Lartigue G, Dimaline R, Varro A, Dockray GJ. Cocaine- and amphetamine-regulated transcript: stimulation of expression in rat vagal afferent neurons by cholecystokinin and suppression by ghrelin. *J Neurosci* (2007) 27:2876–82. doi:10.1523/JNEUROSCI.5508-06.2007
- McMinn JE, Sindelar DK, Havel PJ, Schwartz MW. Leptin deficiency induced by fasting impairs the satiety response to cholecystokinin. *Endocrinology* (2000) 141:4442–8. doi:10.1210/en.141.12.4442
- Savastano DM, Covasa M. Adaptation to a high-fat diet leads to hyperphagia and diminished sensitivity to cholecystokinin in rats. *J Nutr* (2005) 135:1953–9.
- de Lartigue G, Barbier de la Serre C, Espero E, Lee J, Raybould HE. Leptin resistance in vagal afferent neurons inhibits cholecystokinin signaling and

Anthony Pagniez and Isabelle Grit for their assistance to perform biochemical analyses. The authors are very grateful to the MicroPiCell-Biogenouest platform for its assistance in fluorescence microscopy.

FUNDING

This study was supported by a grant from Région Pays de La Loire (PARIMAD project) and LCL (Le Crédit Lyonnais) contribution to Santedige foundation. MN thesis was co-funded by Région Pays de La Loire and INRA, France.

SUPPLEMENTARY MATERIAL

The Supplementary Material for this article can be found online at <http://journal.frontiersin.org/article/10.3389/fendo.2017.00065/full#supplementary-material>.

- satiation in diet induced obese rats. *PLoS One* (2012) 7:e32967. doi:10.1371/journal.pone.0032967
30. Blevins JE, Morton GJ, Williams DL, Caldwell DW, Bastian LS, Wisse BE, et al. Forebrain melanocortin signaling enhances the hindbrain satiety response to CCK-8. *Am J Physiol Regul Integr Comp Physiol* (2009) 296:R476–84. doi:10.1152/ajpregu.90544.2008
 31. Buyse M, Ovesjo ML, Goiot H, Guilmeau S, Peranzo G, Moizo L, et al. Expression and regulation of leptin receptor proteins in afferent and efferent neurons of the vagus nerve. *Eur J Neurosci* (2001) 14:64–72. doi:10.1046/j.0953-816x.2001.01628.x
 32. Broberger C, Holmberg K, Shi T-J, Dockray G, Hökfelt T. Expression and regulation of cholecystokinin and cholecystokinin receptors in rat nodose and dorsal root ganglia. *Brain Res* (2001) 903:128–40. doi:10.1016/S0006-8993(01)02468-4
 33. Berthoud HR, Sutton GM, Townsend RL, Patterson LM, Zheng H. Brainstem mechanisms integrating gut-derived satiety signals and descending forebrain information in the control of meal size. *Physiol Behav* (2006) 89:517–24. doi:10.1016/j.physbeh.2006.08.018
 34. Lopes de Souza S, Orozco-Solis R, Grit I, de Castro R, Bolanos-Jimenez F. Perinatal protein restriction reduces the inhibitory action of serotonin on food intake. *Eur J Neurosci* (2008) 27:1400–8. doi:10.1111/j.1460-9568.2008.06105.x
 35. Qasem RJ, Li J, Tang HM, Pontiggia L, D'Mello AP. Maternal protein restriction during pregnancy and lactation alters central leptin signalling, increases food intake, and decreases bone mass in 1 year old rat offspring. *Clin Exp Pharmacol Physiol* (2016) 43:494–502. doi:10.1111/1440-1681.12545
 36. Camilleri M. Peripheral mechanisms in appetite regulation. *Gastroenterology* (2015) 148:1219–33. doi:10.1053/j.gastro.2014.09.016
 37. Nagata E, Nakagawa Y, Yamaguchi R, Fujisawa Y, Sano S, Satake E, et al. Altered gene expressions of ghrelin, PYY, and CCK in the gastrointestinal tract of the hyperphagic intrauterine growth restriction rat offspring. *Horm Metab Res* (2011) 43(3):178–82. doi:10.1055/s-0030-1270528
 38. Desai M, Gayle D, Babu J, Ross MG. Programmed obesity in intrauterine growth-restricted newborns: modulation by newborn nutrition. *Am J Physiol Regul Integr Comp Physiol* (2005) 288:R91–6. doi:10.1152/ajpregu.00340.2004
 39. Swartz TD, Duca FA, Covasa M. Differential feeding behavior and neuronal responses to CCK in obesity-prone and -resistant rats. *Brain Res* (2010) 1308:79–86. doi:10.1016/j.brainres.2009.10.045
 40. Swartz TD, Savastano DM, Covasa M. Reduced sensitivity to cholecystokinin in male rats fed a high-fat diet is reversible. *J Nutr* (2010) 140:1698–703. doi:10.3945/jn.110.124149
 41. Daly DM, Park SJ, Valinsky WC, Beyak MJ. Impaired intestinal afferent nerve satiety signalling and vagal afferent excitability in diet induced obesity in the mouse. *J Physiol* (2011) 589:2857–70. doi:10.1113/jphysiol.2010.204594
 42. de Oliveira JC, Scomparin DX, Andreazzi AE, Branco RC, Martins AG, Gravena C, et al. Metabolic imprinting by maternal protein malnourishment impairs vagal activity in adult rats. *J Neuroendocrinol* (2011) 23:148–57. doi:10.1111/j.1365-2826.2010.02095.x
 43. Burdyga G, Lal S, Varro A, Dimaline R, Thompson DG, Dockray GJ. Expression of cannabinoid CB1 receptors by vagal afferent neurons is inhibited by cholecystokinin. *J Neurosci* (2004) 24:2708–15. doi:10.1523/JNEUROSCI.5404-03.2004
 44. Yuan X, Huang Y, Shah S, Wu H, Gautron L. Levels of cocaine- and amphetamine-regulated transcript in vagal afferents in the mouse are unaltered in response to metabolic challenges. *eNeuro* (2016) 3. doi:10.1523/euro.0174-16.2016
 45. Owyang C, Heldsinger A. Vagal control of satiety and hormonal regulation of appetite. *J Neurogastroenterol Motil* (2011) 17:338–48. doi:10.5056/jnm.2011.17.4.338
 46. Flores O, Perez H, Valladares L, Morgan C, Gatica A, Burgos H, et al. Hidden prenatal malnutrition in the rat: role of beta(1)-adrenoceptors on synaptic plasticity in the frontal cortex. *J Neurochem* (2011) 119:314–23. doi:10.1111/j.1471-4159.2011.07429.x
 47. Liu F, Liu Y, Liu J, Ma LY. Antenatal taurine improves intrauterine growth-restricted fetal rat brain development which is associated with increasing the activity of PKA-CaMKII/c-fos signal pathway. *Neuropediatrics* (2015) 46:299–306. doi:10.1055/s-0035-1558434
 48. Miller SL, Huppi PS, Mallard C. The consequences of fetal growth restriction on brain structure and neurodevelopmental outcome. *J Physiol* (2016) 594:807–23. doi:10.1113/jphysiol.2015.201502
 49. Simasko SM, Wiens J, Karpel A, Covasa M, Ritter RC. Cholecystokinin increases cytosolic calcium in a subpopulation of cultured vagal afferent neurons. *Am J Physiol Regul Integr Comp Physiol* (2002) 283:R1303–13. doi:10.1152/ajpregu.00050.2002
 50. Cohen JE, Fields RD. CaMKII inactivation by extracellular Ca(2+) depletion in dorsal root ganglion neurons. *Cell Calcium* (2006) 39:445–54. doi:10.1016/j.ceca.2006.01.005

Conflict of Interest Statement: The authors declare that the research was conducted in the absence of any commercial or financial relationships that could be construed as a potential conflict of interest.

Copyright © 2017 Ndjim, Poinsignon, Parnet and Le Dréan. This is an open-access article distributed under the terms of the Creative Commons Attribution License (CC BY). The use, distribution or reproduction in other forums is permitted, provided the original author(s) or licensor are credited and that the original publication in this journal is cited, in accordance with accepted academic practice. No use, distribution or reproduction is permitted which does not comply with these terms.



Enhanced Mortality to Metastatic Bladder Cancer Cell Line MB49 in Vasoactive Intestinal Peptide Gene Knockout Mice

Niely Mirsaidi^{1,2†}, Matthew P. Burns^{1,2†}, Steve A. McClain³, Edward Forsyth⁴, Jonathan Li^{1,2}, Brittany Dukes^{1,2}, David Lin^{1,2}, Roxanna Nahvi^{1,2}, Jheison Giraldo^{1,2}, Megan Patton², Ping Wang⁵, Ke Lin⁵, Edmund Miller^{5,6,7}, Timothy Ratliff^{8,9}, Sayyed Hamidi¹⁰, Scott Crist^{8,9}, Ken-Ichi Takemaru¹¹ and Anthony Szema^{1,2,5,12,13,14*}

OPEN ACCESS

Edited by:

Hubert Vaudry,
University of Rouen, France

Reviewed by:

Rafael Vazquez-Martinez,
Instituto Maimónides de
Investigación Biomédica de
Córdoba, Spain
Terry Moody,
NCI, United States

*Correspondence:

Anthony Szema
aszema@northwell.edu

[†]These authors have
contributed equally
to this work.

Specialty section:

This article was submitted
to Neuroendocrine Science,
a section of the journal
Frontiers in Endocrinology

Received: 22 August 2016

Accepted: 23 June 2017

Published: 07 August 2017

Citation:

Mirsaidi N, Burns MP, McClain SA,
Forsyth E, Li J, Dukes B, Lin D,
Nahvi R, Giraldo J, Patton M,
Wang P, Lin K, Miller E, Ratliff T,
Hamidi S, Crist S, Takemaru K-I and
Szema A (2017) Enhanced Mortality
to Metastatic Bladder Cancer Cell
Line MB49 in Vasoactive Intestinal
Peptide Gene Knockout Mice.
Front. Endocrinol. 8:162.
doi: 10.3389/fendo.2017.00162

¹Department of Technology and Society, College of Engineering and Applied Sciences, Stony Brook University, Stony Brook, NY, United States, ²Three Village Allergy & Asthma, PLLC, South Setauket, NY, United States, ³McClain Laboratories, LLC, Smithtown, NY, United States, ⁴Department of Urology, Stony Brook University School of Medicine, Stony Brook, NY, United States, ⁵The Feinstein Institute for Medical Research, Center for Heart and Lung Research, Manhasset, NY, United States,

⁶The Elmezzi Graduate School of Molecular Medicine, Manhasset, NY, United States, ⁷Hofstra Northwell School of Medicine, Hempstead, NY, United States, ⁸Purdue University, Center for Cancer Research, West Lafayette, IN, United States,

⁹Department of Comparative Pathobiology, College of Veterinary Medicine, Purdue University, West Lafayette, IN, United States, ¹⁰James J. Peters Veterans Affairs Medical Center, Bronx, NY, United States, ¹¹Department of Pharmacological Sciences, Stony Brook University School of Medicine, Stony Brook, NY, United States, ¹²Department of Occupational Medicine, Epidemiology, and Prevention, Hofstra Northwell School of Medicine, Hempstead, NY, United States, ¹³Northwell Health, Department of Medicine, Division of Pulmonary and Critical Care, Manhasset, NY, United States, ¹⁴Northwell Health, Department of Medicine, Division of Allergy and Immunology, Manhasset, NY, United States

To identify if the absence of the vasoactive intestinal peptide (VIP) gene enhances susceptibility to death from metastatic bladder cancer, two strains of mice were injected with MB49 murine bladder cancer cells. The growth and spread of the cancer was measured over a period of 4 weeks in C57BL/6 mice and 5 weeks in VIP knockout (KO) mice. A Kaplan–Meier plot was constructed to compare control C57BL/6 mice and C57BL/6 mice with MB49 vs. VIP KO controls and VIP KO mice with MB49. The wild-type (WT) strain (C57BL/6) contained the VIP gene, while the other strain, VIP knockout backcrossed to C57BL/6 (VIP KO) did not and was thus unable to endogenously produce VIP. VIP KO mice had increased mortality compared to C57BL/6 mice at 4 weeks. The number of ulcers between both groups was not statistically significant. *In vitro* studies indicated that the presence VIP in high doses reduced MB49 cell growth, as well as macrophage inhibitory factor (MIF), a growth factor in bladder cancer cells. These findings support the concept that VIP may attenuate susceptibility to death from bladder cancer, and that it exerts its effect via downregulation of MIF.

Keywords: vasoactive intestinal peptide gene knockout mice, MB49 murine bladder cancer, mortality, metastases, vasoactive intestinal peptide

INTRODUCTION

Bladder cancer is a disease which affects approximately 600,000 patients in the United States. An estimated 74,000 cases are newly diagnosed each year; and 16,000 patients die from complications due to bladder cancer annually (1). From the time of diagnosis, there is a 77.4% 5-year survival rate (1);

however, survival depends on the stage at the time of diagnosis. Regional lymph node spread at the time of diagnosis yields a 34% 5-year survival. Distant metastases at the time of diagnosis entail a 5%, 5-year survival (1). Treatment often entails a combination of surgery, radiation therapy, and chemotherapy (2).

A potential novel therapeutic agent for bladder cancer is vasoactive intestinal peptide (VIP), which is a 28-amino acid peptide that has multiple therapeutic actions, including bronchodilatory and anti-inflammatory properties (3, 4). VIP inhibits the proliferation of small-cell lung cancer *in vitro* and *in vivo* in mice (5) and has been shown to upregulate nuclear expression of p53 in mouse renal cell carcinomas (6). Loss of expression of p53, a tumor suppressor, and its analogs leads to tumor growth and can also be found in patients with bladder cancer (7, 8). The finding that VIP receptors are present in bladder carcinomas (9) lends support to the concept that we may plausibly treat bladder cancer with VIP.

With the recent availability of VIP knockout (VIP KO) mice, we hypothesized that these animals have enhanced mortality to bladder cancer. VIP KO mice lack the VIP gene and thus do not have endogenous VIP.

Using a mouse bladder cancer cell line, MB49, obtained from Timothy Ratliff (Purdue University College of Veterinary Medicine), we created a model using leg injections of the cancer cells to test whether loss of the VIP gene leads to increased mortality and/or morbidity from bladder cancer metastases, compared to control C57BL/6 mice.

We then performed *in vitro* analyses of the effect on VIP on MB49 cells. We hypothesized that VIP would decrease cell growth by decreasing the activity of macrophage inhibitory factor (MIF), a known growth factor in bladder cancer cells (10).

MATERIALS AND METHODS

General Procedures

Using 0.1 mL isoflurane, we anesthetized the VIP KO mice ($n = 11$) at a rate of 4 L/min *via* nosecone technique. We subsequently injected anesthetized animals with 0.1 mL (1E-6/100 microliters) MB49 bladder cancer cells in the right hind leg. A control group of untreated VIP KO mice (3 mice) received 0.1 mL 0.9% saline also in the right hind leg. Similarly, we anesthetized 14 C57BL/6 mice with 0.1 mL ketamine/xylazine mixture followed by 0.1 mL (1E-6/100 microliters) MB49 bladder cancer cells in the right hind leg. An untreated group of five C57BL/6 did not receive bladder cancer cells. As approved by the IACUC, mice that expressed any signs of undue distress were euthanized immediately and counted as non-survivors. Mice that did not succumb to death prior to the end of the study were euthanized at the end of the study period.

Animal Assessment

In both cancer-injected VIP KO and C57BL/6 mice, we measured the size of tumors, visible chest wall metastases, and ulcers using a caliper. Both groups of mice were weighed during the course of the study.

Tissue Preparation

Necropsy included lungs, heart, leg, and bladder. Samples were formalin-fixed and embedded in paraffin. 5 μ m sections were cut and stained with hematoxylin & eosin (H&E). Analysis was done with all observers blinded to the conditions.

In Vitro Study

MB49 mouse bladder cancer cells were cultured in RPMI 1640 containing 10% fetal bovine serum, and 1% penicillin/streptomycin (11). The cells were seeded in 35 mm dishes at a density of 10^4 cells per well, and cultured for 5 days at 37°C in a 5% CO₂ atmosphere, in the presence or absence of VIP. At the end of the culture period, the adherent cells in each culture vessel were counted, and expressed as a percentage of control (no VIP). Cell culture medium was collected and assayed for the concentration of macrophage MIF using a commercially available ELISA (R&D Systems, Minneapolis, MN, USA).

Statistical Analysis

A Kaplan–Meier curve was constructed to compare mortality rates between VIP KO and C57BL/6 mice.

RESULTS

Tumor Burden Effects on Animal Weight

Over a period of 5 weeks, 6 out of 11 (55%) VIP KO mice experienced slight weight loss, and the remaining mice experienced weight gain. While the majority of this weight gain was slight, one of the VIP KO mice (9%) had a significant weight gain by comparison (approximately 13 g). Similarly, the majority of wild-type (WT) mice experienced slight decreases in weight over a period of 4 weeks. However, 3/19 (16%) WT mice experienced a slight increase in weight, and 1 mouse (5%) experienced a significant (approximately 7 grams) increase in weight and 1 mouse (5%) did not change in weight.

The mean weight of the VIP KO mice were less than those of the WT mice at the beginning of the experiments, as previously reported (12). At the time of death, there was no significant change in weight in either group, despite increase in leg girth from tumor growth (Table 1).

Animal Activity and Survivability

Four out of 11 VIP KO mice expired by 5 weeks, including the 4/11 (36%) with leg ulcers. All C57BL/6 mice survived at 4 weeks despite the presence of a tumor in their right legs. Aside from the 5/19 (26%) C57BL/6 mice with ulcerated tumors, the majority of C57BL/6 mice did not particularly appear to be in distress during

TABLE 1 | Weight changes in wild-type (WT) and vasoactive intestinal peptide knockout (KO) mice.

	WT	KO
Average initial weight (g)	32.8	26.3
Average final weight (g)	32.4	27
Average percent change weight	-1	2.75

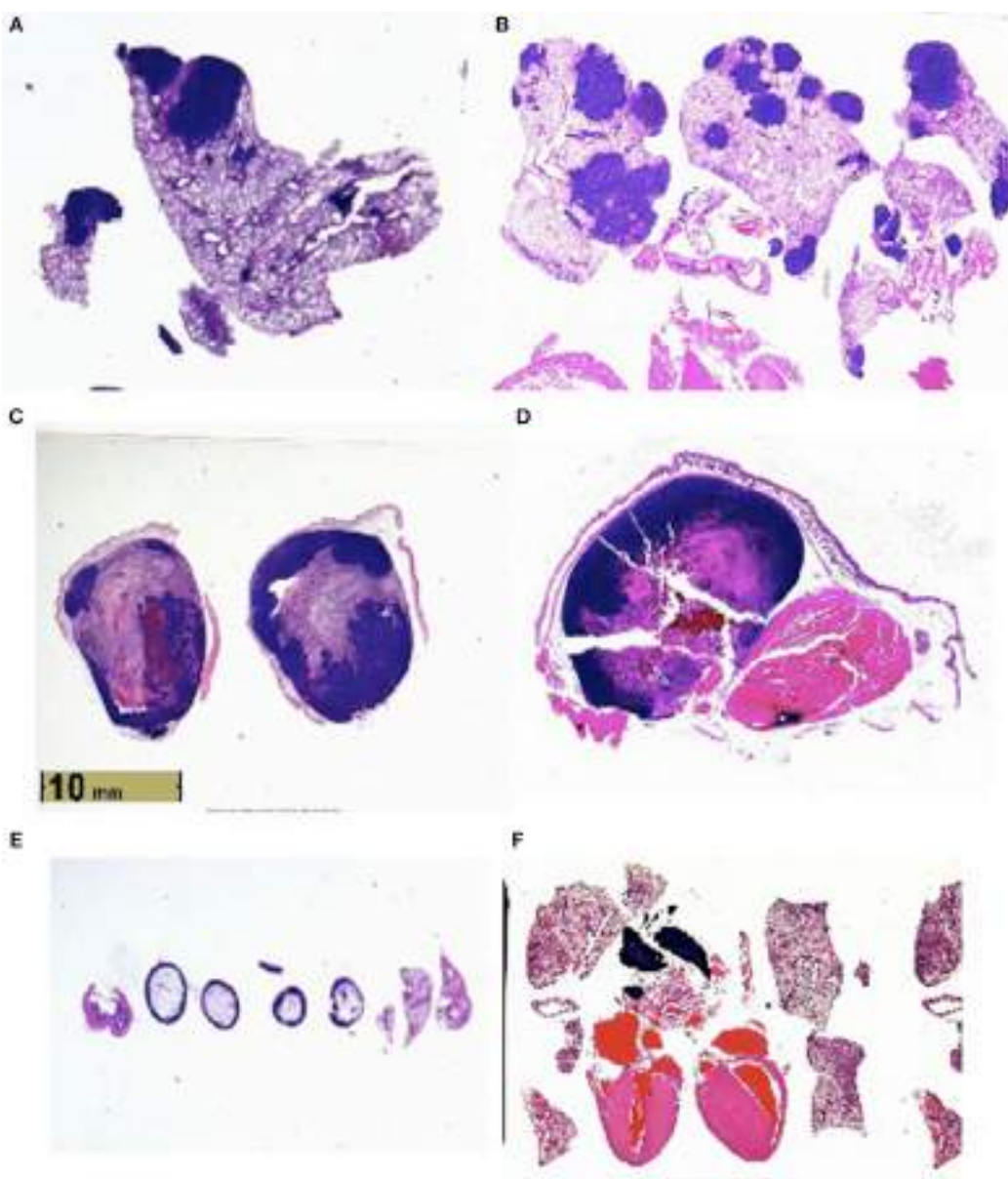


FIGURE 1 | (A) Lung metastases in vasoactive intestinal peptide knockout (VIP KO) mouse. **(B)** Lung metastases in C57BL/6 mouse. **(C)** Leg tumor in VIP KO mouse. **(D)** Leg tumor of C57BL/6 mouse. **(E)** Histology of healthy VIP KO mouse, including lungs. **(F)** Histology of healthy C57BL/6 mouse, including heart and lungs.

the growth of their carcinomas. Most were still mobile but walked with a limp due to the large size of the tumors.

Tumor Progression

Histologic examination (Figure 1) reveals metastases to the lungs, and in certain animals' perithymic, pericardiac, intracardiac, and intravascular lesions.

Tumor Measurement *In Vitro*

MB49 cells grown *in vitro* in the presence of 150 mg/ml VIP showed decreased cell growth when compared to cells grown in

the absence of VIP (Figure 3). Compared to cells grown in the absence of VIP, those grown in the presence of VIP also showed decreased extracellular MIF accumulation (Figure 4), a molecule known to promote proliferation of bladder cancer cells (10).

DISCUSSION

In a previous study, we determined that loss of VIP gene led to increased mortality in association with progressive right ventricular hypertrophy (12). We additionally determined that VIP KO mice have reduced survival at 20 months (100% mortality), as

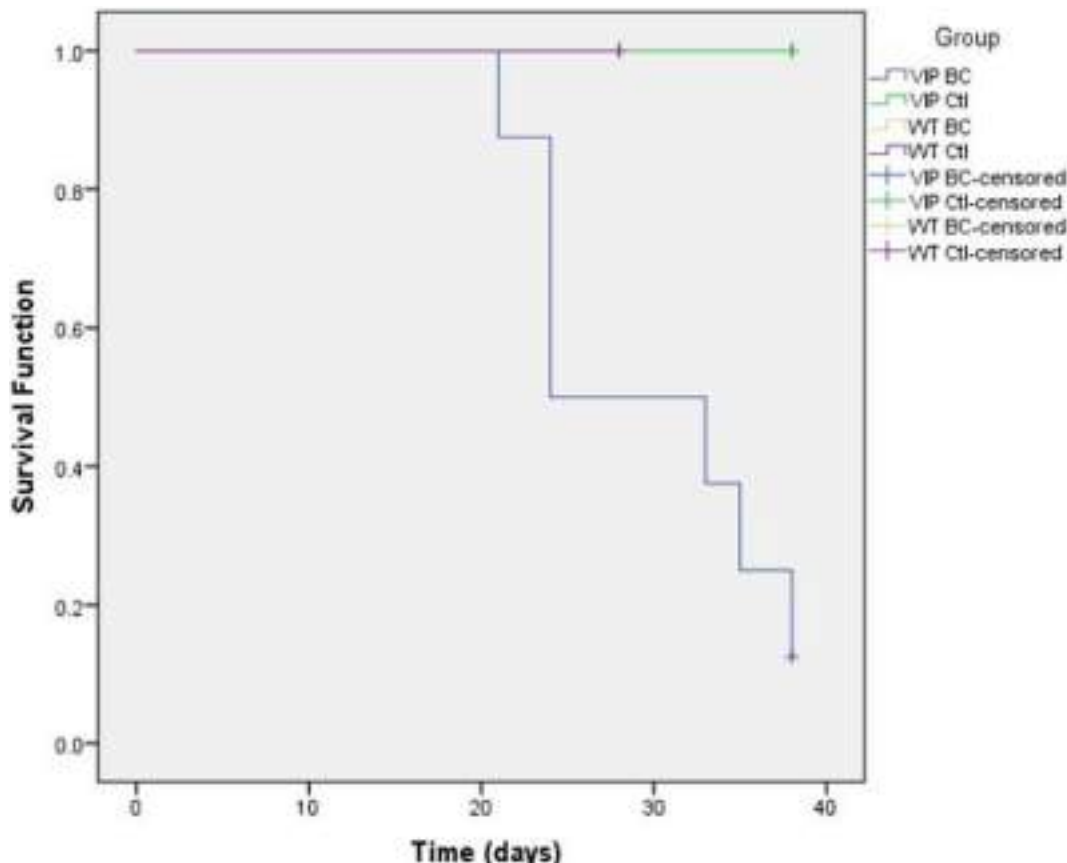


FIGURE 2 | Kaplan–Meier plot comparing death rates between vasoactive intestinal peptide knockout (VIP KO) controls, VIP KO mice with MB49, C57BL/6 controls, and C57BL/6 mice with MB49 ($p = 0.002$).

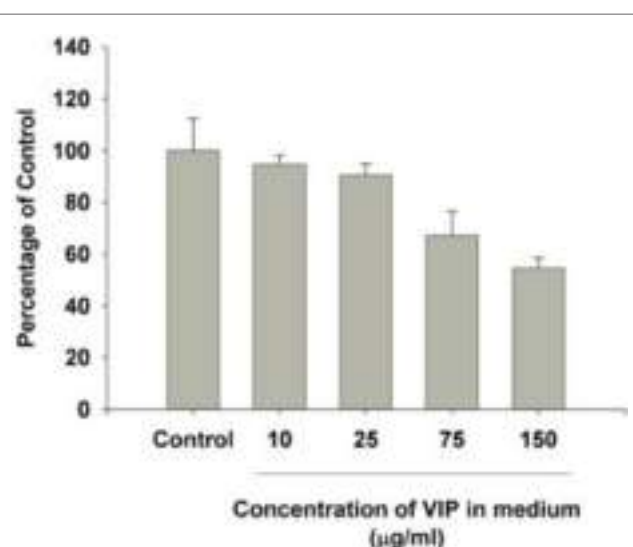
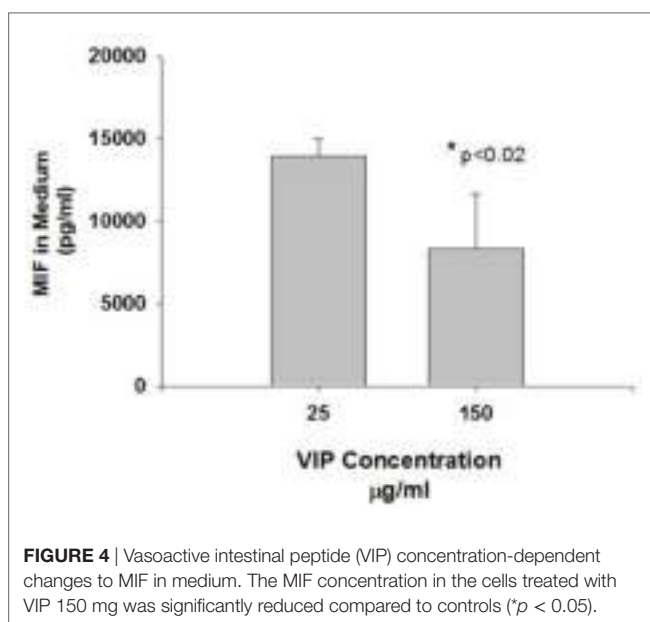


FIGURE 3 | Vasoactive intestinal peptide (VIP) concentration-dependent changes to bladder cancer cell count *in vitro*. The growth in each group was significantly different from control cells grown in the absence of VIP. $p < 0.001$ [multiple comparisons vs. control group (Holm–Šidák method)].

opposed to 100% survival among WT C57BL/6 mice (12). In this study, VIP KO mice have a higher mortality rate with exposure to MB49 bladder cancer cell line than C57BL/6 mice, supporting the concept that VIP inhibits the susceptibility to death from bladder cancer. Additionally, other studies have shown that PAC1, VPAC1, and VPAC2 receptor transcripts were expressed in the urothelium and detrusor smooth muscle of mouse urinary bladder (13), which suggests VIP's potential role in regulating bladder cancer cell growth. We found that administration of VIP to bladder cancer cells cultured *in vitro* led to decreased cell growth, suggesting that the presence of VIP plays a role in regulating bladder cancer cell proliferation, at least in part through VPAC1 receptor. These findings are supported by our *in vitro* data in which VIP induced a dose dependent decrease in the proliferation of the bladder cancer cell line, and reduced the elaboration of MIF, which is known to increase cancer cell proliferation and angiogenesis (10, 14, 15).

In addition, given that the MB49 and C57BL/6 models share similarities with human bladder cancer regarding cell surface markers, sensitivity to apoptosis and immunological profiles (16, 17), our findings lend plausibility to studying whether human patients with late stage bladder cancer have reduced VIP expression in serum compared to those with early stage disease.



Furthermore, in C57BL/6 mice, tumor growth did not seem to change gross mobility or longevity, despite histology showing the spread of cancer to the lungs, heart, vascular and lymphatic systems, and bone of several mice. The Kaplan–Meier plot (Figure 2) shows statistically significantly ($p = 0.002$) increased mortality among VIP KO mice injected with MB49 bladder cancer, whereas all other mice (VIP KO controls, WT controls, and WT mice injected with cancer) survived until the end of term. This increased mortality in VIP KO mice is not associated with an increased number of pulmonary metastases or weight loss or tumor size.

CONCLUSION

Vasoactive intestinal peptide KO mice have enhanced susceptibility to death from MB49 bladder cancer injected in the hind leg. Despite the growth and spread of tumors in both VIP KO and C57BL/6 groups injected with cancer cells, only VIP KO mice died prior to the end of the study. Neither VIP KO controls nor WT controls developed or succumbed to cancer. The Kaplan–Meier analysis further suggests that the lack of endogenous VIP production significantly increases the likelihood of death to cancer. Both VIP KO and C57BL/6 bladder-injected mice had metastases to the lung; however, larger and more numerous metastases were seen in C57BL/6 mice. Vascular invasion was seen in both groups.

Vasoactive intestinal peptide, which currently does not have a therapeutic indication, may potentially be a novel medicine to treat bladder cancer. Further studies into the mechanism of

VIP's action on bladder cancer are nonetheless warranted to understand the full benefit of *in vivo* VIP administration as well as any potential side effects related to dosage.

ETHICS STATEMENT

Stony Brook University's Institutional Animal Care and Use Committee (IACUC) approved this study.

AUTHOR CONTRIBUTIONS

NM and MB were responsible for injection, husbandry and surgery of C57BL/6 mice, data collection, and manuscript preparation. SM prepared slides and performed histological examination on the animal tissue. EF, JL, BD, and DL were responsible for injection and husbandry of VIP KO mice and data collection. JG was responsible for injection of C57BL/6 mice and animal surgery. RN was responsible for data interpretation and manuscript preparation. MP was responsible for injection and husbandry of C57BL/6 mice and data collection. EM, PW, and KL conducted *in vitro* studies and were responsible for data collection and revision of the manuscript. SH analyzed mortality rates between C57BL/6 mice and VIP KO mice and helped revise the manuscript. TR and SC provided MB49 bladder cancer cells. K-IT provided funding and cultured the MB49 bladder cancer cells. AS was responsible for injection, husbandry and surgery of C57BL/6 mice, data collection, manuscript preparation, and supervision of the study.

ACKNOWLEDGMENTS

We would like to thank David Chatenet, Ph.D., and Myriam Létourneau from the *Institut national de la recherche scientifique-Institut Armand-Frappier* for providing VIP for our *in vitro* studies. We would also like to thank John Chen, Ph.D., Professor, Department of Tropical Medicine, Medical Microbiology and Pharmacology at the University of Hawaii for his statistical analysis of our data.

FUNDING

This research was funded by NIH grant R01HL107493-01 to Dr. K. T. Takemaru and Eddie Van Halen to McClain Laboratories. Supported by Three Village Allergy & Asthma, PLLC.

SUPPLEMENTARY MATERIAL

The Supplementary Material for this article can be found online at <http://journal.frontiersin.org/article/10.3389/fendo.2017.00162/full#supplementary-material>.

2. Bethesda M. *National Cancer Institute: PDQ® Bladder Cancer Treatment*. National Cancer Institute (2015). Available from: www.cancer.gov
3. Szema AM, Hamidi SA, Lyubsky S, Dickman KG, Mathew S, Abdel-Razek T, et al. Mice lacking the VIP gene show airway hyperresponsiveness and airway inflammation, partially reversible by VIP. *Am J Physiol Lung Cell Mol Physiol* (2006) 291:L880–6. doi:10.1152/ajplung.00499.2005

REFERENCES

1. Vacas E, Bajo AM, Schally AV, Sánchez-Chapado M, Prieto JC, Carmena MJ. Vasoactive intestinal peptide induces oxidative stress and suppresses metastatic potential in human clear cell renal cell carcinoma. *Mol Cell Endocrinol* (2013) 365:212–22. doi:10.1016/j.mce.2012.10.021

4. Szema AM, Hamidi SA, Golightly MG, Rueb TP, Chen JJ. VIP regulates the development & proliferation of Treg in vivo in spleen. *Allergy Asthma Clin Immunol* (2011) 7:19. doi:10.1186/1710-1492-7-19
5. Maruno K, Said SI. VIP inhibits the proliferation of small-cell and nonsmall-cell lung carcinoma. *Ann N Y Acad Sci* (1996) 805:389–92; discussion 392–3. doi:10.1111/j.1749-6632.1996.tb17499.x
6. Vacas E, Muñoz-Moreno L, Fernández-Martínez AB, Bajo AM, Sánchez-Chapado M, Prieto JC, et al. Signalling pathways involved in antitumoral effects of VIP in human renal cell carcinoma A498 cells: VIP induction of p53 expression. *Int J Biochem Cell Biol* (2014) 53:295–301. doi:10.1016/j.biocel.2014.05.036
7. Urist MJ, Di Como CJ, Lu ML, Charytonowicz E, Verbel D, Crum CP, et al. Loss of p63 expression is associated with tumor progression in bladder cancer. *Am J Pathol* (2002) 161:1199–206. doi:10.1016/S0002-9440(10)64396-9
8. Puzio-Kuter AM, Castillo-Martin M, Kinkade CW, Wang X, Shen TH, Matos T, et al. Inactivation of p53 and Pten promotes invasive bladder cancer. *Genes Dev* (2009) 23:675–80. doi:10.1101/gad.1772909
9. Reubi JC, Läderach U, Waser B, Gebbers JO, Robberecht P, Laisue JA. Vasoactive intestinal peptide/pituitary adenylate cyclase-activating peptide receptor subtypes in human tumors and their tissues of origin. *Cancer Res* (2000) 60:3105–12.
10. Choudhary S, Hegde P, Pruitt JR, Sielecki TM, Choudhary D, Scarpato K, et al. Macrophage migratory inhibitory factor promotes bladder cancer progression via increasing proliferation and angiogenesis. *Carcinogenesis* (2013) 34:2891–9. doi:10.1093/carcin/bgt239
11. Günther JH, Jurczok A, Wulf T, Brandau S, Deinert I, Jocham D, et al. Optimizing syngeneic orthotopic murine bladder cancer (MB49). *Cancer Res* (1999) 59:2834–7.
12. Szema AM, Hamidi SA. Gene deletion of VIP leads to increased mortality associated with progressive right ventricular hypertrophy. *J Cardiovasc Dis* (2014) 2:131–6.
13. Girard BM, Malley SE, Braas KM, May V, Vizzard MA. PACAP/VIP and receptor characterization in micturition pathways in mice with overexpression of NGF in urothelium. *J Mol Neurosci* (2010) 42:378–89. doi:10.1007/s12031-010-9384-3
14. Shimizu T, Abe R, Nakamura H, Ohkawara A, Suzuki M, Nishihira J. High expression of macrophage migration inhibitory factor in human melanoma cells and its role in tumor cell growth and angiogenesis. *Biochem Biophys Res Commun* (1999) 264:751–8. doi:10.1006/bbrc.1999.1584
15. Nobre CC, de Araújo JM, Fernandes TA, Cobucci RN, Lanza DC, Andrade VS, et al. Macrophage migration inhibitory factor (MIF): biological activities and relation with cancer. *Pathol Oncol Res* (2016) 23(2):235–44. doi:10.1007/s12253-016-0138-6
16. Loskog A, Dzovic H, Vikman S, Ninalga C, Essand M, Korsgren O, et al. Adenovirus CD40 ligand gene therapy counteracts immune escape mechanisms in the tumor microenvironment. *J Immunol* (2004) 172:7200–5. doi:10.4049/jimmunol.172.11.7200
17. O'Donnell MA, Luo Y, Hunter SE, Chen X, Hayes LL, Clinton SK. Interleukin-12 immunotherapy of murine transitional cell carcinoma of the bladder: dose dependent tumor eradication and generation of protective immunity. *J Urol* (2004) 171:1330–5. doi:10.1097/01.ju.0000109742.88380.a2

Conflict of Interest Statement: The authors declare that the research was conducted in the absence of any commercial or financial relationships that could be construed as a potential conflict of interest.

Copyright © 2017 Mirsaidi, Burns, McClain, Forsyth, Li, Dukes, Lin, Nahvi, Giraldo, Patton, Wang, Lin, Miller, Ratliff, Hamidi, Crist, Takemaru and Szema. This is an open-access article distributed under the terms of the Creative Commons Attribution License (CC BY). The use, distribution or reproduction in other forums is permitted, provided the original author(s) or licensor are credited and that the original publication in this journal is cited, in accordance with accepted academic practice. No use, distribution or reproduction is permitted which does not comply with these terms.



AM-37 and ST-36 Are Small Molecule Bombesin Receptor Antagonists

Terry W. Moody^{1*}, Nicole Tashakkori¹, Samuel A. Mantey², Paola Moreno², Irene Ramos-Alvarez², Marcello Leopoldo³ and Robert T. Jensen²

¹Department of Health and Human Services, National Cancer Institute, Center for Cancer Research, Bethesda, MD, United States, ²National Institute of Diabetes, Digestive and Kidney Disease, Digestive Diseases Branch, Bethesda, MD, United States, ³Dipartimento di Farmacia, Scienze del Farmaco, Università degli Studi di Bari Aldo Moro, Bari, Italy

OPEN ACCESS

Edited by:

Hubert Vaudry,
University of Rouen, France

Reviewed by:

Miriam Goebel-Stengel,
HELIOS Klinik Zerbst, Germany
Jana Sopkova-de Oliveira Santos,
Centre d'Etudes et de Recherche sur
le Médicament de Normandie
(CERMN), France

*Correspondence:

Terry W. Moody
moodyt@mail.nih.gov

Specialty section:

This article was submitted to
Neuroendocrine Science,
a section of the journal
Frontiers in Endocrinology

Received: 30 November 2016

Accepted: 05 July 2017

Published: 21 July 2017

Citation:

Moody TW, Tashakkori N,
Mantey SA, Moreno P, Ramos-
Alvarez I, Leopoldo M and Jensen RT
(2017) AM-37 and ST-36 Are Small
Molecule Bombesin
Receptor Antagonists.
Front. Endocrinol. 8:176.
doi: 10.3389/fendo.2017.00176

While peptide antagonists for the gastrin-releasing peptide receptor (BB₂R), neuromedin B receptor (BB₁R), and bombesin (BB) receptor subtype-3 (BRS-3) exist, there is a need to develop non-peptide small molecule inhibitors for all three BBR. The BB agonist (BA)1 binds with high affinity to the BB₁R, BB₂R, and BRS-3. In this communication, small molecule BBR antagonists were evaluated using human lung cancer cells. AM-37 and ST-36 inhibited binding to human BB₁R, BB₂R, and BRS-3 with similar affinity ($K_i = 1.4\text{--}10.8 \mu\text{M}$). AM-13 and AM-14 were approximately an order of magnitude less potent than AM-37 and ST-36. The ability of BA1 to elevate cytosolic Ca²⁺ in human lung cancer cells transfected with BB₁R, BB₂R, and BRS-3 was antagonized by AM-37 and ST-36. BA1 increased tyrosine phosphorylation of the EGFR and ERK in lung cancer cells, which was blocked by AM-37 and ST-36. AM-37 and ST-36 reduced the growth of lung cancer cells that have BBR. The results indicate that AM-37 and ST-36 function as small molecule BB receptor antagonists.

Keywords: small molecule antagonists, GRPR, NMBR, bombesin receptor subtype-3, lung cancer

INTRODUCTION

The bombesin (BB) family of peptides is biologically active in the central nervous system (CNS) and periphery. BB, a 14 amino acid peptide isolated from frog skin, has 9 of the 10 same C-terminal amino acids as does human gastrin-releasing peptide (GRP), a 27 amino acid peptide (1). GRP binds with high affinity to the BB₂R, which regulates pruritus, lung development, and gastrin secretion. Neuromedin B (NMB) is a 10 amino acid peptide with 70% sequence homology to the C-terminal of BB. NMB binds with high affinity to the BB₁R and causes satiety, hypothermia, and thyrotropin (TSH) secretion from the pituitary (2). BB receptor subtype-3 (BRS-3) is an orphan receptor with homology to the BB₁R and BB₂R, and binds the universal agonist, BB agonist (BA)1, with high affinity as does the BB₁R and BB₂R (3). Because BRS-3 knockout mice have impaired energy balance, glucose homeostasis, and increased body weight, BRS-3 agonists may function as satiety agents (4). In the CNS, GRP and NMB may act in a paracrine manner being released from brain neurons in the hypothalamus and dentate gyrus, respectively, activating BB₂R and BB₁R in adjacent cells (5).

In numerous cancers, including lung cancer, GRP and NMB function in an autocrine manner to stimulate cellular proliferation. Small cell lung cancer (SCLC), a neuroendocrine tumor, has high levels of GRP (6, 7). GRP is secreted from SCLC and binds to cell surface BB₂R resulting in increased cellular proliferation (8). NMB is present in both SCLC and non-small cell lung cancer (NSCLC) cells, and after secretion it binds to cell surface BB₁R stimulating proliferation (9). Because

many lung cancer cells have BB₁R, BB₂R, and/or BRS-3 there is a need to develop antagonists that block all three receptors of the BB family.

The human BB₁R, BB₂R, and BRS-3 contain 390, 384, and 399 amino acids and have approximately 50% sequence homology. The BB₁R, BB₂R, and BRS-3 are members of the rhodopsin β group G protein-coupled receptors (GPCR) family, and they interact with Gq causing phosphatidylinositol (PI) turnover (10). PI-4,5-bisphosphate (PIP₂) is metabolized to diacylglycerol, which activates protein kinase C and inositol-trisphosphate (IP₃) which causes elevated cytosolic Ca²⁺. Neuropeptide receptors regulate the transactivation of the epidermal growth factor (EGF) receptor leading to NSCLC proliferation (11). The proliferation of NSCLC cells caused by BA1 can be inhibited by the tyrosine kinase inhibitor (TKI) gefitinib or BBR antagonists. The actions of BA1 on BB₁R, BB₂R, and BRS-3 are antagonized selectively by PD168368, PD176252, and Bantag-1, respectively (12).

In the present study, small molecules were synthesized and their ability to antagonize BB₁R, BB₂R, and BRS-3 in lung cancer cells evaluated. The results indicate that AM-37 and ST-36 are useful agents to inhibit the growth of NSCLC cells which have BB₁R, BB₂R, or BRS-3.

MATERIALS AND METHODS

Cell Culture

Non-small cell lung cancer cell line NCI-H1299 (ATCC, Manassas, VA, USA) was stably transfected with BB₁R, BB₂R, and BRS-3. The transfected cells were grown in RPMI-1640 containing 10% fetal bovine serum (FBS) with 0.3 mg/ml geneticin (Invitrogen, Grand Island, NY, USA). The transfected cells, which contained approximately 100,000 receptors/cell, were weekly split using trypsin/EDTA (13). In addition, lung cancer cell lines NCI-H727, H1299, and H1975 were purchased from ATCC and cultured in RPMI-1640, which contained 10% FBS. The cell types were derived from different human biopsy specimens. These studies were approved by the NIDDK biospecimens and biosafety committees.

Ligand Synthesis

The small molecules were synthesized as described previously (14). **Figure 1D** shows the structural formula of AM-37, (R)-3-(1H-indol-3-yl)-2-[3-(4-methoxyphenyl)ureido]-N-[[1-(3-pyridinyl)cyclohexyl]methyl]propanamide, and of its S-enantiomer ST-36. **Figure 1E** shows the structural formula of AM-13, (R)-N-[[1-(4-fluorophenyl)cyclohexyl]methyl]-3-(1H-indol-3-yl)-2-[3-(4-methoxyphenyl)ureido]propanamide, and its S-enantiomer AM-14. The molecular weight of AM-37 and ST-36 is 525.6 Da, whereas the molecular weight of AM-13 and AM-14 is 542.2 Da.

Receptor Binding

The ability of AM-37, ST-36, AM-13, and AM-14 to inhibit specific ¹²⁵I-BA1 binding to NSCLC cells transfected stably with BB₁R, BB₂R, and BRS-3 was investigated. NSCLC cells were placed in 24 well plates. When confluent, the cells were washed three times with PBS. The cells were incubated with

binding buffer (PBS containing 0.25% bovine serum albumin and 0.025% bacitracin, Sigma-Aldrich, St. Louis, MO, USA). Various concentrations of AM-37, ST-36, AM-13, or AM-14 were added to the cells for 10 min, followed by 100,000 cpm of ¹²⁵I-BA1 (0.16 nM) and incubated at 37°C for 30 min when equilibrium of binding was reached. The cells were rinsed three times with binding buffer for 2 min at 4°C. The cells that contained bound peptide dissolved in 0.2 N NaOH and counted in a Wallac 1470 γ-counter. The K_i was calculated as described (15).

Cytosolic Ca²⁺

The ability of AM-37, ST-36, AM-13, and AM-14 to function as BBR antagonists was investigated. NSCLC cells transfected with BB₁R, BB₂R, and BRS-3 were harvested and loaded with Fura-2AM (Calbiochem, La Jolla, CA, USA) as described previously (16). The excitation ratio was determined at 340 and 380 nm with an emission wavelength of 510 nm. The lung cancer cellular calcium response was determined after the addition of AM-37, ST-36, AM-13, or AM-14 followed by 10 nM BA1.

Tyrosine Phosphorylation

The tyrosine phosphorylation of the EGFR and ERK was investigated by western blot. NSCLC cells transfected with BB₁R, BB₂R, and BRS-3 were placed in 10 cm dishes. When the cells were confluent, they were placed in SIT medium (RPMI-1640 containing 3 × 10⁻⁸ M sodium selenite, 5 µg/ml bovine insulin, and 10 µg/ml apo-transferrin; Sigma-Aldrich, St. Louis, MO, USA) for 3 h. AM-37, ST-36, AM-13, or AM-14 were added for 30 min followed by 100 nM BA1 for 2 min. Cell extracts were made as described previously (16), and 600 µg of protein extract was immunoprecipitated with 4 µg anti-phosphotyrosine antibody (Becton Dickinson, USA). The immunoprecipitates were fractionated using a 4–20% polyacrylamide gel (Novex, San Diego, CA, USA). Proteins were transferred to a nitrocellulose membrane and incubated with 2 µg anti-EGFR or anti-ERK antibody (Cell Signaling Technologies, Danvers, MA, USA). After washing the blot, it was incubated with enhanced chemiluminescence detection reagent (Thermo Scientific) for 5 min and exposed to Biomax XAR film (Carestream, Rochester, NY, USA). The band intensity was determined using a Kodak image station 440 densitometer. Alternatively, 20 µg of protein extract was loaded onto polyacrylamide gels and after transfer to nitrocellulose, the blot was probed with anti-PY^{1,068}-EGFR, anti-EGFR, anti-PY²⁰⁴ERK, or anti-ERK (Cell Signaling Technologies, Danvers, MA, USA).

Proliferation

The proliferation of NSCLC cells was investigated using the 3-(4,5-demethylthiazol-2-yl)-2,3-diphenyl-2H-tetrazolium bromide (MTT) assay as described previously (16). NCI-H727, H1299, and H1975 cells were placed in SIT medium and varying concentration of AM-37, ST-36, AM-13, or AM-14 added. After 2 days, 0.1% MTT solution (15 µl) was added. After 4 h, DMSO (150 µl) was added and the absorbance at 570 nm was determined.

Statistical Analysis

The results are expressed as the mean ± SD. Statistical significance of differences was performed by a one-way or two-way

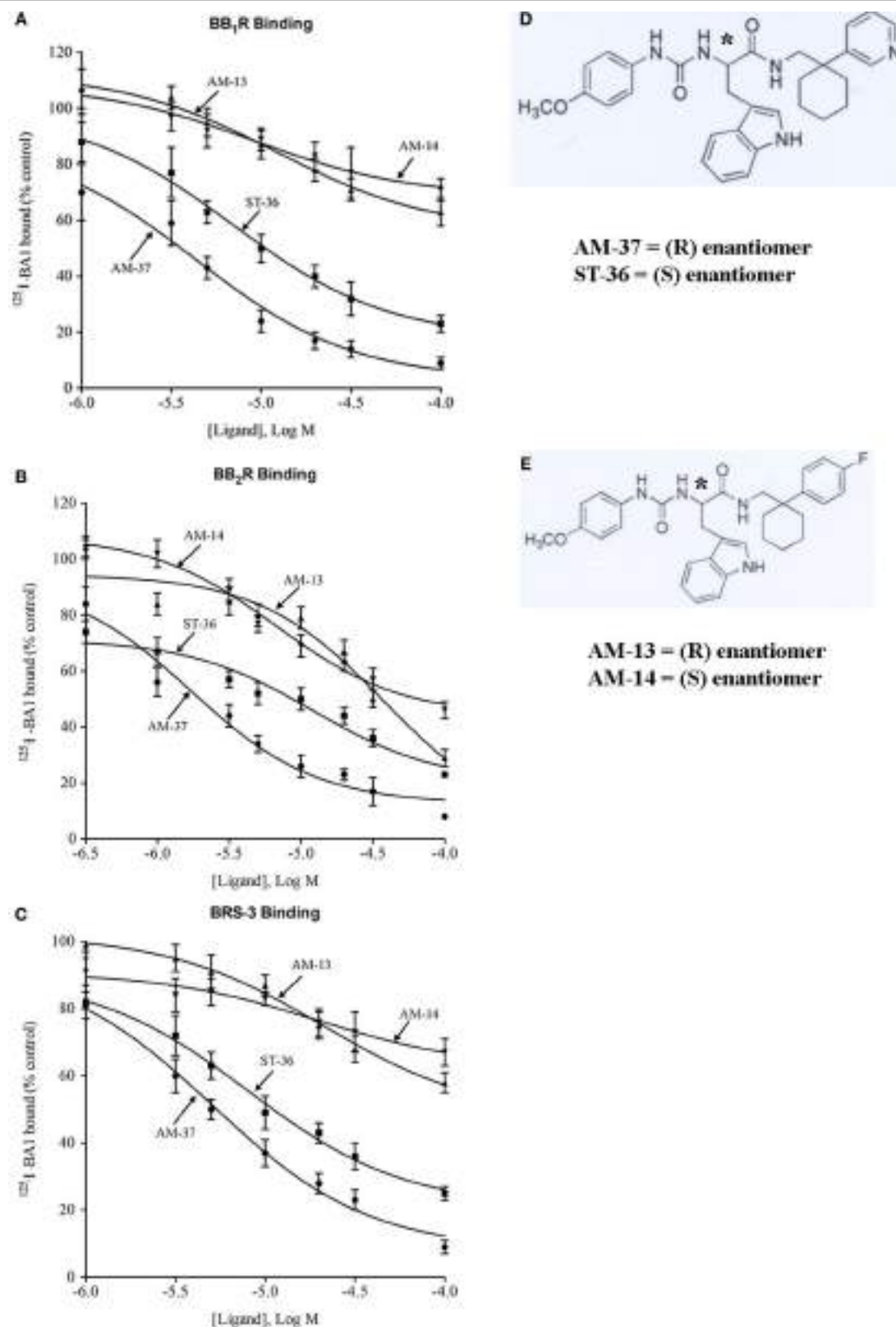


FIGURE 1 | Binding. The ability of varying concentrations of AM-37 (●), ST-36 (■), AM-13 (▲), and AM-14 (▼) to inhibit specific ^{125}I -BA1 binding was investigated using (A) BB₁R-, (B) BB₂R-, and (C) BRS-3-transfected NCI-H1299 cells. The mean value \pm SD of three determinations each repeated in duplicate is shown. (D) The structure of AM-37 and ST-36 is shown. (E) The structure of AM-13 and AM-14 is shown; *indicates the optically active site.

repeated measures of variance. The binding curves were drawn using PRISM.

RESULTS

Receptor Binding

The ability of the small molecules to bind to BB₁R, BB₂R, and BRS-3 was investigated. AM-37 (R-enantiomer) inhibited specific ¹²⁵I-BA1 binding to BB₁R, BB₂R, and BRS-3 in a dose-dependent manner with K_i values 3.6, 1.4, and 5.5 μM, respectively (**Figure 1**). ST-36 (S-enantiomer) inhibited specific ¹²⁵I-BA1 binding to BB₁R, BB₂R, and BRS-3 with K_i values of 7.9, 6.9, and 10.8 μM, respectively (**Figure 1**). In contrast, AM-13 (R-enantiomer) and AM-14 (S-enantiomer) inhibited specific ¹²⁵I-BA1 binding to BB₁R, BB₂R, and BRS-3 with $K_i > 20$ μM. The results indicate that AM-37 and ST-36 bind to BB₁R, BB₂R, and BRS-3 with greater affinity than does AM-13 and AM-14.

The specificity of binding was investigated. **Table 1** shows that BA1 bound with high affinity ($K_i = 0.002$, 0.0005, and 0.004 μM) to BB₁R, BB₂R, and BRS-3. AM-37, ST-36, AM-13, and AM-14 inhibited specific ¹²⁵I-BA1 binding ($K_i = 1.4$, 6.9, 27, and 45 μM) to BB₂R. ST-36 inhibited specific ¹²⁵I-BA1 binding ($K_i = 7.9$ and 10.8 μM) to BB₁R and BRS-3, respectively. AM-13 and AM-14 bind with low affinity to BB₁R and BRS-3 ($K_i > 100$ μM and >100 μM, respectively).

Cytosolic Ca²⁺

The ability of the small molecules to function as BB₁R, BB₂R, and BRS-3 antagonists was investigated. Addition of 10 nM BA1 to NCI-H1299 cells transfected with BB₁R increased the cytosolic Ca²⁺ from 160 to 178 nM within seconds (**Figure 2A**). The response was transient and returned to baseline after 1 min. Addition of 30 μM AM-37 to NCI-H1299 cells transfected with BB₁R had no effect on the basal cytosolic Ca²⁺ but blocked the increase in cytosolic Ca²⁺ caused by BA1 (**Figure 2B**). Addition of 30 μM AM-14 had no effect of basal cytosolic Ca²⁺ but partially blocked the increase caused by 10 nM BA1 (**Figure 2C**). **Table 2** shows that AM-37 and AM-14 significantly inhibited the ability of BA1 to increase cytosolic Ca²⁺ after addition to NCI-H1299 cells transfected with BB₁R. Addition of 10 nM BA1 to NCI-H1299 cells transfected with BB₂R increased the cytosolic Ca²⁺ from 160 to 186 nM (**Figure 2D**). Addition of 30 μM ST-36

to NCI-H1299 cells transfected with BB₂R had no effect on the basal cytosolic Ca²⁺ but blocked the increase in cytosolic Ca²⁺ caused by BA1 (**Figure 2E**). Addition of 30 μM AM-14 had no effect of basal cytosolic Ca²⁺ but partially blocked the increase caused by 10 nM BA1 (**Figure 2F**). **Table 2** shows that ST-36 and AM-14 significantly decreased the ability of 10 nM BA1 to elevate cytosolic Ca²⁺ in NCI-H1299 cells transfected with BB₂R. Addition of 10 nM BA1 to NCI-H1299 cells transfected with BRS-3 increased the cytosolic Ca²⁺ from 170 to 194 nM (**Figure 2G**). Addition of 30 μM ST-36 to NCI-H1299 cells transfected with BRS-3 had no effect on the basal cytosolic Ca²⁺ but blocked the increase in cytosolic Ca²⁺ caused by BA1 (**Figure 2H**). Addition of 30 μM AM-13 had no effect of basal cytosolic Ca²⁺ but partially blocked the increase caused by 10 nM BA1 (**Figure 2I**). **Table 2** shows that ST-36 and AM-13 significantly decreased the ability of 10 nM BA1 to elevate cytosolic Ca²⁺ in NCI-H1299 cells transfected with BRS-3. The results indicate that AM-37 and ST-36 are antagonists for BB₁R, BB₂R, and BRS-3. In contrast, AM-13 and AM-14 are weak antagonists for the BBR family.

The specificity of AM-37, ST-36, AM-13, and AM-14 was investigated. 10 nM neurotensin (NT) or 5 μg/ml ionomycin (ION) strongly increased the cytosolic Ca²⁺ in NSCLC cells. AM-37 or ST-36 had no effect on the ability of NT to increase cytosolic Ca²⁺ in NSCLC cells. AM-13 or AM-14 had no effect on the ability of ION to increase Ca²⁺ in NSCLC cells. Therefore, AM-36 and ST-37 are antagonists for the BBR but not the NTR.

Tyrosine Phosphorylation

The ability of the small molecules to impair EGFR transactivation was investigated. Previously, we found that the BB₁R and BRS-3 regulate EGFR tyrosine phosphorylation (13, 16). **Figure 3** shows that addition of 100 nM BA1 to NCI-H1299 cells transfected with BB₂R increased significantly the EGFR tyrosine phosphorylation to 326%. If the cells were pretreated with 10 μM AM-37 or ST-36, addition of BA1 had little effect. In contrast, if the cells were treated with 10 μM AM-13, BA1 increased strongly EGFR tyrosine phosphorylation. Similarly, BA1 addition to NCI-H1299 cells transfected with BB₂R increased ERK tyrosine phosphorylation to 277%. This increase in ERK tyrosine phosphorylation was decreased significantly in the cells pretreated with AM-37 or ST-36 but not AM-13. Similarly, AM-14 had little effect on EGFR or ERK tyrosine phosphorylation (data not shown). The results indicate that AM-37 and ST-36 antagonize the ability of the BB₂R to regulate tyrosine phosphorylation of the EGFR and ERK. Similar transactivation results were obtained for NSCLC cells transfected with BB₁R or BRS-3 (data not shown).

Proliferation

The ability of the small molecules to inhibit lung cancer proliferation was investigated. AM-37 inhibited NCI-H1299 proliferation in a dose-dependent manner. **Figure 4** shows that AM-37 had little effect at 3 μM but strongly inhibited proliferation at 30 μM. The IC₅₀ for AM-37 was 16 μM. Similarly, ST-36 had an IC₅₀ of 22 μM, whereas AM-14 was less potent (IC₅₀ > 50 μM).

TABLE 1 | Binding to lung cancer cells transfected with human bombesin receptors.

Ligand	K_i , μM		
	BB ₁ R	BB ₂ R	BRS-3
BA1	0.002 ± 0.0002	0.0005 ± 0.0001	0.004 ± 0.0003
AM-37	3.6 ± 0.5	1.4 ± 0.2	5.5 ± 0.6
ST-36	7.9 ± 0.9	6.9 ± 0.3	10.8 ± 0.9
AM-13	>100	27 ± 4	>100
AM-14	>100	45 ± 8	>100

The mean value ± SD of four determinations is indicated. The structure of bombesin agonist 1 is (D-Tyr⁶, β-Ala¹¹, Phe¹³, Nle¹⁴)BB^{6–14}. BRS-3, bombesin receptor subtype-3.

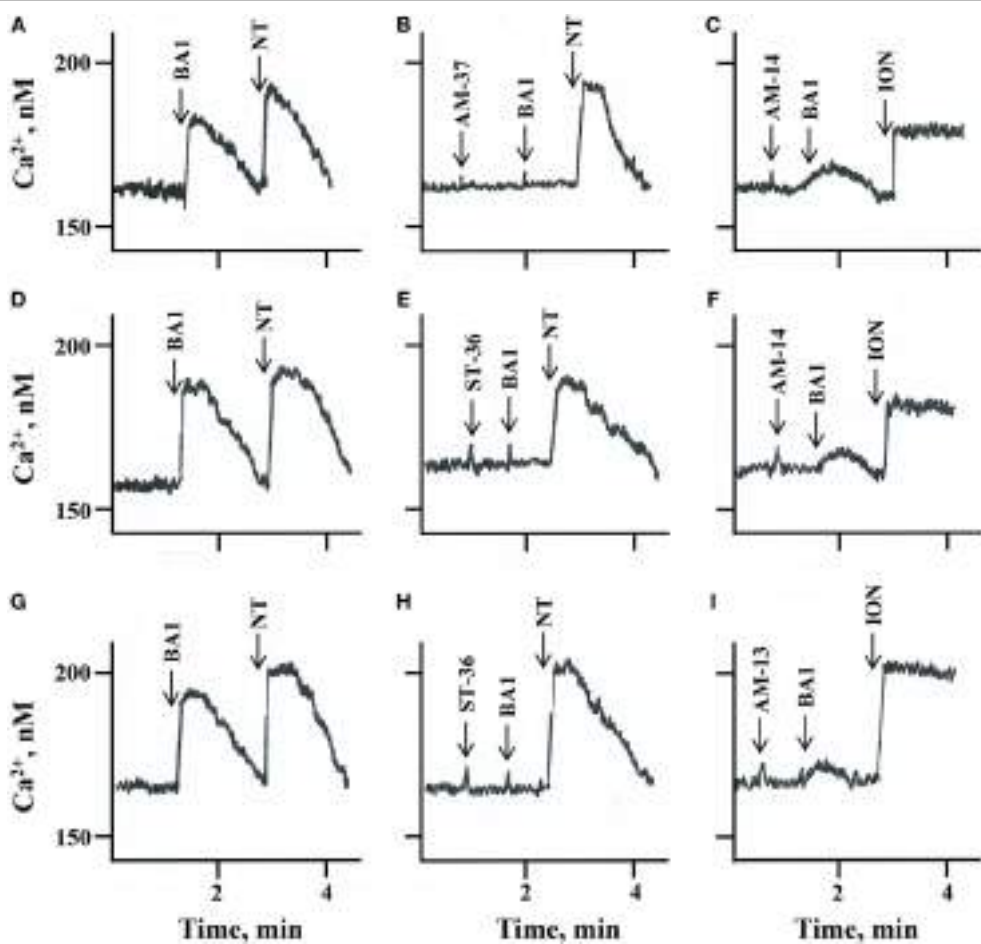


FIGURE 2 | Cytosolic Ca²⁺. The ability of (A) 10 nM bombesin agonist 1 (BA1) and 10 nM neurotensin (NT), (B) 30 μM AM-37 followed by 10 nM BA1 and 10 nM NT, and (C) 30 μM AM-14 followed by 10 nM BA1 and 5 μg/ml ionomycin (ION) to increase cytosolic Ca²⁺ was determined as a function of time after the addition to NCI-H1299 cells transfected with BB₁R. The ability of (D) 10 nM BA1 and 10 nM NT, (E) 30 μM ST-36 followed by 10 nM BA1 and 10 nM NT, and (F) 30 μM AM-14 followed by 10 nM BA1 and 5 μg/ml ION to increase cytosolic Ca²⁺ was determined as a function of time after the addition to NCI-H1299 cells transfected with BB₂R. The ability of (G) 10 nM BA1 and 10 nM NT, (H) 30 μM ST-36 followed by 10 nM BA1 and 10 nM NT, and (I) 30 μM AM-13 followed by 10 nM BA1 and 5 μg/ml ION to increase cytosolic Ca²⁺ was determined as a function of time after the addition to NCI-H1299 cells transfected with bombesin receptor subtype-3. This experiment is representative of three others.

TABLE 2 | Increases in cytosolic Ca²⁺ using human lung cancer cells transfected with bombesin receptors.

Addition	Increase in cytosolic Ca ²⁺ , nM		
	BB ₁ R	BB ₂ R	BRS-3
BA1, 10 nM	18.5 ± 1.1	26.3 ± 1.7	24.4 ± 2.3
BA1 + AM-37, 30 μM	1 ± 0.6 ^a	0 ^a	0 ^a
BA1 + ST-36, 30 μM	0 ^a	0 ^a	0 ^a
BA1 + AM-13, 30 μM	7 ± 0.8 ^a	5 ± 0.6 ^a	2 ± 0.3 ^a
BA1 + AM-14, 30 μM	6 ± 0.6 ^a	6 ± 0.5 ^a	3 ± 0.4 ^a

The initial increase in the cytosolic Ca²⁺ after addition of BA1 to lung cancer cells containing BB₁R, BB₂R, or BRS-3 is indicated. Addition of small molecules significantly inhibited ($p < 0.01$; ^a by ANOVA) the ability of BA1 to increase cytosolic Ca²⁺. This experiment is representative of three others.

BRS-3, bombesin receptor subtype-3; BA1, bombesin agonist 1.

The specificity of the small molecules was investigated. Table 3 shows that AM-37, ST-36, AM-13, and AM-14 (50 μM) inhibited significantly the proliferation of NCI-H727 cells, which have

mRNA for BB₁R, BB₂R, and BRS-3. In contrast, AM-37, ST-36, AM-13, and AM-14 had little effect on NCI-H1975 cells, which lack BB₁R, BB₂R, and BRS-3. These results indicate that the BBR is essential for AM-37, ST-36, AM-13, or AM-14 to inhibit cancer cellular proliferation.

DISCUSSION

While NSCLC patients are traditionally treated with combination chemotherapy, the 5-year survival rate is only 16% (17). Some NSCLC patients (13%) have L858R EGFR mutations, and these patients respond to TKI such as gefitinib or erlotinib; however, secondary EGFR mutations can occur such as T790M resulting in TKI resistance (18). Numerous GPCR are expressed in lung cancer cell lines and biopsy specimens. BB₂R mRNA is expressed in 46–67% of the lung cancer cell lines examined (19). BB₁R mRNA is present in 81% of the NSCLC cell lines examined (20). Using autoradiographic techniques,

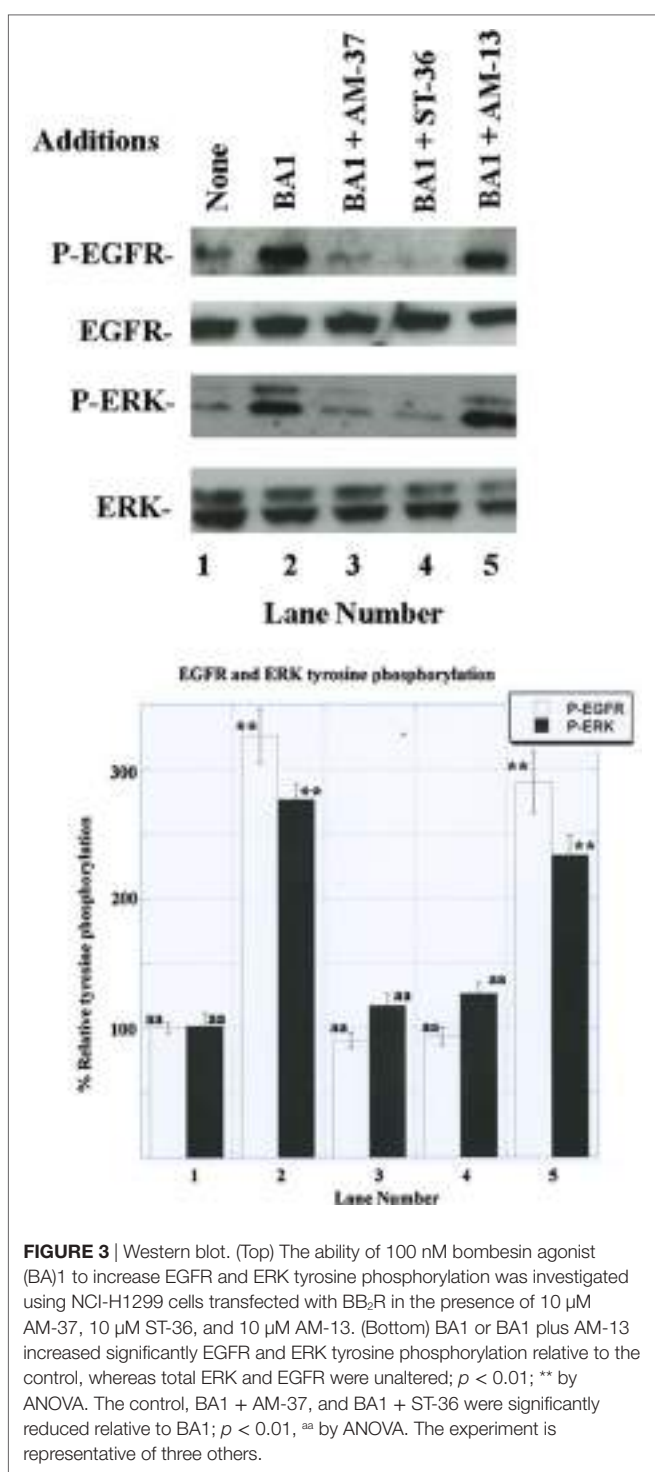


FIGURE 3 | Western blot. (Top) The ability of 100 nM bombesin agonist (BA1) to increase EGFR and ERK tyrosine phosphorylation was investigated using NCI-H1299 cells transfected with BB₂R in the presence of 10 μM AM-37, 10 μM ST-36, and 10 μM AM-13. (Bottom) BA1 or BA1 plus AM-13 increased significantly EGFR and ERK tyrosine phosphorylation relative to the control, whereas total ERK and EGFR were unaltered; $p < 0.01$, ** by ANOVA. The control, BA1 + AM-37, and BA1 + ST-36 were significantly reduced relative to BA1; $p < 0.01$, ^{aa} by ANOVA. The experiment is representative of three others.

BRS-3 binding sites were detected in 40% of the lung cancer biopsy specimens examined (21). The EGFR is abundant on NSCLC (approximately 100,000 EGFR/cell), whereas BBR are present on most native NSCLC cells (approximately 2,000 BBR/cell) (22).

Addition of GRP to NSCLC cells causes transactivation of the EGFR (23). The effects of GRP on NSCLC tyrosine

phosphorylation of the EGFR are impaired by gefitinib, a TKI, and PD176252, a peptoid BB₂R antagonist. Because the ERK and EGFR tyrosine phosphorylation caused by GRP was impaired by marimastat, GM6001 and antibodies to TGF α , matrix metalloproteases may regulate the cellular shedding of TGF α from NSCLC cells. The TGF α may then bind to the EGFR causing its tyrosine phosphorylation. The results indicate that the BB₂R regulates EGFR transactivation in NSCLC cells.

The BB₁R regulates EGFR transactivation (16). The increase in EGFR and ERK tyrosine phosphorylation caused by NMB addition to NSCLC cells was impaired by PD168368, a BB₁R peptoid antagonist, as well as gefitinib. The increase in EGFR tyrosine phosphorylation caused by NMB was impaired by N-acetyl cysteine (NAC), an antioxidant, or tiron, a superoxide scavenger. NMB increased reactive oxygen species (ROS) in NSCLC cells, and the increase was inhibited by Tiron. It remains to be determined if the ROS impair protein tyrosine phosphatases in NSCLC cells, which remove phosphate from the P-EGFR. Activation of BRS-3 with BA1 increased EGFR and ERK tyrosine phosphorylation (13). The increase in EGFR tyrosine phosphorylation caused by BA1 is impaired by NAC, tiron, and diphenyleneiodonium, an inhibitor of NADPH oxidase enzymes.

ML-18 is a small molecule that prefers BRS-3 relative to BB₁R or BB₂R (24). ML-18, an S-enantiomer, inhibits ¹²⁵I-BA1 binding to BRS-3, BB₂R, and BB₁R with IC₅₀ values of 4.8, 16, and >100 μM, respectively, whereas the R-enantiomer EMY-98 is inactive. ML-18 is a BRS-3 antagonist, which inhibits the ability of BA1 to increase cytosolic Ca²⁺, increase ERK and EGFR tyrosine phosphorylation (24). Also, ML-18 inhibited NSCLC growth and increased the cytotoxicity of gefitinib. His¹⁰⁷ is important for BRS-3 to bind antagonists with high affinity (25). Tyr¹⁰¹ of the BB₂R is important for binding of non-peptide antagonists (26). Similarly, this Tyr is conserved in the BB₁R and BRS-3. It remains to be determined if this Tyr is essential for binding of AM-37 to the BB₁R, BB₂R, or BRS-3. ST-36, which is an S-enantiomer, inhibited specific ¹²⁵I-BA1 binding to BB₁R, BB₂R, and BRS-3 with IC₅₀ values of 7.9, 6.9, and 10.8 μM, respectively. It is surprising that AM-37, which is the R-enantiomer, binds with slightly higher affinity to BBR than does ST-36. Previously, the BB₁R was found to prefer PD168,368, which is an S-isomer, relative to the R-isomer (27).

(D-Arg¹, D-Trp^{5,7,9}, Leu¹¹)substance P (SP) is an inhibitor of signal transduction and growth of SCLC cells (28). (D-Arg¹, D-Trp^{5,7,9}, Leu¹¹)SP impaired the ability of BB, vasopressin, or bradykinin to increase cytosolic Ca²⁺ and ERK activity. (D-Arg¹, D-Trp^{5,7,9}, Leu¹¹)SP decreased SCLC growth *in vitro*, and (D-Arg¹, D-Trp^{5,7,9}, Leu¹¹)SP has a unique tertiary structure in with two type IV non-standard turns, which juxtapose the N- and C-terminal adjacent to one another (29). Due to this unique structure (D-Arg¹, D-Trp^{5,7,9}, Leu¹¹)SP may be able to interact with multiple GPCR. In contrast, AM-37 and ST-36 are small molecules that have a different structure from that of (D-Arg¹, D-Trp^{5,7,9}, Leu¹¹)SP.

AM-37 and ST-36 inhibited the proliferation of NSCLC cells such as NCI-H1299 and H727, which have BB₁R, BB₂R, or BRS-3.

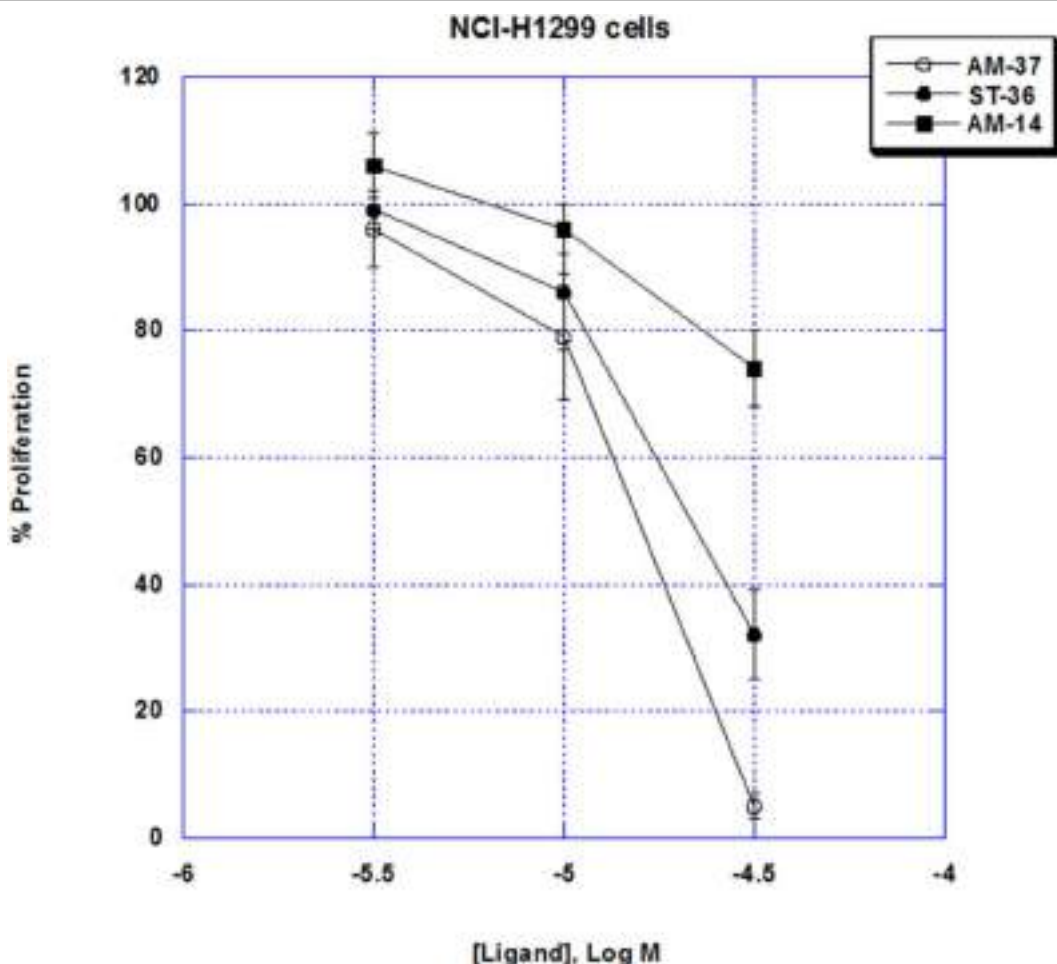


FIGURE 4 | MTT assay. The ability of varying doses of AM-37 (○), ST-36 (●), and AM-14 (■), to inhibit the proliferation of NCI-H1299 cells is shown. The mean value \pm SD of eight determinations is indicated. This experiment is representative of two others.

TABLE 3 | MTT proliferation assay using human lung cancer cell lines.

Addition	% proliferation	
	NCI-H727	NCI-H1975
None	100 \pm 5	100 \pm 6
AM-37, 50 μ M	13 \pm 1 ^{aa}	103 \pm 5
ST-36, 50 μ M	30 \pm 3 ^{aa}	95 \pm 5
AM-13, 50 μ M	67 \pm 4 ^a	89 \pm 5
AM-14, 50 μ M	64 \pm 3 ^a	88 \pm 6

The ability of AM-37, ST-36, AM-13, and AM-14 to inhibit non-small cell lung cancer growth was determined using NCI-H727, which express BB₁R, BB₂R, and bombesin receptor subtype-3 and H1975 cells, which do not express BBR. The mean value \pm SD of eight determinations is indicated. This experiment is representative of two others; ^ap < 0.05, ^{aa}p < 0.01, relative to no additions by ANOVA. Using a test for normality, the data points had a Gaussian distribution.

In contrast, AM-37 and ST-36 have little effect on NSCLC cell line NCI-H1975, which lacks BB₁R, BB₂R, and BRS-3. It remains to be determined if AM-37 or ST-36 are synergistic with gefitinib at inhibiting the growth of NSCLC. A goal is to identify

GPCR antagonists, which potentiate the action of TKI in NSCLC patients.

CONCLUSION

AM-37 and ST-36 are small molecules, which bind to the BB₁R, BB₂R, and BRS-3. Because AM-37 and ST-36 inhibit the ability of BA1 to increase cytosolic Ca²⁺ as well as increase EGFR and ERK tyrosine phosphorylation, they function as BB₁R, BB₂R, and BRS-3 antagonists. A particular advantage of AM-37 and ST-36 is that they will inhibit the growth of NSCLC cells if they have BB₁R, BB₂R, or BRS-3.

AUTHOR CONTRIBUTIONS

TM and SM were responsible for the receptor binding studies. TM and NT were responsible for the cell culture and calcium experiments. TM, PM, and IR-A were responsible for the trans-activation and growth experiments. ML was responsible for the synthesis of the small molecules. TM and RJ were responsible for the writing of the manuscript.

ACKNOWLEDGMENTS

The authors thank Drs. M. Nicklaus, E. Lacivita, D. Venzon, and M. Peach for helpful discussions.

REFERENCES

- Moreno P, Ramos-Alvarez I, Moody TW, Jensen RT. Bombesin related peptides/receptors and their promising therapeutic roles in cancer imaging, targeting and treatment. *Expert Opin Ther Targets* (2016) 20:1055–73. doi:10.1517/14728222.2016.1164694
- Ramos-Alvarez I, Moreno P, Mantey SA, Nakamura T, Nuche-Berenguer B, Moody TW, et al. Insights into bombesin receptors and ligands: highlighting recent advances. *Peptides* (2015) 72:128–44. doi:10.1016/j.peptides.2015.04.026
- Mantey SA, Weber HC, Sainz E, Akeson M, Ryan RR, Pradhan TK, et al. Discovery of a high affinity radioligand for the human orphan receptor, bombesin receptor subtype3, which demonstrates it has a unique pharmacology compared to other mammalian bombesin receptors. *J Biol Chem* (1997) 272:26062–71. doi:10.1074/jbc.272.41.26062
- Majumdar ID, Weber HC. Appetite-modifying effects of bombesin receptor subtype-3 agonists. *Handb Exp Pharmacol* (2012) 209:405–32. doi:10.1007/978-3-642-24716-3_19
- Moody TW, Merali Z. Bombesin-like peptides and associated receptors within the brain: distribution and behavioral implications. *Peptides* (2004) 25:511–20. doi:10.1016/j.peptides.2004.02.012
- Moody TW, Pert CB, Gazdar AF, Carney DN, Minna JD. High levels of intracellular bombesin characterize human small-cell lung carcinoma. *Science* (1981) 214:1246–8. doi:10.1126/science.6272398
- Wood SM, Wood JR, Ghatei MA, Lee YC, O'Shaughnessy D, Bloom SR. Bombesin, somatostatin and neuropeptidyl-like immunoreactivity in bronchial carcinoma. *J Clin Endocrinol Metab* (1981) 53:1310–2. doi:10.1210/jcem-53-6-1310
- Cuttitta F, Carney DN, Mulshine J, Moody TW, Fedorko J, Fischler A, et al. Bombesin-like peptides can function as autocrine growth factors in human small cell lung cancer. *Nature* (1985) 316:823–6. doi:10.1038/316823a0
- Giaccone G, Battey J, Gazdar AF, Oie H, Draoui M, Moody TW. Neuropeptidyl B is present in lung cancer cell lines. *Cancer Res* (1993) 52:2732s–6s.
- Moody TW, Moreno P, Jensen RT. Neuropeptides as lung cancer growth factors. *Peptides* (2015) 72:106–11. doi:10.1016/j.peptides.2015.03.018
- Moody TW, Nuche-Berenguer B, Nakamura T, Jensen RT. EGFR transactivation by peptide G protein-coupled receptors in cancer. *Curr Drug Targets* (2016) 17:520–8. doi:10.2174/138945011666150107153609
- Jensen RT, Battey JF, Spindel ER, Benya RV. Mammalian bombesin receptors: nomenclature, distribution, pharmacology, signaling and functions in normal and disease states. *Pharmacol Rev* (2008) 60:1–42. doi:10.1124/pr.107.07108
- Moody TW, Sancho V, Di Florio A, Nuche-Berenguer B, Mantey SA, Jensen RT. Bombesin receptor subtype-3 agonists stimulate the growth of lung cancer cells and increase EGF receptor tyrosine phosphorylation. *Peptides* (2011) 32:1677–84. doi:10.1016/j.peptides.2011.06.011
- Lacivita E, Schepetkin IA, Stama ML, Kirpotina LN, Colabufo NA, Perrone R, et al. Novel 3-(1H-indoyl-3-yl)-2-[3-(4-methoxyphenyl)ureido] propanamides as selective agonist of human formyl-peptide receptor2. *Bioorg Med Chem* (2015) 23:3913–24. doi:10.1016/j.bmc.2014.12.007
- Chang Y, Prusoff WH. Relationship between the inhibition constant (K_I) and the concentration of inhibitor which causes 50% inhibition (I₅₀) of an enzymatic reaction. *Biochem Pharmacol* (1973) 22:3099–108. doi:10.1016/0006-2952(73)90196-2
- Moody TW, Berna MJ, Mantey S, Sancho V, Ridnour L, Wink DA, et al. Neuromedin B receptors regulate EGF receptor tyrosine phosphorylation in lung cancer cells. *Eur J Pharmacol* (2010) 637:38–45. doi:10.1016/j.ejphar.2010.03.057
- Kaufman J, Horn L, Carbone D. Molecular biology of lung cancer. In: DeVita W Jr, Lawrence T, Rosenberg SA, editors. *Cancer: Principles and Practice of Oncology*. Philadelphia: Lippincott, Williams & Wilkins (2011). p. 789–98.
- Lopes GL, Vattimo EF, Castro Junior GD. Identifying activating mutations in the EGFR gene: prognostic and therapeutic implications in non-small cell lung cancer. *J Bras Pneumol* (2015) 41:365–75. doi:10.1590/S1806-37132015000004531
- Corjay M, Dobrzański DJ, Way JM, Viallet J, Shapira H, Worland P, et al. Two distinct bombesin receptor subtypes are expressed and functional in human lung carcinoma cells. *J Biol Chem* (1991) 266:18771–9.
- Siegfried JM, Krishnamachary N, Gaither Davis A, Gubish C, Hunt JD, Shriver SP. Evidence for autocrine actions of neuromedin B and gastrin-releasing peptide in non-small cell lung cancer. *Pulm Pharmacol Ther* (1999) 12:291–302. doi:10.1006/pupt.1999.0210
- Reubi JC, Wenger S, Schmuckli-Mauer J, Schaefer JC, Gugger M. Bombesin receptor subtypes in human cancers: detection with the universal radioligand [¹²⁵I]-[D-Tyr⁶, β-Ala¹¹, Phe¹³, Nle¹⁴]bombesin(6–14). *Clin Cancer Res* (2002) 8:11139–46.
- Moody TW, Lee M, Kris RM, Bellot F, Bepler G, Oie H, et al. Lung carcinoid cell lines have bombesin-like peptides and EGF receptors. *J Cell Biochem* (1990) 43:139–47. doi:10.1002/jcb.240430205
- Thomas SM, Grandis JR, Wentzel AL, Gooding WE, Lui VWY, Siegfried JM. Gastrin-releasing peptide receptor mediates activation of the epidermal growth factor receptor in lung cancer cells. *Neoplasia* (2006) 7:426–31. doi:10.1593/neo.044454
- Moody TW, Mantey SA, Moreno P, Nakamura T, Lacivita E, Leopoldo M, et al. ML-18 is a non-peptide bombesin receptor subtype-3 antagonist which inhibits lung cancer growth. *Peptides* (2015) 64:55–61. doi:10.1016/j.peptides.2014.12.005
- Nakamura T, Ramos-Alvarez I, Iordanskaia T, Moreno P, Mantey SA, Jensen RT. Molecular basis for high affinity and selectivity of peptide antagonists, Bantag-1, for the orphan BB3 receptor. *Biochem Pharmacol* (2016) 115:64–76. doi:10.1016/j.bcp.2016.06.013
- Carrieri A, Lacivita E, Danilo Belviso B, Caliandro R, Mastorilli P, Gallo V, et al. Structural determinants in the binding of BB2 receptor ligands: in silico, x-ray and NMR studies in PD176252 analogues. *Curr Top Med Chem* (2017) 17:1599–610. doi:10.2174/156802661766161104102459
- Ashwood V, Brownhill V, Higginbottom M, Horwell D, Hughes J, Lewthwaite A, et al. PD176252—the first high affinity non-peptide gastrin-releasing peptide (BB2) receptor antagonist. *Bioorg Med Chem Lett* (1996) 8:2589–94. doi:10.1016/S0960-894X(98)00462-4
- Seckl MJ, Higgins T, Widner F, Rozengurt E. [D-Arg¹, D-Trp^{5,7,9}, Leu¹¹] substance P, A novel potent inhibitor of signal transduction and growth in vitro and in vivo in small cell lung cancer cells. *Cancer Res* (1997) 57:51–4.
- Jeire DA, Kumar M, Hu WS, Sinnott-Smith J, Rozengurt EA. The lipid-associated 3D structure of SPA, a broad-spectrum neuropeptide antagonist with anticancer properties. *Biophys J* (2006) 91:4478–89. doi:10.1529/biophysj.106.089292

FUNDING

This research was supported by the intramural programs of the NCI and NIDDK of the NIH.

Conflict of Interest Statement: The authors declare that the research was conducted in the absence of any commercial or financial relationships that could be construed as potential conflicts of interest.

Copyright © 2017 Moody, Tashakkori, Mantey, Moreno, Ramos-Alvarez, Leopoldo and Jensen. This is an open-access article distributed under the terms of the Creative Commons Attribution License (CC BY). The use, distribution or reproduction in other forums is permitted, provided the original author(s) or licensor are credited and that the original publication in this journal is cited, in accordance with accepted academic practice. No use, distribution or reproduction is permitted which does not comply with these terms.



Gastrin and Gastric Cancer

Helge L. Waldum^{1,2*}, Liv Sagatun^{1,2} and Patricia Mjønes^{2,3,4}

¹Department of Gastroenterology and Hepatology, St Olav's Hospital, Trondheim, Norway, ²Department of Cancer Research and Molecular Medicine, Faculty of Medicine, Norwegian University of Science and Technology, Trondheim, Norway,

³Department of Pathology, St Olav's Hospital, Trondheim, Norway, ⁴Department of Laboratory Medicine, Children and Women's Health, Norwegian University of Science and Technology, Trondheim, Norway

OPEN ACCESS

Edited by:

Hubert Vaudry,
University of Rouen, France

Reviewed by:

Tullio Florio,
University of Genova, Italy
Joseph Pisegna,
University of California Los Angeles,
USA
Terry Moody,
National Cancer Institute, USA

***Correspondence:**

Helge L. Waldum
helge.waldum@ntnu.no

Specialty section:

This article was submitted to
Neuroendocrine Science,
a section of the journal
Frontiers in Endocrinology

Received: 16 November 2016

Accepted: 03 January 2017

Published: 17 January 2017

Citation:

Waldum HL, Sagatun L and Mjønes P (2017) Gastrin and Gastric Cancer. *Front. Endocrinol.* 8:1.
doi: 10.3389/fendo.2017.00001

Gastric cancer although occurring in reduced frequency is still an important disease, partly because of the bad prognosis when occurring in western countries. This decline in occurrence may mainly be due to the reduced prevalence of *Helicobacter pylori* (Hp) infection, which is the most important cause of gastric cancer. There exist many different pathological classifications of gastric carcinomas, but the most useful seems to be the one by Lauren into intestinal and diffuse types since these types seldom transform into the other and also have different epidemiology. During the nearly 30 years that have passed since the groundbreaking description of Hp as the cause of gastritis and gastric cancer, a continuous search for the mechanism by which Hp infection causes gastric cancer has been done. Interestingly, it is mainly atrophic gastritis of the oxytic mucosa that predisposes to gastric cancer possibly by inducing hypoacidity and hypergastrinemia. There are many arguments in favor of an important role of gastrin and its target cell, the enterochromaffin-like cell, in gastric carcinogenesis. The role of gastrin in gastric carcinogenesis implies caution in the long-term treatment with inhibitors of gastric acid secretion inducing secondary hypergastrinemia, in a common disease like gastroesophageal reflux disease.

Keywords: carcinogenesis, classification of cancer, gastric cancer, gastrin, hormones, neuroendocrine neoplasia

Gastric cancer has been one of the most prevalent cancers and combined with a high mortality, gastric cancer has been among the leading causes of cancer death. However, there has been a continuous decline in the prevalence of gastric cancers during the last decades. Unfortunately, in spite of widespread use of upper gastrointestinal endoscopy, the prognosis in patients affected in the western world has not been much improved. This is in contrast to Japan where gastric cancer often is diagnosed at an early phase allowing removal and a better prognosis (1, 2). This is partly due to special screening programs in Japan having a high prevalence of gastric cancer (1, 2), resulting in diagnoses at a curable stage. In most western countries, the prevalence is much lower (3), and therefore, no such program has been implemented. The cause of the geographical differences in the prevalence of gastric cancer most probably is increased prevalence of *Helicobacter pylori* (Hp) in East Asia as well as a higher frequency of atrophic oxytic gastritis (4). The prognosis of gastric cancer is better in patients from East Asia even when living in the west possibly due to less aggressive biology (5). In this review, we will focus on the role of gastrin in the etiology of gastric cancer and at the same time give an explanation of the decline in frequency. We will only cover cancers originating from epithelial cells (carcinomas) and will not discuss the importance of Epstein–Barr virus that plays a role neither in gastric carcinogenesis (6) nor in human papilloma virus, which has a less established impact (7).

THE GASTRIC MUCOSA

The mucosa of the stomach has traditionally been divided into three parts: the cardiac, the oxyntic, and the antral mucosa. During the last decades, it has, however, been discussed whether the cardiac mucosa occurs normally or represents metaplastic mucosa (8, 9). In the oxyntic mucosa, the highly specialized glands contain the acid-producing parietal cell, the pepsinogen-producing chief cell, and the regulatory, histamine-producing [enterochromaffin-like (ECL)] cell, which are specific for the oxyntic glands. These cells are not found in the antral glands where instead the gastrin-producing G-cell is localized. Previously, a sharp border between the oxyntic and antral mucosa was presumed, but recent work has shown that there is overlap with oxyntic glandular elements occurring in the antral mucosa (10). Nevertheless, taking into consideration the differences between the oxyntic and the antral mucosa, it should be obvious that gastric carcinomas should be classified anatomically according to mucosa of origin and not as presently only into cardiac and distal carcinomas with the latter comprising both oxyntic and antral starting point.

EMBRYOLOGY OF THE GASTRIC MUCOSA

The gastrointestinal tract is derived from the endoderm. Stem cells located at the neck of the glands divide and differentiate into specialized cells while moving into the crypts of the glands (parietal and chief cells) or to the surface becoming specialized cells producing mucus and bicarbonate, which make the gastric mucosa like the mucosa of the duodenal bulb, able to resist the highly acidic and proteolytic gastric juice. There are many regulatory neuroendocrine (NE) cells in the gastric mucosa. The NE cells in man were previously claimed not to divide (11) in contrast to similar cells in rodents (12, 13). Now it is, however, established that NE cells also in man do divide as shown for the β-cell (14) and indirectly for the gastric ECL cell by the selective and concentration-dependent trophic effect by gastrin (15). In the gastric mucosa, the ability to self-replicate is unique to the ECL cell and probably the other NE cells and in contrast to other mucosal cells that are formed by differentiation of cells originating from stem cells. Nevertheless, studies have indicated that also the NE cell originate from a common stem cell (16, 17), and thus not coming from the neural crest as proposed by Pearse and Polak (18) based on the similarities between NE cells at different locations and neural cells. Although there seems to be rather firm evidence for stem cell origin of NE cells in the intestine and the antrum (16, 19), this has not been convincingly shown for NE cells in the oxyntic mucosa.

PROPERTIES OF NE CELLS

Whatever the embryology, the NE cells have a unique position among the mucosal cells in their ability to divide. Moreover, they produce signal substances that affect the function of neighboring cells. The signal substances are delivered *via* a paracrine route or *via* synaptic-like transmission from neuron-resembling projections (20, 21) or reaching cells *via* the blood working as

hormones. The NE cells have secretory granules that may be detected by the general markers belonging to the chromogranins (22), and by cell-specific signal substances such as gastrin, ghrelin, somatostatin, enteroglucagon, and many others. Interestingly from an embryological point of view, the synaptic vesicle marker synaptophysin (23) is found in NE cells in common with neurons. In the gastrointestinal tract, there are about 30–40 different NE cells producing separate signal substances. Although the different types of NE cells look quite similar, most of the NE tumors originate from only a few of them, typically the ECL cell in the stomach and the enterochromaffin (EC) cell in the gut. The reason for this discrepancy in tumourigenicity is not known, but could be related to differences in growth regulation as well as to different signal substances with different effect on surrounding tissue. Thus, not only the function (24) but also the proliferation (25) of the ECL cell in the stomach is regulated by the hormone gastrin. Gastrin is often elevated in gastric hypoacidity either due to atrophic gastritis (26) or drug treatment (27). Moreover, the signal substance of the ECL cell is histamine having profound vascular effects, which presumably may favor invasion and spread. In the small intestine, the serotonin-producing EC cell is the principal cell of origin of NE tumors. The regulation of the EC cell function and proliferation is mainly unknown, but it is possible that the serotonin production *via* its vascular effects is the cause of invasion and spread at an early phase, which is in many ways a hallmark of this tumor. Although the NE cells do proliferate, they do so very slowly which was the background for the dispute whether they divide or not (11, 28). The slow proliferation of normal NE cells is reflected in the relatively benign course of NE tumors where the patient may live asymptotically for more than a decade with such a tumor or the first metastasis may manifest itself after more than two decades.

PREDISPOSING CONDITIONS FOR GASTRIC CANCER

Gastritis with metaplasia has for long been known to predispose to gastric cancer (29). In fact, it was shown that gastric cancer virtually only occurred in stomachs with gastritis (29). When Hp was shown to be the cause of most types of gastritis (30), it was natural to examine the role of Hp in gastric cancer, and it was soon shown to be the most important etiological factor of this malignancy (31). Very recently, a meta-analysis showed that Hp eradication reduced the risk of gastric cancer (32). However, also the other type of gastritis, the so-called autoimmune gastritis affecting only the oxyntic mucosa predisposes to gastric cancer (33). Thus, it seems that the gastritis and not Hp itself is the carcinogenic mechanism. Nevertheless, throughout the 25 years since the description of Hp as the cause of gastritis (30) and gastric carcinoma (31), there have been numerous studies on the mechanism by which Hp induces gastric carcinoma, all of them without success. When Hp gastritis is confined to the antral mucosa, it predisposes to duodenal ulcer (34), but not to gastric carcinoma. On the contrary, it is well known that duodenal ulcer in a way protects against development of gastric carcinoma (35). The risk of gastric carcinoma increases only when the gastritis affects the oxyntic mucosa (36) and mainly when oxyntic atrophy

has developed (36). The presence of oxytic gastric atrophy may indirectly be assessed by low serum pepsinogen I (37) and even better when combined with determination of gastrin (38). In atrophic gastritis, intestinal metaplasia may with time develop (39). Intestinal metaplasia has been associated with an additional cancer risk but could also just reflect long-standing oxytic atrophy as patients with intestinal metaplasia are older than those with oxytic atrophy without intestinal metaplasia (39, 40). Anyhow, the sequence in gastric carcinogenesis postulated by Correa where the mucosa goes through phases of gastritis, atrophic gastritis, intestinal metaplasia, dysplasia of different degrees, and finally neoplasia has had great impact for a long time (41). However, in a recent Swedish study, there was little difference in risk of gastric cancer between patients with atrophic gastritis and those with intestinal metaplasia (42). As in other parts of the gastrointestinal tract, polyps in the stomach may predispose to gastric carcinomas, although the polyp carcinoma sequence in the stomach is much less typical than in the colon. Typically, the adenomatous polyps, which are rather seldom, are the polyps with the highest malignant potential. To be complete, it has to be added that ECL cell-derived neuroendocrine tumors (NETs) are associated with both Hp infectious gastritis (43) and autoimmune gastritis (44). Mutation in the gene CDH1 coding for E-cadherin predisposes to gastric carcinoma of diffuse type (45), and quite recently missense mutation of one of the genes of the proton pump, resulting in an acidity from birth was reported to give ECL cell-derived NETs of different degree of malignancy at an early age (46, 47).

CLASSIFICATION OF GASTRIC CARCINOMAS

Quite recently, a molecular classification of gastric carcinomas based on occurrence of mutations was described (48). Although such a system may have impact on the choice of treatment at the time of classification, it may not tell much about the cell of origin, which is mandatory for understanding of carcinogenesis and prophylaxis of tumors. In that respect, older histological classifications may be more useful.

There are many classification systems for gastric carcinomas, but the system proposed by Lauren seems to be the most relevant (49). Thus, his classification into intestinal and diffuse types where the intestinal type shows glandular structures, whereas the diffuse type lacks such differentiation is increasingly used most likely because the carcinomas do not transform into each other over time (49). In fact, the stable phenotype of the carcinomas during the course of the disease may suggest important biological differences that are supported by different epidemiology for the types of cancer (50). The main weakness with Lauren's classification is that about 15% of the carcinomas are difficult to classify due to overlapping traits (49). Although gastric carcinomas of diffuse type lack a hallmark of adenocarcinomas (glandular growth pattern), they have nevertheless been classified as adenocarcinomas due to presumed mucin content of the cancer cells (49). The presence of mucin has been based on PAS positivity. However, PAS positivity is an unspecific histochemical method

reacting with glycoproteins/peptides in general (51), and we have shown that the diffuse gastric carcinomas with the highest content of PAS positive material, the signet ring cells, are positive for NE markers both by immunohistochemistry (52) and *in situ* hybridization (53). In general, gastric carcinomas of diffuse type often show NE differentiation (54, 55), and it might be that this type actually is a NE carcinoma (Figure 1). In this context, it should be recalled that it has for long been known that NETs (formerly called carcinoids) can show glandular growth pattern (56, 57) and mucin positivity (58). Since the gastric carcinomas with endocrine differentiation (which mainly are of diffuse type), more specifically seem to be of ECL cell origin (59), the principal regulator of ECL cell function as well as growth, gastrin, naturally becomes of central interest in gastric carcinogenesis.

GASTRIN AND GASTRIC NETS

More than 30 years ago, gastrin was realized to induce gastric NETs in man whether due to gastrinoma with increased gastric acid secretion (60) or being secondary to hypoacidity

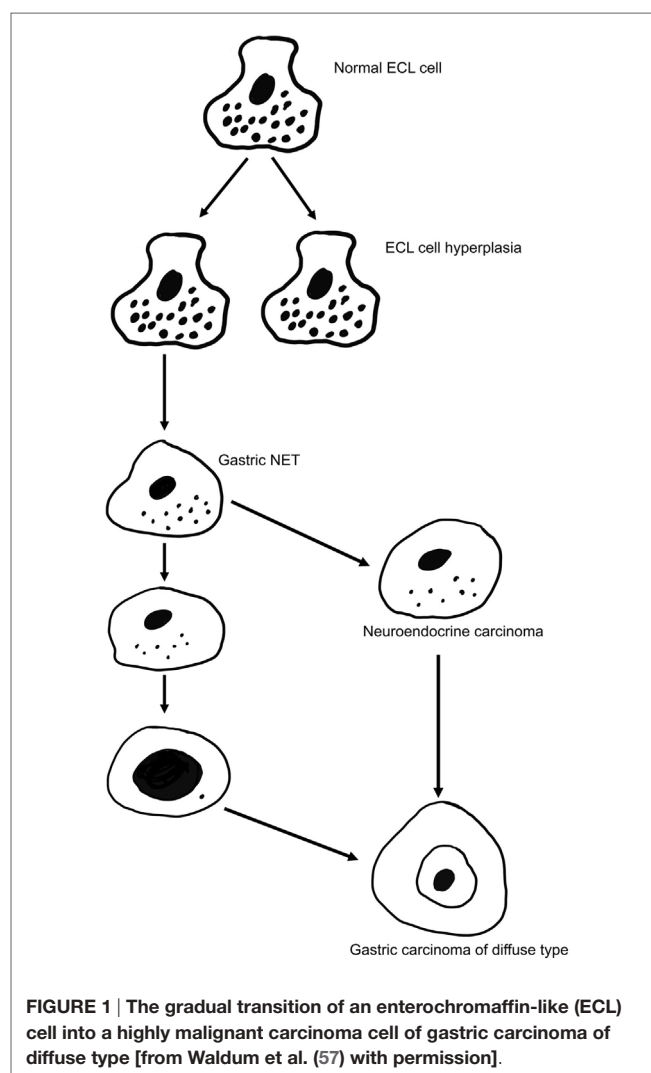


FIGURE 1 | The gradual transition of an enterochromaffin-like (ECL) cell into a highly malignant carcinoma cell of gastric carcinoma of diffuse type [from Waldum et al. (57) with permission].

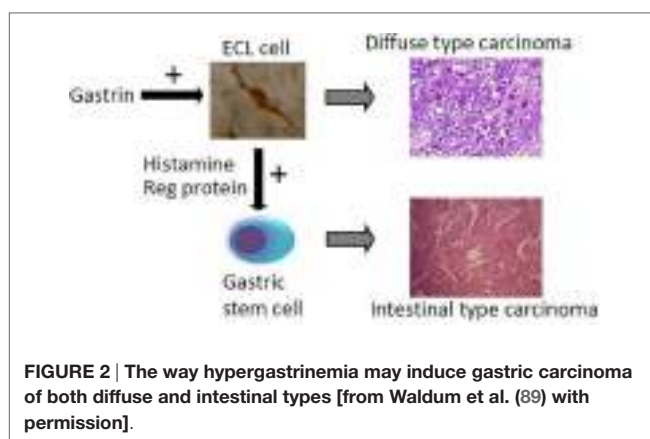
(61) causing Bordi to raise the question whether this was a hormone induced tumor (62). These tumors were regarded as rather benign and also very rare. Gastric NETs were therefore not seen as very important from a clinical point of view. With the description of NETs in the oxyntic mucosa of rodents dosed long term with inhibitors of gastric acid secretion belonging to the histamine receptor-2 blockers (H-2 blockers) like loxidine (63) or the proton pump inhibitors (PPIs) omeprazole (64), the interest increased dramatically since these drugs were so commonly used. It was soon realized that hypergastrinemia was the common pathogenic factor and that the degree and duration of hypoacidity and secondary hypergastrinemia determine the risk of tumor development. Thus, although very high doses of the commonly used H-2 blockers like ranitidine can induce such tumors in rodents (65), the doses used clinically carry little risk since the potency of H-2 blockers in clinical use is too low. Moreover, the tolerance ordinary H-2 blockers induce (66) also protects against long-term marked hypoacidity/hypergastrinemia. Loxidine was the so-called unsurmountable H-2 blocker (63), and this compound was not developed into a drug due to the NETs seen in rodents. The PPIs are very efficient drugs in inhibiting gastric acid secretion (67), but at the same time risky due to hypergastrinemia. Rather early, it was shown that PPI treatment induced ECL cell hyperplasia (68), which caused rebound acid hypersecretion (69). A decade later, it was reported that a period of PPI dosed to healthy individuals induced dyspepsia (70) probably due to rebound acid hypersecretion. Studies based on treatment of PPIs for up to 10 years have not reported occurrence of gastric NETs (71, 72), and thus such treatment has therefore been claimed to be safe with regard to neoplasia. However, it has to be remembered that neoplasia and particularly with respect to tumors originating from NE cells, which are so slow proliferators, may take decades to develop. Moreover, already more than 15 years ago, the producer reported on the occurrence of reversible ECL cell NETs during omeprazole treatment (73), and we (74) and others (75, 76) have reported similar tumors during PPI treatment. Finally, and very importantly, a large kindred from Spain was reported to develop ECL cell tumors of different degree of malignancy at a young age (20s and 30s) due to missense mutation causing lack of function of the proton pump. Thus, the homozygote individuals who all developed tumors had been anacidic and hypergastrinemic from birth (46). Most of the tumors were classified as NETs although one tumor was diagnosed as an adenocarcinoma (46). Later, we have examined these tumors and have concluded that the adenocarcinoma more correctly should have been classified as a NE neoplasm (47). We have also described a gastric NE carcinoma that developed after about 12 years of PPI treatment (77). Oxyntic gastric neoplasia has been reported in all conditions with hypergastrinemia in animals as well as man. It is therefore no doubt that hypergastrinemia may lead to gastric NETs. The dominating role of gastrin in the pathogenesis of gastric NETs is demonstrated by their eradication by the treatment with the gastrin antagonist netazepide (78). We have also demonstrated that treatment with a long-acting somatostatin analog makes gastric NETs disappear or shrink (79). This effect was most probably due to a direct effect on the tumor cells since the reduction

in blood gastrin was only marginal (79). On the other hand, patients operated with antrectomi due to peptic ulcer either as Billroth-I or particularly Billroth-II do develop after long latency carcinomas in the remnant stomach even though they are hypogastrinemic (80). However, not only the ECL cell but also other NE cells in the gastric mucosa could possibly give rise to tumors. Thus, we have described a case where a cancer of the remnant stomach originating from the D cell, developed decades after the Billroth-II procedure (81). It has not yet been examined, but it is conceivable that gastrin has a negative trophic effect on the D cell in the oxyntic mucosa.

GASTRIN AND GASTRIC CARCINOMAS

The main cause of gastric carcinomas is Hp infection (31) and mainly when inducing atrophy of the oxyntic mucosa (36). Atrophic oxyntic gastritis leads to reduced acid secretion, gastric hypoacidity, and secondary hypergastrinemia (26). We have repeatedly shown that gastric carcinomas, especially of diffuse type, express NE markers (54, 55) and more specifically ECL cell markers (59), which incriminate gastrin in the pathogenesis. We have described a patient with pernicious anemia who developed a gastric NET that was removed endoscopically and after 1 year had recurrence of the tumor, resulting in gastrectomy and who died some years later of general metastasis (82). During the 5-year period after the first diagnosis of the gastric NET, the tumor showed progressive loss of NE markers and a dramatic increase in proliferation demonstrating the transition from a gastric NET into a highly malignant carcinoma (82). The close relationship between gastric NETs and gastric carcinomas is also reflected by the co-occurrence of NETs and carcinomas in autoimmune gastritis (83) as well as Hp gastritis predisposing both to gastric cancer (31) and gastric NETs (43). A few studies have reported hypergastrinemia in patients with gastric carcinoma (84–86). The gastric carcinomas of diffuse type quite possibly originate from the ECL cell (54, 55, 59) by dedifferentiation. Carcinomas of intestinal type are also associated to atrophic oxyntic gastritis (87), but this type of gastric carcinoma more seldom express NE markers and therefore more likely develop from the stem cells. However, gastrin may nevertheless be important in the carcinogenic process leading to carcinoma of intestinal type by stimulating the proliferation of the stem cell, either by a possible but not proven gastrin receptor on this cell or indirectly by a positive trophic effect of mediators from the ECL cell, among them Reg protein is the most likely candidate (88) (**Figure 2**).

Since the acknowledgment of the central role of Hp infection in gastric carcinogenesis (31), there has been an unsuccessful search for the mechanism. However, it seems logical to focus on the gastritis since also the so-called autoimmune gastritis predisposes to gastric cancer (33). Moreover, oxyntic gastric atrophy is a common feature in conditions causing gastric cancer (36), and therefore, we recently proposed that hypergastrinemia could be the factor incriminated in Hp gastric carcinogenesis (89). The risk of long-term profound inhibition of gastric acid secretion particularly by the very efficient PPIs is increasingly recognized (90, 91). To conclude this part, gastrin seems to be the most important factor in gastric carcinogenesis.



CONSEQUENCES OF THE DOMINATING ROLE OF GASTRIN IN GASTRIC CARCINOGENESIS

The understanding of the fundamental role of gastrin in gastric carcinogenesis is of clinical importance. Thus, we should avoid long-term treatment particularly in children and young adults due to their long life expectancy, with inhibitors of gastric secretion leading to hypergastrinemia. Presently, long-term treatment with PPI is mainly indicated in patients with gastroesophageal reflux disease (GERD). In young GERD patients, H-2 blocker treatment should be the first choice in order to reach the goals (acceptable symptomatic relief and healing of lesions) at the lowest level of acid inhibition as possible. The alternative of anti-reflux surgery must also be carefully evaluated in these patients.

REFERENCES

- Verdecchia A, Mariotto A, Gatta G, Bustamante-Teixeira MT, Ajiki W. Comparison of stomach cancer incidence and survival in four continents. *Eur J Cancer* (2003) 39:1603–9. doi:10.1016/S0959-8049(03)00360-5
- Suh YS, Yang HK. Screening and early detection of gastric cancer: East versus West. *Surg Clin North Am* (2015) 95:1053–66. doi:10.1016/j.suc.2015.05.012
- Crew KD, Neugut AI. Epidemiology of gastric cancer. *World J Gastroenterol* (2006) 12:354–62. doi:10.3748/wjg.v12.i3.354
- Naylor GM, Gotoda T, Dixon M, Shimoda T, Gatta L, Owen R, et al. Why does Japan have a high incidence of gastric cancer? Comparison of gastritis between UK and Japanese patients. *Gut* (2006) 55:1545–52. doi:10.1136/gut.2005.080358
- Theuer CP, Kurosaki T, Ziogas A, Butler J, Anton-Culver H. Asian patients with gastric carcinoma in the United States exhibit unique clinical features and superior overall and cancer specific survival rates. *Cancer* (2000) 89:1883–92. doi:10.1002/1097-0142(20001101)89:9<1883::AID-CNCR3>3.3.CO;2-8
- Shinozaki-Ushiku A, Kunita A, Fukayama M. Update on Epstein-Barr virus and gastric cancer (review). *Int J Oncol* (2015) 46:1421–34. doi:10.3892/ijo.2015.2856
- Snieters M, Waniczek D, Piglowski W, Kopec A, Nowakowska-Zajdel E, Lorenc Z, et al. Potential role of human papilloma virus in the pathogenesis of gastric cancer. *World J Gastroenterol* (2014) 20:6632–7. doi:10.3748/wjg.v20.i21.6632
- Chandrasoma PT, Der R, Ma Y, Dalton P, Taira M. Histology of the gastroesophageal junction: an autopsy study. *Am J Surg Pathol* (2000) 24:402–9. doi:10.1097/00000478-200003000-00009
- Kilgore SP, Ormsby AH, Gramlich TL, Rice TW, Richter JE, Falk GW, et al. The gastric cardia: fact or fiction? *Am J Gastroenterol* (2000) 95:921–4. doi:10.1111/j.1572-0241.2000.01930.x
- Choi E, Roland JT, Barlow BJ, O’Neal R, Rich AE, Nam KT, et al. Cell lineage distribution atlas of the human stomach reveals heterogeneous gland populations in the gastric antrum. *Gut* (2014) 63:1711–20. doi:10.1136/gutjnl-2013-305964
- Barrett P, Hobbs RC, Coates PJ, Risdon RA, Wright NA, Hall PA. Endocrine cells of the human gastrointestinal tract have no proliferative capacity. *Histochem J* (1995) 27:482–6. doi:10.1007/BF02388805
- Ryberg B, Tielemans Y, Axelson J, Carlsson E, Hakanson R, Mattson H, et al. Gastrin stimulates the self-replication rate of enterochromaffinlike cells in the rat stomach. Effects of omeprazole, ranitidine, and gastrin-17 in intact and antrectomized rats. *Gastroenterology* (1990) 99:935–42. doi:10.1016/0016-5085(90)90610-D
- Tielemans Y, Willem G, Sundler F, Hakanson R. Self-replication of enterochromaffin-like cells in the mouse stomach. *Digestion* (1990) 45:138–46. doi:10.1159/000200235
- Dor Y, Brown J, Martinez OI, Melton DA. Adult pancreatic beta-cells are formed by self-duplication rather than stem-cell differentiation. *Nature* (2004) 429:41–6. doi:10.1038/nature02520
- Delle Fave G, Marignani M, Moretti A, D’Ambra G, Martino G, Annibale B. Hypergastrinemia and enterochromaffin-like cell hyperplasia. *Yale J Biol Med* (1998) 71:291–301.
- Thompson M, Fleming KA, Evans DJ, Fundele R, Surani MA, Wright NA. Gastric endocrine cells share a clonal origin with other gut cell lineages. *Development* (1990) 110:477–81.
- Thompson EM, Price YE, Wright NA. Kinetics of enteroendocrine cells with implications for their origin: a study of the cholecystokinin and gastrin

When PPI treatment is applied, gastrin and chromogranin A, which in this setting are good markers of the ECL cell mass (22, 69, 92), should be monitored. It may in the future be possible to treat young patients with oxytic atrophic gastritis and hypergastrinemia with a gastrin antagonist as prophylaxis against cancer. Furthermore, at which stage of tumor development gastrin loses its effect must be elucidated, in order to determine whether a gastrin antagonist could be used in the treatment. Indirectly, this may be assessed by examination of the tumor cells for the presence of the gastrin receptor either by immunohistochemistry or by *in situ* hybridization.

CONCLUSION

Gastrin and its target cell, the ECL cell, probably play a central role in gastric carcinogenesis.

AUTHOR CONTRIBUTIONS

HW has been the leader of this research throughout many decades. LS has participated in the work during the last years making a thesis on the subject. She has participated active in making the manuscript. PM is a pathologist presently making her doctoral degree on the classification of gastric and renal carcinomas. She has done the evaluation of tumor tissue during the last years and has also participated in the writing of the manuscript.

FUNDING

The funding behind this research has been provided by the hospital and university.

- subpopulations combining tritiated thymidine labelling with immunocytochemistry in the mouse. *Gut* (1990) 31:406–11. doi:10.1136/gut.31.4.406
18. Pearse AG, Polak JM. Neural crest origin of the endocrine polypeptide (APUD) cells of the gastrointestinal tract and pancreas. *Gut* (1971) 12:783–8. doi:10.1136/gut.12.10.783
 19. Andrew A, Kramer B, Rawdon BB. The origin of gut and pancreatic neuroendocrine (APUD) cells – the last word? *J Pathol* (1998) 186:117–8. doi:10.1002/(SICI)1096-9896(1998100)186:2<117::AID-PATH152>3.0.CO;2-J
 20. Larsson LI, Goltermann N, de Magistris L, Rehfeld JF, Schwartz TW. Somatostatin cell processes as pathways for paracrine secretion. *Science* (1979) 205:1393–5. doi:10.1126/science.382360
 21. Gustafsson BI, Bakke I, Hauso O, Kidd M, Modlin IM, Fossmark R, et al. Parietal cell activation by arborization of ECL cell cytoplasmic projections is likely the mechanism for histamine induced secretion of hydrochloric acid. *Scand J Gastroenterol* (2011) 46:531–7. doi:10.3109/00365521.2011.558113
 22. Facer P, Bishop AE, Lloyd RV, Wilson BS, Hennessy RJ, Polak JM. Chromogranin: a newly recognized marker for endocrine cells of the human gastrointestinal tract. *Gastroenterology* (1985) 89:1366–73. doi:10.1016/0016-5085(85)90657-2
 23. Wiedenmann B, Waldherr R, Buhr H, Hille A, Rosa P, Huttner WB. Identification of gastroenteropancreatic neuroendocrine cells in normal and neoplastic human tissue with antibodies against synaptophysin, chromogranin A, secretogranin I (chromogranin B), and secretogranin II. *Gastroenterology* (1988) 95:1364–74. doi:10.1016/0016-5085(88)90374-5
 24. Sandvik AK, Waldum HL, Kleveland PM, Schulze Sognen B. Gastrin produces an immediate and dose-dependent histamine release preceding acid secretion in the totally isolated, vascularly perfused rat stomach. *Scand J Gastroenterol* (1987) 22:803–8. doi:10.3109/00365528708991918
 25. Brenna E, Waldum HL. Trophic effect of gastrin on the enterochromaffin like cells of the rat stomach: establishment of a dose response relationship. *Gut* (1992) 33:1303–6. doi:10.1136/gut.33.10.1303
 26. Korman MG, Strickland RG, Hansky J. Serum gastrin in chronic gastritis. *Br Med J* (1971) 2:16–8. doi:10.1136/bmj.2.5752.16
 27. Pounder R. Changes of plasma gastrin concentration associated with drugs for peptic ulceration. In: Walsh JH, editor. *Gastrin*. New York, NY: Raven Press (1993). p. 319–34.
 28. Waldum HL, Brenna E. Non-proliferative capacity of endocrine cells of the human gastro-intestinal tract. *Histochem J* (1996) 28:397–8. doi:10.1007/BF02331403
 29. Morson BC. Intestinal metaplasia of the gastric mucosa. *Br J Cancer* (1955) 9:365–76. doi:10.1038/bjc.1955.35
 30. Marshall BJ, Warren JR. Unidentified curved bacilli in the stomach of patients with gastritis and peptic ulceration. *Lancet* (1984) 1:1311–5. doi:10.1016/S0140-6736(84)91816-6
 31. Parsonnet J, Friedman GD, Vandersteen DP, Chang Y, Vogelman JH, Orentreich N, et al. *Helicobacter pylori* infection and the risk of gastric carcinoma. *N Engl J Med* (1991) 325:1127–31. doi:10.1056/NEJM199110173251603
 32. Lee YC, Chiang TH, Chou CK, Tu YK, Liao WC, Wu MS, et al. Association between *Helicobacter pylori* eradication and gastric cancer incidence: a systematic review and meta-analysis. *Gastroenterology* (2016) 150:1113–24.e5. doi:10.1053/j.gastro.2016.01.028
 33. Walker IR, Strickland RG, Ungar B, Mackay IR. Simple atrophic gastritis and gastric carcinoma. *Gut* (1971) 12:906–11. doi:10.1136/gut.12.11.906
 34. Levi S, Beardshall K, Haddad G, Playford R, Ghosh P, Calam J. *Campylobacter pylori* and duodenal ulcers: the gastrin link. *Lancet* (1989) 1:1167–8. doi:10.1016/S0140-6736(89)92752-9
 35. Hansson LE, Nyren O, Hsing AW, Bergstrom R, Josefsson S, Chow WH, et al. The risk of stomach cancer in patients with gastric or duodenal ulcer disease. *N Engl J Med* (1996) 335:242–9. doi:10.1056/NEJM199607253350404
 36. Uemura N, Okamoto S, Yamamoto S, Matsumura N, Yamaguchi S, Yamakido M, et al. *Helicobacter pylori* infection and the development of gastric cancer. *N Engl J Med* (2001) 345:784–9. doi:10.1056/NEJMoa001999
 37. Waldum HL, Burhol PG. Serum group I pepsinogens. *Scand J Gastroenterol* (1981) 16:449–51. doi:10.3109/00365528109181996
 38. Sipponen P. Biomarkers in clinical practice: a tool to find subjects at high risk for stomach cancer. A personal view. *Adv Med Sci* (2006) 51:51–3.
 39. Chen XY, van Der Hulst RW, Shi Y, Xiao SD, Tytgat GN, Ten Kate FJ. Comparison of precancerous conditions: atrophy and intestinal metaplasia in *Helicobacter pylori* gastritis among Chinese and Dutch patients. *J Clin Pathol* (2001) 54:367–70. doi:10.1136/jcp.54.5.367
 40. de Vries AC, van Grieken NC, Loosman CW, Casparie MK, de Vries E, Meijer GA, et al. Gastric cancer risk in patients with premalignant gastric lesions: a nationwide cohort study in the Netherlands. *Gastroenterology* (2008) 134:945–52. doi:10.1053/j.gastro.2008.01.071
 41. Correa P. Human gastric carcinogenesis: a multistep and multifactorial process – First American Cancer Society Award Lecture on Cancer Epidemiology and Prevention. *Cancer Res* (1992) 52:6735–40.
 42. Song H, Ekheden IG, Zheng Z, Ericsson J, Nyren O, Ye W. Incidence of gastric cancer among patients with gastric precancerous lesions: observational cohort study in a low risk Western population. *BMJ* (2015) 351:h3867. doi:10.1136/bmj.h3867
 43. Sato Y, Iwafuchi M, Ueki J, Yoshimura A, Mochizuki T, Motoyama H, et al. Gastric carcinoid tumors without autoimmune gastritis in Japan: a relationship with *Helicobacter pylori* infection. *Dig Dis Sci* (2002) 47:579–85. doi:10.1023/A:1017972204219
 44. Hsing AW, Hansson LE, McLaughlin JK, Nyren O, Blot WJ, Ekbom A, et al. Pernicious anemia and subsequent cancer. A population-based cohort study. *Cancer* (1993) 71:745–50. doi:10.1002/1097-0142(19930201)71:3<745::AID-CNCR2820710316>3.0.CO;2-1
 45. Guilford P, Hopkins J, Harraway J, McLeod M, McLeod N, Harawira P, et al. E-cadherin germline mutations in familial gastric cancer. *Nature* (1998) 392:402–5. doi:10.1038/32918
 46. Calvete O, Reyes J, Zuniga S, Paumard-Hernandez B, Fernandez V, Bujanda L, et al. Exome sequencing identifies ATP4A gene as responsible of an atypical familial type I gastric neuroendocrine tumour. *Hum Mol Genet* (2015) 24:2914–22. doi:10.1093/hmg/ddv054
 47. Fossmark R, Calvete O, Mjones P, Benitez J, Waldum HL. ECL-cell carcinoids and carcinoma in patients homozygous for an inactivating mutation in the gastric H(+) K(+) ATPase alpha subunit. *APMIS* (2016) 124:561–6. doi:10.1111/apm.12546
 48. Network TCGAR. Comprehensive molecular characterization of gastric adenocarcinoma. *Nature* (2014) 513:202–9. doi:10.1038/nature13480
 49. Lauren P. The two histological main types of gastric carcinoma: diffuse and so-called intestinal-type carcinoma. An attempt at histo-clinical classification. *Acta Pathol Microbiol Scand* (1965) 64:31–49.
 50. Fuchs CS, Mayer RJ. Gastric carcinoma. *N Engl J Med* (1995) 333:32–41. doi:10.1056/NEJM199507063330107
 51. Karsten FH. The chemistry of Schiff's reagent. In: Bourne GH, editor. *International Review of Cytology*. New York: Academic Press (1960). p. 1–100.
 52. Bakkelund K, Fossmark R, Nordrum I, Waldum H. Signet ring cells in gastric carcinomas are derived from neuroendocrine cells. *J Histochem Cytochem* (2006) 54:615–21. doi:10.1369/jhc.5A6806.2005
 53. Sordal O, Qvigstad G, Nordrum IS, Sandvik AK, Gustafsson BI, Waldum H. The PAS positive material in gastric cancer cells of signet ring type is not mucin. *Exp Mol Pathol* (2014) 96:274–8. doi:10.1016/j.yexmp.2014.02.008
 54. Waldum HL, Aase S, Kvætnoi I, Brenna E, Sandvik AK, Syversen U, et al. Neuroendocrine differentiation in human gastric carcinoma. *Cancer* (1998) 83:435–44. doi:10.1002/(SICI)1097-0142(19980801)83:3<435::AID-CNCR11>3.0.CO;2-X
 55. Waldum H, Haugen O, Isaksen C, Mæcsei R, Sandvik A. Are diffuse gastric carcinomas neuroendocrine tumours (ECL-omas)? *Eur J Gastroenterol Hepatol* (1991) 3:245–9.
 56. Grossi C, Lattes R. Carcinoid tumors of the stomach. *Cancer* (1956) 9:698–711. doi:10.1002/1097-0142(195607/08)9:4<698::AID-CNCR2820090412>3.0.CO;2-I
 57. Waldum HL, Brenna E, Sandvik AK. Relationship of ECL cells and gastric neoplasia. *Yale J Biol Med* (1998) 71:325–35.
 58. Whitehead R, Cosgrove C. Mucins and carcinoid tumours. *Pathology* (1979) 11:473–8. doi:10.3109/00313027909059024
 59. Qvigstad G, Qvigstad T, Westre B, Sandvik AK, Brenna E, Waldum HL. Neuroendocrine differentiation in gastric adenocarcinomas associated with severe hypergastrinemia and/or pernicious anemia. *APMIS* (2002) 110:132–9. doi:10.1034/j.1600-0463.2002.100302.x

60. Solcia E, Capella C, Fiocca R, Rindi G, Rosai J. Gastric argyrophil carcinoidosis in patients with Zollinger-Ellison syndrome due to type 1 multiple endocrine neoplasia. A newly recognized association. *Am J Surg Pathol* (1990) 14:503–13. doi:10.1097/00000478-199006000-00001
61. Borch K, Renwall H, Liedberg G. Gastric endocrine cell hyperplasia and carcinoid tumors in pernicious anemia. *Gastroenterology* (1985) 88:638–48. doi:10.1016/0016-5085(85)90131-3
62. Bordi C, D'Adda T, Pilato FP, Ferrari C. Carcinoid (ECL cell) tumor of the oxytic mucosa of the stomach: a hormone-dependent neoplasm? In: Fenoglio-Preiser C, Wolf M, Rilke R, editors. *Progress in Surgical Pathology*. (Vol. 8), Philadelphia, PA: Field & WOOD (1988). p. 177–95.
63. Poynter D, Pick CR, Harcourt RA, Selway SA, Ainge G, Harman IW, et al. Association of long lasting unsurmountable histamine H₂ blockade and gastric carcinoid tumours in the rat. *Gut* (1985) 26:1284–95. doi:10.1136/gut.26.12.1284
64. Havu N. Enterochromaffin-like cell carcinoids of gastric mucosa in rats after life-long inhibition of gastric secretion. *Digestion* (1986) 35(Suppl 1):42–55. doi:10.1159/000199381
65. Havu N, Mattsson H, Ekman L, Carlsson E. Enterochromaffin-like cell carcinoids in the rat gastric mucosa following long-term administration of ranitidine. *Digestion* (1990) 45:189–95. doi:10.1159/000200245
66. Nwokolo CU, Smith JT, Gaviey C, Sawyerr A, Pounder RE. Tolerance during 29 days of conventional dosing with cimetidine, nizatidine, famotidine or ranitidine. *Aliment Pharmacol Ther* (1990) 4(Suppl 1):29–45.
67. Sharma BK, Walt RP, Pounder RE, Gomes MD, Wood EC, Logan LH. Optimal dose of oral omeprazole for maximal 24 hour decrease of intragastric acidity. *Gut* (1984) 25:957–64. doi:10.1136/gut.25.9.957
68. Lamberts R, Creutzfeldt W, Stockmann F, Jacobaschke U, Maas S, Brunner G. Long-term omeprazole treatment in man: effects on gastric endocrine cell populations. *Digestion* (1988) 39:126–35. doi:10.1159/000199615
69. Waldum HL, Arnestad JS, Brenna E, Eide I, Syversen U, Sandvik AK. Marked increase in gastric acid secretory capacity after omeprazole treatment. *Gut* (1996) 39:649–53. doi:10.1136/gut.39.5.649
70. Reimer C, Sondergaard B, Hilsted L, Bytzer P. Proton-pump inhibitor therapy induces acid-related symptoms in healthy volunteers after withdrawal of therapy. *Gastroenterology* (2009) 137:80–7, 7.e1. doi:10.1053/j.gastro.2009.03.058
71. Laine L, Ahnen D, McClain C, Solcia E, Walsh JH. Review article: potential gastrointestinal effects of long-term acid suppression with proton pump inhibitors. *Aliment Pharmacol Ther* (2000) 14:651–68. doi:10.1046/j.1365-2036.2000.00768.x
72. Lundell L, Vieth M, Gibson F, Nagy P, Kahrilas PJ. Systematic review: the effects of long-term proton pump inhibitor use on serum gastrin levels and gastric histology. *Aliment Pharmacol Ther* (2015) 42:649–63. doi:10.1111/apt.13324
73. Advisory Committee. *Omeprazole Magnesium Tablets*. Wilmington, DE: Astra Zeneca (2000). p. 117–41.
74. Jianu CS, Fossmark R, Viset T, Qvigstad G, Sordal O, Marvik R, et al. Gastric carcinoids after long-term use of a proton pump inhibitor. *Aliment Pharmacol Ther* (2012) 36:644–9. doi:10.1111/apt.12012
75. Cavalcoli F, Zilli A, Conte D, Ciafarini C, Massironi S. Gastric neuroendocrine neoplasms and proton pump inhibitors: fact or coincidence? *Scand J Gastroenterol* (2015) 50:1397–403. doi:10.3109/00365521.2015.1054426
76. Nandy N, Hanson JA, Strickland RG, McCarthy DM. Solitary gastric carcinoid tumor associated with long-term use of omeprazole: a case report and review of the literature. *Dig Dis Sci* (2016) 61:708–12. doi:10.1007/s10620-015-4014-0
77. Jianu CS, Lange OJ, Viset T, Qvigstad G, Martinsen TC, Fougnier R, et al. Gastric neuroendocrine carcinoma after long-term use of proton pump inhibitor. *Scand J Gastroenterol* (2012) 47:64–7. doi:10.3109/00365521.2011.627444
78. Fossmark R, Sordal O, Jianu CS, Qvigstad G, Nordrum IS, Boyce M, et al. Treatment of gastric carcinoids type 1 with the gastrin receptor antagonist netazepide (YF476) results in regression of tumours and normalisation of serum chromogranin A. *Aliment Pharmacol Ther* (2012) 36:1067–75. doi:10.1111/apt.12090
79. Fykse V, Sandvik AK, Qvigstad G, Falkmer SE, Syversen U, Waldum HL. Treatment of ECL cell carcinoids with octreotide LAR. *Scand J Gastroenterol* (2004) 39:621–8. doi:10.1080/00365520410005225
80. Northfield TC, Hall CN. Carcinoma of the gastric stump: risks and pathogenesis. *Gut* (1990) 31:1217–9. doi:10.1136/gut.31.11.1217
81. Waldum HL, Haugen OA, Brenna E. Do neuroendocrine cells, particularly the D-cell, play a role in the development of gastric stump cancer? *Cancer Detect Prev* (1994) 18:431–6.
82. Qvigstad G, Falkmer S, Westre B, Waldum HL. Clinical and histopathological tumour progression in ECL cell carcinoids ("ECLomas"). *APMIS* (1999) 107:1085–92. doi:10.1111/j.1699-0463.1999.tb01513.x
83. Kokkola A, Sjöblom SM, Haapiainen R, Sipponen P, Puolakkainen P, Jarvinen H. The risk of gastric carcinoma and carcinoid tumours in patients with pernicious anaemia. A prospective follow-up study. *Scand J Gastroenterol* (1998) 33:88–92. doi:10.1080/00365529850166266
84. Rakic S, Milicevic MN. Serum gastrin levels in patients with intestinal and diffuse type of gastric cancer. *Br J Cancer* (1991) 64:1189. doi:10.1038/bjc.1991.489
85. Fossmark R, Sagatun L, Nordrum IS, Sandvik AK, Waldum HL. Hypergastrinemia is associated with adenocarcinomas in the gastric corpus and shorter patient survival. *APMIS* (2015) 123:509–14. doi:10.1111/apm.12380
86. McGuigan JE, Trudeau WL. Serum and tissue gastrin concentrations in patients with carcinoma of the stomach. *Gastroenterology* (1973) 64:22–5.
87. El-Zimaity HM, Ota H, Graham DY, Akamatsu T, Katsuyama T. Patterns of gastric atrophy in intestinal type gastric carcinoma. *Cancer* (2002) 94:1428–36. doi:10.1002/cncr.10375
88. Fukui H, Kinoshita Y, Maekawa T, Okada A, Waki S, Hassan S, et al. Regenerating gene protein may mediate gastric mucosal proliferation induced by hypergastrinemia in rats. *Gastroenterology* (1998) 115:1483–93. doi:10.1016/S0016-5085(98)70027-7
89. Waldum HL, Hauso O, Sordal OF, Fossmark R. Gastrin may mediate the carcinogenic effect of *Helicobacter pylori* infection of the stomach. *Dig Dis Sci* (2015) 60:1522–7. doi:10.1007/s10620-014-3468-9
90. Waldum HL, Hauso O, Brenna E, Qvigstad G, Fossmark R. Does long-term profound inhibition of gastric acid secretion increase the risk of ECL cell-derived tumors in man? *Scand J Gastroenterol* (2016) 51:1–7. doi:10.3109/00365521.2016.1143527
91. Aronson JK. Inhibiting the proton pump: mechanisms, benefits, harms, and questions. *BMC Med* (2016) 14:172. doi:10.1186/s12916-016-0724-1
92. Sanduleanu S, De Bruine A, Stridsberg M, Jonkers D, Biemond I, Hameeteman W, et al. Serum chromogranin A as a screening test for gastric enterochromaffin-like cell hyperplasia during acid-suppressive therapy. *Eur J Clin Invest* (2001) 31:802–11. doi:10.1046/j.1365-2362.2001.00890.x

Conflict of Interest Statement: The research behind this publication has been conducted in the absence of any commercial or financial relationship that could be construed as a potential conflict of interest.

Copyright © 2017 Waldum, Sagatun and Mjønes. This is an open-access article distributed under the terms of the Creative Commons Attribution License (CC BY). The use, distribution or reproduction in other forums is permitted, provided the original author(s) or licensor are credited and that the original publication in this journal is cited, in accordance with accepted academic practice. No use, distribution or reproduction is permitted which does not comply with these terms.



Receptor-Mediated Melanoma Targeting with Radiolabeled α -Melanocyte-Stimulating Hormone: Relevance of the Net Charge of the Ligand

Jean-Philippe Bapst^{1†} and Alex N. Eberle^{1,2*}

¹Laboratory of Endocrinology, Department of Biomedicine, University Hospital and University Children's Hospital, University of Basel, Basel, Switzerland, ²Collegium Helveticum, ETH Zurich, Zurich, Switzerland

OPEN ACCESS

Edited by:

Hubert Vaudry,
University of Rouen, France

Reviewed by:

James A. Carr,
Texas Tech University, USA
Akiyoshi Takahashi,
Kitasato University, Japan

*Correspondence:

Alex N. Eberle
alex.n.eberle@unibas.ch

†Present address:

Jean-Philippe Bapst,
Vifor Pharma, Singapore, Singapore

Specialty section:

This article was submitted
to Neuroendocrine Science,
a section of the journal
Frontiers in Endocrinology

Received: 01 February 2017

Accepted: 10 April 2017

Published: 26 April 2017

Citation:

Bapst J-P and Eberle AN (2017)
Receptor-Mediated Melanoma
Targeting with Radiolabeled
 α -Melanocyte-Stimulating
Hormone: Relevance of the Net
Charge of the Ligand.
Front. Endocrinol. 8:93.
doi: 10.3389/fendo.2017.00093

A majority of melanotic and amelanotic melanomas overexpress melanocortin type 1 receptors (MC1Rs) for α -melanocyte-stimulating hormone. Radiolabeled linear or cyclic analogs of α -MSH have a great potential as diagnostic or therapeutic tools for the management of malignant melanoma. Compounds such as [¹¹¹In]DOTA-NAP-amide exhibit high affinity for the MC1R *in vitro*, good tumor uptake *in vivo*, but they may suffer from relatively high kidney uptake and retention *in vivo*. We have shown previously that the introduction of negative charges into radiolabeled DOTA-NAP-amide peptide analogs may enhance their excretion and reduce kidney retention. To address the question of where to place negative charges within the ligand, we have extended these studies by designing two novel peptides, Ac-Nle-Asp-His-D-Phe-Arg-Trp-Gly-Lys(DOTA)-D-Asp-D-Asp-OH (DOTA-NAP-d-Asp-d-Asp) with three negative charges at the C-terminal end (overall net charge of the molecule -2) and DOTA-Gly-Tyr(P)-Nle-Asp-His-D-Phe-Arg-Trp-NH₂ (DOTA-Phospho-MSH₂₋₉) with two negative charges in the *N*-terminal region (net charge -1). The former peptide showed markedly reduced receptor affinity and biological activity by >10-fold compared to DOTA-NAP-amide as reference compound, and the latter peptide displayed similar bioactivity and receptor affinity as the reference compound. The uptake by melanoma tumor tissue of [¹¹¹In]DOTA-Phospho-MSH₂₋₉ was 7.33 ± 0.47 %ID/g 4 h after injection, i.e., almost equally high as with [¹¹¹In]DOTA-NAP-amide. The kidney retention was 2.68 ± 0.18 %ID/g 4 h after injection and hence 44% lower than that of [¹¹¹In]DOTA-NAP-amide. Over an observation period from 4 to 48 h, the tumor-to-kidney ratio of [¹¹¹In]DOTA-Phospho-MSH₂₋₉ was 35% more favorable

Abbreviations: AUC, area under the curve (quantification during a time interval); Boc, *t*-butoxycarbonyl; tBu, *tert*-butyl; DIPEA, *N,N'*-diisopropylethylamine; DIPC, *N,N'*-diisopropyl-carbodiimide; DOTA, 1,4,7,10-tetraazacyclododecane-1,4,7,10-tetra-acetic acid; DTPA, diethylenetriaminepentaacetic acid; Fmoc, fluorenylmethoxycarbonyl; HATU, 0-(7-azabenzotriazole-1-yl)-1,1,3,3-tetramethyluronium hexafluorophosphate; HOEt, hydroxybenzotriazole; ID, injected dose; MBM, mouse binding medium; MC1R, melanocortin type 1 receptor; α -MSH, α -melanocyte-stimulating hormone; MS, mass spectrometry; NOTA, 1,4,7-triazacyclononane-1,4,7-triacetic acid; PAL, 5-(4-aminomethyl-3,5-dimethoxyphenoxy)-valeric acid; Pbf, 2,2,4,6,7-pentamethyldihydrobenzofuran-5-sulfonyl; PBS, phosphate-buffered saline; PEG-PS, poly-ethyleneglycol-polystyrene graft; RP-HPLC, reverse-phase high-pressure liquid chromatography; Suc, succinyl; TBTU, *N,N,N',N'*-tetramethyl-*O*-(benzotriazole-1-yl)uronium tetrafluoroborate; TFA, trifluoroacetic acid; Trt, trityl.

than that of the reference compound. In a comparison of DOTA-NAP-d-Asp-d-Asp, DOTA-Phospho-MSH₂₋₉ and DOTA-NAP-amide with five previously published analogs of DOTA-NAP-amide that altogether cover a range of peptides with an overall net charge between +2 and -2, we now demonstrate that a net charge of -1, with the extra negative charges preferably placed in the *N*-terminal region, has led to the lowest kidney uptake and retention. Charges of +2 or -2 markedly increased kidney uptake and retention. In conclusion, the novel DOTA-Phospho-MSH₂₋₉ may represent a new lead compound for negatively charged linear MC1R ligands that can be further developed into a clinically relevant melanoma targeting radiopeptide.

Keywords: melanoma, α -melanocyte-stimulating hormone, radiolabeled peptide, phosphopeptide, tumor targeting, net charge, tissue distribution, kidney toxicity

INTRODUCTION

In the last 30 years, cutaneous malignant melanoma has become one of the most rapidly advancing tumors in the general population and the most commonly occurring tumor among young adults (1); and today, it still continues to increase (2). The prognosis of metastatic melanoma is usually poor. As melanoma cells overexpress membrane-bound melanocortin type 1 receptors (MC1Rs) (3–5), suitable ligands for MC1R are candidates for targeting melanoma with diagnostic or therapeutic radioisotopes (6) or toxin conjugates (7). The natural ligand for MC1R is α -melanocyte-stimulating hormone (α -MSH) for which a number of peptide analogs with increased binding affinity have been synthesized in the past, such as linear [Nle⁴, d-Phe⁷]- α -MSH (NDP-MSH; melanotan I) (8) or cyclic Ac-Nle-cyclo[Asp-His-d-Phe-Arg-Trp-Lys]-NH₂ (melanotan II) (9) and related peptides (10). For melanoma targeting with radioactive metal isotopes, several linear MSH peptides containing chelators for radiometals were developed (11–15). Of these, ¹¹¹In- or ^{67/68}Ga-labeled DOTA-NAP-amide exhibited the most promising *in vivo* characteristics as it showed the highest tumor uptake paired with minimal non-tumor tissue uptake, except for the kidneys (13).

High uptake and retention of radioactivity by the kidneys and some other organs is a general problem for most peptide radiopharmaceuticals (16). Several strategies have been developed for radiometal-labeled MSH peptides to reduce kidney uptake such as the use of different chelators (e.g., DOTA, NOTA) and radioisotopes and/or variations in the positioning of the chelator within the peptide molecule (6, 17, 18). Alternatively, introduction of a suitable linker between chelator and peptide may be used (19), or the formation of peptide dimers (20) or cyclic peptides (21, 22). Although dimerization produced some very potent high-affinity compounds *in vitro*, their *in vivo* characteristics were disappointing (20). By contrast, analysis of a number of cyclized α -MSH peptides labeled with ¹¹¹In, ¹⁷⁷Lu, ⁹⁰Y, ^{99m}Tc, or ¹⁸⁸Re yielded promising lead candidates (23–28) although these compounds in general suffered equally from high kidney uptake. A direct comparison of a linker-extended ⁶⁴Cu-labeled NOTA-NAP-amide peptide with a related cyclic peptide showed that both radiopeptides displayed excellent melanoma targeting, however paired with relatively high kidney uptake (29); the overall

radiopharmacological characteristics of the linear peptide were superior in this study.

Another approach to reduce uptake of radioactivity by the kidneys is coinjection of radiopeptides with basic amino acids. As the surface of proximal tubular cells in the kidneys is negatively charged and electrostatic interactions contribute greatly to the uptake of positively charged peptide molecules, basic amino acids may compete with the uptake of radiopeptides and hence reduce it (30). This method was first applied for ¹¹¹In-labeled DTPA-octreotide (31, 32) and ⁹⁰Y-labeled DOTA-[Tyr³]-octreotide (32, 33). In particular, coinjection of d-Lys markedly reduced kidney uptake by up to 65% without affecting tumor uptake (32). A lesser reduction was achieved by coinfusion of Lys and Arg with ¹⁸⁸Re-labeled cyclized MSH (34) or with ¹¹¹In-labeled DOTA-NAP-amide (Froidevaux and Eberle, unpublished). Although successful for some of the radiopeptides, coinjection of basic amino acids only partially solved the problem of kidney toxicity by the accumulated radioactivity.

Following basic reabsorption studies in the kidneys with positively, neutrally, and negatively charged proteins (35, 36), Kok et al. (37) demonstrated that the excretion of succinylated lysozyme is dramatically increased compared to the non-succinylated molecule with six amino groups, suggesting that reduction of the positive net charge of lysozyme had a beneficial effect on urinary excretion. Akizawa et al. (38) confirmed the influence of negative charges on the excretion of ¹¹¹In-labeled DTPA-octreotide peptides containing modifications in position 1 (Asp vs. Phe or Met vs. Lys): the lowest radioactivity counts in the kidneys were found with [¹¹¹In]DTPA-[Asp¹]-octreotide, whereas the highest were seen with [¹¹¹In]DTPA-[Lys¹]-octreotide. Less conspicuous data were obtained with [¹¹¹In]DOTA-NAP-amide containing different charges in the C-terminal region: although with the DOTA-NAP-amide analog [DOTA-Nle⁴,Asp⁵, d-Phe⁷,Lys¹¹(Suc)]- α -MSH₄₋₁₁-carboxylate, a negative charge in the C-terminus reduced kidney uptake of the radiopeptide, tumor uptake was also affected, and hence, the tumor-to-kidney ratio was even lower than that of the parent molecule with non-charged C-terminal amide (14). By contrast, introduction of a Glu residue at the *N*-terminus of a Re-cyclized DOTA-containing MSH peptide increased the tumor-to-kidney ratio, demonstrating the beneficial effect of an additional negative charge (26).

To compare the pharmacokinetic properties of linear ^{111}In -labeled DOTA-MSH peptide analogs containing a net charge ranging from +2 to -2, we synthesized and biologically characterized two new peptides, Ac-Nle-Asp-His-d-Phe-Arg-Trp-Gly-Lys(DOTA)-d-Asp-d-Asp-OH (abbreviated name: DOTA-NAP-d-Asp-d-Asp) and DOTA-Gly-Tyr(P)-Nle-Asp-His-d-Phe-Arg-Trp-NH₂ (DOTA-Phospho-MSH₂₋₉), and we also included DOTA-NAP-amide as a reference compound in this study (**Figure 1**). Biodistribution data obtained in tumor-bearing mice were compared with the data of the previously published linear MSH analogs (14). The analysis showed that DOTA-Phospho-MSH₂₋₉ yielded the best tumor-to-kidney ratio of all linear MSH peptides so far investigated, demonstrating that an overall net charge of the peptide of -1 with a negatively charged N-terminal region resulted in the most favorable biodistribution properties.

MATERIALS AND METHODS

Reagents

α -Melanocyte-stimulating hormone was a gift from the Novartis Institutes of Biomedical Research (Basel, Switzerland). [Nle⁴,D-Phe⁷]- α -MSH (NDP-MSH) was obtained from Bachem (Bubendorf, Switzerland). DOTA-tris(*tert*-butyl ester) (1,4,7,10-tetraazacyclododecane-1,4,7-tris-*tert*-butyl acetate-10-acetic acid) was purchased from Macrocylics (Dallas, TX, USA), Fmoc-PAL-PEG-PS resin from Applied Biosystems (Rotkreuz, Switzerland), Fmoc-d-Asp(tBu)-TentaGel S AC resin from Rapp-Polymer (Tübingen, Germany), Fmoc-amino acids from Novabiochem (Läufelfingen, Switzerland), and Kaiser test kits from Sigma-Aldrich (Buchs, Switzerland). *N*-Succinimidyl iodoacetate and iodogen tubes were from Pierce Biotechnology (Rockford, IL, USA), Na¹²⁵I (3.7 GBq/mL) from Perkin Elmer (Waltham, MA, USA), and $^{111}\text{InCl}_3$ (370 MBq/mL) from Mallinckrodt (Petten, The Netherlands). 1,10-Phenanthroline was

bought from Merck (Darmstadt, Germany), and all other organic reagents were obtained from Sigma-Aldrich. All reagents were of highest purity available. Cell culture media were from Biochrom AG (Berlin, Germany) and Sigma-Aldrich. Penicillin, streptomycin, vitamins, and non-essential amino acids were bought from Gibco/Invitrogen (Carlsbad, CA, USA) or Sigma-Aldrich.

Instrumentation

Continuous-flow peptide synthesis was carried out on a Pioneer peptide synthesizer from PerSeptive Biosystems (Framingham, MA, USA). Analytical reverse-phase high-pressure liquid chromatography (RP-HPLC) was performed on a PU-980 system from Jasco (Easton, MD, USA) using a Vydac 218TP54 C18 (5 μm , 4.6 mm \times 250 mm) or a Phenomenex Jupiter C18 300 Å (5 μm , 4.6 mm \times 250 mm) analytical column. DOTA-NAP-amide-d-Asp-d-Asp was chromatographed with a gradient between solvent A [0.1% trifluoroacetic acid (TFA) in H₂O] and solvent B (0.1% TFA in 70:30 acetonitrile/H₂O). The 40-min gradient cycle consisted of the following parts: 95% A (0–2 min), 95–70% A (2–10 min), 70–30% A (10–30 min), 30–5% A (30–34 min), 5% A (34–36 min), 5–95% A (36–38 min), and 95% A (38–40 min); the flow rate was 1 mL/min. UV absorption was recorded at 280 nm using a Jasco UV-1570 detector. DOTA-Phospho-MSH₂₋₉ was chromatographed on a Phenomenex Jupiter column using the same gradient, except that solvent A was replaced by 0.02 M ammonium acetate. Mass spectra were determined on a Finnigan LCQ Deca electrospray ion trap mass spectrometry (MS) system.

The purity of the *radioligands* was assessed by RP-HPLC using a dedicated Jasco PU-980 chromatography system equipped with a Spherisorb ODS2/5- μm column and a Radiomatic 500TR LB506C1 γ -detector (Packard, Meriden, CT, USA). Solvent A was 0.1% TFA in H₂O; solvent B was 0.1% TFA in acetonitrile; the gradient consisted of 96% A (0–2 min), 96–45% A (2–22 min), 45–25% A (22–30 min), 25% A (30–32 min), and 25–96% A (32–34 min);

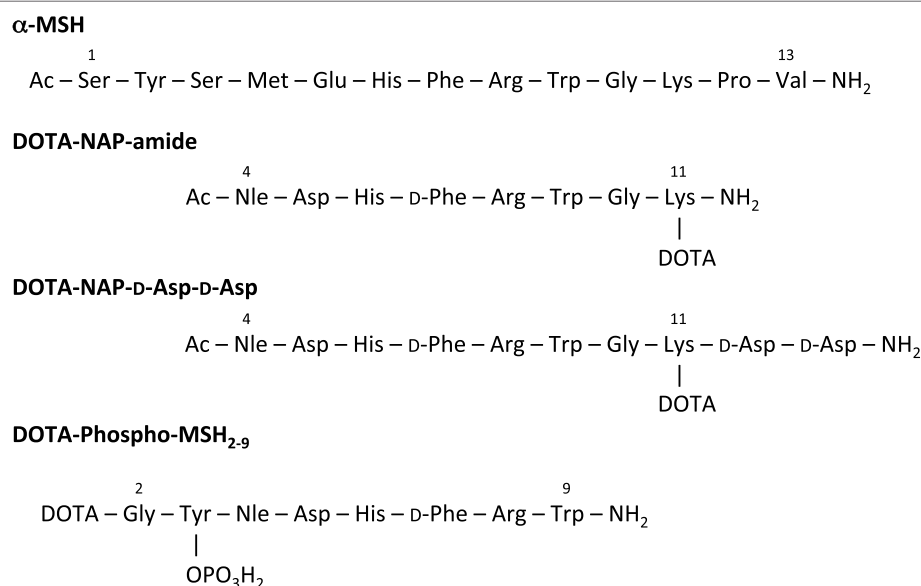


FIGURE 1 | Amino acid sequence of α -MSH, DOTA-NAP-amide, DOTA-NAP-d-Asp-d-Asp, and DOTA-Phospho-MSH₂₋₉.

the flow rate was 1.0 mL/min. A cell harvester (Packard) was used to collect cell-bound radioactivity from binding assays on filters. Their radioactivity was measured on a TopCount microplate scintillation counter (Packard). Radioactivity in internalization and biodistribution assays was measured on a Cobra II Auto-Gamma γ -counter (Packard). For bioassays, melanin content in cell culture media of each well was quantified on a Spectra Max 190 microplate reader (Molecular Devices, Menlo Park, CA, USA) using a wavelength of 310 nm.

Peptide Synthesis

General

Continuous-flow solid-phase peptide synthesis was used, combined with Fmoc strategy and the following resins: Flow-compatible Fmoc-PAL-PEG-PS polystyrene resin containing the acid-labile amide linker 5-(4-aminomethyl-3,5-dimethoxyphenoxy)-valeric acid (substitution 0.21 mmol/g) for NAP-amide and DOTA-Phospho-MSH₂₋₉, and Fmoc-d-Asp(*t*Bu)-TentaGel S AC resin, a low crosslinked polystyrene matrix resin, for NAP-amide-d-Asp-d-Asp-OH. Amino acid side chains were protected as follows: Trt for Cys and His, *t*-butoxycarbonyl (Boc) for Lys and Trp, *tert*-butyl (*t*Bu) for Asp and d-Asp, and Pbf for Arg. Manual Fmoc deprotection was done in 20% piperidine/DMF for 20 min, followed by a short wash with 20% piperidine/DMF and five washes with DMF; completion of deprotection was assessed by Kaiser test. Cleavage of the peptide from the resin was performed with a solution of 90% TFA, 5% thioanisole, 4.5% H₂O, and 0.5% 1,2-ethanedithiol. After 2 h, the solution was filtrated, and the peptide precipitated with a 10-fold volume of *t*Bu-methyl ether or diethylether. All reactions and manipulations with DOTA were carried out in acid-treated (1 M HCl, >1 h) glassware.

DOTA-NAP-Amide

NAP-amide (13) was assembled as described above. The free N-terminus was acetylated at room temperature for 24 h by incubation of the peptide-resin with 2 equivalents of *p*-nitrophenyl acetate, preactivated with hydroxybenzotriazole (HOBT) (1 eq) in DMF for 10 min. The resin was filtrated and washed 5× with DMF and 4× with isopropanol and then submitted to cleavage as described above. The DOTA moiety was coupled to the ϵ -amino group of the C-terminal Lys residue, the peptide conjugate deprotected (90% TFA, 4 h) and purified by RP-HPLC (*t*_R = 9.53 min). Calculated monoisotopic mass: 1,485.64/gmol; found: 1,485.65/gmol.

DOTA-NAP-d-Asp-d-Asp

NAP-amide-d-Asp-d-Asp-OH was synthesized, acetylated, and cleaved from the resin as described for NAP-amide (Figure 2A). NAP-amide-d-Asp-d-Asp-OH was purified by HPLC (*t*_R = 16.1 min) and lyophilized. Calculated monoisotopic mass: 1,330.40/gmol; found: 1,329.9/gmol. The deprotected peptide (1 eq) was conjugated with DOTA-tris(*t*-butyl ester) (1 eq) and preincubated with HATU (1.2 eq) for 10 min, in the presence of DIPEA (2 eq) using DMF as a solvent. After 1 h at room temperature, half of the initial quantity of preactivated DOTA-tris(*t*-butyl ester) was added to the mixture, and after a

total reaction time of 2 h, the peptide was precipitated in ice-cold diethylether. The DOTA moiety was then deprotected by addition of 90% TFA (4 mL per 5 mg of peptide). The mixture was stirred for 4 h, and deprotected DOTA-peptide was precipitated in ice-cold diethylether, resuspended in 10% acetic acid, and purified by RP-HPLC (*t*_R = 16.7 min). Calculated monoisotopic mass: 1,716.80/gmol; found: 1,716.79/gmol.

DOTA-Phospho-MSH₂₋₉

The first amino acid was coupled to the Fmoc-PAL-PEG-PS resin manually; Fmoc-Trp(Boc)-OH (3 eq) was preactivated with HOBT (3 eq + 15%) for 10 min (Figure 2B). This mixture was added to a suspension of the Fmoc-deprotected resin, followed by DIPC (3 eq) for overnight reaction. The resin was washed 5× with DMF, and completion was checked by Kaiser test. The subsequent synthesis steps up to Nle³ were done on the peptide synthesizer. After deprotection of the N-terminal Fmoc-protecting group, Fmoc-Tyr(PO(OBzl)-OH)-OH (5 eq) was preactivated with HOBT (1 eq) and then manually coupled to the peptide (1 eq peptide on resin) by addition of TBTU (1 eq) and DIPEA (15 eq). After overnight incubation, the reaction was repeated under the same conditions, and then the Fmoc-protecting group was cleaved. The final amino acid Fmoc-Gly-OH was coupled in the same way. After Fmoc deprotection, DOTA was coupled to the peptide still on the resin by preactivating DOTA (3 eq) with HATU (3 eq) for 10 min and then by adding DIPEA (9 eq) to the resin suspension (1 eq peptide) for overnight reaction. The peptide was simultaneously cleaved from the resin and deprotected by addition of 90% TFA for 4 h and precipitated with ice-cold diethylether. DOTA-Phospho-MSH₂₋₉ was finally purified by RP-HPLC (*t*_R = 16.5 min). Calculated monoisotopic mass: 1,558.59/gmol; found: 1,558.30/gmol.

Radiolabeling of Peptides

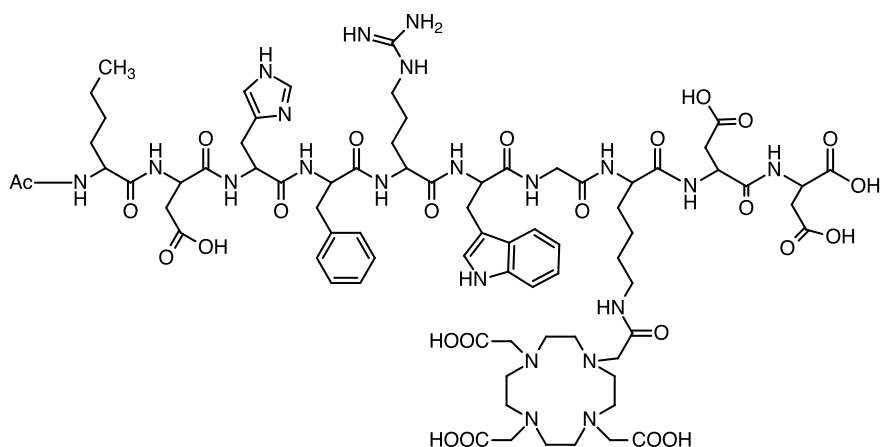
Labeling with ^{111}In

Incorporation of ^{111}In into DOTA-peptides was performed by the addition of 55.5 MBq of $^{111}\text{InCl}_3$ to the DOTA-peptides (10 nmol) that had been dissolved in 54 μL acetate buffer (0.4 M, pH 5) containing 2 mg of gentisic acid. Incubation for 10 min at 95°C allowed completion of the reaction. The radiolabeled DOTA-peptides were purified on a small RP cartridge (Sep-Pak C18, Waters) by first washing the column with 0.4 M sodium acetate buffer (pH 7) and then eluting the peptides with ethanol. The purity of the radioligands was assessed by RP-HPLC/ γ detection as described above. The specific activity of the radioligand was always >7.4 GBq/ μmol .

Radioiodination

NDP-MSH (12.14 nmol) was mixed with Na¹²⁵I (37 MBq; Perkin Elmer) in 60 μL phosphate buffer (0.3 M, pH 7.4) in a Iodogen® precoated tube. After a 15-min incubation at room temperature under agitation, the iodination mixture was loaded onto a Sep-Pak C18 cartridge, which was washed consecutively with water and acetic acid (0.5 M). Finally, the peptide was eluted with methanol. The collected fractions containing [¹²⁵I]NDP-MSH were supplemented with dithiothreitol (1.5 mg/mL) and stored at -20°C. Each binding experiment was preceded by an additional

A Ac-Nle-Asp-His-D-Phe-Arg-Trp-Gly-Lys(DOTA)-D-Asp-D-Asp-OH
[DOTA-NAP-D-Asp-D-Asp]



B DOTA-Gly-Tyr(OPO₃)-Nle-Asp-His-D-Phe-Arg-Trp-NH₂
[DOTA-Phospho-MSH₂₋₉]

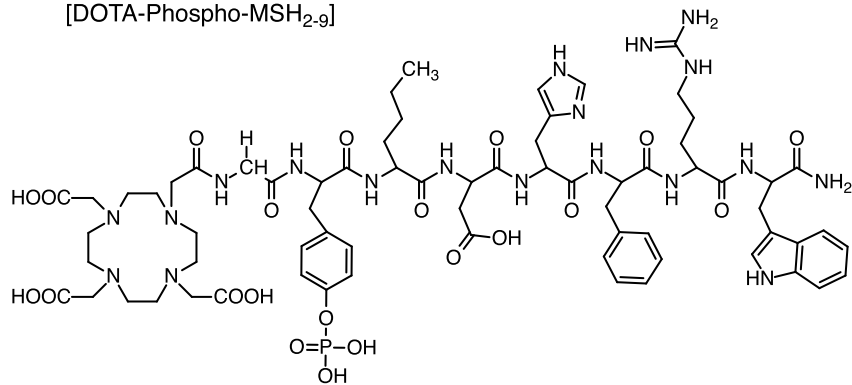


FIGURE 2 | Chemical structure of DOTA-NAP-D-Asp-D-Asp (A) and DOTA-Phospho-MSH₂₋₉ (B).

purification of the radiotracer by RP-HPLC and subsequent lyophilization from lactose/bovine serum albumin (BSA) (20 mg of each per milliliter of tracer solution).

Cell Culture

Mouse B16-F1 melanoma cells (39) were cultured in modified Eagle's medium (MEM) containing 10% heat-inactivated fetal calf serum, 2 mmol/L L-glutamine, 1% non-essential amino acids, 1% vitamin solution, 50 IU/mL penicillin, and 50 μ g/mL streptomycin, in a humidified atmosphere consisting of 95% air and 5% CO₂ at 37°C. For cell expansion or experiments with isolated cells, the B16-F1 cells were detached with 0.02% EDTA in phosphate-buffered saline (PBS) (150 mM, pH 7.2–7.4). The human HBL melanoma cell line (3, 4) was cultured in modified RPMI medium supplemented with 10% heat-inactivated fetal calf serum, 2 mM L-glutamine, 50 IU/mL penicillin, and 50 μ g/mL streptomycin in the same conditions as for B16-F1 cells.

In Vitro Binding Assay

Triplicates of 100- μ L volumes of B16-F1 or HBL cell suspensions adjusted to 4×10^6 /mL were incubated in 96-well U-bottom

microplates (Falcon 3077). The binding medium consisted of MEM with Earle's salts, 0.2% BSA, and 0.3 mM 1,10-phenanthroline. This binding medium was called mouse binding medium (MBM). Triplicates of competitor peptide solution (50 μ L) yielding final concentrations ranging from 1×10^{-6} to 1×10^{-12} M were added. [¹²⁵I]NDP-MSH (50,000 cpm) in 50 μ L was finally added to each well. The plates were incubated at 15°C for 3 h for B16-F1 cells and at 37°C for 2 h for HBL cells. The incubation was stopped by covering the plates with ice for 10 min. A cell harvester was used to collect cell-bound radioactivity on filters (Packard Unifilter-96 GF/B). The collected radioactivity was counted on a TopCount scintillation counter (Packard) after addition of 50 μ L Microscint-20 scintillation cocktail (Perkin Elmer). The IC₅₀ values were calculated with the Prism 6 software (GraphPad Software Inc., San Diego CA, USA).

In Vitro Melanin Assay

The biological activity of the α -MSH derivatives was assessed with an *in situ* melanin assay (40). Briefly, B16-F1 cells (2,500 cells per well in 100 μ L) were distributed into 96-well flat-bottom cell culture plates. MEM without phenol red, supplemented

with 10% heat-inactivated fetal calf serum, 2 mM L-glutamine, 0.31 mmol/L L-tyrosine, 1% non-essential amino acids, 1% vitamin solution, 50 IU/mL penicillin, and 50 μ g/mL streptomycin, was used as culture medium. After overnight incubation at cell culture conditions mentioned above, concentrations of α -MSH derivatives ranging from 1×10^{-8} to 1×10^{-12} in 100- μ L volumes were added (in threefold dilution steps), and the incubation was continued for an additional 72 h. Melanin production was quantified by determining the absorbance at 310 nm in a microplate reader.

In Vitro Internalization Assay

B16-F1 cells were seeded in six-well plates and incubated overnight in MEM at 37°C. For the internalization experiments, MEM was replaced by 1 mL MBM (see above) as internalization buffer. After a 1-h incubation at 37°C, 74 kBq of radioligand (^{111}In -labeled peptides) was added, and the plates were incubated for different time periods. Non-specific internalization was determined by addition of 50 μ L of a 1 μ M α -MSH solution to the incubation mixture. After the desired incubation times, the cells were extensively washed with MBM kept at 37°C to remove excess radioligand. Incubation in 2 mL ice-cold acid buffer (acetate-buffered Hank's balanced salt solution, pH 5) for 10 min allowed dissociation of surface-bound ligand. After collection of the acid buffer fraction, the cells were rinsed once with cold MBM, and the washings were pooled with the acid buffer fraction. The cells were washed again with MBM kept at 37°C, lysed in a 1% Triton X-100 solution, and finally transferred to tubes for quantification. The radioactivity of all collected fractions was measured in a γ -counter. A counting plate underwent the same treatment as the plate incubated for the longest time, but its cells were detached with 0.02% EDTA in PBS instead of being lysed with the Triton X-100 solution. Cells from three wells were collected, counted, and thus allowed for normalization of the results obtained. Results were expressed as percent of the added dose per million cells.

In Vivo Biodistribution and Stability of the Radioligands in B16-F1

Tumor-Bearing Mice

About 5×10^5 B16-F1 cells were implanted subcutaneously to female B6D2F1 mice (C57BL/6 \times DBA/2F1 hybrids; breeding pairs obtained from IFFA-CREDO, France). Seven days later, 185 kBq of ^{111}In -labeled ligand in 200 μ L PBS/0.1% BSA were injected intravenously into the lateral tail vein of each mouse. Control mice were injected with a mixture of the tracer and 50 μ g α -MSH to determine the non-specific uptake of radioligand. The animals were sacrificed 4, 24, and 48 h postinjection, dissected, and the tissues of interest collected, rinsed of excess blood, and weighed. The radioactivity emitted by each organ was measured in a γ -counter to determine the tissue uptake as percentage of the injected dose (ID) per gram of tissue. The total of injected radioactivity per animal was determined by extrapolation from the counts of a standard collected from the injection solution for each animal. Urine samples were collected at 10, 15, and 20 min and 4 h after injection and kept frozen at -80°C until use. Urine (1 vol) was mixed with methanol (2 vol) to precipitate proteins,

and the supernatant was analyzed by RP-HPLC/ γ -detection, as described in Ref. (12).

Analysis of Data

Results are expressed as means \pm SEM, unless otherwise stated. The statistical evaluation of data was performed using the one- or two-way ANOVA test. When significant overall effects were obtained by ANOVA, multiple comparisons were made with the Bonferroni correction. $P < 0.05$ was considered statistically significant. The area under the curve (AUC) was calculated with the GraphPad Prism 6 software for the indicated period of time, using the mean tissue uptake value at each time point.

RESULTS

Peptide Synthesis

All DOTA-peptides were obtained in >99% purity. The synthesis of DOTA-NAP-amide had an overall yield (after RP-HPLC purification) of 15%, DOTA-NAP-D-Asp-D-Asp 8.3%, and DOTA-Phospho-MSH₂₋₉ 5.3%. The expected molecular weights were confirmed by MS. The net charges of DOTA-NAP-D-Asp-D-Asp and DOTA-Phospho-MSH₂₋₉ at physiological pH are -2 and -1, respectively, calculated on the basis of known pK_a values for amino acid residues and functional groups.

In Vitro Receptor-Binding Affinity and Biologic Activity

The binding affinity of the peptides to MC1R was assessed by competition binding assays using [^{125}I]-NDP-MSH as radioligand and both murine B16-F1 and human HBL cells. Table 1 summarizes the IC₅₀ values obtained for the tested peptide compared to the values of the native ligand α -MSH and the reference peptide DOTA-NAP-amide. DOTA-Phospho-MSH₂₋₉ displayed affinities in the nanomolar range on both cell lines. Although the IC₅₀ obtained for DOTA-Phospho-MSH₂₋₉ with B16-F1 cell line was slightly lower than that of DOTA-NAP-amide (2.32 \pm 0.80 vs. 1.38 \pm 0.35 nmol/L), the binding affinity with HBL cells was

TABLE 1 | Receptor-binding potency and biological activity of DOTA-MSH analogs using mouse B16-F1 and human HBL melanoma cells.

Peptide	Receptor-binding potency		Biological activity rEC_{50} [α -melanocyte-stimulating hormone (α -MSH) = 1] ^b
	IC ₅₀ (nmol/L) ^a	B16-F1	
		HBL	B16-F1
α -MSH	1.50 \pm 0.14	1.91 \pm 0.26	1
DOTA-NAP-amide	1.38 \pm 0.35	3.09 \pm 1.11	0.66 \pm 0.35
DOTA-NAP-D-Asp-	19.67 \pm 4.48 ^c	29.80 \pm 7.96 ^c	7.66 \pm 0.33 ^c
D-Asp			
DOTA-Phospho-MSH ₂₋₉	2.32 \pm 0.80	3.03 \pm 0.59	0.85 \pm 0.11

^aIC₅₀ values are the concentrations inducing half-maximal binding inhibition of the MSH analogs and were determined in competition binding experiments using [^{125}I]-NDP-MSH as radioligand and mouse B16-F1 and human HBL human melanoma cells ($n = 3-20$).

^bRE_{C50} values represent the relative concentrations compared to α -MSH (=1) inducing half-maximal melanin production by B16-F1 cells ($n = 3-13$).

^c $P < 0.05$ vs. DOTA-NAP-amide.

comparable (3.03 ± 0.59 vs. 3.09 ± 1.11 nmol/L). DOTA-Phospho-MSH_{2,9} displayed good α -MSH agonist activity (Table 1), as demonstrated by the induction of melanin synthesis by B16-F1 cells at a dose matching its IC₅₀. By contrast, C-terminal extension of DOTA-NAP by d-Asp-d-Asp led to a ~10-fold lower MC1R affinity compared to that of DOTA-NAP-amide with both B16-F1 and HBL cells. The biological activity in the melanin assay was also around 11-fold lower than the reference peptide.

Internalization

[¹¹¹In]DOTA-NAP-d-Asp-d-Asp and [¹¹¹In]DOTA-Phospho-MSH_{2,9} exhibited excellent internalization profiles when studied *in vitro* with cultured B16-F1 cells (Figure 3). The plateau phase was not quite reached by the first peptide after 3.5 h, probably because of the lower receptor affinity; this may predict lower *in vivo* tumor uptake. By contrast, the plateau phase for [¹¹¹In]DOTA-Phospho-MSH_{2,9} was almost complete after 3.5 h, indicating that maximal internalization of the peptide was reached after 4 h, the first test point with *in vivo* biodistribution studies. It appears that MC1R internalization was not altered by the negatively charged ligands.

Biodistribution in Tumor-Bearing Mice

Tissue distributions in B16-F1 melanoma-bearing mice of [¹¹¹In]DOTA-NAP-d-Asp-d-Asp and [¹¹¹In]DOTA-Phospho-MSH_{2,9}

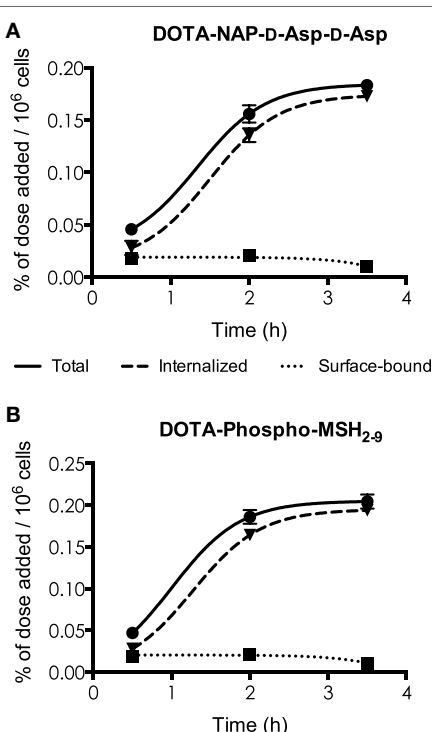


FIGURE 3 | Determination of internalization of [¹¹¹In] DOTA-NAP-d-Asp-d-Asp (A) and [¹¹¹In]DOTA-Phospho-MSH_{2,9} (B) by cultured B16-F1 cells exposed to the peptides at 37°C for 0.5, 2, and 3.5 h. Surface-bound radioligand was released by an acid buffer wash, and internalized radioligand was determined by lysing cells with detergent. Results are expressed in percent of the added dose per million cells.

were compared with the reference peptide [¹¹¹In]DOTA-NAP-amide (Table 2). Tissues, including melanoma tumors, were collected 4, 24, and 48 after injection of the radiopeptides. Clearance from the blood was faster for the two new radiopeptides compared with the reference peptide as almost no radioactivity could be detected after 4 h. Kidney uptake of [¹¹¹In]DOTA-NAP-d-Asp-d-Asp was 5.95 ± 0.85 %ID/g 4 h after injection, i.e., the uptake was 25% higher than that of [¹¹¹In]DOTA-NAP-amide (4.77 ± 0.26 %ID/g), which was not expected. After 24 h, the radioactive load was even 70% higher than with the reference

TABLE 2 | Tissue biodistribution of ¹¹¹In-labeled DOTA-NAP-amide, DOTA-NAP-d-Asp-d-Asp, and DOTA-Phospho-MSH_{2,9} at 4, 24, and 48 h after injection into tumor-bearing mice.

Organ	Time (h)	Uptake (%ID/g of tissue \pm SEM) ^a		
		DOTA-NAP-amide	DOTA-NAP-d-Asp-d-Asp	DOTA-Phospho-MSH _{2,9}
Blood	4	0.09 \pm 0.02	0.01 \pm 0.00	0.02 \pm 0.00
	24	0.02 \pm 0.00	0.01 \pm 0.00	0.01 \pm 0.00
	48	0.00 \pm 0.00	0.01 \pm 0.00	0.00 \pm 0.00
Tumor	4	7.77 \pm 0.35	1.93 \pm 0.11	7.33 \pm 0.47
	24	2.32 \pm 0.15	0.63 \pm 0.03	2.92 \pm 0.12
	48	1.41 \pm 0.12	0.23 \pm 0.02	1.21 \pm 0.18
Stomach	4	0.09 \pm 0.01	0.11 \pm 0.00	0.17 \pm 0.08
	24	0.12 \pm 0.02	0.03 \pm 0.00	0.16 \pm 0.02
	48	0.11 \pm 0.05	0.02 \pm 0.00	0.07 \pm 0.00
Kidney	4	4.77 \pm 0.26	5.95 \pm 0.85	2.68 \pm 0.18
	24	2.41 \pm 0.20	4.09 \pm 0.16	1.88 \pm 0.11
	48	1.55 \pm 0.07	2.02 \pm 0.08	1.04 \pm 0.07
Liver	4	0.34 \pm 0.05	0.10 \pm 0.00	0.20 \pm 0.01
	24	0.31 \pm 0.02	0.09 \pm 0.00	0.16 \pm 0.02
	48	0.27 \pm 0.07	0.07 \pm 0.00	0.12 \pm 0.01
Spleen	4	0.14 \pm 0.01	0.07 \pm 0.00	0.11 \pm 0.01
	24	0.11 \pm 0.01	0.07 \pm 0.00	0.10 \pm 0.01
	48	0.10 \pm 0.01	0.07 \pm 0.00	0.09 \pm 0.01
Lung	4	0.08 \pm 0.01	0.06 \pm 0.00	0.07 \pm 0.02
	24	0.05 \pm 0.01	0.04 \pm 0.00	0.04 \pm 0.00
	48	0.03 \pm 0.00	0.03 \pm 0.00	0.03 \pm 0.00
Small intestines	4	0.07 \pm 0.01	0.05 \pm 0.01	0.11 \pm 0.03
	24	0.08 \pm 0.01	0.04 \pm 0.01	0.06 \pm 0.00
	48	0.05 \pm 0.01	0.03 \pm 0.00	0.06 \pm 0.00
Pancreas	4	0.04 \pm 0.00	0.03 \pm 0.00	0.05 \pm 0.01
	24	0.03 \pm 0.00	0.02 \pm 0.00	0.03 \pm 0.00
	48	0.02 \pm 0.00	0.03 \pm 0.00	0.03 \pm 0.00
Heart	4	0.05 \pm 0.01	0.03 \pm 0.00	0.04 \pm 0.00
	24	0.03 \pm 0.00	0.03 \pm 0.00	0.03 \pm 0.00
	48	0.01 \pm 0.00	0.03 \pm 0.00	0.03 \pm 0.00
Bone	4	0.11 \pm 0.02	0.07 \pm 0.01	0.08 \pm 0.01
	24	0.14 \pm 0.02	0.06 \pm 0.01	0.11 \pm 0.02
	48	0.05 \pm 0.01	0.07 \pm 0.01	0.06 \pm 0.01
Muscle	4	0.05 \pm 0.01	0.02 \pm 0.00	0.02 \pm 0.00
	24	0.02 \pm 0.00	0.02 \pm 0.00	0.02 \pm 0.00
	48	0.01 \pm 0.00	0.03 \pm 0.00	0.02 \pm 0.00
Skin	4	—	0.06 \pm 0.01	0.12 \pm 0.03
	24	—	0.06 \pm 0.00	0.07 \pm 0.02
	48	—	0.04 \pm 0.00	0.08 \pm 0.02

^aThe values are the means of three experiments each of which consisted of $n = 5$ animals per compound.

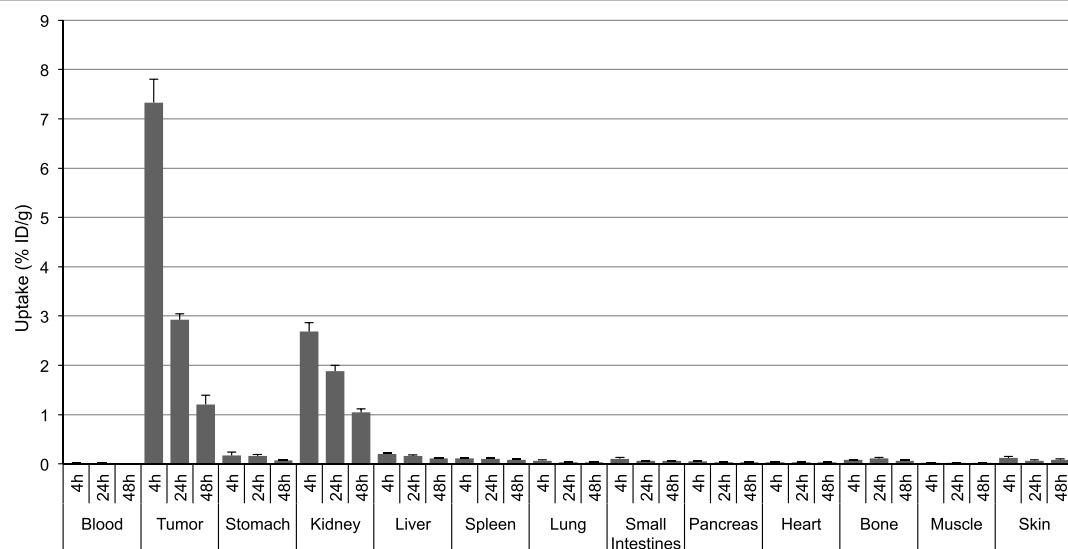


FIGURE 4 | Tissue distribution of $[^{111}\text{In}]$ DOTA-Phospho-MSH₂₋₉ in B16-F1 melanoma tumor-bearing mice at 4, 24, and 48 h postinjection. Results are expressed as percent of injected dose per g of tissue (%ID/g; means \pm SEM; $n = 3$ experiments).

peptide. On the other hand, owing to the lower receptor affinity of $[^{111}\text{In}]$ DOTA-NAP-d-Asp-d-Asp, it was anticipated that tumor uptake (1.93 ± 0.11 %ID/g after 4 h) was lower than that of $[^{111}\text{In}]$ DOTA-NAP-amide (7.77 ± 0.35 %ID/g). Other organs did not substantially accumulate the radiopeptide.

$[^{111}\text{In}]$ DOTA-Phospho-MSH₂₋₉ displayed more promising data: after 4 h, tumor uptake was 7.33 ± 0.47 %ID/g, i.e., almost identical with that of $[^{111}\text{In}]$ DOTA-NAP-amide, and kidney uptake was 2.68 ± 0.18 %ID/g, which corresponds to 56% of that of the reference peptide (Table 2). Non-specific uptake by other organs was very low and did not exceed the values found with $[^{111}\text{In}]$ DOTA-NAP-amide (Figure 4), thus excluding an altered excretion pathway. Coinjection of 50 μg of α -MSH together with the radiopeptide significantly blocked melanoma uptake and confirmed MC1R-mediated internalization (data not shown). The retention of radioactivity by the tumor was decreased to 40% at 24 h postinjection and to 15% at 48 h postinjection. These data are similar to those found with other MSH radiopeptides. On the other hand, clearance from the kidney appeared to be slightly slower. The tumor-to-kidney ratios calculated for 4, 24, and 48 h were 2.75, 1.55, and 1.16, respectively (Table 3). This results in an AUC (4–48 h) of 1.81 compared with 1.17 for $[^{111}\text{In}]$ DOTA-NAP-amide.

Uptake by the Kidneys and Liver in Relation to the Overall Net Charge of MSH Analogs

Kidney and liver uptake of $[^{111}\text{In}]$ DOTA-NAP-d-Asp-d-Asp, $[^{111}\text{In}]$ DOTA-Phospho-MSH₂₋₉, and $[^{111}\text{In}]$ DOTA-NAP-amide (reference peptide) was compared with that of five previously published peptides (14) that altogether cover an overall net charge ranging between +2 and -2 (Table 4). As shown in Figure 5, kidney uptake is lowest for net charge -1; it is considerably

TABLE 3 | Tumor-to-kidney ratios for tissue uptake of $[^{111}\text{In}]$ DOTA-NAP-amide, $[^{111}\text{In}]$ DOTA-NAP-d-Asp-d-Asp, and $[^{111}\text{In}]$ DOTA-Phospho-MSH₂₋₉ after 4, 24, and 48 h postinjection.

Peptide	Tumor-to-kidney ratios ^a		
	4 h	24 h	48 h
$[^{111}\text{In}]$ DOTA-NAP-amide	1.63	0.96	0.91
$[^{111}\text{In}]$ DOTA-NAP-d-Asp-d-Asp	0.32	0.15	0.11
$[^{111}\text{In}]$ DOTA-Phospho-MSH ₂₋₉	2.74	1.55	1.16

^aRatios are presented as quotient between the means of tumor uptake divided by means of kidney uptake (Table 2).

increased for -2 and +2 and moderately for +1 or 0. Of the two peptides with a net charge of -1, $[^{111}\text{In}]$ DOTA-Phospho-MSH₂₋₉ showed a slightly lower kidney uptake than $[^{111}\text{In}]$ DOTA-Nle⁴,Asp⁵,D-Phe⁷,Lys¹¹(Suc)- α -MSH₄₋₁₁-carboxylate, indicating that incorporating the negative charges in the N-terminal region is more advantageous than in the C-terminal region. In addition, the AUC (4–48 h) for $[^{111}\text{In}]$ DOTA-Phospho-MSH₂₋₉ was 1.81, i.e., the tumor-to-kidney ratio was threefold higher than that of $[^{111}\text{In}]$ DOTA-Nle⁴,Asp⁵,D-Phe⁷,Lys¹¹(Suc)- α -MSH₄₋₁₁-carboxylate exhibiting an AUC (4–48 h) of 0.62 (14). With respect to the liver, non-specific uptake does not follow the same pattern as outlined for the kidneys (Figure 6). Other factors such as differences in lipophilicity may play a more important role. It should be stressed, however, that liver uptake is about 20-fold lower than that reported for the kidneys and therefore of minor importance for these peptides.

DISCUSSION

The net charge of radiolabeled peptides appears to be a crucial factor with respect to excretion via the urinary tract. The

TABLE 4 | Comparison of DOTA-NAP-d-Asp-d-Asp and DOTA-Phospho-MSH₂₋₉ with different analogs of MSH-NAP-amide containing modifications at the C-terminal or N-terminal end or in the N^c-lysine side chain that yield different overall net charges.

Peptide	N-terminal	C-terminal	N ^c -Lys	Net charge	Reference
A {[Ac-Nle ⁴ ,Asp ⁵ ,d-Phe ⁷ ,Lys ¹¹ (DOTA)]- α -MSH ₄₋₁₁ }-d-Asp-d-Asp-OH	Ac	d-Asp-d-Asp	DOTA	-2	
B [DOTA-Gly ² ,Tyr(P) ³ ,Nle ⁴ ,Asp ⁵ ,d-Phe ⁷]- α -MSH ₂₋₉ [DOTA-Phospho-MSH ₂₋₉]	DOTA	Trp-amide	-	-1	
C [DOTA-Nle ⁴ ,Asp ⁵ ,d-Phe ⁷ ,Lys ¹¹ (Suc)]- α -MSH ₄₋₁₁ -carboxylate	DOTA	OH	Suc	-1	(14)
D [DOTA-Nle ⁴ ,Asp ⁵ ,d-Phe ⁷ ,Lys ¹¹ (Suc)]- α -MSH ₄₋₁₁	DOTA	Amide	Suc	0	(14)
E {[Ac-Nle ⁴ ,Asp ⁵ ,d-Phe ⁷ ,Lys ¹¹ (DOTA)]- α -MSH ₄₋₁₁ -carboxylate}	Ac	OH	DOTA	0	(14)
F {[Ac-Nle ⁴ ,Asp ⁵ ,d-Phe ⁷ ,Lys ¹¹ (DOTA)]- α -MSH ₄₋₁₁ [DOTA-NAP-amide]}	Ac	Amide	DOTA	+1	(13)
G [DOTA-Nle ⁴ ,Asp ⁵ ,d-Phe ⁷ ,Lys ¹¹ (Ac)]- α -MSH ₄₋₁₁	DOTA	Amide	Ac	+1	(14)
H [DOTA-Nle ⁴ ,Asp ⁵ ,d-Phe ⁷]- α -MSH ₄₋₁₁	DOTA	Amide	H	+2	(14)

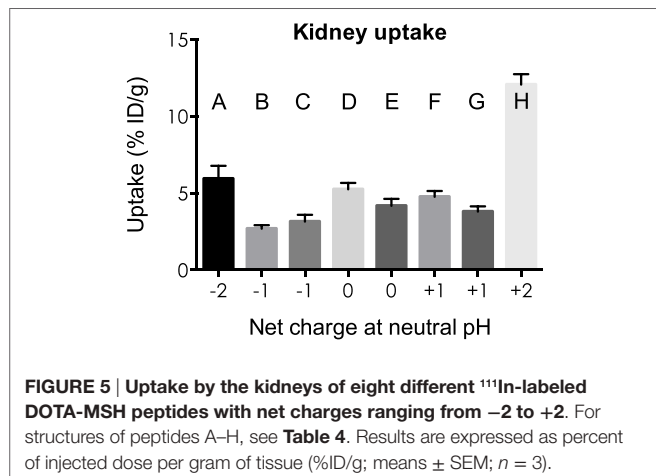


FIGURE 5 | Uptake by the kidneys of eight different ^{111}In -labeled DOTA-MSH peptides with net charges ranging from -2 to $+2$. For structures of peptides A–H, see Table 4. Results are expressed as percent of injected dose per gram of tissue (%ID/g; means \pm SEM; $n = 3$).

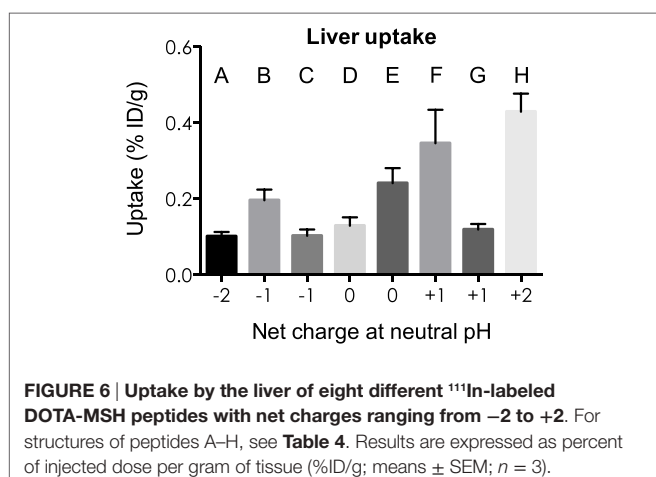


FIGURE 6 | Uptake by the liver of eight different ^{111}In -labeled DOTA-MSH peptides with net charges ranging from -2 to $+2$. For structures of peptides A–H, see Table 4. Results are expressed as percent of injected dose per gram of tissue (%ID/g; means \pm SEM; $n = 3$).

negatively charged surface of tubular cells of the kidneys involves repulsing electrostatic effects on negatively charged molecules passing in the luminal part of the proximal tubules, thus reducing their (re-)uptake (30, 41). As already mentioned, this effect can be further enhanced by the presence of positively charged amino acids such as Lys and Arg (42). An earlier study in our laboratory comparing differently charged DOTA-NAP-amide type of peptides demonstrated that $[^{111}\text{In}$ -DOTA-Nle⁴,Asp⁵,d-Phe⁷,Lys¹¹(Suc)]- α -MSH₄₋₁₁-carboxylate with a net charge of -1 had a tumor-to-kidney ratio of ~ 10 compared to a ratio of ~ 1 for the reference compound DOTA-NAP-amide (14). This finding was explained by the fact that the peptide with a net charge of -1 was rapidly internalized by cultured B16-F1 melanoma cells despite an ~ 10 -fold reduced MC1R affinity compared to DOTA-NAP-amide. In vivo, uptake by melanoma tumors was ~ 4 -fold lower, but uptake/retention by the kidneys was markedly increased. These findings would contradict the expectation of an even higher electrostatic repulsion on the surface of tubular cells. It is possible that once internalized, the fragmentation of the C-terminal region of DOTA-NAP-d-Asp-d-Asp is retarded by the d-Asp residues and excretion of Lys($[^{111}\text{In}$]DOTA), a metabolite of internalized $[^{111}\text{In}$]DOTA-NAP-amide occurring 4 h after injection (Froidevaux and Eberle, unpublished), is slower than for the reference compound. In summary, addition of a total of three negative charges to the C-terminus of DOTA-NAP-amide, yielding a net charge of -2 of the molecule, impairs its pharmacokinetic properties.

To find an alternative to $[^{111}\text{In}$ -DOTA-Nle⁴,Asp⁵,d-Phe⁷,Lys¹¹(Suc)]- α -MSH₄₋₁₁-carboxylate with a net charge of -1 but higher tumor uptake, we aimed at incorporating the negative charges in the N-terminal region of the molecule. To this end, DOTA-Phospho-MSH₂₋₉ was prepared, which contains a phosphate group in the phenolic ring of Tyr² of the MSH₂₋₉ peptide fragment. This peptide exhibited almost the same *in vitro* characteristics as the reference compound DOTA-NAP-amide. In particular, $[^{111}\text{In}$]DOTA-Phospho-MSH₂₋₉ was very rapidly internalized by cultured B16-F1 cells and reached the plateau after 3.5 h. *In vivo*, tumor uptake was about as high as for the reference compound but kidney uptake was markedly lower leading to the most favorable tumor-to-kidney ratio of a linear DOTA-MSH radiopeptide reported to date. All other compounds with net charges from $+2$ to 0 displayed less favorable tumor-to-kidney ratios. In conclusion, linear DOTA-MSH peptides preferably have an overall net charge of -1 , and the additional negative charges are incorporated in the N-terminal region.

While the experimental work with the two new ^{111}In -labeled MSH radiopeptides described here was already completed, the group of Miao and collaborators published several new lactam-bridged cyclized MSH analogs containing DOTA and NOTA chelators (for ^{111}In , $^{67/68}\text{Ga}$, ^{90}Y) or MAG₃ and HYNIC chelators

(for 99m Tc, 188 Re) for which they found considerably superior biodistribution data (43–46) compared to those with previously published cyclic MSH analogs. These novel cyclic MSH analogs may even be superior to DOTA-Phospho-MSH_{2,9}, but this would have to be examined in a comparative study under the same experimental conditions with DOTA-Phospho-MSH_{2,9} to define a potentially even more attractive novel lead compound.

ETHICS STATEMENT

All animal experiments were performed in compliance with Swiss animal welfare regulations and were ethically approved by the Ethics Committee for Animal Experimentation of the University Hospital Basel, followed by review and approval by the Cantonal

Commission for Animal Experimentation of Basel. No human data were used in this study.

AUTHOR CONTRIBUTIONS

J-PB and AE contributed substantially to the conception and design of the work, the acquisition, analysis and interpretation of data, and the drafting of the work.

ACKNOWLEDGMENTS

The authors thank the Swiss National Science Foundation for financial support (project no. 3100A0-102169) and Dr. Martine Christe and Mrs. Heidi Tanner for expert technical assistance.

REFERENCES

- Dennis LK. Analysis of the melanoma epidemic, both apparent and real: data from the 1973 through 1994 surveillance, epidemiology, and end results program registry. *Arch Dermatol* (1999) 135:275–80. doi:10.1001/archderm.135.3.275
- Wick MR. Cutaneous melanoma: a current overview. *Semin Diagn Pathol* (2016) 33:225–41. doi:10.1053/j.semdp.2016.04.007
- Ghanem GE, Comunale G, Libert A, Vercammen-Grandjean A, Lejeune FJ. Evidence for α -melanocyte-stimulating hormone (α -MSH) receptors on human malignant melanoma cells. *Int J Cancer* (1988) 41:248–55. doi:10.1002/ijc.2910410216
- Siegrist W, Solca F, Stutz S, Giuffre L, Carrel S, Girard J, et al. Characterization of receptors for α -melanocyte-stimulating hormone on human melanoma cells. *Cancer Res* (1989) 49:6352–8.
- Loir B, Pérez Sánchez C, Ghanem G, Lozano JA, García-Borrón JC, Jiménez-Cervantes G. Expression of the MC1 receptor gene in normal and malignant human melanocytes. A semiquantitative RT-PCR study. *Cell Mol Biol* (1999) 45:1083–92.
- Eberle AN, Bapst JP, Calame M, Tanner H, Froidevaux S. MSH radiopeptides for melanoma targeting. *Adv Exp Med Biol* (2010) 681:133–42. doi:10.1007/978-1-4419-6354-3_11
- Rozenkrants AA, Lunin VG, Sergienko OV, Giliazova DG, Voronina OL, Ians DE, et al. Targeted intracellular site-specific drug delivery: photosensitizer targeting to melanoma cell nuclei. *Genetika* (2003) 39:259–68.
- Sawyer TK, Sanfilippo PJ, Hruby VJ, Engel MH, Heward CB, Burnett JB, et al. 4-Norleucine, 7-D-phenylalanine- α -melanocyte-stimulating hormone: a highly potent α -melanotropin with ultralong biological activity. *Proc Natl Acad Sci U S A* (1980) 77:5754–8. doi:10.1073/pnas.77.10.5754
- Al-Obeidi F, Castrucci AM, Hadley ME, Hruby VJ. Potent and prolonged acting cyclic lactam analogues of α -melanotropin: design based on molecular dynamics. *J Med Chem* (1989) 32:2555–61. doi:10.1021/jm00132a010
- Cai M, Hruby VJ. Design of cyclized selective melanotropins. *Biopolymers* (2016) 106:873–86. doi:10.1002/bip.22976
- Bagutti C, Stoltz B, Albert R, Bruns C, Pless J, Eberle AN. [111 In]-DTPA-labeled analogues of α -melanocyte-stimulating hormone for melanoma targeting: receptor binding in vitro and in vivo. *Int J Cancer* (1994) 58:749–55. doi:10.1002/ijc.2910580521
- Froidevaux S, Calame-Christe M, Tanner H, Sumanovski L, Eberle AN. A novel DOTA- α -melanocyte-stimulating hormone analog for metastatic melanoma diagnosis. *J Nucl Med* (2002) 43:1699–706.
- Froidevaux S, Calame-Christe M, Schuhmacher J, Tanner H, Saffrich R, Henze M, et al. A gallium-labeled DOTA- α -melanocyte-stimulating hormone analog for PET imaging of melanoma metastases. *J Nucl Med* (2004) 45:116–23.
- Froidevaux S, Calame-Christe M, Tanner H, Eberle AN. Melanoma targeting with DOTA- α -melanocyte-stimulating hormone analogs: structural parameters affecting tumor uptake and kidney uptake. *J Nucl Med* (2005) 46:887–95.
- Bapst JP, Calame M, Tanner H, Eberle AN. Glycosylated DOTA- α -melanocyte-stimulating hormone analogues for melanoma targeting: influence of the site of glycosylation on in vivo biodistribution. *Bioconjug Chem* (2009) 20:984–93. doi:10.1021/bc900007u
- De Visser M, Verwijnen SM, de Jong M. Update: improvement strategies for peptide receptor scintigraphy and radionuclide therapy. *Cancer Biother Radiopharm* (2008) 23:137–57. doi:10.1089/cbr.2007.0435
- Eberle AN, Mild G. Receptor-mediated tumor targeting with radiopeptides. Part 1. General principles and methods. *J Recept Signal Transduct Res* (2009) 29:1–37. doi:10.1080/10799890902732823
- Guo H, Yang J, Gallazzi F, Prossnitz ER, Sklar LA, Miao Y. Effect of DOTA position on melanoma targeting and pharmacokinetic properties of 111 In-labeled lactam bridge-cyclized α -melanocyte stimulating hormone peptide. *Bioconjug Chem* (2009) 20:2162–8. doi:10.1021/bc9003475
- Yang J, Guo H, Padilla RS, Berwick M, Miao Y. Replacement of the Lys linker with an Arg linker resulting in improved melanoma uptake and reduced renal uptake of 99m Tc-labeled Arg-Gly-Asp-conjugated α -melanocyte stimulating hormone hybrid peptide. *Bioorg Med Chem* (2010) 18:6695–700. doi:10.1016/j.bmc.2010.07.061
- Bapst JP, Froidevaux S, Calame M, Tanner H, Eberle AN. Dimeric DOTA- α -melanocyte-stimulating hormone analogs: synthesis and in vivo characteristics of radiopeptides with high in vitro activity. *J Recept Signal Transduct Res* (2007) 27:383–409. doi:10.1080/10799890701723528
- Giblin MF, Wang N, Hoffman TJ, Jurisso SS, Quinn TP. Design and characterization of α -melanotropin peptide analogs cyclized through rhenium and technetium metal coordination. *Proc Natl Acad Sci U S A* (1998) 95:12814–8. doi:10.1073/pnas.95.22.12814
- Chen J, Cheng Z, Owen NK, Hoffman TJ, Miao Y, Jurisso SS, et al. Evaluation of an 111 In-DOTA-rhenium cyclized α -MSH analog: a novel cyclic-peptide analog with improved tumor-targeting properties. *J Nucl Med* (2001) 42:1847–55.
- Cheng Z, Chen J, Miao Y, Owen NK, Quinn TP, Jurisso SS. Modification of the structure of a metallopeptide: synthesis and biological evaluation of 111 In-labeled DOTA-conjugated rhenium-cyclized α -MSH analogues. *J Med Chem* (2002) 45:3048–56. doi:10.1021/jm010408m
- Miao Y, Whitener D, Feng W, Owen NK, Chen J, Quinn TP. Evaluation of the human melanoma targeting properties of radiolabeled α -melanocyte stimulating hormone peptide analogues. *Bioconjug Chem* (2003) 14:1177–84. doi:10.1021/bc034069i
- Miao Y, Hoffman TJ, Quinn TP. Tumor-targeting properties of 90 Y- and 177 Lu-labeled α -melanocyte-stimulating hormone peptide analogues in a murine melanoma model. *Nucl Med Biol* (2005) 32:485–93. doi:10.1016/j.nucmedbio.2005.03.007
- Miao Y, Fisher DR, Quinn TP. Reducing renal uptake of 90 Y- and 177 Lu-labeled α -melanocyte-stimulating hormone peptide analogues. *Nucl Med Biol* (2006) 33:723–33. doi:10.1016/j.nucmedbio.2006.06.005
- Miao Y, Benwell K, Quinn TP. 99m Tc- and 111 In-labeled α -melanocyte-stimulating hormone peptides as imaging probes for primary and pulmonary metastatic melanoma detection. *J Nucl Med* (2007) 48:73–80.
- Miao Y, Gallazzi F, Guo H, Quinn TP. 111 In-labeled lactam bridge-cyclized α -melanocyte stimulating hormone peptide analogues for

- melanoma imaging. *Bioconjug Chem* (2008) 19:539–47. doi:10.1021/bc700317w
29. Gao F, Sihver W, Jurischka C, Bergmann R, Haase-Kohn C, Mosch B, et al. Radiopharmacological characterization of ^{64}Cu -labeled α -MSH analogs for potential use in imaging of malignant melanoma. *Amino Acids* (2016) 48:833–47. doi:10.1007/s00276-015-2131-x
30. Behr TM, Goldenberg DM, Becker W. Reducing the renal uptake of radio-labeled antibody fragments and peptides for diagnosis and therapy: present status, future prospects and limitations. *Eur J Nucl Med* (1998) 25:201–12. doi:10.1007/s002590050216
31. Hammond PJ, Wade AF, Gwilliam ME, Peters AM, Myers MJ, Gilbey SG, et al. Amino acid infusion blocks renal tubular uptake of an indium-labelled somatostatin analogue. *Br J Cancer* (1993) 67:1437–9. doi:10.1038/bjc.1993.266
32. Bernard BF, Krenning EP, Breeman WA, Rolleman EJ, Bakker WH, Visser TJ, et al. D-lysine reduction of indium-111 octreotide and yttrium-90 octreotide renal uptake. *J Nucl Med* (1997) 38:1929–33.
33. Bodei L, Cremonesi M, Zoboli S, Grana C, Bartolomei M, Rocca P, et al. Receptor-mediated radionuclide therapy with ^{90}Y -DOTATOC in association with amino acid infusion: a phase I study. *Eur J Nucl Med Mol Imaging* (2003) 30:207–16. doi:10.1007/s00259-002-1023-y
34. Miao Y, Owern NK, Whitenet D, Gallazzi F, Hoffman TJ, Quinn TP. In vivo evaluation of ^{188}Re -labeled α -melanocyte stimulating hormone peptide analogs for melanoma therapy. *Int J Cancer* (2002) 101:480–7. doi:10.1002/ijc.10640
35. Christensen EI, Rennke HG, Carone FA. Renal tubular uptake of protein: effect of molecular charge. *Am J Physiol* (1983) 244:F436–41.
36. Lawrence GM, Brewer DB. Glomerular ultrafiltration and tubular reabsorption of bovine serum albumin and derivatives with increased negative charge in the normal female Wistar rat. *Clin Sci (Lond)* (1984) 66:47–54. doi:10.1042/cs0660047
37. Kok RJ, Haas M, Moolenaar F, de Zeeuw D, Meijer DK. Drug delivery to the kidneys and the bladder with the low molecular weight protein lysozyme. *Ren Fail* (1998) 20:211–7. doi:10.3109/08860229809045104
38. Akizawa H, Arano Y, Mifune M, Iwado A, Saito Y, Mukai T, et al. Effect of molecular charges on renal uptake of ^{111}In -DTPA-conjugated peptides. *Nucl Med Biol* (2001) 28:761–8. doi:10.1016/S0969-8051(01)00241-4
39. Fidler IJ. Selection of successive tumour lines for metastasis. *Nat New Biol* (1973) 242:148–9. doi:10.1038/newbio242148a0
40. Siegrist W, Eberle AN. In situ melanin assay for MSH using mouse B16 melanoma cells in culture. *Anal Biochem* (1986) 159:191–7. doi:10.1016/0003-2697(86)90327-1
41. Deen WM, Satvat B, Jamieson JM. Theoretical model for glomerular filtration of charged solutes. *Am J Physiol* (1980) 238:F126–39.
42. Rolleman EJ, Valkema R, de Jong M, Kooij PP, Krenning EP. Safe and effective inhibition of renal uptake of radiolabelled octreotide by a combination of lysine and arginine. *Eur J Nucl Med Mol Imaging* (2003) 30:9–15. doi:10.1007/s00259-002-0982-3
43. Guo H, Gallazzi F, Miao Y. Gallium-67-labeled lactam bridge-cyclized α -MSH peptides with enhanced melanoma uptake and reduced renal uptake. *Bioconjug Chem* (2012) 23:1341–8. doi:10.1021/bc300191z
44. Guo H, Miao Y. Cu-64-labeled lactam bridge-cyclized α -MSH peptides for PET imaging of melanoma. *Mol Pharm* (2012) 9:2322–30. doi:10.1021/mp300246j
45. Guo H, Gallazzi F, Miao Y. Design and evaluation of new $^{99\text{m}}\text{Tc}$ -labeled lactam-bridge-cyclized α -MSH peptides for melanoma imaging. *Mol Pharm* (2013) 10:1400–8. doi:10.1021/mp3006984
46. Guo H, Miao Y. Introduction of an 8-aminoctanoic acid linker enhances the melanoma uptake of $^{99\text{m}}\text{Tc}$ -labeled lactam-bridge-cyclized α -MSH peptide. *J Nucl Med* (2014) 55:2057–63. doi:10.2967/jnumed.114.145896

Conflict of Interest Statement: The authors declare that the research was conducted in the absence of any commercial or financial relationships that could be construed as a potential conflict of interest.

Copyright © 2017 Bapst and Eberle. This is an open-access article distributed under the terms of the Creative Commons Attribution License (CC BY). The use, distribution or reproduction in other forums is permitted, provided the original author(s) or licensor are credited and that the original publication in this journal is cited, in accordance with accepted academic practice. No use, distribution or reproduction is permitted which does not comply with these terms.



Inhibition of Ectopic Arginine Vasopressin Production by Phenytoin in the Small Cell Lung Cancer Cell Line Lu-165

Takahiro Ohta^{1,2}, Mitsuo Mita¹, Shigeru Hishinuma¹, Reiko Ishii-Nozawa³, Kazuhisa Takahashi⁴ and Masaru Shoji^{1*}

¹ Department of Pharmacodynamics, Meiji Pharmaceutical University, Kiyose, Japan, ² Department of Pharmacy, National Cancer Center Hospital East, Kashiwa, Japan, ³ Department of Clinical Pharmaceutics, Meiji Pharmaceutical University, Kiyose, Japan, ⁴ Faculty of Medicine, Department of Respiratory Medicine, Juntendo University, Tokyo, Japan

OPEN ACCESS

Edited by:

Hubert Vaudry,
University of Rouen, France

Reviewed by:

Gábor B. Makara,
Hungarian Academy of
Sciences, Hungary
Stanko S. Stojilkovic,
National Institutes of Health, USA

***Correspondence:**

Masaru Shoji
msji@my-pharm.ac.jp

Specialty section:

This article was submitted to
Neuroendocrine Science,
a section of the journal
Frontiers in Endocrinology

Received: 20 January 2017

Accepted: 11 April 2017

Published: 28 April 2017

Citation:

Ohta T, Mita M, Hishinuma S, Ishii-Nozawa R, Takahashi K and Shoji M (2017) Inhibition of Ectopic Arginine Vasopressin Production by Phenytoin in the Small Cell Lung Cancer Cell Line Lu-165. *Front. Endocrinol.* 8:94.
doi: 10.3389/fendo.2017.00094

Phenytoin, a voltage-gated sodium channel (Na_v channel) antagonist, reportedly inhibits arginine vasopressin (AVP) release from an isolated rat neurohypophysis. So far, it is uncertain whether phenytoin has a direct action on ectopic AVP-producing neuroendocrine tumors. We studied the effect of phenytoin on the release of copeptin, the C-terminal fragment of pro-AVP, and expression of AVP gene in the human small cell lung cancer cell line Lu-165. Cells were maintained in RPMI1640 medium with 10% fetal bovine serum and were used within the fifth passage. Copeptin was detected using a new sandwich immunoassay, and AVP mRNA levels were measured using real-time reverse transcription polymerase chain reaction. Treatment with phenytoin at a concentration of 25 $\mu\text{g}/\text{mL}$, but not at 5 or 10 $\mu\text{g}/\text{mL}$, had an inhibitory effect on copeptin levels in the medium at 48 h. At the same concentration, AVP mRNA levels in Lu-165 cells also decreased. Although a sodium challenge with added sodium at 20 mEq/L increased copeptin levels in the medium, a sodium challenge with added sodium at 10 and 20 mEq/L had no effect on AVP mRNA levels. Phenytoin at a concentration of 25 $\mu\text{g}/\text{mL}$ suppressed copeptin levels in the medium under the sodium challenge with added sodium at 10 and 20 mEq/L. Phenytoin at a concentration of 25 $\mu\text{g}/\text{mL}$ also decreased AVP mRNA levels in Lu-165 cells under the sodium challenge with added sodium at 10 mEq/L, but not at 20 mEq/L. Among five tested Na_v channel subunits, $\text{Na}_v1.3$ was highly expressed in Lu-165 cells. However, phenytoin significantly decreased $\text{Na}_v1.3$ mRNA levels under the sodium challenge with added sodium at 10 and 20 mEq/L. These results suggest that Lu-165 cells are sensitive to phenytoin and sodium to control of AVP release and its gene expression. Phenytoin might have a direct action on ectopic AVP-producing tumors, suggesting the importance of Na_v channels in AVP-producing neuroendocrine tumors.

Keywords: phenytoin, vasopressin, copeptin, voltage-gated sodium channel, small cell lung cancer, syndrome of inappropriate antidiuretic hormone secretion

INTRODUCTION

Phenytoin, a voltage-gated sodium channel (Na_v channel) antagonist, is widely used as an anticonvulsant drug in epileptic patients (1). In addition, phenytoin is effective in the treatment of syndrome of inappropriate antidiuretic hormone [arginine vasopressin (AVP)] secretion (SIADH) with abnormalities of the hypothalamic–pituitary axis (2). Phenytoin was found to inhibit AVP release from an isolated rat neurohypophysis (3). It is well known that small cell lung cancer (SCLC), one of the most aggressive forms of cancer, is sometimes complicated with refractory hyponatremia because SCLC is one of neuroendocrine tumors with capability of producing AVP (4–6). However, so far, it is uncertain whether phenytoin has a direct action on ectopic AVP-producing SCLC cells.

Na_v channel is a heterodimer composed of a single pore-forming α subunit and two associated β subunits (7). To date, nine α subunits and four β subunits have been identified. Na_v channels play a critical role in the depolarization of excitable cells, including skeletal muscle cells, cardiomyocytes, and neurons. Indeed, four Na_v channel subunits were found in magnocellular neurons in the hypothalamic supraoptic nucleus, and the expression and electrical activity of these subunits appeared to be salt sensitive (8). Recently, the role of Na_v channels in non-excitable cells has drawn attention (9). Cancer cells express certain Na_v channel subtypes. Cancer cell lines with higher Na_v channel expression show increased cell motility and metastatic potential; however, conflicting results have been reported (7). Notwithstanding, there is little evidence on the expression and role of Na_v channels in AVP-producing SCLC cells.

In the present study, we examined the effect of phenytoin with and without a sodium challenge on AVP mRNA expression and the release of copeptin, the C-terminal fragment of pro-AVP (10), in the human SCLC cell line Lu-165. Lu-165 cells were previously established from a 50-year-old SCLC patient with SIADH (11).

MATERIALS AND METHODS

Cell Culture

The AVP-producing SCLC cell line Lu-165 and three AVP non-producing SCLC cell lines, Lu-24, Lu-134A, and MS-1, were provided by RIKEN BRC through the National BioResource Project of the MEXT, Japan. These cells were maintained in RPMI1640 medium with 10% fetal bovine serum (FBS) in a humidified incubator at 37°C with 5% CO_2 . All cells were used during exponential growth within the fifth passage for experiments without FBS.

Phenytoin Treatment and the Sodium Challenge

Small cell lung cancer Lu-165 cells were counted and inoculated at a density of approximately 5×10^5 cells/well in 24-well cell culture plates containing RPMI1640 medium (980 μL). After a 48-h exposure to either the drug vehicle (dimethyl sulfoxide) or three concentrations of phenytoin (Sigma Chemical Co., St. Louis,

MO, USA) (5, 10, or 25 $\mu\text{g}/\text{mL}$) that span the therapeutic range (10–20 $\mu\text{g}/\text{mL}$), cells and culture media were separately collected and stored at -20°C for later measurement. For the sodium challenge, RPMI1640 media with high sodium concentrations were prepared by adding sodium chloride (Sigma-Aldrich, St. Louis, MO, USA) at 10 mEq/L (added 10 mEq/L) or at 20 mEq/L (added 20 mEq/L) to the basal RPMI1640 medium. The sodium concentration of the basal RPMI1640 medium was 139.5 ± 0.1 mEq/L (mean \pm SE, $n = 6$). For the sodium challenge, cells were treated with the vehicle or phenytoin (25 $\mu\text{g}/\text{mL}$) in RPMI1640 media with added sodium at 10 or 20 mEq/L for 48 h.

Copeptin Measurement

The copeptin level (picomoles per liter) in the medium was detected with a new sandwich immunoassay (Peninsula Laboratories International, San Carlos, CA, USA) after C18 Sep-Column extraction following the manufacturer's recommendations, as previously reported (12).

Real-time Polymerase Chain Reaction

The mRNA levels of AVP and Na_v channel subunits were measured using real-time reverse transcription polymerase chain reaction (RT-PCR). Complementary DNA was obtained from cultured cells using a FastLane Cell cDNA Kit (QIAGEN, Tokyo, Japan) following the manufacturer's protocol. Custom Applied Biosystem TaqMan® Expression Assays (Thermo Fisher Scientific Inc., Yokohama, Japan) were used with Applied Biosystems® 7500 Fast real-time PCR system (Thermo Fisher Scientific Inc., Yokohama, Japan) following the manufacturer's protocol. All RT-PCR reagents contained a TaqMan FAM-MGB probe and two unlabeled, specific custom primers for each target sequence. For the relative quantification of RNA expression, the mRNAs of human AVP and the following human Na_v channel subunits were tested: $\beta 1$, $\text{Na}_v1.3$, $\text{Na}_v1.5$, $\text{Na}_v1.6$, and $\text{Na}_v1.7$. Human 18S-ribosomal RNA (18S rRNA) was used as an internal control. The difference between the cycle threshold values of each gene and the 18S rRNA gene was calculated for each experimental sample using the software of 7500 Fast System.

Statistical Analysis

Continuous variables were expressed as means \pm SEs. For group comparisons, the Tukey multiple comparison test or the paired *t*-test was used following one-way or two-way analysis of variance where appropriate. The data of RT-PCR were normalized by logarithmic transformation. Statistical analyses were performed using GraphPad Prism 6.0 (GraphPad Software Inc., CA, USA). A two-tailed probability value of <0.05 was considered statistically significant.

RESULTS

Comparison of AVP mRNA Levels among the Four SCLC Cell Lines

Reverse transcription polymerase chain reaction showed high levels of AVP mRNA in Lu-165 cells, but not in Lu-24, Lu-134A, or MS-1 cells (Figure 1).

Effects of Phenytoin on Copeptin Levels in the Medium and AVP mRNA Levels in Lu-165 Cells

Copeptin levels in the medium significantly decreased after the 48-h treatment of phenytoin at doses of 25 µg/mL, but not of 5 or 10 µg/mL (Figure 2A). Copeptin levels in the group without phenytoin were 6.7 ± 0.5 pmol/L, which were significantly different ($p < 0.01$) from 3.9 ± 0.3 pmol/L in the group with phenytoin at doses of 25 µg/mL (Figure 2A). Relative AVP mRNA levels in Lu-165 cells also decreased after the 48-h treatment of phenytoin at doses of 25 µg/mL (Figure 2B). There was a significant difference ($p < 0.01$) in relative AVP mRNA levels between the group without phenytoin (1.00 ± 0.36) and the group with phenytoin at doses of 25 µg/mL (0.13 ± 0.04) (Figure 2B).

Effects of Phenytoin on Copeptin Levels in the Medium and AVP mRNA Levels in Lu-165 Cells under the Sodium Challenge

The sodium challenge with added sodium at 10 and 20 mEq/L increased copeptin levels in the medium in an upward trend.

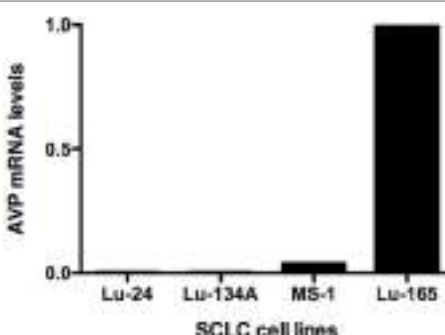


FIGURE 1 | Comparison of arginine vasopressin (AVP) mRNA levels among the four small cell lung cancer (SCLC) cell lines Lu-24, Lu-134A, MS-1, and Lu-165 ($n = 1$).

The copeptin levels of 17.7 ± 1.2 pmol/L at added 20 mEq/L was significantly higher ($p < 0.05$) than those of 9.2 ± 2.3 pmol/L without sodium challenge (added 0 mEq/L). The 48-h treatment of phenytoin at a dose of 25 µg/mL significantly decreased copeptin levels in the medium under the sodium challenge with added sodium at 10 mEq/L ($p < 0.01$) and at 20 mEq/L ($p < 0.05$) (Figure 3A). Although AVP expression levels did not change under the sodium challenges, they significantly decreased in the presence of 25 µg/mL phenytoin under the sodium challenge at added 10 mEq/L ($p < 0.05$) (Figure 3B).

Nav Channel Subunit mRNA Levels in Lu-165 Cells

We measured the mRNA levels of Nav channel subunits, including $\beta 1$, Nav1.3, Nav1.5, Nav1.6, and Nav1.7 in Lu-165 cells. Among the five subunits, Nav1.3 was dominantly expressed. The Nav1.3 mRNA levels in Lu-165 cells were significantly higher than the mRNA levels in any other Nav channel subunits ($p < 0.05$ – 0.01) (Figure 4).

Effects of Phenytoin on mRNA Levels of Nav1.3 in Lu-165 Cells under the Sodium Challenge

The sodium challenge with added sodium at 10 and 20 mEq/L did not affect Nav1.3 mRNA levels. The 48-h treatment of phenytoin at a dose of 25 µg/mL significantly ($p < 0.05$) reduced Nav1.3 mRNA levels under the sodium challenge with added sodium at 10 and 20 mEq/L (Figure 5).

DISCUSSION

It was previously uncertain whether phenytoin has a direct action on ectopic AVP-producing neuroendocrine tumors. The present study clearly demonstrates that Lu-165 cells expressed AVP mRNA and released copeptin and that a slightly greater than therapeutic dose of phenytoin reduced intracellular AVP mRNA levels and AVP surrogate copeptin concentrations in the medium

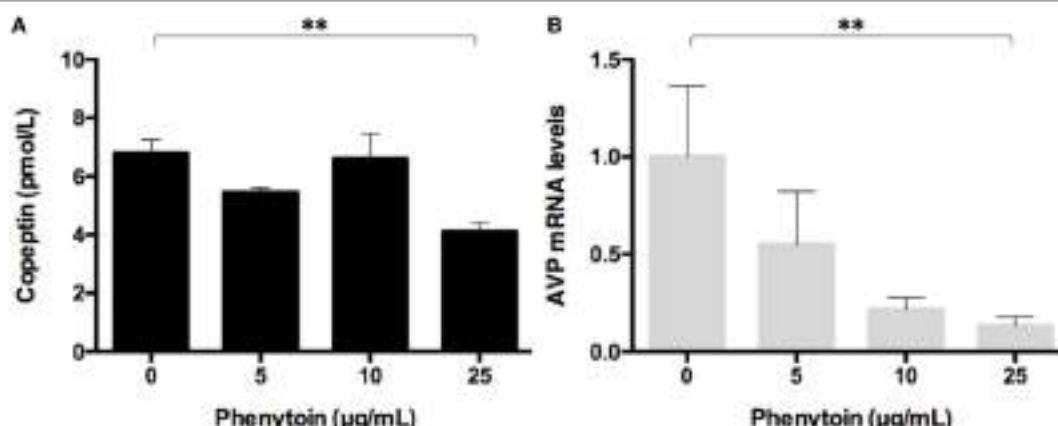


FIGURE 2 | Effect of three doses of phenytoin treatment (48 h) on copeptin levels in the medium ($n = 4$) (A) and arginine vasopressin (AVP) mRNA levels in Lu-165 cells ($n = 5$) (B) (** $p < 0.01$).

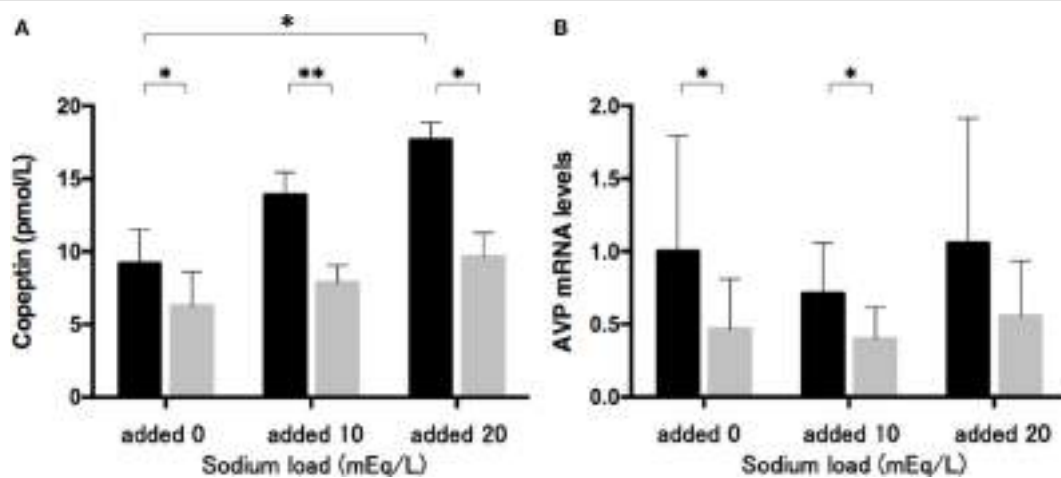


FIGURE 3 | Effects of phenytoin on copeptin levels in the medium ($n = 4$) (A) and arginine vasopressin (AVP) mRNA levels in Lu-165 cells under the sodium challenge ($n = 6$) (B). Black columns for phenytoin (−) and gray columns for phenytoin (+) (* $p < 0.05$, ** $p < 0.01$).

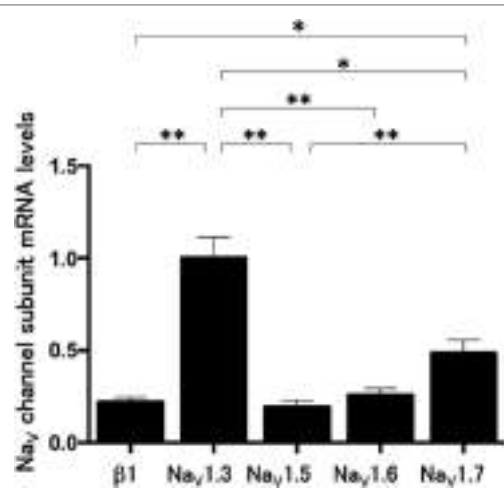


FIGURE 4 | Voltage-gated sodium channel (Nav channel) subunit mRNA levels in small cell lung cancer Lu-165 cells ($n = 6$) (* $p < 0.05$, ** $p < 0.01$).

of SCLC Lu-165 cells. SCLC Lu-165 cells were sensitive to the sodium load for increasing copeptin secretion and insensitive to increase AVP mRNA expression. Phenytoin downregulated those responses in Lu-165 cells.

Physiologically, AVP biosynthesis in the hypothalamic–pituitary axis and its secretion from the posterior pituitary is mainly regulated by peripheral signals from the osmoreceptors and baroreceptors (13). Conversely, ectopic AVP biosynthesis in AVP-producing neuroendocrine tumors appeared autonomous. However, there are some factors for controlling ectopic AVP biosynthesis (5). Verbeeck et al. (14) showed that cAMP and protein kinase-C pathways as well as glucocorticoid receptors are involved in the regulation of AVP mRNA levels in human SCLC GLC-8 cells. The present study indicates the involvement of phenytoin action in AVP gene expression and release in SCLC cells.

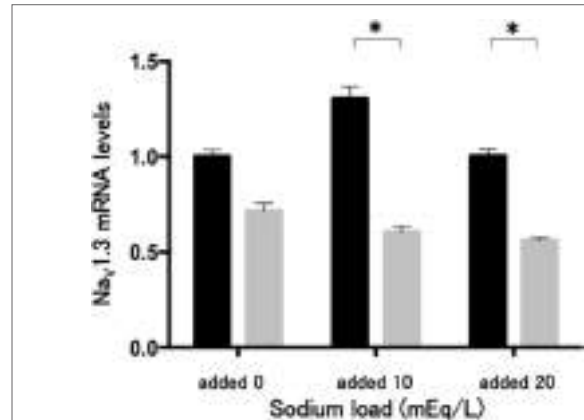


FIGURE 5 | Effects of phenytoin dose of 25 $\mu\text{g}/\text{mL}$ on mRNA levels of voltage-gated sodium channel subunit $\text{Na}_v1.3$ in Lu-165 cells under the sodium challenge ($n = 6$). Black columns for phenytoin (−) and gray columns for phenytoin (+) (* $p < 0.05$).

Guzek et al. (3) reported that 40 $\mu\text{g}/\text{mL}$ of phenytoin inhibited AVP release from an isolated rat neurohypophysis. Niewiadomski (15) found that the intraperitoneal administration of phenytoin at a dose of 100 mg/100 g body weight diminished the vasopressin level in the hypothalamus and neurohypophysis of euhydrated and dehydrated rats. These findings are consistent with the results of the present study. Therefore, there seems to be common mechanisms mediating the phenytoin-induced inhibition of AVP biosynthesis and release in the hypothalamo-neurohypophysis and malignant cells.

Since 1968, phenytoin has been widely used with much clinical success against all types of epileptiform seizures except absence seizures (1). At therapeutic concentrations in blood, the effect of phenytoin is mediated by slowing the rate of recovery of Na_v channel from activation (1, 16). However, at toxic concentrations, 10 times higher than therapeutic concentrations, multiple

effects of phenytoin are evident, including the enhancement of responses to GABA (16). As the phenytoin dose of 25 µg/mL used in the present study is slightly higher than the therapeutic range, there may be mechanisms other than Nav channel that mediate the effect of phenytoin on AVP gene expression and secretion in Lu-165 cells, which may be elucidated by electrophysiological analysis and sodium transport evaluation in future studies.

In the present study, we confirmed the gene expression of Nav channel subunits, including β1, Nav1.3, Nav1.5, Nav1.6, and Nav1.7, in SCLC Lu-165 cells; however, other subunits were not examined. Among these subunits, Nav1.3 was dominantly expressed in SCLC Lu-165 cells. Under the sodium challenged condition, Nav1.3 was found to be downregulated by a phenytoin dose of 25 µg/mL. Nav1.3 is one of the six tetrodotoxin-sensitive Nav channel α subunits (7). Kwong and Carr (9) reported that antiepileptic drugs, including phenytoin, target the local anesthetic site located in domain IVS6. This site is highly conserved among α subunits. Lucas et al. (17) reported that phenytoin suppressed the membrane potential in Nav1.3 that is overexpressed in Chinese hamster ovary cells. These findings suggest that Nav1.3 is one of the candidate molecules for mediating phenytoin action in Lu-165 cells.

Conflicting relationships between Nav channel expression and metastatic potential have been identified in several cell lines and clinical situations using biopsy samples (7, 18). In addition, there has been a discrepancy in the efficacy of phenytoin for controlling epileptic seizures (1). Even with optimal treatment, 20–30% of all epilepsy patients are pharmacoresistant (19). Mutations in genes encoding Nav channel subunits are anticipated to explain drug resistance. Variability in Nav channel genotypes is likely to account for the heterogeneity of the clinical effects of phenytoin (19). In addition, the effects of phenytoin in treating SIADH are controversial (20–22). The relationship between the pharmacotherapeutic effects of phenytoin and gene variations is uncertain. Therefore, SCLC cells and tissues other than Lu-165 cells may not respond to phenytoin. The present findings suggest that at least some forms of SCLC respond to phenytoin treatment. We speculated that the genotype analysis of the phenytoin responsive domain in Lu-165 cells is the key to predicting favorable clinical responses to phenytoin in patients with SIADH. Additionally, the mutational analysis and RNA interference study of Nav channels could confirm the direct involvement of Nav channels in controlling ectopic AVP expression in neuroendocrine tumors.

REFERENCES

- Vajda FJ, Eadie MJ. The clinical pharmacology of traditional antiepileptic drugs. *Epileptic Disord* (2014) 16:395. doi:10.1684/epd.2014.0704
- Miyagawa CI. The pharmacologic management of the syndrome of inappropriate secretion of antidiuretic hormone. *Drug Intell Clin Pharm* (1986) 20:527–31.
- Guzek JW, Russel JT, Thorn NA. Inhibition of diphenylhydantoin of vasopressin release from isolated rat neurohypophyses. *Acta Pharmacol Toxicol (Copenh)* (1974) 34:1–4. doi:10.1111/j.1600-0773.1974.tb01550.x
- Shoji M, Kimura T, Ota K, Yamaji T, Ishibashi M, Ohta M, et al. Genotype analysis of prepro-vasopressin signal peptide in vasopressin-producing and -non-producing lung tumors. *Life Sci* (1997) 61:2561–6. doi:10.1016/S0024-3205(97)01010-2

CONCLUSION

The results of the present study suggest that the SCLC cell line Lu-165 is sensitive to the phenytoin regulation of AVP release and gene expression. In Lu-165 cells, the Nav channel subunit Nav1.3 was dominantly expressed and it might be one of the candidate molecules for mediating phenytoin action. Further studies are required to elucidate the underlying mechanisms of phenytoin action.

ETHICS STATEMENT

Because the present study used established non-infectious cell lines without gene manipulation, ethics approval was not needed as per the institutional guidelines. In addition, the supplier Riken BRC stated that there is no restriction regarding academic use of four cell lines.

AUTHOR CONTRIBUTIONS

TO and MS contributed to the study design, data collection and analysis, interpretation of results, and writing and revising the manuscript. MM and SH contributed to the study design, data collection and interpretation of results and assisted in revising the manuscript. RI-N contributed to data collection and interpretation of results and assisted in revising the manuscript. KT contributed to the study design and interpretation of results and assisted in writing and revising the manuscript.

ACKNOWLEDGMENTS

The authors would like to thank Takayuki Nakai, Takahide Tsuda, Hiroki Takahashi, Hiroshi Kushibe, Wakana Niitsu, Mariko Iwai, Asuka Shimura, Mai Mutou, Kenji Yuasa, and Hiroki Ohori for their technical contribution.

FUNDING

The study was supported in part by MEXT's Promotion Plan for the Platform of Human Resource Development for Cancer project. Four cells were supplied by Riken BRC.

- Keegan BP, Memoli VA, North WG. Targeting the neurophysin-related cell surface antigen on small cell lung cancer cells using a monoclonal antibody against the glycopeptide region (cMAG-1) of provasopressin. *Mol Cancer Ther* (2002) 1:1153–9.
- Castillo JJ, Vincent M, Justice E. Diagnosis and management of hyponatremia in cancer patients. *Oncologist* (2012) 17:756. doi:10.1634/theoncologist.2011-0400
- Kruger LC, Isom LL. Voltage-gated Na⁺ channels: not just for conduction. *Cold Spring Harb Perspect Biol* (2016) 8:6. doi:10.1101/cshperspect.a029264
- Tanaka M, Cummins TR, Ishikawa K, Black JA, Ibata Y, Waxman SG. Molecular and functional remodeling of electrogenic membrane of hypothalamic neurons in response to changes in their input. *Proc Natl Acad Sci U S A* (1999) 96:1088–93. doi:10.1073/pnas.96.3.1088

9. Kwong K, Carr MJ. Voltage-gated sodium channels. *Curr Opin Pharmacol* (2015) 22:131. doi:10.1016/j.coph.2015.04.007
10. Morgenstaler NG, Struck J, Alonso C, Bergmann A. Assay for the measurement of copeptin, a stable peptide derived from the precursor of vasopressin. *Clin Chem* (2006) 52:112–9. doi:10.1373/clinchem.2005.060038
11. Terasaki T, Matsuno Y, Shimosato Y, Yamaguchi K, Ichinose H, Nagatsu T, et al. Establishment of a human small cell lung cancer cell line producing a large amount of anti-diuretic hormone. *Jpn J Cancer Res* (1994) 85:718–22. doi:10.1111/j.1349-7006.1994.tb02420.x
12. Iwashita N, Nara N, Sato R, Nakatogawa T, Kobayashi S, Zama S, et al. Differential regulation of plasma copeptin levels in patients with heart failure: a single-center prospective study. *Tohoku J Exp Med* (2016) 239:213. doi:10.1620/tjem.239.213
13. Share L. Role of vasopressin in cardiovascular regulation. *Physiol Rev* (1988) 68:1248–84.
14. Verbeeck MA, Sutanto W, Burbach JP. Regulation of vasopressin messenger RNA levels in the small cell lung carcinoma cell line GLC-8: interactions between glucocorticoids and second messengers. *Mol Endocrinol* (1991) 5:795–801. doi:10.1210/mend-5-6-795
15. Niewiadomski JS. The hypothalamic and neurohypophysial vasopressin content as influenced by diphenylhydantoin in dehydrated rats. *Acta Physiol Pol* (1979) 30:351–8.
16. Tunnicliff G. Basis of the antiseizure action of phenytoin. *Gen Pharmacol* (1996) 27:1091–7. doi:10.1016/S0306-3623(96)00062-6
17. Lucas PT, Meadows LS, Nicholls J, Ragsdale DS. An epilepsy mutation in the beta1 subunit of the voltage-gated sodium channel results in reduced channel sensitivity to phenytoin. *Epilepsy Res* (2005) 64:77–84. doi:10.1016/j.eplepsyres.2005.03.003
18. Fraser SP, Ozerlat-Gunduz I, Brackenbury WJ, Fitzgerald EM, Campbell TM, Coombes RC, et al. Regulation of voltage-gated sodium channel expression in cancer: hormones, growth factors and auto-regulation. *Philos Trans R Soc Lond B Biol Sci* (2014) 3:1638. doi:10.1098/rstb.2013.0105
19. Sharma AK, Rani E, Waheed A, Rajput SK. Pharmacoresistant epilepsy: a current update on non-conventional pharmacological and non-pharmacological interventions. *J Epilepsy Res* (2015) 5:1. doi:10.14581/jer.15001
20. Okamoto M, Nako Y, Tachibana A, Fujii T, Ohki Y, Tomomasa T, et al. Efficacy of phenytoin against hyponatremic seizures due to SIADH after administration of anticancer drugs in a neonate. *J Perinatol* (2002) 22:247–8. doi:10.1038/sj.jp.7210657
21. Fichman MP, Kleeman CR, Bethune JE. Inhibition of antidiuretic hormone secretion by diphenylhydantoin. *Arch Neurol* (1970) 22:45–53. doi:10.1001/archneur.1970.00480190049008
22. Decaux G, Przedborski S, Soupart A. Lack of efficacy of phenytoin in the syndrome of inappropriate anti-diuretic hormone secretion of neurological origin. *Postgrad Med J* (1989) 65:456–8. doi:10.1136/pgmj.65.765.456

Conflict of Interest Statement: The authors declare that the research was conducted in the absence of any commercial or financial relationships that could be construed as a potential conflict of interest.

Copyright © 2017 Ohta, Mita, Hishinuma, Ishii-Nozawa, Takahashi and Shoji. This is an open-access article distributed under the terms of the Creative Commons Attribution License (CC BY). The use, distribution or reproduction in other forums is permitted, provided the original author(s) or licensor are credited and that the original publication in this journal is cited, in accordance with accepted academic practice. No use, distribution or reproduction is permitted which does not comply with these terms.



The Role of Endocrine G Protein-Coupled Receptors in Ovarian Cancer Progression

Qingyu Zhang¹, Nadine Ellen Madden¹, Alice Sze Tsai Wong², Billy Kwok Chong Chow² and Leo Tsz On Lee^{1*}

¹Centre of Reproduction, Development and Aging, Faculty of Health Sciences, University of Macau, Taipa, Macau,

²School of Biological Sciences, The University of Hong Kong, Pokfulam, Hong Kong

OPEN ACCESS

Edited by:

Hubert Vaudry,
University of Rouen,
France

Reviewed by:

Rafael Vazquez-Martinez,
Instituto Maimónides
de Investigación Biomédica
de Córdoba, Spain
Vance Trudeau,
University of Ottawa, Canada

*Correspondence:

Leo Tsz On Lee
LTOLee@umac.mo

Specialty section:

This article was submitted to
Neuroendocrine Science,
a section of the journal
Frontiers in Endocrinology

Received: 22 December 2016

Accepted: 23 March 2017

Published: 07 April 2017

Citation:

Zhang Q, Madden NE, Wong AST, Chow BKC and Lee LTO (2017)
The Role of Endocrine G Protein-Coupled Receptors in Ovarian Cancer Progression.
Front. Endocrinol. 8:66.
doi: 10.3389/fendo.2017.00066

Ovarian cancer is the seventh most common cancer in women and the most lethal gynecological cancer, causing over 151,000 deaths worldwide each year. Dysregulated production of endocrine hormones, known to have pluripotent effects on cell function through the activation of receptor signaling pathways, is believed to be a high-risk factor for ovarian cancer. An increasing body of evidence suggests that endocrine G protein-coupled receptors (GPCRs) are involved in the progression and metastasis of ovarian neoplasms. GPCRs are attractive drug targets because their activities are regulated by more than 25% of all drugs approved by the Food and Drug Administration. Therefore, understanding the role of endocrine GPCRs during ovarian cancer progression and metastasis will allow for the development of novel strategies to design effective chemotherapeutic drugs against malignant ovarian tumors. In this review, we address the signaling pathways and functional roles of several key endocrine GPCRs that are related to the cause, progression, and metastasis of ovarian cancer.

Keywords: G protein-coupled receptor, ovarian cancer, endocrine system, peptide hormone, cell signaling

G PROTEIN-COUPLED RECEPTORS (GPCRs) AND OVARIAN CANCER

According to the 2012 global cancer statistical report from the World Health Organization (WHO) BLOBOCAN project, approximately 200,000 new cases of ovarian cancer are reported annually (1–3). It is the second most common gynecological cancer and is associated with the higher mortality rate of any gynecological cancer. The high mortality rate is due to the aggressive but asymptomatic progression of cancer cells throughout the peritoneal cavity, with more than 70% of patients being diagnosed at an advanced/metastatic stage (stage III or IV) (4). Because ovarian cancers are frequently diagnosed late, most patients present with extensive intraperitoneal tumors. Surgical debulking followed by chemotherapy is the mainstay of treatment for ovarian cancer, but it has not proven to be effective. The 5-year survival rate of patients undergoing salvage therapies is less than 25%. More than 70% of patients are initially sensitive to platinum- and taxane-based chemotherapy, but recurrence and peritoneal metastases are found in more than half of these patients, leading to low overall survival rates (5). The WHO classifies ovarian cancer into epithelial, sex cord-stromal, and germ cell neoplasms. More than 90% of ovarian cancers arise from epithelial cells (6).

Fertility drugs, androgens, and other hormones used in replacement therapies are widely recognized as risk factors for gynecological cancers (7, 8). Therefore, it has been proposed that endocrine hormones are critical to the development of malignant gynecological neoplasms. Hormone receptors are classified into three superfamilies: GPCRs, cytokine receptors, and nuclear receptors. Generally, water-soluble hormones bind GPCRs and cytokine receptors located on the cell membrane surface,

triggering a cascade of signaling events. Lipid-soluble hormones enter the cell and bind to nuclear receptors that can directly regulate gene transcription. The role of the nuclear and cytokine receptor families in ovarian cancer has been well established. For example, estrogen has been implicated in the progression of ovarian cancer, where estrogen transduces pro-metastatic pathways *via* the nuclear estrogen receptor (ER). Recent epidemiological studies have demonstrated an elevation of ovarian cancer incidence with the postmenopausal use of estrogen (7, 9).

G protein-coupled receptors are involved in many aspects of tumorigenesis, including the promotion of aberrant growth, increased cell viability, angiogenesis, and metastasis (10). Recent large-scale genomic analyses have discovered an abundance of mutations in G proteins and GPCRs (11). For instance, 20% of all sequenced human tumors contain mutations in GPCRs, including mutations in the thyroid-stimulating hormone receptor (TSHR) (12), the luteinizing hormone receptor (LHR), and the follicle-stimulating hormone receptor (FSHR), known to be involved in thyroid, breast, lung, and colon cancers, respectively (13). In another study, a mutant allele of GPRC5A was found to affect breast cancer risk (14), as lower levels of GPRC5A had adverse effect on the expression and function of *BRCA1*. Alterations in gene expression and promoter methylation of GPCRs in tumors have also been reported (10), and these changes appear to promote cancer proliferation, immune evasion, invasion of surrounding tissues, and increased resistance to hostile environments, such as hypoxia (15). In a study describing glioblastoma GPCR transcriptomes, 138 GPCRs were found to be aberrantly expressed, including several orphan receptors, such as GPR19, GPR82, GPR171, and GPR128 (16). Moreover, the orphan receptor GPR161 was shown to be overexpressed in triple-negative breast cancer and correlated with poor prognosis (17). In the same study, GPR161 was found to be a major regulator of cell proliferation and migration through induction of rapamycin signaling.

Here, we will review the role of endocrine GPCRs in ovarian cancer. The term “endocrine GPCRs” refers to a subgroup of GPCRs with endogenous ligands (i.e., it excludes the G-protein-coupled olfactory receptor). This review will focus on the following: (1) reproductive hormone receptors, including the G protein-coupled estrogen receptor (GPER), FSHR, and LHR; (2) hormone receptors that are involved in gonadotropin release, including the kisspeptin receptor (Kiss1R) and gonadotropin-releasing hormone receptor (GnRHR); (3) other hormone receptors including endothelin receptors (ETRs) and angiotensin II type 1 receptor (AGTR1). The signaling network in different receptors is also described, and perspectives on the future of GPCR research in ovarian cancer research are given.

G PROTEIN-COUPLED ESTROGEN RECEPTOR

Estrogens are sex hormones involved in regulating cell growth and differentiation in mammalian ovaries. A large-scale prospective cohort study conducted in the United States showed a strong link between ovarian cancer and estrogen. An increase in the

risk of ovarian cancer was found in patients who had undergone estrogen replacement therapy (ERT), with the rate ratio (RR) rising to 1.23 [95% confidence interval (CI), 1.06–1.43]. For patients who had undergone ERT for more than 10 years, the RR increased to 2.2 (95% CI, 1.53–3.17) (7). This prospective study provided strong evidence that estrogen is a high-risk factor in postmenopausal women. However, a meta-analysis of 15 case studies did not find any correlation between ERT and ovarian cancer. The apparent contrast in results between each study may be due to the different genetic backgrounds of the patients tested or the sample sizes of each study. It is worth noting that ERT consists of treatment with both estrogen and another sex hormone, progesterone. These two hormones have opposing effects on ovarian epithelial cells. Therefore, the effects of estrogen and progesterone should be considered and investigated separately.

Estrogens bind to two different types of receptors in mammalian cells. Two well-known ERs, ER α and ER β , are nuclear receptors that affect gene expression by binding to estrogen responsive elements in the promoter region of target genes. Another is GPER (also known as GPR30), which belongs to the GPCR family of receptors, and mediates the non-genomic signaling of estrogens. GPER is expressed in various cancer cell lines and primary tumors of the breast, endometrium, ovaries, thyroid, lung, prostate, testicular germ cells, and brain (18). Even though GPER is widely expressed in tumors, its role in ovarian cancer is controversial. An early report proposed that elevated expression levels of GPER correlate with poor prognosis (19). Activation of GPER in ER-negative cells has also been shown to promote cell migration and invasion (20). However, contradictory results suggesting that high GPER expression is associated with a favorable prognosis have also been published (21, 22). In fact, the GPER selective agonist, G-1, significantly inhibited the proliferation of ovarian cancer cells by suppressing tubulin polymerization and arresting cell cycle progression (2, 23). These conflicting results indicate that the role of GPER in ovarian cancer may vary from case to case. Several recent studies have suggested that cross talk between GPCRs might clarify the role of GPER during tumorigenesis. For example, the ability of GPER to serve as a prognosticator of cancer prognosis depends on gonadotropin receptor status. Increased expression of GPER predicted a longer survival period in patients negative for either FSHR or LHR compared to patients who were positive for FSHR and LHR. In addition, patients who tested negative for both FSHR and LHR had a more favorable prognosis than single-receptor negative patients (21). This observation suggests a mutually exclusive effect of GPER in association with LHR and FSHR during ovarian cancer progression.

With regards to the mechanistic activity of GPER, it appears that a signal transduction occurs primarily through the extracellular signal-regulated and mitogen-activated protein kinase pathway. It has been shown that activation of GPER by estradiol induces ERK1/2 phosphorylation and promotes ovarian cancer proliferation regardless of ER status (24). In addition, GPER also activates cAMP and PIP2 signaling, inducing expression of matrix metalloproteinase 2 (MMP2) and MMP9, which, in turn, promote cancer metastasis (25). In breast and thyroid cancer cells, as well as endometrial cells, GPER exerts its effects through

the transactivation of the epidermal growth factor receptor (EGFR). For example, GPER activates the ERK1/2 pathway *via* the transactivation of EGFR in breast cancer cell lines (26). In ovarian cancer cells, activation of GPER promotes cell survival *via* the transactivation of EGFR and cross talk with the PI3K/AKT signaling pathway (27).

The expression level of GPER is tightly associated with cell survival in epithelial ovarian cancer cells; a higher expression of GPER is correlated with a lower survival rate. Long et al. found that GPER expression correlates with tumor size and stage, lymph metastasis, and MMP9 expression (20, 28). ER-negative cells provide a clear picture of the role of GPER in ovarian cancer cell proliferation. 17 β -Estradiol is a strong agonist of GPER that can enhance S-phase promotion and cell migration in ER-negative ovarian cancer cells (19, 20). Selective activation of GPER by G-1 can also activate EGFR, upregulate c-fos, cyclin D1, cyclin E, and cyclin A, and promote cell proliferation (23). These *in vitro* studies provide strong evidence that GPER promotes ovarian cancer cell proliferation. However, a clinical study involving 40 ovarian cancer patients with higher GPER expression found no association between clinical stage, pathological stage, and survival time (29). Tissue specimens from 124 ovarian cancers, 35 benign tumors, and 35 low-malignant tumors revealed that GPER is downregulated in ovarian cancer and that elevated expression of GPER correlates with a longer survival time. Additionally, GPER overexpression can induce G2/M cell cycle arrest *via* cyclin B1 and CDC2 (22). Therefore, the ultimate result of GPER activation varies when co-expressed with other hormone receptors. For example, the effect of GPER activation is not only regulated by FSHR and LHR but also ER. It is apparent then that the role of GPER during ovarian cancer progression is highly complex and requires further investigation.

GONADOTROPIN-RELEASING HORMONE RECEPTOR

Two forms of GnRHR have been discovered in mammals: GnRHR1 and GnRHR2. GnRHR1 is predominantly expressed in the hypothalamus and the pituitary and regulates reproduction in response to gonadotropin-releasing hormone (30). GnRHR2 is mainly expressed in the midbrain. GnRHR2 appears to be involved in the regulation of sexual behavior and food intake (30). However, human GnRHR2 acquires frame shift mutations resulting in the appearance of an early stop codon and the production of a truncated version of the protein. Therefore, in this review, we will primarily focus on GnRHR1, hereby referred to as GnRHR.

Upon activation by its ligand (GnRH), GnRHR stimulates the synthesis and release of the gonadotropic hormones, FSH and LH. Because GnRHR is expressed in the ovary (31, 32), it is widely believed to be involved in ovarian cancer development and metastasis. The potential role of GnRHR as a tumor suppressor in ovarian cancer has been hypothesized because ovarian cancer patients with lower tumor expression levels of GnRHR showed more favorable survival rates (31). *In vitro* experiments also support this relationship as treatment with a specific GnRHR agonist (Buserelin) inhibited phosphatidylinositol kinase and

exhibited a strong anti-mitogenic effect on ovarian carcinoma cells (33). In another study, the GnRHR agonist, [D-Ala6] GnRH, directly inhibited the growth of ovarian cancer cells in a time- and dose-dependent manner, whereas a GnRHR antagonist (Antide) reversed this effect (34).

Estradiol (E2) downregulated the expression of GnRHR and reduced GnRHR-mediated inhibition of proliferation in the ovarian cancer cell line, OVCAR-3. However, in human ovary surface epithelial (hOSE) cells, estradiol did not affect the expression of GnRHR, and thus GnRH did not affect cell proliferation (35). These results indicate that GnRHR expression in ovarian cancer can be suppressed by the estrogen signaling pathway. Another study found that estrogen repressed GnRHR-mediated inhibition of proliferation in an ER α dependent manner *via* the upregulation of c-Jun and the recruitment of the cAMP response element binding (CREB) protein (36). These results provide evidence that estradiol promotes the proliferation of ovarian cancer cells and overrides the antineoplastic effects of GnRHR. Because the role of GPER in OVACR-3 and hOSE cell proliferation and migration is unclear, further studies are required to explore the potential cross talk between GnRHR and GPER in regulating ovarian cancer progression.

The signaling pathways regulated by GnRHR appear to be tissue specific. Classic GnRHR signaling in pituitary gonadotrophs is responsible for the activation of protein kinase C (PKC), phospholipase C (PLC), and adenylyl cyclase. Upon ligand binding, GnRHR activates phosphotyrosine phosphatase (PTP), which inactivates the epidermal growth factor receptor/mitogen-activated protein kinase signaling pathway *via* dephosphorylation of the EGFR. GnRHR inhibits proliferation through the activation of PKC, which is followed by phosphorylation and activation of ERK1/2. Interestingly, this antiproliferative effect can be reversed by blocking GnRHR, which has been shown to play a critical role in this process. With respect to GnRHR2, it has been reported that this receptor is non-functional (37). However, the role of GnRHR2 in ovarian cancer requires further investigation. One study showed that treatment with GnRH-I or GnRH-II inhibits PTP and subsequently inactivates MAPK signaling. More specifically, analogs of GnRH-I and GnRH-II reduced EGF-triggered mitogenic signal transduction (38). Transcriptomic and proteomic approaches were used to investigate the effects of triptorelin, an agonist of GnRHR, on ovarian cancer cells. Triptorelin has been shown to be an effective promoter of cell cycle arrest by inhibiting G2/M phase progression, eventually leading to apoptosis. This effect appears to be mediated by NF- κ B phosphorylation and AKT inactivation (39).

In contrast to the studies listed above, it has been shown that GnRHR antagonists exhibit antiproliferative properties in ovarian cancer cells by inducing cell apoptosis *via* the activation of p38 and c-Jun mediated Bax expression. Increased Bax expression ultimately leads to mitochondrial dysfunction and subsequent activation of the intrinsic pathway of apoptosis (40). Intriguingly, GnRHR antagonists appear to be less cytotoxic and more potent in mouse models of cervical cancer compared to GnRHR agonists (41). The uniformity of the GnRH-II agonist and antagonist on cancer cell proliferation probably result from cell stress caused

by hyperactive or over deterrence related signaling. Cross talk between EGF and GnRH-II signaling also appears to promote ovarian cancer metastasis. Specifically, EGF induces the expression of GnRH-II by promoting CREB-dependent transcription, resulting in ovarian cancer invasion (42). Other studies have shown that GnRH-II can enhance cancer cell adhesion, thereby promoting migration and invasion, by increasing laminin receptor expression levels (43).

In conclusion, GnRHR is a critical regulator of ovarian cancer cell proliferation. Both hyperactivity (i.e., high doses of GnRH, ~100 nM) and inhibition of GnRHR can suppress cancer cell proliferation and induce apoptosis. However, lower doses of GnRH-II (~10 nM) can promote cancer cell invasion and migration. Therefore, imbalances in the levels of GnRHR activity appear to modulate the rate of cancer cell proliferation and metastasis.

FOLLICLE-STIMULATING HORMONE RECEPTOR

All ovarian epithelial tumors express FSHR, and the expression level of FSHR is positively correlated with tumor grade (44). FSH is known to stimulate ovarian cancer cell proliferation, and this effect can be reversed by exposure to LH. These observations may explain why FSH treatment does not increase ovarian cancer risk in postmenopausal women (45). LHR and FSHR are generally co-expressed in the ovaries of postmenopausal women, and the co-regulation of LHR and FSHR signaling is essential to maintain normal function of the ovaries. Investigation into the underlying molecular pathogenesis of ovarian cancer has provided evidence that FSHR activation can influence cancer related gene expression. For example, FSH can downregulate tumor suppressor genes, including RB1 and BRCA1 (46), and overexpression of FSHR increased protein levels of Her2, c-myc, EGFR, and ERK1/2 (47), resulting in ovarian cancer cell proliferation. In addition, FSH was found to regulate ovarian cancer mitosis *via* the PI3K/AKT/HIF-1/cyclin-D1 signaling pathway (48). It appears that FSHR not only enhances cell growth but also promotes the invasiveness of ovarian cancer cells. Furthermore, it has been shown that activation of FSHR triggers the PI3K/AKT/Snail signaling pathway, activates ERK1/2, and upregulates expression of OCT4, thereby promoting cancer cell epithelial–mesenchymal transition, migration, and distant invasion (49, 50).

Several groups have already begun testing FSHR inhibitors for their ability to inhibit the progression of ovarian cancer. In one study, an FSH analog complexed with either paclitaxel or cisplatin inside nanoparticles enhanced the potency and selectivity of the chemotherapeutic drug to target ovarian cancer cells, while showing a reduction of unwanted side effects. Here, the selectivity of these complexed nanoparticles for ovarian cancer cells was enhanced using an FSH peptide conjugated to poly-amidoamine dendrimers. These particles have been previously shown to perform better than non-targeted administration with regards to inhibition of ovarian cancer proliferation and lymphatic metastasis (51, 52). Moreover, FSHR-based targeting has shown to have potent anticancer effects in both *in vitro* and *in vivo* models (53). In another study, anti-FSHR immune receptors were used to

redirect T cells to ovarian tumors by inducing the expression of anti-FSHR immune receptors in the patient's T lymphocytes. The anti-FSHR immune receptor then triggered T-mediated cytotoxicity in ovarian cancer cells (54). This promising approach could potentially recruit T lymphocytes to ovarian cancer tumors and not only initiate T cytotoxicity and continuous tumor immune responses but also reduce adverse side effects by limiting cytotoxicity to the site of the tumor.

LUTEINIZING HORMONE RECEPTOR

Previous studies have shown LHR to be expressed abundantly in the plasma membrane of ovarian epithelial cells (55). Moreover, low-grade ovarian cancer tumors express LHR to a higher degree than high-grade tumors, which suggests that LHR may play a role in ovarian cancer progression. LH is known to regulate the expression of several genes related to cell growth and apoptosis. It is worth noting that LH generally upregulates genes related to proliferation. Studies have shown that LH induces the expression of ERBB receptor tyrosine kinase 2 (ERBB2), which promotes cell proliferation. However, upregulation of ERBB2 alone was insufficient to enhance cell proliferation and survival of ovarian cancer cells (56). Interestingly, it was also found that activation of the LHR reduces cell invasion and proliferation. Studies have shown that MMP family members, such as MMP2 and MMP9, are downregulated by LHR activation, while cell adhesion and basement membrane proteins (COL4A3, COL4A4, NID2, ITGB8, and LAMA3) were upregulated (56). These results might explain why treatment with LH suppresses ovarian cancer invasion. By screening using an miRNA-specific array, several antiproliferation miRNAs, including miR-101, miR-301, and miR-210, were found to be upregulated by LH treatment (57). Furthermore, LH appears to activate the PTP pathway *via* Ga(i) and counteracts mitogenic signal transduction induced by EGF (58), suggesting that the interaction of LHR and EGFR is essential for determining the fate of ovarian cancer cells.

Because LHR localizes to the cell surface of ovarian cancer cells, several studies have used LHR as a cancer biomarker for targeted therapy and have obtained moderately positive results. For example, using a nanoparticle that links CD44-siRNA to an LH analog in combination with paclitaxel significantly enhanced cell death in ovarian tumors (59). However, as LHR expression is generally decreased during tumorigenesis, this treatment would not be suitable for advanced stages of ovarian cancer.

THYROID-STIMULATING HORMONE RECEPTOR

Because TSHR is mainly found in the thyroid, scientists have primarily focused on the role of TSHR in thyroid cancer progression. However, recent evidence suggests that TSHR is highly expressed in ovarian cancer tumors (60). Patients with high tumor TSHR expression levels had lower survival rates compared to patients with low TSHR tumor expression levels (61). There remain discrepancies about the role of TSHR in thyroid and ovarian cancers: (1) TSHR was found to be downregulated in

thyroid cancer but highly expressed in ovarian cancer and (2) high TSHR expression was found to predict increased survival rates for thyroid cancer patients but poorer outcomes for patients with ovarian cancer (62). Therefore, TSHR activity appears to be correlated to ovarian cancer progression. However, further investigation is required to discern the role of TSHR in ovarian tumorigenesis.

KISSPEPTIN RECEPTOR

Kisspeptin receptor has been identified as a tumor suppressor in breast cancer and melanoma (63, 64). However, recent evidence suggests that kisspeptin (Kiss1) and Kiss1R are involved in ovarian cancer progression. Despite the similarity of Kiss1R expressions levels between malignant and benign ovarian tumors, the expression of Kiss1 was found to be significantly higher in malignant ovarian tumors. More importantly, Kiss1 expression levels negatively correlated with the clinical stage diagnosis (65). Immunohistochemical analysis of 518 ovarian cancer tumor samples suggested a favorable prognostic role of Kiss1R with regards to the total survival duration as well as the disease-free survival period. Therefore, it appears that the activation of Kiss1/Kiss1R indicates a favorable prognosis. Patient plasma kisspeptin levels also correlated with cancer metastasis, and levels of kisspeptin lower than 20 pmol/L have been associated with a higher risk of ovarian cancer metastasis (66). Additionally, high expression levels of Kiss1R decreased the lysophosphatidic acid induced migration of ovarian cancer cells. In another study, kisspeptin treatment inhibited cancer cell migration in a PKC-dependent manner (67), and decreased stromal cell-derived factor 1 (SDF-1) mediated tumor migration by suppressing AKT phosphorylation (63). Kisspeptin-10 can also activate Kiss1R and influence the binding efficiency of SDF-1/CXCL12 with its cell surface receptor, CXCR4, thereby inhibiting metastasis. Altogether, these results are indicative of the tumor suppressing nature of Kiss1 and its receptor, Kiss1R, in ovarian cancer.

ANGIOTENSIN II TYPE 1 RECEPTOR

Angiotensin II type 1 receptor is a key member of the renin-angiotensin system. This receptor is mainly expressed in the liver, lungs, kidneys, and adrenal glands. Recently, a study demonstrated, by immunohistochemical staining, that ovarian tumors express AGTR1. Survival analysis (from The Cancer Genome Atlas database) found that the expression level of AGTR1 is directly related to the overall survival and disease-free survival rate and that high AGTR1 expression indicates an unfavorable prognosis. Pathologic analysis showed that elevated expression of AGTR1 correlated with high microvessel density and an increased secretion of vascular endothelial growth factor (VEGF) (68). Serum levels of angiotensin II converting enzyme (ACE), the key enzyme responsible for production of angiotensin II, were shown to be significantly increased in ovarian cancer patients. However, no correlation was found between angiotensin II and Ca-125, a glycoprotein biomarker of advanced ovarian cancer. These results suggest that changes in the expression levels

of ACE are an early event during carcinogenesis and could be used as an efficient biomarker for the diagnosis of ovarian cancer compared to angiotensin II or Ca-125. Because ovarian cancer cells invade surrounding tissues through the peritoneal cavity, understanding the role of angiotensin II and ACE during metastasis will be essential to assess how AGTR1 regulates cancer progression. Future studies will determine the correlation between serum and peritoneal fluid angiotensin II levels and ovarian tumorigenesis.

BRCA1, one of the most well-studied tumor suppressor genes, is responsible for DNA repair post injury. Studies have shown that there is a positive correlation between BRCA1 and AGTR1 levels in ovarian tumors. Wild-type BRCA1 patients show higher tumor expression levels of AGTR1 compared to patients with BRCA1 mutations. Elevated expression of BRCA1 has been shown to significantly promote the expression of AGTR1. However, knockdown of BRCA1 did not affect AGTR1 expression. The positive regulation of AGTR1 by BRCA1 implies that AGTR1 might maintain the integrity of the cell's genome and reduce apoptotic signaling throughout carcinogenesis, without promoting cell mitosis (69). Other studies have demonstrated that angiotensin II can increase endothelial nitric oxide (eNOS) and upregulate cyclooxygenase-2, thereby enhancing angiogenesis (70). In mesenchymal stem cells, AGTR1 induced HIF-1 α expression and resulted in the upregulation of VEGF and ACE. In general, VEGF stimulates endothelial cell proliferation and migration, processes which contribute to tumor angiogenesis, while ACE accelerates the *de novo* production of angiotensin II, which forms a positive feedback loop (71). Therefore, AGTR1 antagonists might be useful for suppressing tumor angiogenesis in ovarian cancer. Targeting AGTR1 could significantly inhibit tumor growth via inactivation of the phosphorylation of PLC β 3, which could disrupt tumor angiogenesis by reducing the VEGF production, thus inhibiting endothelial cell survival (72). However, the source of the VEGF secretion (either endothelial cells or ovarian cancer cells) and the molecular mechanism responsible for angiotensin II-mediated endothelial cell migration and microvessel formation remain unknown. Thus, elucidating the role of AGTR1 during ovarian cancer metastasis will prove integral to developing AGTR1-targeted drugs for the treatment of ovarian cancer.

ENDOTHELIN RECEPTOR

There exist two types of ETRs: the endothelin A receptor (ETAR) and the endothelin B receptor (ETBR). All metastatic ovarian cancers and 90% of primary ovarian cancers express ETAR, whereas around 40% of ovarian tumors express ETBR. The ovarian cancer cell lines, PEO4 and PEO14, not only express ET-1 (endothelin 1) and ET-3 (endothelin 3) but also ETAR and ETBR, which suggests that ovarian cancer cells stimulate the ETR pathway in an autocrine fashion. ETAR agonists have been shown to exhibit strong antitumor activities compared to ETBR agonists, indicating that ETAR plays a more significant role during cancer progression in response to endothelin exposure compared to ETBR (73). One study found that endothelin could induce VEGF production via the HIF-1 α pathway, resulting

TABLE 1 | Summary of the role and pathways of G-protein-coupled receptors in ovarian cancer.

Receptor	Ligand	Function	Pathway	Reference
G-protein-coupled estrogen receptor	Estradiol	Regulate metastasis, and proliferation	PI3K/AKT/MMP-9	(24–27)
GnRHR1	GnRH-I, GnRH-II	Antiproliferation	P38/c-Jun/MAPK, Bax/caspase9	(37–39)
Follicle-stimulating hormone receptor	Follicle-stimulating hormone	Enhance proliferation, cell survival, metastasis	PI3K/AKT/HIF-1/cyclin-D1, ERK1/2MAPK	(47–50)
Luteinizing hormone receptor	Luteinizing hormone	Inhibits metastasis, suppress proliferation	cAMP/phosphotyrosine phosphatase/EGFR	(56, 58)
Thyroid-stimulating hormone receptor	Thyrotropin	Predict good outcome	Unknown	(61, 62)
Angiotensin II type 1 receptor	Angiotensin II	Enhance angiogenesis	eNOS/cyclooxygenase-2 (COX2)/HIF-1 α /vascular endothelial growth factor (VEGF)	(68, 70, 71)
Kisspeptin receptor	Kisspeptin	Inhibits proliferation and migration	Stromal cell-derived factor 1/CXCL12/CXCR4/AKT	(63, 67)
Endothelin receptor	Endothelin	Enhance angiogenesis and metastasis	PI3K/integrin-linked kinase/AKT, COX2/PE/HIF-1 α /VEGF	(74–77)

in neovascularization of ovarian tumors (74). Endothelin also induced cyclooxygenase 1/2 expression and increased expression levels of prostaglandin E2 and prostaglandin E4, resulting in VEGF production and promotion of angiogenesis. Furthermore, the activation of ETRs upregulated MMP-2, -3, -7, -9, and -13, critical mediators of cellular invasion. Integrin-linked kinase (ILK) also appears to be involved in transducing extracellular endothelin signals, mediating the activation of PI3K/AKT and promoting cell motility and invasion (74). It was also found that β -arrestin acts as an ETAR signal transducer by inactivating GSK-3 β through the PI3K/ILK/AKT pathway, thereby promoting WNT signaling and contributing to the chemoresistance, invasion, and metastasis of ovarian tumors.

Drug resistance is a major challenge in the treatment of ovarian cancer with paclitaxel therapy. Because endothelial cells generally enhance ovarian cancer cell survival, previous attempts to target ovarian tumors included the use of an ETR agonist (Atrasentan, ABT-627) to inhibit cell proliferation and VEGF production and to reduce ILK expression and phosphorylation of GSK-3 β (75). Ovarian tumors are known to become resistant to paclitaxel. However, administration of ABT-627 in combination with paclitaxel yielded improved results with regards to the inhibition of angiogenesis and the induction of apoptosis. In a separate study, the endothelial receptor antagonist, ZD4054, reduced cancer cell survival, invasion and angiogenesis and enhanced the chemotherapeutic sensitivity of ovarian tumors. ZD4054 effectively induced apoptosis by inhibiting Bcl-2 and activating caspase 3 (76). Furthermore, it was found that gene silencing of the endothelial converting enzyme resulted in the suppression of endothelial mediated cell proliferation and invasion via inhibition of MAPK phosphorylation, which suppressed MMP2 activity and upregulated the ratio of E-cadherin to N-cadherin (77). Finally, epigallocatechin-3-gallate, a polyphenol derived from green tea considered to be a potent natural anticancer small molecule, has been shown to reduce ovarian cancer progression by targeting ETAR, making it a potentially cost effective method of preventing ovarian cancer.

THE RECEPTOR NETWORK IN OVARIAN CANCER

The physiology of the ovary is precisely regulated by the reproductive hormones and receptors of the HPG axis. These receptor signaling cascades are not only found in the ovary but also in ovarian tumors. Evidence suggests that ovarian cancer development is tightly associated with dysregulated hormonal signaling. More importantly, hormone receptor expression patterns and the modulation of intricate signaling networks appear to determine the fate of cancer cells. The role of GPCRs in regulating ovarian cancer development is summarized in **Table 1**. In our model, Kiss1R, GnRHR, and LHR act as cancer suppressors by inhibiting proliferation and metastasis. FSHR acts as an oncogene in ovarian cancer by promoting cell proliferation and survival and antagonizes the tumor suppressing effects of LHR. GPCRs involved in cardiovascular function, such as AGTR1 and ETR, can also modulate the progression of ovarian cancer. Activation of AGTR1 and ETR has been shown to enhance angiogenesis and promote metastasis. While the effects of AGTR1 and ETR activity during tumorigenesis have been well studied, the relationship between these receptors and classic reproductive hormone GPCRs requires further investigation. In conclusion, numerous GPCRs and their specific ligands are likely important in ovarian cancer development and metastasis. Therefore, fully characterizing the roles of these GPCRs during tumorigenesis will greatly benefit the development of novel therapeutics.

AUTHOR CONTRIBUTIONS

All authors have made substantial, direct, and intellectual contribution to the work and approved it for publication.

FUNDING

LL was supported by FDCT grant, Macao (FDCT101/2015/A3) and MYRG2016-00075-FHS.

REFERENCES

- Siegel R, Naishadham D, Jemal A. Cancer statistics, 2012. *CA Cancer J Clin* (2012) 62:10–29. doi:10.3322/caac.20138
- Albanito L, Madeo A, Lappano R, Vivacqua A, Rago V, Carpino A, et al. G protein-coupled receptor 30 (GPR30) mediates gene expression changes and growth response to 17 β -estradiol and selective GPR30 ligand G-1 in ovarian cancer cells. *Cancer Res* (2007) 67:1859–66. doi:10.1158/0008-5472.CAN-06-2909
- Torre LA, Bray F, Siegel RL, Ferlay J, Lortet-Tieulent J, Jemal A. Global cancer statistics, 2012. *CA Cancer J Clin* (2015) 65:87–108. doi:10.3322/caac.21262
- Lengyel E, Burdette JE, Kenny HA, Matei D, Pilrose J, Haluska P, et al. Epithelial ovarian cancer experimental models. *Oncogene* (2014) 33:3619–33. doi:10.1038/onc.2013.321
- Bast RC Jr, Hennessy B, Mills GB. The biology of ovarian cancer: new opportunities for translation. *Nat Rev Cancer* (2009) 9:415–28. doi:10.1038/nrc2644
- Feeley KM, Wells M. Precursor lesions of ovarian epithelial malignancy. *Histopathology* (2001) 38:87–95. doi:10.1046/j.1365-2559.2001.01042.x
- Rodriguez C, Patel AV, Calle EE, Jacob EJ, Thun MJ. Estrogen replacement therapy and ovarian cancer mortality in a large prospective study of US women. *JAMA* (2001) 285:1460–5. doi:10.1001/jama.285.11.1460
- Tomao F, Lo Russo G, Spinelli GP, Stati V, Prete AA, Prinzi N, et al. Fertility drugs, reproductive strategies and ovarian cancer risk. *J Ovarian Res* (2014) 7:51–51. doi:10.1186/1757-2215-7-51
- Hein A, Thiel FC, Bayer CM, Fasching PA, Haberle L, Lux MP, et al. Hormone replacement therapy and prognosis in ovarian cancer patients. *Eur J Cancer Prev* (2013) 22:52–8. doi:10.1097/CEJ.0b013e328355ec22
- Dorsam RT, Gutkind JS. G-protein-coupled receptors and cancer. *Nat Rev Cancer* (2007) 7:79–94. doi:10.1038/nrc2069
- Liang H, Cheung LW, Li J, Ju Z, Yu S, Stemke-Hale K, et al. Whole-exome sequencing combined with functional genomics reveals novel candidate driver cancer genes in endometrial cancer. *Genome Res* (2012) 22:2120–9. doi:10.1101/gr.137596.112
- Russo D, Arturi F, Schlumberger M, Caillou B, Monier R, Filetti S, et al. Activating mutations of the TSH receptor in differentiated thyroid carcinomas. *Oncogene* (1995) 11:1907–11.
- Piersma D, Verhoeft Post M, Look MP, Uitterlinden AG, Pols HA, Berns EM, et al. Polymorphic variations in exon 10 of the luteinizing hormone receptor: functional consequences and associations with breast cancer. *Mol Cell Endocrinol* (2007) 276:63–70. doi:10.1016/j.mce.2007.06.007
- Sokolenko AP, Bulanova DR, Iyevleva AG, Aleksakhina SN, Preobrazhenskaya EV, Ivantsov AO, et al. High prevalence of GPRC5A germline mutations in BRCA1-mutant breast cancer patients. *Int J Cancer* (2014) 134:2352–8. doi:10.1002/ijc.28569
- Liu X, Liu C, Laurini E, Posocco P, Prich S, Qu F, et al. Efficient delivery of sticky siRNA and potent gene silencing in a prostate cancer model using a generation 5 triethanolamine-core PAMAM dendrimer. *Mol Pharm* (2012) 9:470–81. doi:10.1021/mp2006104
- Feve M, Saliou JM, Zeniou M, Lennon S, Carapito C, Dong J, et al. Comparative expression study of the endo-G protein coupled receptor (GPCR) repertoire in human glioblastoma cancer stem-like cells, U87-MG cells and non malignant cells of neural origin unveils new potential therapeutic targets. *PLoS One* (2014) 9:e91519. doi:10.1371/journal.pone.0091519
- Feigin ME, Xue B, Hammell MC, Muthuswamy SK. G-protein-coupled receptor GPR161 is overexpressed in breast cancer and is a promoter of cell proliferation and invasion. *Proc Natl Acad Sci U S A* (2014) 111:4191–6. doi:10.1073/pnas.1320239111
- Prossnitz ER, Barton M. The G-protein-coupled estrogen receptor GPER in health and disease. *Nat Rev Endocrinol* (2011) 7:715–26. doi:10.1038/nrendo.2011.122
- Liu H, Yan Y, Wen H, Jiang X, Cao X, Zhang G, et al. A novel estrogen receptor GPER mediates proliferation induced by 17 β -estradiol and selective GPER agonist G-1 in estrogen receptor alpha (ERalpha)-negative ovarian cancer cells. *Cell Biol Int* (2014) 38:631–8. doi:10.1002/cbin.10243
- Yan Y, Liu H, Wen H, Jiang X, Cao X, Zhang G, et al. The novel estrogen receptor GPER regulates the migration and invasion of ovarian cancer cells. *Mol Cell Biochem* (2013) 378:1–7. doi:10.1007/s11010-013-1579-9
- Heublein S, Mayr D, Vrekoussis T, Friese K, Hofmann SS, Jeschke U, et al. The G-protein coupled estrogen receptor (GPER/GPR30) is a gonadotropin receptor dependent positive prognosticator in ovarian carcinoma patients. *PLoS One* (2013) 8:e71791. doi:10.1371/journal.pone.0071791
- Ignatov T, Modl S, Thulig M, Weissenborn C, Treeck O, Ortmann O, et al. GPER-1 acts as a tumor suppressor in ovarian cancer. *J Ovarian Res* (2013) 6:51. doi:10.1186/1757-2215-6-51
- Wang C, Lv X, He C, Hua G, Tsai MY, Davis JS. The G-protein-coupled estrogen receptor agonist G-1 suppresses proliferation of ovarian cancer cells by blocking tubulin polymerization. *Cell Death Dis* (2013) 4:e869. doi:10.1038/cddis.2013.397
- Yu T, Liu M, Luo H, Wu C, Tang X, Tang S, et al. GPER mediates enhanced cell viability and motility via non-genomic signaling induced by 17 β -estradiol in triple-negative breast cancer cells. *J Steroid Biochem Mol Biol* (2014) 143:392–403. doi:10.1016/j.jsbmb.2014.05.003
- Yu X, Li F, Klussmann E, Stallone JN, Han G. G protein-coupled estrogen receptor 1 mediates relaxation of coronary arteries via cAMP/PKA-dependent activation of MLCP. *Am J Physiol Endocrinol Metab* (2014) 307:E398–407. doi:10.1152/ajpendo.00534.2013
- Wei W, Chen ZJ, Zhang KS, Yang XL, Wu YM, Chen XH, et al. The activation of G protein-coupled receptor 30 (GPR30) inhibits proliferation of estrogen receptor-negative breast cancer cells in vitro and in vivo. *Cell Death Dis* (2014) 5:e1428. doi:10.1038/cddis.2014.398
- Petrie WK, Dennis MK, Hu C, Dai D, Arterburn JB, Smith HO, et al. G protein-coupled estrogen receptor-selective ligands modulate endometrial tumorgrowth. *Obstet Gynecol Int* (2013) 2013:472720. doi:10.1155/2013/472720
- Long L, Cao Y, Tang LD. Transmembrane estrogen receptor GPR30 is more frequently expressed in malignant than benign ovarian endometriotic cysts and correlates with MMP-9 expression. *Int J Gynecol Cancer* (2012) 22:539–45. doi:10.1097/IGC.0b013e318247323d
- Kolkova Z, Casslen V, Henic E, Ahmadi S, Ehinger A, Jirstrom K, et al. The G protein-coupled estrogen receptor 1 (GPER/GPR30) does not predict survival in patients with ovarian cancer. *J Ovarian Res* (2012) 5:9. doi:10.1186/1757-2215-5-9
- Chen CC, Fernald R. GnRH and GnRH receptors: distribution, function and evolution. *J Fish Biol* (2008) 73:1099–120. doi:10.1111/j.1095-8649.2008.01936.x
- Wilkinson SJ, Kucukmetin A, Cross P, Darby S, Gnanapragasam VJ, Calvert AH, et al. Expression of gonadotropin releasing hormone receptor I is a favorable prognostic factor in epithelial ovarian cancer. *Hum Pathol* (2008) 39:1197–204. doi:10.1016/j.humpath.2007.12.011
- Minarets D, Jakubowski M, Mortola JF, Pavlou S. Gonadotropin-releasing hormone receptor gene expression in human ovary and granulosa-lutein cells. *J Clin Endocrinol Metab* (1995) 80:430–4. doi:10.1210/jc.80.2.430
- Takagi H, Imai A, Furui T, Horibe S, Fuseya T, Tamaya T. Evidence for tight coupling of gonadotropin-releasing hormone receptors to phosphatidylinositol kinase in plasma membrane from ovarian carcinomas. *Gynecol Oncol* (1995) 58:110–5. doi:10.1006/gyno.1995.1192
- Kang SK, Choi KC, Cheng KW, Nathwani PS, Auersperg N, Leung PC. Role of gonadotropin-releasing hormone as an autocrine growth factor in human ovarian surface epithelium. *Endocrinology* (2000) 141:72–80. doi:10.1210/en.141.1.72
- Kang SK, Choi KC, Tai CJ, Auersperg N, Leung PC. Estradiol regulates gonadotropin-releasing hormone (GnRH) and its receptor gene expression and antagonizes the growth inhibitory effects of GnRH in human ovarian surface epithelial and ovarian cancer cells. *Endocrinology* (2001) 142:580–8. doi:10.1210/endo.142.2.7982
- Cheng CK, Chow BK, Leung PC. An activator protein 1-like motif mediates 17 β -estradiol repression of gonadotropin-releasing hormone receptor promoter via an estrogen receptor alpha-dependent mechanism in ovarian and breast cancer cells. *Mol Endocrinol* (2003) 17:2613–29. doi:10.1210/me.2003-0217
- Kim KY, Choi KC, Auersperg N, Leung PC. Mechanism of gonadotropin-releasing hormone (GnRH)-I and -II-induced cell growth inhibition in ovarian cancer cells: role of the GnRH-I receptor and protein kinase C pathway. *Endocr Relat Cancer* (2006) 13:211–20. doi:10.1677/erc.1.01033
- Eicke N, Gunthert AR, Emons G, Grundker C. GnRH-II agonist [D-Lys6] GnRH-II inhibits the EGF-induced mitogenic signal transduction in human endometrial and ovarian cancer cells. *Int J Oncol* (2006) 29:1223–9. doi:10.3892/ijo.29.5.1223

39. Meyer C, Sims AH, Morgan K, Harrison B, Muir M, Bai J, et al. Transcript and protein profiling identifies signaling, growth arrest, apoptosis, and NF-kappaB survival signatures following GnRH receptor activation. *Endocr Relat Cancer* (2013) 20:123–36. doi:10.1530/ERC-12-0192
40. Fister S, Gunthert AR, Aicher B, Paulini KW, Emons G, Grundker C. GnRH-II antagonists induce apoptosis in human endometrial, ovarian, and breast cancer cells via activation of stress-induced MAPKs p38 and JNK and proapoptotic protein Bax. *Cancer Res* (2009) 69:6473–81. doi:10.1158/0008-5472.CAN-08-4657
41. Fister S, Gunthert AR, Emons G, Grundker C. Gonadotropin-releasing hormone type II antagonists induce apoptotic cell death in human endometrial and ovarian cancer cells in vitro and in vivo. *Cancer Res* (2007) 67:1750–6. doi:10.1158/0008-5472.CAN-06-3222
42. Poon SL, Hammond GT, Leung PC. Epidermal growth factor-induced GnRH-II synthesis contributes to ovarian cancer cell invasion. *Mol Endocrinol* (2009) 23:1646–56. doi:10.1210/me.2009-0147
43. Poon SL, Klausen C, Hammond GL, Leung PC. 37-kDa laminin receptor precursor mediates GnRH-II-induced MMP-2 expression and invasiveness in ovarian cancer cells. *Mol Endocrinol* (2011) 25:327–38. doi:10.1210/me.2010-0334
44. Prentice LM, Klausen C, Kalloger S, Köbel M, McKinney S, Santos JL, et al. Kisspeptin and GPR54 immunoreactivity in a cohort of 518 patients defines favourable prognosis and clear cell subtype in ovarian carcinoma. *BMC Med* (2007) 5:33. doi:10.1186/1741-7015-5-33
45. Zheng W, Lu JJ, Luo F, Zheng Y, Feng Y, Felix JC, et al. Ovarian epithelial tumor growth promotion by follicle-stimulating hormone and inhibition of the effect by luteinizing hormone. *Gynecol Oncol* (2000) 76:80–8. doi:10.1006/gyno.1999.5628
46. Ji Q, Liu PI, Chen PK, Aoyama C. Follicle stimulating hormone-induced growth promotion and gene expression profiles on ovarian surface epithelial cells. *Int J Cancer* (2004) 112:803–14. doi:10.1002/ijc.20478
47. Zhang Z, Jia L, Feng Y, Zheng W. Overexpression of follicle-stimulating hormone receptor facilitates the development of ovarian epithelial cancer. *Cancer Lett* (2009) 278:56–64. doi:10.1016/j.canlet.2008.12.024
48. Chen J, Bai M, Ning C, Xie B, Zhang J, Liao H, et al. Gankyrin facilitates follicle-stimulating hormone-driven ovarian cancer cell proliferation through the PI3K/AKT/HIF-1alpha/cyclin D1 pathway. *Oncogene* (2016) 35:2506–17. doi:10.1038/onc.2015.316
49. Yang Y, Zhang J, Zhu Y, Zhang Z, Sun H, Feng Y. Follicle-stimulating hormone induced epithelial-mesenchymal transition of epithelial ovarian cancer cells through follicle-stimulating hormone receptor PI3K/Akt-Snail signaling pathway. *Int J Gynecol Cancer* (2014) 24:1564–74. doi:10.1097/IGC.0000000000000279
50. Liu L, Zhang J, Fang C, Zhang Z, Feng Y, Xi X. OCT4 mediates FSH-induced epithelial-mesenchymal transition and invasion through the ERK1/2 signalling pathway in epithelial ovarian cancer. *Biochem Biophys Res Commun* (2015) 461:525–32. doi:10.1016/j.bbrc.2015.04.061
51. Modi DA, Sunoqrot S, Bugno J, Lantvit DD, Hong S, Burdette JE. Targeting of follicle stimulating hormone peptide-conjugated dendrimers to ovarian cancer cells. *Nanoscale* (2014) 6:2812–20. doi:10.1039/c3nr05042d
52. Fan L, Chen J, Zhang X, Liu Y, Xu C. Follicle-stimulating hormone polypeptide modified nanoparticle drug delivery system in the treatment of lymphatic metastasis during ovarian carcinoma therapy. *Gynecol Oncol* (2014) 135:125–32. doi:10.1016/j.ygyno.2014.06.030
53. Zhang XY, Chen J, Zheng YF, Gao XL, Kang Y, Liu JC, et al. Follicle-stimulating hormone peptide can facilitate paclitaxel nanoparticles to target ovarian carcinoma in vivo. *Cancer Res* (2009) 69:6506–14. doi:10.1158/0008-5472.CAN-08-4721
54. Urbanska K, Stashwick C, Poussin M, Powell DJ Jr. Follicle-stimulating hormone receptor as a target in the redirected T-cell therapy for cancer. *Cancer Immunol Res* (2015) 3:1130–7. doi:10.1158/2326-6066.CIR-15-0047
55. Lu JJ, Zheng Y, Kang X, Yuan JM, Lauchlan SC, Pike MC, et al. Decreased luteinizing hormone receptor mRNA expression in human ovarian epithelial cancer. *Gynecol Oncol* (2000) 79:158–68. doi:10.1006/gyno.2000.5928
56. Puett D, Angelova K, da Costa MR, Warrenfeltz SW, Fanelli F. The luteinizing hormone receptor: insights into structure-function relationships and hormone-receptor-mediated changes in gene expression in ovarian cancer cells. *Mol Cell Endocrinol* (2010) 329:47–55. doi:10.1016/j.mce.2010.04.025
57. Cui J, Eldredge JB, Xu Y, Puett D. microRNA expression and regulation in human ovarian carcinoma cells by luteinizing hormone. *PLoS One* (2011) 6:e21730. doi:10.1371/journal.pone.0021730
58. Grundker C, Volker P, Emons G. Antiproliferative signaling of luteinizing hormone-releasing hormone in human endometrial and ovarian cancer cells through G protein alpha(I)-mediated activation of phosphotyrosine phosphatase. *Endocrinology* (2001) 142:2369–80. doi:10.1210/en.142.6.2369
59. Shah V, Taratula O, Garбуza OB, Taratula OR, Rodriguez-Rodriguez L, Minko T. Targeted nanomedicine for suppression of CD44 and simultaneous cell death induction in ovarian cancer: an optimal delivery of siRNA and anticancer drug. *Clin Cancer Res* (2013) 19:6193–204. doi:10.1158/1078-0432.CCR-13-1536
60. Huang W-L, Li Z, Lin T-Y, Wang S-W, Wu F-J, Luo C-W. Thyrostimulin-TSHR signaling promotes the proliferation of NIH:OVCAR-3 ovarian cancer cells via trans-regulation of the EGFR pathway. *Sci Rep* (2016) 6:27471. doi:10.1038/srep27471
61. Seagle BL, Eng KH, Yeh JY, Dandapani M, Schiller E, Samuelson R, et al. Discovery of candidate tumor biomarkers for treatment with intraperitoneal chemotherapy for ovarian cancer. *Sci Rep* (2016) 6:21591. doi:10.1038/srep21591
62. Gyftaki R, Liacos C, Politis E, Liantos M, Saltiki K, Papageorgiou T, et al. Differential transcriptional and protein expression of thyroid-stimulating hormone receptor in ovarian carcinomas. *Int J Gynecol Cancer* (2014) 24:851–6. doi:10.1097/IGC.0000000000000139
63. Navenot J-M, Wang Z, Chopin M, Fujii N, Peiper SC. Kisspeptin-10-induced signaling of GPR54 negatively regulates chemotactic responses mediated by CXCR4: a potential mechanism for the metastasis suppressor activity of kisspeptides. *Cancer Res* (2005) 65:10450–6. doi:10.1158/0008-5472.CAN-05-1757
64. Sanchez-Carbayo M, Capodieci P, Cordon-Cardo C. Tumor suppressor role of KiSS-1 in bladder cancer: loss of KiSS-1 expression is associated with bladder cancer progression and clinical outcome. *Am J Pathol* (2003) 162:609–17. doi:10.1016/S0002-9440(10)63854-0
65. Zhang SL, Yu Y, Jiang T, Lin B, Gao H. [Expression and significance of KiSS-1 and its receptor GPR54 mRNA in epithelial ovarian cancer]. *Zhonghua Fu Chan Ke Za Zhi* (2005) 40:689–92. doi:10.3760/j.issn:0529-567x.2005.10.013
66. Jayasena CN, Commissaris AN, Januszewski A, Gabra H, Taylor A, Harvey RA, et al. Plasma kisspeptin: a potential biomarker of tumor metastasis in patients with ovarian carcinoma. *Clin Chem* (2012) 58:1061–3. doi:10.1373/clinchem.2011.177667
67. Jiang Y, Berk M, Singh LS, Tan H, Yin L, Powell CT, et al. KiSS1 suppresses metastasis in human ovarian cancer via inhibition of protein kinase C alpha. *Clin Exp Metastasis* (2005) 22:369–76. doi:10.1007/s10585-005-8186-4
68. Ino K, Shibata K, Kajiyama H, Yamamoto E, Nagasaka T, Nawa A, et al. Angiotensin II type 1 receptor expression in ovarian cancer and its correlation with tumour angiogenesis and patient survival. *Br J Cancer* (2006) 94:552–60. doi:10.1038/sj.bjc.6602961
69. Bi FF, Li D, Cao C, Li CY, Yang Q. Regulation of angiotensin II type 1 receptor expression in ovarian cancer: a potential role for BRCA1. *J Ovarian Res* (2013) 6:89. doi:10.1186/1757-2215-6-89
70. Tamarat R, Silvestre JS, Durie M, Levy BI. Angiotensin II angiogenic effect in vivo involves vascular endothelial growth factor- and inflammation-related pathways. *Lab Invest* (2002) 82:747–56. doi:10.1097/01.LAB.0000017372.76297.EB
71. Liu C, Zhang JW, Hu L, Song YC, Zhou L, Fan Y, et al. Activation of the AT1R/HIF-1 alpha/ACE axis mediates angiotensin II-induced VEGF synthesis in mesenchymal stem cells. *Biomed Res Int* (2014) 2014:627380. doi:10.1155/2014/627380
72. Park YA, Choi CH, Do IG, Song SY, Lee JK, Cho YJ, et al. Dual targeting of angiotensin receptors (AGTR1 and AGTR2) in epithelial ovarian carcinoma. *Gynecol Oncol* (2014) 135:108–17. doi:10.1016/j.ygyno.2014.06.031
73. Bagnato A, Salani D, Di Castro V, Wu-Wong JR, Tecce R, Nicotra MR, et al. Expression of endothelin 1 and endothelin A receptor in ovarian carcinoma: evidence for an autocrine role in tumor growth. *Cancer Res* (1999) 59:720–7.
74. Spinella F, Rosano L, Di Castro V, Natali PG, Bagnato A. Endothelin-1 induces vascular endothelial growth factor by increasing hypoxia-inducible factor-1alpha in ovarian carcinoma cells. *J Biol Chem* (2002) 277:27850–5. doi:10.1074/jbc.M202421200
75. Rosano L, Spinella F, Di Castro V, Dedhar S, Nicotra MR, Natali PG, et al. Integrin-linked kinase functions as a downstream mediator of endothelin-1

- to promote invasive behavior in ovarian carcinoma. *Mol Cancer Ther* (2006) 5:833–42. doi:10.1158/1535-7163.MCT-05-0523
76. Rosano L, Di Castro V, Spinella F, Nicotra MR, Natali PG, Bagnato A. ZD4054, a specific antagonist of the endothelin A receptor, inhibits tumor growth and enhances paclitaxel activity in human ovarian carcinoma in vitro and in vivo. *Mol Cancer Ther* (2007) 6:2003–11. doi:10.1158/1535-7163.MCT-07-0151
77. Rayhman O, Klipper E, Muller L, Davidson B, Reich R, Meidan R. Small interfering RNA molecules targeting endothelin-converting enzyme-1 inhibit endothelin-1 synthesis and the invasive phenotype of ovarian carcinoma cells. *Cancer Res* (2008) 68:9265–73. doi:10.1158/0008-5472.CAN-08-2093

Conflict of Interest Statement: The authors declare that the research was conducted in the absence of any commercial or financial relationships that could be construed as a potential conflict of interest.

Copyright © 2017 Zhang, Madden, Wong, Chow and Lee. This is an open-access article distributed under the terms of the Creative Commons Attribution License (CC BY). The use, distribution or reproduction in other forums is permitted, provided the original author(s) or licensor are credited and that the original publication in this journal is cited, in accordance with accepted academic practice. No use, distribution or reproduction is permitted which does not comply with these terms.



The Autophagy Machinery: A New Player in Chemotactic Cell Migration

Pierre-Michaël Coly^{1,2}, Pierrick Gandolfo^{1,2}, Hélène Castel^{1,2} and Fabrice Morin^{1,2*}

¹ Normandie Univ, UNIROUEN, Institut National de la Santé et de la Recherche Médicale (INSERM), DC2N, Rouen, France

² Institute for Research and Innovation in Biomedicine, Rouen, France

Autophagy is a highly conserved self-degradative process that plays a key role in diverse cellular processes such as stress response or differentiation. A growing body of work highlights the direct involvement of autophagy in cell migration and cancer metastasis. Specifically, autophagy has been shown to be involved in modulating cell adhesion dynamics as well as epithelial-to-mesenchymal transition. After providing a general overview of the mechanisms controlling autophagosome biogenesis and cell migration, we discuss how chemotactic G protein-coupled receptors, through the repression of autophagy, may orchestrate membrane trafficking and compartmentation of specific proteins at the cell front in order to support the critical steps of directional migration.

OPEN ACCESS

Edited by:

Eric W. Roubos,
Radboud University Nijmegen,
Netherlands

Reviewed by:

Tullio Florio,
University of Genoa, Italy
Anil Kumar Challa,
University of Alabama at Birmingham,
USA
Ciro Isidoro,
University of Eastern Piedmont, Italy

*Correspondence:

Fabrice Morin
fabrice.morin@univ-rouen.fr

Specialty section:

This article was submitted to
Neuroendocrine Science,
a section of the journal
Frontiers in Neuroscience

Received: 01 December 2016

Accepted: 03 February 2017

Published: 16 February 2017

Citation:

Coly P-M, Gandolfo P, Castel H and
Morin F (2017) The Autophagy
Machinery: A New Player in
Chemotactic Cell Migration.
Front. Neurosci. 11:78.
doi: 10.3389/fnins.2017.00078

Keywords: autophagosome biogenesis, cell adhesion, chemotactic migration, CXCR4, GPCR, urotensin II

CHEMOTACTIC MIGRATION: CONTROL BY G PROTEIN-COUPLED RECEPTORS

Steps of Chemotactic Migration

Chemotactic cell migration is a highly coordinated process that is crucial to the function of many cell types. As such, it is a fundamental property of a variety of physiological and pathological phenomena. Chemotactic migration is first observable during embryonic development, as sheets of cells undergo migration to form the different layers of the embryo and later, the different tissues that constitute organs (Keller, 2005). In the central nervous system, chemotactic migration allows cells such as new neurons to localize to the appropriate cortical layer, and guides the elongation of their growth cones to facilitate circuit formation (Cooper, 2013). Cell migration is also involved in immune response and angiogenesis allowing cells to infiltrate and navigate through tissues (Imhof and Dunon, 1997). A few pathological processes can also take advantage of a cell's migration abilities to spread through the organism. This is the case in cancer progression, during which parenchyma invasion and metastasis formation heavily rely on chemotactic migration (Bravo-Cordero et al., 2012).

Previous studies have shown that chemotactic migration can be broken down into a few successive steps. Surface receptors pick up on chemotactic cues in the extracellular environment and orient chemotaxis. These receptors can activate signaling cascades that establish a front-rear polarity. The class I phosphatidylinositol 3-kinase (PI3K) is a vital player during this step. The lipid kinase forms phosphatidylinositol (3,4,5)-triphosphate (PIP3) at the cell front, which serves as a signal for several pathways that converge toward reorganizing the actin cytoskeleton (Weiner, 2002). This allows the formation of actin-dependent membrane protrusions toward the chemotactic signal. The lamellipodium is probably the most characterized type of cell protrusion involved in migration. It is composed of a dense dendritic network of actin filaments that pushes the plasma membrane forward, but also serves as an intracellular scaffold favoring the appearance of links with the extracellular matrix (ECM). These links, called adhesion complexes, stabilize the

lamellipodium and act as a molecular clutch allowing the cell body to pull itself forward (Ridley et al., 2003).

Adhesion complexes are highly dynamic structures that are formed by the hierarchical recruitment of different scaffolding proteins. At their base we find integrins, heterodimer transmembrane proteins with long extracellular heads that can bind to ECM components such as fibronectin. This link, coupled with intracellular cues, activates integrins by modifying the conformation of their extracellular heads, thereby increasing their affinity for the ECM (Tadokoro et al., 2003; Campbell and Humphries, 2011). Activated integrins also cluster together to form more robust structures that are linked to actin filaments by talin and paxillin (Ridley et al., 2003). During migration, the retrograde flow of actin filaments applies forces to the adhesion complexes that seem to be essential to their sustainability and maturation, by allowing the addition of strengthening proteins such as vinculin (Choi et al., 2008). A rearward motion of these adhesion complexes can be observed as the cell body moves forward. Once they reach a certain point, they begin to disassemble, as to not impede with migration. Cells that cannot effectively disassemble adhesion complexes are considerably slowed in their advance since they cannot detach from the substratum (Kaverina et al., 1999; Ezratty et al., 2005). Adhesion turnover also serves to recycle adhesion proteins to the cell front so that they may aid in the construction of new complexes (Margadant et al., 2011).

Disassembly seems to rely on “relaxation” signals carried by microtubules. Early observations showed that adhesions are destabilized as microtubules grow toward them. These filaments may in fact stimulate loss of tension by bringing focal adhesion kinase (FAK) and calpains to the adhesion site. Phosphorylation of paxillin by FAK contributes to the weakening of the structure, whereas calpains physically disrupt the link between actin and the ECM by cleaving talin (Franco S. J. et al., 2004; Webb et al., 2004). Ubiquitination also seems to partake in adhesion disassembly, as several proteins, such as FAK, paxillin, and integrins are ubiquitinylated during this process (Huang, 2014). The final step involves the endocytosis of integrins, mainly by a clathrin-dependent pathway (Ezratty et al., 2009). Once internalized, integrins can either be transported to the cell front for the formation of new adhesion complexes, or directed to autophagosomes and lysosomes for degradation (Tulou-Minguez et al., 2013; Maritzen et al., 2015).

Chemotactic G Protein-Coupled Receptors

With over 800 genes in Human, G-protein coupled receptors (GPCR) constitute the largest surface receptor family (Fredriksson et al., 2003). Their role is to help the cell

adapt to its environment by translating extracellular cues to intracellular responses. GPCRs are involved in a wide assortment of physiological processes and as such, their ligands vary from hormones to lipids and even photons. Many GPCRs can drive cell migration by enhancing motility and guiding the orientation of actin polymerization and adhesion complexes formation. Three main types of GPCRs have been found to induce chemotaxis. These include receptors for chemokines, some vasoactive peptides and bioactive lipids (Cotton and Claing, 2009).

Chemokines constitute a large family of chemotactic cytokines that can stimulate directed cell migration upon binding to their GPCR. They are characterized by the presence of four cysteine residues in their sequence and are named according to the position of the two first ones. Therefore, they are classified in four groups (CC, CXC, C, and CX3C) which bind to GPCRs named accordingly (Murphy et al., 2000). Few chemokine GPCRs have received as much attention as the C-X-C motif chemokine receptor 4 (CXCR4). CXCR4 plays pleiotropic functions in the peripheral immune system by stimulating the migration of monocytes and lymphocytes (Bleul et al., 1996). It is also an important regulator for homing of hematopoietic progenitor cells to the bone marrow microenvironment (Lapidot et al., 2005). In the central nervous system, CXCR4 participates in guiding developing interneurons to their proper cortical layer, as well as recruiting microglial cells during cortical development (Li and Ransohoff, 2008; Tiveron and Cremer, 2008; Nash and Meucci, 2014). Moreover, in CXCR4^{-/-} mice, most GnRH neurons fail to exit the vomeronasal organ during embryonic development, and comparatively few GnRH neurons reach the forebrain (Schwarting et al., 2006). In the adult brain, this GPCR is believed to influence regeneration by recruiting brain-resident and circulating cells to the site of the lesion (Stumm and Höllt, 2007). CXCR4 is also notable for its involvement in the internalization of the HIV as well as in the progression of a wide range of cancers (Feng et al., 1996; Chatterjee et al., 2014). As such, studies have shown that CXCR4 increases the migration rate of several types of cancer cells (Salcedo et al., 2003).

A few vasoactive peptides, initially characterized for the effects on the cardiovascular system, have more recently been shown to increase cell migration. For example, by binding to their cognate GPCRs, angiotensin II and endothelins can drive the migration of smooth muscle cells and endothelial cells (Xi et al., 1999; Daher et al., 2008). Urotensin II, the most potent vasoactive peptide identified so far, is able to induce directed cell migration of monocytes, endothelial cells as well as glioma cells (Segain et al., 2007; Xu et al., 2009; Brûlé et al., 2014; Lecointre et al., 2015). Several bioactive lipids have also been found to induce chemotaxis. One of them is lysophosphatidic acid, which, in the nervous system, has been shown to stimulate the migration of embryonic schwann cells and astrocytes (Sato et al., 2011; Anliker et al., 2013; Yung et al., 2015). Lysophosphatidic acid also drastically accelerates tumor growth by inducing angiogenesis and tumor invasion, two processes that rely on increased migration (Contos et al., 2000; Blackburn and Mansell, 2012).

Chemotactic GPCRs initiate signaling cascades that regulate cell migration by activating heterotrimeric G proteins, composed

Abbreviations: CXCR4, C-X-C motif chemokine receptor 4; DFC1, double FYVE domain-containing protein 1; ECM, extracellular matrix; EMT, epithelial-to-mesenchymal transition; ER, endoplasmic reticulum; ERGIC, ER-Golgi intermediate compartment; GPCR, G protein-coupled receptor; LC3, microtubule associated protein 1 light chain 3; mTOR, mechanistic target of rapamycin (serine/threonine kinase); NBR1, neighbor of BRCA1 gene 1; PI3K, phosphatidylinositol 3-kinase; PI3P, phosphatidylinositol 3-phosphate; PIP3, phosphatidylinositol (3,4,5)-triphosphate; PKA, protein kinase A; UT, urotensin II receptor; WIP1, WD repeat domain phosphoinositide interacting protein.

of three subunits, α , β , and γ . Activation of a GPCR switches out the GDP for a GTP in the $G\alpha$ subunit, which causes the dissociation of $G\alpha$ from $G\beta\gamma$. Each subunit can then go on to regulate different intracellular signaling pathways (Wilkie et al., 1992). Based on their sequences, $G\alpha$ proteins can be split into four main subtypes: α_s , α_i/o , $\alpha_q/11$, and $\alpha_{12/13}$ (Simon et al., 1991). Though previous studies have shown that all of these subtypes can, in one way or another, modulate cell migration, it appears that GPCR-induced chemotaxis is mainly relayed by $G\alpha_i$ and $G\alpha_{12/13}$ (Cotton and Claing, 2009; Lecointre et al., 2015). These G proteins have been linked to the activation of GTPases belonging to the Rho family: RhoA, Rac1, and Cdc42. Together, the GTPases orchestrate the construction of the dendritic actin network in the lamellipodium, as well as the formation and maturation of adhesions.

THE AUTOPHAGY MACHINERY

General Mechanisms of Autophagosome Biogenesis

Macroautophagy (hereafter referred to as autophagy) is an evolutionarily conserved lysosomal pathway involved in the degradation of long lived proteins and cytoplasmic organelles (Hale et al., 2013). This process, which is essential for normal turnover of cellular compartments, is up-regulated in response to nutrient starvation. The mechanistic target of rapamycin (mTOR) kinase is a key regulator of cell metabolism that represses autophagic activity when nutrient conditions are adequate. mTOR is itself inhibited upon nutrient starvation, which results in autophagy induction (Kim et al., 2011). One of the first events in autophagy is the formation of the phagophore, a cup-shaped isolation membrane. The edges of these phagophore membranes elongate and thereby engulf portions of cytoplasm. After the fusion of the membrane edges, the structure becomes a completed autophagosome, which later fuses with lysosomes, resulting in the degradation of its luminal content. Several highly conserved autophagy (ATG) proteins, which control key steps in the autophagy process, have been identified (Nakatogawa et al., 2009). Initiation of the phagophore requires the Beclin1-containing class-III PI3K complex, generation of phosphatidylinositol 3-phosphate (PI3P), and recruitment of the PI3P-binding proteins called WD repeat domain phosphoinositide interacting (WIPI) and double FYVE domain-containing protein 1 (DFCP1). These are followed by the recruitment of the ATG5-ATG12-ATG16L1 ternary complex, along with phosphatidylethanolamine-conjugated microtubule-associated protein 1 light chain 3 beta (LC3-II), which are essential for elongation of the phagophore membrane. While the ATG5-ATG12-ATG16L1 complex decorates the phagophore and dissociates after completion of autophagosome formation, part of LC3-II remains associated with fully formed autophagosomes (Abada and Elazar, 2014). In addition to its bulk degradation property, autophagy also partakes in the clearance of specific substrates. This selective autophagy mainly depends on cargo receptors such as neighbor of BRCA1 gene 1 (NBR1) and p62, which can bind to ubiquitin-tagged substrates. These cargo

receptors can also bind to LC3 via a LC3-interacting region (LIR) motif, which therefore targets them to autophagosomes (Bjørkøy et al., 2005; Pankiv et al., 2007; Kirkin et al., 2009; Zaffagnini and Martens, 2016).

Sources of Membrane for the Expansion of the Phagophore

Phagophores require lipids to mature into autophagosomes. After more than 50 years of investigations, the origin of the autophagosomal membranes is still a critical question. Originally, the endoplasmic reticulum (ER) was proposed to be the primary source of these membranes. Early electron microscopy studies identified a close relationship between the ER and autophagic structures, suggesting that autophagosomal membranes are mainly delivered from the ER (Novikoff and Shin, 1978; Hayashi-Nishino et al., 2009). Consistent with this idea, Axe et al. (2008) showed that, in response to amino acid starvation, the PI3P-binding protein DFCP1, translocates to PI3P-enriched subdomains of the ER. These subdomains then constitute a platform for accumulation of autophagosomal proteins, expansion of autophagosomal membranes and emergence of fully formed autophagosomes. Subsequent three-dimensional tomography studies (Hayashi-Nishino et al., 2009; Ylä-Anttila et al., 2009) demonstrated that subdomains of the ER form a cradle-like curve encircling isolation membranes. The associated ER and isolation membranes are interconnected by a narrow membrane extension from the isolation membrane. Recent studies found evidence that apart from the ER, numerous other membrane sources are involved in the formation of autophagosomes, including mitochondria, the Golgi, recycling endosomes and endocytic vesicles budding from the plasma membrane. Hailey et al. (2010) elegantly demonstrated that, in starved cells, mitochondria directly participate in autophagosome biogenesis. They found that the early autophagosomal marker, ATG5, transiently localizes to puncta on mitochondria, followed by the late autophagosomal marker LC3. This study further showed that cell starvation drives the delivery of lipid components from the mitochondrial outer membrane to newly formed autophagosomes. It has recently been reported that the Golgi may also contribute to the formation of autophagosomes. Following starvation, activation of the class-III PI3K complex promotes re-localization of COPII adaptors from the ER exit sites to the ER-Golgi intermediate compartment (ERGIC). The process leads to the generation of ERGIC-derived COPII vesicles which becomes LC3-positive and contribute to autophagosome biogenesis (Ge et al., 2015).

Recent reports demonstrated that recycling endosomes, through the formation of tubular structures accumulating autophagy proteins, also supply membrane for autophagosome biogenesis. In a siRNA-mediated screen, Knævelsrød et al. identified the PX domain-containing protein, SNX18, as a positive regulator of autophagy (Knævelsrød et al., 2013). The membrane binding and tubulation activities of SNX18, as well as its direct interaction with LC3, allow the formation of LC3-ATG16L1-positive tubules emanating for recycling endosomes that provide membrane input to forming autophagosomes. This

study is in line with other findings (Longatti et al., 2012) showing that vesicular transport from recycling endosomes, negatively regulated by the Rab11 effector protein TBC1D14, contributes to starvation-induced autophagy. Together, these data indicate that the recycling compartment is not solely responsible for recycling of plasma membrane receptors but also serves as a sorting station for controlled delivery of membrane for autophagosome biogenesis.

Work from Rubinsztein's lab identified endocytic vesicles, trafficking to recycling endosomes, as an important source of membrane for autophagosome biogenesis. Endocytic vesicles can form from regions of the plasma membrane through different mechanisms, i.e., clathrin-dependent and clathrin-independent vesicle budding (Ravikumar et al., 2010; Moreau et al., 2012). Accumulation of ATG16L1 at clathrin-coated endocytic structures, through an interaction between ATG16L1 and the clathrin adaptor AP2, and vesiculation of ATG16L1-positive precursors have been found to contribute to autophagosome formation. Inhibition of clathrin-mediated endocytosis, using siRNAs targeting the clathrin heavy-chain or the clathrin adaptor AP2, causes defective autophagosome biogenesis, which is associated with impaired uptake of plasma membrane into pre-autophagosomal vesicles (Ravikumar et al., 2010). These ATG16L1-positive vesicles then undergo SNARE-mediated homotypic fusion, generating tubulovesicular structures that increase in size, enabling the acquisition of LC3 protein (Moreau et al., 2011). Similarly to ATG16L1-positive vesicles, generation of clathrin-coated ATG9-positive vesicles from the plasma membrane also participates in autophagosome formation. Surprisingly, ATG16L1 and ATG9 proteins have been found to localize to distinct clathrin-coated vesicles and to traffic through different routes inside the cell. Although both ATG9 and ATG16L1 proteins end up in recycling endosomes, ATG9 is trafficked via EEA1-positive early endosomes, whereas ATG16L1 has minimal residence in early endosomes (Puri et al., 2013; Zavodszky et al., 2013). The SNARE protein named VAMP3, which co-traffics with ATG9, seems to be critical for the coalescence of ATG16L1 and ATG9 vesicles in recycling endosomes (Puri et al., 2013). The impact of this coalescence on the formation of tubules emanating from recycling endosomes, driven by SNX18, deserves further investigations.

REGULATION OF THE AUTOPHAGY MACHINERY BY G PROTEIN-COUPLED RECEPTORS

To this day, very few GPCRs have been shown to directly affect autophagic activity. These mainly include nutrient sensing receptors that increase anabolic processes via stimulation of the mTOR kinase, a well-known autophagy repressor (Jung et al., 2010; Wauson et al., 2014). The amino-acid responsive T1R1/T1R3 receptor is present in most tissues and acts as a sensor for the fed state and amino acid availability. It has been suggested that this GPCR may impact autophagic activity through mTOR stimulation. Reducing T1R3 levels in HeLa cells is sufficient to impair mTOR activity and activate autophagy (Wauson et al.,

2012). Angiotensin receptors have also been found to modulate autophagic activity in cardiomyocytes (Porrello et al., 2009), podocytes (Yadav et al., 2010) and in vascular smooth muscle cells (Yu et al., 2014), mainly through the generation of reactive oxygen species.

We recently found that chemotactic GPCRs CXCR4 and the urotensin II receptor (UT) also reduce autophagic activity by inhibiting autophagosome biogenesis (Coly et al., 2016). Unlike the studies cited above, these anti-autophagic effects do not seem to be relayed by mTOR modulation, but rather by inhibiting ATG16L1 recruitment to pre-autophagic vesicles budding from the plasma membrane. While Ravikumar et al. (Bjørkøy et al., 2005) demonstrated that ATG16L1 recruitment is dependent on its interaction with the AP2-clathrin complex, the data we obtained indicate that ATG5 is also implicated. We demonstrated that activation of CXCR4 or UT reduces the pool of ATG5 protein located at the plasma membrane, thereby reducing the recruitment of ATG16L1. Accordingly, overexpression of recombinant ATG5 totally abrogates the anti-autophagic activities of CXCR4 and UT, and siRNA-mediated knockdown of ATG5 mimics the inhibitory effects of these GPCRs on the formation of pre-autophagic endosomes. What is the exact role of ATG5 in mediating the formation of pre-autophagic endosomes? We can speculate that ATG5's membrane binding activity (Romanov et al., 2012) might allow the initial docking of an ATG5-ATG16L1 complex to the plasma membrane in order to maximize the probability of interaction between ATG16L1 and AP2-clathrin. Alternatively, since ATG5 can co-immunoprecipitate from cell lysates with ATG16L1 and clathrin, and since the N-terminus region of ATG16L1 allows both AP2-clathrin co-immunoprecipitation (Ravikumar et al., 2010) and direct ATG5 binding (Mizushima et al., 1999; Otomo et al., 2013; Kim et al., 2015), it is conceivable that ATG5 may act as a bridge between ATG16L1 and AP2-clathrin.

G PROTEIN-COUPLED RECEPTOR-INDUCED ACTIVATION OF CALPAINS: A CRITICAL EVENT THAT RELAYS PRO-MIGRATORY AND ANTI-AUTOPHAGIC PROPERTIES

Pro-Migratory Properties of Calpains

Calpains are a ubiquitously expressed family of cysteine proteases that mediate cleavage of specific substrates. Although calpain proteolysis can lead to full degradation of some of its substrates, others are cleaved in a limited fashion, resulting in protein fragments that have altered distributions and/or functions. Calpains have thus been found to be involved in a number of processes such as development, cell death, and motility (Goll et al., 2003). Modulating cell migration is one of the better known roles of these proteases. Studies conducted in neutrophils have shown that calpain inhibition increases random migration, but decreases GPCR-induced directional migration upon exposure to a gradient of interleukin 8 (Lokuta et al., 2003). In neurons, calpain activity was also shown to be essential for SDF1-induced actin reorganization and directional migration (Lysko et al.,

2014). These results are in line with work highlighting the role of the calpain 2 isoform during lamellipodium formation. Calpain 2 controls the formation of cell protrusions by cleaving cortactin, a key modulator of actin filament branching at the cell front. Expression of a calpain-resistant form of cortactin reduces the migration of fibroblasts by increasing the number of transient and inefficient cell protrusions (Perrin et al., 2006). Calpains also play an important role in the dynamics of adhesion formation and disassembly. By modifying the cytoplasmic tail of β -integrins, calpains seem to be essential for the formation of integrin clusters at an early stage of adhesion complex assembly (Bialkowska et al., 2000) Talin is another calpain target during these initial steps. Once cleaved, talin can bind to β -integrin tails, therefore constituting the first link between integrins and actin filaments (Yan et al., 2001) In addition to their role during this assembly phase, calpains are also one of the main actors of adhesion disassembly. They contribute to adhesion turnover by destabilizing the structural integrity of the complex. Several proteins such as paxillin, vinculin and talin are in fact targeted by calpains during this stage (Carragher et al., 1999; Franco S. et al., 2004; Serrano and Devine, 2004). Inhibiting calpains with either calpastatin or pharmacological means significantly slows adhesion turnover (Bhatt et al., 2002). Similar results can be obtained following calpain 2 knockdown, which results in large, long lasting adhesion complexes that inhibit cell detachment and therefore impair cell migration (Franco S. J. et al., 2004). Despite the many roles of calpains during cell migration, their regulation by chemotactic GPCRs remains unclear. However, previous work revealed that calpain 2 is recruited at the plasma membrane and activated following its phosphorylation by ERK and dephosphorylation on a protein kinase A (PKA) site (Glading et al., 2000; Shiraha et al., 2002). Interestingly, as mentioned earlier, the pro-migratory properties of many chemotactic GPCRs are relayed by G_i coupling, which has the ability to activate ERK, through $\beta\gamma$ subunits, and to inhibit PKA, through the α_i subunit (Goldsmith and Dhanasekaran, 2007; Cotton and Claing, 2009). We can therefore speculate that the simultaneous induction of these signaling pathways by chemotactic GPCRs may be determinant for the activation of calpain 2 at the plasma membrane and regulation of adhesion dynamics.

Anti-Autophagic Properties of Calpains

A growing amount of data suggests that calpains are major inhibitors of the autophagy machinery. SiRNA-mediated knockdown of calpain 1 is sufficient to induce autophagy under nutrient rich conditions, correlated with increased levels of LC3-II and ATG5-ATG12 complex (Xia et al., 2010). Using a cell-free system, Yousefi et al. demonstrated that ATG5 can be cleaved by both calpain 1 and calpain 2 (Yousefi et al., 2006). Cleavage of ATG5 then generates a 24 kDa N-terminal product that can translocate to the mitochondria and enhance susceptibility toward apoptotic stimuli (Yousefi et al., 2006). *In vitro* experiments also identified ATG3, ATG4, ATG7, ATG9, ATG10, ATG12, and Beclin1 as direct calpain substrates (Norman et al., 2010; Yang et al., 2010). It should be noted that calpains may also exert their anti-autophagic properties by targeting non-ATG

proteins. The clathrin adaptors AP2 and PICALM, which are critical for the formation of pre-autophagosomal vesicles from the plasma membrane, have been described as calpain substrates (Kim and Kim, 2001; Rudinskiy et al., 2009; Ando et al., 2013). Does calpain-dependent repression of autophagy then constitute a critical event for chemotaxis? In favor of this hypothesis, we found that the anti-autophagic and pro-migratory properties of two chemotactic GPCR, CXCR4, and UT, were abrogated by pharmacological inhibition or siRNA knockdown of calpains (Coly et al., 2016). We further demonstrated that calpain activation, induced by CXCR4 or UT, reduces the pool of ATG5 at the plasma membrane and inhibits the recruitment of ATG16L1 protein to endocytic vesicles, thereby limiting the formation of pre-autophagosomal precursors required for the expansion of the phagophore and formation of mature autophagosomes. In addition to reversing the anti-autophagic effects of chemotactic GPCRs, calpain inhibition or ATG5 overexpression is also sufficient to block their pro-migratory properties, as both these approaches reduce the cells' migration rate, as well as the number of adhesions per cell (Coly et al., 2016). Despite early reports pointing to ATG5 as a calpain target, our attempts at demonstrating its direct cleavage following CXCR4 or UT activation were unsuccessful. One hypothesis is that only a minor, plasma membrane-associated fraction of ATG5 is cleaved by calpains. The cleaved products may also be highly unstable, thereby hindering their detection. Alternatively, the anti-autophagic action of calpains following GPCR activation could depend on the cleavage of the adaptor proteins AP2 and PICALM, or on the cleavage of ATG7, which is essential for conjugation of ATG5-ATG12 (Mizushima et al., 1998). Since the recruitment of calpains at the plasma membrane constitutes an early event during chemotaxis (Franco and Huttenlocher, 2005), it can be anticipated that GPCR-induced inhibition of autophagy may tightly control early steps of cell polarization.

G PROTEIN-COUPLED RECEPTOR-INDUCED INHIBITION OF AUTOPHAGY: POTENTIAL IMPACT ON CHEMOTACTIC MIGRATION AND INVASION

Lamellipodium Expansion vs. Autophagosome Biogenesis: Competition for a Common Source of Membrane?

During GPCR-induced chemotactic migration, efficient expansion of the lamellipodium requires addition of extra membrane at the leading edge, through polarized, microtubule-dependent exocytosis (Bretscher and Aguado-Velasco, 1998; Pierini et al., 2000; Schmoranz et al., 2003). Work from Veale et al. identified VAMP3-positive recycling endosomes as an important source of internal membrane that is incorporated at the leading edge during macrophage migration (Veale et al., 2010). The authors further demonstrated that, in order for this to happen, the R-SNARE VAMP3 needs

to form a complex with its cognate Q-SNARE complex Stx4/SNAP23 located at the cell surface. Loss of any one of the components of the VAMP3/Stx4/SNAP23 complex inhibits efficient lamellipodium formation and alters cell migration. Along with the incorporation of extra membrane, this mechanism also allows the recycling of cell adhesion components at the leading edge, including integrins (Veale et al., 2010).

Since recycling endosomes, through the SNX18-dependent formation of tubules, supply membrane for phagophore expansion, it is conceivable that this compartment may constitute a sorting station that deliver phospholipids in a competitive manner, for either lamellipodium expansion or autophagosome synthesis. The dynamic increase in plasma membrane surface triggered by chemotactic GPCRs may then directly impact the pool of phospholipids available for autophagic activity. How could activation of GPCRs, located at the cell surface, affect the trafficking of membrane from recycling endosomes? Chemotactic GPCRs CXCR4 and UT alter, through the activation of calpains, the recruitment of ATG16L1 in pre-autophagosomal vesicles budding from the plasma membrane (Coly et al., 2016). This may reduce the pool of ATG16L1 targeted to the recycling compartment and limit the coalescence of ATG16L1 and ATG9 vesicles. Inhibition of ATG16L1 and ATG9 coalescence would then favor the delivery of VAMP3-positive vesicles at the cell front, at the expense of the phagophore (**Figure 1**).

Front Cell's Accumulation of Focal Adhesion Components

Among the hallmarks of cell migration, the formation of adhesion complexes at the cell's leading edge is among the most notable. Adhesions are critical in generating the traction required for the cell's forward movement. Several data have demonstrated autophagic degradation of key proteins involved in the initiation and the maturation of adhesion complexes, indicating that autophagy can regulate adhesion dynamics. The Src kinase, which is involved in adhesion signaling, was shown to co-immunoprecipitate with LC3 and to be degraded by autophagy (Sandilands et al., 2012). In fibroblasts, $\beta 1$ integrin-containing vesicles co-localize with LC3-stained autophagic structures. Inhibition of autophagy by ATG5 or ATG3 knockdown is able to slow $\beta 1$ integrin degradation and to promote its recycling to the plasma membrane (Tuloupinguez et al., 2013). Kenific et al. (Shiraha et al., 2002) recently demonstrated that the selective autophagy cargo receptor NBR1 is essential for adhesion turnover and for the autophagic capture of multiple adhesion proteins including paxillin, vinculin and zyxin. Furthermore, paxillin was shown to have its own LIR domain, which is also involved in its autophagic degradation (Sharifi et al., 2016). In agreement with a role of autophagy in adhesion disassembly, global inhibition of autophagosome biogenesis, using knockdown strategies against ATG proteins, results in the accumulation of large and unproductive adhesions at the entire cell periphery that reduce cell migration (Kenific et al., 2016a,b; Sharifi

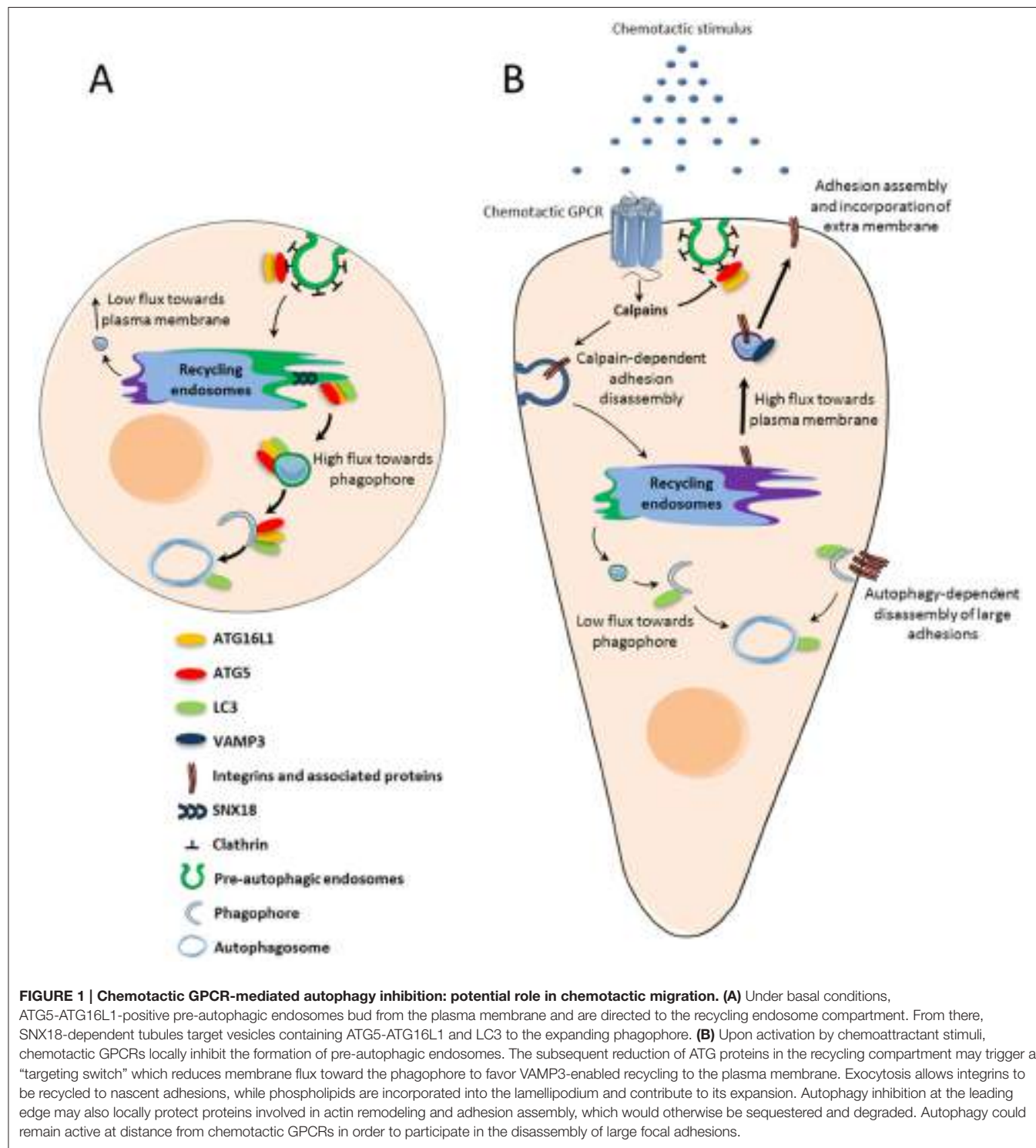
et al., 2016). Also these migration studies could appear to conflict with our report, (Coly et al., 2016) indicating that autophagy inhibition by CXCR4 or UT stimulates migration, they actually stress the fact that efficient chemotactic migration may imply compartmentalized rather than general inhibition of the autophagic machinery (Lecointre et al., 2015). We can propose that, at the front-most part of the cell, chemotactic GPCRs activated by a gradient of ligand could inhibit autophagy to favor the efficient formation of adhesions, while autophagy would remain active at distance from the site of GPCR activation/signaling in order to enable focal adhesion disassembly.

Front Cell's Accumulation of Proteins Participating in Actin Remodeling

Chemotactic GPCRs are known to induce actin polymerization at the cell's leading edge to allow the lamellipodium to protrude toward the chemoattractant stimulus. Interestingly, a number of proteins involved in actin dynamics and lamellipodium expansion have been shown to be degraded by autophagy. A Proteomic analysis allowed the identification of the actin regulators twinfilin, WIPF1, cortactin and cofilin 1 in ATG16L1-positive pre-autophagic vesicles budding from the plasma membrane (Morozova et al., 2015). Recent studies also indicate that the Rho GTPases Rac1 and RhoA can be regulated by autophagy. Using keratinocytes, Carroll et al. showed that Rac1 is inactivated during starvation induced autophagy (Carroll et al., 2013). LC3 is able to block Rac1 activation by binding to one of its effectors, Armus. LC3 can also directly interact with Rac1, though whether this leads to Rac1 degradation remains to be determined. Active RhoA and its regulator GEF-H1, can be ubiquitinated and recognized by p62, therefore leading to their selective degradation by the autophagic machinery (Belaid et al., 2014; Yoshida et al., 2016). Autophagy inhibition by shRNA targeting of ATG5 leads to an accumulation of RhoA at the cell surface and to the formation of actin rich lamellipodia. Interestingly, Belaid et al. (Ando et al., 2013) found that the intense actin polymerization caused by RhoA accumulation actually impairs cell motility. Once again, this implies that autophagy inhibition by chemotactic GPCRs may be fine-tuned and compartmentalized at the cell front in order to support effective cell migration.

Induction of the EMT

Epithelial to mesenchymal transition (EMT) plays a fundamental role in embryonic development and tissue repair. Numerous lines of evidence indicate that EMT also participates in tumor progression and metastasis. Once undergoing EMT, tumoral cells lose their apical-basal polarity, and acquire a mesenchymal phenotype characterized by an elongated morphology and increased motility (Kalluri and Weinberg, 2009). This allows them to detach from the primary site and invade the surrounding tissues and blood vessels. Interestingly, recent publications also link EMT to glioblastoma progression. Although not of epithelial origin, glioblastoma cells can engage an EMT-like process that increases their invasive properties (Kahlert et al., 2013). EMT



has been shown to be driven by a variety of signals, such as transforming growth factor- β , insulin growth factor II, or epidermal growth factor (Thiery et al., 2009). These EMT inducers then lead to the activation of core transcription factors, including Snail and Slug, ZEB1/2, and Twist (Tam and Weinberg, 2013).

A complex relationship exists between autophagy and EMT. On one hand, cells that have undergone EMT require increased autophagy to survive stressful environmental conditions during their migration. On the other hand, recent observations indicate that autophagy acts as an oncosuppressive mechanism by inhibiting early steps of EMT (Gugnani et al., 2016).

This latter idea was first proposed by Lv et al. (2012) who demonstrated that, in breast cancer cells, the intracellular signaling protein DEDD (death-effector domain-containing DNA-binding protein) inhibits EMT through the activation of autophagy and consecutive degradation of Snail and Twist. Snail and Twist were found to colocalize with the autophagosomal marker LC3, and inhibition of autophagy using 3-methyladenine significantly reduced their degradation rates (Lv et al., 2012). Using mouse embryonic fibroblast (MEF) cells, Qiang et al. found that ATG3, ATG5, ATG9, or ATG12 knockout cells exhibit much higher invasive properties than wild-type cells (Qiang et al., 2014). The authors demonstrated that autophagy deficiency promotes EMT events through the accumulation of p62 in the cytosol. Accumulating p62 then binds to Twist1 and prevents its proteasomal degradation. A recent study obtained in glioblastoma indicates that autophagy inhibition, through the knockdown of ATG5 or ATG7, stimulates the expression of the EMT regulators Snail and Slug, as well as cell invasion (Catalano et al., 2015).

From these data, it can be expected that inhibition of autophagy by chemotactic GPCRs, such as CXCR4 or UT (Coly et al., 2016), may constitute a critical event participating in EMT during tumor progression. This hypothesis is reinforced by recent reports demonstrating that, in addition to classical EMT inducers, CXCR4's ligand, CXCL12, drives Twist-dependent EMT-like events in human glioblastoma cells (Yao et al., 2016), as well as EMT in numerous peripheral cancers (Hu et al., 2014; Li et al., 2014; Roccaro et al., 2015) and UT's ligand, urotensin II, promotes the expression of EMT markers in renal tubular epithelial cells (Pang et al., 2016).

REFERENCES

- Abada, A., and Elazar, Z. (2014). Getting ready for building: signaling and autophagosome biogenesis. *EMBO Rep.* 15, 839–852. doi: 10.15252/embr.201439076
- Ando, K., Brion, J. P., Stygelbout, V., Suain, V., Authelet, M., Dedecker, R., et al. (2013). Clathrin adaptor CALM/PICALM is associated with neurofibrillary tangles and is cleaved in Alzheimer's brains. *Acta Neuropathol.* 125, 861–878. doi: 10.1007/s00401-013-1111-z
- Anliker, B., Choi, J. W., Lin, M. E., Gardell, S. E., Rivera, R. R., Kennedy, G., et al. (2013). Lysophosphatidic acid (LPA) and its receptor, LPA1, influence embryonic schwann cell migration, myelination, and cell-to-axon segregation. *Glia* 61, 2009–2022. doi: 10.1002/glia.22572
- Axe, E. L., Walker, S. A., Manifava, M., Chandra, P., Roderick, H. L., Habermann, A., et al. (2008). Autophagosome formation from membrane compartments enriched in phosphatidylinositol 3-phosphate and dynamically connected to the endoplasmic reticulum. *J. Cell Biol.* 182, 685–701. doi: 10.1083/jcb.200803137
- Belaid, A., Ndiaye, P. D., Cerezo, M., Cailleteau, L., Brest, P., Klionsky, D. J., et al. (2014). Autophagy and SQSTM1 on the RHOA(d) again: emerging roles of autophagy in the degradation of signaling proteins. *Autophagy* 10, 201–208. doi: 10.4161/auto.27198
- Bhatt, A., Kaverina, I., Otey, C., and Huttenlocher, A. (2002). Regulation of focal complex composition and disassembly by the calcium-dependent protease calpain. *J. Cell Sci.* 115, 3415–3425.
- Bialkowska, K., Kulkarni, S., Du, X., Goll, D. E., Saido, T. C., and Fox, J. E. (2000). Evidence that beta3 integrin-induced Rac activation involves the calpain-dependent formation of integrin clusters that are distinct from the focal complexes and focal adhesions that form as Rac and RhoA become active. *J. Cell Biol.* 151, 685–695. doi: 10.1083/jcb.151.3.685
- Bjorkoy, G., Lamark, T., Brech, A., Outzen, H., Perander, M., Øvervatn, A., et al. (2005). p62/SQSTM1 forms protein aggregates degraded by autophagy and has a protective effect on huntingtin-induced cell death. *J. Cell Biol.* 171, 603–614. doi: 10.1083/jcb.200507002
- Blackburn, J., and Mansell, J. P. (2012). The emerging role of lysophosphatidic acid (LPA) in skeletal biology. *Bone* 50, 756–762. doi: 10.1016/j.bone.2011.12.002
- Bleul, C. C., Fuhlbrigge, R. C., Casasnovas, J. M., Aiuti, A., and Springer, T. A. (1996). A highly efficacious lymphocyte chemoattractant, stromal cell-derived factor 1 (SDF-1). *J. Exp. Med.* 184, 1101–1109. doi: 10.1084/jem.184.3.1101
- Bravo-Cordero, J. J., Hodgson, L., and Condeelis, J. (2012). Directed cell invasion and migration during metastasis. *Curr. Opin. Cell Biol.* 24, 277–283. doi: 10.1016/j.cub.2011.12.004
- Bretscher, M. S., and Aguado-Velasco, C. (1998). Membrane traffic during cell locomotion. *Curr. Opin. Cell Biol.* 10, 537–541. doi: 10.1016/S0955-0674(98)80070-7
- Brûlé, C., Perzo, N., Joubert, J. E., Sainsily, X., Leduc, R., Castel, H., et al. (2014). Biased signaling regulates the pleiotropic effects of the urotensin II receptor to modulate its cellular behaviors. *FASEB J.* 28, 5148–5162. doi: 10.1096/fj.14-249771

CONCLUDING REMARKS

Although there are still many gaps in our understanding of how Atg proteins control chemotactic migration and cancer cell invasion, it is now clear that the autophagy machinery has major impacts on these processes. Specifically, degradation of focal adhesion components, through selective autophagy, has already been shown to participate in the turnover of adhesions during cancer cell migration. Autophagic degradation of key proteins participating in actin remodeling may also constitute an efficient way of clearing these proteins from the cell rear and concentrating them at the cell front, in order to initiate the expansion of a single lamellipodium in the direction of the chemotactic stimulus. The recent identification of the plasma membrane as a donor compartment for the expansion of the phagophore constituted an essential step in the comprehension of how chemotactic receptors could locally control autophagic flux. Deciphering the signaling cascades triggered by these receptors, and their impacts on the trafficking and/or processing of the core Atg proteins is an exciting challenge for the future and will help to envisage innovative strategies to halt cancer metastasis.

AUTHOR CONTRIBUTIONS

PC, PG, HC, and FM wrote manuscript.

FUNDING

This work was supported by INSERM, Gefluc, TC2N network, the Ligue Contre le Cancer Normandie, the French Agence Nationale de la Recherche, and the University of Rouen. PC is recipient of a fellowship from the French ministry.

- Campbell, I. D., and Humphries, M. J. (2011). Integrin structure, activation, and interactions. *Cold Spring Harb. Perspect. Biol.* 3, 1–15. doi: 10.1101/csdperspect.a004994
- Carragher, N. O., Levkau, B., Ross, R., and Raines, E. W. (1999). Degraded collagen fragments promote rapid disassembly of smooth muscle focal adhesions that correlates with cleavage of pp125(FAK), paxillin, and talin. *J. Cell Biol.* 147, 619–629. doi: 10.1083/jcb.147.3.619
- Carroll, B., Mohd-Naim, N., Maximiano, F., Frasa, M. A., McCormack, J., Finelli, M., et al. (2013). The TBC/RabGAP Armus coordinates Rac1 and Rab7 functions during autophagy. *Dev. Cell* 25, 15–28. doi: 10.1016/j.devcel.2013.03.005
- Catalano, M., D'Alessandro, G., Lepore, F., Corazzari, M., Caldarola, S., Valacca, C., et al. (2015). Autophagy induction impairs migration and invasion by reversing EMT in glioblastoma cells. *Mol. Oncol.* 9, 1612–1625. doi: 10.1016/j.molonc.2015.04.016
- Chatterjee, S., Behnam Azad, B., and Nimmagadda, S. (2014). The intricate role of CXCR4 in cancer. *Adv. Cancer Res.* 124, 31–82. doi: 10.1016/B978-0-12-411638-2.00002-1
- Choi, C. K., Vicente-Manzanares, M., Zareno, J., Whitmore, L. A., Mogilner, A., and Horwitz, A. R. (2008). Actin and alpha-actinin orchestrate the assembly and maturation of nascent adhesions in a myosin II motor-independent manner. *Nat. Cell Biol.* 10, 1039–1050. doi: 10.1038/ncb1763
- Coly, P.-M., Perzo, N., Le Joncour, V., Lecointre, C., Schouft, M.-T., Desrues, L., et al. (2016). Chemotactic G protein-coupled receptors control cell migration by repressing autophagosome biogenesis. *Autophagy* 12, 1–19. doi: 10.1080/15548627.2016.1235125
- Contos, J. J., Ishii, I., and Chun, J. (2000). Lysophosphatidic acid receptors. *Mol. Pharmacol.* 58, 1188–1196. doi: 10.1124/mol.58.6.1188
- Cooper, J. A. (2013). Mechanisms of cell migration in the nervous system. *J. Cell Biol.* 205, 725–734. doi: 10.1083/jcb.201305021
- Cotton, M., and Claing, A. (2009). G protein-coupled receptors stimulation and the control of cell migration. *Cell. Signal.* 21, 1045–1053. doi: 10.1016/j.cellsig.2009.02.008
- Daher, Z., Noël, J., and Claing, A. (2008). Endothelin-1 promotes migration of endothelial cells through the activation of ARF6 and the regulation of FAK activity. *Cell. Signal.* 20, 2256–2265. doi: 10.1016/j.cellsig.2008.08.021
- Ezraty, E. J., Bertaux, C., Marcantonio, E. E., and Gundersen, G. G. (2009). Clathrin mediates integrin endocytosis for focal adhesion disassembly in migrating cells. *J. Cell Biol.* 187, 733–747. doi: 10.1083/jcb.200904054
- Ezraty, E. J., Partridge, M. A., and Gundersen, G. G. (2005). Microtubule-induced focal adhesion disassembly is mediated by dynamin and focal adhesion kinase. *Nat. Cell Biol.* 7, 581–590. doi: 10.1038/ncb1262
- Feng, Y., Broder, C. C., Kennedy, P. E., and Berger, E. A. (1996). HIV-1 entry cofactor: functional cDNA cloning of a seven-transmembrane, G protein-coupled receptor. *Science* 272, 872–877. doi: 10.1126/science.272.5263.872
- Franco, S. J., and Huttenlocher, A. (2005). Regulating cell migration: calpains make the cut. *J. Cell Sci.* 118, 3829–3838. doi: 10.1242/jcs.02562
- Franco, S. J., Rodgers, M. A., Perrin, B. J., Han, J., Bennin, D. A., Critchley, D. R., et al. (2004). Calpain-mediated proteolysis of talin regulates adhesion dynamics. *Nat. Cell Biol.* 6, 977–983. doi: 10.1038/ncb1175
- Franco, S., Perrin, B., and Huttenlocher, A. (2004). Isoform specific function of calpain 2 in regulating membrane protrusion. *Exp. Cell Res.* 299, 179–187. doi: 10.1016/j.yexcr.2004.05.021
- Fredriksson, R., Lagerström, M. C., Lundin, L.-G., and Schiöth, H. B. (2003). The G-protein-coupled receptors in the human genome form five main families. Phylogenetic analysis, paralogon groups, and fingerprints. *Mol. Pharmacol.* 63, 1256–1272. doi: 10.1124/mol.63.6.1256
- Ge, L., Wilz, L., and Schekman, R. (2015). ER-Golgi intermediate compartment. *Autophagy* 11, 2372–2374. doi: 10.1080/15548627.2015.1105422
- Glading, A., Chang, P., Lauffenburger, D. A., and Wells, A. (2000). Epidermal growth factor receptor activation of calpain is required for fibroblast motility and occurs via an ERK/MAP kinase signaling pathway. *J. Biol. Chem.* 275, 2390–2398. doi: 10.1074/jbc.275.4.2390
- Goldsmith, Z. G., and Dhanasekaran, D. N. (2007). G protein regulation of MAPK networks. *Oncogene* 26, 3122–3142. doi: 10.1038/sj.onc.1210407
- Goll, D. E., Thompson, V. F., Li, H., Wei, W., and Cong, J. (2003). The calpain system. *Physiol. Rev.* 83, 731–801. doi: 10.1152/physrev.00029.2002
- Gugnani, M., Sancisi, V., Manzotti, G., Gandolfi, G., and Ciarrocchi, A. (2016). Autophagy and epithelial-mesenchymal transition: an intricate interplay in cancer. *Cell Death Dis.* 7, 2520–2531. doi: 10.1038/cddis.2016.415
- Hailey, D. W., Kim, P. K., Satpute-Krishnan, P., Rambold, A. S., Sougrat, R., and Lippincott-Schwartz, J. (2010). Mitochondria supply membranes for autophagosome biogenesis during starvation. *Cell. Cell* 141, 656–667. doi: 10.1016/j.cell.2010.04.009
- Hale, A. N., Ledbetter, D. J., Gawriluk, T. R., and Rucker, E. B. III. (2013). Autophagy: regulation and role in development. *Autophagy* 9, 951–972. doi: 10.4161/auto.24273
- Hayashi-Nishino, M., Fujita, N., Noda, T., Yamaguchi, A., Yoshimori, T., and Yamamoto, A. (2009). A subdomain of the endoplasmic reticulum forms a cradle for autophagosome formation. *Nat. Cell Biol.* 11, 1433–1437. doi: 10.1038/ncb1991
- Hu, T. H., Yao, Y., Yu, S., Han, L. L., Wang, W. J., Guo, H., et al. (2014). SDF-1/CXCR4 promotes epithelial-mesenchymal transition and progression of colorectal cancer by activation of the Wnt/β-catenin signaling pathway. *Cancer Lett.* 354, 417–426. doi: 10.1016/j.canlet.2014.08.012
- Huang, C. (2014). Roles of E3 ubiquitin ligases in cell adhesion and migration. *Cell Adh. Migr.* 4, 10–18. doi: 10.4161/cam.4.1.9834
- Imhof, B., and Dunon, D. (1997). Basic mechanism of leukocyte migration. *Horm. Metab. Res.* 29, 614–621. doi: 10.1055/s-2007-979112
- Jung, C. H., Ro, S.-H., Cao, J., Otto, N. M., and Kim, D.-H. (2010). mTOR regulation of autophagy. *FEBS Lett.* 584, 1287–1295. doi: 10.1016/j.febslet.2010.01.017
- Kahlert, U. D., Nikkhah, G., and Maciaczyk, J. (2013). Epithelial-to-mesenchymal(-like) transition as a relevant molecular event in malignant gliomas. *Cancer Lett.* 331, 131–138. doi: 10.1016/j.canlet.2012.12.010
- Kalluri, R., and Weinberg, R. A. (2009). The basics of epithelial-mesenchymal transition. *J. Clin. Invest.* 119, 1420–1428. doi: 10.1172/JCI39104
- Kaverina, I., Krylyshkina, O., and Small, J. V. (1999). Microtubule targeting of substrate contacts promotes their relaxation. *J. Cell Biol.* 146, 1033–1043. doi: 10.1083/jcb.146.5.1033
- Keller, R. (2005). Cell migration during gastrulation. *Curr. Opin. Cell Biol.* 17, 533–541. doi: 10.1016/j.celb.2005.08.006
- Kenific, C. M., Stehbens, S. J., Goldsmith, J., Leidal, A. M., Faure, N., Ye, J., et al. (2016a). NBR1 enables autophagy-dependent focal adhesion turnover. *J. Cell Biol.* 212, 577–590. doi: 10.1083/jcb.201503075
- Kenific, C. M., Wittmann, T., and Debnath, J. (2016b). Autophagy in adhesion and migration. *J. Cell Sci.* 129, 3685–3693. doi: 10.1242/jcs.188490
- Kim, J. A., and Kim, H. L. (2001). Cleavage of purified neuronal clathrin assembly protein (CALM) by caspase 3 and calpain. *Exp. Mol. Med.* 33, 245–250. doi: 10.1038/emm.2001.40
- Kim, J. H., Hong, S. B., Lee, J. K., Han, S., Roh, K.-H., Lee, K.-E., et al. (2015). Insights into autophagosome maturation revealed by the structures of ATG5 with its interacting partners. *Autophagy* 11, 75–87. doi: 10.4161/15548627.2014.984276
- Kim, J., Kundu, M., Viollet, B., and Guan, K. (2011). AMPK and mTOR regulate autophagy through direct phosphorylation of Ulk1. *Nat. Cell Biol.* 13, 132–141. doi: 10.1038/ncb2152
- Kirkin, V., Lamark, T., Sou, Y. S., Bjørkoy, G., Nunn, J. L., Bruun, J. A., et al. (2009). A role for NBR1 in autophagosomal degradation of ubiquitinated substrates. *Mol. Cell* 33, 505–516. doi: 10.1016/j.molcel.2009.01.020
- Knævelsrød, H., Sørensen, K., Raiborg, C., Häberg, K., Rasmussen, F., Brech, A., et al. (2013). Membrane remodeling by the PX-BAR protein SNX18 promotes autophagosome formation. *J. Cell Biol.* 202, 331–349. doi: 10.1083/jcb.201205129
- Lapidot, T., Dar, A., and Kollet, O. (2005). How do stem cells find their way home? *Blood* 106, 1901–1910. doi: 10.1182/blood-2005-04-1417
- Lecointre, C., Desrues, L., Joubert, J. E., Perzo, N., Guichet, P.-O., Le Joncour, V., et al. (2015). Signaling switch of the urotensin II vasoactive peptide GPCR: prototypic chemotoxic mechanism in glioma. *Oncogene* 34, 5080–5094. doi: 10.1038/onc.2014.433
- Li, M., and Ransohoff, R. M. (2008). Multiple roles of chemokine CXCL12 in the central nervous system: A migration from immunology to neurobiology. *Prog. Neurobiol.* 84, 116–131. doi: 10.1016/j.pneurobio.2007.11.003

- Li, X., Li, P., Chang, Y., Xu, Q., Wu, Z., Ma, Q., et al. (2014). The SDF-1/CXCR4 axis induces epithelial-mesenchymal transition in hepatocellular carcinoma. *Mol. Cell. Biochem.* 392, 77–84. doi: 10.1007/s11010-014-2020-8
- Lokuta, M. A., Nuzzi, P. A., and Huttenlocher, A. (2003). Calpain regulates neutrophil chemotaxis. *Proc. Natl. Acad. Sci. U.S.A.* 100, 4006–4011. doi: 10.1073/pnas.0636533100
- Longatti, A., Lamb, C. A., Razi, M., Yoshimura, S., Barr, F. A., and Tooze, S. A. (2012). TBC1D14 regulates autophagosome formation via Rab11- and ULK1-positive recycling endosomes. *J. Cell Biol.* 197, 659–675. doi: 10.1083/jcb.201111079
- Lv, Q., Wang, W., Xue, J., Hua, F., Mu, R., Lin, H., et al. (2012). DEDD interacts with PI3KC3 to activate autophagy and attenuate epithelial-mesenchymal transition in human breast cancer. *Cancer Res.* 72, 3238–3250. doi: 10.1158/0008-5472.CAN-11-3832
- Lysko, D. E., Putt, M., and Golden, J. A. (2014). SDF1 reduces interneuron leading process branching through dual regulation of actin and microtubules. *J. Neurosci.* 34, 4941–4962. doi: 10.1523/JNEUROSCI.4351-12.2014
- Margadant, C., Monsuur, H. N., Norman, J. C., and Sonnenberg, A. (2011). Mechanisms of integrin activation and trafficking. *Curr. Opin. Cell Biol.* 23, 607–614. doi: 10.1016/j.ceb.2011.08.005
- Maritzzen, T., Schachtner, H., and Legler, D. F. (2015). On the move: endocytic trafficking in cell migration. *Cell. Mol. Life Sci.* 72, 2119–2134. doi: 10.1007/s0018-015-1855-9
- Mizushima, N., Noda, T., and Ohsumi, Y. (1999). Apg16p is required for the function of the Apg12p-Apg5p conjugate in the yeast autophagy pathway. *EMBO J.* 18, 3888–3896. doi: 10.1093/emboj/18.14.3888
- Mizushima, N., Sugita, H., Yoshimori, T., and Ohsumi, Y. (1998). A new protein conjugation system in human. The counterpart of the yeast Apg12p conjugation system essential for autophagy. *J. Biol. Chem.* 273, 33889–33892. doi: 10.1074/jbc.273.51.33889
- Moreau, K., Ravikumar, B., Puri, C., and Rubinsztein, D. C. (2012). Arf6 promotes autophagosome formation via effects on phosphatidylinositol 4,5-bisphosphate and phospholipase. *D. J. Cell Biol.* 196, 483–496. doi: 10.1083/jcb.201110114
- Moreau, K., Ravikumar, B., Renna, M., Puri, C., and Rubinsztein, D. C. (2011). Autophagosome precursor maturation requires homotypic fusion. *Cell* 146, 303–317. doi: 10.1016/j.cell.2011.06.023
- Morozova, K., Sidhar, S., Zolla, V., Clement, C. C., Scharf, B., Verzani, Z., et al. (2015). Annexin A2 promotes phagophore assembly by enhancing Atg16L+ vesicle biogenesis and homotypic fusion. *Nat. Commun.* 6, 5856–5868. doi: 10.1038/ncomms6856
- Murphy, P. M., Baggolini, M., Charo, I. F., Hébert, C. A., Horuk, R., Matsushima, K., et al. (2000). International union of pharmacology. XXII. Nomenclature for chemokine receptors. *Pharmacol. Rev.* 52, 145–176.
- Nakatogawa, H., Suzuki, K., Kamada, Y., and Ohsumi, Y. (2009). Dynamics and diversity in autophagy mechanisms: lessons from yeast. *Mol. Cell. Biol.* 10, 458–467. doi: 10.1038/nrm2708
- Nash, B., and Meucci, O. (2014). Functions of the chemokine receptor CXCR4 in the central nervous system and its regulation by μ -opioid receptors. *Int. Rev. Neurobiol.* 118, 105–128. doi: 10.1016/B978-0-12-801284-0-0005-1
- Norman, J. M., Cohen, G. M., and Bampton, E. T. (2010). The in vitro cleavage of the hAtg proteins by cell death proteases. *Autophagy* 6, 1042–1056. doi: 10.4161/auto.6.8.13337
- Novikoff, A. B., and Shin, W.-Y. (1978). Endoplasmic reticulum and autophagy in rat hepatocytes. *Proc. Natl. Acad. Sci. U.S.A.* 75, 5039–5042. doi: 10.1073/pnas.75.10.5039
- Otomo, C., Metlagel, Z., Takaesu, G., and Otomo, T. (2013). Structure of the human ATG12~ATG5 conjugate required for LC3 lipidation in autophagy. *Nat. Struct. Mol. Biol.* 20, 59–66. doi: 10.1038/nsmb.2431
- Pang, X. X., Bai, Q., Wu, F., Chen, G. J., Zhang, A. H., and Tang, C. S. (2016). Urotensin II induces ER stress and EMT and increase extracellular matrix production in renal tubular epithelial cell in early diabetic mice. *Kidney Blood Press. Res.* 41, 434–449. doi: 10.1159/000443445
- Pankiv, S., Clausen, T. H., Lamark, T., Brech, A., Bruun, J.-A., Outzen, H., et al. (2007). p62/SQSTM1 binds directly to Atg8/LC3 to facilitate degradation of ubiquitinated protein aggregates by autophagy. *J. Biol. Chem.* 282, 24131–24145. doi: 10.1074/jbc.M702824200
- Perrin, B. J., Amann, K. J., and Huttenlocher, A. (2006). Proteolysis of cortactin by calpain regulates membrane protrusion during cell migration. *Mol. Biol. Cell* 17, 239–250. doi: 10.1091/mbc.E05-06-0488
- Pierini, L. M., Lawson, M. A., Eddy, R. J., Hendey, B., and Maxfield, F. R. (2000). Oriented endocytic recycling of $\alpha 5\beta 1$ in motile neutrophils. *Blood* 95, 2471–2480.
- Porrello, E. R., D'Amore, A., Curl, C. L., Allen, A. M., Harrap, S. B., Thomas, W. G., et al. (2009). Angiotensin II type 2 receptor antagonizes angiotensin II type 1 receptor-mediated cardiomyocyte autophagy. *Hypertension* 53, 1032–1040. doi: 10.1161/HYPERTENSIONHA.108.128488
- Puri, C., Renna, M., Bento, C. F., Moreau, K., and Rubinsztein, D. C. (2013). Diverse autophagosome membrane sources coalesce in recycling endosomes. *Cell* 154, 1285–1299. doi: 10.1016/j.cell.2013.08.044
- Qiang, L., Zhao, B., Ming, M., Wang, N., He, T.-C., Hwang, S., et al. (2014). Regulation of cell proliferation and migration by p62 through stabilization of Twist1. *Proc. Natl. Acad. Sci. U.S.A.* 111, 9241–9246. doi: 10.1073/pnas.1322913111
- Ravikumar, B., Moreau, K., Jahreiss, L., Puri, C., and Rubinsztein, D. C. (2010). Plasma membrane contributes to the formation of pre-autophagosomal structures. *Nat. Cell Biol.* 12, 747–757. doi: 10.1038/ncb2078
- Ridley, A. J., Schwartz, M. A., Burridge, K., Firtel, R. A., Ginsberg, M. H., Borisy, G. G., et al. (2003). Cell migration: integrating signals from front to back. *Science* 302, 1704–1710. doi: 10.1126/science.1092053
- Roccaro, A. M., Mishima, Y., Sacco, A., Moschetta, M., Tai, Y. T., Shi, J., et al. (2015). CXCR4 regulates extra-medullary myeloma through epithelial-mesenchymal-transition-like transcriptional activation. *Cell Rep.* 12, 622–635. doi: 10.1016/j.celrep.2015.06.059
- Romanov, J., Walczak, M., Ibiricu, I., Schüchner, S., Ogris, E., Kraft, C., et al. (2012). Mechanism and functions of membrane binding by the Atg5-Atg12/Atg16 complex during autophagosome formation. *EMBO J.* 31, 4304–4317. doi: 10.1038/emboj.2012.278
- Rudinskiy, N., Grishchuk, Y., Vaslin, A., Puyal, J., Delacourte, A., Hirling, H., et al. (2009). Calpain hydrolysis of α - and β -adaptins decreases clathrin-dependent endocytosis and may promote neurodegeneration. *J. Biol. Chem.* 284, 12447–12458. doi: 10.1074/jbc.M804740200
- Salcedo, R., Zhang, X., Young, H. A., Michael, N., Wasserman, K., Ma, W.-H., et al. (2003). Angiogenic effects of prostaglandin E2 are mediated by up-regulation of CXCR4 on human microvascular endothelial cells. *Blood* 102, 1966–1977. doi: 10.1182/blood-2002-11-3400
- Sandilands, E., Serrels, B., McEwan, D. G., Morton, J. P., Macagno, J. P., McLeod, K., et al. (2012). Autophagic targeting of Src promotes cancer cell survival following reduced FAK signalling. *Nat. Cell Biol.* 14, 51–60. doi: 10.1038/ncb2386
- Sato, K., Horiuchi, Y., Jin, Y., Malchinkhuu, E., Komachi, M., Kondo, T., et al. (2011). Unmasking of LPA1 receptor-mediated migration response to lysophosphatidic acid by interleukin-1 β -induced attenuation of Rho signaling pathways in rat astrocytes. *J. Neurochem.* 117, 164–174. doi: 10.1111/j.1471-4159.2011.07188.x
- Schmoranz, J., Kreitzer, G., and Simon, S. (2003). Migrating fibroblasts perform polarized, microtubule-dependent exocytosis towards the leading edge. *J. Cell Sci.* 116, 4513–4519. doi: 10.1242/jcs.00748
- Schwartz, G. A., Henion, T. R., Nugent, J. D., Caplan, B., and Tobet, S. (2006). Stromal cell-derived factor-1 (chemokine C-X-C motif ligand 12) and chemokine C-X-C motif receptor 4 are required for migration of gonadotropin-releasing hormone neurons to the forebrain. *J. Neurosci.* 26, 6834–6840. doi: 10.1523/JNEUROSCI.1728-06.2006
- Segain, J.-P., Rolli-Derkinderen, M., Gervois, N., Raingeard de la Blétière, D., Loirand, G., and Pacaud, P. (2007). Urotensin II is a new chemotactic factor for UT receptor-expressing monocytes. *J. Immunol.* 179, 901–909. doi: 10.4049/jimmunol.179.2.901
- Serrano, K., and Devine, D. V. (2004). Vinculin is proteolyzed by calpain during platelet aggregation: 95 kDa cleavage fragment associates with the platelet cytoskeleton. *Cell Motil. Cytoskeleton* 58, 242–252. doi: 10.1002/cm.20011
- Sharifi, M. N., Mowers, E. E., Drake, L. E., Collier, C., Chen, H., Zamora, M., et al. (2016). Autophagy promotes focal adhesion disassembly and cell motility of

- metastatic tumor cells through the direct interaction of paxillin with LC3. *Cell Rep.* 15, 1660–1672. doi: 10.1016/j.celrep.2016.04.065
- Shiraha, H., Glading, A., Chou, J., Wells, A., and Jia, Z. (2002). Activation of m-Calpain (Calpain II) by epidermal growth factor is limited by protein kinase A phosphorylation of m-Calpain. *Mol. Cell. Biol.* 22, 2716–2727. doi: 10.1128/MCB.22.8.2716-2727.2002
- Simon, M. I., Strathmann, M. P., and Gautam, N. (1991). Diversity of G proteins. *Science* 252, 802–808. doi: 10.1126/science.1902986
- Stumm, R., and Höllt, V. (2007). CXC chemokine receptor 4 regulates neuronal migration and axonal pathfinding in the developing nervous system: implications for neuronal regeneration in the adult brain. *J. Mol. Endocrinol.* 38, 377–382. doi: 10.1677/JME-06-0032
- Tadokoro, S., Shattil, S. J., Eto, K., Tai, V., Liddington, R. C., de Pereda, J. M., et al. (2003). Talin binding to integrin beta tails: a final common step in integrin activation. *Science* 302, 103–106. doi: 10.1126/science.1086652
- Tam, W. L., and Weinberg, R. A. (2013). The epigenetics of epithelial-mesenchymal plasticity in cancer. *Nat. Med.* 19, 1438–1449. doi: 10.1038/nm.3336
- Thiery, J. P., Acloque, H., Huang, R. Y., and Nieto, M. A. (2009). Epithelial-mesenchymal transitions in development and disease. *Cell* 139, 871–890. doi: 10.1016/j.cell.2009.11.007
- Tiveron, M. C., and Cremer, H. (2008). CXCL12/CXCR4 signalling in neuronal cell migration. *Curr. Opin. Neurobiol.* 18, 237–244. doi: 10.1016/j.conb.2008.06.004
- Tuloup-Minguez, V., Hamai, A., Greffard, A., Nicolas, V., Codogno, P., and Botti, J. (2013). Autophagy modulates cell migration and $\beta 1$ integrin membrane recycling. *Cell Cycle* 12, 3317–3328. doi: 10.4161/cc.26298
- Veale, K. J., Offenhäuser, C., Whittaker, S. P., Estrella, R. P., and Murray, R. Z. (2010). Recycling endosome membrane incorporation into the leading edge regulates lamellipodia formation and macrophage migration. *Traffic* 11, 1370–1379. doi: 10.1111/j.1600-0854.2010.01094.x
- Wauson, E. M., Dbouk, H. A., Ghosh, A. B., and Cobb, M. H. (2014). G protein-coupled receptors and the regulation of autophagy. *Trends Endocrinol. Metab.* 25, 274–282. doi: 10.1016/j.tem.2014.03.006
- Wauson, E. M., Zaganjor, E., Lee, A. Y., Guerra, M. L., Ghosh, A. B., Bookout, A. L., et al. (2012). The G protein-coupled taste receptor T1R1/T1R3 regulates mTORC1 and autophagy. *Mol. Cell* 47, 851–862. doi: 10.1016/j.molcel.2012.08.001
- Webb, D. J., Donais, K., Whitmore, L. A., Thomas, S. M., Turner, C. E., Parsons, J. T., et al. (2004). FAK-Src signalling through paxillin, ERK and MLCK regulates adhesion disassembly. *Nat. Cell Biol.* 6, 154–161. doi: 10.1038/ncb1094
- Weiner, O. D. (2002). Regulation of cell polarity during eukaryotic chemotaxis: The chemotactic compass. *Curr. Opin. Cell Biol.* 14, 196–202. doi: 10.1016/S0955-0674(02)00310-1
- Wilkie, T. M., Gilbert, D. J., Olsen, A. S., Chen, X. N., Amatruda, T. T., Korenberg, J. R., et al. (1992). Evolution of the mammalian G protein alpha subunit multigene family. *Nat. Genet.* 1, 85–91. doi: 10.1038/ng0592-85
- Xi, X. P., Graf, K., Goetze, S., Fleck, E., Hsueh, W. A., and Law, R. E. (1999). Central role of the MAPK pathway in Ang II-mediated DNA synthesis and migration in rat vascular smooth muscle cells. *Arterioscler. Thromb. Vasc. Biol.* 19, 73–82. doi: 10.1161/01.ATV.19.1.73
- Xia, H.-G., Zhang, L., Chen, G., Zhang, T., Liu, J., Jin, M., et al. (2010). Control of basal autophagy by calpain1 mediated cleavage of ATG5. *Autophagy* 6, 61–66. doi: 10.4161/auto.6.1.10326
- Xu, S., Jiang, H., Wu, B., Yang, J., and Chen, S. (2009). Urotensin II induces migration of endothelial progenitor cells via activation of the RhoA/Rho kinase pathway. *Tohoku J. Exp. Med.* 219, 283–288. doi: 10.1620/tjem.219.283
- Yadav, A., Vallabu, S., Arora, S., Tandon, P., Slahan, D., Teichberg, S., et al. (2010). ANG II promotes autophagy in podocytes. *Am. J. Cell Physiol.* 299, C488–C496. doi: 10.1152/ajpcell.00424.2009
- Yan, B., Calderwood, D. A., Yaspan, B., and Ginsberg, M. H. (2001). Calpain cleavage promotes talin binding to the beta3 integrin cytoplasmic domain. *J. Biol. Chem.* 276, 28164–28170. doi: 10.1074/jbc.M104161200
- Yang, L., Li, P., Fu, S., Calay, E. S., and Hotamisligil, G. S. (2010). Defective hepatic autophagy in obesity promotes ER stress and causes insulin resistance. *Cell Metab.* 11, 467–478. doi: 10.1016/j.cmet.2010.04.005
- Yao, C., Li, P., Song, H., Song, F., Qu, Y., Ma, X., et al. (2016). CXCL12/CXCR4 axis upregulates twist to induce EMT in human glioblastoma. *Mol. Neurobiol.* 53, 3948–3953. doi: 10.1007/s12035-015-9340-x
- Ylä-Anttila, P., Vihinen, H., Jokitalo, E., and Eskelinen, E. L. (2009). 3D tomography reveals connections between the phagophore and endoplasmic reticulum. *Autophagy* 5, 1180–1185. doi: 10.4161/auto.5.8.10274
- Yoshida, T., Tsujioka, M., Honda, S., and Tanaka, M. (2016). Autophagy suppresses cell migration by degrading GEF-H1, a RhoA GEF. *Oncotarget* 7, 34420–34429. doi: 10.18632/oncotarget.8883
- Yousefi, S., Perozzo, R., Schmid, I., Ziemiacki, A., Schaffner, T., Scapozza, L., et al. (2006). Calpain-mediated cleavage of Atg5 switches autophagy to apoptosis. *Nat. Cell Biol.* 8, 1124–1132. doi: 10.1038/ncb1482
- Yu, K.-Y., Wang, Y.-P., Wang, L.-H., Jian, Y., Zhao, X.-D., Chen, J.-W., et al. (2014). Mitochondrial KATP channel involvement in angiotensin II-induced autophagy in vascular smooth muscle cells. *Basic Res. Cardiol.* 109, 416–431. doi: 10.1007/s00395-014-0416-y
- Yung, Y. C., Stoddard, N. C., Mirendil, H., and Chun, J. (2015). Lysophosphatidic acid signaling in the nervous system. *Neuron* 85, 669–682. doi: 10.1016/j.neuron.2015.01.009
- Zaffagnini, G., and Martens, S. (2016). Mechanisms of selective autophagy. *J. Mol. Biol.* 428, 1714–1724. doi: 10.1016/j.jmb.2016.02.004
- Zavodszky, E., Vicinanza, M., and Rubinstein, D. C. (2013). Biology and trafficking of ATG9 and ATG16L1, two proteins that regulate autophagosome formation. *FEBS Lett.* 587, 1988–1996. doi: 10.1016/j.febslet.2013.04.025

Conflict of Interest Statement: The authors declare that the research was conducted in the absence of any commercial or financial relationships that could be construed as a potential conflict of interest.

Copyright © 2017 Coly, Gandolfo, Castel and Morin. This is an open-access article distributed under the terms of the Creative Commons Attribution License (CC BY). The use, distribution or reproduction in other forums is permitted, provided the original author(s) or licensor are credited and that the original publication in this journal is cited, in accordance with accepted academic practice. No use, distribution or reproduction is permitted which does not comply with these terms.



[Pyr¹]Apelin-13_(1–12) Is a Biologically Active ACE2 Metabolite of the Endogenous Cardiovascular Peptide [Pyr¹]Apelin-13

Peiran Yang¹, Rhoda E. Kuc¹, Aimée L. Brame¹, Alex Dyson², Mervyn Singer², Robert C. Glen^{3,4}, Joseph Cherian¹, Ian B. Wilkinson¹, Anthony P. Davenport¹ and Janet J. Maguire^{1*}

¹ Department of Medicine, Experimental Medicine and Immunotherapeutics, University of Cambridge, Cambridge, UK

² Division of Medicine, Bloomsbury Institute of Intensive Care Medicine, University College London, London, UK

³ Department of Chemistry, Centre for Molecular Informatics, University of Cambridge, Cambridge, UK, ⁴ Department of Surgery and Cancer, Biomolecular Medicine, Imperial College London, London, UK

OPEN ACCESS

Edited by:

Hubert Vaudry,
University of Rouen, France

Reviewed by:

Kazuhiro Takahashi,
Tohoku University, Japan
Nils Lambrecht,

VA Long Beach Healthcare System
and University of California Irvine, USA

*Correspondence:

Janet J. Maguire
jjm1003@medsch.cam.ac.uk

Specialty section:

This article was submitted to
Neuroendocrine Science,
a section of the journal
Frontiers in Neuroscience

Received: 02 December 2016

Accepted: 10 February 2017

Published: 28 February 2017

Citation:

Yang P, Kuc RE, Brame AL, Dyson A, Singer M, Glen RC, Cherian J, Wilkinson IB, Davenport AP and Maguire JJ (2017)

[Pyr¹]Apelin-13_(1–12) Is a Biologically Active ACE2 Metabolite of the Endogenous Cardiovascular Peptide [Pyr¹]Apelin-13.

Front. Neurosci. 11:92.

doi: 10.3389/fnins.2017.00092

Aims: Apelin is a predicted substrate for ACE2, a novel therapeutic target. Our aim was to demonstrate the endogenous presence of the putative ACE2 product [Pyr¹]apelin-13_(1–12) in human cardiovascular tissues and to confirm it retains significant biological activity for the apelin receptor *in vitro* and *in vivo*. The minimum active apelin fragment was also investigated.

Methods and Results: [Pyr¹]apelin-13 incubated with recombinant human ACE2 resulted in de novo generation of [Pyr¹]apelin-13_(1–12) identified by mass spectrometry. Endogenous [Pyr¹]apelin-13_(1–12) was detected by immunostaining in human heart and lung localized to the endothelium. Expression was undetectable in lung from patients with pulmonary arterial hypertension. In human heart [Pyr¹]apelin-13_(1–12) ($pK_i = 8.04 \pm 0.06$) and apelin-13(F13A) ($pK_i = 8.07 \pm 0.24$) competed with [¹²⁵I]apelin-13 binding with nanomolar affinity, 4-fold lower than for [Pyr¹]apelin-13 ($pK_i = 8.83 \pm 0.06$) whereas apelin-17 exhibited highest affinity ($pK_i = 9.63 \pm 0.17$). The rank order of potency of peptides to inhibit forskolin-stimulated cAMP was apelin-17 ($pD_2 = 10.31 \pm 0.28$) > [Pyr¹]apelin-13 ($pD_2 = 9.67 \pm 0.04$) ≥ apelin-13(F13A) ($pD_2 = 9.54 \pm 0.05$) > [Pyr¹]apelin-13_(1–12) ($pD_2 = 9.30 \pm 0.06$). The truncated peptide apelin-13(R10M) retained nanomolar potency ($pD_2 = 8.70 \pm 0.04$) but shorter fragments exhibited low micromolar potency. In a β-arrestin recruitment assay the rank order of potency was apelin-17 ($pD_2 = 10.26 \pm 0.09$) >> [Pyr¹]apelin-13 ($pD_2 = 8.43 \pm 0.08$) > apelin-13(R10M) ($pD_2 = 8.26 \pm 0.17$) > apelin-13(F13A) ($pD_2 = 7.98 \pm 0.04$) ≥ [Pyr¹]apelin-13_(1–12) ($pD_2 = 7.84 \pm 0.06$) >> shorter fragments ($pD_2 < 6$). [Pyr¹]apelin-13_(1–12) and apelin-13(F13A) contracted human saphenous vein with similar sub-nanomolar potencies and [Pyr¹]apelin-13_(1–12) was a potent inotrope in paced mouse right ventricle and human atria. [Pyr¹]apelin-13_(1–12) elicited a dose-dependent decrease in blood pressure in anesthetized rat and dose-dependent increase in forearm blood flow in human volunteers.

Conclusions: We provide evidence that ACE2 cleaves [Pyr¹]apelin-13 to [Pyr¹]apelin-13_(1–12) and this cleavage product is expressed in human cardiovascular tissues. We have demonstrated biological activity of [Pyr¹]apelin-13_(1–12) at the human and rodent apelin receptor *in vitro* and *in vivo*. Our data show that reported enhanced ACE2 activity in cardiovascular disease should not significantly compromise the beneficial effects of apelin based therapies for example in PAH.

Keywords: apelin, apelin receptor, [Pyr¹]apelin-13(1–12), ACE2, human heart, pulmonary arterial hypertension, forearm plethysmography, biased signaling

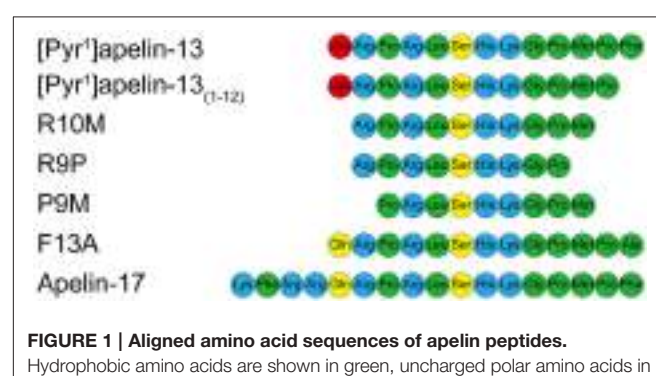
INTRODUCTION

Apelins are a family of peptides that activate the apelin receptor (also known as APJ) and have an emerging importance in the physiology and pathophysiology of the cardiovascular system (Yang et al., 2015). Apelin peptides are present in human vascular and cardiac endothelial cells (Klein and Davenport, 2004) and plasma, with [Pyr¹]apelin-13 identified as the most abundant cardiovascular isoform (De Mota et al., 2004; Maguire et al., 2009; Zhen et al., 2013). Apelins mediate three major actions *in vitro*. Interaction with the apelin receptor on cardiac myocytes causes increased cardiac contractility and inotropic action, with apelin an order of magnitude more potent than endothelin-1. In vessels with an intact endothelium, apelin acts to release vasodilators that may oppose the actions of vasoconstrictors. We have also shown that removal of endothelium unmasks a constrictor response mediated by apelin receptors present on the vascular smooth muscle (Maguire et al., 2009). Importantly, in healthy volunteers and heart failure patients, the major effect of apelin infused into the forearm *in vivo* was nitric oxide dependent arterial dilatation (Japp et al., 2008, 2010; Barnes et al., 2013; Brame et al., 2015). In heart failure patients, intracoronary [Pyr¹]apelin-13 caused coronary vasodilatation and increased cardiac contractility (Japp et al., 2010; Barnes et al., 2013). Systemic infusions of [Pyr¹]apelin-13 in both volunteers and patients increased cardiac index and lowered mean arterial blood pressure and peripheral vascular resistance (Japp et al., 2010; Barnes et al., 2013). Apelin is down-regulated in pulmonary arterial hypertension (PAH), a devastating disease characterized by vascular remodeling resulting in progressive obliteration of the pulmonary circulation, leading to right ventricle (RV) hypertrophy and right heart failure (Alastalo et al., 2011; Chandra et al., 2011). Therefore the apelin receptor may represent a novel target for future drug development.

Human angiotensin converting enzyme 2 (ACE2) has 40% sequence similarity with the C-terminal dipeptidyl-peptidase, ACE (Donoghue et al., 2000; Timpis et al., 2000). ACE2 is expressed for example in heart, kidney and lung (Donoghue et al., 2000; Hamming et al., 2004) and is implicated in pathological conditions such as heart failure where it is up-regulated (Zisman et al., 2003; Goulter et al., 2004). A major role of ACE2 is to degrade angiotensin II to angiotensin (1–7) which then acts as a beneficial vasodilator and anti-proliferation agent, counter-balancing the actions of the vasoconstrictor angiotensin II (Santos et al., 2003, 2008). ACE2 is also a viral receptor for the

severe acute respiratory syndrome coronavirus (Li et al., 2008) which down-regulates the enzyme from the cell surface resulting in angiotensin II-induced lung injury (Kuba et al., 2005). This has been the rational for the development of recombinant human ACE2 (rhACE2) in clinical trials for acute lung injury (Haschke et al., 2013). Interestingly, enhancing ACE2 activity pharmacologically or by gene transfer was effective in preventing or reversing PAH (Shenoy et al., 2011; Dai et al., 2015). Some beneficial actions of ACE2 are thought to be mediated by the conversion of angiotensin II to angiotensin(1–7). However, the possibility of interaction of ACE2 with other peptides was not clear until a screen of over 120 biologically active peptides reported only two others to be hydrolyzed with high catalytic efficiency by ACE2; dynorphin A 1–13, which has no reported vasoactivity and apelin-13, or apelin-36, resulting in the removal of the C-terminal phenylalanine, producing the metabolites apelin-13_(1–12) or apelin-36_(1–35) (Vickers et al., 2002). The loss of the terminal phenylalanine in apelin has been assumed to be a mechanism of degradation and inactivation of the peptide. Our aim was to understand the impact of this ACE2 cleavage reaction on the apelin signaling pathway.

Specifically, our objectives were firstly to confirm that [Pyr¹]apelin-13_(1–12) (**Figure 1**) can be produced by ACE2 hydrolysis of [Pyr¹]apelin-13 and find evidence that [Pyr¹]apelin-13_(1–12) is an endogenous peptide and determine its distribution in human cardiovascular tissues. Secondly, to demonstrate that [Pyr¹]apelin-13_(1–12) binds to the apelin receptor and can activate down-stream signaling pathways in cell based assays. Thirdly, we have determined that [Pyr¹]apelin-13_(1–12) retains significant biological activity, compared with



our previously reported data (Maguire et al., 2009; Brame et al., 2015) for [Pyr¹]apelin-13, *in vitro* using vascular and cardiac human and rodent tissues and by systemic infusions of [Pyr¹]apelin-13(1–12) *in vivo* in the rat; finally, since the predominant action of apelin infused into the human forearm is vasodilatation, we have performed first-in-man studies with [Pyr¹]apelin-13(1–12) to explore the physiological action of the peptide in healthy volunteers. We also wished to explore the structure activity relationship (SAR) of the apelin peptides and therefore additional experiments were performed with the N-terminal extended putative endogenous peptide apelin-17, alanine substituted apelin-13(F13A), and the shorter fragments apelin-13(R10M), apelin-13(R9P) and apelin-13(P9M) (Figure 1). Our data expand our knowledge on the structure activity relationship of apelin peptides and demonstrate the significant biological activity of the ACE2 metabolite [Pyr¹]apelin-13(1–12). These data support the hypothesis that therapeutic strategies enhancing ACE2 activity or up-regulation of ACE2 in cardiovascular disease, both of which may result in enhanced breakdown of [Pyr¹]apelin-13, may not significantly compromise the beneficial effects of endogenous apelin signaling via generation of [Pyr¹]apelin-13(1–12).

METHODS

Cardiovascular Tissue Collection

Human tissues samples were obtained with informed consent (Papworth Hospital Research Tissue Bank REC08/H0304/56) and local ethical approval (REC05/Q0104/142).

Synthesis of [Pyr¹]Apelin-13(1–12) from [Pyr¹]Apelin-13

Synthesis of [Pyr¹]apelin-13(1–12) from [Pyr¹]apelin-13 was confirmed by incubating [Pyr¹]apelin-13 (5 nmol) with rhACE2 enzyme (5 pmol, GSK, Ware, UK) in buffer (pH 6.5) containing 2-(N-morpholino)ethanesulfonic acid (MES, 500 mmol/L), NaCl (300 mmol/L) and ZnCl₂ (10 μmol/L) for 2 h at 37°C followed by quenching with 10 μmol ethylenediaminetetraacetic acid (EDTA) (see Vickers et al., 2002 for similar protocol). The reaction mixture was analyzed by Maldi-TOF mass spectrometry after samples were desalting using Millipore μC18ZipTip (MA, USA), washed with 5% acetic acid and eluted with CHCA matrix (in 50% aqueous acetonitrile containing 0.1% trifluoroacetic acid) to a stainless steel sample slide. Samples were air dried and analyzed using a Waters Maldi MicroMX time-of-flight mass spectrometer (MA, USA). Calibration was external using polyethylene glycol. The 10 Hz-laser power was just above threshold. The spectra were the sum of 1,000 shots collected from a spiral track of the sample area. Data were processed using Waters MassLynx software (MA, USA). Control reactions included incubation of [Pyr¹]apelin-13(1–12) (5 nmol) with rhACE2, incubation of [Pyr¹]apelin-13 (5 nmol) or [Pyr¹]apelin-13(1–12) (5 nmol) without rhACE2 and incubation of rhACE2 (5 pmol) without peptides.

Localization of Endogenous [Pyr¹]Apelin-13(1–12) by Immunostaining

Peroxidase-anti-peroxidase and dual-labeling immunofluorescent staining were conducted as described (Klein et al., 2005) using frozen sections of human cardiomyopathy heart ($n = 4$), histologically normal ($n = 6$) and PAH ($n = 4$) lung. Affinity purified rabbit anti-[Pyr¹]apelin-13(1–12) antiserum (1:25–1:100 dilution) was custom synthesized (antibody raised against the relevant apelin peptide fragment CKGPMP, that lacks the C-terminal phenylalanine) and selectivity confirmed by comparison with the corresponding fragment containing the C-terminal phenylalanine (CKGPMPF) by ELISA (Figure 2A). In contrast the commercially available apelin-12 antibody (Phoenix Pharmaceuticals Inc. CA, USA) crossed reacted with [Pyr¹]apelin-13 but not [Pyr¹]apelin-13(1–12) (Figure 2B). ACE2 (1:50, R&D Systems, MN, USA and 1:200, Abcam, Cambridge, UK) antisera were also used. Von Willebrand factor (vWF) (1:50, Dako, Glostrup, Denmark) was used as an endothelial marker. The peroxidase stained sections were examined with a bright field microscope (Olympus, Southend-on-Sea, UK) and imaged using a CC12 camera and CellID Soft Imaging System (Olympus), whereas fluorescent staining were imaged using a Leica Scanning Confocal Microscope (TCS SP2, Leica Microsystems, Milton Keynes, UK). Image processing with rolling ball method and histogram redistribution were applied equally to the entire image and channel overlay were carried out using ImageJ.

Competition Binding Assays

Assays were performed in human heart as previously described (Brame et al., 2015). Briefly, homogenate of human left ventricle (LV) was incubated for 90 min with 0.1 nmol/L [Glp⁶⁵, Nle⁷⁵, Tyr⁷⁷]^{[125]I]apelin-13 in assay buffer (mmol/L; Tris 50, MgCl₂ 5, pH 7.4, 22°C), in the presence of increasing concentrations of [Pyr¹]apelin-13, [Pyr¹]apelin-13(1–12), apelin-13(F13A), and apelin-17 (0.01 nmol/L–100 μmol/L) or, for SAR, a single concentration (1 μmol/L) apelin-13(R10M), apelin-13(R9P) and apelin-13(P9M). Non-specific binding was defined using 2 μmol/L [Pyr¹]apelin-13. Equilibrium was broken by centrifugation (20,000 g for 10 min, 4°C) and pellets washed with Tris-HCl buffer (50 mmol/L, pH 7.4, 4°C), re-centrifuged and pellets counted for detection of bound radioactivity. Competition binding data were analyzed using GraphPad Prism 6 (GraphPad Software, Inc. La Jolla, CA, USA) to obtain values of pK_i (the negative log₁₀ of the dissociation constant derived from the IC₅₀ for the competing ligands, the radioligand concentration and radioligand affinity by the Cheng and Prusoff equation). Experiments were performed in triplicate.}

Cell-Based Functional Assays

Inhibition of cAMP accumulation, β-arrestin recruitment and receptor internalization by apelin isoforms, modified and truncated apelin peptides were studied using cells expressing the human apelin receptor (DiscoverX, CA, USA) as per the manufacturer's instructions. In all assays the resulting chemiluminescent signal was measured as relative light units (RLU) using a LumiLITE™ Microplate Reader (DiscoverX, Fremont, CA). In the cAMP assay 15 μmol/L forskolin was

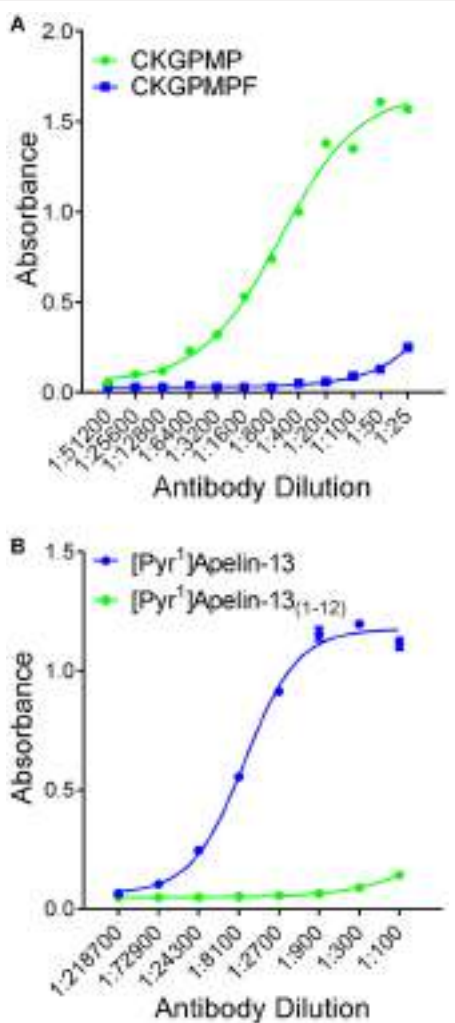


FIGURE 2 | Selectivity of antisera determined by ELISA. (A) [Pyr¹]apelin-13_(1–12) antiserum demonstrated selectivity to the antigen CKGPMPM (●, corresponding to [Pyr¹]Apelin-13_(1–12)) relative to CKGPMPF (■, corresponding to [Pyr¹]Apelin-13). **(B)** The apelin-12 antiserum demonstrated selectivity to [Pyr¹]Apelin-13 (■) relative to [Pyr¹]Apelin-13_(1–12) (●).

used to stimulate cAMP production and concentration-response curves were constructed to [Pyr¹]apelin-13, [Pyr¹]apelin-13_(1–12), apelin-17, apelin-13(F13A) (all 1 pmol/L–30 nmol/L), apelin-13(R10M), apelin-13 (R9P) and apelin-13(P9M) (all 1 nmol/L–10 μmol/L). Agonist responses were expressed as a % of the forskolin response. In the β-arrestin and internalization assays concentration-response curves were constructed to [Pyr¹]apelin-13, [Pyr¹]apelin-13_(1–12), apelin-13(F13A), apelin-13(R10M), (all 10 pmol/L–1 μmol/L), apelin-17 (1 pmol/L–100 nmol/L), apelin-13 (R9P) and apelin-13(P9M) (both 1 nmol/L–300 μmol/L). Agonist responses were expressed as a % of the maximum response to [Pyr¹]apelin-13. Data were analyzed using a 4-parameter logistic equation using GraphPad Prism 6 to determine values of potency, pD₂ ($-\log_{10}$ EC₅₀, where EC₅₀ is the concentration producing half maximal response) and

maximum response (E_{MAX}). n-Values are given as number of replicates/number of experiments.

Using the data from the cAMP and β-arrestin assays with the predominant cardiac isoform [Pyr¹]apelin-13 used as the reference ligand, the relative activation of G protein-dependent and -independent signaling pathways by [Pyr¹]apelin-13, [Pyr¹]apelin-13_(1–12) and apelin-17 were compared using bias analysis as described by van der Westhuizen et al. (2014).

Additional β-arrestin assay experiments were performed with [Pyr¹]apelin-13 that had been incubated with ACE2 as described above. In this assay control concentration-response curves were constructed to [Pyr¹]apelin-13 and [Pyr¹]apelin-13_(1–12) and these were compared to concentration-response curves constructed to both agonists following pre-incubation with rhACE2.

In vitro Functional Studies

Vascular smooth muscle apelin receptor-mediated contraction was exploited in a bioassay to compare the *in vitro* potency of apelin peptides. Experiments were carried out as previously described (Maguire, 2002) in endothelium-denuded saphenous vein with concentration-response curves constructed to [Pyr¹]apelin-13_(1–12) and apelin-13(F13A) (1 pmol/L–300 nmol/L). Agonist responses were expressed as a % of a terminal response to KCl (100 mmol/L). The inotropic action of [Pyr¹]apelin-13_(1–12) was determined in mouse paced RV ($n = 6$) and for comparison in two samples of human paced atrial appendage strips as described (Maguire et al., 2009). Data were expressed as % of the terminal response to CaCl₂. Data from vascular and cardiac experiments were analyzed using a 4-parameter logistic curve (GraphPad Prism 6) to determine values of pD₂ and E_{MAX}.

Systemic Infusions in Rat and Echocardiography

All experiments were performed according to local ethics committee (University College, London) and Home Office (UK) guidelines under the 1986 Scientific Procedures Act and conformed to the Directive 2010/63/EU. The effects of systemic infusion of [Pyr¹]apelin-13_(1–12) (incremental bolus doses 1–300 nmol/300 μL) on blood pressure, heart rate, stroke volume and cardiac output were assessed in male Wistar rats (300 ± 25 g body weight) as described (Brame et al., 2015), that were anesthetized with isoflurane (5% induction, 2% maintenance, continuous monitoring throughout). The left carotid artery and right jugular vein were cannulated (0.96 mm polyvinyl chloride tubing). Mean arterial pressure (MAP) was measured throughout the procedure via a pressure transducer (Powerlab AD Instruments, Chalgrove, UK) connected to the arterial line. Baseline hemodynamics were recorded using Chart 7.0 acquisition software and a 16 channel Powerlab system (AD Instruments, Chalgrove, UK) after a 30 min stabilization period. Thoracic echocardiography was performed at a scanning depth of 0–2 cm using a 14 MHz probe (Vivid 7 Dimension, GE Healthcare, Bedford, UK). Pulsed-wave Doppler was used to determine aortic blood flow velocities in the aortic arch. Stroke volume (SV) was determined as the product of the velocity-time integral (VTI) and vessel cross-sectional area.

Data from six consecutive cardiac cycles were used to determine heart rate (HR) and a marker of left ventricular contractility, peak velocity (PV). Values of SV and HR were used to calculate cardiac output (CO). Respiration rate was determined from movement of the diaphragm using time-motion (M)-model. At the end of the study rats were euthanized by intravenous pentobarbitone and exsanguination.

Forearm Venous Occlusion Plethysmography in Human Volunteers

Studies were performed in healthy volunteers ($n = 12$) in the University of Cambridge Vascular Research Unit, Addenbrooke's Hospital, Cambridge, UK. Volunteer characteristics are given in **Table 1**. This study was carried out in accordance with the recommendations of the National Research Ethics Service Committee East of England-Cambridge Central with written informed consent from all subjects. All subjects gave written informed consent in accordance with the Declaration of Helsinki. The protocol was approved by the National Research Ethics Service Committee East of England-Cambridge Central (REC 11/EE/0305). Changes in forearm blood flow (FBF) in response to [Pyr¹]apelin-13(1–12) (1, 10, 100 nmol/min) were measured as previously described (Brame et al., 2015).

Exclusion criteria were ischemic heart disease, respiratory, renal or neurological disease, diabetes mellitus, hypertension, BMI > 30, BMI < 18; smoker; pregnant; use of vasoactive medication or NSAIDS/aspirin within 48 h of study; current involvement in other research studies. An Omron HEM705CP oscillometric sphygmomanometer was used to measure blood pressure and heart rate at baseline and then every 6 min in the contralateral arm. Periodically, a cuff around the upper arm was inflated for ~8 s to 40 mmHg then deflated for 4 s to interrupt venous return and during a 3 min measurement hand circulation was excluded by inflation of wrist cuffs to 200 mmHg. Changes in forearm volume were measured by mercury-in-silastic strain gauge with FBF subsequently expressed as ml/100 ml forearm volume per min. For infusion of peptides via a 16-gauge catheter (Portex, Kent, UK), the brachial artery (non-dominant arm) was cannulated (27-gauge needle, Cooper's Needle Works, Birmingham, UK) under local anesthesia (lignocaine 1%, Hameln Pharmaceuticals Ltd., Gloucester, UK). FBF was measured in both arms and the response to [Pyr¹]apelin-13(1–12) presented as absolute change in forearm blood flow from the pre-infusion baseline value.

[Pyr¹]apelin-13(1–12), supplied in sealed glass vials and stored at -40°C until required, was allowed to warm to room temperature and diluted with physiological saline to produce stock solutions that were then filtered (0.2 μm flat filter, Portex, Hythe, UK) before further dilution in saline. [Pyr¹]apelin-13(1–12) was infused in three incremental doses during each visit. Doses were previously optimized in a pilot study. Each dose was infused for 6 min with a 20 min saline infusion washout period before the next dose was administered. At the end of the study sodium nitroprusside was infused at 3 $\mu\text{g}/\text{min}$ for 6 min as a positive control followed by a saline infusion as a negative control.

TABLE 1 | Volunteer characteristics.

N =	12
Age (y)	27 \pm 2
Gender (m/f)	6/6
Height (cm)	173 \pm 3
Weight (kg)	70.4 \pm 2.8
BMI (kg/m^2)	23.6 \pm 1
HR (bpm)	68 \pm 3
SBP (mmHg)	127 \pm 6
DBP (mmHg)	72 \pm 4
MAP (mmHg)	90 \pm 4

Values are mean \pm SEM.

Statistical Analyses

Measurements are mean \pm standard error of the mean (SEM). Data analysis and statistical testing were performed using GraphPad Prism 6 to determine values of affinity (pK_i) calculated from competition IC₅₀ values using the Cheng and Prusoff equation, potency [pD_2 ($-\log_{10}$ EC₅₀, the concentration producing 50% of maximum response)] and maximum response (E_{MAX}) as appropriate. Cell assay pD₂ values were compared by one-way ANOVA followed by Tukey's multiple comparison test. For rat *in vivo* experiments the effect of [Pyr¹]apelin-13(1–12) on BP, PV and VTI were expressed as % change from vehicle control in the same animal with other variables (SV and CO) expressed in absolute values. The effect of increasing doses of [Pyr¹]apelin-13(1–12) on each parameter was compared to baseline vehicle control using repeated measures one way ANOVA followed by Dunnett's multiple comparison test. Similarly in the human FBF study the response to successive increasing doses of [Pyr¹]apelin-13(1–12) was compared to pre-infusion baseline value using repeated measures one-way ANOVA followed by Dunnett's multiple comparison test.

Materials

All chemical reagents were purchased from Sigma (Poole, UK), unless otherwise stated. [Pyr¹]apelin-13(1–12) was custom synthesized to GLP standard using Fmoc chemistry on a solid phase support matrix to 98% purity by Maldi-TOF Mass spectroscopy and RP-HPLC analysis. Peptides were tested for sterility and demonstrated to be pyrogen free and biological activity confirmed using the β -arrestin assay. All apelin peptides were synthesized by Severn Biotech (Kidderminster, UK).

RESULTS

[Pyr¹]Apelin-13(1–12) Is Synthesized from [Pyr¹]Apelin-13 by ACE2

As shown in the mass spectra, [Pyr¹]apelin-13 (**Figure 3A**) and [Pyr¹]apelin-13(1–12) (**Figure 3B**) alone produced signals at 1533.8 and 1386.7 m/z, respectively. Incubating [Pyr¹]apelin-13 with rhACE2 resulted in a signal at the mass-to-charge ratio of 1386.7, corresponding to de novo generation of [Pyr¹]apelin-13(1–12), with a weak signal representing the remaining parent

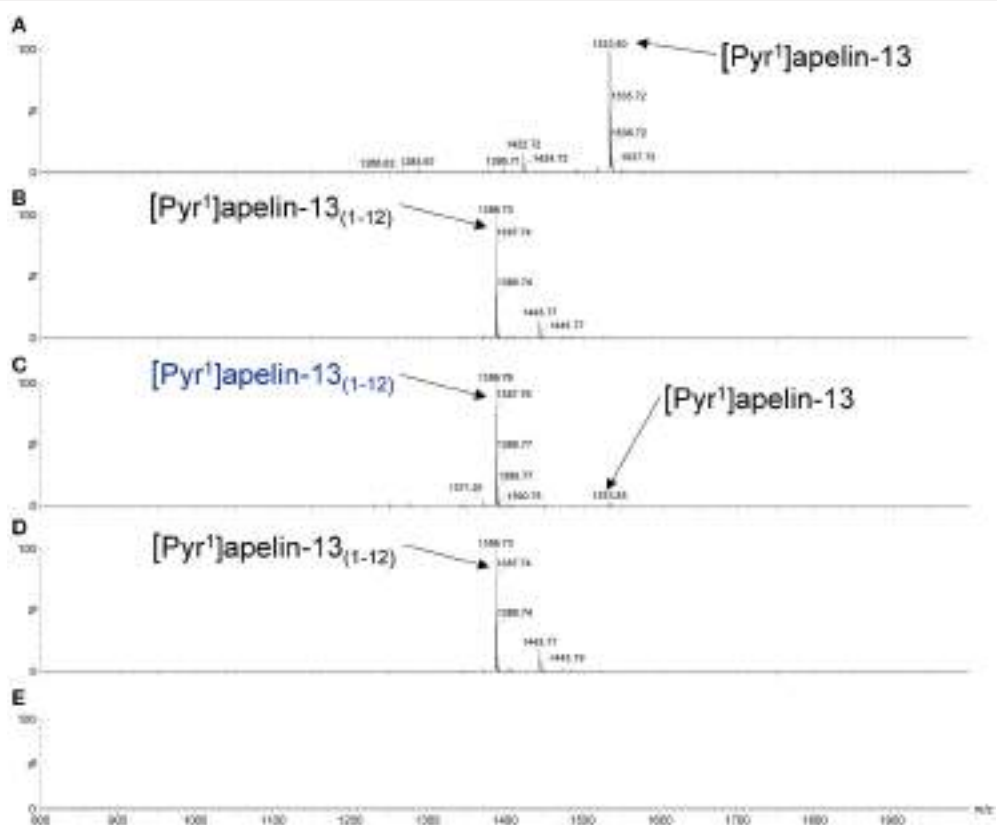


FIGURE 3 | Cleavage of [Pyr¹]apelin-13 to [Pyr¹]apelin-13(1–12) by rhACE2 *in vitro*. Maldi-TOF spectra for (A) [Pyr¹]apelin-13, (B) [Pyr¹]apelin-13(1–12), (C) [Pyr¹]apelin-13 incubated with rhACE2, (D) [Pyr¹]apelin-13(1–12) incubated with rhACE2, (E) rhACE2 alone.

peptide (**Figure 3C**). In contrast, incubating [Pyr^1]apelin-13_(1–12) with rhACE2 (**Figure 3D**) did not produce shorter apelin fragments. Finally, rhACE2 enzyme alone (**Figure 3E**) did not result in interfering signals in the relevant mass range.

[Pyr¹]Apelin-13_(1–12) Is an Endogenous Apelin Peptide Localized to the Endothelium

Endogenous [Pyr^1]apelin-13₍₁₋₁₂₎ peptide was detectable in human cardiovascular tissues and localized to the endothelium (**Figure 4**). [Pyr^1]apelin-13₍₁₋₁₂₎-like immunoreactivity (-LI) was detected in vascular (**Figure 4A**) and endocardial (**Figure 4B**) endothelium identified by positive staining with vWF (**Figure 4C**) in sections of human cardiomyopathy heart, where ACE2 expression has been reported to be increased (Zisman et al., 2003; Goulter et al., 2004). [Pyr^1]apelin-13₍₁₋₁₂₎-LI (**Figure 4D**) and vWF-LI (**Figure 4E**) were also co-expressed (**Figure 4F**) in human lung. Importantly, [Pyr^1]apelin-13₍₁₋₁₂₎-LI (**Figure 4G**) and ACE2-LI (**Figure 4H**) co-localized (**Figure 4I**) in pulmonary blood vessels. Importantly, as apelin is reduced in PAH, the presence of [Pyr^1]apelin-13₍₁₋₁₂₎ was investigated in sections of human PAH lung. Compared to normal lung (**Figure 4J**), [Pyr^1]apelin-13₍₁₋₁₂₎-LI was

not detectable in the vascular endothelium of PAH lung (**Figures 4K,L**).

[Pyr¹]Apelin-13₍₁₋₁₂₎ Binds to and Activates the Human Apelin Receptor

[Pyr¹]apelin-13_(1–12) competed with [¹²⁵I]apelin-13 binding with nanomolar affinity, pK_i = 8.04 ± 0.06 (*n* = 3), that was 4-fold lower than the parent molecule [Pyr¹]apelin-13 (pK_i = 8.83 ± 0.06, *n* = 3) (Figure 5A). Apelin-13(F13A) exhibited comparable affinity to [Pyr¹]apelin-13_(1–12) (pK_i = 8.07 ± 0.24, *n* = 3) whereas the extended peptide apelin-17 competed with highest affinity (pK_i = 9.63 ± 0.17, *n* = 3). Of the shorter fragments apelin-13(R10M) (1 μM) competed for 100% of specific binding whereas apelin-13(R9P) and apelin-13(P9M) were less effective competing for 38% and 62% respectively.

In the signaling assays, [Pyr^1]apelin-13_(1–12) inhibited forskolin-stimulated cAMP production with sub-nanomolar potency, $pD_2 = 9.30 \pm 0.06$ ($n = 8/3$) and was 2-fold less potent than the reference agonist [Pyr^1]apelin-13, $pD_2 = 9.67 \pm 0.04$ ($n = 7/5$) but comparable to apelin-13(F13A) ($pD_2 = 9.54 \pm 0.05$, $n = 2/1$). Apelin-17 ($pD_2 = 10.31 \pm 0.28$, $n = 5/2$) was ~5 times more potent than [Pyr^1]apelin-13. All ligands fully inhibited cAMP production (Figure 5B). Apelin-13(R10M)

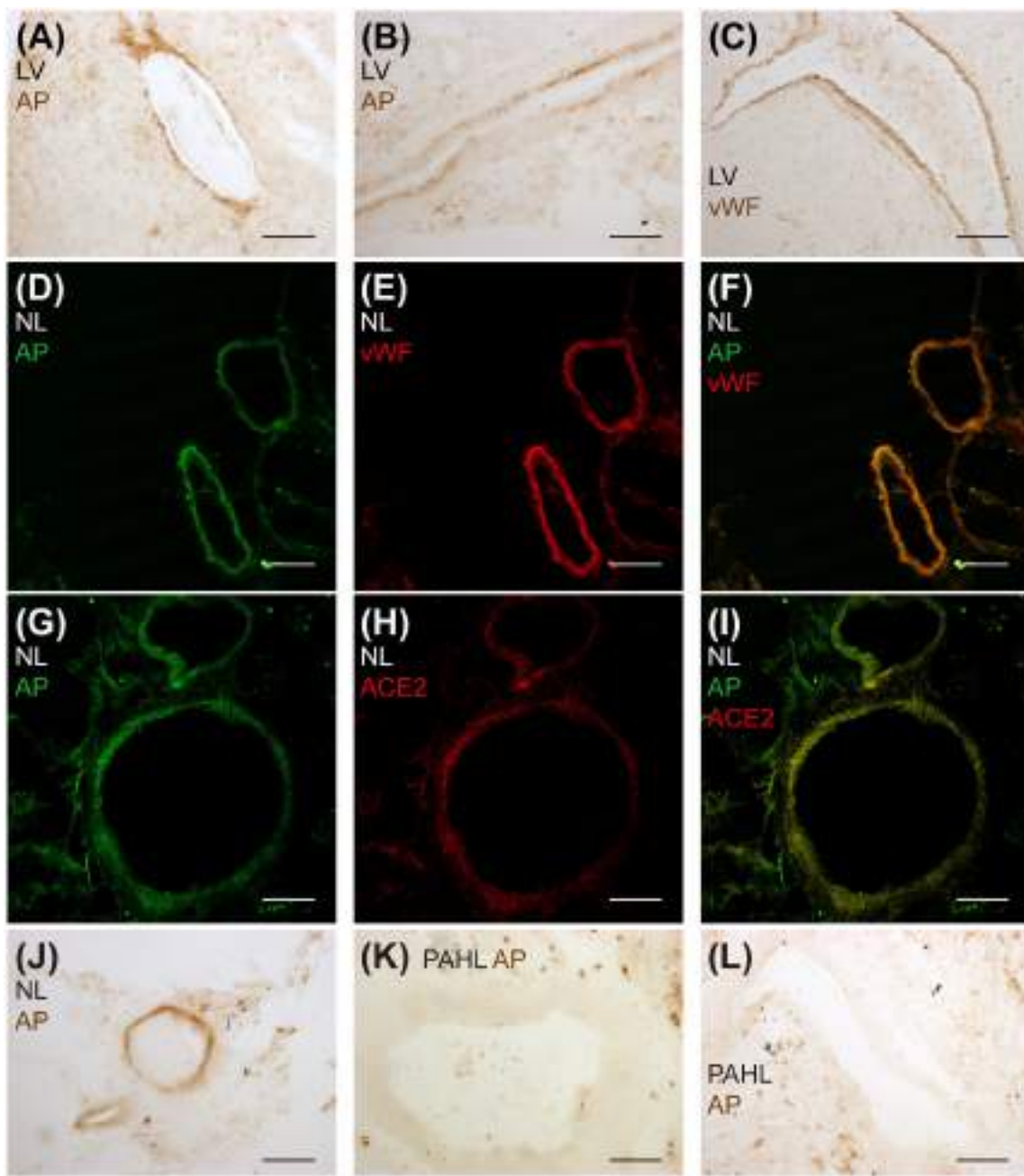


FIGURE 4 | Detection of endogenous [Pyr¹]apelin-13_(1–12) peptide in human cardiovascular tissues. Bright field microphotographs of [Pyr¹]apelin-13_(1–12)-LI in (A) vascular and (B) endocardial endothelium and (C) vWF-LI in cardiomyopathy human heart. Confocal microphotographs of (D) [Pyr¹]apelin-13_(1–12)-LI (green), (E) vWF-LI (red) and (F) their overlay in normal human lung. (G) [Pyr¹]apelin-13_(1–12)-LI (green), (H) ACE2-LI (red) and (I) their overlay in normal human lung. Bright field microphotographs of (J) [Pyr¹]apelin-13_(1–12)-LI in normal human lung and (K,L) the absence of [Pyr¹]apelin-13_(1–12)-LI in PAH human lung tissue. LV, cardiomyopathy human heart; AP, [Pyr¹]apelin-13_(1–12); NL, normal human lung; PAHL, PAH human lung. Scale bar = 200 μ m.

retained nanomolar potency ($pD_2 = 8.70 \pm 0.04, n = 3/1$) whereas inhibition was incomplete for apelin-13(R9P) and apelin-13(P9M) at 10 μ M.

In the G protein-independent β -arrestin recruitment assay [Pyr¹]apelin-13 ($pD_2 = 8.43 \pm 0.08, n = 25/10$,

[Pyr¹]apelin-13_(1–12) ($pD_2 = 7.84 \pm 0.06, n = 17/6$) and apelin-13(F13A) ($pD_2 = 7.98 \pm 0.04, n = 6/2$) were 15-40-fold less potent than in the cAMP assay, with [Pyr¹]apelin-13 ~4-fold more potent than [Pyr¹]apelin-13_(1–12) and apelin-13(F13A). Interestingly, unlike the shorter peptides, apelin-17 exhibited

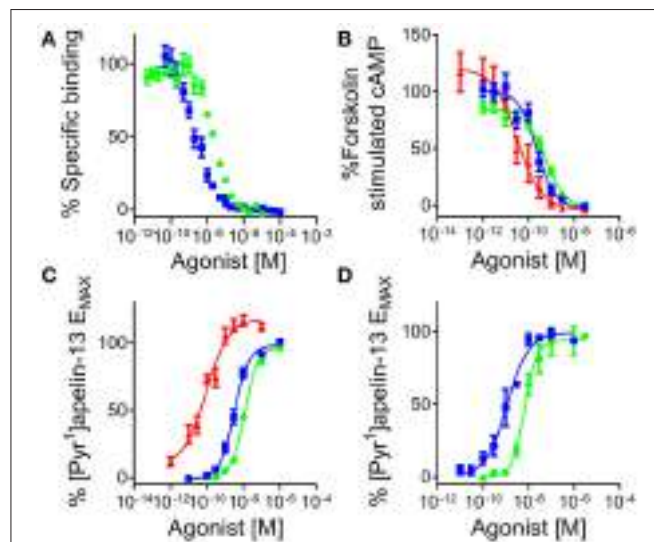


FIGURE 5 | [Pyr¹]apelin-13(1–12) binds to and activates the human apelin receptor. **(A)** Competition binding curve for [Pyr¹]apelin-13 (■) and [Pyr¹]apelin-13(1–12) (●) in human left ventricle ($n = 3$). In cell based assays [Pyr¹]apelin-13 (■), [Pyr¹]apelin-13(1–12) (●), and apelin-17 (▲) **(B)** inhibited forskolin-stimulated cAMP production; **(C)** induced β-arrestin recruitment and **(D)** triggered apelin receptor internalization.

comparable potency as an agonist in both the β-arrestin and cAMP assays with a $pD_2 = 10.26 \pm 0.09$ ($n = 11/4$) (Figure 5C). Apelin-13(R10M) ($pD_2 = 8.26 \pm 0.17$, $n = 9/3$) was ~2-fold less potent than [Pyr¹]apelin-13 and curves were incomplete for apelin-13(R9P) and apelin-13(P9M) at 300 μM.

Similar to the β-arrestin assay, in the internalization assay [Pyr¹]apelin-13(1–12) ($pD_2 = 8.19 \pm 0.06$) was 5-fold less potent than [Pyr¹]apelin-13 ($pD_2 = 8.94 \pm 0.17$). Both peptides were full agonists with comparable efficacy values (E_{MAX} values were $97 \pm 2\%$ and $99 \pm 3\%$ respectively) (Figure 5D).

Comparing the cAMP and β-arrestin data for the three endogenous peptides with [Pyr¹]apelin-13 as the reference agonist, analysis (Table 2) demonstrated a bias factor of 0.24 for [Pyr¹]apelin-13(1–12) and 68 for apelin-17 indicating that compared to [Pyr¹]apelin-13, [Pyr¹]apelin-13(1–12) was 4-fold G protein biased and apelin-17 was markedly β-arrestin biased.

In the β-arrestin recruitment assay [Pyr¹]apelin-13 was significantly more potent than [Pyr¹]apelin-13(1–12) ($p < 0.0001$), [Pyr¹]apelin-13 incubated with rhACE2 ($p < 0.001$) or [Pyr¹]apelin-13(1–12) incubated with rhACE2 ($p < 0.0001$). Both of the rhACE2 combinations exhibited comparable potency to [Pyr¹]apelin-13(1–12) ($p > 0.05$) (Table 3). Therefore the reaction product of [Pyr¹]apelin-13 and rhACE2 more closely resembled [Pyr¹]apelin-13(1–12) than [Pyr¹]apelin-13.

Cardiovascular Actions of Apelin Peptides *In vitro*

[Pyr¹]apelin-13(1–12) ($pD_2 = 9.63 \pm 0.35$, $E_{MAX} = 24 \pm 6\%$, $n = 9$) and apelin-13(F13A) ($pD_2 = 9.72 \pm 0.36$, $E_{MAX} = 23$

TABLE 2 | Pathway bias analysis for [Pyr¹]apelin-13(1–12) and apelin-17 compared to [Pyr¹]apelin-13.

Pathway		[Pyr ¹]apelin-13	[Pyr ¹]apelin-13(1–12)	Apelin-17
cAMP	LogR	9.70 ± 0.05	9.43 ± 0.10	10.28 ± 0.23
	ΔLogR	0.00 ± 0.08	-0.20 ± 0.11	0.48 ± 0.24
	RE	1	0.63	3
β-Arrestin	LogR	8.02 ± 0.13	7.89 ± 0.17	10.34 ± 0.19
	ΔLogR	0.00 ± 0.06	-0.82 ± 0.10	2.32 ± 0.07
	RE	1	0.15	208
cAMP vs. β-Arrestin	ΔΔLogR	0.00 ± 0.10	-0.62 ± 0.15	1.83 ± 0.25
	Bias Factor	1	0.24	68

TABLE 3 | Relative potencies of apelin peptides without and with pre-incubation with recombinant human ACE2 in a β-arrestin assay.

	Potency (pD_2)	E_{MAX} (% [Pyr ¹]apelin-13)
[Pyr ¹]apelin-13	$8.82 \pm 0.03^{\dagger}$	103 ± 4
[Pyr ¹]apelin-13+rhACE2	$7.81 \pm 0.10^{***}$	80 ± 7
[Pyr ¹]apelin-13(1–12)	$7.27 \pm 0.30^{***}$	98 ± 5
[Pyr ¹]apelin-13(1–12)+rhACE2	$7.42 \pm 0.04^{***}$	97 ± 3

Significantly different from [Pyr¹]apelin-13; $^{***}P < 0.001$, $^{****}P < 0.0001$. Significantly different from [Pyr¹]apelin-13(1–12); $^{\dagger}P < 0.001$. One-way ANOVA with Tukey's multiple comparisons test.

± 4%, $n = 9$) contracted saphenous vein with comparable sub-nanomolar potencies and maximum responses (Figure 6A) to the data that we had previously obtained with [Pyr¹]apelin-13 in this assay (Brame et al., 2015).

In mouse paced RV [Pyr¹]apelin-13(1–12) produced a concentration-dependent increase in force of contraction with $pD_2 = 11.68 \pm 0.33$, $E_{MAX} 49 \pm 16\%$ CaCl₂ ($n = 6$) (Figure 6B), compared to isoprenaline with $pD_2 = 7.88 \pm 0.42$, $E_{MAX} = 78 \pm 17\%$ CaCl₂ ($n = 4$) (Figure 6C). Limited human atrial appendage strips were available to test for the inotropic action of [Pyr¹]apelin-13(1–12). In tissue from two patients [Pyr¹]apelin-13(1–12) acted as a positive inotrope with a sub-nanomolar potency value ($pD_2 = 9.61$, $E_{MAX} = 38\%$ CaCl₂, $n = 2$).

Cardiovascular Actions of Apelin Peptides *In vivo*

In anesthetized rat, [Pyr¹]apelin-13(1–12) ($n = 5$) elicited a dose-dependent decrease in BP (Figure 7A). The decrease in BP was significantly different ($P < 0.0001$) from baseline at doses of 10–300 nmol. Other cardiac parameters, SV, CO, PV and VTI were not altered by [Pyr¹]apelin-13(1–12) (Figures 7B–E).

In human volunteers ($n = 12$), [Pyr¹]apelin-13(1–12) (Figure 8) produced comparable dose-dependent increases in forearm blood flow to that which we have shown for [Pyr¹]apelin-13 (Brame et al., 2015). No significant effects of either peptide on heart rate or blood pressure were observed at any dose (data not shown).

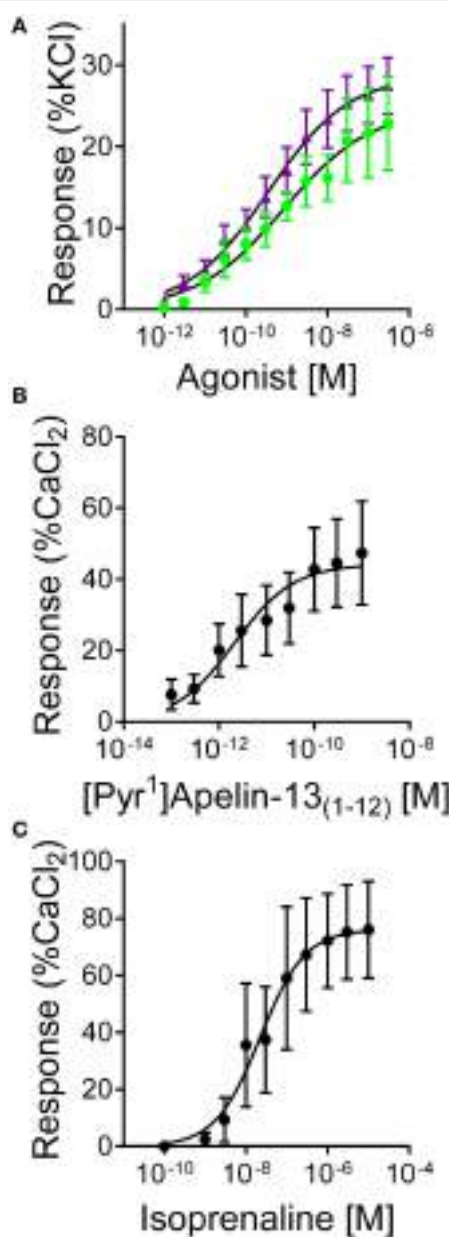


FIGURE 6 | Responses to (A) [Pyr¹]apelin-13(1–12) (●, $n = 9$) and apelin-13(F13A) (▲, $n = 9$) in endothelium-denuded human saphenous vein *in vitro*. **(B)** Inotropic responses to **(B)** [Pyr¹]apelin-13(1–12) ($n = 6$) and **(C)** isoprenaline ($n = 4$) in mouse paced right ventricle.

DISCUSSION

We have characterized the synthesis, receptor pharmacology and functional activity of the ACE2 metabolite of [Pyr¹]apelin-13, [Pyr¹]apelin-13(1–12), *in vitro* and *in vivo*. For the first time we have detected endogenous [Pyr¹]apelin-13(1–12) in human cardiovascular tissues and demonstrated biological activity of this metabolite *in vitro* and in a first-in-man study.

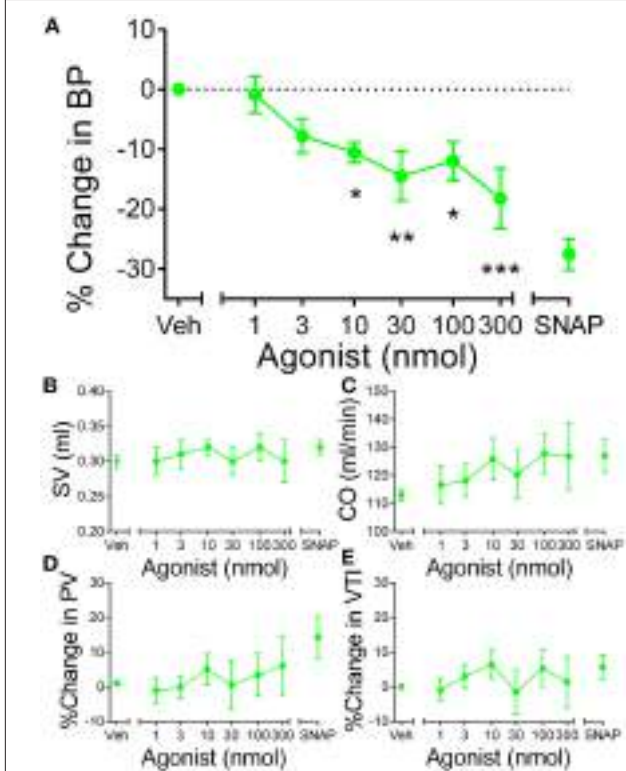


FIGURE 7 | In vivo actions of [Pyr¹]apelin-13(1–12) in rat. (A)

Administration of intravenous [Pyr¹]apelin-13(1–12) (●, $n = 5$) resulted in a significant dose-dependent decrease in blood pressure in rat *in vivo*. Other parameters **(B)** stroke volume (SV), **(C)** cardiac output (CO), **(D)** peak velocity (PV) and velocity-time interval (VTI) were unaffected at any dose of [Pyr¹]apelin-13(1–12). Significantly different from baseline; * $P < 0.05$, ** $P < 0.01$, *** $P < 0.001$. One-way ANOVA repeated measures compared to baseline with Dunnett's multiple comparison test.

Synthesis of [Pyr¹]Apelin-13(1–12) from [Pyr¹]Apelin-13 by ACE2

Apelin-13 and apelin-36 peptides were previously reported to be substrates of purified human ACE2 enzyme (Vickers et al., 2002). In this study, we confirmed (Wang et al., 2016) that ACE2 also catalyzed the conversion of [Pyr¹]apelin-13, the predominant cardiovascular form of apelin, to [Pyr¹]apelin-13(1–12) *in vitro*. This result was not unexpected since the PMPF sequence of [Pyr¹]apelin-13 (Figure 1) conforms to the consensus sequence for ACE2-mediated hydrolysis; Pro-X_(1–3 residues)-Pro-Hydrophobic (Vickers et al., 2002). In support, in the β-arrestin assay the product of *de novo* ACE2 metabolism demonstrated comparable potency to synthetic [Pyr¹]apelin-13(1–12) (Table 3). Our results are consistent with a study reporting that a small proportion of [Pyr¹]apelin-13 was cleaved into [Pyr¹]apelin-13(1–12) in rat *in vivo* (Murza et al., 2014).

We have previously demonstrated endothelial expression of apelin (Kleinz and Davenport, 2004; Kleinz et al., 2005) using an antibody specific for apelin isoforms containing the C-terminal phenylalanine (Figure 2B). This is consistently reported by others using alternative strategies to detect apelin

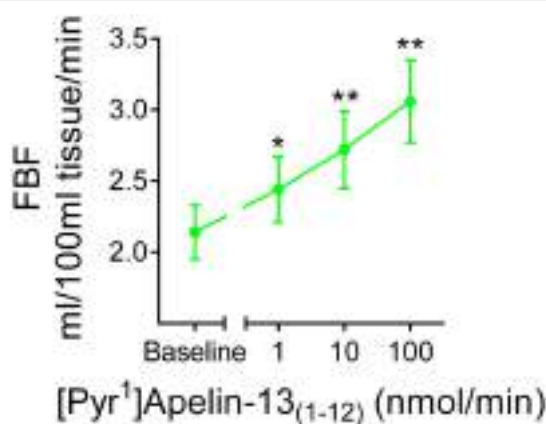


FIGURE 8 | *In vivo* actions of [Pyr¹]apelin-13_(1–12) in human volunteers.

Infusion of [Pyr¹]apelin-13_(1–12) in healthy human volunteers (●, n = 12) resulted in a dose-dependent increase in forearm blood flow. Significantly different from baseline; *P < 0.05, **P < 0.01. One-way ANOVA repeated measures compared to baseline with Dunnett's multiple comparison test.

expression (Sheikh et al., 2008). ACE2 is also expressed in the endothelium (Donoghue et al., 2000; Hamming et al., 2004), raising the possibility of endothelial processing of [Pyr¹]apelin-13 to produce [Pyr¹]apelin-13_(1–12). For this study, we generated an antibody that cross-reacts with apelin isoforms without the C-terminal phenylalanine that has allowed selective identification of [Pyr¹]apelin-13_(1–12) in human heart and lung. [Pyr¹]apelin-13_(1–12)-LI was specifically localized to the endothelium, where the apelin receptor was also expressed, suggesting the possibility of autocrine signaling by this metabolite in these tissues. Importantly, in human PAH lung, where endothelial apelin expression is known to be reduced (Alastalo et al., 2011; Kim et al., 2013), no staining for [Pyr¹]apelin-13_(1–12) was detected.

Biological Activity of [Pyr¹]Apelin-13_(1–12)

ACE2-mediated hydrolysis has been assumed to inactivate apelin peptides. Wang and colleagues have recently reported that the ACE2 product of [Pyr¹]apelin-13 exhibits reduced or absent cardiovascular actions compared to the parent molecule (Wang et al., 2016). However, emerging evidence from structure activity studies suggested that the C-terminal phenylalanine was not a critical residue for apelin biological activity (Fan et al., 2003; Medhurst et al., 2003) and our hypothesis was that compared to [Pyr¹]apelin-13, [Pyr¹]apelin-13_(1–12) may retain significant activity. Indeed, our results showed that [Pyr¹]apelin-13_(1–12) has nanomolar affinity for the native human apelin receptor exhibiting only a 3-fold reduction in binding affinity compared the parent peptide. This is consistent with previous studies where the C-terminal phenylalanine of [Pyr¹]apelin-13 or apelin-13 was replaced with alanine (F13A) (Fan et al., 2003; Medhurst et al., 2003) or removed from apelin-17 (K16P)(El Messari et al., 2004; Iturrioz et al., 2010) with only minimal loss of receptor affinity. Similarly, substitution of the C-terminal phenylalanine

of [Pyr¹]apelin-13 with D-phenylalanine resulted in only a 20-fold decrease in receptor binding affinity, which was modest compared to substitution of other residues known to be important for binding (Murza et al., 2012). Overall, these studies show that loss of the C-terminal phenylalanine from apelin isoforms does not significantly alter receptor binding.

The apelin receptor is G_{αi}-coupled (Habata et al., 1999) therefore we next showed that [Pyr¹]apelin-13_(1–12) inhibited forskolin-stimulated cAMP with potency only 2-fold less than [Pyr¹]apelin-13. This is in agreement with the previous reports of alanine and D-phenylalanine substituted [Pyr¹]apelin-13 (Medhurst et al., 2003; Murza et al., 2012) and K16P (El Messari et al., 2004; Iturrioz et al., 2010; Ceraudo et al., 2014). Therefore, our study confirms that G_{αi}-induced signaling is preserved in response to [Pyr¹]apelin-13_(1–12) receptor binding. In addition to G protein-dependent signaling, activation of the apelin receptor causes β-arrestin recruitment and receptor internalization (Evans et al., 2001). In these assays, [Pyr¹]apelin-13_(1–12) again behaved as a full agonist at the human apelin receptor with only a 5-fold reduction in potency compared to [Pyr¹]apelin-13. This ability to induce receptor internalization without the C-terminal phenylalanine was reported for apelin-13(F13A) (Fan et al., 2003), however, K16P was shown by a second group to exhibit markedly reduced potency and efficacy in β-arrestin recruitment and internalization of rat apelin receptor (El Messari et al., 2004; Iturrioz et al., 2010; Ceraudo et al., 2014). Importantly, compared to [Pyr¹]apelin-13, [Pyr¹]apelin-13_(1–12) is not a biased agonist in G protein-dependent and -independent signaling.

Apelins are modulators of vascular tone and cardiac contractility *in vitro* and *in vivo* (Japp et al., 2008, 2010; Maguire et al., 2009; Barnes et al., 2013; Brame et al., 2015). Therefore, as expected we found that [Pyr¹]apelin-13_(1–12) contracted human saphenous vein with equal potency and efficacy compared with our previous data for [Pyr¹]apelin-13 (Maguire et al., 2009; Brame et al., 2015) and was a potent inotrope in mouse paced right ventricle and human paced atria. We next investigated the *in vivo* actions of [Pyr¹]apelin-13_(1–12). In anesthetized rat compared to our previously published data for [Pyr¹]apelin-13 (Brame et al., 2015), the ACE2 metabolite caused a smaller but significant drop in blood pressure which contrasts with Wang and colleagues (Wang et al., 2016) who reported that [Pyr¹]apelin-13, but not [Pyr¹]apelin-13_(1–12), showed a sustained effect on blood pressure for up to 60 min after administration to mice *in vivo*, although both peptides appear to show an initial comparable reduction in blood pressure over the first 10–15 min in these experiments. Interestingly, these authors also showed that [Pyr¹]apelin-13 is rapidly cleaved by ACE2 *in vitro* and *in vivo* suggesting that the ACE2 cleavage product may contribute to their observed sustained response to [Pyr¹]apelin-13 and as might be expected the half-life of the cleavage product is likely to be short and therefore the response to infused [Pyr¹]apelin-13_(1–12) is observed for only the initial 10–15 min of the experiment. In agreement with this hypothesis, in our rat studies (Brame et al., 2015) the half-life of [Pyr¹]apelin-13 was less than 3 min and in humans

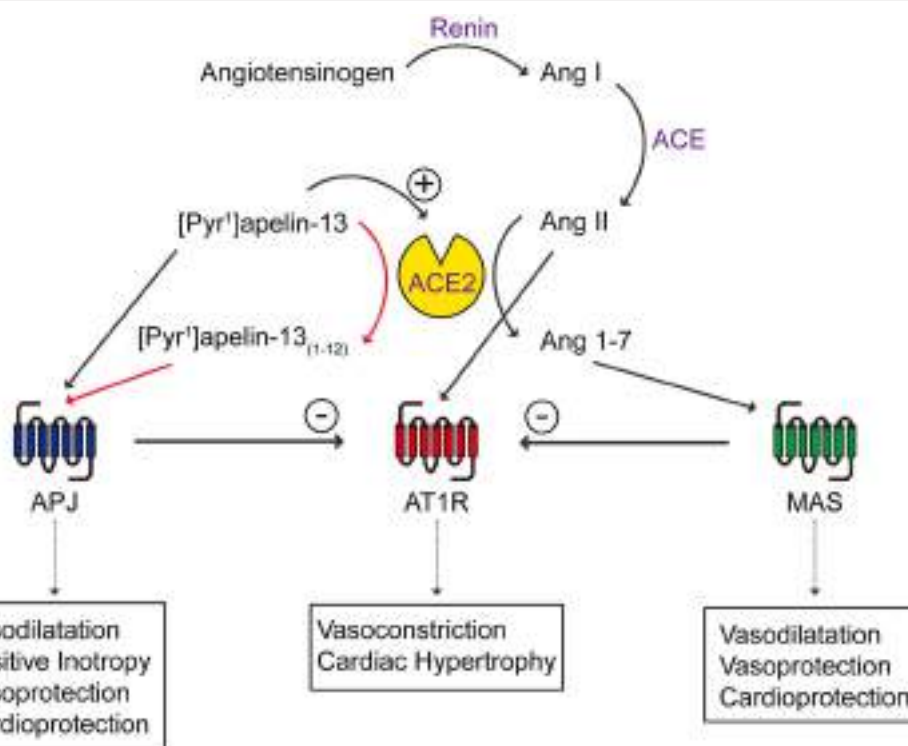


FIGURE 9 | Schematic diagram showing the interactions between apelin/apelin receptor with ACE2 of the renin angiotensin system. New contributions of this study are shown in red arrows. Ang, angiotensin; APJ, apelin receptor; AT1R, angiotensin receptor type I; MAS, Mas receptor.

less than 8 min (Japp et al., 2008). Importantly, in a first-in-man study, infusion of [Pyr¹]apelin-13(1–12) resulted in an increase in forearm blood flow that was the same magnitude as we had previously obtained with [Pyr¹]apelin-13 (Brame et al., 2015), confirming that this metabolite is a vasodilator in humans *in vivo*.

Structure Activity Relationships of Apelin Peptides

The 55-amino acid proapelin, derived from the 77-residue prepropeptide, contains a number of paired basic amino acids residues that are possible cleavage sites for endopeptidases to produce 13 to 36-residue isoforms (Tatemoto et al., 1998; Habata et al., 1999). While the identities of these peptidases remain unknown, a study reported the direct cleavage of proapelin to apelin-13 by proprotein convertase subtilisin/kexin 3 (PCSK3, or furin), bypassing the generation of longer isoforms (Shin et al., 2013). Post-translational modification results in the predominant apelin isoform detected in human cardiovascular tissue and plasma, [Pyr¹]apelin-13 (De Mota et al., 2004; Kleinz and Davenport, 2004; Maguire et al., 2009; Zhen et al., 2013). The putative ACE2 metabolite of this cardiac peptide, [Pyr¹]apelin-13(1–12), is the focus of our study but we have also explored the pharmacology of several other important apelin isoforms to better understand the apelin structure activity relationships, namely the minimum active fragment apelin-13(R10M), apelin-13(F13A) and apelin-17.

As described above, amino acid substitution studies have proposed a consensus on those amino acids within apelin-13 that are important for receptor binding and activation (Narayanan et al., 2015). The C-terminal phenylalanine (F13), adjacent proline and the N-terminal pyroglutamic acid were not identified as important. We have investigated whether the truncated peptides apelin-13(R10M), apelin-13(R9P) and apelin-13(P9M) retained significant binding and functional activity with the hypothesis that apelin-13(R10M) was likely to represent the minimum active fragment as it was the shortest fragment containing all the identified important amino acids. Results of the competition binding experiments and β -arrestin recruitment assays supported this hypothesis as do data from previous publications showing diminished G_{αi}-mediated signaling and calcium mobilization when the methionine (position 11 in apelin-13) was removed (Medhurst et al., 2003; Zhang et al., 2014), while others have demonstrated activity of apelin-12 (apelin-13 without the N-terminal pyroglutamic acid) *in vivo* (Pisarenko et al., 2011). Residues arginine 2 and methionine 11 are indispensable as they are required to form the crucial RPRL motif or provide steric volume (Langelaan et al., 2009; Macaluso and Glen, 2010; Gerbier et al., 2015). In contrast, although the C-terminal phenylalanine has been shown to make specific contacts within the binding pocket of the apelin receptor (Iturrioz et al., 2010), our experimental data suggested that its removal did not abolish binding or functional activity.

Early alanine scanning studies indicated that replacing the C-terminal phenylalanine with alanine did not abolish G_{αi}-mediated signaling, calcium mobilization (Medhurst et al., 2003) and receptor internalization (Fan et al., 2003). However, conflicting data have been reported for F13A, suggesting that it was an antagonist of the apelin receptor in terms of G_{αi}-mediated signaling ([Pyr¹]apelin-13(F13A); De Mota et al., 2000) and hypotensive effect (apelin-13(F13A); Lee et al., 2005). In this study, we found that apelin-13(F13A) resembled [Pyr¹]apelin-13_(1–12) in receptor binding, cell based assays and the vasoconstrictor bioassay. Based on our results apelin-13(F13A) behaves as an apelin agonist with no evidence of receptor antagonism.

Apelin-17, despite its unclear biosynthetic pathway, has been reported to have equal or higher binding affinity and potency in inhibiting cAMP accumulation and inducing receptor internalization compared with [Pyr¹]apelin-13 (Medhurst et al., 2003; El Messari et al., 2004). We investigated apelin-17 in our assays and consistently found higher binding affinity and higher potency than [Pyr¹]apelin-13 in the cAMP and β-arrestin assays. Intriguingly, apelin-17 appeared to be more biased for β-arrestin compared to G protein signaling relative to the reference agonist [Pyr¹]apelin-13. This suggests that N-terminal extension of apelin-13 may result in peptides that stabilize different conformations of the apelin receptor and may be a mechanism by which apelin receptor activation is fine-tuned at the cellular level.

Implication on the Interactions between the Apelin and Renin-Angiotensin Systems

Past studies have suggested a possible link between apelin, its receptor, ACE2 and the renin angiotensin system. For example, apelin knockout mice showed aging or stress-associated cardiac contractility defects, similar to the cardiac phenotype of ACE2 knockout mice (Kuba et al., 2007) and apelin receptor knockout mice are more sensitive to the pressor effect of angiotensin II (Ishida et al., 2004). Interestingly, ACE2 expression is reduced in apelin knockout mice and apelin up-regulates ACE2 expression, indicating that apelin may reciprocally impact ACE2 (Sato et al., 2013). At the receptor level, the apelin receptor has been shown to physically interact with the angiotensin receptor type I (AT1R) (Chun et al., 2008), forcing it into a low affinity state and reducing the binding and signaling of angiotensin II (Siddiquee et al., 2013). Reduced apelin expression due to heart failure or angiotensin II administration can be restored by AT1R blockade (Iwanaga et al., 2006). The opposing effects of apelin/ACE2 and angiotensin II have been shown in health and

REFERENCES

- Alastalo, T. P., Li, M., Perez Ve, J., Pham, D., Sawada, H., Wang, J. K., et al. (2011). Disruption of PPARγ/β-catenin-mediated regulation of apelin impairs BMP-induced mouse and human pulmonary arterial EC survival. *J. Clin. Invest.* 121, 3735–3746. doi: 10.1172/JCI43382
- Ashley, E., Chun, H. J., and Quertermous, T. (2006). Opposing cardiovascular roles for the angiotensin and apelin signaling pathways. *J. Mol. Cell. Cardiol.* 41, 778–781. doi: 10.1016/j.yjmcc.2006.08.013

diseases such as heart failure, atherosclerosis and obesity/diabetes (Ashley et al., 2006; Gurzu et al., 2006; Iwanaga et al., 2006; Zhong et al., 2007; Chun et al., 2008; Barnes et al., 2013; Siddiquee et al., 2013) (**Figure 9**). Our study contributes further evidence that ACE2, that is up-regulated in disease, acting on [Pyr¹]apelin-13 may result in the generation of the active metabolite, [Pyr¹]apelin-13_(1–12), and therefore a compensatory maintenance of apelin receptor signaling. However, a limitation of our study is that we have not measured levels of apelin peptides in plasma of patients receiving rhACE2 therapy, but we would hypothesize that levels of [Pyr¹]apelin-13_(1–12) would be elevated and [Pyr¹]apelin-13 decreased compared to controls.

In conclusion, this study confirmed that ACE2 cleaves [Pyr¹]apelin-13 into [Pyr¹]apelin-13_(1–12) and has demonstrated biological activity of [Pyr¹]apelin-13_(1–12) at the human apelin receptor *in vitro* and in the cardiovascular system of rat and human *in vivo*. The results also clarify R10M as the shortest active apelin fragment, apelin-13(F13A) as an agonist and apelin-17 as a more potent agonist than [Pyr¹]apelin-13. Therefore, our study shows that reported enhanced ACE2 activity in cardiovascular disease should not significantly compromise the beneficial effects of apelin based therapies for example in PAH.

AUTHOR CONTRIBUTIONS

All authors contributed either to the conception or design of the work (PY, AB, AD, MS, RG, JC, IW, APD, and JM), or acquired and analyzed data or interpreted data (PY, RK, AB, AD, MS, APD, and JM). All authors agree to be accountable for all aspects of the work.

FUNDING

This work was supported by the Wellcome Trust Programme in Metabolic and Cardiovascular Disease [096822/Z/11/Z to APD]; Wellcome Trust [WT 107715 to APD]; Medical Research Council [MC_PC_14116 to APD]; Wellcome Trust Programme in Translational Medicines and Therapeutics [085686 to APD], and in part by the National Institute for Health Research Cambridge Biomedical Research Centre; and the Pulmonary Hypertension Association UK.

ACKNOWLEDGMENTS

We thank the theater and consultant staff of Papworth hospital for tissue collection.

- Barnes, G. D., Alam, S., Carter, G., Pedersen, C. M., Lee, K. M., Hubbard, T. J., et al. (2013). Sustained cardiovascular actions of APJ agonism during renin-angiotensin system activation and in patients with heart failure. *Circ. Heart Fail.* 6, 482–491. doi: 10.1161/CIRCHEARTFAILURE.111.000077
- Brame, A. L., Maguire, J. J., Yang, P., Dyson, A., Torella, R., Cherian, J., et al. (2015). Design, characterization, and first-in-human study of the vascular actions of a novel biased apelin receptor agonist. *Hypertension*. 65, 834–840. doi: 10.1161/HYPERTENSIONHA.114.05099

- Ceraudo, E., Galanth, C., Carpentier, E., Banegas-Font, I., Schonegge, A. M., Alvear-Perez, R., et al. (2014). Biased signaling favoring G_i over β -arrestin promoted by an apelin fragment lacking the C-terminal phenylalanine. *J. Biol. Chem.* 289, 24599–24610. doi: 10.1074/jbc.M113.541698
- Chandra, S. M., Razavi, H., Kim, J., Agrawal, R., Kundu, R. K., de Jesus Perez, V., et al. (2011). Disruption of the apelin-APJ system worsens hypoxia-induced pulmonary hypertension. *Arterioscler. Thromb. Vasc. Biol.* 31, 814–820. doi: 10.1161/ATVBAHA.110.219980
- Chun, H. J., Ali, Z. A., Kojima, Y., Kundu, R. K., Sheikh, A. Y., Agrawal, R., et al. (2008). Apelin signaling antagonizes Ang II effects in mouse models of atherosclerosis. *J. Clin. Invest.* 118, 3343–3354. doi: 10.1172/jci34871
- Dai, H., Jiang, L., Xiao, Z., and Guang, X. (2015). ACE2-angiotensin-(1-7)-Mas axis might be a promising therapeutic target for pulmonary arterial hypertension. *Nat. Rev. Cardiol.* 12:374. doi: 10.1038/nrcardio.2015.6.c1
- De Mota, N., Lenkei, Z., and Llorens-Cortés, C. (2000). Cloning, pharmacological characterization and brain distribution of the rat apelin receptor. *Neuroendocrinology* 72, 400–407. doi: 10.1159/000054609
- De Mota, N., Reaux-Le Goazigo, A., El Messari, S., Chartrel, N., Roesch, D., Dujardin, C., et al. (2004). Apelin, a potent diuretic neuropeptide counteracting vasopressin actions through inhibition of vasopressin neuron activity and vasopressin release. *Proc. Natl. Acad. Sci. U.S.A.* 101, 10464–10469. doi: 10.1073/pnas.0403518101
- Donoghue, M., Hsieh, F., Baronas, E., Godbout, K., Gosselin, M., Stagliano, N., et al. (2000). A novel angiotensin-converting enzyme-related carboxypeptidase (ACE2) converts angiotensin I to angiotensin 1–9. *Circ. Res.* 87, E1–E9. doi: 10.1161/01.RES.87.5.e1
- El Messari, S., Iturrioz, X., Fassot, C., De Mota, N., Roesch, D., and Llorens-Cortés, C. (2004). Functional dissociation of apelin receptor signaling and endocytosis: implications for the effects of apelin on arterial blood pressure. *J. Neurochem.* 90, 1290–1301. doi: 10.1111/j.1471-4159.2004.02591.x
- Evans, N. A., Groarke, D. A., Warrack, J., Greenwood, C. J., Dodgson, K., Milligan, G., et al. (2001). Visualizing differences in ligand-induced beta-arrestin-GFP interactions and trafficking between three recently characterized G protein-coupled receptors. *J. Neurochem.* 77, 476–485. doi: 10.1046/j.1471-4159.2001.00269.x
- Fan, X., Zhou, N., Zhang, X., Mukhtar, M., Lu, Z., Fang, J., et al. (2003). Structural and functional study of the apelin-13 peptide, an endogenous ligand of the HIV-1 coreceptor, APJ. *Biochemistry* 42, 10163–10168. doi: 10.1021/bi030049s
- Gerbier, R., Leroux, V., Couvineau, P., Alvear-Perez, R., Maigret, B., Llorens-Cortés, C., et al. (2015). New structural insights into the apelin receptor: identification of key residues for apelin binding. *FASEB J.* 29, 314–322. doi: 10.1096/fj.14-256339
- Goulter, A. B., Goddard, M. J., Allen, J. C., and Clark, K. L. (2004). ACE2 gene expression is up-regulated in the human failing heart. *BMC Med.* 2:19. doi: 10.1186/1741-7015-2-19
- Gurzu, B., Petrescu, B. C., Costuleanu, M., and Petrescu, G. (2006). Interactions between apelin and angiotensin II on rat portal vein. *J. Renin Angiotensin Aldosterone Syst.* 7, 212–216. doi: 10.3317/jraas.2006.040
- Habata, Y., Fujii, R., Hosoya, M., Fukusumi, S., Kawamata, Y., Hinuma, S., et al. (1999). Apelin, the natural ligand of the orphan receptor APJ, is abundantly secreted in the colostrum. *Biochim. Biophys. Acta* 1452, 25–35. doi: 10.1016/S0167-4889(99)00114-7
- Hamming, I., Timens, W., Bulthuis, M. L., Lely, A. T., Navis, G. J., and van Goor, H. (2004). Tissue distribution of ACE2 protein, the functional receptor for SARS coronavirus. A first step in understanding SARS pathogenesis. *J. Pathol.* 203, 631–637. doi: 10.1002/path.1570
- Haschke, M., Schuster, M., Poglitsch, M., Loibner, H., Salzberg, M., Bruggisser, M., et al. (2013). Pharmacokinetics and pharmacodynamics of recombinant human angiotensin-converting enzyme 2 in healthy human subjects. *Clin. Pharmacokinet.* 52, 783–792. doi: 10.1007/s40262-013-0072-7
- Ishida, J., Hashimoto, T., Hashimoto, Y., Nishiwaki, S., Iguchi, T., Harada, S., et al. (2004). Regulatory roles for APJ, a seven-transmembrane receptor related to angiotensin-type 1 receptor in blood pressure *in vivo*. *J. Biol. Chem.* 279, 26274–26279. doi: 10.1074/jbc.M404149200
- Iturrioz, X., Gerbier, R., Leroux, V., Alvear-Perez, R., Maigret, B., and Llorens-Cortés, C. (2010). By interacting with the C-terminal Phe of apelin, Phe255 and Trp259 in helix VI of the apelin receptor are critical for internalization. *J. Biol. Chem.* 285, 32627–32637. doi: 10.1074/jbc.M110.127167
- Iwanaga, Y., Kihara, Y., Takenaka, H., and Kita, T. (2006). Down-regulation of cardiac apelin system in hypertrophied and failing hearts: possible role of angiotensin II-angiotensin type 1 receptor system. *J. Mol. Cell. Cardiol.* 41, 798–806. doi: 10.1016/j.yjmcc.2006.07.004
- Japp, A. G., Cruden, N. L., Amer, D. A., Li, V. K., Goudie, E. B., Johnston, N. R., et al. (2008). Vascular effects of apelin *in vivo* in man. *J. Am. Coll. Cardiol.* 52, 908–913. doi: 10.1016/j.jacc.2008.06.013
- Japp, A. G., Cruden, N. L., Barnes, G., van Gemeren, N., Mathews, J., Adamson, J., et al. (2010). Acute cardiovascular effects of apelin in humans: potential role in patients with chronic heart failure. *Circulation* 121, 1818–1827. doi: 10.1161/CIRCULATIONAHA.109.911339
- Kim, J., Kang, Y., Kojima, Y., Lighthouse, J. K., Hu, X., Aldred, M. A., et al. (2013). An endothelial apelin-FGF link mediated by miR-424 and miR-503 is disrupted in pulmonary arterial hypertension. *Nat. Med.* 19, 74–82. doi: 10.1038/nm.3040
- Klein, M. J., and Davenport, A. P. (2004). Immunocytochemical localization of the endogenous vasoactive peptide apelin to human vascular and endocardial endothelial cells. *Regul. Pept.* 118, 119–125. doi: 10.1016/j.regpep.2003.11.002
- Klein, M. J., Skepper, J. N., and Davenport, A. P. (2005). Immunocytochemical localisation of the apelin receptor, APJ, to human cardiomyocytes, vascular smooth muscle and endothelial cells. *Regul. Pept.* 126, 233–240. doi: 10.1016/j.regpep.2004.10.019
- Kuba, K., Imai, Y., Rao, S., Gao, H., Guo, F., Guan, B., et al. (2005). A crucial role of angiotensin converting enzyme 2 (ACE2) in SARS coronavirus-induced lung injury. *Nat. Med.* 11, 875–879. doi: 10.1038/nm1267
- Kuba, K., Zhang, L., Imai, Y., Arab, S., Chen, M., Maekawa, Y., et al. (2007). Impaired heart contractility in Apelin gene-deficient mice associated with aging and pressure overload. *Circ. Res.* 101, e32–e42. doi: 10.1161/CIRCRESAHA.107.158659
- Langelaan, D. N., Bebbington, E. M., Reddy, T., and Rainey, J. K. (2009). Structural insight into G-protein coupled receptor binding by apelin. *Biochemistry* 48, 537–548. doi: 10.1021/bi801864b
- Lee, D. K., Saldivia, V. R., Nguyen, T., Cheng, R., George, S. R., and O'Dowd, B. F. (2005). Modification of the terminal residue of apelin-13 antagonizes its hypotensive action. *Endocrinology* 146, 231–236. doi: 10.1210/en.2004-0359
- Li, F., Li, L., Qin, X., Pan, W., Feng, F., Chen, F., et al. (2008). Apelin-induced vascular smooth muscle cell proliferation: the regulation of cyclin D1. *Front. Biosci.* 13, 3786–3792. doi: 10.2741/2967
- Macaluso, N. J., and Glen, R. C. (2010). Exploring the 'RPRL' motif of apelin-13 through molecular simulation and biological evaluation of cyclic peptide analogues. *Chem. Med. Chem.* 5, 1247–1253. doi: 10.1002/cmdc.201000061
- Maguire, J. J. (2002). Endothelin-converting enzyme activity in vascular smooth muscle preparations *in vitro*. *Methods Mol. Biol.* 206, 165–177. doi: 10.1385/1-59259-289-9:165
- Maguire, J. J., Klein, M. J., Pitkin, S. L., and Davenport, A. P. (2009). [Pyr1]apelin-13 identified as the predominant apelin isoform in the human heart: vasoactive mechanisms and inotropic action in disease. *Hypertension* 54, 598–604. doi: 10.1161/HYPERTENSIONAHA.109.134619
- Medhurst, A. D., Jennings, C. A., Robbins, M. J., Davis, R. P., Ellis, C., Winborn, K. Y., et al. (2003). Pharmacological and immunohistochemical characterization of the APJ receptor and its endogenous ligand apelin. *J. Neurochem.* 84, 1162–1172. doi: 10.1046/j.1471-4159.2003.01587.x
- Murza, A., Belleville, K., Longpré, J. M., Sarret, P., and Marsault, E. (2014). Stability and degradation patterns of chemically modified analogs of apelin-13 in plasma and cerebrospinal fluid. *Biopolymers* 101, 297–303. doi: 10.1002/bip.22498
- Murza, A., Parent, A., Besserer-Offroy, E., Tremblay, H., Karadereye, F., Beaudet, N., et al. (2012). Elucidation of the structure-activity relationships of apelin: influence of unnatural amino acids on binding, signaling, and plasma stability. *ChemMedChem* 7, 318–325. doi: 10.1002/cmdc.201100492
- Narayanan, S., Harris, D. L., Maitra, R., and Runyon, S. P. (2015). Regulation of the apelinergic system and its potential in cardiovascular disease: peptides and small molecules as tools for discovery. *J. Med. Chem.* 58, 7913–7927. doi: 10.1021/acs.jmedchem.5b00527
- Pisarenko, O. I., Serebryakova, L. I., Pelogeykina, Y. A., Studneva, I. M., Khatri, D. N., Tskitishvili, O. V., et al. (2011). *In vivo* reduction of reperfusion injury

- to the heart with apelin-12 peptide in rats. *Bull. Exp. Biol. Med.* 152, 79–82. doi: 10.1007/s10517-011-1459-9
- Santos, R. A., Ferreira, A. J., Simões, E., and Silva, A. C. (2008). Recent advances in the angiotensin-converting enzyme 2-angiotensin(1–7)-Mas axis. *Exp. Physiol.* 93, 519–527. doi: 10.1113/expphysiol.2008.042002
- Santos, R. A., Simões e Silva, A. C., Maric, C., Silva, D. M., Machado, R. P., de Buhr, I., et al. (2003). Angiotensin-(1–7) is an endogenous ligand for the G protein-coupled receptor Mas. *Proc. Natl. Acad. Sci. U.S.A.* 100, 8258–8263. doi: 10.1073/pnas.1432869100
- Sato, T., Suzuki, T., Watanabe, H., Kadowaki, A., Fukamizu, A., Liu, P. P., et al. (2013). Apelin is a positive regulator of ACE2 in failing hearts. *J. Clin. Invest.* 123, 5203–5211. doi: 10.1172/JCI69608
- Sheikh, A. Y., Chun, H. J., Glassford, A. J., Kundu, R. K., Kutschka, I., Ardigo, D., et al. (2008). *In vivo* genetic profiling and cellular localization of apelin reveals a hypoxia-sensitive, endothelial-centered pathway activated in ischemic heart failure. *Am. J. Physiol. Heart Circ. Physiol.* 294, H88–H98. doi: 10.1152/ajpheart.00935.2007
- Shenoy, V., Qi, Y., Katovich, M. J., and Raizada, M. K. (2011). ACE2, a promising therapeutic target for pulmonary hypertension. *Curr. Opin. Pharmacol.* 11, 150–155. doi: 10.1016/j.coph.2010.12.002
- Shin, K., Pandey, A., Liu, X. Q., Anini, Y., and Rainey, J. K. (2013). Preferential apelin-13 production by the proprotein convertase PCSK3 is implicated in obesity. *FEBS Open Bio* 3, 328–333. doi: 10.1016/j.fob.2013.08.001
- Siddiquee, K., Hampton, J., McAnally, D., May, L., and Smith, L. (2013). The apelin receptor inhibits the angiotensin II type 1 receptor via allosteric trans-inhibition. *Br. J. Pharmacol.* 168, 1104–1117. doi: 10.1111/j.1476-5381.2012.02192.x
- Tatemoto, K., Hosoya, M., Habata, Y., Fujii, R., Kakegawa, T., Zou, M. X., et al. (1998). Isolation and characterization of a novel endogenous peptide ligand for the human APJ receptor. *Biochem. Biophys. Res. Commun.* 251, 471–476. doi: 10.1006/bbrc.1998.9489
- Tipnis, S. R., Hooper, N. M., Hyde, R., Karran, E., Christie, G., and Turner, A. J. (2000). A human homolog of angiotensin-converting enzyme. Cloning and functional expression as a captopril-insensitive carboxypeptidase. *J. Biol. Chem.* 275, 33238–33243. doi: 10.1074/jbc.M002615200
- van der Westhuizen, E. T., Breton, B., Christopoulos, A., and Bouvier, M. (2014). Quantification of ligand bias for clinically relevant $\beta 2$ -adrenergic receptor ligands: implications for drug taxonomy. *Mol. Pharmacol.* 85, 492–509. doi: 10.1124/mol.113.088880
- Vickers, C., Hales, P., Kaushik, V., Dick, L., Gavin, J., Tang, J., et al. (2002). Hydrolysis of biological peptides by human angiotensin-converting enzyme-related carboxypeptidase. *J. Biol. Chem.* 277, 14838–14843. doi: 10.1074/jbc.M200581200
- Wang, W., McKinnie, S. M., Farhan, M., Paul, M., McDonald, T., McLean, B., et al. (2016). Angiotensin-converting enzyme 2 metabolizes and partially inactivates Pyr-Aelin-13 and Apelin-17: physiological effects in the cardiovascular system. *Hypertension* 68, 365–377. doi: 10.1161/HYPERTENSIONAHA.115.06892
- Yang, P., Maguire, J. J., and Davenport, A. P. (2015). Apelin, Elabel/Toddler, and biased agonists as novel therapeutic agents in the cardiovascular system. *Trends Pharmacol. Sci.* 36, 560–567. doi: 10.1016/j.tips.2015.06.002
- Zhang, Y., Maitra, R., Harris, D. L., Dhungana, S., Snyder, R., and Runyon, S. P. (2014). Identifying structural determinants of potency for analogs of apelin-13: integration of C-terminal truncation with structure-activity. *Bioorg. Med. Chem.* 22, 2992–2997. doi: 10.1016/j.bmc.2014.04.001
- Zhen, E. Y., Higgs, R. E., and Gutierrez, J. A. (2013). Pyroglutamyl apelin-13 identified as the major apelin isoform in human plasma. *Anal. Biochem.* 442, 1–9. doi: 10.1016/j.ab.2013.07.006
- Zhong, J. C., Yu, X. Y., Huang, Y., Yung, L. M., Lau, C. W., and Lin, S. G. (2007). Apelin modulates aortic vascular tone via endothelial nitric oxide synthase phosphorylation pathway in diabetic mice. *Cardiovasc. Res.* 74, 388–395. doi: 10.1016/j.cardiores.2007.02.002
- Zisman, L. S., Keller, R. S., Weaver, B., Lin, Q., Speth, R., Bristow, M. R., et al. (2003). Increased angiotensin-(1–7)-forming activity in failing human heart ventricles: evidence for upregulation of the angiotensin-converting enzyme Homologue ACE2. *Circulation* 108, 1707–1712. doi: 10.1161/01.CIR.0000094734.67990.99

Conflict of Interest Statement: The authors declare that the research was conducted in the absence of any commercial or financial relationships that could be construed as a potential conflict of interest.

Copyright © 2017 Yang, Kuc, Brame, Dyson, Singer, Glen, Cheriyan, Wilkinson, Davenport and Maguire. This is an open-access article distributed under the terms of the Creative Commons Attribution License (CC BY). The use, distribution or reproduction in other forums is permitted, provided the original author(s) or licensor are credited and that the original publication in this journal is cited, in accordance with accepted academic practice. No use, distribution or reproduction is permitted which does not comply with these terms.



Role of the Vasopressin/Aelin Balance and Potential Use of Metabolically Stable Apelin Analogs in Water Metabolism Disorders

Adrien Flahault[†], Pierre Couvineau[†], Rodrigo Alvear-Perez, Xavier Iturrioz and Catherine Llorens-Cortes*

Laboratory of Central Neuropeptides in the Regulation of Body Fluid Homeostasis and Cardiovascular Functions, Center for Interdisciplinary Research in Biology (CIRB), INSERM, U1050/CNRS, UMR 7241, College de France, Paris, France

OPEN ACCESS

Edited by:

Hubert Vaudry,
University of Rouen, France

Reviewed by:

Catherine S. Hubbard,
Massachusetts General Hospital/Harvard Medical School, United States
Leo T. O. Lee,
University of Macau, China

*Correspondence:

Catherine Llorens-Cortes
c.llorens-cortes@college-de-france.fr

[†]These authors have contributed equally to this work and are both cofirst authors.

Specialty section:

This article was submitted to
Neuroendocrine Science,
a section of the journal
Frontiers in Endocrinology

Received: 25 January 2017

Accepted: 16 May 2017

Published: 31 May 2017

Citation:

Flahault A, Couvineau P, Alvear-Perez R, Iturrioz X and Llorens-Cortes C (2017) Role of the Vasopressin/Aelin Balance and Potential Use of Metabolically Stable Apelin Analogs in Water Metabolism Disorders. *Front. Endocrinol.* 8:120. doi: 10.3389/fendo.2017.00120

Apelin, a (neuro)vasoactive peptide, plays a prominent role in controlling body fluid homeostasis and cardiovascular functions. In animal models, experimental data demonstrate that intracerebroventricular injection of apelin into lactating rats inhibits the phasic electrical activity of arginine vasopressin (AVP) neurons, reduces plasma AVP levels, and increases aqueous diuresis. In the kidney, apelin increases diuresis by increasing the renal microcirculation and by counteracting the antidiuretic effect of AVP at the tubular level. Moreover, after water deprivation or salt loading, in humans and in rodents, AVP and apelin are conversely regulated to facilitate systemic AVP release and to avoid additional water loss from the kidney. Furthermore, apelin and vasopressin secretion are significantly altered in various water metabolism disorders including hyponatremia and polyuria-polydipsia syndrome. Since the *in vivo* half-life of apelin is in the minute range, metabolically stable apelin analogs were developed. The efficacy of these lead compounds for decreasing AVP release and increasing both renal blood flow and diuresis, make them promising candidates for the treatment of water retention and/or hyponatremic disorders.

Keywords: apelin, vasopressin, apelin receptor, metabolically stable apelin analogs, G protein-coupled receptor, diuresis, osmolality, apelin water metabolism disorders

DISCOVERY

The apelin story began in 1993 with the cloning of the cDNA for the APJ receptor putative receptor protein related to the angiotensin II receptor type 1 (AT1) from a human genomic library (1). This receptor is a type A G protein-coupled receptor (GPCR) that shares 31% of amino acid sequence identity with the sequence of the human AT1 receptor. The human and the rat APJ receptors are 380 and 377 amino acids long, respectively. Studies have been performed to see if APJ receptor could bind angiotensin peptides due to its close homology with AT1 receptor. Binding experiments with angiotensin peptides were performed on Chinese Hamster Ovary (CHO) cells stably expressing the rat APJ receptor fused to enhanced Green Fluorescent Protein (EGFP). No specific binding for angiotensin II (Ang-II), angiotensin III (Ang-III), or angiotensin IV (Ang-IV) was observed in these cells. Moreover, stimulation of the rat APJ receptor by Ang-II or Ang-III at a concentration of 10^{-7} M did not alter forskolin (FSK)-induced cAMP production, showing no activation of the rat APJ receptor by angiotensin peptides (2). These results showed that APJ receptor was not related to

angiotensin peptides and remained an orphan GPCR for which the endogenous ligand had to be discovered.

In 1998, Tatsumoto et al. isolated the endogenous ligand of the orphan APJ receptor from bovine stomach extracts. They used a Cytosensor microphysiometer to detect the metabolic activation of cells expressing the human APJ receptor through measurement of the extracellular acidification rate (3). This 36-amino acid peptide was called apelin for *APJ Endogenous Ligand*. Following the discovery of apelin, the APJ receptor was renamed the apelin receptor (ApelinR).

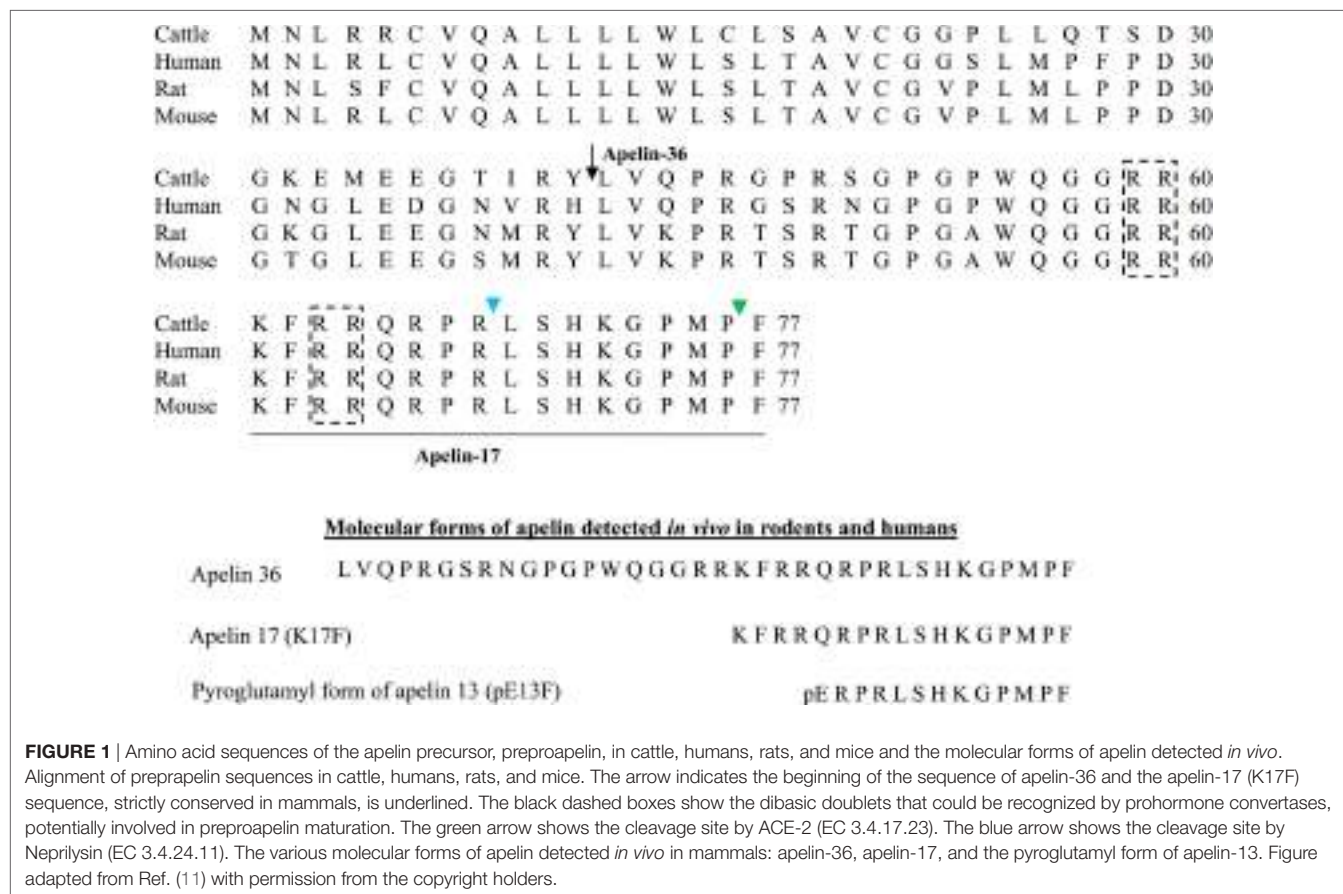
GENE ENCODING/PROCESSING FOR APELIN AND THE ApelinR

Apelin is generated from a 77-amino acid precursor, preproapelin (**Figure 1**). The gene encoding preproapelin is located on chromosome X at locus Xq25-26.1 in human, Xq35 in rat and XA3.2 in mouse (4). The human gene contains three exons, with the coding region spanning exons 1 and 2. The 3' untranslated region also spans two exons (2 and 3) (4). This may account for the presence of two different sizes of transcripts (≈ 3 and ≈ 3.6 kb) in various tissues (4, 5). Alignment of preproapelin amino acid sequences from cattle, humans, rats, and mice shows strict conservation of the C-terminal 17 amino acids (amino acids 61–77 of preproapelin sequence), known as apelin-17 or K17F (**Figure 1**). *In vivo*,

various molecular forms of apelin are present, differing only in length (either 36, 17, or 13 amino acids at the C-terminal part of the precursor) (6–10) (**Figure 1**).

The presence of pairs of basic residues within the cattle, human, rat, and mouse preproapelin sequences suggests that prohormone convertases could be responsible for the processing of the precursor to give birth to K17F and pE13F (pyroglutamyl form of apelin-13: amino acids 65–77 of the preproapelin sequence). More recently, it has been shown *in vitro* that protein convertase subtilisin/kexin 3 (also named furin) may cleave proapelin (amino acids 23–77 of preproapelin sequence) directly into apelin 13 without generating longer isoforms (12). For apelin-36 (amino acids 42–77 of the preproapelin sequence) because of the absence of dibasic motifs upstream the apelin-36 cleavage site, the maturation mechanism remains to be defined. Apelin-36 predominates in rat lung, testis, uterus, and in bovine colostrums, whereas both apelin-36 and pE13F have been detected in the rat mammary gland (6, 8). In rat brain as well as in rat and human plasma, the predominant forms of apelin are pE13F and K17F, whereas the concentration of apelin-36 is much lower (9, 10).

The gene encoding for the ApelinR is intronless in human and rodents and it is located on chromosome 11q12 in human (1), 2E1 in mouse, and 3q24 in rat (2, 5, 6). The human and the rat ApelinRs are 380 and 377 amino acids long, respectively. The ApelinR amino acid sequence is conserved across species, with



more than 90% of homology between human and rodents, and up to 50% of homology with other non-mammalian species such as zebrafish or frog (2, 5, 6, 13). In contrast, Ang-II and apelin-13 do not show much homology; in fact, Ang-II (amino acid sequence: D-R-V-Y-I-H-P-F) only has in common with pE13F (pE-R-P-R-L-S-H-K-G-P-M-P-F) its two C-terminal amino acid residues (P-F). This explains why both peptides are cleaved by the carboxypeptidase, angiotensin-converting enzyme type-2 (ACE-2, EC 3.4.17.23) (14, 15).

METABOLISM OF APELIN PEPTIDES AND PHARMACOLOGICAL CHARACTERIZATION OF THE ApelinR

ACE-2 removes the C-terminal phenylalanine of either apelin-36 K17F or pE13F (14, 15). Finally, it has been recently shown that neutral endopeptidase 24.11 or Neprilysin (EC 3.4.24.11) hydrolyzes the scissile peptide-bond Arg⁸-Leu⁹ of K17F and Arg⁴-Leu⁵ of pE13F leading to two truncated inactive peptides (16).

Apelin peptides exhibit subnanomolar affinities for the ApelinR (17, 18). Alascan studies of pE13F showed that Arg², Arg⁴, Leu⁵ of the RPRL motif of pE13F are key elements for ApelinR binding together with Ser⁶, Lys⁸, and Met¹¹ but with a lesser extent (17). Later structure-function studies by molecular modeling and site-directed mutagenesis demonstrated that Arg², Arg⁴, and Lys⁸ of pE13F interact with residues located at the top of the receptor, Glu¹⁷², Asp²⁸², and Asp⁹², respectively (19).

Several studies have explored the signaling pathways activated by the apelin/ApelinR system. Apelin-36, K17F, apelin-13 (Q13F), and pE13F have been shown to have a similar potency (in the subnanomolar range) to inhibit FSK-induced cAMP production in CHO cells expressing the rat ApelinR and human embryonic kidney (HEK) cells expressing the human ApelinR (2, 7, 17, 20). Hosoya et al. (6) showed that Pertussis toxin was able to inhibit apelin-36 and pE13F responses demonstrating that ApelinR was coupled to Gα_i. This was confirmed by Masri et al. who showed that ApelinR is preferentially coupled to Gα_{i1} and Gα_{i2} protein, which leads to the inhibition of adenylate cyclase and ERK1/2 phosphorylation but was not coupled to Gα_{i3} protein (21, 22).

Apelin-36, K17F, and pE13F have also been shown to increase [Ca²⁺]_i mobilization in Ntera 2 human teratocarcinoma (NT2N) cells, which differentiate into postmitotic neurons following retinoic acid stimulation and also in cells derived from basophils (RBL-2H3) or HEK 293 cells stably expressing human ApelinR (17, 23–25). However, the mechanisms underlying this production of calcium remain unknown. Moreover, Hus-Citharel et al. (26) showed that K17F decreases Ang-II-induced [Ca²⁺]_i mobilization in glomerular arterioles in a nitric oxide (NO)-dependent manner. Interestingly, several studies have shown that the stimulation of ApelinR by apelin induces vasodilation and modulates vascular tone through NO production (22–24, 27, 28). Furthermore, several kinases have been reported to be activated following apelin-induced ApelinR activation. Among these, the extracellular-regulated kinases (ERKs) are phosphorylated in CHO cells stably expressing the mouse ApelinR in a Gα_i-protein-dependent, protein kinase C (PKC)-dependent,

and Ras-independent manner (21, 29). Apelin also stimulates phosphorylation of S6 ribosomal protein kinase (p70S6K) in human umbilical vein endothelial cells (HUVECs) and in CHO cells expressing the mouse ApelinR via two distinct signaling pathways—the phosphatidylinositol 3-kinase (PI3K)/Akt pathway and the ERK1/2 pathway (29, 30). Later on, D'Aniello et al. (31) have shown that apelin induces phosphorylation of p70S6 kinase in murine embryonic stem cells via an ERK1/2-dependent pathway.

Finally, as for most GPCRs, rat and human ApelinRs internalize upon the action of agonist ligands such as apelin-36, K17F, and pE13F (17, 18, 20, 25, 32). However, K17F is 30 times more potent in inducing rat ApelinR internalization when compared to pE13F (33). Deletion of the C-terminal Phe of K17F (K16P) or its substitution by an alanine (K17A) strongly decreases the ability of the peptide to trigger ApelinR internalization without effect on its affinity for the ApelinR or its ability to activate Gα_i-coupling (18, 20). This suggested that the C-terminal Phe of K17F or pE13F is a key residue to trigger ApelinR internalization (20). These results were supported by structure-function studies combining molecular modeling and site-directed mutagenesis of the ApelinR.

Docking of K17F into the three homology three-dimensional (3D) model of the ApelinR using the validated cholecystokinin receptor-1 3D model as a template revealed the presence at the bottom of the binding site of a hydrophobic cavity in which the C-terminal Phe of pE13F was embedded by Trp¹⁵² in TMIV and Trp²⁵⁹ and Phe²⁵⁵ in TMVI (18) (Figure 2). Using site-directed mutagenesis, Phe²⁵⁵ and Trp²⁵⁹ were shown to be crucial for

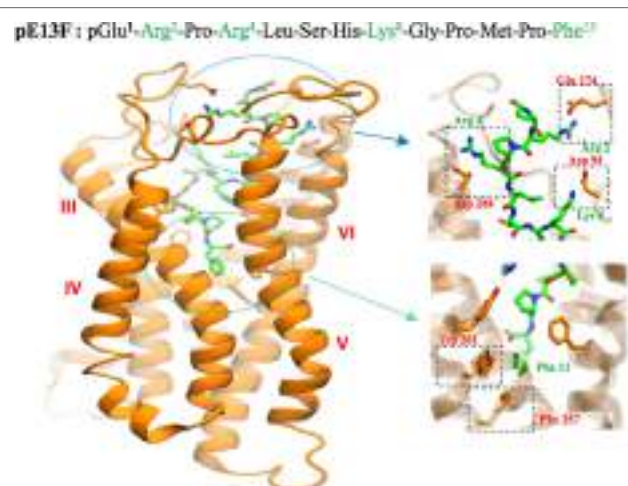


FIGURE 2 | Representation of the human ApelinR three-dimensional model complexed with pE13F. The peptide backbone of the ApelinR is in orange while pE13F is in green. The blue dashed circle shows a detailed view of the binding site of pE13F with interactions (square dashed boxes) between basic residues of pE13F (Arg², Arg⁴, and Lys⁸, in green) and acidic residues of ApelinR (Asp⁹⁴, Glu¹⁷⁴, and Asp²⁸⁴, in orange). The green dashed circle shows a detailed view of the hydrophobic cavity within ApelinR in which the C-terminal Phe of pE13F (Phe¹³, in green) interacts with aromatic residues of ApelinR (Phe²⁵⁷ and Trp²⁶¹, in orange). Figure adapted from Ref. (19) with permission from the copyright holders.

ApelinR internalization without playing a role in apelin binding or $\text{G}\alpha_i$ -protein coupling, by interacting with the C-terminal Phe of pE13F.

All these data indicate functional dissociation between ApelinR G_i -coupling and receptor internalization. This implies that the ApelinR exists in different active conformations depending on the ligand fitting into the binding site leading to the activation of different signaling pathways and subsequent different biological effects (18). Altogether, this suggests that ApelinR may exhibit “functional selectivity” or “biased signaling” by, on one hand, coupling with G protein and on the other hand by recruiting β -arrestins 1 and 2 (34). This hypothesis has been confirmed by Ceraudo et al. (34) who have shown that K17F activates ERK1/2 in a β -arrestin-dependent and G_i protein-dependent manner whereas K16P only activates G_i protein. This functional selectivity of apelin peptides indicates that the β -arrestin-dependent ERK1/2 activation and not the G_i -dependent signaling may participate in K17F-induced BP decrease. Indeed, when pE13A and K16P are injected intravenously in rats, they lost their capacity to decrease arterial blood pressure (BP) when compared with the corresponding natural peptides pE13F and K17F (20, 35).

The characterization of the internalization pattern of the ApelinR induced by apelin-36 or pE13F demonstrates that the internalized ApelinR/pE13F complex is rapidly recycled to the cell surface *via* a Rab4 pathway. The internalized ApelinR/apelin-36 complex is targeted to lysosomes through a Rab7 pathway. Both of these pathways are linked to β -arrestin 1 association with differences in spatio-temporal association (36). These differences are in agreement with studies showing that apelin-36 leads to a strong and sustained desensitization whereas the pE13F-induced desensitization is transient (21). Therefore, subtle differences exist between the apelin isoforms regarding their pharmacological properties, which may influence their physiological actions.

As numerous GPCRs, ApelinR may also form heterodimers *in vitro* with other GPCRs. ApelinR has been shown to dimerize with AT1, leading to an inhibition of Ang-II signaling by apelin (37–39). ApelinR may also heterodimerize with κ -opioid receptor, leading to an increase in cell proliferation through an increase of PKC and a decrease of protein kinase A (PKA) activity (40). In HUVEC cells, ApelinR has been shown to heterodimerize with bradykinin type 1 receptor, leading to an increase in cell proliferation and in phosphorylation of eNOs through a G_q protein-dependent PKC signaling pathway (41).

DEVELOPMENT OF METABOLICALLY STABLE APELIN ANALOGS

The *in vivo* transient effects of apelin fragments suggested that endogenous apelin peptides have a short half-life. In addition, Gerbier et al. (33) showed that K17F and pE13F have a half-life in mouse plasma of 4.6 and 7.2 min, respectively, and Murza et al. (42) showed that pE13F has a 14 min half-life in rat plasma. Regarding apelin-36, Japp et al. (43) suggested from experiments conducted in healthy human subjects that the half-life of apelin 36 is lower than 5 min. This short half-life could be attributed to the action of metabolic enzymes including exo- and endo-peptidases.

The short *in vivo* half-life of apelin encouraged the development of metabolically stable apelin analogs for potential therapeutic applications.

Numerous technologies, such as PEGylation (44, 45), palmytoylation (46) conjugation to albumin, N-terminal acetylation (33), C-terminal amidation (47), use of unnatural amino acids (15, 33, 42, 48), or main chain modifications (cyclization) (49–51) have now been set up to increase the *in vivo* plasma half-life of peptides (52). **Table 1** summarizes the pharmacological characteristics of the main metabolically stable apelin analogs described in this section.

Most studies that aim to develop apelin analogs have focused on pE13F (15, 42, 46, 48, 50, 51, 53) or apelin-36 (44, 45); however, K17F, which had an affinity 10 times higher than that of pE13F for human ApelinR, was 10 times more efficient at inducing internalization of rat ApelinR and also decreased arterial BP more strongly than did pE13F (20).

Given these findings, metabolically stable K17F analogs were recently developed (15, 33). For this purpose, each amino acid of the sequence of K17F, which includes that of pE13F, was replaced with its D-isomer or with an unnatural amino acid. It was found in agreement with previous alanine scanning pE13F studies (17, 54) that replacement of the Arg², Arg⁴, Ser⁶, Lys⁸, and Gly⁹ residues of pE13F with corresponding D-amino acids greatly decreased the ability of these compounds to bind to ApelinR or to inhibit FSK-induced cAMP production. Thus, combination of acetylation of Lys¹ and the introduction of D-Arg³ and D-Gln⁵, D-Leu⁹, Aib¹¹, D-Ala¹³, Nle¹⁵, and 4Br-Phe¹⁷ in K17F, generating P92, which had an affinity of 0.09 nM for the ApelinR, similar to that of K17F (0.06 nM). On the other hand, an original strategy for improving the protection of endogenous peptides against enzymatic degradation on the basis of the introduction of a fluorocarbon chain (FC) directly into the N-terminal part of K17F was used to generate LIT01-196. The presence of the FC on the apelin peptide had no impact on the affinity of LIT01-196 for ApelinR ($K_i = 0.08$ nM), or on its solubility in water (>10 mM).

Altogether these chemical modifications allowed to extend the plasma half-lives of P92 by a factor of 6–11 and that of LIT01-196 by a factor of >100 relative to that of K17F. LIT01-196 displayed remarkable resistance to degradation by plasma enzymes, as >90% of the peptide remained unchanged after 24 h of incubation at 37°C. FC acylation of an endogenous peptide therefore seems to be an efficient way to extend its half-life in plasma.

P92 and LIT01-196 displayed full agonist activity for cAMP production, ERK1/2 phosphorylation (nanomolar range), induction of ApelinR internalization (subnanomolar range), and β -arrestin recruitment (33).

PHYSIOLOGICAL EFFECTS OF APELIN

Distribution of Apelin and Its Receptor Brain

RT-PCR (8, 17), *in situ* hybridization (55) and *Northern blot* (4, 5) studies have shown that mRNAs coding for preproapelin and the ApelinR were distributed heterogeneously in different brain structures. The distribution of apelinergic neurons in the

TABLE 1 | Metabolically stable apelin analogs.

	Reference	Affinity (K_i , nM)	cAMP production inhibition (IC_{50} , nM)	Half-life in plasma ^a (min)
Apelin-13				
pE-R-P-R-L-S-H-K-G-P-M-P-F (pE13F)	(33)	0.56 ± 0.07	1.68 ± 0.47	7.2
E-R-P-R-L-S-H-K-G-P-Nle-P-2Nal	(48)	1.2 ± 0.1	20.5 ± 6	<120
E-R-P-R-L-S-H-K-G-P-Nle-P-4Br(F)	(48)	1.2 ± 0.1	12.4 ± 3	<60
E-R-P-R-L-S-H-K-G-P-Nle-Aib-F	(48)	1.8 ± 0.2	20.9 ± 7	<60
pE-R-P-R-L-S-H-K-G-P-Nle-P-Bpa	(42, 53)	0.38 ± 0.04	0.04 ± 0.02	55
pE-R-P-R-L-S-H-K-G-P-Nle-P-Y(O)Bn	(42, 53)	0.016 ± 0.002	0.35 ± 0.09	66
pE-R-P-R-L-S-H-K-G-P-Nle-P-F(L-αCH3)	(42, 53)	0.34 ± 0.02	0.07 ± 0.02	>120
Cyclo(1-6)C-R-P-R-L-C-H-K-G-P-M-P	(50)	300	2.7 ± 0.8	ND
Palmitoyl-E-R-P-R-L-S-H-K-G-P-Nle-Aib-F	(46)	ND	21.6 ± 4.5	1,740
Cyclo(7-11)pE-R-P-R-L-S-AllyG-K-G-P-AllyG-P-Y(O)Bn	(51)	1.7 ± 0.25	35 ± 11	ND
Ac-E-R-P-R-(D)-S-Aib-K-(D)A-P-Nle-P-4Br(F)	(33)	2.11 ± 0.40	2.22 ± 1.00	86
pE-R-P-R-L-S-H-K-G-P-Nle-Aib-Br(F)	(15)	ND	ND	>60
Apelin-17				
K-F-R-R-Q-R-P-R-L-S-H-K-G-P-M-P-F (K17F)	(33)	0.06 ± 0.01	0.30 ± 0.10	4.6
Ac-K-F-(D)R-R-(D)Q-R-P-R-(D)L-S-Aib-K-(D)A-P-Nle-P-4Br(F) (P92)	(33)	0.09 ± 0.02	0.56 ± 0.32	24
CF3((CF2)7(CH2)2C(O)-K-F-R-R-Q-R-P-R-L-S-H-K-G-P-M-P-F (LIT01-196)	(33)	0.08 ± 0.01	1.71 ± 0.28	>1,440
K-F-R-R-Q-R-P-R-L-S-H-K-G-P-Nle-Aib-Br(F)	(15)	ND	ND	30
Apelin-36				
L-V-Q-P-R-G-S-R-N-G-P-G-P-W-Q-G-G-R-	(6, 7, 43)	4.8 ± 0.24	0.52	<5^b
R-K-F-R-R-Q-R-P-R-L-S-H-K-G-P-M-P-F				
40 kDa-PEG-Apelin-36	(44)	0.3	1.5	ND
Apelin-36-[L28C(30 kDa-PEG)]	(45)	ND	3,050 ± 2,100	ND

^aEx vivo plasma half-life (unless otherwise specified).^bIn vivo plasma half-life.

ND, not determined; G, glycine; AllyG, allylglycine; P, proline; A, alanine; V, valine; L, leucine; I, isoleucine; M, methionine; C, cysteine; F, phenylalanine; Y, tyrosine; W, tryptophan; H, histidine; K, lysine; R, arginine; Q, glutamine; N, asparagine; E, glutamic acid; D, aspartic acid; S, serine; T, threonine; Aib, aminoisobutyric acid; Y(O)Bn, tyrosine(O)benzyl; Bpa, benzylphenyl; Nle, norleucine; 2Nal, naphtalen-2-yl-propanoic acid; 4Br(F), 4-bromo-phenylalanine; PEG, polyethyleneglycol.

In bold and italic characters: native apelin peptides.

In bold characters: name of the analog as it is referred in the article.

adult rat brain has been studied using a polyclonal antibody with a high affinity and selectivity for K17F, which also recognizes pE13F and apelin-36 (9, 32, 56). Apelin-immunoreactive (IR) neuronal cell bodies are abundant in brain structures that are involved in neuroendocrine control, food intake, drinking behavior, and regulation of BP, such as the hypothalamus and the medulla oblongata. They are particularly present in the supraoptic nucleus (SON), the magnocellular part of the paraventricular nucleus (PVN), the arcuate nucleus, the nucleus ambiguus, and the lateral reticular nucleus (56). Conversely, apelin-IR nerve fibers and nerve endings are more widely distributed in the brain: a high density was observed in the inner layer of the median eminence and in the posterior pituitary (32, 57). This suggests that, similarly to magnocellular vasopressinergic and oxytocinergic neurons, the apelinergic neurons of the PVN and the SON project into the posterior pituitary. This hypothesis was verified using double immunofluorescence staining showing that apelin was colocalized with arginine vasopressin (AVP) (9, 58) and oxytocin (57, 59) in magnocellular neurons. Apelin-IR cell bodies and fibers were also identified along the lamina terminalis, which is located in a region along the third ventricle and contains the subfornical organ (SFO), the organum vasculosum of the lamina terminalis (OVLT), and the median preoptic nucleus, which are involved in the control of drinking behavior (60, 61). The SFO and the OVLT, which contain fenestrated capillaries and no blood–brain barrier, constitute a link between peripheral

events such as severe dehydration or hypovolemia and adaptive brain responses such as water intake or AVP release. **Figure 3A** shows the neuroanatomical distribution of apelin-IR cell bodies and nerve fibers on a parasagittal section of adult colchicine-treated rat brain.

The ApelinR is also widely distributed in the rat central nervous system **Figure 3B** (2, 4, 5). ApelinR mRNA has been identified using *in situ* hybridization in the piriform and the entorinal cortices, the hippocampus and in the pars compacta of the substantia nigra, the dorsal raphe nucleus and the locus coeruleus, which contain the monoaminergic neuronal cell bodies. The level of expression of ApelinR mRNA is high in the hypothalamic nuclei, including the SON and the PVN, the arcuate nucleus, the pineal gland, and the anterior and intermediate lobes of the pituitary gland (2). Moreover, double labeling studies combining *in situ* hybridization and immunohistochemistry have shown that, in the SON and PVN, mRNAs coding for the ApelinR (32, 62) as well as AVP receptors type 1a (V1a) and 1b (V1b), but not type 2 (V2R) (63), are coexpressed by magnocellular AVP neurons. This strongly strengthens the existence of an interaction between AVP and apelin.

Kidney

RT-PCR studies have shown that mRNA coding for preproapelin, as well as for ApelinR, is expressed in rat and human kidney (5, 17). Apelin-like immunoreactivity was also detected in human

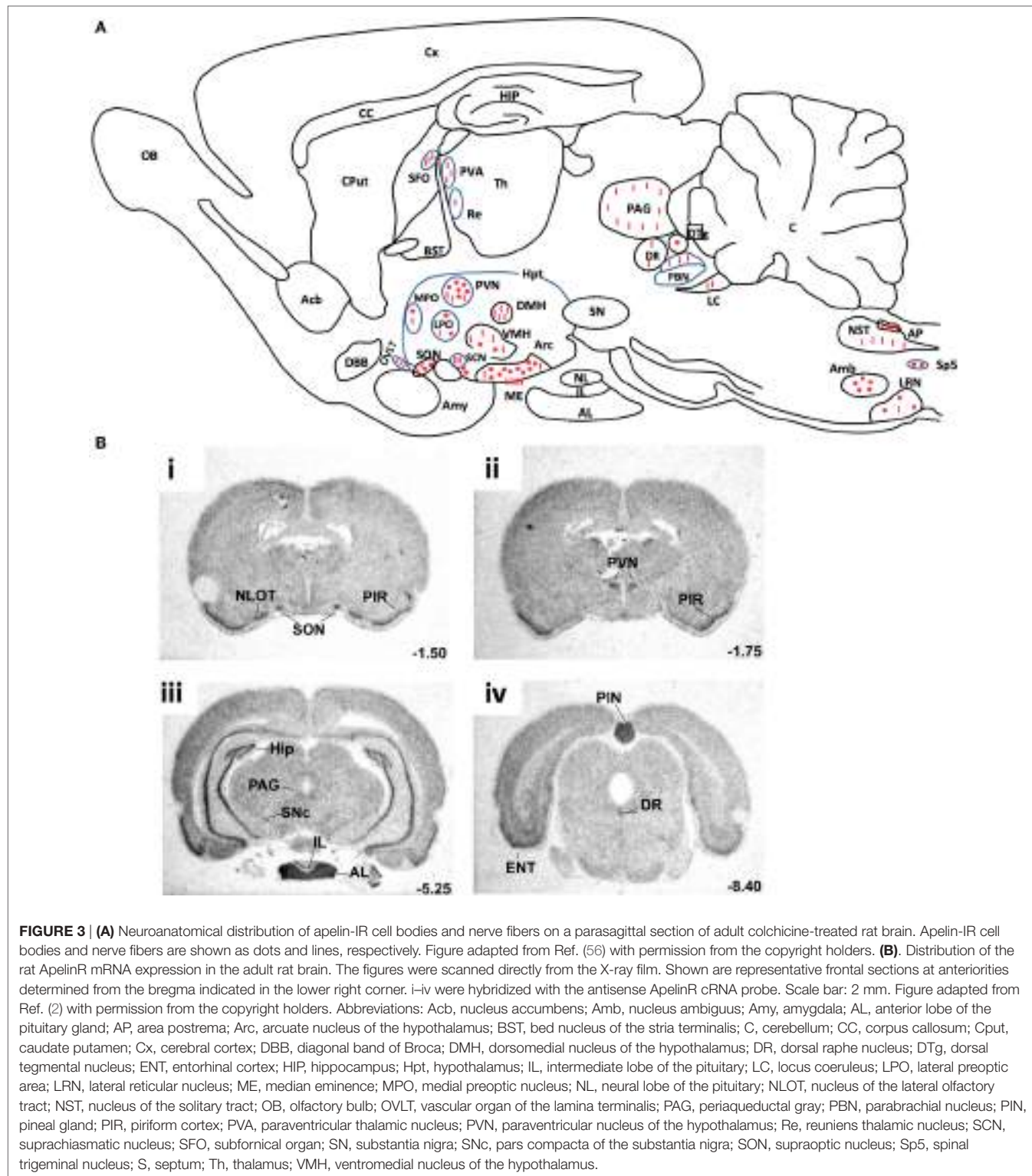


FIGURE 3 | (A) Neuroanatomical distribution of apelin-IR cell bodies and nerve fibers on a parasagittal section of adult colchicine-treated rat brain. Apelin-IR cell bodies and nerve fibers are shown as dots and lines, respectively. Figure adapted from Ref. (56) with permission from the copyright holders. **(B)**. Distribution of the rat ApelinR mRNA expression in the adult rat brain. The figures were scanned directly from the X-ray film. Shown are representative frontal sections at anteriorities determined from the bregma indicated in the lower right corner. i–iv were hybridized with the antisense ApelinR cRNA probe. Scale bar: 2 mm. Figure adapted from Ref. (2) with permission from the copyright holders. Abbreviations: Acb, nucleus accumbens; Amb, nucleus ambiguus; Amy, amygdala; AL, anterior lobe of the pituitary gland; AP, area postrema; Arc, arcuate nucleus of the hypothalamus; BST, bed nucleus of the stria terminalis; C, cerebellum; CC, corpus callosum; Cput, caudate putamen; Cx, cerebral cortex; DBB, diagonal band of Broca; DMH, dorsomedial nucleus of the hypothalamus; DR, dorsal raphe nucleus; DTg, dorsal tegmental nucleus; ENT, entorhinal cortex; HIP, hippocampus; Hpt, hypothalamus; IL, intermediate lobe of the pituitary; LC, locus coeruleus; LPO, lateral preoptic area; LRN, lateral reticular nucleus; ME, median eminence; MPO, medial preoptic nucleus; NL, neural lobe of the pituitary; NLOT, nucleus of the lateral olfactory tract; NST, nucleus of the solitary tract; OB, olfactory bulb; OVLT, vascular organ of the lamina terminalis; PAG, periaqueductal gray; PBN, parabrachial nucleus; PIN, pineal gland; PIR, piriform cortex; PVA, paraventricular thalamic nucleus; PVN, paraventricular nucleus of the hypothalamus; Re, reunions thalamic nucleus; SCN, suprachiasmatic nucleus; SFO, subfornical organ; SN, substantia nigra; SNC, pars compacta of the substantia nigra; SON, supraoptic nucleus; Sp5, spinal trigeminal nucleus; S, septum; Th, thalamus; VMH, ventromedial nucleus of the hypothalamus.

endothelial cells obtained from small intrarenal vessels (64). *In situ* hybridization studies in the rat kidney showed that ApelinR mRNA was expressed in the endothelial cells and vascular smooth muscle cells of the rat glomerular arterioles. ApelinR mRNA has also been detected and in all renal zones (26), most abundantly in

the inner stripe (IS) and the outer stripe (OS) of the outer medulla (OM) (26). Furthermore, a high ApelinR mRNA expression was found in glomeruli and moderate in all the nephron segments including the collecting duct (CD) (26) where the V2R are also expressed (65).

Maintenance of Water Balance by Apelin and Vasopressin through Central and Renal Effects

Central Effects of Apelin on AVP Neuronal Activity, AVP Release and Diuresis

Arginine vasopressin, also known as anti-diuretic hormone, is a peptide that has antidiuretic and vasoconstricting effects. It is synthesized and released by hypothalamic magnocellular AVP neurons in the blood circulation from the fenestrated capillaries of the posterior pituitary in response to variations in plasma osmolality and volemia (66, 67) or under the influence of neurohormones including natriuretic and angiotensin peptides (68, 69). The colocalization of AVP, apelin, V₁, and ApelinR in magnocellular neurons suggests an interaction between apelin and AVP. This raises the possibility of an effect of apelin in response to osmotic or volemic stimuli. It has been hypothesized that independently from the feedback control exerted by AVP on its own release (69, 70), apelin may regulate AVP release. This hypothesis was checked in two animal models. First, the lactating rat, which exhibits an increase in the activity of magnocellular AVP neurons,

leading to an increase in AVP synthesis and release in order to preserve water of the organism for maximal milk production (71, 72). In this model, the intracerebroventricular (i.c.v.) administration of apelin (K17F) (9) induces an inhibition of the phasic electrical activity of AVP neurons, reduces the release of AVP in the bloodstream and increases diuresis, without changes in sodium and potassium excretion (Figure 4). Second, in mice deprived of water for 24/48 h, a condition known to increase AVP neuron activity and systemic AVP release (73, 74), i.c.v. administration of K17F induced a significant decrease in systemic AVP release. These results suggest that apelin is probably released from the SON and PVN AVP cell bodies and inhibits AVP neuron activity and release through a direct action on the apelin autoreceptors expressed by AVP/apelin-containing neurons. This mechanism probably involves apelin acting as a natural inhibitor of the antidiuretic effect of AVP.

Effects of Apelin and Vasopressin on the Maintenance of Water Balance at the Kidney Level

In addition to a central action, the aquaretic effect of apelin probably involves a renal action because of the expression of ApelinR

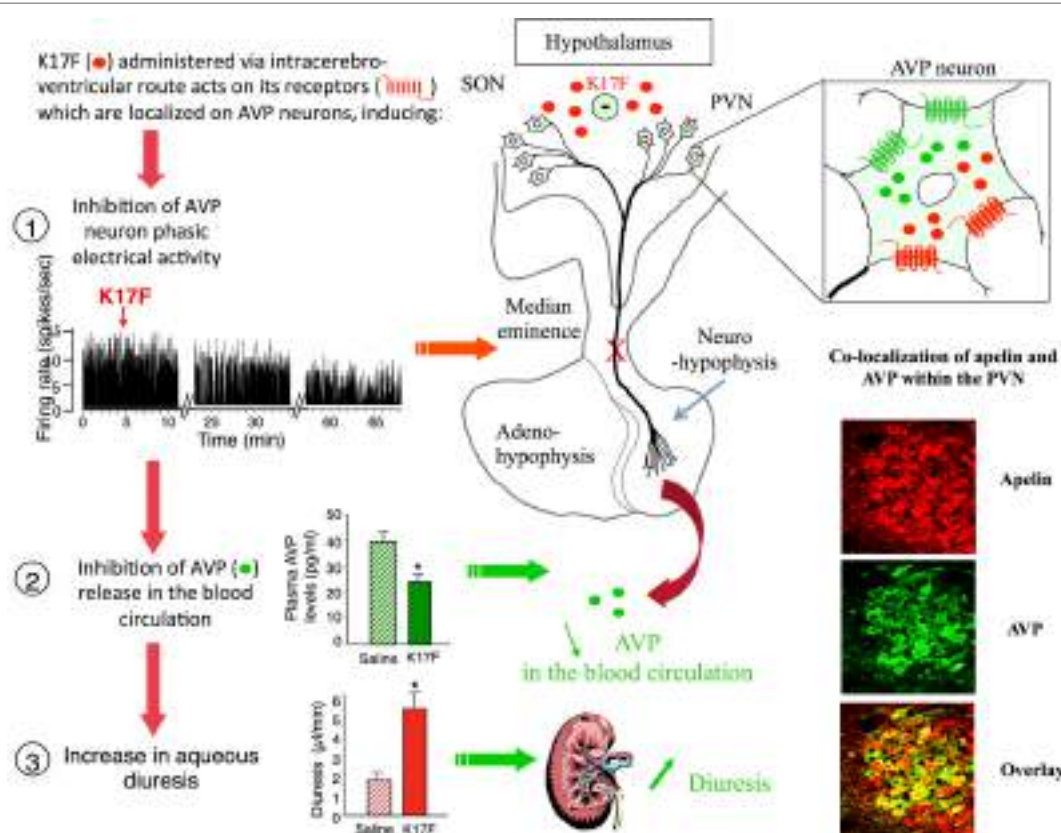


FIGURE 4 | Central action of apelin on vasopressinergic neuron activity. Apelin and its receptor (ApelinR, red) are colocalized in magnocellular vasopressinergic neurons of the supraoptic nucleus and paraventricular nucleus (PVN), with arginine vasopressin (AVP) and vasopressin receptor type 1 (green). In lactating rats, i.c.v. injection of apelin 17 (K17F) inhibits the phasic electrical activity of AVP magnocellular neurons, leading to a decrease in AVP release in the bloodstream and an increase in aqueous diuresis. On the right of the figure are represented confocal images illustrating the distribution of apelin and AVP IR cell bodies within the rat PVN. A high colocalization of apelin (red) and AVP (green) has been detected in PVN magnocellular neurons. Dually labeled cells stand out in yellow when images are merged. Figure adapted from Ref. (11, 58) with permission from the copyright holders.

and preproapelin, as well as apelin immunoreactivity in the kidney (5, 17, 64). ApelinR mRNA has been detected in all renal zones, most abundantly in the IS of the OM (26). A high level of expression was also detected in the glomeruli and a moderate expression was observed in all nephron segments, especially in CD that express V2R. In agreement with the presence of ApelinR mRNA in juxtamedullary efferent (EA) and afferent (AA) arterioles, application on glomerular arterioles precontracted by Ang-II of K17F, induced NO-dependent vasorelaxation by inhibiting the Ang-II induced rise in intracellular calcium mobilization (26). The apelin-dependent vasorelaxation observed in muscular EA, which gives rise to vasa recta, therefore strongly supports a key role of apelin in the control of renal medullary circulation (26).

On the other hand, it is well known that AVP by stimulating V2R in CD induces an increase in cAMP production and activates PKA which phosphorylates aquaporin type 2 (AQP2). This results in the insertion of AQP2 at the apical membrane of the principal cells of the CD (75, 76), leading to water reabsorption, decreasing diuresis, and plasma osmolality. The expression of ApelinR mRNA in the CD suggests that apelin could act as an aquuretic peptide through a direct action on this nephron segment. In agreement with this hypothesis, application of K17F on medullary CD inhibits cAMP production induced by dDAVP (a specific and selective V2R agonist) and decreased the dDAVP-induced calcium influx in CD cells (77). Finally, intravenous injection of K17F in increasing doses in lactating rats increases diuresis in a dose-dependent manner concomitantly with a significant decrease in urine osmolality and a decrease in AQP2 insertion at the apical membrane of CD (77), showing that K17F-induced diuresis is linked to a direct action of apelin on CD. Similarly, in other studies (78, 79), acute or chronic intravenous treatment with apelin-13 potently increased diuresis in male Sprague-Dawley rats.

Thus, the aquuretic effect of apelin is not only due to a central effect by inhibiting AVP release in the blood circulation but also to a direct action of apelin at the kidney level by increasing renal blood flow and counteracting the antidiuretic effect of AVP occurring via V2R in CD.

These results also show that apelin and AVP have opposite effects on the CD and contribute to control plasma osmolality by regulating the reabsorption of water by the kidney (**Figure 5**).

Recent studies have underlined the role of apelin in controlling fluid homeostasis. As previously reported, water deprivation significantly decreases urine volume and increases urine osmolality in wild-type mice, whereas mice deficient for the ApelinR ($\text{ApelinR}^{-/-}$) were unable to concentrate their urine to the same extent (80, 81). This lack of effect is likely not due to an inability of these mice to increase plasma AVP levels since similar increases in plasma AVP levels are seen in wild-type and $\text{ApelinR}^{-/-}$ mice following water deprivation, suggesting the presence of an intact central vasopressinergic system in $\text{ApelinR}^{-/-}$ mice. These observations have therefore led the authors to suggest that since the defect in water metabolism observed in $\text{ApelinR}^{-/-}$ mice is not due to altered AVP neurosecretory function, it could be due to a defect in urine concentration at the kidney level. These results contrast with other studies published showing an aquuretic role of apelin in rodents. A possible explanation for this discrepancy

is that in knock-out models, the total absence of ApelinRs during fetal and adult life could elicit compensatory mechanisms, leading to this opposite effects on urine output observed following an exogenous administration of apelin via i.c.v (9) and i.v. (26, 33, 77–79) routes. In addition, apelin gene expression in the brain has been also reported as a hydration-sensitive gene expression (82).

Effects of the Metabolically Stable Apelin Analogs, P92 and LIT01-196, at the Central and Kidney Levels

Central administration of P92 and LIT01-196 decreases dehydration-induced systemic AVP release in a dose-dependent manner and they are 6 and 160 times, respectively, more effective than K17F (33). These data suggest that P92 and LIT01-196, like K17F, rapidly reach the hypothalamic structures that are involved in AVP release from the posterior pituitary into the bloodstream after i.c.v. injection. They subsequently act on ApelinR expressed by AVP neurons to inhibit their phasic electrical activity, thereby preventing AVP release into the bloodstream. Furthermore, intravenous administration of P92 and LIT01-196 in anesthetized rats, at a dose in the nmol/kg range, potently increased urine output. In parallel, P92 and LIT01-196-induced vasorelaxation of rat glomerular arterioles, respectively, precontracted with Ang-II (33). This strongly suggests that these apelin analogs can act like K17F to increase medullary blood flow (26). Thus, by decreasing AVP release into the bloodstream and by increasing both renal blood flow and urine output, these new compounds should also have an aquuretic effect similar to that previously reported for K17F in lactating rats (9, 26). ApelinR agonists of this type would be particularly useful for the treatment of water retention and hyponatremia, making it possible to avoid the excessive sodium loss that is frequently reported in patients receiving thiazidic or loop diuretics.

Opposite Regulation of Vasopressin and Apelin following Water Deprivation

In Rodents

The colocalization and opposing actions of apelin and AVP on diuresis raise questions concerning how they are regulated to maintain body fluid homeostasis. To this end, the effect of water deprivation on the neuronal content and release of apelin and AVP were studied in rodents, and the effects of different states of hydration on plasma AVP and apelin levels were studied in human volunteers.

Following water deprivation in rodents, AVP is released into the blood circulation faster than it is synthesized, causing a depletion of AVP magnocellular neuronal stores (83). In parallel, water deprivation decreases plasma apelin levels and induces an increase in hypothalamic apelin neuronal content, especially in the PVN and SON AVP magnocellular neurons (9, 58). Following water deprivation, apelin therefore accumulates within AVP neurons rather than being released. This increase in neuronal apelin concentration observed in dehydrated rats is markedly reduced by the i.c.v. administration of a selective V1 receptor antagonist whereas the i.c.v. infusion of AVP has similar effects to dehydration on neuronal apelin content (58).

The apelin response to dehydration is therefore opposite to that of AVP (9, 83). These results imply that AVP and apelin are

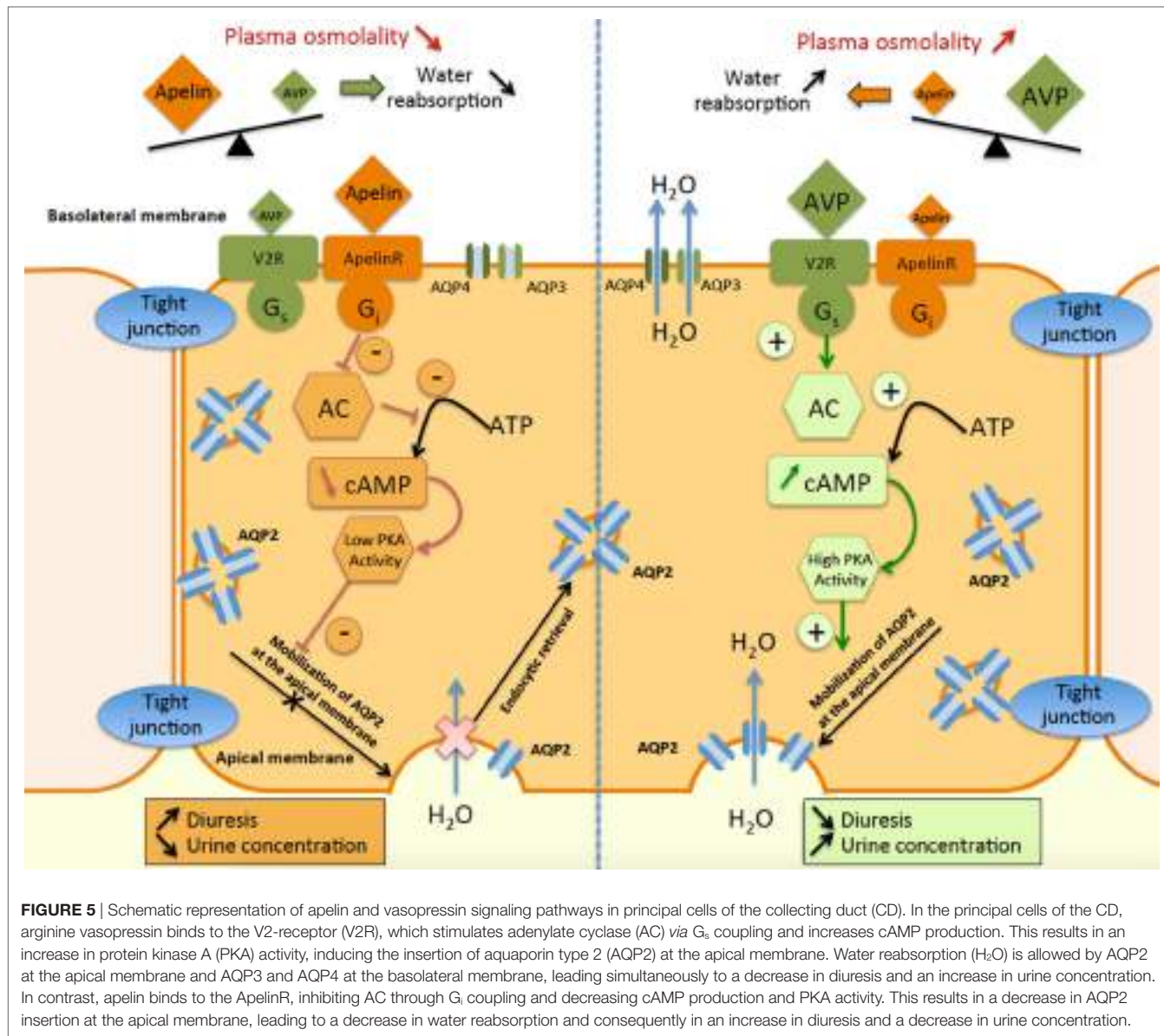


FIGURE 5 | Schematic representation of apelin and vasopressin signaling pathways in principal cells of the collecting duct (CD). In the principal cells of the CD, arginine vasopressin binds to the V2-receptor (V2R), which stimulates adenylate cyclase (AC) via G_s coupling and increases cAMP production. This results in an increase in protein kinase A (PKA) activity, inducing the insertion of aquaporin type 2 (AQP2) at the apical membrane. Water reabsorption (H₂O) is allowed by AQP2 at the apical membrane and AQP3 and AQP4 at the basolateral membrane, leading simultaneously to a decrease in diuresis and an increase in urine concentration. In contrast, apelin binds to the ApelinR, inhibiting AC through G_i coupling and decreasing cAMP production and PKA activity. This results in a decrease in AQP2 insertion at the apical membrane, leading to a decrease in water reabsorption and consequently in an increase in diuresis and a decrease in urine concentration.

released separately by the AVP magnocellular neurons in which they are produced. In agreement with this hypothesis, double immunolabeling confocal microscopy studies show that a large proportion of apelin immunoreactivity colocalizes with AVP in magnocellular neurons in the SON and the PVN (Figure 4), although each peptide is found within distinct subcellular compartments (9, 58).

These *in vivo* animal studies show that the cross-regulation of apelin and AVP following osmotic stimuli has a physiologic purpose, allowing the maintenance of the organism water balance by preventing water excretion by the kidney after water deprivation.

In Humans

Such cross-regulation of apelin and AVP following osmotic stimuli has also been studied in humans. The relationship between

osmolality, apelin, and AVP in the plasma was investigated in healthy men (10) following 2 h of hypertonic saline infusion to increase plasma osmolality or 30 min of oral water loading to decrease plasma osmolality.

Increased plasma osmolality simultaneously raised plasma AVP levels and decreased plasma apelin levels. Conversely, decreased plasma osmolality reduced plasma AVP levels and rapidly increased plasma apelin levels (10). These observations are consistent with plasma osmolality being a major physiologic regulator of plasma apelin levels in humans. Furthermore, the inverse relationship between the regulation of apelin and AVP is consistent with the findings in animal models following water deprivation. This strongly suggests that, like AVP, apelin helps to maintain body fluid homeostasis in humans and rodents.

Effects of Aging on the Cross Regulation of Apelin and Vasopressin

It has been shown in humans that elderly have a higher risk of dehydration, due to lower levels of water intake and excessive water loss (84, 85). Both apelin and AVP contribute to maintain water homeostasis, and their regulation has therefore been investigated during aging.

Aging has been associated with an increase in the size of the magnocellular AVP neuron cell bodies (86), nucleoli (87), and Golgi apparatus (88, 89) in aged humans, and numerous studies have shown higher plasma AVP levels in aged rodents (90–93). In a recent study conducted in adult (3 weeks of age) or aged (22 weeks of age) male Wistar rats (94), intracellular AVP mRNA levels in the SON were lower in aged rats whereas intracellular apelin mRNA levels in the SON were higher. The authors then investigated the effect of dehydration on plasma AVP and apelin levels and showed an impaired response to dehydration of aged rats on both plasma AVP levels, which did not increase significantly after dehydration in aged rats, as well as on plasma apelin levels, which did not decrease significantly after dehydration as previously shown in adult rats (9).

Thus, there may be an absence of additional up- and down-regulation of AVP and apelin in response to a sustained osmotic challenge, as the neuronal system may already be functioning at maximal capacity. Microglial inflammation and overproduction of interleukins have been proposed to contribute to the observed modifications of central apelin and AVP responses to osmotic changes in aged rats. The age-dependent impairment of the AVP/apelin response after an osmotic challenge could explain the poor tolerance of older patients to dehydration, although these results are yet to be confirmed in clinical studies involving elderly.

Apelin and Vasopressin Balance in Different Pathologies

Hyponatremia

Hyponatremia, defined by a plasma sodium concentration below 135 mmol/l, is a common metabolic disorder associated with an increased risk in mortality in hospitalized patients. It is usually secondary to free water retention rather than insufficient sodium intake. Various conditions have been associated with hyponatremia, including drug adverse events (diuretics, antidepressants), chronic heart failure (CHF), chronic liver disease, and the syndrome of inappropriate antidiuretic hormone secretion (SIADH). Copeptin corresponds to the C-terminal part of the AVP precursor and is composed of 77 amino acids. Copeptin is released mole to mole with AVP from the posterior pituitary in the blood circulation and plasma copeptin levels are used as a surrogate marker for AVP release in humans (95, 96). Copeptin measurement alone has proven useful in hyponatremic disorders to differentiate patients with primary polydipsia (PP), who have low copeptin plasma concentration and low urine osmolality, from other causes of hyponatremia such as SIADH, but do not allow to differentiate SIADH from other causes hyponatremic disorders such as diuretic-induced

hyponatremia, hypovolemic hyponatremia, and hypervolemic hyponatremia (97).

Syndrome of Inappropriate Antidiuretic Hormone (SIADH)

In SIADH, abnormal AVP osmoregulation is the primary defect (98). A recent study showed that copeptin was useful to characterize five different subtypes of SIADH, according to plasma copeptin concentration response to hypertonic saline infusion (99). Since an opposite relationship is observed in healthy subjects between plasma apelin and AVP concentrations following osmotic stimuli, the apelin response to the AVP osmoregulation defect in SIADH was investigated (100). Expected ranges of plasma apelin, copeptin levels, and plasma to copeptin ratio for a given plasma sodium concentration were established in healthy subjects. In patients with SIADH, the sex- and age-adjusted apelin and copeptin levels were higher than in healthy subjects, by 26 and 75%, respectively. However, during an acute osmotic challenge, plasma copeptin levels were higher and plasma apelin levels lower than expected from plasma sodium and the plasma apelin to copeptin ratio decreased exponentially with natremia. Apelin to copeptin ratios as a function of natremia were outside the 95% predicted physiological limits for 86% of SIADH patients.

This study showed that apelin levels and apelin to copeptin ratios were inappropriate to natremia in SIADH patients, suggesting that the increase in plasma apelin secretion cannot compensate for the higher levels of vasopressin release and may contribute to the corresponding water metabolism defect.

Heart Failure

In CHF, the decrease in cardiac output and in effective circulating volume results in activation of baroreceptors. These activate the sympathetic nervous system, the renin-angiotensin-aldosterone system, and the release of AVP in the bloodstream. The increase in plasma AVP concentration leads to water reabsorption by the kidney (101). Mild to moderate hyponatremia is present in approximately 10% of CHF patients (102). Hyponatremic patients with advanced CHF often exhibit abnormally elevated AVP plasma levels (103), and hyponatremia has been associated with reduced survival and increased complications in CHF (104). Similarly to SIADH, the apelin to copeptin balance was investigated in hyponatremic CHF patients (100). In this study, plasma copeptin levels were increased by 190% compared to healthy subjects in hyponatremic patients. Plasma apelin levels were also slightly increased (by 25%). The plasma apelin to copeptin ratio was lower in CHF patients than in controls, suggesting that the mild increase in apelin secretion could not counteract the major increase in AVP secretion, leading to abnormal water metabolism and hyponatremia (100).

Polyuria-Polydipsia

In response to an increase in plasma osmolality, i.e. in case of dehydration or of hypertonic saline infusion, it has been shown both in humans and in animals that AVP secretion is increased and apelin secretion is decreased, allowing the reabsorption of water by the kidney. Thirst is also stimulated by the increase

in plasma osmolality. In human pathology, an increase in both fluid intake (polydipsia) and diuresis (hypotonic urine output) is characteristic of the polyuria-polydipsia syndrome (PPS). Three entities are comprised in the PPS: central (complete or partial), diabetes insipidus (DI), nephrogenic (complete or partial) DI, and PP. Central DI (CDI) is secondary to complete or partial brain AVP deficiency mirrored by low plasma copeptin levels. In most cases, thirst perception is intact, resulting in polyuria, polydipsia. Severe hyperosmolality only occurs in case of fluid deprivation. Nephrogenic DI (NDI) is secondary to renal insensitivity to AVP and can be acquired or hereditary, due to mutations of the V2R or of AQP2. PP is not due to a deficiency or resistance of AVP but rather results from an excessive fluid intake over an extended period of time, in the absence of plasma osmolality regulation disorder. PP results from an abnormal thirst mechanism or a psychiatric disorder (105). Plasma copeptin measurement before and after water deprivation can be used to establish the differential diagnosis between each entity with good sensitivity and specificity (106). In order to determine if, similarly to what was observed in hypoosmolar disorders, apelin secretion was also impaired in PPS, the plasma apelin and copeptin levels were measured in PPS patients with complete CDI, complete NDI and PP(107). In patients with NDI, plasma copeptin levels were higher than those measured in healthy volunteers and plasma apelin levels were also increased by 61% compared to control values, probably in an effort of the apelin/AVP system to reestablish the water balance mediated by the two hormones. However, since in NDI AVP is unable to exert its antidiuretic effect at the kidney level, it is likely that only apelin exerts its deleterious effect, which results in polyuria.

In CDI, plasma copeptin levels were decreased by 52% compared to healthy volunteers whereas plasma apelin levels were only decreased by 18%. However, the plasma apelin to copeptin ratio was higher in CDI patients than in healthy volunteers. Possibly, the decrease in plasma apelin levels of patients with CDI is insufficient as compared to the decrease of AVP/copeptin to reestablish a balance between the antidiuretic effect of AVP and the diuretic effect of apelin, resulting in polyuria.

Patients with PP had normal plasma copeptin and slightly but significantly lower plasma apelin levels compared to healthy volunteers. However, the apelin to copeptin ratio was similar to that measured in healthy volunteers. This suggests that the normal apelin to copeptin ratio attests for balanced water homeostasis, whereas plasma apelin to copeptin ratio in CDI or NDI is increased or decreased compared to healthy volunteers, reflecting a disturbed water homeostasis.

Another interesting explanation is that apelin itself might also be involved directly in the pathogenesis of PP. Indeed, the decrease in plasma apelin levels in PP patients could account for altered drinking behavior (leading to an inadequate fluid intake in these patients) since i.c.v. injection of apelin into water deprived rats decreases drinking behavior (32). Further studies need to be conducted in order to determine if the use of the apelin

to copeptin ratio could be a useful diagnosis tool in hyperosmolar disorders.

CONCLUSION AND PERSPECTIVES

The discovery of apelin as the endogenous ligand of the ApelinR is an important step in basic research and has clinical implications. In animal models, experimental data demonstrate that central injection of apelin into lactating rats inhibits the phasic electrical activity of AVP neurons, reduces plasma AVP levels, and increases aqueous diuresis. In the kidney, apelin increases diuresis by increasing renal blood flow and by counteracting the antidiuretic effect of AVP at the tubular level. Moreover, following water deprivation or salt loading, in humans and in rodents, AVP and apelin are conversely regulated to facilitate systemic AVP release and to avoid additional water loss at the kidney level. These data show that, together with AVP, apelin play a crucial role in the maintenance of body fluid homeostasis. In addition, in SIADH or CHF patients with hyponatremia, the apelin to copeptin balance is altered contributing to the water metabolism defect. The administration of apelin agonists in these patients could induce aqueous diuresis and therefore increase water excretion, reversing hyponatremia.

To date, there are no published preclinical or clinical studies utilizing ApelinR agonists/analogs in pathological animal models or patients with water metabolism disorders. The development of metabolically stable apelin analogs that exert longer-lasting and more potent effects than the endogenous peptide on aqueous diuresis and which additionally could only target the G_i signaling pathway like the endogenous apelin fragment K16P (biased agonist), represent promising candidates for the treatment of water retention/hyponatremic disorders.

AUTHOR NOTES

All appropriate permissions have been obtained from the copyright holders of **Figures 1–4** that were adapted and reproduced for this manuscript.

AUTHOR CONTRIBUTIONS

All authors listed have made substantial, direct, and intellectual contribution to the work and approved it for publication.

FUNDING

These studies were supported by INSERM (through financial support for Proof of Concept, CoPoC, INSERM Transfert, in particular), the Centre National de la Recherche Scientifique, the Université de Strasbourg, the Collège de France, and the Agence Nationale pour la Recherche “Physique et Chimie du Vivant 2009.” AF was supported by a Poste d’Accueil INSERM grant.

REFERENCES

- O'Dowd BF, Heiber M, Chan A, Heng HH, Tsui LC, Kennedy JL, et al. A human gene that shows identity with the gene encoding the angiotensin receptor is located on chromosome 11. *Gene* (1993) 136:355–60. doi:10.1016/0378-1119(93)90495-O
- De Mota N, Lenkei Z, Llorens-Cortès C. Cloning, pharmacological characterization and brain distribution of the rat apelin receptor. *Neuroendocrinology* (2000) 72:400–7. doi:10.1159/000054609
- Tatemoto K, Hosoya M, Habata Y, Fujii R, Kakegawa T, Zou MX, et al. Isolation and characterization of a novel endogenous peptide ligand for the human APJ receptor. *Biochem Biophys Res Commun* (1998) 251:471–6. doi:10.1006/bbrc.1998.9489
- Lee DK, Cheng R, Nguyen T, Fan T, Kariyawasam AP, Liu Y, et al. Characterization of apelin, the ligand for the APJ receptor. *J Neurochem* (2000) 74:34–41. doi:10.1046/j.1471-4159.2000.0740034.x
- O'Carroll AM, Selby TL, Palkovits M, Lolait SJ. Distribution of mRNA encoding B78/apj, the rat homologue of the human APJ receptor, and its endogenous ligand apelin in brain and peripheral tissues. *Biochim Biophys Acta* (2000) 1492:72–80. doi:10.1016/S0167-4781(00)00072-5
- Hosoya M, Kawamata Y, Fukusumi S, Fujii R, Habata Y, Hinuma S, et al. Molecular and functional characteristics of APJ. Tissue distribution of mRNA and interaction with the endogenous ligand apelin. *J Biol Chem* (2000) 275:21061–7. doi:10.1074/jbc.M908417199
- Habata Y, Fujii R, Hosoya M, Fukusumi S, Kawamata Y, Hinuma S, et al. Apelin, the natural ligand of the orphan receptor APJ, is abundantly secreted in the colostrum. *Biochim Biophys Acta* (1999) 1452:25–35. doi:10.1016/S0167-4889(99)00114-7
- Kawamata Y, Habata Y, Fukusumi S, Hosoya M, Fujii R, Hinuma S, et al. Molecular properties of apelin: tissue distribution and receptor binding. *Biochim Biophys Acta* (2001) 1538:162–71. doi:10.1016/S0167-4889(00)00143-9
- De Mota N, Reaux-Le Goazigo A, El Messari S, Chartrel N, Roesch D, Dujardin C, et al. Apelin, a potent diuretic neuropeptide counteracting vasopressin actions through inhibition of vasopressin neuron activity and vasopressin release. *Proc Natl Acad Sci U S A* (2004) 101:10464–9. doi:10.1073/pnas.0403518101
- Azimi M, Iturrioz X, Blanchard A, Peyrard S, De Mota N, Chartrel N, et al. Reciprocal regulation of plasma apelin and vasopressin by osmotic stimuli. *J Am Soc Nephrol* (2008) 19:1015–24. doi:10.1681/ASN.2007070816
- Galanth C, Hus-Citharel A, Li B, Llorens-Cortès C. Apelin in the control of body fluid homeostasis and cardiovascular functions. *Curr Pharm Des* (2012) 18:789–98. doi:10.2174/138161212799277770
- Shin K, Pandey A, Liu X-Q, Anini Y, Rainey JK. Preferential apelin-13 production by the proprotein convertase PCSK3 is implicated in obesity. *FEBS Open Bio* (2013) 3:328–33. doi:10.1016/j.fob.2013.08.001
- Devic E, Rizzotti K, Bodin S, Knibiehler B, Audigier Y. Amino acid sequence and embryonic expression of msr/apj, the mouse homolog of Xenopus X-msr and human APJ. *Mech Dev* (1999) 84:199–203. doi:10.1016/S0925-4773(99)00081-7
- Vickers C, Hales P, Kaushik V, Dick L, Gavin J, Tang J, et al. Hydrolysis of biological peptides by human angiotensin-converting enzyme-related carboxypeptidase. *J Biol Chem* (2002) 277:14838–43. doi:10.1074/jbc.M200581200
- Wang W, McKinnie SMK, Farhan M, Paul M, McDonald T, McLean B, et al. Angiotensin-converting enzyme 2 metabolizes and partially inactivates Pyr-apelin-13 and apelin-17: physiological effects in the cardiovascular system. *Hypertension* (2016) 68:365–77. doi:10.1161/HYPERTENSIONAHA.115.06892
- McKinnie SMK, Fischer C, Tran KMH, Wang W, Mosquera F, Oudit GY, et al. The metalloprotease neprilysin degrades and inactivates apelin peptides. *Chembiochem* (2016) 17:1495–8. doi:10.1002/cbic.201600244
- Medhurst AD, Jennings CA, Robbins MJ, Davis RP, Ellis C, Winborn KY, et al. Pharmacological and immunohistochemical characterization of the APJ receptor and its endogenous ligand apelin. *J Neurochem* (2003) 84:1162–72. doi:10.1046/j.1471-4159.2003.01587.x
- Iturrioz X, Gerbier R, Leroux V, Alvear-Perez R, Maigret B, Llorens-Cortès C. By interacting with the C-terminal Phe of apelin, Phe(255) and Trp(259) in helix VI of the apelin receptor are critical for internalization. *J Biol Chem* (2010) 285:32627–37. doi:10.1074/jbc.M110.127167
- Gerbier R, Leroux V, Couvineau P, Alvear-Perez R, Maigret B, Llorens-Cortès C, et al. New structural insights into the apelin receptor: identification of key residues for apelin binding. *FASEB J* (2015) 29:314–22. doi:10.1096/fj.14-256339
- El Messari S, Iturrioz X, Fassot C, De Mota N, Roesch D, Llorens-Cortès C. Functional dissociation of apelin receptor signaling and endocytosis: implications for the effects of apelin on arterial blood pressure. *J Neurochem* (2004) 90:1290–301. doi:10.1111/j.1471-4159.2004.02591.x
- Masri B, Morin N, Pedebernade L, Knibiehler B, Audigier Y. The apelin receptor is coupled to Gi1 or Gi2 protein and is differentially desensitized by apelin fragments. *J Biol Chem* (2006) 281:18317–26. doi:10.1074/jbc.M600606200
- Bai B, Tang J, Liu H, Chen J, Li Y, Song W. Apelin-13 induces ERK1/2 but not p38 MAPK activation through coupling of the human apelin receptor to the Gi2 pathway. *Acta Biochim Biophys Sin (Shanghai)* (2008) 40:311–8. doi:10.1111/j.1745-7270.2008.00403.x
- Choe W, Albright A, Sulcove J, Jaffer S, Hesselgesser J, Lavi E, et al. Functional expression of the seven-transmembrane HIV-1 co-receptor APJ in neural cells. *J Neurovirol* (2000) 6(Suppl 1):S61–9.
- Zhou N, Fan X, Mukhtar M, Fang J, Patel CA, DuBois GC, et al. Cell-cell fusion and internalization of the CNS-based, HIV-1 co-receptor, APJ. *Virology* (2003) 307:22–36. doi:10.1016/S0042-6822(02)00021-1
- Zhou N, Zhang X, Fan X, Argyris E, Fang J, Acheampong E, et al. The N-terminal domain of APJ, a CNS-based coreceptor for HIV-1, is essential for its receptor function and coreceptor activity. *Virology* (2003) 317:84–94. doi:10.1016/j.virol.2003.08.026
- Hus-Citharel A, Bouby N, Frugiére A, Bodineau L, Gasc J-M, Llorens-Cortès C. Effect of apelin on glomerular hemodynamic function in the rat kidney. *Kidney Int* (2008) 74:486–94. doi:10.1038/ki.2008.199
- Szokodi I, Tavi P, Földes G, Voutilainen-Myllylä S, Ilves M, Tokola H, et al. Apelin, the novel endogenous ligand of the orphan receptor APJ, regulates cardiac contractility. *Circ Res* (2002) 91:434–40. doi:10.1161/01.RES.0000033522.37861.69
- Langelaan DN, Bebbington EM, Reddy T, Rainey JK. Structural insight into G-protein coupled receptor binding by apelin. *Biochemistry* (2009) 48:537–48. doi:10.1021/bi801864b
- Masri B, Lahou H, Mazarguil H, Knibiehler B, Audigier Y. Apelin (65–77) activates extracellular signal-regulated kinases via a PTX-sensitive G protein. *Biochim Biophys Res Commun* (2002) 290:539–45. doi:10.1006/bbrc.2001.6230
- Eyries M, Siegfried G, Ciomas M, Montagne K, Agrapart M, Lebrin F, et al. Hypoxia-induced apelin expression regulates endothelial cell proliferation and regenerative angiogenesis. *Circ Res* (2008) 103:432–40. doi:10.1161/CIRCRESAHA.108.179333
- D'Aniello C, Lonardo E, Iaconis S, Guardiola O, Liguoro AM, Liguori GL, et al. G protein-coupled receptor APJ and its ligand apelin act downstream of Cripto to specify embryonic stem cells toward the cardiac lineage through extracellular signal-regulated kinase/p70S6 kinase signaling pathway. *Circ Res* (2009) 105:231–8. doi:10.1161/CIRCRESAHA.109.201186
- Reaux A, De Mota N, Skultetyova I, Lenkei Z, El Messari S, Gallatz K, et al. Physiological role of a novel neuropeptide, apelin, and its receptor in the rat brain. *J Neurochem* (2001) 77:1085–96. doi:10.1046/j.1471-4159.2001.00320.x
- Gerbier R, Alvear-Perez R, Margaté J-F, Flahault A, Couvineau P, Gao J, et al. Development of original metabolically-stable apelin-17 analogs with diuretic and cardiovascular effects. *FASEB J* (2017) 31(2):687–700. doi:10.1096/fj.201600784R
- Ceraudo E, Galanth C, Carpentier E, Banegas-Font I, Schonegger A-M, Alvear-Perez R, et al. Biased signaling favoring Gi over β-arrestin promoted by an apelin fragment lacking the C-terminal phenylalanine. *J Biol Chem* (2014) 289:24599–610. doi:10.1074/jbc.M113.541698
- Lee DK, Saldivia VR, Nguyen T, Cheng R, George SR, O'Dowd BF. Modification of the terminal residue of apelin-13 antagonizes its hypotensive action. *Endocrinology* (2005) 146:231–6. doi:10.1210/en.2004-0359
- Lee DK, Ferguson SSG, George SR, O'Dowd BF. The fate of the internalized apelin receptor is determined by different isoforms of apelin mediating

- differential interaction with beta-arrestin. *Biochem Biophys Res Commun* (2010) 395:185–9. doi:10.1016/j.bbrc.2010.03.151
37. Chun HJ, Ali ZA, Kojima Y, Kundu RK, Sheikh AY, Agrawal R, et al. Apelin signaling antagonizes Ang II effects in mouse models of atherosclerosis. *J Clin Invest* (2008) 118:3343–54. doi:10.1172/JCI34871
38. Sun X, Iida S, Yoshikawa A, Senbomatsu R, Imanaka K, Maruyama K, et al. Non-activated APJ suppresses the angiotensin II type 1 receptor, whereas apelin-activated APJ acts conversely. *Hypertens Res* (2011) 34:701–6. doi:10.1038/hr.2011.19
39. Siddiquee K, Hampton J, McAnally D, May L, Smith L. The apelin receptor inhibits the angiotensin II type 1 receptor via allosteric trans-inhibition. *Br J Pharmacol* (2013) 168:1104–17. doi:10.1111/j.1476-5381.2012.02192.x
40. Li Y, Chen J, Bai B, Du H, Liu Y, Liu H. Heterodimerization of human apelin and kappa opioid receptors: roles in signal transduction. *Cell Signal* (2012) 24:991–1001. doi:10.1016/j.cellsig.2011.12.012
41. Bai B, Liu L, Zhang N, Wang C, Jiang Y, Chen J. Heterodimerization of human apelin and bradykinin 1 receptors: novel signal transduction characteristics. *Cell Signal* (2014) 26:1549–59. doi:10.1016/j.cellsig.2014.03.022
42. Murza A, Belleville K, Longpré J-M, Sarret P, Marsault É. Stability and degradation patterns of chemically modified analogs of apelin-13 in plasma and cerebrospinal fluid. *Biopolymers* (2014) 102:297–303. doi:10.1002/bip.22498
43. Japp AG, Cruden NL, Barnes G, van Gemeren N, Mathews J, Adamson J, et al. Acute cardiovascular effects of apelin in humans: potential role in patients with chronic heart failure. *Circulation* (2010) 121:1818–27. doi:10.1161/CIRCULATIONAHA.109.911339
44. Jia ZQ, Hou L, Leger A, Wu I, Kudej AB, Stefano J, et al. Cardiovascular effects of a PEGylated apelin. *Peptides* (2012) 38:181–8. doi:10.1016/j.peptides.2012.09.003
45. Galon-Tilleman H, Yang H, Bednarek MA, Spurlock SM, Paavola KJ, Ko B, et al. Apelin-36 modulates blood glucose and body weight independently of canonical APJ receptor signaling. *J Biol Chem* (2017) 292:1925–33. doi:10.1074/jbc.M116.748103
46. Juhl C, Els-Heindl S, Schönauer R, Redlich G, Haaf E, Wunder F, et al. Development of potent and metabolically stable APJ ligands with high therapeutic potential. *ChemMedChem* (2016) 11(21):2378–84. doi:10.1002/cmdc.201600307
47. Sidorova MV, Az'muko AA, Pal'keeva ME, Molokoedov AS, Bushuev VN, Dvorantsev SN, et al. [Synthesis and cardioprotective properties of apelin-12 and its structural analogs]. *Bioorg Khim* (2012) 38:40–51. doi:10.1134/S1068162012010177
48. Murza A, Parent A, Besserer-Offroy E, Tremblay H, Karadereye F, Beaudet N, et al. Elucidation of the structure-activity relationships of apelin: influence of unnatural amino acids on binding, signaling, and plasma stability. *ChemMedChem* (2012) 7:318–25. doi:10.1002/cmdc.201100492
49. Hamada J, Kimura J, Ishida J, Kohda T, Morishita S, Ichihara S, et al. Evaluation of novel cyclic analogues of apelin. *Int J Mol Med* (2008) 22:547–52. doi:10.3892/ijmm.00000054
50. Brame AL, Maguire JJ, Yang P, Dyson A, Torella R, Cherian J, et al. Design, characterization, and first-in-human study of the vascular actions of a novel biased apelin receptor agonist. *Hypertension* (2015) 65:834–40. doi:10.1161/HYPERTENSIONAHA.114.05099
51. Murza A, Sainsily X, Côté J, Bruneau-Cossette L, Besserer-Offroy É, Longpré J-M, et al. Structure-activity relationship of novel macrocyclic biased apelin receptor agonists. *Org Biomol Chem* (2017) 15:449–58. doi:10.1039/c6ob02247b
52. Fosgerau K, Hoffmann T. Peptide therapeutics: current status and future directions. *Drug Discov Today* (2015) 20:122–8. doi:10.1016/j.drudis.2014.10.003
53. Murza A, Besserer-Offroy É, Côté J, Bérubé P, Longpré J-M, Dumaine R, et al. C-Terminal modifications of apelin-13 significantly change ligand binding, receptor signaling, and hypotensive action. *J Med Chem* (2015) 58:2431–40. doi:10.1021/jm501916k
54. Fan X, Zhou N, Zhang X, Mukhtar M, Lu Z, Fang J, et al. Structural and functional study of the apelin-13 peptide, an endogenous ligand of the HIV-1 coreceptor, APJ. *Biochemistry* (2003) 42:10163–8. doi:10.1021/bi030049s
55. Pope GR, Roberts EM, Lolait SJ, O'Carroll A-M. Central and peripheral apelin receptor distribution in the mouse: species differences with rat. *Peptides* (2012) 33:139–48. doi:10.1016/j.peptides.2011.12.005
56. Reaux A, Gallatz K, Palkovits M, Llorens-Cortes C. Distribution of apelin-synthesizing neurons in the adult rat brain. *Neuroscience* (2002) 113:653–62. doi:10.1016/S0306-4522(02)00192-6
57. Brailoiu GC, Dun SL, Yang J, Ohsawa M, Chang JK, Dun NJ. Apelin-immunoreactivity in the rat hypothalamus and pituitary. *Neurosci Lett* (2002) 327:193–7. doi:10.1016/S0304-3940(02)00411-1
58. Reaux A, Morinville A, Burlet A, Llorens-Cortes C, Beaudet A. Dehydration-induced cross-regulation of apelin and vasopressin immunoreactivity levels in magnocellular hypothalamic neurons. *Endocrinology* (2004) 145:4392–400. doi:10.1210/en.2004-0384
59. Bodineau L, Taveau C, Lê Quan Sang H-H, Osterstock G, Queguiner I, Moos F, et al. Data supporting a new physiological role for brain apelin in the regulation of hypothalamic oxytocin neurons in lactating rats. *Endocrinology* (2011) 152:3492–503. doi:10.1210/en.2011-0206
60. Buggy J, Fink GD, Johnson AK, Brody MJ. Prevention of the development of renal hypertension by anteroventral third ventricular tissue lesions. *Circ Res* (1977) 40:I110–7.
61. Johnson AK, Cunningham JT, Thunhorst RL. Integrative role of the lamina terminalis in the regulation of cardiovascular and body fluid homeostasis. *Clin Exp Pharmacol Physiol* (1996) 23:183–91. doi:10.1111/j.1440-1681.1996.tb02594.x
62. O'Carroll A-M, Lolait SJ. Regulation of rat APJ receptor messenger ribonucleic acid expression in magnocellular neurones of the paraventricular and supraoptic nuclei by osmotic stimuli. *J Neuroendocrinol* (2003) 15:661–6. doi:10.1046/j.1365-2826.2003.01044.x
63. Hurbin A, Boissin-Agasse L, Orcel H, Rabié A, Joux N, Desarménien MG, et al. The V1a and V1b, but not V2, vasopressin receptor genes are expressed in the supraoptic nucleus of the rat hypothalamus, and the transcripts are essentially colocalized in the vasopressinergic magnocellular neurons. *Endocrinology* (1998) 139:4701–7. doi:10.1210/endo.139.11.6320
64. Kleinz MJ, Skepper JN, Davenport AP. Immunocytochemical localisation of the apelin receptor, APJ, to human cardiomyocytes, vascular smooth muscle and endothelial cells. *Regul Pept* (2005) 126:233–40. doi:10.1016/j.regpep.2004.10.019
65. Ostrowski NL, Lolait SJ, Bradley DJ, O'Carroll AM, Brownstein MJ, Young WS. Distribution of V1a and V2 vasopressin receptor messenger ribonucleic acids in rat liver, kidney, pituitary and brain. *Endocrinology* (1992) 131:533–5. doi:10.1210/endo.131.1.1535312
66. Brownstein MJ, Russell JT, Gainer H. Synthesis, transport, and release of posterior pituitary hormones. *Science* (1980) 207:373–8. doi:10.1126/science.6153132
67. Manning M, Lowbridge J, Haldar J, Sawyer WH. Design of neurohypophyseal peptides that exhibit selective agonistic and antagonistic properties. *Fed Proc* (1977) 36:1848–52.
68. Zini S, Fournie-Zaluski MC, Chauvel E, Roques BP, Corvol P, Llorens-Cortes C. Identification of metabolic pathways of brain angiotensin II and III using specific aminopeptidase inhibitors: predominant role of angiotensin III in the control of vasopressin release. *Proc Natl Acad Sci U S A* (1996) 93:11968–73. doi:10.1073/pnas.93.21.11968
69. Gouzènes L, Desarménien MG, Hussy N, Richard P, Moos FC. Vasopressin regularizes the phasic firing pattern of rat hypothalamic magnocellular vasopressin neurons. *J Neurosci* (1998) 18:1879–85.
70. Ludwig M. Dendritic release of vasopressin and oxytocin. *J Neuroendocrinol* (1998) 10:881–95. doi:10.1046/j.1365-2826.1998.00279.x
71. Poulain DA, Wakerley JB, Dyball RE. Electrophysiological differentiation of oxytocin- and vasopressin-secreting neurones. *Proc R Soc Lond B Biol Sci* (1977) 196:367–84. doi:10.1098/rspb.1977.0046
72. Gimpl G, Fahrenholz F. The oxytocin receptor system: structure, function, and regulation. *Physiol Rev* (2001) 81:629–83.
73. Hogarty DC, Speakman EA, Puig V, Phillips MI. The role of angiotensin, AT1 and AT2 receptors in the pressor, drinking and vasopressin responses to central angiotensin. *Brain Res* (1992) 586:289–94. doi:10.1016/0006-8993(92)91638-U
74. Kadekaro M, Summy-Long JY, Freeman S, Harris JS, Terrell ML, Eisenberg HM. Cerebral metabolic responses and vasopressin and oxytocin secretions during progressive water deprivation in rats. *Am J Physiol* (1992) 262:R310–7.
75. Nielsen S, Chou CL, Marples D, Christensen EI, Kishore BK, Knepper MA. Vasopressin increases water permeability of kidney collecting duct by

- inducing translocation of aquaporin-CD water channels to plasma membrane. *Proc Natl Acad Sci USA* (1995) 92:1013–7. doi:10.1073/pnas.92.4.1013
76. Sands JM, Naruse M, Baum M, Jo I, Hebert SC, Brown EM, et al. Apical extracellular calcium/polyvalent cation-sensing receptor regulates vasopressin-elicited water permeability in rat kidney inner medullary collecting duct. *J Clin Invest* (1997) 99:1399–405. doi:10.1172/JCI119299
77. Hus-Citharel A, Bodineau L, Frugiére A, Joubert F, Bouby N, Llorens-Cortes C. Apelin Counteracts Vasopressin-Induced Water Reabsorption via Cross Talk Between Apelin and Vasopressin Receptor Signaling Pathways in the Rat Collecting Duct. *Endocrinology* (2014) 155:4483–93. doi:10.1210/en.2014-1257
78. Murza A, Sainsily X, Coquerel D, Côté J, Marx P, Besserer-Offroy É, et al. Discovery and structure-activity relationship of a bioactive fragment of ELABELA that modulates vascular and cardiac functions. *J Med Chem* (2016) 59:2962–72. doi:10.1021/acs.jmedchem.5b01549
79. Deng C, Chen H, Yang N, Feng Y, Hsueh AJW. Apela regulates fluid homeostasis by binding to the APJ receptor to activate Gi signaling. *J Biol Chem* (2015) 290:18261–8. doi:10.1074/jbc.M115.648238
80. Roberts EM, Newson MJF, Pope GR, Landgraf R, Lolait SJ, O'Carroll A-M. Abnormal fluid homeostasis in apelin receptor knockout mice. *J Endocrinol* (2009) 202:453–62. doi:10.1677/JOE-09-0134
81. Roberts EM, Pope GR, Newson MJF, Landgraf R, Lolait SJ, O'Carroll A-M. Stimulus-specific neuroendocrine responses to osmotic challenges in apelin receptor knockout mice. *J Neuroendocrinol* (2010) 22:301–8. doi:10.1111/j.1365-2826.2010.01968.x
82. Tang C, Zelenak C, Völkl J, Eichenmüller M, Regel I, Fröhlich H, et al. Hydration-sensitive gene expression in brain. *Cell Physiol Biochem* (2011) 27:757–68. doi:10.1159/000330084
83. Zingg HH, Lefebvre D, Almazan G. Regulation of vasopressin gene expression in rat hypothalamic neurons. Response to osmotic stimulation. *J Biol Chem* (1986) 261:12956–9.
84. Jéquier E, Constant F. Water as an essential nutrient: the physiological basis of hydration. *Eur J Clin Nutr* (2010) 64:115–23. doi:10.1038/ejcn.2009.111
85. Phillips PA, Rolls BJ, Ledingham JG, Forsling ML, Morton JJ, Crowe MJ, et al. Reduced thirst after water deprivation in healthy elderly men. *N Engl J Med* (1984) 311:753–9. doi:10.1056/NEJM198409203111202
86. Fliers E, Swaab DF, Pool CW, Verwer RW. The vasopressin and oxytocin neurons in the human supraoptic and paraventricular nucleus; changes with aging and in senile dementia. *Brain Res* (1985) 342:45–53. doi:10.1016/0006-8993(85)91351-4
87. Hoogendoijk JE, Fliers E, Swaab DF, Verwer RW. Activation of vasopressin neurons in the human supraoptic and paraventricular nucleus in senescence and senile dementia. *J Neurol Sci* (1985) 69:291–9. doi:10.1016/0022-510X(85)90141-8
88. Lucassen PJ, Salehi A, Pool CW, Gonatas NK, Swaab DF. Activation of vasopressin neurons in aging and Alzheimer's disease. *J Neuroendocrinol* (1994) 6:673–9. doi:10.1111/j.1365-2826.1994.tb00634.x
89. Palin K, Moreau ML, Orcel H, Duvoid-Guillou A, Rabié A, Kelley KW, et al. Age-impaired fluid homeostasis depends on the balance of IL-6/IGF-I in the rat supraoptic nuclei. *Neurobiol Aging* (2009) 30:1677–92. doi:10.1016/j.neurobiolaging.2007.12.006
90. Fliers E, Swaab DF. Activation of vasopressinergic and oxytocinergic neurons during aging in the Wistar rat. *Peptides* (1983) 4:165–70. doi:10.1016/0196-9781(83)90108-0
91. Terwel D, ten Haaf JA, Markerink M, Jolles J. Changes in plasma vasopressin concentration and plasma osmolality in relation to age and time of day in the male Wistar rat. *Acta Endocrinol* (1992) 126:357–62.
92. Sladek CD, Olschowka JA. Dehydration induces Fos, but not increased vasopressin mRNA in the supraoptic nucleus of aged rats. *Brain Res* (1994) 652:207–15. doi:10.1016/0006-8993(94)90229-1
93. Palin K, Moreau ML, Sauvant J, Orcel H, Nadjar A, Duvoid-Guillou A, et al. Interleukin-6 activates arginine vasopressin neurons in the supraoptic nucleus during immune challenge in rats. *Am J Physiol Endocrinol Metab* (2009) 296:E1289–99. doi:10.1152/ajpendo.90489.2008
94. Sauvant J, Delpech J-C, Palin K, De Mota N, Dudit J, Aubert A, et al. Mechanisms involved in dual vasopressin/apelin neuron dysfunction during aging. *PLoS One* (2014) 9:e87421. doi:10.1371/journal.pone.0087421
95. Morgenthaler NG, Struck J, Jochberger S, Dünser MW. Copeptin: clinical use of a new biomarker. *Trends Endocrinol Metab* (2008) 19:43–9. doi:10.1016/j.tem.2007.11.001
96. Balanescu S, Kopp P, Gaskill MB, Morgenthaler NG, Schindler C, Rutishauser J. Correlation of plasma copeptin and vasopressin concentrations in hypo-, iso-, and hyperosmolar states. *J Clin Endocrinol Metab* (2011) 96:1046–52. doi:10.1210/jc.2010-2499
97. Fenske W, Störk S, Blechschmidt A, Maier SGK, Morgenthaler NG, Allolio B. Copeptin in the differential diagnosis of hyponatremia. *J Clin Endocrinol Metab* (2009) 94:123–9. doi:10.1210/jc.2008-1426
98. Ellison DH, Berl T. Clinical practice. The syndrome of inappropriate anti-diuresis. *N Engl J Med* (2007) 356:2064–72. doi:10.1056/NEJMcp066837
99. Fenske WK, Christ-Crain M, Hörning A, Simet J, Szinnai G, Fassnacht M, et al. A copeptin-based classification of the osmoregulatory defects in the syndrome of inappropriate antidiuresis. *J Am Soc Nephrol* (2014) 25:2376–83. doi:10.1681/ASN.2013080895
100. Blanchard A, Steichen O, De Mota N, Curis E, Gauci C, Frank M, et al. An abnormal apelin/vasopressin balance may contribute to water retention in patients with the syndrome of inappropriate antidiuretic hormone (SIADH) and heart failure. *J Clin Endocrinol Metab* (2013) 98:2084–9. doi:10.1210/jc.2012-3794
101. Urso C, Bruculeri S, Caimi G. Acid-base and electrolyte abnormalities in heart failure: pathophysiology and implications. *Heart Fail Rev* (2015) 20:493–503. doi:10.1007/s10741-015-9482-y
102. Sica DA. Hyponatremia and heart failure – pathophysiology and implications. *Congest Heart Fail* (2005) 11:274–7. doi:10.1111/j.1527-5299.2005.04180.x
103. Goldsmith SR, Francis GS, Cowley AW. Arginine vasopressin and the renal response to water loading in congestive heart failure. *Am J Cardiol* (1986) 58:295–9. doi:10.1016/0002-9149(86)90065-2
104. Chin MH, Goldman L. Correlates of major complications or death in patients admitted to the hospital with congestive heart failure. *Arch Intern Med* (1996) 156:1814–20. doi:10.1001/archinte.156.16.1814
105. Christ-Crain M, Fenske W. Copeptin in the diagnosis of vasopressin-dependent disorders of fluid homeostasis. *Nat Rev Endocrinol* (2016) 12:168–76. doi:10.1038/nrendo.2015.224
106. Timper K, Fenske W, Kühn F, Frech N, Arici B, Rutishauser J, et al. Diagnostic accuracy of copeptin in the differential diagnosis of the polyuria-polydipsia syndrome: a prospective multicenter study. *J Clin Endocrinol Metab* (2015) 100:2268–74. doi:10.1210/jc.2014-4507
107. Urwyler SA, Timper K, Fenske W, de Mota N, Blanchard A, Kühn F, et al. Plasma apelin concentrations in patients with polyuria-polydipsia syndrome. *J Clin Endocrinol Metab* (2016) 101(5):1917–23. doi:10.1210/jc.2016-1158

Conflict of Interest Statement: The authors declare that the research was conducted in the absence of any commercial or financial relationships that could be construed as a potential conflict of interest.

Copyright © 2017 Flahault, Couvineau, Alvear-Perez, Iturrioz and Llorens-Cortes. This is an open-access article distributed under the terms of the Creative Commons Attribution License (CC BY). The use, distribution or reproduction in other forums is permitted, provided the original author(s) or licensor are credited and that the original publication in this journal is cited, in accordance with accepted academic practice. No use, distribution or reproduction is permitted which does not comply with these terms.



Central and Peripheral Effects of Urotensin II and Urotensin II-Related Peptides on Cardiac Baroreflex Sensitivity in Trout

Frédéric Lancien^{1*}, Gilmer Vanegas¹, Jérôme Leprince², Hubert Vaudry² and Jean-Claude Le Mével¹

¹ Institut National de la Santé et de la Recherche Médicale UMR1101, Laboratoire de Neurophysiologie, SFR ScInBioS, Université de Brest, Faculté de Médecine et des Sciences de la Santé, Brest, France, ² Institut National de la Santé et de la Recherche Médicale U982, UA Centre National de la Recherche Scientifique, Différenciation et Communication Neuronale et Neuroendocrine, Normandie Université, Rouen, France

OPEN ACCESS

Edited by:

Riccarda Granata,
University of Turin, Italy

Reviewed by:

David Chatenet,
Institut National de la Recherche
Scientifique (INRS), Canada
Anna M. D. Watson,
Monash University, Australia

*Correspondence:

Frédéric Lancien
frédéric.lancien@univ-brest.fr

Specialty section:

This article was submitted to
Neuroendocrine Science,
a section of the journal
Frontiers in Neuroscience

Received: 24 November 2016

Accepted: 24 January 2017

Published: 10 February 2017

Citation:

Lancien F, Vanegas G, Leprince J, Vaudry H and Le Mével J-C (2017)
Central and Peripheral Effects of Urotensin II and Urotensin II-Related Peptides on Cardiac Baroreflex Sensitivity in Trout.
Front. Neurosci. 11:51.
doi: 10.3389/fnins.2017.00051

The baroreflex response is an essential component of the cardiovascular regulation that buffers abrupt changes in blood pressure to maintain homeostasis. Urotensin II (UII) and its receptor UT are present in the brain and in peripheral cardiovascular tissues of fish and mammals. Intracerebroventricular (ICV) injection of UII in these vertebrates provokes hypertension and tachycardia, suggesting that the cardio-inhibitory baroreflex response is impaired. Since nothing is known about the effect of UII on the cardiac baroreflex sensitivity (BRS), we decided to clarify the changes in spontaneous BRS using a cross spectral analysis technique of systolic blood pressure (SBP) and R-R interval variabilities after ICV and intra-arterial (IA) injections of trout UII in the unanesthetized trout. We contrasted the effects of UII with those observed for the UII-related peptides (URP), URP1 and URP2. Compared with vehicle-injected trout, ICV injection of UII (5–500 pmol) produced a gradual increase in SBP, a decrease in the R-R interval (reflecting a tachycardia) associated with a dose-dependent reduction of the BRS. The threshold dose for a significant effect on these parameters was 50 pmol (BRS; –55%; 1450 ± 165 ms/kPa vs. 3240 ± 300 ms/kPa; $P < 0.05$). Only the 500-pmol dose of URP2 caused a significant increase in SBP without changing significantly the R-R interval but reduced the BRS. IA injection of UII (5–500 pmol) caused a dose-dependent elevation of SBP. Contrasting with the ICV effects of UII, the R-R interval increased (reflecting a bradycardia) up to the 50-pmol dose while the BRS remained unchanged (50 pmol; 2530 ± 270 ms/kPa vs. 2600 ± 180 ms/kPa; $P < 0.05$). Nonetheless, the highest dose of UII reduced the BRS as did the highest dose of URP1. In conclusion, the contrasting effect of low picomolar doses of UII after central and peripheral injection on the BRS suggests that only the central urotensinergic system is involved in the attenuation of the BRS. The limited and quite divergent effects of URP1 and URP2 on the BRS, indicate

that the action of UII is specific for this peptide. Further studies are required to elucidate the site(s) and mechanisms of action of UII on the baroreflex pathways. Whether such effects of central UII on the BRS exist in mammals including humans warrants further investigations.

Keywords: urotensin II, urotensin II-related peptide 1, urotensin II-related peptide 2, intracerebroventricular injection, peripheral injection, baroreflex, autonomic nervous system, trout

INTRODUCTION

Urotensin II (UII) is a cyclic neuropeptide that was originally isolated and purified from the caudal neurosecretory system of the teleost fish *Gillichthys mirabilis* and later characterized in mammals (Pearson et al., 1980; Vaudry et al., 2010, 2015). UII belongs to a family of structurally related peptides that includes UII and UII-related peptides (URPs) called URP, URP1, and URP2. In the teleost lineage, the four peptides are present but only two of them, UII and URP, are found in tetrapods (Tostivint et al., 2013). UII and URP bind to an ancestral (UII) receptor, termed UT, and the two peptides activate this receptor with similar potency. In teleost fish, which possess different UT subtypes (Tostivint et al., 2014), UII, URP, and UT are present in the central nervous system (CNS) i.e., in the brainstem and spinal cord (Lu et al., 2006; Nobata et al., 2011; Parmentier et al., 2011; Quan et al., 2015) and UT has been identified in various peripheral organs including the cardiovascular system (Lu et al., 2006). In mammals, UII and URP genes are mostly and differentially expressed in cholinergic motor neurons of the brainstem and spinal cord, and UII and UT immunoreactivity are present in neurons of the brainstem involved in cardiovascular functions (Dun et al., 2001; Pelletier et al., 2002; Jégou et al., 2006). UII, URP, and UT mRNAs are also differentially expressed in peripheral tissues, including notably the cardiovascular system (Ames et al., 1999; Vaudry et al., 2010, 2015). These observations suggest that, in fish as in mammals, UII/URPs may act centrally and peripherally to control cardiovascular activity. Indeed, intracerebroventricular (ICV) injection of UII and to a lesser extent URP in the rainbow trout *Oncorhynchus mykiss* (Le Mével et al., 1996; Vanegas et al., 2015) and in the eel *Anguilla japonica* (Nobata et al., 2011), and UII in mammals (Watson and May, 2004) elevates blood pressure but also accelerates heart rate. Since, in these studies, heart rate did not counter-regulate blood pressure elevation as might be expected, it appears that the cardiac baroreflex was impaired following ICV injection of UII/URPs. In mammals, the cardiovascular effects of peripherally administered UII are variable, depending upon the species used and the presence or absence of anesthesia, inasmuch as increase or decrease in blood pressure mostly associated with cardiac positive chronotropic action are observed in rats, sheep and monkeys (Watson and

May, 2004). In trout and eel however, a consistent increase in the dorsal aortic blood pressure is observed following intra-arterial (IA) injection of UII and to a lesser extent URP1 but not URP2 (Le Mével et al., 1996; Nobata et al., 2011; Vanegas et al., 2015), but the baroreflexogenic bradycardia only occurs after UII injection in trout. Since the cardiac baroreflex response is an essential component of the cardiovascular regulation that buffers abrupt changes in blood pressure to maintain homeostasis (La Rovere et al., 2008; Olson, 2011), we decided to clarify the change in the cardiac baroreflex sensitivity (BRS) after ICV and IA injections of trout UII in our established trout model (Lancien et al., 2011). We contrasted the effects of UII with those of the two paralogs URP1 and URP2.

MATERIALS AND METHODS

Peptides and Chemicals

Trout UII, zebrafish URP1, and URP2 (Waugh and Conlon, 1993; Tostivint et al., 2013) were synthesized as previously described (Chatenet et al., 2004; Lancien et al., 2004). **Table 1** summarizes the physico-chemical characteristics of the synthetic peptides. The peptides were dissolved in Ringer's solution (vehicle) and stored in stock solutions at -25°C . Immediately before use, UII, URP1, or URP2 were diluted to the desired concentration with Ringer's solution. The composition of the Ringer's solution was (in mM): NaCl 124, KCl 3, CaCl₂ 0.75, MgSO₄ 1.30, KH₂PO₄ 1.24, NaHCO₃ 12, glucose 10 (pH 7.8). All solutions were sterilized by filtration through 0.22 μm filters (Millipore, Molsheim, France) before injection.

Animals

Adults rainbow trout *Oncorhynchus mykiss* ($251 \pm 26\text{ g}$ body wt, mean \pm SEM, $n = 98$) of both sexes were purchased

TABLE 1 | Physico-chemical characteristics of the synthesized peptides.

Peptide	Sequence	RP-HPLC		MS	
		t _R (min) ^a	Purity (%)	Calcd. ^b	Obsd. ^c
Trout UII	GGNSEC <u>FWKYCVTN</u>	20.33	99.9	1389.55	1390.48
Zebrafish URP1	AC <u>FWKYCVTN</u>	19.40	96.6	1231.51	1232.69
Zebrafish URP2	V <u>CFWKYCSQN</u>	19.92	99.9	1274.52	1275.64

^aRetention time determined by RP-HPLC on a Vydac 218TP54 C18 column (0.46 x 25 cm) using a linear gradient (10–60% over 25 min) of acetonitrile/TFA (99.9:0.1, v/v) at a flow rate of 1 mL/min.

^bTheoretical monoisotopic molecular weight.

^cm/z value assessed by MALDI-TOF-MS on a Voyager DE-PRO in the reflector mode with α -cyano-4-hydroxycinnamic acid as a matrix.

Abbreviations: BRS, baroreflex sensitivity; CNS, central nervous system; DVMN, dorsal vagal motor nucleus; ECG, electrocardiographic; IA, intra-arterial; ICV, intracerebroventricular; NTS, nucleus tractus solitarii; P_{DA}, dorsal aortic blood pressure; SBP, systolic blood pressure; UII, urotensin II; URP, urotensin II-related peptide; URP1, urotensin II-related peptide 1; URP2, urotensin II-related peptide 2; UT, urotensin II receptor.

locally and transferred in a well-oxygenated and thermostatically controlled water tank to the laboratory. All fish were kept in a 1000-liter tank containing circulating dechlorinated and aerated tap water ($11\text{--}12^\circ\text{C}$), under a standard photoperiod (lights on 09:00 AM–08:00 PM). The fish were allowed at least 3 weeks to acclimate under these conditions before the experiments were started. Animal manipulations and experimental protocols were approved by the Comité d'Ethique Finistérien en Expérimentation Animale (authorization number 02142.01).

Experimental Procedures

The surgical procedures have previously been described in detail (Lancien et al., 2004; Le Mével et al., 2012; Vanegas et al., 2015). Briefly, anesthetized rainbow trout were equipped with two electrocardiographic electrodes, a dorsal aortic cannula, an ICV microguide, and a buccal catheter that was used to record the buccal ventilatory pressure (not quantified in the present study). After surgery, the animals were transferred to a 6-liter blackened chamber supplied with dechlorinated and aerated tap water ($10\text{--}11^\circ\text{C}$) that was both recirculating and through-flowing. Oxygen pressure within the water tank (P_{wO_2}) and pH were continuously recorded and maintained at constant levels ($P_{\text{wO}_2} = 20 \text{ kPa}$; pH = 7.4–7.6). The trout were allowed to recover from surgery and to become accustomed to their new environment for 48–72 h.

Each day, after dorsal aortic blood pressure (P_{DA}) and heart rate were stabilized for at least 90 min, parameters were recorded for 30 min and the different injection protocols begun. The

animals received no more than two ICV or IA injections of peptide per day with a delay of at least 5 h between the injections. Some trout received both ICV and IA injections, and in this case, the delay between the two injections was 1 day, and the type of injections was randomized among animals. No single fish was studied for more than 2 days and control experiments revealed that there was no significant change in performance over this period.

Intracerebroventricular and Intra-Arterial Administration of Peptides

For the ICV protocols, the injector was introduced within the ICV guide prior to the beginning of a recording session which lasted 30 min. All injections were made at the 5 min of the test and the injector was left in place for a further 5 min to allow for complete diffusion of the agent and to minimize the spread of substances upwards in the cannula tract. The fish received first an ICV injection of vehicle (0.5 μl) and, 30 min later, an ICV injection of UII, URP1, or URP2 (5, 50 or 500 pmol in 0.5 μl). For IA injections, 5 min after the beginning of the recording session, 50 μl of vehicle, UII at doses of 5, 50 or 500 pmol, URP1 or URP2 at doses of 50 or 500 pmol was injected through the dorsal aorta and immediately flushed by 150 μl of vehicle.

Data Acquisition and Analysis of Cardiovascular Variables

The ECG and P_{DA} signals were recorded using standardized electronic devices whose output were digitalized at 1000 Hz,

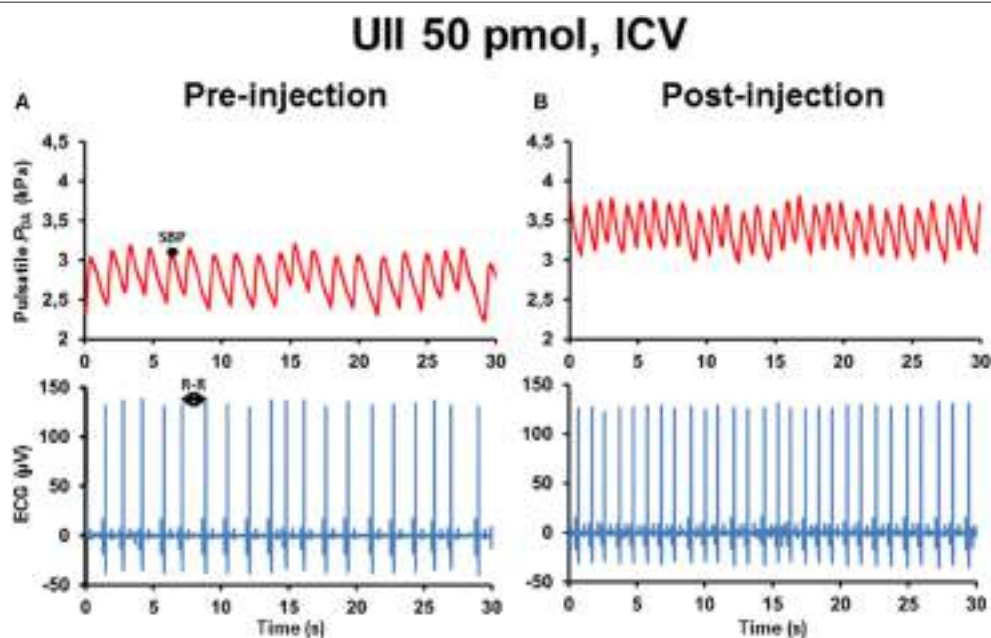


FIGURE 1 | Raw tracings of 30-s duration in a single unanesthetized trout illustrating the changes observed in pulsatile dorsal aortic blood pressure (P_{DA}) and electrocardiographic (ECG) signals between the pre-injection period (A) and the post-injection period (B) after intracerebroventricular (ICV) injection of 50 pmol UII. Note that, compared with the pre-injection period, ICV injection of UII produces an elevation of systolic blood pressure (SBP) but a decrease in the R-R interval of the ECG (reflecting a tachycardia).

visualized on the screen of a PC during the 30-min recording period and finally stored using PowerLab 4/30 data acquisition system (ADIInstruments, Oxford, England) and LabChart Pro software (v.7.0; ADIInstruments, Oxford, England) (Vanegas et al., 2015). ECG and P_{DA} signals were then processed off-line with custom-made programs written in LabView 6.1 (Laboratory Virtual Instrument Engineering Workbench, National Instruments, Austin, USA). Recordings were excluded from the analysis if they contained excessive artifacts on ECG and P_{DA} signals. For all protocols, the entire 25-min post-injection segments of ECG and P_{DA} signals were selected after ICV or IA injections of vehicle, UII, URP1, or URP2.

The R-R intervals (reflecting the time between each R wave of the ECG), systolic blood pressure (SBP) and cardiac baroreflex were calculated as previously described (Lancien et al., 2011). The R-R intervals were determined after detection of the R waves from the ECG recordings and SBP was identified from the pulsatile P_{DA} . Their mean values were calculated. R-R interval and SBP time series were resampled at 2.56 Hz to obtain equidistant data points. The linear trend was removed from the new time series and 29 segments of 256 data points (100 s) overlapping by half were subjected to a Hanning window. To investigate to what extend the input signal, SBP, influences the output signal, the R-R interval, the coherence, phase and transfer function spectra of SBP against the R-R interval were determined (Lancien et al., 2011). A relatively high coherence between the two signals and a negative phase shift (SBP changes precedes R-R interval fluctuations) indicates that the SBP mediates the changes in the R-R intervals. The cardiac BRS was estimated as the mean of the gain of the transfer function when the coherence was high and the phase negative.

All calculations for R-R interval (in ms), SBP (in kPa), and cardiac BRS (in kPa/ms) were made for the entire post-injection period of 25 min and the results were averaged for trout subjected to the same protocol.

Statistical Analysis

Data are expressed as means + or \pm SEM (standard error of the mean) on histograms or in percentage change in the text. For comparison between groups, the data were initially analyzed using a one-way ANOVA followed by the Dunnett's test for comparisons between vehicle-injected trout and trout receiving peptides. A value of $P < 0.05$ was considered significant. The statistical tests were performed and the graphs constructed using GraphPad Prism 5.0 (GraphPad, San Diego, CA).

RESULTS

Cardiac Baroreflex Sensitivity to Central UII, URP1, and URP2

Figure 1 illustrates 30-s recordings of pulsatile P_{DA} and ECG signals taken during the pre-injection period (**Figure 1A**) and during the post-injection period (**Figure 1B**) after ICV injection of 50 pmol UII. Comparison of the post-injection and the pre-injection signals revealed that UII caused a marked elevation in

SBP associated with a sharp reduction of the R-R interval of the ECG.

The histograms in **Figure 2** summarize the average changes in R-R interval and SBP (**Figure 2A**) and in BRS (**Figure 2B**) after ICV injection of vehicle or a range of doses (5–500 pmol) of UII. Compared with vehicle-injected trout, UII produced a gradual increase in SBP. The threshold dose for a statistically significant effect on SBP was 50 pmol and, at this dose, the R-R interval decreased significantly (**Figure 2A**). These effects on the two cardiovascular variables remained significant up to the 500-pmol dose (**Figure 2A**). **Figure 2B** demonstrates that the BRS was dose-dependently reduced following ICV injection of UII. The threshold dose for a statistically significant effect on BRS was 50 pmol (-55% ; 1450 ± 165 ms/kPa vs. 3240 ± 300 ms/kPa; $P < 0.05$) and the maximum decrease was observed for the 500-pmol dose.

The effect of URP1 and URP2 on the cardiovascular variables and cardiac BRS are summarized in **Figures 3, 4**, respectively. In contrast to UII, ICV injection of URP1 provoked no significant change in SBP and the R-R interval (**Figure 3A**). URP1 tended to reduce BRS but this effect was not statistically significant even at the highest dose (**Figure 3B**). Only the 500-pmol dose of URP2 caused a significant increase in SBP without changing significantly the R-R interval (**Figure 4A**) but, at this 500-pmol

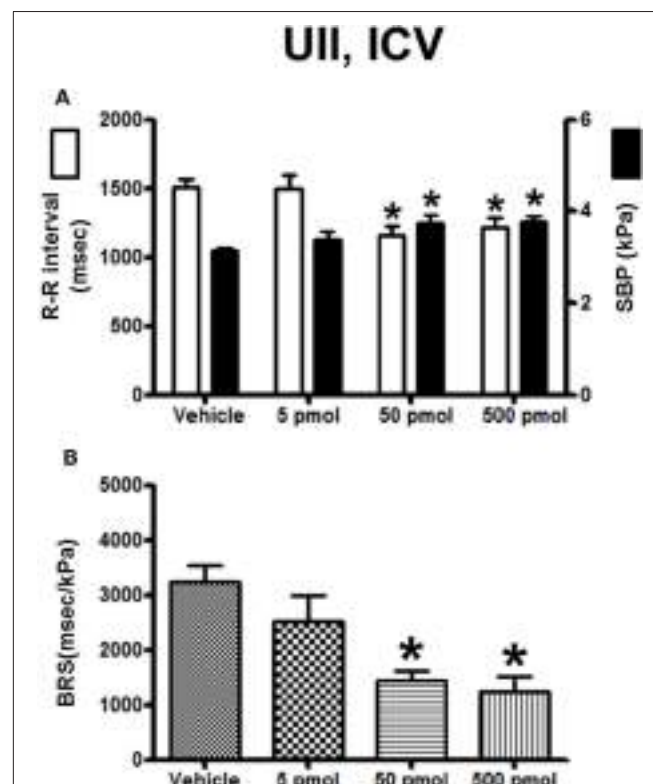


FIGURE 2 | Histograms showing (A) the R-R intervals (scale on the left) and the SBP values (scale on the right), **(B)** the BRS during the 5–30 min period after intracerebroventricular injection of 0 (vehicle, $n = 24$), 5 pmol ($n = 8$), 50 pmol ($n = 7$) and 500 pmol ($n = 9$) UII. n , number of trout. * $P < 0.05$ vs. vehicle.

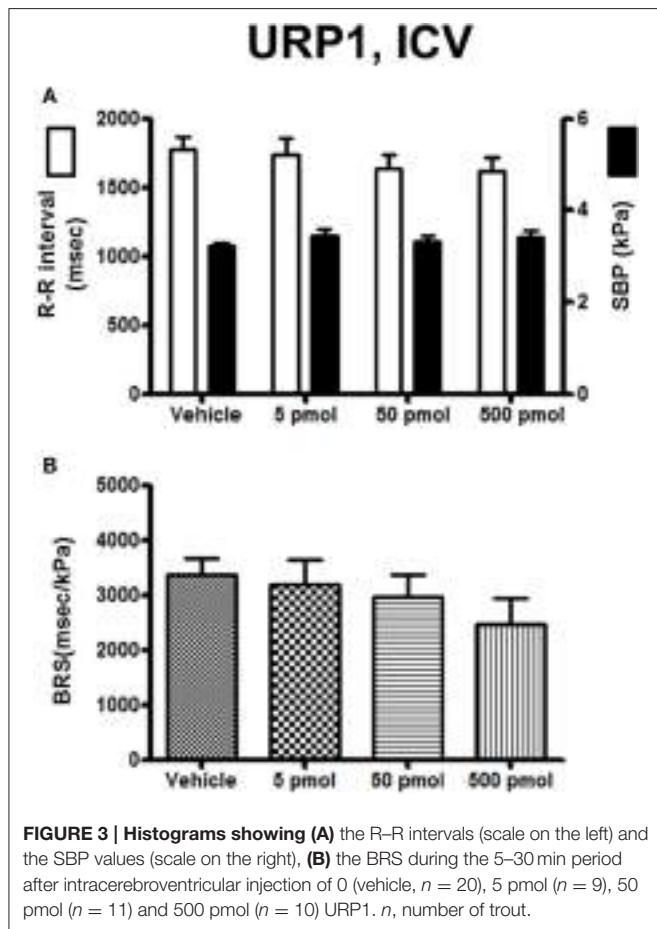


FIGURE 3 | Histograms showing (A) the R-R intervals (scale on the left) and the SBP values (scale on the right), **(B)** the BRS during the 5–30 min period after intracerebroventricular injection of 0 (vehicle, $n = 20$), 5 pmol ($n = 9$), 50 pmol ($n = 11$) and 500 pmol ($n = 10$) URP1. n , number of trout.

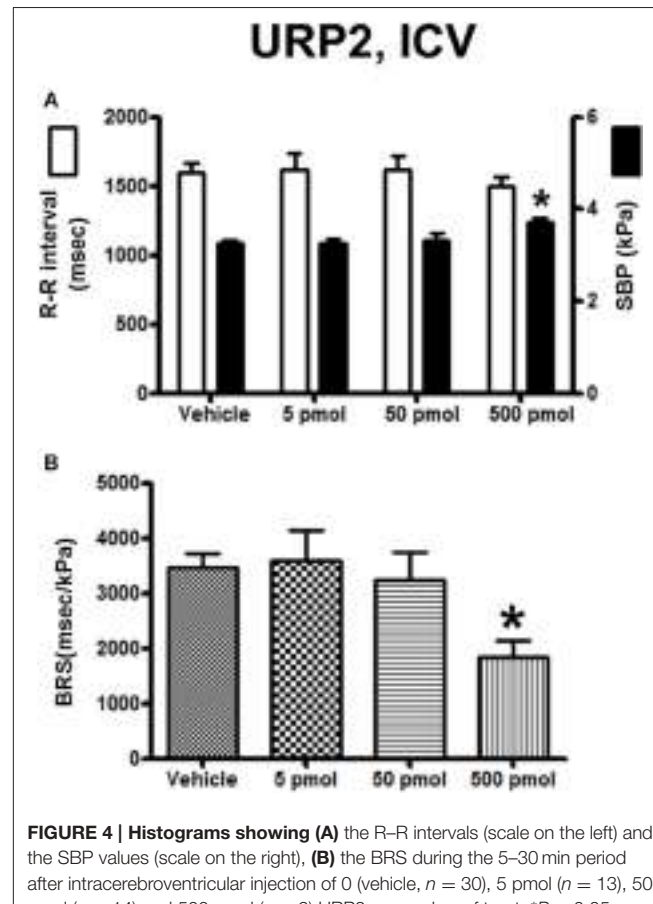


FIGURE 4 | Histograms showing (A) the R-R intervals (scale on the left) and the SBP values (scale on the right), **(B)** the BRS during the 5–30 min period after intracerebroventricular injection of 0 (vehicle, $n = 30$), 5 pmol ($n = 13$), 50 pmol ($n = 14$) and 500 pmol ($n = 9$) URP2. n , number of trout. * $P < 0.05$ vs. vehicle.

dose, URP2 evoked a significant depression in BRS (-47% , 1850 ± 290 ms/kPa vs. 3470 ± 240 ms/kPa, $P < 0.05$; **Figure 4B**).

Cardiac Baroreflex Sensitivity to Peripheral UII, URP1, and URP2

Figure 5 illustrates 30-s recordings of pulsatile P_{DA} and ECG signals taken during the pre-injection period (**Figure 5A**) and during the post-injection period (**Figure 5B**) after IA injection of 50 pmol UII. Comparison of the post-injection and the pre-injection signals revealed that UII caused a marked elevation in SBP associated with a potent increase in the R-R interval of the ECG.

The effects of IA injection of vehicle or a range of doses of UII (5–500 pmol) on the cardiovascular variables and BRS are summarized in **Figure 6**. UII provoked a clear dose-dependent increase in SBP with a threshold dose of 50 pmol for a significant effect and a maximum hypertension at the 500-pmol dose (**Figure 6A**). In marked contrast with the response observed after ICV injection, the R-R interval increased up to the 50-pmol dose and then returned to baseline level at the 500-pmol dose (**Figure 6A**). Interestingly, and compared to vehicle-injected trout, there was no change in the BRS using the lowest picomolar doses of UII (50 pmol; 2530 ± 270 ms/kPa vs.

2600 ± 180 ms/kPa; $P < 0.05$) but the highest dose of UII caused a 2-fold decrease in the BRS (**Figure 6B**).

The effect of URP1 and URP2 on the cardiovascular variables and cardiac BRS are depicted in **Figures 7, 8**, respectively. Only the highest dose of URP1 (500 pmol) elevated SBP but decreased the R-R interval (**Figure 7A**). The attenuation of the BRS was only significant after IA injection of this highest dose of URP1 (-53% ; 1540 ± 250 ms/kPa vs. 3330 ± 290 ms/kPa, $P < 0.05$; **Figure 7B**). The IA injection of URP2 was devoid of effect on the cardiovascular variables and BRS (**Figure 8**).

DISCUSSION

Our study represents the first attempt in any animal species to quantify the changes in spontaneous cardiac BRS after ICV and IA injections of UII and URP. The inhibitory effect of UII on the BRS after ICV injection of low picomolar doses, and its absence of effect after peripheral injection of equimolar doses suggests that only the central urotensinergic system is involved in the attenuation of the BRS. In addition, the limited and quite divergent BRS effects of the two structurally UII-related peptides URP1 and URP2, that share the cyclic hexapeptide core sequence

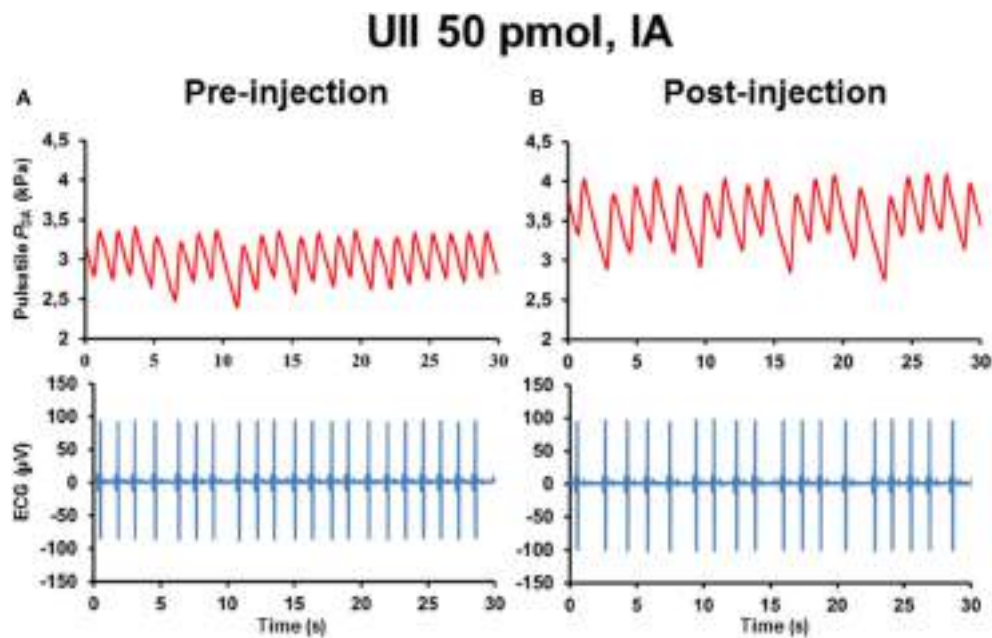


FIGURE 5 | Raw tracings of 30-s duration in a single unanesthetized trout showing the changes observed in pulsatile dorsal aortic blood pressure (P_{DA}) and electrocardiographic (ECG) signals between the pre-injection period (A) and the post-injection period (B) after intra-arterial (IA) injection of 50 pmol UII. Note that, compared with the pre-injection period, IA injection of UII provokes an increase in SBP and in the R-R interval of the ECG (reflecting a bradycardia).

of UII but differ in the N- and C-terminal regions (Table 1), emphasize the importance of the amino-acid residues flanking the N- and C-terminus of the cyclic region of the fish UII-molecule for full interaction with the fish UT receptor. This observation also indicates that the action of UII is specific for this peptide.

The baroreflex has been conserved across vertebrate's evolution (Bagshaw, 1985; Van Vliet and West, 1994) and, in fish as in mammals, the spontaneous BRS can be measured by means of cross spectrum analysis of R-R interval and SBP variabilities (Head et al., 2001; La Rovere et al., 2008; Lancien et al., 2011). This technique offers the great advantage to prevent the use of any stressful surgical interventions for loading or unloading the baroreceptors and circumvents the use of vasoactive drugs to evoke a baroreflex response, drugs that may interfere with baroreflex functioning. However, using this approach, we assessed only one aspect of the baroreflex loop, i.e., the baroreflex regulation of heart rate, but not the baroreflex regulation of vascular tone.

Central Effects of UII and URP

In fish, the primary baroreceptor sites are the gills (Ristori and Dessaix, 1970; Nilsson and Sundin, 1998; Armelin et al., 2016). Afferent baroreceptive activity runs along the glossopharyngeal (IXth cranial nerve) and along the vagus (Xth cranial nerve) to reach the medulla oblongata. Little is known regarding the central neuroregulatory mechanisms involved in the baroreflex responses in fish, except that glutamatergic pathways within the caudal part of the nucleus tractus solitarii (NTS) play a key role to transmit baroreceptive information to the dorsal

vagal motor nucleus (DVMN) and hence, to control the cardiac vagal outflow (Taylor et al., 1999; Sundin et al., 2003). In trout, we previously demonstrated that spontaneous increases or decreases in SBP provoke a bradycardia or a tachycardia, respectively, that are exclusively mediated by the parasympathetic nervous system and thus that the spontaneous BRS can be considered as an index of parasympathetic activity to the heart (Lancien and Le Mével, 2007). The level at which UII/URPs upon ICV injection mimic the possible action of the endogenous urotensinergic system(s) on the neural networks involved in the baroreflex response in trout, and notably on its cardio-vagal inhibitory component, cannot be established from the present experiments. However, some working hypotheses can be proposed. Since the exogenous peptides were injected into the third ventricle at the level of the nucleus preopticus, a nucleus homologous to the paraventricular nucleus of mammals, it is reasonable to speculate that UII/URPs might primarily affect the activity of preoptic neuropeptidergic neurons like arginine vasotocin and isotocin neurons that project toward critical cardiovascular brainstem nuclei including the NTS and the DVMN (Batten et al., 1990; Saito et al., 2004). In addition, the urotensin peptides may diffuse within the cerebrospinal fluid toward the fourth ventricle to control the activity of these cardiovascular nuclei. Since we previously demonstrated that, after peripheral injection of UII, bradycardia may arise from adrenergic-mediated activation of the cardio-inhibitory baroreflex (Le Mével et al., 1996), we can speculate that the reduced BRS after ICV injection of UII may also be due to blockage of central adrenergic pathways. Neuroanatomical and molecular data from various teleost species provide some clues

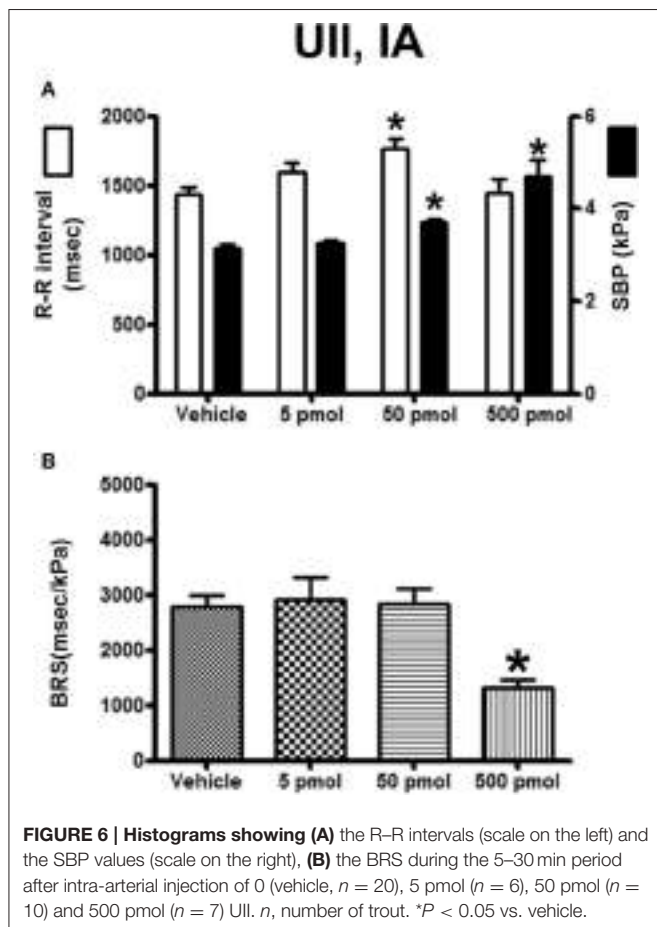


FIGURE 6 | Histograms showing (A) the R-R intervals (scale on the left) and the SBP values (scale on the right), **(B)** the BRS during the 5–30 min period after intra-arterial injection of 0 (vehicle, $n = 20$), 5 pmol ($n = 6$), 50 pmol ($n = 10$) and 500 pmol ($n = 7$) UII. n , number of trout. * $P < 0.05$ vs. vehicle.

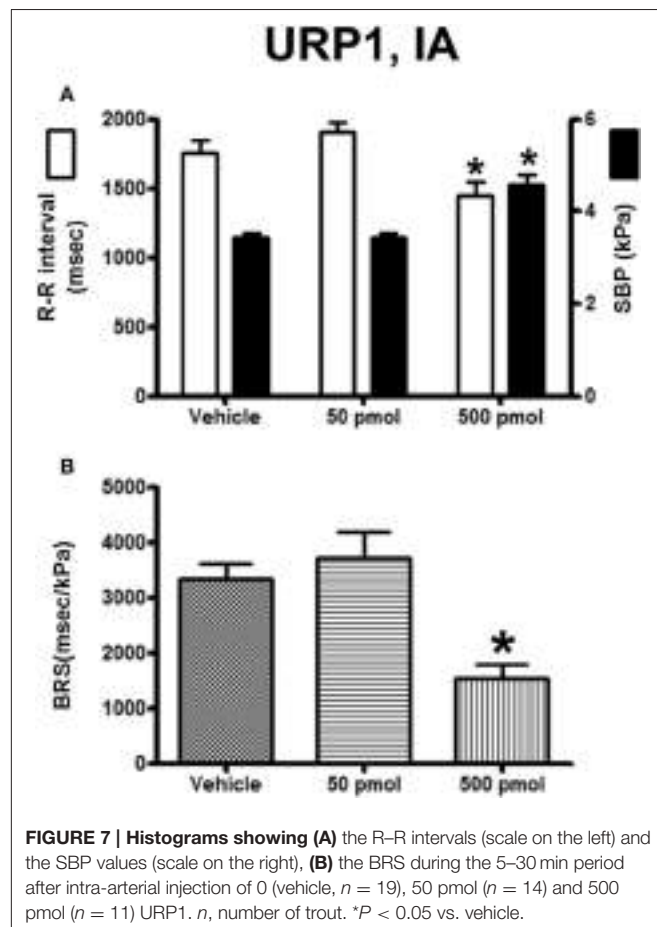
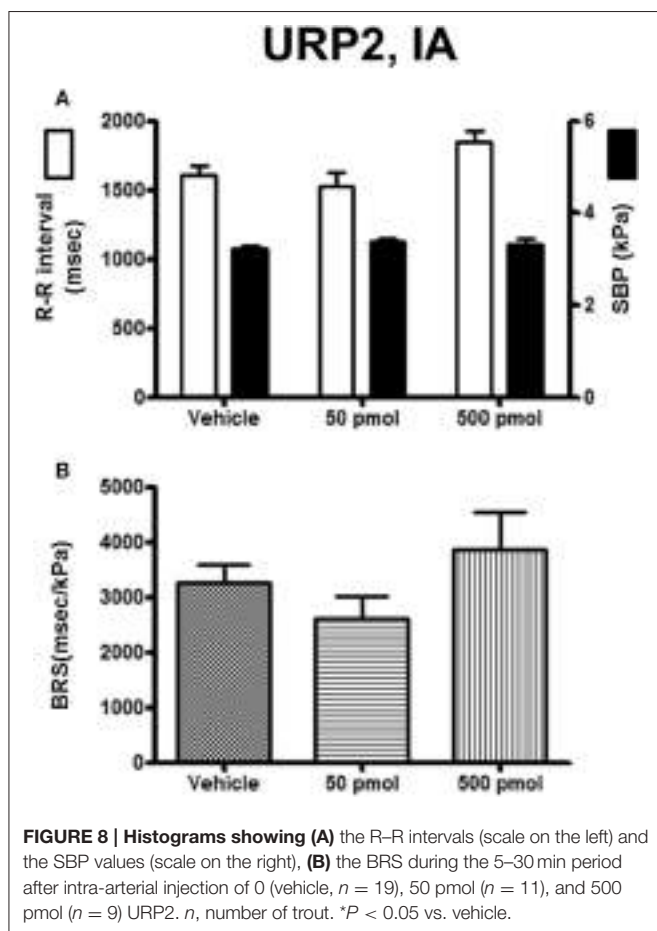


FIGURE 7 | Histograms showing (A) the R-R intervals (scale on the left) and the SBP values (scale on the right), **(B)** the BRS during the 5–30 min period after intra-arterial injection of 0 (vehicle, $n = 19$), 50 pmol ($n = 14$) and 500 pmol ($n = 11$) URP1. n , number of trout. * $P < 0.05$ vs. vehicle.

for these hypotheses. UT is expressed in the teleost brain (Lu et al., 2006) and UII immunoreactivity and URP2 expression are seen in the region surrounding the fourth ventricle (Yulis and Lederis, 1988; Parmentier et al., 2011; Quan et al., 2015) while URP1 is notably expressed in the NTS and the glossopharyngeal motor nuclei (Nobata et al., 2011; Quan et al., 2015). Whether UII/URP neurons present within the brainstem contribute more precisely to the control of the BRS by interacting with baroreflex afferent inputs at the level of the NTS remains to be elucidated.

Our results demonstrating that third ventricle injection of native UII in trout causes an attenuation of the BRS can be compared with previous cardiovascular studies conducted with UII in mammals. As previously mentioned, in normotensive and hypertensive unanesthetized rats (Lin et al., 2003) and in unanesthetized sheep (Watson et al., 2003), ICV administration of UII causes pressor and tachycardic responses through activation of the sympathetic system indicating that, in these species, also the cardiac baroreflex response is impaired. Studies conducted on unanesthetized sheep to test this hypothesis demonstrated that, after ICV infusion of UII, the cardiac baroreflex response is effectively blunted since no changes occur in the cardiac sympathetic nerve activity in spite of an increase in blood pressure (Hood et al., 2005). Since,

in sheep, ICV UII also stimulates the sympatho-adrenal axis resulting in elevation of plasma epinephrine (Watson et al., 2003) and since propranolol blocks UII-induced tachycardia (Hood et al., 2005), an increase in plasma level of epinephrine together with preservation of cardiac sympathetic nerve activity levels was postulated to be responsible for the chronotropic effect of centrally administered UII (Hood et al., 2005). Consequently, the cardiac baroreflex response to an increase in blood pressure after ICV injection of UII, in mammals, is probably impaired through the inability of central baroreflex networks to drive sufficient vagal cardiac inhibitory influx and to block cardiac sympathetic activity. It is known that, in mammals, the central cardiomodulatory action of UII is site-dependent as local administration of UII in discrete brain nuclei produces differential heart rate responses (Lin et al., 2003). Interestingly, a recent study in conscious rat demonstrates that micro-injection of UII within the nucleus ambiguus, a key site controlling parasympathetic cardiac tone, elicits a bradycardia, indicating the involvement of UII in controlling vagal outflow (Brailoiu et al., 2014). The regulation of the baroreflex in fish is probably as complex as in mammals, and further studies are required to determine more precisely the impact of UII/URPs on the cardio-vagal component of the baroreflex, as well as the potential effects of these peptides on sympathetic



outflow to cardiovascular and chromaffin tissues. We previously demonstrated that, after ICV injection of native neuropeptides in trout, angiotensin II (Lancien and Le Mével, 2007), pituitary adenylate cyclase-activating polypeptide and vasoactive intestinal peptide (Lancien et al., 2011) decrease BRS. The present study adds UII and to a lesser extend URP2 as new candidates acting centrally as neuromodulators or neurotransmitters to control the cardiac baroreflex.

Peripheral Effects of UII and URPs

The bradycardic response to UII-induced hypertension is parasympathetically-mediated since, in atropinized trout, this bradycardia is abolished (Vanegas et al., 2016). In the present study, ICV or IA administration of UII at its lowest doses caused similar hypertension but in contrast to its ICV effects, peripheral UII provoked a bradycardia and the BRS was not disturbed. These data support the idea that, after peripheral administration, UII does not affect vagal feedback gain on the heart. Nonetheless, a significant decrease in BRS was observed with the largest dose of UII. Since the BRS reduction to the highest dose of IA administered UII was very similar to that

observed after ICV injection of the same dose, we assume that this effect was mediated through a neurogenic pathway after diffusion of UII to critical target sites in the brain. However, because UT is also strongly expressed in the teleost heart (Lu et al., 2006), we cannot exclude a possible direct positive chronotropic effect of large doses of UII counter-acting the baroreflex response. According to the route of administration the highest dose of URP1 and URP2 had opposite effect on the BRS, URP2 being more efficient than URP1 in the brain and inversely at the periphery. It remains to be determined whether these opposite effects of URP1 and URP2 can be ascribed to differential interaction with UT or to binding to distinct UT subtypes. Moreover, since the two URPs are exclusively expressed in the CNS, the physiological significance of URP1 on BRS remains also to be ascertained.

Possible Physiological Significance

In humans, a decrease in the BRS is associated with hypertension and cardiovascular tissue damages (La Rovere et al., 2008). In fish, the essential role of the baroreflex is to prevent damage to organs primarily at risk, such as the delicate respiratory vasculature of the gills (Bagshaw, 1985). Consequently, endogenous UII, a peptide that provokes inhibition of BRS after central exogenous injection, may contribute to exacerbate the increase in blood pressure and may have deleterious effects. In the periphery, UII also causes hypertension but the maintenance of the BRS may be beneficial to prevent excessive elevation of blood pressure. This hypertension might be useful to correct hypotensive situations in order to maintain tissue perfusion pressure. Further studies are required to elucidate the site(s) and mechanisms of action of UII/URPs on the baroreflex pathways in trout and to determine under which circumstances the central and peripheral urotensinergic systems are recruited to regulate blood pressure.

In conclusion, our study has shown that UII and to a lesser extent URPs interact with CNS blood pressure-regulating structures, not only to elevate blood pressure and heart rate but also to reduce BRS. Conversely, at the periphery, UII at low picomolar doses increases blood pressure and decreases heart rate but does not alter BRS.

AUTHOR CONTRIBUTIONS

FL, GV, and JM, performed the experiments. JL synthetized the peptides. FL analyzed the data. FL and JM, wrote the manuscript. GV, JL, and HV, edited and revised critically the manuscript. All authors approved the final version of the manuscript.

ACKNOWLEDGMENTS

We thank Stéphanie Deshayes for her excellent technical assistance and care in the maintenance of the animals. This work was supported by the European Regional Development Fund (ERDF) for the Peptide Research Network of Excellence (PeReNE).

REFERENCES

- Ames, R. S., Sarau, H. M., Chambers, J. K., Willette, R. N., Aiyar, N. V., Romanic, A. M., et al. (1999). Human urotensin-II is a potent vasoconstrictor and agonist for the orphan receptor GPR14. *Nature* 401, 282–286. doi: 10.1038/45809
- Armelin, V. A., Braga, V. H., Teixeira, M. T., Rantin, F. T., Florindo, L. H., and Kalinin, A. L. (2016). Gill denervation eliminates the barostatic reflex in a neotropical teleost, the tambaqui (*Colossoma macropomum*). *Fish Physiol. Biochem.* 42, 1213–1224. doi: 10.1007/s10695-016-0211-9
- Bagshaw, R. J. (1985). Evolution of cardiovascular baroreceptor control. *Biol. Rev. Camb. Philos. Soc.* 60, 121–162.
- Batten, T. F., Cambre, M. L., Moons, L., and Vandesande, F. (1990). Comparative distribution of neuropeptide-immunoreactive systems in the brain of the green molly, *Poecilia latipinna*. *J. Comp. Neurol.* 302, 893–919. doi: 10.1002/cne.903020416
- Brailoiu, G. C., Deliu, E., Rabinowitz, J. E., Tilley, D. G., Koch, W. J., and Brailoiu, E. (2014). Urotensin II promotes vagal-mediated bradycardia by activating cardiac-projecting parasympathetic neurons of nucleus ambiguus. *J. Neurochem.* 129, 628–636. doi: 10.1111/jnc.12679
- Chatenet, D., Dubessy, C., Leprince, J., Boulanian, C., Carlier, L., Ségalas-Milazzo, I., et al. (2004). Structure-activity relationships and structural conformation of a novel urotensin II-related peptide. *Peptides* 25, 1819–1830. doi: 10.1016/j.peptides.2004.04.019
- Dun, S. L., Brailoiu, G. C., Yang, J., Chang, J. K., and Dun, N. J. (2001). Urotensin II-immunoreactivity in the brainstem and spinal cord of the rat. *Neurosci. Lett.* 305, 9–12. doi: 10.1016/S0304-3940(01)01804-3
- Head, G. A., Lukoshkova, E. V., Burke, S. L., Malpas, S. C., Lambert, E. A., and Janssen, B. J. (2001). Comparing spectral and invasive estimates of baroreflex gain. *IEEE Eng. Med. Biol. Mag.* 20, 43–52. doi: 10.1109/51.917723
- Hood, S. G., Watson, A. M., and May, C. N. (2005). Cardiac actions of central but not peripheral urotensin II are prevented by beta-adrenoceptor blockade. *Peptides* 26, 1248–1256. doi: 10.1016/j.peptides.2005.01.005
- Jégou, S., Cartier, D., Dubessy, C., Gonzalez, B. J., Chatenet, D., Tostivint, H., et al. (2006). Localization of the urotensin II receptor in the rat central nervous system. *J. Comp. Neurol.* 495, 21–36. doi: 10.1002/cne.20845
- Lancien, F., and Le Mével, J. C. (2007). Central actions of angiotensin II on spontaneous baroreflex sensitivity in the trout *Oncorhynchus mykiss*. *Regul. Pept.* 138, 94–102. doi: 10.1016/j.regpep.2006.08.008
- Lancien, F., Leprince, J., Mimassi, N., Mabin, D., Vaudry, H., and Le Mével, J. C. (2004). Central effects of native urotensin II on motor activity, ventilatory movements, and heart rate in the trout *Oncorhynchus mykiss*. *Brain Res.* 1023, 167–174. doi: 10.1016/j.brainres.2004.07.008
- Lancien, F., Mimassi, N., Conlon, J. M., and Le Mével, J. C. (2011). Central pituitary adenylate cyclase-activating polypeptide (PACAP) and vasoactive intestinal peptide (VIP) decrease the baroreflex sensitivity in trout. *Gen. Comp. Endocrinol.* 171, 245–251. doi: 10.1016/j.ygcen.2011.02.006
- La Rovere, M. T., Pinna, G. D., and Raczak, G. (2008). Baroreflex sensitivity: measurement and clinical implications. *Ann. Noninvasive Electrocardiol.* 13, 191–207. doi: 10.1111/j.1542-474X.2008.00219.x
- Le Mével, J. C., Lancien, F., Mimassi, N., and Conlon, J. M. (2012). Brain neuropeptides in central ventilatory and cardiovascular regulation in trout. *Front. Endocrinol. (Lausanne)*. 3:124. doi: 10.3389/fendo.2012.00124
- Le Mével, J. C., Olson, K. R., Conklin, D., Waugh, D., Smith, D. D., Vaudry, H., et al. (1996). Cardiovascular actions of trout urotensin I in the conscious trout, *Oncorhynchus mykiss*. *Am. J. Physiol.* 271(5 Pt 2), R1335–R1343.
- Lin, Y., Tsuchihashi, T., Matsumura, K., Abe, I., and Iida, M. (2003). Central cardiovascular action of urotensin II in conscious rats. *J. Hypertens.* 21, 159–165. doi: 10.1097/01.hjh.0000045518.21915.ec
- Lu, W., Greenwood, M., Dow, L., Yuill, J., Worthington, J., Brierley, M. J., et al. (2006). Molecular characterization and expression of urotensin II and its receptor in the flounder (*Platichthys flesus*): a hormone system supporting body fluid homeostasis in euryhaline fish. *Endocrinology* 147, 3692–3708. doi: 10.1210/en.2005-1457
- Nilsson, S., and Sundin, L. (1998). Gill blood flow control. *Comp. Biochem. Physiol. A Mol. Integr. Physiol.* 119, 137–147.
- Nobata, S., Donald, J. A., Balment, R. J., and Takei, Y. (2011). Potent cardiovascular effects of homologous urotensin II (UII)-related peptide and UII in unanesthetized eels after peripheral and central injections. *Am. J. Physiol. Regul. Integr. Comp. Physiol.* 300, R437–R446. doi: 10.1152/ajpregu.00629.2010
- Olson, K. (2011). “Integrated control and response of the circulatory system. Integrated control of the circulatory system,” in *Encyclopedia of Fish Physiology: From Genome to Environment*, ed P. Farrell (South Bend: Elsevier Inc.), 1169–1177.
- Parmentier, C., Hameury, E., Dubessy, C., Quan, F. B., Habert, D., Calas, A., et al. (2011). Occurrence of two distinct urotensin II-related peptides in zebrafish provides new insight into the evolutionary history of the urotensin II gene family. *Endocrinology* 152, 2330–2341. doi: 10.1210/en.2010-1500
- Pearson, D., Shively, J. E., Clark, B. R., Geschwind, I. I., Barkley, M., Nishioka, R. S., et al. (1980). Urotensin II: a somatostatin-like peptide in the caudal neurosecretory system of fishes. *Proc. Natl. Acad. Sci. U.S.A.* 77, 5021–5024.
- Pelletier, G., Lührmann, I., and Vaudry, H. (2002). Role of androgens in the regulation of urotensin II precursor mRNA expression in the rat brainstem and spinal cord. *Neuroscience* 115, 525–532. doi: 10.1016/S0306-4522(02)00413-X
- Quan, F. B., Dubessy, C., Galant, S., Kenigfest, N. B., Djennoune, L., Leprince, J., et al. (2015). Comparative distribution and *in vitro* activities of the urotensin II-related peptides URP1 and URP2 in zebrafish: evidence for their colocalization in spinal cerebrospinal fluid-contacting neurons. *PLoS ONE* 10:e0119290. doi: 10.1371/journal.pone.0119290
- Ristori, M. T., and Dessaux, G. (1970). Sur l'existence d'un gradient de sensibilité dans les récepteurs branchiaux de *Cyprinus carpio* L. C. R. Séances Soc. Biol. Fil. 164, 1517–1519.
- Saito, D., Komatsuda, M., and Urano, A. (2004). Functional organization of preoptic vasotocin and isotocin neurons in the brain of rainbow trout: central and neurohypophysial projections of single neurons. *Neuroscience* 124, 973–984. doi: 10.1016/j.neuroscience.2003.12.038
- Sundin, L., Turesson, J., and Taylor, E. W. (2003). Evidence for glutamatergic mechanisms in the vagal sensory pathway initiating cardiorespiratory reflexes in the shorthorn sculpin *Myoxocephalus scorpius*. *J. Exp. Biol.* 206(Pt 5), 867–876. doi: 10.1242/jeb.00179
- Taylor, E. W., Jordan, D., and Coote, J. H. (1999). Central control of the cardiovascular and respiratory systems and their interactions in vertebrates. *Physiol. Rev.* 79, 855–916.
- Tostivint, H., Ocampo Daza, D., Bergqvist, C. A., Quan, F. B., Bougerol, M., Lührmann, I., et al. (2014). Molecular evolution of GPCRs: somatostatin/urotensin II receptors. *J. Mol. Endocrinol.* 52, T61–T86. doi: 10.1530/jme-13-0274
- Tostivint, H., Quan, F. B., Bougerol, M., Kenigfest, N. B., and Lührmann, I. (2013). Impact of gene/genome duplications on the evolution of the urotensin II and somatostatin families. *Gen. Comp. Endocrinol.* 188, 110–117. doi: 10.1016/j.ygcen.2012.12.015
- Vanegas, G., Lancien, F., Leprince, J., Vaudry, H., and Le Mével, J. C. (2016). Effects of peripherally administered urotensin II and arginine vasotocin on the QT interval of the electrocardiogram in trout. *Comp. Biochem. Physiol. C Toxicol. Pharmacol.* 183–184, 53–60. doi: 10.1016/j.cbpc.2016.01.006
- Vanegas, G., Leprince, J., Lancien, F., Mimassi, N., Vaudry, H., and Le Mével, J. C. (2015). Divergent cardio-ventilatory and locomotor effects of centrally and peripherally administered urotensin II and urotensin II-related peptides in trout. *Front. Neurosci.* 9:142. doi: 10.3389/fnins.2015.00142
- Van Vliet, B. N., and West, N. H. (1994). Phylogenetic trends in the baroreceptor control of arterial blood pressure. *Physiol. Zool.* 67, 1284–1304.
- Vaudry, H., Do Rego, J. C., Le Mével, J. C., Chatenet, D., Tostivint, H., Fournier, A., et al. (2010). Urotensin II, from fish to human. *Ann. N. Y. Acad. Sci.* 1200, 53–66. doi: 10.1111/j.1749-6632.2010.05514.x
- Vaudry, H., Leprince, J., Chatenet, D., Fournier, A., Lambert, D. G., Le Mével, J. C., et al. (2015). International union of basic and clinical pharmacology. XCII. Urotensin II, urotensin II-related peptide, and their receptor: from structure to function. *Pharmacol. Rev.* 67, 214–258. doi: 10.1124/pr.114.009480
- Watson, A. M., Lambert, G. W., Smith, K. J., and May, C. N. (2003). Urotensin II acts centrally to increase epinephrine and ACTH release and cause potent inotropic and chronotropic actions. *Hypertension* 42, 373–379. doi: 10.1161/01.hyp.0000084633.85427.e6

- Watson, A. M., and May, C. N. (2004). Urotensin II, a novel peptide in central and peripheral cardiovascular control. *Peptides* 25, 1759–1766. doi: 10.1016/j.peptides.2004.04.016
- Waugh, D., and Conlon, J. M. (1993). Purification and characterization of urotensin II from the brain of a teleost (trout, *Oncorhynchus mykiss*) and an elasmobranch (skate, *Raja rhina*). *Gen. Comp. Endocrinol.* 92, 419–427. doi: 10.1006/gcen.1993.1178
- Yulis, C. R., and Lederis, K. (1988). Occurrence of an anterior spinal, cerebrospinal fluid-contacting, urotensin II neuronal system in various fish species. *Gen. Comp. Endocrinol.* 70, 301–311.

Conflict of Interest Statement: The authors declare that the research was conducted in the absence of any commercial or financial relationships that could be construed as a potential conflict of interest.

Copyright © 2017 Lancien, Vanegas, Leprince, Vaudry and Le Mével. This is an open-access article distributed under the terms of the Creative Commons Attribution License (CC BY). The use, distribution or reproduction in other forums is permitted, provided the original author(s) or licensor are credited and that the original publication in this journal is cited, in accordance with accepted academic practice. No use, distribution or reproduction is permitted which does not comply with these terms.



The G Protein-Coupled Receptor UT of the Neuropeptide Urotensin II Displays Structural and Functional Chemokine Features

Hélène Castel^{1,2*†}, Laurence Desrues^{1,2†}, Jane-Eileen Joubert^{1,2}, Marie-Christine Tonon^{1,2}, Laurent Prézeau³, Marie Chabbert⁴, Fabrice Morin^{1,2} and Pierrick Gandolfo^{1,2}

¹ Normandie University, UNIROUEN, INSERM, DC2N, Rouen, France, ² Institute for Research and Innovation in Biomedicine (IRIB), Rouen, France, ³ CNRS UMR 5203, INSERM U661, Institute of Functional Genomic (IGF), University of Montpellier 1 and 2, Montpellier, France, ⁴ UMR CNRS 6214, INSERM 1083, Faculté de Médecine 3, Angers, France

OPEN ACCESS

Edited by:

Stephane Gasman,
Centre national de la recherche
scientifique (CNRS), France

Reviewed by:

Carole ROVERE-JOVENE,
Centre national de la recherche
scientifique (CNRS), France
Leo T. O. Lee,
University of Macau, China

*Correspondence:

Hélène Castel
helene.castel@univ-rouen.fr

[†]Co-first authors.

Specialty section:

This article was submitted
to Neuroendocrine Science,
a section of the journal
Frontiers in Endocrinology

Received: 19 December 2016

Accepted: 28 March 2017

Published: 25 April 2017

Citation:

Castel H, Desrues L, Joubert J-E, Tonon M-C, Prézeau L, Chabbert M, Morin F and Gandolfo P (2017) The G Protein-Coupled Receptor UT of the Neuropeptide Urotensin II Displays Structural and Functional Chemokine Features. *Front. Endocrinol.* 8:76. doi: 10.3389/fendo.2017.00076

The urotensinergic system was previously considered as being linked to numerous physiopathological states, including atherosclerosis, heart failure, hypertension, pre-eclampsia, diabetes, renal disease, as well as brain vascular lesions. Thus, it turns out that the actions of the urotensin II (UII)/G protein-coupled receptor UT system in animal models are currently not predictive enough in regard to their effects in human clinical trials and that UII analogs, established to target UT, were not as beneficial as expected in pathological situations. Thus, many questions remain regarding the overall signaling profiles of UT leading to complex involvement in cardiovascular and inflammatory responses as well as cancer. We address the potential UT chemotactic structural and functional definition under an evolutionary angle, by the existence of a common conserved structural feature among chemokine receptorsopioïdergic receptors and UT, i.e., a specific proline position in the transmembrane domain-2 TM2 (P2.58) likely responsible for a kink helical structure that would play a key role in chemokine functions. Even if the last decade was devoted to the elucidation of the cardiovascular control by the urotensinergic system, we also attempt here to discuss the role of UII on inflammation and migration, likely providing a peptide chemokine status for UII. Indeed, our recent work established that activation of UT by a gradient concentration of UII recruits Gαi/o and Gα13 couplings in a spatiotemporal way, controlling key signaling events leading to chemotaxis. We think that this new vision of the urotensinergic system should help considering UT as a chemotactic therapeutic target in pathological situations involving cell chemoattraction.

Keywords: G protein-coupled receptor, UT, urotensin II, proline, chemokine, migration

INTRODUCTION

The urotensinergic system was previously considered as being linked to numerous pathophysiological states, including atherosclerosis, heart failure, hypertension, pre-eclampsia, diabetes, renal disease, as well as brain vascular lesions. Based on this expectation, validation of urotensin II (UII) receptor (UT) antagonism in cell lines expressing rat or human UT, observations in animal models, and even clinical results were not as beneficial as expected, probably because of the complex effects of the urotensinergic system depending on the vascular bed, the studied animal species, and/or

the administration route. Thus, it turns out that the actions of the UII/UT system in animal models are currently not predictive enough in regard to their effects in human clinical trials, thus many questions remain regarding the overall signaling profiles of UT leading to complex involvement in cardiovascular, inflammatory responses, and cancer. We, here, propose that UII may rather play chemokine functions leading to long-term tissue remodeling and tumorigenesis, at least in part due to the pleiotropic functions of UT oriented toward chemoattractant activities.

THE UII PEPTIDE SYSTEM

Endogenous Urotensinergic Peptide Ligands, from Gene to Sequence

At the end of the 1960s, Drs. Bern and Lederis attributed the name “urotensins” to a series of biologically active peptides isolated from the urophysis neurosecretory system of the teleost fish *Gillichthys mirabilis*. Among those, UII was characterized through its ability to stimulate smooth muscle cells (1). Then, the amino acid sequence of UII was subsequently identified in a number of other fish species, and the presence of the UII peptide was discovered in the brain of a tetrapod, the frog *Rana ridibunda* (2, 3) two decades later (Table 1). Based on these observations, the gene encoding UII has been the subject of more research and was successfully identified in various mammalian species including in monkey and human (Table 1) (4, 5). The neuropeptide UII is composed of 11 amino acids in primates (including *Homo sapiens*) to 17 amino acids in the mouse and shows remarkable conservation of the C-terminal CFWKYC hexapeptide portion formed by the

covalent disulfide bridge (Table 1) during evolution, suggesting a crucial importance of the cycle in biological activity. To date, UII has been characterized in a single species of invertebrates, the *Aplysia californica* (6), in a form composed of 20 amino acids and whose cyclic hexapeptide differs from vertebrates by only two residues (F→L and Y→V) (7).

All the amino acid sequences of UII identified so far are mostly deduced from cDNAs and correspond to the C-terminal part of its precursor. In human, the deduced sequence of prepro-UII, cloned from colon tumor or placental library, evolved from alternative splicing of the human UTS2 gene, yielding a 124 (isoform b, NP_006777) and 139 (isoform a, NP_068835.1) amino acid variants. The two encoded isoforms are identical for the last 97 amino acids but differ at their N-terminal end exhibiting the signal peptide. The mature peptide UII results from the proteolysis of preproprotein UII at the tribasic site KKR by a specific urotensin converting enzyme (UCE), which is not still identified (4, 5). Study on the conversion of a 25 amino acid C-terminal fragment of preproprotein to mature peptide revealed that the endoprotease Furin and the serine protease trypsin, may act, respectively, as intracellular and extracellular UCE (12). This enzymatic cleavage appears necessary to confer biological activity (13).

In comparison with primate prepro-UII, precursors of rat and mouse UII markedly diverge by the amino acid composition of the N-flanking domain of the cyclic hexapeptide and by the absence of a typical cleavage site (KKR) for pro-hormone converting enzymes in the upstream region of UII sequence (10). These observations led Sugo and collaborators to characterize UII immunoreactivity detected in the brain of the two rodent species and to isolate, in 2003, a peptide similar to UII, the

TABLE 1 | Comparison of the sequences of urotensin II (UII) and urotensin II-related peptide (URP) in different species of tetrapods.

Family	Species		Peptide sequences	
	Scientific names	Common names	UII	URP
Tetrapods	<i>Pelophylax ridibundus</i>	Frog	AGNLSECFWKYCV(2)	
	<i>Hyla arborea</i>	Tree frog	AGNLSECFWKYCV(2)	
	<i>Xenopus laevis</i>	Xenope	GNLSECFWKYCV	ACFWKYCV
	<i>Gallus gallus</i>	Chicken	GNLSECFWKYCV	ACFWKYCI
	<i>Taeniopygia guttata</i>	Zebra finch	GNLSECFWKYCV	ACFWKYCI
	<i>Felis catus</i>	Cat	GPSPSECFWKYCV	
	<i>Sus scrofa</i>	Pig	GPPSECFWKYCV(8)	
	<i>Ovis aries</i>	Sheep	GPSSECFWKYCV	
	<i>Bos taurus</i>	Cattle	GPSSECFWKYCV	
	<i>Rattus norvegicus</i>	Rat	QHGTAPECFWKYCI (5)	ACFWKYCV (9)
	<i>Mus musculus</i>	Mouse	QHKQHGAAPCFWKYCI (10)	ACFWKYCV (9)
	<i>Otolemur garnettii</i>	Galago	GTPSECFWKYCV	ACFWKYCV
	<i>Callithrix jacchus</i>	Marmoset	ETPDCFWKYCV	
	<i>Papio anubis</i>	Baboon	ETPDCFWKYCV	ACFWKYCV
	<i>Macaca mulatta</i>	Rhesus monkey	ETPDCFWKYCV	ACFWKYCV
	<i>Macaca fascicularis</i>	Macaque	ETPDCFWKYCV	
	<i>Nomascus leucogenys</i>	Gibbon	ETPDCFWKYCV	
	<i>Pongo abelii</i>	Orangutan	ETPDCFWKYCV	ACFWKYCV
	<i>Gorilla gorilla</i>	Gorilla	ETPDCFWKYCV	ACFWKYCV
	<i>Homo sapiens</i>	Human	ETPDCFWKYCV (5)	ACFWKYCV
	<i>Pan paniscus</i>	Bonobo	ETPDCFWKYCV	ACFWKYCV
	<i>Pan troglodytes</i>	Chimpanzee	ETPDCFWKYCV (11)	ACFWKYCV

The biologically active sequence of the peptides, highlighted in red, is conserved in all tetrapods.

urotensin II-related peptide (URP) (9). Later on, the cloning of the prepro-URP cDNAs, in human, mouse, and rat revealed 54% homology between human and rat vs 47% homology between human and mouse (14). However, the URP sequence is identical in all mammals and corresponds to human Ala¹-UII₄₋₁₁. Finally, although URP was initially thought to exist only in tetrapods, its gene has been identified in the genome of several teleost fishes (15, 16). Together, the sequences of UII, URP, and somastostatin display high homology in particular at the level of the cyclic hexapeptide sequence and it was established that URP is a peptide paralog of UII (17).

General Distribution of UII and Urotensin II-Related Peptide

Urotensin II and URP are widely distributed in the cardiovascular, renal, and endocrine systems. In humans, high expression levels of UII are found in the myocardium (18), the atria, and the ventricles (19–21). UII has also been detected in the heart of rats (4, 9, 20) and mice (11, 22). At the vascular level, the presence of mRNA for prepro-UII has been demonstrated in the arterial network, primarily in the thoracic aorta, pulmonary arteries, and arterioles. In contrast, it is almost absent in the venous network, with the exception of the saphenous and umbilical veins (19–21).

Several studies show that kidney is a major site of production of circulating UII in humans (9, 20, 21, 23, 24). The peptide is particularly abundant in glomerular epithelial cells, convoluted tubules, and collecting ducts (20, 25). Surprisingly, the level of expression of UII in the kidney of monkey and mice is weak (11), stressing some important differences between species. UII is also expressed in endocrine glands, such as pancreas or adrenal gland, in humans and rats (5, 23, 26). Nevertheless, the mRNA for UII is undetectable in these tissues in monkey and mice (11, 22), again raising the question of the occurrence of a conserved cardiovascular and/or endocrine role of UII among the different species.

Even though the identification of URP has been done more than 10 years ago, data concerning this peptide are considerably much more incomplete. Nevertheless, it is worth noting that the expression of prepro-URP is predominant in the gonads and placenta of humans and in the testis of rats (9). URP and its mRNA are also expressed in kidney (8, 9) and in the ventricles and myocardium of the rat heart (27, 28). The expression of the two peptides extends to the spleen, thymus, liver, stomach, and intestines (5, 9, 11, 20, 22, 23, 29, 30).

Within the central nervous system (CNS), UII immunoreactivity is mainly associated with motoneurons of the hypoglossal nucleus of the brainstem and the ventral horn of the spinal cord. This neuronal subpopulation also strongly expresses UII in the nuclei of the abducens, facial, trigeminal, and hypoglossal cranial nerves in rats (10, 31) and those of the caudal part of the spinal cord in mice (10, 32), rats (10, 31), and humans (4, 5). Surprisingly, UII is apparently absent from the brainstem of monkey (4, 11). URP mRNAs are localized in the spinal cord of humans and rats, at expression levels considerably lower than those of UII (9). In mice, URP mRNA is found in the brainstem and in motoneurons of the anterior horn of the spinal cord (22). Finally, URP is present in neuronal cell bodies of the preoptic region and in fibers of the

median eminence and the organum vasculosum of the lamina terminalis, which is involved in thermoregulation (33).

Thus, UII and URP are not ubiquitously expressed within the peripheral and central nervous systems and likely show key expression levels in heart, arterial networks, and kidney with discrepancies between species, suggesting a non-conserved role in the vasomotor tone regulation.

UII RECEPTOR UT RECONSIDERED IN LIGHT OF CONSERVED STRUCTURAL PROPERTIES

The UT receptor was initially discovered and cloned in 1995 from rat sensory tissue extracts (34) and a rat genomic library (35). At this stage, this G protein-coupled receptor (GPCR) was named sensory epithelium neuropeptide-like by Tal et al. (34) and GPR14 (according to the current nomenclature) by Marchese et al. (35). Whereas Ames et al. identified the UII peptide as the endogenous ligand of the human receptor homologous to GPR14 by reverse pharmacology (4), other research teams in the same year corroborate the existence of the UII/GPR14 system in various species (8, 36, 37). It is on the basis of these studies that the receptor was renamed UII receptor or UT, by the International Union of Basic and Clinical Pharmacology (IUPHAR).

Distribution of UT Varies Depending on Species and Systems

The presence of substantial amounts of UII in the cardiovascular system has led several groups to investigate the expression of UT mRNA in different component tissues in rat (37–39) and mouse (36). In human and monkey, high levels of mRNA-encoding UT have been detected in the myocardium (18), the atria (4, 11, 21, 23), and the ventricles (4, 20, 23). At the vascular level, the presence of UT has been detected in the thoracic aorta (4, 21, 40) as well in the pulmonary and coronary arteries (41). In addition, UT, like UII, is strongly expressed in kidney from rat (27, 38, 42–46) and human (21, 23, 24, 41, 47), although it is only moderately expressed in monkey (44). UT is also present in the endocrine system, notably in the pituitary, pancreas, and adrenal gland in human (4, 23), monkey, and mice (11). Other peripheral tissues show significant levels of UT expression, which varies according to the species studied. The CNS shows widespread expression of UT mRNA, which is particularly abundant in the brainstem and spinal cord (23, 24, 36, 38, 48).

Other regions of the CNS, e.g., the cortex, hypothalamus, and thalamus, display relatively weak expression levels that vary between species. UT is also associated with cerebral blood vessels and is expressed mainly in the endothelial cells of microvessels (49). Finally, the expression of the receptor has been detected both in neurons (48) and in a subpopulation of astrocytes in the brainstem and hypothalamus (50) and in cultured cortical astrocytes (51).

Together, this UT distribution highly resembles the UII/URP distribution in cardiovascular endocrine and also nervous tissues, naturally leading several groups to investigate the effects of UT on the cardiovascular system, even if the data remain

multiple and complex. In human, circulating levels of UII and/or URP (“UII-like”) are higher in patients with heart failure (52, 53), systemic (54) or portal hypertension (55, 56), or atherosclerosis (57), than in plasma of healthy volunteers. In fact, the UT-related mechanisms appear associated with tissue remodeling processes during the course of the disease (58), including cardiac hypertrophy and fibrosis (59). Thus, we here question whether UT may play an alternative chemokine-like function in primates than vasomotor regulatory activities as previously proposed in rats.

The UT Positioning Depends on the Different GPCR Classifications

Although GPCRs share a common structure, certain characteristics make it possible to distinguish and to classify them in different families. However, based on the homology of sequence, structure, ligand binding mode, or phylogenetic relationships, the large number of GPCRs makes it difficult to develop a global classification system. The human UT receptor was shown to belong to the class A (Rhodopsin) GPCR family (60) according to the widely used structural classification in the past, based on the identification, by analysis of protein sequences of the TMs of the GPCRs listed in vertebrates and invertebrates, of fingerprints preserved within certain GPCR groups (61). GPCR members of class A (the largest family of GPCRs with 80% of GPCRs listed) share homologies of sequence, structure, and ligand-binding mode. The homologies of sequence between the receptors of class A can be very low since they rely on the conservation of a few residues mainly located in the TMs, which would play a primordial role in their structure and functionality. Within this classification, UT displays sequence homology not only with certain somatostatin receptors (SST), in particular with SST4 (27%), but also opioïdergic receptors (MOR: 26%, DOR: 26%, and KOR: 25%) (35), which are now crystallized (62, 63) and would constitute the best prototypes for UT modeling.

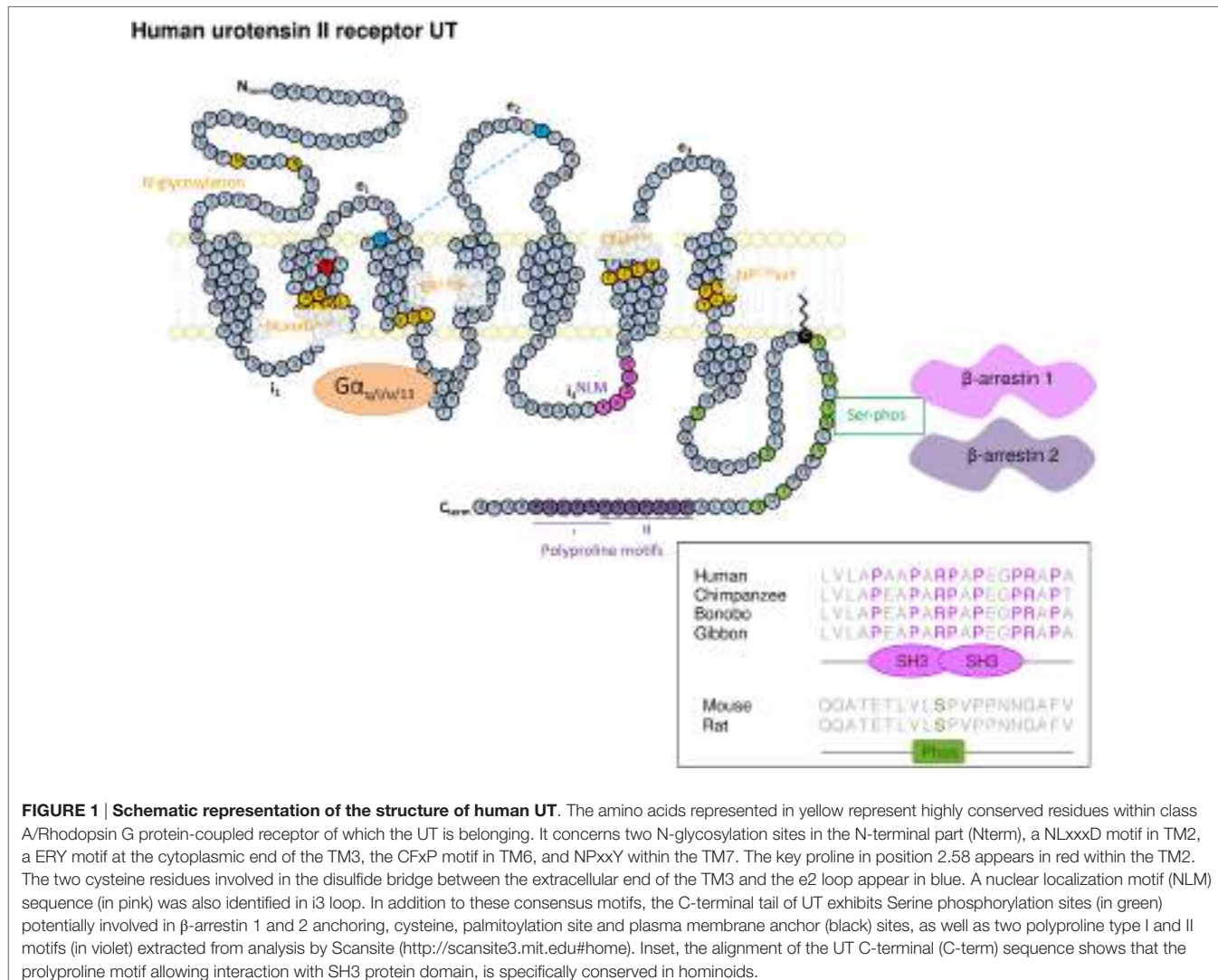
More recently, Fredriksson et al. (64) proposed from the GPCR sequences a yet commonly used systematic classification system named GRAFS formed by the five distinct families of Glutamate (G), Rhodopsin-like (R), Adhesion (A), Frizzled/Taste (F), and Secretin (S). The Rhodopsin-like family showed a clear evolutionary success since containing around 90% of the GPCRs and is divided into four (α , β , γ , and δ) subclasses in Fredriksson's classification. The crystallographic structures of Rhodopsin-like family indicate a common firm core corresponding to high conserved sequence motifs, i.e., E/DRY in TM3, NPXXY on TM7, WXP on TM6, D2.50 in TM2 (X.50, according to the Ballesteros classification: X, numbering of TM; 50, the most conserved residue in the concerned TM) (65), and a water network that can be seen in the binding pocket mediating ligand interactions with the receptor (66). It can be noticed that the γ group includes 59 GPCRs, divided into three different clusters, i.e., SOG (15 GPCRs like SST, OR or GPR54 receptor also named KISS1R), melanin-concentrating hormone receptors (MCHR) (2 GPCRs), and CHEM (42 GPCRs) including chemokine receptors, such as the CXCR4, angiotensin (ANG), and bradykinin (BK) receptors, as well as a large number of orphan receptors. However, the neighbor-joining and maximum parsimony method used in sequence

analysis failed to affect 23 receptors into one family/group/cluster, and this is the case for UT (named GPR14 in this study). These difficulties were due to an unusual part of the GPCR gene sequence in question [usually coding for intra- (i) or extracellular (e) loops] that would result from a chimeric origin of the receptor and/or progressive pressure not shared by neighboring receptors (64). However, UT shares the sequence pattern characteristic of Rhodopsin-like GPCRs. When comparing different sub-families of GPCRs from the conserved ligand binding pocket or from conserved endogenous agonist ligands (67), UT can be found near GPR109A or purinergic P2Y receptors listed in orphan receptors from the SOG or PUR cluster group by Fredriksson et al. (64, 67). In light of these results, we suggest that UT possesses specific structures and functions related to the chemokine receptors of the SOG and PUR families.

Thus, as members of the Rhodopsin SOG and PUR family, UT has a relatively short N-terminal domain with two N-glycosylation sites (N29 and N33), a NLxxxD2.50 motif within its TM2, a disulfide bridge between cysteine residues in the extracellular end of TM3 and the e2 loop, a ER3.50Y motif at the cytoplasmic end of the TM3, a CFxP6.50 motif within the TM6, the highly conserved NP7.50xxY motif at the TM7 level, and a palmitoylation site at the C-terminal tail (C334) (68). Other specific motifs are observed, namely (i) a KRARR nuclear localization motif at the i3 loop (69), (ii) potential sites of phosphorylation by protein kinases A and C, kinase I, and glycogen synthase kinase 3 at i2 and i3 loops (35, 68, 70), (iii) serine potential phosphorylation sites at the C-terminal end involved in β -arrestin interaction and internalization of the receptor (71, 72), and (iv) polyproline type I and II motifs within the C-terminal tail potentially allowing the interaction with proteins harboring src homology 3 type domains (Figure 1).

UT Shares a Structural Feature with Chemotactic GPCRs: An Evolutionary Lighting

These human GPCR classifications were proposed from constructions of phylogenetic trees, which require the use of several methods to assess the robustness of the obtained results. However, other strategies should be used when a position dependency hypothesis is questioned, the size of the dataset becomes large, and/or the relationships between proteins of the same family but of different genomes must be compared. Thus, to address some ambiguities concerning GPCRs classification, as highlighted for UT, analyses of gene sequences by the metric multidimensional scaling (MDS) were conducted. MDS is also called “principal coordinates analysis” and corresponds to an exploratory multivariate procedure designed to identify patterns, within proteins for example, in a distance matrix (73, 74). With MDS, protein sequences can be considered all at once, and individually represented in a low-dimensional space whose respective distances best approximate the original distances. In addition, MDS allows the projection of supplementary information allowing a straightforward comparison of the active and supplementary data. Therefore, MDS was used to explore the sequence space of GPCR families and to interpret patterns in relation with evolution, with projection of GPCR



sequences from distant species onto the active space of human GPCRs (75, 76), based on the assumption that GPCR evolution could follow a radial rather than bifurcated path (represented by the classical phylogenetic tree system). The phylogenetic links between GPCRs of the same species were represented in three dimensions, and the results were shown superimposed between several species (75). By means of this evolutionary-based classification, the work of the Chabbert's group succeeded in identifying GPCRs of the Rhodopsin class in the same clusters as those found by Fredriksson et al. (76), but some differences at the margin were also identified and likely stressed the way how some GPCRs may be activated and function. The differences are as follows: galanin receptors and Kiss1R belonging to the SOG cluster in the Fredriksson et al. classification, are likely rather connected to the PEP cluster according to Chabbert et al., and then SOG becomes SO cluster. In addition, the MCHR and UT appeared in this new classification, grouped in this SO cluster (76).

This is probably the evolutionary point of view that gives the best indications about UT membership and structural characteristics. Indeed, MDS analysis of GPCRs of the Rhodopsin family

allowed the receptors to be sorted into four groups (G0–G3) comprising different clusters (76). The group G0 represents the central group and includes the clusters PEP, OPN, and MRN, the group G1 includes the cluster SO (SST, OR, and UT), CHEM, and PUR (**Table 2**), the group G2 contained AMIN and AD clusters and finally G3 involves LGR, MEC, PTG, and MRG clusters (**Table 2**). It is interesting to note that in *C. intestinalis*, the CHEM cluster only slightly differs from the SO cluster, thus suggesting that this SO/CHEM group gave rise, in vertebrates, to SO, CHEM, and PUR clusters, suggesting a common origin. Moreover, the cluster SO and PEP are close in the most distant ancestral species from human and their distance increases during evolution (75). These observations argue in favor of a common origin between PEP and SO, CHEM, and PUR clusters (76) and allow the repositioning of UT from a “peptide family (PEP)” group to a chemokine receptor family.

Sequence comparison of the different groups (G0–G3) shows that the main characteristic of the G1 group receptors, including UT is a proline within the TM2 in position 2.58 (P2.58), often preceded by an aliphatic residue whereas G0 group mainly comprises

TABLE 2 | Assignment of the 13 non-olfactory human G protein-coupled receptor clusters from the rhodopsin class into four groups, G0, G1, G2, and G3, in addition to an UC.

Group	Family	Pattern	Homo sapiens
G0	PEP <i>Peptide</i>	P2.58	MTLR, GHSR
		P2.59	NMUR1, NMUR2, NTR1, NTR2, GPR39, EDNRA, EDNRB, ETBR2, GPR37, PKR1, PKR2, NPY1R, NPY2R, NPY4R, NPY5R, BRS3, GRPR, NMBR, CCKAR, GASR, QRFP, OX1R, OX2R, NPFF1, NPFF2, PRLHR, GNRR2, GNRHR, GPR83, GALR1, GALR2, GALR3, KISSR, GP151, GP173, GPR19, GPR27, GPR84, GPR85
		P2.60	V1AR, V1BR, V2R, OXYR, TRFR
	OPN <i>Opsin</i>	NoP	NK1R, NK2R, NK3R, GP150
		P2.59	OPN4, OPSX
		P2.60	OPSB
		NoP	OPN3, OPN5, RGR, OPSR, OPSD
	MTN <i>Melatonin</i>	P2.59	MTR1A, MTR1B, MTR1L
G1	SO <i>Somatostatinergic opiodergic</i>	P2.58	OPRM, OPRD, OPRK, OPRX, SSR1, SSR2, SSR3, SSR4, SSR5, NPBW1, NPBW2, UT , MCHR1, MCHR2
	CHEM <i>Chemokine</i>	P2.58	CCR5, CCR2, CCR3, CCR1, CCR4, CCR8, CX3C1, CCRL2, CCPB2, XCR1, CCR9, CCR7, CCR6, CCRL1, CXCR4, CXCR2, CXCR1, CXCR5, CCR10, CXCR3, CXCR6, CXCR7, RL3R1, RL3R2, ADMR, AGTR1, AGTR2, BKRB1, BKRB2, APJ, GPR25, GPR15, C5ARL, C5AR, C3AR, GPR44, FPRL1, FPRL2, FPR1, LT4R1, LT4R2, CML1, GPR32, GPR33, GPR1
		NoP	GP152
	PUR <i>Purinergic</i>	P2.58	P2RY1, P2RY2, P2RY4, P2RY5, P2RY6, P2RY8, P2RY9, P2Y10, P2Y12, P2Y13, P2Y14, PTAFR, SUCR1, OXER1, OXGR1, G109A, PSYR, SPR1, CLTR1, CLTR2, PAR1, PAR2, PAR3, EBI2, FFAR1, FFAR2, FFAR3, GPR4, GPR17, GPR18, GPR20, GPR31, GPR34, GPR35, GPR55, GPR81, GPR87, GPR92, GP132, GP141, GP174, GP171, Q5KU21, GPR82
		P2.58P2.59	P2Y11, PAR4
G2	AMIN <i>Aminergic</i>	P2.59	5HT1B, 5HT1D, 5HT1E, 5HT1F, 5HT1A, 5HT7R, 5HT4R, 5HT2A, 5HT2C, 5HT2B, 5HT5A, HRH1, HRH2, HRH3, HRH4, DRD1, DRD2, DRD3, DRD4, DRD5, ADA1A, ADA1B, ADA1D, ADA2A, ADA2B, ADA2C, ADRB1, ADRB2, TAAR1, TAAR2, TAAR3, TAAR5, TAAR6, TAAR9
		P2.59P2.60	5HT6R, ADRB3
		NoP	TAAR8, ACM1, ACM2, ACM3, ACM4, ACM5
	AD <i>Adrenergic</i>	P2.59	AA2AR, AA2BR, AA1R, AA3R
G3	LGR <i>Glycoproteins</i>	NoP	LGR4, LGR5, LGR6, RXFP1, RXFP2, TSHR, LSHR, FSHR
	MEC <i>Melanocortin Cannabinoid</i>	NoP	ACTHR, MSHR, MC3R, MC4R, MC5R, CNR1, CNR2, EDG1, EDG2, EDG3, EDG4, EDG5, EDG6, EDG7, EDG8, GPR3, GPR6, GPR12
		P2.59	PE2R2, PE2R3, PE2R4, PD2R, PI2R
	PTGR <i>Prostaglandin</i>	NoP	TA2R, PF2R, PE2R1
UC	MRG <i>Mas-related</i>	NoP	MAS, MAS1L, MRGRF, MRGX1, MRGX2, MRGX3, MRGX4, MRGRD, MRGRE
		P2.58	GPBAR, GP120, Q5KU14, GP146
		P2.59	GPR22, GPR26, GPR45, GPR61, GPR62, GPR63, GPR75, GPR78, GPR88, GP101, GP135, GP161, GP176
	UC	P2.60	GPR21, GPR52

Abbreviations of the SO, CHEM, and PUR clusters of the G1 group displaying a P2.58 are in bold. The SO family containing UT is shown in red. The receptors with their most common abbreviations belonging to each of the clusters in the G0–4 and unclassified group (UC) groups are listed [from Pelé et al. (76)].

receptors harboring a proline in position 2.59. Together, only the G1 group, which includes the SO containing UT, CHEM, and PUR clusters, is therefore characterized by a proline P2.58 (75, 76) (**Figure 2A**). Given the phylogenetic links between the PEP, SO, CHEM, and PUR clusters, it is proposed that the position of the proline in 2.58 for the SO, CHEM, and PUR clusters results

from a codon deletion in the TM2 of receptors of the PEP family. This proline in TM2 either on P2.58 or P2.59 induces a typical elbow observable by modeling (77, 78) and confirmed by crystallographic studies (79–81), yielding bulge and kink structures, in P2.59 and P2.58 receptors, respectively (**Figures 2A,B**). In fact, by plotting the curvature and flexibility of the TM2, the position

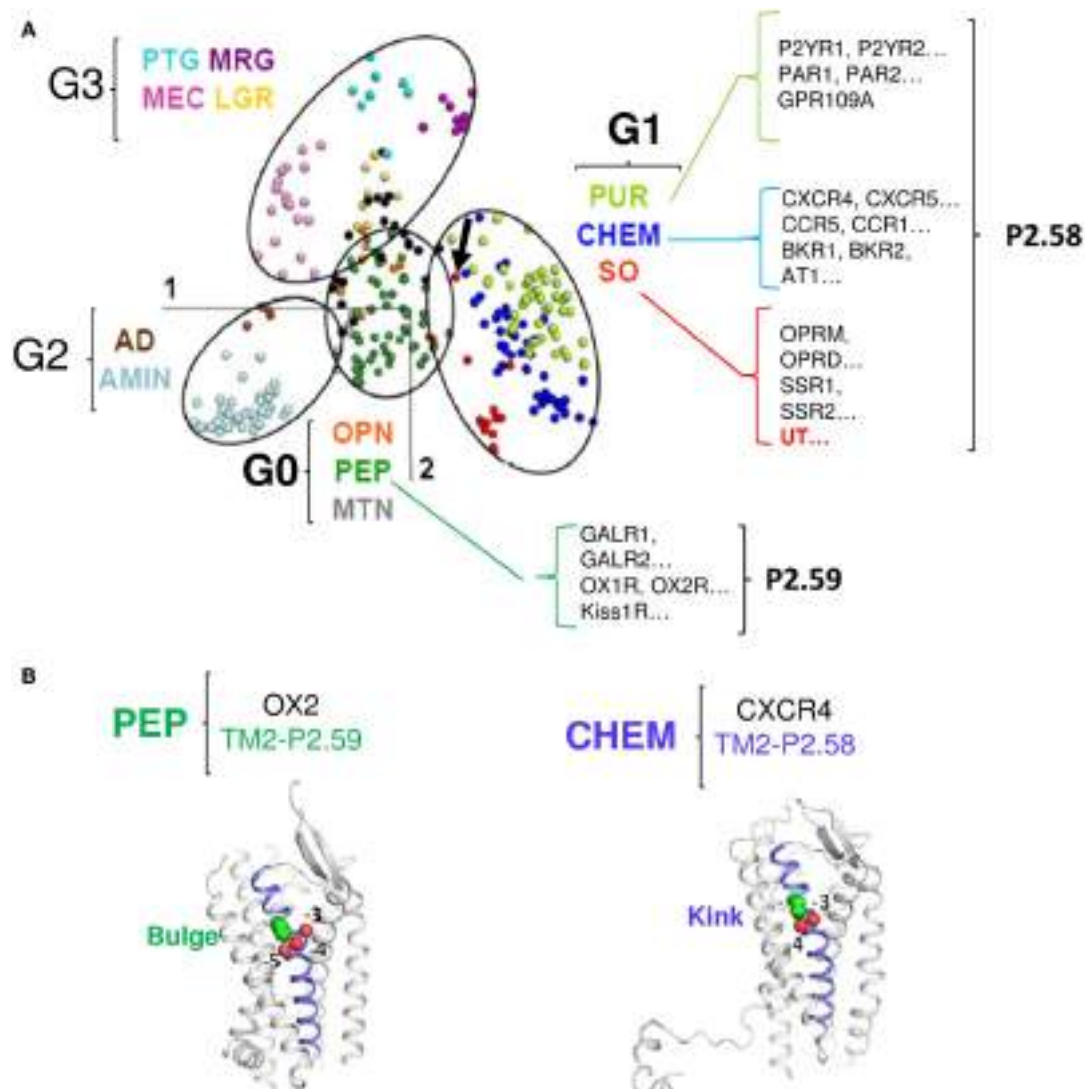


FIGURE 2 | Classification of the different G protein-coupled receptor (GPCR) sub-families according to the multidimensional scaling (MDS) analysis and focus on the proline position in TM2 of receptors from the G0 and G1 groups. (A) In the MDS representation of Rhodopsin-like GPCRs, receptors are visualized as points, with the distances between points as close as possible to the distance in the identity matrix [from Ref. (76)]. The points cluster into four groups, highlighted by ellipses. The color code indicates receptor sub-families and is given in the Figure along with the group the sub-family belongs to. Examples of receptors with the position of the TM2 proline are shown for the G0 and G1 groups. The arrow indicates the position of UT [modified from Ref. (76)]. **(B)** Cartoon view of the PEP receptor OX2 (P2.59, PDB access number: 4S0V, left panel) and of the CHEM receptor CXCR4 (P2.58, PDB access number: 3ODU, right panel). TM2 is slate. The TM2 proline (green) and the preceding oxygen (red) are shown as spheres. In CXCR4, P2.58 is close to the carbonyl groups at positions -3 and -4 (proline kink). In OX2, P2.59 is close to the carbonyl groups at positions -4 and -5 (proline bulge). Thus, according to the position 2.58 or 2.59 of the TM2 proline, the structure of TM2 presents a kink or a bulge.

of the proline could affect the degree of opening of the GPCR-binding pocket and their activation mechanisms (82). Thus, the change in conformation of the TM2, following the deletion of a residue within the TM2 helix, would contribute to the emergence of activation mechanisms specific to SO, CHEM, and PUR cluster receptors.

As many CHEM and PUR receptors are widely recognized as mediating chemotaxis and chemoattractant behaviors, we propose that the P2.58 and kink feature the TM2 of UT, has allowed the capacity of UII gradient sensitivity and chemotactic behavior, leading to cell migration and invasion.

UII/UT SYSTEM, FROM CARDIOVASCULAR FUNCTIONS TO CHEMOKINE PROPERTIES

Physiological and Pathophysiological Effects of the Urotensinergic System on the Cardiovascular Functions

The distribution of UT and its endogenous ligands has naturally led several groups to investigate the effects of UT on the cardiovascular system. When applied to de-endothelialized aortic rings from

rats (4, 36, 83, 84), rabbits (85), macaques (4), or humans (20, 41, 42, 86–88), UII induces dose-dependent constriction. This effect is observed at doses so low that this neuropeptide was considered the most potent naturally occurring vasoactive compound (4, 20). For example, in a murine model, UII is 660 and 16 times as powerful as serotonin and endothelin, respectively (4). This vasoconstrictive activity is primarily relayed by the mobilization of cytosolic calcium (4, 36). Calcium recruited by UT is derived partly from an intracellular pool *via* the activation of channel receptors sensitive to inositol triphosphate (IP_3) and partly from the extracellular pool *via* L-type calcium channels (89–92). Calcium activates calmodulin, whose blockade inhibits the effects of UII on the contraction of rat aortic rings (89). Calmodulin in turn activates myosine light-chain kinase, responsible for the phosphorylation of MLC-2 and the contraction of actomyosin (93, 94). In the sidelines of this principal intracellular signaling pathway, other pathways involved in the contractile activity of UII, such as the PKC/ERK and the RhoA/ROCK pathways, have also been identified (92–95).

However, when injected as an intravenous bolus in anesthetized or conscious rats, UII and URP provoke a slow and prolonged decrease in arterial pressure due to vasodilatation (9, 96–98). In contrast, chronic administration of UII to these animals has no effect (99). In primates, intravenous administration of UII exerts a strong vasodilatation, responsible for cardiovascular collapse and cardiac arrest at high doses (4, 100). However, results in humans are more controversial, since the intravenous injection of UII leads to local vasoconstriction (101) or has no apparent effect (102–104). Studies investigating skin microcirculation even showed that UII infusion through iontophoresis induces a dose-dependent vasodilatation in healthy volunteers but a dose-dependent vasoconstriction in patients with chronic heart failure, systemic hypertension, cirrhosis, or diabetes without cardiovascular pathology (54, 105–107). Finally, endothelium alterations observed in these pathologies could alter vasodilator properties of UII and explain, at least in part, the differences between patients and healthy volunteers.

Overexpression of UII, URP, and UT in the heart of rats and humans with heart failure has also been demonstrated (13, 28) with a correlation between UII plasma level and the cardiac dysfunction (108). A strong “UII-like” immunoreactivity was seen in coronary artery endothelial cells from patients with atherosclerosis (20, 109), associated with a significant effect of UII on the proliferation of vascular smooth muscle cells (95, 110) or the formation of foam cells (111, 112). Moreover, in rat models, treatment by a UT antagonist reduces mortality and improves cardiac function after myocardial infarction (113), decreases coronary angioplasty restenosis (114), pulmonary arterial hypertension (115) and aortic inflammation, and atherosclerosis (116).

Taken together, these data suggest that this peptide could participate rather in tissue remodeling processes during the course of the vascular disease (58) than in tonic vasculo-motor functions. This hypothesis is reinforced by the absence of modification of the vascular tone, and the appearance of a reduced metabolic syndrome and atherosclerotic lesions in UII knockout in comparison with wild-type mice (117).

Effects of UII on Cell Proliferation, Survival, and Hypertrophy

More related to tissue remodeling, the urotensinergic system exerts promitogenic effects on a number of native and recombinant cell types and hypertrophic functions only on cardiomyocytes (Table 3). The activation of ERK is a central element of these effects, either in cell lines transfected with cDNA encoding human UT (118) or in native cells expressing the receptor, i.e., pig renal epithelial cells (119) or rat smooth muscle cells (120). Several signaling pathways leading to the activation of ERK and cell proliferation, survival, or hypertrophy have been described in the literature. One of these pathways involves the transactivation of the epidermal growth factor receptor (EGFR) (121–123). This is often dependent on the production of reactive oxygen species (ROS) by an NADPH oxidase activated by UT (124). The ROS relieve the inhibition exerted by src homology 2-containing tyrosine phosphatase (SHP-2) on EGFR, allowing the transduction of the mitogenic signal (123, 125). This phenomenon of transactivation can also be underpinned by the activation of a disintegrin and metalloproteinase (ADAM) which cleaves the precursor of EGF, the heparin-binding EGF-like growth factor, and releases the active ligand EGFR accordingly (122, 126) (Table 3). The promising effects of UT are also relayed by other second messengers than previously described (PLC and PI3K), *via* receptor coupling to a pertussis toxin-sensitive $G_{i/o}$ proteins in native (45, 118, 127, 128), tumoral human rhabdomyosarcoma (129), or recombinant cell lines (130). These last observations suggest that the ability of UT to coupled $G_{i/o}$ in addition to G_q may have provided acquisition of specific skills important for other activities than cardiovascular tone regulation.

Effects of UII on the Immune System, Relevant to Chemokine-Like Activity

There are few data concerning the link between urotensinergic and immune systems. Some studies have demonstrated the presence of UT on the surface of selected immune cells, i.e., B and NK lymphocytes, monocytes, and macrophages (145, 156), which infiltrate zones displaying high levels of immunoreactivity for UII (20). UII acts as a chemoattractant for human monocytes (145) and induces the extravasation of plasma in mice (157) and rats (158) (Table 3). Pro-inflammatory signals, such as tumor necrosis factor- α (TNF- α), lipopolysaccharide (LPS), or interferon- γ (IFN- γ), promote the expression of UT (145), while UII induces the secretion of cytokines, such as interleukine-6 (IL-6), in UT transfected human cardiomyocytes and lung adenocarcinoma cells (159, 160). Moreover, UII favors acetyl-coenzyme A acetyl-transferase 1 activity in human monocyte (112). On coronary smooth muscle cells or endothelial cells in culture, UII increases the synthesis of inflammatory and pro-thrombotic markers like the plasminogen activator inhibitor-1, the inter-cellular adhesion molecule-1, and the tissue factor through activation of the necrosis factor NF- κ B, a pro-inflammatory transcription factor (124, 161). Finally, expression of UT in human leukocytes, especially monocytes and NK cells, is strongly stimulated after exposure to LPS and requires NF- κ B (145). In addition, in a mouse model of inflammatory acute liver failure, the expression of UII and

TABLE 3 | Transduction pathways associated with UT receptor activation and involved mitogenic and chemokine functions other than cardiovascular tone regulation.

Effect	Cell type	Species	Transduction pathways	Reference
Proliferation	Arterial SMC	Rabbit	PKC, src, MAPK	(110)
	CHO-UT	Rat	RhoA, ROCK	(95)
	Renal epithelial cells	Hamster	G _{i/o} , PI3K, PLC, calmodulin, MEK, extracellular Ca ²⁺	(118)
	Airway SMC	Pig	Ca ²⁺ (voltage-dependent channels), PKC, MAPK, ERK, c-myc	(119)
	Cardiac fibroblasts	Rat	PKC, MAPK, Ca ²⁺ , calcineurin	(131)
	Renal tubular cell line		EGFR transactivation, ERK, ROS	(121)
	SMC		ROS, inhibition of SHP-2, EGFP transactivation via HB-EGF	(122)
	Endothelial precursors		Ca ²⁺ , CaMK, ERK, PKD	(132)
	Airway SMC		ERK, p38MAPK	(133)
	Airway SMC	Human	ERK, TGF β	(120)
Survival	Astrocytes	Rat	NOX, ROS, ERK, p38MAPK, c-Jun, Akt, expression of PAI-1	(124)
	Fibroblasts		NOX4, ROS, FoxO3, JNK, MMP-2	(134)
	Aortic SMC		PLC, intra- and extracellular Ca ²⁺ (T-type channel), IP ₃ , G _{i/o}	(128)
	HUVEC	Human	MAPK, VEGF expression, collagen production	(135)
	Cardiac precursors	Mouse	ROS, SHP-2 inhibition, EGFR transactivation	(123)
Hypertrophy	Vascular SMC	Rat	p38MAPK, ERK	(136)
	Cardiomyocytes		JNK, LRP6	(137)
	Cardiomyocytes-UT	Rat	N. D.	(138)
	Cardiomyocytes		PI3K, ERK	(139)
Angiogenesis	HUVEC	Human	G _q , Ras	(59)
			EGFR transactivation via HB-EGF, ERK, p38MAPK	(126)
			ROS, SHP-2 inhibition, EGFR transactivation	(125)
			PI3K, Akt, GSK-3 β	(140)
			ROS, NADPH oxidase, Akt, GSK-3 β , PTEN	(141)
	Neuromicrovascular endothelial cells	Rat	PLC, Ca ²⁺ , PKC, PI3K, ERK1/2, FAK	(142)
	Chick embryo chorioallantoic membrane	Chicken	VEGF, endothelin-1 and adrenomedullin expression	(143)
			HIF-1, ROS, NOX-2	(144)
Migration, motility, adhesion	HEK293	Human	N.D.	(49)
	Monocytes	Human	RhoA, ROCK	(49)
	Endothelial progenitors	Rat	RhoA/ROCK, MLC	(145)
	Prostatic adenocarcinoma (LNCaP)	Human	RhoA, FAK	(146)
	Vascular SMC		MEK	(147)
	Vascular fibroblasts	Rat	PKC, ROCK, calcineurin, MAPK	(148)
			MLC, myosin light chain	(149)
	Endothelial progenitors		MMP-2, matrix metalloprotease type 2; NOX, NADPH oxidase; p38MAPK, p38 mitogen-activated protein kinase; PAI-1, plasminogen activator inhibitor-1; PI3K, phosphatidylinositol-3 kinase; PKC, protein kinase C; PKD, protein kinase D; PLC, phospholipase C; PTEN, phosphatase and tensin homolog; Ras, small GTPases; RhoA, Ras homolog gene family, member A; ROCK, rho-associated protein kinase; ROS, reactive oxygen species; SHP-2, src-homology 2-containing tyrosine phosphatase; SMC, smooth muscle cells; TGF β , transforming growth factor- β ; VEGF, vascular endothelial growth factor; N.D., not determined.	(150)
	Colorectal carcinoma	Human	N.D.	(151)
	Bladder cancer		N.D.	(152)
	Glioblastoma cell line		N.D.	(153)
			G ₁₃ /Rho/ROCK, G _{i/o} /PI3K	(154)
			Inhibition of pre-autophagic endosomes	(155)

Akt, protein kinase B; CaMK, calmodulin kinase; CHO-UT, Chinese hamster ovary line transfected with the human form of the UT receptor; EGFR, epidermal growth factor receptor; ERK, extracellular signal-regulated kinase; FAK, focal adhesion kinase; FoxO3, forkhead box O3; G_{i/o}, G_q, G₁₃, G proteins type I/o, q and 13; GSK-3 β , glycogen synthase kinase 3 β ; HB-EGF, heparin-binding EGF-like growth factor; HIF-1, hypoxia inducible factor-1; HUVEC, human umbilical vein endothelial cells; IP₃, inositol triphosphate; LRP6, low density lipoprotein receptor-related protein 6; JNK, c-Jun N-terminal kinase; MAPK, mitogen-activated protein kinase; MEK, extracellular signal-regulated kinase; MLC, myosin light chain; MMP-2, matrix metalloprotease type 2; NOX, NADPH oxidase; p38MAPK, p38 mitogen-activated protein kinase; PAI-1, plasminogen activator inhibitor-1; PI3K, phosphatidylinositol-3 kinase; PKC, protein kinase C; PKD, protein kinase D; PLC, phospholipase C; PTEN, phosphatase and tensin homolog; Ras, small GTPases; RhoA, Ras homolog gene family, member A; ROCK, rho-associated protein kinase; ROS, reactive oxygen species; SHP-2, src-homology 2-containing tyrosine phosphatase; SMC, smooth muscle cells; TGF β , transforming growth factor- β ; VEGF, vascular endothelial growth factor; N.D., not determined.

UT was significantly increased in liver endothelial cells, and a pretreatment by the UT biased ligand (130) urantide decreased NF- κ B activation and inflammatory cytokine (TNF- α , IL-1 β , IFN- γ) expression (162).

These data indicate that UII is involved in the immune response and, notably, participates in the production of cytokines and the promotion of immune cell infiltration, suggestive of a chemokine functional activity relayed by the peptide UII, raising a more conserved role in chemotactic attraction of immune cells in pathological situations.

Chemokine Activity of UII in the Context of Tissue Remodeling and Cancer

Chemotaxis is currently known as the fundamental phenomenon highly conserved from bacteria to eukaryotic cells, implying cell directed migration along an extracellular chemical gradient (163–165), a mechanism essential for a number of physiological and pathological processes including embryogenesis and wiring of the CNS (166, 167), the immune system inflammatory response (168), angiogenesis and cancer cell metastasis, and invasion

(165, 169). The “professional” players of chemotaxis, chemokines, are subdivided into C, CC, CXC, and CX3C families, based on the number and spacing of the conserved cysteine residues in their amino termini. Members of the CXC, containing CXCL12 (stromal derived factor-1 or SDF-1) and CC including CCL2 (monocyte chemoattractant protein-1, MCP-1) or CCL5 (regulated upon activation normal T cell, RANTES) chemokine families are known to chemoattract neutrophils, T/B lymphocytes, or natural killer cells and monocytes, macrophages, or T lymphocytes, respectively (170). Through activation of chemotaxis, CXCL12, CCL2, CCL5, or CXCL1 chemokines were shown to stimulate growth, migration/invasion/metastasis as well as angiogenesis and tube formation (171, 172). The CXCL12 and its CXCR4 have long been shown to constitute a promising therapeutic based-system in pre-clinical models and in early clinical trials, but other prototypic chemokines emerge as new potential players in cancer. CCL2 together with its cognate CCR2 play key

roles in cancer metastasis by sustaining cancer cell proliferation and survival, stimulating cancer cell migration and invasion, and inducing deleterious inflammation and angiogenesis (173, 174). In addition, various cancer cells produced CCL5 but also expressed CCR1, CCR3, and CCR5, suggesting autocrine/paracrine mechanisms, associated with metalloproteinase activation and invasion (175, 176).

Consistent with this, a growing number of independent studies show that UII exerts a stimulatory effect on cell migration (Table 3). The Rho/ROCK signaling pathway appears to play a major role in the effects of UII on the migration of rat fibroblasts (149) and endothelial progenitor cells (146) as well as human monocytes (145). In the latter case, the authors consider UII to be a chemotactic factor that acts on the reorganization of the actin cytoskeleton (Figure 3).

The expression of UT at the endothelial level associated with the pro-migration- and mitotic effects of UII, suggested the

Chemotactic directional migration

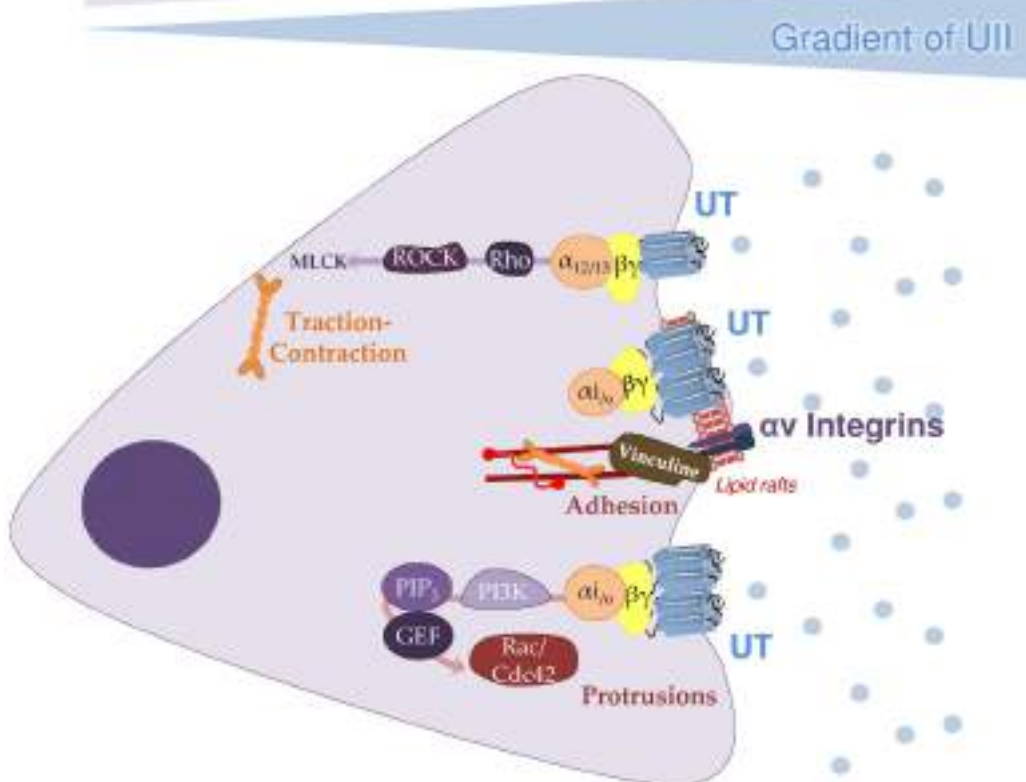


FIGURE 3 | A hypothetical outline of chemokine signaling cascade relayed by the urotensinergic system inducing cell migration. Illustration of a pathophysiological situation involving directional migration/invasion of cells expressing UT in response to a urotensin II (UII) gradient concentration. It is proposed that mobile high-affinity UT coupled to both $\text{G}\alpha_i/\text{o}$ and $\text{G}\alpha_{13}$ is activated by a low concentration of UII, would promote the formation of protrusions and adhesions at the front of the cell through PI3K/PIP3/GEF/Rac/Cdc42 signaling cascade. At the back of the migrating cell, concomitant activation of G13, likely allows actomyosin contraction via the Rho/ROCK/MLCK pathway. To favor cell progression toward the emission source of UII, mobile or engaged UT coupled to $\text{G}\alpha_i/\text{o}$ in lipid rafts may activate proteins responsible for the formation and maturation of focal adhesions composed of αv integrins and vinculin. Together, this pleiotropic UT associated signaling events represents a prototypic chemokine-mediated mechanism shared by P2.58 GPCRs allowing chemotactic migration. Cdc42, cell division control protein 42; GEF, guanine nucleotide exchange factor; MAP1A, microtubule-associated protein 1A; MLCK, myosin light-chain kinase; PI3K, phosphatidylinositol-3 kinase; PIP3, phosphatidylinositol 4,5-trisphosphate; ROCK, rho-associated protein kinase [from Ref. (154)].

involvement of the urotensinergic system in angiogenesis. The first evidence for a proangiogenic effect of UII was obtained by Spinazzi et al., demonstrating that UII leads to the reorganization or tubulogenesis of endothelial cells derived from rat brain microvessels, and stimulates *in vitro* angiogenesis (49). Application of UII in a gelatin implant to the chorioallantoic membrane of chick embryos evokes an increased number of blood vessels (49). Accordingly, studies on human umbilical vein endothelial cells confirmed these data (142, 144, 177) and converge toward chemoattraction of cultured endothelial cells by UII.

The major demonstration of the chemotactic role of the UII/UT system comes from studies on cancer cell lines. The expression of UII and UT is observed in numerous cell lines and tumor samples (**Table 3**), notably in extracts of adrenal gland tumors, such as adrenocortical carcinomas or pheochromocytomas (178, 179), tumors of the CNS such as glioblastomas or neuroblastomas (44, 180, 181), or tumors of muscular tissue, such as rhabdomyosarcomas (129, 182). To date, few isolated studies have investigated the role of the urotensinergic system in tumorigenesis. For example, UII has been shown to stimulate the proliferation of cells of a pulmonary adenocarcinoma cell line *in vitro* and *in vivo* in a xenograft model in immunodeficient nude mice (183). The same team has more recently shown that UII stimulates the release of pro-inflammatory cytokines, such as IL-6, TNF- α , or matrix metalloproteinase-9 and participates in macrophage infiltration of the tumor (160). In human cell lines derived from prostatic or colorectal tumors, application of urantide, Rho pathway inhibitor, or shRNA against UT leads to a decrease in their motility and invasiveness (147, 152). More recently, the expression of UII and UT was also observed in other solid tumors from colon, bladder, and breast (152, 153, 184). The activation of UT with the agonist UII_{4–11} in colon cancer cell lines resulted in stimulation of cell growth whereas the treatment with three biased ligand/antagonists (urantide, UPG83 and UPG85) induced growth inhibition (152). As macrophages have been associated with tumor progression, metastasis, and resistance to treatments (185), these results suggested an important role of UII in chemokine functions associated with tumor development (**Table 3**).

Definitely, the urotensinergic system appears to be involved in cancer cell motility and invasion. Indeed, our recent work demonstrated in glioma cell lines and in recombinant HEK293 cells, that activation of UT by UII involves a signaling switch through the couplings to G α 13/Rho/ROCK kinases and G α i/o/PI3K pathways, involved in actin stress fibers, lamellipodia formation and vinculin-stained focal adhesions to initiate directional migration and cell adhesion, sequential mechanisms in tumor invasion (154). This type of mixed couplings were thus proposed for the CCR2/CCR2 system in human bone marrow stem cells in which activation of CCR2 regulates PI3K likely contributing to cell polarity and migration and Rho/ROCK leading to cell retraction (186). Moreover, we provide evidence that UT-induced inhibition of the autophagic process is also a

key element in the migration of HEK293 cells expressing UT or CXCR4 as well as U87 glioblastoma cells. Autophagy inhibition after activation of UT or CXCR4 at the leading edge may also locally protect proteins involved in actin remodeling and adhesion assembly, whereas autophagy could remain active at distance from chemotactic GPCRs in order to participate in the disassembly of large focal adhesions (155). Together, the more recent pro-migratory, pro-inflammatory and invasiveness role of the urotensinergic system bring it closer to the chemokine systems, such as CXCL12/CXCR4 or the CCL2/CCR2 pair, widening the therapeutic field of pathologies characterized by cellular migratory events, such development, inflammation, invasion and metastasis.

CONCLUSION

In this review, we address the putative UT chemotactic structural and functional definition under an evolutionary angle. According to the postulated evolutionary mechanism, a deletion in TM2 of an ancestral PEP receptor with the P2.59 pattern led by divergence to receptors of the G1 groups with the P2.58 pattern, including UT and chemokine receptors, such as CXCR4. In view of the evolutionary history and chemotactic properties of UT, we propose that UII/UT may rather be considered as a new chemokine system. Indeed, even if the last decade was mainly devoted to the elucidation of the cardiovascular control by the urotensinergic system, interesting investigations on the pro-inflammatory and pro-migratory properties of UII lead us to stipulate that urotensinergic system must be now considered in a new chemokine therapeutic target in pathological situations involving cell chemoattraction.

AUTHOR CONTRIBUTIONS

HC and LD wrote the review and prepared the figures and tables. J-EJ, M-CT, FM, and PG made the bibliography to build the review and constructed the tables and figures. LP and MC participated in the clarification of the UT classification and the establishment of the UT couplings.

ACKNOWLEDGMENTS

The authors thank INSERM, The French Agence National pour la Recherche ANR Chemot-xProG, the Normandie Rouen Université, Géfluc and ligue régionale contre le Cancer charities that aided the efforts of the authors.

FUNDING

Some of the original works cited in the manuscript are supported by INSERM, ANR, Normandie Rouen University, Géfluc and Ligue Régionale contre le Cancer.

REFERENCES

- Bern HA, Lederis K. A reference preparation for the study of active substances in the caudal neurosecretory system of teleosts. *J Endocrinol* (1969) 45:Sxi–xii.
- Conlon JM, O'Harte F, Smith DD, Tonon MC, Vaudry H. Isolation and primary structure of urotensin II from the brain of a tetrapod, the frog *Rana ridibunda*. *Biochem Biophys Res Commun* (1992) 188:578–83. doi:10.1016/0006-291X(92)91095-8
- Pearson D, Shively JE, Clark BR, Geschwind II, Barkley M, Nishioka RS, et al. Urotensin II: a somatostatin-like peptide in the caudal neurosecretory system of fishes. *Proc Natl Acad Sci U S A* (1980) 77:5021–4. doi:10.1073/pnas.77.8.5021
- Ames RS, Sarau HM, Chambers JK, Willette RN, Aiyar NV, Romanic AM, et al. Human urotensin-II is a potent vasoconstrictor and agonist for the orphan receptor GPR14. *Nature* (1999) 401:282–6. doi:10.1038/45809
- Couloarn Y, Lihrmann I, Jegou S, Anouar Y, Tostivint H, Beauvillain JC, et al. Cloning of the cDNA encoding the urotensin II precursor in frog and human reveals intense expression of the urotensin II gene in motoneurons of the spinal cord. *Proc Natl Acad Sci U S A* (1998) 95:15803–8. doi:10.1073/pnas.95.26.15803
- González GC, Martínez-Padrón M, Lederis K, Lukowiak K. Distribution and coexistence of urotensin I and urotensin II peptides in the cerebral ganglia of *Aplysia californica*. *Peptides* (1992) 13:695–703. doi:10.1016/0196-9781(92)90175-3
- Romanova EV, Sasaki K, Alexeeva V, Vilim FS, Jing J, Richmond TA, et al. Urotensin II in invertebrates: from structure to function in *Aplysia californica*. *PLoS One* (2012) 7:e48764. doi:10.1371/journal.pone.0048764
- Mori M, Sugo T, Abe M, Shimomura Y, Kurihara M, Kitada C, et al. Urotensin II is the endogenous ligand of a G-protein-coupled orphan receptor, SENR (GPR14). *Biochem Biophys Res Commun* (1999) 265:123–9. doi:10.1006/bbrc.1999.1640
- Sugo T, Murakami Y, Shimomura Y, Harada M, Abe M, Ishibashi Y, et al. Identification of urotensin II-related peptide as the urotensin II-immunoreactive molecule in the rat brain. *Biochem Biophys Res Commun* (2003) 310:860–8. doi:10.1016/j.bbrc.2003.09.102
- Couloarn Y, Jégou S, Tostivint H, Vaudry H, Lihrmann I. Cloning, sequence analysis and tissue distribution of the mouse and rat urotensin II precursors. *FEBS Lett* (1999) 457:28–32. doi:10.1016/S0014-5793(99)01003-0
- Elshourbagy NA, Douglas SA, Shabon U, Harrison S, Duddy G, Sechler JL, et al. Molecular and pharmacological characterization of genes encoding urotensin-II peptides and their cognate G-protein-coupled receptors from the mouse and monkey. *Br J Pharmacol* (2002) 136:9–22. doi:10.1038/sj.bjp.0704671
- Russell FD, Kearns P, Toth I, Molenaar P. Urotensin-II-converting enzyme activity of furin and trypsin in human cells in vitro. *J Pharmacol Exp Ther* (2004) 310:209–14. doi:10.1124/jpet.104.065425
- Russell FD, Meyers D, Galbraith AJ, Bett N, Toth I, Kearns P, et al. Elevated plasma levels of human urotensin-II immunoreactivity in congestive heart failure. *Am J Physiol Heart Circ Physiol* (2003) 285:H1576–81. doi:10.1152/ajpheart.00217.2003
- Sugo T, Mori M. Another ligand fishing for G protein-coupled receptor 14. Discovery of urotensin II-related peptide in the rat brain. *Peptides* (2008) 29:809–12. doi:10.1016/j.peptides.2007.06.005
- Nobata S, Donald JA, Balment RJ, Takei Y. Potent cardiovascular effects of homologous urotensin II (UII)-related peptide and UII in unanesthetized eels after peripheral and central injections. *Am J Physiol Regul Integr Comp Physiol* (2011) 300:R437–46. doi:10.1152/ajpregu.00629.2010
- Quan FB, Bougerol M, Rigour F, Kenigfest NB, Tostivint H. Characterization of the true ortholog of the urotensin II-related peptide (URP) gene in teleosts. *Gen Comp Endocrinol* (2012) 177:205–12. doi:10.1016/j.ygenc.2012.02.018
- Tostivint H, Joly L, Lihrmann I, Parmentier C, Lebon A, Morisson M, et al. Comparative genomics provides evidence for close evolutionary relationships between the urotensin II and somatostatin gene families. *Proc Natl Acad Sci U S A* (2006) 103:2237–42. doi:10.1073/pnas.0510700103
- Douglas SA, Tayara L, Ohlstein EH, Halawa N, Giaid A. Congestive heart failure and expression of myocardial urotensin II. *Lancet* (2002) 359:1990–7. doi:10.1016/S0140-6736(02)08831-1
- Dschietzig T, Bartsch C, Pregla R, Zurbrügg HR, Armbruster FP, Richter C, et al. Plasma levels and cardiovascular gene expression of urotensin-II in human heart failure. *Regul Pept* (2002) 110:33–8. doi:10.1016/S0167-0115(02)00158-1
- Maguire JJ, Kuc RE, Wiley KE, Kleinz MJ, Davenport AP. Cellular distribution of immunoreactive urotensin-II in human tissues with evidence of increased expression in atherosclerosis and a greater constrictor response of small compared to large coronary arteries. *Peptides* (2004) 25:1767–74. doi:10.1016/j.peptides.2004.01.028
- Matsushita M, Shichiri M, Imai T, Iwashina M, Tanaka H, Takasu N, et al. Co-expression of urotensin II and its receptor (GPR14) in human cardiovascular and renal tissues. *J Hypertens* (2001) 19:2185–90. doi:10.1097/00004872-200112000-00011
- Dubessy C, Cartier D, Lectez B, Bucharles C, Chartrel N, Montero-Hadjadje M, et al. Characterization of urotensin II, distribution of urotensin II, urotensin II-related peptide and UT receptor mRNAs in mouse: evidence of urotensin II at the neuromuscular junction. *J Neurochem* (2008) 107:361–74. doi:10.1111/j.1471-4159.2008.05624.x
- Totsune K, Takahashi K, Arihara Z, Sone M, Satoh F, Ito S, et al. Role of urotensin II in patients on dialysis. *Lancet* (2001) 358:810–1. doi:10.1016/S0140-6736(01)06002-0
- Totsune K, Takahashi K, Arihara Z, Sone M, Ito S, Murakami O. Increased plasma urotensin II levels in patients with diabetes mellitus. *Clin Sci (Lond)* (2003) 104:1–5. doi:10.1042/cs1040001
- Shenouda A, Douglas SA, Ohlstein EH, Giaid A. Localization of urotensin-II immunoreactivity in normal human kidneys and renal carcinoma. *J Histochem Cytochem* (2002) 50:885–9. doi:10.1177/002215540205000702
- Silvestre RA, Rodríguez-Gallardo J, Egido EM, Marco J. Inhibition of insulin release by urotensin II – a study on the perfused rat pancreas. *Horm Metab Res* (2001) 33:379–81. doi:10.1055/s-2001-15414
- Hirose T, Takahashi K, Mori N, Nakayama T, Kikuya M, Ohkubo T, et al. Increased expression of urotensin II, urotensin II-related peptide and urotensin II receptor mRNAs in the cardiovascular organs of hypertensive rats: comparison with endothelin-1. *Peptides* (2009) 30:1124–9. doi:10.1016/j.peptides.2009.02.009
- Nakayama T, Hirose T, Totsune K, Mori N, Maruyama Y, Maejima T, et al. Increased gene expression of urotensin II-related peptide in the hearts of rats with congestive heart failure. *Peptides* (2008) 29:801–8. doi:10.1016/j.peptides.2007.12.018
- Kristof AS, You Z, Han Y-S, Giaid A. Protein expression of urotensin II, urotensin-related peptide and their receptor in the lungs of patients with lymphangioleiomyomatosis. *Peptides* (2010) 31:1511–6. doi:10.1016/j.peptides.2010.04.017
- Wang H, Dong K, Xue X, Feng P, Wang X. Elevated expression of urotensin II and its receptor in diethylnitrosamine-mediated precancerous lesions in rat liver. *Peptides* (2011) 32:382–7. doi:10.1016/j.peptides.2010.10.032
- DunSL, BrailoiuGC, YangJ, ChangJK, DunNJ. UrotensinII-immunoreactivity in the brainstem and spinal cord of the rat. *Neurosci Lett* (2001) 305:9–12. doi:10.1016/S0304-3940(01)01804-3
- Eggerer J-G, Camus A, Calas A. Urotensin-II expression in the mouse spinal cord. *J Chem Neuroanat* (2006) 31:146–54. doi:10.1016/j.jchemneu.2005.10.004
- Eggerer J-G, Calas A. A novel hypothalamic neuroendocrine peptide: URP (urotensin-II-related peptide)? *C R Biol* (2005) 328:724–31. doi:10.1016/j.crvi.2005.06.002
- Tal M, Ammar DA, Karpurj M, Krizhanovsky V, Naim M, Thompson DA. A novel putative neuropeptide receptor expressed in neural tissue, including sensory epithelia. *Biochem Biophys Res Commun* (1995) 209:752–9. doi:10.1006/bbrc.1995.1563
- Marchese A, Heiber M, Nguyen T, Heng HHQ, Saldivia VR, Cheng R, et al. Cloning and chromosomal mapping of three novel genes, GPR9, GPR10, and GPR14, encoding receptors related to interleukin 8, neuropeptide Y, and somatostatin receptors. *Genomics* (1995) 29:335–44. doi:10.1006/geno.1995.9996
- Liu Q, Pong SS, Zeng Z, Zhang Q, Howard AD, Williams DL, et al. Identification of urotensin II as the endogenous ligand for the orphan

- G-protein-coupled receptor GPR14. *Biochem Biophys Res Commun* (1999) 266:174–8. doi:10.1006/bbrc.1999.1796
37. Nothacker H-P, Wang Z, McNeill AM, Saito Y, Merten S, O'Dowd B, et al. Identification of the natural ligand of an orphan G-protein-coupled receptor involved in the regulation of vasoconstriction. *Nat Cell Biol* (1999) 1:383–5. doi:10.1038/14081
 38. Gartlon J, Parker F, Harrison DC, Douglas SA, Ashmeade TE, Riley GJ, et al. Central effects of urotensin-II following ICV administration in rats. *Psychopharmacology (Berl)* (2001) 155:426–33. doi:10.1007/s002130100715
 39. Gong H, Wang Y-X, Zhu Y-Z, Wang W-W, Wang M-J, Yao T, et al. Cellular distribution of GPR14 and the positive inotropic role of urotensin II in the myocardium in adult rat. *J Appl Physiol* (2004) 97:2228–35. doi:10.1152/japplphysiol.00540.2004
 40. Leonard AD, Thompson JP, Hutchinson EL, Young SP, McDonald J, Swanevelder J, et al. Urotensin II receptor expression in human right atrium and aorta: effects of ischaemic heart disease. *Br J Anaesth* (2009) 102:477–84. doi:10.1093/bja/aep011
 41. Maguire JJ, Kuc RE, Davenport AP. Orphan-receptor ligand human urotensin II: receptor localization in human tissues and comparison of vasoconstrictor responses with endothelin-1. *Br J Pharmacol* (2000) 131:441–6. doi:10.1038/sj.bjp.0703601
 42. Maguire JJ, Kuc RE, Kleint MJ, Davenport AP. Immunocytochemical localization of the urotensin-II receptor, UT, to rat and human tissues: relevance to function. *Peptides* (2008) 29:735–42. doi:10.1016/j.peptides.2007.08.021
 43. Mori N, Hirose T, Nakayama T, Ito O, Kanazawa M, Imai Y, et al. Increased expression of urotensin II-related peptide and its receptor in kidney with hypertension or renal failure. *Peptides* (2009) 30:400–8. doi:10.1016/j.peptides.2008.09.021
 44. Nguyen T-TM, Létourneau M, Chatenet D, Fournier A. Presence of urotensin-II receptors at the cell nucleus: specific tissue distribution and hypoxia-induced modulation. *Int J Biochem Cell Biol* (2012) 44:639–47. doi:10.1016/j.biocel.2011.12.022
 45. Song W, McDonald J, Camarda V, Calo G, Guerrini R, Marzola E, et al. Cell and tissue responses of a range of Urotensin II analogs at cloned and native urotensin II receptors. Evidence for coupling promiscuity. *Naunyn Schmiedebergs Arch Pharmacol* (2006) 373:148–57. doi:10.1007/s00210-006-0057-2
 46. Tian L, Li C, Qi J, Fu P, Yu X, Li X, et al. Diabetes-induced upregulation of urotensin II and its receptor plays an important role in TGF-beta1-mediated renal fibrosis and dysfunction. *Am J Physiol Endocrinol Metab* (2008) 295:E1234–42. doi:10.1152/ajpendo.90672.2008
 47. Langham RG, Kelly DJ, Gow RM, Zhang Y, Dowling JK, Thomson NM, et al. Increased expression of urotensin II and urotensin II receptor in human diabetic nephropathy. *Am J Kidney Dis* (2004) 44:826–31. doi:10.1016/S0272-6386(04)01130-8
 48. Jégou S, Cartier D, Dubessy C, Gonzalez BJ, Chatenet D, Tostivint H, et al. Localization of the urotensin II receptor in the rat central nervous system. *J Comp Neurol* (2006) 495:21–36. doi:10.1002/cne.20845
 49. Spinazzi R, Albertin G, Nico B, Guidolin D, Di Liddo R, Rossi GP, et al. Urotensin-II and its receptor (UT-R) are expressed in rat brain endothelial cells, and urotensin-II via UT-R stimulates angiogenesis in vivo and in vitro. *Int J Mol Med* (2006) 18:1107–12. doi:10.3892/ijmm.18.6.1107
 50. Lin Y, Tsuchihashi T, Matsumura K, Fukuhara M, Ohya Y, Fujii K, et al. Central cardiovascular action of urotensin II in spontaneously hypertensive rats. *Hypertens* (2003) 26:839–45. doi:10.1291/hypres.26.839
 51. Castel H, Diallo M, Chatenet D, Leprince J, Desrues L, Schouft M-T, et al. Biochemical and functional characterization of high-affinity urotensin II receptors in rat cortical astrocytes. *J Neurochem* (2006) 99:582–95. doi:10.1111/j.1471-4159.2006.04130.x
 52. Jani PP, Narayan H, Ng LL. The differential extraction and immunoluminometric assay of urotensin II and urotensin-related peptide in heart failure. *Peptides* (2013) 40:72–6. doi:10.1016/j.peptides.2012.12.014
 53. Ng LL, Loke I, O'Brien RJ, Squire IB, Davies JE. Plasma urotensin in human systolic heart failure. *Circulation* (2002) 106:2877–80. doi:10.1161/01.CIR.0000044388.19119.02
 54. Kemp W, Roberts S, Krum H. Increased circulating urotensin II in cirrhosis: potential implications in liver disease. *Peptides* (2008) 29:868–72. doi:10.1016/j.peptides.2007.08.020
 55. Heller J, Schepke M, Neef M, Woitas R, Rabe C, Sauerbruch T. Increased urotensin II plasma levels in patients with cirrhosis and portal hypertension. *J Hepatol* (2002) 37:767–72. doi:10.1016/S0168-8278(02)00295-7
 56. Pawar R, Kemp W, Roberts S, Krum H, Yandle T, Hardikar W. Urotensin II levels are an important marker for the severity of portal hypertension in children. *J Pediatr Gastroenterol Nutr* (2011) 53:88–92. doi:10.1097/MPG.0b013e3182153900
 57. Suguro T, Watanabe T, Ban Y, Kodate S, Misaki A, Hirano T, et al. Increased human urotensin II levels are correlated with carotid atherosclerosis in essential hypertension. *Am J Hypertens* (2007) 20:211–7. doi:10.1016/j.amjhyper.2006.08.001
 58. Pakala R. Role of urotensin II in atherosclerotic cardiovascular diseases. *Cardiovasc Revasc Med* (2008) 9:166–78. doi:10.1016/j.carrev.2008.02.001
 59. Tzanidis A, Hannan RD, Thomas WG, Onan D, Autelitano DJ, See F, et al. Direct actions of urotensin II on the heart: implications for cardiac fibrosis and hypertrophy. *Circ Res* (2003) 93:246–53. doi:10.1161/01.RES.0000084382.64418.BC
 60. Bockaert J, Pin JP. Molecular tinkering of G protein-coupled receptors: an evolutionary success. *EMBO J* (1999) 18:1723–9. doi:10.1093/emboj/18.7.1723
 61. Attwood TK, Findlay JBC. Fingerprinting G-protein-coupled receptors. *Protein Eng* (1994) 7:195–203. doi:10.1093/protein/7.2.195
 62. Fenalti G, Giguere PM, Katritch V, Huang X-P, Thompson AA, Cherezov V, et al. Molecular control of d-opioid receptor signalling. *Nature* (2014) 506:191–6. doi:10.1038/nature12944
 63. Manglik A, Kruse AC, Kobikta TS, Thian FS, Mathiesen JM, Sunahara RK, et al. Crystal structure of the μ -opioid receptor bound to a morphinan antagonist. *Nature* (2012) 485:321–6. doi:10.1038/nature10954
 64. Fredriksson R, Lagerström MC, Lundin L-G, Schiöth HB. The G-protein-coupled receptors in the human genome form five main families. Phylogenetic analysis, paralogon groups, and fingerprints. *Mol Pharmacol* (2003) 63:1256–72. doi:10.1124/mol.63.6.1256
 65. Ballesteros JA, Weinstein H. Integrated methods for the construction of three-dimensional models and computational probing of structure-function relations in G protein-coupled receptors. *Methods Neurosci* (1995) 25:366–428. doi:10.1016/S1043-9471(05)80049-7
 66. Tautermann CS. GPCR structures in drug design, emerging opportunities with new structures. *Bioorg Med Chem Lett* (2014) 24:4073–9. doi:10.1016/j.bmcl.2014.07.009
 67. Lin H, Sassano MF, Roth BL, Shoichet BK. A pharmacological organization of G protein-coupled receptors. *Nat Methods* (2013) 10:140–6. doi:10.1038/nmeth.2324
 68. Onan D, Hannan RD, Thomas WG. Urotensin II: the old kid in town. *Trends Endocrinol Metab* (2004) 15:175–82. doi:10.1016/j.tem.2004.03.007
 69. Chatenet D, Nguyen T-TM, Létourneau M, Fournier A. Update on the urotensinergic system: new trends in receptor localization, activation, and drug design. *Front Endocrinol* (2012) 3:174. doi:10.3389/fendo.2012.00174
 70. Proulx CD, Holleran BJ, Boucard AA, Escher E, Guillemette G, Leduc R. Mutational analysis of the conserved Asp2.50 and ERY motif reveals signaling bias of the urotensin II receptor. *Mol Pharmacol* (2008) 74:552–61. doi:10.1124/mol.108.045054
 71. Oakley RH, Laporte SA, Holt JA, Barak LS, Caron MG. Molecular determinants underlying the formation of stable intracellular G protein-coupled receptor- β -arrestin complexes after receptor endocytosis*. *J Biol Chem* (2001) 276:19452–60. doi:10.1074/jbc.M101450200
 72. Proulx CD, Holleran BJ, Lavigne P, Escher E, Guillemette G, Leduc R. Biological properties and functional determinants of the urotensin II receptor. *Peptides* (2008) 29:691–9. doi:10.1016/j.peptides.2007.10.027
 73. Chen Y, Shang Y, Xu D. Multi-dimensional scaling and MODELLER-based evolutionary algorithms for protein model refinement. *Proc Congr Evol Comput* (2014) 2014:1038–45. doi:10.1109/CEC.2014.6900443
 74. Hout MC, Papesh MH, Goldinger SD. Multidimensional scaling. *Wiley Interdiscip Rev Cogn Sci* (2013) 4:93–103. doi:10.1002/wics.1203
 75. Chabbert M, Castel H, Pele J, Deville J, Legende R, Rodien P. Evolution of class A G-protein-coupled receptors: implications for molecular modeling. *Curr Med Chem* (2012) 19:1110–8. doi:10.2174/092986712799320600
 76. Pelé J, Abdi H, Moreau M, Thybert D, Chabbert M. Multidimensional scaling reveals the main evolutionary pathways of class A G-protein-coupled receptors. *PLoS One* (2011) 6:e19094. doi:10.1371/journal.pone.0019094

77. Devillé J, Rey J, Chabbert M. An indel in transmembrane helix 2 helps to trace the molecular evolution of class A G-protein-coupled receptors. *J Mol Evol* (2009) 68:475–89. doi:10.1007/s00239-009-9214-9
78. Visiers I, Ballesteros JA, Weinstein H. Three-dimensional representations of G protein-coupled receptor structures and mechanisms. *Methods Enzymol* (2002) 343:329–71. doi:10.1016/S0076-6879(02)43145-X
79. Palczewski K, Kumada T, Hori T, Behnke CA, Motoshima H, Fox BA, et al. Crystal structure of rhodopsin: a G protein-coupled receptor. *Science* (2000) 289:739–45. doi:10.1126/science.289.5480.739
80. Rasmussen SGF, Choi H-J, Rosenbaum DM, Kobilka TS, Thian FS, Edwards PC, et al. Crystal structure of the human $\beta 2$ adrenergic G-protein-coupled receptor. *Nature* (2007) 450:383–7. doi:10.1038/nature06325
81. Wu B, Chien EYT, Mol CD, Fenalti G, Liu W, Katritch V, et al. Structures of the CXCR4 chemokine GPCR with small-molecule and cyclic peptide antagonists. *Science* (2010) 330:1066–71. doi:10.1126/science.1194396
82. Yohannan S, Faham S, Yang D, Whitelegge JP, Bowie JU. The evolution of transmembrane helix kinks and the structural diversity of G protein-coupled receptors. *Proc Natl Acad Sci U S A* (2004) 101:959–63. doi:10.1073/pnas.0306077101
83. Chatenet D, Dubessy C, Leprince J, Boullaran C, Carlier L, Ségalas-Milazzo I, et al. Structure-activity relationships and structural conformation of a novel urotensin II-related peptide. *Peptides* (2004) 25:1819–30. doi:10.1016/j.peptides.2004.04.019
84. Labarrère P, Chatenet D, Leprince J, Marionneau C, Loirand G, Tonon M-C, et al. Structure-activity relationships of human urotensin II and related analogues on rat aortic ring contraction. *J Enzyme Inhib Med Chem* (2003) 18:77–88. doi:10.1080/1475636031000093507
85. Opggaard OS, Nothacker H-P, Ehlert FJ, Krause DN. Human urotensin II mediates vasoconstriction via an increase in inositol phosphates. *Eur J Pharmacol* (2000) 406:265–71. doi:10.1016/S0014-2999(00)00672-5
86. Camarda V, Guerrini R, Kostenis E, Rizzi A, Calò G, Hattenberger A, et al. A new ligand for the urotensin II receptor. *Br J Pharmacol* (2002) 137:311–4. doi:10.1038/sj.bjp.0704895
87. MacLean MR, Alexander D, Stirrat A, Gallagher M, Douglas SA, Ohlstein EH, et al. Contractile responses to human urotensin-II in rat and human pulmonary arteries: effect of endothelial factors and chronic hypoxia in the rat. *Br J Pharmacol* (2000) 130:201–4. doi:10.1038/sj.bjp.0703314
88. Russell FD, Molenaar P, O'Brien DM. Cardiostimulant effects of urotensin-II in human heart in vitro. *Br J Pharmacol* (2001) 132:5–9. doi:10.1038/sj.bjp.0703811
89. Gibson A. Complex effects of *Gillichthys* urotensin II on rat aortic strips. *Br J Pharmacol* (1987) 91:205–12. doi:10.1111/j.1476-5381.1987.tb09000.x
90. Gibson A, Conyers S, Bern HA. The influence of urotensin II on calcium flux in rat aorta. *J Pharm Pharmacol* (1988) 40:893–5. doi:10.1111/j.2042-7158.1988.tb06298.x
91. Itoh H, Itoh Y, Rivier J, Lederis K. Contraction of major artery segments of rat by fish neuropeptide urotensin II. *Am J Physiol* (1987) 252:R361–6.
92. Rossowski WJ, Cheng B-L, Taylor JE, Datta R, Coy DH. Human urotensin II-induced aorta ring contractions are mediated by protein kinase C, tyrosine kinases and Rho-kinase: inhibition by somatostatin receptor antagonists. *Eur J Pharmacol* (2002) 438:159–70. doi:10.1016/S0014-2999(02)01341-9
93. Russell FD, Molenaar P. Investigation of signaling pathways that mediate the inotropic effect of urotensin-II in human heart. *Cardiovasc Res* (2004) 63:673–81. doi:10.1016/j.cardiores.2004.05.009
94. Tasaki K, Hori M, Ozaki H, Karaki H, Wakabayashi I. Mechanism of human urotensin II-induced contraction in rat aorta. *J Pharmacol Sci* (2004) 94:376–83. doi:10.1254/jphs.94.376
95. Sauzeau V, Le Mellionne E, Bertoglio J, Scalbert E, Pacaud P, Loirand G. Human urotensin II-induced contraction and arterial smooth muscle cell proliferation are mediated by RhoA and Rho-kinase. *Circ Res* (2001) 88:1102–4. doi:10.1161/hh1101.092034
96. Abdelrahman AM, Pang CCY. Involvement of the nitric oxide/l-arginine and sympathetic nervous systems on the vasodepressor action of human urotensin II in anesthetized rats. *Life Sci* (2002) 71:819–25. doi:10.1016/S0024-3205(02)01743-5
97. Gardiner SM, March JE, Kemp PA, Davenport AP, Bennett T. Depressor and regionally-selective vasodilator effects of human and rat urotensin II in conscious rats. *Br J Pharmacol* (2001) 132:1625–9. doi:10.1038/sj.bjp.0704051
98. Hassan GS, Chouiali F, Saito T, Hu F, Douglas SA, Ao Z, et al. Effect of human urotensin-II infusion on hemodynamics and cardiac function. *Can J Physiol Pharmacol* (2003) 81:125–8. doi:10.1139/y03-004
99. Kompa AR, Thomas WG, See F, Tzanidis A, Hannan RD, Krum H. Cardiovascular role of urotensin II: effect of chronic infusion in the rat. *Peptides* (2004) 25:1783–8. doi:10.1016/j.peptides.2004.03.029
100. Zhu YZ, Wang ZJ, Zhu YC, Zhang L, Oakley RME, Chung CW, et al. Urotensin II causes fatal circulatory collapse in anesthetized monkeys in vivo: a “vasoconstrictor” with a unique hemodynamic profile. *Am J Physiol Heart Circ Physiol* (2004) 286:H830–6. doi:10.1152/ajpheart.00406.2003
101. Böhm F, Pernow J. Urotensin II evokes potent vasoconstriction in humans in vivo. *Br J Pharmacol* (2002) 135:25–7. doi:10.1038/sj.bjp.0704448
102. Affolter JT, Newby DE, Wilkinson IB, Winter MJ, Balment RJ, Webb DJ. No effect on central or peripheral blood pressure of systemic urotensin II infusion in humans. *Br J Clin Pharmacol* (2002) 54:617–21. doi:10.1046/j.1365-2125.2002.t01-1-01704.x
103. Cherian J, Burton TJ, Bradley TJ, Wallace SML, Mäki-Petäjä KM, Mackenzie IS, et al. The effects of urotensin II and urantide on forearm blood flow and systemic haemodynamics in humans. *Br J Clin Pharmacol* (2009) 68:518–23. doi:10.1111/j.1365-2125.2009.03475.x
104. Wilkinson IB, Affolter JT, de Haas SL, Pellegrini MP, Boyd J, Winter MJ, et al. High plasma concentrations of human urotensin II do not alter local or systemic hemodynamics in man. *Cardiovasc Res* (2002) 53:341–7. doi:10.1016/S0008-6363(01)00485-0
105. Lim M, Honisett S, Sparkes CD, Komesaroff P, Kompa A, Krum H. Differential effect of urotensin II on vascular tone in normal subjects and patients with chronic heart failure. *Circulation* (2004) 109:1212–4. doi:10.1161/01.CIR.0000121326.69153.98
106. Sondermeijer B, Kompa A, Komesaroff P, Krum H. Effect of exogenous urotensin-II on vascular tone in skin microcirculation of patients with essential hypertension. *Am J Hypertens* (2005) 18:1195–9. doi:10.1016/j.amjhyper.2005.03.748
107. Zomer E, de Ridder I, Kompa A, Komesaroff P, Gilbert R, Krum H. Effect of urotensin II on skin microvessel tone in diabetic patients without heart failure or essential hypertension. *Clin Exp Pharmacol Physiol* (2008) 35:1147–50. doi:10.1111/j.1440-1681.2008.04960.x
108. Lapp H, Boerrigter G, Costello-Boerrigter LC, Jaekel K, Scheffold T, Krakau I, et al. Elevated plasma human urotensin-II-like immunoreactivity in ischemic cardiomyopathy. *Int J Cardiol* (2004) 94:93–7. doi:10.1016/j.ijcard.2003.05.008
109. Hassan GS, Douglas SA, Ohlstein EH, Giaid A. Expression of urotensin-II in human coronary atherosclerosis. *Peptides* (2005) 26:2464–72. doi:10.1016/j.peptides.2005.05.028
110. Watanabe T, Pakala R, Katagiri T, Benedict CR. Synergistic effect of urotensin II with serotonin on vascular smooth muscle cell proliferation. *J Hypertens* (2001) 19:2191–6. doi:10.1097/00004872-200112000-00012
111. Shiraishi Y, Watanabe T, Suguro T, Nagashima M, Kato R, Hongo S, et al. Chronic urotensin II infusion enhances macrophage foam cell formation and atherosclerosis in apolipoprotein E-knockout mice. *J Hypertens* (2008) 26:1955–65. doi:10.1097/HJH.0b013e32830b61d8
112. Watanabe T, Suguro T, Kanome T, Sakamoto Y-I, Kodate S, Hagiwara T, et al. Human urotensin II accelerates foam cell formation in human monocyte-derived macrophages. *Hypertension* (2005) 1979(46):738–44. doi:10.1161/01.HYP.0000184226.99196.b5
113. Boussette N, Giaid A. Urotensin-II and cardiovascular diseases. *Curr Hypertens Rep* (2006) 8:479–83. doi:10.1007/s11906-006-0026-7
114. Rakowski E, Hassan GS, Dhanak D, Ohlstein EH, Douglas SA, Giaid A. A role for urotensin II in restenosis following balloon angioplasty: use of a selective UT receptor blocker. *J Mol Cell Cardiol* (2005) 39:785–91. doi:10.1016/j.yjmcc.2005.07.002
115. Pehlivani Y, Dokuyucu R, Demir T, Kaplan DS, Koc I, Orkmez M, et al. Palosuran treatment effective as bosentan in the treatment model of pulmonary arterial hypertension. *Inflammation* (2014) 37:1280–8. doi:10.1007/s10753-014-9855-8
116. Zhao J, Xie L-D, Song C-J, Mao X-X, Yu H-R, Yu Q-X, et al. Urantide improves atherosclerosis by controlling C-reactive protein, monocyte chemotactic protein-1 and transforming growth factor- β expression in rats. *Exp Ther Med* (2014) 7:1647–52. doi:10.3892/etm.2014.1654

117. You Z, Genest J, Barrette P-O, Hafiane A, Behm DJ, D'Orleans-Juste P, et al. Genetic and pharmacological manipulation of urotensin II ameliorate the metabolic and atherosclerosis sequelae in mice. *Arterioscler Thromb Vasc Biol* (2012) 32:1809–16. doi:10.1161/ATVBAHA.112.252973
118. Ziltener P, Mueller C, Haenig B, Scherz MW, Nayler O. Urotensin II mediates Erk1/2 phosphorylation and proliferation in GPR14-transfected cell lines. *J Recept Signal Transduct Res* (2002) 22:155–68. doi:10.1081/RRS-120014593
119. Matsushita M, Shichiri M, Fukai N, Ozawa N, Yoshimoto T, Takasu N, et al. Urotensin II is an autocrine/paracrine growth factor for the porcine renal epithelial cell line, LLCPK1. *Endocrinology* (2003) 144:1825–31. doi:10.1210/en.2003-0029
120. Zhang W-X, Liang Y-F, Wang X-M, Nie Y, Chong L, Lin L, et al. Urotensin upregulates transforming growth factor- β 1 expression of asthma airway through ERK-dependent pathway. *Mol Cell Biochem* (2012) 364:291–8. doi:10.1007/s11010-012-1229-7
121. Chen Y-L, Liu J-C, Loh S-H, Chen C-H, Hong C-Y, Chen J-J, et al. Involvement of reactive oxygen species in urotensin II-induced proliferation of cardiac fibroblasts. *Eur J Pharmacol* (2008) 593:24–9. doi:10.1016/j.ejphar.2008.07.025
122. Sue Y-M, Chen C-H, Hsu Y-H, Hou C-C, Cheng C-Y, Chen Y-C, et al. Urotensin II induces transactivation of the epidermal growth factor receptor via transient oxidation of SHP-2 in the rat renal tubular cell line NRK-52E. *Growth Factors* (2009) 27:155–62. doi:10.1080/08977190902879866
123. Tsai C-S, Loh S-H, Liu J-C, Lin J-W, Chen Y-L, Chen C-H, et al. Urotensin II-induced endothelin-1 expression and cell proliferation via epidermal growth factor receptor transactivation in rat aortic smooth muscle cells. *Atherosclerosis* (2009) 206:86–94. doi:10.1016/j.atherosclerosis.2009.02.013
124. Djordjevic T, BelAiba RS, Bonello S, Pfeilschifter J, Hess J, Görlach A. Human urotensin II is a novel activator of NADPH oxidase in human pulmonary artery smooth muscle cells. *Arterioscler Thromb Vasc Biol* (2005) 25:519–25. doi:10.1161/01.ATV.0000154279.98244.eb
125. Liu J-C, Chen C-H, Chen J-J, Cheng T-H. Urotensin II induces rat cardiomyocyte hypertrophy via the transient oxidization of Src homology 2-containing tyrosine phosphatase and transactivation of epidermal growth factor receptor. *Mol Pharmacol* (2009) 76:1186–95. doi:10.1124/mol.109.058297
126. Onan D, Pipolo L, Yang E, Hannan RD, Thomas WG. Urotensin II promotes hypertrophy of cardiac myocytes via mitogen-activated protein kinases. *Mol Endocrinol* (2004) 18:2344–54. doi:10.1210/me.2003-0309
127. Desrues L, Lefebvre T, Diallo M, Gandolfo P, Leprince J, Chatenet D, et al. Effect of GABA A receptor activation on UT-coupled signaling pathways in rat cortical astrocytes. *Peptides* (2008) 29:727–34. doi:10.1016/j.peptides.2008.01.024
128. Jarry M, Diallo M, Lecointre C, Desrues L, Tokay T, Chatenet D, et al. The vasoactive peptides urotensin II and urotensin II-related peptide regulate astrocyte activity through common and distinct mechanisms: involvement in cell proliferation. *Biochem J* (2010) 428:113–24. doi:10.1042/BJ20090867
129. Douglas SA, Naselsky D, Ao Z, Disa J, Herold CL, Lynch F, et al. Identification and pharmacological characterization of native, functional human urotensin-II receptors in rhabdomyosarcoma cell lines. *Br J Pharmacol* (2004) 142:921–32. doi:10.1038/sj.bjp.0705743
130. Brûlé C, Perzo N, Joubert J-E, Sainsily X, Leduc R, Castel H, et al. Biased signaling regulates the pleiotropic effects of the urotensin II receptor to modulate its cellular behaviors. *FASEB J* (2014) 28:5148–62. doi:10.1096/fj.14-249771
131. Chen Y, Zhao M, Liu X, Yao W, Yang J, Zhang Z, et al. Urotensin II receptor in the rat airway smooth muscle and its effect on the rat airway smooth muscle cells proliferation. *Chin Med Sci J* (2001) 16:231–5.
132. Iglesias M, Grant SR. Urotensin II-induced signaling involved in proliferation of vascular smooth muscle cells. *Vasc Health Risk Manag* (2010) 6:723–34. doi:10.2147/VHRM.S11129
133. Xu S, Wen H, Jiang H. Urotensin II promotes the proliferation of endothelial progenitor cells through p38 and p44/42 MAPK activation. *Mol Med Rep* (2012) 6:197–200. doi:10.3892/mmr.2012.899
134. Diebold I, Petry A, Burger M, Hess J, Görlach A. NOX4 mediates activation of FoxO3a and matrix metalloproteinase-2 expression by urotensin-II. *Mol Biol Cell* (2011) 22:4424–34. doi:10.1091/mbc.E10-12-0971
135. Song N, Ding W, Chu S, Zhao J, Dong X, Di B, et al. Urotensin II stimulates vascular endothelial growth factor secretion from adventitial fibroblasts in synergy with angiotensin II. *Circ J* (2012) 76:1267–73. doi:10.1253/circj.CJ-11-0870
136. Lee S-J, Jung YH, Oh SY, Yun SP, Han HJ. Melatonin enhances the human mesenchymal stem cells motility via melatonin receptor 2 coupling with G α q in skin wound healing. *J Pineal Res* (2014) 57:393–407. doi:10.1111/jpi.12179
137. Chen G, Wang W, Meng S, Zhang L, Wang W, Jiang Z, et al. CXC chemokine CXCL12 and its receptor CXCR4 in tree shrews (*Tupaia belangeri*): structure, expression and function. *PLoS One* (2014) 9:e98231. doi:10.1371/journal.pone.0098231
138. Esposito G, Perrino C, Cannava A, Schiattarella GG, Borgia F, Sannino A, et al. EGFR trans-activation by urotensin II receptor is mediated by β -arrestin recruitment and confers cardioprotection in pressure overload-induced cardiac hypertrophy. *Basic Res Cardiol* (2011) 106:577–89. doi:10.1007/s00395-011-0163-2
139. Chen L, Jin L, Zhou N. An update of novel screening methods for GPCR in drug discovery. *Expert Opin Drug Discov* (2012) 7:791–806. doi:10.1517/17460441.2012.699036
140. Gruson D, Ginon A, Decroly N, Lause P, Vanoverschelde JL, Ketelslegers JM, et al. Urotensin II induction of adult cardiomyocytes hypertrophy involves the Akt/GSK-3beta signaling pathway. *Peptides* (2010) 31:1326–33. doi:10.1016/j.peptides.2010.04.009
141. Chao H-H, Sung L-C, Chen C-H, Liu J-C, Chen J-J, Cheng T-H. Lycopene inhibits urotensin-II-induced cardiomyocyte hypertrophy in neonatal rat cardiomyocytes. *Evid Based Complement Alternat Med* (2014) 2014:724670. doi:10.1155/2014/724670
142. Guidolin D, Albertin G, Ribatti D. Urotensin-II as an angiogenic factor. *Peptides* (2010) 31:1219–24. doi:10.1016/j.peptides.2010.03.022
143. Albertin G, Guidolin D, Sorato E, Oselladore B, Tortorella C, Ribatti D. Urotensin-II-stimulated expression of pro-angiogenic factors in human vascular endothelial cells. *Regul Pept* (2011) 172:16–22. doi:10.1016/j.regpep.2011.08.001
144. Diebold I, Petry A, Sabrane K, Djordjevic T, Hess J, Görlach A. The HIF1 target gene NOX2 promotes angiogenesis through urotensin-II. *J Cell Sci* (2012) 125:956–64. doi:10.1242/jcs.094060
145. Segain J-P, Rolli-Derkinderen M, Gervois N, Raingeard de la Blétière D, Loirand G, Pacaud P. Urotensin II is a new chemotactic factor for UT receptor-expressing monocytes. *J Immunol* (2007) 179:901–9. doi:10.4049/jimmunol.179.2.901
146. Xu S, Jiang H, Wu B, Yang J, Chen S. Urotensin II induces migration of endothelial progenitor cells via activation of the RhoA/Rho kinase pathway. *Tohoku J Exp Med* (2009) 219:283–8. doi:10.1620/tjem.219.283
147. Grieco P, Franco R, Bozzuto G, Tocaccieli L, Sgambato A, Marra M, et al. Urotensin II receptor predicts the clinical outcome of prostate cancer patients and is involved in the regulation of motility of prostate adenocarcinoma cells. *J Cell Biochem* (2011) 112:341–53. doi:10.1002/jcb.22933
148. Matsusaka S, Wakabayashi I. Enhancement of vascular smooth muscle cell migration by urotensin II. *Naunyn Schmiedebergs Arch Pharmacol* (2006) 373:381–6. doi:10.1007/s00210-006-0086-x
149. Zhang Y-G, Li J, Li Y-G, Wei R-H. Urotensin II induces phenotypic differentiation, migration, and collagen synthesis of adventitial fibroblasts from rat aorta. *J Hypertens* (2008) 26:1119–26. doi:10.1097/HJH.0b013e3282fa1412
150. Zhang Y-G, Kuang Z-J, Mao Y-Y, Wei R-H, Bao S-L, Wu L-B, et al. Osteopontin is involved in urotensin II-induced migration of rat aortic adventitial fibroblasts. *Peptides* (2011) 32:2452–8. doi:10.1016/j.peptides.2011.10.018
151. Yi K, Yu M, Wu L, Tan X. Effects of urotensin II on functional activity of late endothelial progenitor cells. *Peptides* (2012) 33:87–91. doi:10.1016/j.peptides.2011.11.016
152. Federico A, Zappavigna S, Romano M, Grieco P, Luce A, Marra M, et al. Urotensin-II receptor is over-expressed in colon cancer cell lines and in colon carcinoma in humans. *Eur J Clin Invest* (2014) 44:285–94. doi:10.1111/eci.12231
153. Franco R, Zappavigna S, Gigantino V, Luce A, Cantile M, Cerrone M, et al. Urotensin II receptor determines prognosis of bladder cancer regulating cell motility/invasion. *J Exp Clin Cancer Res* (2014) 33:48. doi:10.1186/1756-9966-33-48

154. Lecointre C, Desrues L, Joubert JE, Perzo N, Guichet P-O, Le Joncour V, et al. Signaling switch of the urotensin II vasosactive peptide GPCR: prototypic chemotactic mechanism in glioma. *Oncogene* (2015) 34:5080–94. doi:10.1038/onc.2014.433
155. Coly P-M, Perzo N, Le Joncour V, Lecointre C, Schouft M-T, Desrues L, et al. Chemotactic G protein-coupled receptors control cell migration by repressing autophagosome biogenesis. *Autophagy* (2016) 12(12):2344–62. doi:10.1080/15548627.2016.1235125
156. Boussette N, Patel L, Douglas SA, Ohlstein EH, Giard A. Increased expression of urotensin II and its cognate receptor GPR14 in atherosclerotic lesions of the human aorta. *Atherosclerosis* (2004) 176:117–23. doi:10.1016/j.atherosclerosis.2004.03.023
157. Vergura R, Camarda V, Rizzi A, Spagnol M, Guerrini R, Calò G, et al. Urotensin II stimulates plasma extravasation in mice via UT receptor activation. *Naunyn Schmiedebergs Arch Pharmacol* (2004) 370:347–52. doi:10.1007/s00210-004-0991-9
158. Gendron G, Simard B, Gobeil F, Sirois P, D'Orléans-Juste P, Regoli D. Human urotensin-II enhances plasma extravasation in specific vascular districts in Wistar rats. *Can J Physiol Pharmacol* (2004) 82:16–21. doi:10.1139/y03-122
159. Johns DG, Ao Z, Naselsky D, Herold CL, Maniscalco K, Sarov-Blat L, et al. Urotensin-II-mediated cardiomyocyte hypertrophy: effect of receptor antagonism and role of inflammatory mediators. *Naunyn Schmiedebergs Arch Pharmacol* (2004) 370:238–50. doi:10.1007/s00210-004-0980-z
160. Zhou C-H, Wan Y-Y, Chu X-H, Song Z, Xing S-H, Wu Y-Q, et al. Urotensin II contributes to the formation of lung adenocarcinoma inflammatory microenvironment through the NF-κB pathway in tumor-bearing nude mice. *Oncol Lett* (2012) 4:1259–63. doi:10.3892/ol.2012.932
161. Cirillo P, De Rosa S, Pacileo M, Gargiulo A, Angri V, Fiorentino I, et al. Human urotensin II induces tissue factor and cellular adhesion molecules expression in human coronary endothelial cells: an emerging role for urotensin II in cardiovascular disease. *J Thromb Haemost* (2008) 6:726–36. doi:10.1111/j.1538-7836.2008.02923.x
162. Liang D, Liu L, Ye C, Zhao L, Yu F, Gao D, et al. Inhibition of UII/UTR system relieves acute inflammation of liver through preventing activation of NF-κB pathway in ALF mice. *PLoS One* (2013) 8:e64895. doi:10.1371/journal.pone.0064895
163. Artemenko Y, Lampert TJ, Devreotes PN. Moving towards a paradigm: common mechanisms of chemotactic signaling in *Dictyostelium* and mammalian leukocytes. *Cell Mol Life Sci* (2014) 71:3711–47. doi:10.1007/s00018-014-1638-8
164. Pierce KL, Tohgo A, Ahn S, Field ME, Luttrell LM, Lefkowitz RJ. Epidermal growth factor (EGF) receptor-dependent ERK activation by G protein-coupled receptors: a co-culture system for identifying intermediates upstream and downstream of heparin-binding EGF shedding. *J Biol Chem* (2001) 276:23155–60. doi:10.1074/jbc.M101303200
165. Roussos ET, Condeelis JS, Patsialou A. Chemotaxis in cancer. *Nat Rev Cancer* (2011) 11:573–87. doi:10.1038/nrc3078
166. Richardson BE, Lehmann R. Mechanisms guiding primordial germ cell migration: strategies from different organisms. *Nat Rev Mol Cell Biol* (2010) 11:37–49. doi:10.1038/nrm2815
167. Théveneau E, Mayor R. Neural crest migration: interplay between chemo-repellents, chemoattractants, contact inhibition, epithelial-mesenchymal transition, and collective cell migration. *Wiley Interdiscip Rev Dev Biol* (2012) 1:435–45. doi:10.1002/wdev.28
168. Sadik CD, Luster AD. Lipid-cytokine-chemokine cascades orchestrate leukocyte recruitment in inflammation. *J Leukoc Biol* (2012) 91:207–15. doi:10.1189/jlb.0811402
169. Bravo-Cordero JJ, Hodgson L, Condeelis J. Directed cell invasion and migration during metastasis. *Curr Opin Cell Biol* (2012) 24:277–83. doi:10.1016/j.ceb.2011.12.004
170. Rostène W, Kitabgi P, Parsadanianz SM. Chemokines: a new class of neuro-modulator? *Nat Rev Neurosci* (2007) 8:895–903. doi:10.1038/nrn2255
171. Borsig L, Wolf MJ, Roblek M, Lorentzen A, Heikenwalder M. Inflammatory chemokines and metastasis – tracing the accessory. *Oncogene* (2014) 33:3217–24. doi:10.1038/onc.2013.272
172. Hembruff SL, Cheng N. Chemokine signaling in cancer: implications on the tumor microenvironment and therapeutic targeting. *Cancer Ther* (2009) 7:254–67.
173. Lim SY, Yuzhalin AE, Gordon-Weeks AN, Muschel RJ. Targeting the CCL2-CCR2 signaling axis in cancer metastasis. *Oncotarget* (2016) 7:28697–710. doi:10.18632/oncotarget.7376
174. Maolake A, Izumi K, Shigebara K, Natsagdorj A, Iwamoto H, Kadomoto S, et al. Tumor-associated macrophages promote prostate cancer migration through activation of the CCL22-CCR4 axis. *Oncotarget* (2017) 8:9739–51. doi:10.18632/oncotarget.14185
175. Kato T, Fujita Y, Nakane K, Mizutani K, Terazawa R, Ehara H, et al. CC1/CC15 interaction promotes invasion of taxane-resistant PC3 prostate cancer cells by increasing secretion of MMPs 2/9 and by activating ERK and Rac signaling. *Cytokine* (2013) 64:251–7. doi:10.1016/j.cyto.2013.06.313
176. Long H, Xiang T, Qi W, Huang J, Chen J, He L, et al. CD133+ ovarian cancer stem-like cells promote non-stem cancer cell metastasis via CCL5 induced epithelial-mesenchymal transition. *Oncotarget* (2015) 6:5846–59. doi:10.18632/oncotarget.3462
177. Albertin G, Guidolin D, Sorato E, Spinazzi R, Mascarin A, Oselladore B, et al. Pro-angiogenic activity of urotensin-II on different human vascular endothelial cell populations. *Regul Pept* (2009) 157:64–71. doi:10.1016/j.regpep.2009.04.006
178. Morimoto R, Satoh F, Murakami O, Totsune K, Arai Y, Suzuki T, et al. Immunolocalization of urotensin II and its receptor in human adrenal tumors and attached non-neoplastic adrenal tissues. *Peptides* (2008) 29:873–80. doi:10.1016/j.peptides.2007.06.025
179. Takahashi K, Totsune K, Murakami O, Arihara Z, Noshiro T, Hayashi Y, et al. Expression of urotensin II and its receptor in adrenal tumors and stimulation of proliferation of cultured tumor cells by urotensin II. *Peptides* (2003) 24:301–6. doi:10.1016/S0196-9781(03)00039-1
180. Desrues L, Lefebvre T, Lecointre C, Schouft M-T, Leprince J, Compère V, et al. Down-regulation of GABA(A) receptor via promiscuity with the vasoactive peptide urotensin II receptor. Potential involvement in astrocyte plasticity. *PLoS One* (2012) 7:e36319. doi:10.1371/journal.pone.0036319
181. Takahashi K, Totsune K, Murakami O, Shibahara S. Expression of urotensin II and urotensin II receptor mRNAs in various human tumor cell lines and secretion of urotensin II-like immunoreactivity by SW-13 adrenocortical carcinoma cells. *Peptides* (2001) 22:1175–9. doi:10.1016/S0196-9781(01)00441-7
182. Birker-Robaczewska M, Boukhadra C, Studer R, Mueller C, Binkert C, Nayler O. The expression of urotensin II receptor (U2R) is up-regulated by interferon-gamma. *J Recept Signal Transduct Res* (2003) 23:289–305. doi:10.1081/RRS-120026972
183. Wu Y-Q, Song Z, Zhou C-H, Xing S-H, Pei D-S, Zheng J-N. Expression of urotensin II and its receptor in human lung adenocarcinoma A549 cells and the effect of urotensin II on lung adenocarcinoma growth in vitro and in vivo. *Oncol Rep* (2010) 24:1179–84.
184. Balakan O, Kalender ME, Suner A, Cengiz B, Oztuzcu S, Bayraktar R, et al. The relationship between urotensin II and its receptor and the clinicopathological parameters of breast cancer. *Med Sci Monit* (2014) 20:1419–25. doi:10.12659/MSM.890459
185. Cook J, Hagemann T. Tumour-associated macrophages and cancer. *Curr Opin Pharmacol* (2013) 13:595–601. doi:10.1016/j.coph.2013.05.017
186. Ryan CM, Brown JAL, Bourke E, Prendergast ÁM, Kavanagh C, Liu Z, et al. ROCK activity and the G β γ complex mediate chemotactic migration of mouse bone marrow-derived stromal cells. *Stem Cell Res Ther* (2015) 6:136. doi:10.1186/s13287-015-0125-y

Disclaimer: All appropriate permissions have been obtained from the copyright holders of any work that has been reproduced in this manuscript.

Conflict of Interest Statement: The authors declare that the research was conducted in the absence of any commercial or financial relationships that could be construed as a potential conflict of interest.

Copyright © 2017 Castel, Desrues, Joubert, Tonon, Prézeau, Chabbert, Morin and Gandolfo. This is an open-access article distributed under the terms of the Creative Commons Attribution License (CC BY). The use, distribution or reproduction in other forums is permitted, provided the original author(s) or licensor are credited and that the original publication in this journal is cited, in accordance with accepted academic practice. No use, distribution or reproduction is permitted which does not comply with these terms.



Membrane Active Antimicrobial Peptides: Translating Mechanistic Insights to Design

Jianguo Li^{1,2,3}, Jun-Jie Koh¹, Shouping Liu¹, Rajamani Lakshminarayanan¹, Chandra S. Verma^{1,2,4,5} and Roger W. Beuerman^{1,3*}

¹ Ocular Chemistry and Anti-Infectives, Singapore Eye Research Institute, Singapore, Singapore, ² Agency for Science, Technology and Research (A*STAR), Bioinformatics Institute, Singapore, Singapore, ³ Duke-NUS Graduate Medical School, SRP Neuroscience and BD, Singapore, Singapore, ⁴ Department of Biological Sciences, National University of Singapore, Singapore, Singapore, ⁵ School of Biological Sciences, Nanyang Technological University, Singapore, Singapore

OPEN ACCESS

Edited by:

Hubert Vaudry,
University of Rouen, France

Reviewed by:

Nils Lambrecht,
Veterans Administration Long Beach
and University of California Irvine, USA

John Michael Conlon,
Ulster University, UK

***Correspondence:**

Roger W. Beuerman
rwbeuerman@gmail.com

Specialty section:

This article was submitted to
Neuroendocrine Science,
a section of the journal
Frontiers in Neuroscience

Received: 29 November 2016

Accepted: 31 January 2017

Published: 14 February 2017

Citation:

Li J, Koh J-J, Liu S, Lakshminarayanan R, Verma CS and Beuerman RW (2017) Membrane Active Antimicrobial Peptides: Translating Mechanistic Insights to Design. *Front. Neurosci.* 11:73.
doi: 10.3389/fnins.2017.00073

Antimicrobial peptides (AMPs) are promising next generation antibiotics that hold great potential for combating bacterial resistance. AMPs can be both bacteriostatic and bactericidal, induce rapid killing and display a lower propensity to develop resistance than do conventional antibiotics. Despite significant progress in the past 30 years, no peptide antibiotic has reached the clinic yet. Poor understanding of the action mechanisms and lack of rational design principles have been the two major obstacles that have slowed progress. Technological developments are now enabling multidisciplinary approaches including molecular dynamics simulations combined with biophysics and microbiology toward providing valuable insights into the interactions of AMPs with membranes at atomic level. This has led to increasingly robust models of the mechanisms of action of AMPs and has begun to contribute meaningfully toward the discovery of new AMPs. This review discusses the detailed action mechanisms that have been put forward, with detailed atomistic insights into how the AMPs interact with bacterial membranes. The review further discusses how this knowledge is exploited toward developing design principles for novel AMPs. Finally, the current status, associated challenges, and future directions for the development of AMP therapeutics are discussed.

Keywords: antimicrobial peptides, action mechanism, membrane, antibiotic resistance, peptide antibiotics

INTRODUCTION

The continued emergence of resistant pathogens world-wide, particularly among Gram-negative bacteria, has become a leading health care challenge (McKenna, 2013). Resistant strains of bacteria/fungus/yeast are regularly being found for almost every antimicrobial used clinically. On the other hand, a decline in the approval of new antibiotics has further exacerbated the problem, leading to an “antibiotic crisis” (Livermore, 2004). Persistence of the current situation is driving clinicians to use drugs that are associated with significant toxicity. In contrast to small molecule antibiotics, antimicrobial peptides (AMPs) act on the bacterial membrane which is

Abbreviations: AMP, Antimicrobial peptide; POPE, Phosphatidylethanolamine; POPG, Phosphatidylglycerol; POPC, Phosphatidylcholine; POPS, Phosphatidylserine; CL, Cardiolipin; LPS, Lipopolysaccharide; SAR, Structure-activity relationship; CD, Circular dichroism; MD, Molecular dynamics; MRSA, methicillin-resistant *Staphylococcus aureus*; MIC, minimum inhibitory concentration.

an evolutionarily conserved component of bacterial cells (Yeaman and Yount, 2003). Bacterial membranes define the phenotype and membrane mutations would likely be costly for bacteria, therefore AMPs are less likely to induce bacterial resistance (Zasloff, 2002). Moreover, AMPs are bactericidal and they kill bacteria much more rapidly than conventional antibiotics (Zasloff, 1987; Romeo et al., 1988; Mygind et al., 2005; Marr et al., 2006; Bai et al., 2012; Deslouches et al., 2013).

There are more than 2,000 naturally occurring and synthetic AMPs (Wang G. et al., 2016). Naturally occurring AMPs, including defensins, are produced in various living organisms including humans and are part of the innate immune system (Diamond et al., 2009). In humans, these molecules are found in lymphocytes and epithelial surfaces (e.g., skin, eye, lung, and intestines etc.). For example, Paneth cells, the specialized secretory epithelial cells in the small intestine, produce high levels of AMPs (e.g., alpha-defensins, lysozyme etc.), resulting in a controlled number of bacteria in the small intestine (Ayabe et al., 2004; Bevins and Salzman, 2011). The tear fluid of the eye is also a rich source of AMPs and include the defensins, lysozyme, and cathelicidins, protecting the eyes from infections (McDermott, 2013). Other AMPs can be either synthesized ribosomally or produced non-ribosomally in bacteria and fungi during cultivation on various carbon sources (Makovitzki et al., 2006). Lipopeptides such as polymyxins are produced as metabolites in bacteria or fungi. However, these are also membrane targeting, so, in this review, the general term, AMP will be used to refer to them. In addition to their antimicrobial-activity, some AMPs have other important roles in immune regulation, inflammation, anti-cancer, sepsis, and wound healing. Indeed, some AMPs demonstrate not only antimicrobial, but also anti-inflammatory and immune regulatory activities (Sjogren, 2004; Gordon et al., 2005). The non-antimicrobial functions of AMPs are out of the scope of this review, and the interested reader can refer to relevant references (Ganz, 2003a,b; Marta Guarna et al., 2006; Van Lenten et al., 2008; McCormick and Weinberg, 2010; Shin and Jo, 2011; Li et al., 2012; Schuerholz et al., 2012; Gaspar et al., 2013; Hilchie et al., 2013; Martin et al., 2015a,b; Brandenburg et al., 2016).

AMPs are generally short peptides with <50 amino acids. Although there are more than 2,000 naturally occurring or synthetic AMPs, their lengths, sequences and 3-dimensional (3-D) conformations differ significantly, making it difficult to relate the sequence/structure to antimicrobial activity. Moreover, AMPs can undergo conformational changes upon adsorption onto the bacterial membrane and have evolved several mechanisms of action, which further complicate the analysis of a structure-activity relationship (SAR). As there is insufficient detailed knowledge of the action mechanisms in bacteria, synthetic AMPs are generally designed by trial and error (Epand and Vogel, 1999). Overcoming this gap in understanding could make antibiotic design closer to what is the common structure based approach for drug design and the action mechanism is crucial to this goal. Although the action mechanism for AMPs have been discussed in earlier reviews, most of them focus on the description of the general features of empirical models (e.g., pore-forming and carpet

models), few discuss the detailed atomistic events and the dynamic processes of AMP mechanisms of action (Epand and Vogel, 1999; Shai, 2002; Guilhelmelli et al., 2013; Lee et al., 2016). Recently, the employment of molecular dynamics (MD) simulations has deepened our understanding of the underlying action mechanism at a molecular level. Based on insights at atomic level, rational molecular principles have been put forward for the development of AMP therapeutics. Our primary focus in this review is to provide a fundamental understanding of the atomistic mechanisms of various AMPs and discuss molecular principles for practical AMP design. In addition, the current status of development of AMP antibiotics as well as challenges and future prospects for AMP therapeutics are discussed.

MODES OF ACTION OF AMPs

Structure of the Bacterial Membrane: The Target of AMPs

To understand the mode of action of AMPs, we begin with a discussion of the structure and physical properties of the bacterial membrane—the target of AMPs. Bacteria are broadly classified as either Gram-positive or Gram-negative, characterized by significant differences in their cell envelopes (Figure 1). The inner or cytoplasmic membranes of both bacteria groups are similar. However, the outer cell envelopes are significantly different. In Gram-positive bacteria, there is a layer of crosslinked peptidoglycan decorated with negatively charged teichoic acid surrounding the cytoplasmic membrane, forming a thick matrix which maintains the rigidity of the bacterial cell. Nano-sized pores penetrate into the peptidoglycan layers, allowing AMPs to diffuse through (Meroueh et al., 2006). In contrast, the peptidoglycan layer in Gram-negative bacteria is much thinner and less cross-linked. In addition, Gram-negative bacteria have an additional outer membrane outside the peptidoglycan layer. The inner leaflet consists purely of phosphate lipids while the outer leaflet is primarily a coat of lipopolysaccharide (LPS; Ruiz et al., 2006). LPS molecules are decorated with a high number of negatively charged phosphate groups that are engaged in salt-bridges with divalent cations (e.g., Ca^{2+} and Mg^{2+}), resulting in an electrostatic network (Nikaido, 2003). This electrostatic region serves as a primary barrier to most hydrophobic antibiotics, resulting in low permeability. Therefore, the details as to how AMPs penetrate into Gram-positive and Gram-negative bacteria must vary in their atomistic interactions. In the case of Gram-positive bacteria, AMPs need to diffuse across the peptidoglycan matrix first and then act on the cytoplasmic membrane. In contrast, killing Gram-negative bacteria involves perturbation or disruption of both outer and cytoplasmic membranes. Inability to permeabilize or disrupt the outer membrane results in the loss of antimicrobial activity. Daptomycin is able to disrupt the cytoplasmic membrane, but not able to permeabilize/disrupt the outer membrane of Gram-negative bacteria. As such, it is highly active against Gram-positive bacteria such as methicillin-resistant *Staphylococcus aureus* (MRSA), but has no activity against Gram-negative bacteria (Tally and DeBruin, 2000).

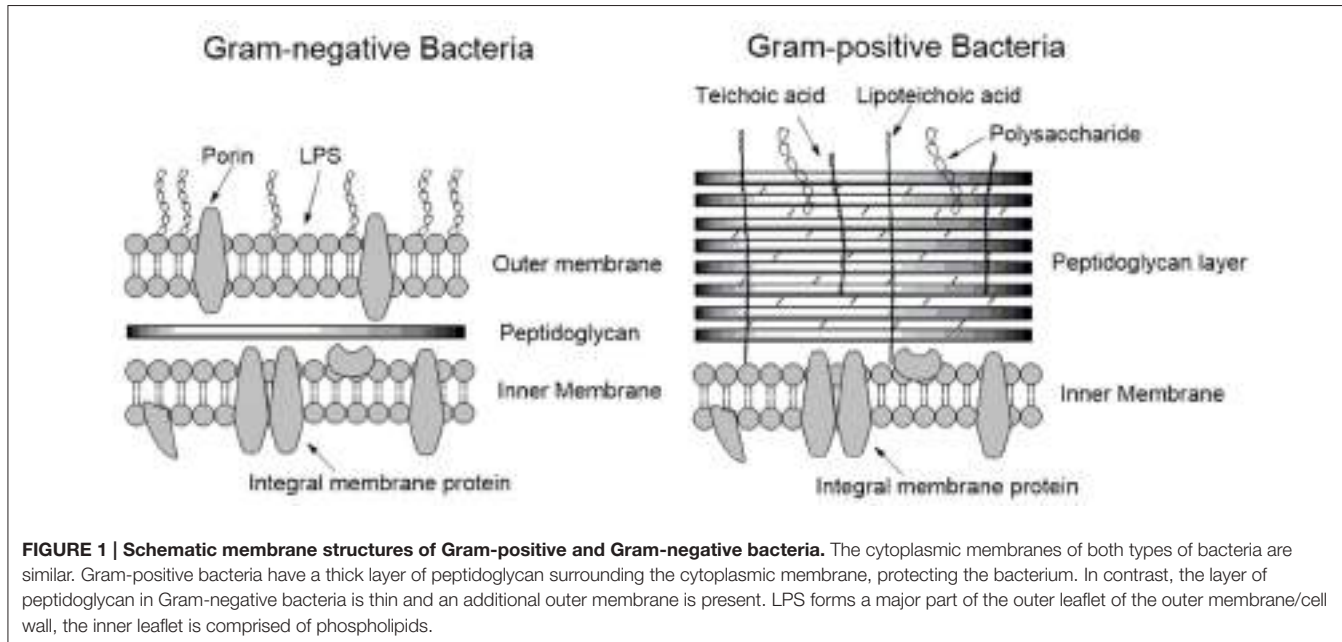


FIGURE 1 | Schematic membrane structures of Gram-positive and Gram-negative bacteria. The cytoplasmic membranes of both types of bacteria are similar. Gram-positive bacteria have a thick layer of peptidoglycan surrounding the cytoplasmic membrane, protecting the bacterium. In contrast, the layer of peptidoglycan in Gram-negative bacteria is thin and an additional outer membrane is present. LPS forms a major part of the outer leaflet of the outer membrane/cell wall, the inner leaflet is comprised of phospholipids.

Parameters Affecting AMP Movement to the Cytoplasmic Membrane

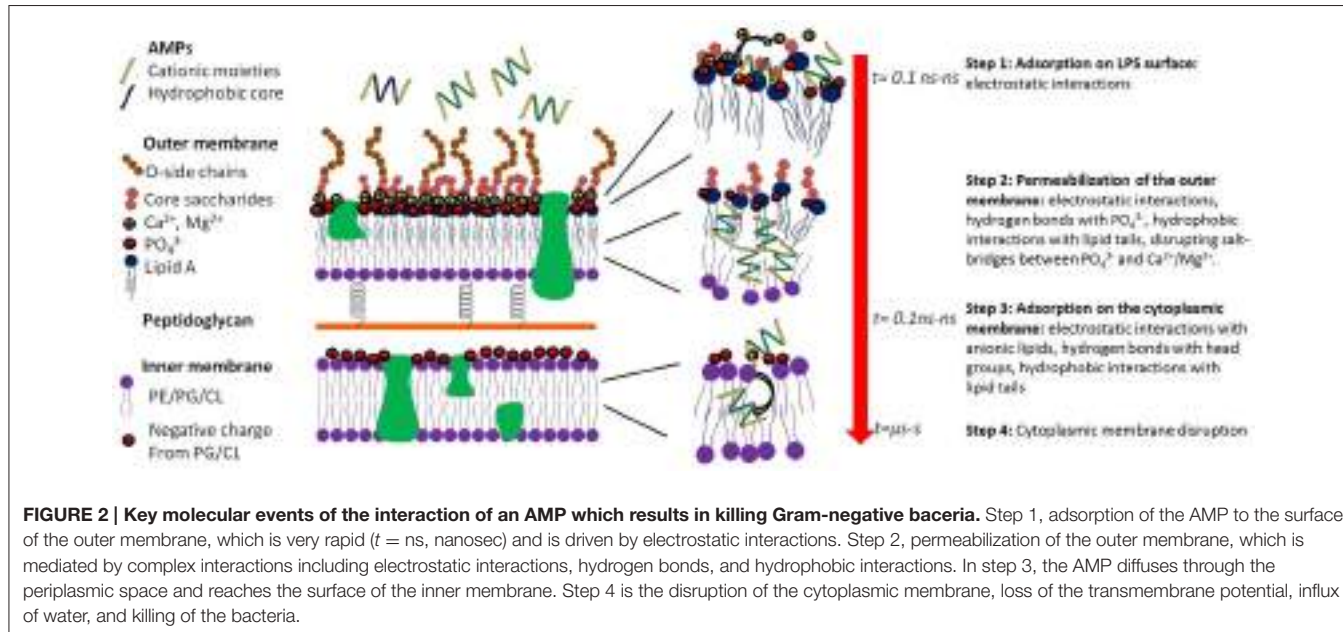
The cytoplasmic membrane (also called as the inner membrane) of Gram-positive and Gram-negative bacteria are comprised of a mixture of zwitterionic and anionic phospholipids, such as phosphatidylethanolamine (POPE), phosphatidylglycerol (POPG), and cardiolipin (CL). Models of action for AMPs acting on the cytoplasmic membrane include pore formation (e.g., barrel stave or toroidal pores) and carpet mechanism (Brogden, 2005; Melo et al., 2009). For an AMP to disrupt the cytoplasmic membrane, the AMP molecules must first accumulate on the membrane surface up to a critical concentration. However, diffusion barriers in either the outer membrane or the periplasmic space affect their partition onto the membrane. This is a more direct path for Gram-positive bacteria as the AMPs only need to diffuse through nano-sized pores in the peptidoglycan, which in most cases is not a rate-limiting step (Vollmer et al., 2008). In fact, the peptidoglycan layer can facilitate AMP accumulation on the surface of the cytoplasmic membrane due to favorable interactions between teichoic acid and cationic AMPs (Malanovic and Lohner, 2016).

In the case of Gram-negative pathogens, AMPs need to permeabilize or disrupt both the outer and cytoplasmic membranes, resulting in a two-step process (Figure 2; Schwechheimer and Kuehn, 2015). Although the outer membrane of Gram-negative pathogens significantly modulates the antimicrobial activity of AMPs, in most cases, the inner membrane is the rate-limiting step. For example, polymyxin B has strong antimicrobial activity against Gram-negative pathogens due to its ability to disrupt both the outer and the cytoplasmic membranes. However, removing the lipid tail resulting in polymyxin B nonapeptide, and only the outer

membrane is permeabilized. As a result, the nonapeptide also loses antimicrobial activity (Ofek et al., 1994).

The detailed mode of interactions between AMPs and the outer membrane of Gram-negative bacteria is poorly understood due to the complex structure of the LPS molecules, which consists of a lipid A component, an inner and an outer core portion and a sugar portion (Figure 2). The initial event is the adsorption onto the outer membrane surface, which can occur within tens of nanoseconds and is largely mediated by electrostatic interactions between cationic AMPs and anionic LPS molecules. Reduction in the electrostatic driving force significantly affects the partition of AMPs to the outer membrane and may result in the loss of antimicrobial activity. For example, modification of the phosphate groups on the LPS molecules such as deacylation, hydroxylation, or addition of phosphoethanolamine endows bacteria resistance to colistin (polymyxin E; Olaitan et al., 2014). Upon adsorption onto the outer membrane, AMPs form hydrogen bonds with the phosphate groups, disrupting the salt-bridges between phosphate groups and divalent cations and destabilizing the outer membrane. In addition to the electrostatic forces, the hydrophobic moieties of an AMP can also interact with the lipid tails of the LPS molecule, further destabilizing the close packing of the outer membrane. After the AMP permeabilizes/disrupts the outer membrane, it diffuses inward to the periplasmic space and adsorbs onto the surface of the cytoplasmic membrane. Once a critical surface concentration on the cytoplasmic membrane is reached, the AMP induces significant perturbations and disorganizations of the cytoplasmic membrane, resulting in loss of the transmembrane potential, and eventual death of the bacterial cell.

Characteristics of the interactions of AMP with the outer and cytoplasmic membranes include: length of the AMP sequence, the total and density of cationic charges, the total number



of hydrogen bonds donors and the 3-D conformation of the AMP in solution and at the membrane (Sitaram and Nagaraj, 1999; Bürck et al., 2008). The AMP structures that have been determined experimentally and deposited into the protein data bank provide little information for SAR as these structures are either in solution or in crystals rather than in the membrane environment. Due to the short sequences of most AMPs, their structures are sensitive to their environment. By comparing the CD spectrum of AMPs in solution and in the presence of liposomes, a large number of AMPs (e.g., melittin, magainin) have been found to undergo conformational transitions from random conformations in solution to helical or beta-sheet conformations on the membrane surface (Ramamoorthy et al., 2006; Hartings et al., 2008). For example, melittin adopts a helical conformation and protegrin adopts a beta-sheet conformation upon adsorption onto the membrane surface (Blazyk et al., 2001; Lu et al., 2005; Rausch et al., 2005, 2007; Dong et al., 2012). *In silico* modeling further reveals that both the alpha-helical and beta-sheet conformations are amphiphilic, with the cationic residues interacting with the anionic head groups and the hydrophobic residues penetrating into the lipid tail region of the membrane. Hence the electrostatic and hydrophobic interactions are two driving forces that steer an AMP toward and into the bacterial membrane.

Early Events in AMP Disruption of the Cytoplasmic Membrane

After adsorption onto the membrane surface, AMPs can induce a variety of membrane perturbations within tens of nanoseconds (Li et al., 2013). For most AMPs, an early event is the formation of hydrogen bonds between the basic residues (e.g., arginine and lysine) and the phosphate groups of the lipids. At physiological conditions, both lysine and arginine are hydrogen bond donors. However, arginine can form more stable bidentate hydrogen

bonds with phosphate groups. Hydrophobic residues can further penetrate and disorganize the lipid tail region of the membrane. As more AMP molecules accumulate at the membrane-water interface, the membrane becomes thin, as observed for most AMPs (Sato and Feix, 2006; Ye et al., 2010). Moreover, as the total volume of the membrane is roughly constant, membrane thinning results in lateral expansion, affecting the mechanical properties of the membrane. For example, with the increase in the area per lipid, the surface tension increases and the bending modulus decreases dramatically, implying membrane deformation (Szleifer et al., 1988; Stevens, 2004). The expansion of the membrane also results in reduction in the packing of the lipid molecules leading to the formation of a large number of cavities, significantly reducing the translocation free energy of water molecules across the lipid tail region. As a result, a large number of water translocations occur, and the membrane becomes leaky with the collapse of the transmembrane potential and additional membrane dysfunction, such as inhibition of ATP production and loss of proton motive force (Dimroth et al., 2000) and rapid death of the bacterium.

Some AMPs, particularly the highly cationic ones can induce lipid re-arrangements and the formation of lipid rafts. B2088, an 18 residue peptide dimer with a high content of basic residues (12 positive charges), once adsorbed on the bacterial membrane, was found to recruit anionic lipids surrounding the peptide, resulting in micro-domains rich in anionic lipids in the outer leaflet of the membrane (Bai et al., 2012). Due to the binding to AMPs, lipid molecules surrounding AMP molecules display slow diffusivity, which not only affects the fluidity and structure of the membrane, but also results in significant tension, particularly along the domain boundaries (Guo et al., 2011). Clustering of anionic lipids in model bacterial membranes was found for other peptides as well (Oreopoulos et al., 2010; Polyansky et al., 2010; Wadhwani et al., 2012; Scheinpflug et al., 2015). Some AMPs were

found to even induce flip-flop of anionic lipids from the inner leaflet to the outer leaflet, resulting in highly negatively charged outer leaflet and less negatively charged inner leaflet (Qian and Heller, 2011). This asymmetric distribution of charged lipids further destroys the membrane potential, resulting in membrane destabilization.

Membrane geometry as measured by the curvature is a fundamental property denoting stability with its basis in lipid organization and protein inclusions. Wong and coworkers suggested that negative Gaussian curvature is a prerequisite topology for the formation of membrane pores (Schmidt et al., 2010, 2011; Schmidt and Wong, 2013). It was found that POPE has the highest tendency to form a negative Gaussian curvature (“saddle-splay”) because of its small head group with respect to its large lipid tails (Yang et al., 2007; Schmidt et al., 2011). Interestingly, bacterial membranes consist of a high percentage of POPE while human membranes are mainly composed of POPC, implying that the preference of AMPS for POPE-rich membranes contributes significantly to the selectivity of AMPs. MD simulation studies have also shown that arginine residues can induce higher negative Gaussian curvature than lysine residues. The guanidinium group of arginine can form bidentate hydrogen bonds and coordinate two phosphate groups at <0.5 nm, while the distance is 0.7 nm for lysine (Schmidt et al., 2012a,b; Wu et al., 2013). Wu et al. employed both coarse-grained and atomistic models to simulate the interactions of poly-arginine and poly-lysine with model bacterial membranes (Wu et al., 2013). Their results revealed the different interactions of arginine and lysine residues with lipid molecules. The

guanidinium group of arginine can simultaneously interact with both phosphate and glycerol groups, and thus induce greater negative Gaussian curvatures than lysine residues, as the latter can only engage interactions with phosphate groups. Wong and coworkers also found that incorporation of hydrophobic moieties further reinforces negative Gaussian curvature, which is consistent with the antimicrobial activity of various arginine-rich AMPs. For example, a series (RW)_n peptides, which consists of only arginine (R) and tryptophan (W), display high antimicrobial activity (Strøm et al., 2002, 2003; Chan et al., 2006). In particular, an analog of (RW)_n peptide LTX-109 has entered into clinical trials (Isaksson et al., 2011b).

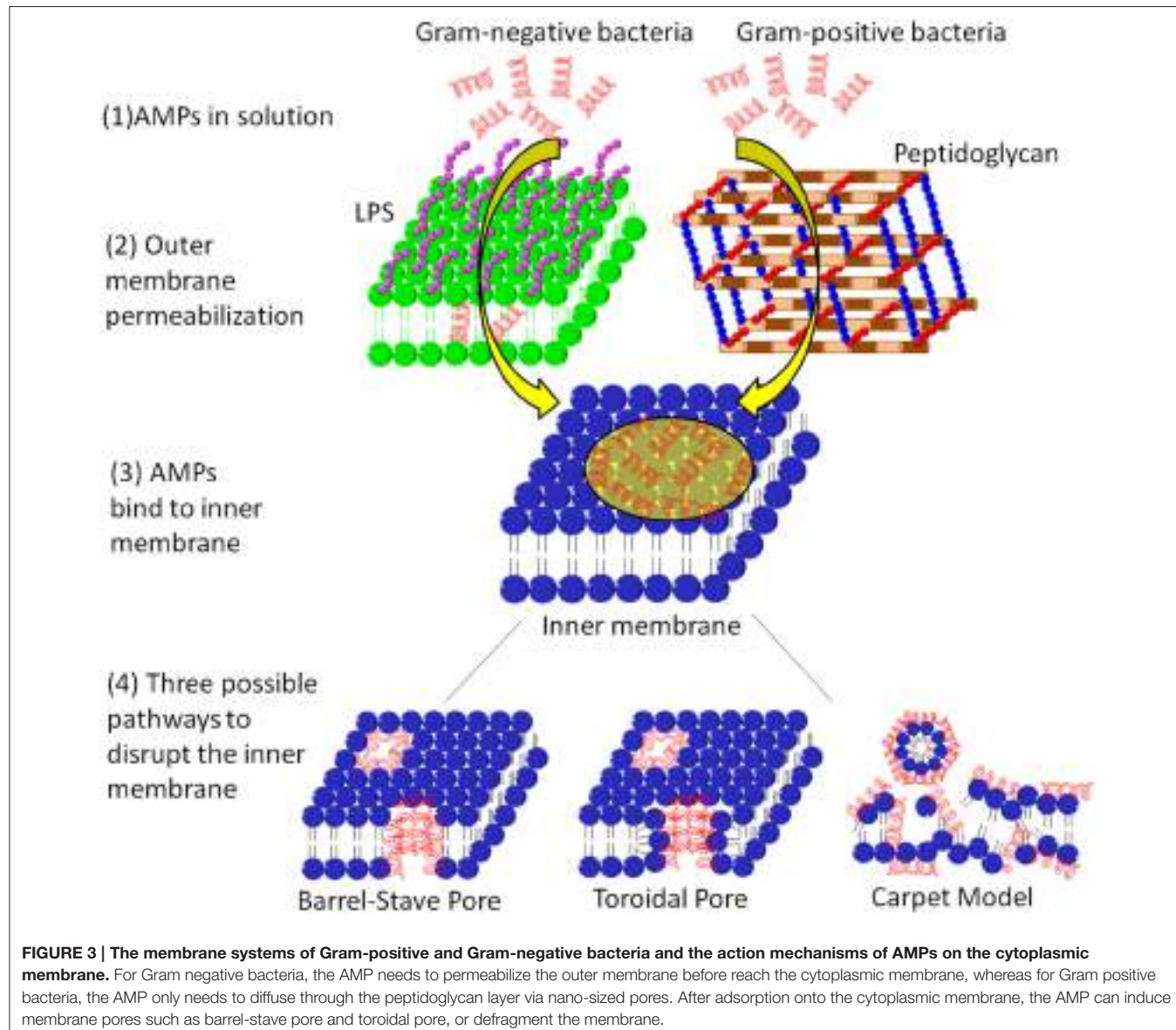
Molecular Models of Pore Formation

A number of AMPs form membrane pores (Table 1). The timescale of pore formation ranges from microseconds to seconds. Membrane pores result in the loss of membrane potential and rapid release of intracellular components and death. Depending on the geometry of the pores as well as the interactions of AMPs with the pores, pores can be described by the barrel-stave or the toroidal model (Figure 3). The formation of barrel-stave pores is driven by hydrophobic match. In this model, the membrane does not display significant curvature and the hydration of the membrane remains unchanged. In the case of the toroidal model, as the AMP molecules penetrate deeper into the membrane, the head groups of the lipids are dragged into the lipid tail region to form toroidal shaped pores while the lipid tails are packed away from the surface of the pore, resulting in significant lipid disorder, and membrane curvature

TABLE 1 | Representative AMPs and their modes of action.

AMPs	Sequence	Mechanism	References
Maculatin 1.1	GLFVGVLAKVAAHVVPAIAEHF	Pore	Dye leakage experiment and MD simulations (Chen and Mark, 2011; Sani et al., 2013)
Caerin 1.1	GLLSVLGSVAKHVLPHVVPIAEHL	Pore	MD simulations (Chen and Mark, 2011)
Cateslytin	RSMRLSFRARGYGFR	Pore	MD simulations and Patch-clamp experiment (Jean-François et al., 2008)
Gramicidin A	VGALAWWWLWLWLW	Pore	NMR (Urry, 1971; Ketcham et al., 1993)
Alamethicin	PAAAAQAVAGLAPVAAEQ	Barrel stave pore	Ion conductance experiment and statistical analysis (Boheim, 1974; Laver, 1994)
Magainin H2	IIKKFLHSIWKFGKAFVGEIMNI	Pore	Ion conductance experiment and MD simulations (Matsuzaki, 1998; Leontiadou et al., 2006)
Melittin	GIGAVLKVLTTGLPALISWIKRKRQQ	Toroidal pore	Dye leakage and grazing-Angle X-Ray Anomalous Diffraction and MD simulations (Yang et al., 2001; Sengupta et al., 2008; Lee et al., 2013; Leveritt et al., 2015)
Protegrin 1	RGGRLCYCRRRCVCVGR	Pore	Ion conductance experiment (Sokolov et al., 1999)
LL-37	LLGDFFRKSKKEKGKEFKRIVQRIKDFLRLNLPRTES	Toroidal pore	NMR (Henzler Wildman et al., 2003)
Indolicidin	ILPWKPWWPWRR	Pore	Ion conductance experiment (Falla et al., 1996)
Pardaxin 1	GFFALIPKIISSPLFKTLLSAVGSAALSSSGEQE	Barrel stave pore	NMR (Porcelli et al., 2004; Ramamoorthy et al., 2010)
MSI peptide	GIGKFLHSAAKFGKAFVGEIMNS	Carpet	NMR (Lee et al., 2015)
Citropin 1.1	GLFDVIKKVASVIGGL	Carpet	MD simulations (Chen and Mark, 2011)
Aurein 1.2	GLFDIIKKIAESF	Carpet	Quartz crystal microbalance with dissipation, vesicle dye leakage and atomic force microscopy experiments and MD simulations (Chen and Mark, 2011; Fernandez et al., 2012)
B2088	(RGRKVVR) ₂ KK	Carpet	MD simulations (Li et al., 2013)
PL-5	Ac-KWKSFLKTFKS-A-AKTVLHTALKAISS-amide		In clinical trials. ProteLight-Pharmaceuticalal, 2016 ^a

^a<http://www.protelight.com/english/Content.asp?Action=ArticleShow&Columns=26&Category=27&Articleid=80>.



change (Sengupta et al., 2008). As a result, toroidal pores are also accompanied by enhanced membrane hydration, as evidenced by significant water penetration into the membrane (Sengupta et al., 2008; Manna and Mukhopadhyay, 2009). In toroidal pores, AMPs primarily interact with the pores electrostatically since the surface of toroidal pores are covered by the phosphate head groups and the AMP molecules have less hydrophobic contact with the lipid tails. In contrast, in barrel stave pores, both electrostatic and hydrophobic interactions are important since the AMP molecules interact with both the head groups and the lipid tails (Mihajlovic and Lazaridis, 2010; Bertelsen et al., 2012).

Although induction of membrane pores is a general mechanism for a large number of AMPs, the morphology of these membrane pores can be quite diverse in terms of pore diameter, lipid conformation surrounding the pore, life time of the pore (e.g., transient pore or permanent pore) and the number

of AMP molecules required to stabilize the pore. Regarding the shape of the pore, AMPs such as alamethicin, dermcidin, and pardaxin induce barrel stave pores (Laver, 1994; Porcelli et al., 2004; Song et al., 2013), while most other AMPs induce toroidal pores (Matsuzaki, 1998; Sokolov et al., 1999; Yang et al., 2001; Henzler Wildman et al., 2003; Sengupta et al., 2008; Lee et al., 2013). In terms of the pore size, magainin induces small toroidal pores of ~2–3 nm in diameter that only allow water and small intracellular molecules to leak out (Takeshima et al., 2003; Brogden, 2005), while lacticin Q and protegrin can form much larger pores of 4.6 and 9 nm in diameter, respectively, allowing the leakage of much large intracellular molecules (Yoneyama et al., 2009; Lam et al., 2012). In addition, the pore size depends on various factors such as the lipid composition and the peptide/lipid ratio. At nanomolar concentrations, melittin can only induce transient pores. As the melittin concentration

increases beyond a critical value (e.g., peptide/lipid ratio of 1/45), it induces stable membrane pores of 2.5–3 nm in diameter, and the pore size further increases with the peptide/lipid ratio (Terwilliger et al., 1982; Matsuzaki et al., 1997; Lee et al., 2013). Another well-studied AMP, maculatin can also form an ensemble of structurally diverse pores (Wang Y. et al., 2016). Moreover, the formation of membrane pores depends on the lipid composition of the membrane as well. Evidence for this lies in the observation that most AMPs induce membrane pores at a much higher concentration in mammalian membranes than in bacterial membranes. The former mainly consists of zwitterionic lipids (e.g., POPC) and cholesterol, which are closely packed and thus have a low tendency to form membrane pores. In contrast, bacterial membranes consist of high percentage of POPE, which has a small head group and thus has higher tendency to form negative Gaussian curvatures, as discussed above (Schmidt and Wong, 2013).

Biophysical methods used to study the pore structure as well as AMP conformations in the pores, include small angle x-ray scattering (SAXS), oriented circular dichroism (OCD, solid-state NMR, quartz crystal microbalance (QCM; Yang et al., 2007; Kwon et al., 2013; Wang et al., 2015; Bürck et al., 2016). However, these methods typically give the early or final states of the AMP-membrane complex, e.g., the static structures of AMPs and membrane pores. The dynamics of the pore formation process is missing because the intermediate states of pore formation are either in non-equilibrium or metastable states and thus have life times that are too short to be observed. To obtain dynamic information on pore formation, MD simulations using atomistic and coarse-grained models have been carried out (Edit et al., 2007; Kirsch and Böckmann, 2016). Due to the complexity of the pore formation process, the sub-microsecond time scales that MD simulations can access and the fact that pore formation is a rare event, it is still difficult to observe the complete process of pore formation in conventional MD simulations. Nevertheless, Leontiadou et al. were the first to successfully simulate the process of toroidal pore formation by magainin (Leontiadou et al., 2006). In the simulations, the toroidal pore displays higher disorder than the normal toroidal pore model, reflecting the dynamic nature of pores in membranes. In another simulation from the same group, similar effects were observed for melittin. One or two melittin molecules were observed to line within the pore axis, while other peptide molecules located at the two ends of the pore (Sengupta et al., 2008). Removing the positive charges of melittin molecules failed to induce membrane pores, revealing the importance of electrostatic interactions. Interestingly, in both simulations, peptides lose their helical conformations when binding to the membrane pores, suggesting that the helical conformation is not necessary for stabilization of the membrane pores, at least for the case of toroidal pores. Coarse-grained MD simulations were also performed for melittin and transient toroidal pores were observed at high peptide/lipid ratios (Santo et al., 2013). It was shown that typically 3–5 melittin molecules are involved in each pore and similar to the atomistic simulations, not all the melittin molecules span across the membrane. The difference in the pores between atomistic and coarse-grained simulations suggests diverse morphologies of melittin induced membrane

pores. These MD simulations, although only carried out at a micro-second time scale, nevertheless provide valuable molecular insights into the action mechanism of AMPs.

Carpet Mechanism

Not all AMPs induce membrane pores. Some AMPs adsorb onto the membrane surface and orient parallel to the membrane. As their surface concentrations reach a critical value, these AMPs disrupt the integrity of the super molecular structure of the membrane via membrane fragmentation, a process called carpet mechanism or detergent model (Figure 3; Gazit et al., 1996). Some examples of AMPs with carpet mechanism are listed in Table 1. In the carpet model, the outer leaflet is covered by a high surface concentration of AMP molecules, while the inner leaflet is free of AMP binding. The large imbalance of charge and surface tension across the membrane eventually leads to catastrophic collapse of membrane integrity and leakage of the cytoplasmic contents, ions, and biomolecules. In contrast, in the pore forming mechanism, only intracellular molecules smaller than the pore can exit. The size of the released molecules can be used to distinguish the pore forming mechanism from a carpet mechanism.

In the carpet mechanism, the complete picture of membrane collapse is not well-understood because (i) the process is highly non-equilibrium; (ii) multiple pathways of membrane lysis exist, making it difficult to be detected in biophysical experiments. However, at a peptide concentration lower than the critical concentration, the membrane undergoes some intrinsic perturbations such as membrane thinning, lateral expansion, clustering of anionic lipids, and membrane deformation, and high surface tension. Interestingly, these membrane perturbations can be used to correlate to the subsequent membrane lysis. For example, Wimley proposed an interfacial activity model to relate these membrane perturbations to the membrane activity of an AMP (Wimley, 2010). In the surface activity model, the membrane activity of an AMP is a function of the surface activity, which depends on two elements: (i) the partition of an AMP to the surface of the bacterial membrane and (ii) the ability to induce membrane perturbations. As the former is mostly driven by electrostatic interactions, AMPs with greater charge are more likely to achieve high concentrations on the membrane surface. The latter depends on many factors such as the 3-D conformation of the AMP, the physical properties of the AMP, and the actual interactions of the AMP with the lipids. Given the fact that the membrane is amphiphilic in nature, AMPs with facial amphiphilicity display high affinity for the membrane. The destabilization of the hydrophobic-water interface is critical for subsequent membrane lysis. In addition, membrane perturbations can be further enhanced via AMP aggregation, a mechanism similar to the toxic effects of an amyloid peptide (Milov et al., 2009; Di Scala et al., 2016). For example, LL-37, HAL-2, and the C-terminal segment of human beta-defensin 3, can achieve high surface concentration via self-aggregation upon adsorption onto the surface (Bai et al., 2009; Wang et al., 2014; Bonucci et al., 2015). The self-aggregation of maculatin 1.1, a membrane-active antimicrobial peptide (AMP) from the Australian tree frog leads to deeper

penetration into the membrane core and significant change of curvature of the membrane (Bond et al., 2008). The self-aggregation of AMPs leads to an enhanced local concentration of AMPs around the membrane and has been used to design multimeric AMPs (Arnusch et al., 2007; Bai et al., 2012; Shin et al., 2013; Lakshminarayanan et al., 2014; Koh et al., 2015a).

METHODS FOR AMP DESIGN

Although research on AMP development has been highly active in the past years, few molecules have entered into the market. For an AMP to be used as a therapeutic agent, it needs to possess several druggable properties: (i) high antimicrobial activity; (ii) low toxicity to the mammalian membrane; (iii) high proteolytic stability; (iv) low serum binding; and (v) low cost. Most AMPs have minimum inhibitory concentration (MIC) values <10 µg/ml, while conventional antibiotics may have MICs in the range of 1–2 µg/ml or even sub µg/ml range, suggesting that significant effort is still needed to design new AMPs with higher activity. Various approaches have been employed to design new AMPs with low MIC, high stability, and low toxicity. These methods include the time-consuming mutation based empirical method, statistically based bioinformatics methods, and more sophisticated mechanism based methods such as MD simulations and biophysical experiments. Recently, multi-disciplinary approaches combining computational predictions, biophysical characterizations and biological validations have proved to be more promising (Bai et al., 2012; Koh et al., 2015a; Lakshminarayanan et al., 2016). This section discusses various experimental and computational methods that have been used for AMP design. Clearly, if the details of the membrane interactions were known design of an appropriate AMP would be facilitated.

Mutation Based Empirical Methods

Early attempts to design AMPs were largely carried out by trial and error due to poor understanding of the action mechanism. Many designed AMPs are actually based on the modifications of existing natural AMPs. A number of approaches can be tried to re-engineer a naturally occurring AMP, such as sequence shuffling and alanine scanning. Sequence shuffling, in which the positions of the amino acids in the sequence are changed can be the simple sequence reversal or via a combinatorial library. Since sequence shuffling does not change the hydrophobicity and the net positive charges, it has been used to optimize the antimicrobial activity of specific AMPs (Monroc et al., 2006; Cherkasov et al., 2009). The technique of alanine scanning mutates each residue or a group of residues to alanine and the antimicrobial activity is monitored for improvement. Alanine scanning has been widely used in AMP design and has proved to be very useful in identifying residues critical for antimicrobial activity (Grieco et al., 2011; Hänchen et al., 2013).

Statistically Based Bioinformatics Methods

AMP databases enhance computer aided AMP design (Fjell et al., 2007; Thomas et al., 2010; Wang G. et al., 2016). Various bioinformatics tools have been developed, including simple statistical modeling, SARs, neural networks, and machine

learning. In general, these bioinformatics based tools need a database with known antimicrobial activity of certain peptides as the training set. By using different bioinformatics algorithms, key structural, and biophysical features are extracted from the training set and can be used to predict the antimicrobial activity of unknown peptides, which is referred to as the test set. For example, Mishra and Wang employed database filtering technology to determine the key parameters of AMPs (e.g., amino acid composition, peptide hydrophobic content, and net charge) and subsequently used these parameters for the ab initio design of potent AMPs against MRSA (Mishra and Wang, 2012). Besides the AMP database, design principles can also be obtained from other sources, such as genomes and proteomes (Li et al., 2007; Brand et al., 2012; Kim et al., 2016).

Mechanism Based Methods

Although the bioinformatics methods are simple and fast, they are still black boxes, as there is little information that reveals the action mechanisms. A more powerful and rational method would be to design new AMPs based on the mode of interaction with the membrane. To this purpose, detailed understanding of the action mechanisms of existing AMPs is required. MD simulation is a powerful method that can give atomistic information regarding the interactions of AMPs with bacterial membranes. If the time scale of the simulation is long enough, membrane disruption or pore formation can be directly observed (Wang Y. et al., 2016). MD simulations have been previously used to decipher the action mechanism of AMPs, and recently have been successfully applied to the design of new AMPs and antimicrobial peptidomimetics (Tsai et al., 2009; Tew et al., 2010a; Li et al., 2013, 2015; John Fox et al., 2016). For example, Bai et al. performed atomistic MD simulations of a short cationic AMP B1088 and found that the charge density plays an important role in its interactions with bacterial membrane mimics (Bai et al., 2009). Based on this information, they subsequently designed a covalent peptide dimer B2088 and a tetramer B4010 which demonstrated enhanced antimicrobial activity and proteolytic stability (Li et al., 2013; Lakshminarayanan et al., 2014). By using coarse-grained MD simulations, Tew et al. successfully designed a number of synthetic mimics of AMPs with high membrane selectivity (Tew et al., 2010a). One of their compounds brilacidin is currently under phase II clinical trials.

NMR can also provide mechanistic details for improved AMP design and in fact complements MD simulations. Similar to MD simulations, NMR, particularly solid state NMR, can provide information regarding the 3-D conformation of the peptide as well as the mode of interactions with model lipid membranes (Strandberg and Ulrich, 2004; Su et al., 2010). These include identification of the biophysical properties of critical residues that mediate the interactions with the membrane. For instance, Saravanan et al. used NMR combined with other biophysical experiments to design tryptophan and arginine rich decamer peptides and potent antimicrobial activity and low toxicity of the decamer peptide were found to arise from an optimal ratio between the positive charges and hydrophobicity (Saravanan et al., 2014). Later the same group used NMR to further design β-boomerang lipo-peptides that neutralized LPS (Mohanram and

Bhattacharjya, 2014). Jeong et al. used NMR experiments not only to design a series of LPcin analogs with potent antimicrobial activities, but also elucidated the 3-D structure of a peptide-membrane complex (Jeong et al., 2016).

Principles for Practical Design of AMPs

Based on the methods discussed above, some general design principles have been proposed which can be directly used to guide AMP design and are briefly discussed below.

Amphiphilicity

Amphiphilicity is perhaps the most striking feature of AMPs, including facial amphiphilicity (Vandenburg et al., 2002), bola-amphiphilicity (Ali, 2007), radial amphiphilicity (Xiong et al., 2015), etc., all with at least one cationic moiety and one hydrophobic moiety. Considering the amphiphilic nature of membranes, amphiphilic peptides are expected to have high membrane affinity. Facially amphiphilic AMPs are usually helical with one side being cationic and the other side being hydrophobic. When adsorbed onto the bacterial membrane, these AMPs locate at the membrane surface, with the cationic face interacting with the head groups and the hydrophobic face penetrating into the lipid tail region, resulting in significant perturbations at the membrane-water interface. On the other hand, bola-amphiphilic peptides are expected to adopt transmembrane conformations, driven by hydrophobic match. In such a case, the two cationic moieties interact with the two head group regions, while the hydrophobic moiety interacts with the lipid tails. When several bola-amphiphilic peptide molecules oligomerize in the bacterial membrane, membrane pores can be formed (Matile et al., 2011).

Peptide Crosslinking

As both the pore forming mechanism and the carpet mechanism depend on the concentration of the peptide on the bacterial membrane surface, various methods have been proposed to enhance the surface concentration of AMPs. An effective way to enhance surface concentration of AMPs is through peptide self-aggregation, which leads to more effective membrane disruption compared to the monomeric peptide. For example, LL-37 self-aggregates on the bacterial membrane leading to the formation of toroidal pores (Bonucci et al., 2015). However, if the peptide is highly cationic, the self-aggregation is inhibited due to electrostatic repulsion between AMP molecules. In such a case, covalent linking can be used to generate covalent peptide aggregates, known as multimeric peptides. As discussed above, the covalent peptide dimer B2088 and tetramer B4010 displayed much higher antimicrobial activity than the peptide monomeric unit comprising these peptides (Bai et al., 2012; Lakshminarayanan et al., 2014, 2016).

Role of Arg

Most AMPs are cationic as a result of a high percentage of basic residues, Lys or Arg. Although both carry positive charges at neutral pH, the pKa values of Arg (12.45) and Lys (10.5) are different, and this will affect their protonation states in the membrane environment. Theoretical calculations found that Arg

will retain its protonation state in the lipid tail region of the membrane, while Lys becomes deprotonated in the bilayer center (Yoo and Cui, 2008, 2010; Gleason et al., 2013). Due to the high pKa and multi-dentate hydrogen bonding property of Arg, Arg-rich peptides are thought to have stronger interactions with membranes. For example, a twin-arginine motif was found to assist peptide translocation and polyarginine itself is an efficient cell penetrating peptide (Chaddock et al., 1995; Bechara and Sagan, 2013). Studies also showed that Arg can induce more negative Gaussian curvatures than Lys due to its bidentate hydrogen bonding with PO₄ groups (Schmidt et al., 2010, 2011; Schmidt and Wong, 2013; Wu et al., 2013). Accordingly, various Arg-rich AMPs have been designed. For example, (RW)_n peptides display excellent antimicrobial activity (Liu et al., 2007). The side chain of Arg residue, the guanidine group was found to greatly enhance the action of antimicrobial peptidomimetics compared to the side chain of Lys residue (Andreev et al., 2014). Although many studies have shown the preference of Arg over Lys in terms of antimicrobial activity, some peptides prefer Lys over Arg residues. For example, arginine modified polymyxin B displayed reduced antimicrobial activity, suggesting that there appears not to be a general rule for selective preference of Arg and Lys by AMPs (Rabanal et al., 2015).

Peptide Truncation

Most of the classical antimicrobial peptides are fairly large and expensive to synthesize. This has led to the design of ultra-short peptides, with only 3–4 amino acids. The sequence of the peptidic moiety and the length of the hydrophobic moiety appear to determine the spectrum of antimicrobial activities. Despite their short lengths, their modes of action involves permeation and disintegration of the membrane organization, similar to that of many classical AMPs (Makovitzki et al., 2006). As electrostatic interactions with the bacterial membrane are still involved, almost all ultrashort peptides designed and synthesized to date contain cationic amino acids, such as arginine and lysine (Findlay et al., 2012; Domalaon et al., 2014; Mishra et al., 2015). For instance, KYR is an amino acid sequence of bovine hemoglobin alpha chain, which was part of the longer amino acid sequence that was obtained from hydrolysing the hemoglobin alpha chain. KYR is one of the shortest AMPs known (Nasompag et al., 2015). Most of the ultrashort peptides are conjugated with a fatty acid tail to provide additional hydrophobicity to kill bacteria efficiently (Makovitzki et al., 2006).

Incorporating Unnatural Amino Acids

The synthetic AMPs are not restricted to the 20 natural amino acids. Instead, they can incorporate various unnatural amino acids or have additional chemical modification. The direct advantage of AMPs containing unnatural amino acids is their high proteolytic stability. More importantly, as AMPs require a delicate balance of cationic and hydrophobic groups, chemical modifications enables easy fine-tuning of the hydrophobic balance. The commonly used approach for chemical modification includes use of more hydrophobic amino acids, lipid, and aromatic modifications. For example, lipid modifications of the above mentioned peptide dimer B2088 results in C8-B2088,

which demonstrated enhanced antimicrobial activity (Koh et al., 2015a). Similarly, modification of the Phe residue with an additional benzene ring significantly enhances the antimicrobial activity of a short peptide FRFR-NH₂, while maintaining its low toxicity to mammalian membranes (Lau et al., 2015). Multiple modifications have been used together to achieve high activity. LTX-109, a short synthetic AMP with both lipid and aromatic modifications, has been in clinical trials (Saravolatz et al., 2012b). Recently, a pharmacophore model has been proposed for the design of short AMP mimetics with the sequence of RXR, where X is a hydrophobic scaffold (Li et al., 2015). Derivatives of the pharmacophore model have shown excellent activity against resistant pathogens, low toxicity to mammalian membranes, and extremely high stability (Koh et al., 2015b).

Current Status: Examples of AMPs/Peptidomimetics in Clinical Trials

In the past 30 years, continuous efforts have been made to develop AMPs as clinically useful antimicrobials due to their advantages over conventional antibiotics such as a rapid bacterial killing, good selectivity toward the bacterial membrane, and a low propensity to give rise to bacterial resistance (Bai et al., 2012). However, to date, no designed AMP antibiotics have yet reached the clinic. Nevertheless, as described below, a number of AMPs and AMP derivatives are already at the pre-clinical stage and in clinical trials.

PL-5 is an α -helical AMP with a sequence of Ac-K-W-K-S-F-L-K-T-F-K-S-A-A-K-T-V-L-H-T-A-L-K-A-I-S-S-amide, where Ac = N-acetyl and amide = C-terminal amide. PL-5 is developed by ProteLight Pharmaceuticals and has recently obtained approval from the China Food and Drug Administration (CFDA) to enter clinical trials for skin infection in the year 2016. It is noteworthy that PL-5 is the first AMP to enter the clinical stage in China. PL-5 is a low toxicity and highly potent AMP against a broad spectrum of drug-resistant bacteria. In addition, PL-5 is able to synergize with conventional antibiotics to improve antibacterial activity *in vitro* and *in vivo* against both Gram-positive and Gram-negative bacteria. This may help prevent or delay the emergence of antibiotic resistance (Feng et al., 2015).

POL7080 is a synthetic cyclic peptide derived from protegrin I. POL7080 is active against Gram-negative bacteria and works by inhibiting a homolog of the β -barrel protein LptD. LptD is an outer-membrane protein widely distributed in Gram-negative bacteria that functions in the assembly of LPS in the outer leaflet of the outer membrane (Braun and Silhavy, 2002). LptD is involved in the outer-membrane biogenesis of lipopolysaccharide. Significantly, POL7080 is highly active on a broad panel of clinical isolates including multi-drug resistant *Pseudomonas* with outstanding *in vivo* efficacy in septicemia, lung and thigh infection models (Polyphor) POL7080 is developed by Polyphor Ltd and has completed a phase I clinical trial with its partner Roche. POL7080 has also completed a phase-II trial in 20 patients with exacerbation of non-cystic fibrosis bronchiectasis in 2015 (Butler et al., 2017). To date, the structure of POL7080 has not been revealed.

DPK-060 is a cationic peptide that has recently completed a Phase II study of topical application for atopic dermatitis. DPK-060 is a broad spectrum cationic peptide active against both Gram-positive and Gram-negative bacteria. Similar to other AMPs, DPK-060 is also membrane targeting (Harvey et al., 2015). DPK-060 is developed by Pergamum AB. The results from a Phase II clinical trial of DPK-060 in outer ear infections showed a statistically significant improvement in a 10-day cure rate compared to placebo and that DPK-060 is safe and tolerable (Lee et al., 2015). However, no recent reports of DPK-060 development have been forthcoming. Pergamum AB has also developed LL-37, a human cathelicidin subunit. Human cathelicidin is synthesized by numerous cells as an inactive precursor, hCAP18/LL-37. It consists of a highly conserved N-terminal signal sequence, a conserved cathelin domain, and a small antimicrobial C-terminal domain. The small antimicrobial C-terminal domain is known as LL-37 (Vandamme et al., 2012). The LL-37 domain is released by cleaving the proteolytic hCAP18/LL-37 precursor. This domain exhibits antimicrobial activities against both Gram-positive and Gram-negative bacteria (Overhage et al., 2008; Barlow et al., 2011). LL-37 has a peptide sequence of LLGDFFRKSKKEKIGKEFKRIVQRIKDFLRNLVPRT. LL-37 is developed for treatment of chronic leg ulcers. The clinical phase results show that LL-37 has a significantly improved healing rate compared to placebo (Lee et al., 2015).

Innate Defense Regulators (IDRs) are a novel class of synthetic peptides that enhance the control of microbial infections. IDRs do not impact the adaptive immune system and do not interfere with chemotherapy, radiation therapy or antibiotic treatments. SGX942 contains the active ingredient dusquetide (also referred to as SGX-94). Dusquetide is a fully synthetic, 5-amino acid peptide derived from Indolicidin with high aqueous solubility and stability (Soligenix) SGX94, has broad-spectrum activity against Gram-negative and Gram-positive bacterial infections caused by intracellular or extracellular bacteria and also complements the actions of standard of care antibiotics (North et al., 2016). Since SGX-94 acts through host pathways to provide both broad-spectrum anti-infective capability as well as control of inflammation, IDRs are unlikely to be impacted by resistance mechanisms. It also offers potential clinical advantages in the fight against emerging and antibiotic resistant bacterial infections (North et al., 2016). SGX-942 was first developed by Inimex and is currently being pursued in a Phase-II trial by Soligenix as treatment for oral mucositis (Butler et al., 2017). SGX942 has previously demonstrated safety and tolerability in a double-blind, placebo-controlled, healthy volunteer Phase I clinical trial. SGX942 has been awarded Fast Track designation from the FDA for the treatment of oral mucositis as a result of radiation and/or chemotherapy treatment in head and neck cancer patients.

There are also several AMPs that were not approved by FDA or failed at an earlier development stage, such as Iseganan, Omiganan, and XMP-629 and Locilex (Ahmad et al., 2012). Dipexium acknowledged that Locilex did not meet the primary clinical endpoint of superiority vs. placebo or “vehicle” namely the cream without its active ingredient of pexiganan. In order to overcome the major limitations of AMPs such as

systemic toxicity and proteolytic instability, the development of small-molecule-based membrane-targeting antimicrobials that maintain the essential key characteristics of AMPs, has received considerable attention (Lohan and Bisht, 2013). Peptidomimetics are a new generation of small-molecule antimicrobials that mimic the structure and antibacterial action of AMPs. Design of peptidomimetics involves the introduction of amide bond isosteres or peptide backbone modifications via non-natural side chains to mimic a peptide structure or function (Niu et al., 2012; Lohan and Bisht, 2013).

Brilacidin is a small-molecule arylamide mimic of AMPs that shows potent antimicrobial activity against a wide range of drug-susceptible and multidrug-resistant Gram-negative and Gram-positive bacteria (Tew et al., 2002, 2010b; Liu et al., 2004) Brilacidin has a planar, conformationally restrained scaffold with four positive guanadiny and pyridinyl substitutions and two trifluoromethane hydrophobic substitutions (**Figure 4**). Brilacidin was first developed by Polymedix Inc. and purchased by Cellceutix corp. in September 2013 (Butler et al., 2017). Brilacidin has completed phase IIa and phase IIb trials for the treatment of acute *S. aureus* skin and skin structure infections. Compared to daptomycin, the results show no serious adverse effects and the efficacy is similar to daptomycin across all brilacidin treatment groups in 215 patients Similar to other AMPs, brilacidin is a membrane targeting antimicrobial. It causes membrane disruption and shows efficacy in a MRSA keratitis model when applied topically. At 0.5% solution, brilacidin shows minimal irritation and is equally efficacious as vancomycin (Kowalski et al., 2016) In addition to brilacidin, Cellceutix is also developing CTIX-1278 (structure not revealed), a

defensin mimetic-compound, against the drug resistant superbug *Klebsiella pneumoniae*. CTIX-1278 is efficacious in a thigh burden study using a mouse model. The results are encouraging as CTIX-1278 shows similar efficacy compared to carbapenem.

LTX-109 is developed by Lytix Biopharma, which focus on topical treatment of skin infections and nasal eradication of staphylococcus. LTX 109 is a synthetic antimicrobial peptidomimetic, which has completed phase 2 trials for the treatment of impetigo in the year 2014 and uncomplicated skin and skin structure infection (uSSI) in the year 2011 (Butler et al., 2017). LTX-109 has the chemical structure Arg-Tbt-Arg-NH-EtPh (**Figure 4**). Arg provides the cationic charge and the tertiary butyl group is important to increase the hydrophobicity. In general, LTX-109 is active against a broad range of bacteria including *E. coli* and *S. aureus* (Isaksson et al., 2011a) Significantly, LTX-109 is also active against a panel of drug-resistant Gram-positive bacteria, such as MRSA, vancomycin-intermediate resistant, daptomycin resistant, and linezolid-resistant strains (Saravolatz et al., 2012a) LTX-109 kills bacteria via the membrane targeting mechanism.

Exeporfinium chloride (XF-73) is a synthetic dicationic porphyrin derivative being developed by Destiny Pharma (Brighton, UK) that has been evaluated in phase-I/II trials for the prevention of post-surgical staphylococcal nasal infections (**Figure 4**; Butler et al., 2017). XF-73 has completed 5 Phase I/IIa clinical studies in Europe/US. XF-73 is a photosensitizer that has broad-spectrum antimicrobial activities against Gram-positive, Gram-negative and *Candida albicans* (Farrell et al., 2010; Gonzales et al., 2013). XF-73 exhibits potent, non-lytic, bactericidal activity against *S. aureus*. Similar to AMPs,

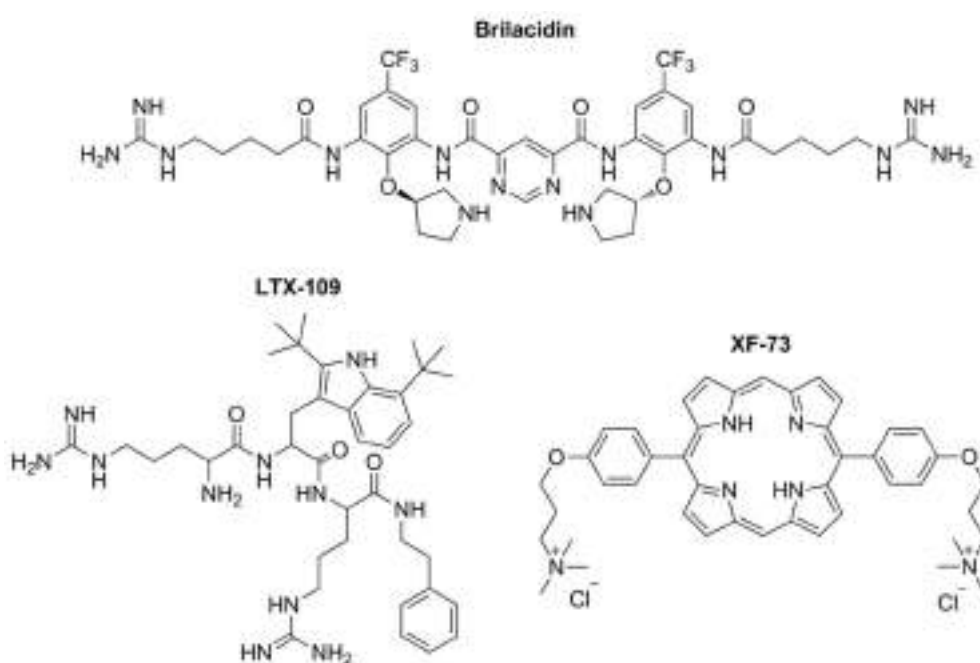


FIGURE 4 | Structures of AMP mimetics in clinical studies. All the three molecules contain a large hydrophobic moiety and two cationic moieties, forming a cationic-hydrophobic-cationic motif, and mimicking the interactions of AMPs with the bacterial membrane.

interaction of XF-73 with the cytoplasmic membrane is lethal to *S. aureus*, leading to release of intracellular components and bacterial cell death (Ooi et al., 2009). In addition, XF-73 showed no drug resistance emergence from four common MRSA strains tested in a multi-step (55 passage) resistance study, as a ≤ 4 -fold increase in MIC against the strains tested (Farrell et al., 2011). On 05 September 2016, Destiny Pharma announced that XF-73 can be delivered safely and is well-tolerated in a two-stage US clinical trial using intra-nasally applied exeporfinium chloride gels (DMID contract number HHSN27220800026C). In addition, no drug was detected in the bloodstream (Destiny Pharma, accessed on 12 January 2017).

Peptides have appeared in a wide range of applications in other clinical areas (Fosgerau and Hoffmann, 2015). For instance, thymalfasin, a short peptide with 28 amino acids, has been used in clinics for its immune regulatory function (Sjogren, 2004). With more and more emerging strategies to design new generation AMPs with improved efficacy, safety, and tolerability, we believe that peptide antibiotic still offer enormous growth potential to reach the clinic in the near future.

CHALLENGES AND FUTURE PERSPECTIVES

Current AMP Development: Challenges and Solutions

AMP development has been an active research area in the past 30 years, but only recently has there been a positive outlook for commercial success. There are challenges that limit the design of potent AMPs, such as the poor understanding of the target-drug interaction and the lack of rational design principles. Besides activity, issues such as toxicity, serum binding, stability, and product cost are also practical considerations. Solutions to overcome these limitations have been proposed and have become hotspots of current AMP research and development. A side benefit of AMP research is that emphasis has changed from screening unknowns in a microbiology setting to defining the target bringing antibiotic development closer to conventional structure based drug development.

Toxicity of AMPs can occur at different levels, including membrane toxicity, cellular toxicity, and systemic toxicity. Membrane selectivity is a widely accepted parameter to characterize *in vitro* membrane toxicity and is defined as the ratio of HC50/MIC, where HC50 is the concentration needed to cause 50% hemolysis of human red blood cells. As stated earlier in this review molecular charge of bacterial membranes and membranes of human cells differ so that AMPs with higher positive charges show enhanced affinity for the bacterial membrane, resulting in higher antimicrobial activity (lower MIC) and conversely less toxicity to human cells (Zelazetsky and Tossi, 2006). Moreover, it is also proposed that AMP hydrophobicity can affect human membrane toxicity, a factor useful in the design of branched lipo-peptides with minimal toxicity (Koh et al., 2015a).

Cellular/metabolic toxicity and systemic toxicity are more difficult to predict as the underlying mechanisms are complex. Cellular toxicity refers to single cell toxicity, which can be

measured for human cells using MTT assays, LDH release, and ATP synthesis (Fotakis and Timbrell, 2006). Systemic toxicity can arise from various effects such as activation of transcription factors, binding to macromolecular receptors in the body, alteration of metabolic pathways, and triggering immune response, making it challenging to predict. For example, polymyxin B, the last resort for the treatment of multi-drug resistant Gram-negative bacteria, although safe at the membrane level, can cause significant nephro- and neurotoxicity (Falagas and Kasiakou, 2006). To address and predict the issues surrounding systemic toxicity, several strategies have been employed. Computational toxicology uses machine learning algorithms to predict toxic outcomes (Valerio, 2009). Another strategy is via formulation (Carmona-Ribeiro and de Melo Carrasco, 2014). For example, Gramicidin, a topical AMP is effective against many Gram-positive bacteria, but has significant hemolysis. However, incorporating gramicidin in a dioctadecyldimethylammonium bromide (DODAB) bilayer not only results in reduced toxicity, but also leads to broader antimicrobial activity against both *E. coli* and *S. aureus* (Ragioto et al., 2014).

AMPs consisting of all natural amino acids may need to enhance their proteolytic stability. This limitation may not be a serious problem for topical applications, but results in significantly reduced half-life in systemic applications. Various approaches can be used to enhance the proteolytic stability of AMPs. The direct way is to mutate key amino acids at the cleavage site to D amino acids or similar analogs. For example, arginine can be replaced by D-Arg or homoarginine, while lysine can be replaced by D-Lys or ornithine. However, the effect of L-to-D mutation on the antimicrobial activity needs to be re-evaluated, although in most cases the L-to-D mutation does not alter the antimicrobial activity significantly (Hong et al., 1999; Berthold et al., 2013; Carmona et al., 2013). In addition, chemical modifications as discussed in Section Principles for Practical Design of AMPs, such as incorporation of unnatural amino acids and cross-linking can function to improve peptide stability.

Cationic AMPs tend to display high affinity for serum proteins, decreasing the available concentration of drug; however, at the same time this is a general issue with most antibiotics. For example, it was shown that AMPs can interact with drug site II of albumin via hydrophobic interactions (Sivertsen et al., 2014). In addition, the cationic residues of most cationic AMPs make them good substrates for the chymotrypsin family of endoproteases (Perona and Craik, 1997). The strong protein binding property significantly reduces the effective concentration of the AMP available to combat bacteria (Svenson et al., 2007). Moreover, host cells can also interfere with the activity of AMPs. Starr et al. pointed out that interactions with host cells can lead to significant loss of activity *in vivo*, in a way very similar to the effects of serum protein binding (Starr et al., 2016). To develop AMPs with less binding to serum proteins/host cells, detailed PK/PD studies are required. Compared to small molecule antibiotics, AMPs may be more expensive to produce; however, this limitation can be overcome by the use of synthetic biology (Cameron et al., 2014). Using genetically engineered microbial fermentation, large amounts of recombinant peptides can be produced. For example,

a fusion protein containing the antimicrobial sequence at its C-terminus was successfully expressed in *E. Coli*, and subsequent cleavage released AMP P2 (Haught et al., 1998).

Future Perspectives

Importantly, AMPs probably represent the best option for the treatment of multi-drug resistant infections. Considerable effort has been expended in this area with progress and a number of AMP/peptidomimetics are in different phases of clinical trials. Since the MIC values for most AMPs are still higher than many conventional antibiotics, the primary task is to improve the antimicrobial activity, reduce the toxicity, and improve delivery efficiency. Another promising area is the design of membrane active peptidomimetics to mimic the action of existing AMPs, which can be achieved by chemical modification of existing AMPs or using unnatural amino acids. Compared to AMPs, peptidomimetics greatly expand the molecular space of membrane active antimicrobials and have the advantages of high proteolytic stability and optimizing the hydrophobicity. However, this needs to be coupled with the more detailed understanding of the molecular and atomistic interactions between AMPs/peptidomimetics and the molecular complex of the Gram-negative membrane system. Computer aided drug design, particularly the mechanism based *in silico* design approach such as MD simulations has a great potential to help overcome some of these limitations.

REFERENCES

- Ahmad, A., Ahmad, E., Rabbani, G., Haque, S., Arshad, M., and Khan, R. H. (2012). Identification and design of antimicrobial peptides for therapeutic applications. *Curr. Protein Pept. Sci.* 13, 211–223. doi: 10.2174/138920312800785076
- Ali, H. E.-S. (2007). Synthesis, surface properties and antimicrobial activity of bolaamphiphile/oppositely charged conventional surfactant mixed systems. *J. Surfactants Deterg.* 10, 117–124. doi: 10.1007/s11743-007-1021-y
- Andreev, K., Bianchi, C., Laursen, J. S., Citterio, L., Hein-Kristensen, L., Gram, L., et al. (2014). Guanidino groups greatly enhance the action of antimicrobial peptidomimetics against bacterial cytoplasmic membranes. *Biochim. Biophys. Acta Biomembranes* 1838, 2492–2502. doi: 10.1016/j.bbamem.2014.05.022
- Arnusch, C. J., Branderhorst, H., de Kruijff, B., Liskamp, R. M. J., Breukink, E., and Pieters, R. J. (2007). Enhanced membrane pore formation by multimeric/oligomeric antimicrobial peptides. *Biochemistry* 46, 13437–13442. doi: 10.1021/bi7015553
- Ayabe, T., Ashida, T., Kohgo, Y., and Kono, T. (2004). The role of Paneth cells and their antimicrobial peptides in innate host defense. *Trends Microbiol.* 12, 394–398. doi: 10.1016/j.tim.2004.06.007
- Bai, Y., Liu, S., Jiang, P., Zhou, L., Li, J., Tang, C., et al. (2009). Structure-dependent charge density as determinant of antimicrobial activity of peptide analogues of defensin. *Biochemistry* 48, 7229–7239. doi: 10.1021/bi900670d
- Bai, Y., Liu, S., Li, J., Lakshminarayanan, R., Sarawathi, P., Tang, C., et al. (2012). Progressive structuring of a branched antimicrobial peptide on the path to the inner membrane target. *J. Biol. Chem.* 287, 26606–26617. doi: 10.1074/jbc.M112.363259
- Barlow, P. G., Svoboda, P., Mackellar, A., Nash, A. A., York, I. A., Pohl, J., et al. (2011). Antiviral activity and increased host defense against influenza infection elicited by the human cathelicidin LL-37. *PLoS ONE* 6:e25333. doi: 10.1371/journal.pone.0025333
- Bechara, C., and Sagan, S. (2013). Cell-penetrating peptides: 20 years later, where do we stand? *FEBS Lett.* 587, 1693–1702. doi: 10.1016/j.febslet.2013.04.031
- Bertelsen, K., Dorosz, J., Hansen, S. K., Nielsen, N. C., and Vosegaard, T. (2012). Mechanisms of peptide-induced pore formation in lipid bilayers investigated by oriented ³¹P solid-state NMR spectroscopy. *PLoS ONE* 7:e47745. doi: 10.1371/journal.pone.0047745
- Berthold, N., Czihal, P., Fritzsche, S., Sauer, U., Schiffer, G., Knappe, D., et al. (2013). Novel Apidaecin 1b analogs with superior serum stabilities for treatment of infections by gram-negative pathogens. *Antimicrob. Agents Chemother.* 57, 402–409. doi: 10.1128/AAC.01923-12
- Bevins, C. L., and Salzman, N. H. (2011). Paneth cells, antimicrobial peptides and maintenance of intestinal homeostasis. *Nat. Rev. Microbiol.* 9, 356–368. doi: 10.1038/nrmicro2546
- Blazyk, J., Wiegand, R., Klein, J., Hammer, J., Epand, R. M., Epand, R. F., et al. (2001). A novel linear amphipathic β -sheet cationic antimicrobial peptide with enhanced selectivity for bacterial lipids. *J. Biol. Chem.* 276, 27899–27906. doi: 10.1074/jbc.M102865200
- Boheim, G. (1974). Statistical analysis of alamethicin channels in black lipid membranes. *J. Membr. Biol.* 19, 277–303. doi: 10.1007/BF01869983
- Bond, P. J., Parton, D. L., Clark, J. F., and Sansom, M. S. P. (2008). Coarse-grained simulations of the membrane-active antimicrobial peptide maculatin 1.1. *Biophys. J.* 95, 3802–3815. doi: 10.1529.biophysj.108.128686
- Bonucci, A., Caldaroni, E., Balducci, E., and Pogni, R. (2015). A spectroscopic study of the aggregation state of the human antimicrobial peptide LL-37 in bacterial versus host cell model membranes. *Biochemistry* 54, 6760–6768. doi: 10.1021/acs.biochem.5b00813
- Brand, G. D., Magalhães, M. T. Q., Tinoco, M. L. P., Aragão, F. J. L., Nicoli, J., Kelly, S. M., et al. (2012). Probing protein sequences as sources for encrypted antimicrobial peptides. *PLoS ONE* 7:e45848. doi: 10.1371/journal.pone.0045848
- Brandenburg, K., Heinbockel, L., Correa, W., and Lohner, K. (2016). Peptides with dual mode of action: killing bacteria and preventing endotoxin-induced sepsis. *Biochim. Biophys. Acta Biomembranes* 1858, 971–979. doi: 10.1016/j.bbamem.2016.01.011
- Braun, M., and Silhavy, T. J. (2002). Imp/OstA is required for cell envelope biogenesis in *Escherichia coli*. *Mol. Microbiol.* 45, 1289–1302. doi: 10.1046/j.1365-2958.2002.03091.x
- When combined with other methods in a multi-disciplinary setting, translation of fundamental knowledge to practical clinical therapeutics can be greatly accelerated. This approach should also be activated to overcome the AMP resistant strains such as the recently appeared colistin (also known as polymyxin E) resistant strains (Fernández et al., 2013; Olaitan et al., 2014; Li et al., 2015). The advantages of combining the *in silico* simulations and NMR is that the approach is adaptable to the challenge of bacteria with modified LPS structure. If successful a new age of antibiotics could be forthcoming with less resistance, longer clinical utility and greater opportunities for special purpose design of antibiotics and other antimicrobials.

AUTHOR CONTRIBUTIONS

JL, JK, and SL wrote the drafted manuscript; RL, CV, and RB modified the manuscript. All authors discussed and contributed to the manuscript.

ACKNOWLEDGMENTS

This work is supported by the grant from NMRC/TCR/002-SERI/2008/R618, NMRC/TCR/R1018 and NMRC/BNIG/2016/2014, Singapore.

- Brogden, K. A. (2005). Antimicrobial peptides: pore formers or metabolic inhibitors in bacteria? *Nat. Rev. Microbiol.* 3, 238–250. doi: 10.1038/nrmicro1098
- Bürck, J., Roth, S., Wadhwanı, P., Afonin, S., Kanithasen, N., Strandberg, E., et al. (2008). Conformation and membrane orientation of amphiphilic helical peptides by oriented circular dichroism. *Biophys. J.* 95, 3872–3881. doi: 10.1529/biophysj.108.136085
- Bürck, J., Wadhwanı, P., Fanghänel, S., and Ulrich, A. S. (2016). Oriented circular dichroism: a method to characterize membrane-active peptides in oriented lipid bilayers. *Accounts Chem. Res.* 49, 184–192. doi: 10.1021/acs.accounts.5b00346
- Butler, M. S., Blaskovich, M. A. T., and Cooper, M. A. (2017). Antibiotics in the clinical pipeline at the end of 2015. *J. Antibi. 70*, 3–24. doi: 10.1038/ja.2016.72
- Cameron, D. E., Bashor, C. J., and Collins, J. J. (2014). A brief history of synthetic biology. *Nat. Rev. Microbiol.* 12, 381–390. doi: 10.1038/nrmicro3239
- Carmona, G., Rodriguez, A., Juarez, D., Corzo, G., and Villegas, E. (2013). Improved protease stability of the antimicrobial peptide pin2 substituted with D-amino acids. *Protein J.* 32, 456–466. doi: 10.1007/s10930-013-9505-2
- Carmona-Ribeiro, A. M., and de Melo Carrasco, L. D. (2014). Novel formulations for antimicrobial peptides. *Int. J. Mol. Sci.* 15, 18040–18083. doi: 10.3390/ijms151018040
- Chaddock, A. M., Mant, A., Karnauchov, I., Brink, S., Herrmann, R. G., Klösgen, R. B., et al. (1995). A new type of signal peptide: central role of a twin-arginine motif in transfer signals for the delta pH-dependent thylakoidal protein translocase. *EMBO J.* 14, 2715–2722.
- Chan, D. I., Prenner, E. J., and Vogel, H. J. (2006). Tryptophan- and arginine-rich antimicrobial peptides: structures and mechanisms of action. *Biochim. Biophys. Acta Biomembranes* 1758, 1184–1202. doi: 10.1016/j.bbamem.2006.04.006
- Chen, R., and Mark, A. E. (2011). The effect of membrane curvature on the conformation of antimicrobial peptides: implications for binding and the mechanism of action. *Eur. Biophys.* 40, 545–553. doi: 10.1007/s00249-011-0677-4
- Cherkasov, A., Hilpert, K., Jenssen, H., Fjell, C. D., Waldbrook, M., Mullaly, S. C., et al. (2009). Use of artificial intelligence in the design of small peptide antibiotics effective against a broad spectrum of highly antibiotic-resistant superbugs. *ACS Chem. Biol.* 4, 65–74. doi: 10.1021/cb800240j
- Deslouches, B., Steckbeck, J. D., Craig, J. K., Doi, Y., Mietzner, T. A., and Montelaro, R. C. (2013). Rational design of engineered cationic antimicrobial peptides consisting exclusively of arginine and tryptophan, and their activity against multidrug-resistant pathogens. *Antimicrob. Agents Chemother.* 57, 2511–2521. doi: 10.1128/AAC.02218-12
- Di Scala, C., Yahi, N., Boutemeur, S., Flores, A., Rodriguez, L., Chahinian, H., et al. (2016). Common molecular mechanism of amyloid pore formation by Alzheimer's β -amyloid peptide and α -synuclein. *Sci. Rep.* 6:28781. doi: 10.1038/srep28781
- Diamond, G., Beckloff, N., Weinberg, A., and Kisich, K. O. (2009). The roles of antimicrobial peptides in innate host defense. *Curr. Pharm. Des.* 15, 2377–2392. doi: 10.2174/138161209788682325
- Dimroth, P., Kaim, G., and Matthey, U. (2000). Crucial role of the membrane potential for ATP synthesis by F(1)F(o) ATP synthases. *J. Exp. Biol.* 203, 51–59. doi: 10.1128/AAC.45.6.1799–1802.2001
- Domalaon, R., Yang, X., O'Neil, J., Zhanal, G. G., Mookherjee, N., and Schweizer, F. (2014). Structure-activity relationships in ultrashort cationic lipopeptides: the effects of amino acid ring constraint on antibacterial activity. *Amino Acids* 46, 2517–2530. doi: 10.1007/s00726-014-1806-z
- Dong, N., Ma, Q., Shan, A., Lv, Y., Hu, W., Gu, Y., et al. (2012). Strand length-dependent antimicrobial activity and membrane-active mechanism of arginine- and valine-rich β -hairpin-like antimicrobial peptides. *Antimicrob. Agents Chemother.* 56, 2994–3003. doi: 10.1128/AAC.06327-11
- Edit, M., Christian, K., and Tieleman, D. P. (2007). Computer simulation of antimicrobial peptides. *Curr. Med. Chem.* 14, 2789–2798. doi: 10.2174/092986707782360105
- Epand, R. M., and Vogel, H. J. (1999). Diversity of antimicrobial peptides and their mechanisms of action. *Biochim. Biophys. Acta Biomembranes* 1462, 11–28. doi: 10.1016/S0005-2736(99)00198-4
- Falagas, M. E., and Kasiakou, S. K. (2006). Toxicity of polymyxins: a systematic review of the evidence from old and recent studies. *Crit. Care.* 10:R27. doi: 10.1186/cc3995
- Falla, T. J., Karunaratne, D. N., and Hancock, R. E. W. (1996). Mode of action of the antimicrobial peptide indolicidin. *J. Biol. Chem.* 271, 19298–19303. doi: 10.1074/jbc.271.32.19298
- Farrell, D. J., Robbins, M., Rhys-Williams, W., and Love, W. G. (2010). *In vitro* activity of XF-73, a novel antibacterial agent, against antibiotic-sensitive and -resistant Gram-positive and Gram-negative bacterial species. *Int. J. Antimicrob. Agents* 35, 531–536. doi: 10.1016/j.ijantimicag.2010.02.008
- Farrell, D. J., Robbins, M., Rhys-Williams, W., and Love, W. G. (2011). Investigation of the potential for mutational resistance to XF-73, retapamulin, mupirocin, fusidic acid, daptomycin, and vancomycin in methicillin-resistant *Staphylococcus aureus* isolates during a 55-passage study. *Antimicrob. Agents Chemother.* 55, 1177–1181. doi: 10.1128/AAC.01285-10
- Feng, Q., Huang, Y., Chen, M., Li, G., and Chen, Y. (2015). Functional synergy of alpha-helical antimicrobial peptides and traditional antibiotics against Gram-negative and Gram-positive bacteria *in vitro* and *in vivo*. *Eur. J. Clin. Microbiol. Infect. Dis.* 34, 197–204. doi: 10.1007/s10096-014-2219-3
- Fernandez, D. I., Le Brun, A. P., Whitwell, T. C., Sani, M.-A., James, M., and Separovic, F. (2012). The antimicrobial peptide aurein 1.2 disrupts model membranes via the carpet mechanism. *Phys. Chem. Chem. Phys.* 14, 15739–15751. doi: 10.1039/c2cp43099a
- Fernández, L., Álvarez-Ortega, C., Wiegand, I., Olivares, J., Kocíková, D., Lam, J. S., et al. (2013). Characterization of the polymyxin B resistome of *Pseudomonas aeruginosa*. *Antimicrob. Agents Chemother.* 57, 110–119. doi: 10.1128/AAC.01583-12
- Findlay, B., Zhanal, G. G., and Schweizer, F. (2012). Investigating the antimicrobial peptide window of activity using cationic lipopeptides with hydrocarbon and fluorinated tails. *Int. J. Antimicrob. Agents* 40, 36–42. doi: 10.1016/j.ijantimicag.2012.03.013
- Fjell, C. D., Hancock, R. E. W., and Cherkasov, A. (2007). AMPer: a database and an automated discovery tool for antimicrobial peptides. *Bioinformatics* 23, 1148–1155. doi: 10.1093/bioinformatics/btm068
- Fosgerau, K., and Hoffmann, T. (2015). Peptide therapeutics: current status and future directions. *Drug Discov. Today* 20, 122–128. doi: 10.1016/j.drudis.2014.10.003
- Fotakis, G., and Timbrell, J. A. (2006). *In vitro* cytotoxicity assays: comparison of LDH, neutral red, MTT and protein assay in hepatoma cell lines following exposure to cadmium chloride. *Toxicol. Lett.* 160, 171–177. doi: 10.1016/j.toxlet.2005.07.001
- Ganz, T. (2003a). Defensins: antimicrobial peptides of innate immunity. *Nat. Rev. Immunol.* 3, 710–720. doi: 10.1038/nri1180
- Ganz, T. (2003b). The role of antimicrobial peptides in innate immunity. *Integr. Comp. Biol.* 43, 300–304. doi: 10.1093/icb/43.2.300
- Gaspar, D., Veiga, A. S., and Castanho, M. A. (2013). From antimicrobial to anticancer peptides. a review. *Front. Microbiol.* 4:294. doi: 10.3389/fmicb.2013.00294
- Gazit, E., Miller, I. R., Biggin, P. C., Sansom, M. S. P., and Shai, Y. (1996). Structure and orientation of the mammalian antibacterial peptide cecropin P1 within phospholipid membranes. *J. Mol. Biol.* 258, 860–870. doi: 10.1006/jmbi.1996.0293
- Gleason, N. J., Vostrikov, V. V., Greathouse, D. V., and Koeppe, R. E. (2013). Buried lysine, but not arginine, titrates and alters transmembrane helix tilt. *Proc. Natl. Acad. Sci. U.S.A.* 110, 1692–1695. doi: 10.1073/pnas.1215400110
- Gonzales, F. P., Felgenträger, A., Baumler, W., and Maisch, T. (2013). Fungicidal photodynamic effect of a twofold positively charged porphyrin against *Candida albicans* planktonic cells and biofilms. *Future Microbiol.* 8, 785–797. doi: 10.2217/fmb.13.44
- Gordon, Y. J., Romanowski, E. G., and McDermott, A. M. (2005). A Review of antimicrobial peptides and their therapeutic potential as anti-infective drugs. *Curr. Eye Res.* 30, 505–515. doi: 10.1080/02713680590968637
- Grieco, P., Luca, V., Auriemma, L., Carotenuto, A., Saviello, M. R., Campiglia, P., et al. (2011). Alanine scanning analysis and structure-function relationships of the frog-skin antimicrobial peptide temporin-1Ta. *J. Pept. Sci.* 17, 358–365. doi: 10.1002/psc.1350
- Guilhelmelli, F., Vilela, N., Albuquerque, P., Derengowski, L. da S., and Silva-Pereira, I., Kyaw, C. M. (2013). Antibiotic development challenges: the various mechanisms of action of antimicrobial peptides and of bacterial resistance. *Front. Microbiol.* 4:353. doi: 10.3389/fmicb.2013.00353

- Guo, L., Smith-Dupont, K. B., and Gai, F. (2011). Diffusion as a probe of peptide-induced membrane domain formation. *Biochemistry* 50, 2291–2297. doi: 10.1021/bi102068j
- Hänen, A., Rausch, S., Landmann, B., Toti, L., Nusser, A., and Süßmuth, R. D. (2013). Alanine scan of the peptide antibiotic feglymycin: assessment of amino acid side chains contributing to antimicrobial activity. *ChemBioChem* 14, 625–632. doi: 10.1002/cbic.201300032
- Hartings, M. R., Gray, H. B., and Winkler, J. R. (2008). Probing melittin helix–coil equilibria in solutions and vesicles. *J. Phys. Chem. B* 112, 3202–3207. doi: 10.1021/jp709866g
- Harvey, A. L., Edrada-Ebel, R., and Quinn, R. J. (2015). The re-emergence of natural products for drug discovery in the genomics era. *Nat. Rev. Drug Discov.* 14, 111–129. doi: 10.1038/nrd4510
- Haught, C., Davis, G. D., Subramanian, R., Jackson, K. W., and Harrison, R. G. (1998). Recombinant production and purification of novel antisense antimicrobial peptide in *Escherichia coli*. *Biotechnol. Bioeng.* 57, 55–61. doi: 10.1002/(SICI)1097-0290(19980105)57:1<55::AID-BIT7>3.0.CO;2-U
- Henzler Wildman, K. A., Lee, D.-K., and Ramamoorthy, A. (2003). Mechanism of lipid bilayer disruption by the human antimicrobial peptide, LL-37. *Biochemistry* 42, 6545–6558. doi: 10.1021/bi0273563
- Hilchie, A. L., Wuert, K., and Hancock, R. E. W. (2013). Immune modulation by multifaceted cationic host defense (antimicrobial) peptides. *Nat. Chem. Biol.* 9, 761–768. doi: 10.1038/nchembio.1393
- Hong, S. Y., Oh, J. E., and Lee, K.-H. (1999). Effect of d-amino acid substitution on the stability, the secondary structure, and the activity of membrane-active peptide. *Biochem. Pharmacol.* 58, 1775–1780. doi: 10.1016/S0006-2952(99)00259-2
- Isaksson, J., Brandsdal, B. O., Engqvist, M., Flaten, G. E., Svendsen, J. S., and Stensen, W. (2011a). A synthetic antimicrobial peptidomimetic (LTX 109): stereochemical impact on membrane disruption. *J. Med. Chem.* 54, 5786–5795. doi: 10.1021/jm200450h
- Isaksson, J., Brandsdal, B. O., Engqvist, M., Flaten, G. E., Svendsen, J. S. M., and Stensen, W. (2011b). A synthetic antimicrobial peptidomimetic (LTX 109): stereochemical impact on membrane disruption. *J. Med. Chem.* 54, 5786–5795. doi: 10.1021/jm200450h
- Jean-François, F., Elezgaray, J., Berson, P., Vacher, P., and Dufourc, E. J. (2008). Pore formation induced by an antimicrobial peptide: electrostatic effects. *Biophys. J.* 95, 5748–5756. doi: 10.1529/biophysj.108.136655
- Jeong, J.-H., Kim, J.-S., Choi, S.-S., and Kim, Y. (2016). NMR structural studies of antimicrobial peptides: LPcin analogs. *Biophys. J.* 110, 423–430. doi: 10.1016/j.bpj.2015.12.006
- John Fox, S., Li, J., Tan, Y. S. N., Nguyen, M., Pal, A., Ouaray, Z., et al. (2016). The multifaceted roles of molecular dynamics simulations in drug discovery. *Curr. Pharm. Des.* 22, 3585–3600. doi: 10.2174/1381612822666160425120507
- Ketcham, R., Hu, W., and Cross, T. (1993). High-resolution conformation of gramicidin A in a lipid bilayer by solid-state NMR. *Science* 261, 1457–1460. doi: 10.1126/science.7690158
- Kim, I.-W., Lee, J. H., Subramaniyam, S., Yun, E.-Y., Kim, I., Park, J., et al. (2016). *In vivo* transcriptome analysis and detection of antimicrobial peptides of the American cockroach *Periplaneta americana* (Linnaeus). *PLoS ONE* 11:e0155304. doi: 10.1371/journal.pone.0155304
- Kirsch, S. A., and Böckmann, R. A. (2016). Membrane pore formation in atomistic and coarse-grained simulations. *Biochim. Biophys. Acta Biomembranes* 1858, 2266–2277. doi: 10.1016/j.bbamem.2015.12.031
- Koh, J.-J., Lin, H., Caroline, V., Chew, Y. S., Pang, L. M., Aung, T. T., et al. (2015a). N-lipidated peptide dimers: effective antibacterial agents against gram-negative pathogens through lipopolysaccharide permeabilization. *J. Med. Chem.* 58, 6533–6548. doi: 10.1021/acs.jmedchem.5b00628
- Koh, J.-J., Lin, S., Aung, T. T., Lim, F., Zou, H., Bai, Y., et al. (2015b). Amino acid modified xanthone derivatives: novel, highly promising membrane-active antimicrobials for multidrug-resistant gram-positive bacterial infections. *J. Med. Chem.* 58, 739–752. doi: 10.1021/jm501285x
- Kowalski, R. P., Romanowski, E. G., Yates, K. A., and Mah, F. S. (2016). An independent evaluation of a novel peptide mimetic, brilacidin (PMX30063), for ocular anti-infective. *J. Ocul. Pharmacol. Ther.* 32, 23–27. doi: 10.1089/jop.2015.0098
- Kwon, B., Waring, A., and J., Hong, M. (2013). A 2H solid-state NMR study of lipid clustering by cationic antimicrobial and cell-penetrating peptides in model bacterial membranes. *Biophys. J.* 105, 2333–2342. doi: 10.1016/j.bpj.2013.08.020
- Lakshminarayanan, R., Liu, S., Li, J., Nandhakumar, M., Aung, T. T., Goh, E., et al. (2014). Synthetic multivalent antifungal peptides effective against fungi. *PLoS ONE* 9:e87730. doi: 10.1371/journal.pone.0087730
- Lakshminarayanan, R., Tan, W. X., Aung, T. T., Goh, E. T. L., Muruganantham, N., Li, J., et al. (2016). Branched peptide, B2088, disrupts the supramolecular organization of lipopolysaccharides and sensitizes the gram-negative bacteria. *Sci. Rep.* 6:25905. doi: 10.1038/srep25905
- Lam, K. L. H., Wang, H., Siaw, T. A., Chapman, M. R., Waring, A. J., Kindt, J. T., et al. (2012). Mechanism of structural transformations induced by antimicrobial peptides in lipid membranes. *Biochim. Biophys. Acta Biomembranes* 1818, 194–204. doi: 10.1016/j.bbamem.2011.11.002
- Lau, Q. Y., Ng, F. M., Cheong, J. W. D., Yap, Y. Y. A., Tan, Y. Y. F., Jureen, R., et al. (2015). Discovery of an ultra-short linear antibacterial tetrapeptide with anti-MRSA activity from a structure–activity relationship study. *Eur. J. Med. Chem.* 105, 138–144. doi: 10.1016/j.ejmchem.2015.10.015
- Laver, D. R. (1994). The barrel-stave model as applied to alamethicin and its analogs reevaluated. *Biophys. J.* 66(Pt 1), 355–359. doi: 10.1016/S0006-3495(94)80784-2
- Lee, D.-K., Bhunia, A., Kotler, S. A., and Ramamoorthy, A. (2015). Detergent-type membrane fragmentation by MSI-78, MSI-367, MSI-594, and MSI-843 antimicrobial peptides and inhibition by cholesterol: a solid-state nuclear magnetic resonance study. *Biochemistry* 54, 1897–1907. doi: 10.1021/bi501418m
- Lee, M.-T., Sun, T.-L., Hung, W.-C., and Huang, H. W. (2013). Process of inducing pores in membranes by melittin. *Proc. Natl. Acad. Sci. U.S.A.* 110, 14243–14248. doi: 10.1073/pnas.1307010110
- Lee, T. H., Hall, K. N., and Aguilar, M. I. (2016). Antimicrobial peptide structure and mechanism of action: a focus on the role of membrane structure. *Curr. Top. Med. Chem.* 16, 25–39. doi: 10.2174/1568026615666150703121700
- Leontiadou, H., Mark, A. E., and Marrink, S. J. (2006). Antimicrobial peptides in action. *J. Am. Chem. Soc.* 128, 12156–12161. doi: 10.1021/ja062927q
- Leveritt, J. M. III., John, M., Pino-Angeles, A., and Lazaridis, T. (2015). The structure of a melittin-stabilized pore. *Biophys. J.* 108, 2424–2426. doi: 10.1016/j.bpj.2015.04.006
- Li, J., Liu, S., Koh, J.-J., Zou, H., Lakshminarayanan, R., Bai, Y., et al. (2015). A novel fragment based strategy for membrane active antimicrobials against MRSA. *Biochim. Biophys. Acta Biomembranes* 1848, 1023–1031. doi: 10.1016/j.bbamem.2015.01.001
- Li, J., Liu, S., Lakshminarayanan, R., Bai, Y., Pervushin, K., Verma, C., et al. (2013). Molecular simulations suggest how a branched antimicrobial peptide perturbs a bacterial membrane and enhances permeability. *Biochim. Biophys. Acta Biomembranes* 1828, 1112–1121. doi: 10.1016/j.bbamem.2012.12.015
- Li, J., Xu, X., Xu, C., Zhou, W., Zhang, K., Yu, H., et al. (2007). Anti-infection peptidomics of amphibian skin. *Mol. Cell. Proteomics* 6, 882–894. doi: 10.1074/mcp.M600334-MCP200
- Li, Y., Xiang, Q., Zhang, Q., Huang, Y., and Su, Z. (2012). Overview on the recent study of antimicrobial peptides: origins, functions, relative mechanisms and application. *Peptides* 37, 207–215. doi: 10.1016/j.peptides.2012.07.001
- Liu, D., Choi, S., Chen, B., Doerksen, R. J., Clements, D. J., Winkler, J. D., et al. (2004). Nontoxic membrane-active antimicrobial arylamide oligomers. *Angew. Chem. Int. Ed. Engl.* 43, 1158–1162. doi: 10.1002/anie.200352791
- Liu, Z., Brady, A., Young, A., Rasimick, B., Chen, K., Zhou, C., et al. (2007). Length effects in antimicrobial peptides of the (RW)(n) series. *Antimicrob. Agents Chemother.* 51, 597–603. doi: 10.1128/AAC.00828-06
- Livermore, D. M. (2004). The need for new antibiotics. *Clin. Microbiol. Infect.* 10, 1–9. doi: 10.1111/j.1465-0691.2004.1004.x
- Lohan, S., and Bisht, G. S. (2013). Recent approaches in design of peptidomimetics for antimicrobial drug discovery research. *Mini Rev. Med. Chem.* 13, 1073–1088. doi: 10.2174/1389557511313070010
- Lu, J.-X., Damodaran, K., Blazyk, J., and Lorigan, G. A. (2005). Solid-state nuclear magnetic resonance relaxation studies of the interaction mechanism of antimicrobial peptides with phospholipid bilayer membranes. *Biochemistry* 44, 10208–10217. doi: 10.1021/bi050730p

- Makovitzki, A., Avrahami, D., and Shai, Y. (2006). Ultrashort antibacterial and antifungal lipopeptides. *Proc. Natl. Acad. Sci. U.S.A.* 103, 15997–16002. doi: 10.1073/pnas.0606129103
- Malanovic, N. and Lohner, K. (2016). Gram-positive bacterial cell envelopes: the impact on the activity of antimicrobial peptides. *Biochim. Biophys. Acta Biomembranes* 1858, 936–946. doi: 10.1016/j.bbamem.2015.11.004
- Manna, M., and Mukhopadhyay, C. (2009). Cause and effect of melittin-induced pore formation: a computational approach. *Langmuir* 25, 12235–12242. doi: 10.1021/la902660q
- Marr, A. K., Gooperham, W. J., and Hancock, R. E. W. (2006). Antibacterial peptides for therapeutic use: obstacles and realistic outlook. *Curr. Opin. Pharmacol.* 6, 468–472. doi: 10.1016/j.coph.2006.04.006
- Marta Guarra, M., Coulson, R., and Rubinchik, E. (2006). Anti-inflammatory activity of cationic peptides: application to the treatment of acne vulgaris. *FEMS Microbiol. Lett.* 257, 1–6. doi: 10.1111/j.1574-6968.2006.00156.x
- Martin, L., De Santis, R., Koczera, P., Simons, N., Haase, H., Heinbockel, L., et al. (2015a). The synthetic antimicrobial peptide 19-2.5 interacts with heparanase and heparan sulfate in murine and human sepsis. *PLoS ONE* 10:e0143583. doi: 10.1371/journal.pone.0143583
- Martin, L., van Meegern, A., Doemming, S., and Schuerholz, T. (2015b). Antimicrobial peptides in human sepsis. *Front. Immunol.* 6:404. doi: 10.3389/fimmu.2015.00404
- Matile, S., Vargas Jentzsch, A., Montenegro, J., and Fin, A. (2011). Recent synthetic transport systems. *Chem. Soc. Rev.* 40, 2453–2474. doi: 10.1039/c0cs00209g
- Matsuzaki, K. (1998). Magainins as paradigm for the mode of action of pore forming polypeptides. *Biochim. Biophys. Acta Biomembranes* 1376, 391–400. doi: 10.1016/s0304-4157(98)00014-8
- Matsuzaki, K., Yoneyama, S., and Miyajima, K. (1997). Pore formation and translocation of melittin. *Biophys. J.* 73, 831–838. doi: 10.1016/S0006-3495(97)78115-3
- McCormick, T. S., and Weinberg, A. (2010). Epithelial cell-derived antimicrobial peptides are multi-functional agents that bridge innate and adaptive immunity. *Periodontol. 2000* 54, 195–206. doi: 10.1111/j.1600-0757.2010.00373.x
- McDermott, A. M. (2013). Antimicrobial compounds in tears. *Exp. Eye Res.* 117, 53–61. doi: 10.1016/j.exer.2013.07.014
- McKenna, M. (2013). Antibiotic resistance: the last resort. *Nature* 499, 394–396. doi: 10.1038/499394a
- Melo, M. N., Ferre, R., and Castanho, M. A. (2009). Antimicrobial peptides: linking partition, activity and high membrane-bound concentrations. *Nat. Rev. Microbiol.* 7, 245–250. doi: 10.1038/nrmicro2095
- Meroueh, S. O., Bencze, K. Z., Hesek, D., Lee, M., Fisher, J. F., Stemmler, T. L., et al. (2006). Three-dimensional structure of the bacterial cell wall peptidoglycan. *Proc. Natl. Acad. Sci. U.S.A.* 103, 4404–4409. doi: 10.1073/pnas.0510182103
- Mihajlovic, M., and Lazaridis, T. (2010). Antimicrobial peptides in toroidal and cylindrical pores. *Biochim. Biophys. Acta* 1798, 1485–1493. doi: 10.1016/j.bbamem.2010.04.004
- Milov, A. D., Samoilova, R. I., Tsvetkov, Y. D., De Zotti, M., Formaggio, F., Toniolo, C., et al. (2009). Structure of self-aggregated alamethicin in ePC membranes detected by pulsed electron-electron double resonance and electron spin echo envelope modulation spectroscopies. *Biophys. J.* 96, 3197–3209. doi: 10.1016/j.bpj.2009.01.026
- Mishra, B., and Wang, G. (2012). Ab initio design of potent anti-MRSA peptides based on database filtering technology. *J. Am. Chem. Soc.* 134, 12426–12429. doi: 10.1021/ja305644e
- Mishra, B., Lushnikova, T., and Wang, G. (2015). Small lipopeptides possess anti-biofilm capability comparable to daptomycin and vancomycin. *RSC Adv.* 5, 59758–59769. doi: 10.1039/C5RA07896B
- Mohanram, H., and Bhattacharjya, S. (2014). β -boomerang antimicrobial and antiendotoxic peptides: lipidation and disulfide bond effects on activity and structure. *Pharmaceutics* 7, 482–501. doi: 10.3390/ph7040482
- Monroc, S., Badosa, E., Besalú, E., Planas, M., Bardaji, E., Montesinos, E., et al. (2006). Improvement of cyclic decapeptides against plant pathogenic bacteria using a combinatorial chemistry approach. *Peptides* 27, 2575–2584. doi: 10.1016/j.peptides.2006.05.001
- Mygind, P. H., Fischer, R. L., Schnorr, K. M., Hansen, M. T., Sonksen, C. P., Ludvigsen, S., et al. (2005). Plectasin is a peptide antibiotic with therapeutic potential from a saprophytic fungus. *Nature* 437, 975–980. doi: 10.1038/nature04051
- Nasompag, S., Dechsiri, P., Hongsing, N., Phonimdaeng, P., Daduang, S., Klaynongsruang, S., et al. (2015). Effect of acyl chain length on therapeutic activity and mode of action of the CX-KYR-NH₂ antimicrobial lipopeptide. *Biochim. Biophys. Acta* 1848(Pt A), 2351–2364. doi: 10.1016/j.bbamem.2015.07.004
- Nikaido, H. (2003). Molecular basis of bacterial outer membrane permeability revisited. *Microbiol. Mol. Biol. Rev.* 67, 593–656. doi: 10.1128/MMBR.67.4.593-656.2003
- Niu, Y., Wang, R. E., Wu, H., and Cai, J. (2012). Recent development of small antimicrobial peptidomimetics. *Future Med. Chem.* 4, 1853–1862. doi: 10.4155/fmc.12.111
- North, J. R., Takenaka, S., Rozek, A., Kielczewska, A., Opal, S., Morici, L. A., et al. (2016). A novel approach for emerging and antibiotic resistant infections: innate defense regulators as an agnostic therapy. *J. Biotechnol.* 226, 24–34. doi: 10.1016/j.jbiotec.2016.03.032
- Ofek, I., Cohen, S., Rahmani, R., Kabha, K., Tamarkin, D., Herzig, Y., et al. (1994). Antibacterial synergism of polymyxin B nonapeptide and hydrophobic antibiotics in experimental gram-negative infections in mice. *Antimicrob. Agents Chemother.* 38, 374–377. doi: 10.1128/AAC.38.2.374
- Olaitan, A. O., Morand, S., and Rolain, J.-M. (2014). Mechanisms of polymyxin resistance: acquired and intrinsic resistance in bacteria. *Front. Microbiol.* 5:643. doi: 10.3389/fmicb.2014.00643
- Ooi, N., Miller, K., Hobbs, J., Rhys-Williams, W., Love, W., and Chopra, I. (2009). XF-73, a novel antistaphylococcal membrane-active agent with rapid bactericidal activity. *J. Antimicrob. Chemother.* 64, 735–740. doi: 10.1093/jac/dkp299
- Oreopoulos, J., Epand, R. F., Epand, R. M., and Yip, C. M. (2010). Peptide-induced domain formation in supported lipid bilayers: direct evidence by combined atomic force and polarized total internal reflection fluorescence microscopy. *Biophys. J.* 98, 815–823. doi: 10.1016/j.bpj.2009.12.4327
- Overhage, J., Campisano, A., Bains, M., Torfs, E. C., Rehm, B. H., and Hancock, R. E. (2008). Human host defense peptide LL-37 prevents bacterial biofilm formation. *Infect. Immun.* 76, 4176–4182. doi: 10.1128/IAI.00318-08
- Perona, J. J., and Craik, C. S. (1997). Evolutionary divergence of substrate specificity within the chymotrypsin-like serine protease fold. *J. Biol. Chem.* 272, 29987–29990. doi: 10.1074/jbc.272.48.29987
- Polyansky, A. A., Ramaswamy, R., Volynsky, P. E., Sbalzarini, I. F., Marrink, S. J., and Efremov, R. G. (2010). Antimicrobial peptides induce growth of phosphatidylglycerol domains in a model bacterial membrane. *J. Phys. Chem. Lett.* 1, 3108–3111. doi: 10.1021/jz101163e
- Porcelli, F., Buck, B., Lee, D.-K., Hallock, K. J., Ramamoorthy, A., and Veglia, G. (2004). Structure and orientation of pardaxin determined by NMR experiments in model membranes. *J. Biol. Chem.* 279, 45815–45823. doi: 10.1074/jbc.M405454200
- Qian, S., and Heller, W. T. (2011). Peptide-induced asymmetric distribution of charged lipids in a vesicle bilayer revealed by small-angle neutron scattering. *J. Phys. Chem. B* 115, 9831–9837. doi: 10.1021/jp204045t
- Rabanal, F., Grau-Campistany, A., Vila-Farrés, X., Gonzalez-Linares, J., Borràs, M., Vila, J., et al. (2015). A bioinspired peptide scaffold with high antibiotic activity and low *in vivo* toxicity. *Sci. Rep.* 5:10558. doi: 10.1038/srep10558
- Ragioli, D. A. M. T., Carrasco, L. D. M., and Carmona-Ribeiro, A. M. (2014). Novel gramicidin formulations in cationic lipid as broad-spectrum microbial agents. *Int. J. Nanomedicine* 9, 3183–3192. doi: 10.2147/IJN.S65289
- Ramamoorthy, A., Lee, D.-K., Narasimhaswamy, T., and Nanga, R. P. R. (2010). Cholesterol reduces pardaxin's dynamics—a barrel-stave mechanism of membrane disruption investigated by solid-state NMR. *Biochim. Biophys. Acta Biomembranes* 1798, 223–227. doi: 10.1016/j.bbamem.2009.08.012
- Ramamoorthy, A., Thennarasu, S., Lee, D.-K., Tan, A., and Maloy, L. (2006). Solid-state NMR investigation of the membrane-disrupting mechanism of antimicrobial peptides MSI-78 and MSI-594 derived from magainin 2 and melittin. *Biophys. J.* 91, 206–216. doi: 10.1529/biophysj.105.073890
- Rausch, J. M., Marks, J. R., and Wimley, W. C. (2005). Rational combinatorial design of pore-forming β -sheet peptides. *Proc. Natl. Acad. Sci. U.S.A.* 102, 10511–10515. doi: 10.1073/pnas.0502013102
- Rausch, J. M., Marks, J. R., Rathnakumar, R., and Wimley, W. C. (2007). β -sheet pore-forming peptides selected from a rational combinatorial library:

- mechanism of pore formation in lipid vesicles and activity in biological membranes. *Biochemistry* 46, 12124–12139. doi: 10.1021/bi700978h
- Romeo, D., Skerlavaj, B., Bolognesi, M., and Gennaro, R. (1988). Structure and bactericidal activity of an antibiotic dodecapeptide purified from bovine neutrophils. *J. Biol. Chem.* 263, 9573–9575.
- Ruiz, N., Kahne, D., and Silhavy, T. J. (2006). Advances in understanding bacterial outer-membrane biogenesis. *Nat. Rev. Microbiol.* 4, 57–66. doi: 10.1038/nrmicro1322
- Sani, M. A., Whitwell, T. C., Gehman, J. D., Robins-Browne, R. M., Pantaratt, N., Attard, T. J., et al. (2013). Maculatin 1.1 disrupts *Staphylococcus aureus* lipid membranes via a pore mechanism. *Antimicrob. Agents Chemother.* 57, 3593–3600. doi: 10.1128/AAC.00195-13
- Santo, K. P., Irudayam, S. J., and Berkowitz, M. L. (2013). Melittin creates transient pores in a lipid bilayer: results from computer simulations. *J. Phys. Chem. B* 117, 5031–5042. doi: 10.1021/jp312328n
- Saravanan, R., Li, X., Lim, K., Mohanram, H., Peng, L., Mishra, B., et al. (2014). Design of short membrane selective antimicrobial peptides containing tryptophan and arginine residues for improved activity, salt-resistance, and biocompatibility. *Biotechnol. Bioeng.* 111, 37–49. doi: 10.1002/bit.25003
- Saravolatz, L. D., Pawlak, J., Johnson, L., Bonilla, H., Saravolatz, L. D. II, Fakih, M. G., et al. (2012a). *In vitro* activities of LTX-109, a synthetic antimicrobial peptide, against methicillin-resistant, vancomycin-intermediate, vancomycin-resistant, daptomycin-nonsusceptible, and linezolid-nonsusceptible *Staphylococcus aureus*. *Antimicrob. Agents Chemother.* 56, 4478–4482. doi: 10.1128/AAC.00194-12
- Saravolatz, L. D., Pawlak, J., Johnson, L., Bonilla, H., Saravolatz, L. D., Fakih, M. G., et al. (2012b). *In vitro* Activities of LTX-109, a synthetic antimicrobial peptide, against methicillin-resistant, vancomycin-intermediate, vancomycin-resistant, daptomycin-nonsusceptible, and linezolid-nonsusceptible *Staphylococcus aureus*. *Antimicrob. Agents Chemother.* 56, 4478–4482. doi: 10.1128/AAC.00194-12
- Sato, H., and Feix, J. B. (2006). Peptide-membrane interactions and mechanisms of membrane destruction by amphipathic α -helical antimicrobial peptides. *Biochim. Biophys. Acta Biomembranes* 1758, 1245–1256. doi: 10.1016/j.bbamem.2006.02.021
- Scheinflug, K., Krylova, O., Nikolenko, H., Thurm, C., and Dathe, M. (2015). Evidence for a novel mechanism of antimicrobial action of a cyclic R-,W-rich hexapeptide. *PLoS ONE* 10:e0125056. doi: 10.1371/journal.pone.0125056
- Schmidt, N. W., and Wong, G. C. L. (2013). Antimicrobial peptides and induced membrane curvature: geometry, coordination chemistry, and molecular engineering. *Curr. Opin. Solid State Mater. Sci.* 17, 151–163. doi: 10.1016/j.cossc.2013.09.004
- Schmidt, N. W., Lis, M., Zhao, K., Lai, G. H., Alexandrova, A. N., Tew, G. N., et al. (2012a). Molecular basis for nanoscopic membrane curvature generation from quantum mechanical models and synthetic transporter sequences. *J. Am. Chem. Soc.* 134, 19207–19216. doi: 10.1021/ja308459j
- Schmidt, N. W., Mishra, A., Lai, G. H., Davis, M., Sanders, L. K., Tran, D., et al. (2011). Criterion for amino acid composition of defensins and antimicrobial peptides based on geometry of membrane destabilization. *J. Am. Chem. Soc.* 133, 6720–6727. doi: 10.1021/ja200079a
- Schmidt, N. W., Tai, K. P., Kamdar, K., Mishra, A., Lai, G. H., Zhao, K., et al. (2012b). Arginine in α -defensins: differential effects on bactericidal activity correspond to geometry of membrane curvature generation and peptide-lipid phase behavior. *J. Biol. Chem.* 287, 21866–21872. doi: 10.1074/jbc.M112.358721
- Schmidt, N., Mishra, A., Lai, G. H., and Wong, G. C. L. (2010). Arginine-rich cell-penetrating peptides. *FEBS Lett.* 584, 1806–1813. doi: 10.1016/j.febslet.2009.11.046
- Schuerholz, T., Brandenburg, K., and Marx, G. (2012). Antimicrobial peptides and their potential application in inflammation and sepsis. *Crit. Care* 16, 207–207. doi: 10.1186/cc11220
- Schwechheimer, C., and Kuehn, M. J. (2015). Outer-membrane vesicles from Gram-negative bacteria: biogenesis and functions. *Nat. Rev. Microbiol.* 13, 605–619. doi: 10.1038/nrmicro3525
- Sengupta, D., Leontiadou, H., Mark, A. E., and Marrink, S.-J. (2008). Toroidal pores formed by antimicrobial peptides show significant disorder. *Biochim. Biophys. Acta Biomembranes* 1778, 2308–2317. doi: 10.1016/j.bbamem.2008.06.007
- Shai, Y. (2002). Mode of action of membrane active antimicrobial peptides. *Biopolymers* 66, 236–248. doi: 10.1002/bip.10260
- Shin, D.-M., and Jo, E.-K. (2011). Antimicrobial peptides in innate immunity against mycobacteria. *Immune Netw.* 11, 245–252. doi: 10.4110/in.2011.11.5.245
- Shin, J. R., Lim, K. J., Kim, D. J., Cho, J. H., and Kim, S. C. (2013). Display of multimeric antimicrobial peptides on the *Escherichia coli* cell surface and its application as whole-cell antibiotics. *PLoS ONE* 8:e58997. doi: 10.1371/journal.pone.0058997
- Sitaram, N., and Nagaraj, R. (1999). Interaction of antimicrobial peptides with biological and model membranes: structural and charge requirements for activity. *Biochim. Biophys. Acta Biomembranes* 1462, 29–54. doi: 10.1016/S0005-2736(99)00199-6
- Sivertsen, A., Isaksson, J., Leiros, H.-K. S., Svenson, J., Svendsen, J.-S., and Brandsdal, B. O. (2014). Synthetic cationic antimicrobial peptides bind with their hydrophobic parts to drug site II of human serum albumin. *BMC Struct. Biol.* 14, 4–4. doi: 10.1186/1472-6807-14-4
- Sjogren, M. H. (2004). Thymalfasin: an immune system enhancer for the treatment of liver disease. *J. Gastroenterol. Hepatol.* 19, S69–S72. doi: 10.1111/j.1440-1746.2004.03635.x
- Sokolov, Y., Mirzabekov, T., Martin, D. W., Lehrer, R. I., and Kagan, B. L. (1999). Membrane channel formation by antimicrobial protegrins. *Biochim. Biophys. Acta Biomembranes* 1420, 23–29. doi: 10.1016/S0005-2736(99)00086-3
- Song, C., Weichbrodt, C., Salnikov, E. S., Dynowski, M., Forsberg, B. O., Bechinger, B., et al. (2013). Crystal structure and functional mechanism of a human antimicrobial membrane channel. *Proc. Natl. Acad. Sci. U.S.A.* 12, 4586–4591. doi: 10.1073/pnas.1214739110
- Starr, C. G., He, J., and Wimley, W. C. (2016). Host cell interactions are a significant barrier to the clinical utility of peptide antibiotics. *ACS Chem. Biol.* 11, 3391–3399. doi: 10.1021/acschembio.6b00843
- Stevens, M. J. (2004). Coarse-grained simulations of lipid bilayers. *J. Chem. Phys.* 121, 11942–11948. doi: 10.1063/1.1814058
- Strandberg, E., and Ulrich, A. S. (2004). NMR methods for studying membrane-active antimicrobial peptides. *Concepts Magn. Reson. Part A* 23A, 89–120. doi: 10.1002/cmr.a.20024
- Strøm, M. B., Haug, B. E., Skar, M. L., Stensen, W., Stiberg, T., and Svendsen, J. S. (2003). The pharmacophore of short cationic antibacterial peptides. *J. Med. Chem.* 46, 1567–1570. doi: 10.1021/jm0340039
- Strøm, M. B., Rekdal, Ø., and Svendsen, J. S. (2002). Antimicrobial activity of short arginine- and tryptophan-rich peptides. *J. Pept. Sci.* 8, 431–437. doi: 10.1002/psc.398
- Su, Y., DeGrado, W. F., and Hong, M. (2010). Orientation, dynamics and lipid interaction of an antimicrobial arylamide investigated by ^{19}F and ^{31}P solid-state NMR spectroscopy. *J. Am. Chem. Soc.* 132, 9197–9205. doi: 10.1021/ja103658h
- Svenson, J., Brandsdal, B.-O., Stensen, W., and Svendsen, J. S. (2007). Albumin binding of short cationic antimicrobial micropeptides and its influence on the *in vitro* bactericidal effect. *J. Med. Chem.* 50, 3334–3339. doi: 10.1021/jm0703542
- Szleifer, I., Kramer, D., Ben-Shaul, A., Roux, D., and Gelbart, W. M. (1988). Curvature elasticity of pure and mixed surfactant films. *Phys. Rev. Lett.* 60, 1966–1969. doi: 10.1103/PhysRevLett.60.1966
- Takeshima, K., Chikushi, A., Lee, K.-K., Yonehara, S., and Matsuzaki, K. (2003). Translocation of analogues of the antimicrobial peptides magainin and buforin across human cell membranes. *J. Biol. Chem.* 278, 1310–1315. doi: 10.1074/jbc.M208762200
- Tally, F. P., and DeBruin, M. F. (2000). Development of daptomycin for Gram-positive infections. *J. Antimicrob. Chemother.* 46, 523–526. doi: 10.1093/jac/46.4.523
- Terwilliger, T. C., Weissman, L., and Eisenberg, D. (1982). The structure of melittin in the form I crystals and its implication for melittin's lytic and surface activities. *Biophys. J.* 37, 353–361. doi: 10.1016/S0006-3495(82)84683-3
- Tew, G. N., Liu, D., Chen, B., Doerksen, R. J., Kaplan, J., Carroll, P. J., et al. (2002). *De novo* design of biomimetic antimicrobial polymers. *Proc. Natl. Acad. Sci. U.S.A.* 99, 5110–5114. doi: 10.1073/pnas.082046199
- Tew, G. N., Scott, R. W., Klein, M. L., and Degrad, W. F. (2010a). *De novo* design of antimicrobial polymers, foldamers, and small molecules: from

- discovery to practical applications. *Acc. Chem. Res.* 43, 30–39. doi: 10.1021/ar90036b
- Tew, G. N., Scott, R. W., Klein, M. L., and DeGrado, W. F. (2010b). *In vivo* design of antimicrobial polymers, foldamers, and small molecules: from discovery to practical applications. *Acc. Chem. Res.* 43, 30–39. doi: 10.1021/ar90036b
- Thomas, S., Karnik, S., Barai, R. S., Jayaraman, V. K., and Idicula-Thomas, S. (2010). CAMP: a useful resource for research on antimicrobial peptides. *Nucleic Acids Res.* 38, D774–D780. doi: 10.1093/nar/gkp1021
- Tsai, C.-W., Hsu, N.-Y., Wang, C.-H., Lu, C.-Y., Chang, Y., Tsai, H.-H. G., et al. (2009). Coupling molecular dynamics simulations with experiments for the rational design of indolicidin-analogous antimicrobial peptides. *J. Mol. Biol.* 392, 837–854. doi: 10.1016/j.jmb.2009.06.071
- Urry, D. W. (1971). The gramicidin A transmembrane Channel: a proposed $\pi((L,D))$ helix. *Proc. Natl. Acad. Sci. U.S.A.* 68, 672–676. doi: 10.1073/pnas.68.3.672
- Valerio, L. G. Jr. (2009). *In silico* toxicology for the pharmaceutical sciences. *Toxicol. Appl. Pharmacol.* 241, 356–370. doi: 10.1016/j.taap.2009.08.022
- Van Lenten, B. J., Navab, M., Anantharamaiah, G. M., Buga, G. M., Reddy, S. T., and Fogelman, A. M. (2008). Multiple indications for anti-inflammatory peptides. *Curr. Opin. Investig. Drugs* 9, 1157–1162.
- Vandamme, D., Landuyt, B., Luyten, W., and Schoofs, L. (2012). A comprehensive summary of LL-37, the factotum human cathelicidin peptide. *Cell Immunol.* 280, 22–35. doi: 10.1016/j.cellimm.2012.11.009
- Vandenburg, Y. R., Smith, B. D., Biron, E., and Voyer, N. (2002). Membrane disruption ability of facially amphiphilic helical peptides. *Chem. Commun.* 16, 1694–1695. doi: 10.1039/b204640g
- Vollmer, W., Blanot, D., and De Pedro, M. A. (2008). Peptidoglycan structure and architecture. *FEMS Microbiol. Rev.* 32, 149–167. doi: 10.1111/j.1574-6976.2007.00094.x
- Wadhwania, P., Epand, R. F., Heidenreich, N., Bürck, J., Ulrich, A. S., and Epand, R. M. (2012). Membrane-active peptides and the clustering of anionic lipids. *Biophys. J.* 103, 265–274. doi: 10.1016/j.bpj.2012.06.004
- Wang, G., Li, X., and Wang, Z. (2016). APD3: the antimicrobial peptide database as a tool for research and education. *Nucleic Acids Res.* 44, D1087–D1093. doi: 10.1093/nar/gkv1278
- Wang, J., Li, Y., Wang, X., Chen, W., Sun, H., and Wang, J. (2014). Lipopolysaccharide induces amyloid formation of antimicrobial peptide HAL-2. *Biochim. Biophys. Acta Biomembranes* 1838, 2910–2918. doi: 10.1016/j.bbamem.2014.07.028
- Wang, K. F., Nagarajan, R., and Camesano, T. A. (2015). Differentiating antimicrobial peptides interacting with lipid bilayer: molecular signatures derived from quartz crystal microbalance with dissipation monitoring. *Biophys. Chem.* 196, 53–67. doi: 10.1016/j.bpc.2014.09.003
- Wang, Y., Chen, C. H., Hu, D., Ulmschneider, M. B., and Ulmschneider, J. P. (2016). Spontaneous formation of structurally diverse membrane channel architectures from a single antimicrobial peptide. *Nat. Commun.* 7:13535. doi: 10.1038/ncomms13535
- Wimley, W. C. (2010). Describing the mechanism of antimicrobial peptide action with the interfacial activity model. *ACS Chem. Biol.* 5, 905–917. doi: 10.1021/cb1001558
- Wu, Z., Cui, Q., and Yethiraj, A. (2013). Why do arginine and lysine organize lipids differently? insights from coarse-grained and atomistic simulations. *J. Phys. Chem. B* 117, 12145–12156. doi: 10.1021/jp4068729
- Xiong, M., Lee, M. W., Mansbach, R. A., Song, Z., Bao, Y., Peek, R. M., et al. (2015). Helical antimicrobial polypeptides with radial amphiphilicity. *Proc. Natl. Acad. Sci. U.S.A.* 112, 13155–13160. doi: 10.1073/pnas.1507893112
- Yang, L., Gordon, V. D., Mishra, A., Som, A., Purdy, K. R., Davis, M. A., et al. (2007). Synthetic antimicrobial oligomers induce a composition-dependent topological transition in membranes. *J. Am. Chem. Soc.* 129, 12141–12147. doi: 10.1021/ja072310o
- Yang, L., Harroun, T. A., Weiss, T. M., Ding, L., and Huang, H. W. (2001). Barrel-stave model or toroidal model? a case study on melittin pores. *Biophys. J.* 81, 1475–1485. doi: 10.1016/S0006-3495(01)75802-X
- Ye, G., Gupta, A., DeLuca, R., Parang, K., and Bothun, G. D. (2010). Bilayer disruption and liposome restructuring by a homologous series of small Arg-rich synthetic peptides. *Colloids Surf. B Biointerfaces* 76, 76–81. doi: 10.1016/j.colsurfb.2009.10.016
- Yeaman, M. R., and Yount, N. Y. (2003). Mechanisms of antimicrobial peptide action and resistance. *Pharmacol. Res.* 55, 27–55. doi: 10.1124/pr.55.1.2
- Yoneyama, F., Imura, Y., Ohno, K., Zendo, T., Nakayama, J., Matsuzaki, K., et al. (2009). Peptide-lipid huge toroidal pore, a new antimicrobial mechanism mediated by a lactococcal bacteriocin, lacticin Q. *Antimicrob. Agents Chemother.* 53, 3211–3217. doi: 10.1128/AAC.00209-09
- Yoo, J., and Cui, Q. (2008). Does arginine remain protonated in the lipid membrane? insights from microscopic pK(a) calculations. *Biophys. J.* 94, L61–L63. doi: 10.1529/biophysj.107.122945
- Yoo, J., and Cui, Q. (2010). Chemical versus mechanical perturbations on the protonation state of arginine in complex lipid membranes: insights from microscopic pK(a) calculations. *Biophys. J.* 99, 1529–1538. doi: 10.1016/j.bpj.2010.06.048
- Zasloff, M. (1987). Magainins, a class of antimicrobial peptides from *Xenopus* skin: isolation, characterization of two active forms, and partial cDNA sequence of a precursor. *Proc. Natl. Acad. Sci. U.S.A.* 84, 5449–5453. doi: 10.1073/pnas.84.15.5449
- Zasloff, M. (2002). Antimicrobial peptides of multicellular organisms. *Nature* 415, 389–395. doi: 10.1038/415389a
- Zelezetsky, I., and Tossi, A. (2006). Alpha-helical antimicrobial peptides—Using a sequence template to guide structure–activity relationship studies. *Biochim. Biophys. Acta Biomembranes* 1758, 1436–1449. doi: 10.1016/j.bbamem.2006.03.021

Conflict of Interest Statement: The authors declare that the research was conducted in the absence of any commercial or financial relationships that could be construed as a potential conflict of interest.

Copyright © 2017 Li, Koh, Liu, Lakshminarayanan, Verma and Beuerman. This is an open-access article distributed under the terms of the Creative Commons Attribution License (CC BY). The use, distribution or reproduction in other forums is permitted, provided the original author(s) or licensor are credited and that the original publication in this journal is cited, in accordance with accepted academic practice. No use, distribution or reproduction is permitted which does not comply with these terms.



Substance P and Calcitonin Gene-Related Peptide: Key Regulators of Cutaneous Microbiota Homeostasis

Awa N'Diaye¹, Andrei Gannessen^{1,2}, Valérie Borrel¹, Olivier Maillot¹, Jeremy Enault¹, Pierre-Jean Racine¹, Vladimir Plakunov², Sylvie Chevalier¹, Olivier Lesouhaitier¹ and Marc G. J. Feuilloley^{1*}

¹Laboratory of Microbiology Signals and Microenvironment (LMSM), Normandie Université Rouen, Evreux, France,

²Winogradsky Institute of Microbiology, Research Center of Biotechnology of Russian Academy of Science, Moscow, Russia

OPEN ACCESS

Edited by:

Hubert Vaudry,
University of Rouen, France

Reviewed by:

Kazuhiro Takahashi,
Tohoku University, Japan
John Michael Conlon,
Ulster University, UK

***Correspondence:**

Marc G. J. Feuilloley
marc.feuilloley@univ-rouen.fr

Specialty section:

This article was submitted to
Neuroendocrine Science,
a section of the journal
Frontiers in Endocrinology

Received: 03 November 2016

Accepted: 16 January 2017

Published: 30 January 2017

Citation:

N'Diaye A, Gannessen A, Borrel V,
Maillot O, Enault J, Racine P-J,
Plakunov V, Chevalier S,
Lesouhaitier O and Feuilloley MGJ
(2017) Substance P and Calcitonin
Gene-Related Peptide: Key
Regulators of Cutaneous
Microbiota Homeostasis.
Front. Endocrinol. 8:15.
doi: 10.3389/fendo.2017.00015

Neurohormones diffuse in sweat and epidermis leading skin bacterial microflora to be largely exposed to these host factors. Bacteria can sense a multitude of neurohormones, but their role in skin homeostasis was only investigated recently. The first study focused on substance P (SP), a neuropeptide produced in abundance by skin nerve terminals. SP is without effect on the growth of Gram-positive (*Bacillus cereus*, *Staphylococcus aureus*, and *Staphylococcus epidermidis*) and Gram-negative (*Pseudomonas fluorescens*) bacteria. However, SP is stimulating the virulence of *Bacillus* and *Staphylococci*. The action of SP is highly specific with a threshold below the nanomolar level. Mechanisms involved in the response to SP are different between bacteria although they are all leading to increased adhesion and/or virulence. The moonlighting protein EfTu was identified as the SP-binding site in *B. cereus* and *Staphylococci*. In skin nerve terminals, SP is co-secreted with the calcitonin gene-related peptide (CGRP), which was shown to modulate the virulence of *S. epidermidis*. This effect is antagonized by SP. Identification of the CGRP sensor, DnaK, allowed understanding this phenomenon as EfTu and DnaK are apparently exported from the bacterium through a common system before acting as SP and CGRP sensors. Many other neuropeptides are expressed in skin, and their potential effects on skin bacteria remain to be investigated. Integration of these host signals by the cutaneous microbiota now appears as a key parameter in skin homeostasis.

Keywords: skin bacterial communication, substance P, calcitonin gene-related peptide, DnaK chaperone protein, EfTu thermo unstable ribosomal elongation factor, MsCl mechanosensitive channel, moonlighting proteins, microbial endocrinology

INTRODUCTION

Skin is a complex ecosystem hosting the second most numerous microbial population of the human body (1). Skin-associated bacteria, which represent the essential of this population, are classically divided into two categories, i.e., commensal and transient germs. While commensal bacteria are considered having protective functions, transient ones include opportunistic pathogens. However, this reductive vision is far from reality and germs such as *Staphylococcus*

aureus, originally considered as pathogens, are chronically carried by 35–60% of the human population (2). Other bacterial pathogens, such as *Bacillus cereus*, *Pseudomonas aeruginosa* or even *Neisseria meningitidis*, can also be encountered on normal skin in a total absence of clinical signs (3). In fact, virulence is not a constant trait for the large majority of the bacterial species, and expression of virulence is closely controlled by bacterial communication designated under the general term of quorum sensing (QS) (4). The QS is triggered in Gram-negative bacteria by N-acyl homoserine lactones and in Gram-positive bacteria by cyclic or linear peptides. Sensing these molecules can lead pathogenic, but also non-pathogenic, bacteria to switch from harmless to aggressive by regulating the production of most of their virulence factors. However, communication is not solely based on intra- or interspecies bacterial QS, since bacteria also need adapting to their host, thereby sensing numerous eukaryotic signals, including skin neuropeptides. These mechanisms are acknowledged to be part of interkingdom communication.

Skin is the principal neuroendocrine organ of the human body (5), and since 1930 it is known that neurotransmitters such as catecholamines can modulate bacterial infection (6). However, at this time, bacteria were considered inert, and this observation was attributed to an unknown effect of adrenalin on the human physiology. It was necessary to wait for the work of Lyte and Ernst in 1992 to show that catecholamines can promote the growth of *Escherichia coli* (7) and also bacterial adhesion, biofilm formation, and expression of virulence factors (8, 9). Membrane proteins acting as specific bacterial sensors for catecholamines were identified, and it was then recognized that bacteria can sense human neurotransmitters (10). This concept was extended to neuropeptides and neurohormones, giving birth to microbial endocrinology, which is presently one of the more active fields in microbiology (11). Neuroendocrine factors have multiple effects on bacteria and can regulate their growth, adhesion, invasion, virulence, and/or biofilm formation activity (12). As almost 25% of the microbial population is located deeply into the skin, particularly in hair follicles and sweat or sebaceous glands (13), bacteria are in close contact with eukaryotic cells communication factors. Moreover, it has been shown that neuropeptides diffuse in significant amount in upper epidermal layers and sweat (14, 15). Cutaneous bacteria are then exposed largely to these host factors.

EFFECT OF SUBSTANCE P (SP) ON CUTANEOUS BACTERIA

In skin, SP is essentially released by sensory primary afferent C-fibers (16). This undecapeptide of the tachykinin family has multiple bioactivities other than neurotransmission, such as fibroblast and keratinocyte proliferation, mast cell degranulation, and capillary vasodilatation (5, 17). It is considered as a major mediator of neurogenic inflammation and has central functions in itch (5). Cutaneous neuropeptides, and particularly SP, are contributing to the pathogenesis of different skin diseases, including psoriasis (18), atopic dermatitis (19), immediate and delayed hypersensitivity (20), acne (21), or rosacea (22). These

diseases are of multifactorial origin, and different studies suggest a contribution of the skin microflora but also an involvement of local host factors (23).

SP Sensing by *B. cereus*

In a first step, the effect of SP was studied on a strain of *B. cereus* (MFP01) isolated from normal human skin (23). Even at a micromolar concentration, SP was without effect on the growth kinetic of *B. cereus*. SP was also without effect of its swimming and swarming modes of motility. However, when *B. cereus* was grown in the presence of SP, the bacterium showed a strong increase of cytotoxicity on HaCaT keratinocytes (24). The threshold of SP activity was nanomolar and therefore in the range of the local concentration of the neuropeptide in skin during inflammation or stress. Bacteria were rinsed to remove any trace of free peptide prior to cell infection, and all the controls realized showed that this effect can only be explained by a direct effect of SP on the bacterium. Moreover, the SP reversed sequence peptide and neuropeptid A, which in eukaryotes binds on the same receptor as SP, displayed no activity on cutaneous bacteria (24, 25). *B. cereus* is responding to SP by an over production of collagenase that can explain its effect on HaCaT cells (24). However, a massive cell death, as observed after exposure of keratinocytes to SP-treated bacteria, is associated with the release of high amounts of toxic-oxidizing compounds, and *B. cereus* also reacts to SP by an overproduction of superoxide dismutase (24). This can be considered as a defense reaction of the bacterium. When *B. cereus* was exposed to SP over a long period (13 h), an increase in the release of S-layer proteins was also noted (24). This result was correlated to a peel-off of the S-layer (the outer wall of the bacterium) and to a drop in bacterial surface polarity (24). These events can also be interpreted as a general defense reaction of the bacterium against SP as this peptide has structural homologies with cationic antimicrobial peptides, and S-layer monomers are known to complex and neutralize antimicrobial peptides (26). The response of *B. cereus* to SP being rapid (90.5% of the maximal response in less than 5 min) and the S-layer showing multiple pores allowing the passage of peptides (27), an SP surface binding site was postulated. By using an original immunoprecipitation technique, a 43 kDa protein, the thermo unstable ribosomal elongation factor EfTu, was identified as the SP sensor in the membrane of *B. cereus* (24) (**Figure 1A**). EfTu is not presenting sequence or structural similarities with the SP (NK1) receptor (**Figure 1B**). However, it was not surprising that EfTu was acting as a surface receptor on the bacterium because this molecule is present in large excess in bacteria (28), and it is now recognized as a “moonlighting protein” (29). These proteins are characterized by multiple functions in different locations between the bacterial stroma and the membrane. Because of their long evolution and history, bacteria have reached a high level of protein fitting (30); expression of moonlighting proteins should be an alternative strategy to counterbalance the absence of alternative splicing in these organisms.

SP Sensing by *Staphylococci*

Further studies revealed that the ability to detect SP is shared by other Gram-positive bacteria such as *S. aureus* and

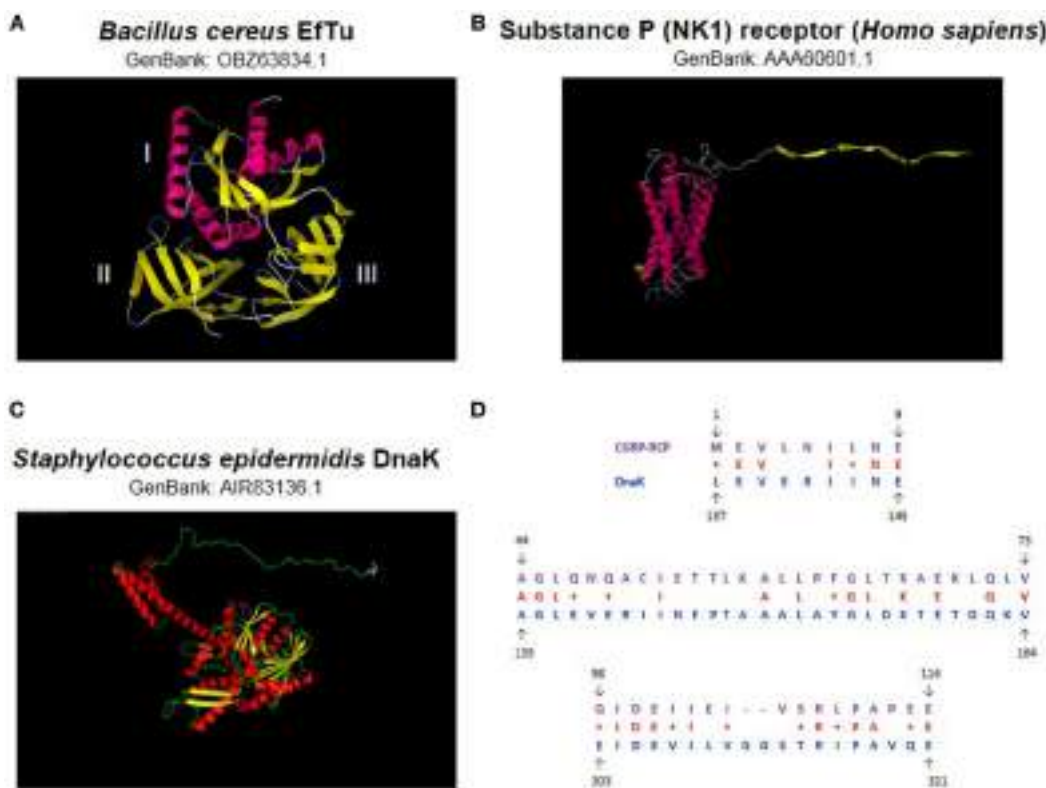


FIGURE 1 | Bacterial substance P (SP) and calcitonin gene-related peptide (CGRP) sensors. The thermo unstable ribosomal elongation factor EfTu identified as SP sensor is a 395 amino acids protein (43 kDa) characterized by three principal domains (**A**). Domain I is essentially organized in alpha helix whereas II and III form beta strands. No signal sequence or transmembrane domain signature is present. EfTu is not showing significant sequence or structural similarities with the NK1 SP human receptor (**B**). The *Staphylococcus epidermidis* chaperone DnaK identified as CGRP sensor is a 609 amino acids protein (70 kDa) (**C**). This protein is showing limited similarity with the human CGRP receptor component protein (CGRP-RCP) but higher similarity with an invertebrate (*Ciona intestinalis*) CGRP-RCP (124 amino acids) where DnaK was found covering 45% of its sequence with 40% identity (**D**). Sequence similarities were investigated by BlastP (<https://blast.ncbi.nlm.nih.gov>). 3D structures were calculated by RaptorX (31) and visualized using Python Molecular Viewer V1.5.6.

Staphylococcus epidermidis. These bacteria react to SP by a marked increase in cytotoxicity and virulence on HaCaT keratinocytes and reconstructed human epithelium (RHE) (25). qRT-PCR arrays revealed that the response of RHE to *S. aureus* and *S. epidermidis* previously exposed to SP is notably different (25). SP-treated *S. aureus* induces an upregulation of CCL5 and CXCL1 chemokines and interleukin 8 expression by RHE suggesting the induction of an inflammatory response. Conversely, SP-treated *S. epidermidis* provoke overexpression of integrin $\alpha 5$ and chemokine ligand 10 CXCL10 (25), two markers of psoriasis (32). Postulating a link between the action of SP on *S. epidermidis* and psoriasis should be a premature conclusion, but this hypothesis is worthy consideration. To get further insights into the role of SP in promoting *S. aureus* and *S. epidermidis* virulence, the effects of the peptide on the adhesion and invasion potential of these bacteria were studied. Exposure of both *Staphylococci* to SP resulted in a marked increase in their adhesion potential on keratinocytes whereas their invasive activities were unchanged (25). Further studies, based on secretome analysis and biofilm formation activities revealed that *S. aureus* and *S. epidermidis* have very

different responses to SP. Indeed, although SP has no effect on the release of exoproteins by *S. epidermidis*, this neuropeptide is stimulating the production of staphylococcal enterotoxin C2 by *S. aureus* (25). In addition, in *S. aureus*, SP induces a decrease in the production of lipase, apparently by inhibiting the processing of its precursor (25). Such a metabolic change should favor lipids' accumulation, and it is well known that a hydrophobic environment is particularly important for the growth of *S. aureus* (33). *Staphylococci* also express the moonlighting protein EfTu and, as in *B. cereus* (24), EfTu was identified as the SP-binding site in *S. aureus* and *S. epidermidis* (25). These results suggest that EfTu should act as an SP sensor in a great variety of Gram-positive bacteria, and potentially also in other eubacteria.

SP Sensing by Gram-negative Bacteria

In agreement with this hypothesis, it was observed that *Pseudomonas fluorescens*, a typical Gram-negative bacterium and member of the commensal skin microflora (1), is also sensitive to SP (34). In this species, the effect of SP is more limited, as no variation of virulence was detected, but SP was found to increase

the adhesion and invasive potentials of the bacterium on HaCaT cells (34). In addition, exposure of *P. fluorescens* to SP is associated with structural rearrangements of the biofilm. Although the SP-binding site was not identified until now in this species, it is interesting to note that, in *Pseudomonas*, EfTu is also known as an environmental sensor (35).

EFFECT OF CALCITONIN GENE-RELATED PEPTIDE (CGRP) ON STAPHYLOCOCCI

Calcitonin gene-related peptide is a neuropeptide abundantly expressed in the skin (9). CGRP is generally co-localized and co-released with SP (36). Two isoforms of this peptide, α -CGRP (or CGRP I) and β -CGRP (or CGRP II), are produced from the same gene by alternative splicing, but α -CGRP is the major form expressed in sensory skin fibers (5). CGRP is known to potentiate the effects of SP on vascular permeability and edema formation. In addition, CGRP exerts trophic effects on endothelial cells and melanocytes. A direct antimicrobial activity of CGRP has been described in *E. coli* and *P. aeruginosa* (37). This effect was explained by structural similarities between CGRP and antimicrobial peptides. However, the antimicrobial spectrum of CGRP is narrow, and this peptide was shown without effect on the viability of *Staphylococci* (37, 38).

Effect of CGRP on *S. epidermidis*

Virulence

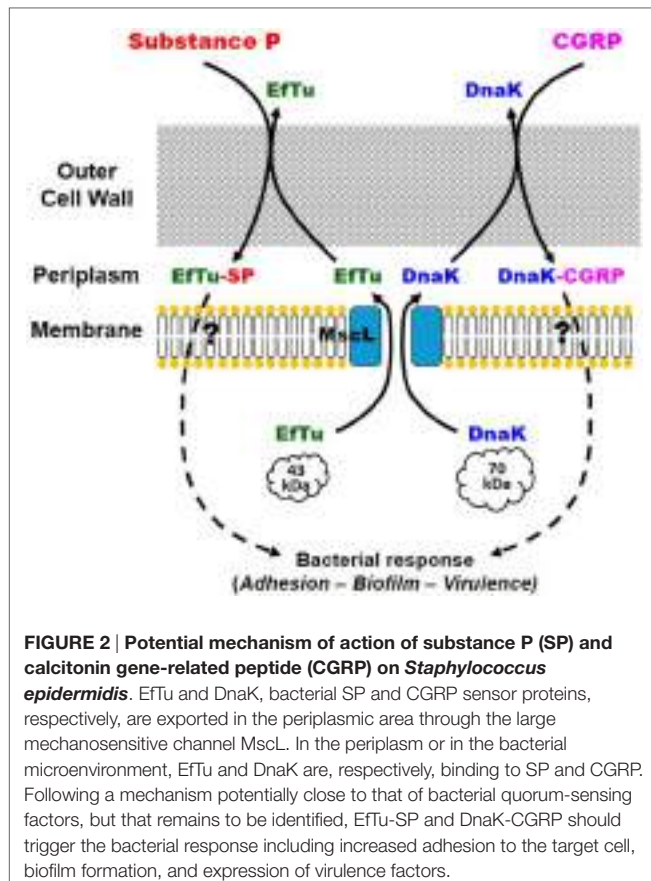
When *S. epidermidis* was exposed to CGRP, an important increase of cytotoxicity and virulence was observed on HaCaT keratinocytes and RHE (38). The threshold of CGRP activity on *S. epidermidis* is remarkably low ($<10^{-12}$ M) suggesting a very specific action. Conversely, no effect of CGRP was found in *S. aureus* (38). As in nerve terminals CGRP is co-secreted with SP, *S. epidermidis* was exposed simultaneously to both neuropeptides, and it was observed that CGRP and SP have antagonistic activities suggesting the existence of a common step in response of the bacterium to these neuropeptides. After exposure to CGRP, *S. epidermidis* is leading to an upregulation of interleukin 8 secretion by keratinocytes and RHE, suggesting that CGRP-treated bacteria are activating an inflammatory response. Then, the normal tolerance of the skin to *S. epidermidis* should be decreased. Because in keratinocytes an inflammatory response is usually associated with the secretion of antimicrobial peptides (39), the production of cathelicidin LL37 and human β defensin 2 (HBD2) by keratinocytes was investigated. However, a limited increase in LL37 secretion and a decrease in HBD2 were observed, suggesting that the effect of CGRP on *S. epidermidis* is not mediated by antimicrobial peptides (38). Analysis of the secretome of CGRP-treated bacteria did not reveal significant variations in the production of known virulence factors. In fact, CGRP appears to modulate the surface properties of *S. epidermidis* as CGRP-treated bacteria showed increased adherence to keratinocytes and reduced internalization and biofilm formation activity. These changes appear to be associated and may be attributed to an increase in surface hydrophobicity (38).

CGRP Sensing in *S. epidermidis*

Investigating the CGRP sensor in *S. epidermidis* was leading to the identification of the chaperone DnaK as a specific CGRP binding protein in this bacterium (38) (Figure 1C). In *Staphylococci*, this protein related to the heat shock protein Hsp70 is known for its multiple functions in environment and stress adaption (40) and was found as a receptor for endothelial cells (41). Moreover, DnaK is showing sequence similarities with the CGRP receptor component protein (CGRP-RCP), a subunit of the eukaryote CGRP receptor that is required for signal transduction (42) (Figure 1D). Altogether these data suggest that DnaK is another member of the moonlighting proteins family. Moreover, a functional relation has been shown between DnaK and EfTu, the SP sensor. Indeed, in *E. coli*, DnaK and EfTu are translocated through the inner membrane by the same large mechanosensitive channel MscL (43). The MscL channels are also expressed in the membrane of *S. epidermidis*, and it was observed that gadolinium chloride, an inhibitor of mechanosensitive channels' activity, was blocking the response of the bacterium to CGRP (38). Complementary studies based on a $\Delta mscL$ mutant confirmed the involvement of MscL in the response of *S. epidermidis* to CGRP (44). These observations were leading to the hypothesis that the export of DnaK and EfTu through MscL is required for the response of the bacterium to CGRP and SP (38). The initial induction of this process remains a major question as the neuropeptides appear acting both as ligands and signals for the export of DnaK and EfTu. However, it was noted that, even in the absence of stimulation, a limited amount of EfTu (and presumably DnaK) is present in the periplasmic area of *S. epidermidis* (38), and this pool of proteins should be sufficient for the initial activation step and induction of the export process. In addition, such ionic channels were first characterized as sensors of membrane mechanical stresses, regulating especially the cell turgor. It could also be conceivable that the interaction of some neuropeptides with the bacterial membrane would lead to cell wall mechanical perturbations, and consequently to the activation of MscL and the export of EfTu and DnaK (Figure 2).

INVOLVEMENT OF OTHER SKIN NEUROPEPTIDES

As mentioned in Section "Introduction," many neuropeptides are produced and released in skin but only a few have been evaluated for their potential effects on cutaneous bacteria. Neuropeptide Y, somatostatin, and even POMC-related peptides have been shown to modulate the growth and virulence of bacteria, but until now, not in the context of skin physiology (12). A particular attention should be given to natriuretic peptides produced locally by endothelial cells that have been studied for their effects on Gram-negative bacteria such as *Pseudomonas*. Indeed, capillary vessels are present in abundance in skin, and especially in a region of the hair follicle, the bulge, at the vicinity of local bacterial populations. Natriuretic peptides, and especially the C type natriuretic peptide (CNP), have been shown to modulate the virulence and adhesion properties of *P. aeruginosa* (45), a common cutaneous opportunistic pathogen, and *P. fluorescens* (46), a member of the



commensal microflora. The CNP bacterial sensor was recently identified in *P. aeruginosa* as another moonlighting protein, the amidase AmiC, an ortholog of natriuretic peptide receptor C (47). In fact, cutaneous bacteria should integrate the signals from a multitude of skin neuropeptides and in response adapt their physiology and virulence. Such local effects are also suspected in the case of a bacterium such as *Propionibacterium acnes* whose

REFERENCES

- Grice EA, Segre JA. The skin microbiome. *Nat Rev Microbiol* (2011) 9(4):244–53. doi:10.1038/nrmicro2537
- Percival SL, Emanuel C, Cutting KF, Williams DW. Microbiology of the skin and the role of biofilms in infection. *Int Wound J* (2012) 9(1):14–32. doi:10.1111/j.1742-481X.2011.00836.x
- Feuilloley MGJ, Doleans-Jordheim A, Freney J. Section III – Chapitre 12: Floremicrobienne de la peau saine. 3ème ed. In: de Riegel P, Favenne L, Paugam A, Pozzetto B, editors. *Précis de Bactériologie Clinique*. Paris: ESKA. (2015). p. 1–15.
- De Kievit TR, Iglewski BH. Bacterial quorum sensing in pathogenic relationships. *Infect Immun* (2000) 68(9):4839–49. doi:10.1128/IAI.68.9.4839-4849.2000
- Roosterman D, Goerge T, Schneider SW, Bunnett NW, Steinhoff M. Neuronal control of skin function: the skin as a neuroimmunoendocrine organ. *Physiol Rev* (2006) 86(4):1309–79. doi:10.1152/physrev.00026.2005
- Renaud M, Miget A. Role favorisant des perturbations locales causes par l'adrénaline sur le développement des infections microbiennes. *CR Soc Biol* (1930) 103:1052–4.
- Lyte M, Ernst S. Catecholamine induced growth of Gram negative bacteria. *Life Sci* (1992) 50(3):203–12. doi:10.1016/0024-3205(92)90273-R
- Lyte M, Freestone PP, Neal CP, Olson BA, Haigh RD, Bayston R, et al. Stimulation of *Staphylococcus epidermidis* growth and biofilm formation by catecholamine inotropes. *Lancet* (2003) 361(9352):130–5. doi:10.1016/S0140-6736(03)12231-3
- Lyte M, Arulanandam BP, Frank CD. Production of Shiga-like toxins by *Escherichia coli* O157:H7 can be influenced by the neuroendocrine hormone norepinephrine. *J Lab Clin Med* (1996) 128(4):392–8. doi:10.1016/S0022-2143(96)80011-4
- Sperandio V, Torres AG, Jarvis B, Nataro JP, Kaper JB. Bacteria-host communication: the language of hormones. *Proc Natl Acad Sci U S A* (2003) 100(15):8951–6. doi:10.1073/pnas.1537100100
- Lyte M. Microbial endocrinology and infectious disease in the 21st century. *Trends Microbiol* (2004) 12(1):14–20. doi:10.1016/j.tim.2003.11.004
- Lesouhaitier O, Veron W, Chapalain A, Madi A, Blier A-S, Dagorn A, et al. Gram-negative bacterial sensors for eukaryotic signal molecules. *Sensors (Basel)* (2009) 9(9):6967–90. doi:10.3390/s90906967
- Lange-Asschenfeldt B, Marenbach D, Lang C, Patzelt A, Ulrich M, Maltusch A, et al. Distribution of bacteria in the epidermal layers and hair

acneic strains are particularly virulent *in situ* but appear without significant virulence when they are grown *in vitro* (48).

CONCLUSION

The physiological meaning of these observations and the reasons for the preservation or emergence of sensor systems for skin neuropeptides in cutaneous bacteria remain hypothetical. However, it appears nowadays that in gut, bacteria use hormones and neurotransmitters as signals for switching from a commensal to a pathogen behavior (49). It is interesting to note that, in skin, SP shows important variations of local concentration under the effect of pain, stress, or infection (15, 50, 51) and even in case of nervous breakdown (14). Then, local changes of SP concentration in skin, and presumably CGRP or other peptides, could trigger an increase in the virulence of cutaneous bacteria. These studies give consistence to the existence of a link between the central nervous system, the cutaneous microbiota, and skin homeostasis. Different products, including a polysaccharide rich in rhamnose and a thermal water of particular ionic composition, were found to be able to antagonize the effects of SP on *B. cereus*, *S. aureus*, and *S. epidermidis* (24). Dermocosmetic products have been developed nowadays on the basis of these observations, which also represent a new strategy for clinical applications in dermatology.

AUTHOR CONTRIBUTIONS

MF wrote the review and designed the figures. MF, OM, and P-JR realized blasts and proteins 3D views. VB, AG, AN, JE, P-JR, VP, SC, and OL revised the manuscript.

FUNDING

LMSM is supported by the Communauté d'Agglomération d'Evreux, Conseil Départemental de l'Eure, Région Normandie, BPI (FUI programs), InterReg Program PeReNe, and UE (FEDER).

- follicles of the human skin. *Skin Pharmacol Physiol* (2011) 24(6):305–11. doi:10.1159/000328728
14. Cizza G, Marques AH, Eskandari F, Christie IC, Torvik S, Silverman MN, et al. Elevated neuroimmune biomarkers in sweat patches and plasma of premenopausal women with major depressive disorder in remission: the POWER study. *Biol Psychiatry* (2008) 64(10):907–11. doi:10.1016/j.biopsych.2008.05.035
 15. Harrison S, Geppetti P. Substance P. *Int J Biochem Cell Biol* (2001) 33(6):555–76. doi:10.1016/S1357-2725(01)00031-0
 16. Severini C, Impronta G, Falconieri-Ersamer G, Salvadori S, Ersamer V. The tachykinin peptide family. *Pharmacol Rev* (2002) 54(2):285–322. doi:10.1124/pr.54.2.285
 17. Peters EM, Ericson ME, Hosoi J, Seiffert K, Hordinsky MK, Ansel JC, et al. Neuropeptide control mechanisms in cutaneous biology: physiological and clinical significance. *J Invest Dermatol* (2006) 126(9):1937–47. doi:10.1038/sj.jid.5700429
 18. Ostrowski SM, Belkadi A, Loyd CM, Diaconu D, Ward NL. Cutaneous denervation of psoriasisform mouse skin improves acanthosis and inflammation in a sensory neuropeptide-dependent manner. *J Invest Dermatol* (2011) 131(7):1530–8. doi:10.1038/jid.2011.60
 19. Misery L. Atopic dermatitis: new trends and perspectives. *Clin Rev Allergy Immunol* (2011) 41(3):296–7. doi:10.1007/s12016-010-8247-6
 20. Wallengren J. Substance P antagonist inhibits immediate and delayed type cutaneous hypersensitivity reactions. *Br J Dermatol* (1991) 124(4):324–8. doi:10.1111/j.1365-2133.1991.tb00591.x
 21. Toyoda M, Morohashi M. Pathogenesis of acne. *Med Electron Microsc* (2001) 34(1):29–40. doi:10.1007/s007950100002
 22. Aubdool AA, Brain SD. Neurovascular aspects of skin neurogenic inflammation. *J Investig Dermatol Symp Proc* (2011) 15(1):33–9. doi:10.1038/jidsymp.2011.8
 23. Hillion M, Mijouin L, Jaouen T, Barreau M, Meunier P, Lefevre L, et al. Comparative study of normal and sensitive skin aerobic bacterial populations. *Microbiolopen* (2013) 2(6):953–61. doi:10.1002/mbo3.138
 24. Mijouin L, Hillion M, Ramdani Y, Jaouen T, Duclairoir-Poc C, Follet-Gueye ML, et al. Effects of a neuropeptide (substance P) on cutaneous microflora. *PLoS One* (2013) 8(11):e78773. doi:10.1371/journal.pone.0078773
 25. N'Diaye A, Mijouin L, Hillion M, Diaz S, Konto-Ghiorghi Y, Percoco G, et al. Effect of substance P in *Staphylococcus aureus* and *Staphylococcus epidermidis* virulence: implication for skin homeostasis. *Front Microbiol* (2016) 7:506. doi:10.3389/fmicb.2016.00506
 26. De la Fuente-Nunez C, Mertens J, Smit J, Hancock REW. Bacterial surface layer protects against antimicrobial peptides. *Appl Environ Microbiol* (2012) 78(15):5452–6. doi:10.1128/AEM.01493-12
 27. Egelseer E, Schocher I, Sára M, Sleytr UB. The S-layer from *Bacillus stearothermophilus* DSM 2358 functions as an adhesion site for a high-molecular-weight amylase. *J Bacteriol* (1995) 177(6):1444–51. doi:10.1128/jb.177.6.1444-1451.1995
 28. Beck BD. Polymerization of the bacterial elongation factor for protein synthesis, EF-Tu. *Eur J Biochem* (1979) 97(2):495–502. doi:10.1111/j.1432-1033.1979.tb13137.x
 29. Amblee V, Jeffery CJ. Physical features of intracellular proteins that moonlight on the cell surface. *PLoS One* (2015) 10(6):e0130575. doi:10.1371/journal.pone.0130575
 30. Sela I, Wolf YI, Koonin EV. Theory of prokaryotic genome evolution. *Proc Natl Acad Sci U S A* (2016) 113(41):11399–407. doi:10.1073/pnas.1614083113
 31. Källberg M, Wang H, Wang S, Peng J, Wang Z, Lu H, et al. Template-based protein structure modeling using the RaptorX web server. *Nat Protoc* (2012) 7(8):1511–22. doi:10.1038/nprot.2012.085
 32. Ferrari SM, Ruffilli I, Colaci M, Antonelli A, Ferri C, Fallahi P. CXCL10 in psoriasis. *Adv Med Sci* (2015) 60:349–54. doi:10.1016/j.admms.2015.07.011
 33. Wright JS, Lyon GJ, George EA, Muir TW, Novick RP. Hydrophobic interactions drive ligand-receptor recognition for activation and inhibition of staphylococcal quorum sensing. *Proc Natl Acad Sci U S A* (2004) 101:16168–73. doi:10.1073/pnas.0404039101
 34. Hillion M, Mijouin L, N'Diaye A, Percoco G, Enault J, Follet-Gueye M-L, et al. *Pseudomonas fluorescens*, a forgotten member of the human cutaneous microbiota sensible to skin communication and defense peptides. *Int J Curr Microbiol Appl Sci* (2014) 3(7):910–25.
 35. Dagorn A, Hillion M, Chapalain A, Lesouhaitier O, Duclairoir-Poc C, Vieillard J, et al. Gamma-aminobutyric acid acts as a specific virulence regulator in *Pseudomonas aeruginosa*. *Microbiology* (2013) 159:339–51. doi:10.1099/mic.0.061267-0
 36. Gibbins IL, Wattchow D, Coventry B. Two immunohistochemically identified populations of calcitonin gene-related peptide (CGRP)-immunoreactive axons in human skin. *Brain Res* (1987) 414(1):143–8. doi:10.1016/0006-8993(87)91335-7
 37. El Karim IA, Linden GJ, Orr DF, Lundy FT. Antimicrobial activity of neuropeptides against a range of micro-organisms from skin, oral, respiratory and gastrointestinal tract sites. *J Neuroimmunol* (2008) 200(1–2):11–6. doi:10.1016/j.jneuroim.2008.05.014
 38. N'Diaye AR, Leclerc C, Kentache T, Hardouin J, Duclairoir Poc C, Konto-Ghiorghi Y, et al. Skin-bacteria communication: involvement of the neurohormone calcitonin gene related peptide (CGRP) in the regulation of *Staphylococcus epidermidis* virulence. *Sci Rep* (2016) 6:35379. doi:10.1038/srep35379
 39. Angrisano T, Pero R, Paoletti I, Keller S, Lembo L, Baroni A, et al. Epigenetic regulation of IL-8 and β-defensin genes in human keratinocytes in response to *Malassezia furfur*. *J Invest Dermatol* (2013) 133(8):2101–4. doi:10.1038/jid.2013.143
 40. Singh VK, Syring M, Singh A, Singhal K, Dalecki A, Johansson T. An insight into the significance of the DnaK heat shock system in *Staphylococcus aureus*. *Int J Med Microbiol* (2012) 302(6):242–52. doi:10.1016/j.ijmm.2012.05.001
 41. Hirschhausen N, Schlesier T, Schmidt MA, Götz F, Peters G, Heilmann C. A novel staphylococcal internalization mechanism involves the major autolysin Atl and heat shock cognate protein Hsc70 as host cell receptor. *Cell Microbiol* (2010) 12(12):1746–64. doi:10.1111/j.1462-5822.2010.01506.x
 42. Evans BN, Rosenblatt MI, Mnayer LO, Oliver KR, Dickerson IM. CGRP-RCP, a novel protein required for signal transduction at calcitonin gene-related peptide and adrenomedullin receptors. *J Biol Chem* (2000) 275(40):31438–43. doi:10.1074/jbc.M005604200
 43. Berrier C, Garrigues A, Richarme G, Ghazi A. Elongation factor Tu and DnaK are transferred from the cytoplasm to the periplasm of *Escherichia coli* during osmotic downshock presumably via the mechanosensitive channel MscL. *J Bacteriol* (2000) 182(1):248–51. doi:10.1128/JB.182.1.248-251.2000
 44. N'Diaye AR. Skin microbial endocrinology: influence of endogenous peptides on the virulence of cutaneous microflora bacteria. PhD Thesis (2016).
 45. Veron W, Lesouhaitier O, Pennanec X, Rehel K, Leroux P, Orange N, et al. Natriuretic peptides affect *Pseudomonas aeruginosa* and specifically modify lipopolysaccharide biosynthesis. *FEBS J* (2007) 274(22):5852–64. doi:10.1111/j.1742-4658.2007.06109.x
 46. Veron W, Orange N, Feuilloley MG, Lesouhaitier O. Natriuretic peptides modify *Pseudomonas fluorescens* cytotoxicity by regulating cyclic nucleotides and modifying LPS structure. *BMC Microbiol* (2008) 8:114. doi:10.1186/1471-2180-8-114
 47. Rosay T, Bazire A, Diaz S, Clamens T, Blier AS, Mijouin L, et al. *Pseudomonas aeruginosa* expresses a functional human natriuretic peptide receptor ortholog: involvement in biofilm formation. *MBio* (2015) 6(4):e1033–1015. doi:10.1128/mBio.01033-15
 48. Ionescu MA, Feuilloley M, Enault J, Saguet T, Robert G, Lefevre L. La modulation du microbiote et du *P. acnes* ribotypes 4 et 5 dans l'acné polymorphe: étude microbiologique et clinique dans une série de 70 adultes acnéiques. *Ann Dermato Venereo* (2015) 142:S434–5. doi:10.1016/j.annder.2015.10.030
 49. Sandrini S, Aldriwesh M, Alruways M, Freestone P. Microbial endocrinology: host-bacteria communication within the gut microbiome. *J Endocrinol* (2015) 225(2):R21–34. doi:10.1530/JOE-14-0615
 50. Nakano Y. Stress-induced modulation of skin immune function: two types of antigen-presenting cells in the epidermis are differentially regulated by chronic stress. *Br J Dermatol* (2004) 151(1):50–64. doi:10.1111/j.1365-2133.2004.05980.x
 51. O'Connor TM, O'Connell J, O'Brien DI, Goode T, Bredin CP, Shanahan F. The role of substance P in inflammatory disease. *J Cell Physiol* (2004) 201(2):167–80. doi:10.1002/jcp.20061

Conflict of Interest Statement: The authors declare that the research was conducted in the absence of any commercial or financial relationships that could be construed as a potential conflict of interest.

The handling Editor declared a shared affiliation, though no other collaboration, with several of the authors AN, AG, VB, JE, P-JR, SC, OL, MF and states that the process nevertheless met the standards of a fair and objective review.

Copyright © 2017 N'Diaye, Gannessen, Borrel, Maillot, Enault, Racine, Plakunov, Chevalier, Lesouhaitier and Feuilloley. This is an open-access article distributed under the terms of the Creative Commons Attribution License (CC BY). The use, distribution or reproduction in other forums is permitted, provided the original author(s) or licensor are credited and that the original publication in this journal is cited, in accordance with accepted academic practice. No use, distribution or reproduction is permitted which does not comply with these terms.



Peptides as Quorum Sensing Molecules: Measurement Techniques and Obtained Levels *In vitro* and *In vivo*

Frederick Verbeke¹, Severine De Craemer¹, Nathan Debuinne¹, Yorick Janssens¹, Evelien Wynendaele¹, Christophe Van de Wiele^{2,3} and Bart De Spiegeleer^{1*}

¹ Drug Quality and Registration Group, Faculty of Pharmaceutical Sciences, Ghent University, Ghent, Belgium, ² Department of Nuclear Medicine, AZ Groeninge, Kortrijk, Belgium, ³ Department of Nuclear Medicine and Radiology, Faculty of Medicine and Health Sciences, Ghent University, Ghent, Belgium

OPEN ACCESS

Edited by:

Hubert Vaudry,
University of Rouen, France

Reviewed by:

Sergueï O. Fetissov,
University of Rouen, France

Gustavo M. Somoza,
Instituto de Investigaciones

Biotecnologicas-Instituto Tecnológico
de Chascomus, Argentina

*Correspondence:

Bart De Spiegeleer
bart.despiegeleer@ugent.be

Specialty section:

This article was submitted to
Neuroendocrine Science,
a section of the journal
Frontiers in Neuroscience

Received: 20 January 2017

Accepted: 20 March 2017

Published: 12 April 2017

Citation:

Verbeke F, De Craemer S, Debuinne N, Janssens Y, Wynendaele E, Van de Wiele C and De Spiegeleer B (2017) Peptides as Quorum Sensing Molecules: Measurement Techniques and Obtained Levels *In vitro* and *In vivo*. *Front. Neurosci.* 11:183.
doi: 10.3389/fnins.2017.00183

The expression of certain bacterial genes is regulated in a cell-density dependent way, a phenomenon called quorum sensing. Both Gram-negative and Gram-positive bacteria use this type of communication, though the signal molecules (auto-inducers) used by them differ between both groups: Gram-negative bacteria use predominantly *N*-acyl homoserine lacton (AHL) molecules (autoinducer-1, AI-1) while Gram-positive bacteria use mainly peptides (autoinducer peptides, AIP or quorum sensing peptides). These quorum sensing molecules are not only involved in the inter-microbial communication, but can also possibly cross-talk directly or indirectly with their host. This review summarizes the currently applied analytical approaches for quorum sensing identification and quantification with additionally summarizing the experimentally found *in vivo* concentrations of these molecules in humans.

Keywords: quorum sensing peptides, analytical methods, reporter bacteria, biosensors, chromatography, microbiome

INTRODUCTION

The idea of bacteria being single isolated organisms has been outdated for many years. In the late 1960s, a cell-density dependent bioluminescence was observed in the marine symbiotic bacterium *Vibrio fisheri* (Nealson et al., 1970; Nealson and Hastings, 1979). This cell-density dependent regulation of gene expression is defined as quorum sensing and consists of at least four steps: (I) synthesis of signal molecules, called autoinducers, (II) excretion of the signal molecules, (III) at a certain threshold concentration, activation of a specific receptor and as a result (IV) activation or suppression of gene expression (Sifri, 2008). For example, with the increase of the number of *Vibrio fisheri* bacteria, the amount of autoinducer in the external environment reaches a certain level and triggers the production of the enzyme luciferase resulting in bioluminescence (Engebrect and Silverman, 1984). The genes involved in quorum sensing, are responsible for activities that are only of use when performed by a large number of cells, for example: bioluminescence, antibiotic production, formation of biofilms, and production of virulence factors (Rutherford and Bassler, 2012).

Both Gram-negative and Gram-positive bacteria apply quorum sensing for communication, but they produce different auto-inducers. Gram-negative bacteria mainly depend on *N*-acyl homoserine lacton (AHL) molecules (autoinducer-1, AI-1) while Gram-positive bacteria use

modified oligopeptides (autoinducer peptides, AIP) (Taga and Bassler, 2003). These peptides possess a large structural diversity and frequently undergo post-translational modifications (Sturme et al., 2002). A third type of autoinducers are boron-furan-derived signal molecules (autoinducer-2, AI-2) and are produced and detected by both Gram-negative and Gram-positive bacteria (Li and Nair, 2012). Besides these 3 main groups, there is also a fourth group of miscellaneous quorum sensing molecules (Barber et al., 1997; Flavier et al., 1997; Holden et al., 1999; Pesci et al., 1999; Higgins et al., 2007; Wei et al., 2011).

In this review, the focus will be on the production of quorum sensing molecules belonging to the first three groups, i.e., AHL molecules, AI-2 molecules and quorum sensing peptides.

The quorum sensing mechanism of Gram-negative bacteria can be described using the example of *Vibrio fisheri*: an intracellular autoinducer synthase (LuxI) synthesizes AHL signal molecules by catalyzing a reaction between S-adenosylmethionine and an acyl carrier protein (Sifri, 2008; Rutherford and Bassler, 2012). Due to the small size and lipophilicity of AHL autoinducers, they readily pass the cell membrane by means of passive diffusion (Sifri, 2008). If the concentration of AHL is sufficiently high, the AHL autoinducer binds to the intracellular LuxR protein and provokes the LuxR DNA binding domain to reveal. Subsequently, the LuxR protein binds to DNA, causing activation of target gene transcription (Figure 1 left panel, Rutherford and Bassler, 2012). More than 100 Gram-negative bacterial species apply a LuxI/LuxR-type system with an autoinducer synthase (e.g., LuxI) and a transcriptional regulator (e.g., LuxR, Sifri, 2008).

Gram-positive bacteria apply peptides as autoinducers for quorum sensing (Figure 1 right panel). Examples of this heterogeneous group of peptides are given in Figure 2. These peptides are synthesized by ribosomes as precursor peptides and undergo posttranslational modifications during excretion to become activated and stabilized (Sturme et al., 2002). In general, the secretion of the AIP is facilitated by a membrane associated ATP-binding cassette (ABC) transporter (Sturme et al., 2002). As the population density increases, the AIPs accumulate in the environment. When a certain threshold level is reached, binding of an AIP to a receptor initiates activation of the receptor kinase by phosphorylation on a conserved histidine residue (Bassler, 1999; Sturme et al., 2002). Subsequently, the activated receptor kinase transfers the phosphoryl group to a conserved aspartate residue of the intracellular response regulator, which in turn will be activated (Bassler, 1999). The activated response regulator influences the transcription of target genes, including the AIP genes, genes for the receptor kinase and response regulator and genes for the ABC transporter. Based on the species, the nomenclature of the quorum sensing mechanisms can be different, due to the involved genes and receptor(s). For example, *Staphylococci* species employ the *agr*-quorum sensing system, *Streptococci* species employ the *ComX*-quorum sensing system and *Bacilli* species use the *Rap*-quorum sensing system.

The current mainstream opinion is that the AIPs only serve as inter-microbial communication molecules, but other biological actions are known and being explored as well, for example the lantibiotic nisin peptide of *Lactococcus lactis*, also has known

antimicrobial properties (Sturme et al., 2002). The influence of quorum sensing peptides on human tumor progression has recently also been investigated (De Spiegeleer et al., 2015; Wynendaele et al., 2015a).

Quorum sensing molecules do not only serve as intra-species communication molecules. It has been demonstrated that certain AHLs are secreted and recognized by several species of Gram-negative bacteria, hereby potentially acting as “cross-talk” signals (interspecies communication). Another indication is the presence of AI-2 in both Gram-positive and Gram-negative bacteria. Co-culture systems of *V. harveyi* and *E. coli* have indicated that AI-2 production by one species affects gene expression in the other (McNab and Lamont, 2003; Ryan and Dow, 2008; Pereira et al., 2013). For example, cell culture supernatant of *P. aeruginosa* is capable of mediating cell death of *E. coli* via a quorum sensing mediated process (Kumar et al., 2013).

INTER-KINGDOM COMMUNICATION

Inter-kingdom communication, due to co-evolution, between bacteria and eukaryotes is readily known (Lyte and Ernst, 1993). The knowledge of the inter-kingdom communication between bacteria and the human host has extended remarkably during recent years [reviewed in references Hughes and Sperandio, 2008; Karavolos et al., 2013; Clarke et al., 2014; O’Mahony et al., 2015; Kendall and Sperandio, 2016; Moos et al., 2016; Oleskin et al., 2016; Stilling et al., 2016]. For example, to modulate the expression of virulence factors, bacteria have shown the remarkable capacity to monitor neuroendocrine hormones produced by the host, e.g., adrenaline and noradrenaline (Lyte, 1993, 2004; Lyte and Ernst, 1993; Sperandio et al., 2003; Freestone et al., 2008; Karavolos et al., 2008, 2011; Pacheco and Sperandio, 2009; Spencer et al., 2010; Lyte et al., 2011). For example, Enterohaemorrhagic *E. coli* (EHEC) is able to modify its mobility and virulence expression in relationship to adrenaline and noradrenaline concentration (Rasko et al., 2008; Pacheco and Sperandio, 2009). Moreover, the mouse gut microbiome itself is capable of producing catecholamines, thus possessing the ability to interact with the host (Asano et al., 2012). The neurotransmitter γ -aminobutyric acid (GABA) produced by various *Lactobacilli* plays an important role in our brains (Barrett et al., 2012; Clarke et al., 2014). Another important group of messenger molecules in the gut-brain communication are the bacterial short chain fatty acids, fermentation products of bacterial metabolism as these molecules are capable of triggering peptide YY release (Holzer et al., 2012). Bacteria are also capable of sensing a variety of human peptide hormones, e.g., somatostatin (Yamashita et al., 1998) and gastrin (Chowers et al., 1999). Both bacteria and humans apply cyclic dipeptides for communication purposes and hence these molecules might be of extreme interest for the gut-brain communication axis [opinionated in reference (Belleza et al., 2014)]. It has also been demonstrated that some quorum sensing peptides are capable to penetrate the blood-brain barrier in a mouse model, without significant subsequent efflux from the brain (Wynendaele et al.,

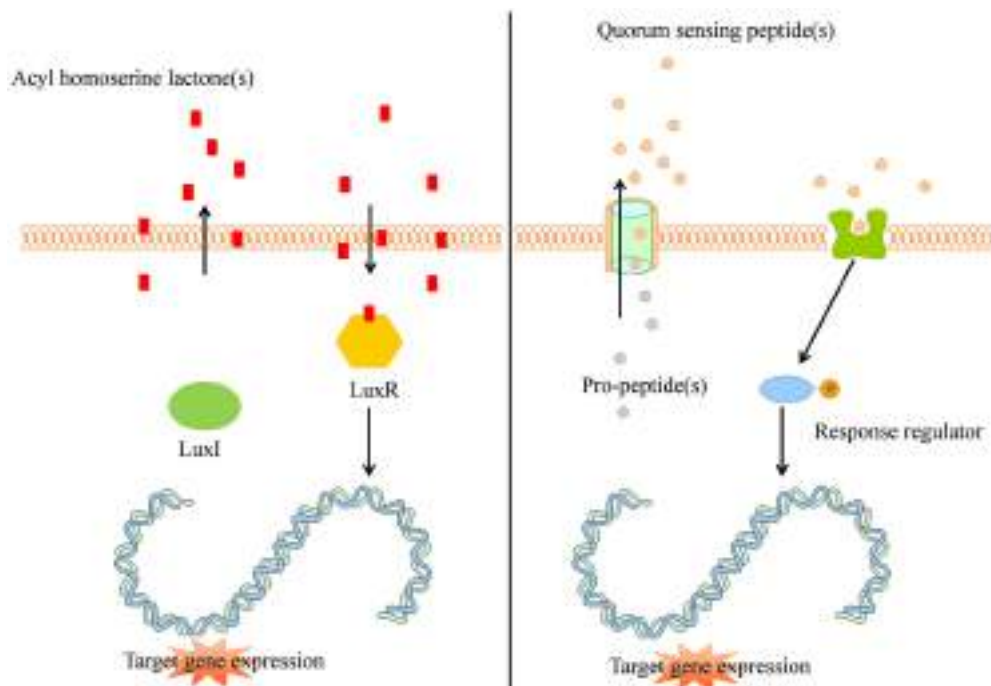


FIGURE 1 | (Left panel) Typical Gram-negative quorum sensing mechanism. Acyl homoserine lactone molecules, synthesized by LuxI, passively pass the bacterial cell membrane and when a sufficient concentration is reached (threshold level) activate the intracellular LuxR which subsequently activates target gene expression in a coordinated way. **(Right panel)** Quorum sensing peptides are synthesized by the bacterial ribosomes as pro-peptidic proteins and undergo posttranslational modifications during excretion by active transport. The quorum sensing peptides bind membrane associated receptors which get autophosphorylated and activate intracellular response regulators via phosphor-transfer. These phosphorylated response regulators induce increased target gene expression.

2015b). The Gram-negative quorum sensing molecules, i.e., N-acylhomoserinelactones (AHLs), easily pass eukaryotic cell membranes, due to their lipophilic nature (Fuqua et al., 1994).

Immunomodulation by odHL (*N*-3-oxo-dodecanoyl-L-homoserine lactone) has been reported (Pritchard, 2006a; Teplitski et al., 2011) and occurs in a TLR4-independent manner (Kravchenko et al., 2006). The activity of macrophages (Gomi et al., 2006; Kravchenko et al., 2006, 2008; Miyairi et al., 2006; Thomas et al., 2006), epithelial cells (Kravchenko et al., 2006, 2008; Jahoor et al., 2008; Cooley et al., 2010), mast cells (Li et al., 2009), fibroblasts (Kravchenko et al., 2006, 2008; Miyairi et al., 2006; Jahoor et al., 2008), T-lymphocytes (Wagner et al., 2007), B-lymphocytes (Telford et al., 1998a), and neutrophils (Zimmermann et al., 2006) is influenced by odHL. The outcome of the immunomodulatory properties of odHL are not straightforward, as some studies suggest a proinflammatory response (Smith et al., 2001, 2002a,b; Vikström et al., 2005; Thomas et al., 2006; Jahoor et al., 2008; Mayer et al., 2011), whereas others point out an anti-inflammatory effect (Telford et al., 1998a; Chhabra et al., 2003; Hooi et al., 2004; Kravchenko et al., 2008; Skinderoe et al., 2009), thus facilitating persistent infection. As a rationale to elucidate this apparent discrepancy, a concentration-dependent effect has been proposed (Teplitski et al., 2011; Pritchard, 2006a). Besides odHL, *P. aeruginosa* also produces an aromatic quorum sensing molecule, i.e., 2-amino-acetophenon. This molecule contributes to the establishment of a chronic

infection by damping the inflammatory immune response (Bandyopadhyaya et al., 2012). A third quorum sensing molecule from *P. aeruginosa*, 2-heptyl-3-hydroxy-4(1H)-quinolone, has shown to inhibit T cell proliferation (Pritchard, 2006b), possibly via the IL-2 receptor pathway (Hooi et al., 2004). As a direct effect of its immunomodulating properties, odHL evokes IL-8 production on fibroblasts and bronchial epithelial cells, resulting in an accelerated apoptosis by mammalian macrophages and neutrophils (DiMango et al., 1995; Smith et al., 2002a; Tateda et al., 2003). Growth of human colorectal and prostate cancer cells is inhibited by odHL and analogs (Dolnick et al., 2005; Oliver et al., 2009), whereas down-modulation of STAT3 by odHL induces apoptosis in breast carcinoma cells (Li et al., 2004). Additionally, quorum sensing molecules produced by the Gram-negative *P. aeruginosa* in nosocomial urinary tract infection (UTI) might also be accountable for renal damage. As an opportunistic pathogen, *P. aeruginosa* especially affects immunocompromised patients and treatment is further hindered by its ability to form biofilms on urinary catheters (Gupta et al., 2013). Immunomodulation by these quorum sensing molecules can also have implications via the neuroendocrine-immune system axis, which is frequently involved in various diseases (Procaccini et al., 2014).

The clinical significance of the microbiome-host relationship is becoming increasingly apparent. Differences between the microbiome of healthy individuals and cancer patients have

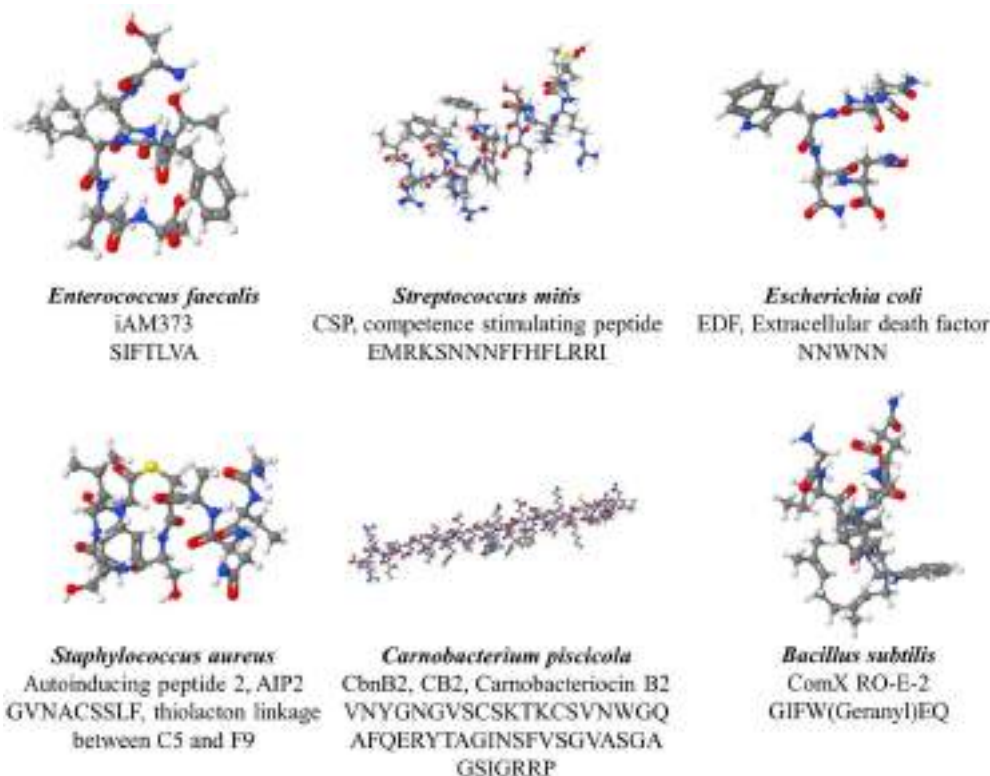


FIGURE 2 | Various quorum sensing peptides, illustrating the structural diversity observed among quorum sensing peptide.

been related to susceptibility to cancer (Bultman, 2014), e.g., an increase in fecal *E. coli* has been associated with development of colon cancer (Wynendaele et al., 2015a). Strong indications have been found that changes in the microbiome are not only associated with tumorigenesis, but also directly contribute to tumorigenesis (Zackular et al., 2013; Baxter et al., 2014). The microbiome has been shown to alter the tumor-environment by influencing the host's neuroendocrine system (Erdman and Poutahidis, 2014). *Helicobacter pylori* is, besides causing gastroduodenal ulcers, accountable for the majority of stomach cancers (Ernst and Gold, 2000). Moreover, the association between inflammatory bowel diseases, e.g., chronic ulcerative colitis and Crohn's disease, and colon carcinoma is widely accepted (Balkwill and Mantovani, 2001). The microbiome is relevantly involved in alterations of the human immune system and host's metabolism (Thaiss et al., 2016). Quorum sensing molecules also affect human health via quorum sensing mediated biofilms (Kalia, 2013) which are associated with a wide array of infections (Beloin et al., 2014). These infections contribute to an increase in morbidity, mortality, and public costs (Haas et al., 2014). Alterations in the human microbiome have also been linked to several central nervous disorders, e.g., autism (Finegold et al., 2010; Tomova et al., 2015), depression (Naseribafrouei et al., 2014; Jiang et al., 2015), and schizophrenia (Castro-Nallar et al., 2015). The gut microbiome is likely associated with various conditions via the gut-brain axis, e.g., anxiety and altered neurochemistry (Cryan and O'Mahony, 2011).

and increasing evidence points toward the influence of the microbiome in neuroendocrine diseases, e.g., as a mediator in diabetes mellitus via the cholinergic nervous system (Parekh et al., 2016). Additionally, aging has also been linked to alterations of the gut microbiome, which are, among others, related to immunosenescence and immune aging (De Spiegeleer et al., 2016; Mello et al., 2016).

ANALYTICAL TECHNIQUES

A variety of analytical techniques have been reported in literature for the qualitative and quantitative analysis of quorum sensing molecules. Generally, these techniques can be considered as chromatographic/mass spectroscopic techniques or based on biosensor systems using (genetically modified) reporter bacteria and will be discussed in more detail in the following sections regarding the detection and quantification of quorum sensing molecules in human biological samples and bacterial cell culture broths.

Biosensor Systems Using Reporter Bacteria

In these systems, the presence of a compound of interest is qualitatively and/or quantitatively detected based on a signal produced by the bacterial reporter. The produced signal can be colorimetric, fluorimetric, bioluminescent, chemiluminescent,

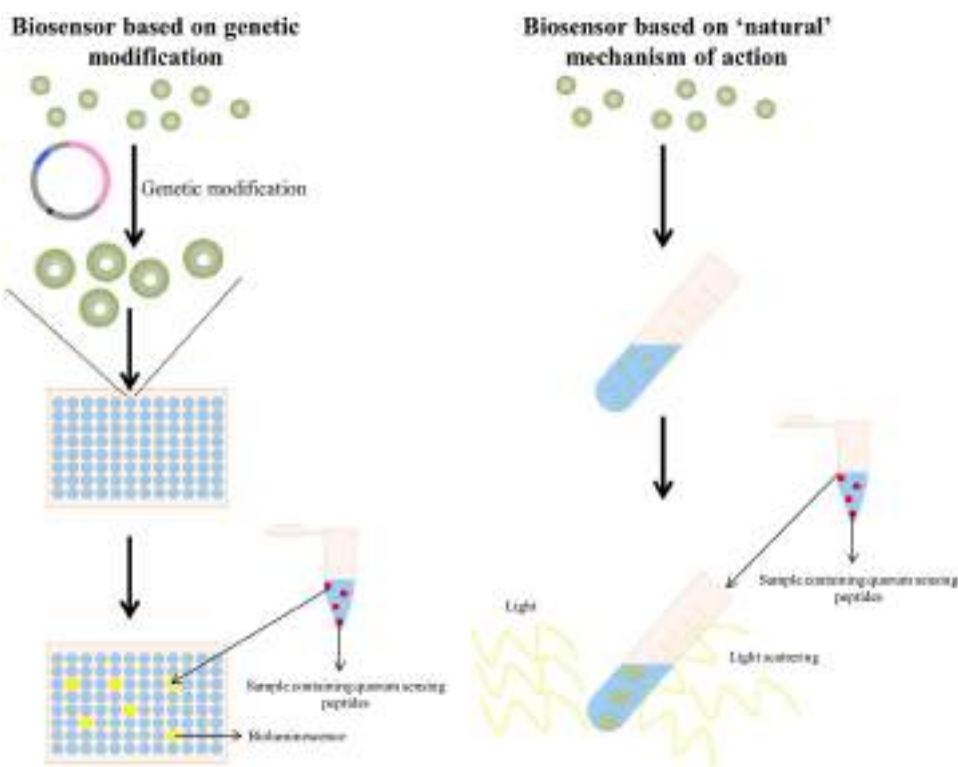


FIGURE 3 | (Left panel) A quorum sensing reporter strain based on genetic modification: bacteria are genetically modified to make them competent to detect the specific quorum sensing peptide. Upon addition of a sample containing the quorum sensing peptide, the activated quorum sensing peptide receptor triggers in this example bioluminescence, allowing detection and quantification of the quorum sensing peptide (La Rosa et al., 2015). **(Right panel)** A quorum sensing reporter strain based on the naturally observed quorum sensing mechanism of a quorum sensing peptide (in this example the clumping induction assay as observed with various *E. faecalis* quorum sensing peptides Suzuki et al., 1984; Mori et al., 1988; Nakayama et al., 1995a). A sample containing the quorum sensing peptide is added to a bacterial strain capable of detecting the quorum sensing peptide and the formation of clumps is observed via light scattering.

turbidimetric, colony forming units to name a few (van der Meer and Belkin, 2010).

Regarding quorum sensing bacterial reporters, two approaches are currently being used, i.e. (I) those based on the “natural” provoked effect by the specific quorum sensing peptide and (II) by applying genetically modified bacteria acting as detecting strains (Figure 3). The clumping assay (Suzuki et al., 1984; Mori et al., 1988; Nakayama et al., 1995a) can be considered as a system based on the “natural” provoked effects of some quorum sensing peptides: the bacteria applied as reporter strain are wild-type bacteria and have not been genetically altered to obtain receptiveness toward the specific quorum sensing peptide(s). When certain enterococcal quorum sensing peptides are added to receptive *Enterococci*, these quorum sensing peptides provoke clumping of the *Enterococci*. Consecutively, the turbidity of the bacterial suspension enhances and provides a quantifiable result via turbidimetry. The second type of bacterial reporters consists of bacteria that have been genetically modified to produce a signal in the presence of the quorum sensing molecule of interest; this type of reporter bacteria is more elaborately explained in the following sections.

Acyl Homoserine Lactones

Detection of quorum sensing molecules is often performed by using quorum sensing reporter bacteria strains, of which most are sensitive to either autoinducer-1 (AHLs) or autoinducer-2 (Steindler and Venturi, 2007; Rai et al., 2015). As mentioned previously, these bacterial reporters can be based on non-genetically modified or genetically-modified bacteria.

Genetic modifications consist of altering the bacterial genome, in order to obtain a detectable signal in the presence of the quorum sensing molecule of interest. This genetic modification consists of coupling a suitable promoter to a desired reporter gene, and hence the desired detection signal. The detection signal is produced by a reporter protein, e.g., bioluminescence, chemiluminescence, fluorescence, colorimetric response, etc. Production of the reporter protein depends on activation of the promoter, which initiates transcription of the reporter gene.

Inherent to genetic modifications of the bacteria, is the need of selecting those bacteria that are successfully genetically modified [e.g., those bacterial cells that have acquired the plasmid(s)]. Selecting these correctly, genetically modified bacteria can be performed by for example antibiotic resistance genes (O’Connor et al., 2016).

TABLE 1 | Overview of some plasmid-based AHL reporter strains (Steindler and Venturi, 2007; Rai et al., 2015; O'Connor et al., 2016).

Plasmid	Bacterial strain	Analyte	Promoter	Reporter
pSB401	<i>E. coli</i>	3-oxo-C4- to 3-oxo-C14-HSL C4- to C12-HSL	<i>luxI</i>	<i>luxCDABE</i>
pSB1075	<i>E. coli</i>	3-oxo-C12- to 3-oxo-C16-HSL C12- to C16-HSL	<i>lasI</i>	<i>luxCDABE</i>
pECP61.5	<i>P. aeruginosa</i>	C4-HSL	<i>rhlA</i>	<i>lacZ</i>
pKDT17	<i>E. coli</i>	3-oxo-C10- to 3-oxo-C12-HSL C10- to C12-HSL	<i>lasB</i>	<i>lacZ</i>
pCF218, pMV26	<i>A. tumefaciens</i>	3-oxo-C6- to 3-oxo-C12-HSL C4- to C12-HSL	<i>tral</i>	<i>luxCDABE</i>
pCF218, pCF372	<i>A. tumefaciens</i>	3-oxo-C4- to 3-oxo-C12-HSL C5- to C10-HSL	<i>tral</i>	<i>lacZ</i>
pSB406	<i>E. coli</i>	3-oxo-C4- to 3-oxo-C14-HSL C4- to C12-HSL	<i>rhlI</i>	<i>luxCDABE</i>
	<i>C. violaceum</i>	3-oxo-C6- to 3-oxo-C8-HSL C4- to C8-HSL	<i>cviI</i>	Violacein
pAL105	<i>E. coli</i>	3-oxo-C12-HSL	<i>lasI</i>	<i>luxCDABE</i>
pAL101	<i>E. coli</i>	C4-HSL	<i>rhlI</i>	<i>luxCDABE</i>
pSB536	<i>E. coli</i>	C4-HSL	<i>ahyl</i>	<i>luxCDABE</i>
pSB403	Broad host range	3-oxo-C4- to 3-oxo-C14-HSL C4- to C12-HSL	<i>luxI</i>	<i>luxCDABE</i>
pHV2001	<i>E. coli</i>	3-oxo-C6- to 3-oxo-C8-HSL C6- to C8-HSL	<i>luxI</i>	<i>luxCDABE</i>
pZLR4	<i>A. tumefaciens</i>	All 3-oxo-HSLs C6- to C14-HSL 3-OH-C6- to 3-OH-C10-HSL	<i>tral</i>	<i>lacZ</i>
pJZ384, pJZ410, pJZ372	<i>A. tumefaciens</i>	3-oxo-C4- to 3-oxo-C18-HSL C4- to C18-HSL	<i>tral</i>	<i>lacZ</i>
pSF105, pSF107	<i>P. fluorescens</i>	3-OH-C6-HSL C6-HSL 3-OH-C8-HSL	<i>phzI</i>	<i>lacZ</i>
pUCP18	<i>P. aeruginosa</i>	3-oxo-C12-HSL	<i>rsaL</i>	<i>luxCDABE</i>
pMS402	<i>P. aeruginosa</i>	3-oxo-C12-HSL	<i>rsaL</i>	<i>luxCDABE</i>
pUCGMAT1-4	<i>E. coli</i>	3-oxo-C6-HSL	<i>ahII</i>	<i>mcherry</i>
pREC-FF	<i>E. coli</i>	3-oxo-C6-HSL	<i>luxI</i>	<i>cfp</i>
M71LZ	<i>P. aeruginosa lasI</i> –	3-oxo-C10 to 3-oxo-C12-HSL	<i>lasI</i>	<i>lacZ</i>
pAS-C8	Broad host range	C8- to C10-HSL	<i>cepl</i>	<i>gfp</i>
pKR-C12	Broad host range	3-oxo-C10- to 3-oxo-C12-HSL	<i>lasI</i>	<i>gfp</i>
pJBA-132	Broad host range	3-oxo-C6-HSL C6- to C10-HSL	<i>luxI</i>	<i>gfp</i>

Table 1 provides an overview of plasmid-based AHL reporter bacteria.

Autoinducer-2

The *Vibrio harveyi* BB170 bioluminescence assay is an example of a reporter bacteria constructed by modifications of the bacterial genome to prevent production of and/or response to certain quorum sensing molecules. It is a frequently used reporter strain for quantification of autoinducer-2 molecules. Genetic modifications of the BB170 strain ensure it does not produce endogenous autoinducer-1 (AHL's) or autoinducer-2 and is insensitive for autoinducer-1. Hence, bioluminescence only occurs when autoinducer-2 is added, where the light intensity correlates with the amount of autoinducer-2 that is added (O'Connor et al., 2016).

Quorum Sensing Peptides

A variety of approaches are applied to proof the presence of, and in rare cases, eventually identify quorum sensing peptides (see **Table 2**). Currently, ~300 quorum sensing peptides and structural analogs have been published (Wynendaele et al., 2013). The majority of these peptides have been tested by the researchers on a system considered a reporter bacteria based biosensor system. While peptide structure elucidation was frequently performed by liquid chromatography-mass spectroscopy and/or Edman degradation. Analogs of the cognate quorum sensing peptides are also frequently evaluated using a specific biosensor.

For example, two reporter strains in *S. mutans* GS5, capable of detecting the competence stimulating peptide (21-CSP) UA159sp4 have been described. The CSP-mediated quorum sensing system of *S. mutans* involves the genes *comCDE*, *comAB*, and *comX*. In brief, the CSP precursor, encoded by *comC*, is cleaved and exported to form CSP by an ABC-transporter encoded by *comAB*. Additionally, the *comDE* gene encodes a two-component signal transduction system that recognizes CSP and initiates a response. *ComX* encodes a sigma factor that regulates transcription of several genes needed for uptake of foreign DNA and the ComE protein is activated by autophosphorylation upon binding of CSP with the ComD histidine kinase receptor. Phosphorylated ComE activates target genes such as *comCDE*, *comAB*, and *comX*, thereby generating a positive feedback quorum sensing system (Svytski et al., 2007). The reporter strain is composed of a *comC* mutant *S. mutans* GS5, resulting in a mutant strain which is unable to produce CSP itself, but still able to respond to exogenous CSP, named SMdC. Mutation of the *comC* gene is obtained by inserting a spectinomycin (*Specr*) resistance gene in the *comC* gene of *S. mutans* GS5. This mutant was used to develop two *lacZ* transcriptional reporter strains in which the *lacZ* gene is fused to the *comDE* promoter or the *nlmAB* promoter. To generate the first reporter strain, a vector pYH2 was formed by fusion of the *comDE* promoter with a promoterless *lacZ* gene in the *Streptococcus-Escherichia coli* shuttle vector pSL; subsequently, pYH2 was transformed into SMdC, resulting in the SMdC-pYH2 reporter strain. The

TABLE 2 | Summary of quorum sensing peptide bio-sensor detection systems.

Quorum sensing molecule (amino acid sequence)	Species	LOD	Operational principle
21-CSP (SGSLSTFFRLFNRSFTQALGK)	<i>S. mutans</i>	Not specified	β -galactosidase assay, Bacteriocin production, Transformation assay (Syvitski et al., 2007; Tian et al., 2009)
Gelatinase Biosynthesis-Activating Pheromone (QNSPNIFGQWM, lacton linkage between S3 and M11)	<i>E. faecalis</i>	Not specified	Bioluminescence (La Rosa et al., 2015)
EntF (AGTKPQGKPASNVLFCVFSFKKCN)	<i>E. faecium</i>	10 aM	Bacteriocin induction (Dunny et al., 1979)
cAM373 (AIFILAS)	<i>E. faecalis</i>	50 pM	Microtiter dilution method (Mori et al., 1986a)
cAD1 (LFSLVLAG)	<i>E. faecalis</i>	50 pM	Microtiter dilution method (Mori et al., 1984)
cCF10 (LVTLVFV)	<i>E. faecalis</i>	25 pM	Clumping induction assay (Mori et al., 1988)
cPD1 (FLVMFLSG)	<i>E. faecalis</i>	40 pM	Clumping induction assay (Suzuki et al., 1984)
cOB1 (VAVLVLGA)	<i>E. faecalis</i>	Not specified	Clumping induction assay (Nakayama et al., 1995a)
iPD1 (ALILTLVS)	<i>E. faecalis</i>	Not specified	Microtiter dilution method (Mori et al., 1987)
iAD1 (LFVVTLVG)	<i>E. faecalis</i>	Not specified	Microtiter dilution method (Mori et al., 1986b)
iAM373 (SIFTLVA)	<i>E. faecalis</i>	200 pM	Clumping induction assay (Nakayama et al., 1995b)
iCF10 (AITLIFI)	<i>E. faecalis</i>	10 nM	Inhibition of induced self-clumping (Nakayama et al., 1994)
CSP (DSRIRRMGFDFSKLFGK)	<i>S. constellatus</i> , <i>S. anginosus</i> , <i>S. thermophilus</i>	0.2 nM	Biofilm formation assay (Petersen et al., 2004)
CSP (DRRDPRGIIGIGKKLFG)	<i>S. milleri</i>	200 ng/ml \approx 105 nM	Transformation assay (Håvarstein et al., 1997)
CSP (SQKGVYASQRSPVPSWFRKIFRN)	<i>S. gordonii</i>	200 ng/ml \approx 72 nM	Transformation assay (Håvarstein et al., 1997)
CSP (EMRISRIILDFLFLRKK)	<i>S. pneumoniae</i>	100 ng/ml \approx 46 nM	Transformation assay (Pozzi et al., 1996)
CSP (EMRLSKFFRDFILQRKK)	<i>S. pneumoniae</i>	100 ng/ml \approx 45 nM	Transformation assay (Pozzi et al., 1996)
EDF (NNWNIN)	<i>E. coli</i>	<100 ng/ml \approx 150 nM	Colony forming units assay (Kolodkin-Gal et al., 2007)

second reporter strain is constructed by fusion of the *nlmAB* promoter with a promoter-lacking *lacZ* gene and transformation of this pOMZ47 plasmid into SMdC, resulting in the SMdC-PnlmAB reporter strain (Steindler and Venturi, 2007). Following addition of exogenous CSP (UA159sp), due to transcription of the *lacZ* gene, both SMdC-pYH2 and SMdC-PnlmAB express β -galactosidase (Syvitski et al., 2007; Tian et al., 2009). Cleavage of O-nitrophenyl- β -D-galactoside by β -galactosidase renders O-nitrophenol, with the yellow color proportional to the enzyme activity and hence the quorum sensing peptide concentration (Syvitski et al., 2007).

The ability of CSP (0.2–100 nM) to induce competence in *S. intermedius* NCTC 11324 was tested: overnight cells of *S. intermedius* NCTC 11324 were diluted 1:200 and subsequently, quorum sensing peptide and a plasmid expressing erythromycin resistance genes were added. After incubation for 24 h, transformants were selected by growth on THB agar plates containing erythromycin. The amount of transformants/mL

increased when increasing concentrations of CSP were added (Wynendaele et al., 2015a). Comparable transformation assays were performed by Håvarstein et al. (1997) with two other synthetic CSPs from *Streptococcus milleri* and from *Streptococcus gordonii* (Håvarstein et al., 1997) and by Pozzi et al. (1996).

The reporter strain for the Gram-negative *E. coli* quorum sensing peptide “extracellular death factor” (EDF) was described by Kolodkin-Gal et al. (2007). They studied the influence of the quorum sensing peptide on mazEF-mediated cell death in *E. coli*. The mazEF module encodes the stable toxin MazF, which exerts its toxic effects by cleavage of single-stranded mRNA at ACA sequences, and the labile antitoxin MazE, which counteracts the effect of MazF. The mazEF module is induced by stress. Stressful conditions that prevent transcription/translation of mazEF, such as inhibition of transcription and/or translation by antibiotics (e.g., rifampicin, chloramphenicol, spectinomycin) or DNA damage, reduces the level of the labile MazE, hereby reducing the counteracting effect on MazF. However, mazEF-mediated

cell death only occurs in dense cultures since it requires the quorum sensing peptide EDF. Addition of rifampicin provokes mazEF-mediated cell death in dense cultures, but not in diluted cultures. The mazEF-mediated cell death in these diluted cultures could be restored by addition of supernatant of a dense culture. The bioassay for detection and quantification of EDF activity is based on this principle. Different dilutions of the supernatant of a dense culture of the *E. coli* strain MC4100relA+, containing EDF, were added to a diluted culture of MC4100relA+, after which stressful conditions (e.g., addition of chloramphenicol) were induced. The percentage of surviving colony forming units (CFUs) was determined after overnight incubation (Kolodkin-Gal et al., 2007).

Quorum sensing peptides can also be detected quantitatively (limit of detection 10 aM) by demonstrating a product of which formation is regulated by a quorum sensing peptide. Nilsen et al. (1998) studied the production of the bacteriocins enterocin A and enterocin B in *Enterococcus faecium* CTC492, regulated by the quorum sensing peptide EntF. Without EntF, a non-bacteriocin-producing culture (Bac-) of *Enterococcus faecium* CTC492 was obtained. Upon addition of induction factor EntF, production of enterocin A and enterocin B is induced and after 20–24 h incubation, bacteriocin activity is assayed by addition of sterilized supernatant to a culture of an indicator organism, e.g., *Lactobacillus sakei* NCDO 2714 (sensitive to both enterocin A and enterocin B), *Pediococcus pentosaceus* FBB 63 (sensitive to enterocin A) or *Lactobacillus sakei* FVM 148 (sensitive to enterocin B). Growth inhibition of these strains indicates presence of bacteriocins in the supernatant and thus, presence of induction factor EntF in the sample added to the non-bacteriocin-producing culture (Nilsen et al., 1998).

A different approach uses the phenomenon of plasmid transfer to demonstrate the presence of quorum sensing peptides. Genes located on plasmids and encoding for hemolysins, bacteriocins, and antibiotic resistance genes are transferable. Several *Enterococcus faecalis* strains are able to transfer plasmids, facilitated by sex pheromones (i.e., quorum sensing peptides) (Dunny et al., 1979). Certain quorum sensing peptides, excreted by recipient strains, induce donor strains, containing conjugative plasmids, to produce a proteinaceous substance on their surface. Thereby, mating aggregates are formed, facilitating plasmid transfer. These quorum sensing peptides are also called clumping-inducing agents (CIA) since they cause self-aggregation of donor cells when culture filtrate of recipients is added (Dunny et al., 1979). Mori et al. (1984, 1986a, 1988), Suzuki et al. (1984) and Nakayama et al. (1995a), isolated and determined the sequence of several of these CIAs. Once the recipient strain acquires the conjugative plasmid, the excretion of the specific CIA, corresponding with the acquired plasmid, stops and the strain becomes sensitive to exogenous quorum sensing peptides. However, production of other CIAs, specific for donor strains containing other conjugative plasmids, still continues (Ike et al., 1983). Quantification of CIA can be performed by means of a microtiter system. Serial dilutions of recipient strain filtrates (or sample) are added to responder cells (donor cells with the appropriate conjugative plasmid) and incubated for 90–120 min, after which clumping is observed in dilutions (samples)

containing sufficient amount of CIA (quorum sensing peptide) (Dunny et al., 1979). The same principle can be applied to other quorum sensing peptides facilitating plasmid transfer in *E. faecalis* e.g., cAD1 (Mori et al., 1984), cCF10 (Mori et al., 1988), cPD1 (Suzuki et al., 1984), and cOB1 (Nakayama et al., 1995a). Quorum sensing peptides cOB1 and cAD1 are an exception to the assumption of one pheromone (cX) specifically activating plasmid transfer of its corresponding plasmid (pX) since both pOB1 and pY11 respond to cOB1 and both pBEM10 and pAD1 respond to cAD1 (Murray et al., 1988; Nakayama et al., 1995a).

The production stop of quorum sensing peptide, once the recipient strain acquires the corresponding plasmid, is due to the production of a quorum sensing inhibitor encoded on the plasmid, which inhibits the activity of its corresponding quorum sensing peptide (Mori et al., 1987). Inhibitory activity of iPD1 (Mori et al., 1986b, 1987) and iAM373 (Nakayama et al., 1995b) can be quantitatively measured by modifying the microtiter system described above. Using iAD1 as example, serially diluted sample solutions containing iAD1 are added to a mixture of responder cells OG1S(pAD1::Tn917) and cAD1. After incubation for 2–3 h, inhibition of cAD1-induced clumping of responder cells is observed (Mori et al., 1986b).

Chromatographic Techniques

Liquid Chromatography

A variety of liquid-chromatographic methods have been reported, especially for the *N*-acyl homoserine lactones (see Table 3) (Morin et al., 2003; Li et al., 2006; Fekete et al., 2007; Kumari et al., 2008; Ortori et al., 2011; Wang et al., 2011; Cataldi et al., 2013), including methods allowing the simultaneous analysis of various *N*-acyl homoserine lactones via a non-targeted LC-MS/MS method (Patel et al., 2016). Generally, these methods are capable of generating limits of detection (LOD) in the broad nM-range (median LOD of 2.3 nM for 19 *N*-acyl homoserine lactone standards; range: 0.6 nM–2838.9 nM), with some compounds owing a limit of detection around 0.6 nM (for C10-HSL) (Patel et al., 2016).

Besides the closely related cyclodipeptides demonstrated qualitatively, the presence of quorum sensing peptides has not yet been demonstrated *in vivo* (Marchesan et al., 2015), except for one report (Darkoh et al., 2015) where the presence of a thiolacton peptide, without structural elucidation, is suggested in feces of patients suffering from *C. difficile* infection. Nevertheless, the presence of these peptides in cell culture broths has already been proven via reporter strains (see Table 2). Additionally, various authors have reported quorum sensing peptide levels in bacterial cell culture broths via chromatographic techniques, hence applying an orthogonal detection method compared to the biological reporter bacteria.

Additional to reporter bacteria based biosensors, several quorum sensing peptides have been qualitatively or quantitatively determined in bacterial cell culture broths (see Table 4). For example, the currently reported *E. faecalis* quorum sensing peptides have been quantified in cell culture broths. Based on the reports, the concentration of these quorum sensing peptides is in the broad picomolar range, though caution should be paid to

TABLE 3 | Summary of reported concentrations of quorum sensing molecules in different matrices.

Quorum sensing molecule	Matrix	Detection method	Concentration
AUTOINDUCER-2			
AI-2	<i>S. oralis</i> 34 <i>in vitro</i> biofilm	<i>V. harveyi</i> BB170 bioluminescence assay	69–123 nM over 48 h (Rickard et al., 2008)
	<i>A. naeslundii</i> T14V <i>in vitro</i> biofilm	<i>V. harveyi</i> BB170 bioluminescence assay	153–382 nM over 48 h (Rickard et al., 2008)
	<i>S. oralis</i> 34 and <i>A. naeslundii</i> T14V <i>in vitro</i> dual-species biofilm	<i>V. harveyi</i> BB170 bioluminescence assay	124–197 nM over 48 h (Rickard et al., 2008)
	<i>S. oralis</i> 34 <i>luxS</i> mutant and <i>A. naeslundii</i> T14V <i>in vitro</i> dual-species biofilm	<i>V. harveyi</i> BB170 bioluminescence assay	122–140 nM over 48 h (Rickard et al., 2008)
	Saliva (<i>n</i> = 8)	HPLC-MS	244–965 nM (mean = 526 nM) (Campagna et al., 2009)
	Saliva IBD patients (<i>n</i> = 3)	<i>V. harveyi</i> BB170 bioluminescence assay	1.67–2.29 μM (mean = 2.05 μM) (Raut et al., 2013)
	Stool IBD patients (<i>n</i> = 2)	<i>V. harveyi</i> BB170 bioluminescence assay	1.57–3.59 μM (mean = 2.76 μM) (Raut et al., 2013)
	Ileal washing IBD patients (<i>n</i> = 1)	<i>V. harveyi</i> BB170 bioluminescence assay	2.29 μM (Raut et al., 2013)
	Saliva healthy volunteers (<i>n</i> = 3)	<i>V. harveyi</i> BB170 bioluminescence assay	0.998–2.07 μM (mean = 1.39 μM) (Raut et al., 2013)
AHL			
3-oxo-C12-HSL	Sputum samples (<i>n</i> = 47) (20 CF patients + 2 healthy volunteers)	LC-MS	20.24–6833.20 nM (Struss et al., 2013)
	<i>P. aeruginosa</i> <i>in vitro</i> biofilms (<i>n</i> = 4)	LC-MS	Mean = 0.95 ± 0.68 μM (Struss et al., 2013)
	Sputum CF patients (<i>n</i> = 38/59)	LC-MS/MS	LLOQ (not specified)–410 nM (Barr et al., 2015)
	Sputum CF patients (<i>n</i> = 10/12)	pKDT17 with <i>lasB:lacZ</i> fusion in <i>E. coli</i>	0.92–21.20 nM (mean = 5.04 nM) (Marchesan et al., 2015)
HHQ	Sputum CF patients (<i>n</i> = 35/59)	LC-MS/MS	LLOQ (not specified)–1066 nM (Barr et al., 2015)
	Plasma CF patients (<i>n</i> = 40/56)	LC-MS/MS	0.01 nM (i.e., LLOQ)–2.744 nM (Barr et al., 2015)
	Urine CF patients (<i>n</i> = 31/59)	LC-MS/MS	0.02 nM (i.e., LLOQ)–4.028 nM (Barr et al., 2015)
NHQ	Sputum CF patients (<i>n</i> = 43/59)	LC-MS/MS	LLOQ (not specified)–1563 nM (Barr et al., 2015)
	Plasma CF patients (<i>n</i> = 25/56)	LC-MS/MS	0.01 nM (i.e., LLOQ)–0.222 nM (Barr et al., 2015)
	Urine CF patients (<i>n</i> = 19/59)	LC-MS/MS	0.01 nM (i.e., LLOQ)–0.347 nM (Barr et al., 2015)
HQNO	Sputum CF patients (<i>n</i> = 47/59)	LC-MS/MS	LLOQ (not specified)–780 nM (Barr et al., 2015)
	Plasma CF patients (<i>n</i> = 21/56)	LC-MS/MS	0.03 nM (i.e., LLOQ)–0.904 nM (Barr et al., 2015)
	Urine CF patients (<i>n</i> = 48/59)	LC-MS/MS	0.03 nM (i.e., LLOQ)–12.511 nM (Barr et al., 2015)
NQNO	Sputum CF patients (<i>n</i> = 26/59)	LC-MS/MS	LLOQ (not specified)–1075 nM (Barr et al., 2015)
	Plasma CF patients (<i>n</i> = 15/56)	LC-MS/MS	0.04 nM (i.e., LLOQ)–0.705 nM (Barr et al., 2015)
	Urine CF patients (<i>n</i> = 16/59)	LC-MS/MS	0.05 nM (i.e., LLOQ)–2.067 nM (Barr et al., 2015)
C7-PQS	Sputum CF patients (<i>n</i> = 21/59)	LC-MS/MS	LLOQ (not specified)–873 nM (Barr et al., 2015)
	Plasma CF patients (<i>n</i> = 8/56)	LC-MS/MS	0.1 nM (i.e., LLOQ)–0.571 nM (Barr et al., 2015)
C9-PQS	Sputum CF patients (<i>n</i> = 16/59)	LC-MS/MS	LLOQ (not specified)–4302 nM (Barr et al., 2015)

(Continued)

TABLE 3 | Continued

Quorum sensing molecule	Matrix	Detection method	Concentration
C4-HSL	Sputum CF patients (<i>n</i> = 18/59)	LC-MS/MS	LLOQ (not specified)–145 nM (Barr et al., 2015)
	Sputum CF patients (<i>n</i> = 6/12)	pECP61.5 with <i>rhlA:lacZ</i> fusion in <i>P. aeruginosa</i>	0.84–5.00 nM (mean = 1.04 nM) (Erickson et al., 2002)
C10-HSL	<i>Burkholderia cepacia</i> JA-8 cell culture broth (<i>n</i> = 4)	LC-MS/MS	260 nM (9% RSD) (Frommberger et al., 2004)
C8-HSL	<i>Burkholderia cepacia</i> JA-8 cell culture broth (<i>n</i> = 4)	LC-MS/MS	180 nM (12% RSD) (Frommberger et al., 2004)

the often elaborate sample preparation methods that have been applied, mostly intended for a qualitative approach.

Besides the presence of *E. faecalis* quorum sensing peptides in cell culture broths, other authors have developed chromatographic methods to demonstrate quorum sensing peptide presence of other species in their respective cell cultures (Junio et al., 2013; Todd et al., 2016). For example, the presence of *Staphylococcus* autoinducing peptide I was demonstrated using a ultra-high performance liquid chromatographic system coupled to a mass spectrophotometer in methicillin-resistant *Staphylococcus aureus* cell cultures with a limit of detection of 3.5 nM and a LOQ of 0.10 μM (Todd et al., 2016). Junio et al. (2013) demonstrated quantitatively (LOD 0.25 μM; LOQ 2.6 μM) the time- and strain dependent synthesis of AIP-1 in cell culture medium in the μM-magnitude, with concentrations as high as $13 \pm 2 \mu\text{M}$ at 16 h incubation of the *S. aureus* LAC strain (Junio et al., 2013).

Additionally, the extracellular death factor quorum sensing peptide from *E. coli* has also been demonstrated in cell culture broths via a qualitative chromatographic method (Kolodkin-Gal et al., 2007).

Quorum sensing is not limited to bacteria, but eukaryotic yeasts have also shown to possess quorum sensing mechanisms. The *C. albicans* quorum sensing molecules farnesol and tyrosol are via a LC-MS/MS method quantifiable with limits of detection of respectively 15.2 and 3.0 nM (Gregus et al., 2010).

Gas Chromatography

Via gas chromatography coupled to a mass spectrometer (GC-MS), an enantiomer-selective method was achieved for the analysis of C8-HSL (LOD: 0.1 mg/L ≈ 0.4 μM for L-C8-HSL), C10-HSL (LOD: 0.1 mg/L ≈ 0.4 μM for L-C10-HSL), and C12-HSL (LOD: 0.3 mg/L ≈ 1.1 μM for L-C12-HSL). By applying this method to *Burkholderia cepacia* LA3 cell culture supernatant, the authors demonstrated the *in vitro* production of D-C10-HSL (Malik et al., 2009). *N*-3-oxoacyl homoserine lactones were determined by derivatizing them into their pentafluorobenzylxime derivatives with subsequent gas chromatography-mass spectrometry analysis. ODHL (biofilm: $3 \pm 2 \mu\text{M}$; effluent: $1 \pm 0.1 \text{nM}$), OdHL (biofilm: $632 \pm 381 \mu\text{M}$; effluent: $14 \pm 3 \text{nM}$), OtDHL (biofilm: $40 \pm 15 \mu\text{M}$; effluent: $1.5 \pm 0.7 \text{nM}$), and OOHL (effluent: $0.1 \pm 0.1 \text{nM}$) were by applying this method found in biofilms and/or effluent (Charlton

et al., 2000). Cataldi et al. (2007) also reported a GC-MS method capable of detecting AHLs in the μM-range with an average LOD of 4.4 μM for the 6 investigated AHLs (Cataldi et al., 2007). The autoinducer-2, following silylation, has also proven to be analyzable by gas chromatography-mass spectrometry (LOD 5.3 nM and limit of quantification (LOQ) 16 nM) (Thiel et al., 2009).

Thin-Layer Chromatography

Besides liquid and gas chromatography, (high performance-) thin-layer chromatography has also been used in the analysis of certain quorum sensing molecules (Shaw et al., 1997; Bala et al., 2013). Shaw et al. (1997) achieved LODs ranging from 0.5 fmol to 300 pmol depending on the specific AHL (Shaw et al., 1997), whereas Bala et al. (2013) reported a lower limit of detection of 0.006 nmol/spot and a lower limit of quantification of 0.01 nmol/spot for PQS (Bala et al., 2013). A hybrid technique, combining bacterial reporters with thin-layer chromatography has been described (Andersen et al., 2001; Charlesworth et al., 2015) (LODs ranging from 0.012 to 1,710 ng depending on the specific AHL) (Charlesworth et al., 2015).

Capillary Electrophoresis

Besides liquid and gas chromatography, some authors reported capillary electrophoresis as a suitable technique to quantify quorum sensing molecules. With partial filling micellar electrokinetic chromatography-electrospray ionization-ion trap mass spectrometry, two acyl homoserine lactone derivatives (i.e., *N*-octanoyl-L-homoserine lactone and *N*-decanoyl-L-homoserine lactone) molecules originating from *Burkholderia cepacia* could be qualitatively detected in bacterial cell culture broths down to a concentration of approximately 1 μM (Frommberger et al., 2003). The same authors were capable of determining quantitatively (LOQ 0.05 μg/ml) C8-HSL ($0.26 \mu\text{g/ml} \approx 1.1 \mu\text{M}$), C10-HSL ($1.93 \mu\text{g/ml} \approx 7.6 \mu\text{M}$), and C12-HSL ($0.16 \mu\text{g/ml} \approx 0.6 \mu\text{M}$) in *Burkholderia cepacia* cell culture broths by means of capillary zone electrophoresis-mass spectrometry following hydrolysis of the homoserine lactones into their corresponding organic acids (Frommberger et al., 2005).

Several *P. aeruginosa*-quinolones are also detectable using capillary electrophoresis with LODs of 65 nM (PQS), 94 nM (HHQ), 61 nM (“Quinolone 1”) and 79 nM (“Quinolone 2”) (Zhou et al., 2012). Noteworthy is the eukaryotic quorum

TABLE 4 | Concentration of selected peptides in bacterial cell culture broths.

Species	Quorum sensing peptide (sequence)	Strain	Concentration	Detection method
<i>Enterococcus faecalis</i>	cAM373 (AIFILAS)	<i>E. faecalis</i> JH2-2 (pAM351)	4.4 µg/16 L = 374 pM	HPLC-UV/VIS (Mori et al., 1986a)
	iPD1 (ALILTLVS)	<i>E. faecalis</i> JH2-2 (pAM351)	6.3 µg/20 L = 378 pM	HPLC-UV/VIS (Mori et al., 1987)
	iCF10 (AITLIFI)	<i>E. faecalis</i> OG1RF(pMSP5011)	15,360 pg/mL = 19,440 pM	Estimated via bio-assay via comparing with synthetic peptide (La Rosa et al., 2015)
	cOB1 (VAVLVG)	<i>E. faecalis</i> FA2-2	1.5 µg/15 L = 135 pM	HPLC-UV/VIS (Nakayama et al., 1995a)
	cAD1 (LFSLVLAG)	<i>E. faecalis</i> JH2-2	200 µg/300 L = 814 pM	HPLC-UV/VIS (Mori et al., 1984)
	iAD1 (LFVVTLVG)	<i>E. faecalis</i> FA2-2 (pAM727)	20 µg/20 L = 787 pM	HPLC-UV/VIS (Mori et al., 1986b)
	cCF10 (LVTLVF)	<i>E. faecalis</i> FA2-2 (pAM351)	4.1 µg/60 L = 86 pM	HPLC-UV/VIS (concentration) FAB-MS (amino acid sequence confirmation) (Mori et al., 1988)
	iAM373 (SIFTLVA)	<i>E. faecalis</i> JSS2 (pAM377)	3 µg/8 L = 500 pM	HPLC-UV/VIS (Nakayama et al., 1995b)

sensing molecule from *C. albicans* farnesol, which is also detectable via capillary electrophoresis. By applying this capillary electrophoresis method, the authors demonstrated the concentration of farnesol to be approximately 2 nM in a cell culture supernatant (Kubesová et al., 2010).

Miscellaneous Analytical Techniques

Cyclic voltammetry and amperometric detection by a bare boron-doped diamond electrode showed, however with selectivity limitations, to be a possible approach to detect 2-heptyl-3-hydroxy-4-quinolone from *P. aeruginosa* at approximately 30 µM in *P. aeruginosa* *pqsL*⁻ mutant strains cell culture medium (Zhou et al., 2011).

Other authors also developed electrochemical biosensors for the detection of AHL's, achieving detection limits down to 2 pM via cyclic voltammetry with a gold microelectrode (Baldrich et al., 2011).

Zhang and Ye (2014) reported a Förster resonance energy transfer-based biosensor for the detection of *N*-(3-oxo-hexanoyl)-L-homoserine lactone. However, the reported method had a limit of detection as high as 100 µM (Zhang and Ye, 2014).

Enzyme-linked immunosorbent assay (ELISA) also proved a suitable approach for AHL-detection. Chen et al. (2010a) developed rat monoclonal antibodies achieving limits of detection of 31 nM concerning 3-oxo-C10-HSL and 476 nM regarding C8-HSL (Chen et al., 2010a). Additionally, Kaufmann et al. (2006) developed an antibody against 3-oxo-C12-HSL (Kaufmann et al., 2006) without aiming to develop an ELISA. However, this antibody could still be suitable for ELISA and has according to Chen et al. (2010a) a limit of detection of 15 nM (Chen et al., 2010a). Another ELISA method has been developed to monitor AHL production in *B. cepacia* LA3 cell cultures (Chen et al., 2010b).

Finally, surface-enhanced Raman spectroscopy also proved a feasible approach for AHL detection with a LOD estimated around 3 nM (Pearman et al., 2007).

IN VIVO CONCENTRATION OF QUORUM SENSING MOLECULES

Autoinducer-2

Streptococcus oralis, *Streptococcus oralis luxS* mutant, and *Actinomyces naeslundii* T14V each produce autoinducer-2 when they are grown in commercial media (Rickard et al., 2006). Rickard et al. (2006, 2008) investigated if each of these species also produce autoinducer-2 when they are part of single- or dual-species biofilms in saliva in an *ex-vivo in-vitro* design. Biofilms were grown within Sorbarods fed with 25% human saliva, after which the autoinducer-2 concentration in the effluent was determined by the *Vibrio harveyi* BB170 bioluminescence assay. Autoinducer-2 concentrations in a single-species biofilm of *S. oralis* 34 or *A. naeslundii* T14V varied between 69–123 and 153–382 nM over 48 h respectively. In the effluent from the *S. oralis* 34 *luxS* mutant biofilm, no autoinducer-2 could be detected. Autoinducer-2 concentrations in the effluent of dual-species biofilms containing *S. oralis* 34 and *A. naeslundii* T14V or *S. oralis* 34 *luxS* mutant and *A. naeslundii* T14V varied respectively between 124–197 and 122–140 nM over 48 h (Rickard et al., 2006, 2008).

Campagna et al. (2009) developed a HPLC-MS method (LOD in the low nM-range) for the detection of autoinducer-2 in human saliva. They asked 8 volunteers to donate approximately 1 ml of saliva and determined the concentration of autoinducer-2 in these samples. The average concentration was found to be 526 nM with individual values ranging from 244 to 965 nM (Campagna et al., 2009).

Autoinducer-2 concentrations in saliva, stool and intestinal samples from patients with irritable bowel disease (IBD), as well as in saliva samples from healthy volunteers, were determined using the *Vibrio harveyi* BB170 bioluminescence assay. Because of genetic modifications, the BB170 strain only emits light when autoinducer-2 is added. Dose-response curves were obtained using 50 nM–0.5 mM dilutions of synthetic autoinducer-2 in saliva or stool matrix. The autoinducer-2 concentration was

quantified in stool ($n = 2$, $2.76 \mu\text{M}$), ileal washing samples ($n = 1$; $2.29 \mu\text{M}$) and saliva from patients with IBD ($n = 3$, $2.05 \mu\text{M}$) and saliva from healthy volunteers ($n = 3$; $1.39 \mu\text{M}$) (Raut et al., 2013).

An overview of the observed *in vivo* concentrations is given in **Table 3**.

Acyl homoserine lactones

Chronic lung disease in cystic fibrosis patients is frequently associated with *Pseudomonas aeruginosa* biofilm formation in the lungs (Singh et al., 2000). Quorum sensing in *P. aeruginosa* is mediated via *N*-3-oxododecanoyl homoserine lactone and *N*-butyryl homoserine lactone (Pesci et al., 1997). *N*-3-oxododecanoyl homoserine lactone is indispensable for the establishment of a persistent *P. aeruginosa* infection; therefore a LC-MS method for the quantitation of this quorum sensing molecule in sputum of cystic fibrosis patients has been developed (LLOQ of 10 nM for 3-oxo-C12-HSL) (Struss et al., 2013). In total, 47 samples originating from 20 cystic fibrosis and 2 healthy donors were collected. Concerning the cystic fibrosis patients, 9 patients donated more than 1 sample, resulting in 34 samples from these patients obtained in total at different time points. Cystic fibrosis patients were allocated into different groups depending on their disease state. Besides patient samples, they also investigated the *N*-3-oxododecanoyl homoserine lactone concentration in *P. aeruginosa* *in vitro* cultured biofilms ($n = 4$) and found a mean concentration of $0.95 \pm 0.68 \mu\text{M}$. Regarding the patient samples, 45 out of 47 samples contained *N*-3-oxododecanoyl homoserine lactone in quantifiable concentrations with concentrations ranging between 20 to $> 1,000 \text{ nM}$; the highest measured concentration was approximately $6,900 \text{ nM}$ (Struss et al., 2013). These results are potentially clinically significant as *N*-3-oxododecanoyl homoserine lactone in a concentration range of 0.1 – $100 \mu\text{M}$ has shown to alter the human immune response (Telford et al., 1998b).

Barr et al. (2015) determined the concentration of several quorum sensing molecules in sputum, plasma and urine of 60 cystic fibrosis patients with chronic *Pseudomonas aeruginosa* infection at the beginning of a pulmonary exacerbation (Barr et al., 2015). All samples were analyzed by liquid chromatography–tandem mass spectrometry (LC-MS/MS). Eight different quorum sensing molecules were observed in sputum: 2-heptyl-4-hydroxyquinoline (HHQ), 2-nonyl-4-hydroxyquinoline (NHQ), 2-heptyl-4-hydroxyquinoline-N-oxide (HQNO), 2-nonyl-4-hydroxyquinoline-N-oxide (NQNO), 2-heptyl-3-hydroxy-4(1H)-quinolone (C7-PQS), 2-nonyl-3-hydroxy-4(1H)-quinolone (C9-PQS), *N*-3-oxododecanoyl-L-homoserine lactone (3-oxo-C12-HSL) and *N*-butanoyl-L-homoserine lactone (C4-HSL). Five of them were also detected in plasma (HHQ, NHQ, HQNO, NQNO, and C7-PQS) and four in urine samples (HHQ, NHQ, HQNO, NQNO). Concentrations in sputum, plasma, and urine varied respectively between lower limit of quantification (LLOQ) (not specified)– $4,302 \text{ nM}$, LLOQ (i.e., 0.01 nM)– 2.744 nM and LLOQ

(i.e., 0.01 nM)– 12.511 nM and do correlate with the disease state of cystic fibrosis (Barr et al., 2015).

The concentration of 3-oxo-C12-HSL and C4-HSL in sputum samples of 12 patients with cystic fibrosis has been assessed. In order to determine the 3-oxo-C12-HSL concentration, a pKDT17 plasmid in *E. coli*, which contains a copy of the *lasR* gene and a *lasB-lacZ* fusion, was used. Concentrations of C4-HSL were determined by means of a pECP61.5 plasmid in *P. aeruginosa*, which contains a copy of the *rhlR* gene and a *rhlA-lacZ* fusion. The measured β -galactosidase activity in both reporter bacteria correlates with the levels of respectively 3-oxo-C12-HSL and C4-HSL. The average concentrations of 3-oxo-C12-HSL and C4-HSL were found to be respectively 5.04 and 1.04 nM with individual values ranging from $< \text{LOD}$ (not specified) to 21.2 nM and $< \text{LOD}$ (not specified) to 5 nM . However, determination of the extraction efficiency by adding synthetic autoinducers to sputum samples that do not contain autoinducer showed only 80% recovery of 3-oxo-C12-HSL and 60–65% recovery of C4-HSL, indicating loss of autoinducer during extraction in sample preparation (Erickson et al., 2002).

A summary of the reported concentrations of quorum sensing molecules in different matrices, together with the method used for detection and the corresponding reference is given in **Table 3**. To our knowledge, quorum sensing peptides have not yet been quantitated nor identified in biological samples from human origin.

DISCUSSION

Detection Methods

A variety of analytical techniques is currently available for many quorum sensing molecules, mainly chromatographic methods and reporter bacteria based biosensors. However, caution must be paid when considering these different methods regarding their analytical characteristics like selectivity. The reporter bacteria are based on the interaction of the molecule of interest with a receptor. Hence, structural analogs can possibly also interact with the receptor and consecutively might impede a straightforward quantitative or qualitative selective analysis of individual quorum sensing molecules, a rather general concern that is also valid for other analytical techniques. For example, applying ELISA as a quantitative analytical method, cannot exclude cross-reactivity toward other structurally analog quorum sensing molecules that are currently not yet discovered. Since these molecules currently might not yet have been identified, it is very difficult to test for cross-reactivity toward these molecules. This can be illustrated by a variety of quorum sensing peptides listed in the Quorumpeps database: various synthetic structural analogs of certain quorum sensing peptides have been tested toward the bacteria receptive for the cognate quorum sensing peptide. The reactivity of the receptors is not solely limited toward synthetic analogs: the receptor(s) have been proven to be activated by various naturally occurring structural analogs (e.g., the *N*-acyl homoserine lactones). This potential pitfall can be omitted by coupling the biosensor with an initial

chromatographic separation by e.g., thin layer chromatography. On the other hand, mass spectroscopy, especially in its targeted modi, allows additional selectivity via quorum sensing molecule fragmentation. Another important method consideration for qualitative and/or quantitative analysis of samples is the achievable limit of detection and its related, always higher, limit of quantification. This analytical characteristic is depending on the analytical method as such, including the sample preparation steps and is also compound-dependent. The latter being illustrated by the large range of limits of detection reported for various methods. The bacteria reporter based biosensors have in some specific cases proven to achieve limits of detection and limits of quantification in the sub-pM range. Chromatography coupled to mass spectroscopy can also achieve limits of detection and quantification in the sub-nM or even below. Hence, the preferred method of detection and/or quantification mainly depends on the desired selectivity and sensitivity for a specific quorum sensing molecule or group of molecules.

In vivo Quorum Sensing Molecule Concentrations

The *in vivo* presence and concentration of quorum sensing peptides have been neglected, while the other classes of quorum sensing molecules (e.g., the *N*-acyl homoserine lactones) have attracted considerable attention. The concentration of these molecules has been demonstrated in both healthy and diseased subjects. Concentrations of AI-2 were found to be in the high nM-low μM range and AHL concentrations were found in a comparable concentration range.

The lack of information related to the large group of quorum sensing peptides in *in vivo* samples cannot be longer justified. Peptides play an important role in all aspects of the immune, endocrine, and neuronal systems, and hence, the biological roles of quorum sensing peptides as produced by our microbiome are expected to be elucidated in the near future. Moreover, taking into consideration the increasing evidence that our microbiome is involved in a variety of biological host processes, both in health as in disease, these quorum sensing peptides could act as biomarkers, similar to recent suggestions of using microbiota as biomarkers (Eloe-Fadrosh and Rasko, 2013). This can be illustrated by the reports of quorum sensing molecules in cystic fibrosis patients (Singh et al., 2000).

CONCLUSION

Quorum sensing molecules are a heterogeneous group of molecules currently only started to be explored in *in vivo* situations. For example, to our knowledge, the bacterial quorum sensing peptides have sparsely qualitatively or quantitatively detected *in vivo* within humans. Conversely, the *N*-acyl homoserine lactones do have attracted considerable scientific interest. They have been quantified *in vivo* at concentrations ranging in the broad nM-μM range. Quorum sensing peptides have, together with the other classes of

quorum sensing molecules, been detected and quantified in bacterial cell culture broths. The concentration of these quorum sensing molecules is highly variable and *in vitro* observed concentrations can reach almost mM concentrations.

A variety of analytical techniques has been described in literature to investigate the major quorum sensing molecule classes. Generally, reporter bacteria based biosensors and chromatography, especially LC(-MS/MS) are most frequently applied for qualitative and quantitative purposes. Selectivity and sensitivity are key analytical characteristics when considering quorum sensing molecule identification and quantification. Concerning selectivity, reporter bacteria based biosensors will potentially be confronted with cross-reactivity, and hence potential false-positives, due to currently unknown quorum sensing molecules that might cross-react with the specific quorum sensing molecule receptor. However, these reporter bacteria biosensors are, in some specific cases, able to achieve very low limits of detection (e.g., pM range), sometimes outperforming the LC(-MS/MS) methods. Opposite, LC-MS/MS methods potentially show a higher degree of selectivity due to both the chromatographic separation and the molecule fragmentation patterns via mass spectroscopy. Hence, the preferred method of analysis does depend on the quorum sensing molecule(s) of interest and the objectives put forward.

Evidence of the role of the human microbiome, both in health and disease, is continuously increasing. Quorum sensing molecules are bacterial languages, and apart from their fundamental biological importance in pathophysiological conditions, they can serve as potential prognostic or diagnostic biomarkers. However, the vast potential field of quorum sensing molecule-biomarkers, especially quorum sensing peptides, have not yet received the attention they deserve.

AUTHOR CONTRIBUTIONS

FV and BD conceived the idea for this manuscript, while FV and SD wrote the manuscript, FV, SD, ND, YJ, EW, CV, and BD made substantial contributions to data interpretation and drafted/revised the manuscript. FV, SD, ND, YJ, EW, CV, and BD approved this manuscript and agree to be held accountable for all aspects of this manuscript.

FUNDING

FV is funded by the “Institute for the Promotion of Innovation through Science and Technology in Flanders (IWT-Vlaanderen)” (Grant number 131356 to FV). ND is funded by “Fonds wetenschappelijk onderzoek-Vlaanderen (Fund Scientific Research-Flanders)” (Grant number 1S21017N to ND). IWT-Vlaanderen or Fonds wetenschappelijk onderzoek-Vlaanderen were not involved in any part of the study, and had no role in the conception, contributions to the consent nor in manuscript writing.

REFERENCES

- Andersen, J. B., Heydorn, A., Hentzer, M., Eberl, L., Geisenberger, O., Christensen, B. B., et al. (2001). gfp-based N-acyl homoserine-lactone sensor systems for detection of bacterial communication. *Appl. Environ. Microbiol.* 67, 575–585. doi: 10.1128/AEM.67.2.575-585.2001
- Asano, Y., Hiramoto, T., Nishino, R., Aiba, Y., Yoshihara, K., Koga, Y., et al. (2012). Critical role of gut microbiota in the production of biologically active, free catecholamines in the gut lumen of mice. *Am. J. Physiol. Gastrointest. Liver Physiol.* 303, G1288–G1295. doi: 10.1152/ajpgi.00341.2012
- Bala, A., Gupta, R. K., Chhibber, S., and Harjai, K. (2013). Detection and quantification of quinolone signalling molecule: a third quorum sensing molecule of *Pseudomonas aeruginosa* by high performance-thin layer chromatography. *J. Chromatogr. B* 930, 30–35. doi: 10.1016/j.jchromb.2013.04.027
- Baldrich, E., Mu-oz, F. X., and García-Aljaro, C. (2011). Electrochemical detection of quorum sensing signaling molecules by dual signal confirmation at microelectrode arrays. *Anal. Chem.* 83, 2097–2103. doi: 10.1021/ac1028243
- Balkwill, F., and Mantovani, A. (2001). Inflammation and cancer: back to Virchow? *Lancet* 357, 539–545. doi: 10.1016/S0140-6736(00)04046-0
- Bandyopadhyaya, A., Keswani, M., Que, Y. A., He, Y., Padfield, K., Tompkins, R., et al. (2012). The quorum sensing volatile molecule 2-amino-acetophenon modulates host immune responses in a manner that promotes life with unwanted guests. *PLOS Pathog.* 11:e1003024. doi: 10.1371/journal.ppat.1003024
- Barber, C. E., Tang, J. L., Feng, J. X., Pan, M. Q., Wilson, T. J., Slater, H., et al. (1997). A novel regulatory system required for pathogenicity of *Xanthomonas campestris* is mediated by a small diffusible signal molecule. *Mol. Microbiol.* 24, 555–566. doi: 10.1046/j.1365-2958.1997.3721736.x
- Barr, H. L., Halliday, N., Cámera, M., Barrett, D. A., Williams, P., Forrester, D. L., et al. (2015). *Pseudomonas aeruginosa* quorum sensing molecules correlate with clinical status in cystic fibrosis. *Eur. Respir. J.* 46, 1046–1054. doi: 10.1183/09031936.00225214
- Barrett, E., Ross, R. P., O'Toole, P. W., Fitzgerald, G. F., and Stanton, C. (2012). Gamma-aminobutyric acid production by culturable bacteria from the human intestine. *J. Appl. Microbiol.* 113, 411–417. doi: 10.1111/j.1365-2672.2012.05344.x
- Bassler, B. L. (1999). How bacteria talk to each other: regulation of gene expression by quorum sensing. *Curr. Opin. Microbiol.* 2, 582–587. doi: 10.1016/S1369-5274(99)00025-9
- Baxter, N. T., Zackular, J. P., Chen, G. Y., and Schloss, P. D. (2014). Structure of the gut microbiome following colonization with human feces determines colonic tumor burden. *Microbiome* 2:20. doi: 10.1186/2049-2618-2-20
- Belleza, I., Peirce, M. J., and Minelli, A. (2014). Cyclic dipeptides: from bugs to brain. *Trends Mol. Med.* 20, 551–558. doi: 10.1016/j.molmed.2014.08.003
- Beloin, C., Renard, S., Ghigo, J. M., and Lebeaux, D. (2014). Novel approaches to combat bacterial biofilms. *Curr. Opin. Pharmacol.* 18C, 61–68. doi: 10.1016/j.coph.2014.09.005
- Bultman, S. J. (2014). Emerging roles of the microbiome in cancer. *Carcinogenesis* 35, 249–255. doi: 10.1093/carcin/bgt392
- Campagna, S. R., Gooding, J. R., and May, A. L. (2009). Direct Quantitation of the quorum sensing signal, autoinducer-2, in clinically relevant samples by Liquid chromatography-tandem mass spectrometry. *Anal. Chem.* 81, 6374–6381. doi: 10.1021/ac900824j
- Castro-Nallar, E., Bendall, M. L., Pérez-Losada, M., Sabuncyan, S., Severance, E. G., Dickerson, F. B., et al. (2015). Composition, taxonomy and functional diversity of the oropharynx microbiome in individuals with schizophrenia and controls. *PeerJ* 3:e1140. doi: 10.7717/peerj.1140
- Cataldi, T. R. I., Bianco, G., Fonseca, J., and Schmitt-Kopplin, P. (2013). Perceiving the chemical language of Gram-negative bacteria: listening by high-resolution mass spectrometry. *Anal. Bioanal. Chem.* 405, 493–507. doi: 10.1007/s00216-012-6371-2
- Cataldi, T. R. I., Bianco, G., Palazzo, L., and Quaranta, V. (2007). Occurrence of N-acyl-L-homoserine lactones in extracts of some Gram-negative bacteria evaluated by gas chromatography-mass spectrometry. *Anal. Biochem.* 361, 226–235. doi: 10.1016/j.ab.2006.11.037
- Charlesworth, J., Kimyon, O., Manefield, M., and Burns, B. P. (2015). Detection and characterization of N-acyl-L-homoserine lactones using GFP-based biosensors in conjunction with thin-layer chromatography. *J. Microbiol. Methods* 118, 164–167. doi: 10.1016/j.mimet.2015.09.012
- Charlton, T. S., de Nys, R., Netting, A., Kumar, N., Hentzer, M., Givskov, M., et al. (2000). A novel and sensitive method for the quantification of N-3-oxoacyl homoserine lactones using gas chromatography-mass spectrometry: application to a model bacterial biofilm. *Environ. Microbiol.* 2, 530–541. doi: 10.1046/j.1462-2920.2000.00136.x
- Chen, X., Buddrus-Schiemann, K., Rothbauer, M., Krämer, P. M., and Hartmann, A. (2010b). Detection of quorum sensing molecules in *Burkholderia cepacia* culture supernatants with enzyme-linked immunosorbent assays. *Anal. Bioanal. Chem.* 398, 2669–2676. doi: 10.1007/s00216-010-4045-5
- Chen, X., Kremmer, E., Gouzy, M. F., Clausen, E., Starke, M., Wöllner, K., et al. (2010a). Development and characterization of rat monoclonal antibodies for N-acylated homoserine lactones. *Anal. Bioanal. Chem.* 398, 2655–2667. doi: 10.1007/s00216-010-4017-9
- Chhabra, S. R., Harty, C., Hooi, D. S. W., Daykin, M., Williams, P., Telford, G., et al. (2003). Synthetic analogues of the bacterial signal (quorum sensing) molecule N-(3-oxododecanoyl-L-homoserine lactone as immune modulators. *J. Med. Chem.* 46, 97–104. doi: 10.1021/jm020909n
- Chowers, M. Y., Keller, N., Tal, R., Barshack, I., Lang, R., Bar-Meir, S., et al. (1999). Human gastrin: a *Helicobacter pylori*-specific growth factor. *Gastroenterology* 117, 1113–1118. doi: 10.1016/S0016-5085(99)70396-3
- Clarke, G., Stilling, R. M., Kennedy, P. J., Stanton, C., Cryan, J. F., and Dinan, T. G. (2014). Minireview: gut microbiota: the neglected endocrine organ. *Mol. Endocrinol.* 28, 1221–1238. doi: 10.1210/me.2014-1108
- Cooley, M. A., Whittall, C., and Rolph, M. S. (2010). *Pseudomonas* signal molecule 3-oxo-C12-homoserine lactone interferes with binding of rosiglitazone to human PPARGamma. *Microbes. Infect.* 12, 231–237. doi: 10.1016/j.micinf.2009.12.009
- Cryan, J. F., and O'Mahony, S. M. (2011). The microbiome-gut-brain axis: from bowel to behavior. *Neurogastroenterol. Motil.* 23, 187–192. doi: 10.1111/j.1365-2982.2010.01664.x
- Darkoh, C., DuPont, H. L., Norris, S. J., and Kaplan, H. B. (2015). Toxin synthesis by *Clostridium difficile* is regulated through quorum signaling. *mBio* 6, e02569-e02514. doi: 10.1128/mBio.02569-14
- De Spiegeleer, B., Verbeke, F., D'Hondt, M., Hendrix, A., Van De Wiele, C., Burvenich, C., et al. (2015). The quorum sensing peptides PhrG, CSP and EDF promote angiogenesis and invasion of breast cancer cells *in vitro*. *PLOS ONE* 10:e0119471. doi: 10.1371/journal.pone.0119471
- De Spiegeleer, B., Wynendaele, E., Bracke, N., Veryser, L., Taevernier, L., Degroote, A., et al. (2016). Regulatory development of geriatric medicines: to GIP or not to GIP? *Ageing Res. Rev.* 27, 23–36. doi: 10.1016/j.arr.2016.02.004
- DiMango, E., Zar, H. J., Bryan, R., and Prince, A. J. (1995). Diverse *Pseudomonas aeruginosa* gene products stimulate respiratory epithelial cells to produce interleukin-8. *Clin. Invest.* 96, 2204–2210. doi: 10.1172/JCI118275
- Dolnick, R., Wu, Q., Angelino, N. J., Stephanie, L. V., Chow, K. C., Sufrin, J. R., et al. (2005). Enhancement of 5-fluorouracil sensitivity by an rTS signaling mimic in H630 colon cancer cells. *J. Cancer Res.* 65, 5917–5924. doi: 10.1158/0008-5472.CAN-05-0431
- Dunny, G. M., Craig, R. A., Carron, R. L., and Clewell, D. B. (1979). Plasmid transfer in *Streptococcus faecalis*: production of multiple sex pheromones by recipients. *Plasmid* 2, 454–465. doi: 10.1016/0147-619X(79)90029-5
- Eloe-Fadrosh, E. A., and Rasko, D. A. (2013). The human microbiome: from symbiosis to pathogenesis. *Annu. Rev. Med.* 64, 145–163. doi: 10.1146/annurev-med-010312-133513
- Engelbrecht, J., and Silverman, M. (1984). Identification of genes and gene products necessary for bacterial bioluminescence. *Proc. Natl. Acad. Sci. U.S.A.* 81, 4154–4158. doi: 10.1073/pnas.81.13.4154
- Erdman, S. E., and Poutahidis, T. (2014). The microbiome modulates the macroenvironment. *Oncoimmunology* 3:e28271. doi: 10.4161/onci.28271
- Erickson, D. L., Endersby, R., Kirkham, A., Stuber, K., Vollman, D. D., Rabin, H. R., et al. (2002). *Pseudomonas aeruginosa* quorum-sensing systems may control virulence factor expression in the lungs of patients with cystic fibrosis. *Infect. Immun.* 70, 1783–1790. doi: 10.1128/IAI.70.4.1783-1790.2002
- Ernst, P. B., and Gold, B. D. (2000). The disease spectrum of *Helicobacter pylori*: the immunopathogenesis of gastroduodenal ulcer and cancer. *Annu. Rev. Microbiol.* 54, 615–640. doi: 10.1146/annurev.micro.54.1.615

- Fekete, A., Frommberger, M., Rothballer, M., Li, X., Englmann, M., Fekete, J., et al. (2007). Identification of bacterial N-acylhomoserine lactones (AHLs) with a combination of ultra-performance liquid chromatography (UPLC), ultra-high-resolution mass spectrometry, and *in-situ* biosensors. *Anal. Bioanal. Chem.* 387, 455–467. doi: 10.1007/s00216-006-0970-8
- Finegold, S. M., Dowd, S. E., Gontcharova, V., Liu, C., Henley, K. E., Wolcott, R. D., et al. (2010). Pyrosequencing study of fecal microflora of autistic and control children. *Anaerobe* 16, 444–453. doi: 10.1016/j.anaerobe.2010.06.008
- Flavier, A. B., Clough, S. J., Schell, M. A., and Denny, T. P. (1997). Identification of 3-hydroxypalmitic acid methyl ester as a novel autoregulator controlling virulence in *Ralstonia solanacearum*. *Mol. Microbiol.* 26, 251–259. doi: 10.1046/j.1365-2958.1997.5661945.x
- Freestone, P. E., Sandrini, S. M., Haigh, R. D., and Lyte, M. (2008). Microbial endocrinology: how stress influences susceptibility to infection. *Trends Microbiol.* 16, 55–64. doi: 10.1016/j.tim.2007.11.005
- Frommberger, M., Hertkorn, N., Englmann, M., Jakoby, S., Hartmann, A., Kettrup, A., et al. (2005). Analysis of N-acylhomoserine lactones after alkaline hydrolysis and anion-exchange solid-phase extraction by capillary zone electrophoresis-mass spectrometry. *Electrophoresis* 26, 1523–1532. doi: 10.1002/elps.200410365
- Frommberger, M., Schmitt-Kopplin, P., Menzinger, F., Albrecht, V., Schmid, M., Eberl, L., et al. (2003). Analysis of N-acyl-L-homoserine lactones produced by *Burkholderia cepacia* with partial filling micellar electrikinetic chromatography – electrospray ionization-ion trap mass spectrometry. *Electrophoresis* 24, 3067–3074. doi: 10.1002/elps.200305567
- Frommberger, M., Schmitt-Kopplin, P., Ping, G., Frisch, H., Schmid, M., Zhang, Y., et al. (2004). A simple and robust set-up for on-column sample preconcentration – nano-liquid chromatography – electrospray ionization mass spectrometry for the analysis of N-acylhomoserine lactones. *Anal. Bioanal. Chem.* 378, 1014–1020. doi: 10.1007/s00216-003-2400-5
- Fuqua, W. C., Winans, S., and Greenberg, E. (1994). Quorum sensing in bacteria: the LuxR-LuxI family of cell density-responsive transcriptional regulators. *J. Bacteriol.* 176, 269–275.
- Gomi, K., Kikuchi, T., Tokue, Y., Fujimura, S., Uehara, A., Takada, H., et al. (2006). Mouse and human cell activation by N-dodecanoyl-DL-homoserine lactone, a *Chromobacterium violaceum* auto-inducer. *Infect. Immun.* 74, 7029–7031. doi: 10.1128/IAI.00038-06
- Gregus, P., Vlcková, H., Buchta, V., Kestranek, J., Krivciková, L., and Nováková, L. (2010). Ultra high performance liquid chromatography tandem mass spectrometry analysis of quorum-sensing molecules of *Candida albicans*. *J. Pharm. Biomed. Anal.* 53, 674–681. doi: 10.1016/j.jpba.2010.05.029
- Gupta, R. K., Chhibber, S., and Harjai, K. (2013). Quorum sensing signal molecules cause renal tissue inflammation through local cytokine responses in experimental UTI caused by *Pseudomonas aeruginosa*. *Immunobiology* 218, 181–185. doi: 10.1016/j.imbio.2012.03.001
- Haas, C. F., Eakin, R. M., Konkle, M. A., and Blank, R. (2014). Endotracheal tubes: old and new. *Respir. Care* 59, 933–952. doi: 10.4187/respcare.02868
- Hávarstein, L. S., Hakenbeck, R., and Gaustad, P. (1997). Natural competence in the genus *Streptococcus*: evidence that streptococci can change phenotype by interspecies recombinational exchanges. *J. Bacteriol.* 179, 6589–6594. doi: 10.1128/jb.179.21.6589-6594.1997
- Higgins, D. A., Pomianek, M. E., Kraml, C. M., Taylor, R. K., Semmelhack, M. F., and Bassler, B. L. (2007). The major *Vibrio cholerae* autoinducer and its role in virulence factor production. *Nature* 450, 883–886. doi: 10.1038/nature06284
- Holden, M. T., Chhabra, S. R., de Nys, R., Stead, P., Bainton, N. J., Hill, P. J., et al. (1999). Quorum-sensing cross talk: isolation and chemical characterization of cyclic dipeptides from *Pseudomonas aeruginosa* and other gram-negative bacteria. *Mol. Microbiol.* 33, 1254–1266.
- Holzer, P., Reichmann, F., and Farzi, A. (2012). Neuropeptide, Y, peptide YY and pancreatic polypeptide in the gut-brain axis. *Neuropeptides* 46, 261–274. doi: 10.1016/j.npep.2012.08.005
- Hooi, D. S. W., Bycroft, B. W., Chhabra, S. R., Williams, P., and Pritchard, D. I. (2004). Differential immune modulatory activity of *Pseudomonas aeruginosa* quorum-sensing signal molecules. *Infect. Immun.* 72, 6463–6470. doi: 10.1128/IAI.72.11.6463-6470.2004
- Hughes, D. T., and Sperandio, V. (2008). Inter-kingdom signaling: communication between bacteria and their hosts. *Nat. Rev. Microbiol.* 6, 111–120. doi: 10.1038/nrmicro1836
- Ike, Y., Craig, R. A., Yagi, Y., and Clewell, D. B. (1983). Modification of *Streptococcus faecalis* sex pheromones after acquisition of plasmid DNA. *Proc. Natl. Acad. Sci. U.S.A.* 80, 5369–5373. doi: 10.1073/pnas.80.17.5369
- Jahoor, A., Patel, R. J., Bryan, A., Do, C., Krier, J., Watters, C., et al. (2008). Peroxisome proliferator-activated receptors mediate host cell proinflammatory responses to *Pseudomonas aeruginosa* autoinducer. *J. Bacteriol.* 190, 4408–4415. doi: 10.1128/JB.01444-07
- Jiang, H., Ling, Z., Zhang, Y., Mao, H., Ma, Z., Yin, Y., et al. (2015). Altered fecal microbiota composition in patients with major depressive disorder. *Brain Behav. Immun.* 48, 186–194. doi: 10.1016/j.bbi.2015.03.016
- Junio, H. A., Todd, D. A., Ettefagh, K. A., Ehrmann, B. M., Kavanaugh, J. S., Horswill, A. R., et al. (2013). Quantitative analysis of autoinducing peptide I (AIP-I) from *Staphylococcus aureus* cultures using ultrahigh performance liquid chromatography–high resolving power mass spectrometry. *J. Chromatogr. B. Analyt. Technol. Biomed. Life Sci.* 930, 7–12. doi: 10.1016/j.jchromb.2013.04.019
- Kalia, V. C. (2013). Quorum sensing inhibitors: an overview. *Biotechnol. Adv.* 31, 224–245. doi: 10.1016/j.biotechadv.2012.10.004
- Karavolos, M. H., Bulmer, D. M., Spencer, H., Rampioni, G., Schmalen, I., Baker, S., et al. (2011). *Salmonella typhi* sense host neuroendocrine stress hormones and release the toxin haemolysin E. *EMBO Rep.* 12, 252–258. doi: 10.1038/embor.2011.4
- Karavolos, M. H., Spencer, H., Bulmer, D. M., Thompson, A., Winzer, K., Williams, P., et al. (2008). Adrenaline modulates the global transcriptional profile of *Salmonella* revealing a role in the antimicrobial peptide and oxidative stress resistance responses. *BMC Genomics* 9:458. doi: 10.1186/1471-2164-9-458
- Karavolos, M. H., Winzer, K., Williams, P., and Khan, C. M. (2013). Pathogen espionage: multiple bacterial adrenergic sensors eavesdrop on host communication systems. *Mol. Microbiol.* 87, 455–465. doi: 10.1111/mmi.12110
- Kaufmann, G. F., Sartorio, R., Lee, S. H., Mee, J. M., Altobelli, L. J. I. I. I., Kujawa, D. P., et al. (2006). Antibody interference with N-acyl homoserine lactone-mediated bacterial quorum sensing. *J. Am. Chem. Soc.* 128, 2802–2803. doi: 10.1021/ja0578698
- Kendall, M. M., and Sperandio, V. (2016). What a dinner party! Mechanisms and functions of interkingdom signaling in host-pathogen associations. *mBio* 7:e01748-15. doi: 10.1128/mBio.01748-15
- Kolodkin-Gal, I., Hazan, R., Gaathon, A., Carmeli, S., and Engelberg-Kulkka, H. (2007). A linear pentapeptide is a quorum-sensing factor required for mazEF-mediated cell death in *Escherichia coli*. *Science* 318, 652–654. doi: 10.1126/science.1147248
- Kravchenko, V. V., Kaufmann, G. F., Mathison, J. C., Scott, D. A., Katz, A. Z., Wood, M. R., et al. (2006). N-(3-oxo-acyl)homoserine lactones signal cell activation through a mechanism distinct from the canonical pathogen-associated molecular pattern recognition receptor pathways. *J. Biol. Chem.* 281, 28822–28830. doi: 10.1074/jbc.M606613200
- Kravchenko, V. V., Kaufmann, G. F., Mathison, J. C., Scott, D. A., Katz, A. Z., Grauer, D. C., et al. (2008). Modulation of gene expression via disruption of NF-κappaB signaling by a bacterial small molecule. *Science* 321, 259–263. doi: 10.1126/science.1156499
- Kubesová, A., Horká, M., Ružička, F., Slais, K., and Glatz, Z. (2010). Separation of attogram terpenes by the capillary zone electrophoresis with fluorometric detection. *J. Chromatogr. A* 1217, 7288–7292. doi: 10.1016/j.chroma.2010.09.038
- Kumar, S., Kolodkin-Gal, I., and Engelberg-Kulkka, H. (2013). Novel quorum-sensing peptides mediating interspecies bacterial cell death. *mBio* 4, 1–12 doi: 10.1128/mBio.00314-13
- Kumari, A., Pasini, P., and Daunert, S. (2008). Detection of bacterial quorum sensing N-acyl homoserine lactones in clinical samples. *Anal. Bioanal. Chem.* 391, 1619–1627. doi: 10.1007/s00216-008-2002-3
- La Rosa, S. L., Solheim, M., Diep, D. B., Nes, I. F., and Brede, D. A. (2015). Bioluminescence based biosensors for quantitative detection of enterococcal peptide-pheromone activity reveal inter-strain telesensing *in vivo* during polymicrobial systemic infection. *Sci. Rep.* 5:8339. doi: 10.1038/srep08339
- Li, H., Wang, L., Ye, L., Mao, Y., Xie, X., Xia, C., et al. (2009). Influence of *Pseudomonas aeruginosa* quorum sensing signal molecule N-(3-oxododecanoyl) homoserine lactone on mast cells. *Med. Microbiol. Immunol.* 198, 113–121. doi: 10.1007/s00430-009-0111-z
- Li, L., Hooi, D., Chhabra, S. R., Pritchard, D., and Shaw, P. E. (2004). Bacterial N-acylhomoserine lactone-induced apoptosis in breast carcinoma

- cells correlated with down-modulation of STAT3. *Oncogene* 23, 4894–4902. doi: 10.1038/sj.onc.1207612
- Li, X., Fekete, A., Englmann, M., Götz, C., Rothbäller, M., Frommberger, M., et al. (2006). Development and application of a method for the analysis of N-acylhomoserine lactones by solid-phase extraction and ultra high pressure liquid chromatography. *J. Chromatogr. A* 1134, 186–193. doi: 10.1016/j.chroma.2006.09.047
- Li, Z., and Nair, S. K. (2012). Quorum sensing: how bacteria can coordinate activity and synchronize their response to external signals? *Protein Sci.* 21, 1403–1417. doi: 10.1002/pro.2132
- Lyte, M. (1993). The role of microbial endocrinology in infectious disease. *J. Endocrinol.* 137, 343–345.
- Lyte, M. (2004). Microbial endocrinology and infectious disease in the 21st century. *Trends Microbiol.* 12, 14–20. doi: 10.1016/j.tim.2003.11.004
- Lyte, M., and Ernst, S. (1993). Alpha and beta adrenergic receptor involvement in catecholamine-induced growth of Gram-negative bacteria. *Biochem. Biophys. Res. Commun.* 190, 447–452. doi: 10.1006/bbrc.1993.1068
- Lyte, M., Vulchanova, L., and Brown, D. R. (2011). Stress at the intestinal surface: catecholamines and mucosa-bacteria interactions. *Cell Tissue Res.* 343, 23–32. doi: 10.1007/s00441-010-1050-0
- Malik, A. K., Fekete, A., Gebefuegi, I., Rothbäller, M., and Schmitt-Kopplin, P. (2009). Single drop microextraction of homoserine lactones based quorum sensing signal molecules, and the separation of their enantiomers using gas chromatography mass spectrometry in the presence of biological matrices. *Microchim. Acta* 166, 101–107. doi: 10.1007/s00604-009-0183-x
- Marchesan, J. T., Morelli, T., Moss, K., Barros, S. P., Ward, M., Jenkins, W., et al. (2015). Association of synergistetes and cyclodipeptides with periodontitis. *J. Dent. Res.* 94, 1425–1431. doi: 10.1177/0022034515594779
- Mayer, M. L., Sheridan, J. A., Blohmke, C. J., Turvey, S. E., and Hancock, R. E. W. (2011). The *Pseudomonas* autoinducer 3O-C12 homoserine lactone provokes hyperinflammatory responses from cystic fibrosis airway epithelial cells. *PLOS ONE* 6:e16246. doi: 10.1371/journal.pone.0016246
- McNab, R., and Lamont, R. J. (2003). Microbial dinner-party conversations: the role of LuxS in interspecies communication. *J. Med. Microbiol.* 52, 541–545. doi: 10.1099/jmm.0.05128-0
- Mello, A. M., Paroni, G., Daragjata, J., and Pilotto, A. (2016). Gastrointestinal microbiota and their contribution to healthy aging. *Dig. Dis.* 34, 194–201. doi: 10.1159/000443350
- Miyairi, S., Tateda, K., Fuse, E. T., Ueda, C., Saito, H., Takabatake, T., et al. (2006). Immunization with 3-oxododecanoyl-L-homoserine lactone-protein conjugate protects mice from lethal *Pseudomonas aeruginosa* lung infection. *J. Med. Microbiol.* 55, 1381–1387. doi: 10.1099/jmm.0.46658-0
- Moos, W. H., Faller, D. V., Harpp, D. N., Kanara, I., Pernokas, J., Powers, W. R., et al. (2016). Microbiota and neurological disorders: a gut feeling. *Biores Open Access*, 5, 137–145. doi: 10.1089/biores.2016.0010
- Mori, M., Isogai, A., Sakagami, Y., Fujino, M., Kitada, C., Clewell, D. B., et al. (1986b). Isolation and structure of the *Streptococcus faecalis* sex-pheromone inhibitor, iAD1, that is excreted by the donor strain harboring plasmid pAD1. *Agric. Biol. Chem.* 50, 539–541. doi: 10.1271/bbb1961.50.539
- Mori, M., Sakagami, Y., Ishii, Y., Isogai, A., Kitada, C., Fujino, M., et al. (1988). Structure of cCF10, a peptide sex pheromone which induces conjugative transfer of the *Streptococcus faecalis* tetracycline resistance plasmid, pCF10. *J. Biol. Chem.* 263, 14574–14578.
- Mori, M., Sakagami, Y., Narita, M., Isogai, A., Fujino, M., Kitada, C., et al. (1984). Isolation and structure of the bacterial sex pheromone, cAD1, that induces plasmid transfer in *Streptococcus faecalis*. *FEBS Lett.* 178, 97–100. doi: 10.1016/0014-5793(84)81248-X
- Mori, M., Tanaka, H., Sakagami, Y., Isogai, A., Fujino, M., Kitada, C., et al. (1986a). Isolation and structure of the *Streptococcus faecalis* sex pheromone, cAM373. *FEBS Lett.* 206, 69–72. doi: 10.1016/0014-5793(86)81342-4
- Mori, M., Tanaka, H., Sakagami, Y., Isogai, A., Kitada, C., Clewell, D. B., et al. (1987). Isolation and structure of the sex pheromone inhibitor, iPD1, excreted by *Streptococcus faecalis* donor strains harboring plasmid pPD1. *J. Bacteriol.* 169, 1747–1749.
- Morin, D., Grasland, B., Vallée-Réhel, K., Dufau, C., and Haras, D. (2003). Online high-performance liquid chromatography-mass spectrometric detection and quantification of N-acylhomoserine lactones, quorum sensing signal molecules, in the presence of biological matrices. *J. Chromatogr. A* 1002, 79–92. doi: 10.1016/S0021-9673(03)00730-1
- Murray, B. E., An, F. Y., and Clewell, D. B. (1988). Plasmids and pheromone response of the beta-lactamase producer *Streptococcus (Enterococcus) faecalis* HH22. *Antimicrob. Agents Chemother.* 32, 547–551. doi: 10.1128/AAC.32.4.547
- Nakayama, J., Abe, Y., Ono, Y., Isogai, A., and Suzuki, A. (1995a). Isolation and structure of the *Enterococcus faecalis* sex pheromone, cOB1, that induces conjugal transfer of the hemolysin/bacteriocin plasmids, pOB1 and pYI1. *Biosci. Biotechnol. Biochem.* 59, 703–705. doi: 10.1271/bbb.59.703
- Nakayama, J., Ono, Y., and Suzuki, A. (1995b). Isolation and structure of the sex pheromone inhibitor, iAM373, of *Enterococcus faecalis*. *Biosci. Biotechnol. Biochem.* 59, 1358–1359. doi: 10.1271/bbb.59.1358
- Nakayama, J., Ruhfel, R. E., Dunny, G. M., Isogai, A., and Suzuki, A. J. (1994). The prgQ gene of the *Enterococcus faecalis* tetracycline resistance plasmid pCF10 encodes a peptide inhibitor, iCF10. *J. Bacteriol.* 176, 7405–7408.
- Naseribarzouei, A., Hestad, K., Avershina, E., Sekelja, M., Linløkken, A., Wilson, R., et al. (2014). Correlation between the human fecal microbiota and depression. *Neurogastroenterol. Motil.* 26, 1155–1162. doi: 10.1111/nmo.12378
- Nealson, K. H., Platt, T., and Hastings, J. W. (1970). Cellular control of the synthesis and activity of the bacterial luminescent system. *J. Bacteriol.* 104, 313–322.
- Nealson, K., and Hastings, J. W. (1979). Bacterial bioluminescence: its control and ecological significance. *Microbiol. Rev.* 43, 496.
- Nilsen, T., Nes, I. F., and Holo, H. (1998). An exported inducer peptide regulates bacteriocin production in *Enterococcus faecium* CTC492. *J. Bacteriol.* 180, 1848–1854.
- O'Connor, G., Knecht, L. D., Salgado, N., Strobel, S., Pasini, P., and Daunert, S. (2016). Whole-cell biosensors as tools for the detection of quorum-sensing molecules: uses in diagnostics and the investigation of the quorum-sensing mechanism. *Adv. Biochem. Eng. Biotechnol.* 154, 181–200. doi: 10.1007/10_2015_337
- Oleskin, A. V., El'-registan, G. I., and Shenderov, B. A. (2016). Role of neuromodulators in the functioning of the human microbiota: “business talks” among microorganisms and the microbiota-host dialogue. *Microbiology* 85, 1–22. doi: 10.1134/S0026261716010082
- Oliver, C. M., Schaefer, A. L., Greenberg, E. P., and Sufrin, J. R. (2009). Microwave synthesis and evaluation of phenacylhomoserine lactones as anticancer compounds that minimally activate quorum sensing pathways in *Pseudomonas aeruginosa*. *J. Med. Chem.* 52, 1569–1575. doi: 10.1021/jm8015377
- O'Mahony, S. M., Clarke, G., Borre, Y. E., Dinan, T. G., and Cryan, J. F. (2015). Serotonin, tryptophan metabolism and the brain-gut-microbiome axis. *Behav. Brain Res.* 277, 32–48. doi: 10.1016/j.bbr.2014.07.027
- Ortori, C. A., Dubern, J. F., Chhabra, S. R., Cámará, M., Hardie, K., Williams, P., et al. (2011). Simultaneous quantitative profiling of N-acyl-L-homoserine lactone and 2-alkyl-4(1H)-quinolone families of quorum-sensing signaling molecules using LC-MS/MS. *Anal. Bioanal. Chem.* 399, 839–850. doi: 10.1007/s00216-010-4341-0
- Pacheco, A. R., and Sperandio, V. (2009). Inter-kingdom signaling: chemical language between bacteria and host. *Curr. Opin. Microbiol.* 12, 192–198. doi: 10.1016/j.mib.2009.01.006
- Parekh, P. J., Nayi, V. R., Johnson, D. A., and Vinik, A. I. (2016). The Role of gut microflora and the cholinergic anti-inflammatory neuroendocrine system in diabetes mellitus. *Front. Endocrinol.* 7:55. doi: 10.3389/fendo.2016.00055
- Patel, N. M., Moore, J. D., Blackwell, H. E., and Amador-Noguez, D. (2016). Identification of unanticipated and novel N-acyl L-homoserine lactones (AHLs) using a sensitive non-targeted LC-MS/MS method. *PLOS ONE* 11:e0163469. doi: 10.1371/journal.pone.0163469
- Pearman, W. F., Lawrence-Snyder, M., Angel, S. M., and Decho, A. W. (2007). Surface-enhanced raman spectroscopy for *in situ* measurements of signaling molecules (autoinducers) relevant to bacteria quorum sensing. *Appl. Spectrosc.* 61, 1295–1300. doi: 10.1366/000370207783292244
- Pereira, C. S., Thompson, J. A., and Xavier, K. B. (2013). AI-2-mediated signalling in bacteria. *FEMS Microbiol. Rev.* 37, 156–181. doi: 10.1111/j.1574-6976.2012.00345.x
- Pesci, E. C., Milbank, J. B. J., Pearson, J. P., McKnight, S., Kende, A. S., Greenberg, E. P., et al. (1999). Quinolone signaling in the cell-to-cell communication system of *Pseudomonas aeruginosa*. *Proc. Natl. Acad. Sci. U.S.A.* 96, 11229–11234. doi: 10.1073/pnas.96.20.11229

- Pesci, E. C., Pearson, J. P., Seed, P. C., and Iglesias, B. H. (1997). Regulation of las and rhl quorum sensing in *Pseudomonas aeruginosa*. *J. Bacteriol.* 179, 3127–3132. doi: 10.1128/JB.179.10.3127-3132.1997
- Petersen, F. C., Pecharki, D., and Scheie, A. A. (2004). Biofilm mode of growth of *Streptococcus intermedius* favored by a competence-stimulating signaling peptide. *J. Bacteriol.* 186, 6327–6331. doi: 10.1128/JB.186.18.6327-6331.2004
- Pozzi, G., Masala, L., Lannelli, F., Manganelli, R., Havarstein, L. S., Piccoli, L., et al. (1996). Competence for genetic transformation in encapsulated strains of *Streptococcus pneumoniae*: two allelic variants of the peptide pheromone. *J. Bacteriol.* 178, 6087–6090. doi: 10.1128/jb.178.20.6087-6090.1996
- Pritchard, D. (2006a). Immune modulation by *Pseudomonas aeruginosa* quorum-signal molecules. *Int. J. Med. Microbiol.* 296, 111–1166. doi: 10.1016/j.ijmm.2006.01.037
- Pritchard, Q. I. (2006b). Immune modulation by *Pseudomonas aeruginosa* quorum-sensing signal molecules. *Int. J. Med. Microbiol.* 296, 111–116. doi: 10.1016/j.ijmm.2006.01.037
- Procaccini, C., Pucino, V., De Rosa, V., Marone, G., and Matarese, G. (2014). Neuro-endocrine networks controlling immune system in health and disease. *Front. Immunol.* 5:143. doi: 10.3389/fimmu.2014.00143
- Rai, N., Rai, R., and Venkatesh, K. V. (2015). “Quorum Sensing Biosensors,” in *Quorum Sensing vs. Quorum Quenching: A Battle with No End in Sight*, ed V. C. Kalia (New Delhi: Springer), 173–183.
- Rasko, D. A., Moreira, C. G., Li, D. R., Reading, N. C., Ritchie, J. M., Waldor, M. K., et al. (2008). Targeting QsecC signaling and virulence for antibiotic development. *Science* 321, 1078–1080. doi: 10.1126/science.1160354
- Raut, N., Pasini, P., and Daunert, S. (2013). Deciphering bacterial universal language by detecting the quorum sensing signal, autoinducer-2, with a whole-cell sensing system. *Anal. Chem.* 85, 9604–9609. doi: 10.1021/ac401776k
- Rickard, A. H., Campagna, S. R., and Kolenbrander, P. E. (2008). Autoinducer-2 is produced in saliva-fed flow conditions relevant to natural oral biofilms. *J. Appl. Microbiol.* 105, 2096–2103. doi: 10.1111/j.1365-2672.2008.03910.x
- Rickard, A. H., Palmer, R. J. Jr., Blehert, D. S., Campagna, S. R., Semmelhack, M. F., Egland, P. G., et al. (2006). Autoinducer 2, a concentration-dependent signal for mutualistic bacterial biofilm growth. *Mol. Microbiol.* 60, 1446–1456. doi: 10.1111/j.1365-2958.2006.05202.x
- Rutherford, S. T., and Bassler, B. L. (2012). Bacterial quorum sensing: its role in virulence and possibilities for its control. *Cold Spring Harb. Perspect. Med.* 2, 1–25. doi: 10.1101/cspperspect.a012427
- Ryan, R. P., and Dow, J. M. (2008). Diffusible signals and interspecies communication in bacteria. *Microbiology* 154, 1845–1858. doi: 10.1099/mic.0.2008/017871-0
- Shaw, P. D., Ping, G., Daly, S. L., Cha, C., Cronan, J. E. Jr., Rinehart, K. L., et al. (1997). Detecting and characterizing N-acyl-homoserine lactone signal molecules by thin-layer chromatography. *Proc. Natl. Acad. Sci. U.S.A.* 94, 6036–6041. doi: 10.1073/pnas.94.12.6036
- Sifri, C. D. (2008). Quorum sensing: bacteria talk sense. *Clin. Infect. Dis.* 47, 1070–1076. doi: 10.1086/592072
- Singh, P. K., Schaefer, A. L., Parsek, M. R., Moninger, T. O., Welsh, M. J., and Greenberg, E. P. (2000). Quorum-sensing signals indicate that cystic fibrosis lungs are infected with bacterial biofilms. *Nature* 407, 762–764. doi: 10.1038/35037627
- Skinderoe, M. E., Zeuthen, L. H., Brix, S., Fink, L. N., Lazenby, J., Whittall, C., et al. (2009). *Pseudomonas aeruginosa* quorum-sensing signal molecules interfere with dendritic cell-induced T-cell proliferation. *FEMS Immunol. Med. Microbiol.* 55, 335–345. doi: 10.1111/j.1574-695X.2008.00533.x
- Smith, R. S., Fedyk, E. R., Springer, T. A., Mukaida, N., Iglesias, B. H., and Phipps, R. P. (2001). IL-8 production in human lung fibroblasts and epithelial cells activated by the *Pseudomonas* autoinducer N-3-oxododecanoyl homoserine lactone is transcriptionally regulated by NF-kappa B and activator protein-2. *J. Immunol.* 167, 366–374. doi: 10.4049/jimmunol.167.1.366
- Smith, R. S., Harris, S. G., Phipps, R., and Iglesias, B. (2002a). The *Pseudomonas aeruginosa* quorum-sensing molecule N-(3-oxododecanoyl)homoserine lactone contributes to virulence and induces inflammation *in vivo*. *J. Bacteriol.* 184, 1132–1139. doi: 10.1128/jb.184.4.1132-1139.2002
- Smith, R. S., Kelly, R., Iglesias, B. H., and Phipps, R. P. (2002b). The *Pseudomonas* autoinducer N-(3-oxododecanoyl)homoserine lactone induces cyclooxygenase-2 and prostaglandin E2 production in human lung fibroblasts: implications for inflammation. *J. Immunol.* 169, 2636–2642. doi: 10.4049/jimmunol.169.5.2636
- Spencer, H., Karavolos, M. H., Bulmer, D. M., Aldridge, P., Chhabra, S. R., Winzer, K., et al. (2010). Genome-wide transposon mutagenesis identifies a role for host neuroendocrine stress hormones in regulating the expression of virulence genes in *T. typhimurium*. *J. Bacteriol.* 192, 714–724. doi: 10.1128/JB.01329-09
- Sperandio, V., Torres, A. G., Jarvis, B., Nataro, J. P., and Kaper, J. B. (2003). Bacteria-host communication: the language of hormones. *Proc. Natl. Acad. Sci. U.S.A.* 100, 8951–8956. doi: 10.1073/pnas.1537100100
- Steindler, L., and Venturi, V. (2007). Detection of quorum-sensing N-acyl homoserine lactone signal molecules by bacterial biosensors. *Fems Microbiol. Lett.* 266, 1–9. doi: 10.1111/j.1574-6968.2006.00501.x
- Stilling, R. M., van de Wouw, M., Clarke, G., Stanton, C., Dinan, T. G., and Cryan, J. F. (2016). The neuropharmacology of butyrate: the bread and butter of the microbiota-gut-brain axis. *Neurochem. Int.* 99, 110–132. doi: 10.1016/j.neuint.2016.06.011
- Struss, A. K., Nunes, A., Waalen, J., Lowery, C. A., Pullanikat, P., Denery, J. R., et al. (2013). Toward implementation of quorum sensing autoinducers as biomarkers for infectious disease states. *Anal. Chem.* 85, 3355–3362. doi: 10.1021/ac400032a
- Sturmé, M. H. J., Kleerebezem, M., Nakayama, J., Akkermans, A. D. L., Vaughan, E. E., and de Vos, W. M. (2002). Cell to cell communication by autoinducing peptides in gram-positive bacteria. *Antonie Van Leeuwenhoek* 81, 233–243. doi: 10.1023/A:1020522919555
- Suzuki, A., Mori, M., Sakagami, Y., Isogai, A., Fujino, M., Kitada, C., et al. (1984). Isolation and structure of bacterial sex pheromone, cPD1. *Science* 226, 849–850. doi: 10.1126/science.6436978
- Syvitski, R. T., Tian, X. L., Sampara, K., Salman, A., Lee, S. F., Jakeman, D. L., et al. (2007). Structure-activity analysis of quorum-sensing signaling peptides from *Streptococcus mutans*. *J. Bacteriol.* 189, 1441–1450. doi: 10.1128/JB.00832-06
- Taga, M. E., and Bassler, B. L. (2003). Chemical communication among bacteria. *Proc. Natl. Acad. Sci. U.S.A.* 100, 14549–14554. doi: 10.1073/pnas.1934514100
- Tateda, K., Ishii, Y., Horikawa, M., Matsumoto, T., Miyairi, S., Pechere, J. C., et al. (2003). The *Pseudomonas aeruginosa* autoinducer N-3-dodecanoyl homoserine lactone accelerates apoptosis in macrophages and neutrophils. *Infect. Immun.* 71, 5785–5793. doi: 10.1128/IAI.71.10.5785-5793.2003
- Telford, G., Wheeler, D., Williams, P., Tomkins, P. T., Appleby, P., Sewell, H., et al. (1998a). The *Pseudomonas aeruginosa* Quorum-sensing signal molecule N-(3-oxododecanoyl)-l-homoserine lactone has immunomodulatory activity. *Infect. Immun.* 66, 36–42.
- Telford, G., Wheeler, D., Williams, P., Tomkins, P. T., Appleby, P., Sewell, H., et al. (1998b). The *Pseudomonas aeruginosa* quorum-sensing signal molecule N-(3-oxododecanoyl)-l-homoserine lactone has immunomodulatory activity. *Infect. Immun.* 66, 36–42.
- Teplitski, M., Mathesius, U., and Rumbaugh, K. P. (2011). Perception and degradation of N-acyl homoserine lactone quorum sensing signals by mammalian and plant cells. *Chem. Rev.* 111, 100–116. doi: 10.1021/cr100045m
- Thaissa, C. A., Zmora, N., Levy, M., and Elinav, E. (2016). The microbiome and innate immunity. *Nature* 535, 65–74. doi: 10.1038/nature18847
- Thiel, V., Vilchez, R., Sztajer, H., Wagner-Döbler, I., and Schulz, S. (2009). Identification, quantification, and determination of the absolute configuration of the bacterial quorum-sensing signal autoinducer-2 by gas chromatography-mass spectrometry. *ChemBioChem* 10, 479–485. doi: 10.1002/cbic.200800606
- Thomas, G. L., Böhner, C. M., Williams, H. E., Walsh, C. M., Ladlow, M., Welch, M., et al. (2006). Immunomodulatory effects of *Pseudomonas aeruginosa* quorum sensing small molecule probes on mammalian macrophages. *Mol. Biosyst.* 2, 132–137. doi: 10.1039/B517248A
- Tian, X., Syvitski, R. T., Liu, T., Livingstone, N., Jakeman, D. L., and Li, Y. H. (2009). A method for structure-activity analysis of quorum-sensing signaling peptides from naturally transformable Streptococci. *Biol. Proced. Online* 11, 207–226. doi: 10.1007/s12575-009-9009-9
- Todd, D. A., Zich, D. B., Ettefagh, K. A., Kavanaugh, J. S., Horswill, A. R., and Cech, N. B. (2016). Hybrid Quadrupole-Orbitrap mass spectrometry for quantitative measurement of quorum sensing inhibition. *J. Microbiol. Methods* 127, 89–94. doi: 10.1016/j.mimet.2016.05.024
- Tomova, A., Husarova, V., Lakatosova, S., Bakos, J., Vlkova, B., Babinska, K., et al. (2015). Gastrointestinal microbiota in children with autism in Slovakia. *Physiol. Behav.* 138, 179–187. doi: 10.1016/j.physbeh.2014.10.033

- van der Meer, J. R., and Belkin, S. (2010). Where microbiology meets microengineering: design and applications of reporter bacteria. *Nat. Rev. Microbiol.* 8, 511–522. doi: 10.1038/nrmicro2392
- Vikström, E., Magnusson, K. E., and Pivoriūnas, A. (2005). The *Pseudomonas aeruginosa* quorum-sensing molecule N-(3-oxododecanoyl)-L-homoserine lactone stimulates phagocytic activity in human macrophages through the p38 MAPK pathway. *Microbes Infect.* 7, 1512–1518. doi: 10.1016/j.micinf.2005.05.012
- Wagner, C., Zimmermann, S., Brenner-Weiss, G., Hug, F., Prior, B., Obst, U., et al. (2007). The quorum-sensing molecule N-3-oxododecanoyl homoserine lactone (3OC12-HSL) enhances the host defence by activating human polymorphonuclear neutrophils (PMN). *Anal. Bioanal. Chem.* 387, 481–487. doi: 10.1007/s00216-006-0698-5
- Wang, J., Quan, C., Wang, X., Zhao, P., and Fan, S. (2011). Extraction, purification and identification of bacterial signal molecules based on N-acyl homoserine lactones. *Microb. Biotechnol.* 4, 479–490. doi: 10.1111/j.1751-7915.2010.00197.x
- Wei, Y., Perez, L. J., Ng, W. L., Semmelhack, M. F., and Bassler, B. L. (2011). Mechanism of *Vibrio cholerae* autoinducer-1 biosynthesis. *ACS Chem. Biol.* 6, 356–365. doi: 10.1021/cb1003652
- Wynendaele, E., Bronselaer, A., Nielandt, J., D'Hondt, M., Stalmans, S., Bracke, N., et al. (2013). Quorumpeps database: chemical space, microbial origin and functionality of quorum sensing peptides. *Nucleic Acids Res.* 41, D655–D659. doi: 10.1093/nar/gks1137
- Wynendaele, E., Verbeke, F., D'Hondt, M., Hendrix, A., Van De Wiele, C., Burvenich, C., et al. (2015a). Crosstalk between the microbiome and cancer cells by quorum sensing peptides. *Peptides* 64, 40–48. doi: 10.1016/j.peptides.2014.12.009
- Wynendaele, E., Verbeke, F., Stalmans, S., Gevaert, B., Janssens, Y., Van De Wiele, C., et al. (2015b). Quorum sensing peptides selectively penetrate the blood-brain barrier. *PLoS ONE* 10:e0142071. doi: 10.1371/journal.pone.0142071
- Yamashita, K., Kaneko, H., Yamamoto, S., Konagaya, T., Kusugami, K., and Mitsuma, T. (1998). Inhibitory effect of somatostatin on *Helicobacter pylori* proliferation *in vitro*. *Gastroenterology* 115, 1123–1130. doi: 10.1016/S0016-5085(98)70083-6
- Zackular, J. P., Baxter, N. T., Iverson, K. D., Sadler, W. D., Petrosino, J. F., Chen, G. Y., et al. (2013). The gut microbiome modulates colon tumorigenesis. *mBio* 4, e00692–e00613. doi: 10.1128/mBio.00692-13
- Zhang, C., and Ye, B. C. (2014). Real-time measurement of quorum-sensing signal autoinducer 3OC6HSL by a FRET-based nanosensor. *Bioprocess Biosyst. Eng.* 37, 849–855. doi: 10.1007/s00449-013-1055-7
- Zhou, L., Glennon, J. D., Luong, J. H., Reen, F. J., O'Gara, F., McSweeney, C., et al. (2011). Detection of the *Pseudomonas* Quinolone Signal (PQS) by cyclic voltammetry and amperometry using a boron doped diamond electrode. *Chem. Commun.* 47, 10347–10349. doi: 10.1039/c1cc13997e
- Zhou, L., Reen, F. J., O'Gara, F., McSweeney, C. M., Clarke, S. L., Glennon, J. D., et al. (2012). Analysis of pseudomonas quinolone signal and other bacterial signalling molecules using capillaries coated with highly charged polyelectrolyte monolayers and boron doped diamond electrode. *J. Chromatogr. A* 1251, 169–175. doi: 10.1016/j.chroma.2012.06.064
- Zimmermann, S., Wagner, C., Müller, W., Brenner-Weiss, G., Hug, F., Prior, B., et al. (2006). Induction of neutrophil chemotaxis by the quorum-sensing molecule N-(3-oxododecanoyl)-L-homoserine lactone. *Infect. Immun.* 74, 5687–5692. doi: 10.1128/iai.01940-05

Conflict of Interest Statement: The authors declare that the research was conducted in the absence of any commercial or financial relationships that could be construed as a potential conflict of interest.

The reviewer SOF and handling Editor declared their shared affiliation, and the handling Editor states that the process nevertheless met the standards of a fair and objective review

Copyright © 2017 Verbeke, De Craemer, Debuinne, Janssens, Wynendaele, Van de Wiele and De Spiegeleer. This is an open-access article distributed under the terms of the Creative Commons Attribution License (CC BY). The use, distribution or reproduction in other forums is permitted, provided the original author(s) or licensor are credited and that the original publication in this journal is cited, in accordance with accepted academic practice. No use, distribution or reproduction is permitted which does not comply with these terms.

Advantages of publishing in Frontiers



OPEN ACCESS

Articles are free to read for greatest visibility and readership



FAST PUBLICATION

Around 90 days from submission to decision



HIGH QUALITY PEER-REVIEW

Rigorous, collaborative, and constructive peer-review



TRANSPARENT PEER-REVIEW

Editors and reviewers acknowledged by name on published articles



REPRODUCIBILITY OF RESEARCH

Support open data and methods to enhance research reproducibility



DIGITAL PUBLISHING

Articles designed for optimal readership across devices



FOLLOW US
@frontiersin



IMPACT METRICS
Advanced article metrics track visibility across digital media



EXTENSIVE PROMOTION
Marketing and promotion of impactful research



LOOP RESEARCH NETWORK
Our network increases your article's readership

Frontiers

Avenue du Tribunal-Fédéral 34
1005 Lausanne | Switzerland

Visit us: www.frontiersin.org

Contact us: info@frontiersin.org | +41 21 510 17 00